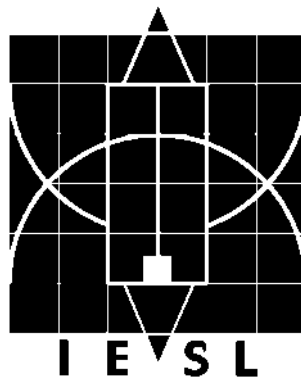


“To promote the acquisition and interchange of technical knowledge,
advance the science and practice of engineering in all its branches and
regulate professional activities in Sri Lanka.”

THE INSTITUTION OF ENGINEERS SRI LANKA



Transactions - 2017

PART B

Technical Papers

This Institution does not, as a body, hold itself responsible for statements made or opinions expressed either in the Papers read or the discussions which have occurred at the Meetings.

CEO / Executive Secretary

The articles published in the Transactions are based on Engineering Research and some are of Professional Interest. All published papers have been refereed in anonymity by at least two subject specialists.

Published by:

**The Institution of Engineers, Sri Lanka
120/15, Wijerama Mawatha
Colombo 07**

Tel : 2 698426, 2685490, 2 699210

Fax : 2 699202

E-mail : iesl@slt.lk

Website : <http://www.iesl.lk>

Printed at:

**Karunaratne & Sons (Pvt) Ltd.
65 C, Midellamulahena,
Thalgahawila Road, Horana.
Info@karusons.com**

CONTENTS

Editor's note	xi
1. Rainfall Thresholds for Initiation of Landslides in Ratnapura District By: Eng. L R Abhayarathne	1
2. Experimental Study on the Effect of Presence of Deep Embedded Retaining Walls on the Settlement of Shallow Foundations By : Eng. M P Amarasinghe and Eng. (Dr.) L I N De Silva	11
3. Shrinkage Behavior of a Liner Material with Expansive Properties for use in an Engineered Landfill By : Eng. (Ms) V Kayaththiry	17
4. Identification of Clayey Properties for Cricket Pitch Surfacing and Analysing the Variation of Surface Crack Densities in different Pitches By : Eng. W S U Perera, Eng. (Dr.)U P Nawagamuwa and Mr. G N U Thilakarathna	25
5. Design of Soil–Cement–Bentonite (SCB) backfill and construction of SCB slurry walls along the earthen dam at Iranamadu Reservoir in Kilinochchi By: Eng. (Dr.) P N Wickramarachchi, Eng. S Weerakoon, Mr. S Semage, Eng. N Madushanka and Eng. T Rajagobu	33
6. Ballast Mats Made of Recycled Tyre Waste to Enhance the Performance of Rail Track Substructure under Cyclic Load By: Eng. (Dr.) S K Navaratnarajah and Eng. (Prof.) B Indraratna	41
7. Analysis of Energy Dissipation in Post-Tensioned Hybrid Precast Concrete Frames By: Eng. K L P S Perera, Eng. W D C R Wanniarachchi and Dr. P Thammarak	51
8. Study on Filler Slab Construction By: Eng. (Dr.) K Baskaran, Eng. A Gopikrishna and Eng. P Thiruvarankan	59
9. Energy Dissipater for Post-Tensioned Steel Frame System By: Eng. Ms. W D C R Wanniarachchi, Eng. K L P S Perera and Dr. P Thammarak	67
10. Simplified Approach for Predicting Fatigue Life of Fillet Welded Joints with FEM By: Eng. (Ms.) S Varakini, Eng. K Ubamanyu and Eng. (Dr.) H M Y C Mallikarachchi	75
11. Growing Colombo: Some Concerns from Wind Engineering Point of View By: Dr. A U Weerasuriya and Mr. K A B Weerasinghe	81
12. Contributory factors for Cost and Time Overruns of Construction Projects By: Eng. Leelanath Daluwatte and Eng. (Prof.) Malik Ranasinghe	89
13. Sub-Contracting and Accident Risk in Construction Industry : A Case Study in Singapore By: Eng. W A Asanka and Eng.(Prof.) Malik Ranasinghe	97



14. Techno-Economic Analysis of Building Energy System with Net Meter Solar PV in Sri Lanka By: Eng. (Dr.) K T M U Hemapala and Eng.(Ms.) T M S C Jayasinghe	105
15. Multi-Functional Floor Cleaning Robot for Domestic Environment By: Eng. H G T Milinda and Eng. B G D A Madhusanka	115
16. Development of CZTS thin Film from Spin Coating for Solar Cell Application By: H A D I Dilshan, W D D Weerasinghe, Eng. N L W Wijewantha, Eng. W P S Wijesinghe and Dr. D Atygalle	121
17. Characterization of Fuel Briquettes Made for Household Cooking from Sawdust and Rice Husk By: M Y A R Ahmed, U M A Devaraja, K A R Mihiranga and Prof. B A J K Premachandra	125
18. Assessing the Performance of a Destructive Measurement System: A Case of an Industrial Glove Manufacturing Environment By: Mrs. H A D Perera and Dr. P Gamage	135
19. Development of ANN Based IMC for Biomass Pack Bed Gasification Plant with Enhanced Efficiency By : Eng. G V C Rasanga, Eng. (Dr.) K T M U Hemapala and Eng. (Dr.) A G Buddhika P Jayasekara	143
20. Organic Rankine Cycle (ORC): Performance of Working Fluids and Energy Recovery Potential in Sri Lankan Thermal Power Plants By : Eng. B S R Fernando, Dr. R A C P Ranasinghe and Dr. H K G Punchihewa	151
21. Mechanized Fertilizer Applicator Operated by Two-wheel Tractor for Coconut Plantation Industry in Sri Lanka By: Eng. S A P S Silva	161
22. Water Loss Reduction by Understanding the Reticulation A Case Study By : Eng. S G G Rajkumar	167
23. Implementation of Water Safety Plans for Rural Water Supply Schemes Managed By CBOs in Sri Lanka - Common Risks and Analysis By: Mr. T R Samaraweera and Eng. (Prof.) (Mrs.) Niranjanie Ratnayake	173
24. A Study on Recontamination Risks in Water Distribution Systems, using A Network Model By : Mr. M H V Lasantha and Eng. (Prof.) (Mrs.) Niranjanie Ratnayake	181
25. Review of Irrigation Ordinance and Identifying the Gaps to fulfil the Current Needs of the Society By: Eng. (Mrs.) Badra Kamaladasa, Eng. Lalith De Alwis and Eng. G D F U Perera	189
26. Analysis of Long-term Trends of Climatological Parameters in Kigali, Rwanda By: Eng. (Dr.) D P C Laknath, Eng. N R Josiah and Eng. T A J G Sirisena	197

27. Development of a Flood Forecasting And Data Dissemination System For Kalu River Basin in Sri Lanka
By: Eng. S Kokularamanan, Eng. (Dr.) A W M Rasmy, Eng. (Dr.) Duminda Perera and Eng. (Prof.) Toshio Koike 205
28. A GIS Based Asset Management Approach to Upgrade the Level of Service to Pipe Borne Water Consumers in Western North Region
By: Eng. A M H K Abeykoon and Eng. B U J Perera 211
29. Application of 3D Physical Modelling for Verification and Optimization of Hydraulic Designs for Salinity Barriers in Sri Lanka
By: Eng. (Mrs.) S M C K Subasinghe, Eng. (Ms.) K P S T Pathirana, Eng. (Ms.) N L Engiliyage and Eng. G H N Rathnasiri 219
30. Numerical Model Investigations on Dispersion of Industrial Effluents in East Coast of Sri Lanka
By: Eng. (Dr.) S Wickramaratne and Eng. (Ms.) K P S T Pathirana 227
31. Numerical Modelling Study for RahfalhuHuraa Resort Development in Maldives
By: Eng. M S L Fernando, Eng. I L Abeygoonasekara and Eng. S M D E Suriyamudali 239
32. Wave Tranquillity Study for a Fishery Harbour using Boussinesq Type Wave Model
By: Eng. (Dr.) D P C Laknath, Eng. D E N Senarathne and Eng. K K P P Ranaweera 247
33. Verification of Wave Transformation to Establish the Nearshore Wave Climate
By: Eng. (Dr.) D P L Ranasinghe, Eng. N L Engiliyage, Eng. H P G M Caldera and Eng. I G I Kumara 255
34. Fabrication and Mechanical Property Analysis of Microcrystalline Cellulose Based Polymer Composite for Engineering Applications
By: Ms. H A D Saumyadi, Mr. L D Rajapaksha, Eng. A M P B Samarasekara, Dr. D A S Amarasinghe and Prof. L Karunanayake 263
35. Synthesis and Characterization of Nanoparticle-Incorporated Antimicrobial Coating for Food Packaging Applications
By: Ms. S P A Madushani, Ms. D P Egodage, Eng. A M P B Samarasekara, Dr. D A S Amarasinghe, Mr. H T S Jayalath and Mr. S M N S Senerath 271
36. Assessing the Impact on Environment, Health and Safety due to Releases from Chemical Process Routes
By: Eng. H B B Anuradha, Eng. (Dr.) Manisha Gunasekera and Dr. Olga Gunapala 277
37. Antecedents of Work Engagement : Case Study of Outsourced Employees in Telecommunication Service Sector of Sri Lanka
By: Eng. K A Chathura S Kumarasinghe 285
38. The Structure of Land Prices in Colombo and its Implications
By : Eng. (Dr.) P I A Gomes and R K Hashan 305



39. Knowledge Management System for Mobile Telecommunication Sector in Sri Lanka
By: Eng. Jeewantha Nadeera, Eng. (Ms.) Shalanika Dayarathna and
Eng. Eranda Ihalagedara 311
40. Effect of Technical and Non-Technical competence on the Job Performance of Private
Sector Engineers in Sri Lanka
With special reference to a group of large scale engineering companies
By : Eng. J R Ekanayake 317
41. Artificial Bone Substitutes and Bone Tissue Engineering as Alternative Methods for
Natural Bone Repair and Regeneration in Severe Traumas and Complex Clinical
Conditions of Bones.
By : Eng. (Miss.) B R M G W U B Balagalla 327
42. Condition Assessment of Power Transformers using Dissolved Gas Analysis
By : Eng. W T D Samarasingha, Eng. (Dr.) J R S S Kumara and
Eng. (Prof.) M A R M Fernando 333
43. Battery - Supercapacitor Hybrid Energy Storage Control for Electric Vehicle
By: Mr. W M J Madhusankha, Mr. G A T P Madhuranga, Mr. S A S Indika,
Eng. (Dr.) B G L T Samaranayake, Eng. (Dr.) P J Binduhewa and
Eng. (Prof.) J B Ekanayake 341
44. Pitch Control of a Twin Rotor System using Error Dynamics Based Nonlinear
Controller
By: Mr. Yasitha Liyanage, Eng. Jagannath Wijekoon, Eng. Shirantha Welikala and
Eng. (Dr.) Lilantha Samaranayake 349
45. Museum Navigation System with Beacons
By: Eng. N D C D Kannangara and Eng. W D S S Bandara 355
46. Adaptation of SCASA Technique for surge Protective Devices for Equatorial Belt
Countries
By : Eng. J P D S Athuraliya, Eng. N L Rathnayake, Eng. N A A N Dilrukshi, Eng. P
Mahadevan, Eng. R Gihara, Mr. T M S Dias, Mr. S R J S Bandara, Ms. H Wijesooriya
and Eng. (Prof.) Nihal Kularatna 363
47. Detecting Key Actors in Multiple SIM Networks Via Centrality Measures and Mobile
Service usage Behaviors
By: Eng. (Dr.) A J M Korale and Mr. N S Weeraman 373
48. Intelligent Pest Repellent System for Sri Lankan Farming Industry
By : Eng. P N Karunanayake, Mr. W H H N de Soysa, Mr. J A C L C Jayasundara,
Mr. Y G Wanniarachchi and Mr. A P I Karunarathne 379
49. Land Cover Classification and Sub Component Analysis Using Hyperspectral
Imagery
By: Ms. A M R Abeysekara, Mr. T S J Oorloff, Ms. S S P Vithana,
Eng. (Dr.) H M V R Herath, Eng. (Dr.) G M R I Godaliyadda and
Eng. (Dr.) M P B Ekanayake 385

50. Spatial Modulation for Indoor MIMO Visible Light Communication System By : Mr. U G R K W S Palitharathna, Mr. A G D U K Samarasinghe, Mr. Y M L D Wijayarathna, Eng. (Dr.) S A H A Suraweera and Eng. (Dr.) G M R I Godaliyadda	391
51. Energy Management System of a Solar Driven DC System By : Mr. H M A A B Herath, Mr. K K S U Kodithuwakku, Eng. Mrs. D R D S Dasanayaka, Dr. P J Binduhewa, Eng. (Prof.) J B Ekanayake and Eng. (Dr.) S M K B Samarakoon	401
52. Laser Ranging Based Intelligent System for Unknown Environment Mapping By: Mr. T H M N C Thelasingha, Mr. U V B L Udugama, Ms. E M S P Ekanayake, Eng. (Dr.) G M R I Godaliyadda, Eng. (Dr.) M P B Ekanayake, Eng. (Dr.) B G L T Samaranayake and Eng. (Dr.) J V Wijayakulasooriya	411
53. A Novel Handover Mechanism for Visible Light Communication Network By : Mr. M A N Perera, Mr. N G K R Wijewardhana, Ms. A A D T Nissanka, Dr. S A H A Suraweera and Eng. (Dr.) G M R I Godaliyadda	421
54. Technical, Economic, Operational and Dispatch Analysis of Optimum Integration of Renewable Energy in to the Sri Lankan Power system By : Eng. Buddhika Samarasekara, Eng. Randika Wijekoon and Eng. Lathika Attanayake	429
55. Optimum Use of Solar Inverter by Feeding Reactive Power at the Night By: Eng. (Ms.) K Kanchanee Navoda and Eng. (Dr.) Asanka S Rodrigo	439
56. Smart Electronic Analyzer for Determination of Chicken Meat Spoilage By: Eng. M P U Isuranga, Mrs. H Pasqual and Dr. N S Weerakkody	447
57. Power Electronic Interface of a Solar Driven DC System By : Mr. W W M D B Wijesinghe, Mr. H M K C B Wijerathne, Ms. B H T S Gunaratne, Dr. P J Binduhewa and Eng. (Prof.) J B Ekanayake	455
58. Indoor Navigation System with RFID Tags for Virtually Impaired Individuals By : Eng. J M K V Jayalath, Mr. D M G C Jayathilake, Mr. M A C I U Yapa, Dr. S A H A Suraweera and Eng. (Dr.) G M R I Godaliyadda	463
59. Energy Efficiency Benchmarking of Pumps in Water and Wastewater Industries in Sri Lanka By: Eng. B G A Dinesh	469
60. Feasibility of Hybrid Reactors for Removal of Heavy Metals in Wastewater By: G S Nallaperuma and Dr. W M K R T W Bandara	475
61. Feasibility of UASB Reactor for Removal of Heavy Metal in Wastewater By: U L N C Jayathileke and Dr. W M K R T W Bandara	485
62. GIS-Based Site Suitability Analysis for Wastewater Treatment Plants By: N A Nusky, S I S Wijesingha, Dr. W M K R T W Bandara, B M L A Basanayake and Dr. Terrance M Rengarasu	493

63. Air Pollution Monitoring Through Crowdsourcing
By : Eng. M I N P Munasinghe, Eng. (Dr.) G I U S Perera, Mr. J K W D B Karunathilaka, Mr. B C S Cooray and Eng. K G D Manupriyal 499
64. A Conceptual Tool for Assessing Building Life Cycle Carbon Emissions in the Context of Sri Lanka
By: Eng. R P Kumanayake, Prof. H B Luo and Eng. R M P S Bandara 507
65. Upgrading of the Existing Sedimentation Tank at Hemmathagama Water Supply Scheme
By: Eng. L Wijesinghe and Eng. (Dr.) D R I B Werellagama 517
66. Risk Assessment of the Active Ingredient, Glyphosate of the Herbicide, *ROUNDUP*® Present in Water Sources of CKDu Prevalent Areas for Humans
By: Eng. (Ms.) S Gunarathna, Eng. (Dr.) (Ms.) B Gunawardana, Eng. (Prof.) M Jayaweera and Mr. K Zoysa 525
67. Field-Scale Study on Treating Landfill Leachate Using Anaerobic Filters Packed with Low-Cost Filter Media
By : Eng. (Dr.) W K C N Dayanthi, Eng. (Mrs.) B S R Nanayakkara, Prof. K Kawamoto, Eng.(Mrs.) M D B A Premathilaka and Mr. O V N Dulvin 531
68. Variations to Key Chemical Parameters during Dried Faecal Sludge and Municipal Solid Waste Co-Composting
By: Eng. H M N Jayawardena, Eng. (Dr.) S C Fernando, Eng. (Dr.) S H P Gunawardena and Eng. N Jayathilake 537
69. Life Cycle Assessment Based Tool to Visualize Environmental Impact of Construction Materials & Products
By : Mr. H M M M Jayawickrama, Mrs. K G N H Weerasinghe, Eng. R L Peiris, Eng. (Dr.) A K Kulatunga 545
70. Safety Analysis of Anaerobic Digestion Plant Operation
By : Eng. (Dr.) Deshai Botheju and Eng. (Dr.) P G Rathnasiri 553
71. Simulating the Effect of Modifying Reversed A2O Process on Combined Removal of Nitrogen, Phosphorous and Organic Matter in Municipal Wastewater
By: Eng. W B Roshen P S Fernando and Eng. (Dr.) P G Rathnasiri 565
72. Extraction of Cellulose from Sri Lankan Agricultural Waste for Engineering Applications
By: Ms. M P A Nanayakkara, Ms. W G A Pabasara, Eng. A M P B Samarasekara, Dr. D A S Amarasinghe and Prof. L Karunanayake 571
73. Environmental Impacts of Organic Fertilizer Produced from Industrial Zone Central Effluent Treatment Plant Sludge using Delta-D Technology
By : Eng. M F H M Aadhil and Eng. (Prof.) S A S Perera 579

74. Field Experiments on Low-Cost Combined-Media an Anaerobic Filter System for the Treatment of Landfill-Leachate
By: Eng. (Ms.) D M T P Fernando, Eng. (Dr.) W K C N Dayanthi, Eng. (Ms.) K G D Chamenuka, Eng. (Mrs.) B S R Nanayakkara and Prof. K Kawamoto 587
75. Low-Cost drinking Water Filter
By: Mr. U A C Perera and Eng. (Dr.) (Ms.) S C S Karunaratne 595
76. Monitoring Carbon Monoxide (CO) Levels at Five Major Schools in Kandy City using Real Time Air Quality Monitoring Sensor Network
By: Eng. R G R N K Ariyaratne, Eng. (Dr.) D G G P Karunaratne, Eng. (Dr.) M A Elangasinghe, Eng. (Dr.) A Manipura, Dr. S P Kodithuwakku, Dr. A D Siribaddana and Mr. K H N Abayalath 605
77. Dense Graded Asphalt for Sri Lanka : Considerations related to Climate and Different Traffic Conditions
By: Eng. W W Bandara and Eng. R P M M Premathilaka 617
78. Suitability of Recycled Pet Fiber and Carbonized Wood Ash in Hot Mix Asphalt Concrete
By : Eng. N Jegatheesan, Eng. (Dr.) T M Rengarasu and Eng. (Dr.) W M K R T Wasala Bandara 623
79. Evaluating Road user Cost for Highway Work Zones – Case Study for Urban Upgrading Projects in Sri Lanka
By: M H M Hamsath and Eng. (Dr.) H R Pasindu 631
80. Development of a Methodology for Road Maintenance Planning of Low Volume Roads Based on Roughness Data
By: Mr. M A D De Silva and Eng. (Dr.) H R Pasindu 641
81. Travel Time Estimation Based on Dynamic Traffic Data and Machine Learning Principles
By: Mr. Sakitha P Kumarage, Mr. V M Jayawardana, Dr. Dimantha De Silva and Eng. (Prof.) J M S J Bandara 649
82. Infrastructure Feasibility Analysis of Inland Water Transportation from Peliyagoda to Hanwella along Kelani River
By: Mr. K P H S Kalahe and Eng. (Dr.) R M N T Sirisoma 659
83. Hydroplaning Risk Evaluation in High Speed Low Traffic Volume Highways
By: Eng. (Ms.) M D M Sheranie and Eng. (Mrs.) S Senevirathne 667





Editor's Note.....

Dear Readers of *Transactions*:

It is my pleasure to introduce *Transactions* (Part B): Technical Papers presented at the 111th Annual Sessions of the Institution of Engineers, Sri Lanka. I am honoured to edit this year's Technical Papers submitted to be presented at the 111th Annual Sessions and sincerely hope that the papers included in here are of value and interest to Engineers and make contributions to the advancement of the Profession of Engineering. As the Editor of the Annual Sessions, I am proud to say that the vision of the IESL in providing our Engineers with a platform to share their research and educational experiences is progressively gaining attention and popularity.

As an engineer, the ability to conduct thorough and accurate research while clearly communicating the results is essential for facilitating the advancement of the acquired knowledge base. Knowing where and how to find different types of information will help solve engineering problems, in both academic as well as the professional career. Lack of investigation into engineering guidelines, standards, and best practices can result in failure with severe repercussions. Traditionally, engineering research has yielded knowledge essential to translating scientific advances into technologies that affect everyday life. Most certainly, engineering research has resulted in the vast progress made by the humanity everywhere in the world. Engineering research, in the future, will generate technological innovations to address enormous challenges in a multitude of areas of the socio-economic systems, in most cases, they will definitely be multi-disciplinary in nature.

All the manuscripts submitted for the Annual Sessions have been reviewed by at least two prominent persons in order to select the highest quality and pertinent research papers that are worthwhile in publishing in the *Transactions*. Many people were involved in this process, beginning with the authors who submit their papers and the reviewers by unrelentingly providing their expertise and time, giving their opinions on the technical and scientific merit of the contents, mathematical and experimental analysis, as well as the scope and contribution to the advancement of the respective field. The reviewers' comments were immensely useful in helping the Editor in making decisions regarding acceptance of a given paper. Their comments helped the authors too, by providing constructive criticisms that enabled them to improve the papers as well as maintaining the quality and higher standards of the *Transactions*. While the Annual Sessions have become a traditional meeting point and forum for engineers, researchers, and professionals, where the discussion topics are recorded as proceeding papers, the *Transactions* is considered a serious reference because the published papers provide a more detailed description of the research work, mainly focused on the current trends in engineering theory and practice. Their validity, relevance, importance, and originality are scrutinised by a peer reviewing process.

I am very grateful to the Council of the IESL for inviting me to be the Editor of this year's Annual Sessions. I extend my sincere appreciations to the staff of the IESL for all their support and help. Finally, once again, I am most appreciative of the efforts of the authors and reviewers, and I am deeply indebted for their commitment, dedication, and creativity.

I wish you all very fruitful deliberations during the Annual Sessions.

Eng. (Professor) Jagath Manatunge

B.Sc. Eng. Hons. (Moratuwa), D.I.C., M.Sc. (Lond.), Ph.D. (Saitama), C. Eng., M.I.E. (SL), MIEPSL

Editor, IESL Transactions (Part B) 2017



Rainfall Thresholds for Initiation of Landslides in Ratnapura District

L. R. Abhayarathne

Abstract: Ratnapura is a district frequently affected by landslides in Sri Lanka and its vulnerability is increased due to its location in the wet zone. The purpose of this study was to find the rainfall thresholds for initiation of landslides in Ratnapura district and the thresholds were based on one day to seven days cumulative rainfall. 225 landslide incidents which occurred from May 1978 to June 2014 were used for the analysis. Probability tables were developed by combining the landslide data with rainfall data. Then, through SPSS a curvilinear Regression model was created for each threshold value using the probability, as the independent variable and the rainfall linked to it as the dependent variable. The correlation of daily rainfall to the cumulative rainfall was calculated up to seven days. The thresholds obtained from the analysis were as follows, for one day threshold ($R = 9.139e^{0.036t}$), for two day cumulative threshold ($R = 15.435e^{0.035t}$) and for three day cumulative threshold ($R = 16.985e^{0.035t}$) where 'R' is the rainfall in millimetres and 't' is the probability of landslide occurrence. The thresholds found for four to seven day cumulative rainfall were not valid due to outliers they contain. When the current NBRO thresholds were compared with the one day threshold value found in the study, the probability received for landslide occurrence was 58.47% for alert level, 66.46% for warning and 77.72% for evacuation level. By looking at the correlation values only the rainfall of the previous day had a significant effect on the cumulative rainfall for occurrence of landslides. In conclusion, the study was able to establish rainfall thresholds for the prediction of landslides based on one day to three day cumulative rainfall.

Keywords: Disaster Management, Landslide, Rainfall Threshold, Ratnapura District

1. Introduction

Sri Lanka is a country prone to handful of natural disasters and one of them is Landslides. A landslide may include a variety of processes that result downward and outward movement of slope forming material that may comprise of rock, artificial fill, soil or a combination of them. They can be very destructive like the one recently happened in Afghanistan which buried more than 2000 people [26] with their property due to the rapid onset that they possess. Similarly in Sri Lanka the landslide event on 29th of October 2014 at Meeriyabeddawatta, in Haldumulla area at Badulla District, shocked the country affecting nearly 1875 people of 521 families, killing 13 people and destroying 66 houses in the area.[32].

Rainfall is one of the recognized triggers of landslides and the fact that Sri Lanka is a tropical country with a mean annual rainfall varying from under 900mm in the dry zone to over 5000mm in the wet zone[28] increases the susceptibility for landslides occurrence. With heavy rainfall the ground water level is increased through infiltration [5] and as a result it increases the pore water pressure thus leading to more landslides[5]. This high and unpredictable precipitation in the wet zone has

created frequent landslide events in over 10 districts including Ratnapura district. Therefore, the minimum amount of rainfall that is needed to trigger a landslide would fall within the interest of disaster analysts, researchers, investigators, disaster responders and the community living in these landslide hazard prone areas.

Currently (August 2017) only a general threshold has been established by NBRO for hourly and daily rainfall which ignores the antecedent rainfall but studies have proven with more antecedent rainfall the current threshold to trigger landslides may reduce [6]. The recent scenario occurred at Meeriyabedda had the highest cumulative rainfall over a period of more than one week proving us the need of having a warning method based on the antecedent rainfall as well.

*Eng. L. R. Abhayarathne, AMIE(SL), AMSSE(SL),
B.Sc. Eng. (Moratuwa), M.Sc. (Colombo), Civil Engineer,
State Engineering Corporation of Sri Lanka*



Current (August 2017) regional landslide thresholds established by NBRO considers only the daily rainfall as follows,

- Alert Level 75mm/day
- Warning Level 100mm/day
- Evacuation Level 75mm/hour or 150mm/day

These thresholds have been defined mainly based on the practical experience supported by statistical analysis and are helpful to issue regional/general warnings to the whole country. However, they do not consider the influence of antecedent rainfall thus making them neither adequate nor accurate to provide a proper warning. Therefore a study to define antecedent rainfall thresholds for local situations is immensely helpful for precise landslide predictions.

2. Literature Review

A threshold could be defined as the minimum or maximum value needed for a certain phenomenon, condition, result or action to occur. The minimum threshold will indicate the lowest level while the maximum threshold will indicate the highest level of the quantity needed and for a rainfall induced landslide a rainfall threshold will indicate the minimum rainfall required to trigger a landslide.

There were two main types of thresholds defined in literature as physical based and empirical based.

- Physical based (process-based, conceptual) ([7]; [8]; [9]; [11])
- Empirical (historical, statistical) based ([12]; [1])

2.1 Physical Based Models

This type of thresholds are based on slope stability models and used extensively in geotechnical engineering ([9]). In order to link the past slope stability data with the rainfall patterns process based models use infiltration models (e.g. [13]). For an example the “leaky barrel” model proposed by Wilson (1989)[2] was used to forecast the accumulation of infiltrated water into the ground.

Further this model was used by Wilson and Wiczorek (1995)[8] to predict debris flow occurrence at La Honda, in the San Francisco Bay region. Apart from this, Crosta and Frattini (2003)[11] also compared three infiltration models given below to forecast the geography and time of debris flows in the Lecco Province, in northern Italy,

- Steady state model ([7])
- Transient “piston-flow” model ([14])
- Transient diffusive model ([10])

These Process-based models can be used to determine the amount of rainfall needed to generate slope failures, the location of the slope failure and the time of occurrence but with limitations,

- They need detailed spatial information on the morphology, soil characteristics, hydrological and lithological data that will control the initiation of landslides
- The difficulty of collecting this type of information accurately over large areas and its rarity because of the lack of testing equipment
- These models can be used in such events where location and time with precipitation measurements are known of slope failures but such information is not commonly available and costly to obtain

As a result of such limitations, physically based models are more suitable to forecast shallow landslides (debris flows and soil slides), but not deep-seated landslides[6].

A different approach was adopted in researches done by Crozier (1999)[14] and Glade et al. (2000)[15] where an antecedent soil water status (ASWS) model was developed and linked with the soil moisture conditions to predict the occurrence of landslides. It was a simplified conceptual model which could estimate soil moisture daily. In addition the model performed a soil water balance which took excess precipitation over a time period up to the day before the landslide occurred and calculated the drainage through the decay function for the evapotranspiration and loss of water through drainage e.g. by analysing hydrograph recession curves (Glade et al., 2000)[15]. Besides this Crozier (1999)[14] by using a calibrated ASWS model was able to successfully forecast days with landslides and days without landslides for a period of 8 months in 1996 though it was not implemented as a landslide warning system [1].

2.2 Empirical Based Models

This type of rainfall thresholds are defined by collecting rainfall data of landslide events and drawing lower bound lines to rainfall events that resulted the landslides in semi-logarithmic, logarithmic or Cartesian coordinates [6]. The thresholds are drawn manually with lesser calculations. When information on rainfall

conditions that did not trigger landslides were available (e.g. [22]), the thresholds would act as a clear cut separators for rainfall events that resulted and did not result in landslides.

Apart from this since the variables change like rainfall, soil type, slope angles etc. with geography, the same threshold couldn't be taken to all locations, therefore thresholds would differ with geography.

When rainfall threshold is defined, the key indicator associated with it is the rainfall intensity. The rainfall intensity is the rainfall accumulated over a period of time which is usually measured in mm/h. However hourly, daily or even longer periods of rainfall had been used depending on the time period considered for the analysis. When the observation period is long it only gives us the average rainfall for that period, neglecting the peak intensities and most of the studies use this mean rainfall rather than the peak intensities.

Further the empirical thresholds can be categorized in accordance to the geological boundaries considered such as the local, regional or global thresholds. All these thresholds will give us the minimum level of rainfall below which landslides do not occur.

Based on the rainfall measurements, the empirical thresholds can be divided in to three groups [6],

- a) Thresholds that use event rainfall measurements
- b) Thresholds that consider the antecedent conditions
- c) Other thresholds

2.2.1 Thresholds that use event rainfall measurements

In event rainfall measurements rainfall from a single or several events were used even though they did not cause landslides. This threshold can be subdivided in to four groups,

1. Rainfall intensity - duration (ID) thresholds
2. Rainfall event - duration (ED) thresholds
3. Rainfall event - intensity (EI) thresholds
4. Thresholds based on the total event rainfall ("Total event rainfall thresholds" or "Rainfall Total event thresholds")

Among them the intensity-duration thresholds were the most popular type of threshold used in literature and they had the form of,

$$I = c + \alpha D^\beta$$

Where: I (mean) rainfall intensity, D is rainfall duration, and $c \geq 0$, α , and β are parameters.

2.2.2 Thresholds that consider the antecedent conditions

Soil Moisture and Ground water conditions affect the occurrence of landslides ([5]). However, the above parameters are hard to measure or predict since they will change abruptly with various factors such as geological, morphological, soil condition and properties, and temperature variations. Antecedent precipitation has a direct impact on the ground water levels and soil moisture; therefore it can be used to predict the initiation of landslides. Here, the simplest way to establish a threshold is to consider the antecedent rainfall. For an example Govi et al. (1985)[17] found that the minimum 60 day cumulative rainfall amount required to initiate landslides in Piedmont region of Italy was 300mm and when the daily rainfall was compared within the 60 days, at least 140mm rainfall was required to initiate a slope failure.

. In literature there are a number of periods considered,

- 3 day period - Kim et al. (1991)[18]
- 4day period - Heyerdahl et al. (2003)[23]
- 10day period Crozier (1999)[14]
- 7, 10 and 15 days period Aleotti (2004) [12]
- 18day period (3-day event rainfall and 15-day antecedent rainfall) Chleborad (2003)[3]
- 2, 5, 15 and 25 day periods Terlien (1998)[19]
- 1 to 59 day period De Vita (2000)[20]

While many authors and researchers accept the fact, a handful of authors have challenged the importance of the antecedent rainfall for the initiation of landslides. Among them, followings are prominent.

- Brand et al. (1984)[24] could not find a correlation in the antecedent rainfall and slope failure events due to high rainfall intensity in Hong Kong
- Corominas and Moya (1999) [16] found that due to large inter-particle voids in slopes covered by coarse debris had a tendency to create debris flow without



the influence of antecedent rainfall in the Pyrenees

- Corominas (2000)[22] investigated the possibility of triggering of shallow landslides due to the existence of large macro pores on slopes mantled by impervious soils without the effect of antecedent rainfall
- Aleotti (2004)[12] could not establish a relationship between cumulative and critical rainfall and the initiating of landslides in the Piedmont region in Italy

2.2.3 Other thresholds

Apart from the above two main threshold types there has been other threshold types defined,

- Reichenbach et al. (1998) [11] related the discharge measurements of different gauging stations in the Tiber River basin, in central Italy to the occurrence (or non-occurrence) of landslides and relevant relationships for the flood volume and maximum mean daily discharge
- Ayalew (1999)[21] investigated the possibility of landslides in Ethiopian Plateau and found that it had a correlation with the number of days with rainfall more than 5mm and the antecedent rainfall up to the date of landslide occurrence

3. Research Methodology

3.1 Data Collection

In order to find the rainfall threshold for the initiation of landslides in Ratnapura district a database was built of rainfall events that resulted landslides in the Ratnapura district.

For this purpose landslide data was obtained from the database maintained by Ministry of Disaster Management (Disinventar.lk) where 225 landslide incidents were obtained which had occurred in Ratnapura district from 13/05/1978 to 02/06/2014. The problem was the difficulty in finding the exact location of the landslides in the database but it provided the division which the landslide occurred in the Ratnapura district. From literature and by using the database the number of deaths, injured and missing people, houses destroyed and damaged, victims and people affected, families affected and evacuated were found but Geology and type of landslide was not mentioned in the detail.

However at the National Building Research Organization (NBRO)web site there were fewer incidents reported when compared to the Ministry of Disaster Management website. Even in this data the type of landslide was not clearly mentioned in all of the entries. Therefore the landslide details were extracted from the Ministry of Disaster Management website.

After collecting the landslide data the rainfall data for the relevant locations and dates were collected from the Meteorological Department of Sri Lanka. The Meteorological Department has stations of its own plus independent stations functioning in estates as well. Out of 225 landslide data collected, 51 landslides occurred at Kalawana Divisional Secretariat Division of Ratnapura (22.67%), 32 landslides occurred at Imbulpe Divisional Secretariat Division (14.22%) and in Ratnapura Divisional Secretariat Division of Ratnapura District had only 21 events (9.33%).

Table 1 - Landslide Events in Divisional Level of Ratnapura

Divisional Secretariat Division	Landslide Events	Percentage %
Kalawana	51	22.67
Imbulpe	32	14.22
Ratnapura	21	9.33
Balangoda	17	7.56
Eheliyagoda	17	7.56
Kolonna	17	7.56
Opanayaka	11	4.89
Nivithigala	10	4.44
Weligepola	9	4.00
Elapatha	8	3.56
Kiriella	8	3.56
Pelmadulla	8	3.56
Kuruvita	6	2.67
Ayagama	5	2.22
Kahawatta	3	1.33
Godakawela	2	0.89

The rainfall of the exact location the landslide occurred was not available since most of the locations were not under observation as landslide prone areas at the moment of landslide so automatic rain gauges were not available. Therefore the rainfall measurements of stations close to the landslide event were used.

Apart from this rainfall data could not be obtained up to the exact moment that the landslides occurred. The rainfall obtained was the daily rainfall on the date that the landslides happened. Hourly rainfall was available for the landslides occurred near the Ratnapura Meteorological office but the daily rainfall was used so a common basis could be maintained for all the landslide events.

3.2 Data Analysis

The 225 landslide incidents were used as seven subsets to find the 7 day cumulative threshold Value, 6 day cumulative threshold Value, 5 day cumulative threshold Value, 4 day cumulative threshold Value, 3 day cumulative threshold Value, 2 day cumulative threshold Value and 1 day threshold Value.

Landslide incidents where rainfall could not be found and the landslide events that did not result from rainfall were neglected. This was achieved by ignoring the addition of rainfall events less than or equal 5mm to the cumulative rainfall and ignoring the rainfall events with a cumulative rainfall less than or equal to 5mm.

Afterwards the calculation of cumulative rainfall for the threshold events was completed as below,

Table 2 - Summary of Thresholds to be analysed

Threshold	Data Used	Code
One Day Threshold	Rainfall data of the day landslide occurred	E1
Two Day Threshold	Cumulative rainfall Data of the day and the previous day the landslide occurred	E2
Three Day Threshold	Cumulative rainfall Data of the day and the previous 2 days the landslide occurred	E3
Four Day Threshold	Cumulative rainfall Data of the day and the previous 3 days the landslide occurred	E4
Five Day Threshold	Cumulative rainfall Data of the day and the previous 4 days the landslide occurred	E5
Six Day Threshold	Cumulative rainfall Data of the day and the previous 5 days the landslide occurred	E6
Seven Day Threshold	Cumulative rainfall Data of the day and the previous 6 days the landslide occurred	E7

Then the cumulative rainfall data was arranged in the ascending order and a frequency distribution was prepared to find the rainfall linked with the probability. After the probability was found the correlation of each daily rainfall with the cumulative rainfall up to that particular day was investigated. Then using SPSS (IBM Statistic Software) a curvilinear Regression model was created for each threshold value using the probability found as the independent variable and the rainfall linked to it as the dependent variable in

$$R = \alpha e^{\beta t} \quad \dots(1)$$

Where 'R' denotes rainfall in millimetres, 't' denotes probability of landslide occurrence and 'α' and 'β' are constants.

4. Results and Discussion

The curvilinear Regression Model obtained using SPSS for one day threshold value is shown in Figure 1 and two day threshold value is shown in Figure 2. Where 'R' is the rainfall in millimetres and 't' is the probability (%). The summary of all the curvilinear regression models developed is shown in Figure 3.



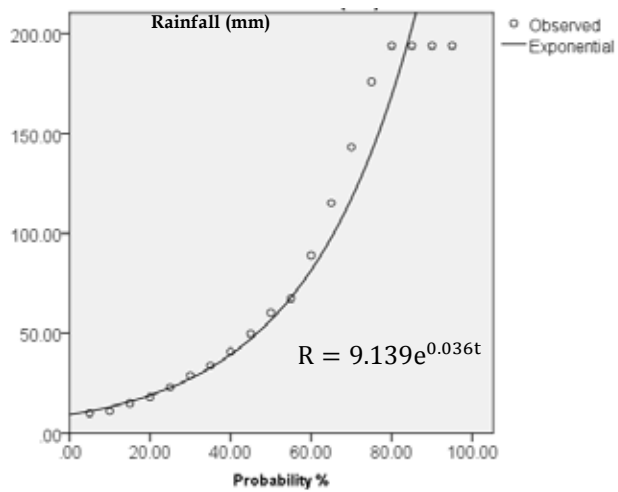


Figure 1 - Probability Distribution Curve for E1

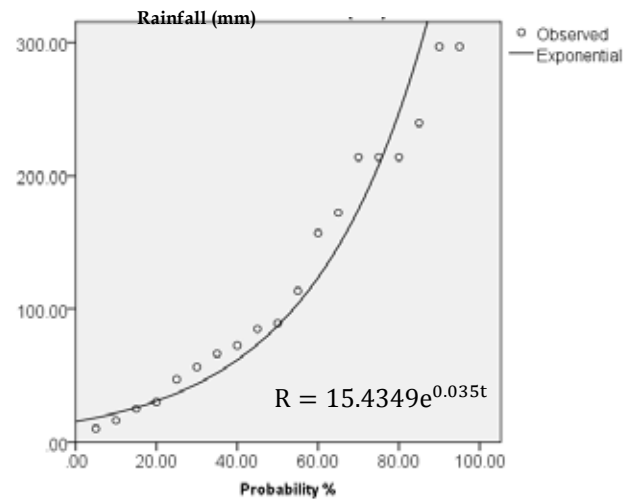


Figure 2 - Probability Distribution Curve for E2

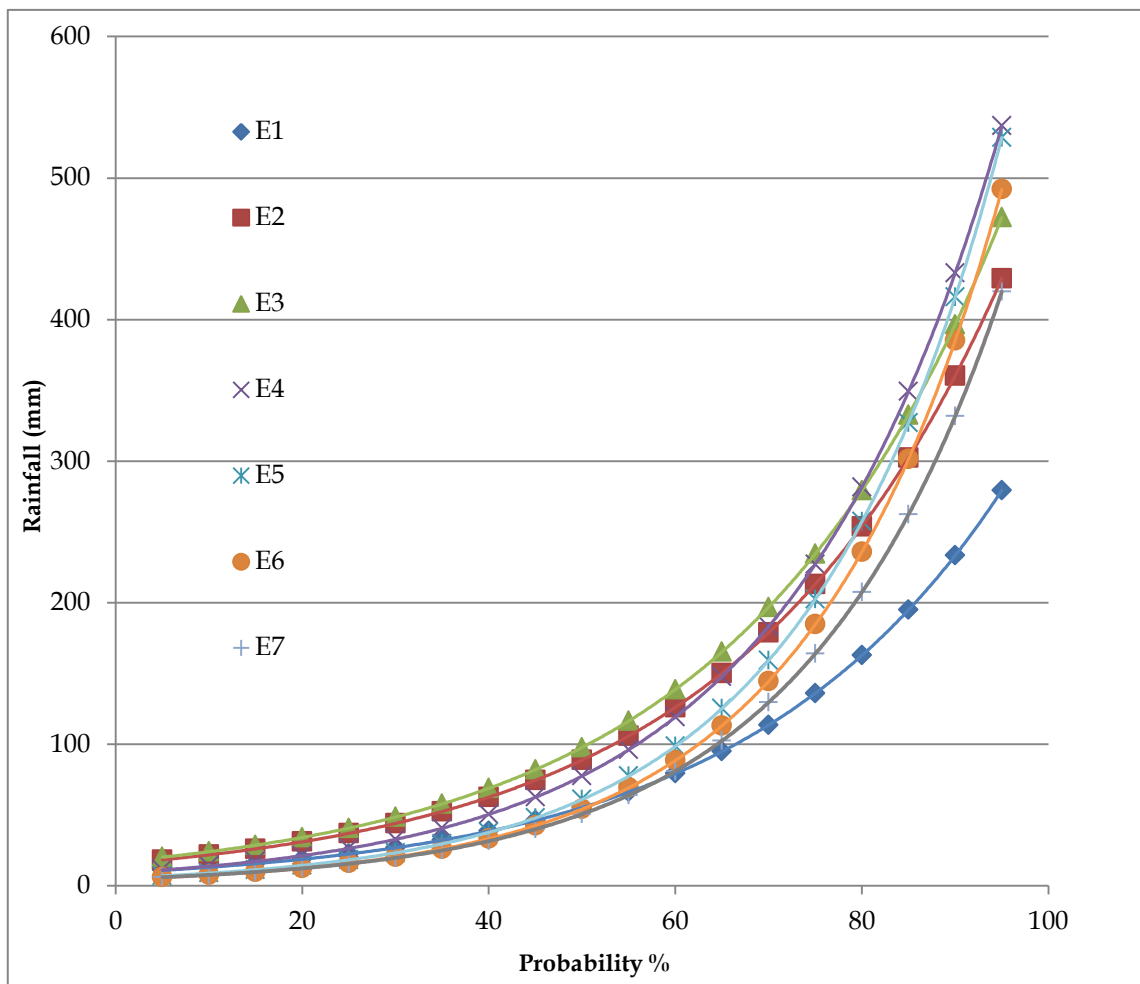


Figure 3 - Summary of Thresholds

Table 3 - Summary of Thresholds

Threshold	Probabilistic Threshold For Rainfall
One day threshold (E1)	$R = 9.139e^{0.036t}$
Two day threshold (E2)	$R = 15.4349e^{0.035t}$
Three day threshold (E3)	$R = 16.985e^{0.035t}$
Four day threshold (E4)	$R = 9.03e^{0.043t}$
Five day threshold (E5)	$R = 5.536e^{0.048t}$
Six day threshold (E6)	$R = 4.681e^{0.049t}$
Seven day threshold (E7)	$R = 4.828e^{0.047t}$

The rainfall thresholds for Ratnapura District found were built by building a curvilinear regression model between the probability (found through frequency distribution) and the respective rainfall. Since the curves showed the shape of an exponential distribution the curvilinear regression model was adapted to interpret the results.

However from E4 to E7 the thresholds were decreasing this could not happen because the thresholds should increase when the rainfalls were cumulating and the reason behind this was the outliers that add up to the frequency distribution when number of rainy days were increasing. In the analysis only events less than 5mm or cumulative events less than 5mm were ignored but this was not sufficient when for 4 day cumulative rainfall and above. Therefore the results in this analysis are not valid from four day cumulative threshold (E4) to seven day cumulative threshold (E7). Comparison of results with the current thresholds established by NBRO is shown in Table 4.

Table 4 - Comparison with Current Thresholds

NBRO Warning and Alert Levels		Probability from established models		
		(E1)	(E2)	(E3)
Alert Level	75mm /day	58.47	45.17	42.43
Warning Level	100m m/day	66.46	53.39	50.65
Evacuation Level	150m m/day	77.72	64.97	62.24

For the determination of acceptable thresholds, the acceptable level of risk which was linked to the probability of the occurrence of landslides was needed to be found. According to UNDP definitions the acceptable amount of risk was defined as "the level of losses that is acceptable without destroying lives, national economy or personal finances"[4]. Since the financial losses occurred due to all the landslide events was not available, the loss of human life due to landslide in Ratnapura was referred. The number of landslide events that caused loss of life was 36 and out of them 10 events occurred due to rainfall less than 75mm on the date of the landslide. If the existing threshold was lowered to at least to 40% probability then the number of events would have dropped to 7 in addition to this the consideration of the antecedent rainfall threshold is important since from the study it is very clear that there is a probability of landslide occurrence in the next few days due to rainfall occurred on the previous day therefore the results of the 40% probability are given in Table 5 below but there is a practical problem in lowering the threshold due to the issuing of alerts more frequently. This could be a nuisance to the public making the alerts less effective. Therefore the thresholds established by NBRO can be agreed upon and further the new thresholds E2 and E3 can be utilized to give warning based on antecedent rainfall.

Table 5 - Proposed Alert Levels for 40% Probability

	Rainfall in (mm)		
	E1	E2	E3
Alert Level	38.57	62.59	68.88
Warning Level	66.19	105.81	116.43
Evacuation Level	94.87	150.15	165.23

Following this antecedent rainfall, the effect of it on the future landslides falls under the interest of this analysis therefore the correlation of the rainfall received on each day (previous day, 2 days back, 3 days back etc.) with the cumulative rainfall was investigated. The summary of the results are given in 'Table 6' and it was evident that only the rainfall of the previous day had a significant effect on the cumulative rainfall of the landslide. The reason behind this observation was the high intensity rainfall received due to the prevailing tropical climate.



Table 6 - Correlation Result Summary

Correlation		Pearson's Coefficient 'r'
Cumulative rainfall up to previous day of landslide	Rainfall in in the previous day	0.65
Cumulative rainfall up to 2 days prior to landslide	Rainfall prior to 2 days before landslide	0.22
Cumulative rainfall up to 3 days prior to landslide	Rainfall prior to 3 days before landslide	0.21
Cumulative rainfall up to 4 days prior to landslide	Rainfall prior to 4 days before landslide	0.15
Cumulative rainfall up to 5 days prior to landslide	Rainfall prior to 5 days before landslide	0.34
Cumulative rainfall up to 6 days prior to landslide	Rainfall prior to 6 days before landslide	0.13

Similar results were observed by Brand et al. (1984)[25] for Hong Kong region where establishment of a correlation between the antecedent rainfall and the occurrence of slope failures failed.

5. Conclusions

It could be agreed that the one day rainfall thresholds ($R = 9.139e^{0.036t}$) that found in this analysis was matching with the practical thresholds established by the NBRO and in addition to that the study was successful in producing thresholds for two day cumulative rainfall ($R = 15.435e^{0.035t}$) and three day cumulative rainfall ($R = 16.985e^{0.035t}$). In the analysis it was evident that when it comes to tropical countries like Sri Lanka most landslides were triggered by the high intensity rainfall despite rare incidents like Meeriyabedda therefore only the rainfall of the previous day has a significant effect on the cumulative rainfall for initiation of landslides. In addition to issuing of warning messages based on probability, a mechanism to report the hourly rainfall using automated rain gauges would be very useful. Only then the process of issuing alert, warning and

evacuation messages based on hourly basis would be possible for the public. Furthermore hourly rainfall data would enable us to create hourly thresholds which would be effective against high intensity rainfalls. Recently NBRO has started collecting hourly rainfall data with automated rain gauges which would pave the way to establish better thresholds on hourly basis. In turn great improvement can be expected when responding to high intensity rainfall events which occur frequently in this region.

The fact that continuous rainfall over a period of time increases the antecedent moisture content in soil which leads to a higher probability of landslides could not be ignored. Therefore continuous monitoring is required for this type of study since new data inputs will give more accurate results for future predictions. With the ongoing worldwide climate change future studies are essential to establish better thresholds.

Acknowledgement

I wish to thank my supervisor Dr. Gamini Jayathissa for his guidance and support to successfully complete my research work. Also I would take this opportunity to thank all the staff members who helped me and guided me to complete my research work as well as academic work specially Dr. Rohan Perera, Dr. Mahesh Edirisinghe, Mr. Niranga Alahakoon, Mr. N. C. Perera and Ms. Kushani De Silva.

References

1. Wieczorek, G. F. and Glade, T., "Climatic Factors Influencing Occurrence of Debris Flows," in *Debris-flow Hazards and Related Phenomena*, Berlin, Heidelberg: Springer Berlin Heidelberg, 2005, pp. 325-362.
2. Wilson, R. C., Torikai, J. D. and Ellen, S. D., "Development of Rainfall Warning Thresholds for Debris Flows in the Honolulu District, Oahu," Dept. of the Interior, U.S. Geological Survey, 1992.
3. A. F. Geological Survey (U.S.), "Preliminary Evaluation of a Precipitation Threshold for Anticipating the Occurrence of Landslides in the Seattle, Washington, area," U.S. Geological Survey Publication, 2003.
4. UNDP, "Disaster Risk Assessment," New York, 2010.
5. Wieczorek, G., "Landslide Triggering Mechanisms," *Landslides Investig. Mitig.*, no. 247, pp. 76-90, 1996.

6. Campbell, R. H., *Soil Slips, Debris Flows, and Rainstorms in the Santa Monica Mountains and Vicinity, Southern California*, U.S. GEOLO. Washington DC: U.S. Government Printing Office, 1975.
7. Guzzetti, F., Peruccacci, S., Rossi, M., and Stark, C. P., "Rainfall Thresholds for the Initiation of Landslides in Central and Southern Europe," *Meteorol. Atmos. Phys.*, vol. 98, no. 3, pp. 239-267, 2007.
8. Montgomery, D. R., and Dietrich, W. E., "A Physically Based Model for the Topographic Control on Shallow Landsliding," *Water Resour. Res.*, vol. 30, no. 4, pp. 1153-1171, Apr. 1994.
9. Wu, W. and Sidle, R. C., "A Distributed Slope Stability Model for Steep Forested Basins," *Water Resour. Res.*, vol. 31, no. 8, pp. 2097-2110, Aug. 1995.
10. Iverson, R. M., "Landslide Triggering by Rain Infiltration," *Water Resour. Res.*, vol. 36, no. 7, pp. 1897-1910, Jul. 2000.
11. Crosta, G. B., and Frattini, P., "Distributed Modelling of Shallow Landslides Triggered by Intense Rainfall," *Nat. Hazards Earth Syst. Sci.*, vol. 3, no. 1/2, pp. 81-93, 2003.
12. Aleotti, P., "A Warning System for Rainfall-Induced Shallow Failures," *Eng. Geol.*, vol. 73, no. 3, pp. 247-265, 2004.
13. Heber Green, W. and Ampt, G. A., "Studies on Soil Physics," *J. Agric. Sci.*, vol. 4, no. 01, p. 1, May 1911.
14. Crozier, M. J., "Prediction of Rainfall-Triggered Landslides: A Test of the Antecedent Water Status Model," *Earth Surf. Process. Landforms*, vol. 24, no. 9, pp. 825-833, Aug. 1999.
15. Glade, T., Crozier, M., and Smith, P., "Applying Probability Determination to Refine Landslide-Triggering Rainfall Thresholds Using an Empirical 'Antecedent Daily Rainfall Model,'" *Pure Appl. Geophys.*, vol. 157, no. 6-8, pp. 1059-1079, Aug. 2000.
16. Corominas, J., and Moya, J., "Reconstructing Recent Landslide Activity in Relation to Rainfall in the Llobregat River basin, Eastern Pyrenees, Spain," *Geomorphology*, vol. 30, no. 1, pp. 79-93, 1999.
17. Cannell, R. Q., Belford, R. K., Blackwell, P. S., Govi, G., and Thomson, R. J., "Effects of Waterlogging on Soil Aeration and on Root and Shoot Growth and Yield of Winter Oats (*Avenasativa L.*)," *Plant Soil*, vol. 85, no. 3, pp. 361-373, Oct. 1985.
18. Kim, S., Hong, W., and Kim, Y., "Prediction of Rainfall-Triggered Landslides in Korea," *Landslides*, vol. 2, pp. 989-994, 1991.
19. Terlien, M. T. J., "The Determination of Statistical and Deterministic Hydrological Landslide-Triggering Thresholds," *Environ. Geol.*, vol. 35, no. 2-3, pp. 124-130, Aug. 1998.
20. De Vita, P., "Fenomeni di instabilità delle coperture piroclastiche dei Monti Lattari, di Sarno e di Salerno (Campania) ed analisi degli eventi pluviometrici determinanti," *Quad. di Geol. Appl.*, vol. 7, no. 2, pp. 213-235, 2000.
21. Ayalew, L., "The Effect of Seasonal Rainfall on Landslides in the Highlands of Ethiopia," *Bull. Eng. Geol. Environ.*, vol. 58, no. 1, pp. 9-19, Aug. 1999.
22. Corominas, J., "Landslides and climate," in *VIII international symposium on landslides, Cardiff, UK*, 2000, p. CD_ROM. 2000.
23. Heyerdahl, H., Harbitz, C., Domaas, U., and Sandersen, F., "Rainfall Induced Lahars in Volcanic Debris in Nicaragua and El Salvador: practical mitigation," in *Proceedings of international conference on fast slope movements - prediction and prevention for risk mitigation*, 2003, pp. 275-282.
24. Brand, E. W., Premchitt, J., and Phillipson, H. B., "Relationship between Rainfall and Landslides in Hong Kong," in *Proceedings of the 4th International Symposium on Landslides*, 1984, vol. 1, pp. 377-384.
25. Brand, E., "Landslides in Southeast Asia: A State-of-the-Art Report," in *Proceedings of the 4th International Symposium on landslides*, 1984.
26. BBC, "BBC News - Afghanistan Landslide Day of Mourning declared," 2014. [Online]. Available: <http://www.bbc.com/news/world-asia-27273684>. [Accessed: 10-Oct-2014].
27. Ministry of Disaster Management, "DMC-SL (Disaster Management Center - Sri Lanka)," 2014. [Online]. Available: http://www.dmc.gov.lk/index_english.htm.
28. Department of Meteorology Sri Lanka, "Climate in Sri Lanka," 2012. [Online]. Available: http://www.meteo.gov.lk/index.php?option=com_content&view=article&id=106&Itemid=81&lang=en. [Accessed: 10-Oct-2014].





Experimental Study on the Effect of Presence of Deep Embedded Retaining Walls on the Settlement of Shallow Foundations

M.P. Amarasinghe and L.I.N. De Silva

Abstract: Most of the foundation designs are conservative, as the failure in foundation will result in failure of the structure. The effects of presence of deep embedded retaining walls on the settlement characteristics of shallow foundations have been investigated to find out whether the effect from embedded retaining walls can be used for an economical design. With the intention to investigate on that behaviour, an experiment on a scaled model was carried out as the field experiments are expensive, complex and time consuming. The behaviour of load with the depth of embedment and the distance to the retaining wall from footing edge was investigated. In the scaled model the load at 25mm settlement increased with the depth of embedment and decreased with the increase of the gap. It was concluded that in shallow footings confined with a deep embedded retaining wall the capacity against settlement failure of the soil can be increased. But when the gap between footing edge and retaining wall is high this effect was minimized.

Keywords: Shallow foundations, Deep embedded retaining walls, Settlement

1. Introduction

Foundations are used to transfer the loads of structures to the ground. A good foundation design can extend the lifetime of a structure. Raft foundation is a concrete slab extended over a large area reducing the contact pressure supporting many concrete columns, beams and slabs, widely used in constructing buildings with basements[1]. Often excavation of great depths is required for raft foundation construction therefore support from embedded retaining walls is required.

Embedded retaining walls are used in many civil engineering applications for embankment stabilization, basement constructions, in underground passes and for waterfront projects. Embedded retaining walls obtain lateral support from penetrating into the ground and may also be supported by structural members. During early days embedded retaining walls were constructed with either soldier piles or steel sheet piles. Later concrete walls were formed using various techniques such as slurry trenches, contiguous or secant piles and diaphragm walls[2].

The purpose of this research is to analyse the effect of presence of deep embedded retaining structures for the settlement characteristics of a shallow rigid foundation using experimental techniques. Actual applications of deep excavations, shallow foundation construction confined with deep embedded retaining walls

are time consuming, expensive and complex. When designing a shallow foundation the bearing capacity and the settlement of it has to be considered. Settlements can be either immediate or consolidation[3].

Not much is known on the effect of deep embedded structures on settlement of shallow foundations. It is planned to analyse and identify whether there is a relationship between load immediately below the footing and settlement of footing with the change of depth of embedment of retaining wall. And the relationship between load and the gap between retaining structure and foundation if footing is confined by a deep embedded retaining wall.

2. Literature Review

It has been found that the "Thickness of the raft has a little influence on the load settlement aspects. However increasing the raft thickness reduces the differential settlement and imposed load". From a 3D numerical analysis it was found that most critical total vertical settlement has occurred at the centre of the raft followed by corner point and at centre of the edge respectively [1].

Eng. M.P. Amarasinghe, B.Sc.Eng(Moratuwa)

Eng. (Dr.) L.I.N. De Silva, B.Sc.Eng(Moratuwa), M.Eng (Tokyo), Ph.D. (Tokyo), MIE(Sri Lanka), Senior Lecturer, Department of Civil Engineering, University of Moratuwa.



It was found that there is an effect from the installation of diaphragm walls on the surrounding and adjacent buildings. "Panel length is the most affecting factor of ground movement and lateral stress reduction during panel installation"[4].

According to [5]"earth retaining structures are influenced by the construction procedure, rigidity of support system and the sequence of excavation. Attributes of the wall, such as height and depth of penetration have a greater influence on the wall movements."

Maximum ground surface settlement takes place near the centre of the excavation and settlements at the corners are smaller. Wall deformation and ground movements are smaller close to the wall corner than around the wall centre[6].

It can be seen that the load-settlement behaviour of an unpiled raft is almost linear and the stiffness of the raft on loose sand is much lower than that on dense sand[7].

3. Objectives

- Experimental investigation on the effect of deep embedded retaining structures on the settlement of shallow foundation using a physical model.
- Propose recommendations on the strength enhancement and settlement reduction due to the presence of deep embedded retaining structure.

4. Methodology

After doing a thorough literature review an experimental procedure is adopted using a model shallow foundation confined by a deep embedded retaining wall.

5. Experimental Procedure

An experiment using a large scale physical model is very difficult. Therefore, an experimental procedure using a scaled model of a shallow foundation confined with a deep embedded retaining wall was used. Two timber boxes of 300mm*300mm and 500mm*500mm of height 600mm were used as the retaining walls. A timber plate of 200mm*200mm was used as the footing.

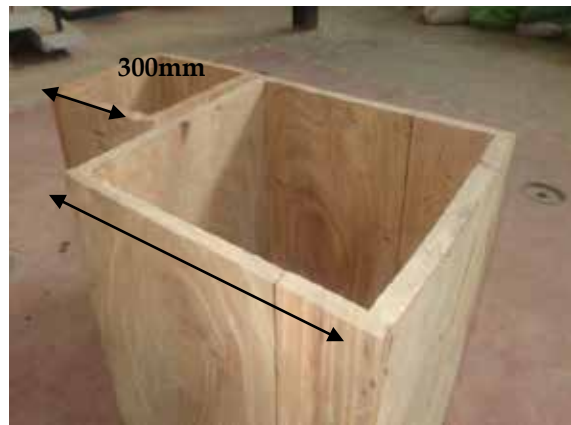


Figure 1 -Timber boxes

A large container was filled with sand up to 100mm. In filling the container the falling height of sand was kept constant to keep the density of sand uniform.



Figure 2 - Timber box placed inside the container

Then the 300mmx300mm timber box was kept inside, levelled and filled with sand for another 500mm from outside and 300mm from inside. After that timber plate was kept at the centre of the box. Because of the practical difficulty in placing the dial gauge on the timber plate few iron plates were first kept on the plate as loads and then using hydraulic jack those plates were loaded.

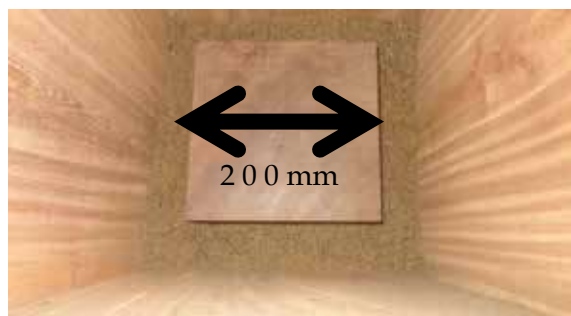


Figure 3 - Timber plate of 200mm*200mm placed at centre



Figure 4 - Filling the container at a constant height



Figure 5 - Placing the steel plate loads



Figure 6- Final arrangement of the experiment

Number of divisions proving ring deflected for every 2mm deflection in dial gauge was measured and converted to a force using calibration data. As there was an initial settlement due to the load from iron plates that load and settlement must be added to the load and deflection. Therefore measured the mass of the steel plates, hydraulic jack and timber plate and graphically calculated the load that would result in a 25mm settlement. The soil unit weight was calculated using the proctor mould. Proctor mould was filled the same way in which the container was filled and from same height. Then the weight of sand that occupy the proctor mould was found and specific weight was calculated.

Similarly a series of experiments were carried out changing the depth of embedment by lifting

the timber box in 100mm steps. The same procedure was followed for the 500mm*500mm timber box and readings were obtained changing the depth of embedment in 100mm step increments starting from a depth of 300mm. The depth of excavation was kept at a constant value of 200mm in all the cases. Finally readings were obtained for the case where there's no embedded retaining wall present.

Table 1- Summary of the experimental procedure

Size of the timber box	Depth of embedment (d)	Depth of excavation (h)
300mmx300mm	100mm	200mm
	200mm	
	300mm	
500mmx500mm	100mm	200mm
	200mm	
	300mm	

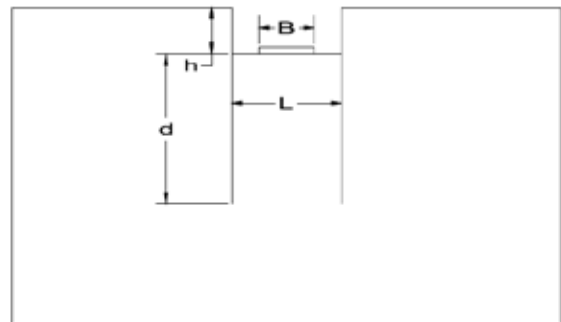


Figure 7 - Experimental setup

Table 1 summarizes the scenarios in the experimental setup where,
h- Depth of excavation
d- Depth of embedment
B- Width of the timber plate
L- Width of the timber box

6. Experiment results

After carrying out the experiment on a small scale model results were obtained. In the experiment for 2mm settlements the load applied was calculated from the proving ring readings using calibration charts. Here it was assumed that the soil is homogeneous and drained. Settlement that was considering is the immediate or elastic settlement as sand was used where pore water dissipation is immediate.

Results were obtained changing the depth of embedment and the distance to the wall from plate edge (i.e. size of the timber boxes). There was an initial settlement due to the steel plates loaded on the timber plate. Therefore in order to get the actual settlement the settlement due to the load from steel plates and hydraulic jack must be added. This settlement values were calculated using a graphical approach assuming the immediate settlement have a linear relationship with the load applied. This linear relationship is identified in [1],[7],[8].

Then at 25mm settlement, the value corresponding to the load was obtained. The results of the experiment for the two timber boxes of size 300mmx300mm and 500mmx500mm are shown in Figure 8 and Figure 9 respectively with the change of depth of embedment of the two timber boxes. Similar pattern was observed in the settlement-stress curves in both the cases of L=300mm and L=500mm. Settlement increasing linearly as the stress applied increased and when the depth of embedment increased the stress required to settle by 25mm was high.

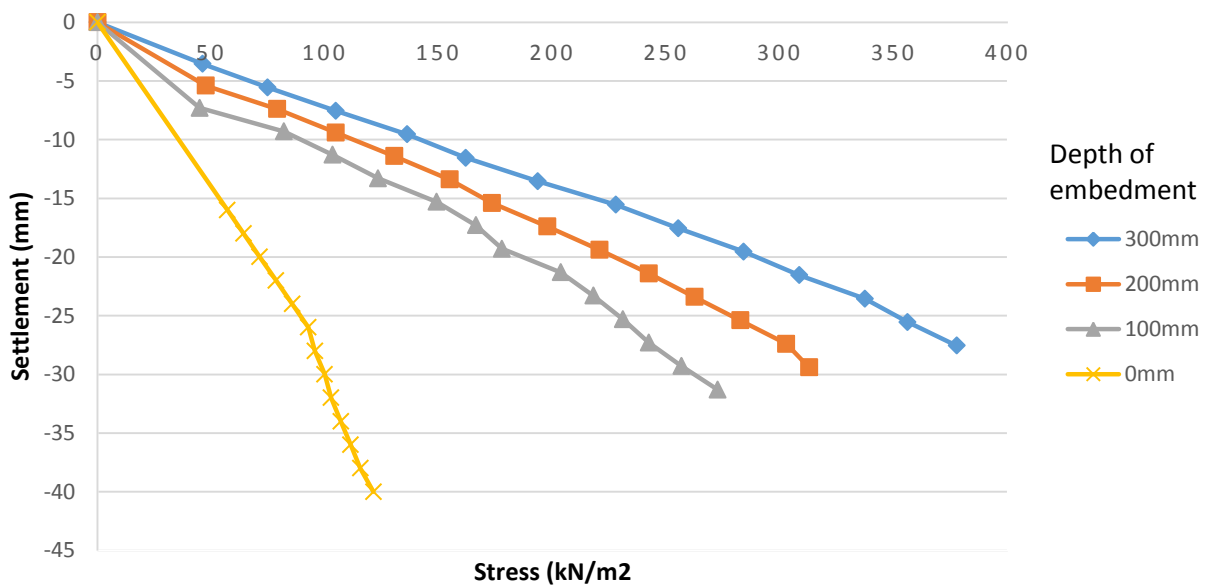


Figure 8 - Settlement- Load chart for L=300 with the variation in depth of embedment

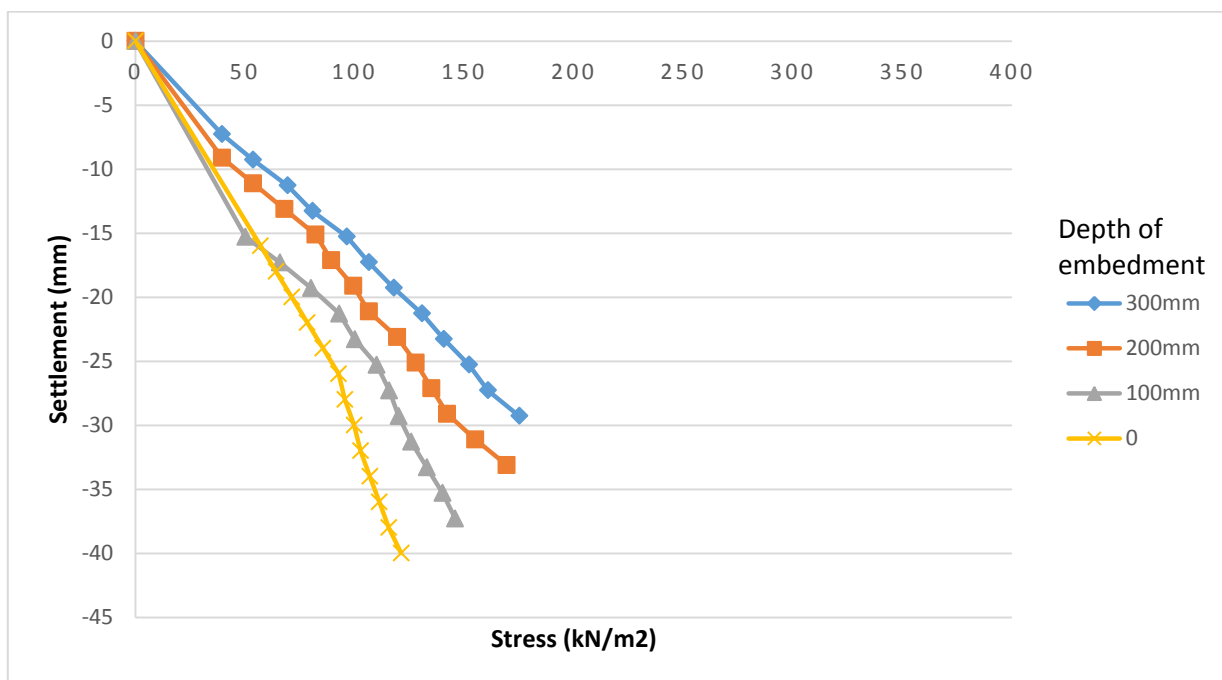


Figure 9 - Settlement- Load chart for L=500 with the variation in depth of embedment

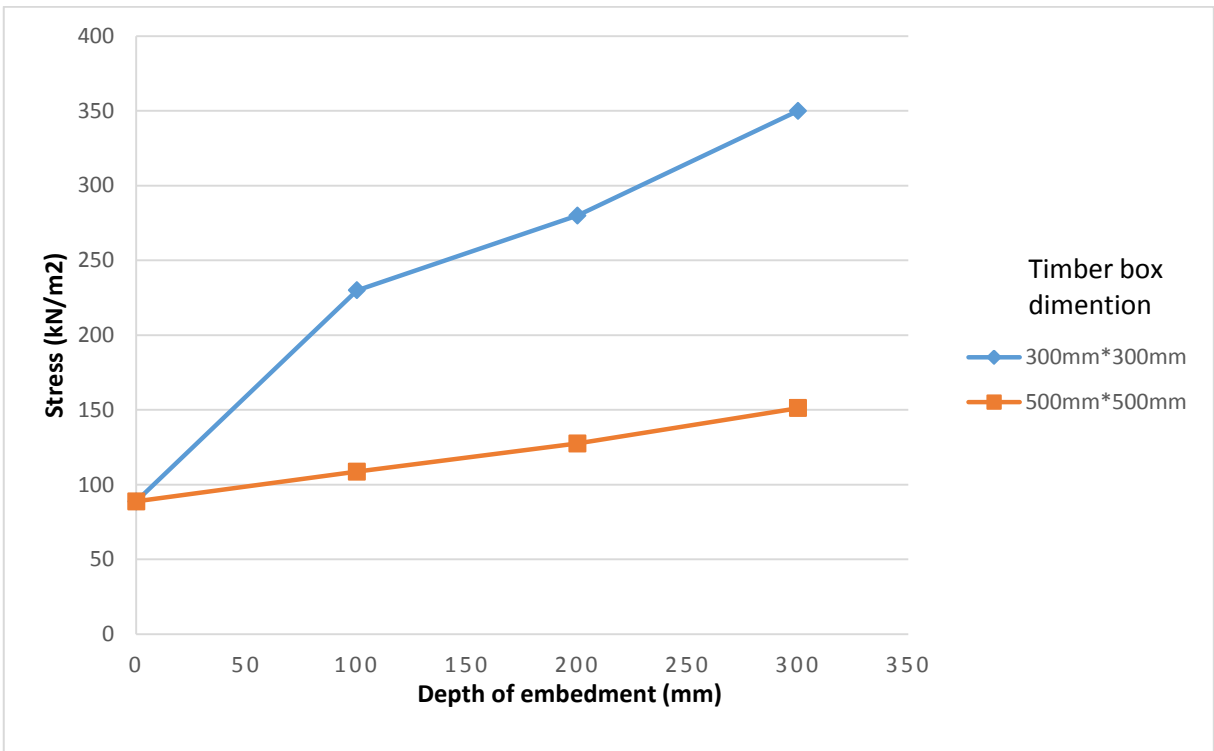


Figure 10 - Stress- depth of embedment for different timber box dimensions

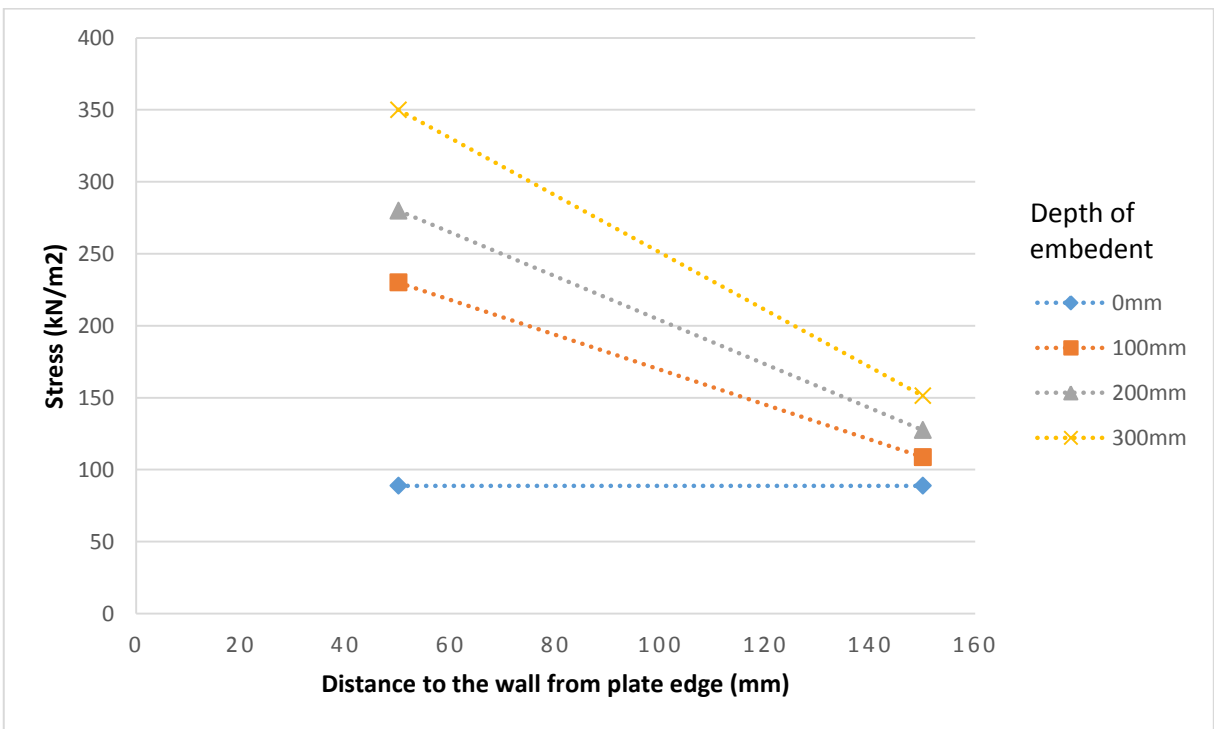


Figure 11 - Stress- distance to the wall from plate edge for various depth of embedment

According to the small scale experimental model the stress required to settle the plate by 25mm is increasing as the depth of embedment increased as discussed. It can be seen that the stress required increases with the decrease in

the size of the timber box used. That means as the distance from wall to plate edge increases the required stress to cause a settlement of 25mm is low.



7. Conclusion

In this study, the effects of presence of deep embedded retaining walls on the settlement characteristics of rigid shallow foundations have been investigated. An experiment was carried out on a scaled model and results were obtained. It was observed that the load at 25mm settlement increases with the depth of embedment as well as when the wall is closer to the shallow foundation.

The reason for the decrease in stress at 25mm settlement as the gap increase is the effect of embedded wall on the slip surface and on stress bulb. As the gap increased the effect was minimized.

It can be concluded that for rigid shallow footings confined with a deep embedded retaining wall, the capacity against settlement failure of the soil can be increased but as the distance between the retaining wall and the footing edge increases the capacity against settlement decreases.

References

1. Leong T. K. and Huat, C. S. "Sustainable design for unpiled-raft foundation structure," in *Procedia Engineering*, 2013, vol. 54, pp. 353-364.
2. Simpson, W. Brian; Powrie, "Embedded retaining walls: theory, practice and understanding," in *15th International Conference on Soil Mechanics and Geotechnical Engineering*, 2001.
3. Rajapakse, R. *Geotechnical Engineering Calculations and Rules of Thumb*. 2008.
4. Comodromos, E. M. Papadopoulou, M. C. and Konstantinidis, G. K. "Effects from diaphragm wall installation to surrounding soil and adjacent buildings," *Comput. Geotech.*, vol. 53, pp. 106-121, 2013.
5. Vaziri, H. H. "A simple numerical model for analysis of propped embedded retaining walls," *Int. J. Solids Struct.*, vol. 33, no. 16, pp. 2357-2376, 1996.
6. Wu, C. H. Ou, C. Y. and Tung, N. "Corner effects in deep excavations-establishment of a forecast model for taipei basin T2 zone," *J. Mar. Sci. Technol.*, vol. 18, no. 1, pp. 1-11, 2010.
7. Nguyen, D. D. C. Jo, S. B. and Kim, D. S. "Design method of piled-raft foundations under vertical load considering interaction effects," *Comput. Geotech.*, vol. 47, pp. 16-27, 2013.
8. Terzaghi, K. Peck, R. B. and Mesri, G. "Soil Mechanics in Engineering Practice, Third Edition," *Wiley-Interscience Publ. John Wiley Sons, Inc.*, p. 664 pp., 1996.

Shrinkage Behavior of a Liner Material with Expansive Properties for use in an Engineered Landfill

V. Kayaththiry

Abstract: Leachate from municipal solid waste landfills contains wide range hazardous compounds; these hazardous compounds have been shown to migrate and contaminate the surrounding environment and impair the use of groundwater. The use of modern landfill liner systems minimizes the migration of hazardous material, it employs a composite liner consisting of a geomembrane overlying a compacted clay liner or a geosynthetic clay liner, but the cost of the geomembrane in Sri Lanka is not affordable. Therefore instead of geomembrane the usage of bentonite-amended expansive soil was considered here and characteristics of the expansive soil were examined. Compared to geosynthetic clay liners (GCL) and high density Polyethylene (HDPE) liners, compacted clay liners (CCL) are less expensive, if the materials are locally available. It is possible to reduce the thickness by using less permeable soil such soil obtained from Moragahakanda, Sri Lanka. This soil is found to be an expansive soil and its hydraulic properties and Shrinkage behavior could be further improved by amending with Bentonite. In addition to the hydraulic conductivity criteria, it is necessary to examine its shrinkage behaviour during drying to investigate the sustainability of its use as a liner. In this examination three different types bentonite-amended expansive soil with following percentage of bentonite content 0, 5 and 10% were analyzed and compared the results. Here analyze was done mainly for variation of moisture contents, volume changes and characteristics of crack with time. For the above purpose following tests were performed, specific gravity test, mechanical analysis, Atterberg limit test, compaction test and shrinkage behavior test. Soil shrinkage and soil compaction represent the dynamics of soil structure with the hydraulic and mechanical stress. An image processing method using ArcGIS 10.2 software was used to determine area reduction and cracked area.

Keywords: Expansive soil, Landfill liner, Shrinkage, Image processing

1. Introduction

In Sri Lanka, there was no any engineered landfills have not been established until the establishment of "PILISARU" for disposal of municipal solid waste. However, the need for engineered landfills cannot be ignored with the increasing quantity of solid waste generation due to rapid urbanization. Municipal solid waste management is a major issue in urban areas. The solid disposal collection is done properly but the final disposal is a major problem in cities. In Colombo disposal of waste is causing major social and political issues. All existing disposal sites are "dumps" as opposed to sanitary landfill sites. As all know the incident of Meethotaramulla landfill slide occurred in April 2017. The people were affected by the incident who were living in the surrounded areas. The officers who are related with waste management have been not worked properly. Hence the

major and long term issue is the generation of leachate which is a liquid produced when water or other liquids come into contact with waste or due to release of moisture present within itself creates one of the major challenges in designing and maintaining an engineered landfill.



Figure 1 - Meethotaramulla landfill slide

Eng. (Ms) V. Kayaththiry, B.Sc. Eng. (University of Peradeniya), Civil Engineer at Central Engineering Consultancy Bureau (CECB),

Therefore, an essential component of an engineered landfill is the liner system which acts as a barrier for leakage of leachate and prevents the transportation of contaminants to the nearby water resources. Synthetic liners consisting of geomembranes or geosynthetic clay liners (GCL) are widely in use as liner materials of engineered landfills constructed in developed and developing countries. However, as geosynthetic materials are not manufactured in Sri Lanka, Compacted Clay Liners (CCL) is an alternative To be considered as a material for a liner. However, in addition to meeting hydraulic conductivity criteria of a liner, one major challenge of using CCL as a liner material is the possibility of developing shrinkage cracks during the dry season. In this regard, use of expansive soils in CCL is advantageous as they exhibit a very high plasticity index (PI) which prolong the initiation of cracking upon drying and have the characteristic of self-healing upon wetting. Kurukulasuriya et.al. ([1], 2013) has investigated expansive soil obtained from Moragahakanda in the Central Province of Sri Lanka and that has amended by 5 and 10% bentonite (Bentofix®, NAUE GmbH & Co. KG, Germany) by weight as candidate materials for a liner and found that they satisfy short and long term hydraulic criteria. In this study, the shrinkage behaviour of the same candidate materials obtained from Moragahakanda is investigated.

2. Materials and Methods

The expansive soil for the study was obtained from the same location (07° 35'32.80 N 80°49'59.90 E) from which soil was obtained for

an earlier study as reported by Wanigaratne et.al. ([2], 2012) in which the hydraulic conductivity was determined on specimens prepared by consolidating one dimensionally to pressures of 46, 92 and 184 kPa. Initially, soil classification tests such as liquid limit, plastic limit, particle size distribution and specific gravity tests were carried out to identify the basic physical soil properties.

In this study, the shrinkage characteristics were investigated on the specimens having the same.

Specimens of diameter 150 mm and thicknesses of 5, 10 and 20 mm were prepared using Moragahakanda expansive soil and they were amended by 5 and 10% bentonite and consolidated to 46.2 and 92.4 kPa. Trimming of compacted specimens to above thicknesses was made possible by using templates of ring shape of required heights (Figure 2) into which the compacted samples were inserted during extraction from the compaction mould. Altogether, 18 specimens were prepared and placed on glass plates and left for air drying (Figure 3).

The change in area of flat surface exposed to the atmosphere and the development of cracks were monitored daily during the drying process. For this purpose, digital photographs were taken using a 14 megapixel camera from a fixed height under almost constant light and ambient temperature conditions. This was facilitated by using a frame as shown in Figure 4. The moisture content too was computed at the time of taking the photograph using the weight of the specimen obtained immediately after taking the photograph.



Figure 2 - Circular shaped templates to prepare specimens of thickness (i) 5 mm, (ii) 10 mm and (iii) 20 mm

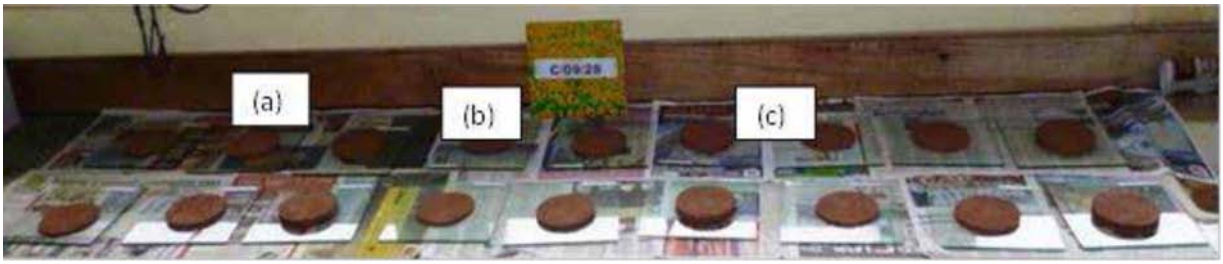


Figure 3 - Compacted specimens of candidate materials left for air drying



Figure 4 - Wooden frame used for photographing the compacted samples during air drying

These images were fed into GIS (ArcMap version 10.2) software and the “IsoCluster Unsupervised Classification” tool was used to multivariate the image. Then, the “Extract by Attributes” tool was used to select the sample from the image and the area was calculated by converting the raster dataset to polygon features using the “Raster to Polygon” tool.

However, the output result of the GIS software will be valid for an image taken at a particular

height. Therefore, it is necessary to calibrate the output result given by the software with reference to the height at which the photograph was taken. This was done by calculating the areas of a square and rectangular shapes placed within a larger circle and photographing at the same height where 5, 10 and 20 mm thick specimens had been photographed (Figure 5).

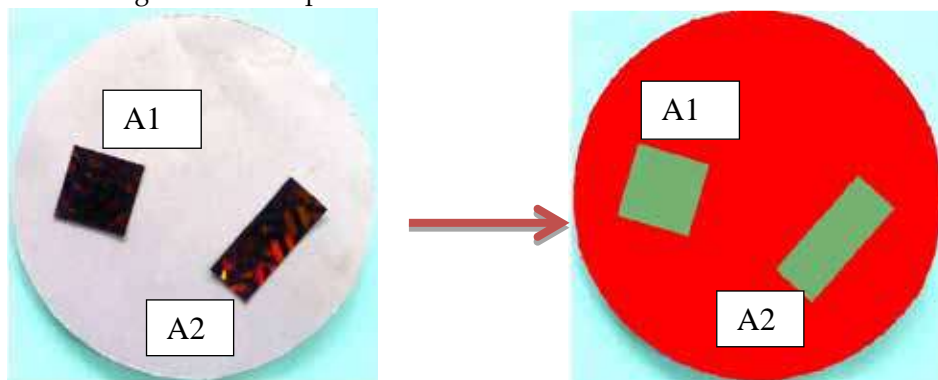


Figure 5 - Image used for calibration of the GIS software computation (a) Object of known area (b) Classification image

3. Results

3.1 Physical and Compaction Properties

Table 1 - Physical and Compaction Properties of Candidate Soils

	Bentonite	Soil M	Soil M+5%	Soil M+10%
Liquid limit (%)	600 *	66	49 *	70 *
Plastic limit (%)	55*	29	21 *	25 *
Plasticity index (%)	545*	37	28 *	50 *
Particle density	2.68*	2.59	2.57	2.55
Swell pressure (kPa)	-	126.1*	267.7 *	357 *
Maximum Dry Density (Mg/m ³)	-	1.65	1.48	1.71
Optimum Moisture Content (%)	-	18.0	26.8	14.0

*- after Wanigaratne et.al, ([2], 2012)

The results of Atterberg limits, specific gravity and swelling pressure tests are given in Table 1 for Moragahakanda expansive soil (Soil M) and that amended by 5% (Soil M+5%) and 10% (Soil M+10%) Bentonite. The Moragahakanda soil was classified as sandy Clay of Intermediate Plasticity (CIS).

The preparation of compacted candidate soil samples was carried out so that the void ratio of the compacted soil sample corresponds to consolidated under 46.2 and 92.4 kPa pressure. Table 2 gives the void ratio of the consolidated soil samples (Wanigaratne et.al. [2], 2012) and the corresponding values of dry density that should be achieved on the compacted soil samples used in this study.

3.2 Shrinkage Characteristics

An example of the transformation of digital images taken during the drying process by the GIS software to compute the surface and crack area (where applicable) is shown in Figure 6. The computed value given by the GIS software was multiplied by the calibration coefficient given in Table 3, which was obtained by the procedure described in the earlier section. As expected, the greatest calibration coefficient was obtained when the object was furthest away from the camera lens.

Table 2 - Target Dry Density of Compacted Candidate Soil Samples

	Soil M		Soil M+5%		Soil M+10%	
Consolidation Pressure (kPa)	46.2	92.4	46.2	92.4	46.2	92.4
Void Ratio	0.74	0.612	0.78	0.729	0.576	0.502
Dry density (Mg/m ³)	1.53	1.65	1.44	1.48	1.62	1.69

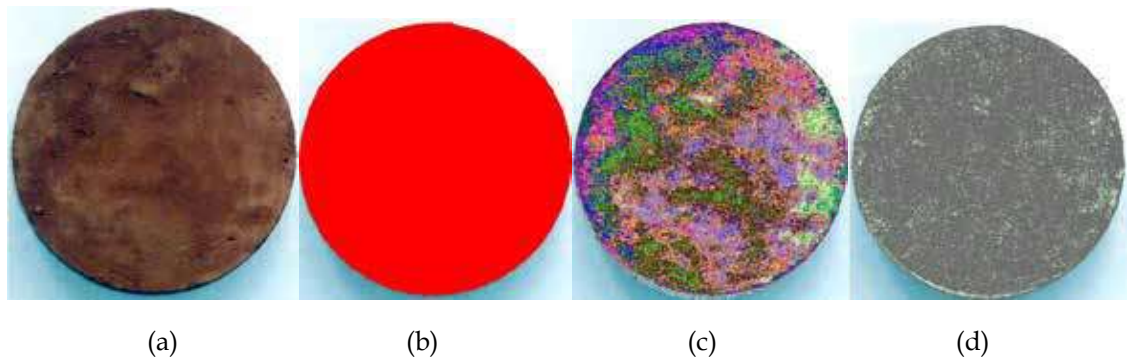


Figure 6 - Steps of image processing in ArcGIS Software, (a) Sample, (b) Classification image, (c) Extracted image and (d) Rastered image

Table 3 - Calibration coefficients used to compute surface areas of compacted specimens

Thickness of specimen (mm)	Calibration Coefficient
20	1.12
10	1.16
5	1.20

The reduction of moisture content is rapid in thin specimens as well as in specimens whose initial void ratio is high as those correspond with samples consolidated to 46.2 kPa. This is understandable as thin specimens and those specimens that correspond with low consolidation pressure contained low amount of moisture and all the specimens had more or less same area of surface exposed to the atmosphere through which the exchange of water molecules and air could take place during the drying process.

Figure 7 shows the variations of percentage area reduction with moisture content of the specimens with an initial voids ratio corresponding to that of specimens consolidated under a pressure of 46.2 and 92.6 kPa. It is seen that although the moisture content is reduced gradually during the drying process of specimens, most of the reduction of area took place once the specimens reached the equilibrium moisture content. It appears that the

shrinkage take place during the drying stage of the specimens does not reduce the area significantly and once the equilibrium moisture content is reached, the specimens continue to undergo contraction at the equilibrium water content. As the drying takes place, the large amount of water absorbed into the diffuse negatively charged layer in montmorillonite clay mineral present in Moragahakanda expansive soil and in Bentonite would be released, thus causing the reduction in the distance between the layers.

Figure 8 shows that for all the 18 specimens, although the reduction of surface area occurred, no shrinkage cracks were developed. This observation is very important as during dry season the liner will lose moisture as the leachate generated is minimal, and it is very advantageous for the liner not to develop shrinkage cracks, although expansive soil has the characteristic of self-healing the cracks when wetted.



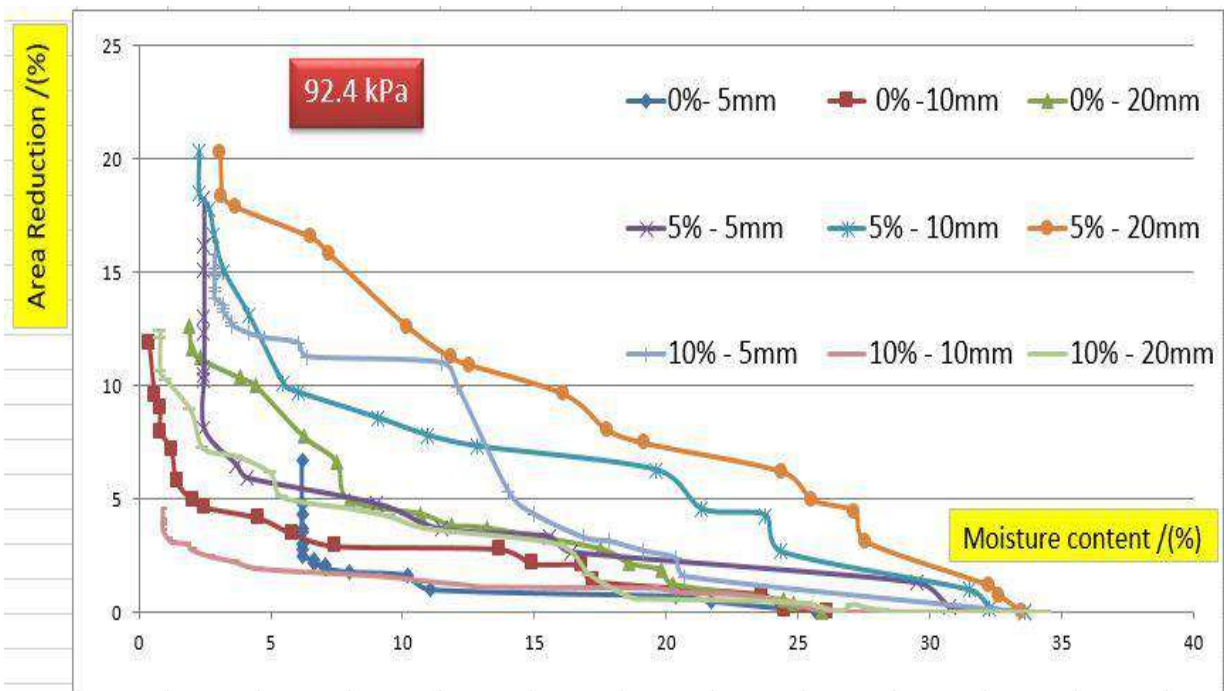
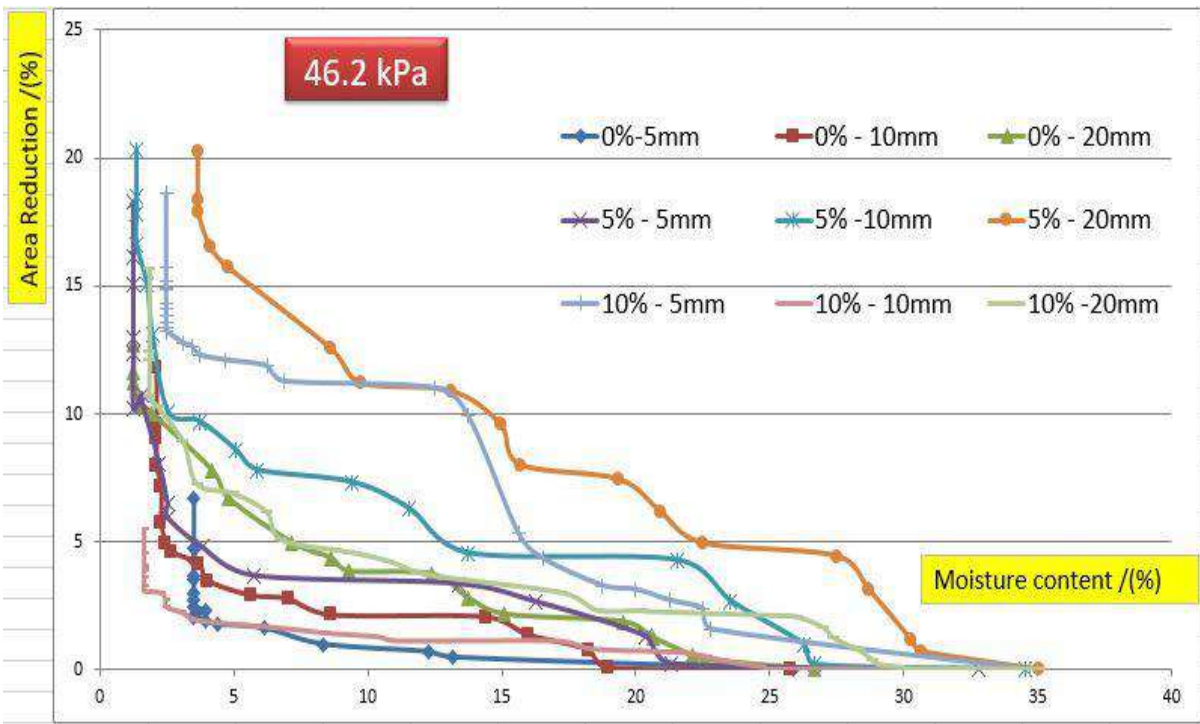


Figure 7 - Variations of percentage area reduction with moisture content of the specimens with an initial voids ratio corresponding to that of specimens consolidated under a pressure of 46.2 kPa and 92.4kPa.



Figure 8 - One of the first day and last day same specimen images.

4. Conclusions

This study was carried out to investigate the shrinkage behaviour of candidate liner materials prepared using expansive soils from Moragahakanda and that was amended by 5 and 10% of Bentonite. The above candidate materials were found to conform to hydraulic criteria of liner materials by a previous study and therefore, the specimens in this study was prepared to the same degree of compaction having the same voids ratio. Based on the outcome of this study, the following conclusions can be made.

- (1) Area reduction takes place, even after reaching the equilibrium water content during drying.
- (2) No shrinkage cracks within the surface of the specimens were visible, thus making the materials highly suitable as a liner material, provided that other criteria to determine the suitability as a liner material such as hydraulic conductivity and durability issues are satisfied.
- (3) Accordingly 10% adding bentonite has been found as most effectively. Noted that the adding percentage more than 10% will work other way as increasing the hydraulic conductivity from 1×10^{-7} cm/sec.

Acknowledgement

I have done this research under the supervision of Dr. L. C. Kurukulasuriya (lecturer, University of Peradeniya) and a great appreciation is given

to IESLAS2017, Reviewers for their assistance to release this paper successfully.

Reference

1. Kurukulasuriya, L. C., Wanigarathna, D., Kawamoto, K., (2013). "Sustainability of liner materials in a municipal landfill constructed using locally available expansive soils". Proceedings of 14th International Waste Management and Landfill Symposium. Sardinia, Italy.
2. Darshika Wanigarathna, Chandana Kurukulasuriya, Shoichiro Hamamoto, Ken Kawamoto (2012) "Locally Available Expansive Soils as a Liner Material for Municipal Landfills". Proceedings, 2nd International Conference on Sustainable Built Environment (ICSBE 2012), Special session on Water and Waste Management, SBE/12/231. Kandy, Sri Lanka.
3. Chao-Sheng Tang, Yu-Jun Cui, Anh-Minh Tang, Bin Shi (2010). *Experiment evidence on the temperature dependence of desiccation cracking*. Elsevier, Issue Engineering Geology, p. 261-266.
4. Abeyrathne, W. K. A. P. et al. (2012). *Development of a landfill clay liner using locally available expansive soil*. Civil Engineering Research Exchange Symposium, Issue Faculty of Engineering, University of Ruhuna, pp. 48-52.
5. Atique, A. & Sanchez, M. (2011). *Analysis of Cracking Behavior of Drying Soil*. Singapore, 2nd International Conference on Environmental Science and Technology.



Identification of Clayey Properties for Cricket Pitch Surfacing and Analysing the Variation of Surface Crack Densities in different Pitches

W.S.U. Perera, U.P. Nawagamuwa and G.N.U. Thilakarathna

Abstract: Clayey top surface of a cricket pitch is the most critical factor which governs the pace and bounce during a match. Previous studies on the same have found out that the soil grading, clay and sand fraction, organic matter content, moisture content (MC%), clay mineralogy and the grass coverage of the top 125mm layer of a cricket pitch are the major governing factors of the playing character of different pitches. This research mainly focuses on the soil grading, clay and sand content and clay mineralogy of the top clayey top surfacing. Laboratory tests were done on three clay samples namely "Grumusol" from Murunkan (MU), a highly expansive soil sample from Kotawehera (KO) and the currently used clay in cricket pitch (TY) preparation by Sri Lanka Cricket. This paper compares the results obtained through the conventional hydrometer test and the laser particle analyser (LPA) method and the clay content is eventually determined. X-Ray diffraction test was done on three samples to investigate their clay mineralogy and the results are compared with the indirect methods used to predict the clay mineralogy. Sample cricket pitches were prepared and the variation of the surface crack densities of cricket pitches made of MU and TY was compared to propose a relationship between clay mineralogy and crack density percentage. The most suitable clay fulfilling the required properties for a fast and bouncy cricket pitch surfacing is identified as MU.

Keywords: Clay content, Crack density, Cricket pitch, Laser particle analyser, X-Ray diffraction

1. Introduction

Cricket is an interesting sporting event which is popular in every nook and corner in Asia. Though it seems like a combat between bat and ball, the cricket pitch plays a huge hidden role in deciding the day's winning team where the ball behaviour is significantly influenced by several factors inherited by the cricket pitch itself.

Ball behaviour after the impact is unpredictable due to several reasons. Studies on this matter have found out that the ball behaviour after the impact is caused by the properties of top most clay layer of the turf. Among these factors clay content, sand content, clay mineralogy, Moisture content (MC %) and top surface grass and cracking conditions are dominant.

This unpredictable ball behaviour of the cricket pitches in different venues in different continents has made the life uneasy for the batsmen over decades. Most of the elegant batsmen in Asian cricket arena who have legendary records in home grounds fail to score big numbers in Australian fast and bouncy wickets. Therefore, development of fast and bouncy cricket pitches is a timely need in Asia. Several studies had been carried out in Sri Lanka regarding the development of fast and bouncy cricket wickets. Laboratory tests were

carried out to find the soil properties of local and foreign soils and the purpose of these efforts was to find a locally available soil which matches with the soil properties of fast pitch material.

In these research studies, most of the soils tested consist of low clay contents and the clay mineralogy of the soils were predicted by indirect methods (Nawagamuwa et al. [4]), (Perera and Nawagamuwa [7]). (Perera et al. [8]).

Prevailing method used in those studies to determine the finer particle content was the conventional hydrometer test in which the output was depended on several assumptions. Assumptions made in hydrometer test have no relation with laser particle analysis (LPA), thus could give a better perspective in determining the clay contents.

Eng. W.S.U. Perera, B.Sc. Eng. (Hons) (Moratuwa), AMIE (SL), M.Sc. (Moratuwa), Lecturer on contract, Department of Civil Engineering, University of Moratuwa.

Eng.(Dr) U.P. Nawagamuwa, B.Sc. Eng. (Hons) (Moratuwa), MEng(AIT), DrEng(YNU), CEng, MIE(SL) Senior Lecturer/Chartered Engineer (Civil)Department of Civil Engineering, University of Moratuwa.

Mr. G.N.U. Thilakarathna, B.Sc. Eng. (Hons) (Moratuwa) Department of Civil Engineering, University of Moratuwa.



Moreover, indirect methods such as high activity and high plasticity characteristics were used to predict the clay mineralogy in the previous research studies. Besides, crack density on the pitch surface is a critical factor which influences the ball behaviour. Crack density on the pitch surface may depend on several factors such as MC%.

This paper compares and contrasts the clay contents obtained by conventional hydrometer and LPA tests in the process of developing fast and bouncy cricket pitches in Sri Lanka. Also the validity of predicting the clay mineralogy by indirect methods was checked by doing X-Ray Diffraction tests. The effect of MC% and the clay mineralogy on the surface crack density was studied and several correlations were identified.

2. Literature Review

2.1 Different types of cricket pitches

Cricket pitches have been categorized into two main categories according to the ball behaviour. The most common categories are “fast” and “slow” pitches (James et al. [3])

“Fast” pitches quite commonly are “Bouncy” pitches while “slow” pitches are “low and spinning” pitches. Therefore, the pitches are of two kinds which are known as fast and bouncy pitches, slow and low pitches (Nawagamuwa et al. [4]).

2.2 Effect of cricket pitch surface

Stewart and Adams [6] had found that the playing characteristics of a cricket pitch were primarily a function of the top 25mm of the soil. This may be an over simplification as the sub base and the sub grade too play an important part in ensuring good bounce but most modern experts believe that the top 100mm-150mm can be considered to be the most crucial [4].

2.3 Previous researches regarding the soil properties of cricket pitches in Sri Lanka

2.3.1 Perera and Nawagamuwa, (2015) [7]

Soil sample taken from Mannar area which is named as “Murunkan soil sample” had been tested for its ability to be used as a fast and bouncy cricket pitch soil.

Figure 1 shows the particle size distribution curves obtained by Perera et al. [7] using

conventional hydrometer tests and wet sieve analysis. Table below shows the clay and silt contents obtained from Figure 1.

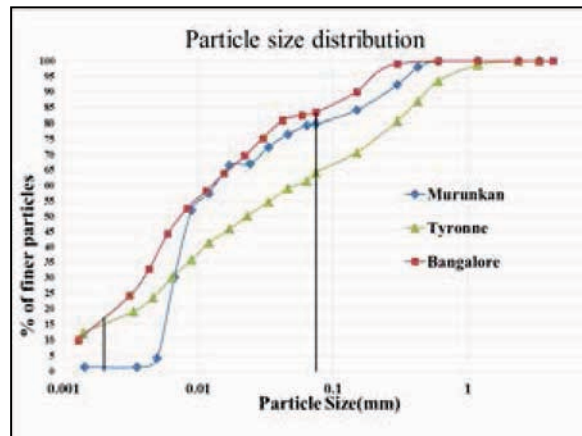


Figure 1 - Particle size distribution graph (Perera & Nawagamuwa, 2015)

Table 1 - Clay and Silt contents, Plastic characteristics [2]

Soil type	% < 0.075 mm	% < 0.002 mm	PL (%)	LL (%)	PI (%)
MU	2	80	70.9	28.1	43.1
Bangalore	15	83	45.6	18.6	26.9
TY	17	64	49.8	30.5	18.3

“Grumusol” soil (MU) is a highly active soil (CH range), hence belongs to the Smectite clay group. MU is known for a soil with high clay content [7]. In contrast the above results showed less clay content in MU when compared to other two soils. In addition the clay content was very much less in all three tested soils.

2.3.2 Perera et al., (2016) [8]

Particle Size distribution

Seven clayey soils from different locations in Sri Lanka were tested in this research for their Particle size distribution, plastic characteristics and degree of colloidal activity etc.

Summary of the particle size distribution is shown in Table 2.

Hydrometer test and the wet sieve analysis were used to obtain the above results. Batticaloa A sample gave the highest clay content of 24% but all the tested soil samples gave comparatively low clay and higher silt percentages. When the particles are bonded together, it will become a larger colloid. Therefore, dry sieve may not provide accurate results in this situation where the accuracy will depend on the clay and silt content to produce

the pace and bounce of a wicket. Hence wet sieve analysis could be treated better.

Table 2 - Comparison of Finer particle percentages [8]

Clay Type	% finer than 0.075 mm	% finer than 0.002 mm
Tyronne	64	15
Murunkan	80	2
Kotawehera	73	8
Bangalore	83	17
Batticaloa A	99	22
Batticaloa B	97	24
Batticaloa C	95	6

Plastic characteristics

Murunkan sample gave the highest LL (74%), PI (47%) from among all tested clays which makes MU an extremely plastic clay. High plasticity is one of the main characteristics of Smectite clays (Herath et al. [1]). Therefore, MU has a high possibility of being a Smectite clay.

Degree of Colloidal activity

Degree of Colloidal activity is one of the indirect methods used to predict the clay mineralogy.

Activity is related to the mineralogy and geological history of clays. (Skempton et al. [8])

$$\text{Activity} = \text{Plasticity Index} / \text{Clay Fraction} \dots (1)$$

Calculated Degree of Colloidal activity values are shown in Table 3.

Error! Not a valid link.

Having a value higher than 1 for the activity implies that soil belongs to Smectite clay mineralogy. Activity (Calculated by equation (1)) was increased due to the low clay contents obtained by the hydrometer. However, MU gave comparatively high value for activity. Authors had predicted both MU and KO to be Montmorillonite clays which belong to Smectite clay group since MU and KO had comparatively high activity values.

2.3.3 Nawagamuwa et al., (2009) [4]

Authors had tested two soils, a soil sample taken from SSC cricket stadium Sri Lanka (Control model) and the same soil mixed with 50% of bentonite (Modified model).

Particle size distribution

Particle size distribution curves were obtained by hydrometer analysis tests. Results were tabulated in Table 3.

Table 3 - Clay percentages [4]

Soil sample	Clay percentage
SSC bulk clay bag	28
SSC pitch	38
Clay from Supplier	16
Modified sample	42

Fairly higher values for the clay percentages were obtained by this research by using hydrometer test.

Plastic characteristics and Activity

Plasticity Index was 14 and Activity was 0.42 in the currently used soil in SSC cricket pitch, which implied that the predominant clay mineral was Kaolinite. Authors have predicted the currently used soil for pitch preparation in Sri Lanka contains Kaolinite clay mineralogy since the activity was less than 1.

Authors recommend the use of expansive clayey soils that can be found in the dry zone of Sri Lanka (Herath et al. [1]) whose primary clay mineralogy is Smectite.

Crack analysis

The crack pattern of the pitch was observed and the maximum crack widths were measured.



Figure 2 - Crack patterns in two soil models [4]

The maximum crack width observed at a MC% of 7.5% for the control model was 1.5mm. In this research, authors had considered only the maximum crack width. Therefore, the factors affecting the crack propagation on the cricket pitch surface should be further studied.

2.4 Comparison of clay mineralogies [1]

Following conclusions were made observing the results made by Herath et al. [1]



Table 4 - Comparison of the properties of Kaolinite and Smectite clays, [1]

Kaolinite	Smectite
Low plasticity	Very high plasticity
Low drying shrinkage	High drying shrinkage
Less cracking density	High cracking density
Low compressive strength	High compressive strength

2.5 Significance of Surface cracking density

Surface cracking of the compacted clayey soil in natural turf pitches is an inherent quality and it adds variations to the behaviour of the cricket ball within different phases of an international test match. Sometimes surface cracks influence the ball to change its trajectory in an unpredictable way which causes difficulties for batsmen and thereby effecting dismissals. Therefore, crack density is one of the dominant characteristics of a cricket pitch which influences the ball behaviour itself. The maximum crack width can be around 10mm however, the playing ability is decided by the umpires. [10].

2.6 Laser Particle Analysis

Laser diffraction method depends upon the diffracted light produced when a laser beam passes through a dispersion of particles in air or in liquid. The angle of diffraction increases as the particle size increases. Therefore, this method is reliable and accurate when measuring the particle sizes distributions between 0.1 and 192 μm (Rathnayake et al. [5]). Also, this method is relatively fast and can be performed on very small sized samples.

3. Objectives

Three objectives of this research could be formulated as follows.

- Comparing the soil grading curves given by hydrometer test and LPA tests and obtaining corrected clay contents.
- Checking the accuracy of the indirect methods such as “Activity of Clays”, used to predict the clay mineralogy by comparing the results with XRD test results.
- Identifying a correlation between clay mineralogy and the crack density.

4. Methodology

- Background of the research was studied through literature review.
- Selection and preparation of samples for the LPA test.
- Obtaining the results of LPA test.
- Comparing the soil grading curves of LPA test with conventional hydrometer test.
- Determining the new clay contents of three clays.
- Calculating the “Activity of clays” and comparing with early results.
- Validating the indirect approaches for predicting clay mineralogy by doing XRD test.
- Preparing model cricket pitches using TY and MU soils.
- Studying the variation of surface crack densities of two model pitches
- Finding a relationship between Clay mineralogy and the variation of crack density.

5. Selection of Samples

Tests were done using 3 samples.

- **Murunkan (MU)** - “Grumusol” clay sample from Murunkan, Mannar, Sri Lanka. The soil plasticity index was more than 60 and the clay activity was higher than one. This soil group has the highest clay content and highest amount of 2:1 clay minerals among Sri Lankan soils classified so far. (Sobana et al. [9])
- **Tyronne (TY)**- Sample from “Tyronne Fernando Stadium” cricket pitch Katubedda which has the same clay used by Sri Lanka Cricket (SLC) for all other cricket pitches in Sri Lanka[7]
- **Kotawehera (KO)**- Sample from Kotawehera in Nikaweratiya region, Sri Lanka [7]

6. Experimental Work

6.1 Laser Particle analysis (LPA)

LPA test was done according to ASTM B822-92 standards by using SHIN-KIGYO PRO OP2. Researches done before gave lower clay percentages due to the conventional hydrometer test. Charged clay particles tend to clog together making heavier particles. Even though charges of clay particles can be

neutralized by the dispersing agent used in Hydrometer test, the organic matters which binds the clay grains together cannot be removed by it. Still clay grains are attached together by organic matter and form larger colloid particles and sedimentation process becomes quick giving lower finer particle percentages in hydrometer test.

However, organic matter inside the finer particles collected from wet sieve analysis was removed by adding H₂O₂ and the charges were neutralized by further adding the dispersing agent during the LPA test (Rathnayake, et al., 2005).

Without organic matter in presence the clay grains get separated without forming heavy particles. Therefore higher clay contents could be obtained for each tested soils.

6.2 Particle size distribution by LPA test

Grading curve of the particle sizes >0.075mm was produced by wet sieve analysis while the LPA was done for collected finer particles, passed through the 0.075mm sieve. Grading curve obtained by LPA test was combined with the grading of wet sieve analysis by overlapping 75µm point of LPA test on the exact point given by wet sieve analysis. Rest of the values of LPA test was modified by multiplying with the ratio obtained at 0.075mm point. Combined particle size distribution was shown in figure 3.

Tabulated result of figure 3 is shown in Table 5.

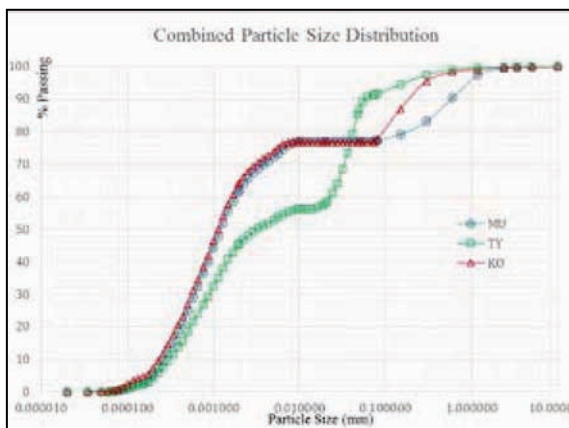


Figure 3 - Modified particle size distribution graphs

Table 5 - New Clay and Silt contents of the clays

Particle Size	MU (%)	TY (%)	KO (%)
2 µm	62.1	45.5	64.2
75 µm	77.2	91.3	76.8
2 -75 µm	15.1	45.8	12.0

6.3 Modified degree of colloidal activity

Since the clay content of the above soils was changed, degree of colloidal activity was calculated as follows in Table 6.

Table 6 - Modified degree of colloidal activity

Clay type	PI (%)	CF (%)	Activity
MU	47.0	62.07	0.75
TY	19.3	45.50	0.42
KO	34.7	64.25	0.54

6.4 USCS Classification

Following abbreviations were used in Figure . Murunkan (MU), Kotavehera (KO), Bangalore (BAN), Batticaloa A{B(A)}, Batticaloa B{B(B)}, Batticaloa C{B(C)}, Soil from Tyronne Fernando stadium(TY).

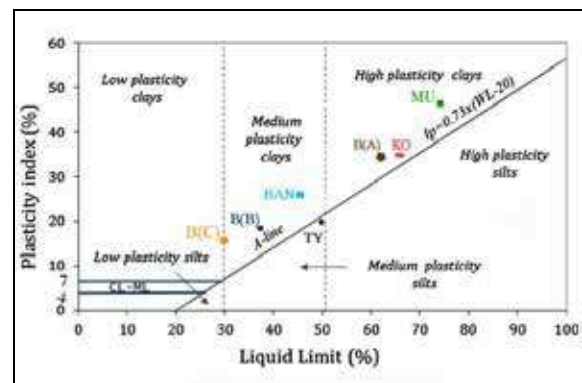


Figure 4 - USCS classification chart for tested soils by Perera , et al., 2016 [8]

6.5 XRD Test

XRD test was adopted in this research to find the clay mineralogy. Powder XRD provides detailed information on the crystallographic structure and physical properties of materials. XRD graphs were given as an output by the XRD test done by BRUKER D8 ADVANCE eco workstation. Summary of the results from the XRD test was summarized in Tables 7, 8 and 9.



Table 7- Summary of the XRD Test for MU

2 Theta Angle	Description	Relative intensity (%)
5.378°	Montmorillonite	30.60
5.627°	Notronite	27.30
20.880°	Notronite	27.60
26.666°	Notronite	100.00

Table 8 - Summary of the XRD Test for KO

2 Theta Angle	Description	Relative intensity (%)
5.613°	Montmorillonite	100.00
19.670°	Sauconite	9.90

Table 9 - Summary of the XRD Test for TY

2 Theta Angle	Description	Relative intensity (%)
12.357°	Kaolinite	14.60
18.321°	Triazine	50.80
26.674°	Triazine	100
20.874°	Quartz	14.10
24.927°	Kaolinite	7.4
50.159°	Quartz	6.4

6.6 Surface crack density analysis

Cracking of the pitch was quantitatively measured during this experiment using an image processing method. Model pitch was prepared in University of Moratuwa grounds and digital photographs were taken on each day of testing and a square of 300mmX300mm was photographed with clear boundaries and the images were processed using MATLAB software to calculate the percentage pixel density which showed cracks.

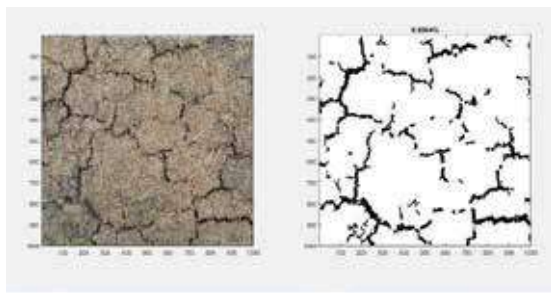


Figure 5 - Actual image of the pitch and image analysis results by MATLAB software.

Model pitches were made from MU and TY soils and the variation of the surface crack patterns were observed for six days. Crack density percentages were calculated by the software and summarized in Table 10.

Table 10 - Surface crack density percentage

Day	MU%	TY%
1	2.79	3.13
2	5.35	3.14
3	7.45	3.94
4	8.75	4.35
5	8.71	5.05
6	8.13	9.63

Crack density depends on the clay mineralogy and MC%. Smectite is a type of an expansive clay which tends to excessively shrink in low moisture environments. Hence it shows a significant cracking when subjected to drying conditions [1].

7. Results and Discussion

7.1 Particle size distribution test

Particle size distribution curves can be obtained by the results of sieve analysis test and conventional Hydrometer test.

Hydrometer test is based on number of assumptions where the accuracy of the results can be less but the LPA test can be more accurate since it is based on digital technology that utilizes diffraction patterns of a laser beam passed through any object ranging from 0.02µm to 2000µm in size.

Laser particle analysis gave a higher value for the clay fraction when compared with the conventional hydrometer test. Both MU and KO had above 60% of clay content while TY had 45.5% of the same. Clearly the two alternative soils (MU and KO) have higher clay content when compared to conventional soil which is used in current cricket pitches. High clay content may lead to proper bonding of pitch material and reduce the crumbling and deteriorating the pitch surface. Therefore, the strength in between the particles of the pitch surface of MU and KO may be higher when compared to TY.

7.2 USCS Classification

According to the Figure , MU, KO and B (A) could be identified as high plasticity clays while BAN and B (B) was medium plasticity clays. High plasticity is one of the main characteristics of Smectite clays. Therefore, according to the indirect way of predicting clay mineralogy by high plasticity MU, KO and B (A) could be Smectite clays [1].

7.3 Degree of colloidal activity

After inserting the corrected value obtained for the clay fraction by LPA, OM content was less than 1% as shown in Table 6. Highest Activity was recorded from MU as 0.75. Since the value is less than “one”, MU cannot be directly categorized in to Smectite clay group. Therefore X Ray Diffraction test should be carried out for further analysis of the clay mineralogy.

7.4 XRD test

Referring to the results given in Table 7, Montmorillonite is a very soft phyllosilicate group of minerals which is a member of the Smectite group. Besides Nontronite is the iron (III) rich member of the Smectite group of clay minerals (Anthony et al. [11]). Majority of the MU sample is in Smectite clay group.

Referring to the results given in Table 8, Sauconite is a complex phyllosilicate mineral of the Smectite clay group [11]. Since the majority of the sample are in Smectite group KO could be named as a Smectite clay.

Referring to the results given in Table 9, Triazine is an organic chemical compound with the formula $(HCN)_3$. Majority of the TY soil are organic compounds, quartz or kaolinite clays. Hence the currently used soil for the cricket pitch preparation in SL is a typical Kaolinite clay with high percentage of organic compounds.

Indirect methods which were used to predict the clay mineralogy gave some close answers. KO and MU gave high PI value which was an indication of a fat clay. Normally clays that belong to Smectite clay groups are high plasticity clays. Therefore, the prediction matches with results given by XRD results.

Activity of clays was determined using the clay content given by the hydrometer test in the previous approach. In that case MU and KO gave higher values for the activity which implied promising results of being a Smectite soil which was later confirmed by the results of XRD test.

Activity of clays was recalculated by corrected clay content obtained from LPA test. All the results were less than 1 and it was an indication of Kaolinite clays. However, MU gave the highest activity value of 0.75 and it was somewhat closer to ‘one’. Majority of this result did not match with the results of XRD test.

7.5 Surface crack density analysis

Crack density variation on the top surface was photographed daily and images processed by MATLAB software were further analysed.

Variation of crack density percentages were plotted against days and shown in Figure 6.

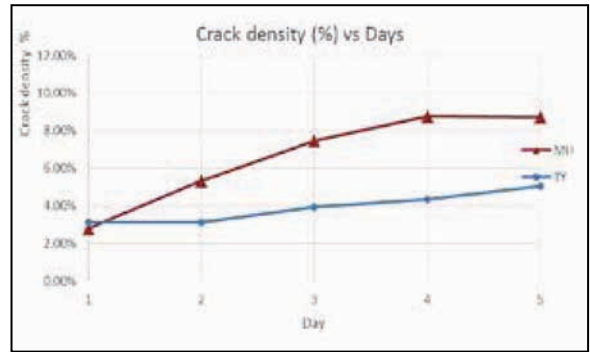


Figure 6 - Crack density percentage vs days

According to Figure 6, Crack density percentage of MU increased with time than that of TY. XRD test revealed that KO and MU belongs to Smectite clay group. Smectite is an expansive clay which tends to shrink in low moisture conditions [1]. Hence it shows a significant cracking when subjected to drying conditions. This would have caused for the higher crack density on the surface of the MU model pitch than TY.

MC is another parameter which governs the crack density [10]. However, MC of the top soil in both pitches reduced with time due to drying caused under direct sun light.

As expected, crack density percentage has a significant negative relationship with moisture content for both pitches. However, the gradient of MU is higher than TY which implies MU generates higher crack densities than TY with the reduction of MC.

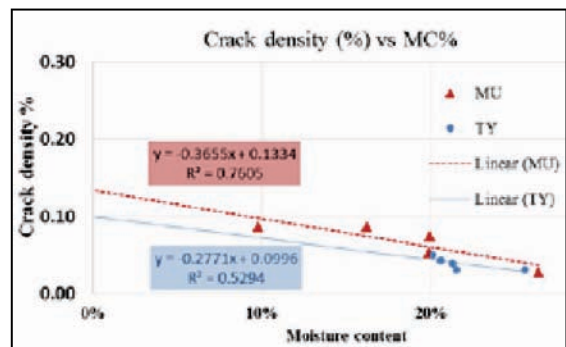


Figure 7 - Crack density% vs MC%

In order to find the relationship between clay mineralogy and crack density the effect of MC should be removed. To remove the effect caused by MC, normalized crack density by MC was plotted against days as shown in Figure 8.



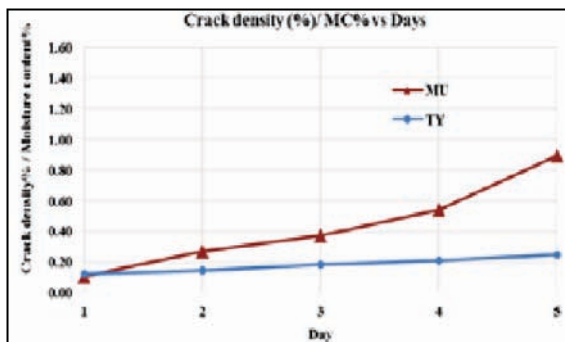


Figure 8 - Crack density (%) / MC% vs Days

According to Figure 8, Crack density % / MC% values of MU was higher than for TY after the 2nd day of the test. Therefore crack density has a significant correlation with the clay mineralogy. This implies that MU which belongs to Smectite clay group is highly expansive clay and it matches with the characteristics of fast and bouncy pitches in Western Australian Cricket Association grounds [4].

8. Conclusions

In this research clay contents were determined by Laser particle analysis since the results given by conventional hydrometer depend on assumptions which may have effect on the lower clay contents. Results by LPA test gave higher clay contents for the tested clays. MU and KO had high values for the clay contents and matches with the soil properties of a fast and bouncy clay.

Activity values which were calculated by the clay contents given by the conventional hydrometer matched with the results given by XRD test where KO and MU with high activity were considered as Smectite clays.

Activity values were recalculated with the results given by LPA test and the results were less than one for each tested soil and slightly deviated from XRD test results.

According to the results of crack density percentage variation MU displayed its highly expansive nature than TY, which is an indication of Smectite clay.

Moreover Crack density percentage showed a significant negative relationship with Moisture content for both soils.

Effect of MC% was removed by normalising the crack density percentage by MC% and plotted against the day. Results showed that Crack density percentage depends on the clay mineralogy where Smectite clay showed higher surface crack densities than Kaolinite clay.

References

1. Herath, J., 1973. Industrial clays of Sri Lanka; Geology, Mineralogy, and Appraisal for Ceramics and other Industries. Economic Bulletin, Geological survey, Sri Lanka, Volume No.1, pp. 1-113.
2. Skempton, A. W., 1953. The Colloidal Activity of Clays. Zurich, s.n., pp. 57-61.
3. James, D., Carré, M. & Haake, S., 2005. Predicting the playing character of cricket pitches. Sports Engineering, Volume 8, pp. 193-207.
4. Nawagamuwa, U., Senanayake, A., Silva, S. & Sanjeewa, D., 2009. Improvement of Local Soils in Order to make "Fast & Bouncy" cricket. Engineer, Institution of Engineers, Sri Lanka, Volume 42(4), pp. 46-55.
5. Rathnayake, N. et al., 2005. Anthropogenic Impacts Recorded in the Sediments of Lunawa, a Small Tropical Estuary, Sri Lanka. Environmental Geology, 48(2), pp. 139-148.
6. Stewart, V. I. & Adams, W. A., 1968. County Cricket Wickets. Journal of Sports Turf Research Institute, Volume 44, pp. 49-60.
7. Perera, W. S. U. & Nawagamuwa, U. P., 2015. Identification of Local Soil for Development Cricket pitches. s.l., Department of Civil Engineering, University of Moratuwa.
8. Perera, W., Nawagamuwa, U. & Wijerathna, H., 2016. Study on Properties of Locally available Clays to be used in Fast and Bouncy Cricket Pitches. s.l., Institute of Engineers' Sri Lanka.
9. Sobana, A., Mapa, R. & Gowthamy, P., 2014. CHARACTERIZATION OF GRUMUSOLS IN MANNAR DISTRICT IN SRI LANKA AND THEIR APPLICABILITY TO AGRICULTURE. Proceedings of the Peradeniya University, p. 527.
10. Tainton, N. et al., 1998. Principles and Practice of Pitch Preparation. [Online] Available at: http://static.espnricinfo.com/db/ABOUT_CRICKET/PITCHES/PREP_OF_PITCHES.html [Accessed 2 June 2016].
11. Anthony, J. W., Bideaux, R. A., Bladh, K. W. & Nichols, M. C., 2010. Handbook of Mineralogy. [Online] Available at: <http://www.handbookofmineralogy.org/> [Accessed June 2016].

Design of Soil-Cement-Bentonite (SCB) Backfill and Construction of SCB Slurry Walls along the Earthen Dam at Iranamadu Reservoir in Kilinochchi

P.N. Wickramarachchi, S. Weerakoon, S. Semage, N. Madushanka and T. Rajagobu

Abstract: Soil-Cement-Bentonite (SCB) slurry walls have been used with increasing frequency in recent years in United States, Canada and European countries to provide barriers to the lateral flow of groundwater or seepage in situations where the strength of a normal soil-bentonite wall would be inadequate to carry foundation loads. However, this technique has been used with less frequency in the Asian region up to date. The addition of cement to the backfill blend allows the backfill to set and form a more rigid system that can support additional overlying loads which the earthen dams undergo.

Construction procedure and quality control for the SCB wall are more demanding than that needed for conventional soil-bentonite slurry walls. Backfill mix design to meet the given strict test parameters, sampling and testing of this type of wall involve more exacting procedures. Designing the SCB backfill is a complex issue involving conflicting actions of the various materials involved. While the SCB wall provides additional strength, permeability is one property that suffers in comparison to soil-bentonite slurry walls. The most demanding tests were a uniaxial compressive strength (UCS) and permeability in this project, and specified values were not less than 100 KPa and not more than 200 KPa for seven days and 1×10^{-7} cm/sec, respectively. The backfill was designed to get the average UCS as 160 KPa and permeability as 1×10^{-8} cm/sec.

The most challenging work involved with this are, mixing in large quantities, transportation and placing the SCB slurry within the specified period to maintain the quality of mixture consistently throughout the project period. However, with greater care and having engineering input, it was possible to successfully construct the SCB slurry wall, 1700 m in length along the earthen dam for the 1st time in Sri Lanka.

Keywords: Permeability, Soil - Cement - Bentonite Slurry, Uniaxial Compressive Strength

1. Introduction

Rehabilitation and improvement of water and irrigation networks are a main strategic movement of any government in order to provide better infrastructure facilities which can be heavily affected by rapid development. The same phenomena were applied during the last two decades in Sri Lanka, and as a result, many areas were developed and facilitating the farmers and villagers. After peace prevails in Northern Province, many such projects were implemented by local and foreign funding agencies.

The Iranamadu tank (the length of the earthen dam is around 2750 m) and its main feature of earth bund have not been rehabilitated in a technically sound manner during last few decades due to many constraints. As a result, the tank was not able to function as it is

supposed to be. The cultivation of paddy was badly affected, and so does the farmers. Therefore, the relevant authorities have identified the urgency and burning desire to rehabilitate the project and comfort the life of common people. At present, the tanks bund is not provided with the required strength to store water up to the full flood level.

Eng.(Dr.)P.N.Wickramarachchi, C.Env.Eng., AMIE(SL), B.Sc.Eng.(Peradeniya), M.Eng.(Tahiland), Dr. Eng.(Saitama), Manger Engineering, Access Engineering PLC.

Eng.S.Weerakoon, AMIE(SL), B.Sc.Eng.(Peradeniya), Project Manager, Access Engineering PLC.

Mr. S. Semage, NCT(SL) Senior Material Engineer, Access Engineering PLC.

Eng. N. Madushanka, AMIE(SL), B.Sc.Eng.(Ruhuna), Site Engineer, Access Engineering PLC.

Eng. T. Rajagobu, C.Eng, MIE(SL), B.Sc.Eng. (Peradeniya), Deputy Project Director, Provincial Irrigation Department, Killinochchi.



Soil-Cement-Bentonite (SCB) slurry walls have often been used in recent years in United States, Canada and European countries to provide barriers to the lateral flow of groundwater or seepage. However, this technique has rarely been used in the Asian region. The addition of cement to the backfill blend allows the backfill to set and form a more rigid system that can support additional overlying loads which the earthen dams are undergone.

While the SCB wall provides additional strength, permeability is one property that generally suffers in comparison to soil-bentonite slurry walls. The most demanding tests are a uniaxial compressive strength (UCS) and permeability.

2. Project Information

The Iranamadu reservoir is the one of most important water body in Northern Province, and the requirement for the new development was a key to develop the area. Though there was a number of main features to rehabilitate and or develop, the SCB wall gained elevated interest among them. The main reason for that one was, it was considered as the very first construction in Sri Lanka.

The earthen dam was 2750 m long, and it was decided to construct only 1700 m length of SCB wall along the dam towards the upstream. The width of SCB wall was 600 mm, and depths were varied from 4 m to 6 m depends on the location and especially the location of existing puddle core.

Figure 1 below shows the basic features of proposed rehabilitation including the SCB wall. The SCB wall was coloured in blue in Figure 1.

The designers have given the dimension of SCB wall, and the contractor was asked to design the SCB backfill mixture and complete construction works. The construction work includes the design of backfill mix and verifies for the given criteria by the contracts especially for the uniaxial compressive strength (UCS) and permeability for the 7 and 28 days, respectively.

3. Materials and Method

Basically, the significant materials for the SCB wall were bentonite, Portland cement and soil. The preliminary investigation showed that the excavated soil of slurry wall trench could be used as soil for the mix (OMC 11.6 %, LL 33, PI 14.3, Clayey loam, MDD 2.024 g/cm³). Even the normal Portland cement was able to utilise with the supplier's source approval. However, the special consideration has to be paid for the bentonite to be used. The project specification clearly mentioned that the proposed bentonite should exhibit the properties as per the API Spec 13 A [1].

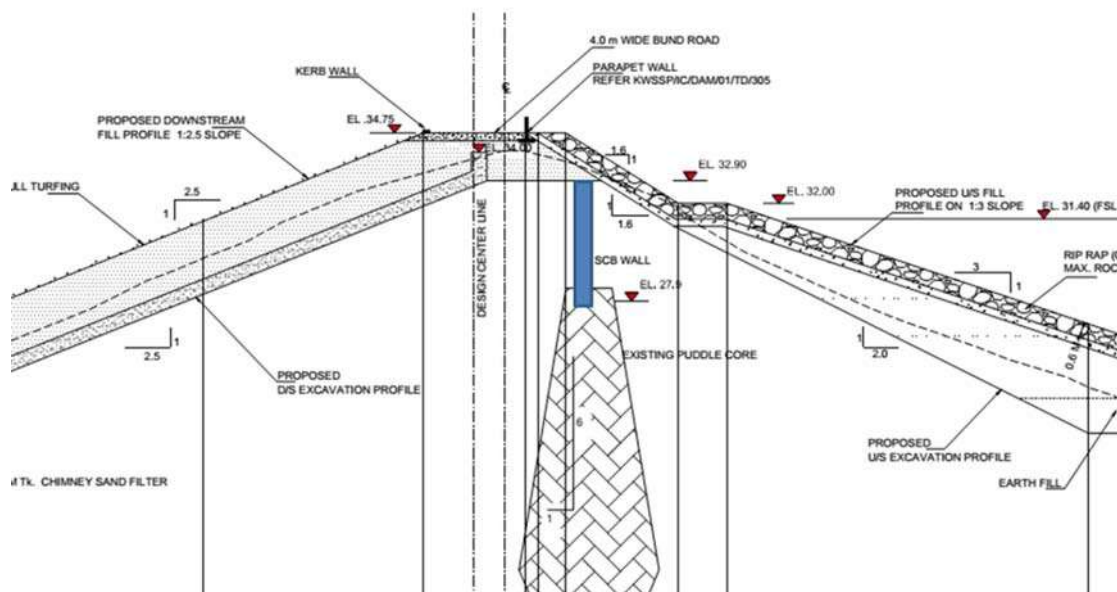


Figure 1 - Basic features of proposed rehabilitation works

Table 1 - Properties of Bentonite Powder

Specification	
Property	Requirement
YP/PV Ratio	> 3
Viscometer at 600 rpm	> 30
Filtrate Loss	< 15 cm ³
Moisture Content	< 10 %
Residue > 75 micrometer	< 4 %
Certification	Meets API 13 A, (4)

3.1 SCB backfill design

Designing the backfill was a major challenge. The key parameter was to maintain the permeability in the range of 10⁻⁷ cm/s range. Rayn and Day [2] have investigated and found that to reach 10⁻⁶ cm/s is also somewhat difficult in SCB backfill mix, however, with the strict quality control procedure, and proper engineering input reaching 10⁻⁷ cm/s is feasible, and they have gotten it in their practical work.

Initially, three types of mixes were considered and performed the required tests. The details are shown in Table 2. The initial composition was based on the literature. It was found that less number of literature and all studies were based on the USA and European region. Owaidat et al., [3] studied several mixes and ranged the mix proportions as 94 %, 2 % and 4 %, soil, bentonite and cement, respectively.

Table 2 - Backfill Mixes

Type of mix	Compositions (%)		
	Soil	Cement	Bentonite
A	93.8	4.0	2.2
B	94.0	3.5	2.5
C	93.0	4.0	2.5

Another important aspect of backfill was the working slump. The accepted range was 120 - 180 mm.

3.2 SCB backfill mixture preparation at site



Figure 2 - Measuring slump of backfill

Once the lab scale tests are passed, the optimum mixture was decided to carry out the construction works at the site. Proper detail plan was prepared considering the required amount per day and construction time was given and site characteristics. Initially, it was planned to carry out 20 m length in the backfilling the slurry trench. However, the required ponds for mixing bentonite slurry and filling slurry were prepared for more lengths. The investigation revealed that the mixture to be backfilled within 3 hrs after mixing. Based on those details, the number of tippers and excavator were selected. The mixing ponds and required machines were placed in the middle of the whole length so that the logistics and transportation activities were easy and comfortable. Based on the calculation for the mix, it was added to the mixing pad, the calculated soil mass, dehydrated bentonite slurry and the calculated amount of cement slurry by 1000 L centrifugal mixer.



Figure 3 - Mixing of soil, cement and bentonite at mixing pad using excavator



3.2 Trench excavation and backfilling

A 600 mm width and 1700 m length trench were excavated to the depths ranging from 4 m to 6 m depending on the location of puddle core along the dam. Initially, borehole investigation was done to identify and locate the existing core paddle. Once it is located then, excavation was commenced stage wise. The trench was filled with bentonite slurry to the depth of 60 cm to the top of the surface to avoid any collapsing the banks because of deep excavation. Approximately 30 - 40 m of the section was excavated each working day.

Backfill mixture was transported using the three cube tippers to the excavated trench and placed with the assistance of skid steer loaders (Bob Cat). The mixture was placed in such a way that in the opposite direction to the excavation. At the initial stage, it was assisted by tremie pipe to place exactly to the place where necessary. Before the transportation, the all required tests were performed including the slump with the presence of Engineer and the client. The approximate mixing time was range from 1 hr to 1.5 hrs depending on the quantity of soil volume.



Figure 4 - Trench excavation

The whole process was carried out as night shifts. It helped the site management not to hinder the daytime progress and work in comparably lower temperatures. During the daytime, the average temperature was over 35° C, and it might cause to lose the calculated moisture and

deviates from specified properties. The excavated trench was filled by the dehydrated bentonite slurry.



Figure 5 - Trench filled with bentonite

The SCB construction was performed as continued work patterns in every day. To continue the previous section, the joint face was scraped up to 100 mm thickness section and face was prepared as fresh section and then continued to backfill new material on top of that face. Once the backfill was done, the top surface was covered by 30 cm thick soil layer by every day.

4. Quality control procedure

The complete performances of SCB wall depend on the states of quality which is maintained at the site. Therefore, very strict quality control procedure was adopted in every aspect to keep the super performance of construction and aftercare. In the site lab with constant supervision by the Engineer and client, the tests were carried out as specified in the contract documents. All tests were performed by experienced lab staff.

The recommendation made by the literature and specification such as API Spec 13 A, ASTM D 5084, ASTM D 4380 [5] and so on.

Table 3 - Tests performed

Tests	Frequency
Initial Bentonite Slurry	
Viscosity	2 /shift
Density	2 /shift
Filtrate Loss	2 /shift
Bentonite Content	1 /project
Trench Slurry	
Unit Weight	2 /shift
Viscosity	2 /shift
Backfill Material	
Slump	1 / shift
Gradation	1 / 2000 m ³
Density	1 / shift
UCS	1/ 500 m
Permeability	1/ 500 m

Table 4 - Test parameters of initial mixes

Type of mix	Compositions (%)			UCS (kPa)		Permeability 10 ⁻⁸ (cm/s)	
	Soil	Cement	Bentonite	7 D	28 D	7 D	28 D
A	93.8	4	2.2	145	225	1.72	1.5
B	94.0	3.5	2.5	125	210	2.93	1.6
C	93.0	4	2.5	155	245	2.88	2.2

Special care was taken to carry out the UCS and permeability tests since these were done at independent third party lab. Sampling was done in a very careful manner and as per the recommendation by Ryan and Day [2] and Cermak and Law [4] and project specifications and standards. Sample preparation and transportation to the labs were done under the special attention on trench specialists and material engineer. Site collected samples were treated not to lose the moisture and kept minimum 4 days at site before transportation to the lab. Once delivered to the lab, then the saturation of samples was carried out, the time period was

nearly 6 -7 days. Then the UCS and permeability tests were commenced in both 7 days and 28 days.

Backfill mixing was carried out in such a way that, pre-determined quantities are met exactly and thorough mixing procedure was done to get the homogeneous mixture. Slump tests were performed to confirm that workability had attained so that filling to continue. If the slump was not gained, based on the reading either bentonite slurry was added or further mixing was done. However, the greater care was done to place the backfill within the specified 3 hr time frame.

5. Results and Discussion

5.1 Results of initial mix design

As per the Table 3, initial 3 mixes were chosen to carry out the testing, namely, type A, B and C. Initial idea was generated through the literature as discussed. Once the mix designs are carefully done, it was easy to finalize the appropriate design for the project. The

main and key parameter was always the permeability, and Unconfined Compressive Strength (UCS) then followed. Based on the results of Table 3, it is clearly demonstrated that UCS values are increasing with cement content. The main purpose of adding cement was to gain additional strength for the mix. On the other hand, the UCS has increased with the setting. That is well-understood phenomena in concrete technology, and here also it has been valid. The specification to achieve was 7 days UCS in between 100 to 200 kPa. All the mixes, that value have been achieved. Figure 6 shows the failure pattern for the one sample.





Figure 6 - Failure pattern for a sample

The most important and interesting parameter was the permeability. Measuring the permeability is also a challengeable task for the lab staff. Experience and knowledgeable

personnel are required to carry out the tests. A tiny error or negligence can be caused to get erroneous values, so that whole work and effort can be wasted. Therefore, permeability experiment should get more close attention. All mixes have exhibited elevated values for the permeability values ranging 1.72 to 2.88×10^{-8} at 7 days and from 1.5 to 2.2×10^{-8} at 28 days, respectively. The values were more than what was expected in the specifications. As expected the permeability has reduced with the time as the material matrix get set. However, the values were not decreased by order, so the permeability values remained in same order.

Based on the satisfactory results, it was decided to move to the type B, where better results with lower cement contents. Therefore, the rest of work carried out with mix B throughout the project.

The figures in the table clearly showed both UCS and permeability values are in proper order so that the construction activities were able to move smoothly. It is our understanding that continuous engineering input and strict quality control procedures were the most important aspect to get much better values.

Table 5 - UCS and Permeability (k) values for mix B

Type of mix	UCS (kPa)		Permeability 10^{-8} (cm/s)	
	7 D	28 D	7 D	28 D
B (Mix design)	125	210	2.93	1.60
B (1st set)	180.3	270	2.89	1.63
B (2nd set)	197.2	277.4	2.78	2.90
B (3rd set)	120.2	238.6	2.65	2.14

Samples and even preservation until to reach to the lab is also very key areas to keep the close eye. In addition, the basic tests as listed in Table 2 are also very vital in order to get the better UCS and k throughout the project.

6. Encountered difficulties and the solution given

Many practical difficulties were encountered in both design and construction aspects during the project.

To initiate a mix design, there are various aspects to consider. During that stage, the considerable time period was consumed to reach a final design, mainly because, to get the 28 days permeability, it had to wait nearly 2 months from the initial working. In practice, in Sri Lanka, very few competent labs are located. As a result, further time consumption can occur. So, better planning and early commencement of such time-consuming tests are highly recommended.

Proper planning and logistics arrangement is also a somewhat problematic area, and it is required constant attention to plan the work smoothly. It is very costly to prepare several mixing ponds and mixing pads along the dam or vicinity. Probably one location to cover approximately 2 km is recommended based on our finding and night shift can be more effective in such work.

Mixing the backfill material is more challengeable in large scale and will be again time-consuming if necessary steps are not being taken. As a result, the productivity and efficiency can be lowered drastically and creating unfavourable condition at the site in terms of finance, time and quality. Mixing time and the way excavator moves are very important aspects. If mixing time passes more

than 2 hr, it is unlikely to get a homogeneous and good slump mixture. Another significant aspect is to select the soil quantity for a batch to mix. Higher quantities can cause to extended time to missing, and non-homogenous mixture and lower quantity can cause the productivity issues.

Placing backfill material is also an area to keep a close eye. Improper placing can lead to creating the non-uniform layers in the trench so that some path can be created and water can move through them once the tank is at full level.

7. Conclusions

For the first time in Sri Lanka, the design and construction work of SCB wall was carried out successfully using only local engineering know how.

Though some literature suggested reaching the permeability values to 10^{-7} cm/s, in this project it has been achieved up to the 10^{-8} cm/s in all case with material composition as 94 %, 3.5 % and 2.5 %, the soil, cement and bentonite, respectively.

The corresponding UCS values were ranged between 100 to 200 kPa at 7 days and over 200 kPa after the 28 days.

Productivity can be increased up to four folds with the same machinery with proper planning. Site observation and feeling are vital aspects in order to increase the productivity and even value engineering.

Acknowledgements

The Authors wish to express their ultimate gratitude for Provincial Irrigation Department in Kilinochchi for their great support given. Further, the laboratory staffs of Access Engineering PLC (PMD 1) are also commended for their valuable services. In addition, the Department of Civil Engineering, University of Moratuwa is highly appreciated for the extended support for the lab services.

References

1. API, Specification for Oil-Well Drilling - Fluids Materials, Specification 13A-4, Washington, DC, 1990,
2. Ryan, C., R, and Day, S. R, Soil-Cement-Bentonite Slurry Walls, *Proceedings of Deep Foundations 2002: An International Perspective on Theory, Design, Construction, and Performance.*, American Society of Civil Engineers, Orlando, CO, 2002, pp. 713-727.
3. Owaidat, L. M., Andromalos, K. B, and Sisley, J.L, Construction of a Soil-Cement-Bentonite Slurry Wall for a Levee Strengthening program, *Proceeding of pan-Am CGS Geotechnical Conferences.*, 2009, pp 512-520.
4. Cermak, J., and Law, M. T, Cut off performances of a Soil - Cement - Bentonite Wall, *Proceedings of Pan-Am CGS Geotechnical Conferences.*, 2011, pp. 713-727.
5. ASTM, Compressive Strength of Molded Soil-Cement Cylinders, Vol. 4.08, West Conshohocken, PA, 2000.



Ballast Mats Made of Recycled Tyre Waste to Enhance the Performance of Rail Track Substructure under Cyclic Load

S.K. Navaratnarajah and B. Indraratna

Abstract: The rail transportation system in many countries plays a significant role in the conveyance of bulk freight and passengers. Increasing demand for high-speed rail and fast heavy haul poses a serious challenge for stability of tracks on the problematic ground. Ballast is a key foundation material placed underneath the sleepers which provides structural support against high cyclically induced stresses imparted by moving trains. Degradation of ballast contributes to a large percentage of maintenance costs, apart from affecting the longevity and stability of track. The problem is more critical in isolated rail track locations such as bridges and tunnels, where the substructure is much stiffer than the surface track assembly. In recent years, use of rubber mats to stabilise the stiffer track foundation has become increasingly popular. These rubber mats placed under the ballast layer is called as Under Ballast Mats (UBMs). Currently, there is a lack of comprehensive assessment on the geotechnical behaviour of ballast using these artificial inclusions under cyclic loading. In this study, a series of large-scale laboratory tests were carried out to verify the performance of ballasted track and understand the use of energy absorbing mats placed on top of a stiff foundation in the attenuation of dynamic stresses and subsequent mitigation of ballast degradation. Cyclic loads were simulated using a large-scale process simulation prismatic triaxial apparatus (PSPTA). The study shows that UBM distributes the stress applied from moving trains more uniformly by increasing effective contact area, which then reduces the dynamic amplification of applied vertical stress and leads to much less ballast degradation. The UBM used in this study was made from recycled tyre waste is a better solution to turn waste into value.

Keywords: Railroad ballast; Cyclic Load; Under Ballast Mat; Deformation; Degradation

1. Introduction

Railways are one of the major modes of transportation in the conveyance of passengers and bulk commodities. The railway industries are emphasizing the implementation of high train speed corridors and heavier freight operations to achieve efficient and cost-effective services. However, increased train speeds and higher freight loads accelerate the deterioration of track foundation, which in turn increases the maintenance costs. A major proportion of track maintenance funds is spent on the geotechnical related problems of the substructure, including the ballast layer [1-3]. The engineering behaviour of ballast is one of the most important aspects governing the stability and performance of a railway track because its progressive degradation under heavy cyclic loads from freight and passenger trains contributes largely to overall track deformation [4]. This, therefore, necessitates a thorough understanding of the geotechnical behaviour of the ballast layer, if the costs of track maintenance are to be reduced.

The ballast provides adequate resiliency when subjected to low-frequency cyclic loading

However, when track vibrations are excessive (for example, high-frequency loading), the resiliency of track diminishes, hence additional substructure inclusions become imperative to restore the original (fresh track) resiliency. Compared to the ballast, the high ductile nature of resilient materials such as rubber mats can absorb a significant amount of energy during cyclic loading at relatively high train speed. Rubber mats placed beneath the ballast layer actively decreases the amount of strain energy transferred to the ballast layer, thereby reducing particle deformation and degradation.

Eng. (Dr.) S.K. Navaratnarajah, Ph.D.(Aus), MSc (USA), B.Sc. Eng.(Hons) (Peradeniya), Senior Lecturer, Department of Civil Engineering, University of Peradeniya.

Eng. (Prof.) B. Indraratna, Ph.D.(Alberta), MSc and BSc-Hons (London), FTSE, FIEAust, FASCE, FGS, FAusIMM, FIES, DIC, C.Eng., CPEng, Distinguished Professor of Civil Engineering and Research Director, Centre for Geomechanics and Railway Engineering; Program Leader, ARC Centre of Excellence for Geotechnical Science and Engineering; University of Wollongong, Australia.



This in effect, improves the overall resiliency, and the longevity of the track.

Under Ballast Mats (UBM) eliminates the hard interface between the ballast and underlying hard layers, which enables the ballast to bed into a relatively softer pad and increase its contact area at the interfaces, which helps to distribute the cyclic load over a larger contact area (Fig. 1). As a consequence, the excessive interface and inter-particle contact forces of ballast are eliminated, which in turn reduces settlement and ballast breakage [5-9]. However, studies conducted to analyse the effectiveness of UBMs in minimising ballast deformation and degradation under cyclic loading are limited.

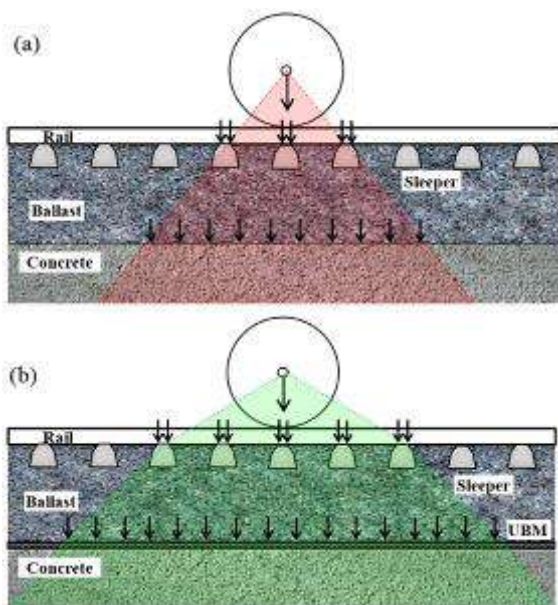


Figure 1 - Cyclic Axle Load Distribution:
(a) Without UBM; (b) With UBM (modified after [8])

The primary objectives of this research study are to assess the stress-strain and degradation behaviour of ballasted rail track and verify its performance when energy absorbing ballast mats are used in track foundation. Large-scale process simulation triaxial testing was conducted to evaluate the stress-strain and degradation characteristics of ballast with and without ballast mats. Empirical models were developed based on the laboratory finding to evaluate the resilient modulus of ballast and ballast breakage index.

2. Large-Scale Laboratory Testing

To assess the role of under ballast mats in more detail, a series of cyclic loading tests were conducted using the state-of-the-art large-scale Process Simulation Prismoidal Triaxial Apparatus (PSPTA) at the University of Wollongong, Australia. The ballast material commonly used in New South Wales (NSW) rail tracks was used for laboratory testing. Details of the test materials and their specifications and the cyclic load test procedures are discussed below.

2.1 Test Materials

The materials used in this study are fresh ballast and recycled tyre waste UBMs. The fresh ballast tested is latite (volcanic) basalt, a common igneous rock found along the south coast of NSW, and obtained from Bombo quarry, near Wollongong, NSW. The ballast samples were prepared in accordance with current Australian practices [10]. The laboratory samples were cleaned by water to remove any dust and clay adhering to the surface of the aggregates and dried before screening through selected sieves and then mixed in desired proportions to obtain the required particle size distribution (PSD). The PSD and grain size characteristics of the ballast material are shown in Figure 2. To simulate a hard subgrade condition such as a rail track over a concrete bridge, a reinforced concrete base was placed underneath the ballast layer.

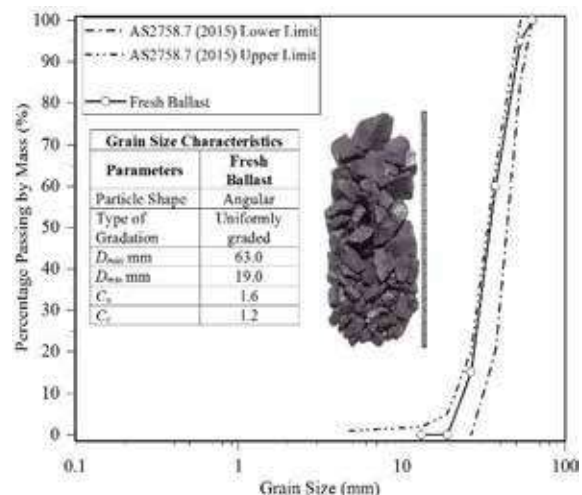


Figure 2 - Particle Size Distribution (PSD) and Grain Size Characteristics of Fresh Ballast

Table 1- Mechanical Properties of UBM

	
Thickness	10 mm
Weight	9.2 kg/m ²
Young's Modulus	6.12 MPa
Tensile Strength	600 kPa
Tensile Strain at Failure	80%
Static Stiffness, C_{stat} (DIN 2010)	0.2 N/mm ³
Dynamic Stiffness, C_{dyn1} (5-30 Hz) (DIN 2010)	0.46-0.59 N/mm ³

The mechanical properties of the UBM used in this study, along with a photograph of the UBM samples are shown in Table 1. The UBM was 10 mm thick and was made from recycled rubber granulates encapsulated within a polyurethane elastomer compound. The mat was placed on top of the concrete base during cyclic loading tests. Even though these polymeric materials deteriorate when exposed to the environment (thermal, oxidation, photolytic, and hydrolysis), they have a handy service life of approximately 20 years [11, 12].

2.2 Cyclic Load Test Procedure

The repeated cyclic loading from wheels moving along a rail track was simulated by the PSPTA shown in Figures. 3a and b. The cubical triaxial chamber is 0.8 m long by 0.6 m wide by 0.6 m high. This apparatus can realistically simulate the stress and boundary conditions found in ballasted track. In a real rail track, lateral movement of the ballast is not fully restrained, particularly parallel to the sleepers [13]. Therefore, the four vertical walls of the PSPTA chamber were built to allow free movement under applied cyclic loading. In this study, only two walls parallel to the sleeper were allowed to move under low confinement, the other two walls were locked in position to simulate a typical straight track (longitudinal deformation parallel to the rail is negligible).

The test specimen consisted of 150 mm thick concrete base overlain by a 300 mm thick layer of ballast to simulate a hard subgrade condition of a rail track. When testing with UBM, a rubber mat was placed on top of the concrete base. Ballast aggregates were placed on top of the concrete base/rubber mat in three equal 100

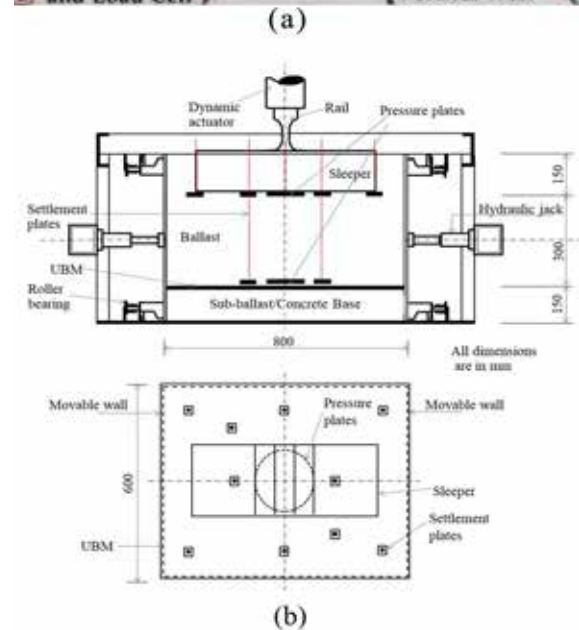
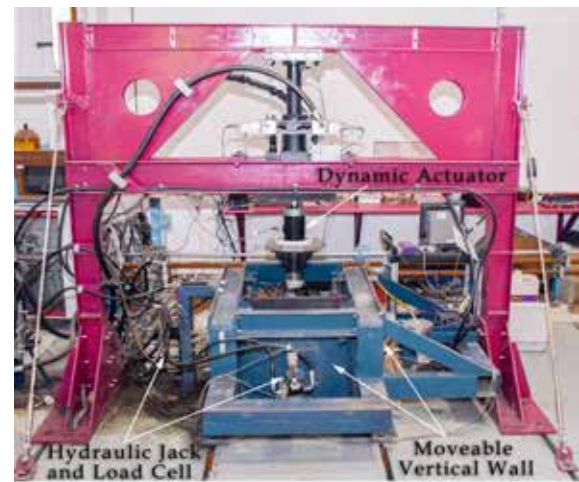


Figure 3 - (a) Photograph of PSPTA; and (b) Schematic Views of PSPTA

mm thick layers, compacted by a rubber padded vibratory hammer to a typical field density of approximately 1560 kg/m³. The rail-sleeper assembly was placed on top of the compacted ballast, and the space around the concrete sleeper was filled with 150 mm thick compacted crib ballast.

Some photographs of sample preparation for testing are shown in Figures. 4 (a)-(f). The cyclic loading was the equivalent of a 25t axle load to simulate a passenger train, and a 35t axle load for a coal train with a frequency of 15 and 20 Hz; this simulated a train traveling at about 110 and 145 km/h, respectively [14]. The corresponding cyclic loading in a sinusoidal wave form is shown in Fig. 5. The amplitude of cyclic loads was determined using American Railway Engineering Association (AREA) method [15].





Figure 4 - (a) The ballast was colour coded to evaluate degradation with depth; (b) Coloured ballast layers compacted inside the triaxial chamber and instrumented with pressure cell and settlement plates; (c) Crib ballast filled around rail-sleeper assembly and potentiometers attached on top of the sleeper; (d) Concrete base is placed at the bottom of the triaxial chamber (e) UBM was placed on top of the concrete base; and (f) Load - frequency controller and data acquisition system.

Lateral confinement was applied by hydraulic jack connected to movable vertical walls that simulated a low confining stress of 10-15 kPa. The walls were locked for movements in the longitudinal direction to ensure plane strain conditions, while the pressure exerted on the walls was measured. Electronic potentiometers and settlement plates were used to measure the deformation of the ballast layer. The vertical and lateral loads and associated deformation

were recorded by data loggers connected to computers. A total of 500,000 load cycles were applied for each cyclic load test.

3. Results and Discussion

Eight cyclic load tests were carried out with and without UBM at varying frequencies (15 Hz and 20 Hz) and axle loads (25t and 35t). The stress-strain response and degradation of

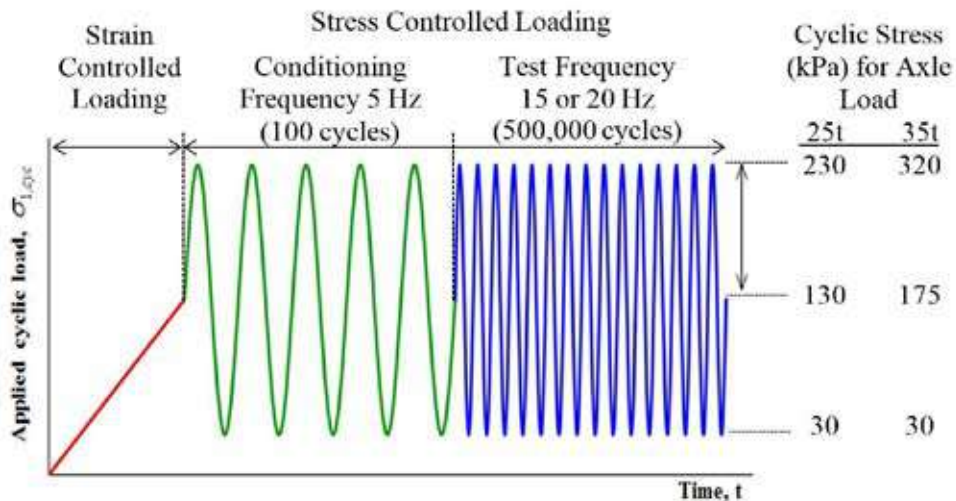


Figure 5 - Applied Cyclic Load

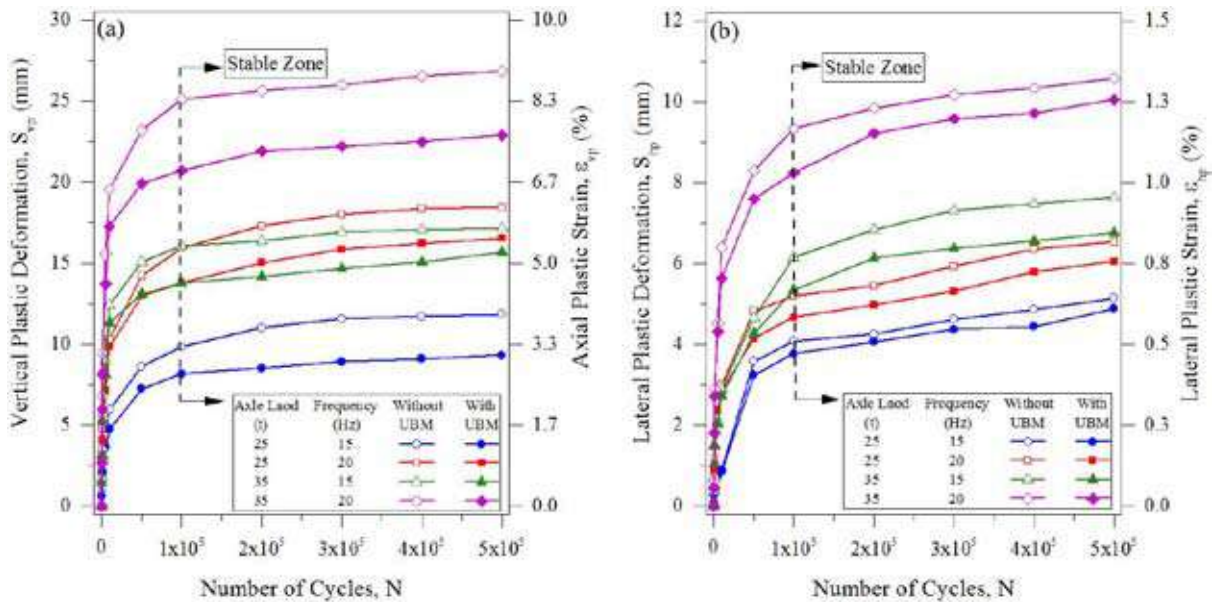


Figure 6 - (a) Vertical; and (b) Lateral Plastic Deformation (and Strain) of ballast with and without UBM (data sourced from Navaratnarajah and Indraratna [1])

ballast observed in these tests and a comparison with and without the use UBM are explained in the following sections.

3.1 Cyclic Deformation and Strain Responses

The vertical and lateral deformations of ballast under cyclic loading with and without shock mats were measured at selected number of load cycles ($N=1, 100, 500, 1000, 5000, 10000, 50000, 100000, \dots, 500000$). Since the longitudinal

vertical walls were restrained (plane strain condition, $\epsilon_2=0$), shear (ϵ_q) and volumetric (ϵ_p) strains were calculated from the following expression by Timoshenko and Goodier [16]:

$$\epsilon_q = \frac{2}{3} \sqrt{(\epsilon_1^2 + \epsilon_3^2 - \epsilon_1 \epsilon_3)} \quad \dots(1)$$

$$\epsilon_p = \epsilon_1 + \epsilon_3 \quad \dots(2)$$

where ϵ_1 , ϵ_2 and ϵ_3 - major, intermediate, and minor principal strains, respectively.

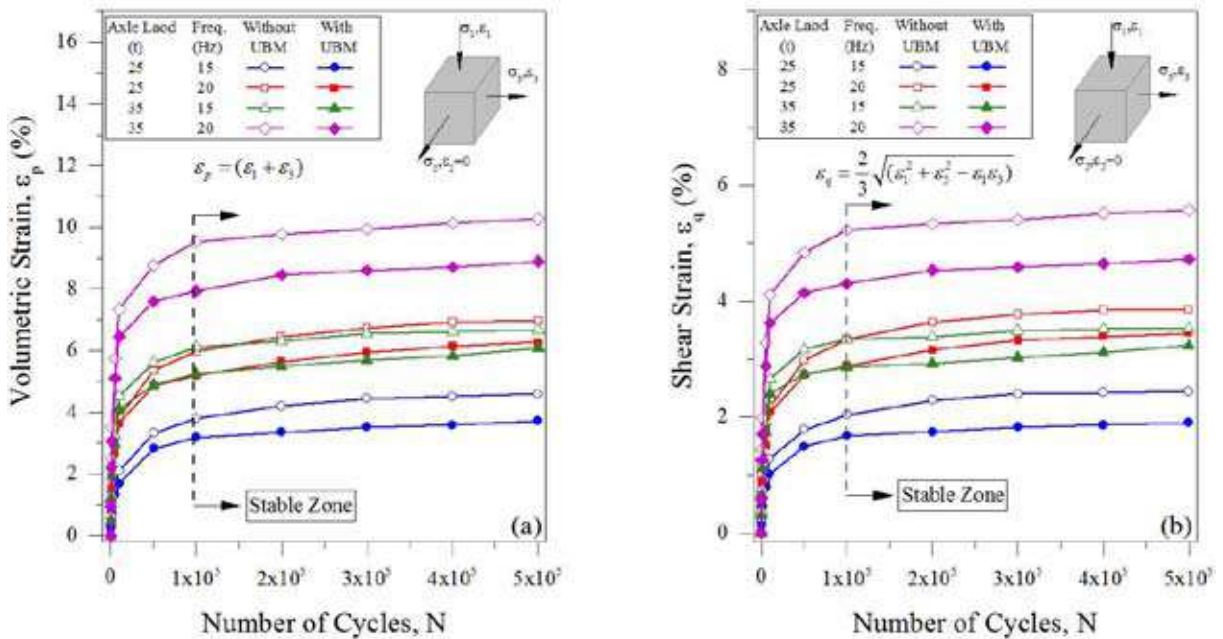


Figure 7- Cyclic strain response of ballast with and without UBM: (a) Volumetric; and (b) Shear Strain (data sourced from Navaratnarajah and Indraratna [1])



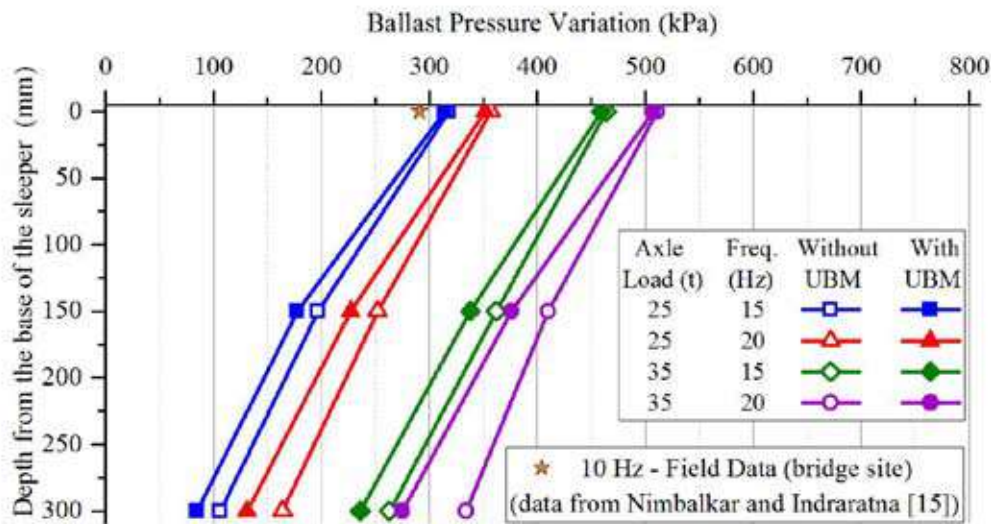


Figure 8 – Ballast Pressure Variation with Depth (data sourced from Navaratnarajah and Indraratna [1])

Vertical and lateral plastic deformation (and strains) with and without the UBM are shown in Figures. 6(a) and (b), and the corresponding volumetric and shear strains are shown in Figs. 7(a) and (b), respectively. As expected, deformation was high due to the hard-concrete base at the bottom of the ballast and the use of UBM on top of the concrete base significantly reduced the ballast deformation. The overall shear and volumetric strains were decreased in the order of 10 to 25% for the applied cyclic loads and frequencies. The test results also indicated that the ballast deformed rapidly up to around 10,000 cycles due to its initial densification and further packing after the corners of the sharp angular aggregates began to break, but once the ballast stabilised after around 100,000 cycles, the rate of ballast strain decreased as the load cycles increased.

Hunt [17] reported that increasing the elastic

elements in the track can cause excessive plastic and elastic deformations of ballast, as well as fatigue damage to other track components. Therefore, a proper design of track stabilised with resilient material with respect to their thickness and stiffness relative to the stiffness of the track substructure is vital.

3.2 Ballast Pressure Variation

In this study, the pressure cells placed at the sleeper-ballast interface, in the middle of the ballast layer, and at the ballast-concrete base interface were used to measure the dynamically induced pressure variation along the depth of the ballast mass. Figure 8 shows the variations in pressure with the depth of the ballast layer. It is observed that the dynamically induced stresses in the ballast increase with the axle load and train speed (loading frequency). These results compare well with the limited field data

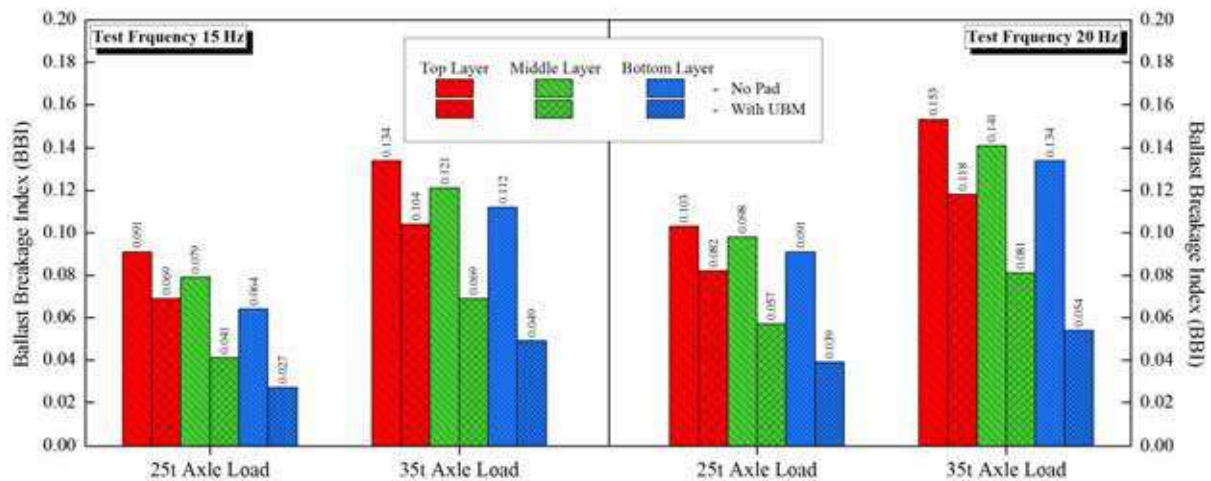


Figure 9 - Ballast Breakage Index, BBI (data sourced from Navaratnarajah and Indraratna [1])

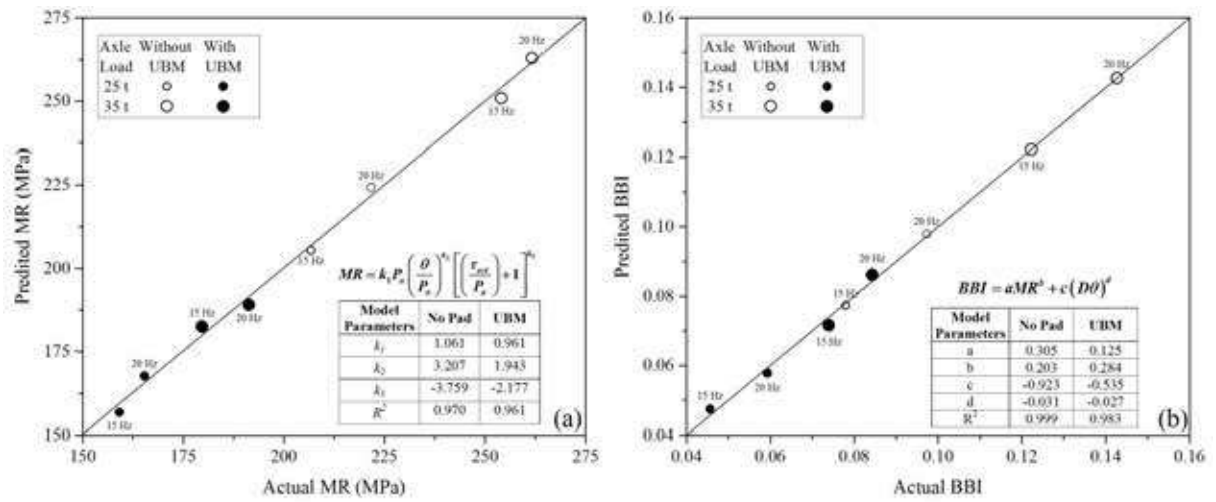


Figure 10 - (a) MR Model; and (b) BBI Model

obtained for a train with a 25 t axle load traveling at a speed of 73km/h (10 Hz) by Nimbalkar and Indraratna [18] at a rail bridge site at the Singleton, NSW, Australia as shown in Figure 8. When a rubber mat is placed on top of a concrete base, there is a notable reduction in stress in the ballast mass, especially at the bottom (ballast-concrete base interface) and middle layers. Stress amplification due to a stiff base is now curtailed by the softer interface introduced by the rubber mat between the ballast and the concrete.

3.3 Ballast Degradation

Progressive particle degradation occurs when a repetitive cyclic load is applied to the ballast mass. Initially, grinding and breakage of corners of the angular ballast at the inter-particle contacts take place, followed by complete fracture across the body of the particles depending on the strength of the parent rock and the level of load increment. This breakage of ballast particles contributes to increased axial and lateral strains and causes differential track settlement. Ballast degradation in this study was quantified using the Ballast Breakage Index (BBI) method proposed by Indraratna, et al. [19]. To quantify particle breakage by this method, particle size analysis was carried out before and after each cyclic triaxial test. To better estimate ballast breakage with depth, the ballast layer was colour coded and divided into three equal thicknesses of 100 mm, and then the BBI values were assessed separately for each layer. The BBI calculated for each layer are presented in Figure 9. As expected, ballast breakage was higher at the top layer due to higher inter-particle contact stress at the top, followed by the middle, and bottom layers. The results shown in Figure 9 indicate that ballast degradation is reduced

significantly by the UBM. On average, when all three layers are considered, UBM reduced the degradation by more than 40% when it was used on top of a concrete base.

3.4 Resilient Modulus and BBI Models

Multiple regression models were developed using MATLAB to predict the Resilient Modulus (MR) and BBI based on the laboratory test results. The MR model is based on Equation (3) and is being adapted from NCHRP [20]. The BBI model is a function of bulk stress (θ), and the damping ratio (D) of the ballast as shown in Equation (4).

$$MR = k_1 P_a \left(\frac{\theta}{P_a} \right)^{k_2} \left[\left(\frac{\tau_{oct}}{P_a} \right) + 1 \right]^{k_3} \quad \dots(3)$$

$$BBI = aMR^b + c(D\theta)^d \quad \dots(4)$$

where, $k_1, k_2, k_3, a, b, c, d$ - Multiple regression constants; P_a - atmospheric pressure (101.3 kPa); $\theta = \sigma_1 + \sigma_2 + \sigma_3$; τ_{oct} - octahedral shear ($\tau_{oct} = \frac{1}{3} \sqrt{(\sigma_1 - \sigma_2)^2 + (\sigma_2 - \sigma_3)^2 + (\sigma_3 - \sigma_1)^2}$); and σ_1, σ_2 and σ_3 - major, intermediate, and minor principal stresses, respectively

The actual and predicted MR and BBI are shown in Figures. 10 (a) and (b), respectively. The coefficient of determination (R^2) is greater than 0.9, which shows that the MR and BBI are predicting well with the variables used in the model.

4. Conclusions

The performance of ballasted rail track under cyclic loads with under ballast mats (UBM) placed on top of a hard foundation (concrete base) was studied through large-scale



laboratory testing. The test results confirmed that UBM reduced the ballast deformation, stress and degradation quite considerably. The overall shear and volumetric strains decreased in the order of 10-25% when UBM was used. The interparticle stress and the interface stress at the ballast-concrete base interface were significantly reduced by the use of UBM. The reduction in ballast degradation was more than 40% when UBM was used on top of a hard track foundation. It is evident from this study that by placing UBM, loads on the ballast bed can be distributed more homogeneously by the hard base and thereby improves track stability. This study confirmed that the recycled UBM used herein had an adequate damping ratio to absorb the energy transmitted to the track, thus preventing excessive ballast degradation. The benefits of reducing degradation with UBM potentially minimize the number of maintenance operations and reduce the life cycle costs of track foundations. Especially, the rubber mats can be made of recycled material such as tyre waste gives more value to the waste materials.

Acknowledgement

Authors wish to acknowledge the Australian Research Council (ARC) for its financial support. The assistance provided by senior technical officers, Alan Grant, Cameron Neilson and Ritchie Mclean at the University Wollongong, Australia is also much appreciated.

References

1. Navaratnarajah, S. K. and Indraratna, B., "Use of Rubber Mats to Improve the Deformation and Degradation Behavior of Rail Ballast under Cyclic Loading," *Journal of Geotechnical and Geoenvironmental Engineering*, vol. 143, no. 6, p. 04017015, 2017.
2. Ionescu, D., Indraratna, B., and Christie, H. D., "Behaviour of Railway Ballast under Dynamic Loads," in *Proc. 13th South East Asian Geotechnical Conference*, Taipei, 1998, pp. 69-74.
3. Indraratna, B., Salim, W., and Christie, D., "Improvement of Recycled Ballast using Geosynthetics," in *Proc. 7th International Conference on Geosynthetics*, Nice, France, 2002, pp. 1177-1182.
4. Indraratna, B., Salim, W., and Rujikiatkamjorn, C., *Advanced Rail Geotechnology: Ballasted Track*. Rotterdam, Netherlands: CRC Press/Balkema, 2011.
5. Bolmsvik, R., "Influence of USP on Track Response - A Literature Survey," Abetong Teknik ABVäxjö, Sweden, 2005.
6. Loy, H. (2008) Under Sleeper Pads: Improving Track Quality While Reducing Operational Costs. *European Railway Review*.
7. Dahlberg, T., "Railway Track Stiffness Variations - Consequences and Countermeasures," *International Journal of Civil Engineering*, vol. 8, no. 1, pp. 1-12, 2010.
8. Indraratna, B., Navaratnarajah, S. K., Nimbalkar, S., and Rujikiatkamjorn, C., "Use of Shock Mats for Enhanced Stability of Railroad Track Foundation," *Australian Geomechanics Journal, Special Edition: ARC Centre of Excellence for Geotechnical Science and Engineering*, vol. 49, no. 4, pp. 101-111, 2014.
9. Navaratnarajah, S. K., Indraratna, B., and Nimbalkar, S., "Performance of Rail Ballast Stabilized with Resilient Rubber Pads under Cyclic and Impact Loading," presented at the Proceedings of the International Conference on Geotechnical Engineering, Colombo, Sri Lanka, 10-11, August, 2015.
10. AS 2758.7 (2015) "Aggregates and Rock for Engineering Purposes, Part 7: Railway Ballast." Standard Australia, Sydney, New South Wales, Australia.
11. Ito, M. and Nagai, K., "Degradation Issues of Polymer Materials used in Railway Field," *Polymer Degradation and Stability*, vol. 93, no. 10, pp. 1723-1735, 10, 2008.
12. Lakuši, S., Ahac, M., and Haladin, I., "Experimental Investigation of Railway Track with under Sleeper Pad," presented at the 10th Slovenian Road and Transportation Congress, Portoroz, Slovenija, 2010.
13. Indraratna, B., Salim, W., Ionescu, D., and Christie, D., "Stress-Strain and Degradation Behaviour of Railway Ballast under Static and Dynamic Loading, Based on Large-Scale Triaxial Testing," in *Proc. 15th Int. Conference on Soil Mechanics and Geotechnical Engineering*, Istanbul, 2001, vol. 3, pp. 2093-2096.
14. Indraratna, B., Biabani, M., and Nimbalkar, S., "Behavior of Geocell-Reinforced Subballast Subjected to Cyclic Loading in Plane-Strain Condition," *Journal of Geotechnical and Geoenvironmental Engineering*, vol. 141, no. 1, pp. 1-16, 2015.
15. Li, D. and Selig, E., "Method for Railroad Track Foundation Design. I: Development," *Journal of Geotechnical and Geoenvironmental Engineering*, vol. 124, no. 4, pp. 316-322, 1998.

16. Timoshenko, S. and Goodier, J. N., *Theory of Elasticity*, 3rd Edition ed. Singapore: McGraw-Hill 1970.
17. Hunt, G., "Review of the Effect of Track Stiffness on Track Performance," *RSSB, Research Project*, vol. 372, 2005.
18. Nimbalkar, S. and Indraratna, B., "Improved Performance of Ballasted Rail Track Using Geosynthetics and Rubber Shockmat," *Journal of Geotechnical and Geoenvironmental Engineering*, vol. 142, no. 8, p. 04016031, 2016.
19. Indraratna, B., Lackenby, J., and Christie, D., "Effect of Confining Pressure on the Degradation of Ballast under Cyclic Loading," (in En), *Géotechnique*, vol. 55, no. 4, pp. 325-328, 2005.
20. NCHRP, "Guide for Mechanistic-Empirical Design of New and Rehabilitated Pavement Structures - 1-37A Final Report," National Cooperative Highway Research Program, Transportation Research Board, National Research Council, Washington, DC, USA.2004.



Analysis of Energy Dissipation in Post-Tensioned Hybrid Precast Concrete Frames

K.L.P.S. Perera, W.D.C.R. Wanniarachchi and P. Thammarak

Abstract: This paper introduces the analysis of a post-tensioned precast concrete hybrid framing system for providing increased ductility in seismic prone zones in following a damage avoidance design philosophy. A Compression Free Device (CFD) being an externally mounted replaceable steel yielding coupon mounted between a set of grips allowing free movement during compression, is to be used as an energy dissipater to counter the hybrid framing system's inherent lack of energy dissipative capacity. The compression free behaviour allows a lighter, slender energy dissipater allowing higher energy dissipation through tensile yielding without buckling. The analysis was performed using SAP2000 and further component to be performed using ABAQUS, through modelling of a subassembly consisting of a single frame connection with a beam and column cruciform assembly. The analyses were performed as a series of non-linear time history analyses and a non-linear reversed cyclic pushover analysis for the subassembly with the CFD modelled using multi-linear plastic link elements. Due to the compression free behavior, to provide energy dissipation for both directions, two sets of CFDs are required for each frame connection fixed on each column face. The analyses were performed for three models, with one being a monolithic frame connection, and the other two for the hybrid frame system with and without the CFD. Comparing the performance of the three systems, it was observed that CFD was successfully able to reduce the movement of the structure during seismic excitation and dissipate energy successfully. In comparison to the monolithic frame system, showed the ability of the hybrid frame system to allow elastic behaviour up to significant drift ratios through the ability to gap-open at the beam column interface. These indicate its feasibility for smart buildings for earthquake prone zones, allowing greater versatility by allowing faster reoccupation after seismic events through replacement of the yielded coupons.

Keywords: Hybrid Precast Systems, Post-Tensioned Hybrid Systems, Energy Dissipaters, Seismic Design, Finite Element Modelling, Damage Avoidance Design, Compression Free Device

1. Introduction

Designing of structures resistant to seismic loading is a critical component of the design phase of any high-rise building. With the recent boom in the construction of high rises throughout the globe and the importance of considering the effect of dynamic loading on these structures, new advancements to provide economic and practical advantages over conventional systems have become a necessity. A structural system which is able to dissipate the large energy of a seismic event while avoiding damage to the critical structural components would provide large economical savings, while also enabling faster rehabilitation avoiding complex, costly repairs.

Precast construction being a relatively newer technique and owing to its reduced adoption especially in seismically active areas, the amount of research performed on this technology for such applications has been limited. Precast concrete technology when compared to conventional CIP concrete possesses several advantages such as reduced

construction time, higher concrete strength, and greater quality control and facilitates ease of construction. According to the Precast Seismic Structural Systems (PRESS) research program, "To a considerable extent, the reason for the lack of advancement of precast structural systems in the United States can be attributed to uncertainty about their seismic performance...The codes require confirmation of the suitability of new designs by satisfaction of performance criteria provided by expensive and time consuming structural testing. This requirement inhibits innovation and has forced research and design practice into a narrow focus of reinforced [monolithic] concrete emulation instead of expanding the scope to take advantage of the strengths and differences of precast construction." [1]

Eng. K.L.P.S. Perera, B.Sc. Eng.Hons. (AIT), Assistant Lecturer, Department of Civil Engineering, SLIIT

Eng. W.D.C.R. Wanniarachchi, B.Sc.Eng. Hons. (AIT), Civil Engineer(structural), MAGA Engineering (pvt) Ltd.

Dr. P. Thammarak, Ph.D.(Texas) Senior Lecturer, Dept. of Structural Engineering, AIT



1.1 Hybrid Framing System

The hybrid connection is a type of gap-opening system whose behaviour upon being acted on by a lateral force is shown in Figure 1. The opening of the beam-column interface allows drift in the frame while causing minimal damage to the main structural elements.

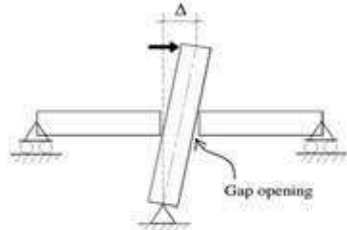


Figure 1 - Gap-Opening Behaviour

The pure hybrid frame system uses a combination of mild-steel and post-tensioning (PT) strands which gives it the hybrid naming. During a seismic event, the PT strands are designed so that they remain elastic and provide a restorative force which will be able to move the frame back to its original position after being acted on by lateral forces, which gives it a self-re-centering behaviour[2]. The mild steel is designed to dissipate the energy during the event by yielding. The compressive forces imposed on the joint by the action of the PT strands gives rise to shear resistance at the joint through friction at the interface, which will aid in the shear force transfer. This is the energy dissipation mechanism which in contrast to the typically preferred beam hinge mechanism where the plastic hinge is formed on the beam, the plastic hinge instead forms in the connection region and in controlled elements which gives it a damage avoidance design concept allowing the main structural elements to avoid being damaged during seismic events. A successful implementation of the hybrid precast connection system is in 'The Paramount' a 39 story 128 m high building; the tallest precast concrete framed building in seismic Zone 4.

1.2 Statement of the Problem

The problem in most systems is that the energy dissipater is situated inside the connection. This will lead to being unable to repair or replace the energy dissipater after it has yielded during an earthquake. This will make the structure not able to resist further seismic events unless costly, labour intensive and time-consuming repairs are done.

1.3 Objectives

The main objective of this paper is to analyse and compare the behaviour of a precast frame under selected loading conditions where the precast frame uses a pure hybrid connection; and as an alternative, the hybrid connection modified with an external energy dissipater. A sacrificial member which can be readily replaced after an earthquake which aims to prolong the viable lifetime of the building as well as reduce repair costs and retrofitting costs by reducing damage sustained by the core structural elements. Also reducing time for re-occupancy after seismic activity.

2. Literature Review

In designing and construction of precast systems, for determination of optimum seismic performance of a given precast structure, the selection of the type and the accurate detailing and specification of the beam-column connections is of paramount importance. The two bodies, which have played a significant role in the process of the development of precast systems having improved seismic performance, have been the programs initiated by the National Institute of Standards and Testing (NIST) and the Precast Seismic Structural Systems (PRESSS). The PRESSS research program was formed by the United States and Japan as a joint effort between the two countries for the "large scale testing for seismic response of precast concrete buildings". [1]

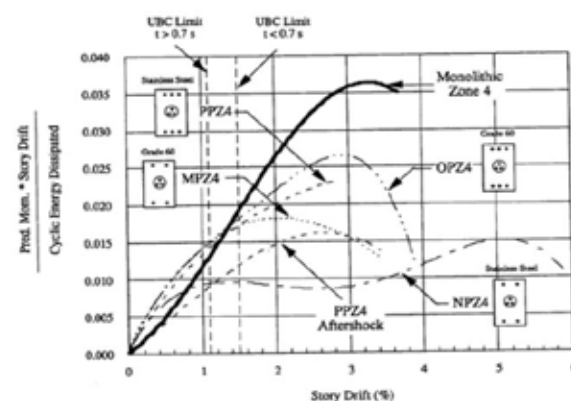


Figure 2 - Comparison of the normalized cyclic energy[3]

As seen in Figure 2 testing of various hybrid-framing system connections with different energy dissipaters provided varying levels of energy dissipation notably being most of them being better than the monolithic framing system at drift ratios below 1.5%. The

advantage seen by the NPZ4 specimen using stainless steel was that the connection was still functional even at an extreme drift ratio of 6%. All the hybrid systems managed to be in a serviceable condition at higher drift ratios compared to the monolithic connection indicating their versatility.[3]

2.1 Energy Dissipaters for Hybrid Frame Systems

The typical energy dissipater in HFS is the mild reinforcing bars inserted at the beam-column interface which yield and provide the nonlinear inelastic energy dissipation of the seismic energy. The disadvantage of the typical methods was that the energy dissipater is situated within the connection, hence difficult to access for maintenance, inspection or replacement, which leads to potential problems.

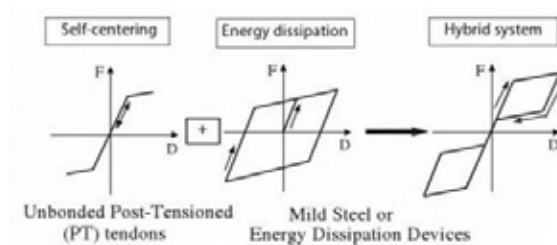


Figure 3 - Energy Dissipation Behaviour

In the Figure 3 it can be observed the components that make up the specific 'flag shaped' hysteretic backbone curve for a hybrid connection with an energy dissipater installed. The PT tendons provides the self-centering force without yielding, which allows it to continuously provide the recentering behavior to the connection. The energy dissipater provides the energy dissipation in this connection as depicted. The combination of the two provides the desired behaviour of the hybrid connection which allows it to both be a highly ductile connection while dissipating adequate energy and preventing residual displacements in the structure.

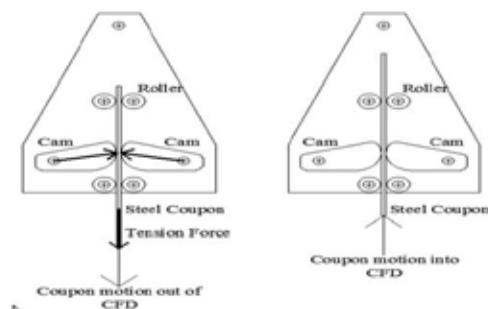


Figure 4 - Behaviour of CGDD system

The Cam Grip Energy Dissipation Device (CGDD) shown in Figure 4 consists of a sacrificial steel member between two cam-grips. When under tension, the grips will lock and allow force to be carried by the member and yield. When a compression occurs, the grips release and allows the member to slide freely preventing buckling. This behaviour allows the use of a thin steel member due to only tensile loads being carried. Also the external installation allows observation and faster replacement of the yielded member after seismic activity.

3. Methodology

For analysis of the proposed structural systems a series of Non-Linear Static and Dynamic Analyses were performed to determine and examine the behaviour and performance of the structures to determine the efficiency of utilising the CFD for the Hybrid Framing Connection.

The following are the key procedures followed during the study:

1. Selection of the subassemblies for the analyses, loading criteria, and other required inputs.
2. Determine method of modelling and analysis for each system.
3. Modelling and Analysis of each system.
4. Evaluation and comparison of the obtained results.

The selected subassembly for the analyses was a cruciform shaped beam and column joint, which was used for the research conducted by Thien, 2015);[4] an experimental test on the efficiency of using a CFD. The beam-column subassembly was selected instead of a full frame to be analysed since during the literature review it was determined that the modelling of a full frame system having a hybrid frame system incorporating gap-opening behaviour, post tensioning strands and external energy dissipating devices is a much complicated task several magnitudes more cumbersome than the modelling of a simple steel or concrete frame structure. Also the required large number of calculations for the design of individual connections at different joints of the frame structure due to varying section sizes, capacity demands and the complexity involved in incorporating these into a full frame model further justified the selection of the cruciform shaped subassembly. Another determining factor was the very high computational



demand involved in the analysis of a full frame structure.

The properties of the test specimen beam was length of 1200mm, width of 170mm and 270mm depth as shown in Figure 5. The column was 2000mm tall with a square section of 320mm x 320mm. The beam was post tensioned with two 7-wire strands in PVC ducts each tensioned up to 8.4 Tons.

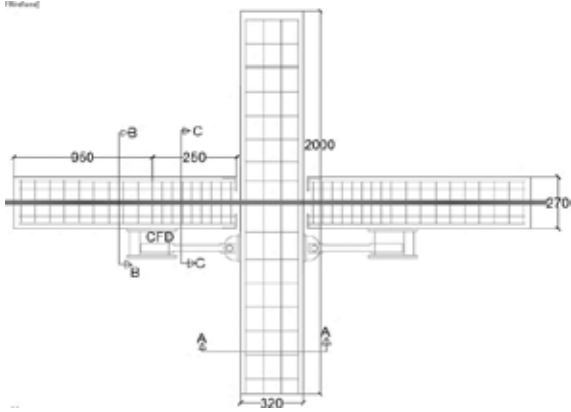


Figure 5 - Test Specimen Details

3.1 Loading and Design Criteria

The support conditions are as shown in Figure 6 with the base pinned and the other ends supported on rollers. Site location was selected as Los Angeles, California due to its high seismicity where Hybrid Frame Systems have been considered for construction. Seismic loading will be carried for Northridge, Kobe and Loma Prieta earthquakes, of which all three have had significant effects on structural designs, and all three sets being used having determined as having 2% probability of exceedence of occurring in 50 years for the Los Angeles area.

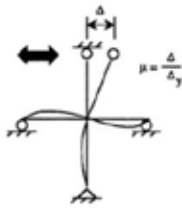


Figure 6 - Support Conditions

A set of Non-Linear Pushover Analyses was also performed. The pushover analysis was done as a reversed cyclic loading based on a drift monitoring approach. For each loading cycle, 30 sub steps were used as a minimum for the loading to improve the data accuracy in reporting and to improve convergence.

3.2 Determine method of modelling and analysis

For the modelling of the subassembly, the literature review revealed three approaches for modelling the hybrid frame connection.

The discrete springs approach as shown in Figure 7, where a number of linear and non-linear link elements are used to emulate the behaviour at the joint was a considered method since it was tested by previous researches as being substantially accurate over the single spring method where a single non-linear rotational spring emulating the combined behaviours of the springs in the discrete model[5]. The complexity in carrying out the large number of calculations for determining the behaviour of the joint in the single rotational spring model indicated that the discrete spring model provided the best approach with suitable fidelity in the computational analysis. Also the level of detail provided by using the discrete spring model allowed finer control over the modelling process with adjustments to the parameters of the individual elements at the connection not resulting in changes to the whole model as with a single spring model. The discrete spring model used also allowed the depiction of the gap-opening behaviour at the beam-column interface for the lateral loading.

The first model attempted was using simple frame elements to model the beam and column and using a similar approach as (Ricles J. , et al.). [6] for discretising the connection into master and slave nodes connected through rigid body constraints to keep plane section hypothesis and enforce the boundary conditions at the joint and through the use of multiple link elements to model the connection region. This model was developed further to incorporate the CFD but the difficulty of incorporating the effect of the gap-opening on the behaviour of the beam led to selection of a new method for the analysis.

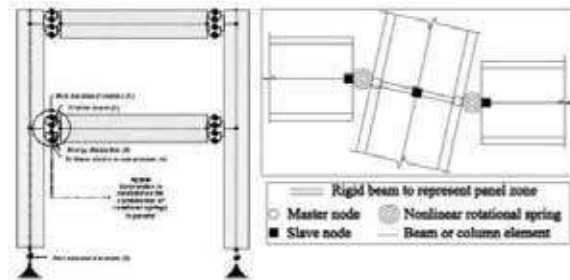


Figure 7 - Discrete springs model [7] (left) and single rotational spring model [8] (right)

The technique used to simulate the gap-opening behaviour at the joint and the non-

linear property of the CFD was a discrete springs approach combined with using of shell elements to model the frame elements.

The frame elements were modelled using thick shell elements using 4000psi (27MPa) concrete with a non-linear mander model utilized for simulating the non-linear behaviour of concrete. Thick shell area property was selected since it provides higher accuracy for shear deformation and since the thickness of each shell element is considerably large compared to its other dimensions.

The gap opening behaviour at the connection interface was emulated by the use of link elements having the "gap" property with very high axial stiffness in compression, but zero stiffness in tension, allowing the beam and column to separate freely, but emulating the actual interaction of compressive crushing when the gap closes.

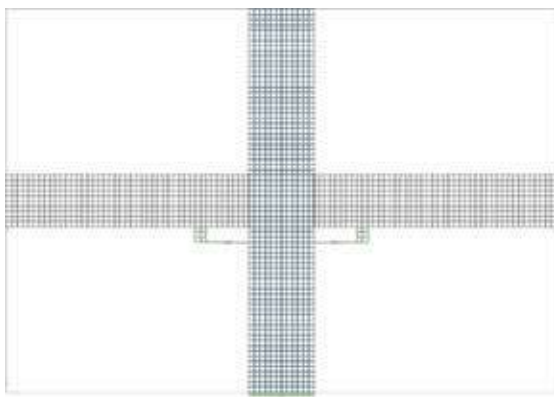


Figure 8- Analysis model of HFC with CFD

The CFD (Compression Free Device) was modelled using a link property using a multi-linear plastic property link element. The material selected for evaluating the properties of the steel coupon was A36 steel with a yield strength (F_y) of 36MPa and ultimate strength (F_u) of 58Mpa and a Poisson's ratio (ν) of 0.26. The force-displacement ($F-\Delta$) behaviour of the sacrificial rod was manually calculated, optimized, and given for the properties of the link as shown in Figure 9. The compression free behaviour was given by providing the link with negligible stiffness when under negative displacement.

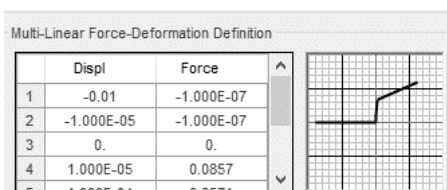


Figure 9 – Force-Displacement graph of CFD

The design for the compression free device was also conducted through a nonlinear FEA through using 'nonlinear' layered shell elements in the software to obtain the force vs. displacement plot for the steel coupon in tension through the application of a monitored displacement force.

4. Results and Discussion

This section presents and examines the results obtained from the various non-linear time history analyses and the non-linear static pushover analysis for reversed cyclic loading. The resulting behaviours were compared to determine if the Hybrid Frame System (HFS) using the CFD provides performance for consideration for practical implementation in real world design and construction of seismic resistant building structures.

For each structure that was analysed, a set of predetermined analysis outputs were obtained. These were then compared to the outputs from the other models to determine the efficiency of each system, specifically to determine the efficiency provided by the CFD, to check if the device is working as intended by dissipating sufficient energy as observed from the energy plots and the hysteresis diagrams for the CFDs.

4.1 Performance of the Hybrid Frame Connection with the Compression Free Device

Upon analysis of each structure, the behaviour of each was observed to be in line with those expected of the structures through the literature review. The gap-opening behaviour at the connection as well as the effect of post tensioning was seen in the analysis results as can be seen in Figure 10.

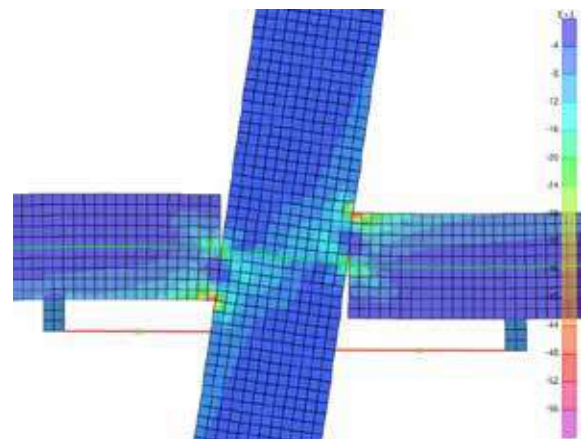


Figure 10- Stresses at 6% drift for HFC



For the Nonlinear Time History Analyses performed on the subassembly with the post-tensioning device installed, results were obtained for the three ground motions that were applied. For the Tab as ground motion the following graphs depicts some of the obtained results for the structural behaviour such as the drifts at the top, and the hysteretic behaviour of the CFD during the loading, including the energy plots for the various energy components through the time period; also in Table 1.

Table 1 - Energy Components(kj)of HFC-CFD

	Input	Kinetic	ModalDamp	Link Hystertrc
TABAS	0.4256	0.0211	0.3837	0.0415
KOBE	0.0291	0.0009	0.0209	0.0041
N.RIDG E	0.1322	0.0190	0.1026	0.0146

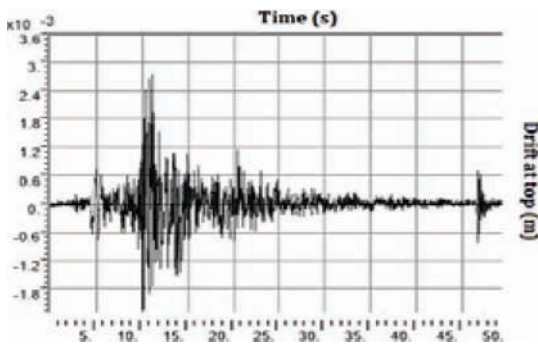


Figure 11 - Drift vs time for LA30 (Tabas)

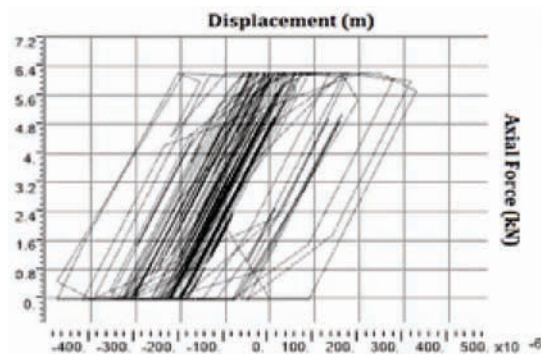


Figure 12 - Hysteresis for CFD for LA30

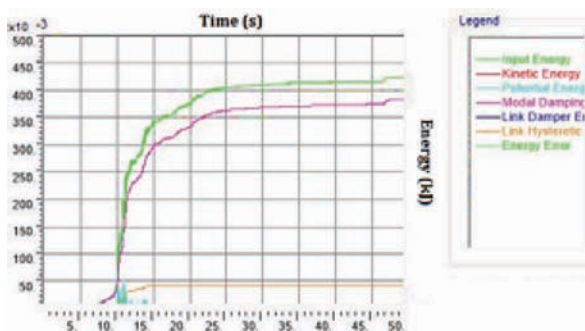


Figure 13 - Energy plots for LA30

4.2 Performance of the Hybrid Frame Connection with the Compression Free Device for NSP

Figure 15 shows the hysteretic behaviour for the CFD obtained from the Non-Linear Static Pushover Analysis conducted on the hybrid precast frame model with the compression free device installed. The recorded drift at the top of the column with each step is shown in Figure 14:

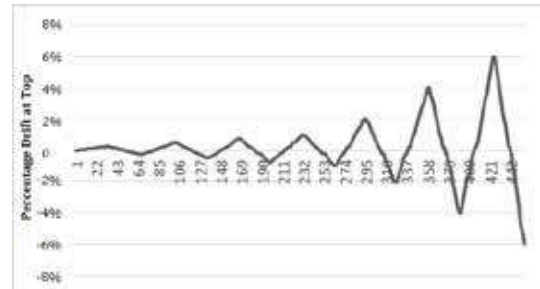


Figure 14 - Imposed drift vs time step for NSP

It was observed from the analysis that the behaviour of the CFD was following the idealized compression free behaviour through the range of motion and was dissipating energy according to the provided parameters though fracture strain was not realized. The Figure 15 depicts the hysteresis behaviour of the east side CFD during the NSP testing.

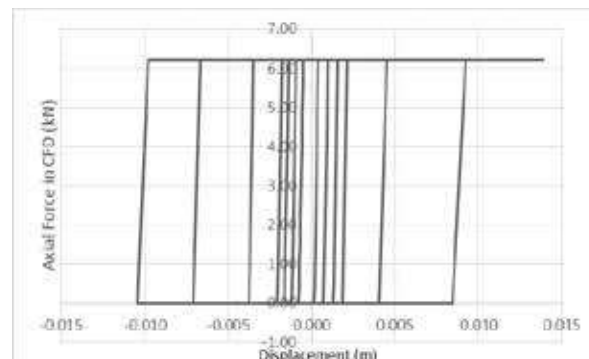


Figure 15 - Hysteresis behaviour of CFD on East side for NSP

4.3 Comparison of the Hybrid Frame System with the CFD and without the CFD

For the tested dynamic analyses, a comparison of the parameters such as the energy components and the drifts was done to identify the efficacy of introducing the CFD to the already versatile Hybrid Framing System. The following figures indicates the comparison of the two systems.

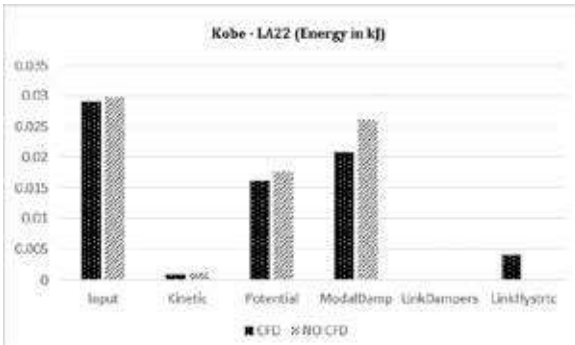


Figure 16 - Energy comparison for Kobe-LA22

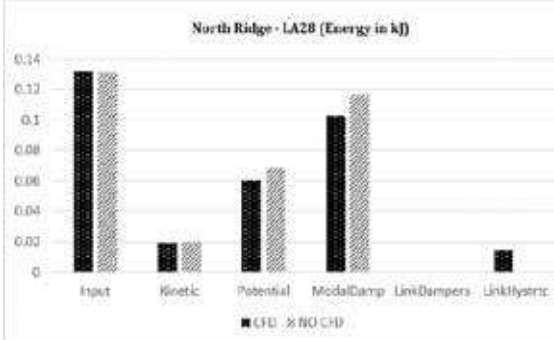


Figure 17 - Energy comparison for Northridge-LA28

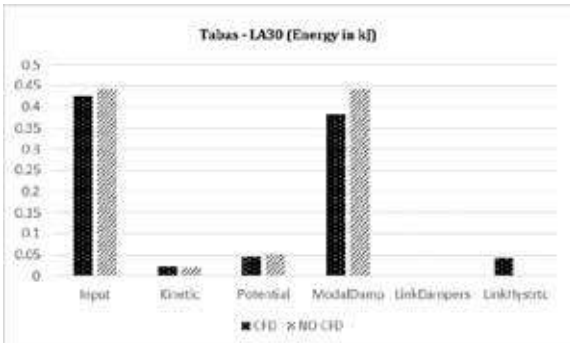


Figure 18 - Energy comparison for Tabas-LA30

Figures 16 to 18 shows the energy component plots for the HFC with and without the CFD. It is observed that in all the ground motions, the presence of the CFD has led to less energy being dissipated through modal damping in the structure, which indicates that less damage will occur to the structure and that the drifts will be minimized. However, from the results we can observe that a majority of damping occurs through modal damping. In the Kobe ground motion, it manages to dissipate a larger amount of energy compared to that occurring in the other ground motions; this can be attributed to the fact that the Kobe ground motion has a greater period with less intense shocks, which allows the link to dissipate energy properly.

When comparing the drifts as in Table 2, it can be seen that the CFD device manages to reduce the drift at the top of the column for all the ground motions, especially in the Kobe ground motion.

Table 2 - Drift at top of column comparison

		NO CFD	CFD	% redu	Avg. %
Tabas	Max	0.00321	0.00275	85.75	75.31
	Min	-0.00349	-0.00226	64.86	
Kobe	Max	0.00304	0.00133	43.65	53.39
	Min	-0.00256	-0.00162	63.13	
North Ridge	Max	0.00144	0.00125	86.75	89.68
	Min	-0.00177	-0.00164	92.60	

5. Conclusion

From the literature review performed of hybrid precast frame systems, it was expected to have higher drift values for the post tensioned hybrid connection, and to observe reduction of the drifts of the hybrid frame connection when using the compression free device. From the inspection of the results of the analyses, the results expected from the literature review were observed successfully. The CFD was observed to be successful at providing energy dissipation to the tested model as observed by the reduction in the drift of the system during the earthquakes applied to the models. The yielding behaviour during tension and the free movement of the CFD during compression and its energy dissipation was successfully observed in the hysteresis diagrams of the CFDs although the energy dissipation capacity was not as good as expected to make it performance efficient.

From the experimental research conducted by Thien [4] it was observed that by using a single CFD passing through the column resulted in the device not being able to provide any energy dissipation due to failure of the steel coupon to reach the yielding strain due to relative movement of the connection elements. The use of two CFDs on either face of the column as tested during this study would give a possible solution to the problem faced when using a single CFD, as well as providing better energy dissipation though being more cumbersome due to requiring two sets of devices for each connection.

From this study, it was confirmed that using the CFDs in a hybrid frame connection can make the hybrid connection dissipate sufficient energy to make it a viable system and combined with the ease of inspection and replacement of the steel coupon makes the use of the CFD even more appealing.

The major drawback faced with this system was in the modelling phase, the highly complex and



computationally expensive procedure required to model the Hybrid Frame System would pose a critical challenge to the widespread adoption of any form of Hybrid Frame System unless significant advances in computing or an alternative method to capture the behaviour of the connection is discovered. The current methods used for the analysis of Hybrid Frame Systems and other Self Centering Moment Resisting Frames in concrete and steel requires expert knowledge in Finite Element Modelling or other alternative unconventional analysis methods, which are typically not used in current mainstream design processes. This makes Hybrid Systems a controversial system with lots of benefits but with limited adoption.

5.1 Recommendations

From the results obtained from the analysis and the methodology followed in this study, it was observed that the analysis and design procedure for hybrid frame systems is computationally expensive in terms of the time and effort required for modelling and analysis. Therefore it would be beneficial to future researches and also would aid in the widespread adoption of the Hybrid Frame System, to develop a commercial software package designed to aid in the analysis and design of Hybrid Frame Systems for both concrete and steel moment resisting frames. This would massively reduce the workload involved in the analysis and design procedure for this type of system which is a highly suitable structural systems solution to highly earthquake prone areas while reducing the post-earthquake damage to the structures.

Future researchers could study how the placement of the device in the system such as the mounting location and the number of devices could affect the performance of the connection where a larger number of devices with elements yielding at certain loadings would be effective. Higher yield devices for reducing damage at large displacements and lesser yield strength devices for controlling drifts for smaller imposed displacements.

For countries like Sri Lanka having recently started on major construction projects such as significant high rises; considering the importance of faster construction, higher quality required, cost effectiveness, the feasibility of precast concrete hybrid frames could be researched upon to evaluate if the

system could provide advantages in the Sri Lankan construction industry context over the CIP system currently used.

Acknowledgement

The authors' wishes to acknowledge the assistance given by the Asian Institute of Technology, Thailand, Dr. Panchet Thammarak and associated masters students for providing the valuable opportunity to pursue this research and for providing guidance and knowledge.

References

1. Priestley, M. N., "Overview of PRESSS Research Program", *PCI Journal*, Vol. 36, No. 04, 1991, pp. 50-57.
2. El-Sheikh, M., Sause, R., Pessiki, S. and L. Lu, "Seismic behaviour and design of unbonded post-tensioned precast concrete frames," *PCI Journal*, vol. 44, no. 3, 1999, pp. 54-71.
3. Cheok, G., and Stone, W., "Performance of 1/3-scale model precast concrete beam-column connections subjected to cyclic inelastic loads – Report No. 4.," National Institute of Standards and Technology, Gaithersburg, 1994.
4. Thammarak, P., Thien, M., Htun, L., and Khine, M., "The Development of a Compression-Free Energy Dissipative Brace," in *Proceedings of the Tenth Pacific Conference on Earthquake Engineering*, Sydney, 2015.
5. Christopoulos, C., Filiatrault, A., Uang, C. and B. and Folz, "Post-tensioned Energy Dissipating Connections for Moment-Resisting Steel Frames," *Journal of Structural Engineering*, vol. 128, no. 9, 2002, pp. 1111-1120.
6. Ricles, J., Sause, R., Garlock, M., and Zhao, C., "Posttensioned Seismic-Resistant Connections for Steel Frames," *Journal of Structural Engineering*, vol. 127, no. 2, pp. 113-121, 2001.
7. Amaris, A., Pampanin, S., Bull, D., & Carr, A. "Experimental Performance Of Hybrid Frames Systems With Non-Tearing Floor Connections" 14th World Conference in Earthquake Engineering (14WCEE). Beijing, China: World Conference in Earthquake Engineering, 2008.
8. Dobossy, M., Garlock, M., & VanMarcke, E. "Comparison Of Two Self-centering Steel Moment Frame Modeling Techniques: Explicit Gap Models, And Non-linear Rotational Spring Models". *4th International Conference on Earthquake Engineering*, (p. Paper No.101). Taipei, Taiwan, 2006.

Study on Filler Slab Construction

K. Baskaran, A. Gopikrishna and P. Thiruvakaran

Abstract: During the design process while fulfilling the functional requirements engineers need to consider ways to reduce the cost of construction. Filler slab construction, which reduces the self-weight of slabs and has reduced loads along the rest of the load path up to foundation, is an effective way for cost reduction. However, application of this technology is found to be limited in Sri Lanka due to the vacuum in knowledge. In the post war resettling program, in the Northern Province of Sri Lanka, roof slabs of few houses were constructed with filler slab technology, similar to those adopted in India. In the present study, filler slab construction is revisited, with the sole objective to throw some light on this approach. Literature survey, field survey, desk study, physical modelling and finite element modelling were some methods adopted in the present study. The purpose of this paper is to share the findings of the present study with the industry. This paper includes brief introduction on filler slab technology, state of the art found from literature and field surveys, design methods adopted in the present study (solid slab approach and flange beam approach), details of two series of experiments on filler slab (specimen with burnt clay tiles as filler material) and solid slab (control specimen), the observations made and subsequent finite element modelling details. The purpose of the two series of experiments is to study the behaviour of filler slab under distributed load and patch load. Flexural failure and post flexural punching shear failure were observed during the physical model testing. The paper briefs on cost comparison and construction difficulties before concluding with summary of findings in the present study.

Keywords: RC solid slab, Flexure, Punching shear

1. Introduction

While transferring the applied loads in a safe manner, reducing the amount of materials needed and controlling the escalating cost are the challenges ahead of structural engineers. As commonly practiced, concrete in tension is considered as cracked and not contribute for flexural load carrying action in a simply supported reinforced concrete slab subjected to transverse loading. Therefore, not much concrete is needed to the bottom part; except to hold the reinforcement together, provide cover to the reinforcement and shear resistance. Therefore significant amount of the concrete can be replaced by the lightweight materials such as mud blocks, bricks, hollow blocks, semi earthen pots, PVC pipes, coconut husks, autoclaved solid blocks and calicut tiles. The amount of replaced concrete depends on the thickness, shape of the filler material and the amount of concrete filled between the voids of the filler materials.

Use of filler materials reduces the self-weight of the slab and results in savings in the required amount of reinforcement and concrete [5]. By using suitable filler materials, aesthetic appearance and thermal comfort inside the building can be improved [6]. According to Jaisingh & Singh [7], sound absorption of the filler slab is greater than the normal reinforced concrete slab therefore it is suitable for class

rooms, lecture halls, conference halls and auditoriums.

Although the filler slab technology was adopted in few buildings constructed in the last century in Sri Lanka, this technology is not practiced in the recent past. Recently for the post war resettling programme, in the Northern province of Sri Lanka roof slabs of few houses were constructed with filler slab technology, after looking at similar construction in India. However, theoretical or experimental evidence are not there for adoption. Hence the aim of the present study is to throw some light on filler slab technology. The objectives of the present study are to

- Identify a design approach
- Find the behaviour up to failure (flexure or punching shear)
- Identify any difficulties during construction and compare cost

2. State of the art

According to the literature review and field survey, calicut tile was selected as a suitable filler material. The parameters considered in the selection process are dimension of the slab,

Eng. (Dr.) K.Baskaran, B.Sc.Eng.(Peradeniya), Dr.Eng. (Cambridge), Senior lecturer of Civil Engineering, Department of Civil Engineering, University of Moratuwa.

Eng. A.Gopikrishna, B.Sc.Eng.(Hons.)(Moratuwa), QA/QC Engineer, Access Engineering PLC.

Eng. P.Thiruvakaran, B.Sc.Eng.(Hons.)(Moratuwa), AMIE(SL).



material cost, fire resistance, water leakage through the filler materials, aesthetic view, thermal comfort and availability. Due to lack of fire resistance, coconut husk and the PVC pipes are not suitable materials for filler slab construction. When considering the dimension of the slab, hollow blocks, semi earthen pots and mud blocks are not suitable in Sri Lanka. Aesthetic view of the slab with calicut tiles is better than other filler materials. Hence, calicut tiles were chosen as the filler material for this study.

3. Theoretical study

In a theoretical study of slabs, both flexure and punching shear are needed to be considered at ULS as they are the governing failure modes. Section 3.1 and 3.2 discuss the flexure theory and the section 3.3 discusses the punching shear theory. Two different approaches were used to determine the flexural resistance of the filler slab and the RC solid slab according to clause 3.4 of BS 8110: part 1: 1985. The considered cross section is shown in Figure 1.

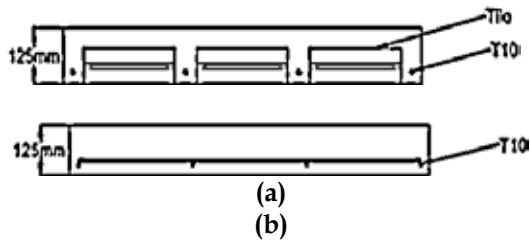


Figure 1 - Cross section of filler slab (a) and RC solid slab (b)

3.1 Solid slab approach

Consider a strip of slab with width “b”. The

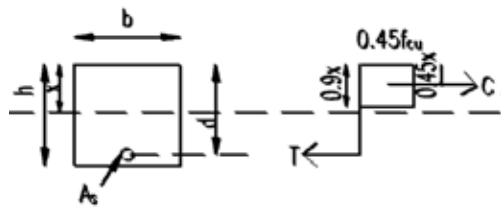


Figure 2 - Solid slab approach diagram

total compressive force in concrete is C. The total tensile force in steel is T (See Figure 2).

$$C = 0.45f_{cu} * b * 0.9x \quad \dots(1)$$

$$T = 0.87f_y * A_s \quad \dots(2)$$

Where, x is the depth of the neutral axis.

By equating forces x was obtained. Hence moment resistance (M) was found.

$$M = 0.87f_y A_s z \quad \dots(3)$$

Then the shear resistance and the deflection check were done according to clause 3.4.5 and clause 3.4.6 of BS 8110: part 1: 1985 ([2]) to ensure that the filler slab will not fail in other modes.

3.2 Flange beam approach

Consider a flange beam for which the web thickness is b_w . The equation for total tensile force in the steel is same as above. To find the total compressive force, the equation (2) is slightly modified since “b” is replaced by “ b_f ” (Figure 3). Here also shear resistance and

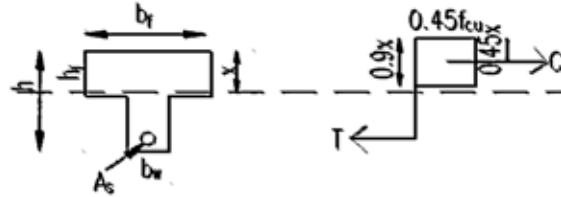


Figure 3 - Flange beam approach diagram

deflection check were done according to clauses mentioned in solid slab approach (section 3.1).

3.3 Punching shear check

a) ACI 318:1995 code ([3])

Shear stress caused around the columns in slabs due to the direct shear and moment is given by,

$$\text{Section 11.12.6.2, } v_u = V_u/A + \gamma * M_u * c \quad \dots(4)$$

Allowable stress

$$\text{Section 11.12.2.1, } v_c = \text{minimum} (0.17(1+2/\beta c) * \sqrt{f_c}, 0.083(2+ \alpha_s * d/u) * \sqrt{f_c}, 0.33 * \sqrt{f_c}) \quad \dots(5)$$

If $v_u < \phi v_c$,

No punching shear reinforcement is required

b) BS EN 1992-1-1:2004(E) code ([4])

$$\text{Equation 6.38, } v_{Ed} = \beta V_{Ed} / u_i d \quad \dots(6)$$

$$\text{Equation 6.9, } V_{Rd,max} = \alpha_{cw} b_w z v_1 f_{ck} / \gamma (\cot \theta + \tan \theta) \quad \dots(7)$$

$$\text{Section 6.4.4, } V_{Rd,c} = C_{Rd,c} k (100 \rho_l f_{ck})^{1/3} + k_1 \sigma_{cp} \geq (v_{min} + k_1 \sigma_{cp}) \quad \dots(8)$$

4. Experimental study

4.1 Materials

Two series of experiments were carried out (one was subjected to line load to check the flexure and other one was subjected to concentrated load to check punching shear capacity). Ordinary Portland cement was used. 10mm diameter ribbed steel bars were used for main bars and distribution bars. The Calicut tile

was used as the filler material. Grade 20 concrete was used and the mix design was done according to DoE method. 10mm and 20mm maximum aggregate sizes were used for Series one experiment and Series two experiment respectively. Here, Series one experiment represents the flexure model (aggregate size immaterial) and Series two experiment represents the punching shear model (aggregate size matters).

4.2 Casting procedure

1.51m length and 1.05m width flexure model slabs and 1.46m length and 0.965m width punching shear model slabs were casted with concrete having w/c ratio of 0.52 and tested in the laboratory. Thickness of the both slabs used in Series one and two experiment were 125mm and the bottom and side cover to reinforcement was 25mm. The dimensions of the both slabs were selected with respect to the size of the test rig. The filler slab and RC solid slab model design was carried out with the concern of the ribbed slab approach which is given in clause 3.6 of BS 8110: part 1: 1985 and clause 3.4.4.4 of BS 8110: part 1: 1985 respectively. Spacing of the main and secondary bars are 330mm and 480mm respectively in Series one experiments and 470mm and 305mm in Series two experiments. Both main bars and distribution bars were tied together and reinforcement mesh was formed. Then it was placed in the timber formwork. Two calicut tiles (one laid on top of the other) were stacked within the rectangular space formed by the reinforcement which is showed in the Figures 4.1 and 4.2. Before placing the tiles, tiles were soaked in water for ten minutes for the saturation purpose to avoid the absorption of water from the concrete. Concrete with high workability was used to spread well between the tiles and reinforcement. Manual compaction method was used because the tiles might be broken by the poker vibrator. The casted slab models are shown in Figure 5.

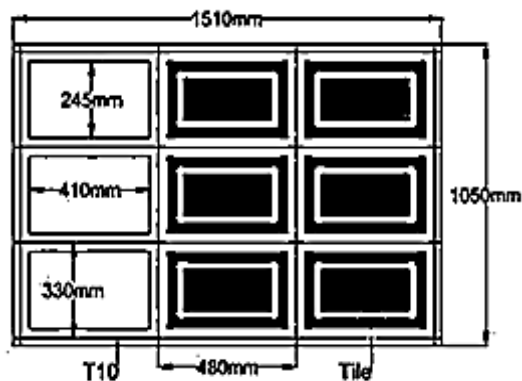


Figure 4.1 - Details of filler slab for Series one experiment

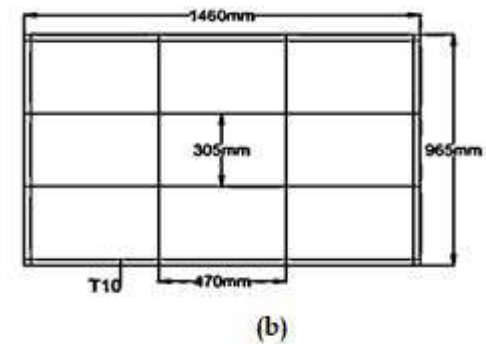
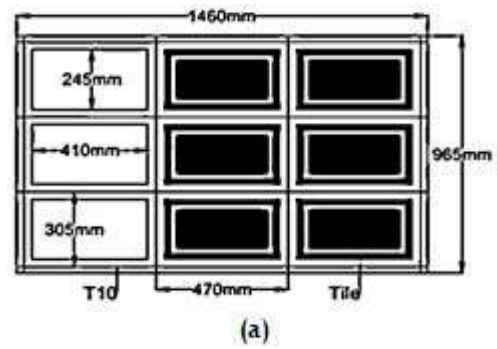


Figure 4.2 - Details of filler slab (a) and RC solid slab (b) for Series two experiment

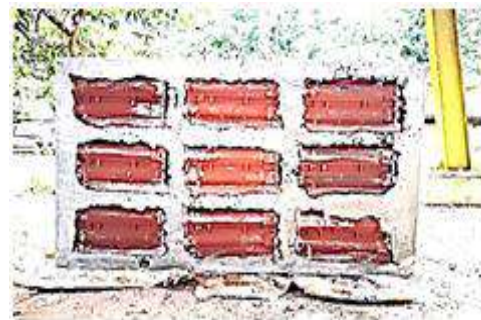


Figure 5 - Casted filler slab (a) and RC solid slab (b)

4.3 Testing arrangement

The RC solid slab and filler slab were tested after 28 days, after ensuring the control cube samples have achieved the desired compressive strength value (Average cubes strength of series one experiment & series two experiment are 21.2 MPa & 26.38 MPa respectively). The slab was simply supported at two edges and



subjected to an increasing concentrated load for punching shear model and distributed load for flexure model at middle. The increasing point load, distributed load was applied with the help of a hydraulic jack to the punching shear model and flexure model respectively.

A proving ring was used in the loading arrangement to measure the applied loads. Dial gauges were fixed at the edge span of the slab for punching shear model and fixed at three points (middle and two edges) of the slab for flexure model as shown in Figure 6, to measure the deflection. The applied load and the corresponding deflections were recorded.



(a)



(b)

Figure 6 - Testing Arrangement for Series one experiment (a) and Series two experiment (b)

4.4 Test results

The effective length between the supports was 865 mm and 1420 mm for punching shear model and flexure model, respectively. The crack was observed at bottom of the middle span of the slab first and propagates diagonally for punching shear model and bottom of the middle span of the slab for flexure model as shown in figures 7.1 and 7.2 respectively. The failure load was considered as ultimate load. Then the serviceability load and the corresponding deflection were determined from Figures 8.1, 8.2 and ensured that the deflection was within the allowable limit.



(a)

(b)

Figure 7.1 - Observed crack pattern of filler slab (a) and RC solid slab (b) for Series one experiment



(c)

(d)

Figure 7.2 - Observed crack pattern of filler slab (c) and RC solid slab (d) for Series two experiment

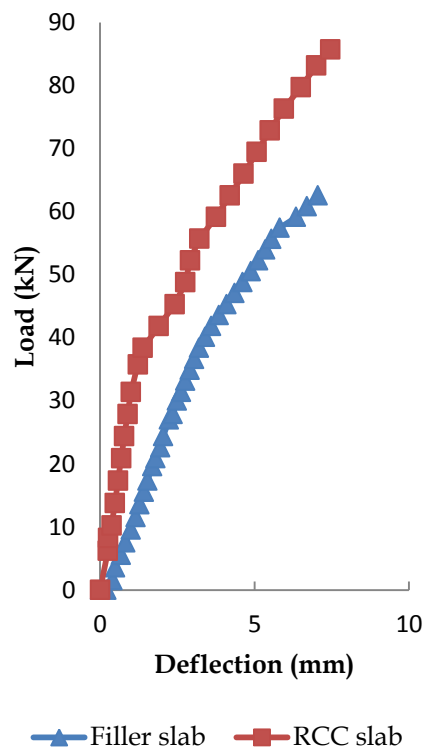


Figure 8.1 - Load Vs Deflection graph for Series one experiment

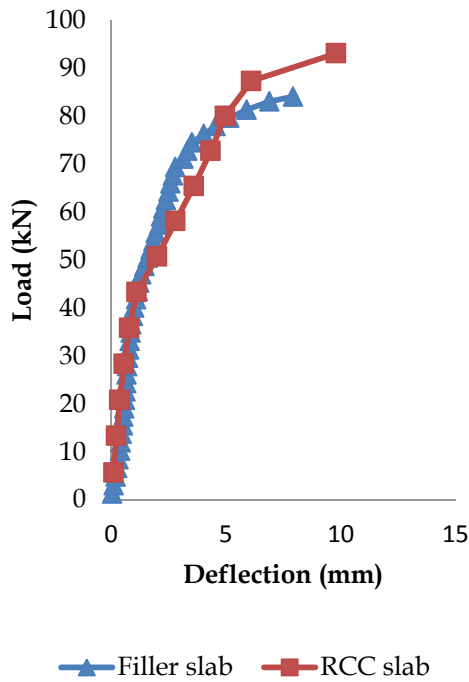


Figure 8.2 - Load Vs Deflection graph for Series two experiment

5. Cost comparison

Both filler slab and RC solid slab of punching shear model was considered for this calculation. Table 1 describes the cost of two types of slabs.

Table 1 - Cost comparison between filler slab and reinforced concrete slab

Slab type	Material	Unit cost (Rs)	Quantity	Total cost (Rs)
Filler slab	Concrete (m ³)	14000	0.11 m ³	2952
	Steel (kg)	120	5.77 kg	
	Calicut tile (one tile)	40	18	
RC solid slab	Concrete (m ³)	14000	0.20 m ³	3492
	Steel (kg)	120	5.77 kg	

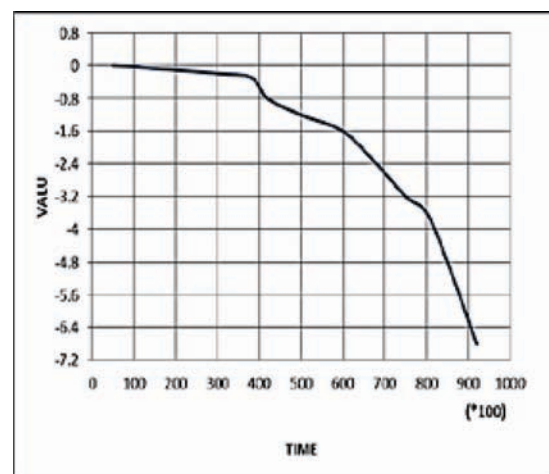
Above total cost was calculated for 1460mm * 965mm slab panel of the casted filler slab and the unit cost of the materials were as of December 2016 ([8], [9]). Cost of the filler material was not considered because unwanted materials with low cost or no cost can be used. According to the table 1, 16% cost can be saved by using filler slab as an alternative.

6. Construction difficulties and feasibility of filler slab

During the casting of the filler slab, manual compaction method was used. Because poker vibrator might break and disturb the alignment of the filler material. In big projects, using manual compaction method is not possible. So, using self-compacting concrete may be a solution to overcome from this issue. High workable concrete for the filler slab was used due to the adequate spreading of concrete between the calicut tiles. Super plasticizers can be used to overcome this problem. Time consumption for the filler slab casting is higher than the reinforced concrete solid slab casting due to time taken for calicut tile laying. It is possible to reduce the time consumption by regular practice in filler slab construction.

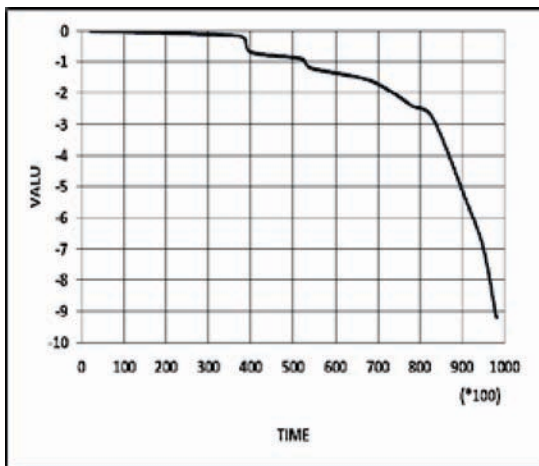
7. Finite element modelling (FEM)

ANSYS 12.1 software was used to analyse the results of load, deflection and crack pattern of both filler and RC slab, whether it is similar to the results of Series two experiment model or not. For concrete and Calicut tiles, solid 65 element and for reinforcement bars link 8 element was used. Loading setup, properties of the materials and boundary conditions were same as from experimental study. Non-linear analysis was done to this model. Load also applied as step by step by using load step option 9 ([1]). Results from ANSYS software are shown in Figures 9 & 10. From ANSYS software analysis, RC solid slab failed at ultimate load of 98.56kN with 9.2mm maximum deflection and filler solid slab failed at 92.51kN ultimate load with 6.9mm maximum deflection.



(a)

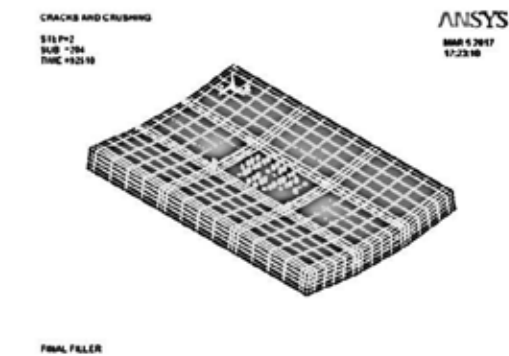




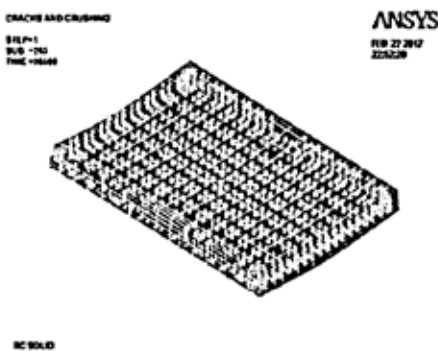
(b)

Figure 9 - Load Vs deflection of filler slab (a) and the RC solid slab (b) for Series two experiment

In above graphs, 'VALU' represents the deflection in millimetres and 'TIME' represents the load in newtons.



(a)



(b)

Figure 10 - Crack pattern of filler slab (a) and the RCC solid slab (b) for Series two experiment

8. Theoretical, experimental and FEM results comparison

Theoretical, experimental and FEM results of Series one and two experiments were compared and checked. Comparison of the results are given in Tables 2 and 3 for Series one and Series two, respectively.

Table 2 - Theoretical and experimental results of moment capacity, deflection, shear for Series one experiment

Analysis	Experimental	Theoretical	
		Solid slab approach	Flange beam approach
Flexural failure load of filler slab (kN)	52.23	40.29	39.99
Flexural failure load of RCC solid slab (kN)	62.56	39.29	38.99
Shear resistance of filler slab (kN)	-	77.9	118.8
Shear resistance of RCC solid slab (kN)	-	76.9	76.9
Deflection of filler slab (mm)	7.05	Actual deflection < Allowable deflection	
Deflection of RCC solid slab (mm)	7.45	Actual deflection < Allowable deflection	

In Series one experiment, experimental flexural failure load of filler slab and RC solid slab are higher than the theoretical value. Reason behind the different values of theoretical and experimental is yield stress of the steel may be increased after the strain hardening. And the flange beam approach shear resistance of the filler slab is higher than the solid beam approach. But the filler slab was considered as set of flange beam is an effective way to analyse. Reason is the reduction in shear area of concrete is considered in this method when analysing for shear stress. Both slabs failed under flexure during the experiment, so that no values in experimental values for shear for Series one experiment. Both experimental and theoretical deflections are in allowable limit.

Table 3 – Theoretical, Experimental and FEM results of moment capacity, deflection, shear and punching shear for series two experiment

Analysis	Experimental	Theoretical		FEM
		Solid slab approach	Flange beam approach	
Flexural failure load of filler slab (kN)	47.04	47.89	48.59	-
Flexural failure load of RCC solid slab (kN)	43.4	46.89	47.59	-
Shear resistance of filler slab (kN)	-	70.5	116.1	-
Shear resistance of RCC solid slab (kN)	-	69.5	69.5	-
Deflection of filler slab (mm)	7.8	Actual deflection < Allowable deflection		6.9
Deflection of RCC solid slab (mm)	9.8	Actual deflection < Allowable deflection		9.2
Punching shear failure load of filler slab (kN)	84.15	41.6 (ACI)		92.51
		68.6 (BS EN 1992)		
Punching shear failure load of RCC slab (kN)	93.2	40.6 (ACI)		98.56
		67.6 (BS EN 1992)		

In Series two experiment, experimental flexural failure load values of both slabs are nearly same as theoretical values. Flange beam approach shear resistance values are higher than the solid approach shear resistance like Series one experiment. Here also, shear failure was not noticed during the experiment. Deflection of

the experimental and theoretical of both slabs are in safe limit and FEM final deflection at failure also approximately same as experimental values. Theoretical punching shear capacity from two different codes (ACI and BS EN 1992) is lower than the experimental values.

9. Yield line Analysis

Main concept behind the upper bound theory is actual collapse load is less than or equal to mechanism load. And also, yield line patterns also can be checked for each boundary and load condition. Yield line analysis was carried out for the punching shear model. For the moment capacity, core cutter test and tensile strength of the steel were measured. The results of the yield line analysis are given in Table 4,

Table 4 - Results of yield line analysis

	Failure mechanism load (kN)	Actual collapse load (kN)
RC slab	102.1	93.2
Filler slab	86.34	84.15

Failure mechanism load > Collapse load (Yield line analysis is satisfied)

10. Conclusions

In the present study only a limited numbers of model slabs were tested in the laboratory. However they revealed both solid slab approach and flange beam approach can be used safely to design filler slabs. In Series one, flexural failures were observed and in Series two, post flexural punching shear failures were observed. For punching shear capacity the prediction from ACI and BS EN are conservative. However use of upper bound yield line analysis gave reasonably close predictions.

In the present study even under patch load post flexural punching shear failures have happened. Mix design and use of compaction need extra care with filler slab approach. Also filler slab construction needs more labour contribution compared to RC solid slab approach. Hence it is recommended to study the whole life cost analysis for filler slab incorporating the thermal, acoustic advantages too.



References

1. ANSYS Theory reference. ANSYS, Inc. *Southpointe, 275 Technology Drive, Canonsbury, 1999.*
2. British Standard Institution. *BS 8110: part 1: Structural use of design and construction, 1985,28-30 p.*
3. American concrete Institute. *ACI 318: Building Code Requirements for Reinforced Concrete, 1995, 169-176 p.*
4. British Standard Institution *Euro code 2: Design of concrete structures - Part 1-1: General rules and rules for buildings, 2004, 97-106 p.*
5. Ayush, S., Cost Effective and Innovative Housing Technology. *International Journal for Scientific Research & Development, Vol. 2, 2014, pp. 27-29.*
6. Harrison, S. W. & Sinha, B. P. A study of alternative building materials and technologies for housing in Bangalore, India. *Construction and building materials, Vol. 9, No. 4, 1995,pp. 211-217.*
7. Jaisingh, M.P, Jaisingh, L. & Singh, B., n.d. "A RC filler slab with non-autoclaved cellular concrete". *Central building research institute, Rotterdam, 1998.*
8. <http://www.siamcitycement.com/>, Visited 10th December 2016
9. <http://www.ceylonsteel.com/>, Visited 10th December 2016

Energy Dissipater for Post-Tensioned Steel Frame System

W.D.C.R. Wanniarachchi, K.L.P.S. Perera and P. Thammarak

Abstract: Following the Northridge earthquake in 1994, connection failures were found in steel moment resisting structures with welded connections. Brittle fractures initiated within the connections at a low level of plastic demand lead to the development of improved welded connections focusing on the rotational ductile capacity. However, due to the limitation of these connections, steel moment-resisting frames(MRF) with post-tensioned(PT) strands running parallel to the beam, which is capable of providing adequate stiffness, ductility and strength during a seismic event are introduced. In this paper, Compression Free Device (CFD), a more advanced alternative to the top and seat angle and friction damper is introduced as the energy dissipating device for the PT MRFs. The CFD device with two major components, sacrificial steel rod and grip is designed with the mechanism of dissipating energy only in tension yielding and free movement during compression to prevent buckling of the steel rod. In this study, detailed shell models of PT beam-column connection, PT connection with CFD and welded moment resisting connection are developed and analysed under cyclic loading using a commercial software and further development of the model to be done using an advanced finite element analysis software. The model, Beam-Column cruciform assembly with two sets of CFDs which is modelled using multi-linear plastic link elements, fixed on each face of the column flange is analysed by performing the nonlinear-dynamic (Non-Linear Time History Analysis) and non-linear static (pushover) analyses to compare the behaviour of three models on the basis of energy dissipation, displacement and hysteresis. Time history analysis results indicate that the PT connection with CFD exceeds the seismic performance of a welded moment-resisting connection subjected to the same earthquake. Efficacy of the device in dissipating energy and ease of repairing and replacement after an earthquake provides pronounced viability for seismic events.

Keywords: Post-Tensioned, Self-Centering Moment-Resisting Frames, Shell Modelling, Energy Dissipaters, Welded Connections, Finite Element Modelling

1. Introduction

The sudden release of energy during an earthquake due to the sudden rupture of the fault within Earth's crust causes seismic waves, low-frequency sound wave to propagate through the Earth's crust or along its surface. This phenomenon of seismic waves reaching the Earth's surface is the main reason for the ground to vibrate at certain frequencies. When the structure and ground share the structure's natural frequency (resonance), it amplifies the effects of an earthquake, causing buildings to suffer more damage. Steel MRFs are designed to resist earthquakes while the building should accommodate extensive yielding and plastic deformations and dissipate large seismic energy. Taking advantage of the ductility of steel material, steel buildings are expected to provide adequate ductility—the ability to withstand large inelastic deformations without significant strength degradation and without the development of collapse and instability [1].

“Prior to the major earthquake of Northridge, welded-flange-bolted-web connections were

considered the most seismic resistant detail of any beam-column connection based on experimental work since it can withstand high plastic rotation” [2], [3]. The top and bottom flanges of the beam are welded directly to the column by full penetration groove welds to transfer moment. The beam web is bolted or welded to a shear plate, which is attached to the column by welding to transfer shear [2].

However, 1994 Northridge earthquake caused unprecedented damage to conventional welded beam-to-column connections in steel MRFs. Many brittle failures were reported. A common failure pattern of beam-to column joints is cracking of the bottom beam flange to column weld. The main causes of this type of failure are weld defects at the root of the weld (downward welding) and high stresses at the exterior of the beam flange.

Eng. Ms. W.D.C.R Wanniarachchi, B.Sc.Eng. Hons. (AIT), Civil Engineer (Structural), MAGA Engineering (pvt) Ltd.

Eng. K.L.P.S Perera, B.Sc. Eng. Hons. (AIT), Assistant Lecturer, Department of Civil Engineering, SLIIT.

Dr. P. Thammarak, Ph.D.(Texas) Senior Lecturer, Dept. of Structural Engineering, AIT.



In most of the tested 'pre-Northridge' joint typologies were observed reduced values of beam plastic rotation (<0.01 rad). Connection failure should be avoided before the member failure because as found in Northridge earthquake the connection failure is not ductile as that of steel member failure.

After evaluation of Northridge earthquake, many efforts have been made find suitable solutions for observed damage in pre-Northridge steel beam-column connections and to improve steel MRFs. Improved welded unreinforced flange connection, Reduced beam section connection, Connection with welded haunches: top and bottom haunch and bottom haunch were few suggestions. Nonetheless, earthquake-induced damage in steel MRFs is still inevitable under moderate-to-severe earthquakes. The repair of damaged buildings with high residual deformations may not be economically feasible; thus, demolishing may be necessary for such intensively damaged buildings.

1.1 PT steel beam-column connection

As an alternative to the welded connections, researchers came up with the idea of using self-centring systems to avoid structural failures and performance weaknesses resulting from local residual drift at connection level and global residual drift at the structural level. Self-centring behaviour was characterised by nearly zero residual deformation at the end of the cyclic loading tests, in which the system also dissipate the energy. The only type of behaviour which ensured these two abilities was the flag-shaped hysteresis behaviour. Two main self-centring strategies have been proposed by researchers: using shape memory alloys (SMAs) or using post-tensioning forces. In the strategy of using post-tensioning force, the technique used to recover the inelastic deformations induced on the structure is pre-stressing the structure before imposing loads. This is considered a very reliable method to pull the structure back to its original position after a seismic event.

A PT connection consists of two main components; post-tensioned strands which provide the self-centering capacity and energy dissipation devices installed in the connection to dissipate energy.

The connection utilizes high strength post-tensioned strands which pass through the frame columns and run parallel to the beam web along the span are anchored against the

column flange. In each connection, either yield-based or friction-based energy dissipation devices are installed.

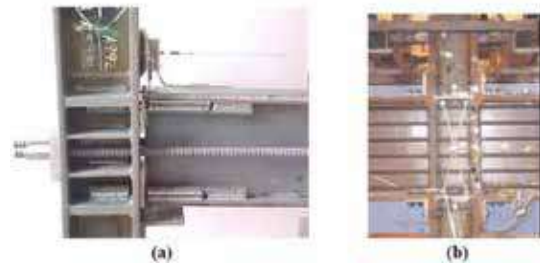


Figure 1 - PT steel connection (a) Energy dissipating bars [4] (b) Top & seat angles [5]

Beam depth, the PT force, strength and the elastic stiffness of the PT strands are the properties affecting the flexural behavior of a post-tensioned connection. There will not be any damage to the beam and beam will not yield significantly till the PT strands remain elastic.

Researchers have proposed several types of energy dissipating devices for post-tensioned connections, such as replaceable energy dissipating bars, top and seat angle and friction dampers. Post-tensioned connections were characterized by their flag-shaped hysteresis behavior and behaved in a similar manner regardless of the energy dissipating device installed in the connection [4]. But discrepancies in the hysteresis behavior, the resistance of the shear force and bending moment depended on the type of the energy dissipater.

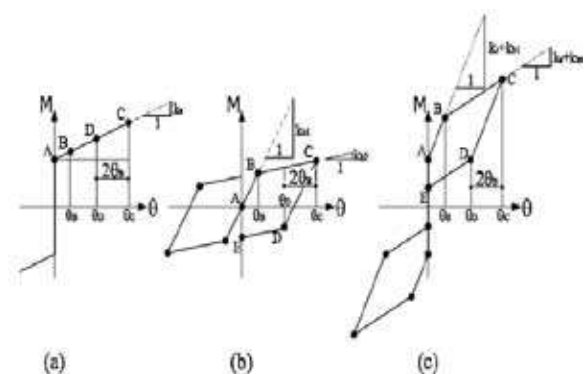


Figure 2 - Hysteretic behavior of PT connection with replaceable energy dissipating bars

As illustrated in Figure 2, the PT connection initially behaved as a fully rigid welded connection experiencing no relative rotation between the beam and the column when the applied moment was less than the moment provided by the PT strands. A gap started

opening between the beam and the column when the applied moment is more than the PT strands moment. Energy dissipating device starts contributing to the system at this instant to resist the moment of the connection.

1.2 Energy dissipaters for PT steel frames

1.2.1 Energy Dissipating Bars

In the PT connection with energy dissipating bars, replaceable steel bars were installed in the connection. In order to avoid buckling energy dissipating bars were confined with steel cylinders [6]. These bars start to elongate and yield when the gap opens. Post-tensioned strand and the energy dissipating bars provide the resistance to the bending moment [4]. Even though shear resistance was provided by friction at the intersection of the beam and column flange, it dropped substantially upon gap opening. Energy dissipating bars contributed to the moment resisting in two stages; first stiffness prior to yielding and second stiffness in the post yielding stage.

1.2.2 Top and Seat Angles

When the gap starts to open, top and seat angles formed plastic hinges at the top and bottom [7]. Since three plastic hinges are formed during the decompression and gap opening of the connection, the hysteretic behavior took a curved shape.

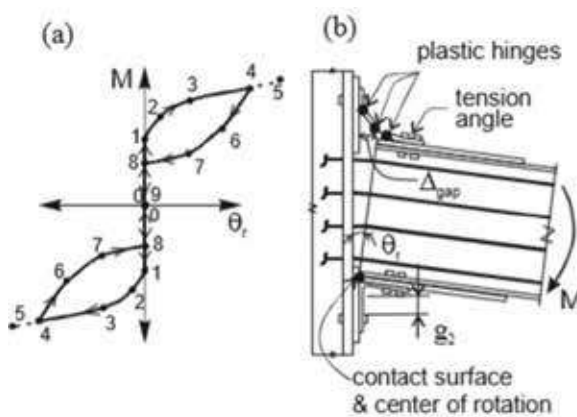


Figure 3 - PT connection with seat angles as energy dissipaters (a) Moment-rotation behavior (b) Configuration [5]

1.2.3 PT Connections with Friction Damper

Even though both yield based energy dissipaters, energy dissipating bars and seat angles have high reliability and energy dissipating capacity, they were required to be replaced after the seismic event due to plastic

deformations. Hence, more durable energy dissipater based on friction was proposed [8].

PT strands and the friction forces in the friction device provided the moment resistance of the connection. If the friction device is installed at the beam web, it is used to provide shear resistance when the gap opens, and the contact area between the beam and the column flange is reduced.

1.3 Compression free energy dissipater (CFD CAM-GRIP device)

In this research CFD device, passive energy dissipating device which increases the energy dissipating capacity and reduces the seismic demand on the structure will be used [9].

As illustrated in Figure 4, the device consists of 2 main parts, one is a sacrificial member, and the other one is grips. When the load is applied on the specimen (or building) the sacrificial member (or steel core) will be in tension, thus, the grips will generate a force to hold the steel core, allow it to yield, then energy is dissipated. Reversely, when the load is removed, the steel core will be in compression but two grips will open up, allow steel core to freely slide in, so no compression force is taken by steel core. The main advantage of CGDD is it will allow the steel core to get rid of compression and its buckling. External installation of the device will provide the ease of repairing or replacement once it's damaged after cycles of loading. The zero internal force is expected in steel coupon when it moves towards the compression free device and energy will only loss in tension yielding. The downward displacement of the steel rod is resisted by inclined forces produced by two cams.

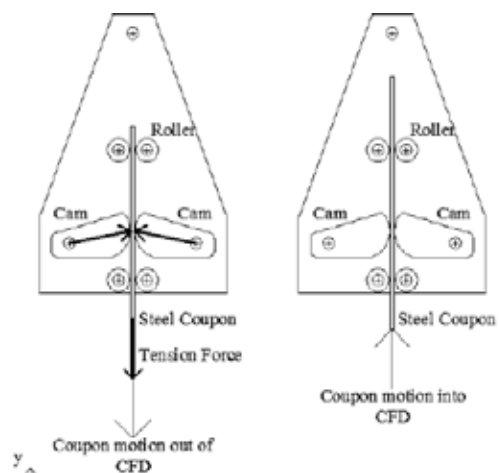


Figure 4 - Cam-Grip device with steel coupon under motion towards CFD and away from CFD



2. Methodology

In order to investigate the behavior of steel frames with PT connection when subjected to a ground motion, Ricles [10] designed a six-story six bay moment-resisting frame using DRAIN-2DX. In Ricles research, the structure was assumed to be an office building situated in seismic design category D. Hence seismic hazard exposure Group III is assumed. In this research cross-section of beam and column was based on the Ricles [10] research paper which focuses on the comparison of the post-tensioned moment-resisting frame with pre-Northridge welded beam-column connection.

A36 and A572 Gr.50 steel were used for the designing of the beams and columns, and the floor dead load of 4.79 kPa, live load of 2.40 kPa are considered.

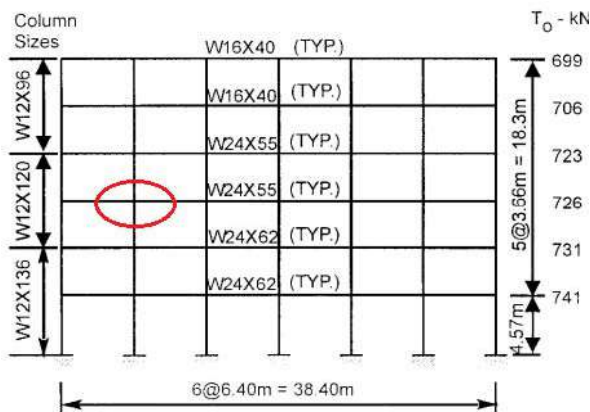


Figure 5 - Selected sub-assembly in elevation of Prototype Six-Story, Six-Bay MRF [10]

Each PT connection had four levels of strands, with two strands, one on each side of the beam web, in each level. A post-tensioned strand designed in this research had an area of 140 mm², a Young's modulus of 200 GPa, and an ultimate strength of 1,860 MPa. Post-tensioning force of 729 kN was used.

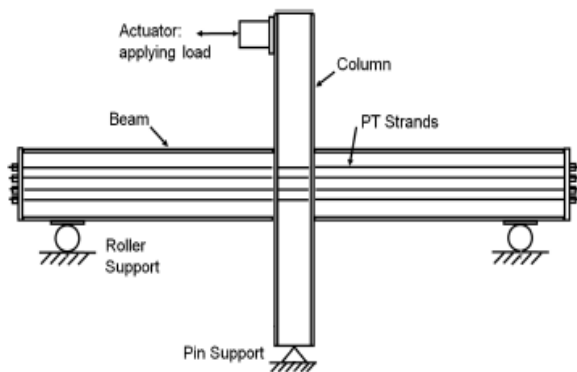


Figure 6 - Schematic of a PT connection

2.1 Mesh Design & Modelling

Even though discrete spring model, integrated single rotational spring model were considered as modelling techniques for this research, due to technical difficulties and complicated calculations combination of the discrete spring model and shell modelling approach is adopted to model the welded beam-column connection and the post-tensioned beam-column connection with Cam-Grip energy dissipating device.

In the welded beam-column model, effect of welding was considered by constraining all degrees of freedom in the beam-column interface. The gap opening behaviour of the post-tensioned beam-column connection is modelled by non-linear link element with one degree of freedom, axial. Self-centring mechanism of high axial stiffness in compression and zero stiffness in tension is illustrated by link element in the software.

Four post-tensioned strands running parallel to the beam web were designed using the cable element. The cable elements were modelled without being bound to the beam web shell elements to simulate their external placement. Each strand had an area of 280 mm², since the referred 3D model had 8 post-tensioning strands, each strand having an area of 140 mm². The material A416Gr270 is assigned for the defined cable element. Post-tensioning force of 729 kN is allocated per a cable element.

Multi-linear plastic link was used for modelling of the compression free energy dissipating device (CFD). The properties of the link were calculated by a manual method using A36 steel as the material of the steel coupon and calculating the force - displacement behaviour of the link element with it having negligible stiffness in compression. Gripping device which used to fix the CFD to the beam flange is depicted by a stiffened steel shell section.

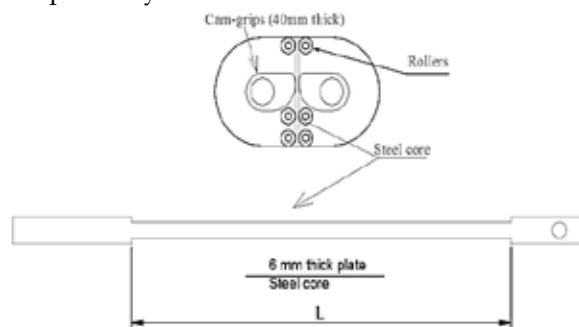


Figure 7 - Cross section of the CFD

2.2 Analysis of the models

The behavior of the post-tensioned beam-column test assembly, PT beam-column with compression free energy dissipating device model and conventional welded moment-resisting connection having the same geometry and element properties were compared with each other. The comparison was based on the data obtained from the non-linear static analysis (Pushover) and non-linear dynamic analysis. Displacement, residual drift and energy dissipating capacity were characteristics observed for the comparison.

Time history analysis was done for nonlinear evaluation of dynamic structural response under loading. The lateral loads will be provided as a time history loading of a selected earthquake. According to the code ASCE/SEI 7-10 [11], minimum 3 time history analysis are to be selected. Hence following seismic events were selected from the Pacific Earthquake Engineering Research (PEER) database;

- Northridge (LA28) (PGA: 1.33g, M: 6.69)
- Loma Prieta (LA21) (PGA: 0.472g, M: 6.93)
- Kobe (LA24) (PGA: 1.282g, M: 6.9)

The design response spectrum was constructed and the selected time histories were converted into the response spectrum using the PRISM software. The scaled time histories were converted from the response spectra and applied to the model, which was analyzed to obtain the maximum results. Pushover analysis will be done by giving displacement controlled force at the top in the both direction.

3. Results & Discussion

In this chapter the results obtained from the Nonlinear Static Pushover analysis and Nonlinear Time History Analyses of the three tested models are depicted and the results are analyzed to compare the differences between the three systems to evaluate their benefits and disadvantages.

3.1 Performance of PT connection with CFD

Evaluation of the analysis results of each system was verified with the predicted behavior of each system from the literature review. The gap-opening behavior (Figure 8) at the connection and the energy dissipation through yielding of the CFDs were clearly observed in the outputs.

Results obtained from the Non-Linear Time History Analyses were taken for the drifts, base shears and energy plots. The following figures depicts the results of the system using the CFD under Northridge EQ loading.

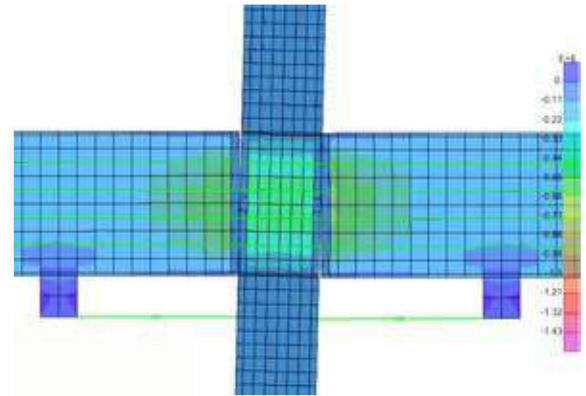


Figure 8 - Gap opening behavior of the PT connection with CFD

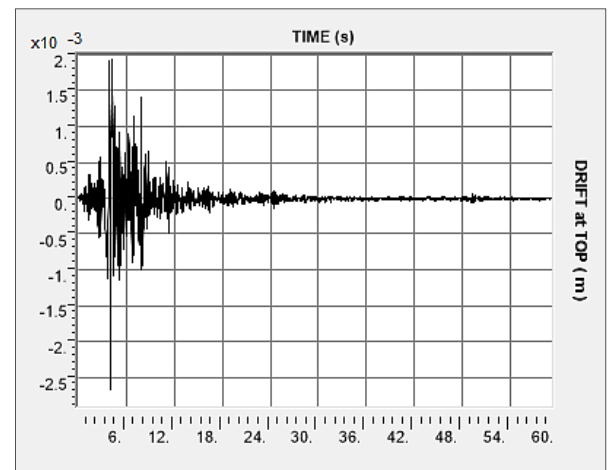


Figure 9 - Drift (m) vs time (s) for LA28 (Northridge)

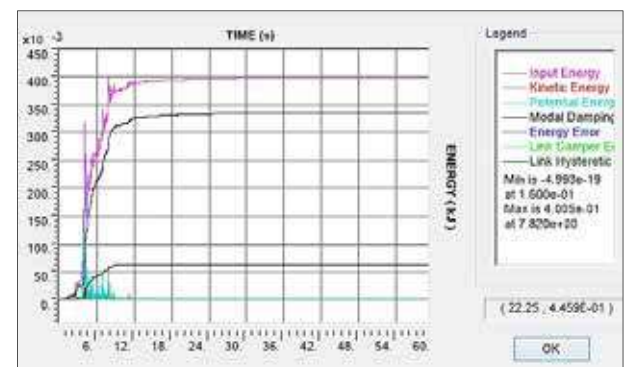


Figure 10 - Energy Plots for LA28 (Northridge) [Energy in kJ vs. time (s)]

From Figure 10 it can be observed that the CFD does manage to dissipate some of the input energy from the ground motion and reduces the modal damping of the structure. In



addition, the hysteresis of the CFD can be observed in Figure 11.

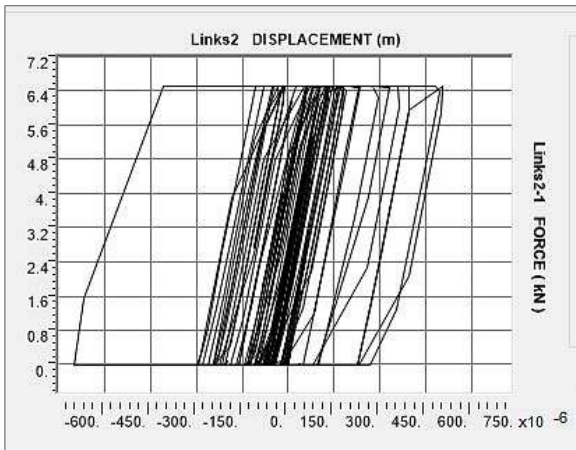


Figure 11 - Force (kN) vs displacement (m) Plots for LA28 (Northridge) for CFD

Table 1 shows the energy components into which the input energy was converted to. The Link Hysteretic column indicates the energy dissipated through the yielding of the CFD.

The energy dissipation through the CFDs was observed to be plateauing at a certain value as observed in Figure 10 indicating that after a certain point, the energy dissipation through the CFDs did not occur. This can be attributed to the resulting significant drift occurring at the plateauing time as seen in Figure 9. This large motion yields the CFD significantly and dissipates energy but afterwards the CFD will not be effective for further smaller movements since it has yielded. This is in comparison to a typical damper, which will provide continuous damping. This is observed as a downside to the CFD system.

Table 1 - Comparison of Energy (kJ)

Output Case	Input	Kinetic	Potential	Modal Damp	Link Hystrtc
LA21	0.2043	0.0329	0.1247	0.1646	0.0392
LA28	0.4005	0.0905	0.2274	0.3365	0.0623
LA24	0.1431	0.0264	0.0376	0.115	0.0194

3.2 Performance of PT connection for NSP

Upon the evaluation of the behaviour of the structure during the non-linear static pushover, the obtained force-displacement behaviour is shown in figure 12. The re-centring behaviour at low drifts and the energy dissipation occurring due to the yielding of the CFD can be seen.

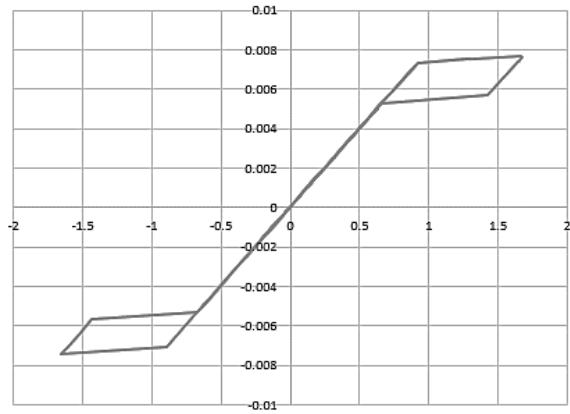


Figure 12 - Force (kN) vs displacement (m) behaviour for NSP

3.3 Comparison of PT system with/without CFD

Input energy, kinetic energy, potential energy, modal damping of PT connection with CFD device is compared with results of the post-tensioned connection without energy dissipating device. Below figures depict the comparison of the results for the three seismic events.

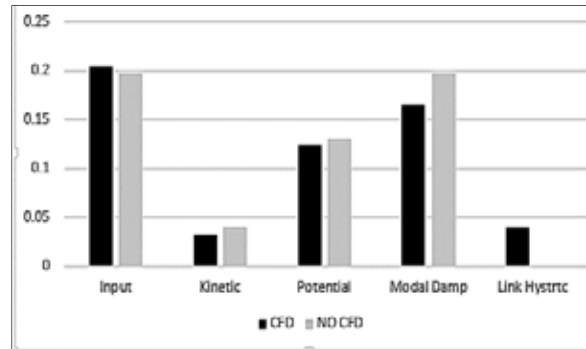


Figure 13 - Energy (kJ) components for Kobe (LA21)

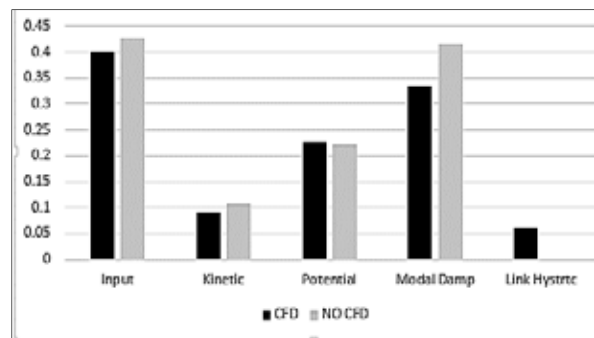


Figure 14 - Energy (kJ) components for Northridge (LA28)

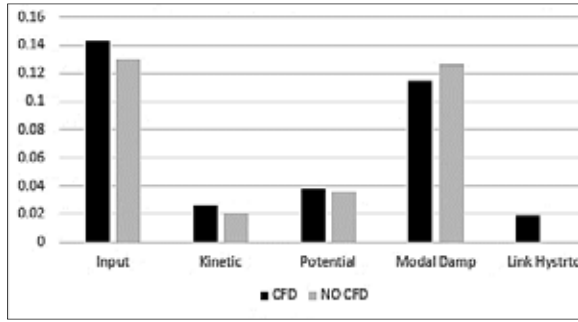


Figure 15 - Energy (kJ) components for Loma Prieta (LA24)

After evaluating the figures 13,14 and 15 it is observed that when the CFD is introduced there is over a 20 percent decrease in the modal energy component showing that the energy dissipation through modal damping is less for PT connection with CFD device for all three ground motions. This prevents the permanent damage to the structure and make the structure more stable after the earthquake. Also the kinetic energy can be observed to have decreased with the addition of the CFDs as shown in Figures 13 and 14 meaning less movement of the structure. Link hysteretic illustrate the energy dissipating capacity of the CFD.

3.4 Performance of Welded Frame Connection

Non-linear dynamic time history analysis was performed for the conventional welded beam-column subassembly to evaluate the behaviour of the connection under the three ground motions. An example of the largely modal damping occurring in welded connections can be observed in the energy plots where almost all the energy is dissipated through modal damping as in Figure 16 and Table 2.

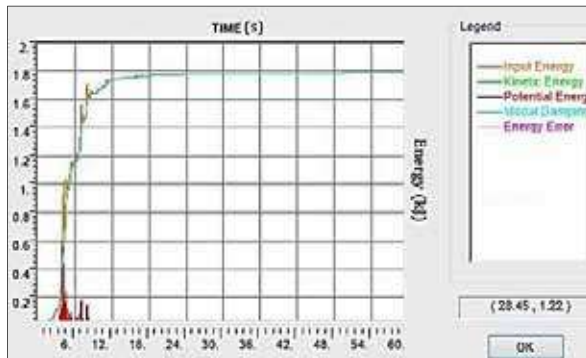


Figure 16 - Energy plot for Northridge (LA28) (Energy in kJ vs. time (s))

Table 2 - Comparison of Energy (kJ) in Welded Frame

Output Case	Input	Kinetic	Potential	Modal Damp
LA21	0.7603	0.0827	0.3518	0.7603
LA28	1.7843	0.2611	0.5524	1.7843
LA24	0.3723	0.0481	0.0724	0.3656

For the Non-Linear Static Pushover test it was observed the expected behaviour of a welded frame connection with the hysteretic behaviour of the connection showing the yielding of the connection as seen in Figure 17. This shows that the energy dissipation occurs throughout the range of motion and that upon force removal the residual deformations will be present, as the plot does not pass through the origin as seen in Figure 12 for the PT frame.

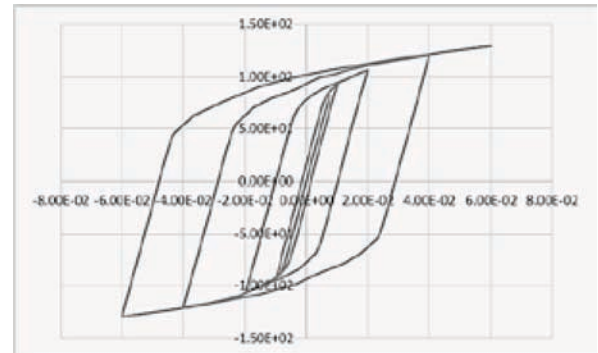


Figure 17 - Force (kN) vs displacement (m) plot

4. Conclusion & Recommendation

Post-tensioned steel connection with Cam-Grip device offers seismic response that is superior to the seismic response of the conventional moment resisting welded connection in terms of reducing the residual displacements and damage in the beam elements but not in the amount of energy dissipation. Conventional welded connection can dissipate significantly higher energy in the early stages of the earthquake which results in damping of the response in the later stages. The dissipated energy in welded connection however is a result of the permanent damage in the frame elements (plastic hinges). In passive PT connection with CFD acceptable levels of response (deformations) can be achieved without severe damage (without plastic hinges).

Seismic response of passive post-tensioned steel frames is heavily dependent on the connection



parameters F_{pt} (post-tensioning force) and β (energy dissipation factor). When these parameters are selected correctly, post-tensioned steel frames exhibit very good dynamic behaviour under seismic actions. It is expected that increasing the initial post-tensioning force in the connection would result in lower energy dissipating capability for the same loading and performance level. In further research this should be considered and should run the analysis using different post-tensioning forces.

Further advanced research should focus on the energy dissipating behaviour of the compression free device (CFD) relative to the existing energy dissipation devices discussed in the literature review. The energy dissipating factor (β) which is the ratio of moment provided by energy dissipation device installed in the connection and moment provided by PT strands before gap opening, should be calculated and compared, since it has a high influence on ductility, moment capacity, energy dissipating capacity and self-centring properties of the post-tensioned connection.

Due to certain limitations, only 2D beam-column subassembly was modelled and analysed to evaluate the seismic performance. To develop this research further, it's quite important to consider an entire structure. Three-dimensional 6 storey frame would be an ideal model for analysis of the PT steel moment-resisting frame since they are proposed as a replacement of conventional MRFs, which are usually designed for low to medium high structures. CFD device installed in the post-tensioned steel MRF model will provide a broader idea of the energy dissipating capacity of the CFD and it would also help to determine the optimum connection location to place the CFD. This determination is quite important since it would be cost effective and more practical than installing the CFD at each joint.

The experimental study should be conducted on this topic and compare the experimental values with analytical values. The yielding behaviour during tension and the free movement of the CFD during compression and its energy dissipation was successfully observed in the hysteresis diagrams of the CFDs.

Acknowledgement

The authors wish to acknowledge Asian Institute of Technology (AIT) for the guidance

and providing the great opportunity to conduct the research

References

- 1 FEMA 335D, "State of the Art Report on Connection Performance," Program to Reduce the Earthquake Hazards of Steel Moment-Frame Structures, California, 2000.
- 2 Popov, E. P., T.-S. Yang and S.-P. Chang, "Design of steel MRF connections before and after 1994 Northridge earthquake," 1998.
- 3 Popov, E., and Stephen, R., "Cyclic Loading of Full-Size Steel Connections," American Iron and Steel Institute,, Washington, D.C., 1972.
- 4 Christopoulos, C., Filiatrault, A., Uang, C. M., and Folz, B., "Posttensioned energy dissipating connections for moment-resisting," *J. Struct. Eng.*, vol. 9, no. 128, p. 1111-1120, 2002.
- 5 Bruneau, M., "Seismic Retrofit of Steel Structures," Tlaxcala, Mexico, 2004.
- 6 Christopoulos, C., Filiatrault, A., and Folz, B., "Seismic Response of Self-centring Hysteretic SDOF Systems," *Earthquake Engineering and Structural Dynamics*, vol. 5, no. 31, pp. 1131-1150, 2002a.
- 7 Garlock, M., Ricles, J., and Sause, R., "Cyclic load tests and analysis of bolted top-and-seat angle connections.," *J. Struct. Eng.*, vol. 12, no. 129, pp. 1615-1625, 2003.
- 8 Rojas, P., Ricles, J., and Sause, R., "Seismic Performance of Post-tensioned Steel Moment Resisting Frames with Friction Devices," *Journal of Structural Engineering*, vol. 131, no. 4, pp. 529-540, 2005.
- 9 Thammarak, P., Thien, M., Htun, L., and K. M.T, "The Development of a Compression-Free Energy Dissipative Brace," Sydney, Australia , 2015.
- 10 Ricles, J., Sause, R., Garlock, M., and Zhao, C., "Posttensioned seismic-resistant connections for steel frames," *J. Struct. Eng.*, vol. 128, no. 7, pp. 113-121, 2001.
- 11 ASCE/SEI 7-10, Minimum Design Loads for Buildings and other Structures, American Society of Civil Engineering, Structural Engineering Institute, 2010.

Simplified Approach for Predicting Fatigue Life of Fillet Welded Joints with FEM

S. Varakini, K. Ubamanyu and H.M.Y.C. Mallikarachchi

Abstract: Subjected to cyclic loading, many materials fail well below their yield strength due to the phenomenon of fatigue. Stress concentrating factors, such as sharp changes in geometry, are especially conducive for fatigue crack initiation. Owing to the inherently complicated nature of the welding process, a weld presents many such sites favourable for initiation and therefore becomes a point of weakness to the whole structure, especially when subjected to a cyclic loading. However, fatigue testing is expensive and time-consuming, and at the same time, computer simulations comprising of the complex details of the welding process can be computationally expensive when combined with fatigue analysis. In this paper, a simplified fatigue crack simulation technique using a two-dimensional model has been explored. A specimen of fillet welded joint was modelled using the commercial finite element software package Abaqus, and it was analysed under various stress conditions in order to obtain the energy release rate at the crack tip (by the J-integral method) at different crack lengths and thereby predict its fatigue life for each stress level.

Keywords: Fatigue life, crack initiation and propagation, J-integral, fillet weld

1. Introduction

Fatigue is a phenomenon related to fracture that causes the material to fail well below their yield strength when a cyclic load is applied. Fatigue life comprises of three main stages: crack initiation, crack propagation and sudden fracture. The initiation and propagation depend on a number of complex factors such as geometric shape, material properties, exposure conditions, surface condition, loading type and production variables like residual stress. The interconnectivity of these factors is still a topic of extensive research.

1.1 Fatigue in Welded Joints

Welds represent an area of weakness with regards to many of the above-mentioned influences. Sharp changes in geometry at the toe of a fillet weld, residual stresses introduced as a result of the welding process and the change of base metal property in the heat affected zone (HAZ) are of major concern in determining the fatigue performance of welds. Furthermore, workmanship is an important factor in deciding the degree of stress concentrators present in a weld. Otegui, Kerr, Burns, & Mohaupt [1] have identified undercuts, slag inclusions and spatter as the main stress concentrators in welded connections.

In order to incorporate the complex factors involved in welding, 3-dimensional finite element models are generally found to have been used. However, processing such complex models can be time-consuming, especially due to a large number of load cycles involved. This paper investigates the suitability of using a simple 2-dimensional finite element model developed using Abaqus, commercial finite element package.

1.2 Theoretical Background

Total fatigue life can be expressed as follows.

$$N_T = N_i + N_p \quad \dots (1)$$

where N_i , N_p and N_T refers to the number of cycles for crack initiation, propagation and total fatigue life respectively.

One of the most common approaches in determining crack initiation is given by Equation 2 and Tricotiaux, Fardoun, Degallaix, & Sauvage [2] have successfully used it in a local approach to deal with N_i of welded joints.

Eng. (Ms.) S. Varakini, B.Sc. Eng. (Hons.) (Moratuwa), Department of Civil Engineering, University of Moratuwa.

Eng. K. Ubamanyu, B.Sc.Eng.(Hons.) (Moratuwa), AMIE (SL), Department of Civil Engineering, University of Moratuwa.

Eng. (Dr.) H.M.Y.C. Mallikarachchi, C.Eng., MIE(SL), B.Sc.Eng.(Hons.)(Moratuwa), Ph.D.(Cantab), Senior Lecturer, Department of Civil Engineering, University of Moratuwa.



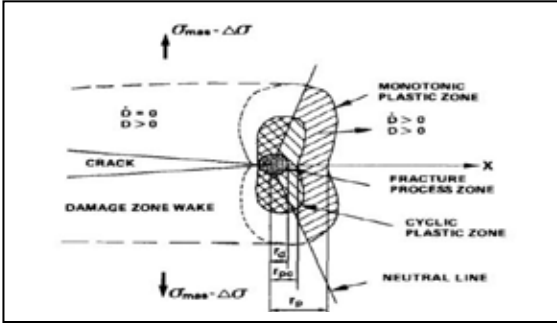


Figure 1 - Crack tip region and the contour used for J-Integral

$$\frac{\Delta\varepsilon}{2} = \frac{\sigma'_f - \sigma_0}{E} (2N_i)^b + \varepsilon'_f (2N_i)^c \quad \dots(2)$$

where $\Delta\varepsilon/2$ is the local total strain amplitude, σ'_f and ε'_f are fatigue strength and ductility coefficients, σ_0 is the initial local mean stress, E is the Young's Modulus and b and c are fatigue strength and ductility exponents.

Another commonly accepted approach for crack initiation period is to assume that a micro crack exists at the location of high-stress concentration and it attains macro crack status when it reaches a depth of 0.3 mm [1]. In this study, this depth is taken as the threshold for crack initiation and the time taken to achieve it is calculated using fracture mechanics models describing micro crack growth up to 0.3 mm.

Linear Elastic Fracture Mechanics (LEFM) cannot be used for the initiation phase since the size of the plastic region surrounding the crack tip is significant at these short crack lengths as illustrated in Figure 1. Effect of plasticity can be addressed by adopting an Elastic Plastic Fracture Mechanics (EPFM) approach. The J-integral based fatigue crack growth rate prediction provides a good approximation of short crack behaviour [3].

Rice [4] initially developed this integral as a path independent approximate method to determine strain concentrations by cracks and notches. A closed contour integral along an arbitrary path around the crack tip is defined as the J-integral, and a formal definition is given by Equation 3.

$$J = \oint [Wn - T_i u_{i,k}] d\Gamma \quad \dots(3)$$

where W is the strain energy density, T_i is traction vector, $u_{i,k}$ is displacement vector, and n is the outward unit normal to the integration path Γ . This could be determined using the contour integral evaluation capabilities

available in finite element software packages. However, it must be noted that the cyclic J-integral ΔJ should be calculated using Equation 4 presented by Ochensberger & Kolednik [5], and it does not denote the range between maximum and minimum values, J_{max} and J_{min} .

$$\Delta J = J_{min} + J_{max} - 2\sqrt{J_{min} \cdot J_{max}} \quad \dots(4)$$

According to the Paris Law [6], crack growth is given by Equation 5 in LEFM. As the effect of the plastic region near the crack tip is of concern in this work, a modification was used. El Haddad, Dowling, Topper, & Smith [7] have shown that the relationship given in Equation 6 gives a good approximation of crack behaviour in this zone for plane stress conditions. This was used to calculate the stress intensity factor ΔK required in the Paris Law relationship.

$$da/dN = C (\Delta K)^m \quad \dots(5)$$

$$\Delta J = (\Delta K)^2/E \quad \dots(6)$$

The number of load cycles (N) for a crack to propagate from an initial crack length a_i to a final length a_f is given by Equation 7.

$$N = \int_{a_i}^{a_f} \frac{da}{C(\Delta K)^m} \quad \dots(7)$$

This paper presents a numerical model that was developed using Abaqus finite element analysis package to determine J-integral. Using Equation 7 the number of cycles required for a micro crack to reach the 0.3 mm threshold depth was determined in an attempt to predict the time taken for fatigue crack initiation.

2. Simulation of Fillet Weld

A 2-dimensional half-model of a fillet weld was created using symmetry boundary conditions along the vertical line of symmetry shown in Figure 2. Ideally, the shape of the weld should correspond to that of the section-cut at the location of minimum toe radius of the weld as this is the critical location for fatigue crack initiation [1]. However, this geometric detail has not been covered in this study. To verify this method, the results from an experimental work carried out by Otegui et al. [1], as illustrated in Figure 2(a) and 2(b) was used. Material properties are listed in Table 1. Residual stress distribution was obtained by a welding process involving a heat input of 2.9×10^6 J/m as used in [1]. The temperature distribution at the end of the welding process.

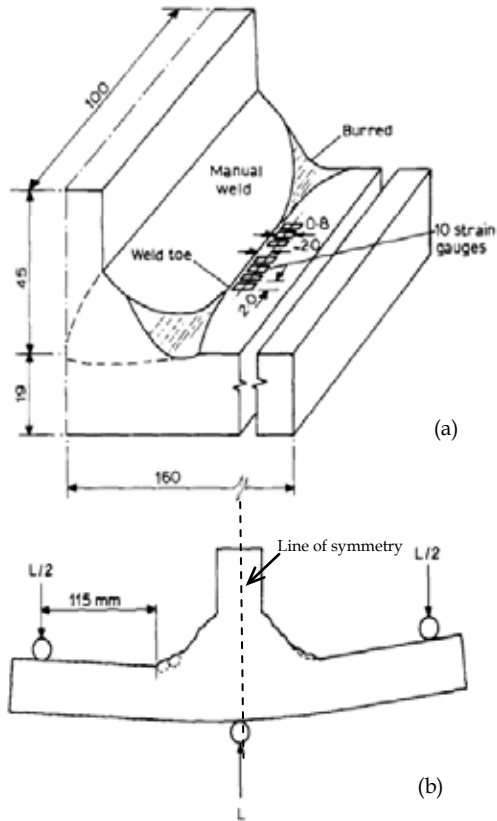


Figure 2 - Fatigue testing by Otegui et al. [1] (a) Geometry of the specimen (b) Experimental set-up (dimensions are in millimetres)

was simulated by means of an uncoupled thermal analysis and this was applied as the initial condition in the successive fatigue analysis.

In the fatigue analysis, the cyclic load was applied at a minimum to maximum load ratio, $R = 0.1$. Using the contour integral nodal enrichment and direct cyclic analysis capability of Abaqus, the J-integral was determined. Ten contour integral were requested, and the stabilized value was taken as the J-integral at that particular load.

A special mesh pattern was used in the crack initiation region to avoid the stress singularity occurring at the crack tip. According to the findings presented in [8] and the recommendations of Abaqus user manual [9], quadrilateral quarter-point elements of type CPS8R belonging to the quadratic order were used to capture the combined effect of $1/\sqrt{r}$ singularity characteristic of the linear elastic

Table 1 - Material Properties of Test Specimen

Property	
Yield Strength (MPa)	421
UTS (MPa)	509
Elongation (%)	53
Young's Modulus (GPa)	210

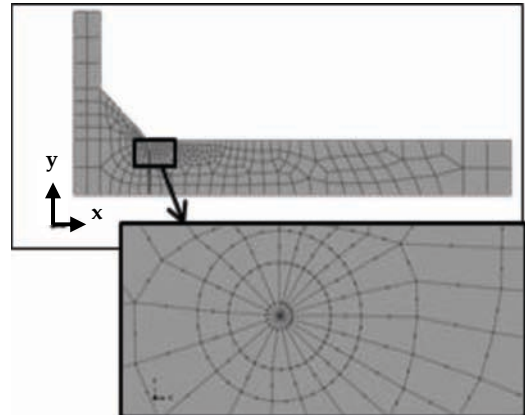


Figure 3 - Meshing scheme used in the numerical model and rosette mesh in the crack tip region

material and $1/r$ singularity of perfectly plastic material. These formed a rosette pattern in the crack tip region, and the rest was meshed using a relatively coarser mesh as shown in Figure 3. Seam cracks were introduced at different depths below 0.3 mm, and the J-integral value was studied. The number of cycles required for crack growth between each depth interval was determined, and the summation was taken as the fatigue crack initiation period, N_i .

To avoid convergence issues, stress was simulated by applying a cyclic displacement at the free end. Stress conditions, similar to that shown in Figure 4, were achieved for each load cycle.

3. Results and Discussion

The J-integral was recorded for each stress amplitude over crack lengths of 0.05 to 0.3 mm, with 0.05 mm increments. J_{min} and J_{max} values were extracted from the J-integral plot produced by Abaqus for each crack length. ΔK was calculated using Equations 4 and 6. The procedure is illustrated for an applied nominal stress amplitude of 190 MPa. The ΔK vs a curve was fitted to a power law relationship as shown in Figure 5. Using experimental data available

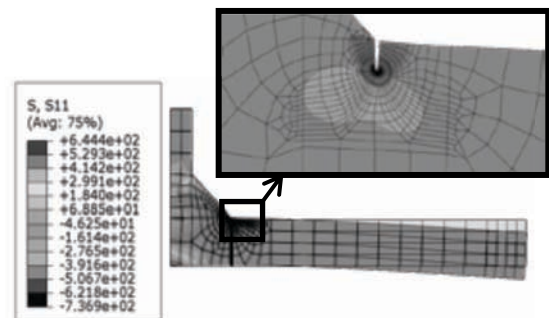


Figure 4 - Stress distribution and stress singularity at the crack tip [1] the values of C and m were determined to be 6×10^{-10} and 8.8071 respectively.

The relationship presented in Figure 5 was applied to the Paris Law and integrated to obtain the number of cycles needed for short crack propagation between each length interval. Results are presented in Table 3 for an applied nominal stress amplitude of 190 MPa.

Table 2 - Calculation of ΔJ and ΔK

a (mm)	J_{min} (W/m ²)	J_{max} (W/m ²)	ΔJ (W/m ²)	ΔK (MPa \sqrt{m})
0.05	0.010	0.058	0.019834	2.04
0.10	0.010	0.066	0.024619	2.27
0.15	0.012	0.077	0.028205	2.43
0.20	0.014	0.087	0.031200	2.56
0.25	0.014	0.090	0.033007	2.63
0.30	0.015	0.095	0.034502	2.69

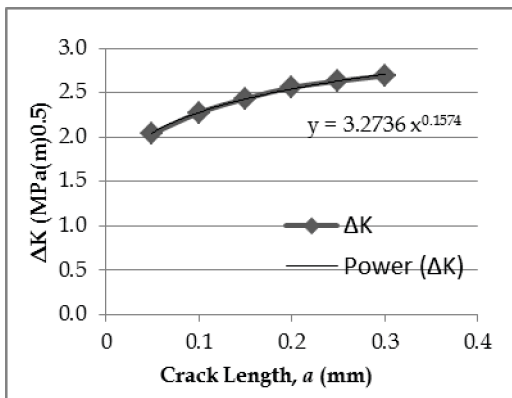


Figure 5 - Variation of ΔK with crack length

Table 3 - Number of Cycles for Short Crack Propagation

Crack Length (mm)	N (kilocycles)
0.05-0.10	93.8
0.10-0.15	44.3
0.15-0.20	27.5
0.20-0.25	19.3
0.25-0.30	14.6

Total time calculated for crack initiation = 199.5 kilocycles

The procedure was repeated for different nominal stress amplitudes, and the results are presented as an S-N Curve shown in Figure 6. Note that two trend lines were drawn by fitting experimental and simulated data, separately using power law. From this, it is seen that for a

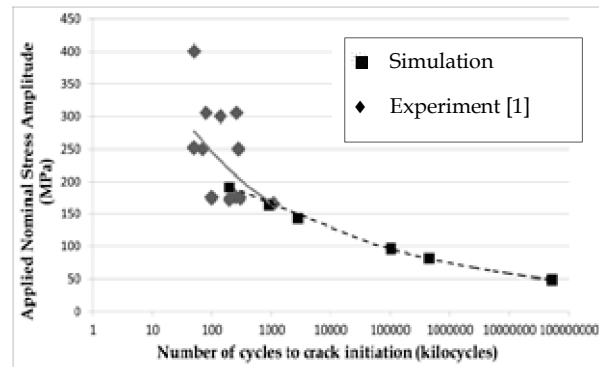


Figure 6 - Comparison of simulated results with experimental results presented by Otegui et al. [1]

particular stress the number of cycles given by the trend line of simulation data is lower than that of experimental data. This could be due to the following reasons.

- The actual welding parameters and cooling conditions were not known, and reasonable boundary conditions and interactions were assumed in the model
- The residual stress distribution was not verified. Detrimental tensile stress distribution was simulated in this study. However, if compressive residual stresses had developed during the actual welding process it would have had a beneficial effect on the fatigue crack initiation life and effectively increased it

4. Conclusions

A technique was developed using elastic plastic fracture mechanics concepts to predict crack initiation life of fatigue cracks at the toe of a welded joint. EPFM parameter ΔJ was obtained using a simple 2D simulation and was used to determine the number of load cycles for small crack growth until a critical 0.3 mm length was reached.

A graphical comparison of experimental and simulation results shows that the numerical results follow a similar trend line to that exhibited by the experimental results. In the overlapping region of both curves between 150 to 200 MPa, experimental data points show close correlation with the simulation results. However, there is room for future work in order to improve the accuracy of the crack initiation life predictions. Special consideration must be given to the effect of residual stresses which can be beneficial or detrimental depending on whether it is tensile or

compressive. Also, means should be explored to fully incorporate the welding parameters and conditions into a two-dimensional model.

This technique proposes a relatively simple and computationally efficient procedure for the determination of fatigue crack initiation period, N_i .

Acknowledgement

The authors are thankful to the National Research Council, Sri Lanka and Senate Research Committee, University of Moratuwa for financial assistance.

References

1. Otegui, J. L., Kerr, H. W., Burns, D. J., & Mohaupt, U. H., "Fatigue Crack Initiation from Defects at Weld Toes in Steel," *Int. J. Press. Vessel. Pip.*, Vol. 38, No. 05, 1989, pp. 385-417.
2. Tricoteaux A., Fardoun, F., Degallaix, S., & Sauvage, F., "Fatigue Crack Initiation Life Prediction in High Strength Structural Steel Welded Joints," *Fatigue Fract. Eng. Mater. Struct.*, Vol. 18, No. 02, February, 1995, pp. 189-200.
3. Suresh, S., Ritchie, R. O., "Propagation of Short Fatigue Cracks," *Int. Met. Rev.*, Vol. 29, No. 01, 1984, pp. 445-475.
4. Rice, J. R., "A Path Independent Integral and the Approximate Analysis of Strain Concentration by Notches and Cracks," *J. Appl. Mech.*, Vol. 35, No. 02, 1968, pp. 379-386.
5. Ochensberger, W., Kolednik O., "A New Basis for the Application of the J-integral for Cyclically Loaded Cracks in Elastic-plastic Materials," *Int. J. Fract.*, Vol. 189, No. 01, September, 2014, pp. 77-101.
6. Paris, P. C., Gomez, M. P., & Anderson, W. E., "A Rational Analytical Theory of Fatigue," *Trend Eng.*, Vol. 13, 1961, pp. 9-14.
7. El Haddad, M. H., Dowling, N. E., Topper, T. H., & Smith, K. N., "J-integral Applications for Short Fatigue Cracks at Notches," *Int. J. Fract.*, Vol. 16, No. 01, February, 1980, pp. 15-30.
8. Dhondt, G., "General Behaviour of Collapsed 8-node 2-d and 20-node 3-d Isoparametric Elements," Vol. 36, November, 1993, pp. 1223-1243.
9. Dassault Systems Simulia Corp., Abaqus 6.14: Abaqus Analysis User's Guide. Providence, RI, 2013.



Growing Colombo: Some Concerns from Wind Engineering Point of View

A. U. Weerasuriya and K.A.B. Weerasinghe

Abstract: Colombo is rapidly developing as a major business centre in the South Asia region. As a result, the city is transforming its urban environment at a great rate of growing numbers in high-rise buildings and the population. The construction of high-rise buildings would induce two types of wind nuisance: high wind speed and low wind speed those are not experienced by citizens before. The impacts of these wind nuisance can be predicted using the knowledge on wind engineering in the absence of the field measurements and simulation data for Colombo. This article aims to demonstrate probable wind nuisances that would be occurred in the Colombo city future using similar experiences in wind-related issues reported in other countries. A number of design strategies and long-term policies are proposed to minimise the anticipated wind nuisances resulting from future development projects in Colombo city. In addition, a set of recommendations is given in this article to increase the awareness of the urban wind climate among the stakeholders of the development projects and is to encourage employing wind data for future building designs and urban planning in Sri Lanka.

Keywords: Building Form, Colombo city, Wind Environment, Wind Nuisance, Urban Planning

1. Introduction

Colombo, the commercial capital of Sri Lanka, undergoes significant modifications on its historical form and the city environment. The Colombo port city project and a number of tall building constructions are two such modifications that could influence the environmental conditions of Colombo. Although the urbanisation is an inevitable and an inherent feature of the modern world, it should be managed well such that it can lead to the sustainable growth of a city with preserving the environment, liveability, and many other factors [1]. The liveability has become a major measure of a sustainable city because of its immense influences on health, life expectancy, and even psychological conditions of citizens.

The wind is one of the major climate factors that determine the city's liveability. Wind contributes many aspects of the liveability including air quality, outdoor thermal comfort, pedestrian wind comfort, natural ventilation, and for recreational activities. Therefore, a city with its properly designed wind environment can easily in achieve a higher level of liveability compared with a city with improper wind conditions.

In this article, the main focus and discussion direct on how Colombo city can achieve a liveable environment in its growth phase from the wind engineering point of view. The anticipated wind-related issues due to the city

development process are presented rationally. A number of solutions for the wind-related issues are proposed and anticipated difficulties, required skills and resources pursuing are discussed in detailed to increase the awareness of the urban wind climate in the development of the Colombo city.

2. The Colombo City

2.1 Geography and the Urban Climate

The Colombo city (6°54' N, 79°52' E) bounds to the Indian Ocean in the west and Muthurajawela marshland in the east by stretching the city in the north-south direction parallel to the coastline. The Colombo city, the main focus of this article, is at as the centre of the Colombo Metropolitan Region (CMR), which extends about 100 km in the north-south direction and 40 km in the east-west direction. The permanent population of the city was about 0.56 million in 2012 while more than 1 million people daily travel to Colombo from other areas of Sri Lanka [2].

Dr. A.U.Weerasuriya, B.Sc. Eng. (Moratuwa), M.Sc. (Moratuwa), Ph.D.(HKUST), Post-Doctoral Fellow, Department of Civil and Environmental Engineering, The Hong Kong University of Science and Technology, Hong Kong, China.

Mr. K.A.B. Weerasinghe, B.Sc. Eng. (Moratuwa), M.Sc. (Moratuwa), Lecturer, Institute of Technology (ITUM), University of Moratuwa.



The climate of Colombo can be classified as the tropical climate with hot and humid conditions that prevail throughout the year. The Asiatic monsoons induce variations in air temperature and humidity such a way that the annual air temperature and humidity are in the range of 23-32 °C, and 80%-85%, respectively [3]. The monsoons define the urban wind climate of Colombo with the prevailing wind direction in southeast and northeast the city as shown in Figure 1.

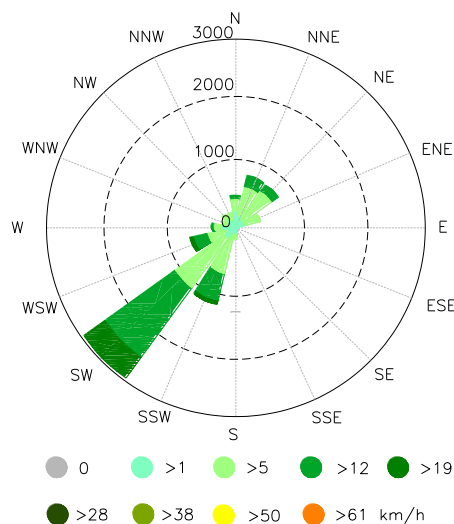


Figure 1 - Annual wind rose of Colombo (radial distances show the number of hours that wind speeds prevailed)[4]

Due to the lack of available data in wind speeds, several researchers made crude estimations of the magnitude of average wind speed in Colombo. The Design Manual “Design building for highwinds, 1978” [5] proposed 2 types of 3-second gust wind speeds: 38 ms⁻¹ and 33 ms⁻¹ for the post-disaster structures and the general structures built in zone 3 where Colombo is located. Although these wind speeds are for the purpose of structural design, the details of wind speed profile or the measurement heights are not presented in the manual. To compensate the absence of background information on the design manual, Holmes and Waller [6] have suggested to assume the design wind speeds are based on 50-year return period and are measured at 10 m height above the ground with the roughness length of 0.02 m. With these two parameters, a designer can calculate the wind speed at any height using empirical wind profile models, the logarithmic or the power-law model. Nandalal and Abeyruwan [7] have fitted the measurements of 3-minute averaged wind speeds taken over 16 years to the Gumbel distribution and have found 20 ms⁻¹ of 3-minute

averaged mean wind speed or 26 ms⁻¹ of the 3-second gust wind speeds with 50-years return period as the design wind speeds for Colombo. Due to, difficulties in setting up measurement locations and conduct field measurement campaigns and the lack of interest create near ground level wind speed data scarce for Colombo. Nevertheless, a field study conducted by Johansson and Emmanuel [8] to measure wind speeds close to the ground shows that 5-minute average wind speed is about 1.9 ms⁻¹ with the minimum wind speed of 0.6 ms⁻¹ at the congested city centre of Colombo. It should be noted that some of these measurements were taken at a height of 10 m or above, thus it is reasonable to assume that the wind speed near the ground is substantially lower than 1.9 ms⁻¹ due to the wind slowdown from the friction between wind and rough surfaces of ground buildings, trees, and vehicles.

2.2 Urban Form of Colombo

The vernacular architecture of Colombo city, which consists of wide eaves, open verandas, and courtyards to cope up with hot and humid climate, has been gradually replaced by the modern architecture. The buildings designed according to the modern architecture are in the shape of a solid vertical slab. These modern buildings are low to medium rise and are concentrated along traffic arteries in the city. Particularly, the medium-rise buildings located along the Colombo-Galle highway (A2), which a main entrance to the city, play a major role in controlling the sea-breeze penetration into the city. At the city centre, buildings are congested along narrow streets and in the outskirts of the city, buildings are separated by sufficient distances between them. Compared to other major cities worldwide, Colombo has only a few high-rise buildings, which were also built in the recent past. The Bank of Ceylon Headquarters building (105 m height), World Trade Centre tower (152 m height), Hilton tower apartments (129 m height), and the Crescat office and Condominium (113 m height) are the buildings taller than 100 m and built before the year 2000. The scarcity of open spaces and green areas (i.e., public parks) within the city is another noticeable difference between Colombo and other major cities worldwide. Most of the major cities are keen to maintain green areas within the city limit such as the central park in New York, USA and several public parks around London, England because of the parks act as ‘lungs of the city’ providing clean air for breathing. In Colombo,

only Viharamahadevi Park is available as a large greenery area that may be a vital factor in controlling microclimate conditions of the city.

2.3 Studies on Urban Climate of Colombo

Most of the wind-related research done in Sri Lanka had focused on structural wind engineering aspects such as calculating wind loading on high-rise buildings [9] or assessing the adoptability of international wind loading standards to the Sri Lankan context [10-12]. An exception is a series of studies done by Emmanuel and his research group [3, 8, 13-16] in which the focuses were on several aspects of the urban climate of Colombo including outdoor thermal comfort, urban heat island (UHI) effect, and air pollution. Although none of these studies directly relate to wind engineering, Emmanuel and his research group were keen to identify wind as a critical factor in the urban climate of Colombo. For example, Emmanuel's research group has identified the importance of sea breeze penetration in achieving outdoor thermal comfort thus, recommended a staggered building arrangement in order to enhance the air circulation in the city [8]. Moreover, their effort to measure wind speeds at the street level is invaluable as these numbers indicate the influence of compact building arrangement on the prevailing low wind speeds in Colombo.

3. Wind Nuisance in Future Colombo City

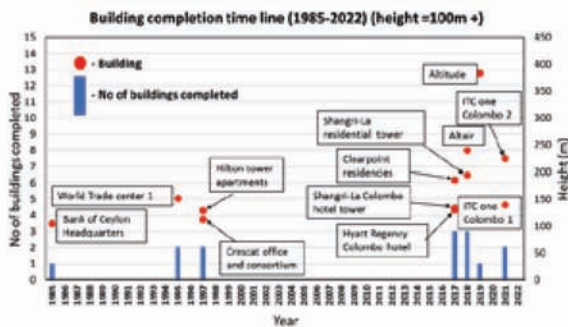


Figure 2 - Details of the completed and proposed high-rise buildings in Colombo[17].

The trend of constructing high-rise buildings, as shown in Figure 2, would be the main cause of wind-related issues in the future Colombo city. The proposed and under-construction high-rise buildings are not only being gigantic but also with atypical shapes and complex building forms. (Figure 3). The unorthodox shapes and superior building heights would

certainly challenge wind engineers when estimating wind loads and predicting building responses. However, this article does not intend to discuss the challenges imposed by high-rise buildings on structural engineers but mainly focuses on the possible environmental issues that can be caused by to the construction of high-rise buildings in Colombo city.



Figure 3 - Proposed two high-rise buildings in Colombo; (a) Altair (240 m) (source: www.altair.lk), and (b) Krish towers (Tower 1 - 420 m height) (source: www.skyscrapercenter.com)

The possible wind nuisance in future Colombo city will depend on the way high-rise buildings arranged in the city. The future high-rise buildings can be arranged as closely-spaced buildings as similar to the skyline in Hong Kong (Figure 4(a)) or as a group of high-rise buildings in the centre of the city forming the central business district (CBD) as in San Francisco, USA (Figure 4(b)) or as the combination of both. A skyline is a possibility in the coastline parallel to the Colombo-Galle road when developers attempt to provide the scenic view of the Indian Ocean for many tenants. On the other hand, the centre of Colombo city including the Fort area is a suitable area to develop as the CBD in Colombo with a number of high-rise buildings built together. Depend on the development type, these two building arrangements will define two types of wind nuisances: (1) unpleasant or dangerous high wind speeds, and (2) undesirable low wind speeds. In the following subsections, causes and repercussions of these two wind nuisances are discussed in detail.



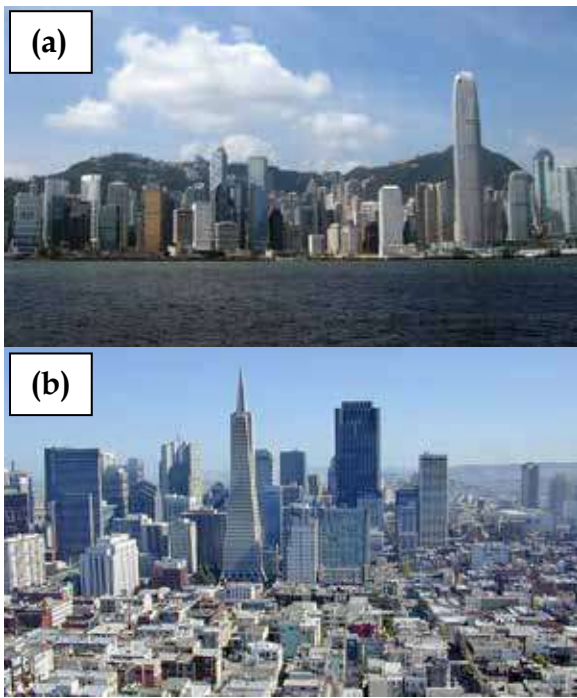


Figure 4 - (a) Skyline of Hong Kong (source: www.wikimedia.org), and (b) high-rise buildings in CBD of San Francisco (source: www.xpressmagazine.org)

3.1 Unpleasant or Dangerous High Wind Speed

The windy areas around tall buildings are formed as a result of deflected high-speed winds from high altitudes to the pedestrian level. There are two pronounced windy areas formed near a high-rise building, first, from the downwash of the windward side, and second, from separated wind flows at the windward corners. The properties of these windy areas (i.e. the intensity and the area) vary with dimensions of the buildings those flow features are attached[18]. Therefore, properly designed building scan easily control the windy areas formed in their vicinity. Another mitigation method is to use passive controllers (discussed in Section 4)but they are less successful against violent high-speed winds and can be applied on case basis rather than universally.

The possible adverse effects of the windy areas are greater difficulty in walking and operating doors, unable to use umbrellas on rainy days, blown down of light vehicles such as bicycles, and in the worst case, people can be injured from falls caused by wind gusts. Due to the low ambient wind speed, accidents to the pedestrians would be unlikely happend in Sri Lanka, nevertheless such an unfortunate incident would lead legal actions against the building

owners, design engineers, architects, and city authorities for mismanaging the wind environment near high-rise buildings. Windy conditions can also cause negative economic impacts for shop owners by preventing customers coming to shopping precincts [19].

3.2 Undesirable Low Wind Speeds

High land prices and limited availability of lands in cities force to construct closely-spaced high-rise buildings, which subsequently induce excessive sheltering causing inadequate city ventilation. Particularly, high-rise buildings built adjoining each other, act like a wall against incoming wind flows and drastically cut down the wind penetration into the city. This phenomenon is referred to as the ‘wall effect of buildings’ [20]and is commonly found in waterfront areas of HongKong, which are similar to the coastal sites in Colombo.

A number of issues including outdoor thermal discomfort exaggerated UHI effect, accumulation of air pollutants near the ground level and favourable conditions to spread airborne pathogens are related to the weak air circulation in a city. None of the above-mentioned issues are standalone problems but they are interconnected with each other causing severe detrimental effects on both citizens and the urban environment. For example, a 3 °C of UHI effect in Hong Kong induces high thermal stresses on inhabitants of the city almost every day and night in summer and consequently, acquires more energy to maintain comfortable indoor temperature, thereby increasing the energy use and CO₂emissions [21]. Therefore, the cities suffering from low wind speeds setup regulations to promote the air circulation at ground level in urban areas.

4. Design strategies, and long-term policies

The following subsections present strategies and long-term policies that Colombo can adopt to mitigate anticipated issues arisen from high/low wind speeds.

4.1 Design Strategies for High Wind Speeds

The design strategies on high wind speeds intend to protect people by shielding the activity areas (e.g. walkways) from dangerous high winds or by assigning suitable areas for certain activities according to prevailing wind

conditions (e.g. threshold wind speeds for shopping areas and lingering areas).

As a design strategy, certain building forms such as buildings with large openings near the ground are not recommended for the locations with high wind speeds. To protect inhabitants from windy areas near high-rise buildings Architectural designs and building features are effectively employed, for example, building's main doors are located away from the windward corners to avoid occupants suddenly exposed to windy areas and podium structures are adopted to deflect the downwash flow away from the building (Figure 4). Aerodynamically favourable building shapes can also be helpful in minimising windy areas forming near high-rise buildings.

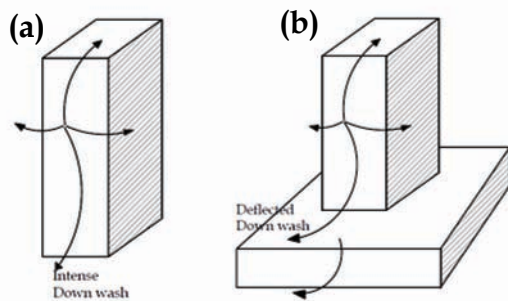


Figure 5 - (a) Intense downwash of a building without a podium structure, and (b) deflected downwash of a building with a podium structure

Economic concerns over the reduced rentable floor area and unattractive appearance are some factors curtail the flexibility of modifications of an architectural design. In such case, designers can use active or passive mitigation methods to protect occupants and pedestrians from high wind speeds created by the building or the nearby buildings. Penwarden and Wise[19] demonstrated several practical solutions including the construction of an additional roof and an installation of glass screens that they had proposed for ill-conditioned shopping precincts in the United Kingdom. But they also reported that these mitigation methods were costly and difficult to implement on the completed buildings and were not capable of solving the wind nuisance completely. The passive mitigations methods can be natural wind breaks such as trees or technically advanced smart, automatic control systems. Less effectiveness and uncertainties in alleviating high wind speeds are the disadvantages of passive mitigation methods.

In the city scale, the design strategies against high wind speeds are controlled by city authorities than by individual designer. An example is that the authorities will design the orientation of street grid, which is generally in the diagonal direction to the prevailing winds to provide the maximum sheltering effect to pedestrians. Another city scale design strategy to reduce high wind speeds at the pedestrian level is building narrow streets with deep street canyons to encourage the skimming flow regime, in which the wind flows over the buildings rather than entering to the canyon.

4.2 Design Strategies for Low Wind Speeds

Design strategies for low wind speeds are completely opposite to the strategies used to mitigate high wind speeds. More specifically, design strategies for low wind speeds promote the air circulation near the ground by opening 'the more wind the better' instead restricting the wind circulation. In order to achieve high air circulation rate, some forbidden building forms and architectural features in windy cities are embraced by cities with low wind speeds. Buildings with an open space at the ground level or commonly known as 'lift-up' buildings are such a favourable building form in cities with low wind speeds [22]. And certain building forms, such as podium structures are not recommended, or only being adopted following special guidelines such as a zero setback for podiums to deflect more high-speed winds from higher altitudes to the street level. It is also recommended to have voids at different heights of buildings, greenery areas at the ground level and intermediate levels, and maintain sufficient separation distances from adjacent buildings in the locations with low ambient wind speeds.

In the city scale planning, major highway arteries are built parallel to the prevailing wind directions creating main breezeways of the city. The secondary streets are designed as wide roads connecting to the main highways by forming minor breezeways and air paths (Figure 5(a)). Greenery areas and open spaces within the city have linked each other to enhance the unobstructed wind air circulation as shown in Figure 5(b). Closely-spaced similar heights tall buildings are prohibited to build in waterfront sites and designers are encouraged to design buildings with varying heights or ascending building heights in the direction parallel to the prevailing wind.



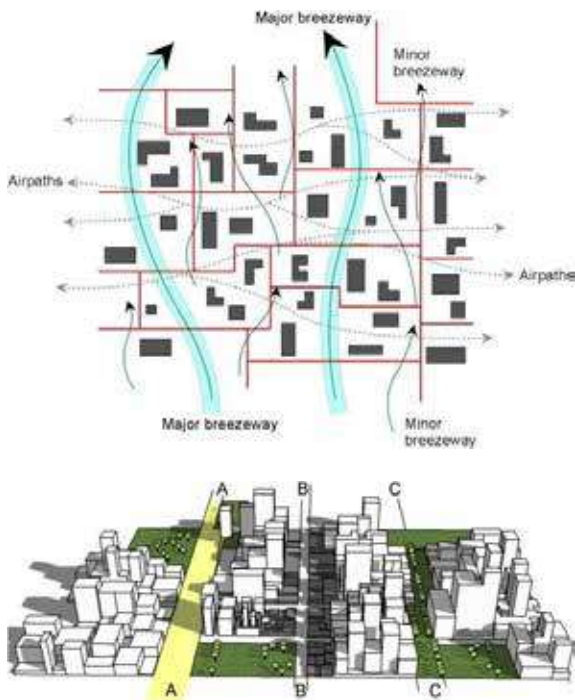


Figure 6- (a) Breezeways and air paths in a city with low wind speeds, (b) linkage of open spaces: air path A-A linking open spaces with a breezeway; air path B-B linking open spaces with low-rise buildings; and air path C-C linking open spaces with a linear park. [23]

4.3 Long-Term Policies

Since Colombo city is still in its early stage of rapid urbanization, it is important to follow a set of well-planned policies to avoid occurring any kind of wind nuisance discussed in this paper. The long-term policies can be extended in a wide range from educating the general public to providing specific design related information for engineers. In this subsection, only the latter will be presented in detailed while non-technological long-term policies will be discussed in section 5.

A Wind Ordinance for Colombo City

As along-term policy, the city authority should stipulate a wind ordinance to address anticipated wind-related issues in future Colombo city. Several researchers [24, 25], have reported the basic contents of a wind ordinance that addresses the two types of wind nuisances. In general, a wind ordinance contains followings; how the city decides which building projects are to be tested, how the testing is to be carried out, criteria for whether the projects meet the city's requirement, and how the results are reported. Among the above-mentioned contents, the criteria to assess the

existing wind conditions with the expectations citizen are a question to be addressed carefully. As the previous sections demonstrated, it is anticipated to experience both high and low wind speeds in future Colombo city, and thus it is recommended to employ criteria to address both types of wind nuisance, simultaneously. For instance, the future wind ordinance of Colombo may propose a minimum wind speed to maintain outdoor thermal comfort, several wind speeds for different areas such as CBD, residential areas, and recreational and a maximum threshold wind speed to ensure the safety of the citizens.

An Urban Map of Colombo City

An urban map should be developed indicating sensitive locations for the urban climate of the city. Such an urban map can be utilised to evaluate the impact of future development on the wind conditions of its neighbourhood. The urban map can also define the areas dedicated for different types of development, for example, for the CBD or for a residential development, and then to regulate design parameters such as building height, and ground covering ratio. By regulating building parameters, the city authority can maintain an acceptable level of wind circulation near the ground. For instance, low building heights and small ground covering ratios recommended for the coastal sites would be advantageous to facilitate the sea breeze penetration in to inland areas.

Building design guidelines for Colombo City

A set of design guidelines should be introduced for designers to design buildings without imposing adverse effects on the urban wind environment. Such building design guidelines can recommend certain building forms for different areas, for instance, podium structures for locations experience high wind speeds and 'lift-up' buildings for locations where the prevailing wind speeds are low. Another advantage of stipulating the building design guidelines is its ability to control minor design concerns such as the required percentage of greenery area, minimum building separation distance, minimum clearance distance from streets, and other parameters related to the wind circulation. On the other hand, design guidelines can set a common platform for both the city authority and developers can agree and it will reduce the risk of being modified the design in a later stage of the project. The format and some of the contents of the sustainable

building design guidelines stipulated by the Building Department of Hong Kong [26] can be set as an example for building design guidelines of Colombo.

5. Applying wind engineering to Colombo city design

Non-technical, long-term policies can be in three major fields; education, research, and meteorology as discussed in the following subsections.

Education

It is necessary to educate all the stakeholders including planners, engineers, authorities and general public involved in the development of the Colombo city to increase the awareness of urban wind climate. Particularly the professional courses for engineers, planners, architects should accommodate wind engineering, and thus recognise wind as a design parameter. Moreover, wind and its interdependency on other climate factors should be illustrated to increase the awareness of technical professionals on the urban climate.

Research

A considerable amount of research is necessary to estimate important design parameters such as the minimum wind speed required to maintain outdoor thermal comfort and favourable buildings forms for Colombo. It is also necessary to follow an integrated research approach to study the urban wind climate of Colombo than following individual research interests. An integrated research approach would prevent establishing conflicting research findings such as promoting deep street canyons, which are favourable in achieving outdoor thermal comfort but have adverse effects on wind circulation within the canyon. The local researchers should be encouraged to collaborate with experts in other countries to exchange the existing knowledge and learn from their past experiences.

Meteorological data

The scarcity of meteorological data is one of the major obstacles in integrating wind into the planning of the future Colombo city. It is advisable to establish a network of anemometers and small-scale weather stations to collect the data of wind speeds (near the ground and high altitudes) and other

meteorological data including air temperature, humidity, and solar irradiation, and roadside air pollution for the planning purpose.

6. Concluding Remarks

This paper presents two types of anticipated wind-related issues: high wind speeds and low wind speeds in the future Colombo city and design strategies, mitigation methods, and long-term policies to eliminate the probable wind nuisances. Moreover, several recommendations are proposed to increase the awareness of wind engineering in the urban planning and possibility of integrating wind data for the future city design. However, with the absence of exact data, the facts presented in this article are based on the similar cases reported in the literature. Therefore this article should be referred as a source of the knowledge on the urban wind climate rather than as a design manual established for Colombo.

References

1. <http://www.worldbank.org/en/news/press-release/2015/09/29/urbanization-offers-sri-lanka-major-economic-opportunity>, accessed on 08th February 2017.
2. Perera D. "The way forward Colombo Metropolitan Transport Master Plan and Areas for International Cooperation", 2014. Available on http://www.uncrd.or.jp/content/documents/22938EST-P5_Sri-Lanka-MOT.pdf
3. Emmanuel, Rohinton, H. Rosenlund, and Erik Johansson. "Urban shading—a design option for the tropics? A study in Colombo, Sri Lanka." *International Journal of Climatology* 27, no. 14 (2007): 1995-2004.
4. https://www.meteoblue.com/en/weather/forecast/modelclimate/colombo-sri-lanka_1248991, accessed on 09th February 2017
5. Clarke, A.G., Swane, R.A., Schneider, L.M., Shaw, P.J.R., "Technical Assistance to Sri Lanka on Cyclone resistant construction-Project Summary", Commonwealth of Australia, Department of Housing and Construction for Australian Development Assistance Bureau, Vol-1, Part 1-4, October 1979.
6. Holmes, John D., and Richard Weller. *Design wind speeds for the Asia-Pacific region*. Standards Australia International, 2002.
7. Nandalal, K.D.W., Abeyruwan, H., "An attempt towards wind zone demarcation for



- Sri Lanka", APECWWReport,Tokyo Polytechnic University, Japan, 2010 (available on <http://www.wind.arch.t.kougei.ac.jp/APECWW/Report/2010/Srilankab.pdf>)
8. Johansson, Erik, and Rohinton Emmanuel. "The influence of urban design on outdoor thermal comfort in the hot, humid city of Colombo, Sri Lanka." *International journal of biometeorology* 51, no. 2 (2006): 119-133.
 9. Wijeratne, M. D., and M. T. R. Jayasinghe. "Wind loads for high-rise buildings constructed in Sri Lanka." *Transactions Part: 58-69*.
 10. Premachandra, W. R. N. R. "Study of new wind loading code to be adopting on Sri Lanka." PhD diss., M. Sc Thesis, Graduate school, Kasetart University, 2008.
 11. Weerasuriya, A. U., and M. T. R. Jayasinghe. "Wind Loads on High-Rise Buildings by Using Five Major International Wind Codes and Standards." *Engineer: Journal of the Institution of Engineers, Sri Lanka* 47, no. 3 (2016).
 12. Weerasuriya, A. U., and M. T. R. Jayasinghe. "Wind Loads on a Medium-Rise Building by Using Five Major International Wind Codes and Standards." *Engineer: Journal of the Institution of Engineers, Sri Lanka* 47, no. 1 (2015).
 13. Emmanuel, Rohinton. "Thermal comfort implications of urbanization in a warm-humid city: the Colombo Metropolitan Region (CMR), Sri Lanka." *Building and Environment* 40, no. 12 (2005): 1591-1601.
 14. Emmanuel, R., and H. J. S. Fernando. "Urban heat islands in humid and arid climates: role of urban form and thermal properties in Colombo, Sri Lanka and Phoenix, USA." *Climate Research* 34, no. 3 (2007): 241-251.
 15. Perera, Bimalka, Rohinton Emmanuel, and Sumal Nandasena. "Urban air pollution and mitigation options in Sri Lanka." *Proceedings of the Institution of Civil Engineers-Urban Design and Planning* 163, no. 3 (2010): 127-138.
 16. Emmanuel, Rohinton, and Erik Johansson. "Influence of urban morphology and sea breeze on hot humid microclimate: the case of Colombo, Sri Lanka." *Climate research* 30, no. 3 (2006): 189-200.
 17. <https://skyscrapercenter.com/city/colombo>, accessed on 09th February 2017.
 18. Tse, K. T., A. U. Weerasuriya, X. Zhang, S. Li, and K. C. S. Kwok. "Pedestrian-level wind environment around isolated buildings under the influence of twisted wind flows." *Journal of Wind Engineering and Industrial Aerodynamics* 162 (2017): 12-23.
 19. Penwarden, Alan David, and Alan Frederick Edward Wise. *Wind environment around buildings*. HMSO, 1975.
 20. Yim, Steve HL, Jimmy Chi Hung Fung, Alexis Kai-Hon Lau, and See Chun Kot. "Air ventilation impacts of the "wall effect" resulting from the alignment of high-rise buildings." *Atmospheric Environment* 43, no. 32 (2009): 4982-4994.
 21. Fung, W. Y., K. S. Lam, W. T. Hung, S. W. Pang, and Y. L. Lee. "Impact of urban temperature on energy consumption of Hong Kong." *Energy* 31, no. 14 (2006): 2623-2637.
 22. Tse, K. T., Xuelin Zhang, A. U. Weerasuriya, S. W. Li, K. C. S. Kwok, Cheuk Ming Mak, and Jianlei Niu. "Adopting 'lift-up' building design to improve the surrounding pedestrian-level wind environment." *Building and Environment* 117 (2017): 154-165.
 23. Ng, E. "An investigation into parameters affecting an optimum ventilation design of high density cities." *International Journal of Ventilation* 6, no. 4 (2008): 349-357.
 24. Arens, Edward, D. Ballanti, C. Bennett, S. Guldman, and B. White. "Developing the San Francisco wind ordinance and its guidelines for compliance." *Building and Environment* 24, no. 4 (1989): 297-303.
 25. Willemsen, Eddy, and Jacob A. Wisse. "Design for wind comfort in The Netherlands: Procedures, criteria and open research issues." *Journal of Wind Engineering and Industrial Aerodynamics* 95, no. 9 (2007): 1541-1550.
 26. *Technical Guide for Air Ventilation Assessment for Developments in Hong Kong*, by Hong Kong Planning Department. Visited on 15th of February 2017 (<http://www.devb.gov.hk/filemanager/technicalcirculars/en/upload/15/1/jtc-2006-01-0-1.pdf>)

Contributory Factors for Cost and Time Overruns of Construction Projects

Leelanath Daluwatte and Malik Ranasinghe

Abstract: Most construction projects experience overruns in cost and time when delivering the agreed scope. Construction projects in Sri Lanka are no exception. As these delays negatively impact the stakeholders of the projects, there is room for research on why such overruns take place and how to control them. It is important to optimize the use of scarce resources (by way of controlling the cost) and opportunity costs for the stakeholders (by way of controlling the time) of the projects. There are many reasons for the overruns of cost and time as identified by this study.

The objectives of this paper were to identify and analyse contributory factors for the cost and time overruns of construction projects. The literature review identified 42 factors that contribute to the overruns of cost and time in construction projects. Most of these were due to the inadequacy of analysis at the preconstruction stage of the projects.

Methodology of the study relied mainly on the literature reviews. Data collected from the review was analysed. The following seven factors, design effects, planning and controlling, material issues, scope change, finance, client influenced changes, and contractor inexperience contributed to 51% occurrences of the contributory factors while top 17 factors contributed to 80% of the occurrences of the contributory factors.

Keywords: Construction projects, Cost, Time, Overrun,

1. Introduction

Construction projects consume significant quantities of scarce resources like building materials, fossil fuels, machinery built using resources, human resources, irrespective of the magnitude of the construction project [1]. However, construction projects are meant to utilize optimum amounts of resources at optimum project duration to deliver effective project output. In most construction projects, utilization of optimum resources or delivery of the project on agreed time does not happen [2]. These require additional costs and time for the project scope to be achieved resulting in lost opportunity costs to stakeholders of the projects. Most construction projects in Sri Lanka contribute to the above scenario, thus creating cost and time overruns.

In preliminary review it was observed that most of the construction projects exceeded the time and cost to deliver the agreed scope. In the end this appear to incur losses to the concerned parties and hence the study was focused in the concerned area. The objectives of this paper are (i) to identify the contributory factors for cost and time overruns of construction projects; (ii) to analyze the

identified contributory factors and (iii) to select the key contributory factors.

The paper describes the extensive literature review conducted in the research area.

This paper is based on ongoing research focused on the cost and time overruns of construction projects and will followed by further research in the industry.

2. Literature Review

A number of publications related to cost and time overruns of construction projects were reviewed and during the research it was revealed that the contributory factors were similar, irrespective of the type, cost, duration, locality etc. of the project.

Eng. Leelanath Daluwatte, B.Sc.Eng.(Hons), FIE(Sri Lanka), C.Eng., P.E., M.ASCE, DBM, Dip HRM (Merit), Dip(Cleaner Production), Dip(Human Rights), Distinguished Toastmaster, Consultant in Project Management / Construction Management / Process Improvements.

Eng. (Prof.) Malik Ranasinghe, B.Sc.Eng.(Hons), M.ASc, Ph.D., FIE(Sri Lanka), C.Eng., Senior Professor, Dept. of Civil Engineering, University of Moratuwa.



Further the findings of the literature review was categorized according to different stages of the construction project are described in this section.

2.1 Findings related to Preconstruction phase

Ineffective investigations during preconstruction caused cost and time overruns in construction projects [3], and inadequate allocation of funds to the preconstruction stage led to shortcomings such as ambiguities, design (errors and omissions) and incurred additional costs during the construction phase [4]. Also, risks taken during preconstruction stage caused errors in processes (bidding, estimating, finance and design) in construction projects [5].

However, provision of all information to stakeholders as appropriate led to stakeholder satisfaction and avoided doubts and conflicts among them regarding matters related to the projects [6] while analysis of stakeholder involvement provided an evaluation of the needs and expectations of stakeholders in relation to the main objectives of the project [7].

It was found that lack of funding for bidding caused cost overruns [2] while limited time given for submission of bids caused time overruns in construction projects [8].

It was also highlighted that contract conditions were the most occurring and impacting risk in construction cost estimating and caused cost and time overruns in construction projects [5] and contract constraint risk caused cost overruns in construction projects [9].

Ineffective project communication [10] and inefficient communication between stakeholders had caused cost and time overruns in construction projects [11]. Unsupportive government policies [25], uncertainties in regulations [13] and bureaucratic indecision [14] caused cost and time overruns. It was also noted that poor site conditions [10], [13], [25] and unforeseen ground conditions caused cost and time overruns in construction projects [15].

2.2 Findings related to Design phase

Design related issues were identified among the most problematic [3], [4] and significant [16], [17], which caused cost and time overruns in construction projects.

The following aspects of design were found to have contributed to cost and time overruns; Design errors [5], [6], [9], [18], [19]; Poor design [14], [16]; Delay in design [16], [20]; Design changes [9], [18], [19]; Delays in approval of design [5], [16], [21]; Client driven design changes [17], [18]; Design changes driven change orders [18]; Failing to identify project risks at design stages [23]; Erroneous design work/process and Attitudes of the designer [17], [18].

It was stated that clarity in design at the early stage and clearly defined scope led to more accurate budget estimates of the projects [17].

As the clients were the main party that impose changes and client-driven design changes caused critical risks that resulted in cost overruns in construction projects [17].

2.3 Findings related to Planning phase

Ineffective planning was most significant and common factor that caused cost overruns [16]. Also, poor planning and controlling [24], [25], [26] insufficient planning and scheduling [27], improper planning [28] and deficiencies in planning and scheduling caused cost and time overruns in construction projects [5], [29].

Slowness in decision-making process caused time overruns in construction projects [30]. Efficient planning was one of the best methods to reduce cost overruns [31].

2.4 Findings related to Implementation phase

Financial difficulties faced by the client was a major factor [14], [15], [21], [28], [32], [33] and financial resource management was among the major contributors to cost and time overrun of construction projects. Also, deficiencies in finance management [34] and poor change management caused cost and time overruns [35].

Delays in payments for contractors to complete the work [25], [36] and cash flow and financial difficulties faced by contractors caused cost and time overruns of construction projects [37]. Long response time from utility agencies had caused time overruns in construction projects [27].

Shortage of workers [28], [37], [38], [39], ineffective relationship between management and labour, [16], low productivity level of workers [25], [40], [41], and poor

communication and coordination between parties caused cost and time overruns in construction projects [40],[42].

Poor site management and supervision [12], [16],[43], faulty contract management, [6],[34],[36],delays in decisions [15],[24], and delays in approval of major changes of scope of work caused cost and time overruns in construction projects [41].

Proper management of site and supervision of the project would be ideal to avoid cost overruns in construction projects [31].

Changes in the scope was a significant factor which incurred cost and time overruns in construction projects [6], [27], [28], [37]. The main source was the change in plans by the client, due to change of mind, which had a critical impact on project cost, time and quality of the projects [18].

As requirements of the client expanded during construction, additional works by the client [40], [22], and the change orders significantly contributed towards cost overrun[26]. Too many owner-generated change orders cause cost and time overruns in construction projects [22].Change orders issued during construction generated cost overruns [26]as they had a critical impact on cost, time and quality of construction and it was concluded change orders increased the contract value by about 10% to 15% [18].

Changes in material specifications [44], changes in quantities of material and substituting material [18], unavailability of material during implementation [45], increase

in the cost of construction material [26] and material related issues [10]caused cost and time overruns in construction projects. Inexperienced[16], [28], [37],and incompetent contractors caused cost and time overruns in construction projects [35].

Though process-related factors influenced and contributed to cost and time overruns [10],methods of construction [31] and cost-effective construction techniques [45] avoided cost overruns in construction projects. Similarly, decreased project duration and increased productivity was achieved by effective use of construction technology [38].

The review highlighted that cost and time overruns spanned across all the phases Preconstruction [4], Planning [25], Design [4]and Implementation [26]) of a construction project and was spread over all five continents Asia [15], Africa [41], America [4], Europe [17] and Australia [29].

3. Methodology and Analysis

After the extensive review of literature in the areas of cost and time overruns of construction projects, the methodology identified and record the contributory factors for cost and time overruns of construction projects as highlighted by previous studies. The review showed that most of the factors identified appeared in many of the other studies too. The research was mostly based on qualitative analysis method.

Table 1 - Contributory Factors Identified from the Literature Review

Rank	Factor	Occurrences	Rank	Factor	Occurrences
1.	Design aspects	29	22.	Consultant's Issues	2
2.	Planning and Controlling	20	23.	Contract Conditions	2
3.	Material Issues	19	24.	Pre-Construction Issues	2
4.	Scope Change	18	25.	Disputes within parties	2
5.	Finance	15	26.	Equipment & Plant Cost	2
6.	Client Influences - Changes	10	27.	Government Policies	2
7.	Management - Site	10	28.	Information- Availability	2
8.	Contractor Inexperience	9	29.	Investigation - early	2
9.	Poor Contract Management	8	30.	Perception on Issues	2
10.	Bid - Time given for	7	31.	Quantities	2



11.	Contractor - Defects	7		32.	Social Issues	2
12.	Construction Methods	7		33.	Worker Productivity -low	2
13.	Construction Technology related	7		34.	Construction - Issues (Implementation)	1
14.	Approval - Delays	6		35.	Equipment - Productivity	1
15.	Communication- Project	6		36.	Estimation Issues	1
16.	Management - Strategies	6		37.	Internal Conflicts	1
17.	Payment to Contractors	5		38.	Optimism biased	1
18.	Decision Delay	4		39.	Procurement - Delays	1
19.	Ground - Site Conditions	4		40.	Records - Lack of	1
20.	Worker Shortage	4		41.	Uncertainties- Risks	1
21.	Change Order Issues	3		42.	Worker (Risky) Behavior	1
					Total occurrences	237

The identified contributory factors for cost and time overruns of construction projects were listed and the number of occurrences in the literature review they were recorded as shown in Table 1 above.

Forty two contributory factors identified had a total of Two hundred and thirty seven (237) occurrences in the literature reviewed (Table-1).

$$\begin{aligned} \text{Percentage Contribution by a factor} &= P \\ \text{Number of Occurrences by a factor} &= n \\ \text{Sum of Occurrences by all factors} &= N \end{aligned}$$

$$\% \text{ of Occurrences by a factor} = (n / N) \times 100\%$$

Sum and % contribution by the top ranking contributory factors are given in Table 2 below.

Table 2- Sum and % Contribution of Top Ranking Factors.

Factors grouped	Sum of Contributions	% from Total Contributions (237)
Top 3 factors	68	~30%
Top 7 factors	121	51%
Top 17 Factors	189	80%

Figure 1 given below indicates the composition of occurrences by the top three contributing factors which account for ~ 30% of the total 237 occurrences.

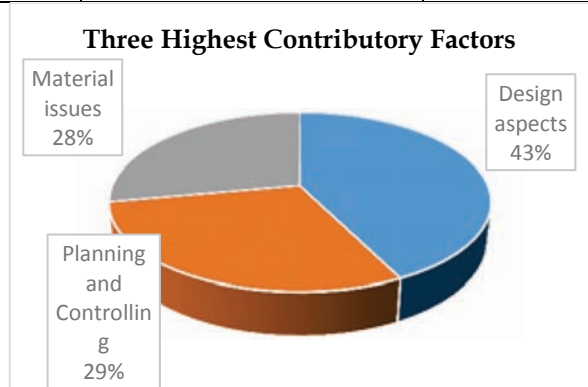


Figure 1 - Three highest contributory factors.

Figure 2 below highlights the composition of occurrences of the top seven contributing factors which account for ~51% of 237 total occurrences.

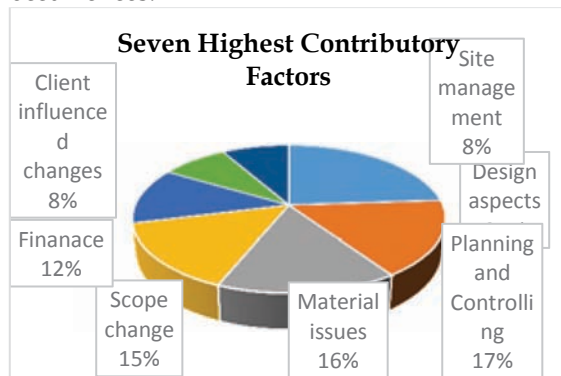


Figure 2 - Seven highest contributory factors

4. Discussion

While 42 contributory factors for cost and time overruns were found, the total sum of the occurrences of the contributory factors in the reviewed literature was found to be 237. The highest occurrence of a contributory factor was identified as 29, for Design aspects, and the

lowest contributory factor 1 was shared by 9 contributory factors (e.g. Optimism biased). (Table 1).

Design aspects, planning and controlling and material issues were found to be the three main contributors to cost and time overruns of construction projects. (Table. 1).

When the factors at the top of the list were grouped, it was observed that sum and the % of the contributions of the selected groups were 68, ~30%; 121, 51% and 189, 80% for the groups of top three factors, top seven factors and top 17 factors respectively (Table 2).

Above analysis indicated that factors ranked high with respect to occurrences dominated the contributions for cost and time overruns of construction projects as indicated in Figure 3 below.

Design aspects, Planning and controlling and Material related issues were identified to be the top three key contributors to cost and time overruns of a construction project (Figure 3).

Some of the aspects found were, Design (delay in design, failing to identify project risks at design stage, design errors, poor design, change orders due to design changes etc.), Planning and Controlling (incomplete planning at the project implementation, insufficient planning, poor planning, inaccurate / incorrect planning, etc.) and Material (change in material specification, material deficiency, delay in material delivery, escalation of cost of material, substituting material by change orders, etc.)

Out of 42 contributory factors identified, only a single contributory factor, i.e. changes influenced by the client, was identified as the factor outside the agreed project scope and hence out of control of the project team. All other 41 factors, i.e. 98% (41 out of 42), were within the agreed project scope and within the control of the project team. Nevertheless, the review carried out identified that all these 41 factors had contributed to causing cost and time overruns in construction projects.

Hence it is observed that the analysis carried out on identified contributory factors were inadequate and ineffective causing cost and time overruns by the identified controllable

(41) contributory factors in construction projects.

However, if an effective analysis was carried out on the said 41 contributory factors, perhaps at a relevant stage of a project (eg. preconstruction stage) cost and time overruns of the projects could have minimised / eliminated.

Further, through the review carried out, it was found that the industry sensitive contributors for cost and time overruns of projects such as shortage of workers (Table 1, Rank 20), low productivity of workers (Table 1, Rank 33) did not appear as significant contributory factors for cost and time overruns of construction projects.

It was revealed that there exist considerable number of common factors contributing to overruns irrespective of the type, cost, duration, locality etc. of the project (Table -1).

Focus of the review was to reveal type of possible contributory factors for overruns in cost and time of construction projects. Hence the factors listed consists of contributions from both cost overruns and/or time overruns. This may be considered as a limitation.

5. Conclusions

The review revealed there are 42 factors that contributed to the overruns of cost and time in construction projects. The analysis highlighted that most of these were due to the inadequacy of proper analysis at pre-construction stage of the projects. The analysis highlighted that seven factors contributed to 51% of the occurrences of contributory factors while top 17 factors contributed to 80% of the occurrences of the contributory factors.

The analysis further revealed, design aspects (12%), planning and controlling (8%) and material (8%) were found to be the top three key contributors with the highest number of occurrences (Table 1). These three factors contributed to ~30% of the occurrences (see Table 2). Further, top 7 factors, design aspects, planning and controlling, material issues, scope change, finance, client influenced changes and contractor inexperience, contributed for 51% of the occurrences and top 17 factors contributed to 80% of the occurrences (see Table 2).



The above indicates that the contribution for cost and time overruns for the construction projects by the identified factors were not equally distributed and the contributory factors ranked high in order contributed heavily (Table 1) for cost and time overruns of construction projects.

However, 98% (41 out of 42) of the contributory factors were within the control of the project team the only exception being the changes made by the owner (see Table 1). Yet these 41 factors within the control of the project team continue to contribute to cost and time overruns of construction projects.

It is concluded that industry sensitive contributory factors like worker shortage and low worker productivity ranked comparatively low in the analysis (Table 1).

Contributory factors appear to have surfaced as the symptoms of the causes inducing cost and time overruns of construction projects. Further research can be carried out to find the root causes and possible corrective actions of such contributory factors.

References

1. EU Technical report 2014-2478, Luxembourg.
2. Shrestha, P. P., Burns, L. A. and Shield, D. R. (2013) Magnitude of construction cost and schedule overruns in public work projects. *Journal of Construction Engineering* Volume 2013 (2013), Article ID 935978, 9 pages <http://dx.do>
3. Jatarona, N. A., Yusof, A. M., Ismail, S. and Saar, C. C. (2016). Public construction projects performance In Malaysia. *Journal of Southeast Asian Research* http://www.ibimapublishing.com/journals/J_SAR/jsar.html Vol. 2016(2016), Article ID 940838, 7 pages DOI: 10.5171/2016.940838.
4. Craigie, E. K., (2015) A framework for estimating preconstruction service costs at the functional level for highway construction projects. Graduate essays and Dissertations. Paper 14752.
5. Ojo, G. K. and Odediran, S. J. (2015). Significance of construction cost estimating risks in Nigeria. *International Journal of Civil Engineering and Construction Science*. Vol. 2, No. 1, 2015, pp. 1-8. 2015; 2(1): 1-8 published online April 20, 2015 (<http://www.aascit.org/journal/ijcecs>)
6. Buys, F (2015) Five causes of project delay and cost overrun, and their mitigation measures. Paper, LinkedIn.com
7. Olander, S. (2007) Stakeholder impact analysis in construction project management, *Construction Management and Economics*, 2007, Vol. 25, Issue 3, 277-287.
8. Patel, C. H., Chaturvedi, H., Rao, M. R., Katta, P. and Prasad, K. N. N. (2015). An analysis of cost and time overruns in construction projects. *NICMAR Journal of Construction Management*, Vol. XXX April - June 2015 No. II
9. Vu H.A., Wang, J., Min, L., Mai, S.H. and Nguyen, H. P. (2016) Research on cost overrun risk of construction phase of Vietnam highway international contracting project, *Engineering*, 2016, 8, 86-98, Published Online March 2016 in SciRes. <http://www.scirp.org/journal/eng> <http://dx.doi.org/10.4236/eng.2016.83011>
10. Adam, A., Josephson, P. and Lindahl, G. (2014) "Implications of cost overruns and time delays on major public construction projects". *Proceedings of the 19th International Symposium on the Advancement of Construction Management and Real Estate*, 7-9 Nov 2014, Chongqing
11. Priyadharshini, N. S. and Kumar S. S. (2015). Project communication: Is key to productive construction and its research needs in the future of construction engineering and management. *International Journal of Science, Technology & Management* www.ijstm.com Volume No 04, Special Issue No. 01, March 2015 ISSN (online): 2394-1537
12. Azhar, A., Farooqui, R. U. and Ahmed, S.M. (2008) Cost overrun factors In construction industry of Pakistan, *First International Conference on Construction In Developing Countries (ICCIDC-I)* August 4-5, 2008, Karachi, Pakistan, Conference paper, <https://www.researchgate.net/publication/277987526>
13. Allahaim and Liu (2013) An empirical classification of cost overrun in infrastructure projects by using analysis, *University of New South Wales, Built Environment*, www.be.unsw.edu.au,
14. Morris, S. (1990), Cost and time overruns in public sector projects. *Economic and Political Weekly*, Vol. 25, No. 47, pp.M154-M168, November 24, 1990.
15. Memon, A. H. (2014) Contractor Perspective on Time Overrun Factors in Malaysian

- Construction Projects. *International Journal of Science, Environment ISSN 2278-3687 (O) and Technology*, Vol. 3, No 3, 2014, 1184 - 1192... 1-
16. Memon, A. H., Rahman, I. A. and Azis, A. A. (2011). Preliminary Study on Causative Factors Leading to Construction Cost Overrun. *International Journal of Sustainable Construction Engineering & Technology* Vol 2, Issue 1, June 2011.
 17. Jackson (2000) Project Cost Overruns and Risk Management, School of Construction Management and Engineering, The University of Reading, Whiteknights, PO Box 219, Reading, RG6 6AW, UK, <https://www.reading.ac.uk/web>files>, Visited 2nd May 2017.
 18. Desai, N. J., S., Pitroda, J. and Bhavsar, J. J. (2015) A Review on Change Order and Assessing Causes Affecting Change Order in Construction, *Journal for International Academic Research for Multidisciplinary* Impact Factor 1.625, ISSN: 2320-5083, Volume 2, Issue 12, January 2015.
 19. Olawale, Y. A. and Sun, M. (2010) Cost and Time Control of Construction Projects: Inhibiting Factors and Mitigating Measures in Practice. *Construction Management and Economics*, 28(5), 509-526.
 20. Akinsiku, O. E. and Akinsulire A. (2012) Stakeholders' Perception of the Causes and Effects of Construction Delays on Project Delivery KICEM *Journal of Construction Engineering and Project Management Online* ISSN 2233-9582 25 www.jcepm.orghttp://dx.doi.org/10.6106/JCEPM.2012.2.4.025.
 21. El-Kholy, A. M. (2015) Predicting Cost Overrun in Construction Projects, *International Journal of Construction Engineering and Management* p-ISSN: 2326-1080 e-ISSN: 2326-1102 2015; 4(4): 95-105.
 22. Kaveen, S., Aleem, M. I. A. and Tharrini, J. (2015) Application of Value Engineering in Construction Project to Predict Time and Cost Overrun - An Overview; *International Journal of Scientific Engineering and Applied Science (IJSEAS)* - Volume-1, Issue-9, December 2015 ISSN: 2395-3470 www.ijseas.com.
 23. Edwards, P., Bowen, P., Hardcastle, C., and Stewart, P. (2009) Identifying and Communicating Project Stakeholder Risks. *Building a Sustainable Future*: pp. 776-785. doi: 10.1061/41020(339)79 ASCE.
 24. Bhatia, D. and Apte, M. R. (2015). Schedule Overrun and Cost Overrun in the Construction of Private Residential Construction Project: Case Study of Pune, India. *International Journal of Technical Research and Applications* e-ISSN: 2320-8163, www.ijtra.com Volume 4, Issue 2 (March-April, 2016), PP. 174-177.
 25. Mulla, S. S. and Waghmare, A. P. (2015) A Study of Factors Caused for Time and Cost Overruns in Construction Project and their Remedial Measures. *International Journal of Engineering Research and Applications*, www.ijera.com ISSN: 2015 Jan; 5(1):48-53.
 26. Patel, A (2014) Effects and Causes of Cost Overrun on Building Construction Projects, Academia.edu.
 27. Emam, H., Farrell, P. and Abdelaal, M. (2015) Causes of Delay on Large Infrastructure Projects in Qatar, Conference: 31st Annual ARCOM Conference, At Lincoln, UK. DOI: 10.13140/RG.2.1.1732.0400.
 28. Bekr., G. A. (2015) Identifying Factors Leading to Cost Overrun in Construction Projects in Jordan, *Journal of Construction engineering, Technology & Management*, Vol 5, No 3 (2015).
 29. Doloi, H.(2013) Cost Overruns and Failure in Project Management: Understanding the Roles of Key Stakeholders in Construction Projects, *Journal of Construction Engineering and Management*, March 2013, Vol. 139, No. 3 : pp. 267-279 doi: 10.1061/(ASCE)CO.1943-7862.0000621).
 30. Mukuka, M., Aigbavboa, C. and Thwala, W. (2015). Effects of Construction Projects Schedule Overruns: A Case of the Gauteng Province, South Africa, <http://creativecommons.org/licenses/by-nc-nd/4.0/>). Peer-review under responsibility of AHFE Conference.
 31. Shibani, A. and Arumugam, K. (2015). Avoiding Cost Overruns in Construction Projects in India. *Management Studies*, August 2015, Vol. 3, No. 7-8, 192-202 D doi: 10.17265/2328-2185/2015.0708.003.
 32. Larsen, J. K., Shen, G. Q., Lindhard, S. M. and Brunoe, T. D. (2015) Cost overrun, Denmark, quality level, schedule delay) [http://dx.doi.org/10.1061/\(ASCE\)ME.1943-5479.0000391](http://dx.doi.org/10.1061/(ASCE)ME.1943-5479.0000391) Publisher: American Society of Civil Engineers.
 33. Ameh, O. J., Soyingbe, A. A. and Odusami, K. T. (2010) Significant Factors Causing Cost



- Overruns in Telecommunication Projects in Nigeria. *Journal of Construction in Developing Countries*, 15 (2). pp. 49-67.
34. Rahman, I. S., Memon, A. H., Nagapan, S. and Latif, Q. B. A.I. (2012). Time and Cost Performance of Construction Projects in Southern and Central Regions of Peninsular Malaysia. 2012 IEEE Colloquium on Humanities, Science and Engineering (CHUSER).
 35. Long, N. D., Ogunlana, S., Quang, T. and Lam, K. C. (2004) Large Construction Projects in Developing Countries: A Case Study from Vietnam, *International Journal of Project Management*, Vol.22: 553-561.
 36. Okpala, D. and Aniekwu, A. (1988). Causes of High Costs of Construction in Nigeria. *Journal of Construction Engineering and Management*, June 1988, Vol. 114, No. 2: pp. 233-244.
 37. Memon, A. H., Abdullah, M. A. H. I. A. M. R. and Azis, A. A. (2010). Factors Affecting Construction Cost in Mara Large Construction Project: Perspective of Project Management Consultant. *International Journal of Construction Engineering & Technology* Vol 1, No 2, December 2010.
 38. Sepasgozar, S. M. E., Razkenari, M. A. and Barati, K. (2015) The Importance of New Technology for Delay Mitigation in Construction Projects in Iran, *American Journal of Civil Engineering and Architecture*, 2015 3 (1), pp 15-20. Doi: 10.12691/ajcea-3-1-3.
 39. KPMG in India - PMI study (2012) Study on project schedule and cost overruns in infrastructure projects in India.
 40. Shibani, A. (2015) Time and Cost Overrun in Construction Projects in Egypt, <https://www.researchgate.net/publication/282219318>, Visited, 2nd May 2017.
 41. Mukuka, M., Aigbavboa, C., and Thwala, W. (2015) Understanding Construction Projects' Schedule Overruns in South Africa. ICCREM 2015: pp. 591-602. doi: 10.1061/9780784479377.068 ASCE.
 42. Ismail, I., Rahman, I. A. and Memon, A. H. (2013) Study of Factors Causing Time and Cost Overrun throughout Life Cycle of Construction Projects, *Proceedings of Malaysian Technical Universities Conference on Engineering & Technology (MUCET)* 3-4 December 2013 , Kuantan, Pahang.
 43. Rahman, I. A., Memon, A. H., Karim, A. T. A. and Tarmizi, A. (2013) Significant Factors Causing Cost Overruns in Large Construction Projects in Malaysia, *Journal of Applied Sciences* 13 (2): 286-293, 2013 ISSN 1812-5654 / DOI: 10.3923/ljas.2013.286.293 O 2013 Asian Network for Scientific Information.
 44. Patil, Y. K. and Bhangale, P.P. (2013) Investigation of Factors Influencing Cost Overrun in High-Rise Building Constructions. *International Journal in Latest Trends in Engineering Technology (IJLTET)*, Volume 6, Issue 3, January 2016, ISSN: 2278-621X.
 45. Mahadik, U. A. (2015). Cost Reduction in Construction Projects. *International Journal of Engineering Technology, Management and Applied Sciences*. September 2015, Volume 3, Special Issue, ISSN 2349-4476.

Sub-Contracting and Accident Risk in Construction Industry : A Case Study in Singapore

W.A. Asanka and Malik Ranasinghe

Abstract: Sub-contracting is a wide spread concept in construction project management. Convenience in mobilization, competitive cost, lower welfare and relaxed management efforts are the main factors that make sub-contracting popular. However, sub-contracting can increase the risk of accidents in construction projects. Accident risk is higher in the construction sector, and it is an adversed is advantages to the industry. Proper investigation and deployment of adequate mitigation measures are key requirements for risk management. Risk factors such as negligence, knowledge, legislations, communication, are aligned with the management system and relate to the sub-contracting process as well.

Subcontractor's contributions to construction projects can be as high as 90% of the total project cost. Main contractors are taking the overall project responsibility and authority of the commence projects work. Then, Sub contractors are invited to take part in specific work packages at execution stage. The interaction between both parties in terms of accident risk, therefore, is an essential and sensitive matter. Quantification of the accident risk is the main objective of this study. This study focuses on subcontractor's experience, communication ability, contribution and maintaining responsibility for risk mitigation, and continuous improvement. Practicing engineers and supervisors were questioned and the data was analysed to draw conclusions in this study. Practical project experience related to the study was collected from Singapore, as the Singaporean construction industry has been considerably successful in implementing safety and health regulations with low dangerous incidents.

Keywords: Subcontracting, Accident risk, Bayesian inference

1 Introduction

1.1 Subcontractor in construction industry

General contractor, the prime contractor, or the main contractor is the main party that undertakes the responsibility for projects. Contract administration, financing, material and equipment procuring, monitoring and managing the progress are some of the main contractor's obligations[1]. Sub-contractors are below the main contractor as they are only responsible for specific work items.

Main contractors are sometimes reluctant to maintain in-house resources (humans and equipment) for construction activities. Sub-contractors, on the other hand,,are small companies, with expertise skills, knowledge and machinery for specific work categories. Supplying materials, manpower, tools, equipment and designs [2] are some of the functions of sub-contractor. Competitiveness in cost, time and quality are key factors for their popularity.

1.2 Issues in the process

Sub-contracting has been identified as one of the causes of workplace accidents[3], [4]. Short operational durations and lack of concern about safety and health aspects in contractual agreements are pushing sub-contractor towards unsatisfactory performances. Ignorance or negligence is high in the process. Declining

quality and productivity standards[5], coordination and supervision difficulties should be expected to due to temporary and insecure relationships among site management team [6].

1.3 Consequences

Minor, major or fatal injuries to employees are consequences in construction incidents. Equipment or machinery damages are secondary effects. However, in terms of cost, all accidents are accountable losses on organizational financial achievements.

Reported fatality rates, around the world, are evidence of the crisis of accidents and its diversified spread[6], [7]. Fatality statistics of Singapore from 2006 to 2013 are presented in Table 1 as an example of the necessity for further investigations on accident risks.

Table 1 - Fatality in construction sector, Singapore
[<http://www.mom.gov.sg/>]

Year	2006	2007	2008	2009	2010	2011	2012	2013
Fatality	24	24	25	31	32	22	26	33

*Eng. W.A.Asanka, AMIE(SL), GMICE,Msc(HW,UK),
Design Manager, Dredging International Asia Pacific,
Singapore.*

*Eng. (Prof.) Malik Ranasinghe, Senior Professor,
Department of Civil Engineering, University of Moratuwa.*



1.4 Objectives

Objectives of this study are the quantification of the accident risk by the application of Bayesian Belief Network (BBN) model and to analyse the predicted accident risk in construction sector due to the performance of subcontractors.

1.5 Scope

The study is an indication of general accident risk associated with the sub-contracting process in Singapore. Sub-contractors daily interactions with site management staff are the main scope of this study.

2 Literature Review

2.1 General

Subletting or sub-contracting is a management process, which divides the workload among specialised contractors. The popularity, as a fraction of the project cost, is between 50% [8] to 90% [2] in total. Subcontracting is cascading down to different layers, called multilayer or latent sub-contracting, sharing work schedules or damages among layers[9] can be highlighted in multilayer sub-contracting.

The sub-contracting is more prevalent in the building construction industry than that of civil engineering or industrial sectors[10]. A Hong Kong based study classified the subcontractors to, equipment-intensive and labour-intensive according to their specialist resource availability[11]. Labour only sub-contractors are reducing the costs on mobilising or mark ups. However, temporary workforce provides the best advantages to the large firms [12], [13]. In Turkey, a study with 35 general contractors and 56 sub-contractors, concluded that work overload and time pressure is leading them towards subcontracting to secondary levels [14].

2.2 Pros and cons of the process

A misunderstanding between both parties (main and sub-contractor) may result in costly litigation or dissatisfied customers [15], while declining standards of quality, falling productivity, coordination difficulties, supervising and monitoring problems due to temporary and insecure relationship [5], [19] cause sub-contracting accidents.

A UK based studies[3], [4], reported that restricting the layers of subcontractors, working with a regular chain of subcontractors, implementing a safety and health reward scheme for subcontractors and insisting on non-working sub-contractor foremen who have direct responsibility for the safety of workers in their trade, improved safety at sites[4].

However, studies of subcontractor and main contractor with safety and health aspects are limited in the literature[16].

Lack of supervision due to distance operation of sub-contractor's official staff makes the working crew less decisive and irresponsible. The inherent risks in sub-contractors in the Singapore Construction Industry are due to low management competency [4]; Subcontracting, Foreign Workers and Job Safety [17].

However, the dependence of time, quality and cost on sub-contractors may lead overall performance of main contractor [8], [18].

Improvements of sub-contracting process can be by registration[20], [21], selection [22], [23], [24], performance rating at construction stage [8], [18], [15], [25], [26], [27], [28].

In terms of stabilising organizational financial risks at business fluctuations, multilayer contracting process is popular [2], [11], [29], [30], [31], [22], [32],[33]. Multilayer contracting makes subcontractor's overall performance more stable at business fluctuations, flexibility in workforce coordination, and reduction of management cost [29] and are highlighted as positive trends in the industry.

2.3 Synopsis of literature review

Sub-contracting process has certain constraints. However, it is a management process and one of necessity in the construction industry. Therefore proper administration, management, and regulatory aspects are required to maintain healthier and safer work places.

Accident risk is one of the key disadvantage inherent with the subcontracting process in the construction industry. Difficulties in the interaction between sub-contractor with the main contractor enhance the health and safety risks, which have less attention from the research community.

3 Methodology

The methodology of this study is, constructing a Bayesian Belief Network (BBN) by gathering both quantitative and qualitative information through expert opinions and literature review. Parent and child nodes of the BBN were defined according to the expert opinions. Then further data will be used to learn BBN to use in accident risk prediction of sub-contractor performance.

A freely available academic version of Uninet software is used to construct BBN. Bayes inference concept as described in Eqn. 1 is inherent with the software. Normal copulas

were used in the current implementation to model influences from parent nodes.

The BBN model is based on the following Bayesian concepts as given in Eqn. 1.,

$$P(e/c) = \sum \frac{P(c/e) \times P(e)}{P(c/e) \times P(e) + P(c/\bar{e}) \times P(\bar{e})} \dots E1$$

P(effect/cause) = posterir probability

P(cause/effect) = likelihood probability

P(cause) = prior/marginal probability

P(cause/effect) = 1 – P(cause/̄effect)

P(effect) = 1 – P(̄effect)

3.1 Model development

Initially, 5 construction industry professionals with over 10 years of experience in Singapore construction industry were interviewed to categorise risk factors related to Sub-contractors. All of them started their career as site engineers and proceeded to project engineer (2 of them) followed by project managers (3 persons).

Five major risk drivers could be identified in the interviews T1.1:Experience, T1.2:Communication ability, T1.3:contributing

to risk mitigation, T1.4:Holding the responsibility, and T1.5:Continual improvement. These factors were taken as Tier 1, the parents of the accident risk in the model.

The construction site is a complex network with anenormous amount of activities. Data collection requires more tangible divisions of risk factors. Therefore, four major site activity ratings (Tier 2) and causes affecting their ratings were proposed in the current study for data collection, i.e.T2.1:Method Statement (MS),T2.2:Risk Assessment (RA),T2.3:Site Work (SW),and T2.4:Site Management (SM). Finally, data were collected for the marginal probability distribution of each cause through expert opinions.

Causes affecting the ratings (Tier 3) have been set up using daily site activities of the site management team. Repetitive occurrences of those causes are much familiar with experts thus expected accuracy could be acceptable. Singapore national statistics were accessed for estimation of accident risk at present. The model is presented in Figure 1.

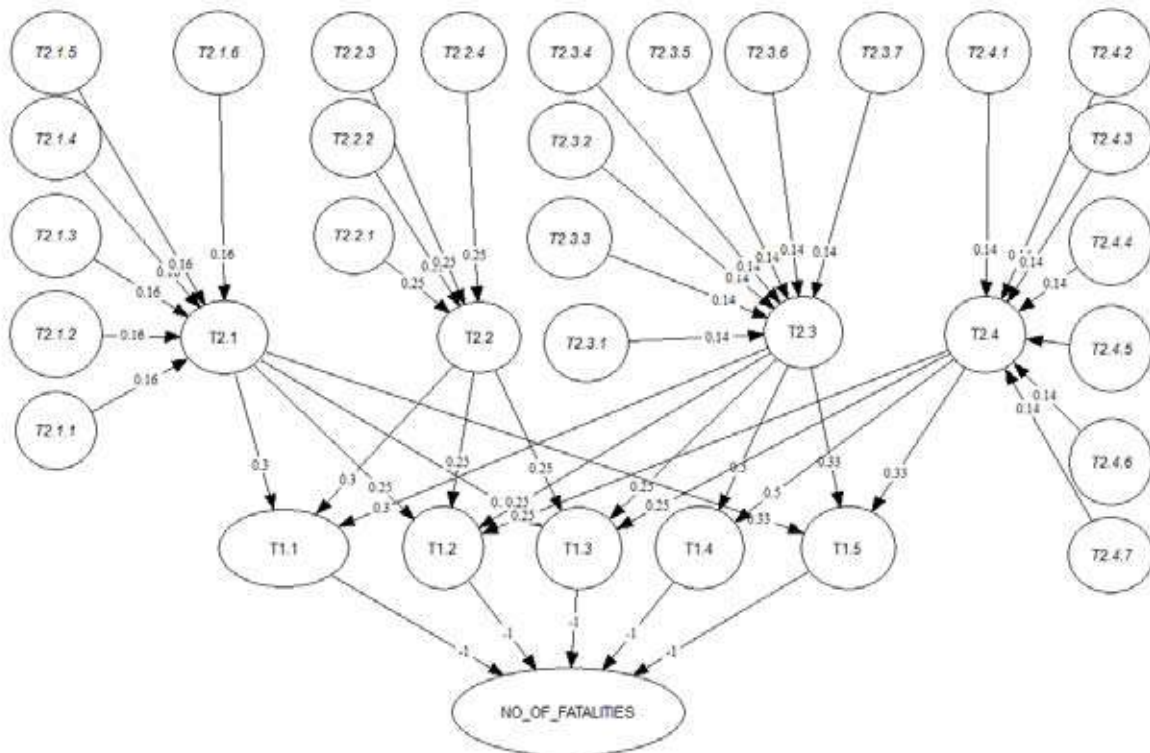


Figure 1 - BBN with dependencies on each effect with cause

4 Data collection

4.1 Nominating the four ratings in Tier 2

Main contractor’s engineers deal with sub-contractors on a daily basis when managing the construction sites. Method Statement (MS) and

Risk Assessment (RA) are two main items in sub-contractors documentation scope.

A method statement is a document expressing sub-contractor’s expertise about the work they are about to engage. Proper reviewing of work scope of which have to be done is a good indication of the sub contractor’s performance.



MS represents industry updates, especially about updated safe work methods and incident studies. are vital in preparation of the content of the MS.

Similarly, the Risk Assessment also caters to determining applicable work sequence for specific site conditions and require expert guidance in assessing and predicting upcoming risks.

Site work is a major concern, and it is the key to control accidents. Responsibility, commitment, and vigilance are key areas investigated in this research study. Following are the brief content of each item that has been studied

Ratings of site work and site management is the second step of sub-contractors involvement with main contractor's site staff. Over 90% of interviewees agree to use of the four ratings as sub-contractors' performance evaluation indexes.

When nominating the tier 2 ratings, 15 site engineers and 20 site supervisors were interviewed. All of them had over 5years of experience in Singapore construction projects.

4.2 Conditional relationship between nodes& prior probabilities

Four ratings at Tier 2 and causes in Tier 3, Risk drivers in Tier 1 with ratings are connected with parent child relationships in Uninet software. Interrelations for more than one parent per child are factorised equally, assuming the same influence from each parent.

Interviews with 3 experts from health and safety departments were convinced about these relationships and followed their guidance. Tier 1 factor's effect on a number of fatalities is taken as negative. Prior probabilities of Tier 1 & 2 factors assumed as uniform distributions with mean value 0.5.

4.3 Status of fatalities

No of fatalities has been modelled using poison distribution (Eqn. 2) as prior information which is to be updated with influence data. Rolling average of cumulative months has been used to enhance the accuracy of predictions. However, as poison distribution is not integrated with Uninet software, therefore equivalent Beta

Table 3 - Tier 2 and 3 Factors& Average ratings

ID	Causes and Effects (Tier 2 & 3)	Rate				
		1	2	3	4	5
T2.1	Method statement (MS) Rating					
T2.1.1	Content relevant to work scope	2%	15%	51%	25%	7%
T2.1.2	Properly reviewed the Main contractors drawings	2%	9%	40%	38%	11%
T2.1.3	Work sequence is relevant	2%	5%	22%	51%	20%
T2.1.4	Up to date safest Work method proposed	2%	13%	39%	33%	13%
T2.1.5	Proper equipment is proposed	5%	33%	44%	16%	2%

distribution (Eqn. 3) was used with alpha and beta fitted with least square fitting method.

$$\lambda^k e^{-\lambda} / k! \dots \dots \dots E2$$

$$\frac{x^{\alpha-1}(1-x)^{\beta-1}}{B(\alpha,\beta)} \dots \dots \dots E3$$

$$B(\alpha,\beta) = \frac{\tau(\alpha)\tau(\beta)}{\tau(\alpha+\beta)}, \alpha = 18.40, \beta = 51.08$$

Table 2 - Fatalities in Singapore, "Work place safety and health report,2015 National statistics."

Year	Fatality rate	Rolling average
2006	24	24.00
2007	24	24.00
2008	25	24.33
2009	31	26.00
2010	32	27.20
2011	22	26.33
2012	26	26.29
2013	33	27.13
2014	27	27.11
2015	26	26.50

4.4 Questionnaire based data collection for Tier 3: marginal distributions of risk factors

A questionnaire was used to collect data for Tier 3 risk factors. Background information of the respondents was questioned at the beginning to confirm respondent's position, work scope and company type followed by risk factors. Then, all tier 3 factors were asked to rate in 1~5 scale. There were 55 respondents participated in the study.

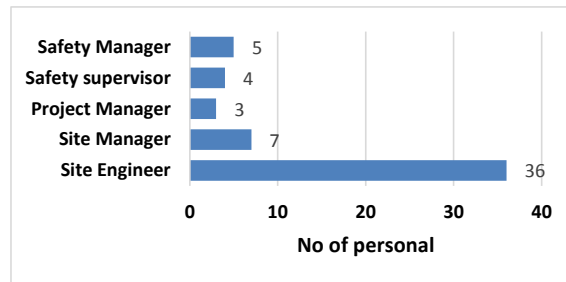


Figure 2 - Positions and number of respondents

All the respondents are selected above 5 years of experience. All of them possesses basic safety and health training which is mandatory in Singapore (www.mom.gov.sg).

Average ratings for each factor are summarized in Table 3.



	T2.1.6	Equipment maintenance is up to date	2%	18%	38%	29%	13%
T2.2		Risk Assessment (RA) Rating					
	T2.2.1	Risk identification	2%	13%	41%	35%	9%
	T2.2.2	Risk estimation	5%	35%	40%	16%	4%
	T2.2.3	Contingency Plan provided & adequate	2%	4%	37%	44%	13%
	T2.2.4	Recovery Plan provided & adequate	2%	11%	36%	40%	11%
T2.3		Site work Rating					
	T2.3.1	Relationship with main contractors site staff	2%	13%	36%	42%	7%
	T2.3.2	Sufficient supervisory staff is deployed	7%	35%	38%	16%	4%
	T2.3.3	Effectiveness of supervision	2%	33%	45%	18%	2%
	T2.3.4	Proper equipment provided	2%	7%	33%	44%	13%
	T2.3.5	Adhered to proposed work method in MS	2%	11%	33%	40%	15%
	T2.3.6	Efficiency of incident reporting	4%	35%	42%	18%	2%
	T2.3.7	Approach on rectification of unsafe acts or conditions	2%	5%	31%	49%	13%
T2.4		Site Management rating					
	T2.4.1	Competency of site staff	2%	2%	27%	51%	18%
	T2.4.2	Actions to rectify unsafe acts / conditions	2%	7%	25%	47%	18%
	T2.4.3	Instruction to site staff	2%	27%	51%	18%	2%
	T2.4.4	Approach on MS review	4%	38%	40%	16%	2%
	T2.4.5	Approach on RA review	7%	36%	36%	16%	4%
	T2.4.6	Extend of foreign workers deployment	0%	0%	5%	29%	65%
	T2.4.7	Awareness of emergency procedures	2%	19%	35%	30%	13%

5 Analysis and Results

The advantage in the Bayesian inference model is learning with available data and predicting the future situations with given initial conditions. Sensitivity analysis option built in with Uninet software evaluates most sensitive factors for current accident occurring. Table 4 summarises the sensitivity data.

Table 4 - Sensitivity analysis

Predicted Variable	Base Variable	Rank Correlation	Remark
Part 1			
NO_OF_FATAL ITIES	T1.1	-0.6003	Highest
	T1.2	-0.5987	
	T1.3	-0.5862	
	T1.4	-0.5232	
	T1.5	-0.5505	
Part 2			
T1.1	T2.1	0.2925	
T1.1	T2.2	0.2947	Highest
T1.1	T2.3	0.2732	
T1.1	T2.4	0.0071	
Part 3			
T1.2	T2.1	0.233	
T1.2	T2.2	0.2494	
T1.2	T2.3	0.2577	Highest
T1.2	T2.4	0.2165	
Part 4			
T1.3	T2.1	0.2587	Highest
T1.3	T2.2	0.2381	
T1.3	T2.3	0.2320	

T1.3	T2.4	0.2308	
Part 5			
T1.4	T2.1	-0.0034	
T1.4	T2.2	0.0121	
T1.4	T2.3	0.4957	Highest
T1.4	T2.4	0.4294	
Part 6			
T1.5	T2.1	0.3084	
T1.5	T2.2	0.0094	
T1.5	T2.3	0.3332	Highest
T1.5	T2.4	0.2908	
Part 7			
T2.1	T2.1.1	0.1551	
T2.1	T2.1.2	0.1556	Highest
T2.1	T2.1.3	0.1481	
T2.1	T2.1.4	0.1467	
T2.1	T2.1.5	0.1379	
T2.1	T2.1.6	0.1481	
Part 8			
T2.2	T2.2.1	0.2342	Highest
T2.2	T2.2.2	0.2267	
T2.2	T2.2.3	0.2234	
T2.2	T2.2.4	0.2083	
Part 9			
T2.3	T2.3.1	0.1212	
T2.3	T2.3.2	0.1257	
T2.3	T2.3.3	0.1346	Highest
T2.3	T2.3.4	0.1308	
T2.3	T2.3.5	0.1315	
T2.3	T2.3.6	0.1274	
T2.3	T2.3.7	0.1254	
Part 10			



T2.4	T2.4.1	0.1311	
T2.4	T2.4.2	0.1375	Highest
T2.4	T2.4.3	0.1302	
T2.4	T2.4.4	0.1289	
T2.4	T2.4.5	0.1272	
T2.4	T2.4.6	0.0950	
T2.4	T2.4.7	0.1110	

Rank correlation of each predicted variable is highlighting the individual contribution to its base variable. With respect to correlations, T1.1 (Experience) is the highest and T1.2 (Communication ability), T1.3 (contributing to risk mitigation), T1.4 (Holding the responsibility), and T1.5 (Continual improvement) have proven their importance through significant ranks.

Each part of the analysis in Table 14 has its own highest correlation to base variable. When considering the tier 3 variables T2.1.2 (Properly reviewed the Main contractors drawings), T2.2.1 (Risk identification), T2.3.3 (Effectiveness of supervision), and T2.4.2 (Actions to rectify unsafe acts / conditions) it is highly clear that effectiveness in day to day work activities or how individuals review their surrounding leads the accidents, paying attention on work is required for mitigation.

All of these factors are management related and there is higher chance to achieve good performance by implementing proper management system.

Singapore achieved good health and safety performance through careful deployment of competent personal to work sites. Required training and inductions prior to work is mandatory. Regulatory framework is smart and wider to capture unpredicted situations of work sites. It is highly recommended to deploy experienced personal for certain works in all construction projects since the experience is essential to deliver quality and reliability tasks successfully.

6 Conclusions

Objectives of this study were to quantify the accident risk by the application of Bayesian Belief Network (BBN) model and to analyse the predicted accident risk in construction sector due to the performance of subcontractors.

The study showed experience is the main cause of accidents and it has -0.6003 correlation with fatalities. Work procedure, work environment, supervision are key elements, which can be the cause of experience, identified in the "Safety

Analysis & Recommendation Report on Work at Height" by MOM, Singapore.

Communication, mitigation, responsibility and continual improvements are also equally important in the prevention of accidents.

Developed model in the current study is the status of Singapore industry. This model with marginal probabilities of risk factors (Tier 3 parameters) can be used for another similar environment, Srilankan industry, to predict fatality risks. The authors would like to extend the study towards Sri Lankan construction industry to identify steps necessary to improve safety and health performance of Sri Lanka.

References

1. Benjaoran, V., "A cost control system development: A collaborative approach for small and medium-sized contractors," *Int. J. Proj. Manag.*, vol. 27, no. 3, pp. 270-277, 2009.
2. Kumaraswamy, M. M., and Matthews, J. D., "Improved subcontractor selection employing partnering principles," *J. Manag. Eng.*, vol. 16, no. 3, pp. 47-57, 2000.
3. Sabet, P. G. P., Aadal, H., Jamshidi, M. H. M., and Rad, K. G., "Application of Domino Theory to Justify and Prevent Accident Occurrence in Construction Sites," *IOSR J. Mech. Civ. Eng.*, vol. 6, no. 2, pp. 72-76, 2013.
4. Manu, P., Ankrah, N., Proverbs, D., and Suresh, S., "Mitigating the health and safety influence of subcontracting in construction: The approach of main contractors," *Int. J. Proj. Manag.*, vol. 31, pp. 1017-1026, 2013.
5. Heery, E., and Salmon, J., "Introduction: The Insecure Workforce," *Manag. Res. NEWS*, vol. 21, pp. 7-8, 1998.
6. Ling, F. F. Y. Y. F. Y. Y. F. Y. Y., Liu, M., and Woo, Y. C. Y. C. Y., "Construction fatalities in Singapore," *Int. J. Proj. Manag.*, vol. 27, pp. 717-726, 2009.
7. Hämäläinen, P., Takala, J., and Saarela, K. L., "Global estimates of occupational accidents," *Saf. Sci.*, vol. 44, pp. 137-156, 2006.
8. Albino, V., and Garavelli, A. C., "A neural network application to subcontractor rating in construction firms," *Int. J. Proj. Manag.*, vol. 16, no. 1, pp. 9-14, 1998.
9. Shimizu, J. Y., and Cardoso, F. F., "Subcontracting and cooperation network in building construction: a literature review," *Proc. IGLC-10, Gramado-RS*, 2002.
10. Clough, A., hr; Sears, "Construction Contracting," *Constr. Contract. Law Manag.*, vol. 7, no. Jan, pp. 12-31, 2005.
11. Thomas Ng, S., Tang, Z., and Palaneeswaran, E., "Factors contributing to the success of equipment-intensive subcontractors in

- construction," *Int. J. Proj. Manag.*, vol. 27, no. 7, pp. 736-744, 2009.
12. Bresnen, M., Wray, K., Bryman, A., Beardsworth, A. D., Ford, J. R., and Keil, E. T., "The Flexibility of Recruitment in the Construction Industry: Formalisation or Re-Casualisation?," *Sociology*, vol. 19, no. 1, pp. 108-124, 1985.
 13. Beardsworth, a D., Keil, E. T., Bresnen, M., and a Bryman, "Management, Transience and Subcontracting: the Case of the Construction Site," *J. Manag. Stud.*, vol. 25, no. 6, pp. 603-625, 1988.
 14. Assaf, S. A., and Al-Hejji, S., "Causes of delay in large construction projects," *Int. J. Proj. Manag.*, vol. 24, no. 4, pp. 349-357, 2006.
 15. Sturts Dossick, C., and Schunk, T. K. "Subcontractor Schedule Control Method," *J. Constr. Eng. Manag.*, vol. 133, no. 3, pp. 262-265, 2007.
 16. Daykin, N., "Workplace health promotion: Issues and strategies for the insecure workforce," 1997.
 17. Debrah, Y. A., and Ofori, G., "Subcontracting, Foreign Workers and Job Safety in the Singapore Construction Industry," *Asia Pacific Bus. Rev.*, vol. 8, no. 1, pp. 145-166, 2001.
 18. Mbachu, J., "Conceptual framework for the assessment of subcontractors' eligibility and performance in the construction industry," *Constr. Manag. Econ.*, vol. 26, no. July 2015, pp. 471-484, 2008.
 19. Costantino, N., Pietroforte, R., and Hamill, P., "Subcontracting in commercial and residential construction: an empirical investigation," *Constr. Manag. Econ.*, vol. 19, no. 4, pp. 439-447, 2001.
 20. Ng, S. T., Luu, C. D. T., and Chu, A. W. K., "Delineating criteria for subcontractors registration considering divergence in skill base and scales," *Int. J. Proj. Manag.*, vol. 26, no. 4, pp. 448-456, 2008.
 21. Ng, S. t T., and Luu, C. D. T., "Modeling subcontractor registration decisions through case-based reasoning approach," *Autom. Constr.*, vol. 17, no. 7, pp. 873-881, 2008.
 22. Okoroh, M. I., and Torrance, V. B., "A model for subcontractor selection in refurbishment projects," *Constr. Manag. Econ.*, vol. 17, pp. 315-327, 1999.
 23. Arslan, G., Kivrak, S., Birgonul, M. T., and Dikmen, I., "Improving sub-contractor selection process in construction projects: Web-based sub-contractor evaluation system (WEBSES)," *Autom. Constr.*, vol. 17, no. 4, pp. 480-488, 2008.
 24. Okoroh, M. I., "A knowledge based decision support and risk management system for the selection of sub-contractors for refurbishment projects," *Beijing, China*, 1996.
 25. Chiang, Y. H., "Subcontracting and its ramifications: A survey of the building industry in Hong Kong," *Int. J. Proj. Manag.*, vol. 27, no. 1, pp. 80-88, 2009.
 26. Ko, C. H., Cheng, M. Y., and Wu, T. K., "Evaluating sub-contractors performance using EFNIM," *Autom. Constr.*, vol. 16, no. 4, pp. 525-530, 2007.
 27. Maturana, S., Alarcón, L. F., Gazmuri, P., and Vrsalovic, M., "On-Site Subcontractor Evaluation Method Based on Lean Principles and Partnering Practices," *J. Manag. Eng.*, vol. 23, no. 2, pp. 67-74, 2007.
 28. Wang, W. C., and Liu, J. J., "Factor-based path analysis to support subcontractor management," *Int. J. Proj. Manag.*, vol. 23, no. 2, pp. 109-120, 2005.
 29. Yik, F. W. H., and Lai, J. H. K., "Multilayer subcontracting of specialist works in buildings in Hong Kong," *Int. J. Proj. Manag.*, vol. 26, no. 4, pp. 399-407, 2008.
 30. Arditi, D., and Chotibhongs, R., "Issues in Subcontracting Practice," *J. Constr. Eng. Manag.*, vol. 131, no. 8, pp. 866-876, 2005.
 31. Hsieh, T.-Y., "The economic implications of subcontracting practice on building prefabrication," *Autom. Constr.*, vol. 6, no. 3, pp. 163-174, 1997.
 32. Olson, R., "Subcontract coordination in construction," *Int. J. Prod. Econ.*, vol. 5273, no. 97, pp. 503-509, 1998.
 33. Perng, Y. H., Chen, S. J., and Lu, H. J., "Potential benefits for collaborating formwork subcontractors based on cooperative game theory," *Build. Environ.*, vol. 40, no. 2, pp. 239-244, 2005.



Techno-Economic Analysis of Building Energy System with Net Meter Solar PV in Sri Lanka

K.T.M.U. Hemapala and T.M.S.C. Jayasinghe

Abstract: Optimum net meter solar PV capacity to be installed is depend on various factors such as tariff category, solar irradiation, building load profile, maximum demand of the building etc. Thus it is essential to do a techno economic analysis for deciding the most feasible PV system capacity. A methodology is proposed to develop an optimum energy solution tool using techno- economic analysis of building energy system with net meter solar PV in Sri Lanka considering three key variable parameters; load profile, tariff scheme and the maximum demand. The software HOMER was used to model the energy system and the tool is developed in Microsoft Excel. HOMER simulation has done for 114 cases by changing the above mentioned key parameters. Selected results from HOMER simulation such as PV system cost, capital cost, replacement cost, O &M cost, cost of energy, renewable fraction, simple payback period, discounted payback period etc., are extracted and stored in an Excel based database. Developed tool has three inputs as key variables; load profile, tariff scheme and the maximum demand. And Optimum solar PV capacity to be installed, related PV system investment cost, cost of energy, payback period are the outputs. If the user cannot go for the optimum PV capacity due to the limitations on cost or area, then this tool can be used to select whatever the other feasible capacity and to compare them. This tool is more convenient for any user even without much knowledge on net meter solar PV installations and can see the feasibility of it without having consultancy from solar panel providers. The tool developed has been verified considering two actual situations.

Keywords: Optimum PV Capacity, Load Profile, Tariff Scheme, Maximum Demand

1. Introduction

Green building concept is widely considered in Sri Lanka. Optimizing the building energy system with renewable energy sources is also play a major role in this concept. Different types of renewable energy technologies can be used depend on their feasibility, and net meter solar Photovoltaic (PV) is very popular in Sri Lanka.

However solar PV installation should be a feasible solution in both economically and technically. Before the installation, a feasibility analysis should be carried out to obtain maximum outcome of it. Solar PV optimum capacity to be installed is depend on various parameters such as tariff category, solar irradiation, PV system technical characteristic, building load profile, maximum demand of the building etc. Thus it is essential do a proper analysis to decide the PV system capacity and also important to know about the investment, cost of energy, payback period etc.

There are many computer software tools capable of analyzing the integration of renewable energy systems. For all those software need various parameters as inputs such as tariff data, solar irradiation levels, PV system cost, load variation pattern and etc.

Thus at the conceptual design stage of a building it is tedious to do such analysis. Instead user friendly method is preferred to obtain optimum combination of net meter PV system with important factors such as cost of energy, installation cost, payback period & etc. and it will be really helpful at the conceptual design stage. During the detailed design stage of PV installation, the results of the conceptual design could be considered as input information.

1.1 Net Meter PV System

In the concept of the net metering, consumers are allowed to connect their on site renewable generators to the grid. Consumers have to pay only for the difference of export and import energy units. Import energy is the amount of energy units which a user consumed from the utility grid per month whereas the export energy is the amount of energy supplied by the on- site generation to the grid. In the concept of net metering input / export energy meter is used instead of normal energy meter. Figure 1 shows an arrangement of net meter solar system. [14]

Eng. (Dr.) K. T. M. U. Hemapala, MIE(SL), B.Sc.Eng. (Moratuwa), Ph.D.(Italy), Senior Lecturer, Department of Electrical Engineering, University of Moratuwa.
Eng. (Ms.) T.M.S.C. Jayasinghe B.Sc.Eng. (Peradeniya), M.Sc.Eng. (Moratuwa. AMIE (SL) Electrical Engineering Department of Buildings.



The billing period is one month. At the end of a billing period the bill is prepared according to the difference between import and export energy units. There may be an excess electricity due to the high number of export units than import units. In such cases, that excess amount will be carried forward to use in future. The energy balancing of export and inputs units is carried out within the same tariff tier and credit in one tier is not transferable to another tier.

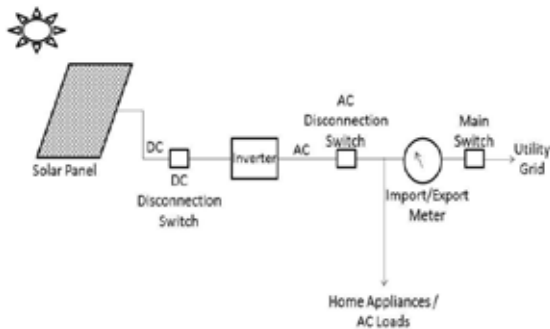


Figure 1 - Solar PV Net Metering Arrangement [14]

1.2 Electricity Load Profile in Buildings

Load profile gives the variation of the electrical load versus time. This will vary according to the customer type such as residential, commercial and industrial. Load profile represents the loading pattern of various electrical loads belong to an electrical installation. When considering the Sri Lankan buildings, there are several load profile based on the building usages such as office buildings, super markets, fashion outlets, banks, hospitals, hotels, prisons etc. Those variation details are obtained from a previous research [13] and shown in Table 1.

2 Literature review

Several researches are carried out to optimize the energy systems and to analyze reliable electricity with renewable energy using various software [2]. Software HOMER is widely used to analyze a stand-alone systems [6], [7]. Many researches have been done to find out optimal renewable energy system parameters including solar PV for grid connected systems [3], [4], [5] and [12]. But in many of these, only a single load variation and one tariff scheme are considered. They are like case studies and no tool was developed to have a general idea for different cases. [9], [10], [11].

There are few tools developed nationally and internationally to find out capital cost and

payback period. But they have limitations such as considered only a single category (Ex: Residential), no load variation pattern is considered etc. Sri Lanka Sustainable Energy Authority (SLSEA) has developed a tool which helps to select the most economical net meter solar panel system based on the investment and the average electricity bill [15]. This tool has no capability to decide the optimum system capacities. And also it is considered only residential buildings and not considered the load variation patterns.

3 Modelling and Simulation

3.1 Model Proposal

Figure 2 shows the proposed model which contains three selectable inputs, a database and an output. The first input is the type of the building (cluster) which is based on the load variation pattern of the building as Commercial, Office, Hotel etc (12 clusters with load curve are considered). The second input is the tariff category which is based on applicable tariff scheme on Commercial, Office, Hotel tariff schemes (GV2, GP2 & H2 are considered; as CEB tariff scheme [16]) and the third input is the maximum load demand range of the building. Optimization model contains a database which contain optimized net meter solar PV system parameters which are analyzed using a micro power system optimization software.

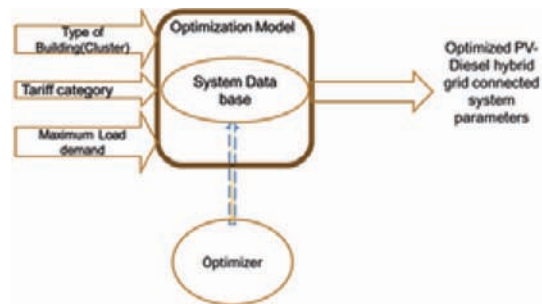


Figure 2 - Proposed Model

3.2 HOMER Simulation

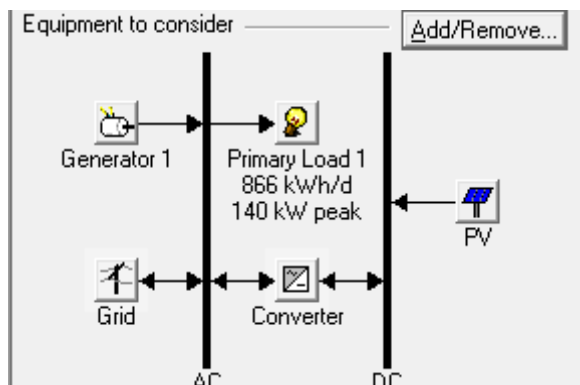


Figure 3 - Developed model in HOMER

Table 1- Cluster Description with Sample Installations [13]

Cluster	Example installations	Possible tariff categories
Cluster 2	Government banks, Government offices, University, Educational Institute type 1 , Embassy offices type 1, High commissioner's offices, Municipal Councils	GV2 , GP2
Cluster 4	Financial institute office, Fashion Outlets type 1	GP2
Cluster 5	Private banks, Private company offices type 1, Insurance offices	GP2
Cluster 6	Show rooms(shoes), Apartments	GP2
Cluster 7	Hospitals type 1, Embassy office type 2, Institute type 2, Private company office type 2	GV2 , GP2
Cluster 8	Utility service officers, Hotel type 1	GP2 , H2
Cluster 9	Hotels type 2, Hospitals	GV2, GP2 , H2
Cluster 12	Hotels type 3	H2
Cluster 13	Prisons	GV2 , GP2
Cluster 14	Super markets(consumer goods, electrical items), Food outlets, Fashion Outlets type 2	GP2
Cluster 16	Railway Stations, Hotel type 4	GP2 , H2
Cluster 17	Fashion Outlets type 3, Private company office type 3	GP2

As shown in Figure 3, HOMER simulation is consisted with a Primary load, Generator, PV, Converter and Grid. Electrical demand of a power system at a time is identified as the primary load in HOMER. But it will add randomness to the synthesized data in order to have a unique pattern for everyday load. Randomness is specified by the user.

HOMER assumes that the diesel generator fuel curve which is shown in Equation 1, is a linear variation [1]. Fuel curve is obtained considering the fuel consumption per hour and respective output power generation capability.

$$F = F_0 Y_{gen} + F_1 P_{gen} \quad \dots(1)$$

Where F_0 is the fuel curve intercept coefficient, F_1 is the fuel curve slope, Y_{gen} the rated capacity of the generator (kW), and P_{gen} the electrical output of the generator (kW). Unit of F is depend on the unit of fuel if fuel is in liters, F is l/h.

Fixed cost of energy of the generator is calculated using the equation 2 [1].

$$C_{gen, fixed} = C_{om, gen} + (C_{rep, gen} / C_{rep, gen}) + F_0 Y_{rep, gen} C_{fuel, eff} \quad \dots(2)$$

where $C_{om, gen}$ is the O&M (Operational and Maintenance) cost in dollars per hour, $C_{rep, gen}$ the replacement cost in dollars, R_{gen} is the generator lifetime in hours, F_0 is the fuel curve intercept coefficient in quantity of fuel per hour per kilowatt, Y_{gen} is the capacity of the generator (kW), and $C_{fuel, eff}$ is the effective price of fuel in dollars per quantity of fuel.

Marginal cost of energy of the generator which is the additional cost other than the fixed cost in dollars per hour is calculated using equation 3 [1] in HOMER.

$$C_{gen, mar} = F_1 C_{fuel, eff} \quad \dots(3)$$

Where F_1 is the fuel curve slope in quantity of fuel per hour per kWh and $C_{fuel, eff}$ is the effective price of fuel in dollars per quantity of fuel.

PV array can produce DC electricity in HOMER. Electricity generation of the PV array is directly proportion to the global solar



irradiation on it. Power output of the PV array is given by equation 4[1].

$$P_{PV} = f_{PV} Y_{PV} (I_T / I_S) \quad \dots(4)$$

Where, f_{PV} is the PV derating factor, Y_{PV} is the rated capacity of the PV array (kW), I_T is the global solar radiation incident on the surface of the PV array (kW/m²), and I_S is the standard amount of radiation used to rate the capacity of the PV array. I_S is 1 kW/m².

Solar resource data should be provided by the user in order to model a system containing a PV array. Monthly average solar irradiation level and the latitude for the location of interest can be given. Then HOMER generates synthetic hourly solar irradiation data. For this HOMER use an algorithm developed by Graham and Hollands [8].

In HOMER, grid is also available. Consumers can purchase AC electricity from grid and sell back to grid. The tariff scheme can be modeled with peak, off-peak, day, etc. To model the purchasing cost from the grid, kVA demand charge can be also modeled. HOMER considers all the tariff charges and demand charges for a billing period. HOMER can also model net metering systems with the one month billing period.

There is no direct method to model the grid outage in HOMER. HOMER generator will not be running unless the cost of grid purchasing power unit exceeds the cost of generator power. Thus a generator to be run in the system grid power unit cost should be higher than generator power unit cost. In order to model the grid outage above mentioned feature in HOMER was used. By making the generator to be forced ON and introducing higher rate for grid power as compared with cost of generator power during that period, 0grid outage has been modeled.

In order to figure out the grid outage percentage and its occurrence two studies are done for real situations; standby generator operation at Geological Survey & Mines Bureau -Pitakotte and at "Suhurupaya", Baththaramulla. Based on above real data grid outage is assumed as 1%.

Based on this assumption, generator and grid inputs are adjusted. New tariff is introduced as 'grid off' and generator is forced 'ON' during that that period. No energy will be purchased

from the grid under the grid off tariff, as shown in Figure 4. This will also require a modification of the grid feed-in tariff schedule to prevent the sale of electricity back to grid that is not available. This can be achieved by altering the HOMER grid inputs for grid feed in tariff to be \$0 when the "Grid off" is scheduled. So this will not affect the net present cost. It affects the net purchases figure, but this aspect has not been considered for the development of the tool in the present study.

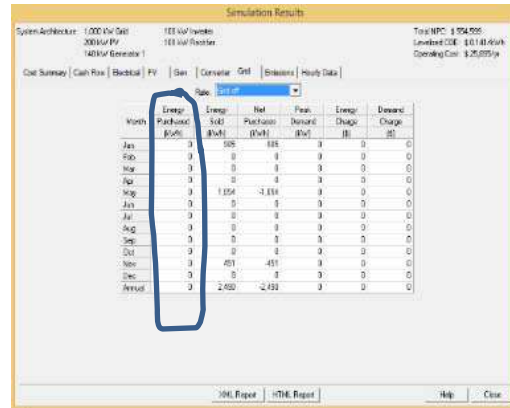


Figure 4 - Simulation Results When Grid Outage

Total net percent cost is the main parameter which represent the system life cycle cost. By considering the capital, maintenance, running (fuel), replacement cost and salvage values of each and every component in the micro power system, net percent cost is calculated in HOMER.

Salvage value for each component is calculated by Equation 5 [1]. This is the component value at the end of the project life time.

$$S = C_{rep} (R_{rem} / R_{comp}) \quad \dots(5)$$

where S is the salvage value, C_{rep} the replacement cost of the component, R_{rem} the remaining life of the component, and R_{comp} the lifetime of the component.

HOMER uses the total Net Present Cost (NPC) as its primary economic figure of merit and calculates using Equation 6 [1].

$$C_{NPC} = C_{ann,tot} / CRF(i, R_{proj}) \quad \dots(6)$$

Where $C_{ann,tot}$ is the total annualized cost, i the annual real interest rate (the discount rate), R_{proj} the project lifetime, and $CRF()$ is the capital recovery factor, given by Equation 7[1].

$$CRF(i, N) = \frac{i(1+i)^N}{(1+i)^N - 1} \quad \dots(7)$$

Where i is the annual real interest rate and N is the number of years. HOMER uses Equation 8 [1] to calculate the levelized cost of energy:

$$COE = \frac{C_{ann,tot}}{E_{prim} + E_{def} + E_{grid,sales}} \dots\dots(8)$$

where $C_{ann,tot}$ is the total annualized cost, E_{prim} and E_{def} are the total amounts of primary and deferrable load, respectively, that the system serves per year, and $E_{grid,sales}$ is the amount of energy sold to the grid per year.

The average cost per kilowatt-hour of electrical energy produced by the energy system is called as levelized cost of energy (CoE).

3.3 Comparison of the Simulation Results

For the simulation, some parameters such as solar irradiance level, economic parameters, PV cost, Inverter cost, Generator cost are considered as constant for all analysis. But the tariff category, maximum load demand and load curve is changing accordingly.

Figure 5 shows, the variation of the optimum PV system capacity with maximum load demand and cluster type in same tariff category (GP2). It clearly shows that the optimum PV capacity is highly consumer based. Thus every building should be analyzed separately to decide the optimum PV capacity.

4 Analysis of the Tool Development

HOMER simulation has done for 114 cases by changing the parameters of base model such as

tariff category, load curve (cluster type) and maximum load demand.

For a single case there is an optimum energy combination. But this optimum point may not be achievable due to the practical limitations such as area limitation, investment cost etc. Therefore other feasible combinations are also considered to develop this database tool.

This tool gives the optimum net meter solar PV capacity with minimum cost of energy and other feasible combinations with payback period. Graphical output shows how the system parameters such as CoE, payback period, area requirement, solar PV system cost and renewable energy percentage varies with feasible PV combinations. And also this can be used to compare other feasible systems with the optimum PV capacity.

Always the best energy combination is the one which gives minimum CoE. User can select other feasible solar PV systems as well but with the net metering concept, solar PV installation beyond the optimum capacity is economically less feasible.

4.1 Tool Development

Figure 6 illustrates the algorithm used for the tool development. Selected results from HOMER simulation such as PV system cost, capital cost, replacement cost, O &M cost, cost of energy, renewable fraction, simple payback period, discounted payback period etc., are extracted and stored in an Excel based database.

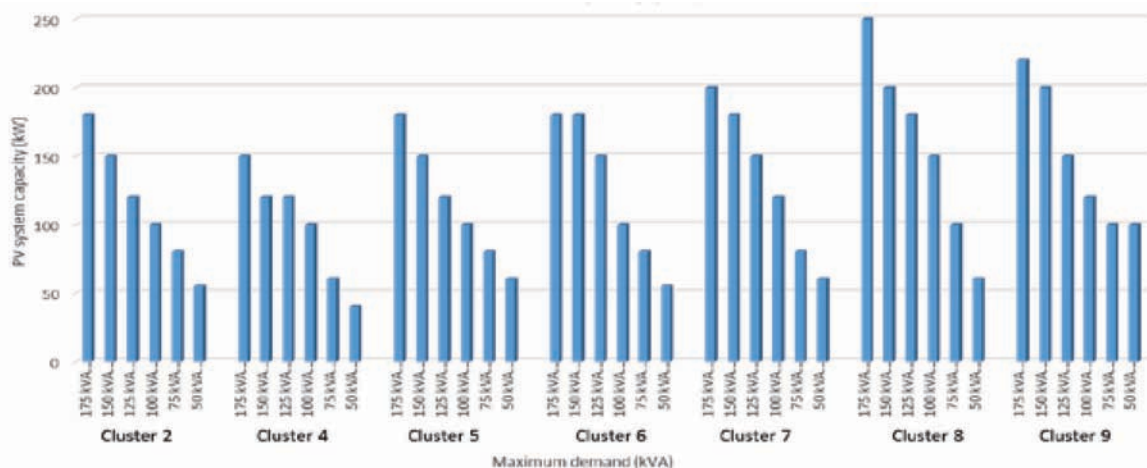


Figure 5 - Optimum PV capacity for different clusters with varying maximum demand



Microsoft visual basic in excel is used for programming. HOMER results are compared to select best suitable energy combination based on system cost and area limitations. Those comparison shows how the CoE and renewable energy fraction varies with solar PV capacity, how the PV system cost and the area requirement varies with solar PV capacity and how the simple and discounted payback periods are varies with solar PV capacity.

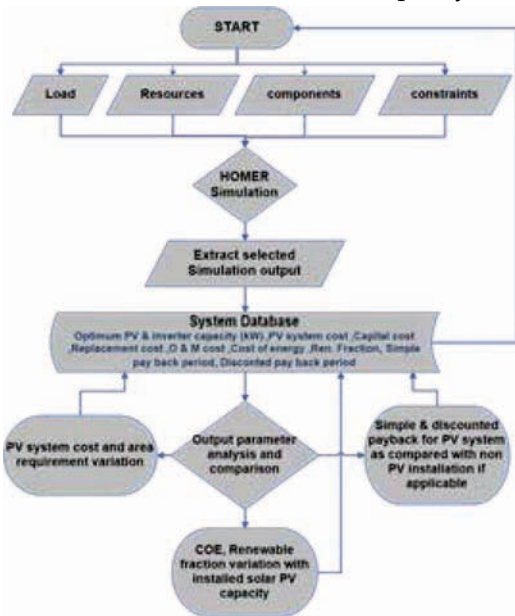


Figure 6 - Tool development algorithm

4.2 Data Retrieval from the Tool

Microsoft visual basic in excel is used for programming to retrieve the relevant data from the database. Front page of the tool contains all necessary instruction to user for data obtaining from this tool. There is a table which describe the cluster with example installations and the applicable tariff category.

By pressing (Ctrl+D), a window will popup which contains 3 selectable inputs. User can select these inputs; tariff category, average maximum demand and load profile (cluster type) based on their building with the details in front page. By pressing the “Build” button, the tool will give the relevant details to the user required building. By pressing the “Clear” button, user can delete his requirement and select parameters again and By pressing the “Exit” button, user can exit from the window. Figure 7 shows the input window with selectable inputs.



Figure 7 - Input Selection Window

If the selectable inputs are possible then the tool will display all possible feasible PV systems and its techno economic details with comparison graphs. Otherwise it give an error message which says “NOT REAL. Check your input parameters as the given table in front page”.

5 Case Studies

To verify the developed tool, two actual buildings considered. This tool gives techno economical details on energy system which is much similar to actual situation. This verifies that the user can use this tool to get correct idea on their building energy system and can be used to decide on future net meter solar PV system.

5.1 Study 1

As the Study 1, “Food City Nawala”, No 264, Nawala Road, Rajagiriya Net meter PV system is selected.60 kW net meter PV system has been installed in 2014 September at cost of 11.8 million rupees. 396 m² area was utilized to install 60 kW solar system. The PV system was expected 6900 kWh average PV units monthly. The applicable tariff category is GP-2. Since this is a supermarket (consumer goods) cluster 14pattern is considered as load profile.

According to the Electricity bill (Acc: 0103133008) at Cargills food city Nawala, their maximum demand is around 75 kVA and they are under GP2 tariff category.

According to the tool output for CoE which is shown in figure 8, optimum solar PV capacity which minimize the CoE is 80 kW. But they have installed 60 kW due to the area limitation. It is also feasible.

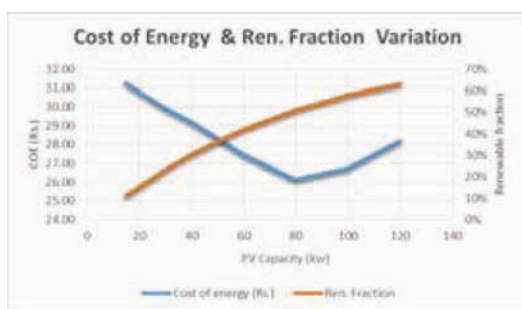


Figure 8 - Tool Output for CoE Period for Study1

Table 2 - Comparison of Actual Data and Tool Output for Study 1

Parameter	Actual data	Tool Results
PV system cost (Rs.)	11,800,000 (in 2014)	10,037,625
Cost of energy (Rs.)	24.15	27.45
Renewable Fraction	39 %	42%
Area requirement (m ²)	396	408
Simple payback period for PV system (years)	6.53 (If project cost is 10,037,625 this become 5.56)	5.03

Table 2 compares actual data which are calculated using actual system performance data and simulation results on PV system cost, CoE, renewable, average area requirement and simple payback period for PV system which validate the tool developed.

5.2 Study 2

Solar PV installation at Geological survey & Mines bureau (GSMB) – Pitakotte is selected as study 2. 25 kW net meter PV system was installed since 2014 investing 4.2 million rupees and expected monthly solar PV generation was 2,750 kWh. Then they have added another two 15 kW systems in 2016 at a cost of 5.15 million rupees with 3400 kWh units monthly production. Expected total PV generation is 6150 kWh per month. This is a government office building which has the cluster 2 load pattern. They are paying for

electricity under the tariff category GP2. Maximum demand is considered as 175 kVA.

Figure 9 shows tool output for the CoE which contain optimum PV capacity and other feasible system capacities as well. Optimum solar PV capacity which minimize the CoE is 180 kW. But they have installed 55 kW. Table 3 compares actual data and simulation results at GSMB on PV system cost, CoE, renewable, average area requirement and simple payback period for PV system which again validate the developed tool.

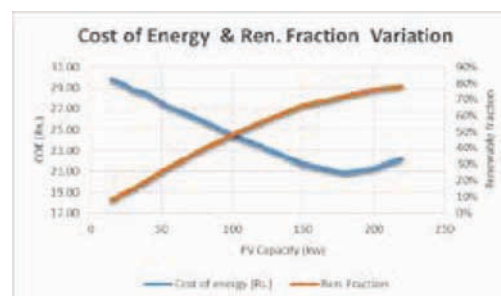


Figure 9 - Tool Output for CoE Period for Study 2

Table 3 - Comparison of Actual Data and Tool Output for Study 2

Parameter	Actual data	Tool Results
PV system cost (Rs.)	9,350,000	9,224,465
Cost of energy (Rs.)	24.48	27.26
Renewable Fraction	28 %	28 %
Average area requirement (m ²)	363	374
Simple payback period for PV system (years)	5.81	4.65

6 Conclusion and Discussion

This research was done to analyze the feasibility of incorporating solar net metering for commercial building in Sri Lanka.

Optimum solar PV capacity to be installed is depend on tariff category, solar irradiation, technical performance of the system, building load profile and maximum demand of the building. But there was no user friendly method to analyze the feasibility of PV installation and its outcomes for commercial buildings in Sri Lanka. This paper present a

tool to analyze solar PV incorporating at the conceptual design stage of the project. Variation of technical performance of PV systems and solar irradiation is not considered in this tool.

- User can select optimum solar PV capacity to be installed and get details on investment cost, cost of energy, payback period etc.
- If the user cannot go for the optimum PV capacity due to the limitations such as cost or area, then he can select whatever the possible capacity using this tool. It can be used to decide whether to install solar and if installed what the payback period is.
- This tool can be used even with the conceptual design stage of the building with estimated electrical demand. That will help to utilize the area for solar panels and the project cost.
- When consider the government sector projects, this tool will help to do proper budgetary allocations for net meter solar PV system at the initial stage. This will avoid price variations.
- Any user without much knowledge on net meter solar PV installations, can see the feasibility of it without having consultancy from solar panel providers.

In this research only the net meter solar PV installation is considered. In 2016 government introduced a concept called “Battle for solar energy” which has three options; net metering, net accounting and net plus. In net plus, the electricity production and the consumption are independent. So no need to optimize the capacity. But this can be included net accounting concept using the same simulation software HOMER. Further this tool can be developed to decide the most feasible solar installation method; net metering, net accounting and net plus.

Sensitivity analysis are not included in this tool. But this tool can be further developed by adding sensitivity analysis for solar irradiation, tariff scheme changes, technical performance of PV panels etc.

The results of this research is only applicable for bulk installations. This is not applicable for domestic sector electrical installations. Also this is not applicable for multi category electrical installations which are consisted as

retail type domestic, commercial and hotel electrical installations (electrical installations where its contract demand is below 42 kVA).

References

1. Lambert, T., Gilman, P. and Lilienthal, P. (2005) Micropower System Modeling with Homer, in Integration of Alternative Sources of Energy (eds F. A. Farret and M. G. Simões), John Wiley & Sons, Inc., Hoboken, NJ, USA. doi: 10.1002/0471755621.ch15.
2. Sunanda Sinha, S.S. Chandel, Review of software tools for hybrid renewable energy systems, Renewable and Sustainable Energy Reviews, Volume 32, April 2014, pp. 192-205, ISSN 1364-0321.
3. Patrick Mark Murphy, Ssenoga Twaha, Inês S. Murphy, Analysis of the cost of reliable electricity: A new method for analyzing grid connected solar, diesel and hybrid distributed electricity systems considering an unreliable electric grid, with examples in Uganda, Energy, Volume 66, 1 March 2014, pp. 523-534, ISSN 0360-5442.
4. Makbul, A. M. Ramli, Ayong Hiendro, Khaled Sedraoui, Ssenoga Twaha, Optimal sizing of grid-connected photovoltaic energy system in Saudi Arabia, Renewable Energy, Volume 75, March 2015, pp. 489-495, ISSN 0960-1481.
5. Kyoung-Ho Lee, Dong-Won Lee, Nam-Choon Baek, Hyeok-Min Kwon, Chang-Jun Lee, Preliminary Determination of Optimal Size for Renewable Energy Resources in Buildings using RETScreen, Energy, Volume 47, Issue 1, November 2012, pp. 83-96, ISSN 0360-5442
6. Shafiqur Rehman, Luai M. Al-Hadhrami, Study of a Solar PV-Diesel-Battery Hybrid Power System for a Remotely Located Population near Rafha, Saudi Arabia, Energy, Volume 35, Issue 12, December 2010, pp. 4986-4995, ISSN 0360-5442.
7. Tamer Khatib, A. Mohamed, K. Sopian, M. Mahmoud, Optimal Sizing of Building Integrated Hybrid PV/Diesel Generator System for Zero Load Rejection for Malaysia, Energy and Buildings, volume 43, issue 12, December 2011, pp. 3430-3435.
8. Graham, V. A., and Hollands, K. G. T., A Method to Generate Synthetic Hourly Solar Radiation Globally, Solar Energy, Vol. 44, No. 6, pp. 333-341, 1990.
9. Mukhtaruddin, R. N. S. R.; Rahman, H. A.; Hassan, M. Y., "Economic Analysis of Grid-Connected Hybrid Photovoltaic-Wind System

- in Malaysia", Clean Electrical Power (ICCEP), 2013 International Conference on June 2013, vol. 11, no.13, pp.577-583.
10. Moniruzzaman, M., Hasan, S., "Cost Analysis of PV/Wind/diesel/grid connected hybrid systems," Informatics, Electronics & Vision (ICIEV), 2012 International Conference on May 2012, vol.18, no.19, pp.727-730.
 11. Kolhe, M., Ranaweera, K. M. I. U., Gunawardana, A. G. B. S., "Techno-Economic Optimum Sizing of Hybrid Renewable Energy System," Industrial Electronics Society, IECON 2013 - 39th Annual Conference of the IEEE , vol.10, no.13, pp.1898-1903, Nov. 2013.
 12. Rashayi, E., Chikuni, E., "The Potential of Grid Connected Photovoltaic Arrays in Zimbabwe," Electrotechnical Conference (MELECON), 2012 16th IEEE Mediterranean, vol.25, no.28, pp.285-288, March 2012.
 13. www.opac.lib.mrt.ac.lk
Methodology to determine the maximum demand of multi category bulk electrical installations - [2015].
 14. <http://www.pucsl.gov.lk/english/wp-content/uploads/2016/03/Net-Metering-Report-Final1.pdf> Visited, 20th June 2016.
 15. www.energy.gov.lk Visited, 20th June 2016.
 16. www.ceb.lk Visited, 20th June 2016.



Multi-Functional Floor Cleaning Robot for Domestic Environment

H.G.T.Milinda and B.G.D.A. Madhusanka

Abstract: Floor cleaning is a major task in the household cleaning process. But nowadays people are very busy with their works they do not have enough time to spend cleaning process. Multi-functional floor cleaning robot was introduced to the world as a solution for above reason. The proposed method is capable to identify and classify the dirt in the domestic environment. According to dirt detected by the floor, the robot can decide and apply most suitable cleaning action among sweeping, mopping and vacuuming. Dirt detection is based on vision system. The vision system is introduced a novel method of mud detection and proposed vision algorithm is used to separate mud and dirt elements. According to this vision base decision robot select cleaning method. The robot can be identified more than 70% of dirt and mud elements in the domestic environment. Many Sensors around the main body are used to avoid collision with the floor obstacles or the fall from the stairs and sharp edges. The automatic floor cleaning action of dynamic mechanism and dust removal equipment is controlled by both electric circuit and single-chip microprocessor. For the operation of functionality and practicality, an Android-based application is added to the robot with three models, including manual operation, automatic operation, and cleaning operation. Our findings suggest that average save more than two hours of people's time per week, floors are cleaner leading to better homes and lives, systematic cleaning is seen as an important feature, and modifications to the domestic environment to support the navigation of the robot are largely accepted.

Keywords: Multi-functional cleaning, Dirt detection, Mud identification, floor cleaning robot

1. Introduction

A mobile robot is an automatic machine which is capable of locomotion and has the capability to move around in their environment. The mobile robots are capable of navigating an uncontrolled environment without any physical or electromechanical guidance. Mobile robots have become more commonplace in commercial and industrial settings. This kind of robot is used in many fields and new researchers also going on several fields as well. Domestic robots are consumer products, including entertainment robots and those that perform certain household tasks such as vacuuming, cleaning or gardening.

Floor cleaning robot is the domestic robot as well as the mobile robot. So it has characteristics of both. People in modern society very busy with their work and they do not have time spent on household cleaning purposes. Nowadays floor cleaning becomes waste of time by comparing his daily routing. Also, modern world manual work is taken over the robot technology and many of the related robot appliances are being used extensively floor cleaning also takeover by the robot.

In the cleaning purpose, robots were introduced for making the efficient cleaning pattern. The present floor cleaning robot comes

with more efficient cleaning using artificial intelligent technology and image processing which able to take its own decision.

In today's market, most of the robot having its own charging and control from any part of the world some robot can control using smart devices. Some of them can be connected to house automation system.

Most of the robot in the current market can only perform one task at each time. Roomba [1], Neato [2] and LG Hom bot [3] are the best-selling brands in the robot market. These robots can only performance sweeping and vacuum functions only. Any robot in the market does not identify what sort of the dirt it is. They are always cleaning the floor and it is the waste of energy of robot. No robot on the market neither tries to clean the floor if it is necessary or all of them.

*Eng. H.G.T. Milinda, BTech(Eng)(Hons)(OUSL),
Student Member of IESL, Department of Mechanical
Engineering, The Open University of Sri Lanka.*

*Eng. B.G.D.A. Madhusanka,
BTech(Eng)(Hons)(OUSL), MSc(Moratuwa),
AMIE(SL), MIEEE, Probational Lecturer, Department of
Mechanical Engineering, The Open University of Sri
Lanka.*



2. Proposed System

Floor cleaning robot available only can identified dirt but dirt is not specifically separate as mud spot or dirt element. Reason for that is no robot able to identify the dirt and separately so it cannot perform correct cleaning action for floor. All the prevailing robot used basically used three method to identified dirt

- Ultrasonic scan
- Laser beam scan
- Image processing techniques

But perform the multi-tasking need the dirt specifically identification using the Ultrasonic and Laser beam it is impossible to separate dirt specifically. Image processing is an only solution for detect the dirt.

So the design the multi-tasking robot first robot should read the collision sensor to check whether robot can move forward and also take the image in front of robot. Then identified objects in the floor. In this research mainly focused on identified object in the floor whether it is dirt or mud and clean it. For that purpose prevailing three methods only image processing techniques can used separate mud. So dirt detect process image processing techniques are going to be used

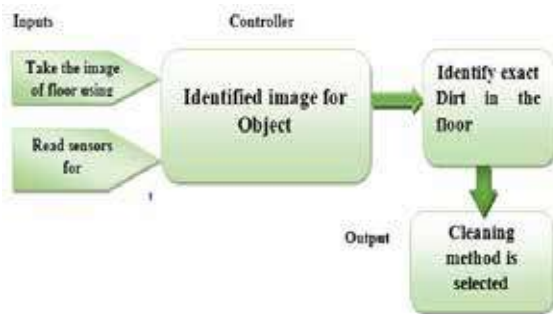


Figure 1- Proposed model diagram

Firstly objects are identified from image using template matching [4]. Then identified objects once again sorted whether dirt or mud. For that purpose expected to use combination of colour matching and pattern recognition techniques coming under the image processing techniques.

According to identification image, cleaning action is automatically decided by the robot and clean specific floor area after that. Mainly robot can perform few cleaning action.

2.1 Overview of cleaning method

Cleaning System has consisted of three main unit mopping, vacuuming and sweeping. Sweeping and vacuum unit are work together mopping function is operated separately. Dirt detection is done using image processing techniques as mention earlier

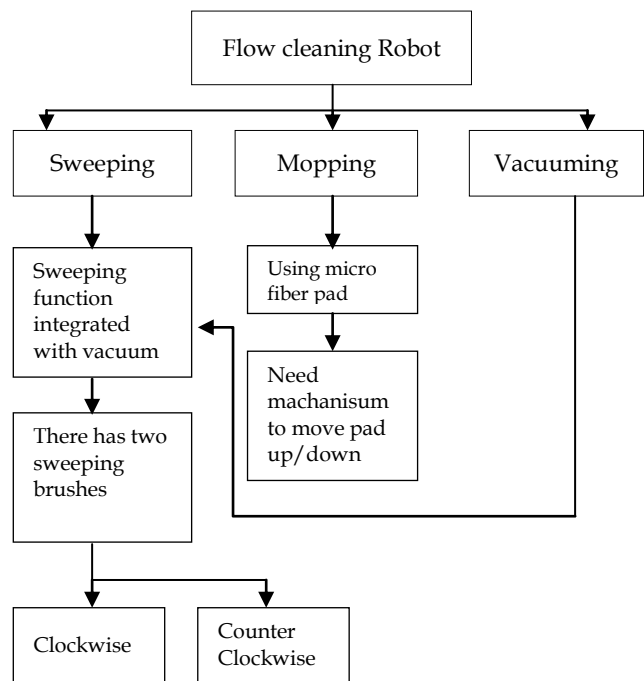


Figure 2 - Overview of Cleaning

The sweeping unit consists of two sweeping brushes one rotates clockwise and other rotate counterclockwise. Vacuum unit consists of dustbin and vacuuming fan this unit is integrated with the sweeping unit as given in figure 3(b). Mopping unit has consisted of microfibre cloth and water tank as in figure 3(a). From the Moping unit and Sweeping unit only one unit work at the time.

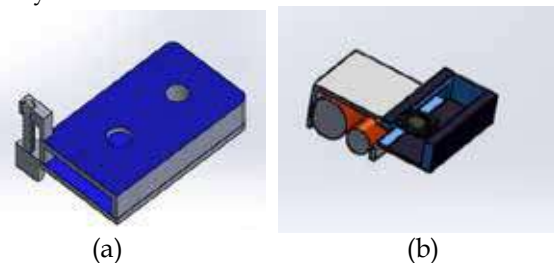


Figure 3-(a) Proposed mopping unit. (b) Proposed sweeping unit

3. Methodology

Floor cleaning robot to process the above task should contain the following units shown in figure 2. This unit should be designed or selected according to requirement. Mopping and Suction units going to be design and sensors and processing and the controlled unit must be selected.

Image Acquisition unit is used to capture the image of floor and collision avoiding sensors are used to detect the object in the working environment. Image processing should be done separately because one controller is not suitable done both image processing and real-time robot

controlling at the same time. If the same controller is used for both purposes working efficiency of controller going to low then it is not satisfied. The motor driving unit is used move robot around the floor. This driver is used control the motor according to the signal given by the controller. Gyro and Accelerometer sensors are used to tracking the navigation on the floor. Robot scan collision sensor first then take an image of ground and processed the image and return the decision to the main controller according to cleaning action is taken and run motors according to that.

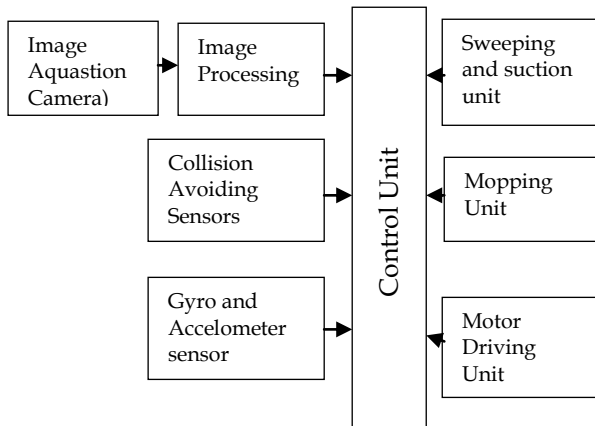


Figure 4 - Block diagram proposed cleaning robot

Read sensor for any kind of collision: - Sonar sensor is used to detect the collision. Though collision can check using the image it not can sudden collision tracking because it takes time to process. So sonar sensor read the collision Read the image first and identified dirt using template machine:-take the image of floor and process the image template matching and identified dirt then identified dirt separate:-This identified dirt especially separate as mud or non-mud dirt using object identification method using colour matching and pattern recognition. Then select most suitable action:-According to dirt speciation activate the mopping unit or sweeping and vacuum unit.

4. Image processing and dirt classification

4.1 Dirt Detection

The concept of MSERs (Maximally Stable Extremal Regions) was proposed by Baek [5]. MSERs denote a set of distinguished regions that are detected in a grey scale image. All of these regions are defined by an extremal property of the intensity function in the region and on its outer boundary. First identified MSE regions and apply several morphological filters.

Then the area of the each MSE region is calculated and checked with the threshold. Mean and standard deviation of each region also checked. If any object is under both threshold identified as dirt. Furthermore MSERs are detected at different scales. Figure 5 shows the MSER detection of floor image.



Figure 5-(a) Original dirt and (b) MSER dirt identified Feature

4.2 Mud Detection

Mud detection novel method is introduced [8]. The new concept is based on the colour and area distribution of mud. Though research is done to service robot for the outdoor environment by A. Rankin and L. Matthies, [6]. That method uses two stereo cameras and it is cannot be implemented for the small robot. MSER function cannot identify mud most of the cases because mud normally having the property of spread on the floor than the dirt particles and difficult a stable sharp point in the mud marks .in this novel method first spectral residual filter[7] is used identified the object from background then apply hue value mask. Resultant image frame apply the morphological operation to make close regions.then calculated area, mean and standard deviation finally checked with threshold values and detected as mud.Figure 6 shows that calculation of varicence and identified mud areas.

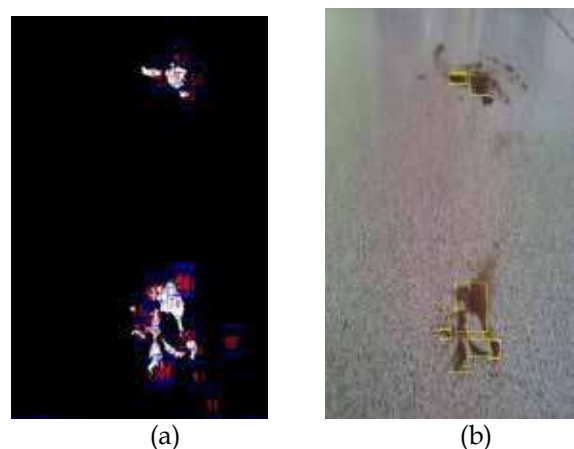


Figure 6-(a) Variance Calculation each region (b) Mud detection according to threshold



5. Prototype implementation and testing

A Real-time working module of the robot was implemented and tested proposed algorithm can identify and dirt and mud separately and cleaning it according to dirt detected. Real time working module of robot is shown in Figure 7.

5.1 Analysis of dirt detection experiments

Several experiment is recoded at domestic environments with a variety of dirt particles of different sizes in different floor to check whether proposed algorithm can identified mud spot and dirt separately.



Figure 7 - Working module of floor cleaning robot.

5.2 Dirt Detection on floor experiment

These experiments were done several household floors like tile, red cement, wood and carpet. In this experiment 1' x1' (one square feet) area of tile floor is selected. Newspaper particles with the different colour are used as dirt particles which are having the area less than 25cm². From these dirt element number of pieces are detected as the dirt by the algorithm. Figure 8 shows that several images of experiment results .

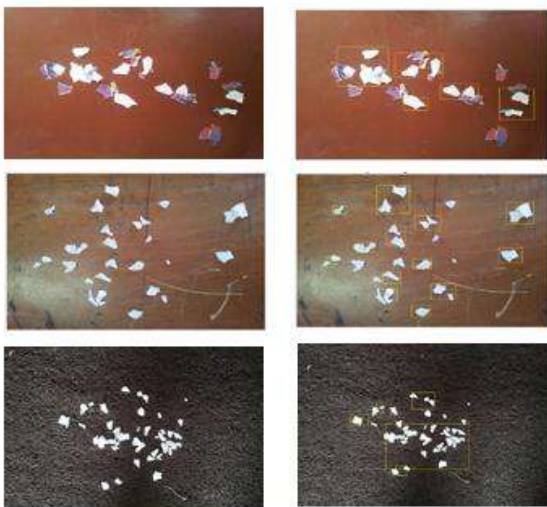


Figure 8 - Example images from house environment surfaces. Left column: original images , Right column: detected dirt indicated by yellow rectangles

5.3 Mud Detection on floor experiment

The experiments are conducted same environments where the dirt detection experiment are done. One square feet area of tile floor is selected. The footprint of the man with mud is used as mud element. There 7cm x10 cm area of mud sign is used. From this mud sign, several areas are detected as the mud by the algorithm. Several kinds of mud sign is also used on the same floor and tested.figure 9 shows some experiment cases.

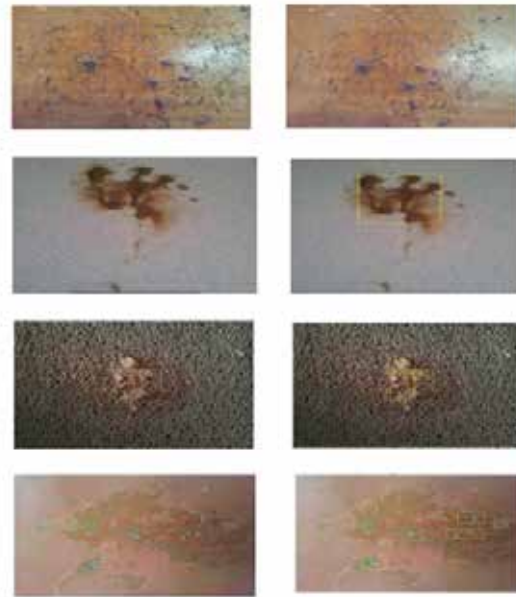


Figure 9 - Example images from house environment surfaces. Left column: original mud spot images I. Right column: detected mud spot indicated by yellow rectangles

5.4 Floor sweeping and vacuuming Experiment

Sweeping and vacuuming action is done several types of floors check whether sweeping is successful done in each floor. Area of the 1' x1' (one square feet) is selected as tested area figure 10 (a) showed that dusty area. After cleaning by the robot floor shown as figure 10(b).



Figure 10 - Experiental result of sweeping fuction

5.5 Floor mopping Experiment

Mopping function is checked on tile floor. Area of the one square feet is selected as tested area figure 5. Mopping function is checked on the tile floor. Area of the one square feet is selected as tested area figure 5.17 (a) showed that mud spot. After cleaning from the robot floor shown in figure 5.17(b).In there robot mopping one time routing its mopping unit in this area. All most all of the mud spot is cleaned by the robot.

6. Results & Discussion

In these experiments try to identify the foreground object of the floor many experiments have been done this experiment values given most accurate values at the present. This algorithm good enough to identified 70% of the solid Dirt in the floor.

6.1 Analysis of mud detection experiments

Table 1 summarizes the sets of surfaces in home environments, provides percentages of dirt detected on them and comments on typical problems with dirt detection. Please notice that the detection results come with a low false positive rate of a few percent. The reported percentages are computed as the number of found dirt spots divided by the number of present dirt spots. The results were counted manually since the labelling of the streams would have been too tedious. A dirt spot was considered to be found by the algorithm if it was detected in several frames.

Table 1 - Summary of the Image processing result

Surface	Detection of Dirt	Remarks
Floor tiles	82.4%	Most of the dirt partials are bigger
Red Cement floor	85.2%	very dark and small black objects
Wood surface	77.6%	fine-grained dirt
Carpet floor	75.3%	some false positives in reflection of light

Red cement floor get the most accurate result in the dirt particles detection carpet floor get minimum accurate results because algorithm compare MSER values it is difficult done in carpet floor because. Many experiments are done in these floors average time values is included into report. Many points is detected as sharp edges in the carpet.

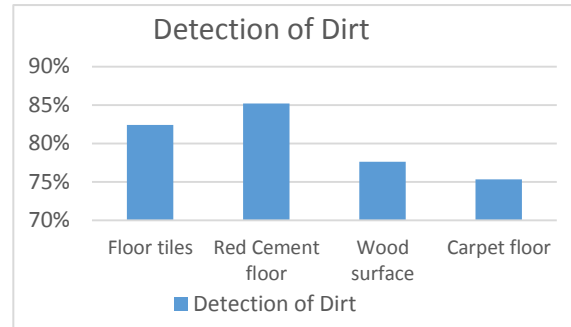


Figure 11- Graphical representation of mud detection result

6.2 Analysis of mud detection experiments

Several experiments are recorded at above environments with a variety of mud particles of different sizes. Table 2 summarizes the sets of surfaces in home environments, provides percentages of mud spot detected on them and comments on typical problems with mud detection. Please notice that the detection results come with a low false positive rate of a few percent. The reported percentages are computed as the area of found mud spots divided by the total area of present mud spots. The results were counted manually since the labelling of the streams would not have been most accurate. A mud spot was considered to be found by the algorithm if it was detected in several frames.

Table 2 - Summary of the mud identification result

Surface	Detection of Mud(Approximately)	Remarks
Floor tiles	80%	Reflection and edges with mud
Red Cement floor	75%	Dark colour difficult to identified mud
Wood surface	70%	Most similar to mud colour so difficult detect
Carpet floor	79%	Design in the carpet made some errors

In there robot sweep two times routing its sweeping brushes and vacuuming unit in this area. More than 98% of the dust is swapped and vacuumed by the robot. Mopping function is checked using the robot floor In there robot mopping one time routing its mopping unit in mud area. All most all of the mud spot is cleaned by the robot.



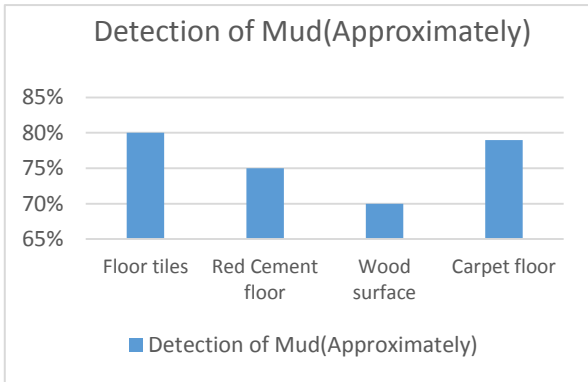


Figure 12 - Graphical representation of mud detection result

7. Conclusion

The implemented low cost solution consists with Raspberry PI cluster, load balancer and intelligent automated management platform. It replaces the current manual process of physical node IaaS configuration and management task of network administrator.

Intelligent management controls the roles of worker nodes and changes worker roles according to the available demand. Therefore cloud can adapt with request types dynamically without interaction of the user.

Dynamically expandable nature provides more flexibility to cloud administrator in expansions and management by reducing server down time and service interruptions. The floor cleaning robot is mainly focused to dirt identification part only. The robot navigation part does not cover in this research. In next stage of this research is develop the vision base auto navigation algorithm. Also the robot should be done auto charging when its battery needed to be recharged. Virtual fence for floor cleaning robot is to be suggested when cleaning area. Advanced dirt identification algorithm is to be developed which is not only for the domestic environment but also adaptive to any environment scenarios with decision taking capabilities.

References

1. C. W. 2009, "How do Roomba robot vacuum cleaners work?," Explain that Stuff, 2016. [Online]. Available: <http://www.explainthatstuff.com/how-roomba-works.html>. Accessed: Feb. 21, 2017.
2. N. Robotics, "Neato robotics," in Wikipedia, Wikimedia Foundation, 2017. [Online]. Available: https://en.wikipedia.org/wiki/Neato_Robotics. Accessed: Feb. 21, 2017.

3. Shanavan, "LG Hom-Bot robotic vacuum - ocean black (VR65704LVM) | LG US," 2017.[Online]. Available: <http://www.lg.com/us/vacuum-cleaners/lg-VR65704LVM>. Accessed: Feb. 21, 2017.
4. V. S and S. A, "Template Matching Technique for Searching Words in Document Images", International Journal on Cybernetics & Informatics, vol. 4, no. 6, pp. 25-35, 2015.
5. I. Baek, "A Method to Detect Object of Interest from Satellite Imagery based on MSER(Maximally Stable Extremal Regions)", Journal of the Korea Institute of Military Science and Technology, vol. 18, no. 5, pp. 510-516, 2015.
6. A. Rankin and L. Matthies, "Passive sensor evaluation for unmanned ground vehicle mud detection", Journal of Field Robotics, vol. 27, no. 4, pp. 473-490, 2010.
7. X. Hou and L. Zhang, "Saliency Detection: A Spectral Residual Approach", 2007 IEEE Conference on Computer Vision and Pattern Recognition, 2007.
8. H. Milinda and B. Madhusanka, "Mud and dirt separation method for floor cleaning robot", 2017 Moratuwa Engineering Research Conference (MERCCon), 2017.
9. [Online].Available: https://en.wikipedia.org/wiki/Kalman_filter. Accessed: Feb. 21, 2017.

Development of CZTS thin Film from Spin Coating for Solar Cell Application

H.A.D.I. Dilshan, W.D.D. Weerasinghe, N.L.W. Wijewantha, W.P.S. Wijesinghe and D. Atygalle

Abstract: Copper Zinc Tin Sulphide (CZTS) layer fabrication was done using the spin coating method and optimum conditions for CZTS layer fabrication were found to be 2000rpm – 6000rpm spin coating speed with 30 seconds of spinning time, 38°C – 42°C precursor solution temperature, 140°C – 160°C drying temperature, and 280°C annealing temperature (30 mins) that promotes the formation of CZTS. The obtained CZTS layers have shown a bandgap in the range of 1.45eV to 1.55eV within which the theoretical bandgap 1.50eV of CZTS lies.

Keywords: Bandgap, Copper Zinc Tin Sulphide (CZTS), Photovoltaic, Spin Coating

1. Introduction

The main objective of manufacturing thin film solar cells is to reduce photovoltaic electricity generation costs while maintaining the conversion efficiencies comparable to first generation bulk material solar cells. Thin film solar cells have an absorber layer of thickness less than few micrometres, which is several orders magnitude thinner compared to hundreds of micrometre thick silicon wafer based solar cells. In other words, thin film solar cells use much less material and thereby saves energy and money.

At present, the efficiencies of thin film solar cells are comparable to that of polycrystalline silicon; for instance in terms of efficiency, 21.3% for multi-crystalline Si and 22.3% for copper indium (gallium) diselenide (CIGS) [1]. Though the Si polycrystalline solar cells dominate the market, the market share of the thin films photovoltaic module is increasing [2]. Thin film solar cells based on polycrystalline cadmium telluride (CdTe), copper indium diselenide (CIS), and copper indium (gallium) diselenide (CIGS) have reached a commercialization stage; however, restrictions on heavy metal usage, such as Cd and scarcity of supply for In and Te have raised concerns on sustainability of certain PV technologies. In this circumstance, Copper Zinc Tin Sulphide (CZTS) quaternary semiconductor compound has identified and promoted as one of the promising candidates.

CZTS is nontoxic, and elements that are contained in CZTS are abundant in the earth crust. CZTS has an absorption coefficient of 10^4 cm^{-1} and the band gap is around 1.5 eV, which makes it a very promising absorber layer for thin-film PV [3]. Theoretically, the predicted

conversion efficiency for single junction CZTS solar cells are more than 30% [4].

A vast variety of CZTS fabrication methods have being studied by different researchers in the past decade. Each of these methods has its advantages and drawbacks. Some are in the high technological set category, which are also costly. Pulsed laser techniques, co- evaporation, sputtering are some of them. Other than them, it is possible to identify, low-cost methods like spray pyrolysis, spin coating and electro deposition, which also reportedly produced encouraging results [5]. In our research, we used spin coating method as our deposition method. It has several advantages over other low-cost deposition methods. It is a simple and cost effective method relative to other methods. Thin and uniform coating can be achieved within few seconds and coating will dry very quickly after deposition due to high airflow during high speed rotating [6].

2. Experimental Procedure

2.1 Preparation of CZTS Precursor solution

The CZTS precursor solutions were prepared by mixing Copper(II) Chloride Dihydrate (98%), Tin(II) Chloride Dihydrate (98%), Zinc(II) Chloride (99%), Thiourea (98%), 2-Methoxy Ethanol (99%) and de ionized water [2]. $\text{CuCl}_2 \cdot 2\text{H}_2\text{O}$ [0.9 M], ZnCl_2 [0.7 M], $\text{SnCl}_2 \cdot 2\text{H}_2\text{O}$ [0.5 M], and Thiourea [4 M] were used for thin films. All the dry chemicals were

H.A.D.I Dilshan, B.Sc.Eng.(Moratuwa),
W.D.D. Weerasinghe, B.Sc.Eng.(Moratuwa),
Eng. N.L.W. Wijewantha, B.Sc.Eng.(Moratuwa),
AMIE(SL).
Eng. W.P.S. Wijesinghe, B.Sc.Eng.(Moratuwa),
AMIE(SL).
Dr. D. Atygalle, B.Sc.(Sp) (Colombo), Ph.D.(Toledo),
Senior Lecturer, Department of Material Science &
Engineering, University of Moratuwa.



measured according to the required concentrations and mixed with the de ionized water and 20 ml of 2-Methoxy Ethanol for a 100ml of the solution. The solution was stirred for 1 hour at 40-45°C until the metal salts were dissolved. Crystal clear yellow coloured solution was obtained

2.2 Thin film fabrication

Thin films were fabricated by the spin-coating method, which involved two steps: first, spin-coating precursor solution on the glass substrate to form a film; and second, annealing thin films in a proper atmosphere [7].

The experiments were carried out under the coating conditions, spin coating speed ranges from 2000rpm - 12000rpm and amount of CZTS ranges from 0.5ml to 1.5ml, to determine optimum fabrication conditions because, according to literature, spin coating speed was a determinant factor when it comes to CZTS thin film thickness. Then, the drying was done at 150°C to promote the formation of CZTS

Table 1- Regulated conditions for CZTS thin film fabrication and annealing

Speed Range (rpm)	Amount of CZTS (ml)	Spin Coating Time (s)	Annealing Temperature
4000 - 8000	1.0	30	310
4000 - 8000	1.0	30	280
4000 - 8000	1.0	30	250
2000 - 6000	0.5	30	310
2000 - 6000	0.5	30	280
2000 - 6000	0.5	30	250
2000 - 8000	1.0	30	310
2000 - 8000	1.0	30	280
2000 - 8000	1.0	30	250

It was identified that the speed of the spin coating plays a dominant role in determining the uniformity and film thickness. Thereafter, samples were annealed at elevated temperatures to promote grain growth and grain refining. Table 1 shows the conditions that were used in making samples.

2.3 Analysis of Thin Films

Prior to getting electrical measurements, thin films on glass slides were visually examined for cracks, unevenness and pinholes to eliminate poor coatings.

Microscopic observations of the thin films were performed using an optical microscope

(Infinity1-MEIJ) to determine if the microstructure is uniform and has a good grain growth. The film thickness of the samples was determined by microscopic observation of the cross section of the glass slide coated with CZTS layer.

Dual Beam Shimadzu UV-1800 Spectrophotometer was used to collect the transmittance data of different CZTS thin films fabricated on glass slides under predetermined conditions. The wave length range used was 300nm to 1, 100nm, and the collected data was analysed to obtain absorbance bandgap of the CZTS thin films. Since the accuracy of calculated band gap value heavily dependent on the film thickness, a Carl ZeissEvo 150 scanning electron microscope (SEM) was used to verify the optical microscopy measurements. The film composition was determined using Energy Dispersive X-Ray Spectroscopy (EDS). Electrical measurements of the CZTS thin films were obtained to evaluate if the layer possesses photoconductivity. Since the CZTS layer thickness was in the micron range, the measurement of the current being generated when exposed to light was done, and the dark current and light current was measured for varying voltages.

3 Results and Discussion

3.1. Microscopic Observations of CZTS Thin Films

Microstructure observations prove that the CZTS thin films fabricated at 40°C show a higher level of uniformity compared to other temperatures. Figure 1 shows that the coating was applied with uniformly distributed grain structure. Uniformity and the film thickness of fabricated CZTS thin films were determined by optical micrograph as shown in figure 2.

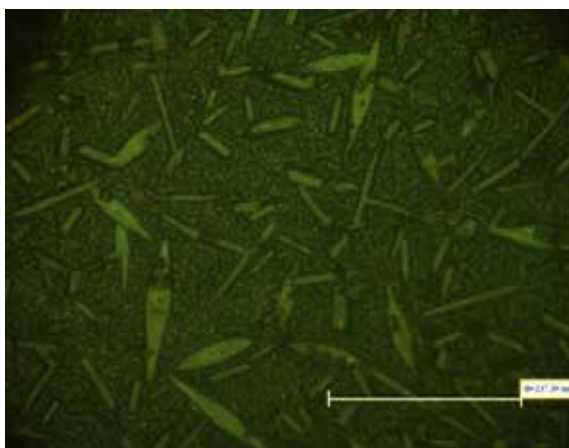


Figure 1- Optical Micrograph of CZTS layer fabricated on glass slides (2000-6000rpm with 3 Coatings)

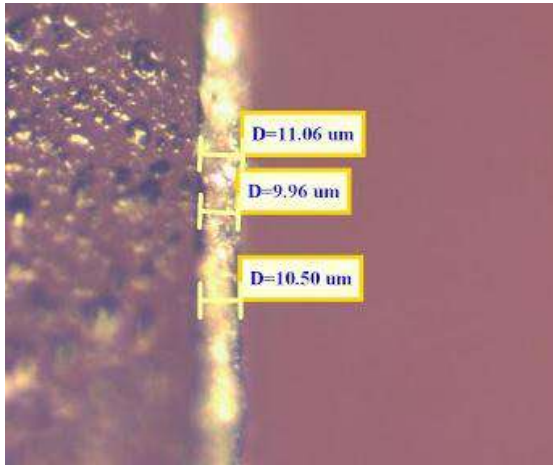


Figure 2 - Micrograph of CZTS thin film fabricated at 40°C with 2000-8000rpm and 0.5ml of CZTS solution

3.2. UV-Vis Spectroscopic Analysis of CZTS Thin Films

Data obtained from UV-Vis Spectrophotometer were analysed and obtained the absorbance curves of different CZTS coatings applied on glass substrates. In Figure 3, the absorbance curves derived for CZTS fabricated on glass slides at 40°C solution temperature for different fabrication conditions were plotted in one graph.

When the bandgap of CZTS thin films was calculated using the obtained graph $(\alpha hv)^2$ vs (hv) , the bandgap was found to be in the range of 1.40eV to 1.60eV, and it proves that the obtained CZTS layer has suitable bandgap for thin-film solar cells.

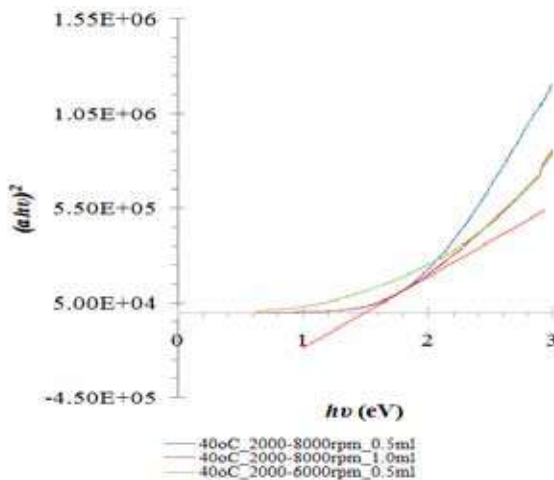


Figure 3 - Bandgap calculations of CZTS thin films fabricated at varying conditions

3.3. Electrical Measurements of CZTS Thin Films

According to the Figure 4, a considerable change of current was observed in dark and light environments of both samples annealed at 280°C. In the illuminated environment, the resistance of the film gets reduced with the generation of electrons due to the interaction of light photons. In dark environment, it is not possible due to unavailability of light photons to generate electrons and holes pairs. Photo resistive nature is a good proof for the photo voltaic effect of CZTS material to use in solar cell applications.

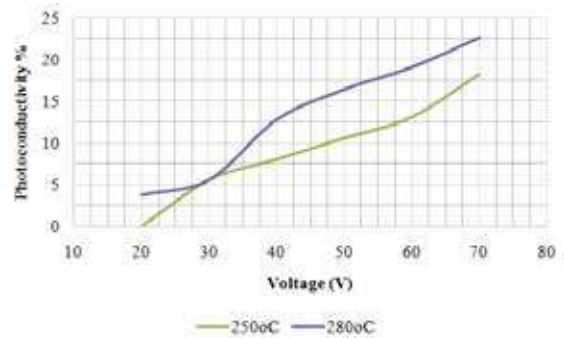


Figure 4 - Voltage vs. Percentage of Photoconductivity graph for CZTS thin film annealed at 250°C and 280°C

3.4. SEM and EDS Analysis of CZTS Thin Films

From the results obtained, it was evident that the CZTS composition was not with the expected atomic ratios. In all the samples, the Zinc content was relatively higher, and Sn content was relatively lower while Cu and S content remained almost constant. This can be attributed to the fact that the Zn content was increased by the researchers to hinder the formation of secondary phases in Cu as described in the literature.

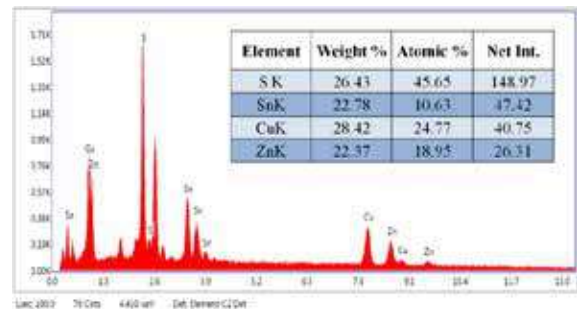


Figure 5 - EDS graph of CZTS thin film annealed at 280°C



Table 2 - Composition of CZTS thin film annealed at 280°C

Element	Weight %	Atomic %	Net Int.
S K	26.43	45.65	148.97
SnL	22.78	10.63	47.42
CuK	28.42	24.77	40.75
ZnK	22.37	18.95	26.31

4. Conclusions

Spin coating is an appropriate method to fabricate thin films from CZTS as an absorption layer for thin film solar cells. The controllable thickness of few micrometres can be achieved for CZTS layer by spin coating method.

Thickness can be conveniently controlled via varying the speed at which the spin coating was done. Optimum conditions for CZTS layer fabrication was 2000rpm-6000rpm spin coating speed with 30 seconds of fabrication time, 38°C-42°C precursor solution temperature, 140°C-160°C drying temperature, and 280°C annealing temperature that promotes the formation of CZTS.

The obtained CZTS layers have shown a bandgap in the range of 1.45eV to 1.55eV within which the theoretical bandgap 1.50eV of CZTS lies. Annealing temperature control was found to be critical because, with the higher temperatures, CZTS thin film tends to be changed in composition and turning into a semi-metallic while deteriorating the semiconductor properties.

CZTS thin film has shown photoconductive properties and temperature dependent resistance variation as expected for a semiconductor material.

References

- Green, M. A., Emery, K., Hishikawa, Y., Warta, W. "Solar Cell Efficiency tables (Version 35)". Progress in Photovoltaics: Research and applications, Vol. 18, pp.144-150, 2010.
- Dr. Gerhard Angerer, Dr. Frank Marscheider, Weideman: "RohstoffefürZukunftstechnologien" [English Translation]. FraunhoferInstitutfür System- und Innovationsforschung ISI. Report published on 15, May, 2009.
- Todorov, T. K., Tang, J., Bag, S., Gunawan, O., Gokmen, T., Zhu, Y., and Mitzi, D. B., "Beyond 11% efficiency: Characteristics of state-of-the-art cu 2 ZnSn(S, se) 4 solar cells," *Advanced Energy Materials*, vol. 3, no. 1, pp. 34-38, Aug. 2012.
- Shockley, W., and Queisser, H. J., "Detailed Balance Limit of Efficiency of p-n Junction Solar Cells," *Journal of Applied Physics*, vol. 32, no. 3, p. 510, 1961.
- Shi, Z., Attygalle, D., Jayatissa, A.H., "Kesterite-Based Next Generation High Performance thin Film Solar Cell: Current Progress and Future Prospects" *Journal of Materials Science: Materials in Electronics*, Vol. 2 (28), pp. 2290-2306, 2016.
- "Spin coating: A guide to theory and techniques." [Online]. Available: <http://www.ossila.com/pages/spin-coating>. [Accessed: 03-Jan-2016].
- Todorov, T., Gunawan, O., Chey, S. J., De Monsabert, T. G., Prabhakar, A., and Mitzi, D. B., "Progress Towards Marketable Earth Abundant Chalcogenide Solar Cells". *Thin Solid Films*, Vol. 519 (21), pp. 7378-7381, 2011.

Characterization of Fuel Briquettes made for Household Cooking from Sawdust and Rice Husk

M.Y.A.R. Ahmed, U.M.A. Devaraja and K.A.R. Mihiranga and
B.A.J.K. Premachandra

Abstract: Fossil fuels are non-renewable source of energy which is commonly used in many applications. Liquid Petroleum Gas (LPG) is a common derivative of Fossil fuels which is widely used for cooking purposes in many households around the world. Alternative sources of energy plays a wider role in many rural households that do not have access to electricity or LPG distribution. Biomass is one of the most commonly used alternative sources of energy in the world for household cooking, and two of the most important reasons for this popularity are low cost and being a solution for waste management. Sawdust and rice husk are abundantly available biomass types in Sri Lanka. About 112,000 MT of sawdust is produced annually, around 3% is used for energy purposes. Annual production of rice husk is estimated around 700,000 MT and around 54% is used for energy purposes. Rest of these are dumped in to the environment or burnt. Since still most of the Sri Lankan houses use traditional fire wood stoves, using these wastes as a fuel for household cooking in an efficient way is a good option for waste disposal problem. Briquetting is the most commonly used technique to use sawdust as a fuel in an efficient manner. The research was carried out to produce and characterize sawdust and rice husk mixed fuel briquettes using a Mount press machine at a pressure of 5000 psi. Physical and mechanical properties of these fuel briquettes such as gross calorific value, moisture content, ash content, volatile matters, density, compressive strength, shatter index, fixed carbon etc. were tested according to ASTM standards. We mainly focused on calorific value variations of the samples and other mechanical properties. After checking all these parameters it is found that sawdust and rice husk mixture is suitable to use as fuel briquettes even though there is a slight reduction in calorific value when compared to briquettes made only with sawdust.

Keywords: Biomass, Sawdust, Rice husk, Briquettes, Fossil Fuel

1. Introduction

Fossil fuel is the most commonly used energy source for industrial and domestic purposes. Generally fossil fuel is categorized as oil, gas and coal. With the growing population of the world, energy demand has increased drastically. According to Ecotricity in UK, fossil fuels are being depleted very fast and it is expected that fossil fuels will be remaining only until 2088[1].

Since fossil fuel is depleting drastically, alternative energy has gained lot more interest to replace fossil fuel. They are widely available and environment friendly also they cause little or almost no pollution. Solar, wind, geothermal, hydroelectric, ocean and biomass can be listed as most widely used alternative energy sources. Among these biomass is one of the most important alternative energy sources.

In Sri Lanka, the city Moratuwa is producing highest amount of furniture. Timber can be categorized as hardwood and softwood. Most of the wood used in Moratuwa such as Teak, Ebony, Halmilla, Jak, Kumbuk, Nedun, Satinwood, Suriya Mara and Mahogani are hard wood and there few saw mills that use

softwood like Pine and Albizia. When comparing the sawdust production, hard wood usually produces more sawdust than soft wood[2]. Since Moratuwa timber industry mostly use hardwood, sawdust production is very high. According to a previous research[3] done in 2005 there are about 4000 sawmills in Sri Lanka. Since the industry is developing this number should be higher than this now. Therefore sawdust is an abundantly available solid waste in Sri Lanka. Among these sawmills there are around 400 sawmills in Moratuwa. It is found in a research done in 2002, the annual production of sawdust in country is about 112,000 MT[4] and in Moratuwa around 1800 MT of sawdust is generated per month. Almost only 2% of this sawdust production in Moratuwa is used for energy purposes and also since there is no proper way to dispose them in an environmental friendly way the remaining 98% is burnt or dumped in to the sea or river[3]. Therefore Moratuwa is under serious environmental threat and need a proper waste management system.

M.Y.A.R. Ahmed, B.Sc. Eng. (Hons)(Moratuwa),
U.M.A. Devaraja, B.Sc. Eng. (Hons)(Moratuwa),
K.A.R. Mihiranga, B.Sc. Eng. (Hons)(Moratuwa),
Prof. B.A.J.K. Premachandra, B.Sc. (Colombo), M.Sc. (Sri
J'pura), Ph.D. (Cincinnati, USA).



Several researches are conducted to find the availability of getting a commercial value from sawdust[2],[5],[6]. Most of these researches are conducted to find the availability of using sawdust as an efficient energy source. But there are some researches done to find the possibility of using sawdust as bricks with some other secondary raw material[2]. Almost all the sawdust used for energy purposes are used for boilers in factories, but not in an efficient way. Manufacturing fuel briquettes using sawdust and rice husk can a viable option for waste management and the rising energy demand in Sri Lanka.

2. Literature Review

Biomass is organic matter derived from living, or recently living organisms and it can be used as a source of energy. Compared to fossil fuel, biomass is a sustainable energy feedstock and supports the reduction of greenhouse gas emission and low impact on climate[7]. Also biomass is highly available in the world and it is cost effective. As well as biomass is considered as an ecofriendly energy source because of its low sulfur content, low nitrogen content and low heavy metal content compared to fossil fuel. When it comes to Sri Lankan context more than 80% of the biomass is consumed for household cooking and heating purposes[3]. Fire wood is a type of biomass and it is an important backup fuel for countries like Sri Lanka as it is cheaper and abundantly available. According to Sri Lanka Sustainable Energy Authority, 77% of the fire wood consumption in Sri Lanka is for household energy requirement[8].

When sawdust is going to be used as an energy source it should be translated into a user friendly, advance manner that can be easily handled[9]. Making densified fuel briquettes is the promising technology to be applied to solid fuel production from these wastes because it is the simply technology which can be adjusted for the local area. The bulk volume of the material can be reduced by applying a compressive load for easy handling, transportation and storage [10]. There are several pressure values for briquetting being used in previous research papers. InTanakorn et al.[10]compression pressure varies between 56-166MPa for 20 seconds for each pellets. In Lela et al.[6]it is mentioned that compression force should be at least 100kN to obtain briquettes with satisfactory strength and in their research applied pressure varies between

147.15kN to 588.16kN. Since the reduction in transportation cost, increment in durability transformation of primary biomass into solid compact fuels, such as pellets and briquettes, is very common in Europe and around the world [7]. Several factors are there which affects compacting biomass, such as raw material type, moisture content, size of sawdust particles, aspects related to manufacturing process (pressure applied, temperature reaching during the compaction). Hardness of briquettes increases moderately as the particle size decreases. When the particle size is large, briquettes tend to fracture easily[11].

Rice husk is a waste of agricultural industry and since agriculture is one of the major industries in Sri Lanka rice husk is abundantly available. According to [3]there were about 7000 rice mills in Sri Lanka in 2005 and the annual production of saw dust is about 2 MT. This number might be nearly the same in 2016. According to the same research, among these 2MT of rice husk about 54% is used for energy purposes, 7% of it is used for other purposes and 39% is not used. With the increasing interest for sustainability these values might be different now and the not used percentage might be less now. But this is a serious environmental threat and need a solution very quickly. Several researches are done around the world to find the availability of using rice husk as a fuel in an efficient way.

Density of rice husk in Sri Lanka varies between 90-110 kg/m³ and moisture content is about 8.5-12% lower heating value varies between 12.5-19 MJ/kg. One of the most important characteristic of rice husk is that it has high volatile matters (68%). Rice husk has nearly 17.4% fixed carbon and 14.1% ash content[3].

2.1 Chemical properties

The main components of the wood are the cellulose, hemi-cellulose and lignin. In addition, main types of natural binding agents of biomass particles are lignin, protein and starch[12]. Protein acts as a binder at plasticized state which needs processing at high temperature. Sawdust contains 40-50% cellulose and 30% lignin[13]. Therefore starch, lignin or water soluble fibers are needed to be added externally in order to increase the bonding of biomass in briquettes. When applying pressure on the briquette, lignin will squeeze out of the biomass cell and agglomerate the fuel briquette. Lignin is not softened at the ambient temperature and pressure [13]. To get to lignin

work as a binding agent, the glass transition point has to be reached[14]. For dry native lignin the temperature is about 200°C and this temperature depends on the moisture content of the biomass. Softening temperature for biomass is around 90-100°C at 30% moisture and around 130°C at 10% moisture[15]. After cooling solid briquette becomes harder. However, previous researches have suggested that binding materials need to be supplied externally for ambient temperature processes[15]. In biomass combustion fuel gases burn and release heat and liquid and other solids do not burn themselves. But they consume heat in the drying and volatilization processes needed for them to be chemically converted into fuel gasses. The main fuel intermediates are volatile hydrocarbons and energy rich organic molecules, Carbon Monoxide (CO) and Hydrogen (H₂)[16]. The process of gas evaluation due to heat is called pyrolysis, and progressively converts the biomass into gasses, volatile liquids, and a carbon rich solid residue called bio char[16]. Biochar is a carbon rich (65 to 90%), fine-grained and porous substance obtained when biomass, such as wood, manure and leaves, is heated or naturally burned under oxygen limited condition and at relatively low temperatures (<700°C). Biochar yield decreased with increasing temperature and the ash and calorific value of the biomass increases with the increment of the heating temperature[17].

2.2 Mechanical properties

- Compressive strength

The maximum compression strength of a briquette is defined as the capacity of a briquette to withstand axially directed pushing forces. This is usually performed to identify the ability of the briquette to withstand the crushing load during handling, transporting and storing. There is no standard method established for testing the compressive strength[15]. In a previous research the compressive strength is measured using a compressive testing machine. The briquettes were placed in between plates of the machine, which ensured uniform stress distribution over the cross sectional area of the biomass fuel. The briquettes were subjected to uniform loading until it failed. The corresponding strengths were recorded from the scale of the compressive strength machine at the time of failure[5].

$$\text{Compressive strength (MPa)} = \frac{\text{Stress (MPa)}}{\text{Strain}} \dots (1)$$

- Shatter index

Shatter index of a briquette is defined as the percentage of a briquette retained on a sieve of stated aperture after being subjected to a free or gravitational resistance to fall or drop[5]. This measures the resistance to mechanical action which affects its transportation and handling. This test is done either in a rotating drum or by repeatedly dropping samples from a specific height. The briquette fraction retained after screening is used as an index of its friability. Shatter should attain a value of higher than 90% according to a previous research results. In a previous research each briquette were subjected to gravitational fall. The initial mass of the briquette was taken and then subjected to the fall of gravitational fall from a constant 2m height three times. Then samples are passed through a 2.36mm sieve while the mass of the briquette retained on the sieve was recorded[18].

Shatter Index

$$= \frac{\text{Mass of the remaining briquette}}{\text{Initial mass of the briquette}} \dots (2)$$

2.3 Physical properties

- Moisture content

Moisture content of a briquette is one of the most important properties to consider for a fuel briquette. Usually the average moisture content of sawdust is about 27% at dry basis. But this number varies with the type of sawdust. Since it's difficult to collect different types of sawdust in pure form from sawmills, a mixture of sawdust has to be collected and therefore an average value for the moisture content should be taken. Moisture content affects briquettes physical properties like durability, density and most importantly the calorific value and the combustion efficiency[6]. After the densification process briquettes should be air dried to remove the moisture. It is found that the optimum moisture content for a briquette is 12-15%[19]. In most of the previous researches briquettes are air dried to reduce the moisture content[10],[5],[15],[20]. In[11] found that if the moisture content is over 50% (wet basis) it's impossible to form a bound aggregate from a forestry or wood residues. Also when the moisture content is less than 12% low comparison strength can be observed[15]. But water is also an important factor in the



compression process, as it can intervene chemically in the particle bonding process, facilitating binding between the hydrogen bridges in the cell wall. Moreover, dry lignocellulose material acts as thermal insulation between which obstructs heat transmission, a key factors in the compacting process[11]. In[6]it is found that moisture content decreases with the increasing drying temperature.

- Density

Density is an indicator of strength and stiffness; it varies widely between wood species and types. There are several methods used in previous researches to determine the density. One method is measuring the height and the diameter of the briquette by a venire calliper and measuring the mass by an electronic balance[15]. Another method is by measuring the volume by water displacement method. To prevent water absorption into the briquette a wax coating is applied to the briquette. Used volume of the wax is measured before using it and from the difference of volumes, the volume of the briquette measured[5]. Second method is the most accurate method to measure the density among these methods since briquette may not be uniform. In[3] it is found that the density of the sawdust is 370 kg/m³.

- Volatile matter

Volatile matter signifies the components of carbon, hydrogen and oxygen present in the biomass that when heated turn to vapour. Usually it is a mixture of short and long chain hydrocarbons.

Volatile content has been shown to influence the thermal behaviour of solid fuels, but this is also influenced by the structure and bonding within the fuel.

- Ash content

Ash has a major influence on the heat transfer to the surface of the fuel, as well as the diffusion of oxygen to the fuel surface during char combustion.

- Fixed carbon

The conversion of inorganic carbon (carbon dioxide) to organic compounds by living organisms is called carbon fixation. The fixed carbon of a fuel not equal to the total amount of carbon in the fuel because there is also a significant amount released as hydrocarbons in the volatiles. It is the percentage of carbon available for char combustion. Fixed carbon

gives an indication of the proportion of char that remains after the depolarization phase.

$$\text{Fixed Carbon} = 100 - (\text{Volatile Content} + \text{Ash Content} + \text{Moisture Content}) \quad \dots (3)$$

- Calorific value

Calorific value can be defined as the amount of energy produced by the complete combustion of a material. This heating value of biomass is depend on the carbon content, ash content and the moisture content and reduces with increasing moisture content and it has a linear relationship with ash content and moisture content[21]. Ash content and fixed carbon content doesn't change with compression process and fixed carbon content depends on the cellulose content of the selected biomass[15]. According to[6] ash content in obtained after the combustion of a briquette is increases with the reduction of the compression load. Therefore according to[21]when the compression load reduces, the calorific value of the briquette reduces. Thus calorific value can be used to evaluate the competitiveness of a processed biomass fuel in a given market situation. But the production cost of a briquette is independent of their calorific value. In previous researches calorific value is given by Lower heating value (LHV) or Higher heating value (HHV). Because of the difficulty to collect pure sawdust types from sawmills, calorific value of different types of sawdust is hard to measure. Therefore in most of the previous researches an average value or rage for calorific value is given. According to[3]average calorific value (HHV) of sawdust collected from Moratuwa at 28% moisture content is 18.8 MJ/kg. But since the HHV is independent from the moisture content, this value has no effect on the moisture content that is mentioned in this research paper. In[6]it's found that the compression doesn't have a significant impact on HHV. But in[13] it is mentioned that briquetting enhances the calorific value. Since there is a contradiction in these statements and in[13] there is no proper argument on this,[13] argument can be taken as the correct one.

- Environmental impact

When considering a fuel environmental impact is one of the most important factor that should be considered. Fossil fuel are the most commonly used energy sources in the world and Petroleum and Coal are the most impactful energy sources among them. But these two non-renewable energy sources are the most important environmental pollutants in the

present time. These are the main reasons for the global warming and greenhouse gas emissions[22]. In a previous research paper[23] it is mentioned that due to the discharge of harmful substances to the environment carbon cycle in the nature is strongly affected. Therefore renewable energy should be given more attention. Since the world is paying more attention towards sustainable energy, several types of renewable energy are introduced and people interest toward biomass has increased. When compared to coal burning wood is more beneficial to the environment point of view due to the lowest total emission of greenhouse gasses (GHG) [7]. Wood combustion is considered as a carbon neutral process since the CO₂ produced in the process of wood combustion is considered as a part of the carbon cycle in nature[23]. Briquetting biomass is one of the most commonly used and efficient way of using them as a fuel. In Poland the government has banned installing coal fired boilers in new family houses. Moreover, boiler users are becoming increasing interested in renewable fuels, mainly briquettes and pellets[7]. Lack of proper sawdust waste management system in Moratuwa one of the major problems that the timber industry in Moratuwa faces. Sawdust is one of the major wastes resulting from wood processing, which stored in uncontrolled manner can be resulting environmental pollution[23]. From about 400 sawmills in Moratuwa around 2000 MT of sawdust has accumulated in Moratuwa over the years and the Not for Profit Organizations (NFPO) currently helps to dispose about 350-400 MT per month[24]. Therefore there are several researches done to find a solution for these two problems in Sri Lanka and also several researches have conducted around the world too. Most of these researches are about manufacturing efficient fuel briquettes from sawdust or developing them. But also there is a research conducted in 2007 to find the availability of manufacturing bricks from sawdust and limestone dust[2]and they have found that it's a viable option.

As well as there are lot of beneficial effect in using sawdust briquettes as a fuel there are some negative impacts on the environment too. These pollutants can be categorized as ash and gaseous pollutants proceed through the combustion gases. Carbon Monoxide (CO), volatile organic compounds, oxides of nitrogen, oxides of sulfur and particulate emissions.

Some of these pollutants can lead to formation of acid rains and snowfalls[23]. Even though sawdust has these negative impacts on the environment, when it comes to densified sawdust briquettes these impacts are comparatively lesser than wood[23].

3. Objectives

Objectives of this research are finding an environmental friendly solution for sawdust and rice husk disposal problem and also introducing an alternative fuel for energy demand with higher calorific value and easy handling for domestic use.

4. Materials and Methodology

4.1 Collection and pre-treatment of raw materials

Saw dust and rice husk are collected from saw mills and rice mills around Moratuwa area and air dried for 3 days. Both raw material were grinded and sieved using a 2 mm mesh.

4.2 Sample Preparation

Dry sawdust and rice husk were blended together according to four mass ratios.

Table 1 - Mixed mass ratios of sawdust and rice husk

Sample Name	Mass ratio of Sawdust	Mass ratio of Rice husk
Sample A	100%	0%
Sample B	75%	25%
Sample C	50%	50%
Sample D	25%	75%

4.3 Briquetting

Briquettes from every samples were made using the Mount Press Machine (Figure 1) which is available in the Department of Material science and Engineering, University of Moratuwa. Few series of samples were prepared using the mount press. Mould was heated to 130 °C and kept for 5 minutes after applying 5 Psi (34.5 KPa) pressure. Then briquettes were removed and kept for cooling for few minutes.





Figure 1 - Mount Press Machine

4.4 Testing Methods

Several tests are conducted to find characteristics of fuel and some of these tests are conducted to find characteristics of sawdust and rice husk mixed saw dust.

- **Density**

Density was determined for each briquette as ratio of briquettes weight to volume.

Apparatus: Vernier calliper, three decimal scale

Procedure:

Measured the weight, diameter and height of samples.

$$\text{Diameter of sample} = \frac{d_1 + d_2 + d_3}{3} = d$$

$$\text{Height of the sample} = \frac{h_1 + h_2 + h_3}{3} = h$$

$$\text{Volume of briquette} = \frac{\pi d^2 h}{4}$$

$$\text{Density} = \frac{\text{Weight of the briquette}}{\text{Volume of the briquette}} \quad \dots (4)$$

- **Moisture Content**

Method: ASTM E871

Moisture content of the briquette is found by using ASTM E871 standard method.

- **Volatile Matters**

Method: ASTM E872

Volatile matters of the briquette is found by using ASTM E872 standard method.

- **Ash content**

Method: ASTM E830

Ash content of the briquette is found by using ASTM E830 standard method.

- **Fixed carbon**

$$\text{FC (\%)} = 100 - (A + B + C) \quad \dots (5)$$

Where,

A = moisture content

B = volatile matter

C = ash content

- **Shatter index**

Procedure: Weight the samples (W_i). Released the samples in to 1 m height at three times. Samples are sieved in to 2 mm sieve and weighted remaining part (W_f)

$$\text{Shatter index} = \frac{W_f}{W_i} \times 100\% \quad \dots (6)$$

- **Compressive strength**

Apparatus: Universal Tensile Testing Machine

Procedure: Samples placed between plates of the machine. The briquette was subjected to uniform loading until it failed / ruptured. Corresponding compressive strengths were recorded from scale of the machine.

Compression strength (MPa) = Stress/Strain ... (7)

- **Water permeability**

Water permeability of the briquette is as the change in volume and weight when the briquette is submerged in water for 2 minutes.

Procedure: Weighted the samples (W_1). Measured the dimension of briquettes (diameter = d_i , height = h_i). Samples are submerged in to water for 2 minutes. After weighted samples (W_f) and measured dimensions (d_2, h_2)

Water permeability (as weight percentage)

$$= \frac{W_f - W_i}{W_i} \times 100\% \quad \dots (8)$$

Water permeability (as volume percentage)

$$= \frac{V_f - V_i}{V_i} \times 100\% \quad \dots (9)$$

Where,

V_i = initial volume

V_f = final volume

5. Results and Discussion

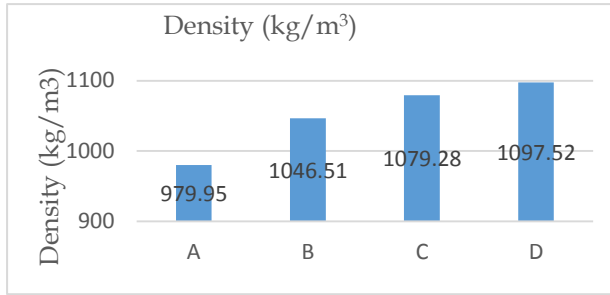


Figure 2 - Density Variation of briquettes

When comparing density variation of briquettes, rise husk helps to increase the density of briquettes. Highest density is found from sample D (25% saw dust and 75% risk husk mixture) (Figure 2).

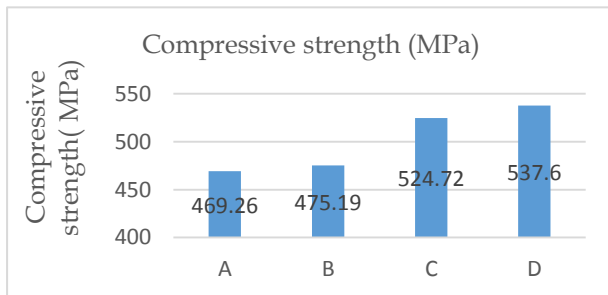


Figure 3 - Compressive Strength Variation of briquettes

The figure 3 shows compressive strength of briquettes vary with different compositions. Sample D is shown highest compressive strength and it implies more rice husk give to high compressive strength.

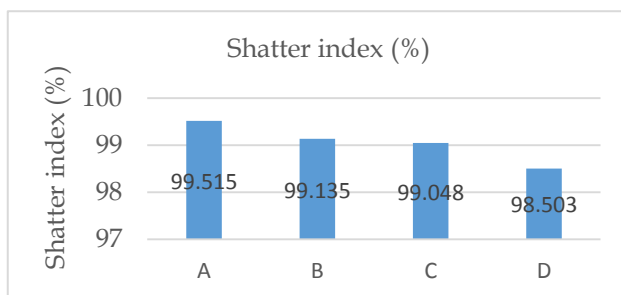


Figure 4 - Shatter Index Variation of briquettes

Figure 4 shows the shatter index of briquettes are decreased with rice husk percentage (Figure 4).

Therefore when the rice husk percentage increased bonding strength of briquettes is also increased.

According to above results mechanical properties of briquettes increase with increasing rice husk percentage.

When considering physical properties such as moisture content, volatile matter, fixed carbon and ash content (Figure 5) sample A is shown positive qualities for combustion. As household fuel briquettes ash content should be reduce. Higher volatile matter and fixed carbon implies higher combustion properties.

Calorific value of saw dust is higher than rice husk and it is shown in figure 6. Therefore when decreasing saw dust percentage, calorific value also decrease.

Figure 7 shows result of water permeability test. According to visual inspections (figure 7) "sample A" has higher water permeability than others. When increasing rice husk, water permeability is decreased.

Physiochemical properties are decreased with rice husk percentage and mechanical properties are increased with rice husk percentage.



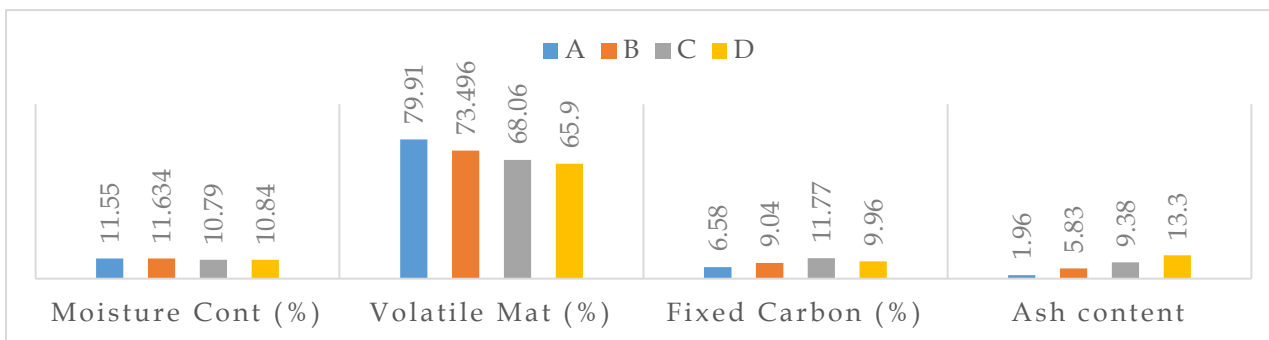


Figure 5 - Variation of briquettes Physical Properties

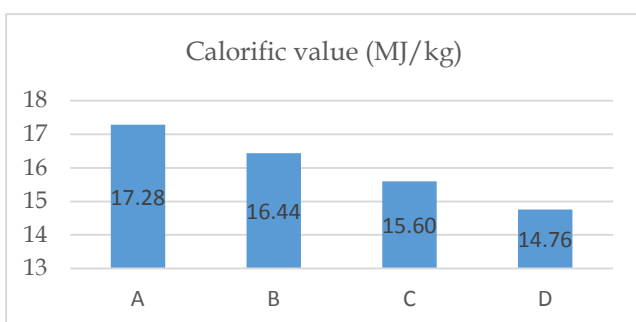


Figure 6 - Calorific Value Variation of briquettes

6. Conclusions

Calorific value is the most important factor that defines the energy available in a fuel. When considering the results, calorific value of sawdust is higher than that in rice husk. So when it comes to the briquette made with sawdust and rice husk mixture, calorific value is less than that of sawdust. Therefore the obtainable energy from the briquette is slightly less than sawdust briquettes.

But durability, ease of transportation and storage are some important factors that has to be considered when manufacturing briquettes. In the present research it is found that stability of the briquette is higher when briquettes are made using sawdust and rice husk mixture than sawdust briquettes. Also when both sawdust and rice husk is mixed, it doesn't require any binding material when the right pressure and temperatures are applied at densification stage.

Therefore to use as a fuel and for a waste management solution, sawdust and rice husk mixed briquettes can be given as a good solution.



100% sawdust briquette after water permeability test



75% sawdust 25% rice husk briquette after water permeability test



50% sawdust 50% rice husk briquette after water permeability test



25% sawdust 75% rice husk briquette after water permeability test

Figure 7 - Water Permeability Variation of briquettes

Acknowledgement

Authors wish to thanks the Department of Chemical and Process Engineering and Department of Material Science Engineering of University of Moratuwa for providing the laboratory facilities and also wish to acknowledge the assistance given by the IESL in preparation of this guide.

References

1. A. Gore, "The end of the fossil fuels - our green energy," 2010. [Online]. Available: <https://www.ecotricity.co.uk/our-green-energy/energy-independence/the-end-of-fossil-fuels>. [Accessed 09 June 2016].
2. H. M. A. Paki Turgut, "Limestone dust and wood sawdust as brick material," *Building and Environment*, vol. 42, no. 9, pp. 3399-3403, 2007.
3. P. R. S. S. A. S. S. B. P. A. S. K.K.C.K. Perera, "Assessment of sustainable energy potential of non-plantation Biomass resources in Sri Lanka," *Biomass and Bioenergy*, no. 29, pp. 199-213, 2005.
4. P. R.M.Amarasekara, "Resource Potential of sawdust and its spatial distribution in Kandy district," Integrated Development Association, Kandy, Sri Lanka, 2002.
5. B. A. C. Antwi-Boasiako, "Strength properties and calorific values of sawdust-briquettes as wood residue energy generation source from tropical hardwoods of different densities," *Biomass and Bioenergy*, vol. 85, pp. 144-152, 2016.
6. M. B. S. N. e. B. Lela, "Cardboard/sawdust briquettes as biomass fuel: Physical-mechanical and thermal characteristics," *Waste Management*, vol. 47, pp. 236-245, 2016.
7. M. K. z. W. Mariusz Jerzy Stolarski, "Energy, economic and environmental assessment of heating a family," *Energy and Buildings*, vol. 66, no. 18/07/2013, pp. 395-404, 2013.
8. S. E. A. S. Lanka, "Sri Lanka Energy Balance," 2014. [Online]. Available: <http://www.info.energy.gov.lk/>. [Accessed 29 09 2016].
9. Nalladuari Kaliyan, R. Vancey Morey, "Natural binders and solid bridge type binding mechanisms in briquettes and pellets made from corn stover and switchgrass," *Biosource Technology*, 2009.
10. T. P. N. S. N. S. M. T. Tanakorn Unpinit, "Fuel Properties of Bio-Pellets Produced from Selected Materials under Various Compacting Pressure," *Energy Procedia*, vol. 79, pp. 657-662, 2015.
11. S. V. M. L. Y. A. I. Relova, "Optimisation of the manufacturing variables of sawdust pellets from the bark of Pinus caribaea Morelet: Particle size, moisture and pressure," *Biomass and bioenergy*, vol. 33, pp. 1351-1357, 2009.
12. R. V. M. Nalladurai Kaliyan, "Factors affecting strength and durability of densified biomass products," *Biomass and bioenergy*, vol. 33, pp. 337-359, 2009.
13. L. L. G. J. M. J. M. E. Granada, "Fuel lignocellulosic briquettes, die design and products study," *Renewable Energy*, vol. 27, pp. 561-573, 2002.
14. M. Stahl, "Improving Wood Fuel Pellets for Household Use," Karlstand University Studeis, 2008.
15. A. A. N. S. Daham Shyamalee, "Evaluation of different binding materials in forming biomass briquettes with sawdust," *International Journal of Scientific and Research Publications*, vol. 5, no. 3, pp. 1-8, 2015.
16. R. P. Overend, "Direct Combustion of Biomass," *Renewable Energy*, vol. 1, pp. 1-9, 2008.
17. G. d. S. A. B. A. Wan Azlina Wan Ab Karim Ghani, "PHYSICO-CHEMICAL CHARACTERIZATIONS OF SAWDUST-DERIVED BIOCHAR AS POTENTIAL SOLID FUELS," *The Malaysian Journal of Analytical Sciences*, vol. 18, no. 3, pp. 724-729, 2014.
18. G. Borowski, "The Possibility of Utilizing Coal Briquettes with a Biomass," in *Environment Protection Engineering*, Lublin, Lublin University of Technology, 2007.
19. A. S. Ayhan Demirbas, "Evaluation of biomass residue: 1. Briquetting waste paper and wheat straw mixtures," *Fuel Processing Technology*, vol. Volume 55, no. Issue 2, 1998.
20. C. H. A. S. B. N. Emre Altun, "Influence of coal briquette size on the combustion kinetics," *Fuel Processing Technology*, vol. 85, pp. 1345-1357, 2004.
21. P. Z. M. V. G. O. D. M. D. Bolortuya, *Physics of Particles and Nuclei Letters*, vol. 10, pp. 723-726, 2013.
22. Rinkesh, "Conserve Energy Future," 2015. [Online]. Available: www.conserve-energy-future.com/NonRenewableEnergySources.php. [Accessed 1 10 2016].
23. L. F.-T. F. G. Teodora Deac, "Environmental impact of sawdust briquettes use - experimental approach," *Energy Procedia*, vol. 85, pp. 178-183, 2016.
24. I. Nizam, "The Island," 5 9 2010. [Online]. Available: http://www.island.lk/index.php?page_cat=article-details&page=article-details&code_title=6011. [Accessed 9 2016].
25. M. S.Ericson, *The briquetting of agricultural wastes for fuel*, Rome: FAO, 1990.



Assessing the Performance of a Destructive Measurement System: A Case of an Industrial Glove Manufacturing Environment

H.A.D. Perera and P. Gamage

Abstract: Quality improvement is a key aspect to gain a competitive advantage by any organisation. The main focus of quality improvement is to reduce the variation of any system which is inherent with product/process variation and the Measurement System Variation (MSV). Thus, Gauge Repeatability and Reproducibility (Gauge R&R) study provides a better solution in verifying the precision of the Measurement System by assessing the MSV as a percentage of total variation in a system. Gauge R&R study is challenging when it is used in assessing destructive measurements where the product is affected by the measurement. Literature suggests that there is a poor focus on destructive Measurement System Analysis (MSA). Hence, this study is focused on assessing the performance of a destructive measurement system for measuring the abrasion resistance level of industrial gloves using Gauge R&R and Analysis of Variance (ANOVA) method. The results show that the percentage study variation of total Gauge R&R is 17.41%, which is acceptable based on the American Automotive Industry Action Group (AIAG) guidelines.

Keywords: Gauge R&R, Destructive Measurement System, Industrial Gloves

1. Introduction

With the growth of the global economy manufacturing organizations strives to be competitive by satisfying customers [18]. Engineers engaged in design, development and actual manufacturing of products, play a vital role in achieving process efficiency and process capability of their manufacturing processes. Another important aspect of process efficiency is minimising the variation of the process output so that the process output or the quality characteristic under consideration stays well within the specification limits [1, 3].

Quality management decisions are depending on the quality of the data and knowledge that could be gain through analytical studies. It is likely to be low or high if the quality of the data is respectively low or high—which is used to make an actionable conclusion [17]. Measurements are considered as the data that is essential for understanding and improving the quality of product/ process or any kind of service [5, 10]. A measurement system is a process used to obtain measurements which are a collection of gauges, appraisers, methods, instruments, etc. [19]. Establishing a correct Measurement System is a key requirement before checking the stability and capability of

the processes as the real process variation can be concealed by the Measurement System Variation (MSV). Therefore, understanding the MSV is essential as it corporates in identifying the real process variation and preventing wrong quality management decisions [19].

MSV can be categorised into accuracy closeness of the mean in measured values to the true value and precision closeness of replicated observations [9, 19]. Precision can be categorised into repeatability measuring the same sample using the same instrument by the same appraiser and reproducibility measuring that includes the same sample using the same instrument by different appraisers as shown in Figure 1.

Gauge R&R study is a designed experiment to assess the capability of the MS to determine the total variability due to gauge, to isolate the

Mrs. H. A. D. Perera, BSc. Eng. Hons (Thailand), MSc. Candidate, Department of Manufacturing and Industrial Engineering, Faculty of Engineering, University of Peradeniya.

Dr. P. Gamage, BSc. Eng. Hons (Peradeniya), Ph.D. (New Zealand), Lecturer, Department of Manufacturing and Industrial Engineering, Faculty of Engineering, University of Peradeniya.



-sources of variability in the system. measurement system to obtain reliable data for quality improvement activities [6].

Measurement systems can be broken down into replicable measurement systems where the reading can be replicated for each part and non-replicable measurement systems [6, 19] where the part is being damaged/destroyed or apply changes to the characteristics of the part by the measurement process [19].

Luo et al. [21] depicted that the requirement of further research on the effective analysis of data obtained from a destructive measurement system is limited in the current literature. Therefore, the aim of this paper is to assess the capability of the measurement System using ANOVA method and few other capability measures such as P/T ratio, Signal-to-Noise ratio (SNR), and discrimination ratio (D_R). Thus, this research is focused on analysing a destructive measurement system with Homogeneity Sample method followed by a case example of an ABC industrial glove manufacturing plant.

2. Literature Review

Total variation of any process and/or product can be categorized into two major components: the process and/or product inherent variation and Measurement System Variation (MSV) as shown in Figure 1.

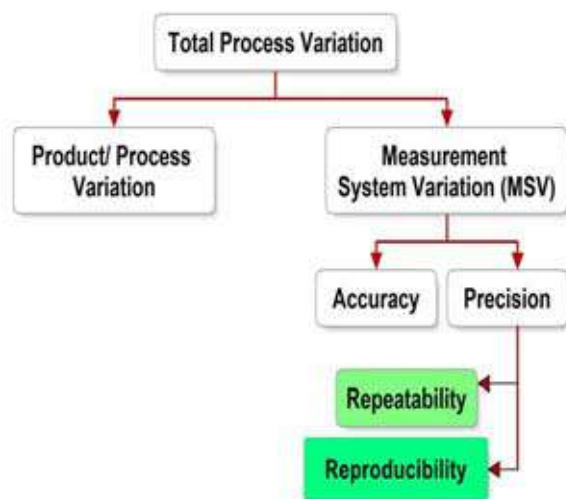


Figure 1 – Total process variation (Source: [9, 19])

Many literatures [2, 6, 10, 12, 19] have been emphasized that conducting a Gauge R&R study to analyse the MSV is important before

collecting any data to understand the process stability, capability or to perform any quality improvements activities of product/ process because these results contain do get obscured by Measurement System variation. Inadequate measurement systems cause loss to the company as well as for the customer due to the wrong quality decision with unreliable data [10, 12, 17].

Gauge R&R study is challenging when it is used in assessing a destructive measurement system where products are damaged when taking the measurements [11, 17]. Measuring reproducibility and repeatability can be performed under a strong assumption on batch homogeneity [16]. De Mast and Trip [11] have explained that good estimate of the measurement system can be obtained if the experimenter can arrange a Gauge R&R study with the homogeneous conditions which is not completely solved the confounding of measurement system variation with other sources of variation.

Lou et al. [17] have studied the application of homogeneity method to analyse destructive measurement system with a case example of electronic industry, and further research is recommended to analyse destructive measurement systems effectively. ANOVA method has the capability of handling any experimental setup, estimating variances more accurately and finding the interaction between parts and appraisers though its numerical computation is complicated [19].

According to AIAG [11] guidelines, (a) < 1% contribution from Gauge R&R is ideal and 1-9% contribution is acceptable, (b) < 10% Study variation is ideal, 10-20% is acceptable, 20-30% is marginal but acceptable if it is not economically feasible to improve the measurement system [4, 19]. Apart from ANOVA method, few other criteria (P/T ratio, SNR, and D_R) are used to validate the results obtained from a Gauge R&R study, for a better conclusion of acceptability of a measurement system [7, 8, 14] Following section describes different capability measures which were used to assess the capability of Gauge R&R study in this case example.

2.1 Capability Measures

Precision to Tolerance ratio (P/T ratio)

The precision to tolerance ratio is one of the quality measures that use to evaluate the capability of a measurement. The P/T ratio can be calculated using the formula shown below [5, 19]:

$$P/T = \frac{K \times \sigma_{R\&R}}{USL - LSL} \quad \dots(1)$$

Where σ_{MS} is the variance of the measurement system, USL and LSL are the upper and lower specification limits of the process respectively, and K is the standard deviations between “natural” tolerance limits of a normal process. According to AIAG [20] guidelines, the measurement system is capable when P/T ratio $\leq 10\%$, and incapable when P/T ratio ≥ 30 .

Montgomery and Runger [10] have explained that there is a risk in relying on P/T ratio which can be made smaller by increasing the specification limits. Therefore measurement system is measured as a function of the ratio of process variance to measurement variance $\hat{\mathcal{V}}$.

Signal-to-Noise Ratio (SNR)

SNR is another capability measure which is a function of $\hat{\mathcal{V}}$ that can be calculated by the formula given below [5, 19].

$$SNR = \sqrt{\hat{\mathcal{V}}} \quad \dots(2)$$

Where;

$$\hat{\mathcal{V}} = \frac{\sigma_p^2}{\sigma_{MS}^2} \quad \dots(3)$$

σ_p^2 : Variance of the process

σ_{MS}^2 : Variance of the measurement system

Further, Wheeler and Lyday [4], and Woodall and Borror [13] have presented Discrimination ratio (D_R) as another capability measure which is also a function of $\hat{\mathcal{V}}$ to examine the applicability of a measurement system. D_R is calculated as follows:

$$D_R = \sqrt{(ndc^2 + 1)} \quad \dots(4)$$

Where, $ndc = 1.41\sqrt{\hat{\mathcal{V}}}$... (5)

Due to the fact that P/T ratio, SNR, and D_R criteria are being subjective to each process and do not explain the capability of the measurement system adequately, Burdick et al. [5] highlights the need of inducing confidence intervals to the assessment process.

Table 1 describes the criteria and their acceptability ranges – extracted from literature – which are discussed in this case research to assess the capability of the measurement system.

Table 1 - Acceptability of evaluation criteria

Criterion	Accepted	Moderately Accepted	Rejected	Source
R&R%	< 10%	10%-30%	> 30%	[5, 14, 15, 19]
P/T ratio	<8%			[17, 15, 19]
ndc	≥ 5	2-4	≤ 4	[5, 14, 19]
SNR	≥ 5		<5	[17, 19]
D_R	> 5	4-5	<4	[5, 6, 13]

Table 1 describes the criteria that are discussed here in this research with their acceptability ranges extracted from the literature.

3. Case Study

XYZ Company is a glove manufacturing company that produces many types of gloves such as industrial gloves, surgical gloves, etc. Abrasion resistance is considered as the major quality characteristic of ABC industrial gloves according to the customers’ requirement. (XYZ and ABC are pseudonyms given by the researcher to prevent the identification of the company and product respectively). Researchers are planning to conduct an experiment to improve the abrasion resistance level of industrial gloves to satisfy the customers by being competitive with other glove manufacturers. An abrasion testing machine is used to measure the abrasion resistance of ABC industrial gloves.





Figure 2 – Abrasion resistance testing process

The Martindale abrasion resistance tester (LIAB007) can test 9 samples at a single run that takes around 4 hours for each set. Figure 2 explains the testing procedures which are following by the operators to determine the abrasion resistance of ABC industrial gloves. Each sample is damaged during abrasion test. Therefore, this measuring system will fall into the category of destructive tests. Gauge R&R study can be conducted with the key assumption that the homogeneity of samples within a batch to analyse the destructive measurement system [17, 19].

Thus this case study example is focused on analysing the measuring system which used to measure the abrasion resistance of ABC industrial gloves as the first step in quality improvement process to make sure that the measurement system variability itself is consistent and comparably small, relative to process variability.

4. Methodology

The methodology of this research can be represented schematically as shown in Figure 3 below.

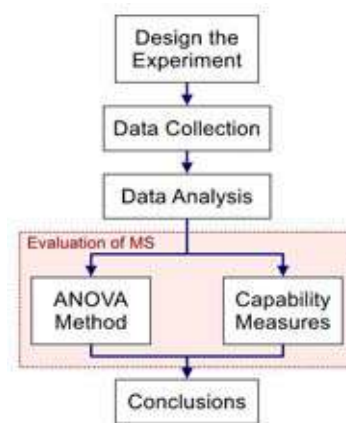


Figure 3 – Research Methodology

4.1 Design the Experiment

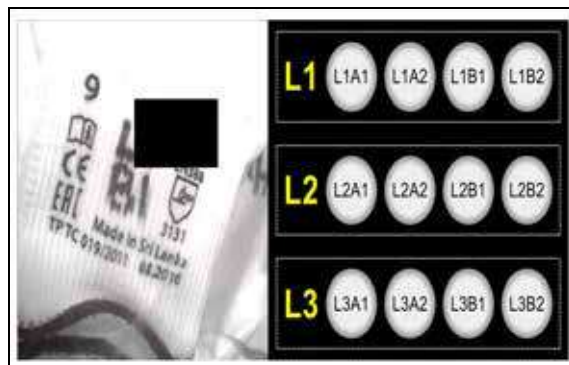


Figure 4 – Selection of homogenous samples

Gauge R&R study is designed with two appraisers (operators A and B) with a single abrading machine using 48 samples of gloves. Since the nature of the test is destructive, Gauge R&R study was conducted with the assumption

that ABC gloves at each dipping row (see Figure 4) have homogeneous properties. This study assumes that researchers used the homogenous batch of parts which can be assigned at least two parts from each batch to each operator to conduct the destructive Gauge R&R study. Figure 5 shows how the batches were selected with the homogeneous properties to conduct the destructive Gauge R&R study. Samples were allocated to each operator, and the measurements were taken in the randomised pattern which generated by a software package (Minitab 17).

5. Results

This research was analysed the measurement system which used to measure abrasion level of ABC industrial gloves as a destructive measurement system using Homogeneity

Sample Method based on ANOVA method and with other criteria (P/T ratio, SNR, and D_R) for a better conclusion of acceptability of a measurement system. Figure 5 and Figure 6 show the graphical plots and ANOVA results which were generated by Minitab 17 software package respectively. Figure 7 shows the percentage study variation of total Gauge R&R is 17.41%. This result shows that the measurement system is acceptable according to the AIAG guidelines [19, 20]. ANOVA results show that causes of gauge variation are due to repeatability. Repeatability is larger compared to reproducibility, and this may cause due to excessive within part variation (96. 97%) [19]. The number of distinct categories (7) is also greater than 5 and shows the acceptance of the measurement system

Assumption : Parts within Lot i (L_i) is homogenous. ($i= 1,2, \dots, 12$)

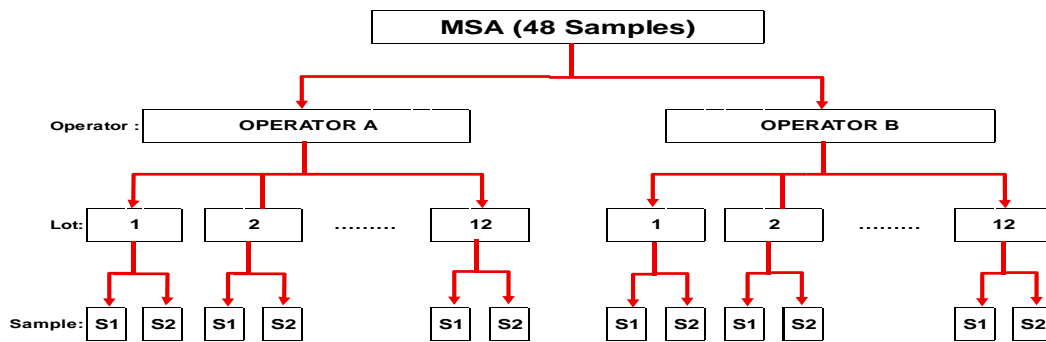


Figure 5 - Crossed model Gauge R&R design

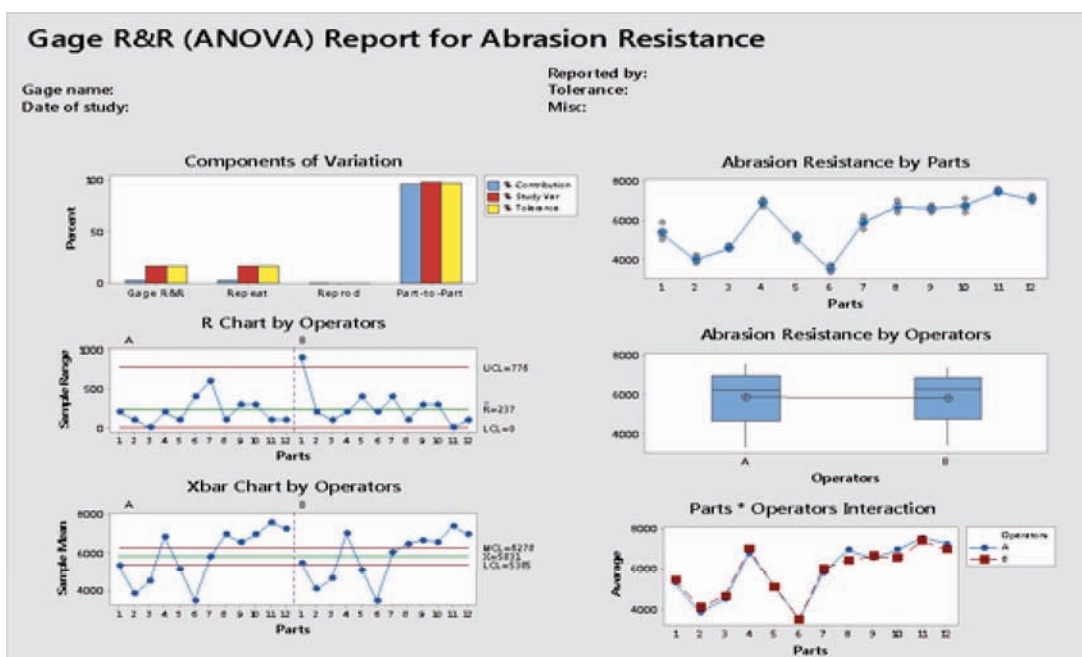


Figure 6 - Graphical representation of Gauge R&R study based on ANOVA method



In Figure 6, the component of the variation graph shows that part-to-part variation is the dominant source of variability, which basically implies that given the degree of part-to-part variation, the measurement gauge is able to produce measurements that are repeatable and reproducible. The R chart shows that there are no points outside the control limits. Therefore, this is indicated that the measurement is repeatable and reproducible. The chart X-bar

chart shows that the precision of the measurement system where the variation due to repeatability is low relative to part-to-part variation. The box plot shows the consistency of the measurements and the variability among the two operators. The Sample \times Operator interaction plot shows that lines do closely follow one another, thus showing high reproducibility.

Gage R&R				%Contribution
Source	VarComp	95% CI		(of VarComp)
Total Gage R&R	53065	(35662.473, 487221.855)		3.03
Repeatability	53065	(34909.300, 90294.018)		3.03
Reproducibility	0	(0.000, 432529.291)		0.00
Operators	0	(0.000, 432529.291)		0.00
Part-To-Part	1697089	(844885.508, 4916977.503)		96.97
Total Variation	1750154	(897998.702, 4999439.393)		100.00

Source	95% CI	
Total Gage R&R	(0.97, 21.78)	
Repeatability	(1.00, 7.03)	
Reproducibility	(0.09, 18.99)	
Operators	(0.09, 18.99)	
Part-To-Part	(78.22, 99.03)	
Total Variation		

Process tolerance = 8000

Source	StdDev (SD)	95% CI		Study Var
				(6 \times SD)
Total Gage R&R	230.36	(188.845, 698.013)		1382.16
Repeatability	230.36	(186.840, 300.490)		1382.16
Reproducibility	0.00	(0.000, 657.670)		0.00
Operators	0.00	(0.000, 657.670)		0.00
Part-To-Part	1302.72	(919.177, 2217.426)		7816.34
Total Variation	1322.93	(947.628, 2235.943)		7937.60

Source	95% CI		%Study Var	95% CI
			(%SV)	
Total Gage R&R	(1133.071, 4188.077)		17.41	(9.82, 46.67)
Repeatability	(1121.042, 1802.938)		17.41	(10.01, 26.52)
Reproducibility	(0.000, 3946.018)		0.00	(3.05, 43.58)
Operators	(0.000, 3946.018)		0.00	(3.05, 43.58)
Part-To-Part	(5515.059, 13304.555)		98.47	(88.44, 99.52)
Total Variation	(5685.768, 13415.656)		100.00	

Source	%Tolerance	95% CI	
	P/T ratio		
	(SV/Toler)		
Total Gage R&R	17.28	(14.16, 52.35)	
Repeatability	17.28	(14.01, 22.54)	
Reproducibility	0.00	(0.00, 49.33)	
Operators	0.00	(0.00, 49.33)	
Part-To-Part	97.70	(68.94, 166.31)	
Total Variation	99.22	(71.07, 167.70)	

Number of Distinct Categories = 7
 95% CI = (2.67991, 14.3260)

Figure 7 - ANOVA results of Gauge R&R study

In addition to this, P/T ratio, SNR, and D_R capability measures and their confidence intervals were calculated as shown in Table 2 to validate the results obtained from this case Gauge R&R study.

Table 2 – Acceptability levels of evaluation criteria

Criterion	Value	95 % CI	Decision
Gauge R&R %	17.41%	(9.82, 46.67)	Moderately accept
P/T ratio	17.28%	(14.16,52.35)	Moderately accept
ndc	7	(2.68,14.32)	Accept
SNR	5.65	(2.81,9.58)	Accept
D_R	7.07	(4.08,13.55)	Accept

6. Discussion and Conclusion

In this research, we considered verifying the appropriateness of the destructive measurement system that measures the abrasion resistance of industrial gloves through use of statistical measures obtained from the Gauge R&R and ANOVA method. The results are presented in Figure 6, 7 and table 2.

As shown in Table 2, R&R % = 17.41 %, ndc = 7, P /T% = 17.28%, SNR = 5.65 and D_R = 7.07%. ANOVA results and the capability measures which were considered in this destructive measurement system analysis are at acceptable levels at a 95% confidence interval. Additionally, from the comparison of all the considered measures, it is evident that this case study example can be shown as a good gauge capability analysis. Thus, the conclusion can be made that the destructive measurement system which used to measure the abrasion level of ABC industrial gloves is capable of obtaining reliable data for any quality improvement activities. Further studies have to be conducted to improve the dimensional measurement process further using Design of Experiment (DoE) methods.

Acknowledgement

Authors would like to acknowledge the assistance and support given by the employers at the case study organization in conducting this research work.

References

- Rao, L. P. Carr, I. Dambolena, R. J. Kopp, J. Martin, F. Rafii, et al., A Cross Functional Perspective. . NY: John Wiley & Sons, 1996.
- Montgomery, D. C., Introduction to Statistical Quality Control, 6 ed. Hoboken, NJ: John Wiley & Sons, 2009.
- Deming, W. E., Out of the Crisis. Cambridge, MA: MIT Press, 2000.
- Wheeler, D. C., and Lyday, R. W., Evaluating the Measurement Process, 2 ed. Knoxville, TN: SPC Press, Inc., 1989.
- Burdick, R. K., Borror, C. M., and Montgomery, D. C., "A Review of Methods for Measurement Systems Capability Analysis," Journal of Quality Technology, vol. 45, October 16-17 2003.
- Hamada, M. S., and Borror, C. M., "Analyzing Unreplicated Gauge R&R Studies," Quality Engineering, vol. 24, pp. 543-551, 2012.
- Burdick, R. K., Borror, C. M., and Montgomery, D. C., "Design and Analysis of Gauge R&R Studies: Making Decisions with Confidence Intervals in Random and Mixed ANOVA Models," American Statistical Association and the Society for Industrial and Applied Mathematics., 2005.
- Al-Refaie, A., and Bata, N., "Evaluating Measurement and Process Capabilities by GR&R with Four Quality Measures," Measurement, vol. 43, pp. 842-851, 2010.
- Hare, L. B., "Gage R&R Reminders: Running Gage Repeatability and Reproducibility Studies Properly," Quality Progress pp. 62-64, 2012.
- Montgomery, D. C., and Runger, G. C., "Gauge Capability and Designed Experiments Part I: Basic Methods," Quality Engineering, vol. 6, pp. 115-135, 1993.
- De Mast, J., and Trip, A., "Gauge R&R studies for Destructive Measurements," Journal of Quality Technology, vol. 37, pp. 40-49, 2005.
- Sarkar, A., Mukhopadhyay, A. R., and Ghosh, S. K., "Measurement System Analysis for Implementing Design for Six Sigma," International Journal of Productivity and Quality Management, vol. 14, pp. 373-386, 2014.
- Woodall, W. H., and Borror, C. M., "Some Relationships between Gage R&R Criteria," Quality and Reliability Engineering International pp. 99-106, 2008.



14. Cagnazzo, L., Sibalija, T., and Majstorovic, V., "The Measurement System Analysis as a Performance Improvement Catalyst: A Case Study," pp. 269-292, 2010.
15. Gunawan, I., and Sirodj, D. A. N., "Validation of the Grader's Ability using Measurement System Analysis," ARPN Journal of Engineering and Applied Sciences, vol. 11, August 2016 2016.
16. Ya-Juan, H., and Zhen, H., "An Applied Study of Destructive Measurement System Analysis," presented at the Second IEEE Conference on Industrial Electronics and Applications, 2007.
17. LOU, Z. B., Shi, L. X., He, Z., and He, Q. M., "The Study of Destructive Measurement Systems," presented at the Industrial Engineering and Engineering Management (IE&EM), 2011.
18. Longo, R. J., "An Assesment of Total Quality Managmeent in the Finanace Services of United Klingdom and Brazil," Doctor of Philosophy, Department of Management Studies, University of Newcastle, Newcastle upon Tyne, UK, 1997.
19. AIAG, "Measurement System Analysis," ed. Detroit: AIAG, 2010.
20. AIAG, "Measurement System Analysis," Chrysler Group LLC, Ford Motor Company, General Motors Corporation USA 978-1-60-534211-5, 2010.

Development of ANN Based IMC for Biomass Pack Bed Gasification Plant with Enhanced Efficiency

G.V.C. Rasanga, K.T.M.U. Hemapala and A.G. Buddhika P. Jayasekara

Abstract: Energy crisis and emerging negative impacts on environment are the driving factors of process industries to increase the share of sustainable resources in energy production. The utilization of biomass has a growing attention as a replacement for fossil fuels due to its wide availability and sustainability. However, biomass gasification has to face most of its drawbacks because of unpredictable variability of biomass properties, process complexity, and controllability of the process which creates additional barriers for a wider utilization of biomass gasification.

This study focusses on the development of biomass gasification plant controller to enhance the process efficiency. The plant control was developed based on internal model controller (IMC) architecture while gasification plant model was developed using neural network based nonlinear autoregressive model with external output (NNARX). Plant inverse model which was developed based on the NNARX was used as the controller. The plant model predicts the output for one time step of five seconds and sends the error between prediction and real output to the controller.

Developed neural network based internal model controller (NNIMC) was tested using 15kW pack bed imbert type downdraft biomass gasifire and controller algorithms development was then analysed for 72 minutes of the plant operation. The analysis showed that with the introduction of NNIMC control solution process, efficiency can be improved up to 12%, with the increase of performance in terms of stability.

Keywords: Biomass, Gasification, Internal Model Controller, Neural Network

1. Introduction

Sri Lankan industrial energy demand is being increased with the population growth and urbanization [1]. Therefore, the cost of electricity and fossil fuel, which are the primary energy sources of current Sri Lanka, is also continuously going up. In this context, usage of renewable energy sources is becoming more popular, particularly, industrial sector is interested in biomass-based solutions to meet their thermal, electricity and other forms of energy demands due to low cost [2].

“Gasification” is one of the process of converting solid fuel, which was invented during World War II [3]. In this process, there is a thermochemical conversion of solid fuel into high calorific and useful gaseous fuel or chemical products [4], which can directly use for internal combustion engine and gas burners. Furthermore, researchers have tried to produce useful chemicals and gases using gasification produced gas and produced gas is also used for fuel cell. The overall efficiency of electricity generation by gasification process is higher than direct combustion of biomass [4]. For power generation, biomass gasification produced gas has to meet some special

technical requirement for an example, partially composition of the produced gas. The composition of CO and H₂ are greater than 20% and 10% respectively, while tar content should be lower than 100mmgNm⁻³.

However, this technology is still not much acquainted for small scale domestic power generation application. Because of complexity and operation difficulties of those processes such as maintaining continuous process output due to process uncertainties and process disturbances like fuel properties.

Most of past researchers tried to overcome those problems by improving reactor geometry and fuel pre - processing. Although there is a considerable practical development in past,

Eng. G. V. C. Rasanga, AMIE (SL), B.Sc.Eng. (Ruhuna), Mechanical Engineer, Sri Lanka Ports Authority, Galle, Sri Lanka.

Eng. (Dr.) K. T. M. U. Hemapala, CEng, MIE (SL), B.Sc.Eng. (Moratuwa), PhD(Italy), Senior Lecturer, Department of Electrical Engineering, University of Moratuwa, Colombo, Sri Lanka.

Eng. (Dr.) A. G. Buddhika P. Jayasekara, AMIE (SL), B.Sc.Eng. (Moratuwa), M.Sc.(Moratuwa), PhD(Saga), Senior Lecturer, Department of Electrical Engineering, University of Moratuwa, Colombo, Sri Lanka.



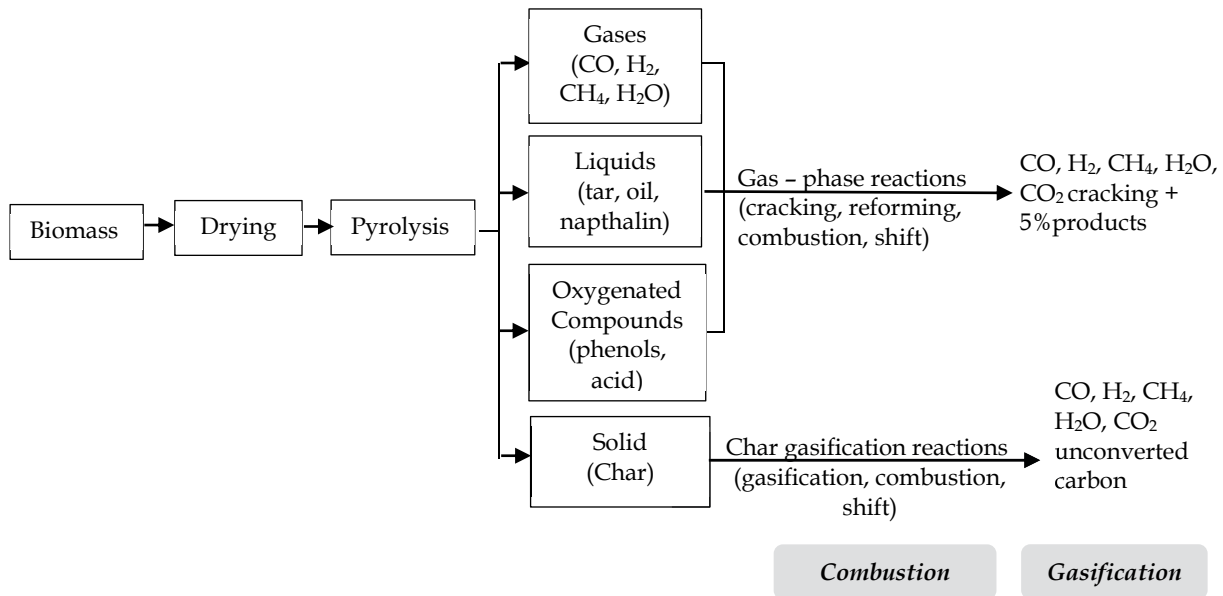


Figure 1 - Schematic Diagram of Gasification Process [3]

number of gasification projects has increased all over the world, especially in Europe.

Typically, biomass gasification includes basic steps as drying, pyrolysis, combustion and char reaction (gasification) as illustrated in Figure 1 [3].

Moisture content of fresh wood and dry biomass are usually varied between 30% - 60% and 10-20% respectively. Drying is the stage where bounded water of biomass irreversibly removes at above 100°C due to heat from high temperature zone (combustion zone)[3].

In the stage of pyrolysis, large hydrocarbon molecules in biomass are broken down in to small hydrocarbons and char, due to lack of oxygen at relatively low temperature as shown in Figure 1. Gasification pyrolysis occurs between 300°C - 650°C, which is called as pyrolysis temperature. Pyrolysis gas reacts with oxygen at combustion zone and results high temperature (1000°C-1350°C). Then combusted gas (CO₂, H₂O) reacts with red hot char and produced syngas (CO, H₂ and CH₄).

According to gas - solid contacting mode and gasification medium, there are several type of gasifires has been developed [3, 4]. Among them, downdraft pack bed gasifire is very much appropriate for small scale power application as it is simple, low cost construction and has low tar production [3, 5].

Biomass gasification influences on several process parameters. The main variable of

uncertainty is related with properties of biomass [6] such as gasification agent, process temperature, moisture content, and air flow rate [3, 4, 7, 8 and 9].

Modelling is very effective in terms of optimizing the operation of existing gasifiers and explore operational limits instead of sizing the reactor. A model can identify the sensitivity of gasifier performance according to the variations of for different operations and design parameters [8]. Furthermore, there are different modelling approaches, such as thermodynamic equilibrium, kinetic, computational fluid dynamics and artificial neural network.

The maximum yield that can be accomplished a desired product in a reacting system can be calculated using a thermodynamic equilibrium model. Equilibrium of thermochemical system is determined based on the equilibrium constant or minimization of Gibbs free energy [8, 10]. Furthermore, there are two equilibrium models such as stoichiometric and non-stoichiometric depending on above two techniques.

Thermal chemical equilibrium cannot be used for gasifire reactor [8], because gasification is a dynamic process. The main advantage of the equilibrium model is that independence from gasification geometry. Different authors had developed gasification equilibrium models both in non-stoichiometric and stoichiometric models for downdraft gasifire [11, 12]. The main purpose of equilibrium modelling is to

predict the performance of gasifier in design stage.

Development of kinetic models to evaluate and imitate the gasifier behaviour is caused by the inadequacy of equilibrium model to correlate the reactor design parameter with the final product gas composition, reaction rate, residence time, reactor geometry.

Ozgun Yucel (2016)[13], has developed a kinetic model for downdraft and predicted the reactor performance for different throat angles. However, due to nonlinearity and complexity of the model, gasifier kinetic model is also difficult to use for online plant control.

Hybrid multilayer feedforward neural networks (HMFNN) were improved by Guo et al. [14] to forecast the plant output of fluidised bed gasifier and they had only considered temperatures of gas and bed as model inputs. Furthermore, Puig- Arnavat et al. [15] developed an artificial neural network (ANN) model for fluidised bed gasifier. That model consisted of input output layer, one hidden layer, and composition of the biomass in terms of C, H, and O, equivalence ratio, gasification temperature, ash and moisture content as model inputs. Predicted outputs were percentage values of CO, CO₂, H₂ and CH₄ in produced gas as illustrated in Figure 2.

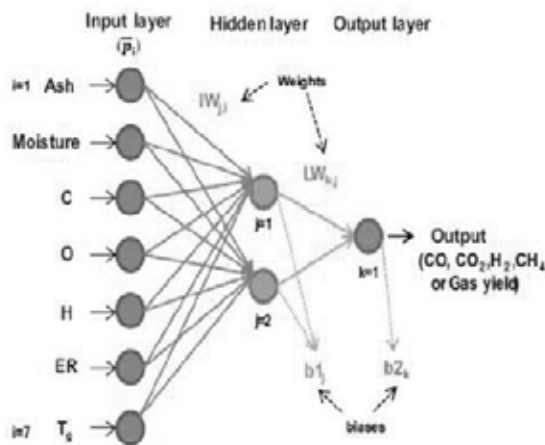


Figure 2 - ANN Model Structure to Predict Produced Gas Composition of CFB Gasifier [15]

Equilibrium and kinetic models are useful in prediction of gasifier performance under number of different stationary operating conditions therefore, they are often used for preliminary design and optimisation purposes. According to Ahmed [16], many equilibrium models have been verified just on several

operating points or with data derived due to lack of extensive measurements. Less number of artificial intelligence systems based on biomass gasification models have been reported because ANN model does not create intensive measurement.

ANN is a universal function approximator that can approximate any continuous function to an arbitrary precision even without a prior knowledge on structure of the function that is approximated [17]. Furthermore, ANN models have proven their potential of forecasting the process parameters in energy related processes such as in biodiesel production process [18] and applied for different thermochemical reactor applications such as flotation column, packed distillation column [19, 20]. For that, ANN models use a non-physical modelling approach which correlates input and output data to form a process prediction.

Macmurray and Himmelbealj (1995) [20], developed ANN based controller for distillation column. After that, Mohanty (2009) [19], developed ANN based model predictive controller for floatation column. Robert (2015) [21], later improved the gasification process efficiency by 25% modifying the plant controller using ANN based control map.

According to the research outcomes of above researches, ANN based predictive, model based controller has proved its capability for nonlinear process and plant control. Among them, internal model controller (IMC) is one of the simplest model based predictive controller which can easily link with ANN [22].

2. Methodology

Methodology is comprised of experimental set up of gasification plant and development of internal model controller.

2.1 Biomass Gasification Plant

Imbret type downdraft gasifier of 15-25kW thermal output was used in the experimental setup as shown in Figure 3.

Plant consists of variable speed driver (VSD), which controls 1hp centrifugal blower that pulls air through the gasifier and a swirl type burner. The temperature of char bed, throat and flue gas out were measured by k type thermocouples as illustrated in Figure 4.





Figure 3 - Experimental Set-up of Downdraft Gasfire

The mass flow rate through the swirl burner was kept constantly using induced blower which is also displayed in Figure 4.



Figure 4 - Swirl Burner

2.2 Artificial Neural Network (ANN) Based Internal Model Controller (IMC)

Architecture of the ANN based IMC is shown in Figure 5.

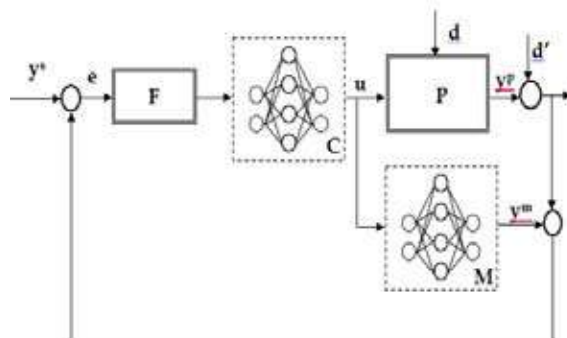


Figure 5 - Structure of Neural Network Based Internal Model Controller

P, C and M in Figure 5, represent nonlinear plant, nonlinear controller and nonlinear plant model respectively. F is first order linear filter. Both M and C are nonlinear autoregressive network with exogenous inputs neural network (NARXNN). Temperature at char bed, and throat, speed control, signal of VSD (which controls blower rpm) and previous predicted plant output are the inputs of the plant model. Gasification plant was operated for 340 minutes at different blower rpms and temperature of char bed, throat, and flue gas were then recorded for every 5 second. Plant model NN was trained using recorded values using Matlab time sires tool.

Best fitted NN for plant model is shown in Figure 6. C is the gasification plant inverse model. It was also trained by the same data set which was used in Matlab time series tool. Best fitted NN for plant inverse model is shown in Figure 7.

Developed NNIMC is shown in Figure 8. There, f_1 denotes logtan function and f_2 represents linear function.

D is delay of inputs and outputs. Similarly, b_x is base value of layers

while IW_x and LW_x are and weights of network respectively. The developed NNIMC was implemented on LabView graphical interface.

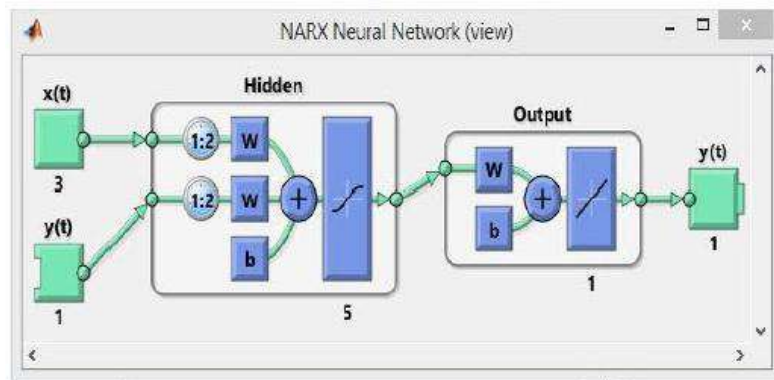


Figure 6 - Neural Network Plant Model (M)

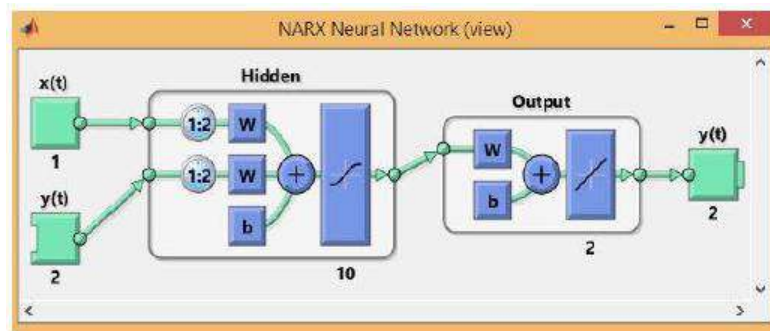


Figure 7 - Neural Network Inverse Model (C)

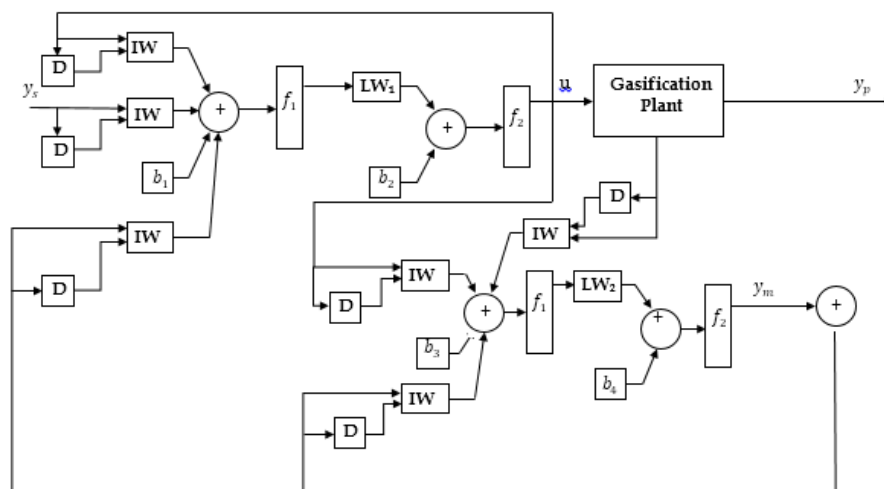


Figure 8 - Developed NNIMC for Gasifire Plant



3. Results and Discussion

Two experiments were arranged to investigate the performance of proposed IMC system for biomass downdraft gasifier. In first experiment, gasifier was operated with the proposed IMC system using 12kg of coconut shells. Set value was fixed during the operation as the dash line in the Figure 9. Step response was provided at $t = 306$, and $t = 465$ to controller within the range of set value from 960 K to 980K. According to the Figure 9, flue gas temperature follows the set value and it levels off all over

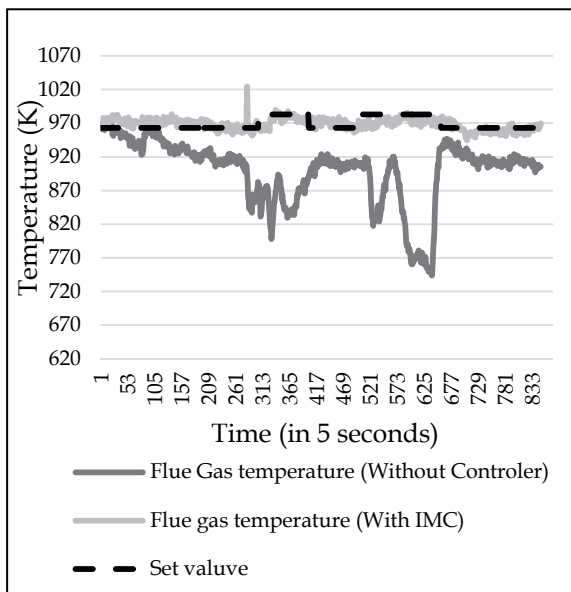


Figure 9 - The Graph of Flue Gas Temperature vs. Time

the operation as indicated in orange line. Secondly, gasifier was operated at constant blower speed of 3260 rpm for 12kg of coconut shells. Black colour continuous line represents the flue gas temperature at burner and it is not stable in the second experiment. Also, ignition was disturbed and flame did not appear particularly at the lowest temperature points.

Figure 10 displays the variation of power output for both experiments. Flue gas flow rate was remained at a constant value of 0.029kg/s, therefore, variation of power output is proportionate to the flue gas temperature changes.

As shown in Figure 10, total energy output of two experiments (With IMC and Without IMC) were 83201.57kJ and 73878.74kJ respectively.

According to the above result, the overall improvement of energy output is 12.60%.

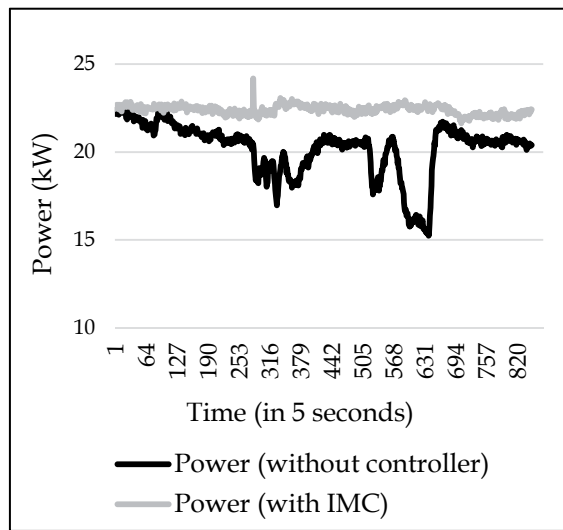


Figure 10 - The graph of Power Output vs. Time

Figure 11 and 12 show temperatures at different locations; char and throat, when gasifier was operated with and without proposed internal

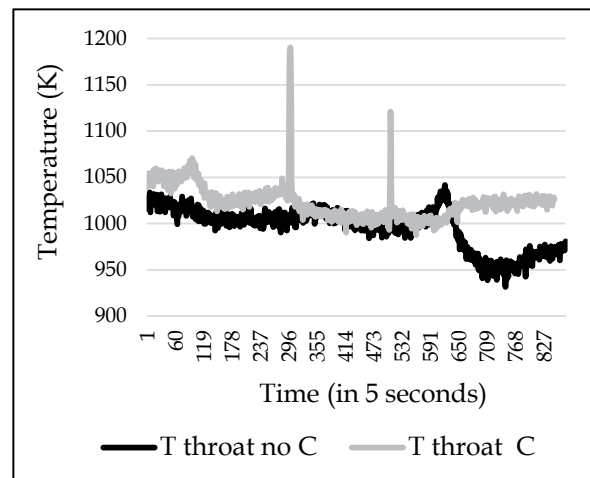


Figure 11 - Temperature Variations at Throat

model control. According to the temperature variations, introduced IMC system operates the gasifier at higher process temperatures. Higher gasification temperatures reflect a better oxidation, low tar production and higher calorific value of syngas [11].

Higher gasification temperatures provide better formation rate of CO, CH₄ and H₂ which lead to higher syngas heating value which is shown in Figure 09. When introduced IMC system operates gasifier, flue gas temperature of the

burner is higher than without IMC. There are high temperature impulses indicated by ash

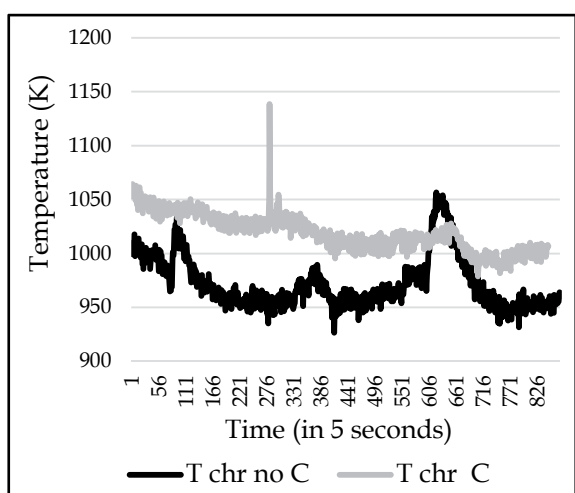


Figure 12 - Temperature Variation at Char

colour line in Figure 11 at around $t = 309$ and 450. Those are resulted by the stuck char particles at throat. When the pressure difference increased by them across the throat, it causes a rapid high air flow and consequently flame at combustion area goes to char burning zone and throat.

4. Conclusions

Internal model based control architecture was used for developing plant controller because of high process nonlinearity of biomass gasification process. Plant inverse model was also developed by using neural network. And developed biomass gasification plant model was then used as the internal model. The neural network technics can be easily combined with IMC control architecture. Furthermore, according to the results, neural network can be effectively used to model and control nonlinearity system.

Figure 9,10 show that the syngas production stability is improved by IMC all over the plant operation. At the same time, IMC increases power output of the gasification. However, the plant output takes more time to reach to the set value because gasification is time delaying process.

During the development of plant model, it revealed the importance of grate shaking effect. However, the effect of grate shaking could not be considered for implementing the control because of a technical problem i.e., burnout of the grate shaking motor.

In this research, the neural network based IMC has been trained only for coconut shells. Therefore, this plant control may not applicable for other biomass types. As future directions, network should be developed for different biomass with different physical properties.

Moreover, gasification plant with internal combustion engine is one of very popular application. However, composition of gasification produced gas is not constant. This issue disturbs for smooth running of internal combustion engine because of the ignition preparation of gas component is different, for an example, ignition propagation of H_2 is high and ignition propagation of CO is very low than H_2 . Therefore, advanced predictive controller will be an effective solution for smooth governor control

References

1. Sri Lanka Sustainable Energy Authority "Sri Lanka Energy Balance 2007 and Analysis of Energy Sector Performance", Chapter 5, 2017.
2. Johansson, T. B.; Kelly, H.; Reddy, A. K. N.; Williams, R.H. Renewables for fuels and electricity, 1992, UNCED.
3. Basu, P., Biomass Gasification and Pyrolysis, 1st Ed.
4. Milieuonderzoek, K. et al, " Review of applications of gases from biomass gasification- ECN Biomass", 2006.
5. Available: <http://biofuelsacademy.org/web-modules/process/gasification/cross-draft-gasification/> accessed on 22/11/2016.
6. Fournel, S., Palacios, J. H., Morrisette, R., Villeneuve, J., Godbout, S., Heitz, M., and Savoie, " Influence of Biomass Properties on Technical and Environmental Performance of a Multi-Fuel Boiler during on-Farm Combustion of Energy Crops", Applied energy, 141, 2015, pp. 247-259.
7. Budhathoki, R., "Three Zone Modeling of Downdraft Biomass Gasification: Equilibrium and Finite Kinetic Approach", 2013.
8. Patra, T. K., and Sheth, P. N., "Biomass Gasification Models for Downdraft Gasifier: A State-of-the-Art Review", Renewable and Sustainable Energy Reviews, 50, 2015, pp. 583-593.
9. Ghassemi, H., and Shahsavan, R., - Markadeh, "Effects of Various Operational Parameters on Biomass Gasification Process; A Modified Equilibrium Model", Energy Conversion and Management, 79, 2014, pp. 18-24.



10. Available: <http://www.bios-bioenergy.at/en/electricity-from-biomass/biomass-gasification.html> accessed on 22/ 11/2016.
11. Mendiburu, A. Z. et al, Thermochemical Equilibrium Modeling of a Biomass Downdraft Gasifier: Constrained and Unconstrained Non-Stoichiometric Models, *Energy* xxx, 2014, pp. 1-14.
12. Mendiburu, A. Z., et al, "Thermochemical Equilibrium Modeling of Biomass Downdraft Gasifier: Stoichiometric Models", *Energy* 66, 2014, pp.189 - 201.
13. Yucel, O., and Hastaoglu, M.A., "Kinetic Modeling and Simulation of Throated Downdraft Gasifier" *Fuel Processing Technology*, 144, 2016, pp.145-154.
14. Bing Guo et al, "Simulation of Biomass Gasification with a Hybrid Neural Network Model" *Bio Resource Technology*, 76, 2001, pp. 77-83.
15. Puig-Arnavat, M. et al, "Artificial Neural Network Models for Biomass Gasification in Fluidized Bed Gasifiers", *Biomass and bioenergy*, 49, 2013, pp. 279-289.
16. Ahmed, T. Y. et al, "Mathematical and Computational Approaches for Design of Biomass Gasification for Hydrogen Production: A Review" *Renewable and Sustainable Energy Reviews*, 16, 2012, pp. 2304- 2315.
17. Robert Mikulandric et al, "Artificial Neural Network Modelling Approach for a Biomass Gasification Process in Fixed Bed Gasifiers" *Energy Conversion and Management*, xxx, 2014, pp. xxx-xxx.
18. Piloto-Rodríguez, R. et al, "Prediction of the Cetane Number of Biodiesel using Artificial Neural Networks and Multiple Linear Regression" *Energy Conversion and Management*, 65, 2013, pp. 255-261.
19. Mohanty, S., "Artificial Neural Network Based System Identification and Model Predictive Control of a Flotation Column", *Journal of Process Control*, 19, 2009, pp. 991-999.
20. Macmurray, J. C., and Himmelbeal, D. M., "Modeling and Control of A Packed Distillation Column Using Artificial Neural Networks", *Computers chem. Engng*, 19(10) 1995, pp.1077-1088.
21. Mikulandric et al, "Process Performance Improvement in a Co-Current, Fixed Bed Biomass Gasification Facility by Control System Modifications" *Energy Conversion and Management*, 104, 2015, pp. 135-146.
22. Hunt, K. J., and Sbarbaro, D., "Neural Networks for Nonlinear Internal Model Control", *IEE Proc.-D*, 138(5), 1991.

Organic Rankine Cycle (ORC): Performance of Working Fluids and Energy Recovery Potential in Sri Lankan Thermal Power Plants

B.S.R. Fernando, R.A.C.P. Ranasinghe and H.K.G. Punchihewa

Abstract: ORC based power generation is becoming popular as a way of generating electricity from low-grade heat sources such as waste heat. Working fluid selection and system optimization based on heat source temperature are two critical aspects of ORC design. In this work, eleven fluids comprised of hydrocarbons and refrigerants were theoretically investigated to maximize the work output for a range of source temperatures. Results show that Heptane, Pentane and Decane show favourable results in terms of work outputs while, in terms of efficiency, Decane and Heptane are better. Further, it was found that Pentane outperforms, when source temperatures are between 45 – 190 °C, while Heptane for 190 – 260 °C. Decane is more suitable for 260 – 340 °C range. Based on the theoretical analysis, a new summarized graphical chart was developed for Pentane, Heptane and Decane, where one point on the graph can denote approximate work output, efficiency, pressure, temperature and other required data for the initial design process and fluid selection of an ORC plant. Subsequently, the economic feasibility of ORC was assessed considering WH data of all the thermal plants of in Sri Lanka. Possible electric power outputs were computed for each selected plant, for selected fluids from the above theoretical analysis. Then, maximum work out of each case was selected for further economic evaluation under seven different scenarios, which represents the future economic situation in the country. Investment cost was estimated pertaining to the maximum work output and payback time was estimated to evaluate the investment feasibility. Interestingly, results show that some of the high volume power stations are very good candidate for ORC, which has very short payback time even with the worst possible economic situations considered.

Keywords: ORC, Thermal power performance, Thermal Energy recovery

1. Introduction

Thermal energy is still the major source for power generation, worldwide. Efficiencies of most of the thermal plants are less than 50% [1]. Consequently, the total emission of CO₂ due to fossil fuel combustion was estimated to be 32,381 Mt in 2014 [4], and many environmental issues related to fossil fuel combustion have also been identified [2, 3]. Dumping of low-grade waste heat to the environment is one of the key issues of such power plants, yet inevitable. One of the solutions would be harnessing back waste heat, but presently, [5,6] the available technologies are less cost-effective for investment [7,8] unless there is a significant volume of heat for recovery.

A number of low-grade heat recovery cycles [9] have been developed: Organic Rankine Cycle (ORC), Kalina Cycle [10], Goswami Cycle [11,12], and Trilateral Flash Cycle [13]. Out of these, one of the promising technology for conversion of low-grade heat is the Organic Rankine Cycle "ORC", where principle operation is similar to the conventional Rankine Cycle, but, with a different organic working

fluid [14-17]. Therefore, the present study aims to investigate the technical and economic potential for low-grade waste heat recovery from thermal power plants in Sri Lanka, using ORC with different working fluids.

2. Organic Rankine Cycle

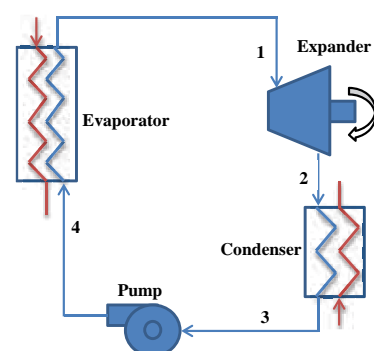


Figure 1- Basic configuration of ORC system

Eng. B. S. R. Fernando, B.Sc. Eng. (Hons), M.Eng. (Energy), CEng (UK), AMIE (SL).

Dr. R. A. C. P. Ranasinghe, Department of Mechanical Engineering, University of Moratuwa.

Dr. H. K. G. Punchihewa, Department of Mechanical Engineering, University of Moratuwa.

ORC has become a field of intense research and appears as a promising technology for conversion of low-grade heat into electricity [18]. It is exactly like the steam Rankine cycle, except that the working fluid in the system will be a refrigerant or a hydrocarbon [19].

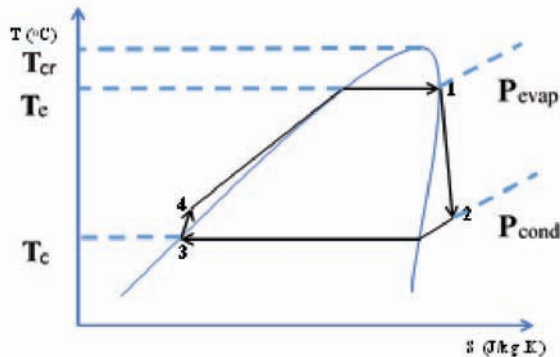


Figure 2 - Basic T-s diagram for ORC system

Figure 1 shows the major components and their connections in a basic ORC configuration, consisting of an expander, condenser, evaporator (heat recovery unit) and a working fluid pump [20]. The cycle consists of four thermodynamic processes shown in the T-s diagram in Figure 2. In process 1 - 2, organic fluid passes through the expander to generate mechanical power. Ideally, this process should be an isentropic process, but in the actual case, isentropic efficiency (η_{is}) is below 100%. Exhaust organic vapour from the expander is fed into the condenser where it is cooled to liquid in isobaric process 2 - 3. In process 3 - 4, condensed liquid is pressurized and sent to the evaporator. In the evaporator, heat absorption takes place from the heat source denoted as process 4 - 1. During the heat absorption, liquid fluid is transferred to saturated or superheated vapour phase in the outlet [20]. In practical ORCs heat required for the process, 4 - 1 can be obtained from waste heat sources such as exhaust flue gas, jacket or condenser cooling water, lubrication oil cooler, blowdown of steam boilers or by direct burning of fuels.

2.1 Wet, Isentropic and Dry working fluids

The operating costs of the ORC system are strictly linked to the thermodynamic properties of the working fluid. Selection of working fluid is the most critical factor of ORC for efficient and economical operation [21]. Further, working fluids can be divided as dry, wet and isentropic, based on the expansion curve gradient (1-2) on T-s diagram [22].

When the line (1-2) slope is positive (i.e. point 2 lies outside the vapour region), droplet formation in the expansion is avoided and hence called dry fluids. In negative slope, the droplet will be formed in expansion and called wet. Normally, the formation of droplets during the expansion is undesirable for turbine operation. Further, the fluids having an infinite slope (1-2 vertical) is considered as isentropic fluid as the entropy remains unchanged during the expansion.

2.2 Superheating and critical point of working fluid

Superheating an ORC can increase the thermal efficiency, but more significantly decreases the second law efficiency [20]. Further, overheating increases the cycle pressure which increases the investment costs of the system. Hence, it is not recommended [24] unless to gain more power at the expense of losing efficiency [20, 25]. Therefore, all the fluids considered in the present work have been analysed on saturated state (prior to expansion) [23].

Closer to the critical condition of the working fluid, sudden abnormal changes of mass flow rate can happen. These changes near critical point may cause instability in the system [26]. However, performance near critical is favourable than supercritical [26], hence, during the present analysis, the maximum possible pressure for a given fluid was considered to be 4 bar less than the fluid's critical pressure.

3. Thermodynamic Modelling of ORC

Based on the work of [21, 27, 28], the ORC is assumed to operate in steady, stable conditions. For the calculated figures to be more realistic, the isentropic efficiency for expansion process 1 - 2 is assumed as 75 % ($\eta_{is} = 0.75$) [29]. Note that expander efficiencies vary between 70-85% in practice. In addition, it is assumed that the mechanical efficiencies of fluid pump, expander and generator are 75% [29], 96% and 98% respectively. It is further assumed that feed pump work is isentropic. For simplification, pressure drops across pipeline, heat exchanger and condenser are assumed negligible for all operating conditions. For calculation and comparison purposes, mass flow rate of the organic fluid is taken from 1.0 kg/s for all fluids in all conditions. The modelling equations used in the present work are

summarized below. Further information and derivation procedures can be found in [20, 29].

The expander work output \dot{W}_{exp} for a mass flow rate \dot{m} of the working fluid is expressed as;

$$\dot{W}_{exp} = \dot{m} \times (h_1 - h_2) \times \eta_{is} \quad \dots(1)$$

Where, h_1 and h_2 are the enthalpies at the state points 1 and 2 respectively in the T-s diagram. The isentropic efficiency of the expander is related to the actual power output \dot{W}_{exp} and the isentropic power output $\dot{W}_{exp,is}$ as given by equation 2.

$$\eta_{is} = \dot{W}_{exp} / \dot{W}_{exp,is} \times 100\% \quad \dots(2)$$

Heat absorption rate of the working fluid at the evaporator \dot{Q}_{evap} can be calculated from equation 3 given below;

$$\dot{Q}_{evap} = \dot{m} (h_1 - h_4) \quad \dots(3)$$

$\dot{W}_{pump,is}$ denotes the power requirement of the pump, which is less than 100% practically, as part of the energy that goes to raise the temperature of outlet fluid. Hence, pump actual pump requirement can be defined as;

$$\dot{W}_{pump} = \frac{\dot{m} v_{pump} (P_4 - P_3)}{\eta_{pump,is}} \times 100 \quad \dots(4)$$

The overall cycle efficiency can be calculated from total energy input (Heat energy absorbed by the evaporator & pump work) and work output from the expander.

$$\dot{W}_{in} = \dot{Q}_{evap} + \dot{W}_{pump} \quad \dots(5)$$

$$\eta_{cycle} = \frac{\dot{W}_{out}}{\dot{W}_{in}} = \frac{\dot{W}_{exp}}{\dot{Q}_{evap} + \dot{W}_{pump}} \quad \dots(6)$$

Amount of heat recovered from the waste heat available depends on the efficiency of the evaporator η_{evap} , which is defined as follows;

$$\eta_{evap} = \frac{\dot{Q}_{evap}}{\dot{Q}_{evap,max}}$$

$$= \frac{\dot{m} \times \bar{c}_{p,f} (T_{f,ev.out} - T_{f,ev.in})}{\dot{m} \times \bar{c}_{p,f} (T_{avg} - T_{f,ev.in})} \quad \dots(7)$$

Where $T_{f,ev.out}$ is mean average temperature at evaporator outlet, $T_{f,ev.in}$ is mean average temperature at evaporator inlet, T_{avg} average source temperature, $T_{f,ev.in}$ is evaporator inlet temperature, $\bar{c}_{p,f}$ denotes the specific heat capacity of the working fluid and \dot{m} denotes the fluid mass flow rate.

4. Fluid Analysis

The fluid analysis here was performed by varying the evaporator temperature. Evaporator temperature denotes the exhaust temperature of the heat source. Hence, evaluating the temperature variation will represent the ORC performance under different source temperatures [35]. This will easily provide maximum effective ranges of each fluid with optimum evaporator temperatures. These factors are critical when designing ORC for heat recovery. Also, this analysis provides a reference for selection of fluids based on heat source temperature.

4.1 Fluid Selection

In the fluid selection, 11 fluids which are commonly recommended in the literature for ORCs were chosen [21], where 06 of them are organic fluids, and other 05 are refrigerants. Table 1 & 2, show the chemical formulae, physical properties and few other important characteristics of selected fluids.

Table 1 - Fluids Molecular Formula and Physical Data

No	Fluid	Molecular Formula	Physical Data [30]		
			NBP(°C)	Tc(°C)	Pc(bar)
1	R 245fa	C ₃ H ₅ F ₅	14.9	154.1	36.4
2	R 123	C ₂ HC ₁₂ F ₃	27.82	183.68	36.62
3	Toluene	C ₆ H ₅ -CH ₃	110.6	318.6	41.26
4	R 113	C ₂ Cl ₃ F ₃	47.58	214.06	33.92
5	Benzenene	C ₆ H ₆	80.08	288.9	48.94
6	R 245ca	C ₃ H ₃ F ₅	25.13	174.42	39.25
7	Decane	C ₁₀ H ₂₂	174.12	344.55	21.03
8	R 134a	CH ₂ FCF ₃	-26.07	101.0	40.59



				6	
9	R 114	ClF ₂ CCF ₂ Cl	3.586	145.68	32.57
10	Pentane	C ₅ H ₁₂	36.06	196.6	33.7
11	Heptane	C ₇ H ₁₆	98.38	266.98	27.36

Table 2 - Physical, Safety and Environmental Data of selected fluids

No	Fluid	Safety Data [36]	Environmental Data [31,32,33]			Expansion [30,34]
		ASHRAE	Atm Life	ODP	GWP (100 yrs)	
1	R 245fa	B1	7.7	0	1050	Dry
2	R 123	B1	1.3	0.01	77	Dry
3	Toluene	-	2.4	-	2.7	Dry
4	R 113	A1	85	0.85	6130	Dry
5	Benzene	-	12.5	-	-	Dry
6	R 245ca		6.5	0	726	Dry
7	Decane	-	-	-	-	Dry
8	R 134a	A1	14	0	1430	Dry
9	R 114	A1	190	0.58	9180	Dry
10	Pentane	A3	0.009	0	20	Dry
11	Heptane	-	-	-	-	Dry

Note: T_c - Temperature at critical point
P_c - Pressure at critical point
NBP - Temperature at normal boiling point (pressure at 1 atm)
ODP - Ozone depletion potential
GWP - Global warming potential

4.2 Evaporator Temperature Variation

The following were also some criteria/conditions used in addition to the assumptions stated previously. The condenser temperature was assumed to maintain at 45 °C which is normally 15 °C higher than the atmospheric temperature in a tropical climate. However, some of the fluids are in gaseous phase at 45 °C, at condenser pressure. Hence, in such cases, the condenser temperature was suitably adjusted to meet the temperature requirements. Further, upon the selection of temperature at the evaporator, corresponding pressure values were fixed. Condenser pressure was maintained higher than the atmospheric level to avoid air mixing in a possible leakage. The output of the evaporator was maintained as saturated vapour and is the input to the expander. The outlet temperature and pressure

of evaporator were maintained within saturated fluid range by controlling the heat input and fluid flow rate. Further, expander outlet also maintained at the saturated state and then fed to the condenser for further cooling.

4.3 Results & Discussion

Power output and efficiency plot for each and every fluid was done with varying the evaporator temperature. Figure 03, shows the plotted graph for fluid Decane, by varying expander power against evaporator temperature. The plot further shows the power in & out a variation with the temperature from 180 °C to 340 °C.

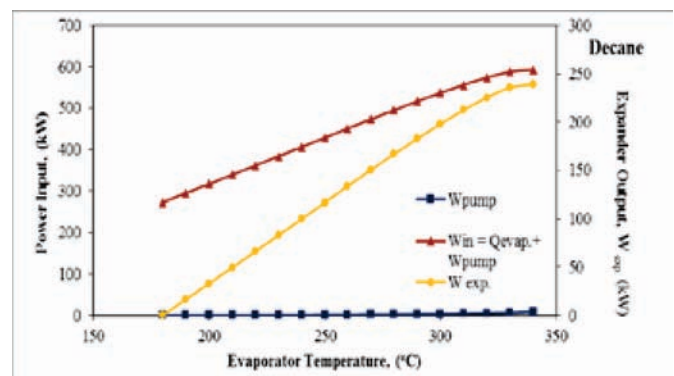


Figure 3 - Variation of Expander work with evaporator temperature variation for Decane

(Note: T_{con} = 180 °C, P_{con} = 1.1739 bar, \dot{m} = 1 kg/s and other parameter fixed including η pump = 0.75, η exp. = 0.96 & η elec. = 0.98)

Efficiency variation also plotted for each fluid accordingly, and Figure 4, shows the sample plot for Decane. When evaporator temperature close to 340 °C, cycle efficiency is around 40%.

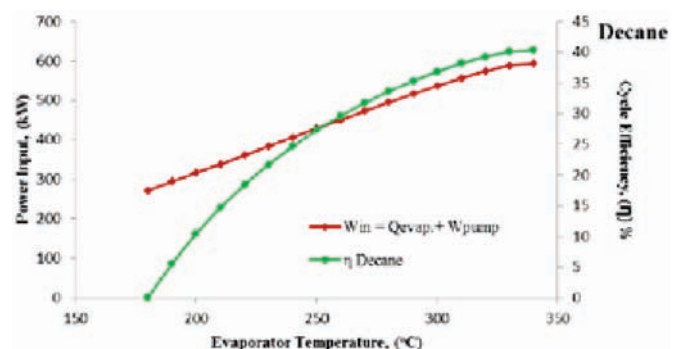


Figure 4 - Variation of Expander work & efficiency with evaporator temperature variation for Decane

(Note: T_{con} = 180 °C, P_{con} = 1.1739 bar, \dot{m} = 1 kg/s and other parameter fixed including η pump = 0.75, η exp. = 0.96 & η elec. = 0.98)

Combining individual plots for each fluid, complete graphs for power output and efficiencies of the ORC fluids were developed and compared as shown in figure 5 & 6 respectively.

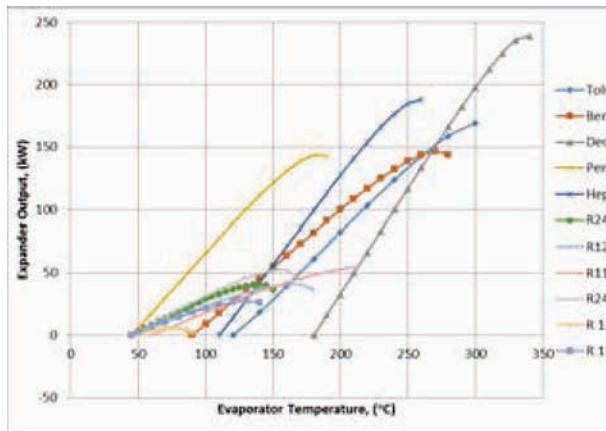


Figure 5 - Work output variation with different evaporator temperatures

(Note: $T_{evap.min} = 45\text{ }^{\circ}\text{C}$, $T_{evap.max} = 340\text{ }^{\circ}\text{C}$, $\eta_{pump} = 0.75$, $\eta_{exp.} = 0.96$ & $\eta_{elec.} = 0.98$)

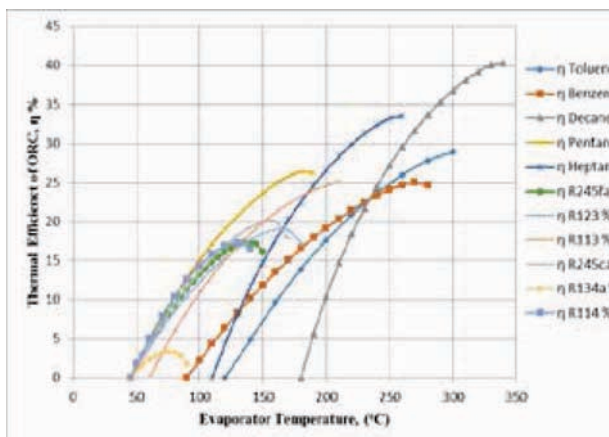


Figure 6 - Cycle efficiency variation with different evaporator temperatures

(Note: $T_{evap.min} = 45\text{ }^{\circ}\text{C}$, $T_{evap.max} = 340\text{ }^{\circ}\text{C}$, $\eta_{pump} = 0.75$, $\eta_{exp.} = 0.96$ & $\eta_{elec.} = 0.98$)

Results show that Heptane, Pentane and Decane show favourable results in terms of work outputs (figure 5) while, in terms of efficiency, Decane and Heptane are better (figure 6). Further, it was found that Pentane outperforms, when waste heat source temperature is between 45 - 190 °C, while for Heptane the temperature should be 190 - 260 °C. Decane is more suitable for 260 - 340 °C range.

In the development of summarized charts for those fluids, evaporator inlet temperatures were varied to obtain theoretical work output at different points. These points were marked on

the same plot against the output on the Y axis and, equal temperature lines were drawn. Further, system efficiencies of each point were obtained, and iso-efficiency lines were drawn. In the calculations of above points, unit mass flow rate (1 kg/s) of ORC fluid has been considered. One point on the developed summarized charts will denote pressure, temperature, work output and efficiency at a given evaporator and condenser temperature for a given fluid.

5. Economic Analysis

Economic feasibility of potential waste heat opportunities of thermal plants in the country was analysed. Then, plant capacities were decided according to available source, and investment costs have been calculated. Total investments with payback were compared considering seven possible scenarios governed by external factors of the economy for better prediction.

5.1 Investment cost of ORC

Based on some worldwide reputed manufacturers of ORC systems, investment costs were derived for each opportunity. Those manufacturers have given some basic guidelines for cost estimation with required source temperatures and cost per kW. The cost of the organic fluid is small compared to component cost, hence working fluid does not have considerable impact. Further, manufacturers have done the cost estimation including the fluid costs.

Based on the evaluation, recommended fluids for individual plants and their economics of output were shown in Table 3.

Table 3 - Estimated plant capacity & investment

Plant	Organic Fluid	Expected Electric Output (kW)	Estimated Plant Capacity (kW)	Investment Cost (USD) per kW	Total Investment (mn USD)
SPS	Decane	769.07	750	2200	1.65
LVJ	Pentane	669.52	650	2200	1.43
JDP	Decane	27.39	25	2500	.06
KLP	Decane	11667.97	11600	1800	20.88
KGT	Decane	2335.20	2300	1900	4.37
LBD	Heptane	103.32	100	2500	.25



Note:	SPS	- Sapugaskanda Power Station
	LVJ	- Lakvijaya Coal Plant
	JDP	- Jaffna Diesel Plant
	KLP	- Kelevarapitiya Plant
	KGT	- Kelanithissa GT Plant
	LBD	- Lakvijaya Boiler Blowdown

Based on manufacturer's criteria [31], following cost factors were defined and investment costs of each WH opportunity are summarized in table 3.

Plants below 250kW	- USD 2500 per kW
Plants above 250kW	- USD 2200 per kW
Plants above 1MW	- USD 1800 - 2000 per kW

5.2 NPV Calculation

Here, cash inflows are the cash generated from the investment and cash outflows are the expenditures including investment. Hence, net cash flow is the difference of cash in and outflow. NPV relationship between net cash flow and the investment can be determined using the following equation;

$$NPV = \sum_{i=1}^n (B - C) i * A^i \quad \dots(8)$$

Where;

NPV	- Net present value
B	- Cash inflow or benefit
C	- Cash outflow or investment
A	- Discount rate

The discount rate can be explained as the interest rate used in discounted cash flow (DCF) analysis to determine the present value of future cash flows. The discount rate in DCF analysis takes into account not just the time value of money, but also the risk or uncertainty of future cash flows. Hence, greater the uncertainty of future cash flows, the higher the discount rate [32,33].

The discount rate can be calculated as follows;

$$A = \frac{1}{(1+i)^p} \quad \dots(9)$$

Where;

i	- Interest rate
p	- Period or years

Approximate capital investment for selected waste heat sources was estimated based on their potential output calculated previously. Further, suitable organic fluid also was selected by referring to the previous calculations.

Most of the country's thermal power plants would generate power, more than 60% during the year. Especially, Lakvijaya coal plant is expected to run more than 80% during the year to minimize power purchasing from private owned plants. For calculations, annual running hours were estimated as 60%, which means 5256 hrs per year. Further, it has been assumed that operation pattern would continue unabated for the next 07 years.

Fluctuation of electricity prices and an inflation rate of the country have made the financial analysis part more critical and complex. The impact of different economic situations arising out of unstable economic conditions referred to as scenarios, on the investment has been considered in evaluating the project. Hence, considering possible future occurrences, seven different scenarios are defined based on average selling price of electricity unit, future economic condition and bank interest. Investments are evaluated with reference to those scenarios, to estimate the financial viability of project implementation.

Table 4 - Different scenarios on which NPV calculations were done for project feasibility

Practical Situations	Average Selling Price of Unit (Rs. Per kWh)	Bank Interest Rate %
Scenario 1	14.00	8%
Scenario 2	15.00	8%
Scenario 3	15.40	8%
Scenario 4	14.00	10%
Scenario 5	15.00	10%
Scenario 6	14.00	12%
Scenario 7	Refer table 5	

Table 5 - Plant running hours and interest rate for scenario 7

Waste Heat Recovery Opportunity	Averaged Annual Running %	Exp. Running Hours per Year	Average Unit Selling Price Rs.	Interest Rate
Sapugaskanda Power Station	60 %	5256	15.00	10%
Lakvijaya Coal Plant	70 %	6132	15.00	10%
Jaffna Diesel Plant	60 %	5256	15.00	10%
Keravalapitiya Plant	60 %	5256	15.00	10%
Kelanithissa GT Plant	40 %	3504	15.00	10%
Lakvijaya Boiler Blow Down	70 %	6132	15.00	10%

Scenario 7 in Table 5 represents the plants average actual running hours for last few years (till 2015). Further, average actual selling price

of a unit is Rs. 15.40, but for scenario 7, unit price was taken as Rs. 15.00. Because, if the evaluation is favourable even with low selling price, it will eventually ensure the profitability during implementation. Additionally, present bank interest rates are low as 6 - 8 % (in 2015), which is not a normal situation in the country. Hence, the average interest rate for next seven years has been taken as 10%. Meanwhile, scenario 7 represent current situation of the country. Further, all overhead costs such as operation and maintenance, spare parts, labour, etc., have been estimated as 1% of the total investment for next 07 years.

5.3 NPV Results

Calculations were done accordingly to investigate the feasibility of ORC systems on selected heat sources, based on different scenarios. Net cash flows were estimated after 07 years and tabulated in Table 6, where negative cash flows are shown as N and positive cash flows shown as P.

Table 6 - NPV results of WHR opportunities

WHR Opportunity	Scenarios						
	1	2	3	4	5	6	7
Sapugaskanda Power Station	P	P	P	P	P	P	P
Lakvijaya Coal Plant	P	P	P	P	P	P	P
Jaffna Diesel Plant	P	P	P	N	P	N	P
Kelevarapitiya Plant	P	P	P	P	P	P	P
Kelanithissa GT Plant	P	P	P	P	P	P	N
Lakvijaya Blowdown	P	P	P	N	P	N	P

6. Conclusion

This paper presents the performance of different ORC working fluids under varying evaporator temperature. The evaluation was done in the subcritical region for all fluids considering waste heat recovery applications. Evaporator temperature was varied from 45 - 340 °C and upon their output, the range was divided into 03. The region between 45 - 190 °C, fluid Pentane has shown higher work output than any other fluids while the region of 190 - 260 °C, fluid Heptane has shown the highest work. Further, temperature between 260 - 340 °C, fluid Decane has shown the highest work. Significantly, these fluids have shown predominantly higher work outputs

along their respective regions and can be recommended for further study in WHR systems. Sample summarized graphs were developed for above fluids as a guideline for interested parties. The developed summarized graphs provide approximate power output against source temperature in a convenient manner for the end user.

Economic evaluation of the implementation of ORC system was done according to net present value method. Expected plant capacities were decided upon maximum power output, and relevant investment costs were estimated accordingly. Based on NPV method, recovery of investment was estimated under different economic situation for 07 years. With reference to evaluation, favourable results are shown for ORC implementation. Detailed financial analysis is further recommended.

Acknowledgement

Author wishes to acknowledge the assistance given by the Ceylon Electricity Board authorities to provide required information.

References

- Hung, T. C., Shai, T. Y., Wang, S. K., (1997, July). A Review of Organic Rankine Cycle (ORC's) for the Recovery of Low-Grade Waste Heat. Energy (issue 7) [Online] 22, Pp. 661-667.
- Qiu, G., (2012, July). Selection of working fluids for micro-CHP systems with ORC, Renewable Energy [Online] 48, pp. 565-570.
- Steinfeld, J. I., (2001, June). Climate Change and Energy Options: Decision Making in the Midst of Uncertainty. Fuel Processing Technology [Online]. 71(issue 1-3), pp. 121-129.
- International Energy Agency. Key World Energy Statistics 2016.
- Smouse, S., Staats, G., Rao, S. N., Goldman, R., Hess, D., (1998, March). Promotion of Biomass Cogeneration with Power Export in the Indian Sugar Industry. Fuel Processing Technology (issue 1-3) [Online] 54, pp. 227-247.
- Tillman, D. A., (1982, January). Cogeneration with Wood Fuels: A Review. Fuel Processing Technology (issue 3-4) [Online] 5, pp. 169-181.
- El Wakil, M. M., Power Plant Technology, 2nd International Edition. New Delhi, India: TATA McGraw-Hill, 1988.



8. Sjoding, D., (2010, September). Overview of Waste Heat Recovery for Power & Heat. U.S. Department of Energy. Chicago, U.S.A.
9. Convert Low Grade Heat into Electric Power; Thermodynamic Cycles for the Conversion.
10. Deepak, K., and Gupta, A.V.S.S.K.S., (2014, June) Thermal Performance of Geothermal Power Plant with Kalina Cycle System. *International Journal of Thermal Technologies*. 4(2).
11. Chen, H., Goswami, D. Y., Stefanakos, E. K., (2010, June). A Review of Thermodynamic Cycles and Working Fluids for the Conversion of Low-Grade Heat. *Renewable and Sustainable Energy Reviews*. [Online] 14 (issue 9), pp. 3059-3067.
12. Vijayaraghavan, S., and Goswami, D. Y., (2006, July). A Combined Power and Cooling Cycle Modified to Improve Resource Utilization Efficiency using a Distillation Stage. *Energy*. [Online]. 31 (issue 8-9), pp. 1177-1196.
13. Smith, I., Stosic, N., and Aldis, C., (1995). Trilateral Flash Cycle System: A high Efficiency Power Plant for Liquid Resources, City University, London - U.K., [Online]. pp. 2109-2114.
14. Thorin, E., *Power Cycles with Ammonia-Water Mixtures as Working Fluid: Analysis of Different Applications and the Influence of Thermo-physical Properties*, Ph.D. dissertation, Department of Chemical Engineering and Technology, Royal Institute of Technology, Stockholm, Sweden, 2000.
15. Matsuda, K., (2013). Low Heat Power Generation System. *Chemical Engineering Transactions*. [Online] 35, pp. 223-228
16. Ferdinand, W. Preliminary Study of Binary Power Plant Output Comparing ORC and Kalina for Low-Temperature Resources in Rusizi Valley, Burundi, Ministry of Energy and Mines, United Nations University, Iceland, 2013.
17. Zamfirescu, C., and Dincer, I., (2008, October) Thermodynamic Analysis of Novel Ammonia-Water Trilateral Rankine cycle. *Thermochemica Acta*. [Online]. 477(issue 1-2). pp. 7-15.
18. Peris, B., Esbri, J. N., Moles, F., and Babiloni, A.M., "ORC Applications from Low Grade Heat Sources," in 3rd International Seminar on ORC Power Systems, October 2015, pp. 12-14.
19. Saadatfar, B., Fakhrai, R., and Fransson, T., (2014) Thermodynamic Vapor Cycles for Converting Low- to Medium-grade Heat to Power: A State-of-the-art Review and Future Research Pathways. *Micro Journals*. [Online]. 2 (issue 1).
20. Velez, F., Segovia, J.J., Martin, M.C., Antolin, G., F. Chejne, and Quijano, A., (2012, November) Comparative Study of Working Fluids for a Rankine Cycle Operation at Low Temperature. *Fuel Processing Technology*. [Online]. 103. pp. 71-77.
21. Quoilin, S., Declaye, S., Tchanche, B. F., and Lemort, V., (2011, October) Thermo-economic optimization of waste heat recovery Organic Rankine Cycles. *Applied Thermal Engineering*. [Online]. 31 (issue 14-15), pp. 2885-2893.
22. Badr, O., Probert, S. D., and O'Callaghan, P.W., (1985). Selecting a Working Fluid for a Rankine Cycle Engine. *Applied Energy*. [Online]. 21(issue 1). pp. 1-42.
23. Bândeian, D. C., Smolen, S., and Cieslinski, J. T., "Working Fluid Selection for Organic Rankine Cycle Applied to Heat Recovery Systems," in *World Renewable Congress*, Sweden, 2011, pp. 772-779.
24. Bombarda, P., Invernizzi, C. M., and Pietra, C., (2010, February). Heat Recovery from Diesel Engines: A Thermodynamic Comparison between Kalina and ORC Cycles. *Applied Thermal Engineering*. [Online]. 30 (issue 2-3), pp. 212-219.
25. Quoilin, S., "Sustainable Energy Conversion Through the Use of Organic Rankine Cycles for Waste Heat Recovery and Solar Application," Ph.D. dissertation, Faculty of Applied Science, University of Liege, Belgium, 2011.
26. Pan, L., Wang, H., and Shi, W., (2012, January). Performance Analysis in Near-Critical Conditions of Organic Rankine Cycle. *Energy*. [Online]. 37 (issue 1), pp. 281-286.
27. Tchanche, B. F., "Low Grade Heat Conversion into Power Using Small Scale Organic Rankine Cycle," Ph.D. dissertation, Dept. Natural Resources and Agricultural Eng., University of Athens, Greece, 2011.
28. Jian, S., and Wenhua, L., (2011, August). Operation Optimization of An Organic Rankine Cycle (ORC) Heat Recovery Power Plant. *Applied Thermal Engineering*. [Online]. 31 (issue 11-12), pp. 2032-2041.
29. Khatita, M. A., Ahmed, T. S., Ashour, F. H., and Ismail, I. M., (2014, January). Power Generation using Waste Heat Recovery by Organic Rankine Cycle in Oil and Gas Sector in Egypt: A Case Study. *Energy*. [Online]. 64, pp. 462-472.
30. National Institute of Standards and Technology, *Chemistry Web Book: Thermodynamic Properties of Fluid Systems*. U.S.A. Web

31. IPCC, 2007: Climate Change 2007: The Physical Science Basis. Contribution of Working Group I to the Fourth Assessment Report of the Intergovernmental Panel on Climate Change [Solomon, S., D. Qin, M. Manning, Z. Chen, M. Marquis, K.B. Averyt, M. Tignor and H.L. Miller (eds.)]. Cambridge University Press, Cambridge, United Kingdom and New York, NY, USA, 996 pp.
32. The Montreal Protocol on Substances that Deplete the Ozone Layer, 9th Edition, UNEP, Printed and bound in Kenya by UNON, 2012.
33. The Pollution Information Site; logged on 05.07.2016 at 15.30 hrs.
34. Rycroft, M., (2016). Organic Rankine Cycle and Waste Heat Recovery. EE Publisher.
35. Korobistyne, M. A., "New & Advanced Energy Conversion Technologies, Analysis of Cogeneration, Combined and Integrated Cycles," Ph.D. dissertation, Energy Research Foundation (ECN), Netherland, 1998.



Mechanized Fertilizer Applicator Operated by Two-wheel Tractor for Coconut Plantation Industry in Sri Lanka

S.A.P.S. Silva

Abstract: Fertilization of coconut trees is a time consuming and labour intensive process, which has become a problem for coconut estate owners due to inadequate availability of human labour and reliable technology for applying fertilizer. This innovative fertilizer applicator improves efficiency of fertilization process, reduces the cost of fertilization process and increases the absorption of fertilizer to plants. This applicator consists of a fertilizer-spreading mechanism, a feed hopper and a modified rotavator. The modified rotavator facilitates loosening the soil surface and damages the feeding roots of the palm tree. Average time taken for application of fertilizer for one palm tree is two minutes with two labourers. According to the field investigation reports, it has been revived that overall saving of cost for fertilization with applicator is about 35%. This paper describes design aspects of innovative fertilizer applicator with performance details.

Keywords: Mechanized fertilizer applicator, Coconut, Fertilization, Two wheel tractor

1. Introduction

Coconut is one of the commercially important plantation crops in Sri Lanka. Currently, the contribution of coconut sector to the Gross Domestic Product (GDP) is about 1.4%. It is also responsible for nearly 3.1% of the total foreign exchange earnings in Sri Lanka in 2009 [1]. Coconut is a tropical perennial plantation crop and the totals of 1 million acres of coconut plantations are available in Sri Lanka. Generally in wet zone around 150 palms are harvested in one hectare due to its canopy structure requires a wide spacing between palms.

Currently production of coconut is going gradually decreased due to fragmentation of lands that has taken place extensively in the recent past. Nevertheless, the potential per capita availability of coconut has been reduced due to the fact that the production has not been increased sufficiently to meet the requirement of growing population [2]. As solutions to increase the coconut yield, it is necessary to introduce higher yielding coconut varieties and also more proper fertilization methods. Considering above the proper fertilization contribute around 5% for increasing yield [3]. Nut yield was taken at two month intervals and the total 120 nut production per palm per year was considered for calculations [4]. From above it was found that yearly around 360Mn yield increase of coconut nut production is possible in Sri Lanka.

At present, the fertility levels of the most of the coconut growing soils have been declined; especially the coconut lands in the coconut triangle where the higher proportion of national yield come from. The inherent capacity to supply adequate nutrients to coconut palms in degraded soils is very low or poor. Therefore nut production in such soils reported to be very low. Improper soil and nutrient management with high exploitation leads to further soil degradation, resulting poor nut production in the existing lands. Therefore proper soil and nutrient management system should be adopted especially for the coconut, in long term as far as the nut yield and the sustainability is concerned [5].

Coconut palm being a perennial with a life span of 60 years or more requires a regular supply of plant nutrients to sustain its growth and yield in its production period. It is revealed that 45% of the variation in yield is influenced by nutrients. In coconut growing soils, considerable amount of nitrogen (N) phosphorus (P), potassium (K) and magnesium (Mg) are depleted from the soil, as a result of continuous removal of Nut and other parts of the palm. [6].

Eng. S.A.P.S.Silva, MEng.(Manufacturing Systems Engineering - Moratuwa), B.Sc.Eng (Mechanical ,First Class Hons-Peradeniya), AMIE, Research Engineer, NERD Centre.



Traditionally the application of fertilizer to coconut trees is a labour intensive and time-consuming activity. In manual method, top soil of the adjacent area of the plant is removed up to 6" depth (within 6' feet diameter circle) and refilled with removed soil and other debris after application of fertilizer. The main disadvantages of the manual method are,

- Non-uniformity of fertilizer distribution
- Considerable wastages of fertilizer
- Low absorptivity due to cutting off of feeding roots
- High cost involvement

2. Development of an innovative fertilizer applicator

The innovative fertilizer applicator shown in Figure 2.1 has been developed by improving the efficiency of fertilization and addressing the above-related issues. Basically equipment is an attachment to the common two-wheel tractor and it is powered by the power transmission output (PTO) of the two-wheel tractor. The rotavator in this attachment loosens the surface soil with damaging the feeding roots while spreading mechanism is applying fertilizer. The above technique is assured the improvements of fertilizer absorption capacity.

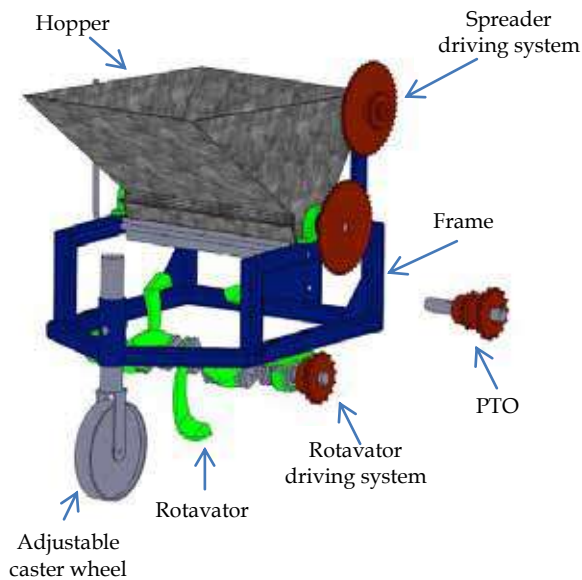


Figure 2.1 - Schematic conceptual design of a fertilizer applicator

2.1 Analytical formulations in the design of fertilizer spreader

For analytical design formulations, it is considered that the tractor speed and the PTO (Power Transmission Output) speeds are synchronized based on the tractor manufacturer's specifications while fertilizer is applied. Further the turning radius of the two

wheel tractor is vital for evaluating the quantity of the applied fertilizer to the palm. In two wheel tractors, turning is done by actuating the clutches in each wheel. As an example, disengaging the left wheel clutch the tractor is turned to left [7]. Maximum turning path is defined by the tractor manufacture and according to that this fertilizer applicator was designed. The PTO speed of a common two-wheel tractor is around 80 rpm. The fertilizer is always filled with the hopper in operation.

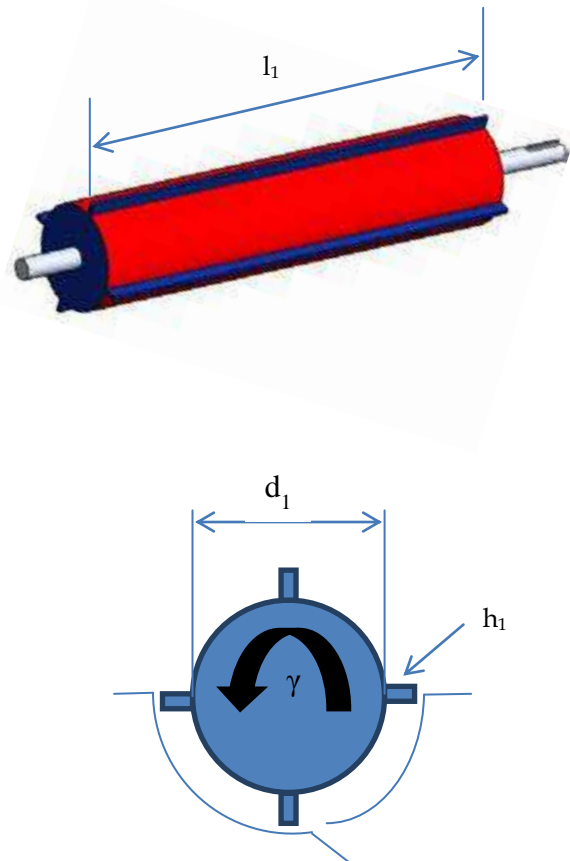


Figure 2.2 - Schematic view of the fertilizer spreader

Where h_1 is the height of the flap, d_1 is the diameter of the cylinder, l_1 is the length of the rotor and γ is the speed of the rotor in rpm.

Volume rate of the fertilizer spread out of the unit,

$$l_1 \pi \left\{ \left(h_1 + \frac{d_1}{2} \right)^2 - \frac{d_1^2}{4} \right\} \frac{\gamma}{60}$$

Weight of the fertilizer spread in unit time,

$$l_1 \pi \left\{ \left(h_1 + \frac{d_1}{2} \right)^2 - \frac{d_1^2}{4} \right\} \frac{\gamma}{60} \rho$$

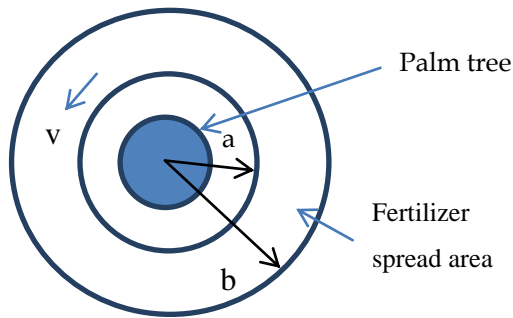


Figure 2.3 - Schematic view of the tractor-driving path

Where v is the tractor travelling speed, a is the inner radius of the fertilizer spreading area and b is the outer radius of the fertilizer spreading area.

Average radius drive around the palm,

$$\left[\frac{a + b}{2} \right]$$

Time taken for one palm,

$$\frac{2\pi \left[\frac{a+b}{2} \right]}{v}$$

Weight of fertilizer applied for one palm,

$$l_1 \pi \left\{ \left(h_1 + \frac{d_1}{2} \right)^2 - \frac{d_1^2}{4} \right\} \frac{\gamma}{60} \rho \times \frac{2\pi \left[\frac{a+b}{2} \right]}{v}$$

From above equation found the height of the flap (h_1) and the diameter of the cylinder (d_1).

Table 2.1 - values obtain from the design calculations

Parameters	Value
Inner radius of the fertilizer spreading area (a)	0.6m
Outer radius of the fertilizer spreading area (b)	1.05m
Tractor travelling speed (v)	10m/min
Diameter of the cylinder (d_1)	100mm
Length of the rotor (l_1)	450mm
Height of the flap (h_1)	10mm
Density of the fertilizer (ρ)	1725 kg/m ³
Required speed of the rotor in rpm (γ)	3 rev/min
Proposed travelling time around palm	31s

3. Fabrication of prototype

By considering the design concept and the formulation in section 2, and by considering the features mentioned in the below table, the prototype of the mechanized fertilizer applicator as shown in figure 3.1 has been fabricated.



Figure 3.1 - fertilizer applicator

Table 3.1 - Overall Features of the developed machine and the results of the field testing

Feature	Value of the feature
Dimensions	Width :550mm Length :700mm Height :850mm
Weight	80kg
Width of the rotavator	450mm
Capacity of fertilizer hopper	40kg
Fuel consumption	depend on the tractor
Application time	max 2 min/tree
No of trees can apply inclusive of travelling in estate	200/day

Note: Above factors depend on the soil condition, palm layout of the estate, Tractor specifications etc.

4. Cost impact analysis

Table 4.1 - Data for calculating the cost in year 2016

Skilled labour cost/day	Rs.1500.00	
Un-skilled labour cost/day	Rs.1250.00	
Labour requirements	Manual	Un-skilled :03
	Developed machine	Skilled :01 Un-skilled :01
Diesel cost per liter	Rs.95.00	
Price of a Chinese brand new two wheel tractor with attachment	Rs.350,000.00	

Note: Pre-mixed coconut fertilizer cost is used and wear and tear is calculated for IMI 7 Two wheel tractor

Table 4.2 - Cost benefit analysis

Description	Traditional method (Manual)	Developed method (Fertilizer applicator)
Fertilized trees per day (8h shift)	30	160
Cost for fertilizer per tree (5kg) /LKR	115	115
Labour cost per palm/LKR	125	17
Diesel cost per palm/LKR	-	12
Wear and tear/LKR	-	16
Total cost per palm/LKR	240	160



- Cost saving respect to the manual

$$\text{method} = \frac{(240-160)}{240} \times 100\% \\ = 34\%$$

- Labour saving respect to the manual

$$\text{method} = \frac{(125-17)}{125} \times 100\% \\ = 86\%$$

- Time saving respect to the manual

$$\text{method} = \frac{(16-4)}{16} \times 100\% \\ = 75\%$$

Normally fertilizer application is done in twice per year and the palms per hectare are 150 nos.

So,

- Minimum payback period for 15 hectare

$$\text{land} = \frac{(350000)}{(240-160) \times 150 \times 15 \times 2} \\ = 0.97 \text{ years} \\ = 01 \text{ year}$$

I.e. The equipment cost is cover within one year for 15 hectare land with twice application per year.

5. Prototype's field evaluation and other advantages - The results

After completing the field trials in different soil conditions (different locations), each around 20 acre lands in Sri Lanka it was found that the following advantages,

- Applying fertilizer within two minutes time period.
- More than 35% of financial saving could be achieved.
- Ability to fertilize at least 10 Nos. of palms with one hopper load of fertilizer.
- Homogeneous spread of fertilizer around the palm tree.
- Ability of applying right quantity of fertilizer.
- Minimizing wastage of fertilizer.
- As the machine damages the feeding roots of the palm tree, absorption of fertilizer becomes more efficient.
- The center caster wheel which connects to the rotavator back side ergonomically affects to the operator.

The lever system which connects and operates the fertilizer ON/OFF chute was also more user friend.

6. Conclusions

The purpose of mechanization in coconut cultivation is to produce more from existing land. Machinery is a complimentary input required to achieve higher land productivity. Additional benefits to the user may be associated with a reduction in drudgery of farm work greater leisure, or reduction of risk.

Use of manpower for the application of fertilizer is uneconomical due to high labor cost. Therefore power tiller operated fertilizer applicator for coconut cultivation was designed and constructed. This machine is not only useful to broadcast fertilizer on the soil but also to mix it with the soil close to the palm on the weeded surface.

The designed machine consists of fertilizer distribution unit and rotary unit. The Maximum spreading width in 0.5 meter, Machine discharge rate in 1.6 kg/min (3.3kg per palm) and Uniformity coefficient of spray distribution were considered as criteria for comparison of merits and demerits. According to the field investigation reports, it has been revived that overall saving of cost for fertilization with applicator is about 35%.

Acknowledgement

Express my warm thanks to Eng. D.D.A. Namal (Director General), Eng. G.G.K.A. De Silva (Deputy Director General), Eng. K.Y.H.D. Shantha (Director), Dr. A. Warahena (Principal Research Engineer), Dr. (Mrs.) K.M.W. Rajawatta (Senior Scientist), Eng. (Mrs) P.M.Y.S. Pathiraja (Senior Research Engineer) and, Mr. P.A.U.W.K. Paranagampola (Engineer) for their support and guidance in National Engineering Research and Development Centre of Sri Lanka.

References

1. Annual report Central Bank of Sri Lanka, 2009
2. http://www.statistics.gov.lk/agriculture/COP/COP_Coconut.html
3. An Empirical Investigation on the Effect of Land Size on its Productivity of Coconut Plantations in Sri Lanka K. V. N. N. Jayalath¹, P. M. E. K. Pathiraja¹, U. K. Jayasinghe-Mudalige² and M. T. N. Fernando³ ¹ Agricultural Economics & Agribusiness Division, Coconut Research

Institute of Sri Lanka, Lunuwila, Sri Lanka, 61150
2 Dept. of Agribusiness Management, Faculty of
Agriculture & Plantation Management Wayamba
University of Sri Lanka, Makandura, Gonawila,
Sri Lanka (NWP) 3 United Nations Development
Project, Asia & Pacific Regional Centre, 23,
Independence Avenue, Colombo 7.

4. Abeywardana, V. (1971). Yield variations in coconut. Coconut Research Institute of Sri Lanka. Ceylon Coconut Quarterly, 22: 97-103. Bardhan, P. K. (1973). Size, productivity and returns to scale: An Analysis of farm-level data in Indian agriculture. J. of Political Economy, 81(6): 1 370-1 386. Central Bank of Sri Lanka (2009).
5. http://www.cri.gov.lk/web/images/stories/statistics/satistics_on_coconut_oil_palm.pdf
6. Senarathne, S.H.S and Costa, M.J.I. (2009). Comparison of several recommended cultural practices for weed management and their effects on yield of coconut in tropical coconut plantations, Proc. 8th Workshop of the EWRS Working Group: Physical and Cultural Weed Control conf., Zaragoza, Spain, 17-23.
7. Peiris, K.&Adikarinayake,T.B. (2005).Design and Analysis od a skidder Type Supporter for a Combine Harvester.Engineer:Journal of the Institution of Engineers,Sri lanka.38(p),pp7-12.
DOI:<http://doi.org/10.4038/engineer.v38i2.72>

10



Water Loss Reduction by Understanding the Reticulation A Case Study

S.G.G. Rajkumar

Abstract: Safe treated water is considered as an economic good, than a social good as scarcity of water is felt in many parts of the world. The situation is made worse with increase in population and climate change. Presently many parts of developing countries are provided with interrupted water supply to share the resources amongst the entire citizen. Traditionally water for piped supplies was obtained from perennial wells and water supply was limited to few households by the respective local authorities. Presently the situation has changed and water authorities are supplying water for which the costs have to be recovered. The consumers are used to paying for water and are conscious of the amount they have to pay while they are aware of their consumption. Presently amount of water consumed, wasted by leaks and unaccounted water are given priority. There are many steps taken to address all those mentioned above from consumer's level to operational level while illegal use is also given due consideration.

Colombo City water supply is over hundred years old, the Non Revenue Water remained high for many years. Many strategies were adopted; having understood the complexities of the reticulation, water loss reduction through visual leak survey became a low cost approach and effective method to make the change. The Non Revenue water reduced from 49% to 46% in Colombo City.

This paper describes the lessons learned to improve water utility efficiency by reduction of water losses. Extensive work carried out in many planned distribution isolation within the city boundary and on engineering judgments. While giving due consideration for holistic approach in dealing with water losses, while considering every drop conserved would be useful for many who are deprived.

Keywords: Visual Leaks survey, Engineering Judgment, Low cost approach, lessons learned, many steps

1. Introduction

The National Water Supply and Drainage Board (NWSDB), is responsible for the supply of drinking water in Sri Lanka. Non Revenue Water (NRW) has been a major issue in Colombo City, where initial pipe lines were laid as far as in 1870's resulting in aged pipes in many parts of the city. The NRW was reported around 49% in Colombo City, which is higher than the nationwide average of 30% set by NWSDB in 2010. In order to resolve this issue, several steps such as leak detection/repair, detection and regularization of illegal connections, removal of public stand posts and converting its users' to be responsible for individual connections and improvement to billing was carried out. However, the NWSDB still faces difficulties to reduce NRW to a satisfactory level.

In view of resolving the NRW, a study area was selected. The area comprised of 5000

connections. Action was taken to identify the causes of losses from part of the system, to replicate the remedial measures to the whole distribution system.

2. Objective

- Detail study done in small area to understand the longstanding NRW issue
- Identify the causes in scientific manner and replicate the finding to whole of Colombo City.

Eng. S.G.G. Rajkumar, B.Sc.Eng(Hons), C.Eng., FIE(Sri Lanka), M.Sc(Denmark), MBA(Sri.J), M.Eng (Moratuwa, Presently, Deputy General Manager(Commercial), National Water Supply & Drainage Board)



3. Methodology

Colombo City has over one hundred thousand connections. Non Revenue water has four contributory factors, Leaks from the system, free water, administrative losses, unauthorized consumption. Even though, many activities had been done to arrest these four factors, NRW remained high, for past 10 years. To identify the main cause of losses indepth study was carried out by selecting a sample area in Colombo city.

The area was selected in such a way where the pipe was over one hundred years old, and the NRW was considered high. The selected area had nearly 5000 connections, this was sub divided into sub zones where each sub-zone has about 500 house connections, was carefully selected paying attention to “less interconnection with the outside of the sub-

zones”[1] and “relatively high pressure”. Table 1 gives the details of the sub zone selection.

Hydraulic isolation was planned based on available drawings. Some, valves were introduced to modify the existing distribution system for hydraulic isolation with one or two feedings [2]. as shown in figure 1.

3.1 Household survey

The customers in the subzones were identified with the available information and all the premises within the subzone were visited. All the premises, the water bills was compared with the water meter; the number of users were identified; the water meter accuracy was tested using a conical can; service leaks were checked using acoustic principles[3], and bypass lines were checked.

Table 1 - Details on No of connections and pipe lengths

Sub-zone		1		2		3&4		5		6		7		9		
No of connections		397		426		1383		115		159		1545		200		
Material		PVC	CI	CI	PVC	CI	CI	PVC	CI	PVC	CI	DI	PVC	CI	DI	
Main Pipe Length (m)	Diameter (inch)	2														
		3			61		963	319					872		148	
		4		407	993		3,168	63	38	1,536	262	2,153			1,589	
		5		300	414		119	314				165				
		6	692				737	171				925		114		
		7					724									
		8				173							212			
		9														
		10					1,449								1,034	
		12									771					
		16								298			290			
		18											304		898	
		24														887
		28														
		Sub Total (m)		692	707	1,468	173	7,160	867	336	2,307	262	4,617	304	114	3,669
Total (m)		1,399		1,468	7,333		867	2,643		5,183			4,670			



In addition more field information was collected on unauthorized consumption, visible leaks along roads and free water outlets etc. Free water outlets were metered and their consumptions were measured.

The initial NRW was established by measuring the inflow to the subzone. The composition of factors contributing to NRW was identified. Remedial work was done and the water saved was monitored. Key areas where large amount of water saved was identified and that was replicated to the Colombo City.

Since the percent NRW was still high, as activity 2 further search was made for possible leaks, which resulted in repairs of 14 service leaks and one main leak and the percent NRW reduced to 72.95. The other observation was the system inflow dropped to 918m³/d, the Minimum Night Flow (MNF) was 330 l/min and the system pressure was 19.47m. Leakage search activity was repeated by segmenting the distribution into further small length and locating leaks adopting step testing technique and repair or replacement of pipes or replace bundle pipes. Table 3 shows the outcome of the four subzones after repeated water loss reduction activity. It became clear one of the main causes of losses is the leakage.

The search was initiated in Colombo city for the visible leaks, during the night time when pressure was high visible leak survey was done in a methodical manner [4], Table 4 shows the number of leaks identified. During day time culverts, road side drains etc. were searched for losses Figure 2 shows the NRW reduction over the years.

4. Outcome

4.1 Water loss reduction in study area

In sub zone 1 under the activity 1, action was taken to regularize the 45 unauthorized use of water; 19 defective meters were replaced; service leaks 52 nos and three main leaks were repaired 14 standpost were metered. After completing the activity 1, the status of NRW is given in Table 2.



Figure 1- Sub-Zone Selection in Study Area

Table 2 - Status of reduction of losses in sub zone 1 after Activity 1&2

Component	Water Balance Before activity	Water Balance After Activity 1	Water Balance After Activity 2
Total System Input (m ³ /d)	1295	1041	918
Billed Authorized consumption (m ³ /d)	190.88	248.29	
NRW	85.26 %	76.15%	72.95%
MNF (l/min)	690	480	330

Table 3 - Water saved by repeated water loss reduction activities

Sub-zone		1	2	3&4
System input volume (m3/d)	Initial	1,295	1,245	4,240
	After activities	571	933	3,989
	Saving	724	312	251
NRW (%)	Initial	85%	78%	73%
	After activities	56%	72%	71%

Table 4 - Visible leaks identified by Night leak survey in Colombo City

OIC Area	Number of Connections in the Area	2013	2014	2015
Pamankada	15,700	81	257	130
Timbirigasyaye	13,911			169
Hulsdrof	14,555	32	304	150
Slave Island	10,910			58
Kotahena	11,338	122	524	94
Mattakkuliya	18,393			205
Maligawatta	18,690	57	277	113
Borella	11,180			126
Total		292	1362	1045

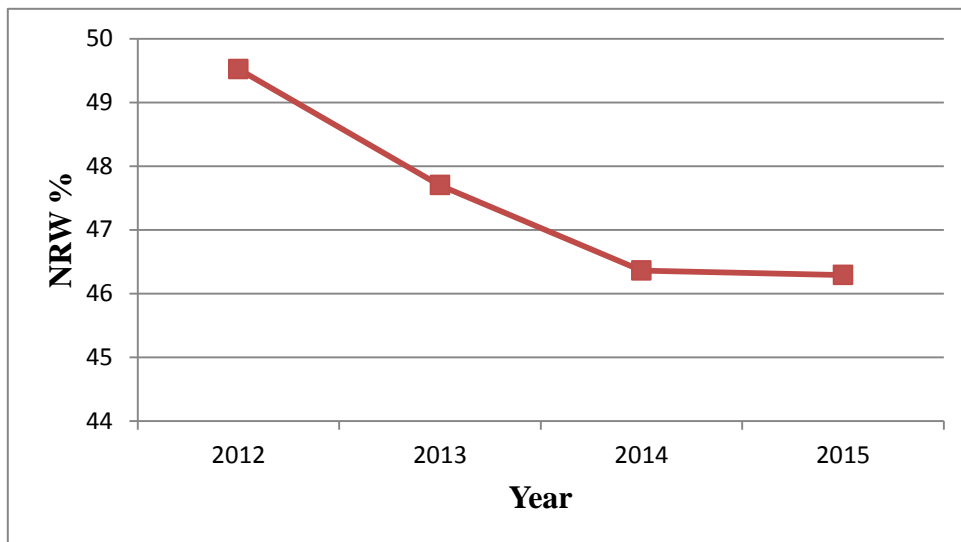


Figure 2 - NRW Reduction after Night Visible Survey Leak Repair

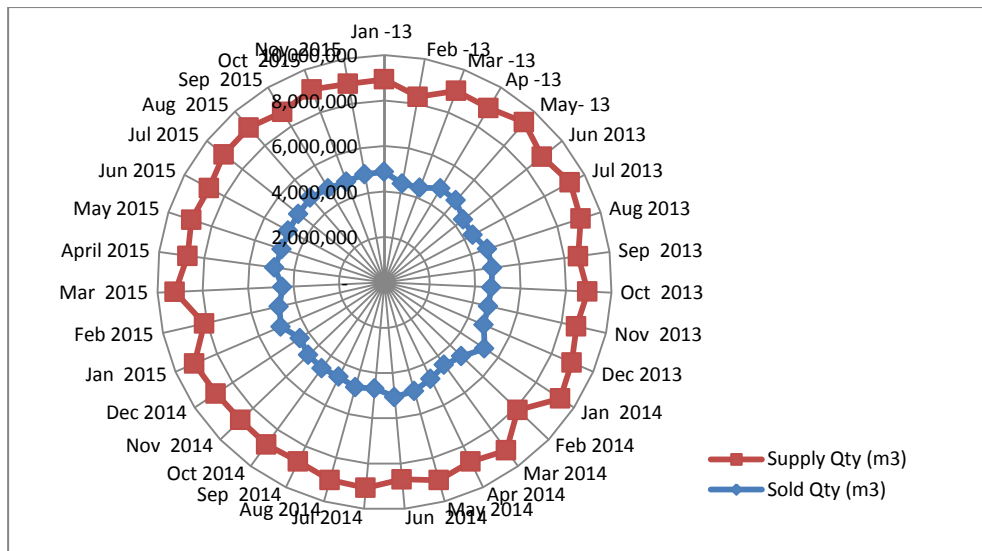


Figure 3 - No change to the inflow to the City, Sold volume has increased

5. Conclusion

It became clear from the study area first round of activity that the NRW could be reduced marginally. More emphasis needs to be given for leakage reduction, search for leaks and repairs need to be continued till satisfactory level of NRW is reached. The process for leakage search and repair needs to be routine work. It confirms that even in an older system, attention to leak reduction brings desired results. The findings from small part of the distribution system could be replicated to other areas so that the whole distribution system could be covered for reduction of percent NRW. The water saved could be supplied to the existing and new customers without bring in additional water as shown in Fig 3. The estimated income from sale of additional water is estimated as Rs 500 million [5] during the period 2012 to 2015.

References

1. Farley, M. and Liemberger, R. "Developing a non-revenue water reduction strategy planning and implementing the strategy" Water Science and Technology: Water Supply Vol 5 No 1 pp. 41-50 © IWA Publishing 2005.
2. International Water Association "District Metering Area" Guidance Notes, Feb 2007, pp. 1-10.
3. Stuart Hamilton, Bambos Charalambous "Leak Detection Technology and Implementation" 2013, pp. 7-9.
4. Rajkumar, S.G.G., "Managing Water Loss by Understanding the Reticulation", 2014 pp. 30-34
5. Rajkumar, S.G.G., "Non Revenue Water Reduction in Colombo City By Adaptation of Low Cost Strategies" Mar 2016 pp 3 of 5.



Implementation of Water Safety Plans for Rural Water Supply Schemes Managed by CBOs in Sri Lanka – Common Risks and Analysis

T. R. Samaraweera and Niranjani Ratnayake

Abstract: Safe water is a major concern in the present global context. Even though water is available and appears as safe, it is important to assure the extent that water can be safely used, especially for drinking purposes. In most countries the urban communities receive drinking water with adequate quality assurance, while the rural areas are receiving water without quality assurance, most of the time. As far as Sri Lanka is concerned, the water quality in urban water supplies, which are managed by the state institution National Water Supply and Drainage Board, is monitored and regulated, and the implementation of Water Safety Plans (WSPs) has commenced. But a considerable population is supplied water by the small community based organizations (CBO's), to whom WSP is a very new concept. However, these are the schemes that are mostly at risk of contamination, as the monitoring and external surveillance of quality is lacking in these schemes. In this research several case studies were conducted to identify and rank the risks according to the World Health Organization (WHO) guidelines, in order to develop specific guidelines to help the CBO's to focus on, in providing safe drinking water to consumers. The study revealed that in water supplies with surface water and spring water as sources, there were inherent typical risks with similar severities, such as residual chlorine being not tested in water (uncertainty of presence of chlorine in water), head variation of the chlorination tank, resulting in variations in the added chlorine amount, rusted GI pipes in the distribution line and source pollution due to tea plantations surrounding the water source. The water supplies that use ground water as the source encountered common risks such as filtration or chlorination not being done, poor practices of water storage and usage, rusted GI pipes, and source pollution due to houses being located close to the dug wells.

Keywords: Water Safety Plan, Rural Water Supply, Community Based Organizations (CBO), Risk Identification and Assessment

1. Introduction

Water is essential to sustain life, and a satisfactory (adequate, safe and accessible) supply must be available to all [3]. Safe drinking water, as defined by the WHO Guidelines, does not represent any significant risk to health over a lifetime of consumption, including different sensitivities that may occur between life stages. Safe drinking-water is suitable for all usual domestic purposes, including personal hygiene [3].

The most effective means of consistently ensuring the safety of a drinking-water supply is through the use of a comprehensive risk assessment and risk management approach that encompasses all steps in water supply from catchment to consumer called WSP. [1].

The objectives of a water safety plan are to ensure safe drinking water through good water supply practice, that is:

- To prevent contamination of source waters;

- To treat the water to reduce or remove contamination that could be present to the extent necessary to meet the water quality targets; and
- To prevent re-contamination during storage, distribution and handling of drinking water. [2]

1.1 Water supply and community based organizations in Sri Lanka

Some of the water supply schemes extract water from a source with good or acceptable quality and distribute to the community while some extract, treat and then distribute to the community (Statistics in NWDB). Since the community is

Eng. (Prof.) (Mrs.) N. Ratnayake, B.Sc.Eng.Hons (Cey), M.Eng. (Wales), C.Eng., FIE(SL), Member IWA, Senior Professor in Civil Engineering, University of Moratuwa.

Mr. T. R. Samaraweera, Department of Civil Engineering, University of Moratuwa.



provided drinking water through such schemes it must be assured they distribute safe water, so the water safety plans (WSPs) are introduced recently to the CBOs. As the concept of WSP is newly introduced to the CBOs in Sri Lanka, apart from a few studies being done on implementation of WSPs in rural scenario in some other countries, there is a knowledge gap in adopting WSPs to the community based organization's water supplies in Sri Lankan context. Thus a proper study carried out on water supply types and identifying the common potential risks of contamination would be worthwhile for improving the process of implementation of WSPs.

1.2 Research and Objectives

- To find out and analyse the variation of the common risks with the common elements of the water supplies via a quantitative risk ranking so that a basis to categorize community based water supplies can be developed for the design and implementation of WSPs.
- To provide an example risk analysis done on CBO managed water supplies to aid WSP team.

2. Methodology

2.1 Desk study and collecting details of different water supply schemes in Kalutara district.

In selecting the CBO managed water supply schemes, major concern was given to cover all main types of water sources such as ground water, surface water and water springs. The collected details of water supplies were analysed and it was found that within Kalutara District all types of sources can be covered. Thus, six CBO managed schemes within Kalutara District with around 100 connections or above were selected. Apart from Kalutara schemes the Kithulgala Liyanoya water supply scheme which has been selected by UNICEF in collaboration with NWSDB as the pilot CBO managed water supply scheme for water safety plan implementation was also selected.

2.2 Visiting the water supply schemes and collection of data

For assuring the reliability of the collected data, site visits were done to each water supply scheme and visual observation of catchment to consumer processes was done. During the visits

demographics and tariff data were also gathered.

2.3 Catchment to consumer process identification

Catchment of each water supply scheme was studied and mapped using Google maps with the aid of the GPS coordinates marked during the visits. The processes from source to consumer were observed and all concerns were noted down.

Finally the attention was given to study water storage and consumption methods at the consumer levels.

2.4 Catchment to consumer risk identification

Using the prepared catchment maps and collected details the probable risks on catchment contamination and pollution were identified. Risks and practices relating to the collection, treatment, storage, distribution and storage at consumer levels were identified via the collected details by interview and informal questionnaire survey at each supply.

2.5 Ranking risks using semi-quantitative risk matrix approach suggested by World Health Organization

As the WSPs are intended to treat and mitigate the risks of contamination, water supplies with similar types of risks can be treated in a similar way in planning and designing the WSP by the WSP team. All schemes studied were subjected to the risk assessment using the semi-quantitative risk matrix approach suggested by WHO [4].

Once the proper risk analysis and ranking was done, trends of the risks were studied and it was attempted to find out whether the risks are varying in a common pattern or patterns among the categories of schemes.

Table 1 - Detail of Water Supply Scheme

Name of the CBO	DS Division	Gram-Niladhari Division	GND No.	Type of Scheme	Address of the CBO	Number of Connections	Source	Chlorination	Treatment Process	Quality
Ridee Nimnaya CBO	Horana	Koralaima	604A	Pumping	Wijayagiri Viharaya, Gonapala Junction	110	Shallow Ground	No	None	Good
Suhada CBO	Horana	Kumbuka East	607	Pumping	158/A/1, Kumbuka East, Gonapala Junction	105	Shallow Ground	No	None	Fair
Janopakara CBO	Horana	Kumbuka West	607A	Pumping	Saranathissa Mw., Kumbuka West, Gonapala Junction	84	Shallow Ground	No	None	Good
Randiya CBO	Ingiriya	Kurana North	627B	Gravity	Siri Nimal Road, Arakavila / Handapanoda	105	Shallow Ground	No	None	Fair
Nagarika Sanwardana Padanama	Bulathsinhala	Bulathsinhala	824B	Gravity	Piriwena Road, Athura, Bulathsinhala	1,323	Surface	Yes	Roughing Filter & Chlorination	Good
Sathsewa CBO	Mathugama	Yatadolawatta East	802D	Gravity	Yatadolawatta, Mathugama	275	Spring	No	None	Good
Randiya Dahara CBO	Mathugama	Welipenna East - North	793B	Pumping	Palliya Road, Welipenna, Mathugama	128	Shallow Ground	No	None	Fair
Kithulgaliyanoya development	Kithulgala	Malwatta	134	Gravity	Malwathara Rd, Kithulgala	515	Surface	Yes	Chlorination only	Good

Source: NWSDB

Table 2 - Semi-Quantitative Risk Matrix

Risk ranking basis				
Likelihood	Severity	Rating	Risk ranking basis	
			Risk score	Risk rating
Almost Certain /Once a day	Catastrophic public health impact	5	>15	very high
Likely/Once a week	Major regulatory impact	4		
Moderate/ Once a month	Moderate aesthetic impact	3	15-10	High
Unlikely/Once a year	Minor compliance impact	2	6 - 9	Medium
Rare/Once every 5 years	insignificant	1	<6	Low



3. Results and Discussions

3.1 Kithulgala Liyanoya Development Water Supply

Table 3 - Example Risk Analysis Done Using Semi-Quantitative Risk Matrix Approach

Process Step	Hazardous Event (Source Of Hazard)	Hazard Type	Likelihood	Severity	Score	Risk Rating(Before Consideration Of Controls)	Basis
Source (surface water)	Tea plantation surrounding the water source	Chemical	3	4	12	High	Potential toxic chemical addition above national standards ex; glyphosate(rating of 4) Can occur more than thrice a year(likelihood rating 3)
Source	People bathing in the source	Chemical & Microbial	4	2	8	Medium	Potential introduction of detergents to water (severity rating 2) Can occur more than once a week(likelihood rating 4)
Source	New hotel being setup in the upstream(addition of waste)	Chemical & Microbial	3	4	12	High	Potential for hazardous waste specially when rainfall is low(severity rating 4) Can occur more than thrice a year(likelihood rating 3)
Source	The impact of Yatiyanthota repeater station(addition of electronic waste)	Chemical	2	5	10	High	Potential of electronic wasted being added potential of mercury or lead addition(severity rating 5) Uncertain likelihood (likelihood rating 2)
Treatment	Residual chlorine is not tested in water(uncertainty of presence of Cl in water)	Chemical	5	5	25	Very high	Potential of pathogens intruding the system without knowing (severity rating 5) Daily occurrence(likelihood rating 5)
Treatment	Head variation of the chlorination tank, hence the added chlorine amount varies		5	4	20	Very high	Not enough disinfectant dosage present in water(severity rating 4) Daily occurrence(likelihood rating 5)
Distribution	Inadequacy of water supply in dry season	Physical	2	3	6	Medium	Potential of people moving for other water sources which may be polluted(severity rating 3) Occurring twice a year(likelihood rating 2)
Treatment	The security fence around the water tanks	Physical microbial and chemical	2	5	10	High	Potential of a deliberately caused risk (severity rating 5) Uncertain likelihood(likelihood rating 2)
Distribution	Rusted GI pipes	Chemical and physical	3	5	15	High	Potential for leakage and corrosion products entering the system(severity rating 5)
Source	Turbidity in water	Chemical	2	5	10	High	Potential of shielding microbes from chlorine (severity rating 5)

The main risks identified with the highest risk score were residual chlorine is not tested in water (uncertainty of presence of Cl in water), head variation of the chlorination tank, hence the added chlorine amount varies and rusted GI pipes in the distribution line. Tea plantation surrounding the water source new hotel being setup in the upstream(addition of waste), possible impact of Yatiyanthota repeater station(addition of electronic waste), broken security fence around the water tanks increased turbidity in water during wet season and people bathing in the source were identified as the risks with moderate impact.



Figure 1 - Kithulgala, Liyanoya Water Supply

3.2 Urban Development Foundation water supply - Bulathsinhala

Residual chlorine is not tested in water (uncertainty of presence of Cl in water), head variation of the chlorination tank, hence the added chlorine amount varies and rusted GI pipes in transmission and distribution were the identified high risk events.

Deforestation surrounding the intake tea plantation surrounding the water source water extraction from dug wells and surrounding houses and possibility of intrusion of septic tank water into the dug wells were the identified moderate risk events. Inadequacy of water supply in dry season and occasionally cleaned consumer level storage tanks were also among the identified risks.



Figure 2 - Bulathsinhala Water Supply

3.3 Yatadolawatta sathsewa CBO's water supply

Filtration or chlorination not being done, rusted GI pipes in the distribution line were the identified high risk events.

Tea plantation surrounding the water source, people bathing in the source, leakages in the tank, high turbidity in water during wet season, lack of maintenance personnel and inadequacy of water supply during dry season were the identified moderate risks.



Figure 3 - Yatadollawaththa Water Supply

3.4 Janopakara Community Based Organization- Kumbuka West

Filtration or chlorination not being done poor practices of water storage and usage and rusted GI pipes were among the prevailing high risk events.

The houses located close by the dug well, fertilizer used in paddy fields and inadequacy of water during dry season were among the moderate risk events.



Figure 4 - Dug Well, Kumbuka West



3.5 Rideenimnaya Community Based Organization- Korallaima

Filtration or chlorination not being done, poor practices of water storage and usage and rusted GI pipes were among the high risk events.

The houses located close by the dug well, fertilizer used in paddy fields and inadequacy of water during dry season were the moderate risk events.



Figure 5 - Dug Well, Korallaima

3.6 Suhada Community Based Organization Kumbuka East

A treatment method not being followed, rusted GI pipes and the houses located very close to the dug wells were the major risks identified. The unavailability of a parallel pump and the poor storage practices were among the mid impact risks.



Figure 6 - Storage Tank, Kumbuka, East

3.7 Randiya Dahara CBO -Welipenna, Mathugama

Filtration or chlorination not being done, poor practices of water storage and usage and rusted GI pipes were the high risk events.

The houses located close by the dug well, fertilizer used in paddy fields and inadequacy of water during dry season were the moderate risk events.



Figure 7 - Storage Tank, Welipenna

4. Discussion

The study showed that rural water supply schemes with similar water sources show typical risks in an almost similar increasing order. Some of these risks, especially on source protection are not within the capacity of the WSP team to be mitigated.

Most water supply schemes faced the issue of inadequacy of water supply during the dry weather. Even though the risk assessment method used resulted in this being of lesser priority, the additional risk of the consumers resorting to less safe sources during these period is not reflected in this analysis. Mitigation of this risk by proper catchment restoration and aquifer recharge are important aspects that need to be emphasized.

During water supply scheme design stage the focus should be given on providing technical assistance on problems on water treatment and head variation problem in chlorination tanks.

Further study is encouraged on how the human factor will affect the implementation of WSPs and to investigate the legal background and support on taking actions by WSP teams in issues such as agrochemical addition.

5. Conclusions

- The common issues identified in all CBO managed water supply schemes regardless of the water source type were rusted GI pipes and the related leakages.
- The treatment process of surface water sources and spring supplies show typical risks of water not being chlorinated, residual chlorine not being tested and effect of head variation of the chlorination tank which

prevents the chlorine dosage being applied at the correct rate during the course of the day. The mitigation measures suggested are introduction of chlorination if possible or else public awareness to boil the drinking water where water is not being chlorinated; try adopting ways for testing residual chlorine or at least check presence of chlorine in water by DPD; chlorine addition to water chlorination tank to be done twice a day so that during peak hours enough water head will be remaining in the tank, respectively.

- In the catchment of surface water source supplies, issues such as tea plantations in the catchment directly discharging water into the streams, people bathing in the upstream and possible threats of future development along the banks were identified. The mitigation measures that can be followed are public awareness & legal actions that can stop contamination by above issues.

- Ground water source supplies show typical risks of proper treatment not being done, houses located very close to the water wells and poor safety practices of water storage at consumer levels, for which adopting treatment methods or at least public awareness for boiling water before drinking, pumping over longer periods at slower pumping rates, usage of screens on side walls of the well are suggested for mitigation of risks.

- As observed in the research the common risks were shown with almost similar risk rankings in the water supplies with similar types of water source. During the WSP initiating stage water supplies may be categorized and the above issues can be commonly addressed depending on the type of the water source of the water supply.

References

1. Bartram, J., Corrales, L., Davison, A., Deere, D., Drury, D., Gordon, B., Howard, G., Rinehold, A., & Stevens M. (2009). *Water safety plan manual: step-by-step risk management for drinking-water suppliers*. Geneva: World Health Organization
2. Davison A., Howard G., Stevens M., Callan P., Fewtrell L., Deere D., and Bartram J., *Water Safety Plans - Managing drinking-water quality from catchment to consumer*, WHO/SDE/WSH/05.06 Water, Sanitation and Health Protection and the Human Environment World Health Organization Geneva (2005)
3. World Health Organization, *Guidelines For Drinking-Water Quality Third Edition Incorporating The First And Second Addenda Volume 1 Recommendation* (2008)
4. World Health Organization, *Water safety planning for small community water supplies; step by step risk management for drinking water supplies in small communities*.



A Study on Recontamination Risks in Water Distribution Systems, using A Network Model

M.H.V. Lasantha and Niranjanie Ratnayake

Abstract: Water supply schemes aim to deliver safe and wholesome water to the consumers in adequate quantities. However due to reasons like inadequate disinfectant residual, leakages, stagnation, intermittent services, low pressures and cross connections, treated water can get re-contaminated before reaching the consumers. In this study, selected contamination scenarios were simulated using the open source network model EPANET developed by the USEPA in order to demonstrate the application of this freely available software to identify safety risks in a distribution system and to study the effects of proposed mitigatory measures.

Municipal water supply scheme of Raddolugama was modelled with EPANET 2.0 as a case study. Presence and remediation of contamination risks such as inadequate disinfectant residual, contamination by a conservative substance, stagnation of water and contaminant entering at a pressure deficient location were studied. Simulation of chlorine level in the network revealed that some sections have inadequate chlorine residual. The proposed chlorine booster provides an adequate safeguard against this risk, showing that a network model can be satisfactorily used to identify and develop mitigation actions for inadequate disinfectant residual. Simulation of transport of a conservative substance helped identify various factors that affect the system's behaviour. Time of addition of the substance, with respect to water demand, is a critical factor that affects the peak concentration. In an event of contamination, the rate of dispersion, especially within first few hours, is a deciding factor on the severity of the outcomes and the mitigatory actions of the risk. This simulation reveals that a contamination occurring at a peak time affects significantly more people. It was also possible to identify the affected sections of the network due to a leaking pipe at a pressure deficient location. The tracer study for determining percentage of water at any node originating from each of the two tanks is useful for determining the affected area due to a contamination.

Keywords: Water supply, pipe networks, water quality modelling, contaminant transport

1. Introduction

Water supply schemes aim to deliver safe and wholesome water to the consumers in adequate quantities. Due to inadequacies of treatment process and distribution infrastructure, and also due to improper usage and lack of maintenance, contaminants can enter the distribution system and degrade the water quality. Changes of physio-chemical and radioactive characteristics of water and presence of harmful microorganisms can make water unsuitable for human consumption. Since the effect of a substance on an organism changes with the dose and the exposure time [1] it is important to know not only the toxicological properties of a contaminant but also the exposure limits for humans. Water quality guidelines and standards establish safe exposure levels substances found in drinking water. Water treatment plants in Sri Lanka produce drinking water following the specifications of SLS 614:2013 standard for potable water.

Common contaminants in water distribution can be mainly categorized as chemical and microbiological. Chemical contaminants in piped water can be either the chemicals added during water treatment and distribution activities or entrants to the system during distribution. Thompson & WHO [2] identifies a large number of chemical contaminants, categorised by the source, along with information useful for risk management. A water treatment process may use various chemicals for purposes like coagulation, softening and disinfection. Aluminium and Iron from coagulants and acrylamides from coagulant aids can be present in the treated water. Treatment chemicals like chlorine, chloramine and ozone can also be present. Pipe materials like iron, lead, copper, zinc and vinyl chloride can be leached in to water.

Mr. M.H.V. Lasantha, B.Sc. Eng. (Hons) (Moratuwa).

Eng. (Prof.) Mrs. Niranjanie. Ratnayake is a Senior Professor in the Department of Civil Engineering, University of Moratuwa and President Elect, IESL for the session 2016/2017.



Some of the above chemicals can give rise to harmful by-products. Toxic and carcinogenic disinfection by-products (DBPs) such as Trihalomethanes (THM), haloacetic acids (HAA) and bromate can be formed when the disinfectants react with natural organic matter or bromide ions.

A significant proportion of reported piped drinking water-related disease outbreaks are due to contaminations during distribution [3]. Contaminations of water distribution networks by pathogenic microorganisms are extremely dangerous in a public health point of view because of the large number of people exposed to the infection risk. Common water borne bacterial diseases include cholera, typhoid, haemorrhagic colitis, paratyphoid, salmonellosis, shigellosis, legionellosis, leptospirosis and dysentery. Hepatitis A and E are caused by the respective viruses. Protozoa can cause amoebiasis and giardiasis. Many types of parasitic worms can also spread through water contaminated with their eggs. Effects of some of these pathogens like *Vibrio cholera*, *Escherichia coli* O157:H7 and hepatitis E can be lethal especially when healthcare is inadequate. Microorganisms are found to cause chronic diseases as well. Diabetes, myocarditis, Guillain-Barré syndrome and gastric cancer have been linked to waterborne pathogens. [3]

1.1 Contamination risks in water distribution networks

Problems with treatment process, improper usage of distribution system and lack of maintenance can lead to chemical or microbiological contaminations in the system. Some of the major contamination risks as identified by WHO & UNICEF [4] are inadequate disinfectant residual, low water pressure, intermittent service, water leaks, cross connections and ageing of infrastructure.

Inadequate disinfection residual

Disinfection as the last step of water treatment is intended for inactivating any microorganisms present in treated water. However, it is important for the water to have a residual disinfection capacity to protect against contamination during distribution. Reasons for absence of disinfection residual can be intentional. Chlorine which is the most commonly used disinfectant, has a residual capacity. Chlorination imparts a taste and odour to the water and there is also the possibility of formation of by-products. These factors may negatively influence the choice of

chlorine as a disinfectant over ozone or UV radiation which however does not have a residual capacity. It is understood that health benefits of disinfection outweigh the harmful effects of chlorination by-products. There have been observed remarkable decreases of waterborne disease outbreaks in water supplies that started chlorination. [5]

Leakages

Leakages are the main constituent of Unaccounted-for Water. Apart from loss of quantity, leakages can cause loss of water quality as well. Leaks in pipes allow contaminants from outside to enter into the system. When paired with low pressures and intermittent supplies, their effect is highly significant. [6]

Intermittent service

Due to increase of population beyond the design capacity, many water supply systems, especially old ones, may not be able to provide a continuous supply. In periods of drought, treatment plants may face shortages of supply and the service may be restricted to a limited period each day. Various studies have found evidence that, continuous supplies are less prone to contaminations than intermittent supplies. [7] During the periods of restricted service, water is stagnant within parts of the system and the pressures are drastically reduced. This increases the chance of contaminants in the surrounding being drawn into the system. Increased occurrence of pressure fluctuations causes additional strains on the pipes increasing the chance of fractures and leaks.

Inadequate pressure

When the capacity of a water supply system becomes insufficient, often the pressures will be inadequate at some regions. When negative pressures occur, water will flow in reversed direction creating a backflow. Backflow can draw in undesired contaminated water into the network. [5]

Cross connections

Another source of contamination is cross connections in the distribution system, particularly where the consumers use dual systems or use hose pipes for delivering water from the tap to various collection vessels. In household level, cross contaminations between water supply pipes and wastewater pipes can occur due to poor plumbing practices. Backflow is another hazard associated with distribution networks. When there is a possibility of harmful substances entering the pipe network by flowing upstream, a backflow protection device need to be installed. EPA [8] and WHO

[9] identifies many common cross connection hazards and presents different backflow prevention methods. Air gap, barometric loop, atmospheric vacuum breaker, hose bib vacuum breaker, pressure vacuum breaker and check valve are some backflow prevention devices. Opening or closing of valves, use of unapproved material, third party access to hydrants, open and unprotected service reservoirs and vandalism have also been identified as water quality hazards within distribution networks. [10]

For controlling growth of micro-organisms in pipe networks, current practice is maintaining a disinfectant residual. WHO [11] identifies importance of rigorous application of good operational and maintenance practices along with providing a disinfectant residual. Strategies for controlling contaminations of distribution systems should start at the design stage of the water supply system. For example, practices such as decentralised treatment and water zoning can facilitate better operational, maintenance and management routines.

Networks models can become useful throughout the life cycle of a water distribution network for different purposes like design, maintenance and troubleshooting. Hydraulic models which simulate the flow (quantity, direction and pressure) in the system, steady-state water quality models which determine the transport of contaminants including flow paths and travel times under steady-state conditions and dynamic water quality models which simulate the movement and transformation of substances in the water under changing conditions are the three types of network models which become useful under different scenarios.

1.2 EPANET

EPANET software package for water distribution network modelling was developed by the United States Environmental Protection Agency's (EPA) Water Supply and Water Resources Division. It can perform extended-period simulation of a network's hydraulic and water-quality behaviour. EPANET supports simulation of spatially and temporally varying water demand, variable speed pumps, and minor head losses for bends and fittings. EPANET is in public domain and its latest version EPANET 2.0 was used for this study.

1.3 Description of the water distribution network

Raddolugama water supply scheme near Seeduwa town in Western province, Sri Lanka was constructed in 1982 along with the housing scheme. Using Dandugam-Oya as the source, a conventional treatment plant produces water to satisfy Sri Lanka Standards for potable water. [12] The distribution network covers an extent of 3 km² and serves 6,000 households. There are two water tanks in the network, each with 1800 m³ capacity.

2. Aim and Objective

The aim of this study was to obtain an understanding on transport of contaminants and predict the behaviour of the system under possible contamination risk events.

The objectives of this study were,

- To study the behavior of residual chlorine level in the network and identify residual chlorine deficient sections
- To propose chlorine boosters to remedy any lack of disinfectant residual
- To simulate the transportation of a conservative contaminant in the network
- To study the transport of a contaminant which enters the system due to a leak at a pressure deficient location
- To determine the percentage of water at any node that originates from either of the two tanks

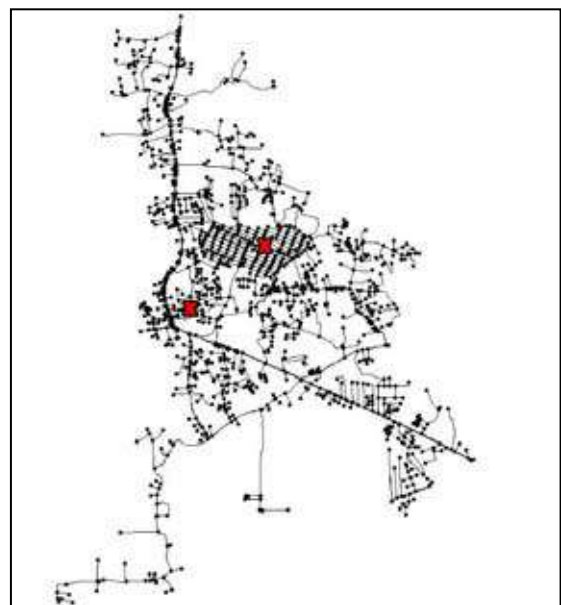


Figure 1 - Raddolugama distribution network model in EPANET 2.0 showing locations of the two tanks

3. Methodology

3.1 Data collection and hydraulic modelling

National Water Supply and Drainage Board (NWSDB) operates the Raddolugama water supply scheme. Data related to pipes and their layout, water demands, demand pattern (figure 2) and tank details were obtained from NWSDB. Using this data, a simplified network having 1608 nodes and 1729 pipes (links) was constructed. Hazen-Williams formula was selected for calculating head loss. A global pipe friction factor of 130 was applied as specified by Clarke [13] for cast iron pipes.

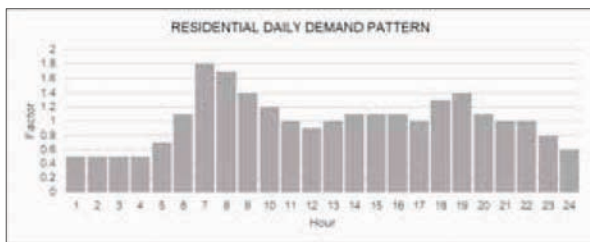


Figure 2 - Demand pattern applied for the system

3.2 Field tests and sampling in Raddolugama

Water samples from ten locations in the study area were tested to identify the prevailing water quality characteristics of the network. Chlorine level maintained in the clarified water sump of Raddolugama water treatment plant is 0.7 mg/l.

3.3 Determination of bulk decay rate

In the laboratory, chlorine levels of water samples from the network were tested over time, to determine bulk decay rate of chlorine in the studied network. Chlorine is known to be consumed in the bulk liquid phase and at the pipe wall following a first order decay [14]. Results of the test, applied to the first order integrated rate law (equation 1), are shown in Figure 3.

$$\ln\left(\frac{C_t}{C_0}\right) = -kt \quad \dots (1)$$

C_t is the chlorine concentration at time, t and C_0 is the initial concentration. Bulk reaction coefficient is k .

Bulk reaction coefficient for chlorine in the network was found to be -0.7/day.

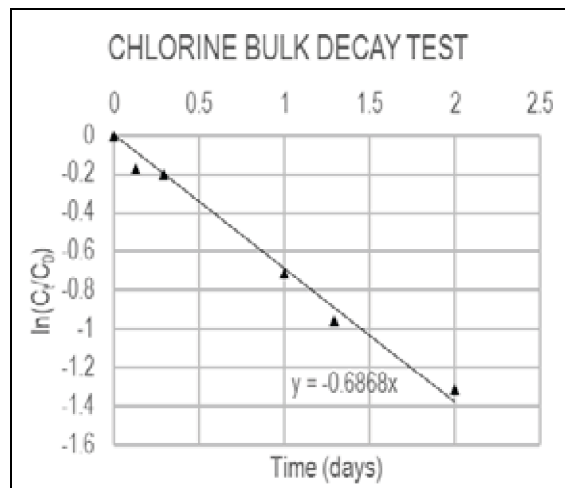


Figure 3 - Graph of $\ln(C_t/C_0)$ vs time

3.4 Application of the model

After the hydraulic model was developed, water quality inputs were defined for the selected scenarios. Hydraulic model was first run using a 1-hour time step. Using the information on flows and pressures in the network from the hydraulic model, water quality study scenarios were planned. Water quality simulations were done using 5 minutes for both hydraulic time step and water quality time step.

Simulation of residual chlorine level in the network

For this simulation, water quality parameter was defined as a non-conservative substance with first-order decay. Global bulk reaction rate for all pipes and tanks was defined -0.7 /day. This simulation was run for progressively longer periods to identify steady state operating conditions.

Determination of a suitable location for a chlorine booster

EPANET allows defining any node as a source of the modelled water quality parameter. Model was run until a suitable location was found for booster dose to produce sufficient chlorine levels at all deficient nodes. Source type was selected as *mass booster* which adds chlorine with a fixed concentration to the water that enters the node. [15]

Simulation of transportation of a conservative contaminant in the network

A conservative substance having zeroth order growth and reaction rate of zero is introduced to the system at the tank of the housing scheme (Node T1). Method of addition is a *mass booster* with a time pattern set to activate for one hour. The Time of addition of the substance was

changed to observe the change in response of the system. Peak demand periods of 0600h to 0700h, and 1800h to 1900h along with low demand periods 1200h to 1300h and 2100h to 2200h were considered in the study.

Simulation of a conservative contaminant entering at a pressure deficient location

Hydraulic simulation reveals that some nodes experience negative pressures. There is an increased risk of contamination as leaking pipes can allow contaminants inside the network when pressure becomes negative. This scenario is simulated by assigning an *emitter* which represents a fracture in a pipe, at a node which experiences negative pressure. Pressure variation shown in *Figure 4* is representative of the general pattern for most nodes that experience negative pressures.

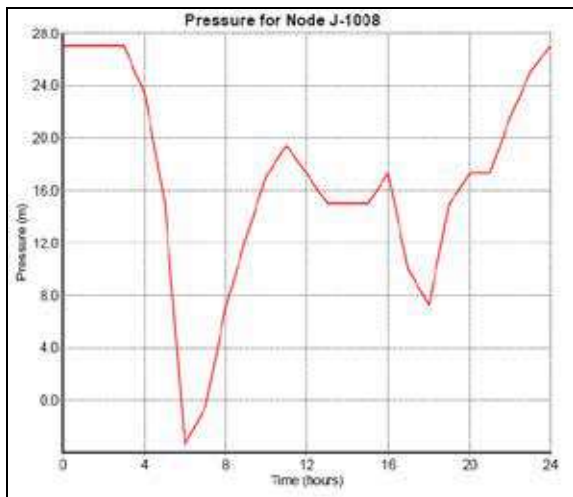


Figure 4 - Pressure variation at node J-1008 throughout 24 hours

Determination of the percentage of water at any node that originates from each tank

By a tracer study, the percentage of water at any node that originates from another node can be determined. [15] In this study, water originating from the two tanks were traced.

4. Results and discussion

Simulation of residual chlorine

The system reached steady chlorine levels after about 700 hours. *Figure 5* shows change of chlorine concentration at a selected node which is representative of the whole network. Results for 30th day were selected as the operating conditions of the system for subsequent studies. When variation of chlorine levels throughout a 24-hour period is examined, a general pattern can be observed. Chlorine level shows a drop during night time (2300 h - 0600 h) and

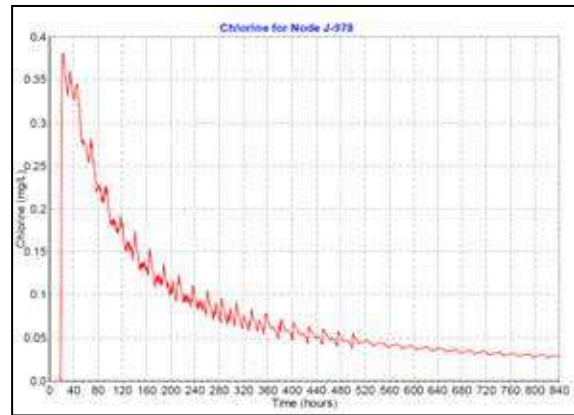


Figure 5 - Change of Chlorine level at node J-978

suddenly during midday (at around 1300 h). This can be correlated with the demand pattern applied to the network (*figure 2*). During the periods of low demand, chlorine levels tend to drop.

Chlorine deficient nodes in the system were identified in this study. Eleven nodes with zero residual chlorine were identified. They are located along two branches of the network close to each other as shown in *figure 6*.

Simulation of Chlorine boosters

After several trial runs, node J-185 located ahead of the chlorine deficient region was selected as the location for chlorine boosting. A chlorine source adding a 0.5 mg per litre of flow through the node was set up. After this there were no zero-chlorine nodes.

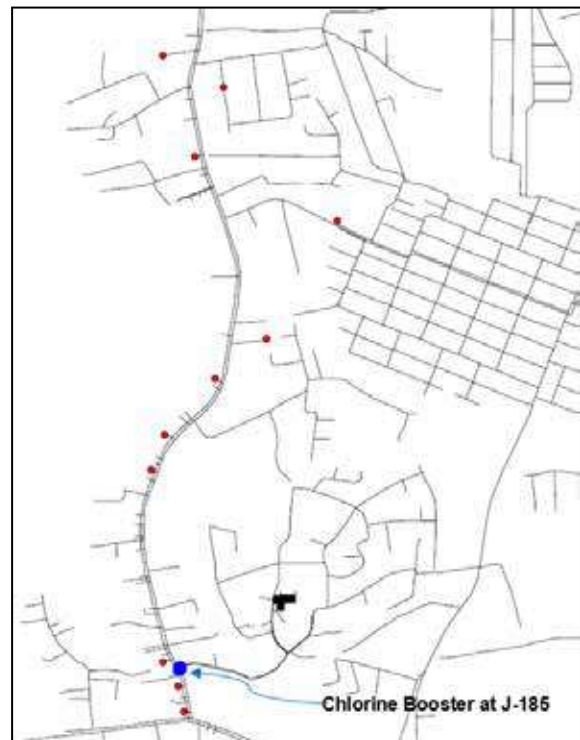


Figure 6 - Chlorine booster at J-185 and the zero-chlorine nodes



Transport of a conservative substance

The dispersion of the substance within the network, and the concentrations at selected nodes were observed in the simulation.

Simulation showed that the peak concentration at a selected node and the time to peak, changes with the time of addition of the substance. When a contamination event occurred during peak time, the contaminant concentration at a selected node was found to be lower than the concentration resulting from a contamination during low-demand period.

The number of nodes to which the contaminant has spread at a certain time after addition, is also affected by the time of addition. When contaminant was added during 0600h and 0700h which is the peak hour, the number of nodes that had got contaminated after one hour i.e. at 0900h was 657. When the contaminant was added during 2100h and 2200h the number of contaminated nodes at 2300h was 387.

Contaminant entering at a pressure deficient location

Negative pressure occurs at the time of peak demand (0600 h – 0700 h) as shown in Figure 3. A contaminant that enters the system during this period disperses along the network. It can be observed that, at end-nodes with smaller demands, contaminants are retained for a longer period.

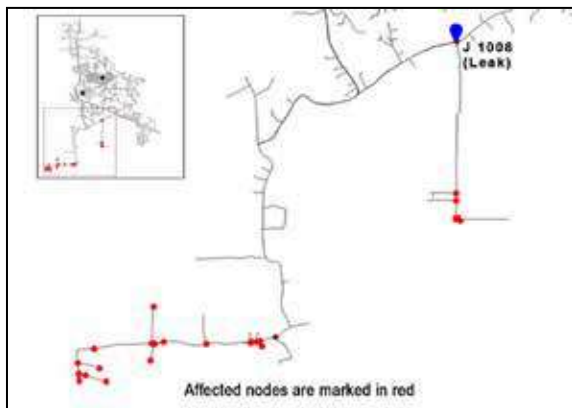


Figure 8 - Contaminated nodes at 0900 h due to the leak at J-1008

Tracer study for determination of percentage of water that originated from a certain node

Figure 9 shows the contour plots for the percentage of water originating from each tank at 1200 h. The two graphs complement each other.

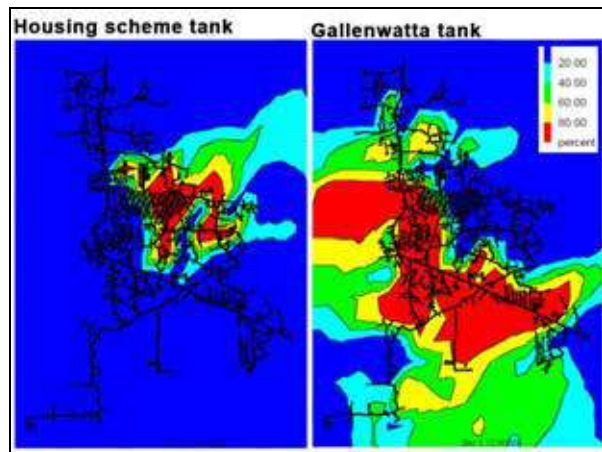


Figure 9 - Contour plots showing the percentages of water originating from the two tanks at 1200h.

5. Conclusion

In this study a water quality modelling approach was taken to assess contamination risks in a water distribution system.

Simulation of chlorine level in the network revealed that some sections have inadequate chlorine residual. The proposed chlorine booster provides an adequate safeguard against this risk.

When the network model was used for predicting the transport of a conservative substance, various factors that affect the system's behaviour could be identified. Time of addition of the substance, with respect to water demand, is found to be a critical factor that determines the peak concentration that occurs at a given node. In an event of contamination, the rate of dispersion, especially within first few hours, is a deciding factor on severity of the outcomes. This simulation reveals that a contamination occurring at a peak time affects significantly more people.

In this study, the network model was successfully used for identifying the affected sections of the network due to a leaking pipe at a pressure deficient location.

Tracer study also presents its practical usefulness especially in a system with multiple sources. For instance, in an event where one of the tanks is contaminated, this information becomes useful for determining the affected area.

Outcomes of above studied scenarios suggest that water quality models of water distribution networks can be useful for designers and operators of such systems by providing information that supports activities like design of pipe networks, troubleshooting, contingency planning and emergency response.

References

1. Crump, KS; Hoel, DG; Langley, CH; Peto, R (1976). "Fundamental carcinogenic processes and their implications for low dose risk assessment"., *Cancer Research*, Volume 36, Issue 9 Part 1, pp. 2973-2979
2. Thompson, T., & World Health Organization., (2007). *Chemical safety of drinking-water*. Geneva: World Health Organization. PP 75-79
3. World Health Organization., Dufour, A., & Organisation for Economic Co-operation and Development, *Assessing Microbial Safety of Drinking Water: Improving Approaches and Methods* (WHO Drinking Water Quality Series), IWA Publishing, 2003, 12p, 179 p.
4. World Health Organization & United Nations Children's Fund, *Global water supply and sanitation assessment 2000 report*, 2000. Retrieved from World Health Organization, http://www.who.int/water_sanitation_health/monitoring/jmp2000.pdf
5. Lee, E. J. & Schwab, K.J., "Deficiencies in drinking water distribution systems indeveloping countries", *Journal of Water and Health*, vol 3, no. 2, 2005, pp. 109-127.
6. Fontanazza, C., Notaro, V., Puleo, V., Nicolosi, P. and Freni, G., "Contaminant Intrusion through Leaks in Water Distribution System: Experimental Analysis", *Procedia Engineering*, 119, 2015, pp.426-433.
7. Kumpel, E. and Nelson, K. "Comparing microbial water quality in an intermittent and continuous piped water supply", *Water Research*, 47(14), 2013, pp.5176-5188.
8. EPA, *Cross connection control manual*, Office of Water, 2003 (4606M)
9. WHO, *Health aspects of plumbing*, 2006, Geneva.
10. Bartram, J., *Water safety plan manual*. Geneva: World Health Organization, 2009, Geneva.
11. World Health Organization, *Safe Piped Water Managing Microbial Water Quality in Piped Distribution*, IWA Publishing, 2004.
12. Rajkumar, S.G.J., *Assessment and suggestions for improvements to the treatment process for the Raddolugama water treatment plant*, 2005
13. Clark, R., *Modeling water quality in distribution systems*. 1st ed. Denver, Colo. American Water Works Association, 2011, 64 p.
14. Ozdemir, O. & Ger, A., "Realistic numerical simulation of chlorine decay in pipes", *Water Research*, 32(11), 1998, pp 3307-3312.
15. Rossman, L. A., *EPANET 2 User's Manual*. Cincinnati, Ohio. US Environmental Protection Agency, 2000, 79 p, 95 p.



Review of Irrigation Ordinance and Identifying the Gaps to fulfil the Current Needs of the Society

Badra Kamaladasa, Lalith De Alwis and G.D.F.U. Perera

Abstract: During a recent intervention on amending Irrigation Ordinance, it was revealed that most of the legislations related with water resources management in Sri Lanka need to be updated to the current context of water usage. Irrigation Ordinance itself is decades old while the organisations with vested power have undergone many structural changes which have not been updated in the legislations. Further the water users and uses have been changed compared to the time formulating the original legislations. Provisions made on dealing of those who violates the conditions are outdated in terms of offences and also charges. This paper intends to discuss provisions in existing water legislations in Sri Lanka, highlight drawback in current legislation related to irrigation management and draw some experience gathered when amending the Irrigation Ordinance during 2016.

Keywords: Irrigation Ordinance, Water legislations, amendments to Acts

1. Introduction

Water is considered a basic human need, globally and nationally. Hence access to water and regulations in usage, abstraction and pollution of this valuable resource should be a primary concern in legislations. Water plays different roles according to the usage, in agriculture as a livelihood supporting ingredient, in domestic use for drinking, sanitation and cooking purposes, as an essential element for environment sustainability and an indispensable component in hydropower generation. Hence when legislations are framed water is considered to have stakes in different dimensions in social welfare, environmental sustainability and national economic development. However, in Sri Lanka legislations on water have been introduced sectorally addressing the issues arising from time to time. The first such ordinance is Irrigation and Paddy lands Ordinance that was enacted in 1856 by colonial rulers to promote traditions and customs in managing water in irrigated agriculture. [8] For other major service or development sectors (such as domestic water supply, power generation, Mahaweli river basin development, inland fishing etc.), legislations were introduced mainly to establish the organisations describing their functions and responsibilities.

This paper describes the process followed in amending the Irrigation Ordinance and also the vital changes proposed in the amendments.

2. Provisions in selected current water Legislations

Being an island country, Sri Lanka has its own Acts conferring at national level to make use of water resources, as no international treaties are required. Hence until 1987 all the enactments approved by the parliament were valid island-wide. After the formation of Provincial Councils (PC) under the 13th amendment to the constitution, PCs were given powers to enact their own statutes subject to the conditions explained in section 2.1.

There are no dedicated national laws pertaining to water, but is covered with several Acts introduced from the colonial period. [9] The existing legal framework consists of many enactments that directly or indirectly influence the water sector in areas such as flood prevention, water resources management, drinking water supply, state lands, coast conservation, inland fisheries, environment protection etc.

Eng. (Mrs.) Badra Kamaladasa, B.Sc.(Eng.) UOMSL, M.Sc. (Development Technologies) University of Melbourne, FIE(SL), Retired Director General of Irrigation.

Eng. Lalith De Alwis, C.Eng., MIE(SL), M.Eng. (EWRE&M) University of Moratuwa., Director (Water Resources Management) Ministry of Irrigation and Water Resources Management.

Eng. G.D.F.U. Perera, IESL (Civil), GCCG (UK) PGDM, Dip.Com. Arb, FIIESL, MIE(SL), MIM(SL), Head of Institute, Kothmale International Training Institute of Water Management.



2.1 Enactments under Provincial Councils (PC)

In the 13th amendments to the constitution, schedules of subject areas were given under the three lists as described below on which PC can have direct control or shared responsibilities or areas that PC do not have authority. [19]

- i) **The Provincial List** specified the subjects in respect of which Provinces could exercise Legislative powers. Water related subjects listed here are Agriculture and agrarian services, rural development, irrigation, animal husbandry, mines and minerals.
- ii) **The Reserved List** specified the subjects in respect of which the Central government could exercise Legislative powers.
- iii) **The Concurrent List** specified the subjects in respect of which either the Centre or the Provinces could exercise Legislative powers. In addition to the subject matters listed in the Provincial List related to water, planning, protection of environment, tourism is included in the concurrence list that would have an impact on water.

PCs can have their own statutes over the subjects in the Provincial list and Concurrence list. However, before the PCs could pass a statute on such a subject, it should consult the Parliament for its opinions on the provisions contained in such a statute. Seven PCs have already constituted their own statutes with regards to Irrigation. The Provincial Councils follow the legal provisions of Central government where there are no statutes adopted yet. [10]

The 13th amendment further specifies that Inter-Provincial Irrigation and Land Development projects will be the responsibility of the Government of Sri Lanka. Such projects would be;

- (a) Within the Province initiated by the State and which utilize water from rivers following through more than one Province; a Provincial Council however, may also initiate irrigation and land development schemes within its province utilizing water from such rivers;
- (b) Within the Province which utilize water through diversions from water systems from outside the Province; and
- (c) All schemes where the command area falls within two or more Provinces such as the Mahaweli Development Project. The administration and management of such projects will be done by the Government of Sri Lanka.

2.2 Water related Law in Sri Lanka

There had been several legislations enacted giving authority to different organizations in the areas such as irrigation, land, environment, coast conservation, agriculture, inland fishing, forests and wildlife that have a stake in water. Forest Ordinance No 16 of 1907, Fauna and Flora Protection Ordinance, No. 2 of 1937 (latest revision in 2009), National Heritage and Wilderness Areas Act No. 3 of 1988, National Environmental (Protection) Act, Soil Conservation Act, Land Development Ordinance, Crown Land Ordinance, Land Settlement Ordinance are among those).

When multi-purpose water resources development in several individual river basins such as Gal Oya, Uda Walawe and Mahaweli were undertaken separate legal enactments were adopted to manage the whole natural resources in the basin. Entirely new institutional setups such as Gal Oya Development Board, Mahaweli Development Board, Mahaweli Authority and River Valley Development Board were established with special powers vested with.

2.3 Integrated Water Resources Management

It is a well accepted fact that management of water to be done in a holistic manner, as it is a cross-sectoral subject.

The Water Resources Board Act (no 29 of 1964) was introduced in view of formation an apex body for regulation of all the water related activities in Sri Lanka. The Board was setup as an advisory body to the Minister on all matters concerning the control and utilization of the Water Resources in the country. The Board did not function assuming the powers vested with it in the Act, but ended up as an implementation organization related to ground water management after when in 1978 Groundwater Division of the Irrigation Department was transferred to the Water Resources Board. [18] The Water Resources Board Act was amended and passed by the Parliament in 1999 to enable the Water Resources Board to pay more emphasis on matters pertaining to Groundwater Resources in Sri Lanka.

In year 2000, an attempt was made to introduce Water Resources Law and introduce an institutional mechanism for regulation in the water sector. However, misinterpretation of certain provisions paved way to the government to abandon the draft proposals.

3. Irrigation Ordinance

Irrigation Ordinance is the oldest prevailing legislation covering the water sector. Provisions that are based on the traditions and customs inherited from ancient hydraulic civilization in Sri Lanka subjected to the regulation of British colonial administrative structure. Hence it has unique features having combined ancient Sri Lankan law and British law. In this chapter the process of developing the current Ordinance, institutional structure, provisions and gaps will be discussed. [11]

3.1 Provisions in current Irrigation Ordinance

The British rulers initiated the establishment of a legal framework and made financial provisions for the restoration of ancient irrigation infrastructure. [6] The first Ordinance related to irrigation was the "Irrigation and Cultivation of Paddy Lands No 9 of 1856". The Government Agent was vested powers to organise meetings to revive the customs and traditions related with paddy cultivation in each District and then adopt a similar legal framework in the relevant area. [4] The following legal enactments or amendments were introduced from time to time spanning to nine decades until the currently valid Ordinance was introduced in 1946, depending on the changes of government policy or demand by the society.

- Paddy Lands Irrigation Ordinance (No. 21 of 1861) [16, 17]
- Paddy Cultivation Ordinance (No 21 of 1867) [12]
- Amendment to above by 42/1884 [13]
- Irrigation and Paddy Cultivation Ordinance no 23 of 1887 [14]
- Irrigation and Paddy Cultivation Ordinance (No 23 of 1889)
- Irrigation and Paddy Cultivation Ordinance (No 6 of 1892)
- Irrigation Ordinance no 16 of 1906

- Irrigation Ordinance (No 45 of 1917) [1]
- Irrigation Ordinance No 32 of 1946

There were a few amendments thereafter to the 1946 Ordinance by Acts 1 of 1951, 48 of 1968, 23 of 1983, 34 of 1990 and 13 of 1994 and Irrigation Law no. 23 of 1973. [15]

But those did not address fully the fast changing scenario in the society. Irrigation engineers face many difficulties in managing limited water resources available and there were many requests to the policy makers to change the legislations to fulfil the current needs. Recognizing these shortcomings, the Ministry of Irrigation and Water Resources Management took initiative in 2016 to identify the current needs in order to amend the Ordinance. Since the irrigation infrastructure serves not only the irrigation sector, but many sectors such as domestic water supply, inland fishing, environment, flood control, power generation etc. comprehensive consultative studies had to be conducted to cover all these areas.

3.2 Institutional Set Up and Responsibilities

Irrigation Development was initially undertaken by the Government Agent in 1850's and then the same was shared with the Public Works Department (PWD) when the technical issues became complicated. Central Irrigation Boards and Provincial Irrigation Boards were formed mainly to develop major irrigation works, when British rulers found that the PWD could not pay much attention to irrigation. [5] In 1900 Irrigation Department was established solely for this purpose. However, the role played by the Government Agent in facilitating and organizing seasonal cultivations, land alienation, collection of irrigation rates etc. were continued in the same spirit in the Ordinance. Even though Irrigation Department was fully responsible for planning and development of water resources, that fact has not been acknowledged in the amendments or in new Irrigation laws that were introduced later.

The focus of the Irrigation Department was mainly on restoration of ancient reservoirs until 1920's. It was later shifted towards development of new reservoirs. Government



Agent was vested with legal powers to sell or alienate lands developed under the irrigation systems, manage lands and water through the village councils and headman, fixing and collection of irrigation rates, taking action against irrigation offences etc. They played a major role in the management of the cultivation while managing the revenue collection through his assistants who were known as Chief Headmen and later on as District Revenue Officers.

When the current Irrigation Ordinance, that had been later revised several times, was enacted in 1946, Government Agent remained a key player. [2] One other reason for continuing the GA's role in irrigation management would have been, and especially the absence of a central coordinator in managing all the two key natural resources, land and water, which was duly filled by the Government Agent.

One successful institutional structure introduced under the Irrigation Ordinance of 1946 was the District Agricultural Committee, popularly known as DAC. In the dry zone of Sri Lanka this is still a strong administrative entity that takes decisions regarding irrigation and agriculture in the districts and also on water resources development. [15]

An Advisory Committee at district level was prescribed in the 1946 Ordinance. However these committees do not exist in any district now.

With the 1968 amendment, the overall supervisory power over the activities defined in the Ordinance was vested with the Commissioner of Agrarian Development. However, this has not been practiced so far and was proven to be an unsuccessful administrative proposal.

Amendment introduced in 1994 empowered the farmer organizations and Project Management Committees to play key roles in seasonal planning and management of Irrigation schemes.

3.3 Methodology Adopted for identifying gaps in the legislation

Ministry of Irrigation and Water Resources Management (M/I&WRM) appointed an expert

panel to study the shortcomings in the current Ordinance and recommend a course of action to rectify them. The panel consisted of two retired Director Generals of Irrigation (both engineers), one of them appointed as the team leader, and two other retired officers of Sri Lanka Administrative Service (one officer a former Secretary to the Prime Minister and the other officer, a former Secretary to the Ministry of Lands). The coordinating officer of the committee was a former Director in the Irrigation Department. The panel conducted a literature survey and had extensive discussions initially with key officials in the M/I&WRM, Irrigation Department and Agrarian Development Department (ADD) to identify the gaps.

A special briefing session was conducted with the Minister of I&WRM to make him aware and get his feedback as the M/I & WM has overall responsibility to redress the shortcomings in irrigation legislations. The expert panel then conducted a series of consultations at District level covering 22 districts where interprovincial major irrigation schemes are operated. For the District level consultations, District Secretaries, Director of Irrigation, Chief engineers, Divisional Irrigation Engineers, Divisional Secretaries, Irrigation officials, Official in line agencies and farmer organization leaders were involved. After briefing the problem the participants were grouped in random and a discussion paper was given for them to discuss and express their views.

Their opinion over the shortcomings of the current legal provisions was very vital since all these groups confront problems associated with irrigation & water resources sector on a daily basis.

A special workshop was conducted with all the key officials of nine Provincial Councils. Discussions were conducted with Ministry of Lands, Ministry of Agriculture and Mahaweli Authority of Sri Lanka. The veteran Irrigation and water sector officers included the retired officials from the Ministry of Irrigation and Department of Irrigation; university academics and representatives from International Water Management Institute were consulted to get their feedback as well. A paper advertisement was also published inviting the views of the public over the shortcomings of the current Irrigation Ordinance and suggestions for improvements.

After listing the feedback from all the stakeholders, the expert panel reviewed the current (consolidated) Ordinance. The amendments were considered in two formats; [15]

- i) Changes to the existing sections in the Ordinance
- ii) Introduction of new sections to fill the gaps.

Representatives from the Department of Legal Draftsmen (D/LD) were then invited and briefed the rationale of each and every proposal of the amendment and obtained their feedback. This was aimed to shorten the time taken for D/LD to draft the amendments and produce the final version of amendments for the approval from the parliament.

3.4 Observed Gaps

The expert panel summarized all the feedback received during the consultations. The issues raised by those who face practical difficulties in the field in managing existing irrigation schemes or by those who do planning and construction of new water development reflected the current gaps in the legislations. The farmer organization leaders were allowed to express their views freely and hence the panel was able to grasp the issues from the beneficiary's point of view as well. The main shortcomings identified in the prevailing irrigation laws were: [15]

- Not introducing timely amendments- Since 1946 from when the current Irrigation Ordinance of was enacted, many changes have occurred in the social, demographic and economic spheres in the country. Demand for water for the increasing population and new livelihood was increased dramatically. Hence the monopoly over water resources initially held by the irrigation sector has been confronted by the demand created by urban water supply, industry, tourism, wildlife, inland fishery, aqua sports and other activities. Amendments to the Irrigation Ordinance made after 1946 do not reflect such matters. Environmental flow that has to be released under the new environmental regulations has also made impacts over the share of the agricultural water user.
- Ambiguity of the definition of "Minister" - The overall power over execution of provisions in the Ordinance is vested with the Commissioner General of Agrarian Development. Hence logically regulations over the matters related in the Ordinance have to be originated from the Minister in charge of Agrarian Development. As most of the matters relevant to major irrigation works are under purview of another Ministry, it is not practical to issue such direction from a minister not responsible directly to the subject.
- Absence of regulations - There are provisions made in the Ordinance to introduce regulations in specific matters. No regulations have been passed in the parliament under this Ordinance. This has created a huge vacuum in the legislations as many important issues were not defined in details there.
- Non-availability of a complete list of irrigation offences - specially some pressing issues such as non-compliance with the agreed decisions with regard to management of the seasonal cultivation, conservation of water, protection of the infrastructure, responsibilities of the stakeholders towards proper maintenance of the infrastructure, encroachments on the reservations, willful damages caused to structures, unauthorized acquisition of water, harmful activities within reservoir bed and reservations, unauthorized constructions, failure to comply with instructions for remedial action. Identification of the offences is the first step which should be followed up with un-delayed action to undo the harmful effects of any such offence committed.
- No clear definition for major and minor irrigation works - classification of major and minor irrigation works requires to be redefined in the Ordinance in view of the current practice. In practice below 200 Acs. (80ha) irrigable area appears to be the criterion for the



classification of minor irrigation schemes which are under the purview of the Agrarian Services Department or Provincial Councils while the larger inter-provincial irrigation schemes are under the purview of the Irrigation Department as major irrigation works. Both categories are governed by the Irrigation Ordinance.

- Entrusting the Government Agent on construction and maintenance of irrigation works for which GA has no supporting institutional structure. According to the Ordinance, where it is proposed to construct any irrigation work or any variation be made for the physical conditions of any irrigation work, a project proposal for that purpose may be prepared by the Government Agent. The Commissioner of Agrarian Services approves the irrigation scheme prepared by the GA. Practically this procedure does not take place as the Irrigation authorities attend the same.
- Time consuming process for the prevention of offences - The Ordinance mentions for the GA to serve a notice for the person who committed an offence (such as encroachment or obstruction of a water courses, channels or tanks) to abate such encroachments or obstructions and if the offender fails to do so cause it to be abated and recover the costs. It has not been much practiced. A quicker and effective procedure is required
- Not sufficient empathy given for protection of reservations - The responsibility of protection of reservations of irrigation reservoirs, structures, canals, drainage canals and spill tail canals or other lands on which buildings or other structures are constructed is not assigned to the Irrigation Department, which is responsible in managing these systems. The ID is currently facing frequent difficulties in taking legal action for the protection of such reservations.
- Difficulties in mobilizing FO to act against the irrigation offenders - Farmer Leaders in the Project Committees and Farmer Organizations show a reluctance to take action against their errant fellow-farmers. They request to be given recognition within the Ordinance so that they could take action against their fellowmen in an official capacity rather than in a personal capacity as at present.
- Lack of provisions for management of irrigation systems have extended beyond district and administrative boundaries - in the present Ordinance decisions over the development and operation of irrigation scheme has been taken at the District level. It does not identify the requirements of the complicated schemes spread beyond the district boundaries.
- Absence of provision for Water resources planning - Planning of water resources has not been addressed in the Ordinance. Irrigation development plans are not merely to serve the irrigation requirements but more needs nowadays such as urban water supply, inland fishing, environmental needs, industrial demand, hydropower, flood mitigation and salt water exclusion. There is a need for holistic approach for comprehensive water resource planning taking into account the needs of all above sectors.
- Absence of regulations in catchment management & riverine management - To ensure sustainable water resources of the country, regulation of catchment and riverine management is a must. This aspect has not been covered in any of the water legislations. Irrigation Ordinance is the most suitable legislation to incorporate these aspects.

4. Observations

Many observations were made by the panel during the process of consultations and literature review. One notable observation is the initiative and active participation taken by the engineers in changing the legislations. Since the irrigation engineers are in the forefront in planning, designing and management of water resources infrastructure in the country, they face immense difficulties in the field and also are subjected to criticisms from the public due to a lack of proper legal support.

Representatives from Provincial Councils too were mainly engineers and they highlighted the lack of legal provisions, training opportunities and interaction with national organisations, which are essential for quality enhancement of their interventions in water sector.

Following additional information were also taken into account when finalizing the proposed amendments to the Irrigation Ordinance.

- i. An extended responsibility has been placed with Irrigation Department in 2014 by the National Policy on "Protection and conservation of water sources, their catchments and reservations". The Irrigation Department will have to take care of riverine management, protection of reservations, protection of watercourses and preservation of water quality etc. With this assigned responsibility, legal support is necessary to be in place.
- ii. Failure in publication of an irrigation scheme in the Gazette as prescribed in the Irrigation Ordinance has not been taken place. The legal acceptability of an irrigation scheme rests upon GA making arrangements to gazette same with the recommendation of Director of Irrigation and /or Survey General due to practical limitations. This has not been attended to in the past due to practical reasons. There is no legal coverage for Irrigation Department to claim boundaries of the infrastructure due to this shortcoming, which has to be attended early.
- iii. Lack of regulatory mechanism is found to be a shortcoming in the whole process where implementing agencies themselves

have become regulatory bodies in water management. Hence it is high time for establishment of an apex body to impose regulatory measures, for each organisation handling bulk water management to make use of water resources in the agricultural sector to be more efficient and productive.

5. Way forward

The panel submitted its recommendations to the Ministry of I&WRM in its final report, after 6 months of deliberations. Amendments proposed to the existing Irrigation Ordinance were submitted to the Department of Legal Draftsmen for their perusal. After review by the Legal Draftsmen, the draft will be referred to the Attorney General's Department to get the views from all the stakeholders. Once this process is cleared, the amendments will have to be passed through the Parliament which will take nearly one year.

6. Conclusion

Systematic approach in identifying the gaps in the current Irrigation Ordinance made a pathway to make proposals for amending the current Irrigation Ordinance. These amendments define the issues in broader context and it is necessary to frame regulations considering detailed requirements. However, legislation for overall water resources management is a need of the country, which cannot be fulfilled without the introduction of the amendments to the Irrigation Ordinance, as emphasized in many consultative discussions.

Acknowledgement

The authors wish to acknowledge with thanks the approval given by the Secretary of Ministry of Irrigation and Water Resources Management in quoting the internal documents of the Ministry and also the input of the specialist panel who conducted a comprehensive study in framing a proposal for amending the Irrigation Ordinance.

References

1. Ceylon Government Gazette, Part II, Dec 21, 1917.
2. Ceylon Government Press, Acts of Ceylon, Chapter 453.



3. Ceylon Government Press, Supplement to Ceylon Government Gazette Feb 16,1951.
4. Ceylon Government Publication, 1856.
5. Ceylon Sessional paper IXLV, 1905, Capt Sir John Keane, Report on Irrigation in Ceylon.
6. House of Commons, Report of Lieutenant-Colonel Colebrooke, 1832, Government of Ceylon.
7. Irrigation Department, Proceedings of Seminar on Irrigation, 2000.
8. Kamaladasa, Badra (1999), "Does the Irrigation Ordinance provide the necessary legal framework for Irrigation Development and Management", Transactions 1999 of annual sessions of The Institution of Engineers of Sri Lanka.
9. Kamaladasa, Badra, 2001, "Integrated Water Resources Management-Need to think both globally and locally", International Seminar on "Engineering management for Accelerated Development in South and South east Asia", Institution of Engineers Sri Lanka, Colombo, 2001.
10. Kamaladasa, Badra, 2015, "Role of the Irrigation Department in irrigation sector in the context of devolution of power under 13th amendment", National seminar on "Impact made in the irrigation sector by devolution power by 13th Amendment", 2007, Seminar Proceedings by HARTI, Colombo.
11. Kamaladasa, Badra, 2015, "What if the first Irrigation Ordinance in Sri Lanka in modern history was implemented?" INWEP symposium, Marawila, Sri Lanka, October.
12. Legislative enactments of Ceylon, Vol II Ceylon Government, Ordinances, 1867.
13. Legislative enactments of Ceylon, Vol III, (pg 454-457) Ordinances, 1884.
14. Legislative enactments of Ceylon, Vol III, (pg 88-92), Ordinances, 1887.
15. Ministry of I & WRM, 2016, Final report on "Amending the Irrigation Ordinance".
16. Ordinances of Ceylon, Ceylon Government Gazette no 3264, 1861, pg 453-458).
17. Ordinances of Ceylon, Ceylon Government Press, Ordinances 21/ 1861.
18. Water Resources Board, Annual report, 2011.
19. www.ep.gov.lk/Documents/13th_Amendment.pdf.

Analysis of Long-term Trends of Climatological Parameters in Kigali, Rwanda

D.P.C. Laknath, N.R. Josiah and T.A.J.G. Sirisena

Abstract: Kigali is the capital city of Rwanda in Africa. Rwanda is located astride two key climate regions (i.e. East Africa and Central Africa). Even though Rwanda is located in the tropical belt, it experiences a temperate climate as a result of its high elevation. To represent the climatic conditions at a proposed dam construction site in the proximity of Kigali City, this study was carried out to identify the long-term variation of climatological parameters in Kigali as it was the most representative hydro-meteorological station within the area. Accordingly, Kigali Airport weather station was selected considering the long length of data availability between 1971 – 2013 periods. For the analysis, meteorological variables such as rainfall, temperature, relative humidity, evaporation, sunshine duration, wind and atmospheric pressure were selected. To identify the trends of each climatic parameter, annual anomalies were calculated. In this study, trend analysis was carried out by using non-parametric Mann-Kendall test (1945). On the basis of Mann-Kendall test and Z_c statistics of each month and seasons, long term trend of each variable between 1971 – 2013 periods was identified. As the outcome of the study, it has been identified that there is an increasing trend in temperature during last 40 years at Kigali-Aero station. Also, rainfall has a decreasing trend during the same period. Further, relative humidity has decreased during the same period. With the increasing temperature and decreasing humidity, an increase in evaporation is expected. According to the present analysis, a positive trend of evaporation was identified. Further, a positive trend in wind speed and atmospheric pressure was identified for the past 40 years. In case of sunshine hours, a significant trend was not identified.

Keywords: Design of dam, climatological data, annual anomalies, Mann-Kendall test, trend analysis

1. Introduction

Generally, in many countries in the African continent, the impact of climate change on the continent's scarce resources such as water resources seems to be completely ignored. Also, as climate change issues are not of immediate importance, there is a lack of enthusiasm to understand about the climate change [1] in the same region. Further, especially in Africa, a knowledge gap has been identified in literature related to water resource management under climate change [2]. However, in African countries, water resources are considered as an important and limiting constraint for economic development. Hence, development of hydraulic infrastructure has been identified as an important task for water resources management and identifying long-term trends and variation of climatic parameters such as rainfall, temperature and atmospheric pressure are crucial for the construction of hydraulic structures like dams.

The present study was carried out focusing a potential dam site at a selected location in the middle reaches of Nyabarongo River in

Rwanda (Figure 1). This dam site is situated approximately 30km north east of Kigali which is the capital and largest city of Rwanda. To represent the climatic conditions at the proposed dam construction site, this study was carried out to identify the long-term variation of climatological parameters for the most representative hydro-meteorological station for the proposed dam within the area. Accordingly, Kigali Airport weather station was selected considering the long length of data availability between 1971 – 2013 periods. For the analysis, meteorological variables such as rainfall, temperature, relative humidity, evaporation, sunshine duration, wind and atmospheric pressure were selected. Thus, trends of each climatic parameter were identified.

Eng. (Dr.) D.P.C. Laknath, B.Sc.Eng. (Moratuwa), M. Eng. (Thailand) Dr. Eng. (Japan), Engineering Manager, Lanka Hydraulic Institute Ltd.

Eng. N.R. Josiah, B.Sc.Eng.(Peradeniya), Research Engineer, Lanka Hydraulic Institute Ltd.

Eng. T.A.J.G. Sirisena, B.Sc.Eng.(Peradeniya), M.Eng (AIT), Ph.D. Candidate, UNESCO-IHE Institute for Water Education, Delft, The Netherlands, University of Twente, Enschede, The Netherlands.



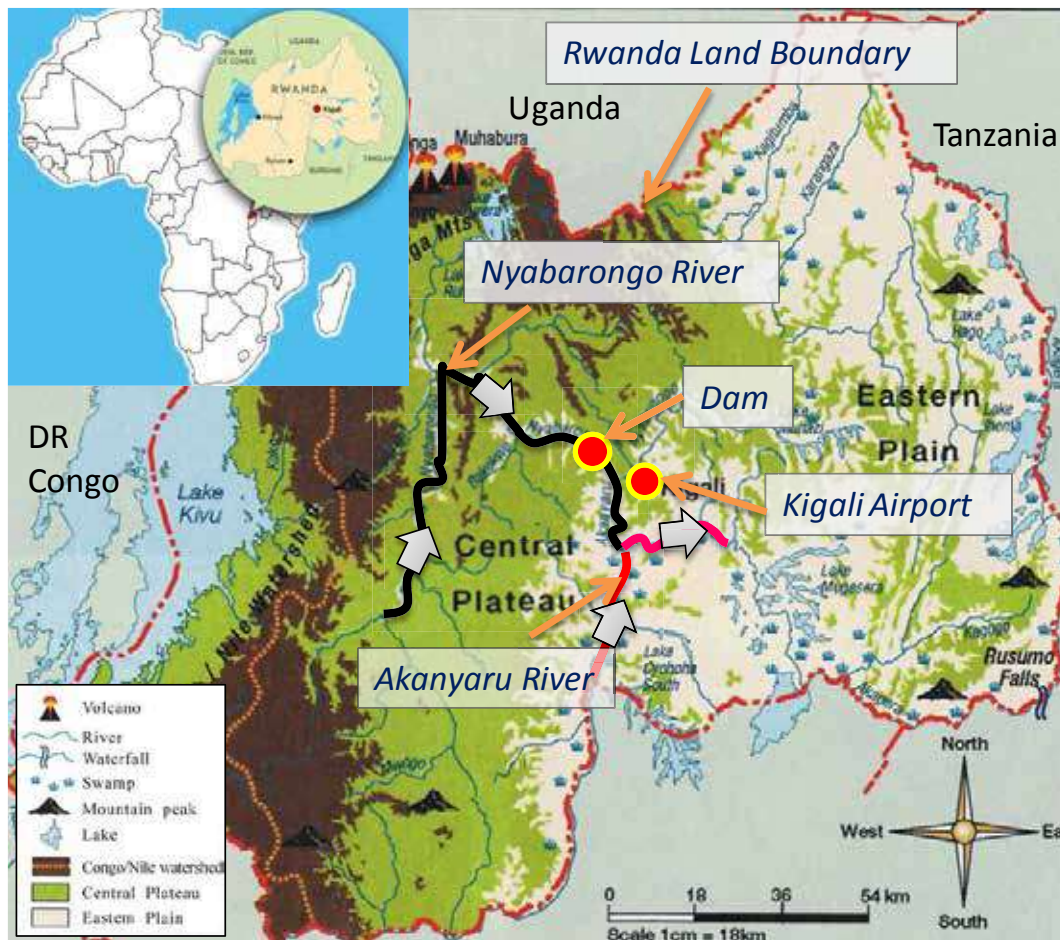


Figure 1 - Study Area: Proposed Dam Site and Kigali Airport Weather Station [3]

2. Study Area

Climatological study was carried out focusing a potential dam site at a suitable location across the Nyabarongo River (Figure 1). This dam site is situated approximately 30km north east of Kigali which is the capital and largest city of Rwanda. Rwanda has two principal basins called eastern Nile basin (85% of entire basin) and the western Congo basin (15% of entire basin). These basins are divided by Congo-Nile alpine regions. The Nyabarongo and Akanyaru rivers belong to the Nile basin. The proposed dam could aim to cater for municipal and irrigation water and power needs of the country and stabilization of Nyabarongo River for flood control. Even though Rwanda is located in the tropical belt, it experiences a temperate climate as a result of its high elevation. The Albertine branch of the Rift Valley runs along the western side of Rwanda. Much of the border with the Democratic Republic of Congo (DRC) is mountainous with elevation over 2000 m. Elevations decline toward the central plateau of Rwanda and again in the eastern plateau towards the border with Tanzania. According

to the SCCE study [4], the average temperature in Rwanda is around 20°C. As a result of topography variation, the warmest annual temperatures are found in the eastern plateau (20°C-21°C) and Imbo and Bugarama Valleys (23°C-24°C). The cooler temperatures are in high elevations of the central plateau (17.5 -19 °C) and highlands (<17 °C). In the case of rainfall, Rwanda experiences bimodal patterns of rainfall, mainly driven by the progression of the Inter-Tropical Convergence Zone (ITCZ). The ITCZ is the area encircling the earth near the equator where the northeast and southeast trade winds come together. Based on precipitation and climate, Rwanda can be divided into four climatic areas (i.e. *low altitude, high altitude, central plains and eastern savanna*). Rwanda experiences four seasons, including two rainy seasons and two dry seasons. Generally, long rains occur during rainy season 1 (March - May) due to the ITCZ moves to the north. Short rains occur during Rainy season 2 (October - December) due to the return of ITCZ to south. January - February and June to September periods are identified as Dry season - 1 and 2, respectively.

3. Methodology

In general, Fifth assessment report of the Intergovernmental Panel on Climate Change (IPCC) [9] set the technical guidelines for assessing climate change impacts and adaptations. It sets the prerequisite characteristics of climate data sets necessary for an adequate analysis of climate changes. For a climatic data analysis, data availability, quality and consistency of the data, observation practices and instrumentation are found to be the governing parameters [10]. Further, Bocchiola [11] was presented different methodologies such as liner regression against time, liner regression against with NAO and global thermal anomalies, Mann-Kendall test, correlation against physiographic and climatic features and correlation against local climate variables to be useful for the prediction of hydro-meteorological trend analysis. With this general idea, the climatic data and the suitable method of analysis were determined and discusses below.

3.1 Climatic Data

In line with the project objective, climatic data analysis was carried out for the most representative hydro-meteorological station within or near the area. Accordingly, Kigali Airport (*Kigali Aero*) weather station at (30.11° E -1.95° N) was selected considering the long length of data availability between 1971 - 2013 periods (Table 1). For the analysis, following meteorological variables were considered.

- Rainfall
- Temperature
- Relative Humidity
- Evaporation
- Sunshine duration
- Wind
- Atmospheric pressure

Percentage availability of meteorological

variables and record lengths at Kigali Aero are tabulated in Table 1.

3.2 Trend Analysis

Before analysis of data, quality control tests were carried out. For the identification of trends of each climatic variable, data record of sufficient length is required. Accordingly, period between 1971 and 2013 was considered for the analysis. After selecting data between suitable time periods, rough screening of the data was done by computing and verifying the totals of each parameter for the water years (hydrological years). By using water years, it removes any risk of the seasons being split over two years. After performing a rough screening of the data, data was plotted for the selected time step (year) to identify trends or discontinuities. Further, to identify trend of each climatic parameter, annual anomalies were calculated. Anomalies defined as deviations from the average in climatology and the average was calculated over some time period of at least 20 or 30 years [8]. To detect the significant trends in climatologic time series parametric and non-parametric methods can be implemented [6]. Independent and normally distributed data is needed to use the parametric tests, while non-parametric tests require only the independent data [6]. In this study, trend analysis was carried out by using non-parametric Mann-Kendall test [5]. The Mann-Kendall test statistic (S) can be calculated [7] as shown in 3.1.

$$S = \sum_{i=1}^{n-1} \sum_{j=i+1}^n \text{sgn}(x_j - x_i) \quad \dots(3.1)$$

where, n is the number of data, x_i, x_j are data values in time series i and j ($>i$) respectively and $\text{sgn}(x_j - x_i)$ is the sign function as,

$$\text{sgn}(x_j - x_i) = \begin{cases} +1, & \text{if } x_j - x_i > 0 \\ 0, & \text{if } x_j - x_i = 0 \\ -1, & \text{if } x_j - x_i < 0 \end{cases} \quad \dots(3.2)$$

Table 1 - Summary of Completeness of Meteorological Variables at Kigali Aero

Climate Parameters	Interval	% Availability	Duration
Rainfall	Daily	98.82	1971 - 2013
Mean Temperature	Daily	98.66	1972 - 2013
Min/Max Temperature	Monthly	98.64	1972 - 2013
Relative Humidity	Daily	98.15	1972 - 2013
Evaporation	Daily	91.63	1972 - 2012
Sunshine Duration	Daily	97.34	1972 - 2001
Wind Speed/ Direction	Daily	98.80	1974 - 2009
Atmospheric Pressure	Daily	98.70	1972 - 2013



The variance can be computed as,

$$Var(S) = \frac{n(n-1)(2n+5)}{18} \dots(3.3)$$

where, n is number of data. For the sample size $n > 10$, Mann-Kendall statistic (Z_c) can be calculated as,

$$Z_c = \begin{cases} \frac{S-1}{\sqrt{Var(S)}}, & \text{if } S > 0 \\ 0, & \text{if } S = 0 \\ \frac{S+1}{\sqrt{Var(S)}}, & \text{if } S < 0 \end{cases} \dots(3.4)$$

Increasing and decreasing trends can be indicated by the positive and negative Z_c values. This statistical test is frequently used to analyse the significance of trends in climatological time series [7] and it is being used for studying the spatial variation and temporal trends of hydro climatic series.

4. Results and Discussion

4.1 Rainfall

Annual average rainfall for water years within 1971- 2013 period at the representative station are illustrated in Figure 2. Further, anomalies for the same period are illustrated in Figure 3. Anomaly shows the departure from the long-term average of rainfall (983 mm). Thus, long term trend and inter-annual variability of rainfall at the representative station were identified.

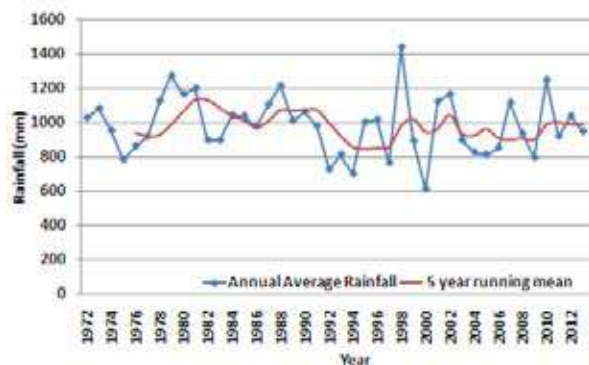


Figure 2 - Annual Average Rainfall and 5 Year Running Mean for 1971- 2013 Period

Considering 5 year running mean rainfall and anomalies, a slight decrease of rainfall over the last 40 years was observed. This trend was further analysed with Mann-Kendall test for each month over considered time period. By applying equations 3.1, 3.2, 3.3 and 3.4 static S , sign, variance and Z_c were estimated.

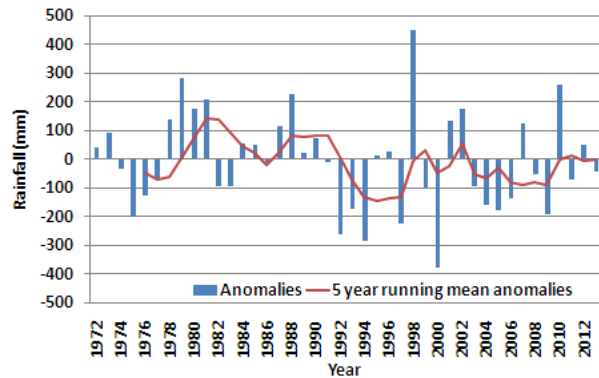


Figure 3- Annual Rainfall Anomaly and 5 Year Running Mean Anomalies for 1971 - 2013 Period

There was a positive trend observed in January, March and October while the other nine months had a negative trend. Thus, in overall, a negative rainfall trend for the considered 40 years has been identified. Table 2 shows the summary of the Mann-Kendall Z_c values and the long-term trend.

4.2 Temperature

Mean, minimum and maximum temperatures for the period 1972-2013 at the representative station were analysed. Average of mean temperature was calculated as 20.5°C. The mean values of the annual temperatures with the 5 year running mean and anomalies are shown in Figure 4 and 5 respectively.

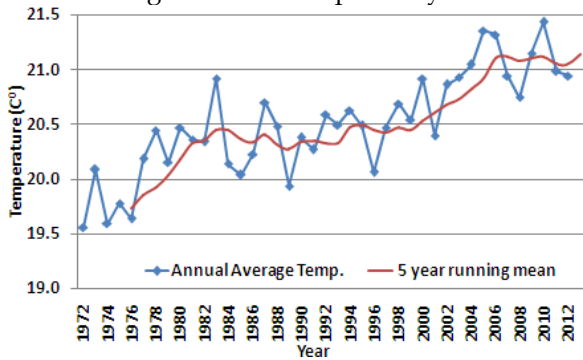


Figure 4 - Average of Annual Mean Temperature and 5 Year Running Mean for 1972 - 2013 Period

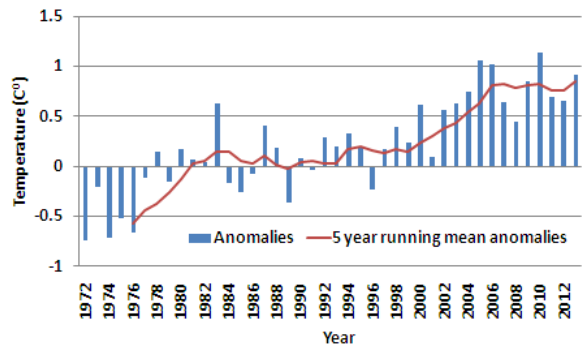


Figure 5 - Annual Average Temperature and 5 Year Running Mean Anomalies for 1972 - 2013 Period

To understand the long term trend and inter-annual variability, Mann-Kendall test was performed for mean, minimum and maximum temperatures for each month over the considered time period.

Mann-Kendall Z_C values are shown in Table 2. It has been noted that there is a positive trend of mean temperature of all months and a gradual increase was identified since 1972. Further, a large increase in minimum temperature than maximum temperature was identified. This implies a reduction in diurnal temperature range during the considered period.

4.3 Relative Humidity

Annual average relative humidity for the years 1972-2013 at the representative station was considered and the average relative humidity was calculated as 73.9%. Figure 6 shows the annual average humidity with 5 year running mean while Figure 7 shows the anomalies.

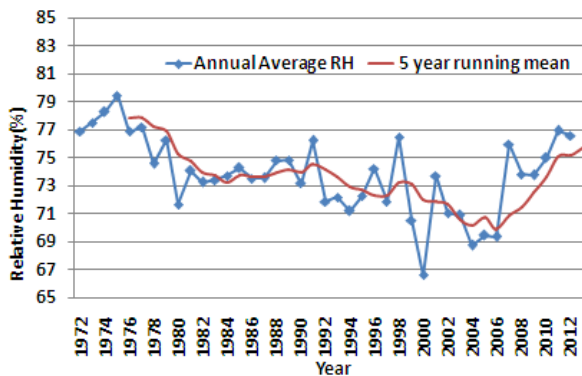


Figure 6 - Annual Average Relative Humidity and 5 Year Running Mean for 1972-2013 Period

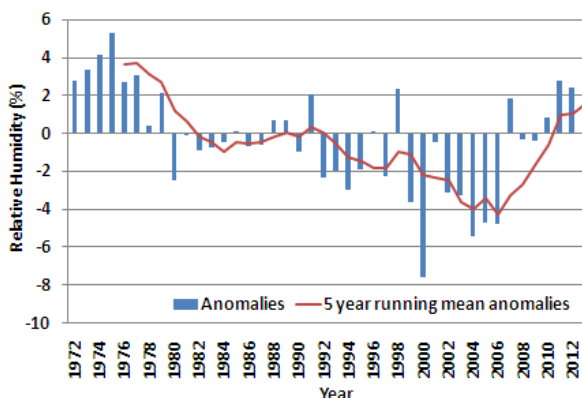


Figure 7 - Annual Average Relative Humidity and 5 Year Running Mean Anomalies for 1972 - 2013 Period

A decrease in relative humidity was observed when considering 5 year running mean and the anomalies. To ensure the trend, Mann-Kendall

test was performed for each month individually. Table 2 presents the Mann-Kendall Z_C values for Relative Humidity.

It has been revealed that, except March, all other months have negative trends. Thus, it was identified that there was a negative trend of relative humidity at the representative location.

4.4 Evaporation

Annual total evaporation for the period of 1972-2013 was considered for the analysis. Average annual total evaporation was calculated as 1438.1 mm. Figure 8 and 9 illustrate the annual total evaporation with 5 year running mean and the anomalies respectively.

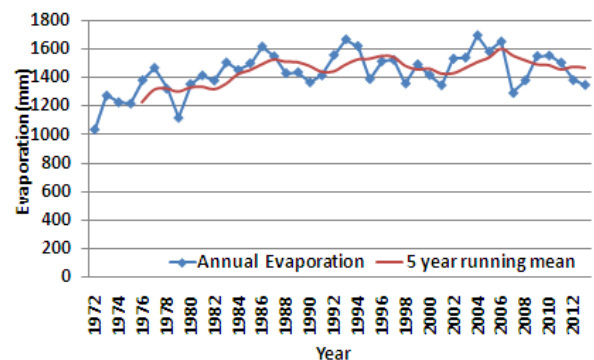


Figure 8 - Annual Total Evaporation and 5 Year Running Mean for 1972-2013 Period

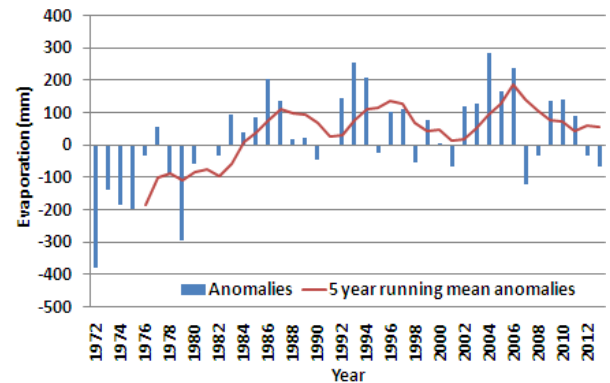


Figure 9 - Annual Evaporation and 5 Year Running Mean Anomalies for 1972 - 2013 Period

There was an increase of annual total evaporation as observed when considering the 5 year running mean and anomalies of total evaporation. The trend was further analysed with Mann-Kendall test for each month individually over the considered time period.

Positive trends were identified for all months for the evaporation (Table 2). Thus, in overall there was a positive trend of evaporation at the representative location.



4.5 Sunshine duration

Annual average sunshine durations for the period of 1972-2001 at the representative location were used in the analysis. Figure 10 shows the annual average sunshine duration with 5 year running mean. Further, average annual sunshine duration was estimated as 5.8 hours.

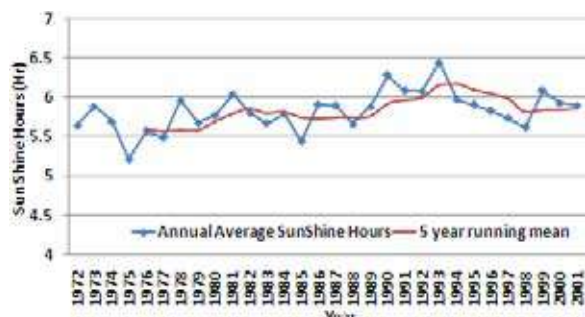


Figure 10 - Annual Average Sunshine Duration and 5 Year Running Mean for 1972-2001 Period

Considering 5 year running mean and the anomalies there were no significant trend identified.

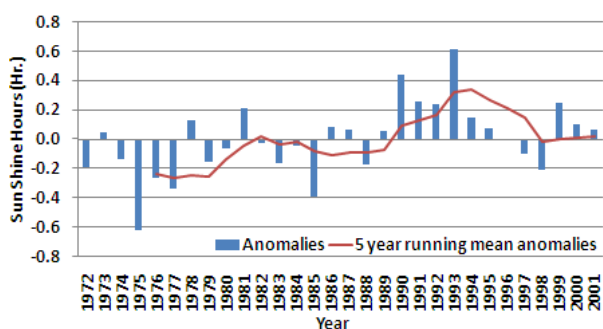


Figure 11 - Annual Average Sunshine Duration Anomaly and 5 Year Running Mean Anomalies for 1972 - 2001 Period

Anomalies of annual average sunshine hours are shown in Figure 11. Further, Mann-Kendall test was performed for each month over the considered period to identify the possible trends.

Except January, March, October and December, negative trends were identified (Table 2). In overall, there were no significant trends identified for the sunshine at the representative location.

4.6 Wind

Annual average wind speeds for the years 1974-2009 at the representative station were considered for the analysis. Figure 12 and 13 show the annual average wind speed and 5 year running mean and the anomalies

respectively. The annual average wind speed was calculated as 2.6 m/s.

An increase in annual average wind speed was observed by considering the 5 year running mean and anomalies. This trend was further examined with Mann-Kendall test. Test was applied for each month individually over the considered period.

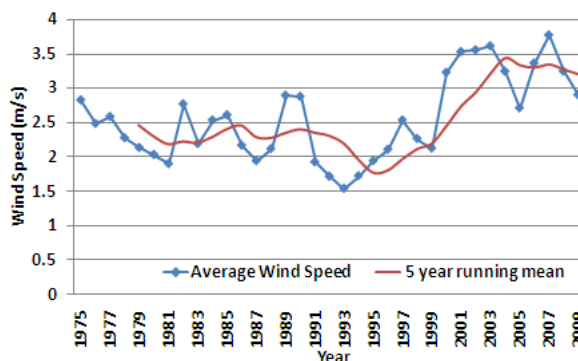


Figure 12 - Annual Average Wind Speed and 5 Year Running Mean for 1974-2009 Period

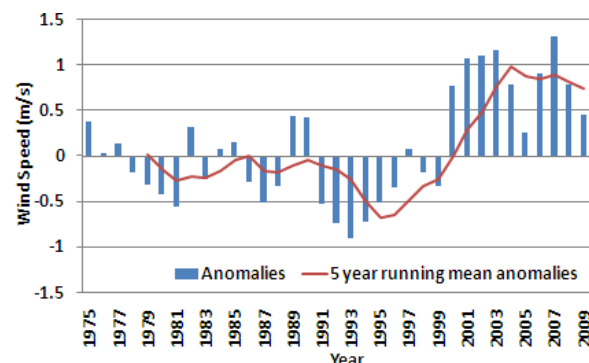


Figure 13 - Annual Average Wind Speed and 5 Year Running Mean Anomalies for 1974 - 2009 Period

The Mann-Kendall trend of annual average wind speed showed positive statistics for all months (Table 2). Thus it was recognized as a positive trend of wind speed at the representative location for considered period.

Further, wind directions for the years 1974-2009 were also considered in the analysis. Winds are dominant between 292.5^o-360.0^o and 22.5^o-90.0^o directions. A 73.74% of wind speeds belonged to 4m/s - 8 m/s range and the percentage occurrence of winds over the speed of 10 m/s was very low during the analysis period.

4.7 Atmospheric pressure

Annual average atmospheric pressure for the years 1972-2013 at the representative station were considered for the analysis. Average annual atmospheric pressure was 851.3 mbar. Figure 14 and 15 show the annual average

atmospheric pressure and 5 year running mean and anomalies respectively.

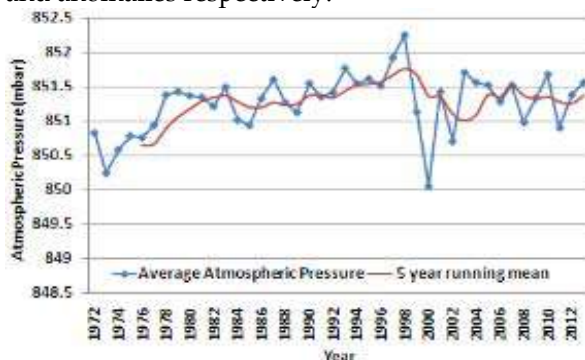


Figure 14 - Annual Average Atmospheric Pressure and 5 Year Running Mean for 1972-2013 Period

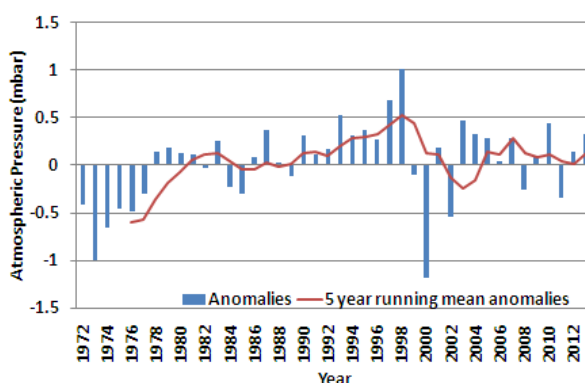


Figure 15 - Annual Average Atmospheric Pressure and 5 Year Running Mean Anomalies for 1972 - 2013 Period

An increase in atmospheric pressure was observed by considering the 5 year running mean and anomalies of atmospheric pressure. Trend was further examined with Mann-Kendall test for each month over the considered period.

A positive trend of atmospheric pressure was identified for all months by Mann-Kendall test.

4.8 Analysis summary

Table 2 illustrates the summary of long term variability of meteorological variables such as rainfall, temperature, relative humidity, evaporation, sunshine hours, wind speed and atmospheric pressure at Kigali-Aero weather station which is a representative location for the study.

On the basis of Mann-Kendall test and Z_c statistics of each month and seasons, the long term trend of each variable between the years 1971-2013 was identified. Identified overall trend of each variable is given under “long term trend (1971-2013)” of Table 2.

5. Conclusions

This study was carried out to understand about the long-term variation of climatological parameters at a proposed dam site in the proximity of Kigali City. Thus, as the representative hydro-meteorological station within the area, Kigali Airport weather station was selected considering the long length of data availability for 1971 - 2013 period. For the analysis, meteorological variables such as rainfall, temperature, relative humidity, evaporation, sunshine duration, wind and atmospheric pressure were selected. As shown in Figure 16, there is an increasing trend in temperature during last 40 years at Kigali-Aero station. Also, rainfall has a decreasing trend during the same period. Further, relative humidity has decreased during the considered period. With the increasing temperature and decreasing humidity, an increase in evaporation is expected and it was confirmed in the subsequent analyses (Figure 17).

Table 2 - Summary of the Long-Term Variability of Meteorological Variable at Kigali Aero Weather Station

Parameter	Units	Average	Mann Kendal Z_c												Long-term Trend (1971 - 2013)
			Dry -1			Rainy -1			Dry - 2				Rainy-2		
			Jan	Feb	Mar	Apr	May	Jun	Jul	Aug	Sep	Oct	Nov	Dec	
Rainfall	mm/year	983.5	1.35	-1.04	1.52	-1.28	-0.54	-0.75	-0.70	-0.18	-1.31	0.93	-0.18	-1.78	Decrease
Temperature	°C	20.5	3.90	3.74	2.40	4.43	4.70	4.58	4.20	4.24	3.10	2.27	5.41	3.88	Increase
Relative Humidity	%	73.9	-1.25	-1.78	0.47	-1.41	-0.76	-1.66	-2.16	-1.94	-1.42	-0.61	-1.11	-1.04	Decrease
Evaporation	mm/year	1438.1	1.80	2.02	0.16	0.36	2.00	3.10	2.57	3.06	1.41	0.67	1.08	0.25	Increase
Sunshine Hours	hours	5.8	-1.64	0.34	-0.82	1.96	0.75	1.46	1.36	2.43	1.57	-1.18	0.71	-0.93	-
Wind Speed	m/sec	2.6	2.49	2.83	1.86	3.58	1.68	2.61	1.26	1.83	1.85	1.59	2.06	1.68	Increase
Atmospheric Pressure	mbar	851.3	1.07	1.29	1.84	3.70	2.53	2.03	1.18	2.21	2.84	2.60	-0.22	0.11	Increase



Further, a positive trend in wind speed and atmospheric pressure is identified. In case of sunshine hours, a significant trend was not identified.

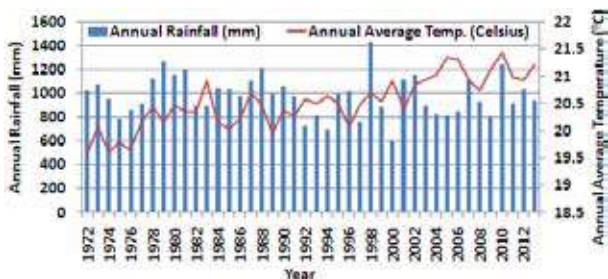


Figure 16 - Annual Trend of Mean Annual Temperature and Annual Rainfall for 40 Years

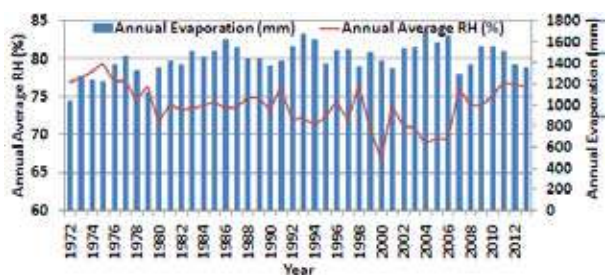


Figure 17 - Annual Trend of Annual Average RH and Annual Evaporation for 40 Years

The methodology of this study can be used for the developing countries in Asia, Africa and other continents, where it has a lack in accurate climatic data and very low technical adequacy. Further, it is a need to improve the present instrumentation techniques in-order to acquire accurate data to do the future studies. It is recommended to develop the study further with the available online climatic data to do the other suggested analysis methods and compare the results.

Acknowledgement

The authors wish to acknowledge to Rwanda Meteorology Agency for providing data for the success of this research.

References

- Nkhonjera, G. K., "Understanding the impact of climate change on the dwindling water resources of South Africa, focusing mainly on Olifants river basin: A review", *Journal of Environmental science and Policy*, Vol.71, 2017, pp:19-29
- Holman, I., "Climate change impacts on groundwater recharge - uncertainty, shortcomings and the way forward?", *Hydrogeology journal*, Vol.14, Issue.5, 2006, pp:637-647.
- Henninger, S., "Does the global warming modify the local Rwandan climate?", *Natural Science*, Vol.5, 2013, pp. 124-129.
- SCEE, "Rwanda's climate: Observations and Projections", *Smith school of enterprise and the environment*, University of Oxford, UK, 2011.
- Mann, H. B., "Nonparametric tests against trend", *Econometrica*, Vol.13, 1945, pp.245-259.
- Gocic, M., and Tajkoviv, S., "Analysis of changes in meteorological variables using Mann-Kendall and Sen's slope estimator statistical tests in Serbia", *Global and Planetary Change*, Vol.100, 2013, pp.172-182.
- Douglas, E. M., Vogel, R. M. and Kroll, C. N., "Trends in floods and low flows in the United States: Impact of spatial correlation", *Journal of Hydrology*, Vol.240, 2000, pp.90-105.
- Jones, P. D and Hulme, M., "Calculating regional climatic time series for temperature and precipitation: methods and illustrations", *International Journal of Climatology*, Vol.16, 1996, pp.361-377.
- IPCC, "Climate Change: The physical science basis, contribution of working group I to the fifth assessment report of the Intergovernmental panel on climate change", Cambridge University press, Cambridge, UK, 2013.
- Richard, R and Heim, Jr., "An overview of weather and climate extremes - Products and trends", *Weather and Climate Extremes*, Vol.10, 2015, pp.1-9.
- Bocchiola, D., "Long term (1921-2011) hydrological regime of Alpine catchments in Northern Italy, *Advances in Water Resources*, Vol.70, 2014, pp.51-64.

Development of a Flood Forecasting and Data Dissemination System for Kalu River Basin in Sri Lanka

S.Kokularamanan, A.W.M. Rasmy, Duminda Perera and Toshio Koike

Abstract: Flood hazard is one of the most frequent hazards in Sri Lanka which brings devastating damages. At present flood forecasting in major river basins was based on upstream water levels. This study focuses on the development of Flood Forecasting System (FFS) and data dissemination system by incorporating improved spatial and temporal resolution of rainfall data and numerical simulation to proactively predict the floods. Kalu River basin was chosen due to the reasons that, high rainfall, more frequent flooding and still many people live in the flood-prone areas of the basin. Since flood forecasting needs forecasted discharge and inundated area, Rainfall Run off Inundation (RRI) model was used to develop FFS in this study. 2014 daily rainfall data was used for calibration and 2013 daily data set was used for validation. Lead-time for this basin was found to be nearly 19.5 hours In order improve spatial and temporal resolution of rainfall data, Global Satellite Mapping of Precipitation (GSMaP) was used. In order to correct the bias of GSMaP, software developed by Japan Aerospace Exploration Agency (JAXA) and International Center for Water Hazard and Risk Management (ICHARM) was used. To determine the minimum number of ground stations (and locations) needed for optimum bias correction, some combinations of ground daily rainfall stations were analyzed. Rainfall stations located along the boundary of the basin gave better results. To disseminate the forecasted data, a web based dissemination system was developed using FORTRAN, Gnuplot, JavaScript, Openlayers and HTML. Combined automated system would be used as emergency operation room tool during flood situations.

Keywords: RRI Model, Near-real time flood mapping, GSMaP, JavaScript, HTML

1. Introduction

Flood occurs due to high intensity rainfall. Since Sri Lanka has many rivers (103 major rivers) with very steep slope and flat lands around river mouth (and sometimes even in upstream) flooding occurs in these flat lands. Kalu River (shown in Figure 1) is affected more severely than any other river due to its

topographic, rainfall trend (highest annual rainfall) and demographic reasons. Furthermore some studies indicate that Rathnapura and Kalutara district flood damages show increasing trend [1] and around 132,000 people were living in flood prone area of this basin [2].

At present, flood forecasts are made using upstream water levels obtained through telephone and often criticized for inefficiency and ineffectiveness. The objective of this study is to develop a flood forecasting system for Kalu River basin. Possibility of achieving this with ground rainfall data and satellite rainfall data would be considered. Even possibility of dissemination of forecasted information through modern information technology also considered. Overall system would enable



Figure 1 - Kalu River basin map

Eng. S.Kokularamanan, B.Sc.Eng.(Peradeniya),C.Eng. MIE(SL), M.Sc.(Grips-Tokyo), M.B.A.(Colombo), Chief Engineer, Irrigation Department, Sri Lanka.

Eng.(Dr.) A.W.M.Rasmy, B.Sc.Eng.(Peradeniya), Senior Researcher, ICHARM, Public Works Research Institute, Japan.

Eng.(Dr.)Duminda Perera, B.Sc.Eng.(Moratuwa), Research Specialist, ICHARM, Public Works Research Institute, Japan.

Eng.(Prof.)Toshio Koike, Director, ICHARM, Public Works Research Institute, Japan.



Irrigation Department(ID) of Sri Lanka to use this system as an operation room tool during flood emergencies and might enable the department to implement similar systems in other flood prone basins in Sri Lanka.

For numerical modeling RRI was selected as it could estimate inundation depth, extend and duration as they were important for flood forecasting. GSMaP rainfall estimates were used as real-time rain gauges are limited. However, it should be noted that if more real time gauges are available, estimation of flood forecasting could be improved and forecast lead time also could be improved by 4.5 hrs.

2. Data and Methodology

Flood event of 1st, June, 2014 is used for model development and calibration. May, 2013 and June data were used for validation. Lead time

Table 1 - Data used for calibration and validation

	Daily Data	Hourly Data
Period	2012 to 2014	01/05/2014 to 31/07/2014
Number of rain gauges	18	2
Number of river gauges	4	4

analysis showed that, discharge from most upstream (Ratnapura) takes about 40 hrs. to reach the most downstream area (Putupaula). However, in the case of tributary (Milakanda) to Putupaula it takes only 24 hours. Hence GSMaP data latency is around 4.5 hrs. brings the overall lead time as 19.5 hrs. Rainfall and discharge data sets used in this study is given in Table 1. In order to validate the flood inundation maps several Moderate Resolution Imaging Spectroradiometer (MODIS) and Landsat data sets were tried and due to cloud coverage good results could not be obtained. Finally and Advanced Land Observing Satellite (ALOS) data set of 3rd, June, 2008 was used for partial validation. Several GSMaP data sets also used for bias correction verification.

Although there were several hydrological models available, in this study based on the available data and purpose simple RRI model was adopted. RRI model is governed by both continuity and momentum equations.

$$\frac{dh^{i,j}}{dt} + \frac{q_x^{i,j-1} - q_x^{i,j}}{\Delta x} + \frac{q_y^{i-1,j} - q_y^{i,j}}{\Delta y} = r^{i,j} - f^{i,j} \quad \dots(1)$$

$$q_x = \begin{cases} -k_a h \frac{\partial H}{\partial x}, & (h \leq d) \\ -\frac{1}{n} (h - d_a)^{5/3} \sqrt{\left| \frac{\partial H}{\partial x} \right|} \text{sgn} \left(\frac{\partial H}{\partial x} \right) - k_a h \frac{\partial H}{\partial x}, & (d_a < h) \end{cases} \quad \dots(2)$$

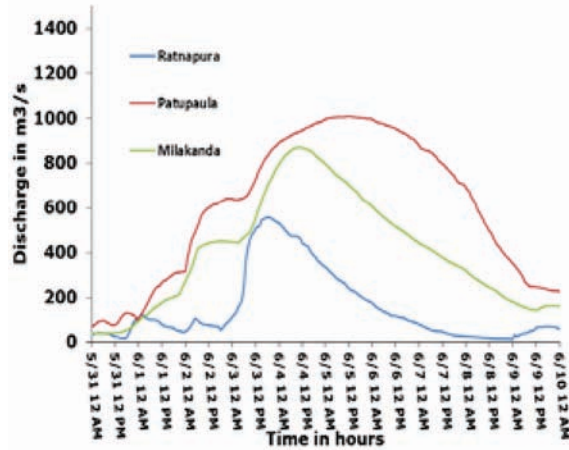


Figure 2 - Lead time comparison based on 1st June 2014 flood event

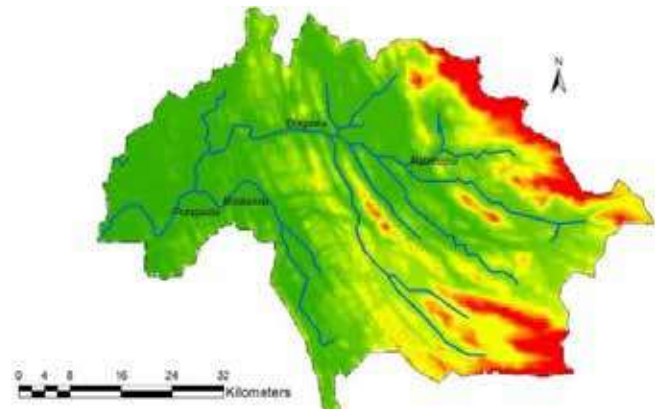


Figure 3 - Edited DEM (Changed river path)

$$q_y = \begin{cases} -k_a h \frac{\partial H}{\partial y}, & (h \leq d) \\ -\frac{1}{n} (h - d_a)^{5/3} \sqrt{\left| \frac{\partial H}{\partial y} \right|} \text{sgn} \left(\frac{\partial H}{\partial y} \right) - k_a h \frac{\partial H}{\partial y}, & (d_a < h) \end{cases} \quad \dots(3)$$

Where equation 1 is discretized mass balance equation and $q_x^{i,j}, q_y^{i,j}$ are discharges in x,y directions. Furthermore, h is height of water from local surface and H is the height of water from datum, r effective rainfall and f is the infiltration rate. Equation 2 and 3 were based on diffusive wave approximation of Saint Venant equation for flood wave propagation and k_a is the lateral saturated hydraulic conductivity and d_a is the soil depth times the effective porosity[4]. Using the RRI model, FFS was developed by following the methodology indicated in Figure 4. Initially 3 arcsec Digital Elevation Model (DEM) was tried and due to noise and computational power requirement 15 arcsec DEM was taken for model development.

DEM had to be edited (Figure 3) for river path and after sensitivity analysis actual river dimensions also incorporated into the model. Simulation was done from 1st,April,2014 to 31st,July,2014. Sensitivity analysis and calibration were done using the ground rainfall in this period and referred to as the flood period. River width and depth parameters showed high sensitivity. Finally it was decided to incorporate the actual river dimensions in order to overcome following problems.

1. Formulae (power formulae which represents the river dimensions) assumes that river is expanding as it reaches the sea, whereas actual river remains with fairly constant width in the upstream reach also.

2. Narrow point at Ellagawa cannot be presented in the formulae method.

After incorporation of actual river dimensions and adjustment of rainfall records, calibration was redone. In order to improve hourly data

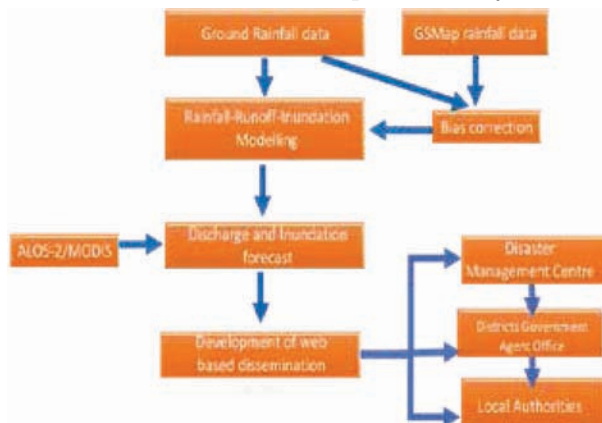


Figure 4 - Steps adopted in the study

resolution GSMaP was used. However GSMaP has some systematic errors and this had to be corrected. This is called bias Correction[5]. For

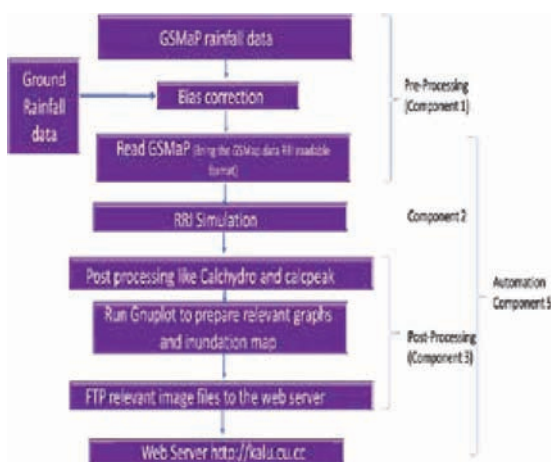


Figure 5 - Flood forecasting and Dissemination system

bias correction JAXA/NTT/ICHARM developed software was used. Normal procedure for dissemination of flood alerts, ID had to convey the initial message by fax and phone call to the DMC. Thereafter DMC had to pass the information to other agencies. However since web based dissemination system is available to other agencies also (like local authorities), they can directly access the information from the system.

3. FFS development details

Flood forecast and hazard information is so dynamic and might be updated each hour based on the rainfall data. Therefore this type of dynamic information might need dynamic information dissemination system. Hence web based forecast dissemination system might be the most suitable. Most important advantage of this system is interactive web based maps. Bias corrected GSMaP real-time data was used to run simulation of RRI as specified in methodology flow chart in Figure 5. In order to make discussion easier system was broken into 5 components. FFS has 5 main components (Figure 5).

Component 1: Pre-processing component of the system details

Since system needs hourly data and hourly rainfall data is sparse GSMaP data was used. First part of GSMaP processing starts with FORTRAN based executable. Based on the input files from GSMaP it rewrite the last hour and number of out files, in RRI control file (RRI_input.txt). Beside this it also modifies certain plot files which would be used as input files for Gnuplot in the rain subfolder in order discharge curves with starting time. Furthermore system would prepare GSMaP rainfall distribution for all 88 points with temporal details.

Component 3 :Post processing

Two important post processing functions were done by FORTRAN based executable. They are,

1. Producing predicted discharge and water level information
2. Automated warning information

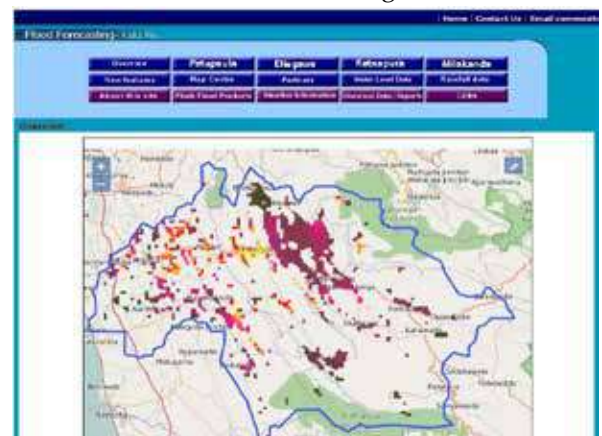


Figure 6 - Inundation map produced at runtime



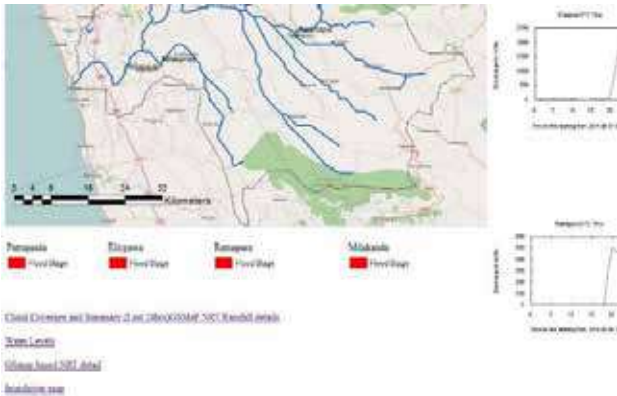


Figure 7 - Warnings issued by the system

based on the threshold values given in the location.txt

Gnuplot prepares the inundation map at runtime with script as shown in Figure 6. User can set two levels of threshold for each station. Hence based on these threshold values, system would raise warning messages in the web site as in Figure 7.

Component 4: Web technologies

Openlayers, JavaScript, HTML and KML were used. Inundation map is based on openlayers and gives the user ability to dynamic zoom and panning of the map. Demo is available on the internet site <http://kalu.cu.cc>. DOS based automation script was also developed. Therefore if the system is able to retrieve the DIAS data web site would be updated hourly automatically.

Component 5: Directory structure and automation

Directory structure of the system designed in fixed manner so that automated script can execute each processes and transfer the relevant files to other processes. Therefore it is a must to keep the sub folders name as it is.

4. Results

All these simulations were done for the

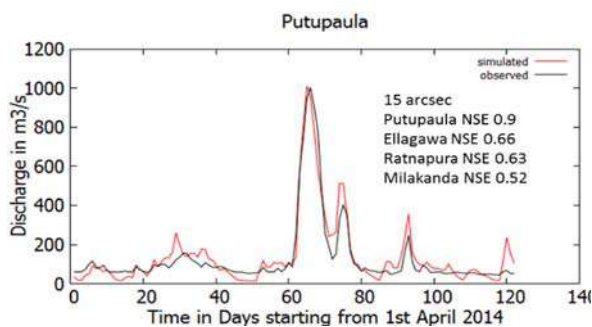


Figure 8 - RRI simulation on 15 arcsec DEM

period of April 1st to July 31st of 2014 using ground rainfall data from Irrigation Department. Initial calibration was not good. However after incorporation of actual river dimensions into RRI and a shift in the daily

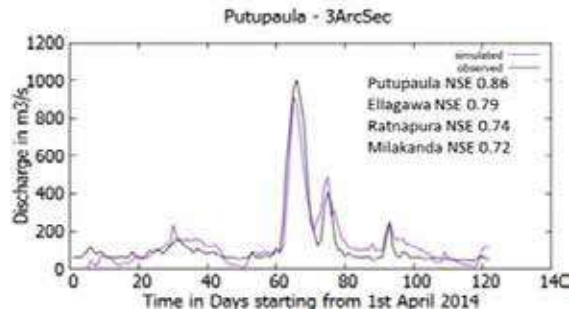


Figure 9 - RRI simulation on 3 arcsec DEM

data was corrected recalibration results were good Nash Sutcliffe Efficiency (NSE) 0.91 and Root Mean Square Error (RMSE) 56 m³/s at Putupaula. For validation 2013 data was used (NSE 0.67 and RMSE 72 m³/s). Similarly 3 arcsec DEM model also was developed and same calibration parameters were applied.

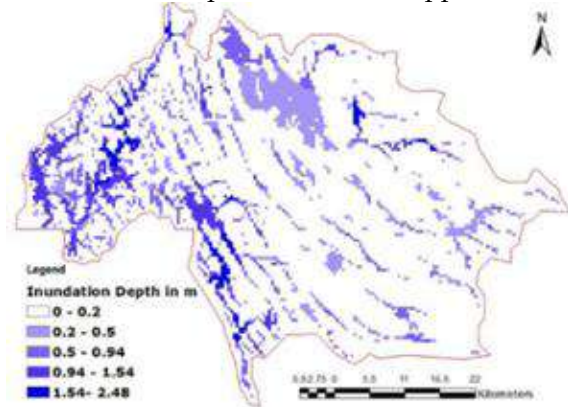


Figure 10 - Inundation Map produced from 15arcsec simulation for the flood period of 2014

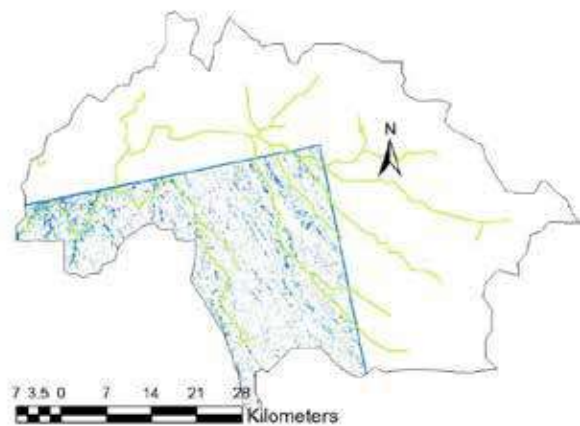


Figure 11 - Inundation area retrieved from ALOS 2008 June 3rd data set in blue colour

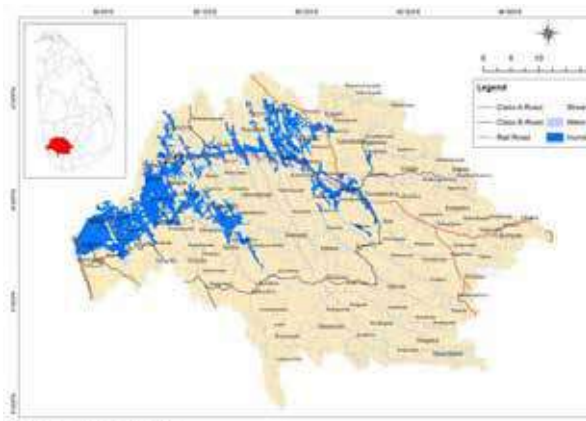


Figure 12 - DMC Sri Lanka report on hazards in 2012 inundation map (DMC, December 2012)

However, first model (15 arcsec- Figure 8) gave good performance mainly Putupaula and other station showed lesser NSE. Second model (3 arcsec -Figure 9) showed similar performance for all four station and showed better average NSE. In order validate the inundation MODIS, Landsat ALOS (Three satellite image sources) data were tried. MODIS and Landsat were covered with clouds and could not get proper inundation maps. However ALOS data for 2008 June 3rd flood event gave partial inundated area of Kalu River basin (Figure 11). However Disaster Management Center (DMC) published inundation Map (Figure 12) also been compared.

GSMaP bias correction

As the hourly data for bias correction is from automated gauges it is necessary to decide the minimum number of stations and location of the gauges to get the optimum bias correction. For this five groups combinations were tried. It was found that gauges located along the boundary gave better bias correction (Figure 13 and 14).

5. Discussion

Sensitivity analysis showed that river dimensions plays important role in model output. For flood inundation validation satellite data was used. Since Landsat and MODIS data during the flood period concerned were mostly covered with cloud, as a final resort 2008 June 3rd ALOS SAR image and DMC [3] published map was used for validation. During initial analysis of bias correction parameter's sensitivity analysis grouping does not work well for this basin. This may be due to the small catchment area. To determine minimum number of the stations required for optimum bias correction, 5 combinations (Figure 13 to 17) of 18 ground stations were used. Basins located around the

basin boundary yielded good result (Figure 18). Based on the basin area, minimum number could be decided. For development of the web based dissemination system, DOS based scripting was used, since DOS based computers are most common in irrigation department. Automation script would run as windows/DOS services for every hour and web site would be updated automatically on hourly interval.



Figure 13 - Group 1



Figure 14 - Group 2



Figure 15 - Group 3



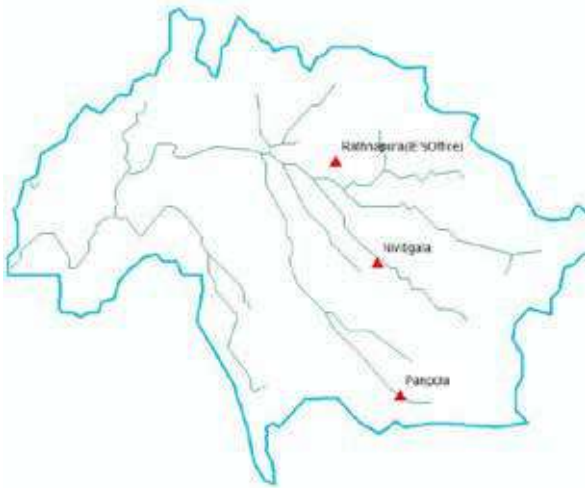


Figure 16 - Group 4



Figure 17 - Group 5

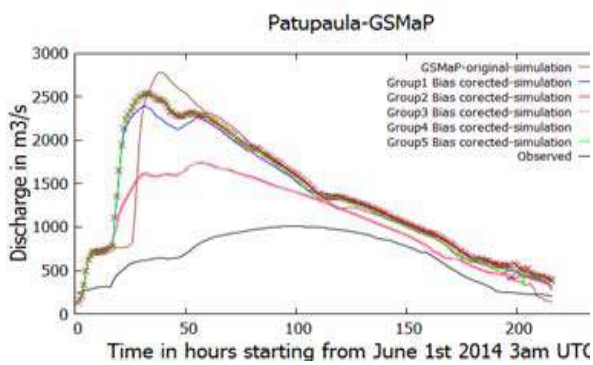


Figure 18 - Comparison 5 group combination

Furthermore, when considering the DEM, due to the noise in the 3 arcsec 15 arcsec was used in this study. 3 arcsec model could be used for forecasting if accurate DEM and enough computational power is available. Dissemination system could be further improved by incorporating SMS and email alerts. Development of simple web integrated RRI model as described in this paper, for flood prone basins might enable the stakeholders of the basin to do better flood management.

Acknowledgement

Author wishes to acknowledge my heartiest gratitude to the supervisors at ICHARM who gave me the guidelines that enabled me to complete this research work. Furthermore, he wishes thank to JICA, which made financial support and this opportunity to undertake this research. He takes this opportunity to thank ID for giving him duty leave for one year for this research.

References

1. ADPC (2016, July 22), Urban Flood Risk Mitigation in Kalutara City Case Study. (Asian Disaster Preparedness Centre) Retrieved July 22, 2016, from Asian Disaster Preparedness Centre: http://www.adpc.net/igo/category/ID222/doc/2013-qvl8PC-ADPC-Safer_Cities_23.pdf
2. ADRC. (March, 2009). Comprehensive study on disaster management in Sri Lanka. GOSL & JICA.
3. DMC. (December 2012). Hazard Profiles of Sri Lanka. Disaster Management Center of Sri Lanka. Colombo: GOSL.
4. Sayama, T. (2015). Rainfall-Runoff-Inundation Model ver. 1.4.2 user manual. Tsukuba, Japan; International Center for Water Hazard and Risk Management (ICHAHM) and Public Works Research Institute (PWRI).
5. JAXA (2014). GSMaP Customization Interface real time correction function Guide. JAXA.

A GIS Based Asset Management Approach to Upgrade the Level of Service to Pipe Borne Water Consumers in Western North Region

A.M.H.K. Abeykoon and B.U.J. Perera

Abstract: Geographic Information System (GIS) is a technology with a powerful set of tools that many organizations are using to get a better grasp on their data. GIS is capable of organizing complex water utility data into a clear visual representation that would allow water utility agencies such as National Water Supply and Drainage Board (NWSDB) to make efficient operational decisions to ensure a sustainable water supply. NWSDB implemented GIS and remote sensing based water utility management project in the Western-North region to address the entire lifecycle and operations of water infrastructure including, distribution and transmission pipeline mapping, design and asset management, leak survey management, customer database management, water hydraulics, outage management, operation & maintenance (O&M) management, field automation and operation intelligence. Using the satellite images, we have prepared the low scale base maps. On top of the base maps, all system components such as water mains, storage reservoirs, pump houses, pipelines, and valves were digitized. Simultaneously, consumer locations and leak locations were marked using GPS instruments. Water consumer related other attributes such as account number, address, contact details were stored in the database. Water leakages related attributes such as diameter, leak type, repair details were also stored there. Subsequently, organized data is utilized for O&M work by the Area Engineer & OIC offices via more interactive interfaces such as Google earth, Google Map etc. Further, we have started hydraulic modelling work. Hydraulic models are vital for the asset related decision making. This whole process is incessant that we need to keep on enhancing & updating the current knowledge base continuously with a trained O&M staff. Successful completion of this project will enable water utility managers to make quick and effective judgments on routine operations that had been extremely resource and time intensive during the past. Future focus areas include integrating information from sensors, meters with the GIS maps, sharing interactive maps in the boardroom and making functional maps available to field devices.

Keywords: GIS, Maps, Operations & Maintenance, Water Utility Management, Water Distribution

1. Introduction

Drinking water supply to the Cities North of Colombo Region is mainly divided into six water supply schemes namely; Biyagama, Mahara, Kelaniya, Welisara, Ragama and Ekala. The main reservoir is Church Hill, which is fed by Kelani Right Bank water treatment plant. The total region is fed by three main transmission pipelines coming down from the Church Hill reservoir and connected to several water towers and ground reservoirs which are located in high elevations. Main transmission systems and distribution system consist of more than 3000 km of DI, CI and PVC pipelines, of which the diameters ranging from 63mm to 1200mm. The system serves more than 175,000 domestic and commercial type consumers. Though the NWSDB maintains a massive quantity of assets such as pipelines, different types of valves, flow meters etc., a suitable asset management

system is yet to be implemented in order to utilize them in the most efficient manner to maintain a high level of service.

Water Asset Management (WAM) is meant to meet the required level of service, in the most cost effective manner. Geographical Information System (GIS) is one of the popular and worldwide accepted asset management set of tools that can be used to achieve a better grasp of spatially located asset data. GIS is capable of organizing complex water utility data into a clear visual representation that would allow water utilities such as National Water Supply and Drainage Board (NWSDB) to make efficient operational decisions to ensure a sustainable water supply. GIS and

Eng. A.M.H.K. Abeykoon, C.Eng., MIE(SL), B.Sc. Eng. (Moratuwa), MSc, Civil Engineer, National Water Supply & Drainage Board.

Eng. B.U.J. Perera, C.Eng., MIE(SL), B.Sc. Eng. (Moratuwa), M.Sc(Netherlands), Chief Engineer, National Water Supply & Drainage Board.



remote sensing based water utility management projects are implemented in the Western-North region to address the entire lifecycle and operations of water infrastructure, including distribution and transmission pipeline mapping, design and asset management, leak survey management, customer database management, water hydraulics, outage management, O&M management, field automation and operational intelligence.

2. Literature Review

Water Asset Management (WAM) has been identified as a responsible and proactive approach for water infrastructure management, efficient water utilisation and minimisation of waste. WAM enables delivery of institutional objectives in the optimal and sustainable manner at the least lifecycle cost. Further more in today's environment of ageing infrastructure, an ageing work force, increasing regulations, and transparency requirements of the communities served, achieving sustainable water and wastewater services require a geography-based platform. Asset management based on GIS transforms a water utility into a more informed, efficient, fiscally responsible, and transparent organization

GIS facilitates water utilities to create, organize, and share geographic information and tools within the organization on multiple devices at both office and field. It enables everyone in the water utility sector to access the information they need and provides means to collaborate with other employees regarding the location and status of assets, staff, and customers. ArcGIS is the most commonly used software for water asset management aspects. ArcGIS can be used in multiple devices from desktops, the web, smart phones, and tablets and may run on any platform (i.e. local network or hosted in clouds). It includes enterprise portal and geospatial content management platform that supports online mapping and geographic analysis. This approach allows institutions to easily and securely manage content, while sharing the information with the key stakeholders.

Functions of water utility are unique per location considered, such as distribution and collection networks, pressure zones, service areas, customers, facilities, and crew locations. Hence, need for geography based data

platform becomes pivotal to ensure sustainable water utility operations. Water utilities can reap following benefits by adopting GIS:

- Comprehensive and up to date asset information reduces time in the field spent locating assets; improves planning for maintenance, renewal, and growth.
- GIS enables network analysis for different functions such as system tracing and hydraulic modelling.
- Field GIS assists logistics through less work force, minimal travel time and costs, integrates work flows, and ensure real-time information flow.
- Web GIS provides a single view of utility that integrates information from multiple sources into intuitive as a map and dashboard. Web GIS applications can be integrated with many other systems used by the organization.
- Portal technology allows data accessible to everyone in the utility, allowing them to collaborate with contractors and other agencies. People across the department can discover, use, make, and share maps on any device, anywhere, anytime.

Water Loss Management

Age of the water system infrastructure is one of the main reasons for major breaks and chronic leaks. Using a properly updated GIS database, high leak prone areas due to the aging pipes could be spatially identified, thus supporting Spatial prioritization of these information to prioritize capital spending with objective evidence.

White House Utility District (WHUD) in the USA, adopted GIS to display water system asset information via interactive web maps. This information helped decision makers in prioritizing projects based on data-driven interpretations of the spatially enabled data. Consequently, WHUD achieved significant operational cost savings in the first year. Enterprise GIS enhanced asset management decision making that saved \$32 million for WHUD customers.

Moreover, undetected leaks cause major resource loss, which can be crucial in water restricted regions. GIS platform offers a suite of water-loss detection and response solutions. By using advanced technology to isolate and repair leaks, utilities avert costly acoustic surveys and step testing as well as the even

costlier consequences of long term undetected leaks. Through the ArcGIS based leak-detection solutions enabled WHUD to save \$37,000 per leak with total annual savings of up to \$219,000.

3 Methodology

Some of the Satellite images of Gampaha District were received from the UNDP, and the balance was downloaded from Google Earth. Those images were geo-referenced using ArcGIS to be used as the background images in the digitizing process. Road centre lines, road edges, railway lines, landmarks, buildings etc. were digitized subsequently and those were used as the base maps to produce the water utility maps. On top of the base maps, all water utilities such as water mains, storage reservoirs, pump houses, distribution pipelines, all kinds of valves were marked and relevant attributes of each type of asset were recorded (Figure 1). Main attributes collected and recorded were the pipe diameter, pipe material, type, constructed year, valve position(open/close), flow meter type etc. Some of those data were collected from the NWSDB mapping section. Data collected from UDA and the Survey Department were also used in succeeding this work, especially for the low scale base maps preparation work. Accuracy of the collected data was verified from the field sources. In certain locations, site

excavations were required to check the actual condition of pipes, valves and their connectivity with each other, especially in junctions.

Above data were centrally stored in a network server in the geodatabase format. After completing the databases of each scheme, it was handed over to O&M staff, and they were trained to update the subsequent system modifications. In addition, they were also trained to map the locations of leaks within the distribution system, and a data format was given to collect details of every leak except service leaks. We commenced marking consumer locations in a spatial database using GPS machines with the help of meter readers(Figure2). They were trained to carryout this work parallel to their routine duties. Building hydraulic models for the existing schemes were started from the Kelaniya Area by using Water GEMs software integrated with ArcGIS. Nodal elevations were extracted from Digital Elevation Models and digital contours obtained from the Survey Department. Consumer pack boundaries were marked in the model with the help of zone officers. Nodal demands were estimated using the relevant pack demands and assigned to the nodes by This sen Polygon method in WaterGEMs software. Peak demand factors were calculated by analysing logged flow data of critical points of the system for several days. Subsequently, the model was calibrated and

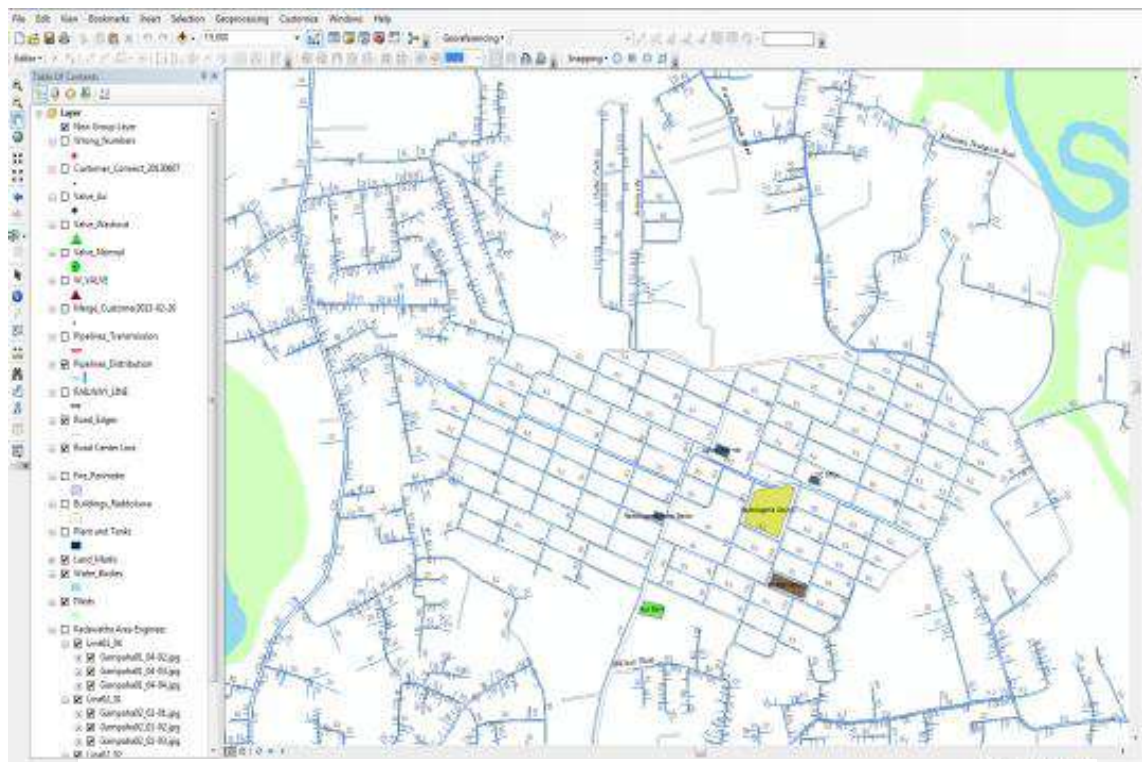


Figure 1 - Digitized Water Assets



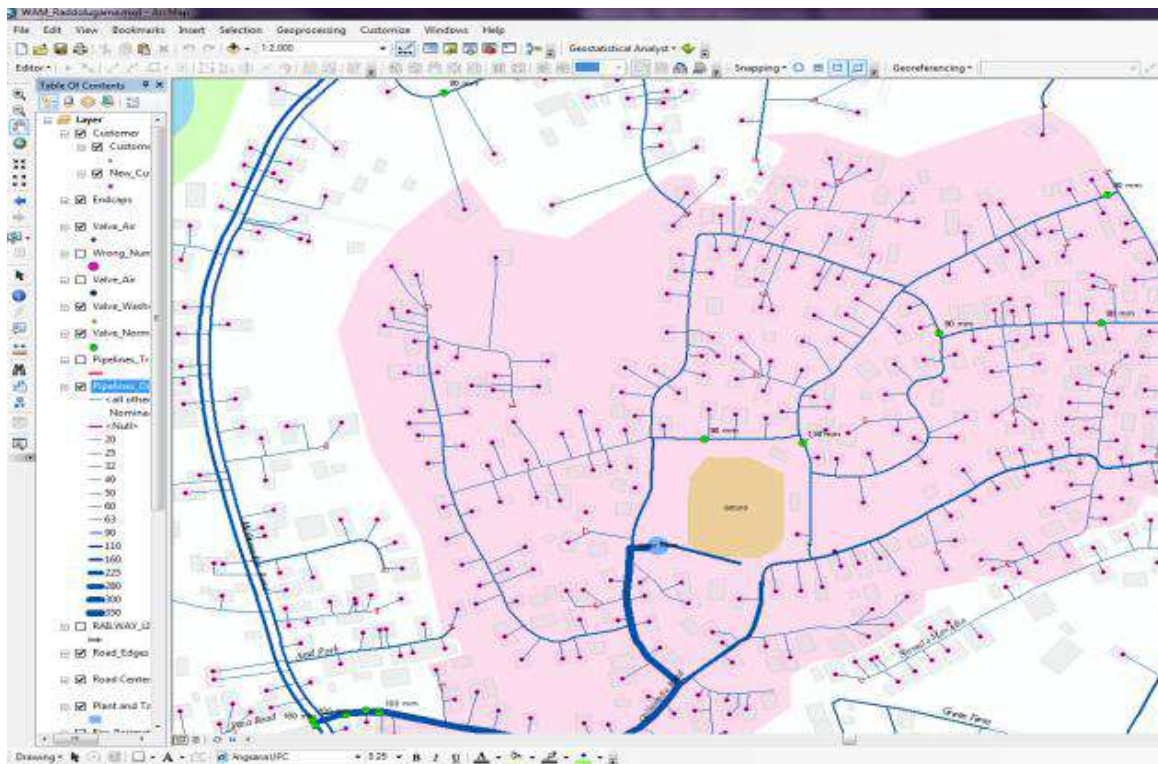


Figure 2 - Consumer Locations

verified using actual field data.

Water quality models were also developed using the relevant parameters to simulate the system water age and residual chlorine variation. Age analysis was performed for water in the system, assigning an initial age as 0 for all nodes. There is an infinite supply of source water (from the reservoir). The age of water elsewhere in the system at a point in time represents the time from the start of the run and when the water left the reservoir. The analysis will be conducted run for 14 days (336 hours), in order to determine the equilibrium point of the system. Water age vs time graph was used to monitor the time taken to stabilize the system age.

Once a repeating pattern is reached, it can be observed that the age of the water fluctuates between two fixed values (for a 24-hour period). After that, the water age of the system is supposed to be in equilibrium. Hence, the age value could be estimated at any given time period. The samples were collected in the morning from 9 am to 12.30 pm. Therefore, the average age within that period was taken for the analysis.

The constituent analysis was carried out to monitor the chlorine residuals in the system over time under present demand as well as

future demands. Following parameter values were used for the analysis.

Bulk Reaction Rate	-0.10(mg/L) ⁽¹⁻ⁿ⁾ /day
First Order Wall Reaction Rate	-0.08 m/day
Diffusivity	1.2e-9m ² /s
Initial chlorine concentration	0.2mg/l

Water quality model was calibrated with the actual RCI values measured at site.

4. Results and Discussion

Using the updated database, we are basically capable of answering any type of query on those assets and make recommendations on system rehabilitations or upgrading based on available data analysis. The O&M staff could make use of these data for their related activities such as pipe extensions, valve location identification in case of a leak, map preparation work etc. Through leakage mapping, vulnerable areas for pipe bursts could be identified, and remedial actions could be proposed. In addition, cost of leakage repairs and loss of water could also be calculated.

NRW management through the establishment of District Meter Areas (DMAs) is also another advantage that could be achieved by utilising these data which we have planned to start

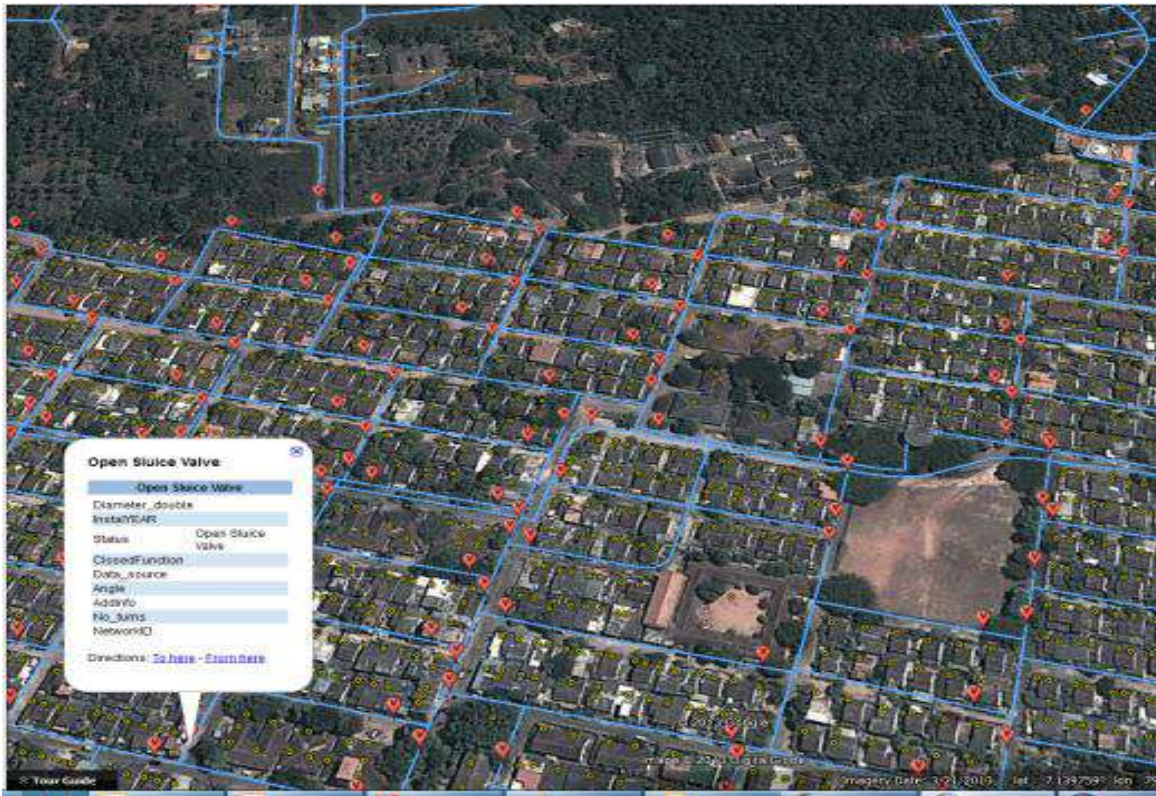


Figure 3 - Displaying Valves on Google Earth

soon. Consumer complaint mapping and water quality mapping are also another two activities we are planning to implement in the near future. Since all these assets could be viewed through Google Earth application, those data has become more interactive and user-friend(Figure 3). Further, we expect to develop a web based utility mapping system in order to benefit the mobile workers.

After completion of consumer location marking work, we can contribute more to the operational and design work, including supporting disconnection programs, identification of defective meter locations, spot estimations for new connections, identification of consumers affected by an interruption, valve detection in case of a leak, demand estimations for hydraulic models etc. Hydraulic behaviour of the system could be identified through hydraulic models and could propose remedial actions for any underperforming situations.

Further, it will replicate the system under various demand loading and operating conditions, thus facilitate the decision making processes. Hydraulic models and water quality models could be used to monitor water quality related parameters associated with RCI and water age. Through that, we are able to trace the areas where water stagnates or not having residual protection (Figure 4,5 & 6).

Conclusions

Water Asset Management is a timely need for the sustainable development of the water sector. The importance and the benefits should be convinced to the higher management of the organization in order to maintain a continuous progress and growth of this particular work. Key advantages are the optimized usage of assets, reduced wastage, water loss reduction, asset renewal planning and communication with customers and enhance the quality of service in respect of pressure, serving hours, consumer response time, accurate and timely billing etc. Further based on the risk and growth assessments renewal, rehabilitation, upgrade, and condition assessments could be justified through a properly implemented asset management process

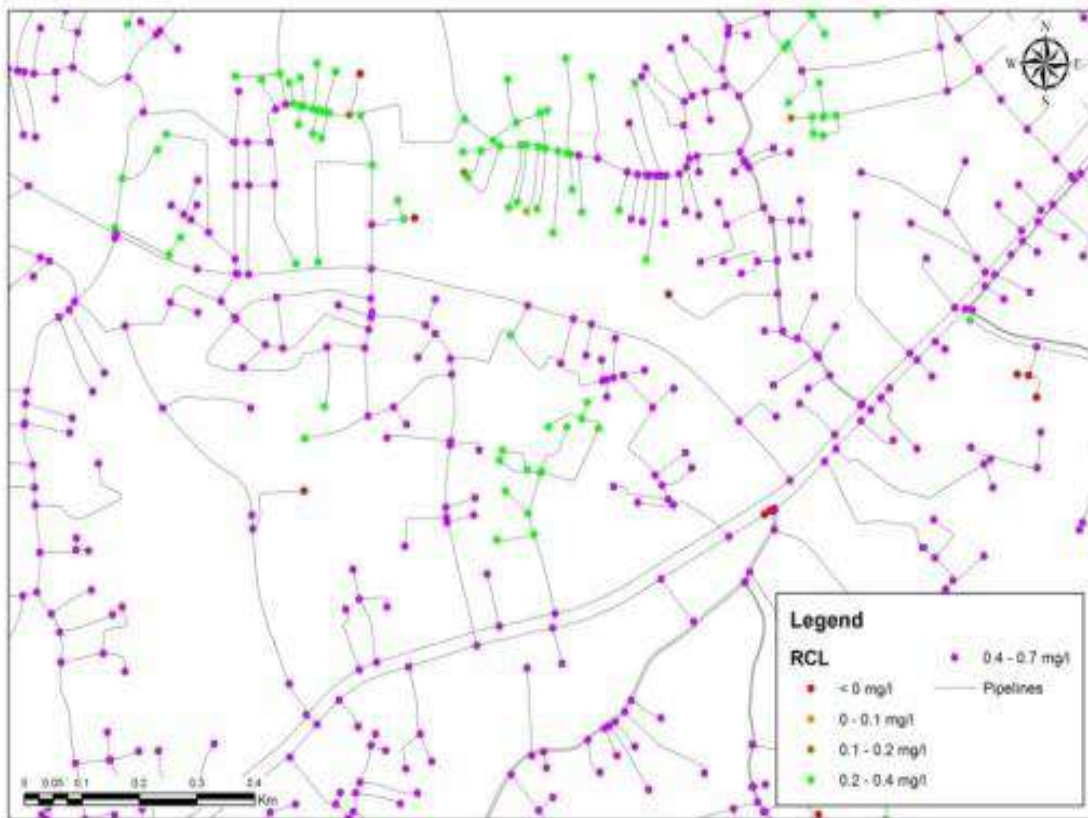


Figure 4 - Pressure Variation of the system at 10.00hrs

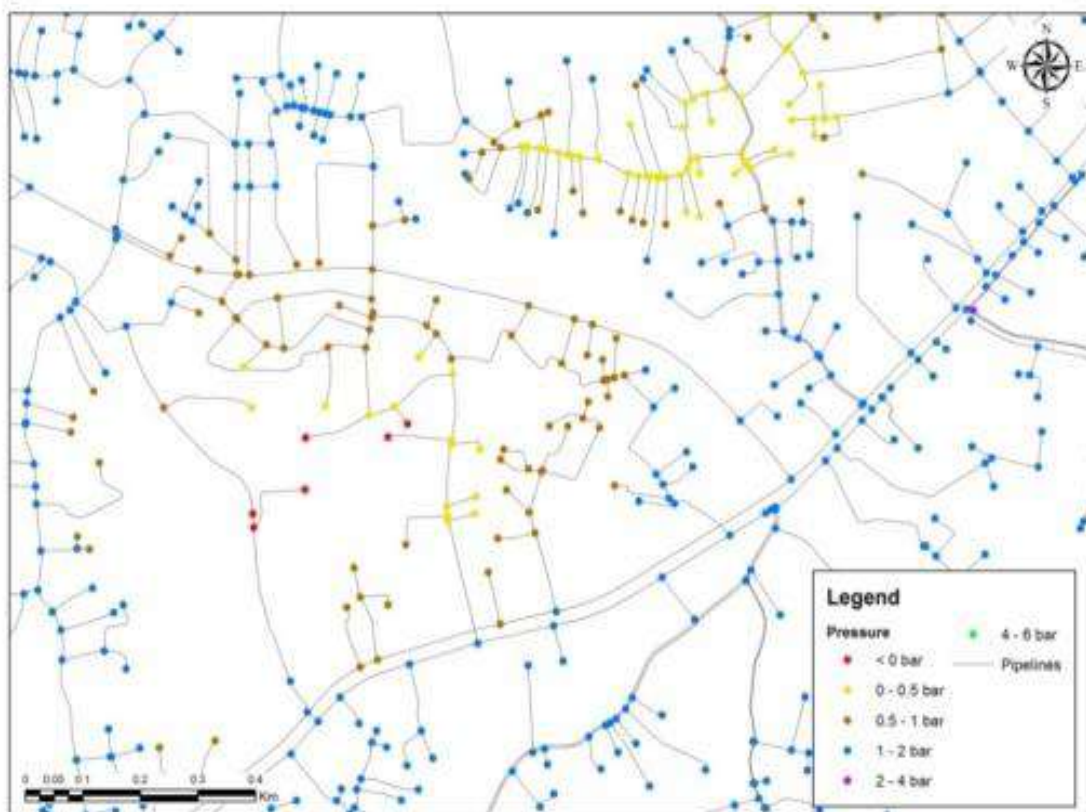


Figure 5 - Water Age Variation of the system at 10.00hrs

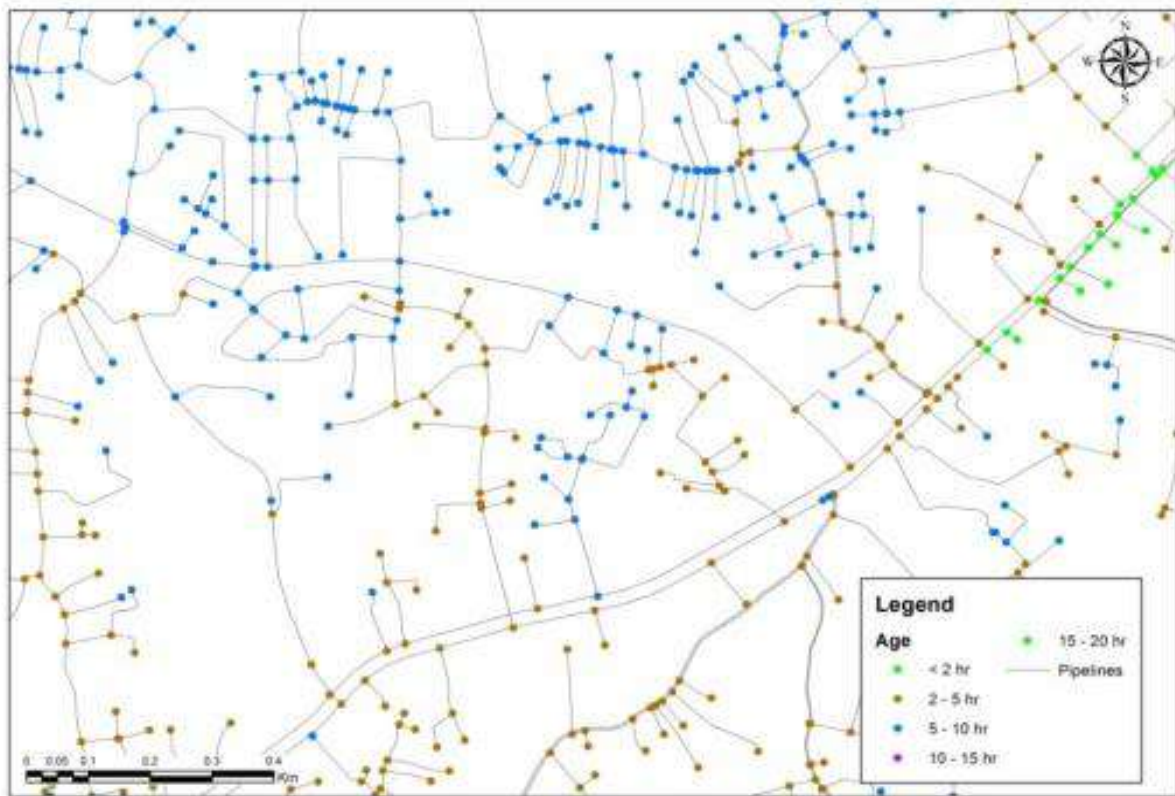


Figure 6 - RCI Variation of the system at 10.00hrs

References

1. Booth, R. and Rogers, R., 2001. Using GIS technology to manage infrastructure capital assets. Journal AWWA, 93(11), 62-68.
2. Ferreira, A. and Duarte, A., 2006. A GIS-based integrated infrastructure management system. FIG Portugal. Proceedings of the Institution of Civil Engineers. ISSN 0965-0903 159(2), 113-120
3. Garaci, M., Sutherland, J. and Mergelas, B.J., 2002. Role of GIS and data management systems for pipeline integrity. Paper presented at Pipeline Division Specialty Conference, Cleveland, OH.
4. Luettinger, J. and Clark, T., 2005. Geographic Information System-Based Pipeline Route selection Process. Journal of Water Resources Planning and Management, 131(3), 193-200.
5. City of Tampa, 2006. Tampa GIS strategic plan. Tampa, FL: City of Tampa.

City of Tampa, 2008a. City of Tampa detailed profile [online]. Available from: <http://www.city-data.com/city/TampaFlorida.html>, Visited 5th September 2009].

City of Tampa, 2008b. City of Tampa GIS strategic plan [online]. Available from: <http://www.tampagov.net>, Visited, 5th April 2008].

6. <http://www.esri.com/industries/water>
<http://www.esri.com/industries/water/water>

<http://solutions.arcgis.com/water/documentati>
[on/](http://solutions.arcgis.com/water/documentati), Visited , 05th May 2017



Application of 3D Physical Modelling for Verification and Optimization of Hydraulic Designs for Salinity Barriers in Sri Lanka

S.M.C.K. Subasinghe, K.P.S.T. Pathirana, N.L. Engiliyage and G.H.N. Rathnasiri

Abstract: Salinity Intrusion has become a major problem in several river basins of Sri Lanka which are immensely used for potable water supplying. At present, the feasibility of non-structural measures to get rid of this salinity intrusion problem is either impractical or economically non-viable for many of these river basins. Hence, all preventive measures involve the construction of a full or partial barrier to prevent the intrusion of saline wedge to main raw water intakes during low flow period. However, the design of salinity barriers need to be done with minimum or zero impact to the environment paying special attention to possible increase of flood levels, morphological changes to river stretch with siltation and bank erosion etc., during flood events. Basic hydraulic design of salinity barriers are carried out and checked by means of hydraulic models of both numerical and 3D physical models. First, the conceptual model is developed and impacts are assessed with numerical models. The physical model studies are carried out to verify or optimize the design parameters. The objectives of the 3D physical modeling are the investigation of river hydraulics in the vicinity of proposed salinity barrier location, estimation of head losses for different flows and suggest necessary improvements to the barrier layout, assessment of possible water level rises during construction stage, investigation of sediment regime in the river and investigation of impact of the barrier on sedimentation and erosion pattern of river bed and bank, and finally the determination of the type of erosion protective measure needed and its extent along the river reach. This paper discussed the capabilities of 3D physical models applied to engineering studies, mainly for the construction of salinity barriers for the purpose of locating water intakes. Further it elaborates the methodology on verification of numerical model results and optimization of the hydraulic design of salinity barrier by means of 3D Physical Model studies.

Keywords: Salinity Intrusion, Structural Solution, Flow Pattern, Siltation, Erosion, Fixed Bed Model Testing, Movable Bed Model Testing

1. Introduction

Salinity intrusion is the sea-water driving upstream of the river through the mouth by rising tides which resembles a form of a saline wedge. Usually the river flow is large enough to keep the salt water front at bay. But during very low flow periods due to drought or upstream water abstraction, salt water can travel upstream. The extent or the length of salinity intrusion depends on the density difference of fresh and seawater, fresh water flow rate, the depth of flow and the tidal range. A higher 'minimum flow' is required to counteract salinity intrusion into the river. Sand mining in rivers has a significant impact on saltwater intrusion due to deepening of the river bed. In certain river basins of Sri Lanka, salinity intrusion has become a major problem and restricts the water abstraction from the river causing difficulties in supplying potable water to public[2,3]. The frequency of occurrence of salinity intrusion has been increased to the

extent that some of the water intakes in rivers are used occasionally. Hence, either non-structural or structural measures are required to be implemented to get rid of this problem and provide safe drinking water.

Comprehensive studies have been carried out in recent past for water intakes that are badly

Eng.(Mrs.) S.M.C.K. Subasinghe, C.Eng., MIE(SL), B.Sc.Eng.(Peradeniya), M.Eng.(AIT), Engineering Manager, Lanka Hydraulic Institute Ltd, Katubedda, Moratuwa.

Eng.(Ms.) K.P.S.T. Pathirana, AMIE(SL), B.Sc.Eng. (Peradeniya), Research Engineer, Lanka Hydraulic Institute Ltd, Katubedda, Moratuwa.

Eng.(Ms.) N.L. Engiliyage, AMIE(SL), B.Sc.Eng. (Moratuwa), Research Engineer, Lanka Hydraulic Institute Ltd, Katubedda, Moratuwa, Sri Lanka.

Eng.G.H.N. Rathnasiri, AMIE(SL), B.Sc.Eng. (Moratuwa), NWS&DB, Water Supply and Sanitation Improvement Project, Badulla District Support Unit, Badulla.



affected by salinity intrusion problem using possible non-structural measures such as relocation of the intakes in further upstream, finding new alternative water sources etc [2].

However, for some of the water intakes located in the river basin like Nilwala etc, the feasibility of non-structural measures to get rid of this salinity intrusion problem is either impractical or economically non-viable under the current context. Therefore, as a solution, structural measures such as salinity barriers have been proposed to get rid of this salinity intrusion problem. In general, the salinity barrier type and location has to be decided with great care for stability of the structure while minimizing the cost of the structure, cost for mitigating the environmental impacts due to the introduction of the structure and minimizing the flood impacts too. When designing salinity barriers, more attention should be paid for estimating key design parameters and other factors such as, locating the gated salinity barrier with small or zero impact on flooding, navigation and the environment considering the 100 year (yr) sea level rise to prevent the salt water intrusion into water intakes. The conceptual design for salinity barriers are formulated to conform to the hydraulic design criteria established subsequent to the hydrologic and hydraulic studies. Design verifications prior to the construction are important as millions of rupees are generally spent on constructions and design failure would be a loss and create harmful impacts to the people.

3D physical models are generally proposed to verify the designs in addition to the application of 1D or 2D numerical models. Application of physical model would produce a physical system of required study area which is scaled down so that the major dominant forces acting on the system are represented in the model in correct proportion to the prototype. Hydraulic model studies with a 3D physical model to verify the design parameters and observations on flood levels, velocities, bank erosions etc., is more suitable as the appropriate equations governing the processes will be considered without simplifications as in numerical models. The results obtained from numerical modelling system are verified by means of physical model for the effectiveness of the design. Further, visual observation can be made during physical model testings and reproduction of complex boundary conditions can be done whereas non-linear effects, major difficulties are encountered during numerical modelling.

This paper describes the application of 3D physical model tests related to construction of salinity barriers across Nilwala and Kalu Rivers. The numerical model studies were done using the MIKE 11 software and results were compared and verified with the physical model studies.

2. Objectives of 3D Physical Model Studies for the Salinity Barriers across Rivers

- Investigation of river hydraulics in the vicinity of proposed salinity barrier locations.
- Investigation of head losses for different flows and suggest necessary improvements to the barrier layout.
- Assessment of possible water level rises during construction stage.
- Investigation of sediment regime in the river and investigation of impact of the barrier on sedimentation and erosion pattern of river bed and bank.
- Determine type, size and length of the upstream and downstream protection of the proposed barrier & effectiveness of bed protection.

3. Theory Related to Physical Modelling

The theory of physical model is related to the laws of similitude. There are three types of similarities; Geometric similarity, Dynamic similarity and Kinematic Similarity. For a proper physical model, all these three similarities need to be satisfied. For flows with a free-surface, inertia and gravity forces are usually dominant, and the Reynolds number effects can be neglected if the flow is turbulent. Consequently, the requirement for hydrodynamic similitude in a river system between the model and the prototype is the Froude similarity:

$$(Fr)_{\text{Model}} = (Fr)_{\text{Prototype}}$$

$$(V/\sqrt{gd})_m = (V/\sqrt{gd})_p$$

Where, d is the depth of water (m), g is the gravitational acceleration (ms^{-2}), V is the mean velocity (ms^{-1}) of flow and the subscripts m and p , denote the model and the prototype, respectively.

The similitude ratios are obtained using the above equations and the necessary model

parameters are calculated. The Reynolds numbers of the flow corresponding to each test condition is calculated to ensure that the flow is turbulent.

The main scale ratios used for model parameters are given in Table 1 where the selected geometrical scale ratio is 1: X.

Table 1 - Similitude ratios for main model parameters

Parameter	Scale (model: prototype)
Length	1: X
Area	1: X ²
Time and Velocity	1: \sqrt{X}
Discharge	1: X ^{5/2}

4. Main Steps of Physical Modelling Process

The main steps related to physical modelling are;

- i) Scaling of the model
- ii) Model approach
- iii) Model construction
- iv) Model calibration
- v) Model testing

4.1 Scaling of the model

A model can be either distorted or undistorted. Both Nilwala and Kalu river models were selected to be undistorted models because these studies required observing the sedimentation patterns with movable bed model. Factors taken into consideration when selecting scale ratios were;

- To minimize scale effects
- Convenience for the observation of flow patterns and discharge characteristics
- Available basin area
- Available pumping capacities

The appropriate model scales for Nilwala and Kalu rivers were 1:40 and 1:60, respectively. Further, these selected model scales ensured that comparatively large pooling area is available at upstream and downstream of the model area to get a smooth flow and a sufficient depth for scour in the bed.

The extent of the flood plain to be modelled and area to be bounded were calculated by considering the 100 year return period flood. Scale down of sediment sizes has been a typical problem in physical model studies as the modelled sediments would eventually fall into

cohesive sediment range whose behaviour would be completely different that of the real situation. Therefore, instead of scaling down the sediments according to the model ratio, the available sand with mean diameter of 0.12 mm was used for both these studies. As the sediment sizes are not scaled down according to the similitude ratio, the model results such as, erosion and deposition patterns were interpreted only in qualitative terms.

4.2 Model Approach

The model tests are usually conducted in two stages; for fixed bed and movable bed. From the fixed bed model, velocity and water level measurements and flow pattern investigations are obtained while the movable bed model is used to get erosion patterns along the river banks and river beds. The fixed bed model tests are carried out with and without the salinity barrier while the movable bed tests are carried out only with the salinity barrier. In order to check the river hydraulic changes during the construction of the barrier, tests are carried out for coffer dam phases. The purposes of each testings are given in Table 2.

Table 2 - Purpose of Model Testing under different Bed conditions

Condition	Purpose
Fixed Bed Without Barrier	Calibration of the model: Observation of flow patterns and velocity distributions under existing condition
Fixed Bed With Barrier (Gates in Open & Gates in Closed position)	Investigate head losses for different flows and suggest necessary improvements to the barrier layout Assessment of the water level rise during flood conditions and construction stage
Mobile Bed With Barrier (Gates in Open, Higher Flows)	Investigate impact of the barrier on sedimentation and erosion pattern of river bed and bank Effectiveness of bed protection

4.3 Model Construction

In order to represent the actual flow conditions in the model properly, the bed surface is



finished in a manner, which would have the same relative roughness as for the prototype condition during the fixed bed model tests. Adequate pooling areas are provided in upstream and downstream of the river (Figure 1).



Figure 1 - Fixed Bed Model with Proposed Salinity Barrier (for Nilwala River)

For movable bed models, only the required river stretch from upstream and downstream of the barrier are filled with appropriate sand. The length to be filled is decided according to the geometry of the river (Figure 2).



Figure 2 - Movable Bed Model with Proposed Salinity Barrier (for Nilwala River)

The water circulation system is planned in a way that it provides a smooth, continuous flow. The required model discharge (upstream inflow) was supplied by means of a regulating weir. A thin plate rectangular weir was used for higher discharges while V –Notch was applied for low discharges [01]. Downstream water levels were also controlled by a regulating weir.

4.4 Model Calibration and Testing

It is required to ensure that physical model represents the actual hydraulic behaviour of the study area without been affected by the scale effects etc. Model calibration is done for existing condition with fixed bed model. Both

water levels and flow velocities are checked with the generated water levels by numerical model studies. In case of any discrepancies incurred, the bed resistance of the river is changed accordingly with appropriate modifications such as applying paints to smooth the bed and make is coarser with the use of sand/silt for the model. Figure 3 and Figure 4 show the calibration check against water levels and velocities respectively.

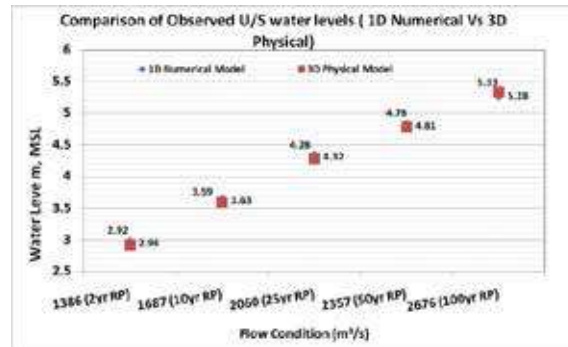


Figure 3 - Comparison of observed U/S water levels under existing condition

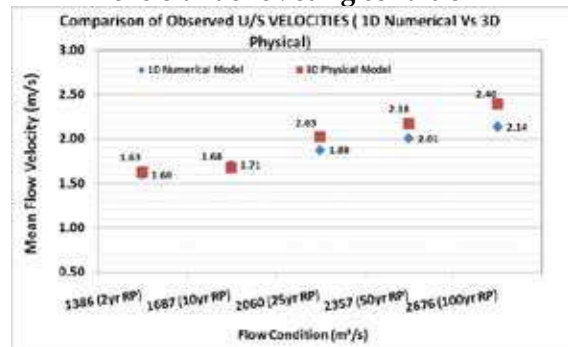


Figure 4 - Comparison of observed U/S velocities under existing condition

Table 3 - Flow Conditions for Model Tests

Flow Condition	Details
Fixed Bed Model	
Flood Flows	2 yr Return Period
	10 yr Return Period
	25 yr Return Period
	50 yr Return Period
	100yr Return Period
High Flows	5% Exceedance Flow of FDC
	10% exceedance Flow of FDC
Low and Average Flows	75 % exceedance Flow of FDC
	Required minimum Flow to flush the salinity wedge
Movable Bed Model	
Flood Flow	50yrReturn Period

Once the model is calibrated, testings are done for the selected flow conditions. The different flow conditions used for both Nilwala and Kalu river models are illustrated in Table 3.

High, low and average flows were defined based on the Flow Duration Curve (FDC) at salinity barrier site. Steady state flow conditions are generated in the model for the selected flow conditions. Once the flow becomes steady, the water levels were measured at the selected locations in the model area.

4.2.1 Observation of River Flow Pattern

Flow velocities were measured across some selected profiles of the river and the flow paths along the river were recorded by means of float tracking. Finally float tracking was carried out to check the streamline flow patterns. Figure 5 shows the observed flow pattern in Nilwala River without and with the proposed salinity barrier corresponding to 5yr return period flood [2]. Streamlines are obtained with float tracking (Figure 5).

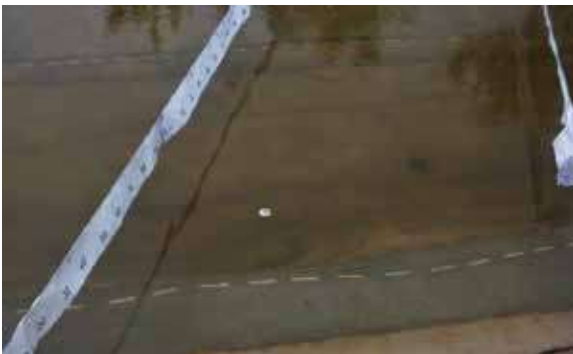


Figure 5 - Float Tracking

The orientation of salinity barrier is proposed in a ways that it does not obstruct the stream lines which were observed under existing condition. According to the Figure 6, it can be seen that the proposed orientation of the salinity barrier is perpendicular to the streamlines. Therefore, no changes had to be done for the location.

4.2.2. Verification of Estimated Flood Water Levels

During the model tests for the existing condition with the fixed bed model, the estimated flood levels from the numerical model studies were verified. Thereafter, tests are carried out with the presence of salinity barrier (Figure 7).



Figure 7 - Simulation of Flood Condition with gates opened position

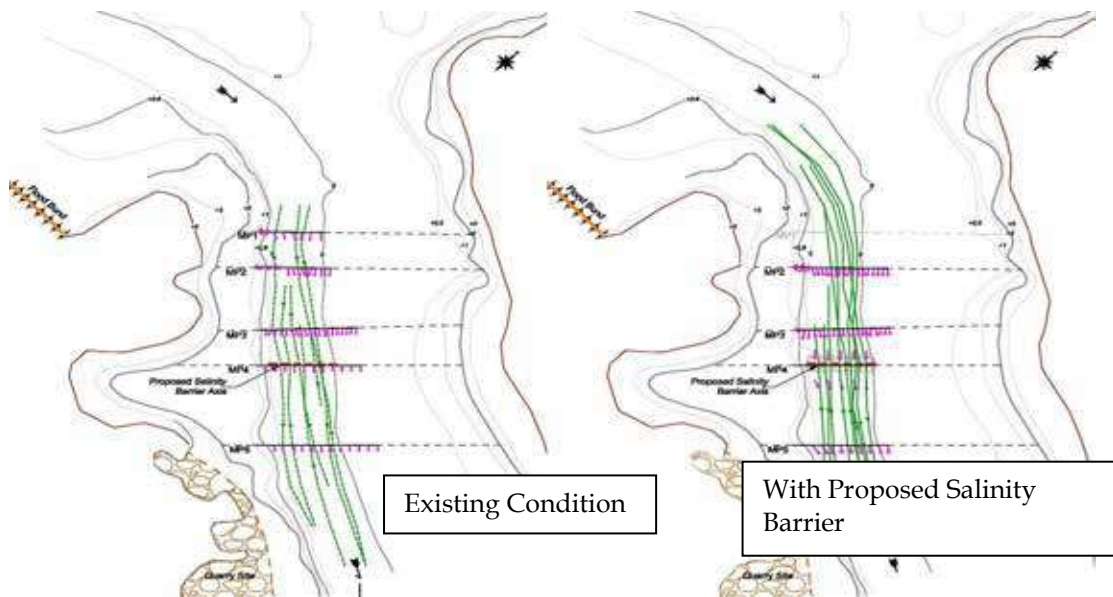


Figure 6 - Streamline pattern for 5yr RP Flow

Once the tests are completed for all scenarios, the results are compared with the numerical model results.

Table 4 - Comparison of Generated Extra Head up with Presence of Salinity Barrier for a Selected River

Flow Condition	Water Level Rise (m) at Upstream location of Observation	
	Numerical Model	3D Physical Model
(2yr RP)	0.09	0.11
(10yr RP)	0.07	0.06
(25yr RP)	0.07	0.06
(50yr RP)	0.07	0.07
(100yr RP)	0.08	0.09

Referring to Table 4, it can be observed that the water level rises due to the presence of the salinity barrier as simulated by the numerical model were validated with the 3D physical model results [03]. The difference of anticipated water level rises for different return periods are interrelated with the stage – area relationship of river cross sections at and in the vicinity of proposed salinity barrier location. Further, once the magnitude of flood is increased, considerable amount of water goes through a larger flood plain and there is a possibility that the sill of the structure will become to fully drowned condition.

Moreover, 3D model simulations facilitate to study the several other scenarios such as, when the gates are kept in partially or fully closed position during a flood scenario (refer Figure 08). With this kind of observations, the significance of having a proper gate operation rule is clearly understandable. In addition, 3D physical models also facilitate the observation of water level rises during the construction stage with coffer dam (Figure 8). This type of model tests would lead to recommend proper construction methodology with minimum impacts.



Figure 8 - Simulation of Flood Condition with partial gate opening condition



Figure 9 - Model Simulations to observe impacts during the construction stage construction

4.2.3. Identification of Vulnerable Areas for Deposition and Erosion

The objectives of the model runs with a movable bed are to investigate the scouring/ deposition patterns at upstream and downstream of the proposed salinity barrier structures and to decide on required lengths for river bank and bed protections. Refer Figure 9.



Figure 10 - Identification of Vulnerable areas for erosion and deposition

5. Conclusions

3D physical model studies facilitate the engineers to observe and understand the river flow patterns before and after construction of salinity barriers across rivers and confirm the hydraulic design of the structure with minimum impacts to the environment. Moreover, the visual observations and measurements of water levels and velocities also provide a guideline for operation of the salinity barriers-

This paper discussed the capabilities of 3D physical models applied to engineering studies, mainly for the construction of salinity barriers for the purpose of locating water intakes. In this regard, physical model studies already carried out for the proposed salinity barriers at Nilwala and Kalu Rivers were taken as examples. With the completion of both fixed and movable bed model tests, following conclusions could be made based on the test results.

- Appropriateness of the selected location; the selected location of the barrier is suitable since it does not change the flow pattern during both average and high river flows significantly. The optimization of the salinity barrier axis was done.
- The dimensions of the proposed structure and sill levels are satisfactory considering the observed water level rises.
- Observed water level rises in the physical model tests are in line with the numerical model observations.
- The shape of the piers, with arcs at upstream and downstream end caused smooth flow. Consequently, the hydraulic performance of the barrier is acceptable.
- The boulder sizes selected for upstream and downstream bed protections are adequate.
- Adequacy of the extents of chosen upstream and downstream river bed protection is verified.
- Estimation of maximum head over the gates during operational conditions i.e. in the closed condition.
- The lengths of upstream & downstream bank protections are assessed.
- Emergency plans are to be well executed to keep the gates open during flood conditions.

Acknowledgement

Authors would like to extend their gratitude for Lanka Hydraulic Institute Ltd for providing the resources needed to carry out this study and NWS&DB for the extended assistance.

References

1. Acker, P., White, W. R, Perkins, J. A., and Harrison, A. J. M., 'Weirs and Flumes for Flow Measurement' 1978.
2. Lanka Hydraulic Institute Ltd. (2016), Consultancy services for construction of Salinity barrier across Nilwala River.
3. Lanka Hydraulic Institute Ltd. (2017), Consultancy services for construction of Salinity barrier across Kalu River.



Numerical Model Investigations on Dispersion of Industrial Effluents in East Coast of Sri Lanka

S. Wickramaratne and K.P.S.T. Pathirana

Abstract: It is proposed to develop eastern Sri Lanka with an industrial zone in Eravur. This planned development requires a proper environmental assessment of the implications arising from discharging accrued industrial effluents to the sea. The discharge includes typical heavy metals generating from multitudinous of industries proposed. The effluent discharge, in addition, is heated, necessitating an investigation on its thermal effect to marine environment. Albeit the discharge is significantly 'neutralized' after being sent through a large treatment plant, one would still need to account for the worst case scenario where a total blackout of the plant occurs, allowing untreated discharge to gush out to the sea.

On this context, a numerical modelling study is formulated to observe probable dispersion patterns of two key physical entities: concentration of solid matters and the effluent temperature. The study aimed at spatially and temporally quantifying the dispersion of let discharge under a variety of tide, wind, and wave conditions typically anticipated in the east coast. Landfalls of thermal or effluent plumes were also monitored for their concentrations and the time durations at which the plumes are in contact with shore are recorded. A state of the art numerical modelling platform MIKE 21 is utilised for simulations and recommendations followed with the model derivations established therein. The entire study provides sufficient guidance for any future studies particularly been the first ever dispersion modelling completed for east coast of Sri Lanka.

Keywords: Dispersion of Effluents, Numerical Simulations, Eravur

1. Introduction

Adding to the number of industrial zones operating in Sri Lanka, the newest is proposed export processing zone at Eravur (Batticaloa) in the Eastern Province of Sri Lanka (Figure 1). The zone includes heavy industrial factories and plants which are expected to discharge a considerable amount of effluents. After passing through a treatment plant, this effluent discharge is significantly 'neutralized' which is then discharged out to the sea via sea outfall. The outfall is approximately 1km from shore.



Figure 1 - Location of the Project

The main issue that rises in an industrial zone is environmental implications occurring due to the discharge of harmful effluents. To address this, dispersions have to be modelled and necessary measures have to be taken depending on the level of concentrations present. As such, a bathymetric survey and a numerical modelling were carried out for simulation of effluent dispersion of the sea outfall related to the proposed export processing zone. A bathymetric survey of area 2 km X 2 km was conducted to gather all important depth information for subsequent planning, design, modelling and construction work of proposed sea outfall (Figure 1).

2. Hydrodynamic Study

2.1 Introduction

Hydrodynamic (HD) study is a priori for dispersion modelling for its distinct resolution of water currents and fluxes which govern the

Eng. (Dr) S. Wickramaratne, C.Eng., MIE(SL), B.Sc.Eng. (Moratuwa), Ph.D.(Calgary), Senior Engineering Manager, Lanka Hydraulic Institute (LHI), Katubedda.

Eng. (Ms)K.P.S.T. Pathirana, B.Sc.Eng. (Peradeniya), AMIE(SL), Research Engineer, Lanka Hydraulic Institute (LHI), Katubedda.

dispersion. In principle, hydrodynamic study is an investigation of the behaviour of water bodies subjected to a variety of natural force fields including tides, winds, and waves etc. This study launched an HD modelling for the prime purpose of,

1. determining water currents, levels that would attain in the study area under probable, selected offshore wave attacks.
2. monitoring variation of the current field based on hydrodynamic parameters, and
3. deriving hydrodynamic input data (fluxes and levels) for dispersion modelling studies.

2.2 MIKE 21 HD Module: Theoretical Formulation

For a given water body with known boundary information, currents and fluxes are resolved through two basic equations of conservation: continuity and momentum (Eq 1 and Eq 2). Required computational platform is created with state of the art computer simulation tool: MIKE 21 HD [1]. This modelling package provides hydrodynamic basis for computations performed in modules of dispersion, sediment processes and environmental hydraulics. Unsteady two dimensional flows in one layer fluids were simulated under the HD module. In particular, three main relationships:

2D continuity equation

$$\frac{\partial \zeta}{\partial t} + \frac{\partial p}{\partial x} + \frac{\partial q}{\partial y} = \frac{\partial d}{\partial t} \quad \dots(1)$$

2D momentum equation in y direction

$$\frac{\partial q}{\partial t} + \frac{\partial}{\partial y} \left(\frac{q^2}{h} \right) + \frac{\partial}{\partial x} \left(\frac{pq}{h} \right) + gh \frac{\partial \zeta}{\partial y} + \frac{gq\sqrt{p^2+q^2}}{C^2 h^2} - \frac{1}{\rho_w} \left[\frac{\partial}{\partial y} (h\tau_{yy}) + \frac{\partial}{\partial x} (h\tau_{xy}) \right] + \Omega_p - fVV_y + \frac{h}{\rho_w} \frac{\partial}{\partial xy} (\rho_a) = 0 \quad \dots(2)$$

2D momentum equation in x direction

$$\frac{\partial p}{\partial t} + \frac{\partial}{\partial x} \left(\frac{p^2}{h} \right) + \frac{\partial}{\partial y} \left(\frac{pq}{h} \right) + gh \frac{\partial \zeta}{\partial x} + \frac{gp\sqrt{p^2+q^2}}{C^2 h^2} - \frac{1}{\rho_w} \left[\frac{\partial}{\partial x} (h\tau_{xx}) + \frac{\partial}{\partial y} (h\tau_{xy}) \right] + \Omega_q - fVV_x + \frac{h}{\rho_w} \frac{\partial}{\partial x} (\rho_a) = 0 \quad \dots(3)$$

where

- h(x, y, t) water depth (= ζ -d, m)
 ζ (x, y, t) surface elevation (m)
d(x, y, t) time varying water depth (m)
p, q(x, y, t) flux densities in x- and y directions

($m^3/s/m$) = (uh,vh); (u,v) = depth averaged velocities in x- and y-directions

C(x, y)	Chezy resistance ($m^{1/2}/s$)
G	acceleration due to gravity (m/s^2)
f(V)	wind friction factor
V, V _x , V _y (x, y, t)	wind speed and components in x- and y directions (m/s)
Ω (x, y)	Coriolis parameter, latitude dependent (s^{-1})
p _a (x, y, t)	atmospheric pressure ($kg/m/s^2$)
ρ_w	density of water (kg/m^3)
x, y	space coordinates (m)
t	time (s)
$\tau_{xx}, \tau_{xy}, \tau_{yy}$	components of effective shear stress

were resolved through the numerical process[1].

2.3 MIKE 21 HD: Model Setup

The approach used in formulating the HD module is nested grid approach starting from a larger "Regional model", gradually reducing to a smaller "Intermediate model" and finally to a much smaller "Local model" (Figure 2). Objective of sticking to the grid approach is to use known tidal constituents to generate distinctive tides in the boundaries to drive the Regional HD model, and to arrive at more accurate and finer grid resolutions towards the area of interest (Local Model). The regional model was set up to be with a resolution of 500m x 500m covering an area of 425km x 260km. Stepping down from the Regional model is to an intermediate model with a grid resolution of 100m x 100m for an area of 105 km x 100 km. With a high grid resolution of 10m x 10m, the local model was set up which had a study area of 14km x 10km.

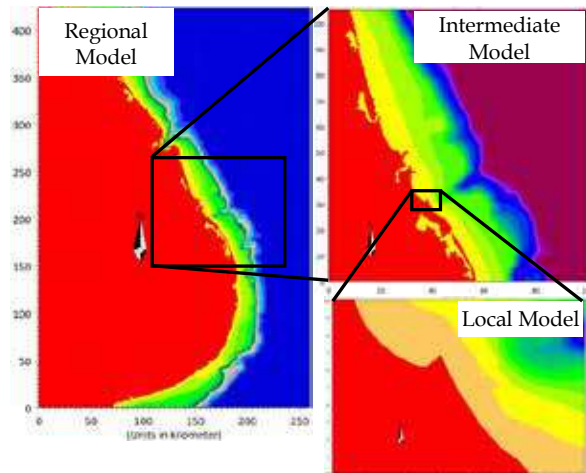


Figure 2 - Nested Grid

2.4 Model Calibration

The regional model was calibrated using constituent-generated tide at Trincomalee. The model predicted water levels were compared with that of Admiralty predicted (constituent-generated) and the best match is obtained via varying Manning's coefficient of the model. Hence calibrated model is utilized for furtherance of HD study.

2.5 Model Simulation

Regional model was purely tide driven, and evaluated overall hydrodynamic characteristics of the region while the intermediate model was tide and wind driven for an accurate model formation. The regional and the intermediate models were simulated for a period of 15 days inclusive of 3hr warm up period. Model scenarios simulated were Southwest monsoon, Northeast monsoon and inter-monsoon. Necessary boundary conditions for the intermediate model were extracted from HD results of the regional model simulations.

Local HD model was simulated for 7 combinations of wind speeds/ directions and spring/neap periods. Selection of wind speed and direction was based on locally measured wind by the Department of Meteorology (SL) and offshore wind provided by Wavewatch III model.

Although the Regional model did not consider wave effect in its hydrodynamics, local model being focused on nearshore was fed with appropriate wave information. In this context, radiation stresses resulting from a series of MIKE 21 PMS simulations provided required wave information to MIKE 21 HD models. Table 1 presents the selected combinations

used for Local Model simulation. Wave and wind have been chosen that they represent average (50%) and extreme (2%) exceedance scenarios.

Table 1 - HD Local Model Scenarios

Scenario Number	Tide	Wave Parameters			Wind (Speed, m/s / Dir, Deg)	
		Wave Condition	Hs (m)	Tp (s)		
1	Spring	NE-Sea	0.90	6.1	63	8/45°
2	Neap	NE-Sea	0.90	6.1	63	8/45°
3	Spring	NE Swell	0.30	10.4	125	8/45°
4	Spring	SW-Sea	0.32	5.8	152	6.5/135°
5	Neap	SW-Sea	0.32	5.8	152	6.5/135°
6	Spring	SW-Swell	0.55	9.9	150	6.5/135°
7	Spring	IM-Swell	0.61	10.2	167	9/67.5°

In all simulations, wind was assumed to be constant in time and space, and applied to the entire model domain. Further, a 3 hour warm up period was allowed for smooth and gradual model computations.

2.6 Hydrodynamic Model Results

The major aim of the water circulation study was to obtain water level and current information to investigate whether any of those parameters attain unacceptably high/low values at any instance in the HD simulation, except probably during the warm up period. Hence, in the model time domain, the instance where maximum currents occur in the generic study area was plotted for each model scenario (Figure 4).

An in depth assessment of current values in each scenario indicates that currents present in the swash zone depict a significant level of irregularities and perturbations due to the local wave breaking. However, the maximum water current in any modelled wave, wind, and tide scenario does not exceed 0.5m/s.

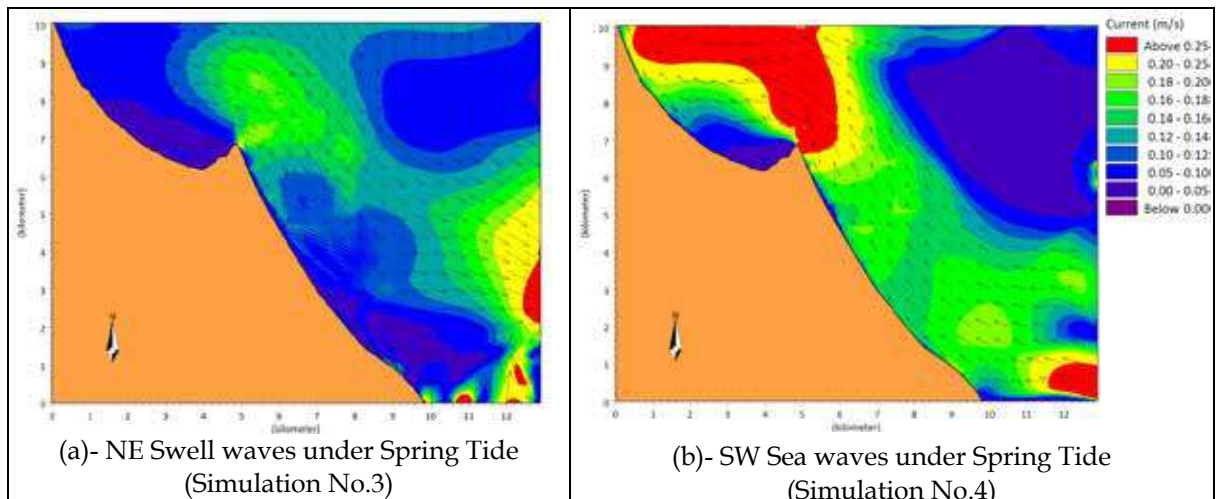


Figure 3 - Maximum Water Currents Attained in the Study Area

3. Effluent Dispersion Study

3.1 Introduction and Theoretic Formation

In general, heat exchange is calculated on basis of the four physical processes.

- i. sensible heat flux (or the heat flux due to Convection)
- ii. latent heat flux (or the heat loss due to Vaporization)
- iii. net Short Wave Radiation
- iv. net Long Wave Radiation

The heat dissipation follows a prescribed function, where the decay factor F may take the form:

$$F = 0.2388 / (r C_p H)(4.6-0.09(T_{ref} + T)+4.06W) \exp(0.033(T_{ref} + T)) \quad \dots(4)$$

T_{ref} is the reference temperature in degrees Celsius (same units as T), r is the density of water, C_p is the specific heat and H is the water depth [2]. W may be given constant or varying in time, following a prescribed function. In units consistent with former ones, r C_p is given the value 106 (Cal/m³ °C) [2].

Conservative matters disperse as,

$$\frac{dc}{dt} = -Fc \quad \text{or} \quad c = c_0 e^{-F(t-t_0)} \quad \dots(5)$$

where c is the concentration and t is the time.

The T_{90} value (the time it takes to reduce matter by 90%), is used to calculate c from,

$$c = c_0 10^{-\frac{t}{T_{90}}} \quad \dots(6)$$

Advection-Dispersion module (MIKE 21 AD) in the MIKE 21 Flow Model provides the basis for computation. The AD model solves two-dimensional, depth-integrated transport equation of the advection (dilution)-dispersion type for heated effluents. The hydrodynamic flow field of the study area is a pre-requisite for this dispersion modelling. Under the dispersion modelling, the dispersion characteristics of effluents, their extension of dispersion and probability of a landfall were checked. Given the very low discharge rate (625m³/hr) anticipated at the outfall, near field dispersion is conservatively excluded in the modelling, paving way for more emphasis on critical far field dispersion.

Modelling of effluent dispersion is not novel and the literature is rich with numerous examples of international case studies [3,4,5,6].

Yet, only a handful of dispersion models have ever been set for Sri Lankan perspective [7,8,9]. Given the distinctive two monsoonal cycle and related wind patterns prevailing in Sri Lanka, a high emphasis has been placed to compare and correlate dispersion characteristics observed in Sampur thermal power project which geographically is the closest available study for Eravur [8].

3.2 Technical details of the Model

Contents of the discharged effluents can be categorized into two main parts.

1. Conservative matter (i.e. typical solid matters present in the discharge measured in mg/l)
2. Heat dissipation

Government of Sri Lanka (GOSL) has published maximum allowable concentrations that can be safely discharged to the sea as wells as maximum allowable intake concentrations of a treatment plant [10]. Since no predicted discharge concentrations of the proposed outfall are available, the worst case scenario: a total blackout of the treatment plant forcing the maximum allowable intake concentrations to be directly discharged to the sea was modelled. In other terms, maximum allowable intake concentrations by the treatment plant have been taken as input concentrations for the dispersion modelling, and resulting maximum dispersed concentrations at sea were checked with maximum allowable marine concentrations adopted [10].

Since there are no individual dispersion differences among the different Conservative Matters, the highest individual concentration of 2100 mg/l at the intake (as published by GOSL) was selected as the representative strength of Conservative Matter. The ratio of observed dispersed concentration versus the intake concentration (2100 mg/l) is then used to scale up and derive the level of dispersion of all individual conservative matters. In terms of temperature, the maximum allowable intake temperature, 40°C was assumed at the discharging point.

Background pollution is not considered in this study as the area concerned does not have any major polluting sources.

3.3 Model Simulation

The seven scenarios used in the Local HD model were simulated in parallel with the AD

model. Model simulations were continued until steady state dispersion was obtained. Observed time duration for this was 2-3 days for most cases. The simulation period included 3hr warm up time during which specified model parameters attained their full values gradually.

3.4 Dispersion of Effluents

3.4.1 Spatial Assessment

Results depicted that the dispersion starts as a speck of the plume which then grows in size over the time. While the outer perimeter grows, conservative concentration or the temperature rise reduces inside the plume, weakening the propagation and eventually letting the plume collapse back to a smaller size. It was also observed that patches of high accumulation of conservative matter are present within the plume span creating multiple foci temporary. After several cycles, a steady state variation, i.e. identical cycles in expansion and retraction of plume is attained.

Maximum plume size in each of the model scenario was plotted in a bid to quantify the worst effect to the neighbourhood during the respective model scenario considered. Further, maximum length spans in which the plume is in contact with the beach (max. landfall lengths) have been measured (Figures 5 and 6).

Following up with similar studies, given the differences exist over the discharge rate of cooling water in proposed Sampur thermal power plant (100,000m³/hr) versus the effluent discharger rate of Eravur treatment plant (625m³/hr), comparison of thermal plumes is plausible only for its dispersion pattern and not the strength. It is rightfully observed that thermal plumes of both studies behave exactly in accordance with the monsoonal wind and wave patterns modelled [8]. Albeit the existence of obstructions for natural dispersion in Colombo Port area, Mutwal dispersion studies completed in 2004 also record similar elongated thermal plume pattern[11,12,13].

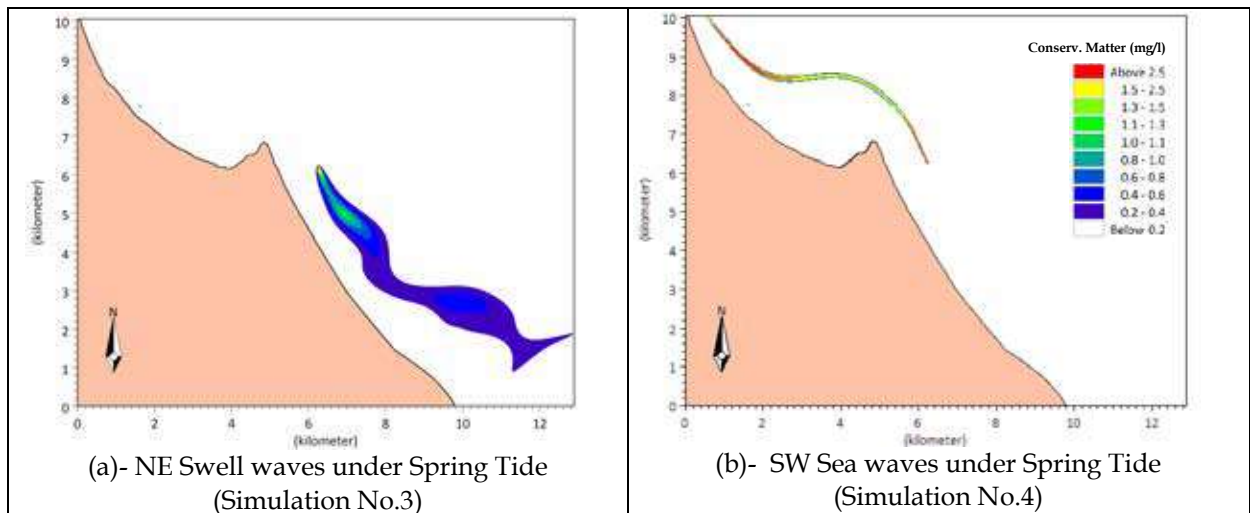


Figure 4 - Maximum Thermal Plumes

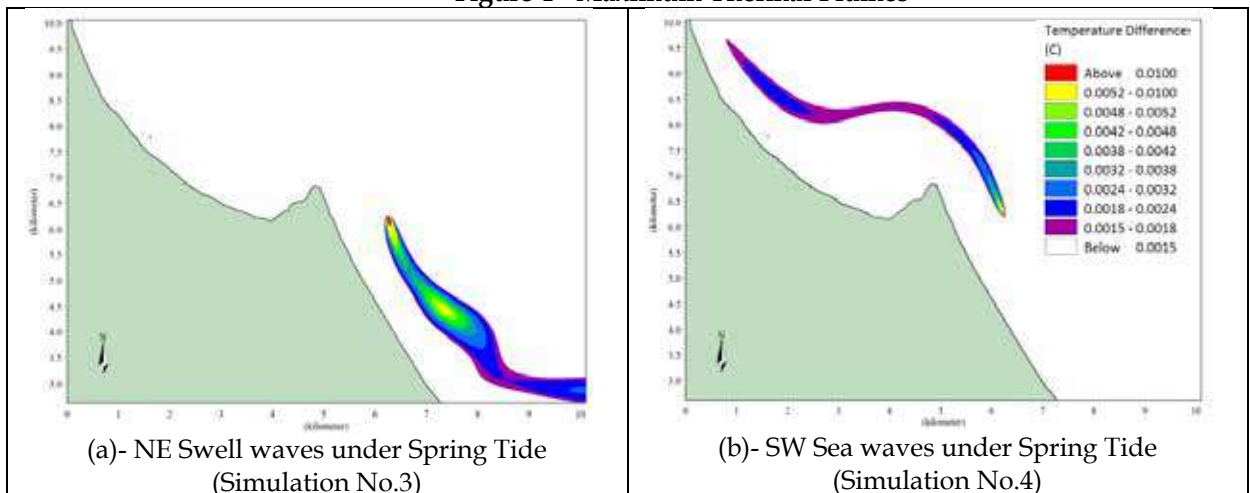


Figure 5 - Maximum Effluent Plumes



3.4.2. Temporal Assessment

In order to gain an understanding of the variation of seawater temperature over the time due to proposed discharge, three representative locations (Figure 7); one offshore of the outfall point, one at south and the other at north of Punnaikudah were considered.

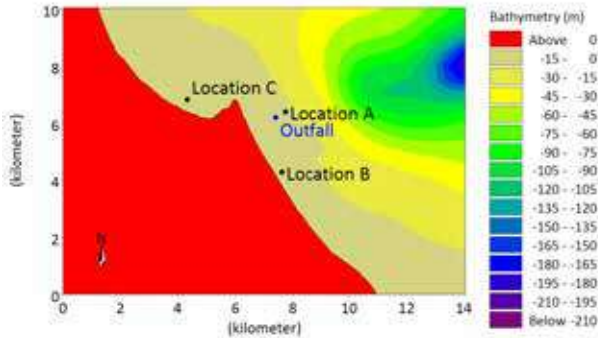
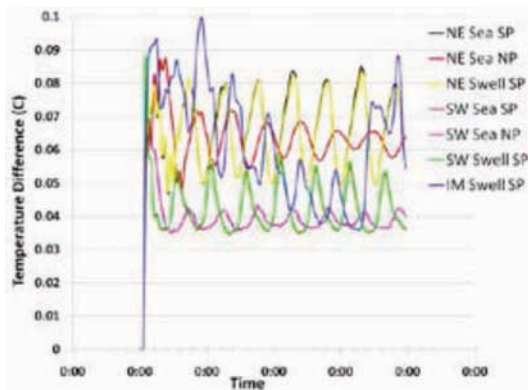
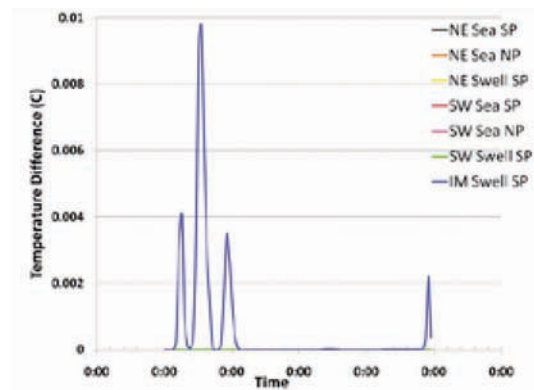


Figure 6 - Representative Locations for Thermal Dispersion Study

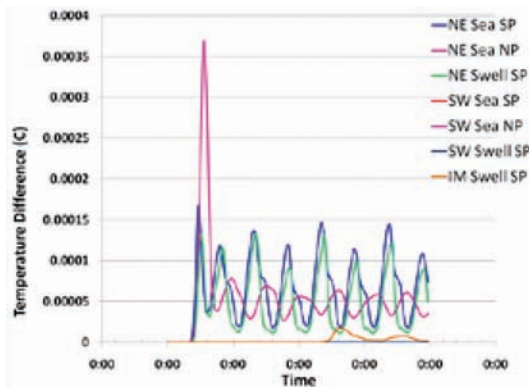
Extracted data related to temperature rise of the sea water and the variation of the conservative matter at the three locations and at outfall were plotted (Figures 8-9). In both temperature and conservative matter scenarios a very desirable dispersion cycle of approx. 12 hrs was achieved for all model scenarios except in the inter-monsoonal condition where the cycle time has increased to 3.0-3.5 days. No accumulation of heated discharge or conservative matter was present. For locations north and south of Punnaikudah, the only effect is from inter-monsoon condition, which too does not record a higher value. Due to low discharge rate of the outfall, the effluent concentrations are too weak to inflict any harm to the marine environment.



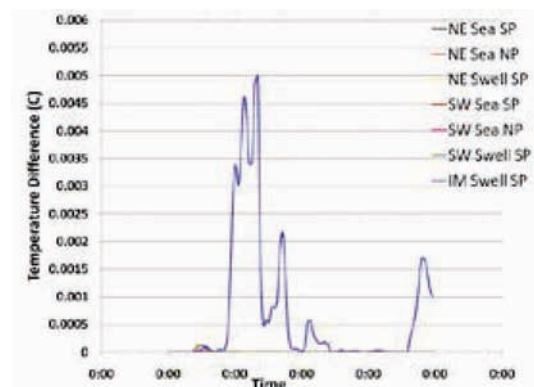
(a)- Temperature Rise at Outfall



(b)- Temperature Rise at Location A

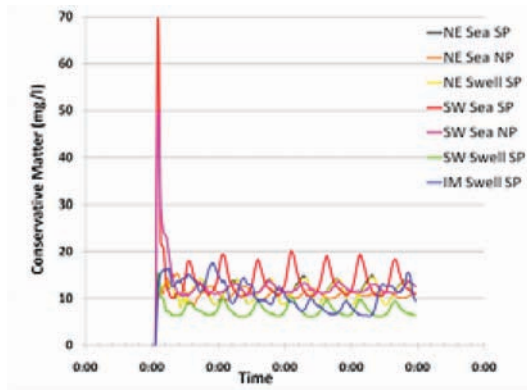


(c)- Temperature Rise at Location B

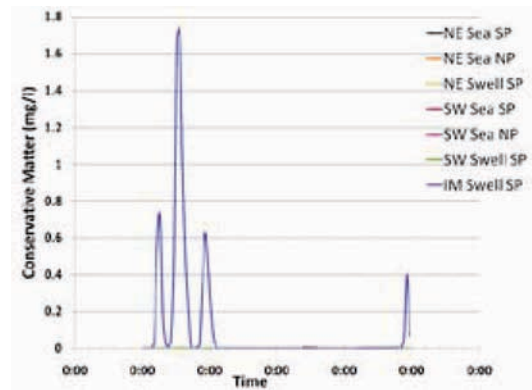


(d)- Temperature Rise at Location C

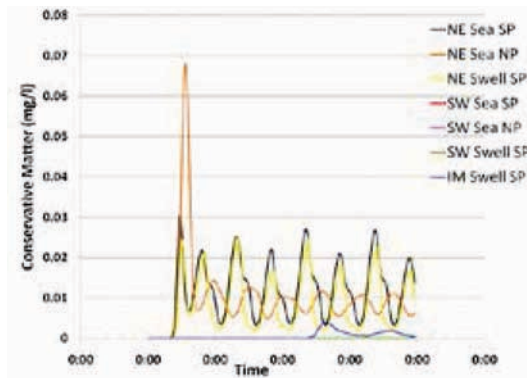
Figure 7 - Temporal Variation of Temperature



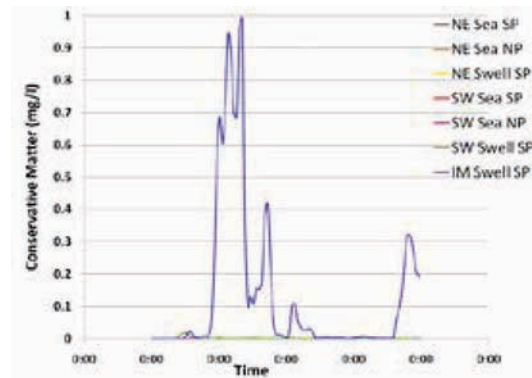
(e)- Conservative Matter at Outfall



(f)- Conservative Matter at Location A



(g)- Conservative Matter at Location B



(h)- Conservative Matter at Location C

Figure 8 - Temporal Variation of Conservative Matters

Although a landfall of the plume was evident in the inter monsoon waves coupled with north westerly wind (simulation no.7), the average temperature that would be felt is only 0.003°C higher than the ambient sea temperature. In general, low outfall discharge rate coupled with high winds and strong monsoonal waves assist the quick dispersion. Events in which wind and wave directions are distinctively apart as is the case in simulation no.7, cause slow dispersion recording relatively larger plumes.

4. Conclusions

In this study, no accumulation of either heated discharge or effluents was observed, as such discharged materials/heat were effectively dispersed within a maximum cycle time of 3.0-3.5 days. In addition, no heated discharge ever reached nearshore areas except for inter-monsoon conditions where a landfall is expected at north Punnaikudah with a maximum temperature rise in the sea water of 0.003°C. In practical terms, this level of temperature rise is hardly detectable and its effect to the environment is negligible. Further the dispersion levels of Conservative Matters have been excellent with no effluents making a

landfall during any of the major monsoon periods. Inter-monsoon period however creates a platform for effluent landfall along northern Punnaikudah beach for a length of approximately 6km. Nonetheless, dispersed concentrations of all effluents have been very low and less than 1 mg/l. Simulated concentrations have been well within the stipulated maxima by CEA and thus, no threat exists over contamination of coastal neighbourhood of Punnaikudah from effluents of proposed outfall discharge.

Computer simulations of effluent dispersion carry distinct advantages. The textbook benefits include being able to predict the final residue concentrations of harmful effluents that may be present in the marine environment. In this instance, the modelling results further indicate that the need of a treatment plant is not mandatory as the model scenario was the total blackout of the treatment plant. Further, this study will bear ramifications for similar dispersion studies in future given the very low number of modelling activities ever carried out for Sri Lanka.



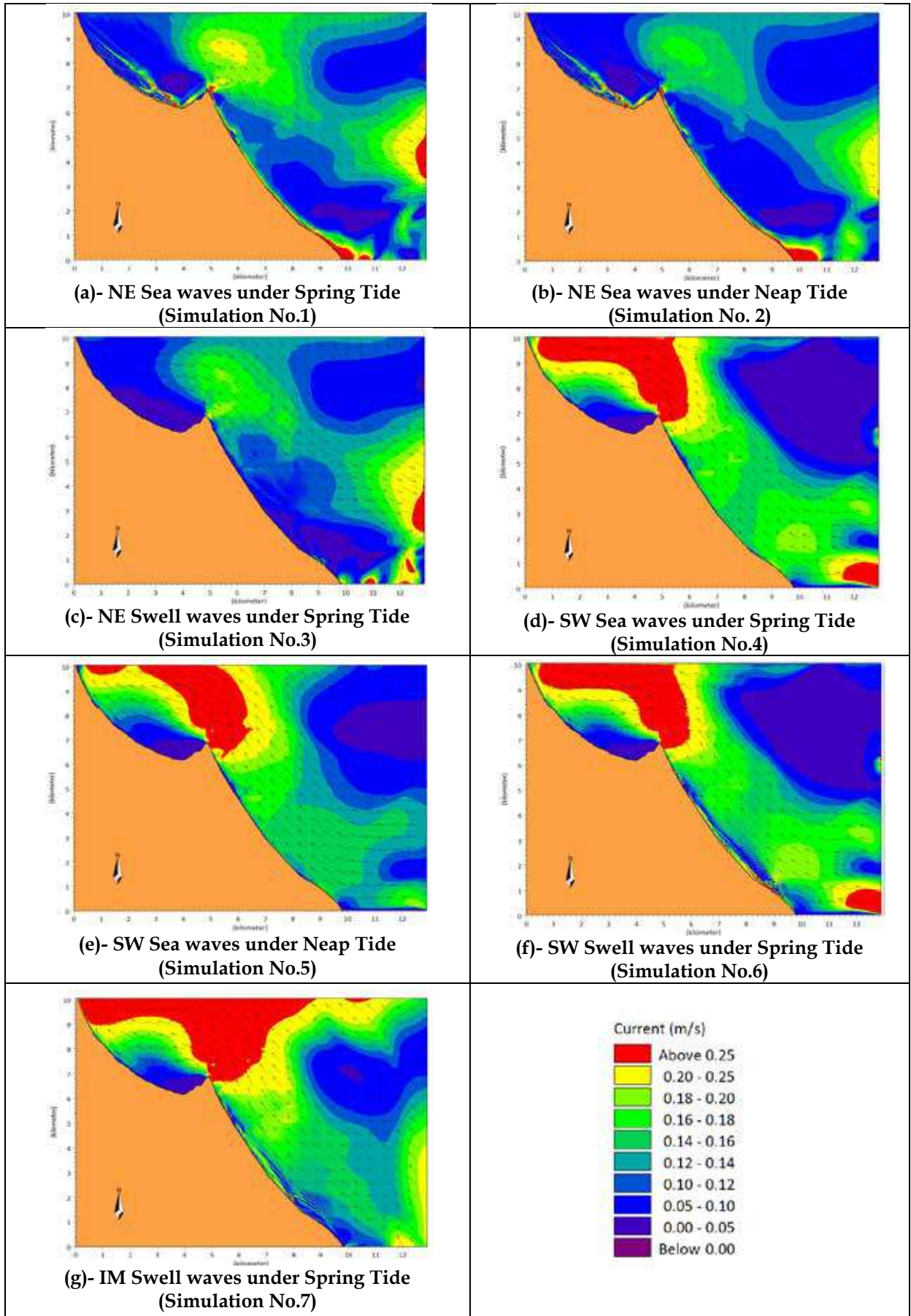
Acknowledgement

Authors wish to thank BOI Sri Lanka and Lanka Hydraulic Institute for their authorization to publish the research findings. Guidance and support rendered by Eng. IGI Kumara for the numerical modelling component is also acknowledged.

References

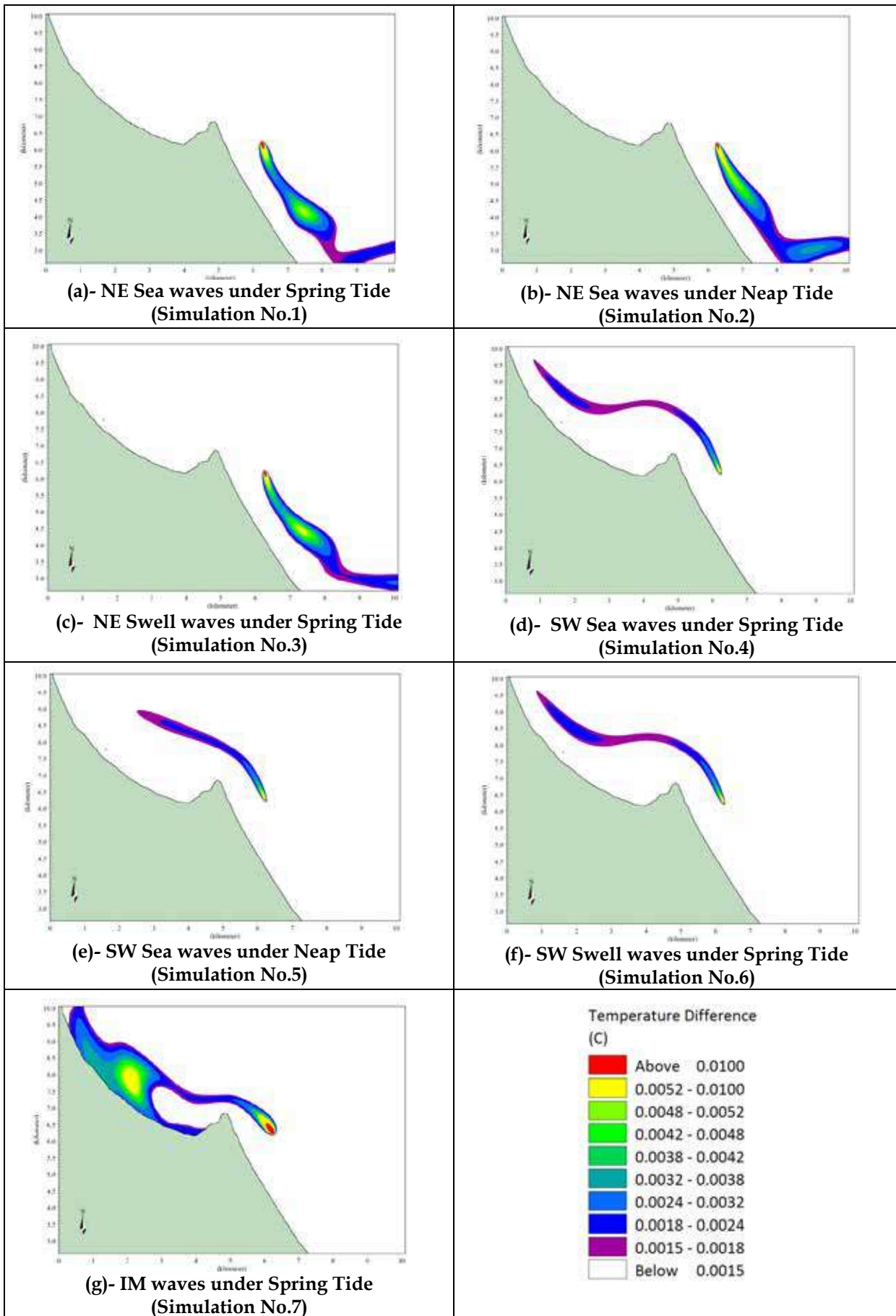
1. DHI (2009). User Manual, MIKE 21 Flow Module, Danish Hydraulic Institute.
2. DHI (2009). User Manual, MIKE 21 AD Module, Danish Hydraulic Institute.
3. Abbaspour, M., Javid, A. H., Moghimi, P., and Kayhan, K. (2005). Modeling of Thermal Pollution in Coastal Area and its Economical and Environmental Assessment. *Int. J. Environ. Sci. Tech.*,2(1):13-26.
4. Monteiro, A. J., Neves, R. J., Sousa, E. R., (1992). Modelling Transport and Dispersion of Effluent Outfalls, *Water Science and Technology*, 25 (9) 143-154;
5. Baumgartner, D. J., Frick, W. E., and Roberts, P. J. W., (1994). *Dilution models for effluent discharges*. 3rd ed. USEPA, Pacific Ocean Systems Branch, Newport, Oregon.
6. James, I. D., 2002. Modeling Pollution Dispersion, the Ecosystem and Water Quality in Coastal Waters: A Review. *Environ. Model.Softw.*17(4): 363-385.
7. LHI (2013). Dispersion Modeling Report, Feasibility Study for Introducing LNG to Sri Lanka.
8. LHI (2014). Final Report-Thermal Dispersion Study, Sampur Thermal Power Project.
9. Samarawickrama, S. P., Hettiarachchi, S. S. L., Jayaweera, M., O'Brian, D., Raveenthiran, K., & Wickramaratne, S. (2008). Modelling the changes in Water Quality due to the Colombo South Harbour, Proc. of the 7th International Conference on Coastal and Port Engineering in Developing Countries (PIANC-COPEDEC VII), Dubai, United Arab Emirates. Feb 24-28.
10. BOI (2011). National Environmental (Protection and Quality) Regulations, No. 1 of 2008, available from www.investsrilanka.com/images/publications/pdf/environmental_norms.pdf, last accessed on Aug 20, 2017.
11. LHI (2011). Development of Modern City at Southern Border of the Colombo Port, Mathematical Modelling Report.
12. Martin, J. L., and McCutcheon, S. C., (1998). Hydrodynamics and Transport for Water Quality Modeling. Lewis Publishers, New York.
13. Scott Wilson (2005). Colombo Port Efficiency and Expansion Project, Colombo South Harbour, Detailed Engineering Report.

Annex

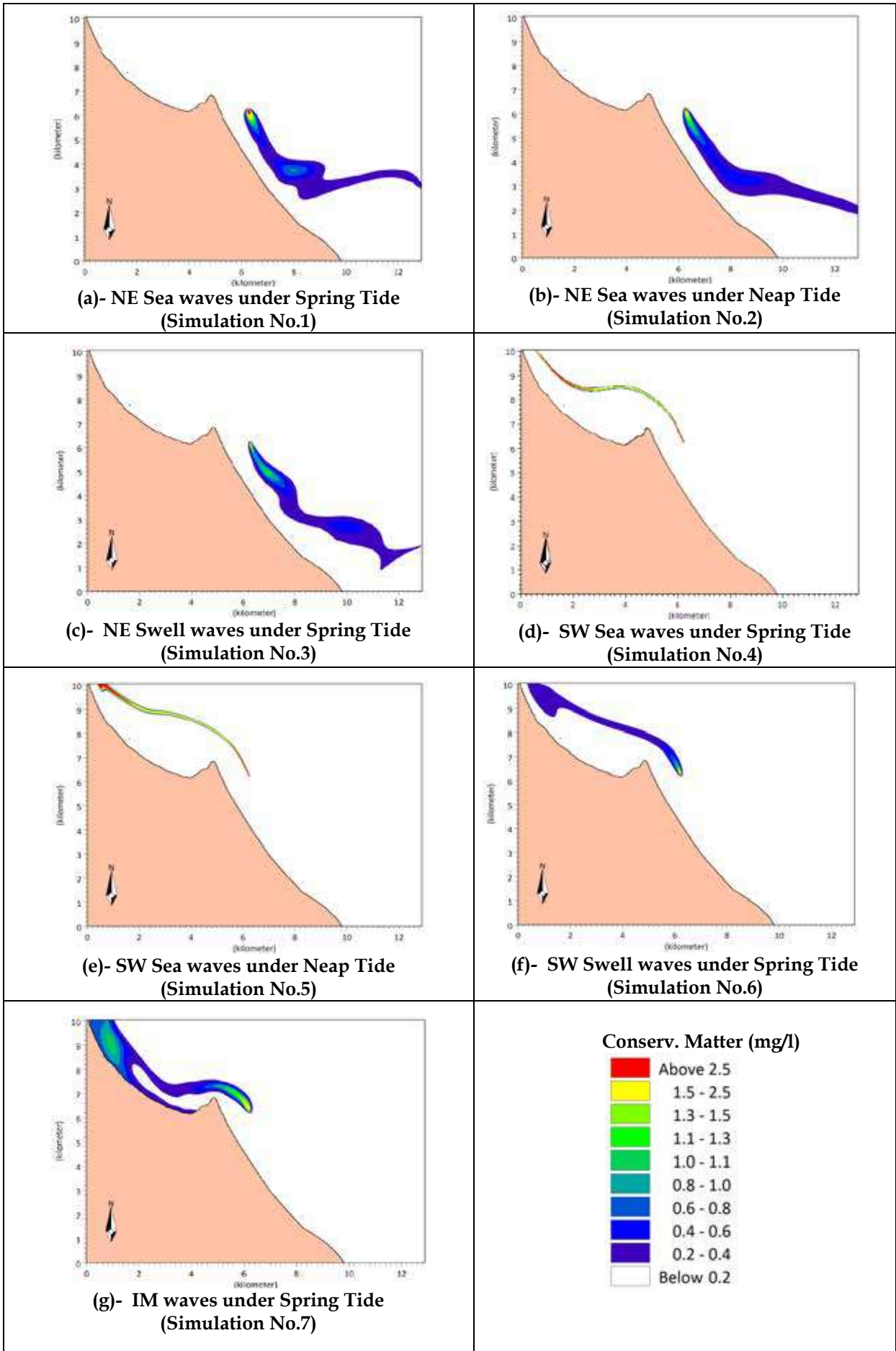


A1 - Maximum Water Currents Attained in the Study Area





A2 - Maximum Concentration of Thermal Plumes



A3 - Maximum Concentration of Effluent Plumes



Numerical Modelling Study for RahfalhuHuraa Resort Development in Maldives

M.S.L. Fernando, I.L. Abeygoonasekara and S.M.D.E. Suriyamudali

Abstract: Unavailability of sufficient land for the development has adversely affected booming tourism industry of Maldives. Although the developers show interest to invest in resort development, lack of land is a dire discouraging factor for them. As a solution, the Government of Maldives has promoted formation of islands on shallow reefs through reclamation. Fulfilling the need, RahfalhuHuraa Resort Development Project surfaced which once constructed will be the largest reclamation undertaken in the Maldives for tourism development.

RahfalhuHuraa reef is located in North Male Atoll, around 50km northward to Male city. The proposed development consists of six main islands which create 77.5ha land on top of the reef area where average water depth is just 1m. In order to obtain design wave parameters, sea currents and max/min water levels, a comprehensive numerical model study was carried out considering different monsoon conditions and layouts. In this process, DHI's MIKE 21 software package available with flexible mesh and finite volume method was utilised for numerical modelling. Offshore wave and wind data, tide elevation, bathymetry and proposed island layout were used as main input parameters whilst wave breaking coefficients and sea bed roughness were used as calibration parameters. Since Maldives is highly vulnerable to storm surge and sea level rise with its low level lands, those factors were also taken into consideration. The study was formed to predict wave heights in front of shore protection structures for different return periods. Further, current patterns with its maximum values were obtained for existing and proposed layouts. In addition, influence for the water level variation by proposed development was also discussed in the study.

Keywords: Wave Transformation, Hydrodynamic, Reclamation

1. Introduction

The Maldives is a South Asian island country, located in the Indian Ocean which consists of 26 ring-shaped atolls. More than 1000 scattered coral islands are existed on top of atoll reefs creating 298 km² of total land area.

There is a shortage of land area for the development and it has severely affected tourism industry. Most of the islands in atolls surrounding Male city (nearly 90%) is being utilized for various land uses and remaining islands are too small for economic activities. Hence, formation of new land on shallow reefs through reclamation is the only option remaining. With this circumstance, the Government of Maldives has promoted this reclamation option to fulfil the requirement of booming tourism industry. As a result, several resort island developments come up for the field. Among them RahfalhuHuraa Resort Developments is a major tourist resort development which was subjected to a comprehensive coastal engineering study.

The orientation of islands with their shapes should be carefully designed to minimise the effect of wave action and sea current. Further, coastal protection structures such as breakwater and revetment should be designed to withstand severe waves. For this purpose, it is essential to estimate wave conditions affected on structures. In this process, numerical models play vital role in order to transfer waves from deep sea to project site. Hence, this paper presents usage of numerical model in wave transformation. Additionally, influence of sea currents and water level variation obtained through a hydrodynamic model were also presented.

Eng. M.S.L. Fernando, AMIE(Sri Lanka), B.Sc. Eng. Hons (Moratuwa), M.Sc. (Moratuwa), Engineering Manager, Lanka Hydraulic Institute Ltd.

Eng. I.L. Abeygoonasekara, AMIE(Sri Lanka), B.Sc. Eng. Hons (Ruhuna), Research Engineer, Lanka Hydraulic Institute Ltd.

Eng. S.M.D.E. Suriyamudali, AMIE(Sri Lanka), B.Sc. Eng. Hons (Peradeniya), Civil Engineer, National Water Supply & Drainage Board.



2. Project Background

The proposed resort island development site is located in north of Kaafu Atoll (North Male Atoll), Maldives, and around 50km northward to Male city (Figure 1). A natural reef is available at site about 1m depth level with a lagoon in the middle. The proposed island formation would be placed on top of the reef.

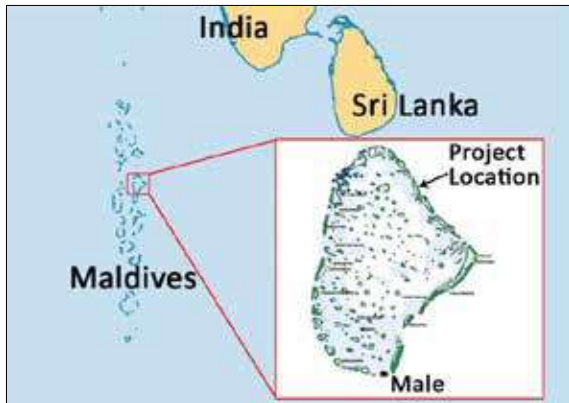


Figure 1 - Project Location

The RahfalhuHuraa Resort Development Project will be the largest reclamation undertaken in the Maldives for tourism development with total area of 77.5ha. The aim of this project is to develop a multi-island resort and marina in North Male Atoll by reclaiming the shallow water lagoon of RahfalhuHuraa. The proponent aims to use the proximity to Male International Airport and continued growth in tourism arrivals in the Maldives to establish a collection of successful and profitable resorts.

The concept master plan encompasses developing six main islands with four as high-end resorts (5 - 12ha in size), one as a marina, hotel and resort (34ha), and the other one as a service island (11.5ha). The proposed project includes land reclamation, shore protection, and infrastructure development of marina and resorts [1].

3. Methodology

Since measured wave data is not available at the vicinity of site, Hind-Cast wind/wave data obtained through a Global Spectral Wind/Wave Model was used for the study. The other data required to set up the numerical models were also obtained through field investigation and reliable sources. The basic procedures of the methodology are given below.

- Obtain and analyze of UK Met Office (UKMO) hind-cast data (wind & wave).
- Carry out field investigations to obtain bathymetry, tide, current and wave data at proposed site and extract model required data from reliable sources.
- Perform numerical modelling for wave transformation from UKMO data location to project site.
- Perform numerical modelling for water circulation (hydrodynamic) for regional model using known tidal data.
- Perform numerical modelling for water circulation (hydrodynamic) for local model using regional model and wave model results.
- Extract the results at suitable locations, analyse and discuss them

4. Data Collection and Analysis

4.1 Field Investigation

In order to find out sea bed levels, tidal variation, wave and current condition at site a set of field investigation was carried out at the beginning of study. Bathymetry survey was done in July 2015 and the other measurements were taken in December 2015. In addition to the field investigation, regional bathymetry was extracted from Admiralty Maps and offshore wind/wave data was obtained from a Global Spectral Wind/Wave Model of UK Met Office (UKMO) [3].

4.2 Offshore Wind/Wave Data

Wave data is very important for the planning and designing of coastal development and it is necessary to measure wave data for a period of 5-10 years. Such a measured data are presently not available for the project site. The visual data, based on ships observations are not adequate for long-term wave characteristics of an area. In order to obtain a uniform spatial-temporal wave data base for estimating wave statistics, the study based on Global Wave Hind Casting Method is the only alternative.

The wind and wave data was obtained based on the hind-cast data from the global wind and wave model of the UK Met Office (UKMO) at offshore of the project area. The available nearest suitable offshore data point (4.453N, 78.180E; UTM 43 N) at 2500m water depth was

selected with considering wave pattern as shown in Figure 2. UKMO is regularly forecasting sea state of global oceans using a 2D Global Spectral Wave Model (GSWAM). The spectral energy changes due to wave generation, propagation, decay, nonlinear wave-wave interaction, etc. is catered in the source term of the model. The input for this spectral type wave model is analyzed global wind fields generated from a Global Spectral Wind Model (GSWIM). The model assimilates wave measurements from the radar altimeter on the ERS-2 satellite and the spectral and statistical outputs are available on 1.5 x 1.5 deg in 3hr / 6hr basis for any region of interest [3].

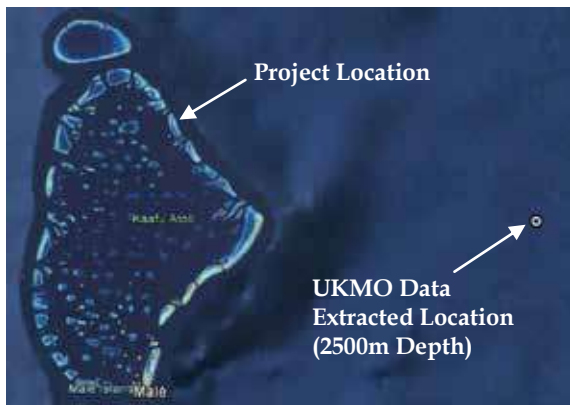


Figure 2 - Offshore Wave Data Extracted Location

Six years data was obtained from UKMO at offshore of proposed site. The wave height, wave period and wave direction are available with wind speed and wind direction during January 2010 to December 2015. The data set contents 8764 no of records with the interval of 6 hours. Analyses were carried out to assess the distribution of wind and wave parameters and annual distribution pattern of wind and wave are given in Figure 3 and 4 respectively.

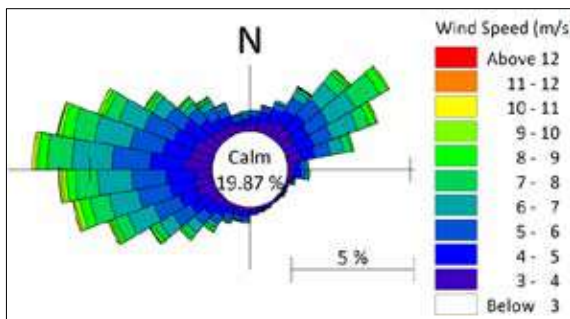


Figure 3 - Annual Distribution of Offshore Wind

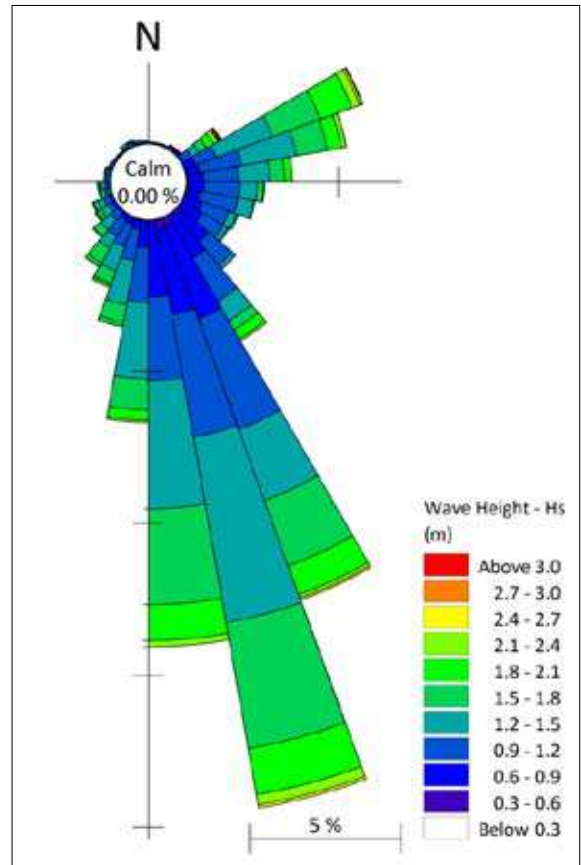


Figure 4 - Annual Distribution of Offshore Wave

5. Wave Climate Model

When implementing new coastal structures, study on wave climate and wave modelling are essential components. The wave data is not available for the desired location on the sea fit for usage. Most of the time wave data measured point is far away from the project location and it has to be transformed to a desired location by a model. In this case, MIKE 21 SW numerical wave model developed by Danish Hydraulic Institute, Denmark was used for wave transformation process. The objectives of the wave climate modelling of this scheme are,

- Establishing nearshore wave climate at the proposed site.
- Evaluating the extreme wave events for different returns periods at different locations considering proposed island formation.

5.1 Wave Model Setup

The model bathymetry was established by digitizing from the Admiralty charts no 1013 & 3323, and near shore measured bathymetry



data. The preparation of model bathymetry was completed using flexible mesh as a requirement of SW model with reference to the UTM 43 coordinate system (for (x, y) coordinates) and Mean Sea Level. Further, a rounded offshore boundary was selected considering the wave and wind approach directions. This rounded boundary was almost fixed to the depth value of UKMO wave point (2500m); thus the wave condition is almost same along the boundary (Figure 5).

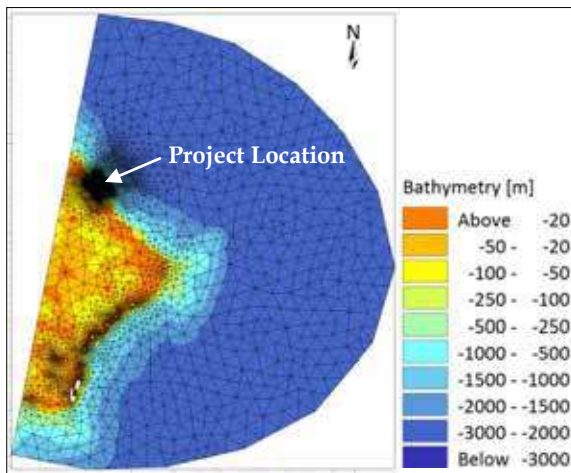


Figure 5 - Wave Model Bathymetry - Regional

Additionally, a local model was also incorporated to improve the performance and accuracy of results. Then UKMO waves were transferred to 1000m depth and applied to the local model. Size of the elements in mesh was reduced while moving to the area of interest with consideration of keeping high resolution near proposed site.

5.2 Wave Model Calibration

Measured wave data at site location was used for the model calibration. Basically, sea bottom friction and wave breaking index were used as the calibration parameter [2]. Since this site is abundant with natural reef, sudden drops of sea bed are available around the reef. Hence, it is not like a normal beach, these steep slopes directly affect to the wave breaking. As a result, wave breaking index would be higher than general values, and then it would be significant in calibration.

Finally, after several test runs, most suitable bottom friction and wave breaking index were set to Nikuradse Roughness value of 0.04m and Gamma value of 1.2 respectively [3]. The calibration curve is given in the Figure 6.

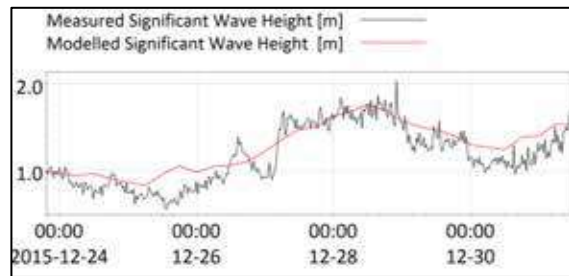


Figure 6 - Calibration Curve for the Wave Model

5.3 Wave Model Results

Accordingly all wave data records were transferred from offshore to site location with applying particular wind conditions. The results were extracted at 8m depth in front of the project site and different locations near the islands as shown in Figure 7.

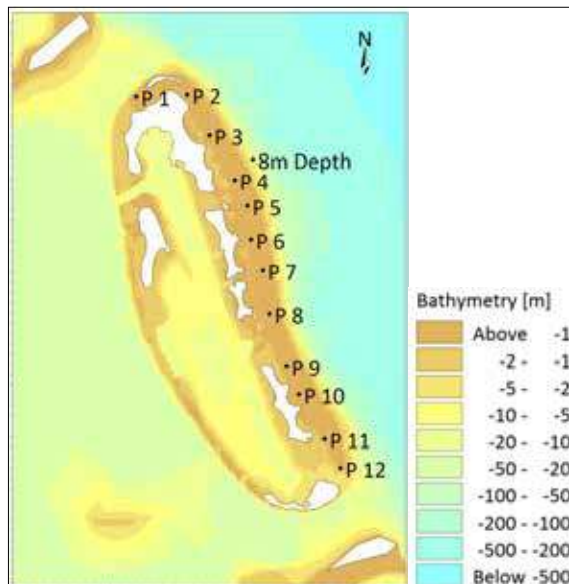


Figure 7 - WaveHeight Extracted Locations

Wave data analysis was done for the extracted data at 8m depth for total year, South-West and North-East monsoon periods. South West monsoon was considered as from May to November while North East as from December to April [1].

Wave statistic at 8m depth (Figure 8) shows that refracted waves have approached the near shore from east side with a narrow band. The most wave occurrence has happened between 90° and 100°, but high waves reach between 60° and 70°. Further, occurrence of high wave was observed during North-East monsoon.

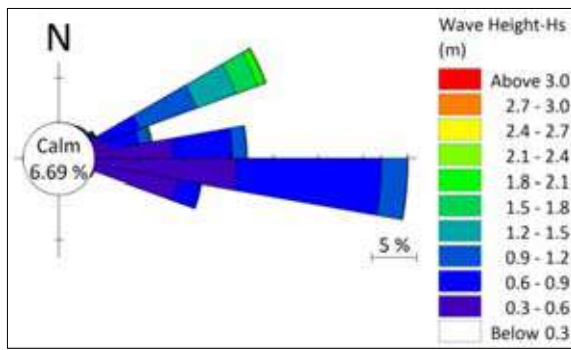


Figure 8 - Annual Wave Height Distribution at 8m Depth

5.4 Extreme Wave Analysis

In the design of any coastal structure, it is necessary to ensure the structural stability against extreme wave events. In general, in the design of structures such as breakwater revetments and quay wall, a significant wave height of 50-100 year return period is considered as the design wave height. However the selection of return period value depends on design life of structure and appropriate probability of extreme event occurrence.

Accordingly the Extreme Wave Analysis was done using the ACES software of the US Army Corps of Engineers (USACE). Analysis was done by fitting the data to distributions of Weibull and Fisher-Tippet with varying K shape parameter.

Mean Sea Level is not desirable to apply as still water level for the modelling of designing purpose. The extreme condition should be considered when designing coastal structures. Therefore the still water level should be decided with considering following factors which are mainly influence the water level variation in the sea environment.

- Astronomical tide variation
- Storm surge
- Sea level rise

Astronomical tide variation was estimated using Admiralty Tide Tables [4]. Since tide data at proposed site is not available in Admiralty tide tables, the data at Girifushi (32 km southward) was used for the estimation. The relevant tide levels at Girifushi are given in Table 1.

Table 1 - Tide Levels at Girifushi [4]

Tidal Level	Level relative to Chart Datum (m)	Level relative to MSL (m)
Highest Astronomical Tide (HAT)	1.2	0.62
Mean Higher High Water (MHHW)	0.9	0.32
Mean Lower High Water (MLHW)	0.7	0.12
Mean Sea Level (MSL)	0.58	-
Mean Higher Low Water (MHLW)	0.4	- 0.18
Mean Lower Low Water (MLLW)	0.3	- 0.28

Mean Higher High Water (MHHW) was applied for all return periods as the tidal elevation. A storm surge of 0.38m water level increment was applied for the still water level according to the UNDP research findings [5]. The sea level rise was taken as 3.6 mm per year with considering regional sea level rise and 0.18m of sea level rise was estimated for 50 years design period for proposed structures [3]. Computation of design water level is expressed in Table 2.

Table 2 - Design Still Water Level relative to MSL

Influence	Water Level Variation (m)
Astronomical Tide	0.32
Storm Surge	0.38
Sea Level Rise	0.18
Design Still Water Level (m MSL)	0.88

Table 3 - Design Wave Height - Hs (m) at Different Locations

Return Period (yr)	Location												
	P1	P2	P3	P4	P5	P6	P7	P8	P9	P10	P11	P12	8m Depth
2	1.24	1.26	1.07	1.09	1.24	1.06	1.31	1.15	1.13	1.01	1.12	2.06	2.75
5	1.33	1.29	1.09	1.12	1.27	1.08	1.34	1.17	1.16	1.03	1.14	2.18	2.98
10	1.4	1.31	1.11	1.13	1.28	1.09	1.36	1.19	1.18	1.05	1.16	2.27	3.15
25	1.49	1.34	1.13	1.15	1.31	1.11	1.39	1.21	1.2	1.07	1.18	2.39	3.38
50	1.56	1.36	1.14	1.17	1.33	1.13	1.41	1.23	1.22	1.08	1.2	2.48	3.55
100	1.63	1.38	1.16	1.18	1.34	1.14	1.43	1.24	1.24	1.1	1.22	2.57	3.72



The results of extreme wave height analysis for different locations in front of islands are given in Table 3. The locations are according to the Figure 7. The results show a significant reduction of wave height in front islands compared to 8m depth. Energy dissipation of low depth submerge reef is the main reason for this wave height reduction. However the location P12 has gained considerable wave height with its higher depth and lower protection of reef.

6. Hydrodynamic (HD) Model

In order to compute water circulation with effect of tidal flow, wave and wind in and around the study area, a hydrodynamic model should be carried out. Hence, the numerical model, MIKE 21 HD was used in this process.

6.1 HD Model Setup

Same as the wave model, Admiralty charts and near shore measured bathymetry data were used for the development of model bathymetry. Since tidal variation would be applied as main boundary condition for the regional model, availability of tidal data was considered when setting up the model. Therefore the regional model extends from Goidhoo (North Boundary) to Male (South Boundary) where tidal boundaries were derived using the tidal constituents. The regional model covers the model area of 77 km in north-south way and 162 km east-west way. Figure 9 illustrates the bathymetry of regional model and position of the local model on it. Local model was selected considering the bathymetry, and kept offshore boundary at 1000m depth.

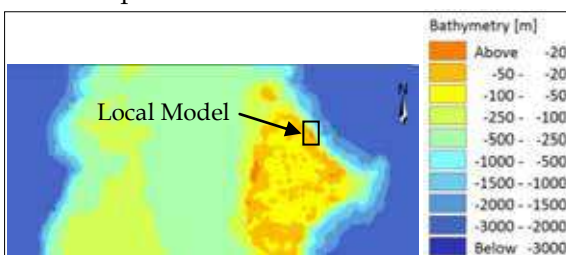


Figure 9 - Bathymetry for Regional Hydrodynamic Model

Triangular flexible mesh was generated by MIKE 21 Bathymetry Creator Tool while considering finer mesh size for more concerned area. Maximum mesh size in regional model is 1×10^6 m² and maximum mesh sizes in local model, deep sea and shallow areas are 500,000m² and 1,000m² respectively. Further very fine mesh with

element area of 100m² was developed in local bathymetry for marina area to observe the water circulation and flushing rates. The UTM 43 coordinate system was used for (x, y) coordinates and Mean Sea Level (MSL) was used as the elevation datum. The local bathymetry with mesh is given in Figure 10.

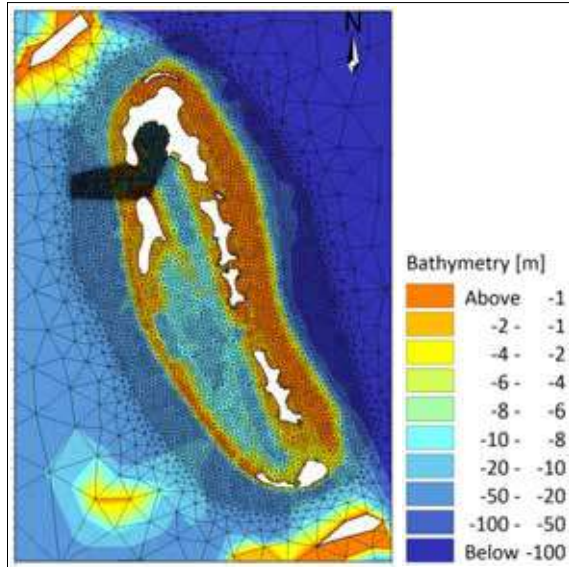


Figure 10 - Local Bathymetry with Mesh

The regional model was run for a period of one year to cover both South-West and North-East monsoon and the local model was run for two set of periods with two weeks for each set which covering spring and neap tide. One set was selected from South-West monsoon and the other one from North-East.

Water levels and discharges extracted from regional model at the boundaries of the local model were used as boundary conditions for the local model. Local model was run for average and extreme wave/wind condition for both monsoons. The average condition was selected considering 50% occurrence of wave height of the wave data extracted at 1000m depth from wave transformation model (MIKE 21 SW). In this process, most dominant directional bands were selected for the calculations. Same as wave, 50% occurrence of wind speed of UKMO wind data was selected to obtain corresponding wind speed. Same method was adopted to select the extreme condition by considering 98% occurrence (2% exceedance of wave height and wind speed). The selected wave and wind conditions are given in following tables.

Table 4 - Applied Wave Conditions for the Hydrodynamic Model

Monsoon	Average (50%)		Extreme (98%)		Dir
	Hs (m)	Tp (s)	Hs (m)	Tp (s)	deg
South West	0.74	9.80	1.33	9.82	120
North East	0.8	9.35	2.18	9.42	75

Table 5 - Applied Wind Conditions for the Hydrodynamic Model

Monsoon	Average (50%)	Extreme (98%)	Dir
	Speed (m/s)	Speed (m/s)	Deg
South West	4.96	8.58	270
North East	4.36	8.55	60

6.2 HD Model Calibration

Calibration was done considering the variation surface elevations. Model predicted tide elevation and measured water level at proposed site were incorporated for the calibration. The bed roughness was used as the calibration parameter and Manning’s Number of 32 was set as the suitable values. Figure 11 shows the calibration curve.

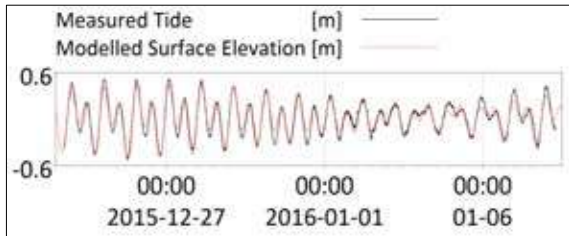


Figure 11 - Calibration Curve for the HD Model

6.3 HD Model Results

The main objective of the HD modelling is to observe the flow pattern in the model area and find out the effect for the current flow by the proposed island. Hence current speeds were extracted in between islands as indicated in Figure 12 and the maximum current speed values are given in Table 6.

Results show that an increment of maximum current speed in between islands relative to the existing condition. That increment comparatively higher in North-East monsoon than South-West.

Furthermore water levels are also extracted in front of proposed island as indicated in Figure 12 and the results are given in Table 7.

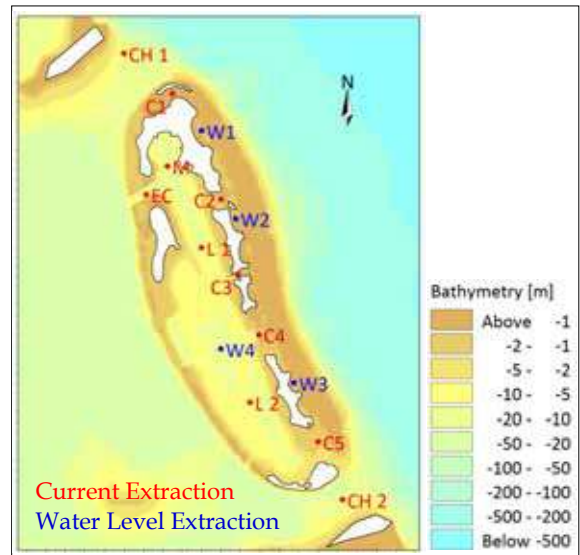


Figure 12 - Current Speed and Water Level Extracted Points

Table 6 - Maximum Current Speed in m/s at Extracted Point

Location	Average				Extreme			
	South-West		North-East		South-West		North-East	
	Existing	Proposed	Existing	Proposed	Existing	Proposed	Existing	Proposed
CH 1	1.04	0.87	1.17	0.94	1.04	0.87	1.12	0.93
CH 2	1.20	1.03	1.35	1.07	1.20	1.03	1.30	1.07
C 1	0.37	0.26	0.48	0.53	0.42	0.32	0.65	0.54
C 2	0.32	0.61	0.39	1.09	0.39	0.76	0.57	1.10
C 3	0.32	0.57	0.38	1.02	0.39	0.72	0.58	1.03
C 4	0.32	0.43	0.40	0.86	0.38	0.54	0.59	0.86
C 5	0.23	0.32	0.33	0.64	0.32	0.39	0.48	0.65
EC	0.23	0.19	0.28	0.32	0.27	0.23	0.44	0.31
M	0.09	0.03	0.11	0.03	0.09	0.05	0.13	0.05
L 1	0.09	0.04	0.09	0.07	0.10	0.05	0.13	0.07
L 2	0.07	0.03	0.09	0.02	0.07	0.05	0.07	0.03



Table 7 - Maximum and Minimum Water Levels (m MSL) in front of Islands

Location	Average								Extreme							
	South-West				North-East				South-West				North-East			
	Max		Min		Max		Min		Max		Min		Max		Min	
	Ext.	Pro.	Ext.	Pro.	Ext.	Pro.	Ext.	Pro.	Ext.	Pro.	Ext.	Pro.	Ext.	Pro.	Ext.	Pro.
W 1	0.45	0.46	-0.51	-0.52	0.48	0.63	-0.47	-0.14	0.46	0.51	-0.5	-0.52	0.54	0.63	-0.42	-0.13
W 2	0.45	0.47	-0.51	-0.51	0.48	0.62	-0.47	-0.18	0.46	0.52	-0.5	-0.51	0.53	0.63	-0.42	-0.18
W 3	0.45	0.46	-0.51	-0.51	0.48	0.62	-0.47	-0.21	0.46	0.51	-0.5	-0.51	0.52	0.62	-0.42	-0.21
W 4	0.44	0.44	-0.51	-0.52	0.48	0.49	-0.47	-0.45	0.45	0.45	-0.51	-0.51	0.51	0.49	-0.43	-0.45

7. Conclusions

A significant reduction of wave height and a directional change were observed at near shore waves compared to offshore waves. Presence of low depth reef has been affected for wave height reduction. Especially considerable energy dissipation happens through depth induce wave braking when waves enter the low depth area. Existence of hard bottom reef bed dissipates more energy through bottom friction as well. The effect of low depth reef for the wave height reduction is clearly illustrated by the results given in Table 3. The reef edge where the 8m depth point located had high waves, but after energy dissipation, low waves appeared on top of reef near islands. Hence this natural reef has provided a good protection to islands by acting as a submerged breakwater.

Diffraction and refraction processes have influenced to narrow the wide range of offshore wave directions. Islands and reefs located in south of atoll cut off southern waves causing diffraction process. Furthermore waves refract with depth reduction limited wave directions to a narrow band.

Current speed of channels either side of reef has been reduced by proposed island formation, but it has been increased in between islands relative to the existing condition. This current speed increment in between island is more significant in North-East monsoon season than South-West. Interruption of the water flow on top of reef would be the reason for this increment of current speed in between islands.

Significant change in maximum water level cannot be observed for the South-West monsoon, but considerable increment has been indicated for the North-East monsoon. Hence

beach crest level should be designed accordance with these water level variations.

Acknowledgement

Authors would like to express their gratitude to Dr. Ahmed Shaig (Director - CDE Consulting, Maldives) for all support given throughout the project duration and Lanka Hydraulic Institute for providing there sources to carry out the study. Also we thank to all friends for their support given in many ways.

References

1. CDE Consultant, "Environment Impact Assessment for the Proposed RafalhuHurra Resort Development, at Mai Falhu, Kaafu Atoll", April, 2016.
2. Danish Hydraulic Institute, MIKE 21 Scientific Document; Spectral Wave Module, 2014.
3. Lanka Hydraulic Institute, Development on RafalhuHurra, Maldives, Numerical Modelling, Final Report, September 2016.
4. United Kingdom Hydrographic Office, Admiralty Tide Tables, Indian Ocean and South China Sea, Vol 03, 2015.
5. United Nation Development Programme, Developing a Disaster Risk Profile for Maldives, Vol 1 & 2, 2006.

Wave Tranquillity Study for a Fishery Harbour using Boussinesq Type Wave Model

D.P.C. Laknath, D.E.N. Senarathne and K.K.P.P. Ranaweera

Abstract: The knowledge about the behaviour of waves inside a harbour basin and entrance is important for fishing boats mooring and handling, navigational purposes as well as handling downtime. During the last 4 decades, Boussinesq-type models became well-known simulation technique among the coastal engineering community. This is because of their ability to represent all main physical phenomena of water waves in shallow seas and harbours. This study was carried out for a fishery harbour planned to be implemented in the North-western coastal stretch of Sri Lanka. The main objective of this study is to carry out a wave tranquillity study for the proposed harbour to ensure the mooring arrangements, safe navigational through the harbour entrance in relation to predefined criteria for acceptable wave disturbance. Boussinesq Wave (BW) module of MIKE 21 modelling system was used to simulate the wave disturbances inside harbour basins and harbour entrance under different characteristics of wave incidences. Boussinesq type equations incorporate frequency dispersion as opposed to the shallow water equations. With the hindcast, nearshore wave climate in the study area, simulations were carried out for representative nearshore wave climate conditions during the southwest and northeast monsoon seasons (for H_s : 0.7m - 1.7m & 265°N - 305°N directional ranges). As the outcome of the simulation, it was identified that maximum significant wave heights are less than 0.4 m for most of scenarios at the harbour entrance, inside and quay wall areas indicating the safe navigation across the harbour entrance and convenient operations. Hence, as per the PIANC Guidelines and simulation results, it was concluded that navigational and mooring operations could be done in the basin with minimum disturbance for all seasons. Thus, suitability of the harbour location and layout in terms of wave tranquillity was justified with the numerically simulated results.

Keywords: Wave disturbances, fishery harbour, numerical simulation, Boussinesq-type model

1. Introduction

In addition to the existing 20 fishery harbours, Sri Lankan government continues to develop new fishery harbours and landing facilities in the coastal zone of the Sri Lanka [1]. Hence, improvement of harbour design methodologies is an important factor to be considered in terms of enhancing the accuracy of the design and saving cost and time with an optimized harbour layout. During the harbour design phase, mathematical modelling is considered as an efficient and cost effective technique for the reproduction of existing coastal phenomenon as well as to select the best harbour configurations out of several alternatives designs through a systematic harbour layout optimization process [2]. Further, understanding about the wave disturbances inside a harbour basin is important for fishing boats mooring and handling during loading/unloading operations as well as navigational purposes. Over the last 40 years, Boussinesq-type models have become well known and are favoured by the coastal engineering community for harbour layout

optimization through wave tranquillity studies. This is because of their ability to represent all main physical phenomena of water waves in shallow seas and harbours [3]. Generally, Boussinesq Wave Model includes non-linearity and frequency dispersion. Also, it has a capability of simulating refraction, shoaling, reflection, diffraction, wave interaction and other important non-linear phenomenon [4]. In this context, MIKE21 Boussinesq Wave (BW) model is a powerful tool for determination and assessment of wave dynamics in ports and harbours in coastal areas. In this study, wave penetrations through a proposed Fishery Port

Eng. (Dr.) D.P.C. Laknath, AMIE(SL), B.Sc.Eng. (Moratuwa), M.Eng. (AIT), Dr. Eng. (Yokohama), Engineering Manager, Lanka Hydraulic Institute Ltd.

Eng. D.E.N. Senarathne, AMIE(SL), B.Sc.Eng. (Moratuwa), Research Engineer, Lanka Hydraulic Institute Ltd.

Eng. K.K.P.P. Ranaweera, C.Eng., MIE(SL), B.Sc.Eng. (Moratuwa), Project Director, Ministry of Fisheries and Aquatic Resources Development.



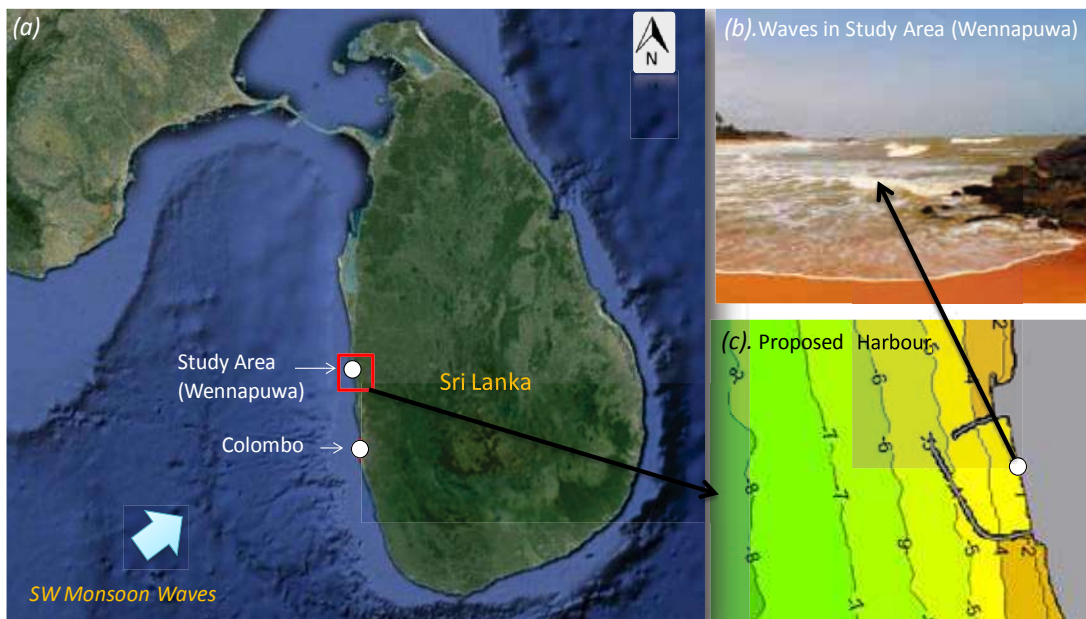


Figure 1 - (a). Study Area (Wennappuwa); (b). Wave Condition in Study Area (c). Proposed Harbour
 (Sources: Field visit in July 2015, <http://maps.google.com>)

entrance and wave disturbance (i.e. agitation) inside harbour basin (especially, quay wall area and harbour entrance) have been studied by MIKE21 BW module. This study was carried out in connection with a fishery harbour planned to be implemented in Wennappuwa in the North-western coastal stretch of Sri Lanka (Figure 1(a)). Accordingly, the main objective of this study is to carry out a wave tranquillity study for the proposed harbour to ensure the mooring arrangements, safe navigational through the harbour entrance in relation to predefined criteria (i.e. *Permanent International Association of Navigation Congresses - PIANC*) for acceptable wave disturbances. Hence, it was an attempt to assess the suitability of the harbour location and layout by wave calmness study with the numerically simulated results.

2. Proposed Harbour and Study Area

In this study, wave tranquillity study was carried out for a proposed Fishery Harbour in Wennappuwa (Figure 1(c)). Considering the general wave and sediment processes in the study area, conceptual harbour layout was initially designed. As per the requirement of the fishermen and other stakeholders, the conceptual layout was further optimized. Thus, proposed harbour layout consists of two breakwaters, quay wall, slipway facilities and onshore facilities. As most important areas, wave disturbances in harbour entrance, basin and quay wall areas are mainly considered for the assessment. Generally, the wave climate in

the west coast of Sri Lanka is mainly governed by the southwest monsoon. Comparatively, northeast monsoon is very much milder. The tides occurring in Sri Lanka is the semi-diurnal type with an average tidal range of less than 1m. Due to that, magnitudes of tidal currents along the coast are not significant. In case of wave induced currents, the long shore coastal currents are strongest during the respective months. Thus, during the southwest monsoon period, wave induced currents are in a northerly direction while currents in a southerly direction could be experienced during the northeast monsoon time [5]. In terms of sediment process, this study area was recognized as a highly sensitive area for coastal erosion before implementing the Coastal Resource Management Project (CRMP) in Sri Lanka between 2000 - 2006 periods. Though this area has been stabilized with beach nourishment and hard structures under the CRMP, still this coast can be considered as a highly sensitive and critical coastal stretch for sediment processes.

Out of several significant coastal processes, we have studied each process with the state-of-the-art technologies to design a high-performance harbour layout with a minimal adverse impact on the existing coastal processes. In this paper, to assess the navigational and mooring capacity of the proposed harbour, we only presented and discussed about the wave penetration through the harbour entrance and resultant wave disturbances inside the harbour basin areas for the identified dominant wave conditions.

3. Methodology

3.1 MIKE 21 BW Model

MIKE 21 BW module is developed by Danish Hydraulic Institute (DHI), offering the required modelling platform to assess the tranquillity of the harbour basin. Boussinesq Wave model is a state-of-the-art numerical tool for calculation and analysis of short and long period wave disturbance in ports and harbours. Madsen and Sørensen [6] explained the theoretical formulation of enhanced Boussinesq equations. The model has been extended into the surf zone by inclusion of wave breaking and moving shoreline as described in Madsen et al. [7, 8] and Sørensen [9]. MIKE 21 BW is capable of reproducing the combined effects of most wave phenomena of interest in ports, harbours and related structures. These include: shoaling, refraction, diffraction, partial reflection and transmission, non-linear wave-wave interaction, frequency spreading and directional spreading. BW simulation requires a series of input parameters (e.g. bathymetry, boundary conditions, simulation period, internal wave generation, eddy viscosity, bottom friction, porosity, and sponge). As the main output, wave parameters (i.e. wave heights, time period and directions) and wave disturbance coefficients (WDC) can be obtained at the interested locations. During the model setup stage, selection of suitable time step and grid resolution is an important factor to ensure efficient model simulation and the accurate results. Time step size determines the frequency at which Boussinesq equations are resolved. The time step should be sufficiently small to resolve the shortest individual wave periods. In

addition, the selection of time step and grid spacing must attest the Courant Number which is a stability indicator, to be less than or equal to unity.

3.2 Wave Climate in the Study Area

To identify dominant wave conditions for wave penetration study, the establishment of the wave climate in the study area is a prerequisite. Detailed description about the hindcasting of wave climate for the study area can be found from the study of Laknath et al. [5]. As per this study, the applied methodology to hindcast wave climate is based on the application of MIKE 21 SW (Spectral Waves) model to simulate wave propagation off the western coast (offshore) and using a Wave Transformation Matrix (WTM) approach to transform wave recordings based on reproduced model results. Wave propagation modelling was carried out to transform wave recordings from Colombo to representative locations in the study area. Thus, representative nearshore wave climate was established at 8 m water depths in the study area (Wennappuwa). All wave measurements in Colombo during 1998 - 2015 periods were transformed to the offshore boundary of the model and thereafter transformed back to the desired destination locations (Wennappuwa). Thus, established wave data at 8 m depth was analysed to use as the boundary conditions of the MIKE 21 BW model simulations.

3.3 Model Scenarios

Wave tranquillity study was performed for the proposed harbour layout for number of wave conditions. Thus, simulations were carried out

Table 1 - Simulation Scenarios for MIKE 21 BW Model

Case No	Season	Condition	% Exceedance		Wave Parameters		
			50	2	Hs(m)	Tp (s)	Dir
1	SW	Average	√		1.10	7.5	265
2	SW	High		√	1.70	6.5	265
3	IM-1	Average	√		0.70	9.2	245
4	IM-1	High		√	1.50	6.2	255
5	NE	Average	√		0.50	9.9	255
6	NE**	Average	√		0.70	5.8	295
7	NE	High		√	0.90	8.9	265
8	NE**	High		√	1.10	4.8	305
9	IM-2	Average	√		0.50	9.8	245
10	IM-2	High		√	1.10	5.7	255

** NB: Additional wave conditions were selected for NE monsoon to represent North - West quadrant.



for different wave boundary conditions at 8 m sea depth. Considering the percentage of exceedance of established wave climate at 8 m sea depth, wave parameters relevant to average and high wave conditions were estimated for each monsoon. Thus, 50 % and 2 % exceedance of wave parameters for considered periods are taken as “average” and “high” wave conditions. Accordingly, wave tranquillity study for proposed harbour layout was carried out for 10 scenarios (Table 1).

4. Results and Discussion

4.1 Variation of Significant Wave Heights
 For all scenarios (see Case No. 1 – Case No. 10 in Table 1), wave height variation in and around the harbour was assessed. Thus, wave agitation and tranquillity areas are identified and illustrated by using 2D plots (see Figure 2, 3, 4 and 5 for Case No. 1,2, 6 and 8). Comparing the prevailing duration of each season, SW monsoons season is the longest season. Also, wave effect is dominant during the same season as a significant amount of waves comprise generally high values. Hence, while analysing 2D plots of wave heights in the harbour area, the outcome of SW monsoon was specially considered. Basically, for the most representative case (Case No. 1: SW – average), significant wave heights (Hs) in basin area varies between 0.1 m – 0.25 m. In harbour entrance area, significant wave heights vary between 0.25 m – 0.75 m. For south west high case (Case No. 2) also, significant wave heights are lesser than 0.25 m, indicating the calmness inside the basin. At the entrance, significant wave height has increased up to 1 m compared to SW – average condition (i.e. Case No. 1). For Case No. 3, 4, 5, 7, 9 and 10, relatively low wave disturbances prevail at harbour basin and entrance. In case of particular NE average and high wave conditions (Case No. 6 and 8 in Figure 4 and 5), slightly elevated significant wave heights up to 0.25 m are observed inside the basin. In front of quay wall area also, same observation can be seen. This is due to the direct penetration of wave during the NE monsoon as wave propagation directions belong to north – west quadrant (i.e. 295° N and 305° N). However, considering the duration of NE monsoon period and percentage of occurrence of Case No. 6 and 8, expected harbour operations are safe for these conditions as wave heights are within the allowable range. In general, the proposed harbour layout provides sufficient wave tranquillity for harbour operations.

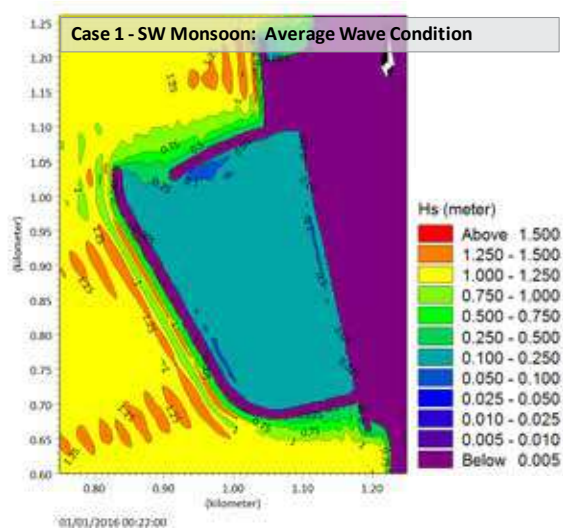


Figure 2 - Significant Wave Heights - Case 1

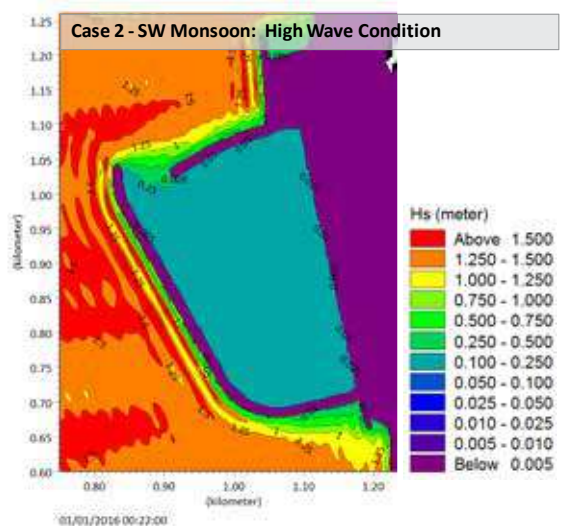


Figure 3 - Significant Wave Heights - Case 2

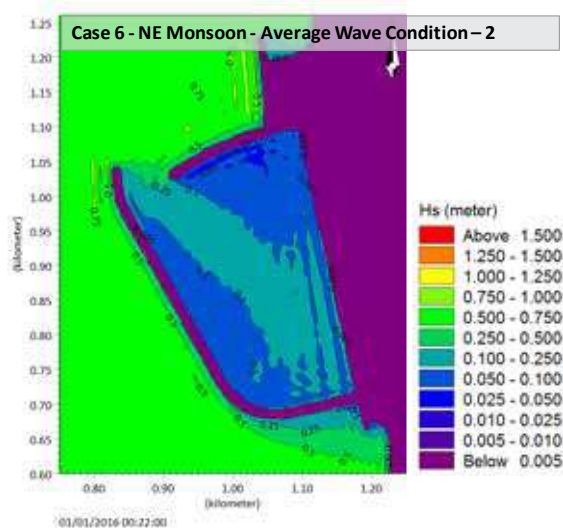


Figure 4 - Significant Wave Heights - Case 6

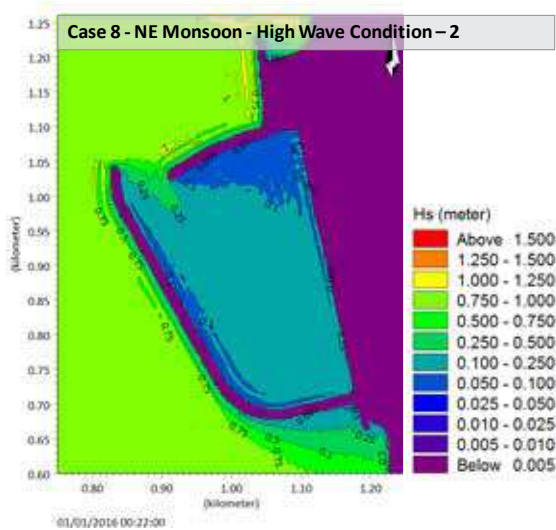


Figure 5 - Significant Wave Heights - Case 8

4.2 Wave Heights at Selected Locations of Harbour

For each scenario (see Case No. 1 – Case No. 10 in Table 1), significant wave heights were extracted at selected locations in the proposed harbour (see Figure 6 (a)). To evaluate whether the simulated wave conditions inside the harbour basin are within the acceptable limits, the criteria tabulated in Table 2 is used. These criteria were suitably adopted from the PIANC Guidelines (Criteria for Movement of Moored Ships in Harbours), giving due consideration to

the sizes of the vessels that will be operated from proposed Wennappuwa Fishery Harbour. The PIANC criteria have been specified for a large fishing craft having a length overall (LOA) 25 – 60 m.

Extracted significant wave heights for each scenario are presented in Table 3. In front of quay wall area, the maximum wave height is 0.25 m for Case No: 8 (i.e. NE High ($H_s = 1.10\text{m}$, $T_p = 4.80\text{ sec}$, $\text{Dir.} = 305^\circ\text{N}$)). This could mainly result as quay wall area is directly exposed to 305°N wave direction. However, as per the allowable values presented in Table 2, loading and unloading operations are safe at quay wall as extracted significant values are lesser than allowable value of 0.4 m. Further, in turning circle area and spending beach area, maximum significant wave heights are 0.18 m and 0.13 m respectively. Hence, mooring operations could be done in the basin with minimum disturbance for all seasons. At harbour entrance, maximum significant wave heights over 0.4 m have been recorded only for Case No: 2 (i.e. SW High ($H_s = 1.70\text{ m}$, $T_p = 6.50\text{ sec}$, $\text{Dir.} = 265^\circ\text{N}$)) and Case No: 8 only (i.e. maximum values of 0.46 m and 0.51 m respectively). Thus, these results indicate the safe navigation across harbour entrance.

Table 2 - Allowable Significant Wave Heights for Safe Mooring and Operations of Vessels within the Harbour Basin

Type of Boat Operation	Allowable Significant Wave Height (H_s)
Loading/unloading operation at a Quay	H_s should not exceed 0.4 m more than 1 week/year
Mooring in the basin	H_s should not exceed 0.6 m more than 1 week/year
Mooring - survival	H_s should not exceed 0.4 m during extreme condition

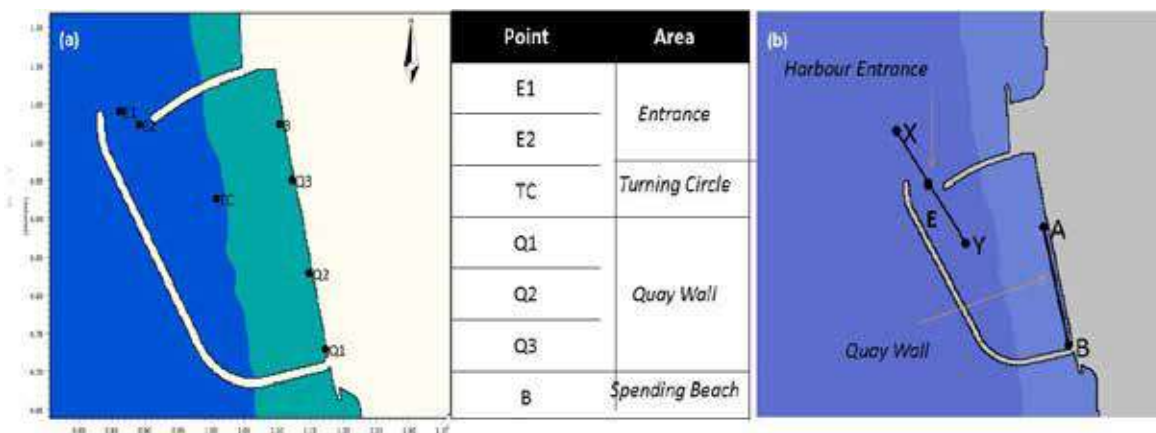


Figure 6 - Wave Extracted Locations and XY, AB Longitudinal Profiles for Wave Analysis



Table 3 - Significant Wave Heights at Selected Points- BW Simulations

Case No	Season	Incoming Wave Height (m)	Extracted Wave Heights (m)						
			E1	E2	TC	Q1	Q2	Q3	B
1	SW	1.10	0.37	0.23	0.13	0.14	0.15	0.13	0.12
2	SW	1.70	0.46	0.27	0.16	0.18	0.19	0.15	0.13
3	IM-1	0.70	0.19	0.12	0.06	0.07	0.08	0.07	0.06
4	IM-1	1.50	0.33	0.19	0.12	0.13	0.13	0.11	0.09
5	NE	0.50	0.17	0.10	0.06	0.06	0.08	0.07	0.05
6	NE**	0.70	0.37	0.23	0.12	0.13	0.13	0.09	0.06
7	NE	0.90	0.33	0.23	0.11	0.13	0.13	0.12	0.11
8	NE**	1.10	0.51	0.36	0.18	0.25	0.18	0.12	0.10
9	IM-2	0.50	0.15	0.09	0.05	0.05	0.06	0.05	0.04
10	IM-2	1.10	0.28	0.16	0.09	0.10	0.10	0.09	0.07

Further analysis of wave disturbances was carried out for the proposed harbour at entrance and quay wall area (see Figure 6 (b)). The analysis was carried out on the basis of extracted wave heights profiles. Accordingly, extracted wave heights along X - Y (i.e. across the entrance) and A - B (i.e. in front of quay wall) longitudinal profiles for Case No. 1 - Case No. 10 were compared (see Figure 7).

Wave height variation along the X - Y longitudinal profile for all wave conditions (i.e. Case No. 1 - Case No. 10) are shown in Figure 7. It is clear that there is a remarkable reduction of wave heights across the harbour entrance. Outside the harbour, the highest wave is observed for Case No. 2 (SW - Average). Inside the harbour, the highest wave is observed for Case No. 8 (NE - High - 305° N direction),

resulting due to the lack of shelter for 305° N direction.

Figure 8 illustrates wave height variation along E - Y longitudinal profile. It further clarifies the observations which have been identified from Figure 7. It is clear that all wave heights inside the harbour are less than 0.4 m.

Figure 9 illustrates wave heights variation in front of quay wall area along E - Y longitudinal axis. Generally, wave heights are below 0.4 m for all cases ensuring safe loading and unloading operations at the proposed quay wall areas. Highest waves are observed for both Case No 2 (SW - Average) and Case No. 8 (NE - High - 305° N direction).

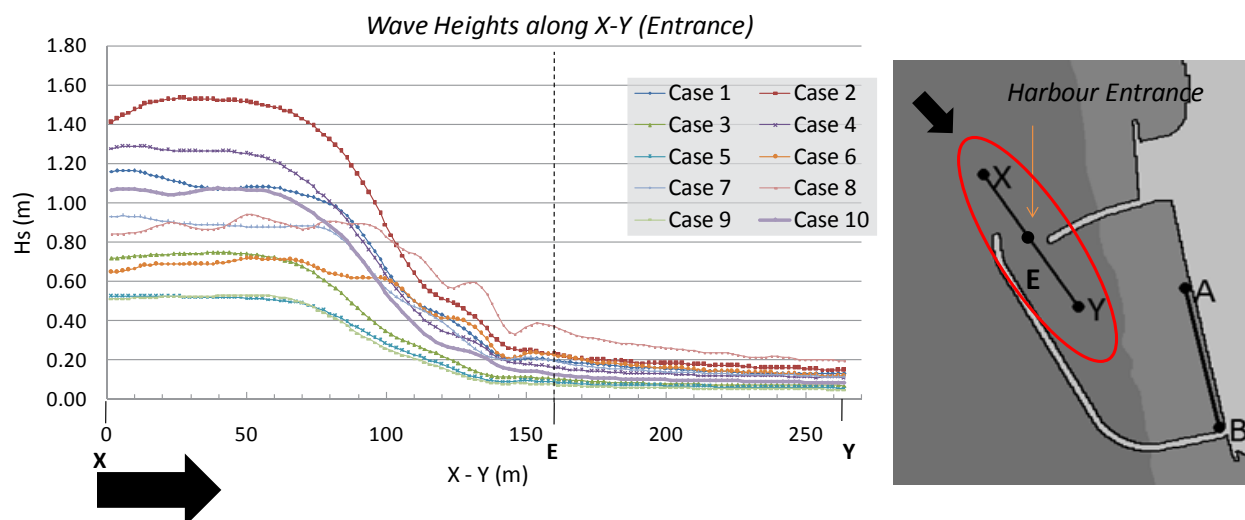


Figure 7 - Wave Heights Variation along Longitudinal Profile X-Y (Entrance - Inside and Outside of the Harbour)

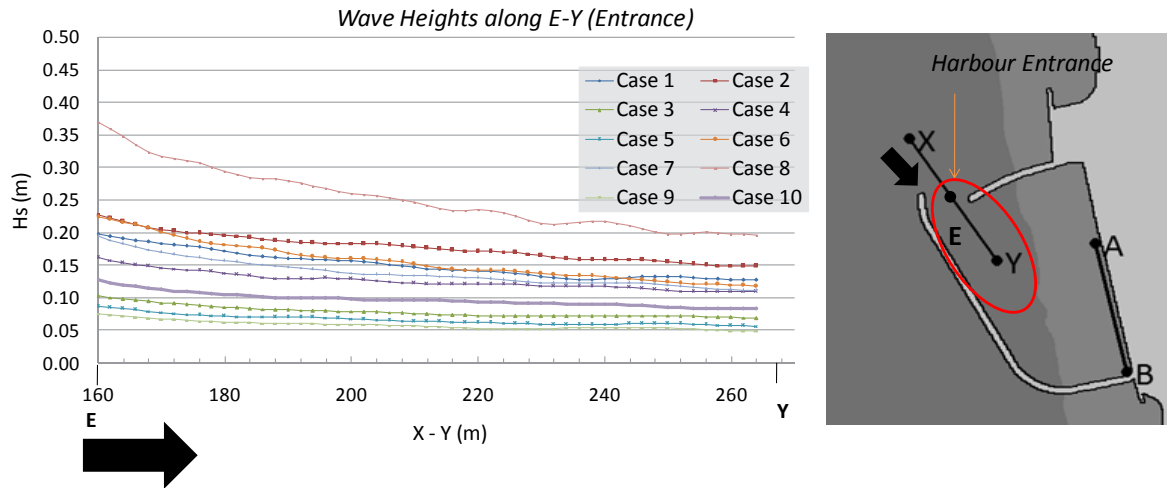


Figure 8 - Wave Heights Variation along Longitudinal Profile E-Y (Entrance)
(Entrance – Inside the Harbour)

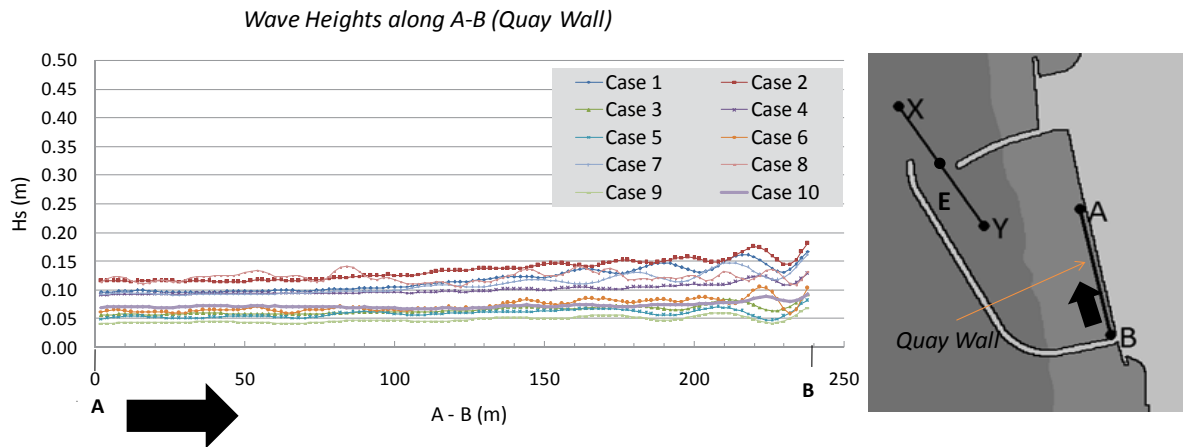


Figure 9 - Wave Heights Variation along Longitudinal Profile A - B (Quay Wall)

5. Conclusions

Wave tranquillity study was carried out for the development of proposed Fishery Harbour in Wennappuwa. The main objective of this study was to carry out a wave calmness study for the proposed harbour to ensure the mooring arrangements and safe navigational through the harbour entrance in relation to predefined criteria for acceptable wave disturbance. For the simulation of wave disturbances inside harbour basins and harbour entrance, Boussinesq Wave (BW) module of MIKE 21 modelling system was used. Comparing with other wave simulation models, Boussinesq type wave model is a powerful tool for determination and assessment of wave dynamics in ports and harbours in coastal areas. Especially, it includes non-linearity and frequency dispersion and has capability of capture and simulate non-linear

phenomenon. On the basis of already established wave climate in the study area, BW simulation was carried out for 10 representative wave conditions which cover southwest (SW), inter-monsoon-1(IM1), northeast (NE) and inter-monsoon-2(IM2) seasons. As the outcome of the simulation, 2-dimensional wave plots, significant wave heights at selected locations and longitudinal wave profiles were extracted and analyzed for all scenarios. From the analysis, it was identified that maximum significant wave heights are less than 0.4 m for most of scenarios at the harbour entrance, inside and quay wall areas indicating the safe navigation across the harbour entrance. Hence, as per the PIANC Guidelines and simulation results, it was concluded that navigational and mooring operations could be done in the basin

with minimum disturbance for all seasons. Thus, suitability of the harbour location and layout in terms of wave tranquillity was justified with the numerically simulated results.

Acknowledgement

The authors wish to acknowledge the "Construction of Fishery Harbours and Anchorages Project" of MFARD (Ministry of Fisheries and Aquatic Resources Development) in Sri Lanka for various supports for the success of this study.

References

1. Laknath, D. P. C., and Weesakul, S. "Natural Harmonize Design Improvements of Hikkaduwa Fishery Harbor". *Proc., Conference on Coastal and Port Engineering in Developing Countries (COPEDEC IX)*, Rio de Janeiro, Brazil, 2016
2. Santosh K. Kori , Amol S. Borkar, Vaidya, A. M., Kudale, M. D., " Design of Fishing Harbour Layout in High Littoral Drift Zone". *Procedia Engineering*, Vol.115, 2015, pp.320-325
3. Barve, K. H., Ranganath, L. R., M. Karthikeyana, Kori, S., and Kudale, M. D., "Wave Tranquility and Littoral Studies for Development of a Mini Fishing Harbour". *Aquatic Procedia*, Vol. 4, 2015, pp. 72-78
4. Jitendra K. Panigrahi, Padhy, C. P., Murty, A. S. N., "Inner Harbour Wave Agitation using Boussinesq Wave Model". *International Journal of Naval Architecture and Ocean Engineering*, Vol. 7, Issue 1, January, 2015, pp. 70-86.
5. Laknath, D. P. C., Caldera, H. P. G. M. and Ranasinghe, D. P. L., "Wave Hindcasting and Extreme Value Analysis for North-western Coast of Sri Lanka", *Proc., 27th International Offshore and Polar Engineering Conference, ISOPE, San Francisco, USA, 2017*
6. Madsen, P. A., and Sorensen, O. R., "A New Form of the Boussinesq Equations with Improved Linear Dispersion Characteristics". *Coastal Engineering*, Vol. 18, 1992, pp. 183-204.
7. Madsen, P. A., Sørensen, O. R., and Schäffer, H. A., "Surf Zone Dynamics Simulated by a Boussinesq Type Model. Part I. Model Description and Cross-Shore Motion of Regular Waves". *Coastal Engineering*, Vol. 32, 1997a, pp. 255-287.
8. Madsen, P. A., Sørensen, O. R. and Schäffer, H. A., "Surf Zone Dynamics Simulated by a Boussinesq Type Model. Part II: Surf Beat and Swash Oscillations for Wave Groups and Irregular Waves". *Coastal Engineering*, Vol. 32, 1997b, pp. 289-319.
9. Sørensen, O. R., Schäffer, H. A. and Sørensen, L. S., "Boussinesq-Type Modelling using An Unstructured Finite Element Technique". *Coastal Engineering*, Vol. 50, 2004, pp. 181-198.

Verification of Wave Transformation to Establish the Nearshore Wave Climate

D.P.L. Ranasinghe, N.L. Engiliyage, H.P.G.M. Caldera and I.G.I. Kumara

Abstract: MIKE 21 SW model simulation and wave transformation matrixes have been used to transform the reordered wave data to desired locations. Both back and forward transformation were carried out since the direct transformations were not possible due to the geophysical features exist between wave sources and the destination. As the first step, all the measured data (Galle and Hambantota) were transferred to a 100 m depth directly located off Gandara coast and then transferred to Gandara and Kudawella (15m depth) which is the nearest location with recorded wave data to Gandara. The comparison depicted that the South-west and Inter-Monsoon 1 monsoonal waves transformed from Galle shows a statistical mismatch with on-site recordings while all the transformed data from Hambantota is in lined with recorded data. Furthermore, it has been observed that local features like headlands decline the southwest sea wave effect in Gandara which is prevailing at southern coast. The transformed wave data which could not be statistically verified were not used to develop wave data base at Gandara. Upon completion of building up of the wave data base for Gandara, the extreme wave occurrences were estimated by extrapolating the wave heights within the built-up data base. Furthermore, relevant peak wave period for extreme wave heights was also obtained through a measured data in the vicinity. The obtained extreme values for 50 years return period ($H_s=3.89$ m, $T_p=14.9$ s) at Gandara 20 m depth were compatible with past relevant studies done on the southern coast. Thus, the importance of verification and screening process of transformed wave data in the establishment of nearshore wave climate was evident.

Keywords: Galle offshore, Gandara, extreme peak wave period

1. Introduction

1.1 General

As the behaviour of a coastal zone is completely different from one to another, site specific parameters are required prior to the design of coastal structures. Furthermore, the designs need to withstand against the extreme events that could be occurred during its design life. Therefore, extreme wave analysis is needed through a long term wave data in order to have a long lasting and cost effective design of coastal structures. Even though the relevant details on the bathymetry and topography could be obtained through a single survey exercise, it is unable to obtain a considerable measured wave data series at each and every location that needs a coastal development. Therefore, numerical models are played a vital role to transform the recorded wave data to the desired location for the purpose of obtaining the design wave parameters which are locally unavailable.

Currently, there are several commercial and non-commercial software that can be used for numerical model simulations to assess the wave transformation process due to shoaling, refraction, wave breaking etc. Among them, MIKE 21 SW module has been used as the

numerical modelling platform in this study. Even though a large number of data is given the higher accuracy on generated wave climate, higher computational time is required to handle the data. The situation will be further complicated and time-consuming when the measured data is available at different locations. In such a situation usage of wave transformation matrix method would be an advantage.

1.2 Study Area

The proposed site Gandara is situated in the Southern coastal belt in Devinuwara Divisional Secretariat division of Matara District (Figure 1). Being a partially sheltered Bay, the proposed location is currently acted like a fish landing centre. However, the navigation difficulties exist near landing site due to the rocky outcrops in the nearshore area.

Eng. (Dr.) D.P.L. Ranasinghe, C.Eng., MIE(SL), B.Sc. Eng.(Ruhuna), M.Sc. (Moratuwa), Ph.D.(Tohoku), Engineering Manager, Lanka Hydraulic Institute.

Eng. N.L. Engiliyage, AMIE(SL), B.Sc.Eng.(Moratuwa), Research Engineer, Lanka Hydraulic Institute.

Eng. H.P.G.M. Caldera, AMIE(SL), B.Sc.Eng. (Peradeniya), Research Engineer, Lanka Hydraulic Institute.

Eng. I.G.I. Kumara, AMIE(SL), B.Sc.Eng.(Moratuwa), Research Engineer, Lanka Hydraulic Institute.



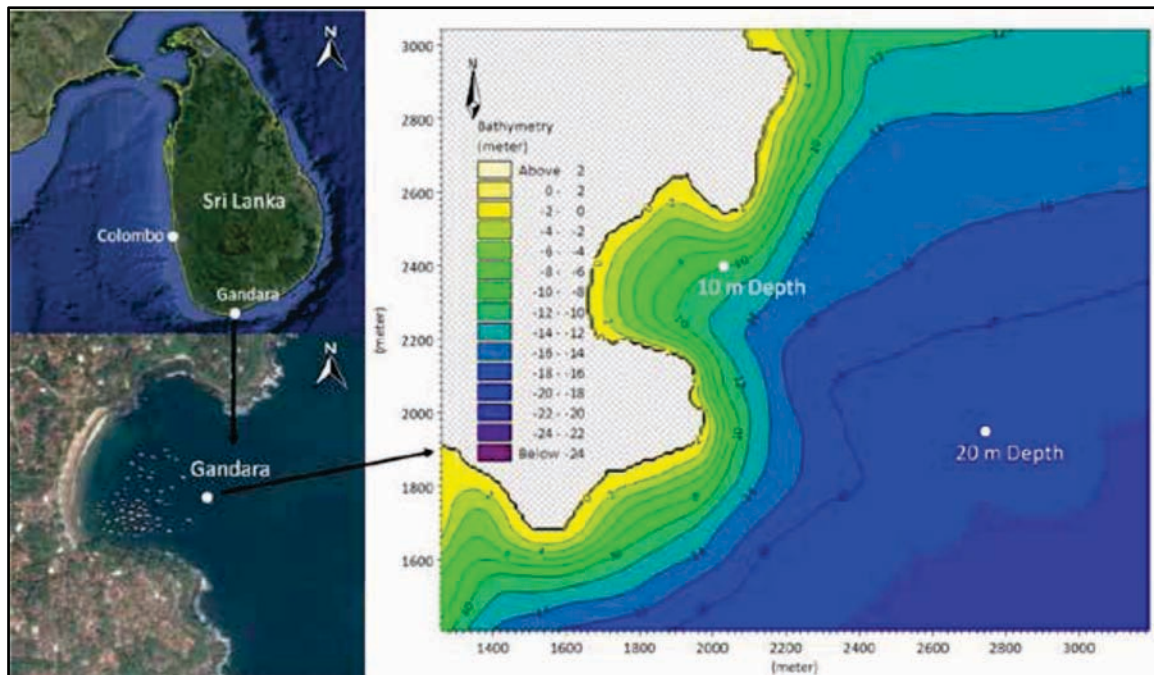


Figure 1 - Location Map and Local Bathymetry [1] (Source: <http://maps.google.com>)

Therefore, the necessity of the maximum utilization of the Bay via breakwater is evident. Both south and north part of the bay is covered by the cliffs while small beach area is situated in the southwest of the bay. Therefore, sediment intrusion due to alongshore transport seems to be a negligible and seasonal variation of the shoreline could be visible from the sandy beach area [1]. Since Gandara on-site wave recordings were not available, the transformation of wave data from other available locations off the southern coast was found to be necessary to establish the data base.

1.3 Objectives

The purpose of this study to establish nearshore wave climate at Gandara (20m and 10m depths) using measured wave data at Galle offshore (70 m depth) and Hambantota near shore (17m and 10m depths) in Sri Lanka through a detailed verification using measured wave data at Kudawella (15 m depth) and hence, to estimate the extreme waves.

2. Wave Data Base and Existing Wave Climate at Southern Coast of Sri Lanka

The southern coast of Sri Lanka is subjected to the dual influence of two distinct wave systems, namely swell waves and sea waves. Swell waves are those generated by wind fields in the vast open sea areas of the Southern Indian Ocean and have propagated beyond the generating fetch to reach the coast. These waves approach from a southerly direction in the deep sea. However, as they approach the shore, the

effect of refraction causes the wave direction to change towards a shore normal direction. Therefore, local variations in swell wave directions are observed in shallow nearshore waters. The sea waves are those waves being generated by the local wind fields. They have shorter periods compared to swell waves and are much steeper representing a chaotic sea state with component waves widely scattered in approach direction. The southern coast of Sri Lanka is primarily subjected to the influence of sea waves generated by south-westerly monsoonal winds. However, moving towards the south-east, progressively increased the influence of north-east monsoonal sea waves is observed.

A summary of available wave data in Southern Sri Lanka that has been considered in this study is given in Table 1, and the wave recording locations are indicated in Figure 2.

Table 1 - Available Wave Data at Southern Coast

Location/Depth	Duration	
	From	To
Galle (70m)	Feb 1989 May 1994	Sep 1992 Sep 1995
Kudawella (15m)	Jan 1996	Feb 1997
Hambantota (17m)	Dec 2002	Mar 2003
Hambantota (17m)	May 2006	May 2009
Hambantota (10m)	Apr 2013	Mar 2014



Figure 2 - Wave Recording Locations and Wave Transformation Sequences
(Source: <http://maps.google.com>)

The most comprehensive wave data base available for the southern coast is that the directional wave recordings conducted around 70 m water depth, about 8 km offshore of Galle under the CCD-GTZ directional wave climate study. Considering the deep sea location used for recording waves, CCD-GTZ wave data can be regarded as representative of swell waves at that depth for the entire southern coast. Furthermore, these data can also be readily used for transformation of monsoons' induced sea waves to other locations [2]. Directional wave recordings at 15 m water depth in Kudawella were carried out in 1996-1997 about 13 km northeast of Gandara. Apart from that, two sources of oceanographic data available from Hambantota near shore at 17 m and 10 m water depths.

Due to close proximity to Gandara, Hambantota wave recordings can be considered to constitute a reliable data base for transformation in the first instance. However, the possible sheltering effect on sea waves by local coastline features like headlands could restrict the usage of whole recorded wave data at Hambantota for deriving wave conditions at Gandara. In some monsoonal sea waves approaching to Gandara exhibit a very weak influence on the Galle offshore wave recording location and vice versa. However, it has been identified that establishment of nearshore data base using overall waves is more appropriate to estimate the design wave parameters. Therefore, waves transformed from Galle offshore and Hambantota near shore to Gandara should be used with caution and requires prior verification comparing with on site wave recordings from Kudawella which is the nearest location with recorded wave data to Gandara.

3. Numerical Model Simulations

Since accurate assessment of wave conditions is very important for designing structures in coastal regions or designing harbour structures, wave modelling is essential. As wave induced currents have a significant role in transporting sediment in coastal areas, knowledge of wave climate is necessary in order to carry out coastal design structures with the minimal impact to the existing littoral movements.

The spectral wave module, DHI MIKE 21 SW developed by Danish Hydraulic Institute, Denmark, is a state-of-the-art spectral wind-wave model. The module enables to simulate growth, decay and transformation of wind-generated waves and swells in offshore and coastal areas. The model includes the main physical phenomena, for example, the processes of wave generation by wind, quadruplet wave-wave interactions, white-capping and bottom friction [3]. Further, this model handles processes that only affect waves in coastal waters such as depth induced wave breaking and triad wave-wave interactions. The formulations for the wave generation processes are based on the wave action balance equation (i.e. in MIKE 21 SW the waves are represented by the wave action density spectrum). MIKE 21 SW uses an unstructured mesh for the numerical solution. An unstructured mesh has the advantage that it is highly flexible and therefore suitable for modelling projects where high resolution is needed in the area of interest, and coarse resolution is sufficient in the surroundings. The necessary model Input data of MIKE 21 SW Model can be divided into groups such as domain and time parameters, equations, discretization and solution technique, forcing parameters, source function



parameters, initial conditions and boundary conditions. Model Output such as significant wave height (Hs), peak wave period (Tp), mean wave direction (MWD) and radiation stress tensor can be obtained from MIKE 21 SW at each mesh point for each time step.

3.1 Wave Transformation

The applied methodology to hind cast wave climate of this study is based on the application of MIKE 21 SW model to simulate wave propagation off the southern coast (offshore) and using a wave transformation matrix approach to transform wave recordings based on reproduced model results. Wave propagation modelling was carried out to transform wave recordings from Galle and Hambantota to representative locations in the study area. Thus, representative nearshore wave climate was established at 20 m and 10 m water depths in the study area (Gandara). Both back and forward transformation were carried out since the direct transformations were not possible due to the geophysical features exist between wave sources and the destination. As the first step, all the measured data were transferred to a 100m depth directly located off Gandara coast and then transformed back to the desired destination locations (Gandara and Kudawella). For minimizing a large number of data transformation of individual wave recordings, a transformation matrix approach which relies on the transformation of a selected set of wave conditions at the offshore boundary was adopted. A set of wave conditions comprising combinations of following wave parameters were specified at the offshore boundary. Thus, MIKE 21 SW model simulation was carried out to transfer combination of wave parameters as presented in Table 2.

Table 2 - MIKE 21 SW Model Setup

Hs (m)	Tp (s)	MWD(°N)
0.5	1,2,.....27	40,50,.....260
1.0	1,2,.....27	40,50,.....260
⋮	⋮	⋮
5.0	1,2,.....27	40,50,.....260

The specific significant wave heights of 0.5 m, 1.5 m.....and 4.5 m were assumed to represent offshore wave height ranges 0 m - 1.0 m, 1.0 m - 2.0 m.....and 4.0 m - 5.0 m respectively. Since

waves are highly influenced by wind field, well established Beaufort Scale standard was used to incorporate the wind speed to the simulation. Accordingly, the wind speed was correlated with the offshore significant wave height based on the Beaufort Scale [4] description of the marine water (Table 3). It is assumed that wind directions are similar to the offshore wave direction over the entire model domain.

Table 3 - Wind Speed for Offshore Significant Wave Height [4]

Significant Wave Height (m)	Speed (m/s)
0.5	2.9
1.0	4.8
1.5	6.6
2.0	8.3
2.5	9.8
3.0	11.2
3.5	12.5
4.0	13.7
4.5	14.8
5.0	15.9
5.5	16.9

The southern coastal belt is influenced by two major monsoons of South West (SW: May – September) and North East (NE: December - February) as well as the two inter monsoons (IM1 and IM2) created due to changing of wind patterns end of the major monsoons. Therefore, all the four seasons were considered for the simulations and the analysis in order get the insight of the seasonal variation in wave climate.

3.2 Assessment and Verification of Wave Transformation

The verification of wave data sets obtained by transformation from different locations and on-site recordings in the time domain is not possible as there is no physical overlap between different data sources. Therefore, the comparison between different wave data sources was made only in a statistical sense. Such comparisons for measured and transformed data sets at Kudawella are illustrated in Figure 3 for overall seasonal waves. In these illustrations, the mean value of a particular wave direction class interval considered (e.g. 155° in the direction class 150° - 160°) represents that particular direction class interval.

It is not realistic to expect similar distributions in wave heights in two data sources covering different durations. A longer duration wave

data source is more likely contain high and extreme waves. However, at a given location a particular wave system is known to approach from a characteristic direction range over different seasons. Therefore, in the statistical comparison, these trends in directional distributions were looked at for different data sources. In this exercise, the two main considerations for satisfactory comparison between two data sets adopted were: similarity in dominant wave approach direction; and similarity in range of wave directions. The magnitude of the percentage of waves representing the dominant wave direction is only of secondary importance, as that will vary with the time duration covered by the wave data source.

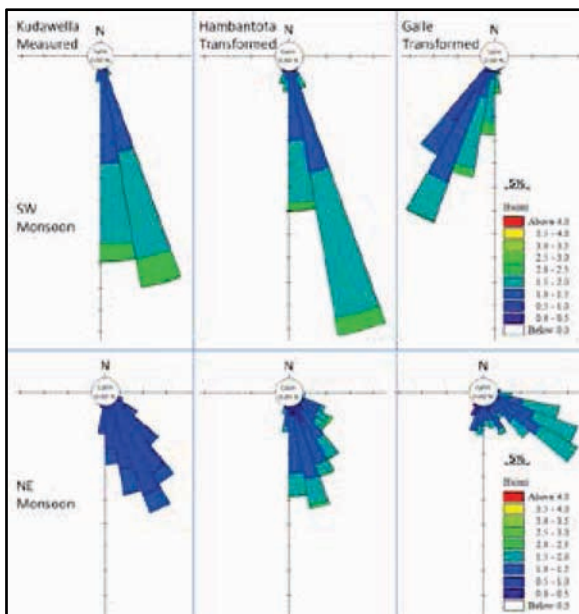


Figure 3 - Wave Roses for Measured and Transformed Data at Kudawella 15 m Depth

As shown in Table 4, the comparisons between different data sets clearly indicate that wave data transformed from Hambantota showed similar directional trends throughout the year as obtained from Kudawella site recordings. Galle offshore transformed wave data, although compared poorly with site recordings during SW and IM1 seasons. In contrast, Galle transformed data indicates the very similar range of approach directions in NE season while IM2 season shows similar dominant direction with wider direction band. These findings indicate that in the SW and IM1 seasons wave data transformed from Hambantota can be combined with on-site recordings, while in the other two seasons of the year additionally, wave data transformed from Galle offshore could also be combined to

constitute a representative directional wave data base.

Table 4 - Comparison of Transformed Wave Data

Season	Measured	
	MWD(°N)	Direction Band(°N)
SW	165	160-180
IM1	175	160-180
NE	155	130-180
IM2	165	150-180
Transformed from Hambantota		
SW	165	160-180
IM1	165	150-190
NE	165	120-180
IM2	165	160-190
Transformed from Galle		
SW	205	190-220
IM1	195	170-220
NE	125	100-160
IM2	175	160-220

4. Nearshore Wave Climate at Gandara

As concluded in Section 3.2, the following wave data sets were combined to constitute the directional wave data bases for overall waves at Gandara 20 m and 10 m water depths (Table 5). Therefore, transformed data from Hambantota for SW and IM1 seasons and transformed data from Hambantota and Galle for NE and IM2 were used to develop the nearshore wave data base at Gandara.

Table 5- Selection of Transformed Wave Data

Season	Transformed From		
	Hambantota 17m	Hambantota 10m	Galle 70m
SW	√	√	X
IM1	√	√	X
NE	√	√	√
IM2	√	√	√

The established wave data series at Gandara nearshore 20 m depth indicates that comparatively high waves are approaching from the southern direction in SW monsoon while during NE monsoon lower magnitude's



wave is dominating with a wider direction band in south-east quadrant (Figure 4). In other words, swell component is higher than the sea component in SW overall waves and vice versa in NE overall waves at 20 m depth of Gandara. Table 6 indicates the characteristics of high and average waves in all four seasons.

Table 6 - Average and High Wave Conditions at Gandara 20 m Depth

20 m Depth	Average (50% Exceedance)			Extreme (2% Exceedance)		
	Hs (m)	Tp (s)	MWD (°N)	Hs (m)	Tp (s)	MWD (°N)
SW	1.7	13.5	187	2.3	14.2	187
IM1	1.5	11.8	187	2.5	15.5	187
NE	1.3	5.6	152	1.9	14.4	184
IM2	1.5	9.6	189	1.9	11.4	187

Due to the effect of local features like headlands and the nearshore bathymetry, all the waves at 10 m of Gandara Bay is approaching from Southeast direction despite monsoonal change (Figure 4).

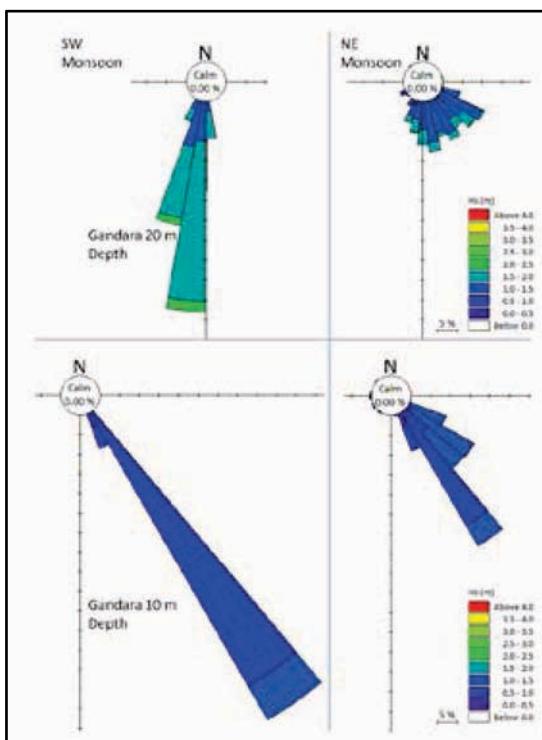


Figure 4 - Wave Statistics at Gandara 20 m and 10 m Depths

5. Extreme Wave Analysis

In the design of breakwater structures for the proposed harbour, it is necessary to ensure the structural stability against extreme wave events. Since it is expected to design the structures for 50 years of design life, a significant wave height of 100 year return period (YRP) is considered as the design wave height. However, very high waves are likely to be attenuated due to breaking before reaching the structure, whereas a wave of somewhat lower return period may approach the structure without significant reduction in height. Therefore, Extreme wave analysis was performed for different return period as well as for both 20 m and 10 m depths. Results obtained at 20 m depth will be used for the harbour tranquillity modelling while 10 m depths data is needed to design the proposed marine structures.

5.1 Significant Wave Heights

The extreme significant wave heights for annual overall waves for Gandara (20 m and 10 m) were determined through extrapolation of time series established a database. In the method adopted, the maximum wave heights occurring during 3 hours storms were selected for extrapolation and data series was controlled for the outliers [5]. This selection of wave heights yields a statistically independent set of data appropriate for making predictions. The inclusion of comparatively low wave heights in an extreme wave analysis would often lead to underprediction. In order to exclude such storms, the Peak Over Threshold (POT) method was applied [5]. Selected storm events were fitted to the standard statistical Extreme Value Probability distributions and evaluated the goodness of fit of each distribution. It was observed that the selected wave data was well fitted with three parameters (Shape parameter- α , Scale Parameter- β , Location Parameter- γ) Weibull Distribution (3P WD) and yielded most consistent results compared with other distributions. Therefore, 3P WD (with $\alpha=1.0$) was adopted to compute the extreme wave heights for different return periods using regression analysis [6].

5.2 Peak Wave Periods

The estimation of peak wave period that can be associated with extreme significant wave height is still a challenging task for the coastal engineers. Since the estimated extreme wave heights are not included in the primary data series, a direct correlation is unable to obtain.

On the other hand, breaking the effect of higher waves could be reduced when the extrapolation of peak period is used in the analysis. Therefore, special care need to be taken while choosing the appropriate extreme wave periods since overtopping behaviour is completely different in short (sea) and long (swell) periods waves. Hence, available data records at the vicinity were carefully analysed in order to obtain a correlation between wave heights and the wave periods. The design wave period for particular extreme significant wave height was estimated using regression analysis [5]. This regression line was generated for the measured data at Hambantota 10 m depth as it contains a robust set of data. Since overall wave heights were considered in this study, mean wave periods (T_z) were considered instead of peak wave period (T_p) to develop the relationship. Because the scatteredness of the peak wave periods are higher than that of the mean wave periods for the same wave heights. In order to develop the better relationship, wave heights were split into the classes of 0.2 m intervals, and the average of each class was plotted against particular mean wave periods, and the regression line was obtained. Computed mean wave periods for extreme wave heights were then transferred to peak wave period using $T_p=1.4T_z$ relationship which was estimated using recorded data in the vicinity. The computed extreme wave heights and the relevant peak wave periods are given in Table 7.

Table 7 - Extreme Waves for Different Return Periods at Gandara 20 m Depth

Return Period	Hs/(m)	Tp/(s)
2	3.28	14.4
10	3.58	14.7
25	3.76	14.8
50	3.89	14.9
100	4.02	15.0

6. Comparison of Results

Since the structural stability and hence its durability depend on the accuracy of the design wave parameters, compatibility of obtained results has been compared with previous studies that have been done for the southern coastal belt. The studies done for the overall waves could be directly compared with the present study while other studies provide the indication of Sea and Swell component of the

overall waves during each monsoon. Extreme waves for the same return period wave illustrated in Table 8 for better comparison. It is observed that the extreme waves for Gandara near shore are in line with the previous studies done for the adjacent locations.

Table 8 - Summarized Results for 50 YRP Extreme Waves in Southern Coast

Location	D (m)	Designed Wave conditions		Wave Type	Ref.
		Hs (m)	Tp (s)		
Suduwella	15	4.37	16.5	AS	[7]
	15	3.85	8.5	ASea	
Kudawella	15	3.41	16.9	AS	[8]
	15	2.52	5.4	ASea	
Kudawella	15	2.74	13.0	AS	[9]
		3.33	5.0	SWS	
		2.86	4.0	NES	
Hambantota	17	3.58	16.8	AS	[10]
		4.92	4.5	SWS	
		2.60	4.5	NES	
Hambantota	17	3.86	13.5	AS	[9]
		4.09	4.5	SWS	
		2.59	5.0	NES	
Gandara Present Study	20	3.89	14.9	AO	
	10	2.97	14.0	AO	

Note: D-Depth, AO- Annual Overall, AS- Annual Swell, SWS-SW Sea, NES-NE Sea, ASea-Annual Sea

7. Conclusions

Model verification using Kudawella wave recordings indicated that the transformed wave data from Hambantota for all seasons and Galle transformed data only for NE and IM2 seasons could be utilized to establish the wave data base at Gandara Nearshore. The wave statistics at Gandara depicted that swell component is higher than the sea component in SW overall waves and vice versa in NE overall waves at 20 m depth of Gandara. Furthermore, all the waves at 10 m of Gandara Bay are approaching from Southeast direction despite the monsoonal change. Estimation of peak wave period which associates with extreme wave heights concluded that swell component of extreme overall waves would be higher than the sea component in Gandara Nearshore.



Acknowledgement

The authors wish to acknowledge the “Construction of Fishery Harbours and Anchorages Project” of MFARD (Ministry of Fisheries and Aquatic Resources Development) in Sri Lanka and the Project Director, Eng. K.K.P.P. Ranaweera as well as to Dr. K. Raveenthiran for the various supports given during this research. Further, the authors' gratitude also extended to Late Dr. P. P. Gunaratne for his involvement and guidance given for wave climate studies in Sri Lanka.

References

1. Lanka Hydraulic Institute, Interim Report 1 on Detailed Design on Gandara Fishery Harbour, 2017.
2. Scheffer, H. J., Fernando, K. R. M. D. and Fittschen, T. Directional Wave Climate Southwest Coast of Sri Lanka. Colombo. CCD-GTZ Coast Conservation Project, 1994.
3. DHI, MIKE21 Spectral Wave Module. Scientific documentation, Danish Hydraulic Institute (DHI), 2009.
4. https://en.wikipedia.org/wiki/Beaufort_scale, Visited, 10th March 2017.
5. Caires, S., Extreme Value Analysis: Wave Data, JCOMM Technical Report No. 57, World Meteorological Organization, 2011.
6. Kamphuis J. W., Introduction to Coastal Engineering and Management 2nd Edition, Advanced Series on Ocean Engineering-Volume 30, World Scientific, 2000
7. Uni Consultancy Services: University of Moratuwa, Final Report on Feasibility Study for the Development of a Fishery Harbour at Suduwella, Kottagoda in Matara District, 2009.
8. Lanka Hydraulic Institute, Final Report on Kudawella Fishery Anchorage Development, 1997.
9. Ranasinghe, D. P. L. and Gunaratne, P. P. Assessment of Nearshore Wave Climate In Southern Coast Of Sri Lanka, Annual Research Journal of SLSAJ, Vol. 11, Japan, 2011.
10. Lanka Hydraulic Institute, Final Report on Mathematical Model Test on Wave Field: Hambantota Seaport Development - Phase I, 2008.

Fabrication and Mechanical Property Analysis of Microcrystalline Cellulose Based Polymer Composite for Engineering Applications

H.A.D. Saumyadi, L.D. Rajapaksha, A.M.P.B. Samarasekara
D.A.S. Amarasinghe and L. Karunanayake

Abstract: In the last several years, polymer composites have been used heavily in aerospace, automotive and other engineering applications. Natural fibers are recently getting attention from researchers and academia to utilize in polymer composites due to their eco-friendly nature and sustainability. In this research, Polypropylene matrix with microcrystalline cellulose (MCC) reinforced composite was investigated for their mechanical properties.

MCC was subjected to surface modification technique to improve compatibility with hydrophobic Polypropylene (PP) using silane treatment. Polypropylene was mixed with surface treated MCC by varying MCC concentration (1% wt. to 5% wt.) in a laboratory type internal mixer. Impact, tensile, hardness and water absorption tests were performed to evaluate the mechanical properties of the developed composites. Experimental results showed that gradual increase of tensile strength, hardness and impact strength with increase of MCC concentration. Polypropylene with 4 wt. % sample showed the maximum impact strength and it was 18.2 KJ/m². Maximum water absorption (0.02%) was observed in 5 wt% MCC containing sample. 5wt% MCC containing sample showed the maximum hardness (74.4 Shore D). Developed composite showed the gradual reduction of density from 1 wt% MCC (0.882 g/cm³) to 5 wt% MCC (0.826 g/cm³). Therefore, Polypropylene with MCC polymer composite can be used for different engineering applications providing attractive benefits.

Keywords: Micro crystalline cellulose, composite, polypropylene

1. Introduction

Cellulose is a naturally occurring polysaccharide and it is the most abundant bio polymer. Microcrystalline cellulose (MCC) is a member of cellulose family. Compared to natural cellulose fibres, MCC possesses several advantages, such as micro scale dimension, high strength per mass and higher modulus, higher specific surface area, unique optical properties, etc. MCC has high strength due to their dense and orderly crystalline structure [1-7].

Other benefits of cellulose crystals include not costly and they are light weight with micro scale dimensions and unique morphologies. MCC can be used as high-quality reinforcing filler for polymers and biodegradable materials. There are researches about glass fibre /polypropylene composites to improving mechanical properties [8-10]. Increasing mechanical properties such as shock absorbance and strength is the aim of this research by using MCC/polypropylene composite than other fibers with polypropylene based composite. Furthermore, bio-based plastics may provide so many advantages such

as reduced petroleum use, life-cycle emissions and part weight while increasing recyclability of polymers. Natural fiber based composites materials are widely used in different industries due to their extraordinary properties. The development and the application of polymeric composite materials filled with micro sized rigid particles has been attracted both scientific and industrial interest [11-13]. The objective of this research was to develop a MCC and polypropylene based composite with improved mechanical properties.

Ms. H.A.D. Saumyadi, B.Sc. Eng. (Moratuwa), Dept. of Materials Science & Engineering, University of Moratuwa.

Mr. L.D. Rajapaksha, B.Sc. Eng. (Moratuwa), Dept. of Materials Science & Engineering, University of Moratuwa.

Eng. A.M.P.B. Samarasekara, B.Sc.Eng.(Moratuwa), M.Phil. (Moratuwa), AMIE(Sri Lanka), Senior Lecturer, Dept. of Materials Science & Engineering, University of Moratuwa.

Dr. D.A.S. Amarasinghe, B.Sc.(Kelaniya), MSc. (Moratuwa), M.Phil. (CUNY, USA), Ph.D.(CUNY, USA), Senior Lecturer, Dept. of Materials Science & Engineering, University of Moratuwa.

Prof. L. Karunanayake, B.Sc. (USJP), Ph.D. (North London), Professor, Department of Chemistry University of Sri Jayewardenepura.



2. Experimental Procedure

2.1 Material

Ethanol ($\text{H}_3\text{CCH}_2\text{OH}$, Min. 99.85 %, ACS, VWR Chemicals), Stearic acid (Sigma-Aldrich), Toluene ($\text{C}_6\text{H}_5\text{CH}_3$, $\geq 99.7\%$, ACS, Sigma-Aldrich) were used for surface modification of MCC.

2.2 Characterization of MCC

MCC was confirmed as pure MCC with correct structure and size by using SEM image, FTIR spectrum (KBr) and TGA techniques.

2.2.1 FTIR Spectroscopy

The MCC sample was mixed with KBr and grinded well to prepare fine powder and compressed to make disc. FTIR spectrum was recorded on FTIR Bruker (α) alpha spectrophotometer in frequency range of 4000-600 cm^{-1} , with a resolution of 4 cm^{-1} , in transmission mode. A total of 30 cumulative scans were taken.

2.2.2 Morphological investigation

The surface morphology of the MCC and surface modified MCC particles were investigated by Scanning Electron Microscope (CARLZEISS EBO - 18). A sample was coated with gold layer until 90 seconds under high vacuum and then observed with an accelerating voltage of 20 kV.

2.2.3 Thermogravimetric analysis (TGA)

Thermo gravimetric analysis was performed with a TAS100 instrument to study the degradation characteristics of the obtained MCC. The samples were dried in oven at 80 $^{\circ}\text{C}$ for more than 8 h before test. The samples were heated from 30 to 800 $^{\circ}\text{C}$ at a heating rate of 10 $^{\circ}\text{C min}^{-1}$ under N_2 atmosphere.

2.3 Surface modification methods

The surface energy of polymer must compatible with MCC. Therefore, modification of MCC is a critical process to develop composite material.

2.3.1 Stearic acid treatment

Stearic acid 1.7 g was mixed with toluene (200 ml). MCC 20 g was added to stearic and toluene solution and subjected to ultrasonic disruption (50 kHz, 10 min) then stirred for one hour at room temperature. Then solution was dried at room temperature to constant weight to remove toluene and residual solvent.

2.3.2 Silane treatment (Si -69 treatment)

20 g of MCC was added into 85 wt% ethanol, dispersed by ultrasonic waves for 20 min, then mixed with mixed solution which was 20 wt% & 30 wt% Si-69(6 g) and 85 wt% ethanol medium for 1 h. The mixture was dispersed by ultrasonic waves for 5min, magnetic stirring at 70 $^{\circ}\text{C}$ for 3 h. The modified material was washed with ethanol and extracted. The mixture was dried at room temperature to constant weight.

2.4 Composite preparation

Modified MCC and PP were mixed by varying composition 1-5 wt.% to obtain good composite properties. Maximum 5 wt% MCC was given the optimum mixing homogeneity. Internal mixing method was used as composite preparation and compression moulding was used for sample preparation.

2.4.1 Composite preparation- Batch preparation

Modified MCC (varying 1-5% wt.) and PP were well mixed by using internal mixer for 5 min. (Brabandary type, Fill factor-0.8, temperature-150 $^{\circ}\text{C}$, rotor speed - 65 rev/min).

3. Testing procedure

3.1 Testing sample preparation

Prepared composite batch samples (by considering MCC percentage variation and modified method variation) were compression moulded under 165 $^{\circ}\text{C}$ for 8 min, with 0.75 psi pressure. Then samples were cooled under room temperature in 15 min.

3.1.1 Impact test

80 mm length, 10 mm width and 2 mm thickness samples were cut from prepared testing samples and cut the notch according to ISO 180 methods. Five specimens were measured for each sample by using Izod impact testing machine.

3.1.2 Tensile Test

Sample dimensions were 2-3 mm thickness, 3-5 mm width and 30 mm length. The strain rate was 30 mm/min, extension range was 400 and applied load was 1 kN at 25 $^{\circ}\text{C}$. The five samples were measured for each MCC percentage. Tensile forces and elongation at break were measured by using universal tensile testing machine. This test was conducted according to the ASTM D638 standard.

3.1.3 Hardness

Hardness of samples was measured using a shore durometer according to the ASTM D2240 standard. Several points of each sample were measured to obtain Hardness values.

3.1.4 Water absorption test

Five samples were selected for each MCC percentage. Samples were weighted and then soaked in distilled water at room temperature. The samples were removed at specific time intervals (24 hrs), and removed the excess water on the surface and immediately weighed. This test was conducted according to the ASTM D570 standard.

3.1.5 Density test

Densities of the samples were measured by Specific gravity (SG) meter. Five samples were tested for each MCC weight percentage up to 5%. This test was conducted according to the ASTM D792 standard.

4. Results and Discussion

4.1 Characterization of MCC

4.1.1 FTIR analysis

As per Figure 1, analysing a FTIR spectrum of the microcrystalline cellulose, it was possible to tell that existence of a wide band in the field of 3348 cm^{-1} . It showed that there are large number of various types of hydrogen bonds, formed by $-\text{OH}$ groups. [14] There was a peak at 2901 cm^{-1} due to the band of symmetric and asymmetric vibrations of CH_2 groups. As well as deformation vibrations of CH_2 and CH groups and angular deformation vibrations of C-O-H were located in the field $1637\text{--}1372\text{ cm}^{-1}$. If there are hemicellulose and lignin, there should be peaks at 1736 cm^{-1} and 1512 cm^{-1} . However, that peaks were not appeared in this spectrum. That means, hemicellulose and lignin have been removed.

The band at 1637 cm^{-1} was assigned to the

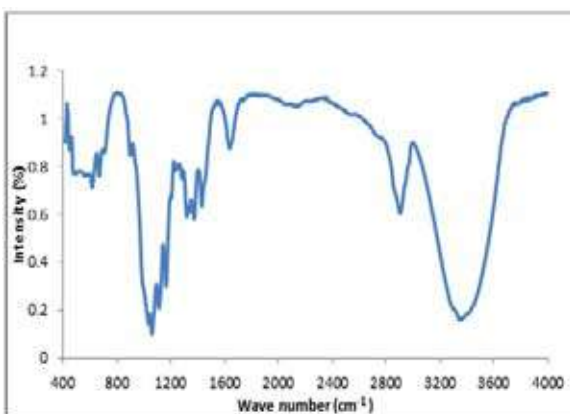


Figure 1 - FTIR Spectrum of Unmodified MCC

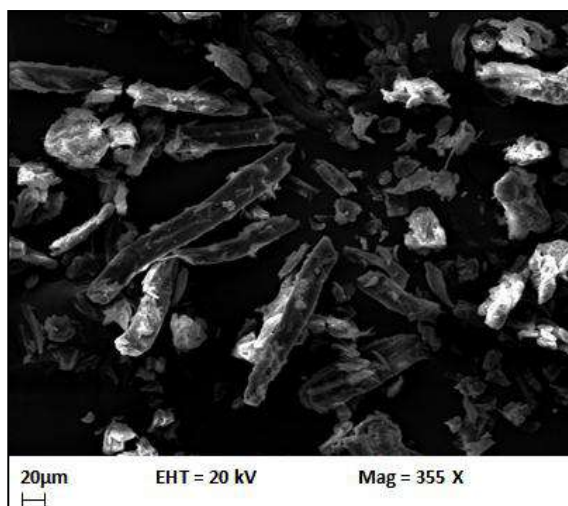


Figure 2 - SEM image of Unmodified MCC

absorbed water [15]. By analysing FTIR spectrum, we could confirm that obtained MCC was pure.

4.1.2 Morphological Investigation

According to the SEM images in Figure 2, needle type structure could be observed. Length and diameter of the microcrystals were differed and had the sizes from 1 to 100 microns [15].

4.1.3 Thermogravimetric Analysis (TGA)

Figure 3 shows the TGA and DTG curves for MCC. MCC sample undergoes mass loss from $30\text{ }^\circ\text{C}$ to $700\text{ }^\circ\text{C}$. There was an endothermic peak at $75\text{ }^\circ\text{C}$ due to the evaporation of water in this sample. So there was a 5.7% of weight loss due to the evaporation of vapour. Additionally to the above degradation stage, there was another degradation stage. The 2nd degradation was believed to be due to the pyrolysis of MCC. There was 88.5 % of weight loss at the 2nd degradation stage. The total weight loss found at 700°C was 94.2%.

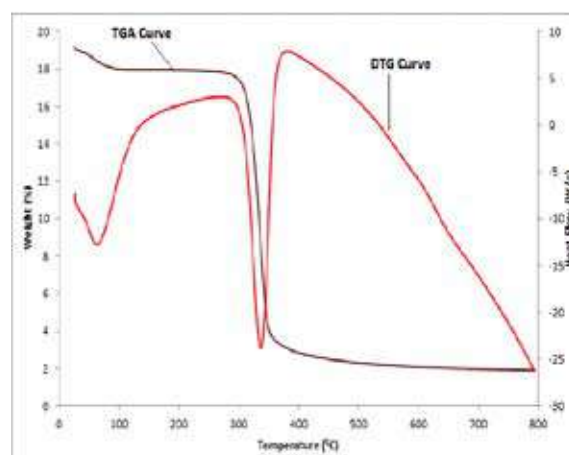


Figure 3 - TGA and DTG Curves

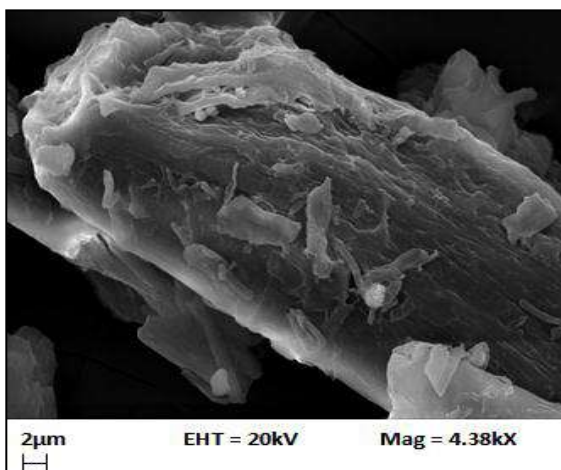


Figure 4 - SEM micrograph of surface modified MCC by (Si-69)

4.2.Characterization of Surface modified MCC

4.2.1 Morphological Investigation

According to the above SEM images, there were bonded parts due to the silane (si-69) on the surface of the MCC. So MCC had been surface modified by Silane 69.

4.2.2 FTIR Analysis

FTIR spectra of MCC (Figure 5) exhibited the typical bands of cellulose. The -OH stretching of intramolecular hydrogen bonds at 3,700–3,000 cm^{-1} , the C-H stretching at 2,901 cm^{-1} , the C-H bending at 1,370 cm^{-1} , the C-O stretching at 1,059 and 1,033 cm^{-1} . The spectral data of pure stearic acid showed (Figure 5) a sharp absorption at (1700-1710) cm^{-1} wave number for carbonyl (C=O). The spectral data of stearic acid treated MCC also showed absorption at 1703 cm^{-1} . This indicates that unreacted stearic acid is remained on the surface of the MCC. The stearic acid treated MCC also showed a small peak at 1732 cm^{-1} , corresponding to the

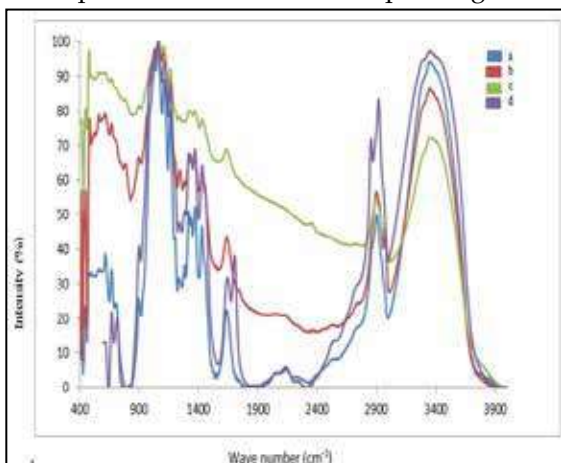


Figure 5 - FTIR spectra of (a) untreated MCC (b) 20%Si-69-treated MCC (c) 30% Si-69-treated MCC (d) stearic acid treated MCC

stretching vibration of the ester linkages (-C=O) expected between 1725 and 1750 cm^{-1} .

This confirmed that the formation of carboxylate linkages between stearic acid and MCC. The reduction of peak intensity was not noticed at 3000-3700 cm^{-1} , corresponding to the -OH group in cellulose structure. According to the Figure 5, stearic acid has been reacted with some amount of -OH group in cellulose. So, there were untreated -OH groups in MCC structure [16].

There should be a peak at 450-500 cm^{-1} assigned to Si-O-C bond in the structure. Spectral of Si-69 treated MCC (Figure 5) showed peak at 468 cm^{-1} for this type of bond. Two absorption band peaks at 2925 cm^{-1} and 1460 cm^{-1} were methylene, and on FTIR of surface modification MCC have been significantly enhanced. As well as, reduction of peak intensity was noticed at 3000-3700 cm^{-1} , corresponding to the -OH group in cellulose structure. According to the mixing percentage of Si-69, reduction of peak intensity corresponding to the -OH group in the cellulose was varied. The amount of reduction of peak intensity corresponding to the -OH group in the cellulose had been greater in 30% Si-69 treated MCC than 20% Si-69 treated MCC (Figure 5). So 30% Si-69 coupling agent has been properly reacted with MCC. So MCC was properly surface modified by 30% Si-69 [17].

4.3 Preparation of Composite.

4.3.1. Casting evaporation

A proper film could not be obtained due to some reasons. Because thickening of the solution could not be kept constant.

4.3.2. Mechanical mixing

Laboratory type internal mixer was used to mix polypropylene and MCC. Better mixed and distributed composite batches were obtained by this method. That means, polypropylene and MCC had been properly bonded and mixed by this method. So this method was used to further composite mixing.

4.4 Physical properties of Composite.

The notched izod impact strength was shown in Figure 6 for PP based silane modified MCC composite. The impact strength was significantly higher in the composites than pure PP. The impact strength of the composites increased when increased modified MCC percentage up to 4% and then decreased furthermore.

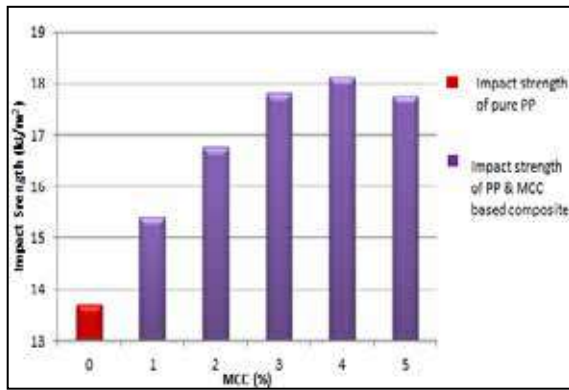


Figure 6 - Impact strength of Developed Composite

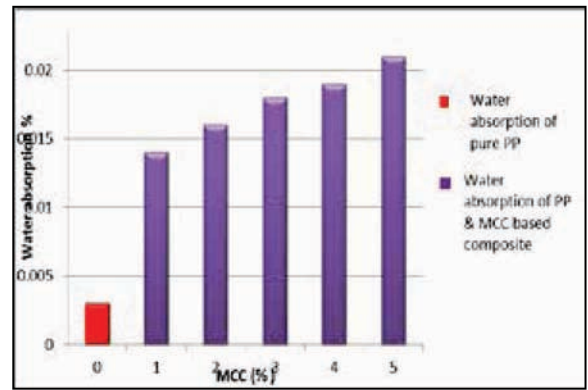


Figure 10 - Water absorption of Developed composite

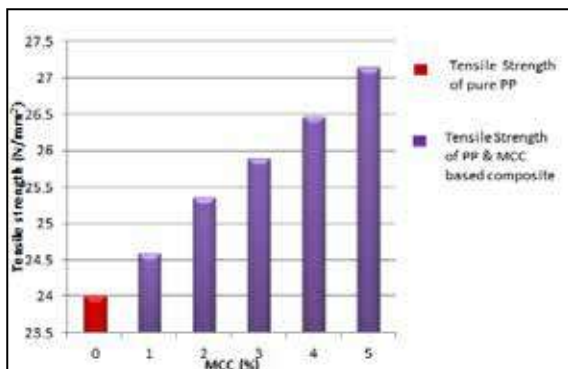


Figure 7 - Tensile Strength of Developed Composite

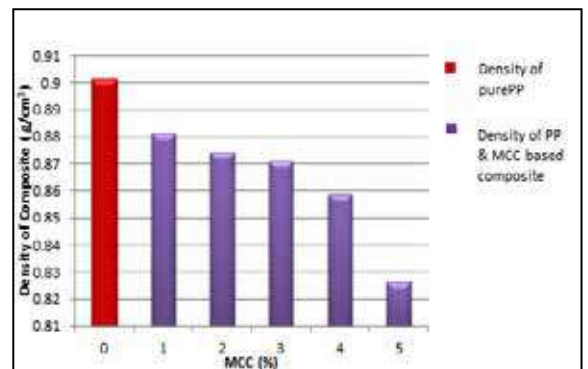


Figure 11 - Density of Developed Composite

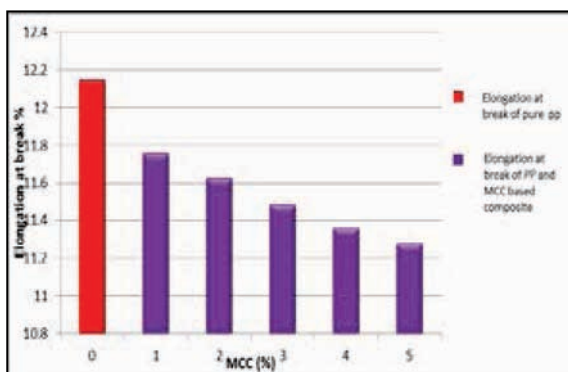


Figure 8 - Elongation at break of Developed composite

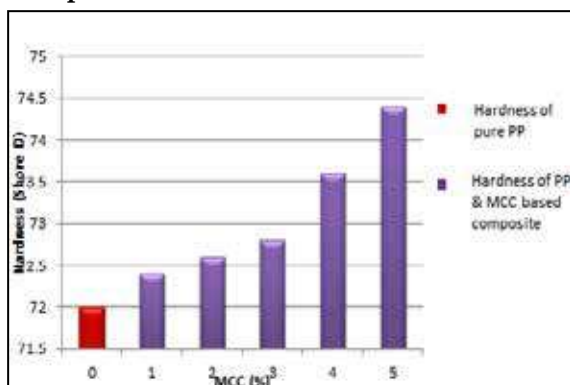


Figure 9 - Hardness of Developed Composite

Composites with modified MCC by silane coupling agent, the impact strength seemed to be dependent on modified MCC content. The results strongly suggest that silane modified MCC, acts as a compatibilizer, improves the compatibility between hydrophilic MCC and the hydrophobic PP matrix. That results strong connections between MCC and PP due to removing OH groups on MCC by silane groups. But beyond 4% MCC was not working as a filler material. Because MCC is a high crystalline material. Therefore, high percentage of MCC is not giving good properties as a filler material to impact force and high crystallinity gives low impact strength.

The tensile strength at break of the composite was shown in Figure 7. The tensile strength at break exhibited sharp increases up to 5 wt% of modified MCC.

The higher tensile strength shows in modified MCC containing samples due to improved compatibility between hydrophilic MCC and the hydrophobic PP matrix. Therefore, a diffuse interlayer can be formed between the PP and MCC exhibiting excellent adhesion to each other. So MCC has been act as a filler material for this composite.

Elongation at break of pure PP was higher than composite. (Figure 8) Elongation at break slightly decreased with an increase of modified MCC percentage. These results were possibly due to the interaction between silane groups onto PP and OH groups of MCC that improve the interfacial adhesion of MCC with the PP matrix.

Due to above reason tensile strength increased and elongation at break slightly decreased with an increase of modified MCC content. MCC acts as a short fibers and distribution is discontinue. These are other major reasons for this slight decrease of elongation at break.

Hardness variation of composite was shown in Figure 9 for Pure PP hardness value was lower than composite and hardness value increased with an increase of modified MCC content. The results imply that resistance to indentation increased with modified MCC content. It can be described as stiffness of composite increases due to MCC gives high crystallinity region for composite. Therefore when MCC content is increased, stiffness of composite slightly increases with MCC content. Therefore results strongly agreed with above hardness variation.

It was important to analyse the water-absorption (Figure 10) qualities of the developed composites, because the dimensional stability of the final products decline as a result of water absorption. Also water absorption rate increased with an increasing of modified MCC content due to increase of slightly presence of hydrophilic OH groups in modified MCC.

Density variation of composite and pure PP was shown in Figure 11. Composite density was always lower than pure PP density and it decreased with MCC content. MCC gave the low density for composite than pure PP. These results imply that MCC based composite can be used for light weight product with high specific properties.

5. Conclusions

Experimental results showed that gradual increase of tensile strength, hardness and impact strength with increase of MCC concentration. Polypropylene with 4 wt.% MCC containing sample showed the maximum impact strength and it was 18.2 KJ/m². Maximum water absorption (0.02%) was observed in 5 wt.% MCC containing sample. 5 wt.% MCC containing sample showed the maximum hardness (74.4 Shore D). Developed composite showed the gradual reduction of density from 1 wt.% MCC (0.882 g/cm³) to 5 wt.% MCC (0.826 g/cm³). Therefore, Polypropylene with MCC polymer composite

can be used for light weight engineering applications due to above tested properties.

References

1. Samarasekara, A. M. P. B., and Jayasuriya, E. A. P. C. D., "Synthesis of Biodegradable Polyolefins Based Polymer Composites Using Degradable Natural Materials." *Proceedings of International Forestry and Environment Symposium*. Vol. 18. 2014.
2. Umadaran, S., Somasuntharam, P., and Samarasekara, A. M. P. B., "Preparation and Characterization of Cellulose and Hemi-Cellulose Based Degradable Composite Material using Sugarcane Waste." *Moratuwa Engineering Research Conference (MERCon)*, 2016. IEEE, 2016.
3. Kahawita, K. D. H. N., and Samarasekara, A. M. P. B., "Extraction and Characterization of Cellulosic Fibers from Sawmill Waste." *Moratuwa Engineering Research Conference (MERCon)*, 2016. IEEE, 2016.
4. Samarasekara, A. M. P. B., Somasuntharam, P., and Umadaran, S., "Development of Environmentally Friendly Cellulose Containing Packaging Products from Waste Materials." (2015).
5. Samarasekara, A. M. P. B., Senavirathne, H. V. H. H., and Sandaruwan, A. H. W. O., "Preparation of Biodegradable Polymer Materials using Agricultural Waste." *Proceedings of International Forestry and Environment Symposium*. Vol. 17. 2012.
6. Medve, József, et al. "Hydrolysis of Microcrystalline Cellulose by Cellobiohydrolase I and Endoglucanase II from *Trichoderma Reesei*: Adsorption, Sugar Production Pattern, and Synergism of the Enzymes." *Biotechnology and bioengineering* 59.5, 1998, 621-634.
7. Lee, H. V., Hamid, S. B. A., and Zain, S. K., "Conversion of Lignocellulosic Biomass to Nanocellulose: Structure and Chemical Process." *The Scientific World Journal* 2014 (2014).
8. Kiziltas, Alper, et al. "Mechanical Properties of Microcrystalline Cellulose (MCC) filled Engineering Thermoplastic Composites." *Journal of Polymers and the Environment* 22.3, 2014, 365-372.
9. El-Sakhawy, Mohamed, and Mohammad L. Hassan. "Physical and Mechanical Properties of Microcrystalline Cellulose Prepared from Agricultural Residues." *Carbohydrate polymers* 67.1, 2007, 1-10.
9. Amarasinghe, D. Shantha, Dehipalawage Sunil, and Harry D. Gafney. "Effect of CO Pressure

- Gradients on the Photochemistry and Thermal Chemistry of Fe (CO) 5 Physisorbed into Porous Vycor Glass." *The Journal of Physical Chemistry C* 115.43 ,2011, 20824-20831.
10. Huang, Jun, and Denis Rodrigue. "Comparison of the Mechanical Properties between Carbon Nanotube and Nanocrystalline Cellulose Polypropylene Based Nano-Composites." *Materials & Design (1980-2015)* 65 , 2015, 974-982.6.
 11. Lokshina, I., et al. "Microcrystalline Cellulose: Extraction and Analysis." *Proceedings of the fourteenth Israeli-Russian Bi-National workshop, Ariel, Israel.* 2015.
 12. Mathew, Aji P., Kristiina Oksman, and Mohini Sain. "Mechanical Properties of Biodegradable Composites from Poly Lactic Acid (PLA) and Microcrystalline Cellulose (MCC)." *Journal of applied polymer science* 97.5, 2005, 2014-2025.
 13. Senevirathna, Sandhya Rani, et al. "The Effect of Change of ionomer/polyol Molar Ratio on Dispersion Stability and Crystalline Structure of films Produced from Hydrophilic Polyurethanes." *Journal of Applied Polymer Science* 134.7, 2017.
 14. Chauhan, Yuvraj P., et al. "Microcrystalline Cellulose from Cotton Rags (waste from garment and Hosiery Industries)." *International Journal of Chemical Sciences* 7.2, 2009.
 15. Spoljaric, Steven, Antonietta Genovese, and Robert A. Shanks. "Polypropylene-Microcrystalline Cellulose Composites with Enhanced Compatibility and Properties." *Composites Part A: Applied Science and Manufacturing* 40.6, 2009, 791-799.
 16. Gao, Tian Ming, et al. "Preparation and Characterization Nano-Cellulose and its Surface Modification by Silane Coupling Agent." *Applied Mechanics and Materials*. Vol. 217. Trans Tech Publications, 2012.



Synthesis and Characterization of Nanoparticle-Incorporated Antimicrobial Coating for Food Packaging Applications

S.P.A. Madushani, D.P. Egodage, A.M.P.B. Samarasekara, D.A.S. Amarasinghe, H.T.S. Jayalath and S.M.N.S. Senerath

Abstract: The rising demand to increase fresh food shelf life, as well as the need of protection against food-borne diseases, urged the development of antimicrobial food packaging. Nanomaterials have increasingly been used in food packaging applications in recent years due to their extraordinary properties when compared to bulk materials. Nanoparticles provide significant antimicrobial properties in different environmental conditions. Nowadays, there is heightened attention in designing nanoparticles incorporated food packaging with the introduction of nanotechnology. Silver nanoparticles (AgNPs) based antimicrobial packaging is an innovative form of food packaging that used to extend shelf-life of food and reduce the risk of pathogens. AgNPs are one of the most powerful antimicrobial agents which can be used for increasing the shelf life of foods due to its capacity to eliminate infectious micro-organisms. The present research work describes the preparation of silver nanoparticles incorporated coating for polymer-based packaging components. Nanosilver impregnated cross-linked polyvinyl alcohol coating was synthesized and applied to the polymer surface. In this study, the wettability of the polymer surface was enhanced by a UV treatment. The contact angle was measured to confirmation of the wettability. The adhesion of the coating to polymer was obtained as load required to peel off the coating. Optimum UV treatment time was selected by considering the contact angle measurements and mechanical properties of the polymer. Thermal degradation of cross-linked nanosilver coating was determined using thermogravimetric analysis. Presence of silver nanoparticles in the coating was confirmed by Surface Plasmon Resonance (SPR) and Scanning Electron Microscopy (SEM). The nanosilver incorporated polymer was tested for its biocidal action against model bacteria *Escherichia coli* using zone inhibition and applying foods in nanosilver coated containers. Developed nanosilver incorporated polymer-based food packaging products showed antimicrobial properties. This developed product can be used to improve the quality of the food and extend shelf life, especially in food packaging applications.

Keywords: AgNPs, food packaging, antimicrobial coating, wettability

1. Introduction

Food packaging plays a vital role in preserving food throughout the distribution. Food containers with antimicrobial properties can withstand longer life than usual food containers. Currently, available polymer food containers can be attacked during the food storage. Thus foods may be toxic or expired. So food containers with antimicrobial properties can be used to improve the quality of the food. The most effective way to improve the antimicrobial properties in food container is applying a surface coating[1]. Antimicrobial agents in food packaging is a full-grown technology, concerns about the risks associated with the potential ingestion of the Ag ions migrated into food still exist. The general requirement is not to exceed 0.05 mg/kg in food. This gives that assessment of silver migration profiles is necessary to assure

antimicrobial usefulness while complying with the current regulations [2].

There are various nanomaterials that exhibit antimicrobial activity.

Ms. S.P.A. Madushani, B.Sc. Eng. (Moratuwa), Dept. of Materials Science & Engineering, University of Moratuwa.

Ms. D.P. Egodage, B.Sc. Eng. (Moratuwa), Dept. of Materials Science & Engineering, University of Moratuwa.

Eng. A.M.P.B. Samarasekara, B.Sc. Eng. (Moratuwa), M.Phil. (Moratuwa), AMIE(Sri Lanka), Senior Lecturer, Dept. of Materials Science & Engineering, University of Moratuwa.

Dr. D.A.S. Amarasinghe, B.Sc. (Kelaniya), MSc. (Moratuwa), M.Phil. (CUNY, USA), Ph.D.(CUNY, USA), Senior Lecturer, Dept. of Materials Science & Engineering, University of Moratuwa.

Mr. H.T.S. Jayalath, B.Sc. Eng. (Moratuwa), Dept. of Materials Science & Engineering, University of Moratuwa.

Mr. S.M.N.S. Senerath, B.Sc.Eng.(Moratuwa), Dept. of Materials Science & Engineering, University of Moratuwa.



Inorganic materials such as silver and gold have been found as antimicrobial materials having nano range. Silver nanoparticles have a high antimicrobial activity because they can insert within the cell membrane due to their small size and release silver ions locally from the silver particle [3].

Nanosilver particles are prepared by chemical and physical methods. A simple and easy method is the chemical reduction of silver ions to nanosilver particles, in the presence of reducing agent and capping agent. Polyvinyl alcohol (PVA) used to prepare silver nanoparticles. Thus it acts as a size reducing agent and as a stabilizer to stabilize the growth of the particles and water-soluble synthetic polymer with excellent film-forming, non-toxic and adhesive properties and biodegradable polymer [3]. Nanoparticles of silver can be prepared in an aqueous medium easily using PVA, thus making the material synthesis non-toxic and environmentally friendly because of the zero solid by-product [4].

However, due to its solubility in water, it is often combined with other polymers in multilayer structures, PVA being located in the core layer. An alternative route to avoid the use of several polymers would be the crosslinking of PVA. For PVA, most commonly used crosslinkers are dialdehydes and polycarboxylic acids such as citric acid, succinic acid and tartaric acid [4,5]). The advantage of using Polycarboxylic acid is that it can be used as food additives. Citric acid is a weak organic tricarboxylic acid. It occurs naturally in citrus fruits. Citric acid used as a food additive (European code E330). The advantage of using citric acid is completely harmless natural crosslinking [5].

Many plastics have non-porous structure and low surface free energy hence most of them are hydrophobic and are not naturally wettable. Wettability studies usually involve the measurement of contact angles as the primary data, which indicates the degree of wetting when a solid and liquid interact. Small contact angles that lesser than 90° correspond to high wettability, while large contact angles that greater than 90° correspond to low wettability [6]. Polypropylene is the second widest used polymeric material for packaging applications due to stability, chemical and moisture resistance, lightness, flexibility, strength, and easiness of process, and suitability of recycling and reuse. For polypropylene has contact angle

approximately 102.1° , for water. Therefore, PP is a hydrophobic polymer. [6].

The main feature of application of a coating is that coatings adhere to the substrate, the surface energy of the substrate must be higher, or surface energy of the coating must be lower. By increasing the surface energy of the substrate, the contact angle will be reduced. To increase the surface energy of polymer surfaces, surface pre-treatments will be done such as chemical treatments, plasma treatments, laser irradiation and ultraviolet (UV) irradiation treatments without affecting bulk properties. The increase in surface energy of plastics occurs through the surface oxidation of polymer chains by UV irradiation. [7,8]

The objective of this paper is intended to describe the preparation of silver nanoparticles incorporated coating for polymer-based packaging components. Nanosilver solution was synthesized by reducing silver nitrate by PVA and crosslinked the coating to avoid solubility. The applicability of UV treatment to increase the surface energy was investigated, and then nanosilver particles were coated on the substrate. The fabricated nanosilver based coating was tested for adhesion. SEM and UV spectrometers were used to investigate the presence of nanosilver on the coating and analyse the thermal degradation of the crosslinks.

Antibacterial properties against *Escherichia coli* were investigated for the developed products. As *Escherichia coli* are a widespread, diverse group of bacteria, it can be found in environment and foods. It is an anaerobic bacteria. Thus it can grow food containers even though they are sealed.[9]

2. Materials and Methods

2.1 Materials

Silver nitrate (AgNO_3 , 99.9% purity) was purchased from Research-Lab Fine Chem industries, Mumbai and Polyvinyl alcohol (PVA, 9000–10000 molecular weight, 88% hydrolysis, and Industrial grade) were purchased from Organic Trading, Sri Lanka. Citric acid was obtained from Glorechem, Sri Lanka and Polypropylene cups were purchased from Starpack plastic product distribution agent, Borupana, Sri Lanka and other chemicals and laboratory equipment were acquired from Department of Materials Science and Engineering and Department of Chemical and Process Engineering University of Moratuwa.

2.2 Preparation of Silver Nanoparticles

Silver nanoparticles were prepared using AgNO_3 as precursor and PVA as reducing and stabilizing agent. 0.1wt% silver was prepared by dissolving silver nitrate in 5ml of de-ionized water. PVA solution was made by adding 0.06gml^{-1} of PVA to 50ml of de-ionized water and stirred magnetically maintaining a temperature between 60-70°C. After PVA completely dissolved in de-ionized water (transparent) the silver nitrate solution was added drop by drop (drop per second) while maintaining the temperature between 60-70°C with continuous stirring. Magnetic stirring continued until the solution became a faint brownish viscous liquid.[4]

2.3 UV-Vis Spectrophotometry

The formation of the nanosilver particles in aqueous solution was verified by recording UV absorbance spectrum between 350-700nm wave range by UV-1800 SHIMADZU spectrometer.

2.4 Preparation of Cross-linked Nano Silver Coating on Polypropylene Substrate

Citric acid was used as a crosslinking agent to crosslink PVA. 0.0066g/ml of Citric acid were added to 50ml of de-ionized water and mixed with pre-prepared PVA/Ag 50ml solution while maintaining the temperature between 65-70°C while stirring magnetically. Then polypropylene samples were coated with the solution and were kept in the oven for 100-130°C for 6 hours.

2.5 Thermo Gravimetric Analysis (TGA)

Thermal degradation of cross-linked polymer coating was determined by using TGA. Thermal decomposition of the coating was obtained by TGA STD Q600 apparatus for coated samples of different crosslinked temperatures (90,100, 120, 130°C). This analysis was done with 800°C ambient temperature with a heating rate of 10°C/min in open ceramic pan under nitrogen environment.

2.6 UV Treatment

For a better adhesion of the coating on a polymer substrate, UV treatment was done. This was done by UV rays having intensity 35 W/m^2 . Samples were UV treated for 24 hours, 48 hours, and 72 hours time periods.

2.7 Contact Angle Analysis

The wettability of the polymer after the UV treatment was analysed by measuring the contact angle of the polymer substrate. The contact angles for de-ionized water were measured by taking photographs which are

taken by 13 Mega Pixel camera, and 0.05ml of de-ionized water drop using and the images were analysed by software.

2.8 Mechanical Property Testing of UV Treated Polypropylene

Mechanical properties of the UV treated and non-treated polypropylene samples were tested by Universal tensile testing machine. The polypropylene samples were cut 500×200mm² size, and the width and thickness of the samples were measured by using Venire calliper. The machine parameters were set as 500N load, 200mm extension. Tensile strength was calculated and compared.

2.9 Measuring UV penetration depth

Absorbance and transmittance spectrum of the 1.7mm thin polypropylene film was taken by using UV-1800 SHIMADZU spectrometer for 200 to 650 nm because mercury lamp spectrum was distributed through this range which used for UV treatment.

Absorbance was calculated by using Beer-Lambert law for each wavelength of the transmission spectrum of polypropylene. Percentage of transmittance was calculated for each mercury peak wavelengths for variable sample penetration depths.

2.10 Measuring Adhesion Load of Nano Silver Coating

The adhesion load on coating was measured for nanosilver impregnated coated 48 hours UV treated samples and non-treated polypropylene substrates by using the universal tensile testing machine.

The load required to peel off the coating was measured by setting the load cell parameters as 500N load, 500mm extension, speed 20 mm/min and dimensions of the sample 4.5 x 4cm². The maximum load to peel off the coating was recorded.

2.11 SEM Analysis

The existence and shape of nanosilver particles in the prepared coating were determined by ZEISS EVO 18 RESEARCH apparatus. The SEM analysis and the energy dispersive X-ray spectroscopy were done by using prepared coating under 10.00kV voltage with the magnification of 3.58K .

2.12 Antimicrobial Activities

Nanosilver coated, and non-coated polypropylene samples were investigated for



antibacterial activity by using Agar diffusion method against Escherichia coli. This method was carried out initially by pouring the Muller Hinton Medium solid agar onto sterilized Petri dishes and 10^6 CFU/mL concentration Escherichia coli bacteria solution was spread uniformly on the plate. The nanosilver coated and non-coated polypropylene samples were cut into a disc shape with 6mm diameter and was placed on plates. The agar plate was incubated for 24 hours at 37 °C, and inhibition zone diameter was recorded.

The antibacterial activity of the nanosilver coating observed visually by including foods in the food packaging container.

3. Results and Discussion

3.1 Characterization of Nanosilver Particles

UV visible adsorption analysis was performed to verify the presence of silver nanoparticles in the prepared solution. Silver nanoparticles have a surface plasmon adsorption between 400 nm and 450nm. Figure 1 shows the adsorption peak at 415.43nm that clarified the formation of nanosilver particles and the presence of spherical or roughly spherical silver nanoparticles.

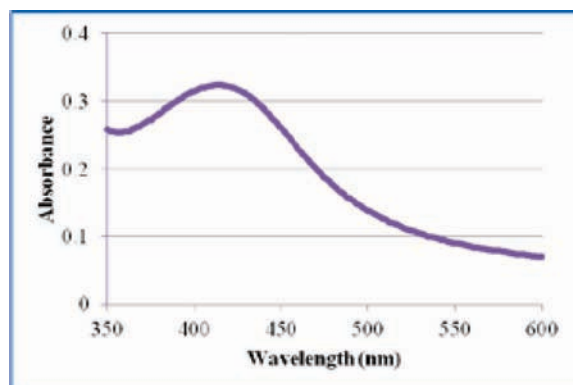


Figure 1 - Adsorption spectrum of the silver nanoparticles colloidal solution.

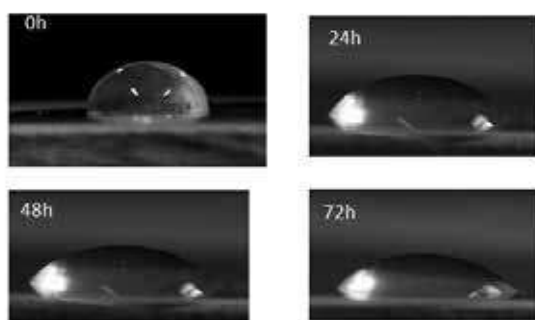


Figure 2 - Contact angle images

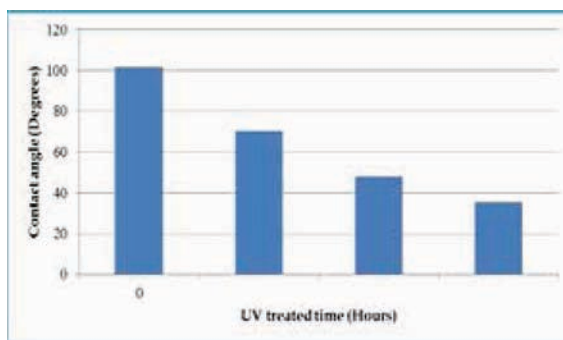


Figure 3 - Graph of contact angle vs UV treated time

3.2 Surface Modification of Polypropylene samples

Figure 2 is shown the images of the contact angle of the UV treated polypropylene samples with de-ionized water and the Figure, 3 is shown the contact angle values reduces with the increase of the UV treated time. When solid and liquid interacts, the contact angle indicates the degree of wetting. The angles less than 90° results to high wettability and vice versa. Therefore, this result shows that increasing of the wettability of the polypropylene samples because of reduction of the contact angle with increasing UV treated time of the polypropylene samples. That was a positive solution for the adhesion difficulty of the coating to the polypropylene surface. To measure the contact angle, de-ionized water was used since the nano silver solution is water based.

3.4 Mechanical Properties of the UV Treated Polypropylene Samples

The average tensile strength and elongation of the polypropylene samples are very important when using UV treatment as surface treatment. According to the results shown in Figure 4 and Figure 5 after 48 hours UV treated time, the tensile strength reduces 3%, but the elongation reduces 47%. It is important to retain the properties of the polypropylene sample up to 90% after the UV treatment. Therefore, 48 hours was selected as best UV treatment time for the polypropylene samples, since after 48 UV treated time, the tensile strength doesn't show significant change but, elongation value reduces drastically.

3.5 Measuring UV penetration depth

Figure 6 shows the resulted transmittance values for each penetration depth at peak values of mercury. That shows the mercury peak values were chosen because 254, 300, 312, 334, 365, 405, 436, 546, 579nm values have the highest tendency to penetrate due to the high-

intensity UV rays will fully penetrate to the sample as the thickness of the polypropylene sample is 1.7mm. When 5% of UV transmitted, 95% UV was absorbed by the sample. Therefore, 48 hours of UV treatment was chosen since this effect will moderate at 48 hours.

3.6 Measuring Adhesion of Nanosilver Coating

The adhesion load of the polypropylene samples (10.6 N) which 48 hours UV treated showed a higher value than the non-UV treated samples (4.7N). That interprets the 48 hours UV treated time polypropylene samples gives the best results of adhesion of the nanosilver coating.

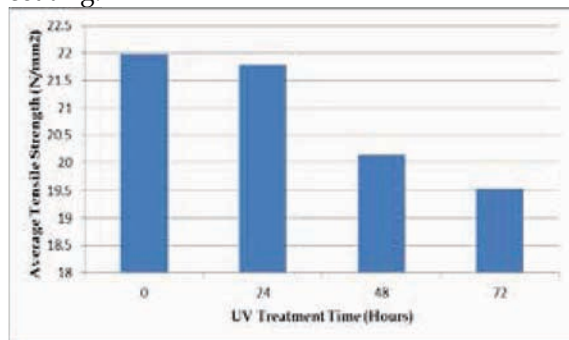


Figure 4 - Graph of Average Tensile Strength Vs. UV Treated Time

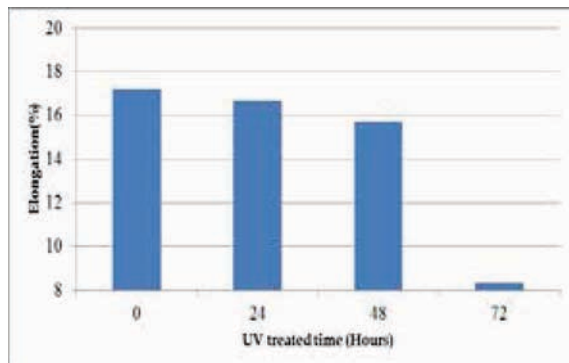


Figure 5 - Graph of Average Elongation Break % Vs. UV Treated Time

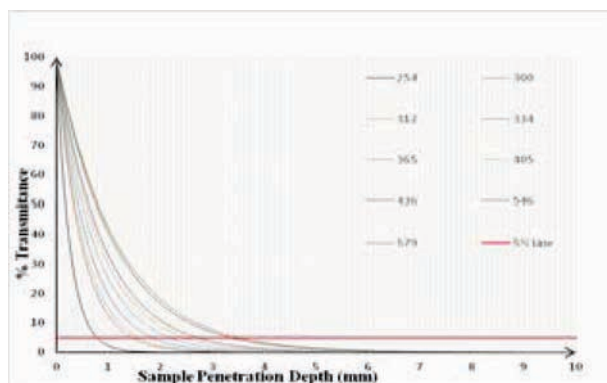


Figure 6 - Graph of Transmittance vs Penetration Depth of Polypropylene

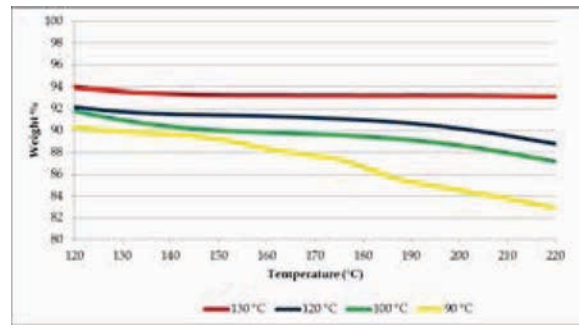


Figure 7 - Temperature curves of TGA

3.7 Thermo Gravimetric Analysis (TGA)

Figure 7 shows the retain weight percentage of the crosslinked polyvinyl alcohol using citric acid with different crosslinking temperatures. The thermal stability was analysed qualitatively. High thermal stability can be observed with increasing crosslinks. The non-cross-linked films show weight loss at about 70°C, whereas the weight loss of the crosslinked films start at about 100 °C. The first major weight loss of both films initiated at about 120°C. But the non-cross-linked films shows slightly more weight loss than the cross-linked films. It can be seen that low weight loss of the cross-linked films between 120 and 220 °C. This can be due to the higher thermal stability of the films. According to the Figure 7, at 130°C temperature crosslinked nano silver coating is most stable due to a higher degree of the crosslinking. Therefore, that is the most favourable temperature for crosslinking.

3.8 SEM Analysis

The SEM microgram confirms that the surface coating contains nanoparticles with around 400nm diameter with a spherical shape. The energy dispersive X-ray spectroscopy confirms that the particles observed in the scanning electron microgram are silver particles. The energy dispersive X-ray spectroscopy confirms that the particles observed in the scanning electron microgram are silver particles.

3.9 Antimicrobial Activity

Nanosilver coated polypropylene sample shows 1mm clear inhibition zone around the substrate and the non-coated polypropylene sample doesn't show any inhibition zone (Figure 10). That interprets that the E-coli bacteria was inhibited because of the nanosilver particles, the clear zone appeared.



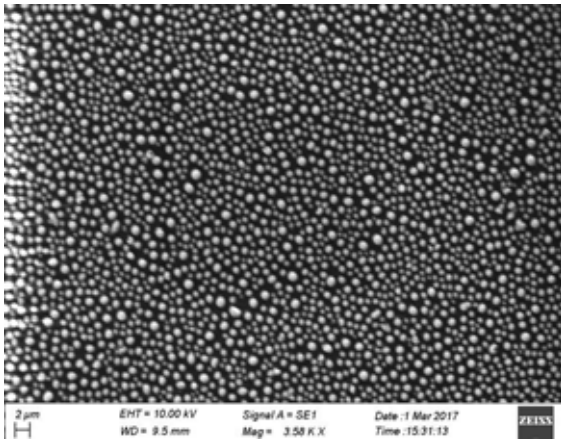


Figure 8 - Scanning Electron Microscopy image of the coating



Figure 9 - Energy Dispersive X-ray Spectrum



Figure 10 - Zone Inhibition of Non-coated Polypropylene and Nansilver Coated Polypropylene



Figure 11 - Microorganism Growth of Non-coated Polypropylene and Nansilver Coated Polypropylene

Figure 11 shows the storage of food in nanosilver coated and control containers. The control sample showed the clear microorganism growth, but developed

nanosilver incorporated polymer-based food packaging product showed antimicrobial properties.

4. Conclusions

The developed nanosilver particle incorporated antimicrobial coated polymer showed significant surface adhesion properties and antimicrobial properties. This product can be used in food packaging applications to extend shelf life.

References

1. Metak and T. Ajaal, "Investigation on Polymer Based Nano-Silver as Food Packaging Materials", *International Journal of Biological, Biomolecular, Agricultural, Food and Biotechnological Engineering*, vol. 7, no. 12, 2013, pp. 1103-1109.
2. Marilena Carbone, Domenica Tommas Donia, Gianfranco Sabbatella, Riccarda Antiochia, "Silver nanoparticles in polymeric matrices for fresh food packaging", *Journal of King Saud University - Science*, Vol. 28, Issue 4, , 2016 pp. 273-279.
3. Yolanda Echegoyen, Cristina Nerín, "Nanoparticle Release from Nano-Silver Antimicrobial Food Containers". *Food and Chemical Toxicology*, vol.62, 2013, pp.16-18.
4. Abdul Kareem, T., Anu Kaliani, A., "Synthesis and Thermal Study of Octahedral Silver Nano-Plates in Polyvinyl Alcohol (PVA)", *Arabian Journal of Chemistry*, vol.4, 2011, pp. 325-331.
5. Birck, S. Degoutin, Tabary, N., Miri, V., Bacquet, M., "New Crosslinked Cast Films Based on Poly(vinyl alcohol): Preparation and physico-chemical properties", *eXPRESS Polymer Letters*, vol.8, no.12, 2014, pp.941-952.
6. Dehnavi, A. Aroujalian, A. Raisi and Fazel, S., "Preparation and Characterization of Polyethylene/Silver Nanocomposite Films with Antibacterial Activity", *Journal of Applied Polymer Science*, vol. 127, no. 2, 2012, pp. 1180-1190.
7. Ebnesajjad, S., Ebnesajjad C., *Surface Treatment of Materials for Adhesion Bonding*, 1st ed., Norwich, NY, U.S.A.,2006, pp. 3-18 .
8. Bracco, G., Holst, B., *Surface Science Techniques*, 1st ed., Berlin, 2013, pp. 3-16.
9. Michael Donnenberg, *Escherichia coli Virulence Mechanisms of a Versatile Pathogen*, 1st ed., California, U.S.A., 2002, pp. 214 .

Assessing the Impact on Environment, Health and Safety due to Releases from Chemical Process Routes

H.B.B. Anuradha, Manisha Gunasekera and Olga Gunapala

Abstract: The chemical process route selection is one of the important decisions that needs to be taken during initial stages of plant design and development. Although conventionally the economic factor has been considered in this selection process, presently the environmental, health and safety (EHS) issues have also become main concerns, since the operational costs related to EHS can be largely reduced by avoiding EHS hazards during initial stages of plant development. Most available methodologies for chemical process routes assessment mainly consider environmental or health or safety hazards individually or a combination of two of them. In this work inherent environmental, health and safety hazard index (IEHSHI) is developed to assess chemical process routes based on integrated EHS hazards due to daily operational activities of the plant as well as accidental releases. The IEHSHI includes information of nine parameters available at the conceptual design stage of process plant development. The environmental hazards and health hazards are assessed considering both accidental and continuous releases from the manufacturing process. The safety assessment is done considering chemical safety and process safety associated with the route. The environmental, health and safety parameter values are combined individually using weights. The routes can be ranked and compared according to IEHSHI values. The IEHSHI was applied in three routes to manufacture methyl methacrylate.

Keywords: Accidental releases, Chemical process, Environmental hazards, Inherent Safety

1. Introduction

Environmental impact, employee health and safety are more concerned than before since they have become important in environmental conservation and human life protection. Chemical process route is considered as the way to achieve a particular product using raw materials and energy [3]. Literature reveals that the operating cost of chemical manufacturing plants can be considerably reduced by selecting environmentally friendlier, healthier and safer chemical routes during the design stage of the chemical process plant [4].

In inherently safer chemical process plants, hazards are avoided or removed rather than controlling them with add-on protective equipment [3]. The inherent safety should be considered or practised as early as possible in the design stages because the impact on design decision is large at this stage.

The chemical process plant development process can be categorized into various stages according to its function involved as they are considered as key design decision-making points. The process design stages are defined considering design stages [12] and process design life cycle [5]. These stages are shown in figure 1.



Figure 1 - Process design stages.

Chemical process route selection is one of the key design decisions taken during process

Eng. H.B.B. Anuradha, B.Sc. Eng. (Moratuwa), Research Student, Department of Chemical and Process Engineering, University of Moratuwa.

Eng. (Dr.) M. Y. Gunasekera, B.Sc. Eng.(Hons) (Moratuwa), M.Eng. (Moratuwa), Ph.D.(UK), MIE(Sri Lanka), Senior Lecturer, Department of Chemical & Process Engineering, University of Moratuwa.

Dr. Olga Gunapala, M.Sc. Eng.(Moscow), Ph.D. (Moscow), Senior Lecturer, Department of Chemical & Process Engineering, University of Moratuwa.

development, and it is taken at the conceptual design stage since it is the earliest stage. The conceptual stage is defined as that contains basic process information such as synthesis process routes, process materials and product specifications.

An index called Inherent environmental (E) health (H), and safety (S) hazards index (IEHSHI) is developed considering information available at the conceptual stage. The IEHSHI index is developed combining environmental, health and safety parameters. Environmental hazard assessment is carried out by considering catastrophic and continuous releases of the plant. Health hazard assessment is carried out assessing acute and chronic hazards associated with the chemical plant. In safety assessment, chemical and process safety are considered.

2. Methodologies available for Hazards Assessment

Inherent hazards assessment of chemical process routes has been done in various ways such as environmental hazards assessment or health hazards assessment or safety assessment and combining two of the above or all of three (EHS assessment). Noteworthy among them are the Environmental hazards index (EHI) [3], Safety weighted hazard index (SWeHI) [6], Fuzzy logic based inherent safety index [10], Integrated inherent safety index (I2SI) [1], Process route healthiness index (PRHI) [7], Inherent benignness indicator (IBI) [4], Health quotient index (HQI) [8], Sustainable assessment of novel chemical process and Risk-based inherent safety index (RISI) [5].

2.1 The Environmental Hazards Assessment Methodologies

The environmental hazards index (EHI) is developed by Cave and Edwards [3] to estimate the environmental impact of a total release of chemical inventory. The EHI of a route is calculated by evaluating the effects and exposure of each chemical in the route. Chemical distribution and toxicity are main parameters of EHI. Predicted environmental concentration is determined by Mackay's fugacity model, and LC50 and LD50 data are used for toxicity evaluation.

2.2 The Health Hazards Assessment Methodologies

The PRHI is developed by Hassim and Edwards [7] for assessing inherent occupational health hazards. In this work, Inherent chemical

and process hazards index (ICPHI), Material harm index (MHI), Health hazards index (HHI) and the ratio between worker exposure concentration (WEC) and occupational exposure limit (OEL) are used as parameters for determining the PRHI. Small leaks and fugitive emission in the workplace have been considered in the assessment. The chemical process route with least PRHI value is considered as the best process.

The HQI [8] is another method which uses airborne chemical concentrations in the working area to assess the impact on health. The fugitive emission rate and air volumetric flow rate are used to estimate airborne chemical concentration. The health risk posed by a mixture of chemicals is given by HQI. The least value of HQI is considered in selecting the chemical route with least health effect.

2.3 The Safety Assessment Methodologies

The I2SI proposed by Khan et al. [1] is composed of two main sub-indices: a hazard index (HI) and an inherent safety potential index (ISPI). The HI is intended to be a measure of the damage potential of the process after taking into account the process and hazards control measures. The ISPI accounts for applicability of the inherent safety principles to the process.

The RISI [5] is an extension of I2SI earlier discussed. The risk involved in a base design (RiskBD) and the inherent safety risk for alternative designs (ISRisk) are integrated to develop the RISI.

2.4 The Environmental, Health and Safety Hazards Combined Assessment Methodologies

The IBI [4] combines 15 parameters related to safety, health and environmental impacts of a route. The chemical safety aspects of the routes have been assessed by three parameters and four parameters have been considered for assessing the processing aspects. The health and environmental impact of each route is assessed by seven parameters. The toxicity is also a property of a substance that is used as a parameter for the IBI. The parameter is scaled to the range of 0 and 1, where 0 means not hazardous, and 1 represents the most hazardous level. The IBI is taken by integrating the 15 normalized values of parameters for each route.

The sustainable assessment [2] evaluate the chemical process based on economic feasibility, environmental impact, human health and risks. Greenhouse gases and cumulative energy demand are considered to assess the environmental impact. EHS index is proposed by Sugiyama based on environmental, health and safety [2]. The individual categories are aggregated using weight factors: environmental- 0.4, health- 0.2 and safety- 0.4.

3. Inherent Environmental Health and Safety Hazards Index

In this work, the proposed inherent environmental health and safety hazards index (IEHSHI) aims to assess the chemical process routes in the early stages of process design. The method evaluates chemical process based on continuous releases and catastrophic releases from the process plant. The process area includes raw materials storage, plant operation area and end product storage. The framework for estimating IEHSHI consists of mainly three categories: environmental hazards, health hazards, and process and chemical safety.

3.1 Conceptual Design Stage Information

The EHSI assessment is carried out at the conceptual design stage which is the earliest stage of process plant design (Figure 1). The chemical route synthesis and their conversion factors, process operating conditions, enthalpy values and process block diagram are known information at this stage.

3.2 Development of Block Diagrams for All Possible Chemical Routes

The block diagram for each chemical route is developed considering main operating units such as reactors and separators. The mass balance is compiled for the route using block diagram, with considering main reactions, side reactions and conversion factors.

3.3 Select a Chemical Route

The EHSI assessment is used to compare the chemical routes which give an expected desirable product. The calculation is begun with considering one chemical route and determining all nine parameter values related to that route. Once calculation for the first chemical route is completed, the other routes are analysed.

3.4 Hazards Assessment

In this analysis, the parameters are categorized into environmental, health, and safety which

contribute to the final index value. The environmental and health hazards are determined based on catastrophic and continuous released from manufacturing plant but in safety assessment, chemical and process safety are considered.

3.4.1 Environmental Hazards Assessment

3.4.1.1 Accidental Release Assessment

The Environmental Hazards Potential (EHP) is proposed in this work which represents the environmental impacts of raw materials, end products and chemicals in the reactors and separation stages. The parameter expects to assess the catastrophic releases from the chemical processing plant, which is the worst case that would happen in the life time of the plant.

The EHP is based on following assumptions:

- The total inventory stocks would be released to the environment during the accident and that chemical released would be most concentrated, and consequently, effects would be most severe in the 1km² area surrounding the plant.
- The released chemicals are accumulated in the air, water and soil compartment within of 0.6 km radius circle around the plant.
- The damage to the environment due to a chemical is directly proportional to the amount of chemical released.
- The damage due to the release of a mixture of chemicals is additive.

The EHP is a function of predicted environmental concentration (PEC) and permissible exposure limit (PEL). The ratio between PEC and PEL values of a mixture of chemicals are added to obtain the EHP value and is shown in equation (1).

$$EHP_r = \sum_{i=1}^n \frac{PEC_i}{PEL_i} \quad (1)$$

The PEC is calculated using Mackay fugacity approach [13] and this model has also been used in inherent environmental hazard assessment by Cave and Edwards [3]. The mass flow of chemical substances in the process are calculated for the production of a unit mass of product using stoichiometric equations. The resident time of chemical in storage is often over 300 times of reaction and separation stage [3]. Furthermore, the material stock is approximately 300 times of feeding rate of raw materials.



In the calculation of this work, the product manufacturing flow rate is considered as one tone per hour and the raw materials in the stock is 300 times of feeding rates, correspondingly, the end products stock is also 300 times of manufacturing flow rate.

The chemical concentration in the air compartment is calculate considering sudden releases of available chemicals in the plant premises according to the above calculation.

The PEL data are collected for all chemical in the plant and the ratios between PEC and PEL calculated. Moreover, the ratio values are simply summed as shown in equation (1) for the mixture of chemicals associated with the considered chemical route.

The above procedure is repeated for all the chemical process routes and the highest EHP value, is used to normalize the EHP values. The normalized value is defined as \overline{EHP}_r and is shown in equation (2).

$$\overline{EHP}_r = \frac{EHP_r}{\text{Max}(EHP_r)} \quad (2)$$

3.4.1.2 Continuous Release Assessment

The environmental hazards involved with the continuous operation are assessed by Greenhouse Gas (GHG) emission. The calculation of GHG emission rate depends on the carbon dioxide production rate (m_i) of the manufacturing process route (i). The stoichiometric equation for all chemical routes is used to calculate the GHG emission rate. This analysis is also carried out for one tone of the main product manufacturing process.

$$GHG_r = \sum_{i=1}^n m_i \quad (3)$$

The same procedure is followed for other chemical process routes to calculate the respective GHG emission values. The maximum value is used in the normalization step. Each GHG emission value is divided by the maximum GHG value, and the result is defined as \overline{GHG}_r .

$$\overline{GHG}_r = \frac{GHG_r}{\text{Max}(GHG_r)} \quad (4)$$

3.4.2 Health Hazards Assessment

3.4.2.1 Acute Toxicity Assessment

The Hazards in Airborne Quantity (HAQ) is assessed by determining airborne quantity (AQ) resulting from small leaks, due to accidental releases. The acute toxicity

parameter, short-term exposure limit (STEL) values are used as a reference for the concentration of airborne materials.

The Dow chemical equation [11] for gaseous releases and liquid releases are used for calculation of AQ values. The hole diameter of gases or liquid release is considered as at its maximum value of 6.35 mm. this is used in other research works as well such as the inherent occupational health hazards index developed by Hassim and Edwards [7].

The volumetric flow rate (VF) is calculated as in Equation 5 considering a typical wind speed of 4m/s inside the plant. The same has been used in Inherent occupational health assessment during preliminary design stage by Hassim and Hurme [8]. Their work refers to a survey of wind speeds in indoor workplaces by Baldwin in arriving at this value [8]. Furthermore, the average height of main unit operations' leak source is taken as less than (h) 7m. The same is also applied in Hassim and Hurmes' development where the reference is made to the Process plant layout by Mecklenburgh [8]. The floor area of the process plant is calculated by considering average floor area required for main unit operations of the plant and are given in Hassim and Hurmes' work [8].

$$VF = V \times h \times \sqrt{A_{\text{Floor}}} \quad (5)$$

The concentrations due to airborne materials (C_{AQ}) are given by largest AQ value dividing volumetric flow rate as shown in Equation 6. The largest AQ value is selected from possible chemical releases in the chemical process plant. The C_{AQ} values for all the chemicals in the mixture are calculated.

$$C_{AQ} = \frac{AQ_i}{VF} \quad \dots(6)$$

The HAQ values are determined by getting the ratio between C_{AQ} and STEL value for relevant chemical as in following equation 7.

$$HAQ_r = \frac{C_{AQ}}{\text{STEL}} \quad (7)$$

The procedure for assessment of \overline{HAQ}_r is continued for all chemical routes and the maximum value, which is defined as a Max (\overline{HAQ}_r) is determined. The normalized value of \overline{HAQ}_r is determined for each \overline{HAQ}_r value by dividing the Max (\overline{HAQ}_r) and the result is defined as $\overline{\overline{HAQ}}_r$ (equation 8).

$$\overline{HAQ}_r = \frac{HAQ_r}{\text{Max}(HAQ_r)} \quad (8)$$

3.4.2.2 Chronic Toxicity Assessment

Chronic toxicity parameter is used for long term exposure to the chemical substance. Health hazards in continuous releases from chemical processing plant are assessed under chronic toxicity assessment.

The fugitive emission is used as a parameter to assess the chronic toxicity hazard. The Hazards in Fugitive Emissions (HFE) is taken as a function of fugitive emission rate (FE), volumetric flow rate and time weight average (TWA). The FE rate is determined by following the procedure applied in inherent occupational health assessment by Hassim and Hurme [8].

In this assessment, the main unit operation such as reactors, separators and compressor are decided considering reactions associated with the chemical process route. The number of piping components is calculated according to the Hassim's work [8].

The pre-calculated emissions data are given in the U.S. Environmental Protection Agency (EPA) for different piping components [14]. The total emission rate is determined by a number of piping component and its emission factor. The individual emission rate of a chemical is determined considering the molar ratio of the reactors and separators.

The VF is assessed following the same procedure as in HAQ assessment, and TWA data for all chemical substance are collected from the literature.

$$HFE_r = \sum_{j=1}^c \frac{FE_j}{VF \times TWA_j} \quad (9)$$

The procedure for assessment of HFE_r is continued for all chemical routes and the maximum value, which is defined as a Max (HFE_r) is determined. The normalized value of HFE_r is determined for each HFE_r value by dividing the Max (HFE_r) and the result is defined as \overline{HFE}_r is shown in Equation (10).

$$\overline{HFE}_r = \frac{HFE_r}{\text{Max}(HFE_r)} \quad (10)$$

3.4.3 Safety Assessment

For safety assessment, chemical safety and process safety are considered separately.

3.4.3.1 Chemical Safety Assessment

The assessment of chemical safety aspects of routes is carried out using two parameters, explosiveness and flammability.

Explosiveness (E)

The explosiveness measures the tendency of chemicals to form an explosive mixture in the air. The explosive nature of chemicals is represented by the difference between the low explosiveness limit (LEL) and the upper explosiveness limit (UEL) of each chemical.

The summed value for explosiveness, E_r of all chemicals (j) involved in the chemical route is considered for assessment of explosiveness of the chemical route. The Equation 11 shows the determination of E_r .

$$E_r = \sum_{j=1}^c E_j \quad (11)$$

The explosiveness value, E_r is determined for all chemical routes and the maximum value is selected for normalization. The normalization is carried out as in Equation 12, and normalized values are defined by the notation, \overline{E}_r .

$$\overline{E}_r = \frac{E_r}{\text{Max}(E_r)} \quad (12)$$

Flammability (F)

The flammability measures the tendency of a chemical to burn. The chemical safety from accidental fires and explosions of flammable mixture could be measured by flammability values.

The flammability ratings of each chemical involved in the route are taken from NFPA fire rating [15]. The NFPA ratings have values ranging from 0 (minimum impact) to 4 (extreme impact) as shown in table 1, which is developed by flash point (FP) and boiling point (BP) values.

The added value for flammability of all chemicals involved in the chemical route are considered for assessment of flammability of the chemical process route and is defined in Equation 13 as F_r .

$$F_r = \sum_{j=1}^c F_j \quad (13)$$



The flammability value, F_r determine for all chemical routes and select the maximum value for normalization of flammability. The normalization is carried out as in Equation 14 and normalized values are defined as a \bar{F}_r .

$$\bar{F}_r = \frac{F_r}{\text{Max}(F_r)} \quad (14)$$

Table 1 - NFPA fire ratings

	Flammability
Non- combustible	0
FP > 60 °C	1
37.78 °C < FP < 60 °C	2
37.78 °C > FP & 37.78 °C < BP	3
37.78 °C > FP & 37.78 °C > BP	4

3.4.3.2 Process safety assessment

For process safety assessment, operating pressure, operating temperature and heat of reaction are considered.

Operating pressure (OP)

The processes that operate under high pressure or sub-atmospheric pressure are generally hazardous. High pressure can cause the leakage of chemicals. The difference of the reaction's pressure range from atmospheric pressure is chosen to represent the hazards due to pressure.

The summed value for gauge pressure of all chemical reactions (i) in the chemical route is considered for hazards assessment due to operating pressure, and it is defined in Equation 15 as P_r .

$$P_r = \sum_{i=1}^n P_i \quad (15)$$

The pressure hazard values (P_i) are summed, and P_r values are determined for all chemical routes. The maximum value is selected for normalization of P_r . The normalization is carried out as shown in Equation 16 and normalized values are defined as \bar{P}_r .

$$\bar{P}_r = \frac{P_r}{\text{Max}(P_r)} \quad (16)$$

Operating Temperature (OT)

The process operating temperature is also a direct measurement of hazards. This represents heat energy available for release. A reaction condition higher or lower than ambient temperature is considered as unsafe.

The summed value of operating temperature difference from ambient temperature (25°C) of all chemicals reactions (n) in the chemical route are considered for hazards assessment and is shown in Equation 17 as T_r .

$$T_r = \sum_{i=1}^n T_i \quad (17)$$

The maximum value of T_r is selected for normalization of T_r . The normalization is carried out as in Equation 18, and the normalized values are denoted by \bar{T}_r .

$$\bar{T}_r = \frac{T_r}{\text{Max}(T_r)} \quad (18)$$

Heat of Reaction (ΔH)

Reaction enthalpy represents the heat changes whether it is heat released or absorbed, and both are potentially hazardous.

The summed value of reaction enthalpy for all chemical reactions (n) involved with the chemical route is considered for the hazards assessment due to the heat of reaction for a chemical route and is defined in Equation 19 as ΔH_r .

$$\Delta H_r = \sum_{i=1}^n \Delta H_i \quad (19)$$

The normalization is carried out as in Equation 20, and the normalized values are defined as $\bar{\Delta H}_r$.

$$\bar{\Delta H}_r = \frac{\Delta H_r}{\text{Max}(\Delta H_r)} \quad (20)$$

3.5 Development of Hazard Scores

Hazard scores for the environment, health and safety are developed by combining normalised values by using equal weights. The equal weight factors have been used by other research works as well such as in the sustainable assessment of novel chemical processes at an early stage by Patel et al. [2].

3.5.1 Environmental Hazards Score (EHS)

The environmental hazards level that is resulting from combining both hazards of catastrophic and continuous releases is represented in EHS. The equal weights of 0.5 are used for both normalized parameters, \bar{EHP}_r and \bar{GHC}_r for chemical route r. The EHS for chemical route r is determined as in Equation 21.

$$EHS_r = 0.5 \times \bar{EHP}_r + 0.5 \times \bar{GHC}_r \quad (21)$$

3.5.2 Health Hazards Score (HHS)

The HHS is the health hazards level of chemical process route r , which is a result of combining both hazards chronic toxicity and acute toxicity. The equal weights of 0.5 are used for both normalized parameters, \overline{HAQ}_r and \overline{HFE}_r for chemical route r . The HHS for chemical route r is determined as shown in Equation 22.

$$HHS_r = 0.5 \times \overline{HAQ}_r + 0.5 \times \overline{HFE}_r \quad (22)$$

3.5.3 Chemical and Process Safety Score (CPSS)

The CPSS is determined by combining five parameters using equal weights each of 0.2 considering that all parameters are equally important. The normalized values of a chemical route r , \overline{E}_r , \overline{F}_r , \overline{P}_r , \overline{T}_r and $\overline{\Delta H}_r$ are combined as shown in Equation 23.

$$CPSS_r = 0.2 \times \overline{E}_r + 0.2 \times \overline{F}_r + 0.2 \times \overline{P}_r + 0.2 \times \overline{T}_r + 0.2 \times \overline{\Delta H}_r \quad (23)$$

3.6 Determine the IEHSH Index

Inherently safe processes allow for the reduction of hazards control costs. The environmental, health and safety aspects of chemical route r , are aggregated to arrive at one score called the IEHSH index. The weight for environmental, health and safety categories are taken as 0.4, 0.2 and 0.4, respectively, which are the weight factors used in work done by Sugiyama [9].

The IEHSH Index for route r is calculated as shown in Equation 24.

$$IEHSH\ Index_r = 0.4 \times EHS_r + 0.2 \times HHS_r + 0.4 \times CPSS_r \quad (24)$$

4. Case Study

The IEHSH index is demonstrated by applying in three potential chemical process routes to manufacture methyl methacrylate (MMA). The definition of each chemical route is considered as the same as that is given by Adu et al. in their work on the comparison of methods for assessing environmental, health and safety hazards [9]. The MMA routes discussed are as follows:

- (A) Acetone cyanohydrin based route (ACH)
- (B) Tertiary butyl alcohol based route (TBA)
- (C) Isobutylene based route (i-C4)

The IEHSH is calculated by using the simple Process Flow Diagram (PFD) that was

developed considering the Reactors and associated separator units. The environmental, health and safety hazard values are tabulated as shown in the following table 2. The model environment for PEC calculation included the air and water compartments. The normalised values of each parameter are shown in Table 3. The environmental, health and safety score values are given in Table 4.

Table 2 - Hazards parameter values

Parameter	Route A	Route B	Route C
EHP _r	9.83	63.93	69.69
GHG _r	0.50	0.79	0.79
HAQ _r	3.74	10.55	10.55
HFE _r	3962.39	1.25	1.25
E _r	109.30	108.3	102.7
F _r	23	20	17
P _r	6	0	0
T _r	1875	645	645
ΔH _r	729.65	595.59	649.09

Table 3 - Normalised values

Parameter	Route A	Route B	Route C
\overline{EHP}_r	0.14	0.92	1
\overline{GHG}_r	0.63	1	1
\overline{HAQ}_r	0.36	1	1
\overline{HFE}_r	1	2.52×10^{-4}	2.52×10^{-4}
\overline{E}_r	1	0.99	0.94
\overline{F}_r	1	0.87	0.74
\overline{P}_r	1	0	0
\overline{T}_r	1	0.34	0.34
$\overline{\Delta H}_r$	1	0.82	0.89

Table 4 - Environmental, health and safety score

Score	Route A	Route B	Route C
EHS _r	0.39	0.96	1
SHS _r	0.68	0.5	0.5
CPSS _r	1	0.6	0.58

The IEHSH index is presented for chemical routes A, B and C in Table 5:

Table 5 - The IEHSH Index values

	Route A	Route B	Route C
IEHSH _r	0.69	0.72	0.73

According to the individual EHS scores (Table 4) route A is the most environmentally friendly, route B and C are the most healthy and route C is the one that is most safe. Considering the final IEHSH index values (Table 5), the route A is the most environmentally friendly, healthy and safe. However, the rank could be different



if the weights are changed based on its importance of each EHS.

5. Conclusions

The proposed method in this work is capable of assessing environmental hazards, health hazards due to both continuous and catastrophic releases and safety risk assessment for both chemical and process safety.

Furthermore, the chemical routes can be ranked considering their environmental hazard level or health hazards level or safety separately. If the process route shows a higher hazard either on the environment, health or safety, the methodology is able to show the total hazard by all three aspects in a single score by using weights on EHSr, HHSr and CPSSr.

Acknowledgement

This research project was supported by the University of Moratuwa Senate Research Grant Number SRC/LT/2015/01.

References

1. Khan, F. I., & Amyotte, P. R., "Integrated inherent safety index (I2SI): A Tool for Inherent Safety Evaluation", *Faculty of Eng. & Applied Science, Memorial University of Newfoundland*, Vol. 23, No. 02, June, 2004, pp. 136-148.
2. Patel, A. D., Meesters, K., Uil, H. D., Jong, E. D., Blok, K., & Patel, M. K., "Sustainable Assessment of Novel Chemical Processes at Early Stage: Application to Biobased Processes", *J. Energy & Environmental Science*, June, 2012, pp. 8430-8444.
3. Cave, S., R., & Edwards, D., W., "Chemical Process Route Selection Based on Assessment of Inherent Environmental Hazard", *Department of chemical engineering, Loughborough, UK*, Vol. 21, 1997, pp. S965-S970.
4. Srinivasan, R., & Nhan, N. T., "A Statistical Approach for Evaluating Inherent Benign-ness of Chemical Process Routes in Early design stages", *J. Process Safety and Environmental Protection*, August, 2007, pp. 163-174.
5. Rathnayaka, S., Khan, F., & Amyotte, P., "Risk-Based Process Plant Design Considering Inherent Safety", *J. Elsevier, Safety Science*, June, 2014, pp. 438-464.
6. Khan, F. I., Husain, T., & Abbasi, S. A., "Safety Weighted Hazard Index (SWeHI)", *J. Institute of Chemical Engineering*, Vol. 79, March, 2001, pp. 65-80.
7. Hassim, M. H., & Edwards, D. W., "Development of Methodology for Assessing Inherent Occupational Health Hazards", *J. Institute of Chemical Engineering*, Vol. 84, September, 2006, pp. 378-390.
8. Hassim, M. H., & Hurme, M., "Inherent Occupational Health Assessment during Preliminary Design Stage", *J. Loss Prevention in the Process Industry*, Vol. 23, December, 2009, pp. 476-482.
9. Adu, I. K., Sugiyama, H., Fischer, U., & Hungerbuhler, K., "Comparison of Methods for Assessing Environmental Health Safety Hazards in Early Phases of Chemical Process Design", *J. Process Safety and Environmental Protection*, Vol. 86, August, 2007, pp. 77-93.
10. Gentile, M., Rogers, W. J., & Mannan, M. S., "Development of a Fuzzy Logic-Based Inherent Safety Index", *J. Institute of Chemical Engineering*, Vol. 81, November, 2003, pp. 444-456.
11. American Institute of Chemical Engineering, "Dow's Chemical Exposure Index", 1st ed., New York, 1988, pp. 8-17.
12. Mannan, S., "Lee's Loss Prevention in the Process Industry", 4th ed., Texas, USA, 2012.
13. Mackay, D., "Multimedia Environmental Models", 2nd ed., USA, 2001.
14. EPA, "Protocol for equipment leak emission estimates", publish no. EPA-453/R-95-017, 1995
15. Edwards, D. W., & Lawrence, D., "Assessing the Inherent Safety of Chemical Process Routes: Is there a Relation between Plant Costs and Inherent Safety?", *J. Institute of Chemical Engineering*, Vol. 71, November, 1993, pp. 252-258.

Antecedents of Work Engagement : Case Study of Outsourced Employees in Telecommunication Service Sector of Sri Lanka

K.A. Chathura S. Kumarasinghe

Abstract: This study evaluates the work engagement level of outsourced employees involved in engineering service delivery in the telecommunication sector of Sri Lanka. It attempts to identify the significant antecedents that have high influence on the work engagement. The conceptual framework of this study was built on the job-demands resources model of work engagement proposed by Bakker and Demerouti (2008a). This study adopts a mixed research approach. The quantitative study involved analysing responses to a questionnaire by 115 outsourced employees to estimate their work engagement level and to identify the significant antecedents. The relationship between work engagement and nine antecedents were investigated through multiple linear regression analysis. Qualitative analysis explored data collected from four interviews to identify the perceived influential antecedents.

This study discovered that the work engagement level of outsourced employees in the telecommunication sector of Sri Lanka was lower than desirable. Both the quantitative and qualitative studies revealed that autonomy, managerial, supervisory coaching and opportunities for professional development were significant influences on work engagement. Though there is no consensus between qualitative and quantitative results, social support, self-efficacy, self-esteem and optimism have also been found to be influential.

There is an increasing trend towards outsourcing engineering services in the telecommunication sector of Sri Lanka. Telecommunication operators depend heavily on these outsourced employees to deliver quality service to their subscribers. Therefore, there is much interest in the performance of these outsourced employees. Though there have been ample academic studies conducted on the financial and contractual aspects of service outsourcing, there are very few academic undertakings that have focused on the human aspects of outsourcing. The study fills this void by investigating the work engagement of outsourced employees and identifying influential antecedents. By knowing the present level of work engagement and the factors that should be focused on, telecommunication operators and outsource service providers should be able to devise an effective strategy to improve the work engagement.

Keywords: Work Engagement, Outsourcing, Telecommunication, Service

1. Introduction

The telecommunication industry is a capital-intensive undertaking, where the operators have to constantly keep investing in coverage expansion, infrastructure development and the introduction of rapidly changing new technologies. Further, a large proportion of operational costs to an operator, such as energy costs, site rentals, spectrum fees paid to government and network maintenance costs, are fixed costs that bear little relationship to the number of customers served by the operator. Hence, operators are constantly looking for avenues for increasing usage of the deployed network, as unused capacity at any given moment is wasteful. Therefore, telecommunication operators have opted to slash their prices in order to win new customers. In fact, a severe price war among the telecommunication operators has resulted with Sri Lanka being placed among those countries

having the lowest telecommunication tariffs in the world (Fitch Rating, 2015).

In this context, operators have adopted measures to reduce the cost of production. One of the key initiatives was to shift from the in-house operation model to outsource model. Different operators have adopted out-sourcing to different degrees. All operators have adopted outsourcing services at some level, and so there is considerable involvement of outsourcing service providers in operating telecommunication networks at present. Outsource service provider may be generally responsible for the day-to-day maintenance of active network elements, maintenance of the passive infrastructure such as

*Eng. K.A.C.S. Kumarasinghe, B.Sc.(Electronic & Telecommunication Engineering - Moratuwa), MBA (Leicester), C.Eng(SL & UK), MIE(SL), MIET (UK).
Email:Chathurak@hotmail.com*



telecommunication towers, network planning, network optimisation activities and technical support services to customers' requests through customer visits. Consequently, the telecommunication operator who has to provide quality services to its subscribers is highly dependent on the outsourcing service provider. Hence, outsourced employees play important and critical roles in the technical service delivery mechanism.

Traditionally, work engagement simply meant employment and organisations believed that employees were engaged in their work. However, over time, this understanding has changed. In a general sense, engagement refers to a combination of involvement, enthusiasm, passion, commitment and dedication (Schaufeli, 2012: 3; Schaufeli, 2014: 15). Work engagement means exhibiting these attributes towards work.

There can be multiple benefits to employees and companies from work engagement. Engaged employees experience positive emotions and enjoy good mental health (Schaufeli, 2012; Schaufeli and Salanova, 2008; Halbesleben, 2010). At the individual employee level, a better work engagement may lead to better performance, increased output and a lower number of absent days from work (Schaufeli, 2012; Schaufeli, 2014; Rich et al., 2010; Halbesleben, 2010). At the organisational level, this may lead to increased customer satisfaction, higher profitability, productivity, turnover, and safety (Harter et al., 2002; Harter et al., 2009). Therefore, work engagement can be identified as a desirable condition for employees and for the organisation for which they work (Schaufeli, 2012).

Normally, in-house employees empathise to a marked degree with their organisations' goals, are familiar with their organisations, engage in direct communication with top management and are subject to direct supervision by their managers (Purcell and Purcell, 1998). In contrast, outsourced employees are involved in the service delivery of organisations that avail themselves of the offerings of third-party service providers. They are not part of the hiring organisation. This means that outsourced employees are relatively less informed, less compensated and operate under less supervision.

Therefore, outsourced employees face more difficulties or challenges in executing their work compared to in-house employees. In this context, there is a high chance that outsourced

employees could be more stressed, leading to lower levels of performance. This may also impact the delivery commitments of the outsource service provider towards the contracting organisation.

On the other hand, increased work engagement might be the solution to overcome these challenges considering the positive impact that works engagement generates. Therefore, telecommunication operators and outsource service providers ought to be keen on improving the work engagement of their staff to improve or maintain their service levels.

Organisations are now seeking to improve the work engagement of their employees by conducting surveys to figure out what needs to be done (Ketter, 2008). By doing so, Saks (2006) suggests that they might discover a few antecedents of the work engagement that could assist in enhancing engagement. There are many antecedents of the work engagement, and some have been empirically tested (Wollard and Shuck, 2011). However, with outsourcing, the main academic attention so far has centred on the economics of this activity, and much less attention has been paid to personal or employee aspects (Raghuram, 2006). Similarly, Purcell (1996: 22 cited in Kessler et al., 1999: 5) notes, "we lack the research to make definite statements about the effect of outsourcing on employees." As such, previous research has provided valuable insights into the work engagement in an in-house context; but only limited studies have been devoted to the outsource environment. This study aims to fill this gap by investigating the work engagement of outsourced employees.

Taking into account the above-mentioned considerations, this study will attempt to identify antecedents that would have a high influence on the work engagement of outsourced employees. Once these influential antecedents of the work engagement are identified, telecommunication operators with the collaboration of outsourcing service providers could devise some mechanism to reinforce these antecedents in order to improve the work engagement of employees.

Therefore, this study primarily focuses on the research questions:

- What would be the work engagement levels of outsourced employees at present in the telecommunication engineering service sector of Sri Lanka?
- What are the significant antecedents of the work engagement in outsourced employees

in the telecommunication engineering service sector of Sri Lanka?

2. Literature Review

2.1 Concept of Engagement at Work

In a general sense, engagement refers to a display of involvement, absorption, commitment, passion, enthusiasm, focused effort, zeal, dedication, and energy of someone or something (Schaufeli, 2014: 15). However, the traditional view of the work engagement simply meant employment. Organisations assumed that employees were fully engaged at their jobs because they happened to be on the pay role (Schumann, 2010). But recent developments in business studies and in academia have altered this simple understanding of the engagement.

In the 1990s, a management consulting firm, Gallup Inc. introduced an employee satisfaction and engagement measurement tool (Harter et al. 2009). This fuelled much interest on work related engagement in both business and academia (Schaufeli, 2014). Schaufeli (2014: 17) also attributed this increase in interest partially to a positive psychology movement, where researchers try to understand the optimal human behaviour to discover the reasons that enable individuals and organisations to succeed.

Employee engagement and work engagement are commonly used concepts in literature. Employee engagement refers to the relationship between the employee and his organisation, whereas the work engagement narrows it down to the relationship between the employee and his work (Schaufeli, 2014: 15). This study mainly focused and developed on the concept of work engagement, which is a narrower and a more specific idea.

The initial reference to the engagement in academia was by Khan (1990: 694) who defined personal engagement as the "harnessing of organisation members' selves to their work roles: in engagement, people employ and express themselves physically, cognitively, emotionally, and mentally during role performances". In this view, employees build an identity for themselves centred on their work, and they put in an effort to develop and maintain this identity.

Alternatively, the work engagement is also viewed as the opposite of burnout. In this

understanding from the viewpoint of occupational health psychology, an employee's psychological relationship with his work is visualised as falling in between the endpoints of the positive experience of engagement and negative experience of burnout in a single continuum (Maslach and Leiter, 2008). Here, the engagement is identified by energy, involvement, and efficacy, which are considered to be the direct opposites of three burnout dimensions, exhaustion, cynicism, and lack of professional efficacy (Maslach and Leiter, 1997, as cited in Maslach and Leiter, 2008). This means that if an employee is low on work engagement, he is high on burnout.

Schaufeli et al. (2002: 74) define the work engagement "as a positive, fulfilling, work-related state of mind that is characterized by vigour, dedication, and absorption." In this definition, vigour is identified as having a higher level of energy at work, ability to weather-out difficulties at work and willingness to invest effort in work. Dedication refers to being strongly involved in work with the feeling of self-importance, enthusiasm, pride, being inspired by work, and feeling challenged. Absorption means fully concentrating and being happily occupied in one's work. This portrays the work engagement as a distinctly different concept from burnout.

Saks (2006: 602) defined employee engagement as "a distinct and unique construct consisting of cognitive, emotional, and behavioural components that are associated with individual role performance." This definition is similar to the definition of Khan (1990) whose focus was on an organisation's employees collectively, while Saks' (2006) focus was on individuals.

Schaufeli (2014: 31) claims that most of the academic studies on engagement have utilised the definition based on vigour, dedication and absorption. For this research, the same work engagement definition proposed by Schaufeli et al. (2002) is adopted.

There are multiple theories available to explain work engagement behaviour. However, as Schaufeli (2014: 25) claims, there is no single theory that explains all aspects of work engagement, but a collection of theories that elaborate on different aspects of work engagement. Kahn (1990) in his Need-Satisfying model proposed that employees will be engaged if three psychological needs are met. He identifies these needs as



meaningfulness, safety, and availability and suggests that employees ask three questions from themselves relating to work to verify whether these needs will be met. These questions are: (i) Is this work meaningful enough for me to get myself personally involved? (ii) How safe will this work be? and (iii) Am I available for this work? In other words, these three questions assess return on self-investment, preservation of self-image or status and possessing of physical or psychological resources, respectively (Kahn, 1990: 705). Simply put, this theory predicts that when the job is meaningful, the environment is safe to work in, and personal resources are available, then employees become engaged deeply in work.

In the Affective Shift Model, Bledow et al. (2011: 1246) propose that work engagement results from an employee moving from a situation in which negative effects are experienced to a situation of high positive effects, attempting to explain changes in work engagement throughout the day, between tasks or events. Positive affect is a signal to self to approach and continue along the line of action while negative affect interrupts the ongoing stream of action, disrupts the mental decision-making process and hinders behaviour (Bledow et al., 2011: 1247). Work engagement will be low if an employee remains in a negative affective state without experiencing positive effects. However, employee motivation will improve if an employee moves to a positive affective state.

Social exchange theory proposes that social behaviour is the result of an exchange process

to maximise benefits and minimise costs. Saks (2006: 603) suggests that when employees receive benefits such as salary or development opportunities, employees also reciprocate in kind; one way of repayment is on their level of engagement. Saks (2006: 603) notes, "bringing oneself more fully into one's work roles and devoting greater amounts of cognitive, emotional, and physical resources is a very profound way for individuals to respond to an organisation's actions." When organisations fail to provide these reassurances, employees will tend to disengage themselves from their roles.

The Job Demands - Resources (JD-R) theory proposes that causes of employee well-being fall under two main categories identified as job demands and job resources (Bakker and Demerouti, 2007: 312). Job demands refer to conditions that generate physiological or psychological stress such as work pressure and unfavourable working environment (Bakker and Demerouti, 2007: 312). Job resources are those factors that mitigate the physiological or psychological stress, stimulate personal growth or assist in achieving work goals (Bakker and Demerouti, 2007: 312). Xanthopoulou et al. (2007, 2009) have expanded this model to include personal resources. Personal resources are positive self-evaluations that are linked to resiliency; they refer to an employee's conviction that he can successfully control and influence his environment (Hobfoll et al., 2003). Building on above findings, Bakker and Demerouti (2008a: 218) propose the JD-R model of work engagement as shown in Figure 1. This model shows that job resources and personal resources can independently and collectively

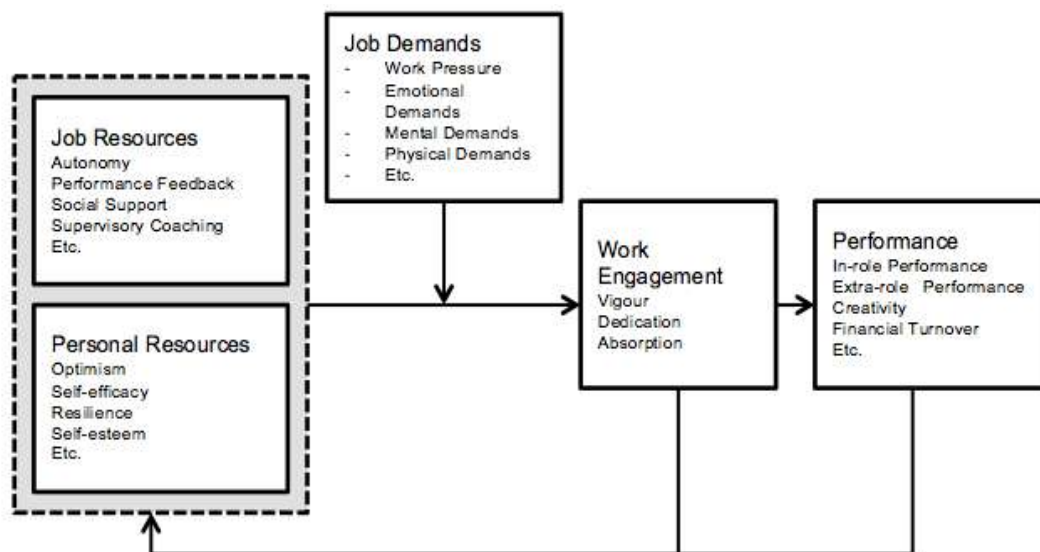


Figure 1 - The JD-R model of work engagement (Bakker and Demerouti, 2008a: 218)

influence work engagement. Bakker and Demerouti (2008a: 218) argue that “job and personal resources particularly have a positive impact on engagement when job demands are high”. This model presents that there is a relationship between work engagement and performance. The JD-R model also includes a feedback loop through which employees who are engaged and perform well, can reciprocally influence their own resources.

In this model, the relationship between job resources and work engagement could be explained in terms of the motivational process (Bakker and Demerouti, 2008a). In accordance with McClelland’s theory of needs (1961, as cited in Robbins et al., 2011), autonomy can be identified as the need for power over oneself. Social support, feedback and supervisory coaching can be linked with the need for affiliation. When these needs are satisfied, employees will be motivated in term of energy, dedication and focus. In fact, work engagement is the presence of these three qualities (Schaufeli et al., 2002). Further, the job characteristics model proposes that core job dimensions such as autonomy or feedback can lead to a critical psychological state (Hacman and Oldham, 1980, as cited in Robbins et al., 2011). This psychological state can be considered as work engagement. This is the intrinsic motivational relationship between job resources and work engagement. Meijman and Mulder (1998, as cited in Bakker and Demerouti, 2008a) also identify an extrinsic motivational relationship where a congenial work environment with supportive colleagues, guidance from supervisor or feedback would motivate employees to work hard and successfully complete tasks. Multiple studies have confirmed this relationship between job resources and work engagement (Schaufeli and Bakker, 2004b; Xanthopoulou et al., 2009).

The relationship between personal resources and work engagement is explained as follows: a person with higher personal resources would have a more positive self-regard and be more goal oriented, which in turn would lead to higher performance (Judge et al., 2005, as cited in Bakker and Demerouti , 2008a: 213-214). Xanthopoulou et al. (2009: 136) having examined the relationship between self-efficacy, self-esteem, optimism and work engagement claim that the motivational process is also active between personal resources and work engagement. They explain that having a high level of personal resources makes employees

feel more confident in controlling their environment, and increase their pride and confidence in the work they do, leading to a better work engagement (Xanthopoulou et al., 2009: 136).

In this model, Job demands refer to job aspects such as work overload or high time pressure, which would require employees to exert additional effort to achieve work goals and to prevent performance decline (Schaufeli, 2014: 27). These job demands would exhaust the energy of employees over time and eventually lead to burnout (Schaufeli, 2014: 27). This negative process is called health impairment process, which counteracts or mediates the motivational process between resources and work engagement within the JD-R model.

The JD-R model also presents the relationship between work engagement and job performance. Bakker and Demerouti (2008a) identified four possible reasons as to why engaged employees perform better than non-engaged employees. These reasons are, (i) positive emotions experienced by engaged employees, (ii) better mental health of engaged employees, (iii) engaged employees to create own job and personal resources, and (iv) engaged employees to induce engagement among other employees (Bakker and Demerouti 2008a: 215-217). According to Bakker and Demerouti (2008a: 214-215), several studies have provided evidence on the relationship between work engagement and performance.

Out of the four models of work, engagement was discussed, the JD-R model of work engagement has received the most empirical support (Schaufeli 2014: 31). Hence, the JD-R model was adopted for this study.

2.2 Measurement of Work Engagement

There are several instruments available for measurement of work engagement. The most widely used instrument to measure employee engagement in the business domain is Gallup’s Q12 questionnaire (Schaufeli, 2012: 4). This questionnaire has items that were developed from an actionable standpoint, including items such as “This last year, I had opportunities at work to learn and grow” (Harter et al., 2009: 8-9). The above question assesses opportunities for professional development, a job resource under the JD-R model. Therefore, rather than evaluating the work engagement as a psychological state, the Q12 questionnaire



directly measures the antecedents of work engagement (Schaufeli, 2012: 4).

Bakker and Demerouti (2008b) propose Oldenburg Burnout Inventory (OLBI) as an alternative measurement of burnout and engagement. They argue that instead of having both positively and negatively worded items to measure two dimensions, exhaustion and disengagement, the OLBI question items could be reverse coded to represent two engagement dimensions, vigour and dedication (Bakker and Demerouti, 2008b). This follows the visualisation of burnout and work engagement as endpoints of a single continuum (Maslach and Leiter, 2008).

Schaufeli et al. (2002) proposed a 17-item Utrecht Work Engagement Scale (UWES-17) questionnaire to evaluate the work engagement by assessing the three dimensions, vigour, dedication, and absorption. This scale includes 6 vigour items, 5 dedication items, and 6 absorption items (Schaufeli et al., 2002). Bakker and Demerouti (2008a: 210) note that multiple researchers in several countries have validated the UWES-17 scale. Later, Schaufeli et al. (2006) have developed a shorter version of the UWES scale and have concluded that this new scale can be satisfactorily utilised to measure work engagement. This compact scale has 3 questions on each of the 3 dimensions of work engagement. Schaufeli and Bakker (2004a: 21) found higher than 0.9 correlations among the three dimensions measured with UWES-17 and UWES-9, with the new scale having an internal reliability measured by Cronbach's alpha at between 0.89 to 0.97 across 25 studies they analysed. For present research, the UWES-9 scale was adopted in view of its alignment with the work engagement definition and the JD-R model.

2.3 Antecedents of Work Engagement

The main purpose of this research revolves around the antecedents of work engagement. Wollard and Shuck (2011: 433) in their review of the literature identified a total of 41 antecedents to employee engagement, 20 of them individual antecedents and balance 21 organisational antecedents. They found that 11 of 20 individual antecedents and 13 out of 21 organisational antecedents were supported by empirical evidence (Wollard and Shuck, 2011: 433). The antecedents with empirical evidence are absorption, dedication, corporate citizenship, involvement in meaningful work, linkage with individual and organisational

goals, perceived organisational support, vigour, work-life balance, core self-evaluation, authentic corporate culture, clear expectations, corporate social responsibility, job characteristics, job fit, task challenge, manager expectation, manager self-efficacy, work place safety, work place climate, rewards, supportive organisational culture and use of strengths (Wollard and Shuck, 2011: 433). It is worth noting that this extensive list includes the three dimensions of work engagement proposed by Schaufeli et al. (2002: 74). This shows that different scholars in different contexts have considered an array of attributes as possible antecedents of work engagement. However, testing and assessing all these 41 antecedents will be an intimidating task for any single study.

Schaufeli and Bakker (2004b) found performance feedback, social support, and supervisory coaching to be important antecedents. Saks (2006: 611) found organisational support and procedural justice to be significant antecedents to employee engagement. Xanthopoulou et al. (2007, 2009) found autonomy, social support, supervisory coaching, professional development, organization-based self-esteem, optimism and self-efficacy to be significant antecedents.

For this study, five job resources, viz. autonomy, social support, managerial, supervisory coaching, performance feedback and professional development opportunities and four job resources, viz. self-efficacy, self-esteem, resilience and optimism were selected as possible antecedents.

In general sense, autonomy is the freedom that an employee has from being governed. Schwalbe (1985: 525) notes autonomy as freedom of movement, freedom to establish and execute plans for task accomplishment, and freedom from immediate supervision. Robbins et al. (2011: 91) identify autonomy as the degree to which the job provides freedom, independence and discretion in work scheduling and on deciding the course of action.

Etzion (1984, as cited in Brough and Pears, 2004: 472) defined social support as an informal social network that provides individuals with expressions of emotional concern or empathy, practical assistance, informational support or appraisal. Brough and Pears (2004: 472) identify behaviour such as collaborative problem

solving, sharing of information, giving advice to and receiving advice from colleagues as workplace social support. When an employee is faced with high work pressure or a difficult problem to solve, he could turn to his colleagues at work who are willing to support.

Fournies (1987, as cited in Ellinger et al., 2005: 621) claim that managerial coaching is a leadership style in which constructive feedback is used to get the most out of employees through demonstration of respect and appreciation. Managerial coaching helps employees to recognise their potential, improve their performance, and develop their skills by empowering them (Ellinger et al., 2005: 622). The employee would receive proper instructions, solutions to problems he faces and guidance on how to be efficient through the supervisory coaching. Further, it also brings clarity to the tasks an employee performs.

Performance feedback means providing direct and clear information on an employee's performance or effectiveness (Robbins et al., 2011: 91). Performance feedback is important if an employee is to perform as expected by the organisation, without having to face surprises at performance appraisals; it also allows him to discuss and find out solutions for difficulties.

Professional development means updating one's skill set or acquiring new knowledge. When an employee is given the opportunity of acquiring new knowledge or mastering a new skill, he will show more competence in performing his job. With advanced skills set or knowledge, the employee will be able to face work pressure or manage difficult situations at work more efficiently and effectively.

Self-efficacy is the employee's belief that he is capable of performing a task competently (Robbins et al., 2011: 80). When an employee has high self-efficacy, he would be more confident in his ability to accomplish a task.

Self-esteem is the employee's own evaluation of his own worth (Rosenberg, 1965, as cited by Robbins et al., 2011: 72). Maslow (1954: 45) asserts that "satisfaction of self-esteem need leads to feelings of self-confidence, worth, strength, capability, and adequacy, of being useful and necessary in the world. But thwarting of these needs produces feelings of inferiority, of weakness, and of helplessness." Stating it differently, when an employee possesses self-respect, believes in himself and

feels important at work, then he would be more confident in taking up challenging tasks.

Resilience is an employee's ability to face difficult situations, cope with adverse conditions without becoming flustered and recover from unsettling situations fast (Hornby, 2005: 1291). When an unfavourable development causes a setback to a resilient employee, he would not continue to be in a discouraged state of mind but would recover quickly and continue to perform well.

In general terms, optimism may be regarded as hopefulness or confidence that the future would be promising (Hornby, 2005: 1067). Optimistic employees will look beyond present difficulties or challenges and remain hopeful.

As already explained, the JD-R model proposes that these nine resources would assist an employee to mitigate the adverse impact of job demands on work engagement. The purpose of this study is to explore the relationship between work engagement and these nine antecedents in an outsource service environment.

2.4 Service Outsourcing

Outsourcing is the transfer of an in-house function to an external service provider, who then provides the outsourcing company with services at least as good as, or hopefully better than the services provided in-house (Godfrey-Faussett, 1997: 179). Telecommunication operators have been increasingly outsourcing their engineering services to outsource service providers. As Belcourt (2006) point out, this trend of outsourcing is primarily prompted by the need to reduce the operational costs of the telecommunication operator in a high price sensitive market, while there are also other benefits such as the following:

- Outsourcing secondary functions allows organisations to focus more and better on their core functions
- Easier access to upgraded and the latest technology through outsource partnership
- Improved performance through enforcing strict performance standards in outsource contracts
- Access to the specialised expertise of outsourced employees

While there are benefits to be reaped through outsourcing, Belcourt (2006) draws attention to several risk factors associated with outsourcing.



Increased inflexibility due to difficulty in changing the terms of the contract, negative impact on employees' morale and performance, and limiting of the organisation's ability to learn and adapt to changes are some of these. Despite these disadvantages, telecommunication operators in Sri Lanka are embracing this practice of outsourcing their engineering functions.

Ramani (2014) has identified five levels of outsourcing in ascending order of involvement of an outsource service provider as shown in Figure 2.

Level-1: Staff Augmentation – Specific skilled resources to supplement in-house workforce are provided by an outsource service provider. Activities that outsourced employees engage in are as instructed by telecommunication operator and outsource service provider does not take any risk or responsibility.

Level-2: Out-Tasking – Outsource service provider only performs certain tasks related to part of the network element and is responsible for those activities.

Level-3: Project Based – Outsource service provider is responsible for the day-to-day running of a particular project. The telecommunication operators' duty is restricted to monitoring and control the project deliveries are as per service level agreement entered into by both parties.

Level-4: Managed Services – Outsource service provider takes complete ownership for delivery. His scope includes achieving technical service delivery and business objectives.

Level-5: Managed Service with Managed Capacity – Outsource service provider takes responsibility for complete service delivery and developing network capacity infrastructure to achieve business objectives of the telecommunication operator.

One telecommunication operator in Sri Lanka has adopted outsourcing at level-5 of above classification. Remaining telecommunication operators have also outsourced their engineering services at level-3 or level-4. Therefore, there is high involvement of outsourced employees in the day-to-day operations of telecommunication operators. Telecommunication operators are therefore highly dependent on the performance of these outsourced employees as their numbers are substantial and form a vital part of the service delivery to subscribers.

As discussed, outsourced employees are a key component of service delivery of telecommunication operators. However, these outsourced employees differ from in-house employees in several aspects. Purcell and Purcell (1998) note that outsourced staff is treated differently from in-house staff. Outsourced staff is paid less, not granted fringe benefits and training is kept to a minimum, in contrast to the much higher pay of in-house staff, who are entitled to fringe benefits such as sick pay and holiday pay. They are also more likely to receive employee training as their organisations are more willing to invest in them. Outsourced employees who typically work alongside the in-house employees are well aware of the differential treatment. Hence, they are likely to be in a rather discontented state of mind.

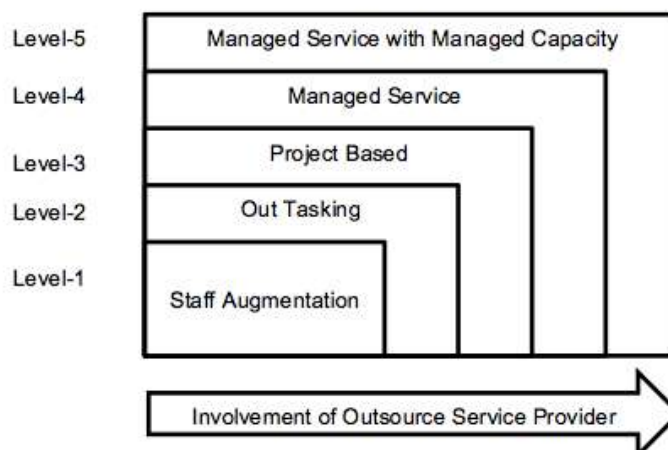


Figure 2 - Levels of Service Outsourcing (Ramani, 2014)

Outsourced employees involved with engineering service delivery on behalf of telecommunication operators require a high level of skills and domain expertise to perform satisfactorily. Whereas, Aron and Singh (2005: 137) point out that outsourced employees engaged in such demanding work tend to make more mistakes in operation compared to in-house staff. This is also an indication that outsourced employees are placed at a disadvantage compared to in-house employees.

While telecommunication operators are increasingly dependent on the services of outsourced employees, it can be seen that due to differences between in-house and outsource employment conditions, outsourced employees are placed in an unfavourable position.

Outsourced employees are faced with additional challenges or difficulties in their work environment. To be specific, they are faced with high job demands, both psychological and physiological. According to the JD-R model of work engagement, a high level of job demands would lead outsourced employees to lower engagement levels in comparison to in-house employees, who do not face similar challenges.

However, as Raghuram (2006) highlights, previous studies on outsourcing mainly focused on the economic aspects of outsourcing and much less on the individuals involved. Purcell (1996: 22, as cited in Kessler et al., 1999: 5) has expressed a similar view stating "we lack the research to make definite statements about the effect of outsourcing on employees." In this context, even though the JD-R model predicts lower engagement level for outsourced employees based on additional job demands they experience while being deprived of resources, there is no empirical evidence to support this claim. Thus, this study attempts to fill this gap by estimating the work engagement of outsourced employees involved in telecommunication service delivery in Sri Lanka.

As discussed, telecommunication operators are heavily dependent on outsourced employees for delivery of engineering services. Considering the positive impact work engagement has on the performance of these outsourced employees, telecommunication operators would be keen on improving the work engagement levels. This could be achieved through stimulating the job resources

and personal resources that act as antecedents to work engagement as identified in the JD-R model. Though literature identifies an array of antecedents to work engagement, the available literature fails to identify significant antecedents that refer specifically to the outsource environment. Therefore, this study also attempts to identify the significant antecedents of the work engagement of outsourced employees involved with telecommunication service delivery. By knowing those significant antecedents, telecommunication operators and outsource service providers could devise a more effective strategy to enhance the work engagement of outsourced employees, which would, in turn, improve the performance level of those employees.

3. Methods

This study adopts a combination of quantitative and qualitative research methods. Use of quantitative and qualitative methods in combination allows the crosschecking and validating of findings, thus allowing the researcher to have greater confidence in the results (Greene et al. 1989: 259; Bryman and Bell, 2007: 413). The quantitative study in this research focuses on establishing the work engagement level of outsourced employees and on identifying significant antecedents of work engagement, while qualitative research is used to verify and correlate with findings of the quantitative study.

3.1 Quantitative Study

A quantitative study was conducted by administering questionnaires to outsourced employees currently engaged in engineering service delivery. These employees were requested to fill in a structured questionnaire on a voluntary basis. This study was conducted with one of the larger outsource service providers, who provide engineering services to telecommunication service providers in Sri Lanka. This company has on its employment role 281 permanent and contractual staff assigned to operations of a single telecommunication operator. Due to time and resource constraints, it was decided to administer the questionnaire to just 50% of the population, totalling 140 participants. For convenience, the questionnaire was administered only to those employees who attended monthly review meetings. This approach assisted in receiving a good response in terms of completing the questionnaire.



A structured questionnaire with 77 questions was drafted to capture the relevant data on work engagement and their antecedents. Work engagement was measured using the UWES-9 (Schaufeli et al., 2006). Items were scored on a Likert scale ranging from 0= Never to 6= Always. Scores of all questions were summed up to determine the overall UWES score, where a high score implies high work engagement. Autonomy was measured using a modified version of the Self-Determination Scale (SDS; Sheldon et al., 1996; Sheldon, 1995) that was designed to assess the extent to which employees tend to function in a self-determined way. SDS has two 5-item subscales, one subscale on awareness of oneself and the other on perceived choice in one's actions. For this study, a 5-item sub-scale on perceived choice is adopted in the employment context. Each item consists of a pair of statements (statement A and statement B), and participants were asked to judge the degree to which statement-A is true against statement-B on a 5-point Likert scale. If statement-A strikes as completely true and statement-B strikes as completely untrue, the appropriate response would be 1. If the two statements are equally true, the appropriate response would be 3. A score of each item would be reversed to arrive at SDS value so that a higher score on every item will indicate a higher level of self-determination.

A six-item scale that was developed based on the social support questionnaire-short form (Sarason et al., 1987) was used to measure social support for employees at work. Each item is scored on a 4-point Likert scale as 1= 'Not true at all' to 4= 'Exactly true'. Scores of individual items were added up to arrive at the total social support score. Ellinger et al. (2005) have introduced an exploratory 8-item measure for managerial coaching based on managerial coaching behavioural themes. Six items in this scale focus on supervisory coaching, while the balance two items focus on supervisory feedback. Therefore, this scale is used to measure both managerial, supervisory coaching and feedback dimensions in the present study. Each item is scored on a 7-point Likert scale where 1= 'Almost never' to 7= 'Almost always'. The scores obtained for question numbers 1,2,3,6,7 and 8 were taken to calculate the total score of managerial, supervisory coaching, while scores for question numbers 4 and 5 were summed up to obtain the supervisory feedback score. Possibilities for professional development were measured using a 3-item scale developed by Bakker et al. (2003, cited in

Xanthopoulou et al., 2009). This item scale ranges from 1= 'Strongly disagree' to 5= 'Strongly agree'. Sum of all three items is taken as a measure of opportunities for professional development.

Self-efficacy is captured through the General Self-Efficacy (GSE) scale developed by Schwarzer and Jerusalem (1995). GSE consists of 10 items scored as 1= 'Not true at all' to 4= 'Exactly true'. The total score is equal to the sum of scores obtained for all items. The Rosenberg Self-Esteem Scale (RSE) with 10-items was used to evaluate self-esteem of employees (Rosenberg, 1965). Each item was scored using a 4-point Likert scale. For items 1,3,4,7 and 10, a score of 1 represents 'strongly disagree' and 4 represents 'strongly agree', while for the balance items the scoring is reversed. Sum of all items after reversing 2,5,6,8 and 9 is computed to arrive at the RSE score. A higher RSE score indicates greater self-esteem. Participants' resilience was measured using a 14-item Resilience scale (Wagnild, 2009) in which each item was scored on a 7-point scale with 1= 'totally disagree' to 7= 'totally agree'. All scores are summed up to compute the total score.

Optimism was measured with the Life Orientation Test - Revised (Scheier et al., 1994). This scale is comprised of six items that measure optimism and four filler items. The four filler items were not considered for computation. Out of the six main items, three items measure optimism as a positive quality, while the other three items measure pessimism as a negative quality. Participants rate each item on a 5-point scale ranging from 0= 'totally disagree' to 4= 'totally agree'. All negative items were reversed before totalling so that higher scores indicate higher optimism.

This study attempts to investigate the relationship between work engagement and 9 independent variables. All 9 independent variables and the dependent variable, work engagement, are measured on a continuous scale. Hence, Multiple Linear Regression technique is employed to investigate the relationship between work engagement and the independent variables.

The total number of fully completed questionnaires received was 116 out of the 140 distributed, a response rate of 83%. However, when checking for outliers while performing multiple linear regression analysis, one outlier (Participant 89) was identified and excluded

from the dataset. In the final dataset, 12% (N=14) were from manager level, 37% (N=42) from engineers and balanced 51% (N=59) from technical officers attached to the outsourcing organisation. Further, 26% (N=30) of the respondents have been at the current employment position for less than 2 years, 63% of them (N=72) from 3 to 5 years and balance 11% (N=13) have been in their positions for more than 5 years.

ANOVA analysis is performed to examine the model fit with regression analysis. Table 1 provides the model summary of regression analysis. The multiple correlation coefficients (R) is the Pearson correlation coefficient between the predicted scores of work engagement by the regression model and actual

A non-probability sample of six participants, viz. two managers, two engineers and two technical officers were selected for interviews out of those who responded to the initial questionnaire, in order to maximize the validity and reliability of results (Bryman and Bell, 2007: 473). Invitations for the interview were sent to all six participants together with a list of five questions. Four out of these six accepted the invitation while two of them refused to participate. All interviews were conducted in a meeting room at their office at a time convenient to them, with the interview lasting approximately 50 minutes. Extensive notes were taken during the interviews. However, all participants had expressed concerns about recording the interviews. Therefore, the

Table 1 - Model Summary of Regression Analysis

R	R ²	Adjusted R ²	Std. Error of the Estimate	Durbin-Watson
0.847	0.717	0.687	0.67155	1.835

Table 2 - ANOVA Statistics

	Sum of Squares	df	Mean Square	F	Sig.
Regression	117.706	11	10.701	23.727	0.000
Residual	46.452	103	0.451		
Total	164.157	114			

values of work engagement. R value of 0.847 suggests a strong association. Further, R² value of 71.7% indicates that inclusion of independent variables in the regression model caused 71.7% variability in the work engagement compared to the mean model. Adjusted to reflect the variability in the population, the Adjusted R² value of 68.6% indicates a large size effect (Lakens, 2013). As shown in Table 2, ANOVA predicts the model's statistical significance at $p < 0.0005$. Through these observations, it can be concluded that the regression model provides a good fit at a statistically significant level.

3.2 Qualitative Study

Qualitative data were obtained from face-to-face semi-structured interviews conducted with five open-ended questions pertaining to the focus of interest of this study and in such a way that the results could be easily interpreted, despite the lack of flexibility that could be caused by novel explanations (Zikmund et al., 2013: 154).

These five open-ended questions invited participants to share their own opinions, beliefs and experiences in relation to work engagement in the outsourced engineering service environment and to share their thoughts on what they believed to influence the work engagement.

interviews were not recorded.

Notes that were taken during the interviews were read over multiple times to identify a possible logical model or themes. These themes were further analyzed with the intention of finding the answers to research questions.

4. Results

4.1 Descriptive Statistics

Table 3 presents means, standard deviations, Cronbach's alphas and correlations among the study variables. In this study, Cronbach's alpha falls between 0.78 and 0.95, which is within the acceptable range, indicating that the measures used are reliable (Tavakol and Dennick, 2011). There is a high correlation ($r > 0.5$) between work engagement and four of the independent variables with high significance ($p < 0.01$). Five of the remaining measures are also sufficiently correlated ($r = 0.26-0.46$) with high significance ($p < 0.01$). These results suggest that certain factors identified as possible antecedents of work engagement are indeed positively related. Further, it should be noted that these results also suggest that there are close relationships between several independent variables. For example, autonomy is positively correlated to self-efficacy ($r = 0.58$, $p < 0.01$) and managerial supervisory coaching is also positively



correlated to resilience ($r= 0.45, p <0.01$). These findings suggest that there can be a relationship between job resources and personal resources. However, no further analysis was performed as this is beyond the scope of the present study.

4.2 Level of Work Engagement

As given in Table 3, work engagement has a mean value of 2.54 with a standard deviation of 1.20. Distribution of samples over the work

	Mean	SD	WES	AUT	SS	MSC	FB	PD	SEF	SES	RES	OPT
WES: Work Engagement	2.54	1.20	0.914									
AUT: Autonomy	3.05	0.70	.629**	0.783								
SS: Social Support	2.51	1.81	.331**	.212*	0.883							
MSC: Managerial Sup. Coaching	3.96	1.45	.635**	.495**	.295**	0.946						
FB: Feedback	3.76	1.68	.382**	.302**	0.148	.190*	0.838					
PD: Professional Development	2.42	0.88	.594**	.330**	.294**	.384**	.306**	0.834				
SEF: Self-Efficacy	2.41	0.82	.632**	.578**	.321**	.486**	.491**	0.937				
SES: Self-Esteem	2.41	0.78	.255**	.219*	0.074	.240**	.251**	0.116	.271**	0.922		
RES: Resilience	3.97	1.31	.456**	.531**	0.103	.447**	0.146	.384**	.343**	.233*	0.939	
OPT: Optimism	2.13	0.96	.290**	0.082	-0.039	0.01	-0.096	.225*	0.123	-0.088	.226*	0.800

** Correlation is significant at the $P < 0.01$ level.

* Correlation is significant at the $P < 0.05$ level.

Table 3: Means, Standard Deviations, Cronbach's Alphas (on the diagonal) and Pearson Correlations among the study variables (N=115)

Work Engagement Level	Range	Frequency	Percent	Cum. Percent
1_Very Low	<=1.93	38	33	33
2_Low	1.94 – 3.06	22	19.1	52.2
3_Average	3.07 – 4.66	54	47	99.1
4_High	4.67 – 5.53	1	0.9	100
5_Very High	>=5.54	0	0	100

Table 4: Work Engagement Levels (N=115)



engagement levels specified by Schaufeli and Bakker (2004a: 40) is presented in Table 4. This shows that 99.1% of samples fall on or below the “Average” work engagement level with 52% in the “Very low” and “Low” categories. The data clearly indicate that the work engagement level of outsourced employees in the telecommunication service delivery sector of Sri Lanka is skewed towards average or lower levels.

4.3 Relationship Analysis

Multiple regression analysis permits prediction of the value of a dependent variable given the independent variables. More importantly, in the current research context, it helps to investigate the corresponding changes in the dependent variable due to variances in independent variables (Keller, 2014). In this study, the corresponding variation of work engagement is explored in relation to 9 independent variables.

Regression coefficients provided in Table 5 indicate that autonomy, professional development, optimism, managerial, supervisory coaching and feedback are statistically significant antecedents that influence work engagement. Remaining four antecedents are not statistically significant, and there is no linear relationship between work engagement and those six antecedents. These results indicate that a unit change in autonomy would result in a 0.462 change in the work engagement. This is the largest influencer of work engagement as per this qualitative analysis. Compared to feedback, the least influential antecedent, autonomy is 5 times more influential. A unit change in professional development would result in a 0.318 change in the work engagement. This is the second largest antecedent, influencing work engagement and is 3.46 times as strong compared to feedback.

Similarly, optimism would influence the work engagement by 0.97, which is again 3.23 times as potent compared to feedback. A unit change in managerial, supervisory coaching would result in a 0.274 change in the work engagement. This is again 2.98 times as influential compared to feedback. The least influential antecedent of the work engagement is feedback. A unit change in feedback would result in a 0.092 change in the work engagement.

In conclusion, based on quantitative analysis, five antecedents that influence work engagement were identified. Of these five antecedents, four are job-related attributes, viz. Autonomy, Professional Development, Managerial Supervisory Coaching and Feedback. The remaining antecedent is a personal attribute: Optimism.

4.4 Qualitative Analysis

Four main themes have emerged as what participants perceived as factors influencing work engagement. These themes were further analysed to identify the factors that impact work engagement in their workplace.

Ambiguity in Instructions and Scope: All four participants have cited the lack of a clear idea about what is expected of each of them and ambiguity in instructions as a major cause of degradation of work engagement. They made statements such as “[supervisor] tells me to do one thing in front of mobile operator’s staff and another privately”, “mobile operator expects me to do certain things, but I cannot do so because of instructions from my company” and “I am afraid to commit to any delivery as I’m not sure how my supervisor would react”. These statements clearly demonstrate the participants’ lack of freedom to take decisions

	Unstandardized Coefficients B	Std. Error	Infl. Comp. to Feedback
Autonomy	0.462 **	0.129	5.02 times
Social Support	0.078	0.086	
Managerial Supervisory Coaching	0.274 ***	0.056	2.98 times
Feedback	0.092 *	0.043	1 time
Professional Development	0.318 **	0.091	3.46 times
Self-Efficacy	0.173	0.109	
Self-Esteem	0.096	0.089	
Resilience	-0.047	0.063	
Optimism	0.297 ***	0.071	3.23 times

*** p < 0.0005, ** p < 0.005, * p < 0.05

Table 5 - Regression Coefficients



or actions on their own. Further, these indicate that there is a lack of proper understanding between supervisor and subordinate. Further, it provides evidence of a lack of proper leadership from the supervisor or senior management in such a way that subordinates are unnecessarily exposed to conflicts between the telecommunication operator and outsource service provider.

High Work Demand / High Work Pressure: Participants have indicated that they are subjected to high work demands by their own supervisors and by the telecommunication operator staff. Expressions such as “I’m asked to adhere to impossible deadlines” and “I’m given impossible tasks to complete” reflect the perception of participants regarding their work and their reluctance to undertake challenges in the work environment. This demonstrates that participants lack the confidence that they can undertake and fulfil the assignments entrusted to them. Hence, these statements could be interpreted as evidence of low self-efficacy as related to the work engagement. It also highlights the fact that participants lack sufficient faith in their abilities and in themselves with respect to completing these tasks. Clearly, these participants associate the feeling of lack of confidence or self-esteem with work engagement.

Lack of Training or Development Opportunities: Participants have a feeling that those who are assigned to outsource service team become stagnant, performing the same tasks over long periods of time without the opportunity for self-development. Statements “same old thing over and over again, nothing new to do or learn” and “technology is changing fast but I’m working on the old technology” were made regarding the lack of opportunity for training and development. Participants have realised that exposure to the latest technology and learning and training on the latest technology is lacking when working in the outsource service delivery domain, which in turn has eroded their enthusiasm for work. All these statements are clear evidence of participants associating the lack of training and development opportunities for work engagement.

Preference over Nationality: In a multinational working environment, where the telecommunication operator is based in one country, and the outsource service provider originates from another; the local employees seemed to feel that preference was given to employees from those two foreign nationalities

over them. Telecommunication operator prefers that senior positions in outsource service team be filled with their nationality. Outsource service provider tend to have their own nationals assigned to senior positions within the service team. In this situation, the local staff felt neglected because they had been given lower preference. Through claims such as “you have to be a [nationality] if you are to get appointed to a senior position” or “only listen to or believe what these people say or do,” participants indirectly highlight the fact that only foreign nationals are given the responsibility or the authority to act as they see fit. The delegation of authority to local employees is perceived as being low. This is an indication that participants feel the lack of authority delegation to local employees as a lack of autonomy in relation to work engagement. Further, these statements indicate a connection between perceived social support for local employees and work engagement. Local employees seem to sense that there is a difference in support available to them in comparison with other nationalities working in the same environment.

The discussion on qualitative analysis can be summarised as follows:

Theme-1: Ambiguity in Instruction and scope

- Lack of freedom to take decisions or actions on their own > Autonomy
- Lack of understanding between subordinate and supervisor; lack of proper leadership > Managerial Supervisory Coaching

Theme-2: High work demand/ work pressure:

- Resistance to undertake challenges in work environment > Self-Efficacy
- Lack self-regard or self-confidence in completing assigned tasks > Self-Esteem

Theme-3: Lack of training or development opportunities:

- Unavailability of exposure to the latest technology, learning and training on the latest technology > Professional Development

Theme-4: Preference over Nationality:

- Perception that only the foreign nationals are given the responsibility or the authority to act as they see fit > Autonomy
- Difference in support extended to locals and foreign employees > Social Support

Above identifies the indicators obtained through qualitative analysis on associations perceived between the work engagement and its antecedents. Based on this, it can be identified that the qualitative study provides

evidence that autonomy, social support, managerial, supervisory coaching, opportunities for professional development, self-efficacy and self-esteem are perceived as influential antecedents of work engagement.

A combined matrix of antecedents and their relationship to the work engagement is shown in Table 6. Both the quantitative and qualitative studies have identified autonomy to be an influencing factor of work engagement. Similarly, both studies identify managerial, supervisory coaching and opportunities for professional development as influencing antecedents. It should be noted that opportunities for professional development have emerged as the main theme in the qualitative study and clear evidence is available to support its influence over the work engagement. Social support, feedback, self-efficacy, self-esteem and optimism were identified as influential antecedents from either the qualitative or quantitative analysis, but not

evidence to support these assumptions (Saks, 2006). Secondly, there has been a minimal investigation into the work engagement in the outsource work environment (Raghuram, 2006). This study has attempted to academically explore the antecedents of the work engagement of employees involved in engineering service delivery, attached to an outsource service provider. The study was built on the JD-R model (Demerouti et al., 2001; Bakker and Demerouti, 2007; Bakker and Demerouti, 2008a), which presents the concept that work engagement as interactions between job resources, personal resources and job demands. Five job resources: autonomy, social support, supervisory coaching, performance feedback and opportunities for professional development and four personal resources: self-efficacy, self-esteem, resilience and optimism were investigated during this study to establish their relationship with work engagement.

This research has resulted in some interesting

Factor	Quantitative Observations	Qualitative Observations
Autonomy	Significant (B= 0.462 **)	Evidence of Association
Social Support	Not Significant	Evidence of Association
Managerial Sup. Coaching	Significant (B= 0.274 ***)	Evidence of Association
Feedback	Significant (B= 0.092 *)	No Evidence
Professional Development	Significant (B= 0.318 **)	Evidence of Association
Self-Efficacy	Not Significant	Evidence of Association
Self-Esteem	Not Significant	Evidence of Association
Resilience	Not Significant	No Evidence
Optimism	Significant (B= 0.297 ***)	No Evidence

B = Unstandardized Regression Slope Coefficient
 *** p < 0.0005, ** p < 0.005, * p < 0.05

Table 6 - Influencing Antecedents of Work Engagement

from both.

5. Discussion

The main purpose of this study is to investigate the relationship between work engagement and nine probable antecedents of work engagement. This relationship is explored to identify which antecedents have the more significant and larger influences on the work engagement.

5.1 Theoretical Implications

There has been a great deal of interest in the work engagement in recent years. Organisations invest in conducting annual surveys to investigate work engagement of their employees.

Despite all this enthusiasm, linking the work engagement with organisational performance and business results, there is little empirical

findings. To start with, the quantitative study finds the work engagement level of outsourced employees to be lower than global norms. This is not surprising considering that the qualitative study points out severe job demands faced by outsourced employees. Such job demands would lead to a degradation of the work engagement levels of employees.

This study has revealed that autonomy is the most influential antecedent of work engagement. This is in line with the claim by Bakker and Demerouti (2007: 316) that autonomy is one of the most important predictors of work engagement. Bakker and Bal (2010: 196) in their study of teachers have also observed that autonomy is positively related to the work engagement. Xanthopoulou et al. (2007: 35 and 2009: 241) have also confirmed that autonomy at work is strongly correlated to



work engagement. This finding also supports the Karasek (1979) job demand-control model that predicts autonomy, or in other words, decision latitude, as the most important resource available to employees to cope with job stress. It should also be noted that high work demands and high work pressure have emerged as a theme in a qualitative study. In that context, the job demand-control model could be considered to be quite relevant, and so it is not surprising to discover that the study identifies decision latitude, i.e. employees' control over their tasks, as a significant factor.

This study also identifies opportunity for professional development as an influential antecedent of work engagement. This is the only job resource that emerged as a main theme in the qualitative study. The importance of professional development opportunities with respect to the work engagement was resoundingly demonstrated from the revelations of the participants. Xanthopoulou et al. (2007: 135 and 2009: 241) have also established that opportunities for professional development correlate strongly with work engagement. Bakker and Bal (2010: 196) also confirm that any opportunity for development is positively related to the work engagement.

Similarly, the quantitative study finds evidence that managerial, supervisory coaching and feedback are antecedents of work engagement. The qualitative study identifies that effective leadership role of supervisor and understanding between supervisor and subordinate as important components of managerial, supervisory coaching. Xanthopoulou et al. (2007: 135 and 2009: 241) have also established that receiving proper coaching has a relationship with work engagement. Further, Van Dierendonck et al. (2004) also found that good leadership behaviour has a direct association with subordinates' sense of well-being and engagement. In contradistinction to above, Saks (2006: 610-611) found that there is no significant relationship between supervisor support and job engagement. In their study, Xanthopoulou et al. (2009: 241) also found that high-quality feedback positively correlates with work engagement. Bakker and Bal (2010: 196) found that exchanges with the supervisor, i.e. a combined measure of both supervisor feedback and supervisory coaching, positively related to the work engagement.

The quantitative study found that there is no significant relationship between social support and work engagement. This is in agreement with Bakker and Bal's (2010: 196) finding that social support was unrelated to work engagement. However, the results of the quantitative study contradict the finding of Xanthopoulou et al. (2009: 241) according to whom having supportive colleagues enhances work engagement. The qualitative results of the present study provide evidence of an association between social support and the work engagement, in agreement with Xanthopoulou et al. (2009: 241).

This study finds optimism to be an antecedent of work engagement. Xanthopoulou et al. (2009, 241) also state that optimistic employees show a high level of work engagement. However, in their study Xanthopoulou et al. (2013) found that in employees facing emotional demands, optimism did not have any significant relationship with work engagement. The quantitative study failed to identify any of the other personal resources as having a significant relationship with work engagement. This contradicts with the result of Xanthopoulou et al. (2009, 241) that observed self-efficacy and self-esteem are related to work engagement. However, the qualitative study agrees with Xanthopoulou et al. (2009, 241), as the present study found evidence that the work engagement is associated with self-efficacy and self-esteem.

5.2 Practical Implications

Telecommunications operators rely heavily on services of outsourced employees for the delivery of service to their subscribers. These outsourced employees are responsible for maintaining the network and ensuring good quality service to subscribers. But this study finds that the work engagement level of those responsible for maintaining the network is lower than is desirable. This low engagement level would invariably lead to performance gaps when executing assigned tasks. As Godfrey-Faussett (1997) notes, problems arising due to poor quality or interrupted service could have a serious and direct impact on the telecommunication operator. Hence, a lower work engagement level of outsourced employees would be a matter of serious concern for telecommunication operators, especially in view of the increasing tendency to outsource more of the engineering services to third party service providers. At present, labour laws and contracts between telecommunication

operators and service providers mainly govern the financial aspects of outsourcing, performance service levels and employee well-being at the point of outsourcing (Godfrey-Faussett, 1997). However, there is a minimal focus on the long-term well-being of outsourced employees. Considering the findings of this study, telecommunications operators should review the contractual frameworks they have with outsourcing service providers to ensure that necessary resources are available to maintain better work engagement levels. However, such modification to existing contracts would certainly come at an increased cost to the telecommunication operator.

This is where the second part of this study becomes very relevant to telecommunication operators. When telecommunication operators attempt to enhance the work engagement of outsourced employees, they should focus on areas that would have a higher impact on the work engagement. By doing so, telecommunication operators could gain more in terms of improving the work engagement. This study helps achieve that by identifying those factors that have the most influence over the work engagement. For example, a telecommunication operator's investments in improving autonomy at work would be five times as effective as the same investment made on feedback process improvement. Based on the findings of this study, telecommunication operators could work out a strategy to bolster significant job and personal resources in such a way as to put outsourced employees in a strong position, where they will be able to face the job demands effectively and with much less negative impact on work engagement levels.

5.3 Limitations of Present Research

Despite obtaining some interesting results, the present study does have certain limitations. This study adopts a non-probability sampling mechanism in this research for its convenience. Even though convenience sampling is widely used (Bryman, 1989: 113-114 cited in Bryman and Bell, 2007: 198) in the field of business and management, it introduces a problem in that with such sampling, it is impossible to generalize the findings because there is no evidence to indicate what population that the sample represents (Bryman and Bell, 2007: 198).

The quantitative study indicates that participants of this research are at the "very low" to "average" level of employee engagement. Statistically, 99.1% of participants are at an average or lower level of engagement.

Therefore, this study sample primarily represents the employee sub-set, whose work engagement is at a low-level and not necessarily outsourced employees in general. This may be due to the error introduced by the convenience sampling technique adopted. Therefore, generalizing the findings of this study to include outsourced employees of the telecommunication service sector of Sri Lanka may lead to erroneous conclusions.

This study employed 10 measurement instruments to estimate work engagement and the antecedents of work engagement. The researcher was careful to use well-established and tested measurement tools with the intention of employing a reliable scale. Reliability of these scales has been tested and found to be satisfactory. However, these measurement instruments were developed and predominantly verified in western countries. Hence, participants may have found it difficult to understand and interpret them. This could have caused some ambiguities in the responses to the questionnaire. Further, this could lead to difficulties in interpreting the meaning of culturally determined work engagement scores given by the UWES scale (Shimazu et al., 2010). All attempts to find a locally developed and tested measurement instruments were unsuccessful.

5.4 Recommendation for Future Studies

In the present study, a high correlation between job resources and personal resources were observed. These inter-correlations between antecedents are of much academic interest (Xanthopoulou et al., 2007, 2009; Saks, 2006; Schaufeli and Bakker, 2004b). This means that there is evidence of a relationship between the motivational process and the health impairment process. However, investigating the relationships between job resources and personal resources or reciprocal relationships is beyond the scope of the present study. Yet, the data set collected for this research can also be analysed to find answers to different sets of questions with a much broader academic scope. Through such an undertaking, it would be possible to contribute much towards building a wider knowledge base on the intricacies of work engagement.

As per its design, this research used convenience sampling and focused on employees of a single organisation. Further, it was evident that the work engagement level of the study sample was relatively low. Hence,



this study sample is biased towards one end of the work engagement spectrum. All these concerns lead to a limitation with generalising of the results of this study. A more comprehensive study involving a larger sample and including employees of multiple outsource organisations could mitigate this limitation.

Future studies should also consider the cultural and language issues discussed earlier. Questionnaire design in local languages and in conformity with the local cultural context might generate more reliable data for the study. However, this would require substantial preliminary work developing and testing new measurement tools in local languages before employing those in a study aimed at exploring relationships.

References

1. Aron, R., Singh, J. V. 2005. Getting offshoring right. *Harvard Business Review*, 83(12): 135-143.
2. Bakker, A. B., Bal, P. M. 2010. Weekly Work Engagement and Performance: A Study among Starting Teachers. *Journal of Occupational and Organizational Psychology*, 83: 189-206.
3. Bakker, A. B., Demerouti, E. 2007. The Job Demands-Resources Model: State of the Art. *Journal of Managerial Psychology*, 22: 309-328.
4. Bakker, A.B., Demerouti, E. 2008a. Towards a Model of Work Engagement. *Career Development International*, 13(3): 209-223.
5. Bakker, A. B., Demerouti, E. 2008b. The Oldenburg Burnout Inventory: A Good Alternative to Measure Burnout and Engagement. In J. Halbesleben (ed.), *Handbook of stress and burnout in health care*. New York: Nova Science Publishers.
6. Belcourt, M. 2006. Outsourcing – The benefits and the risks. *Human Resource Management Review*, 16: 269-279.
7. Bledow, R., Schmitt, A., Frese, M., Kuhnel, J. 2011. The Affective Shift Model of Work Engagement. *Journal of Applied Psychology*, 96(6) 1246-1257.
8. Brough, P., Pears, J. 2004. Evaluating the Influence of the Type of Social Support on Job Satisfaction and Work Related Psychological Well-Being. *International Journal of Organisational Behaviour*, 8(2): 472-485.
9. Bryman, A., Bell, E. 2007. *Business research methods*. 2nd edition. New York: Oxford University Press, Inc.
10. Demerouti, E., Bakker, A. B., Nachreiner, F., Schaufeli, W.B. 2001. The Job Demands-Resources Model of Burnout. *Journal of Applied Psychology*, 86: 499-512.
11. Ellinger, A. E., Ellinger, A. D., Keller, S.B. 2005. Supervisory Coaching in a Logistics Context. *International Journal of Physical Distribution & Logistics Management*, 35(9): 620 – 636.
12. Fitch Ratings. 2015. 2016 Outlook: Sri Lanka Telecommunications Services. Available at: www.fitchratings.lk/download-article-361.pdf; accessed 30 September 2016.
13. Godfrey-Faussett, M. 1997. Outsourcing Telecommunications Outsourcing a Legal Perspective. *Computer Law & Security Report*, 13(3): 176-181.
14. Greene, J. C., Caracelli, V. J., Graham, W. F. 1989. Toward a Conceptual Framework for Mixed-Method Evaluation Designs. *Educational Evaluation and Policy Analysis*, 11(3): 255-274.
15. Halbesleben, J. R. B. 2010. A Meta-Analysis of Work Engagement: Relationships with Burnout, Demands, Resources, and Consequences. In: Bakker, A. B., Leiter, M. P. (eds.), *Work Engagement: A Handbook of Essential Theory and Research*. New York: Psychology Press.
16. Harter, J. K., Schmidt, F. L., Hayes, T. L. 2002. Business-Unit-Level Relationships between Employee Satisfaction, Employee Engagement, and Business Outcomes: A Meta-Analysis. *Journal of Applied Psychology*, 87: 268-279.
17. Harter, J. K., Schmidt, F. L., Killan, E. A., Agrawal, S. 2009. Q12 Meta-Analysis: the Relationship between Engagement at Work and Organizational Outcomes. Gallup Organisation. Available at: http://www.aamga.org/files/hr/MetaAnalysis_Q12_WhitePaper_2009.pdf; Accessed 21 March 2016.
18. Hobfoll, S. E., Johnson, R.J., Ennis, N., Jackson, A.P. 2003. Resource Loss, Resource Gain, and Emotional Outcomes among Inner City Women. *Journal of Personality and Social Psychology*, 84: 632-643.
19. Hornby, A. S. 2005. *Oxford Advanced Learners Dictionary, 7th Edition*. Oxford: Oxford University Press.
20. Kahn, W. A. 1990. Psychological Conditions of Personal Engagement and Disengagement at Work. *Academy of Management Journal*, 33(4): 692 -724.
21. Karasek, R. A., Jr. 1979. Job Demands, Job Decision Latitude and Mental Strain: Implications for Job Redesign. *Administrative Science Quarterly*, 24: 285-308.
22. Kessler, I., Coyle-Shapiro, J., Purcell, J. 1999. Outsourcing and the Employee Perspective. *Human Resource Management Journal*, 9(2): 5-19.
23. Ketter, P. 2008. What's the Big Deal about Employee Engagement? *T and D*, 62(1): 44-49.

24. Keller, G. 2014. *Statistics for Management and Economics*, 10th edition. Delhi: Cengage Learning India Pvt. Ltd.
25. Lakens, D. 2013. Calculating and reporting effect sizes to facilitate cumulative science: a practical primer for t-tests and ANOVAs. *Front Psychol.* 4: 863.
26. Maslach, C., Leiter, M. P. 2008. Early Predictors of Job Burnout and Engagement. *Journal of Applied Psychology*, 93(3): 498-512.
27. Maslow, A. H. 1954. *Motivation and Personality*. New York: Harper & Row, Publishers, Inc.
28. Purcell, K., Purcell, J. 1998. In-sourcing, Outsourcing, and the Growth of Contingent Labour as Evidence of Flexible Employment Strategies. *European Journal of Work and Organizational Psychology*, 7(1): 39-59.
29. Raghuram, S. 2006. Individual effectiveness in outsourcing. *Human Systems Management*, 25: 127-133.
30. Ramani, K. 2014. IT Operations Managed Services - A Perspective. Mindtree Limited; Available at: <http://www.mindtree.com/sites/default/files/mindtree-thought-posts-it-operations-managed-services-perspective.pdf>; accessed 30 September 2016.
31. Rich, B. L., Lepine, J. A., Crawford, E. R. 2010. Job engagement: Antecedents and effects on job performance. *Academy of Management Journal*, 53: 617-635.
32. Robbins, S. P., Judge, T. A., Sanghi, S. 2011. *Essentials of Organizational Behaviour*, 10th edition. New Delhi: Dorling Kindersley (India) Pvt. Ltd.
33. Rosenberg, M. 1965. *Society and the adolescent self-image*. Princeton, NJ: Princeton University Press.
34. Saks, A. M. 2006. Antecedents and consequences of employee engagement. *Journal of Managerial Psychology*, 21: 600-619.
35. Sarason, I. G., Sarason, B. R., Shearin, E. N., Plerce, G. R. 1987. A Brief measurement of social support: Practical and Theoretical Implications. *Journal of Social and Personal Relationships*, 4: 497-510.
36. Schaufeli, W. B. 2012. Work Engagement. What Do We Know and Where Do We Go? *Romanian Journal of Applied Psychology*, 14(1): 3-10.
37. Schaufeli, W. B. 2014. What is engagement? In Truss, C., Delbridge, R., Alfes, K., Shantz, A., Soane, E. (eds.), *Employee Engagement in Theory and Practice*. New York: Routledge.
38. Schaufeli, W. B., Bakker, A. B. 2004a. UWES - Utrecht Work Engagement Scale: Preliminary Manual. Version 1.1 (December 2004). Utrecht: Department of Psychology, Utrecht University. Available at: http://www.wilmarschaufeli.nl/publications/Schaufeli/Test%20Manuals/Test_manual_UWES_English.pdf; accessed 21 March 2016.
39. Schaufeli, W. B., Bakker, A. B. 2004b. Job Demands, Job Resources, and their Relationship with Burnout and Engagement: A Multi-Sample Study. *Journal of Organizational Behavior*, 25: 293-315.
40. Schaufeli, W. B., Bakker, A. B., Salanova, M. 2006. The Measurement of Work Engagement with a Short Questionnaire: A Cross-National Study. *Educational and Psychological Measurement*, 66: 701-716.
41. Schaufeli, W. B., Salanova, M. 2008. Enhancing Work Engagement through the Management of Human Resources. In Näswall, K., Hellgren, J., Sverke, M. (eds.), *The Individual in the Changing Working Life*. Cambridge: Cambridge University Press.
42. Schaufeli, W. B., Salanova, M., González-Roma, V., Bakker, A. B. 2002. The Measurement of Engagement and Burnout: A Two Sample Confirmative Factor Analytic Approach, *Journal of Happiness Studies*, 3: 71-92.
43. Scheier, M. F., Carver, C. S., Bridges, M. W. 1994. Distinguishing Optimism from Neuroticism (and trait anxiety, self-mastery, and self-esteem): A Re-Evaluation of the Life Orientation Test. *Journal of Personality and Social Psychology*, 67: 1063-1078.
44. Schumann, M. 2010. The New Rules of Employee Engagement: How Business Leaders Must Reinvent How they Connect. *Management Today*, 28(1): 44-45.
45. Schwalbe, M. L. 1985. Autonomy in work and self-esteem. *The Sociological Quarterly*, 26(4): 519-535.
46. Schwarzer, R., Jerusalem, M. 1995. Generalized Self-Efficacy Scale. In J. Weinman, J., Wright, S., Johnston, M. (eds.), *Measures in health psychology: A user's portfolio. Causal and control beliefs*. Windsor, UK: NFER-NELSON.
47. Sheldon, K. M. 1995. Creativity and Self-Determination in Personality. *Creativity Research Journal*, 8: 61-72.
48. Sheldon, K. M., Ryan, R. M., Reis, H. 1996. What makes for a Good Day? Competence and Autonomy in the Day and in the Person. *Personality and Social Psychology Bulletin*, 22: 1270-1279.
49. Shimazu, A., Miyataka, D., Schaufeli, W. B. 2010. Work Engagement from a Cultural Perspective. In Albrecht, S. L. (ed.) *Handbook of employee engagement perspectives, issues, research and practice*. Cheltenham, UK: Edward Elgar Publishing Limited.



50. Tavakol, M., Dennick, R. 2011. Making Sense of Cronbach's Alpha. *International Journal of Medical Education*, 2: 53-55.
51. Van Dierendonk, D., Haynes, C., Borrill, C., Stide, C. 2004. Leadership Behavior and Subordinate Well-Being. *Journal of Occupational Health Psychology*, 9(2): 165-175.
52. Wagnild, G. M. 2009. The Resilience Scale User's Guide for the US English Version of the Resilience Scale and the 14-Item Resilience Scale (RS-14). The Resilience Center, Montana. Available at: http://ja.cuyahogacounty.us/pdf_ja/en-us/defendingchildhood/drcharlesfigley-scoring-scalesheets.pdf; accessed 15 September 2016.
53. Wollard, K. K., Shuck, B. 2011. Antecedents to Employee Engagement: A Structured Review of the Literature. *Advances in Developing Human Resources*. 13(4): 429-446.
54. Xanthopoulou, D., Bakker, A. B., Demerouti, E., Schaufeli, W.B. 2007. The Role of Personal Resources in the Job Demands-Resources Model. *International Journal of Stress Management*, 14: 121-141.
55. Xanthopoulou, D., Bakker, A. B., Demerouti, E., Schaufeli, W.B. 2009. Reciprocal Relationships between Job Resources, Personal Resources, and Work Engagement. *Journal of Vocational Behavior*, 74: 235-244.
56. Xanthopoulou, D., Bakker, A. B., Fischbach, A. 2013. Work Engagement Among Employees Facing Emotional Demands The Role of Personal Resources. *Journal of Personnel Psychology*, 12(2): 74-84.
57. Zikmund, W. G., Babin, B. J., Carr, J. C., Adhikari, A., Griffin, M. 2013. *Business Research*

The Structure of Land Prices in Colombo and Its Implications

P. I. A. Gomes and R. K. Hashan

Abstract: Land prices could vary linearly or non-linearly due to several factors such as distance to the regional and zonal commercial centres and major roads, access road width, retail facilities, health facilities, schools and so forth. Whether these factors really impact the prices and if to what extent is unknown. Data for several influencing factors were collected from over 300 land plots on sale from Homagama, Maharagama, Malabe and Moratuwa for the period 2016 to early 2017. Data collection was accomplished through printed and online real estate advertisements and direct contact with the property agents/owners. Data were analyzed using a combination of bivariate and multivariate analyses. Distance to Colombo and land prices showed a strong correlation in Homagama, where closer to Colombo, prices increased. All other suburbs prices were rather independent of the distance to Colombo and showed relative maxima or minima points indicating the impact of within-the-suburb factors. It was the case for variables that represented socio-economic factors such as distance to nearest school, hospital, retail facilities and so forth. Access road width was the only variable that showed uniformity in its impact on prices of all suburbs. Similar results (on important variables and the fact that Homagama's pricing behaves differently) were evident from the linear multiple regression, and detrended correspondence analyses. Other than indicating what factors should be given more prominence when selecting a land, the results clearly indicated a time lag of development in certain closely located suburbs. The results of this study could be important to the government and individuals in deciding their policies and investment decisions, respectively.

Keywords: Colombo suburbs; Distance; Land prices; Major roads

1. Introduction

In traditional societies, the land was considered as a personal/family property and ownership was passed from generation to generation, and no conversion to monetary terms was observed. The land is a finite resource with highly increasing demand. In contrast, the complementary product of lands, buildings due to vertical phasing (thus supply is not limited as lands) may not necessarily have a high demand. Demand for a land could be well understood by its market price. According to Ai [1], the price is the best expression to compare land values in a functional market. The price of land mainly depends on accessibility to present or future services and its production potential (i.e. ability to use the land to produce goods and services, therein by to generate revenue or profits). There is a basic difference between the value and price of a land [2]. Value prescribes an actual benefit of the land in relation to other similar lands. The actual benefits may not necessarily limited to direct monetary benefits, but also includes intrinsic and bequest values. Price (market) of a land prescribes what a land might be sold for at a specific period of time. Firstly, land price heavily relies upon its geographical placement

or location [3]. The research pertaining to the land prices and influencing factors are not as common as other real estate components such as apartments. However, past quantitative and qualitative research suggests some important factors that may govern land prices in large geographical areas. Those research have mainly targeted the differentiation and analyses of land prices with land use (e.g. [4]). Sri Lanka, with the end of civil conflict, is experiencing a booming economy, and an expanding real estate market. On one side, Colombo municipal areas undergo a rapid growth in the condominium market [5]. In tandem, Colombo suburbs came up with many real estate projects. Obviously, most of the lands for sale are from suburbs that contain bare lands (e.g. Homagama, Athurugiriya, Malabe), and are relatively less populated. Nevertheless, suburbs which are already populated, such a

Eng. (Dr.) P. I. A. Gomes, BSc(Eng)Hons., MSc, PhD(Japan), MIE (Sri Lanka), CEng. Senior Lecturer, Department of Civil Engineering, Sri Lanka Institute of Information Technology

R. K. Hashan, BSc(Eng)Hons., Research Assistant, Department of Civil Engineering, Sri Lanka Institute of Information Technology



Moratuwa and Maharagama, too have lands to be sold (e.g. brownfields, old houses), but in relatively less numbers.

This research aims to quantitatively analyse the importance of some factors that are often considered to be vital land transactions. Should be noted, it is not easy to give conclusive judgement on the behaviour of a variable on land prices. As an example, distance to the nearest major (e.g. A class) road may have contrasting impacts on land prices. Noise related issues may indicate lands closer to the road to be less expensive, on the other hand, ease of access may lead to a higher price. Also, the behaviour of a particular variable could be changed or influenced by another variable(s). Therefore, standard models or theories will not help in exploring a price and factor based study. Hence, using up to date real data collected with data modelling is necessary.

2. Materials and Methods

2.1 Study area

Data from land plots in Moratuwa, Maharagama, Homagama, and Malabe were collected during 2016 and early 2017. Other than Malabe all other suburbs (study areas) were bound by the respective local authority limit (Malabe is part of Kaduwella Municipality). These four areas have different socio-economic status quos. Moratuwa and Maharagma are two well recognized human settlements since several decades to a few centuries back (i.e. residential land use is high). Certain areas of Malabe had settlements since a few decades back, but it was only recently the mass settlements started. Homagama, as per Colombo district standards could be considered semi to un-urbanized. Therefore, it was expected these four areas to cover a wide range of socio-economic aspects, and are representative Colombo suburbs.

2.2 Variables (factors) considered and sampling details

A survey conducted for 225 respondents helped to shortlist 20 key variables that they considered important when buying a land. These variables are widely mentioned in land sale market (including mainstream literature) and some are considered important in

traditional architectural Vasthu Vidya design. However, after preliminary investigations, it was observed certain variables were rather unresponsive to the land price (e.g. shape of the land, ground water level, etc.). Unresponsiveness was decided based on the strength of coefficient of correlation on a bivariate platform. The variables that were considered for the comprehensive data collection and analyses included: land plot size; distance to Colombo, distance to the nearest town (economic center); distance to the nearest major road (e.g. A class); access road width; distance to health care and school facilities, and domestic plot ratio.

From each suburb, 60-70 samples were collected (i.e. 60-70 different locations, and some locations were land sale projects with several lands, and considered as a single data point). Data were collected by contacting land sales advertised (printed and online) by different agencies, and individuals (owners). It should be noted all lands were visited by a member of the research team, and details on access road width etc. were taken by in person. Other details such as distance to nearest services were obtained from aerial maps.

The price used in the model is not necessarily the advertised price, but the possible realized (i.e., actual even if its off the records) price at a time of the deed transfer. Price shown in the deed is in many cases the minimum government valuation, and if used will have wrong implications. Land sales by real estate agencies, the advertised price and realized price were the same in almost all cases. However, the prices of land sales by individuals did change. We assume the prices obtained were correct as assurance was given to keep the information anonymous and the respondents were confident that the data would be used merely for an academic research. It is assumed, any misinformation (unavoidable in this kind of research) is minor and proportionate for all suburbs.

2.3 Data analysis

Bivariate plots were used to check the relationships different variables make with the land price (per perch). Then simple multiple linear regression

was used to model the price and influencing factors (variables). All variables were checked for multi collinearity. First, multiple linear regression analyses were conducted excluding variables with $> 10\%$ variation inflation factor. In this step, the variable pairs/groups with multicollinearity were identified and accordingly some variables were excluded before the next modelling. Simple multiple linear regression was repeated again until all variables modelled were $< 5\%$ variation inflation factor. All cases a $P < 0.05$ was considered as the threshold for significance. SPSS statistical package (IBM V21.0) was used for the statistical analyses.

Prices have been arranged in ranges considering price and number of lands available (e.g. Rs. 0 to Rs. 50,000 per perch), and the respective midpoint (i.e., in this case, Rs. 25,000) will assume to represent all values of that range, and the averages of the respective dependent variables (e.g. distance to Colombo) were calculated accordingly.

3. Results and Discussion

3.1 Overview of lands sampled and Distance to Colombo on Land Prices

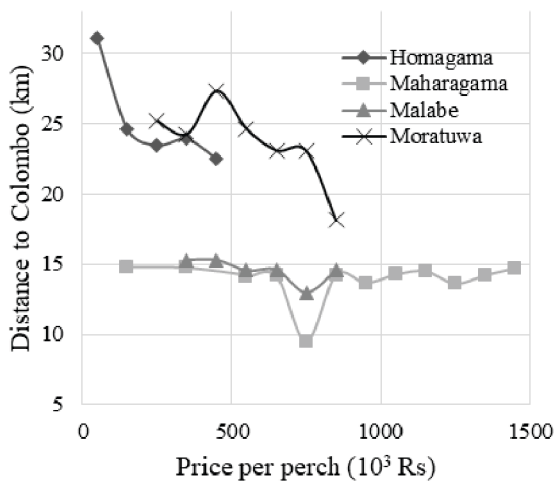


Figure 1 - Price variation with distance to Colombo

Many lands that were sampled in Malabe and Maharagama had more or less the same distance to Colombo. As an example, all sampled land plots in Malabe was about 15 km from Colombo. One reason is the shape and the orientation of the suburb. Also, it could be due to localized reasons (e.g. brownfields/old

settlements ready to be sold). It could also be due to some short comings of not able to identify some other lands for sale during the data collection. In Moratuwa, most of the lands had old houses (or lands with demolished old houses). Homagama, most of the lands were green-field (virgin) lands (i.e., no buildings were constructed before).

Colombo, the commercial capital (also the former official capital) has reputed schools, a large number of government agencies and commercial entities. It has the most important transportation hubs. Colombo has a resident population of about 0.6 million at a given time. The floating population (non-resident or temporary) is about 0.5 million. Because of these reasons lands close to Colombo are expensive. When prices were analyzed taking average land prices of suburbs such as Dehiwala, Mount Lavinia, Ratmalana and Moratuwa, along the Galle road, this was clearly evident (data not shown). Therefore, it was assumed that the distance to Colombo could be a decisive factor governing the land price within a suburb as shown in Figure 1. Equations 1-4 show power functions and the respective coefficient of correlations (R^2) developed for each suburb. Homagama clearly showed a distance dependent price variation, where closer to Colombo prices were high. Moratuwa too showed a similar, but a very weak relationship and the variation was rather sinusoid. These two contrasting views could be well understood considering the connectivity to Colombo. Moratuwa enjoys good connectivity to Colombo via road (A2), and railway. Both these modes are well catered by public and private vehicles/transport modes (also there are several railway stations within Moratuwa). In addition, road width and number of rail tracks are satisfactory. In case of Homagama, the connectivity is not so good, and the train services though scheduled, the number of trains are a few. The data samples managed to collect from Malabe and Maharagama were not very suitable to derive a relationship between distance to Colombo and prices, as many lands had the same distance. However, even with more or less the same distance, in both suburbs, especially Maharagama showed a huge price difference. Therefore, the macroscopic view that prices closer to Colombo is high is conclusively true, only for Homagama.

$$D_{(Homagama)} = 52P^{-0.14} ; R^2 = 0.91 \quad \text{--- (1)}$$

$$D_{(Maharagama)} = 16P^{-0.02} ; R^2 = 0.01 \quad \text{--- (2)}$$

$$D_{(Malabe)} = 31P^{-0.12} ; R^2 = 0.45 \quad \text{--- (3)}$$

$$D_{(Moratuwa)} = 77P^{-0.19} ; R^2 = 0.39 \quad \text{--- (4)}$$

3.2 Impact of distance to the nearest major road on land prices

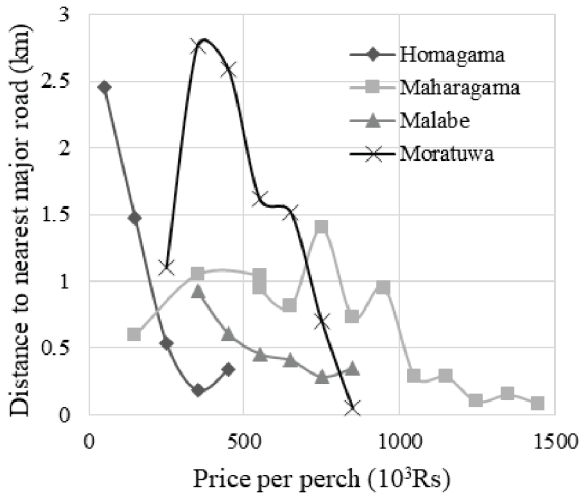


Figure 2 - Price variation with distance to nearest major road

Homagama and Malabe showed strong negative correlations between the distance to the major road and price (Figure 2), as greater the distance lesser the price. The other two suburbs, Moratuwa and Maharagama, showed a quadratic relationship, with a peak (for Moratuwa the peak was left skewed, i.e. towards low price side). Therefore, in these two suburbs, certain areas showed to have optimum choices of land. This meant, the price and the distance to nearest road were distorted by different factors, as such certain land plots irrespective of remoteness to a major road showed relatively high prices. The less decisiveness of distance to the nearest road in Moratuwa and Maharagama could be further explained due to the availability of widespread (alternative) road network.

3.3 Availability of socio-economic facilities (retail facilities, schools, medical centres), and building foot print on land prices

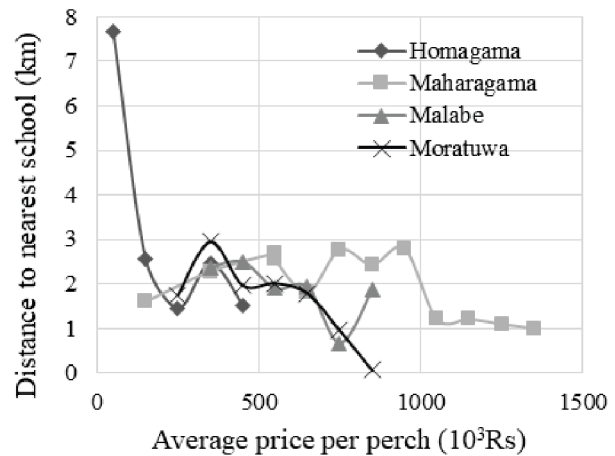


Figure 3 - Price variation with distance to nearest school

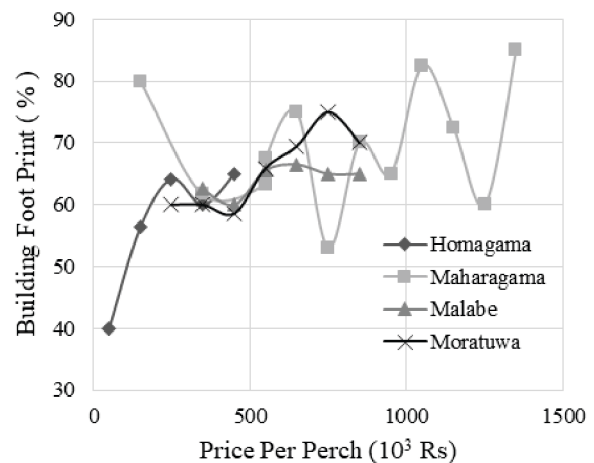


Figure 4 - Price variation with distance to nearest school

The relationships between nearest retail and medical facilities with the price were similar to the relationship between nearest school and price (Figure 3). Only Homagama showed a clear linear relationship (close the socio-economic facility greater the price). All other suburbs the prices were independent of such facilities.

Building foot print and price also showed all suburbs other than Homagama, to be independent (Figure 4), and the relationships were same as with the socio-economic facilities.

The main reason for this is due to the centralized nature of facilities available in Homagama and otherwise in Moratuwa and Maharagama. Importantly, same as in the relationship with distance to the nearest major road, these two suburbs showed optimum locations. This in a way indicated the accessibility and capacity to satisfy certain needs outside their municipal boundaries (e.g. considerable number of students attend to schools in Colombo).

3.4 Effect of access road width on land prices

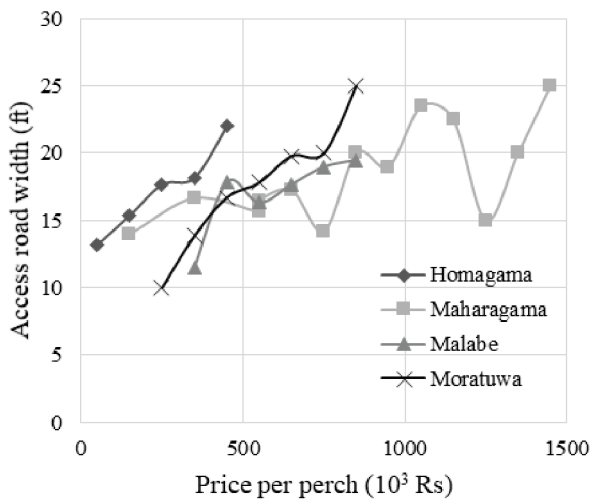


Figure 5 - Price variation with the access road width

The access road width was the only variable that showed a similar relationship across all suburbs, indicating the common perspective of buyers, that the access road width is an important factor of a land (Figure 5). Perhaps, this could be due to convenience in day to day activities and importantly ease of getting bank loan facilities.

3.5 Relating price with variables on a multivariable approach

The simple multiple linear regression analyses conducted validated the results of bivariate analyses (Figure 1 to 5) as well as pave the way to identify the significant ($P < 0.05$) and influencing ($R^2 > 0.4$) variables. Equations (5) to (8) show the simple multiple linear regression equations. Where, X_1 is the access road width; X_2 is the distance to nearest socio economic

centre; and X_3 is the distance to the nearest major road.

$$P_{Homagama} = 6241X_1 - 27334X_2 - 37844X_3 + 355360; R^2 = 0.79 \text{ --- (5)}$$

$$P_{Maharagama} = 68997X_1 - 394346; R^2 = 0.65 \text{ --- (6)}$$

$$P_{Malabe} = -176647X_3 - 693838; R^2 = 0.43 \text{ --- (7)}$$

$$P_{Moratuwa} = 27417X_1 - 29104X_3 + 120201; R^2 = 0.84 \text{ --- (8)}$$

Figure 6 shows the detrended correspondence analysis scatter plot. Samples (data points) with similar responses are grouped together. The scatter plot is cluttered and congested due to the inclusion of large number of data points. Therefore, small axis lengths were used to identify the ownership of the data point. Circled area 1 mainly consisted of Maharagama samples, whereas 2 mainly consisted of Moratuwa. Malabe samples were distributed among these two encircled areas. However, most of the Homagama samples were located outside.

3.6 Land prices, influential factors and government policies

Considering the polarization of suburbs like Maharagama and Moratuwa, and clear linear relationship Homagama lands show between price and the respective dependent variables, it was obvious Homagama has a different socio-economic signature. This is particularly important considering the government policies of hosting several IT and higher educational institutes there. Still in the Sri Lankan context startups and also higher education students/staff prefer domiciling close to major socio-economic centers. Improved infrastructure that connects well with Colombo would make lands in areas like Homagama on par with well-sorted places like Moratuwa and Maharagama.



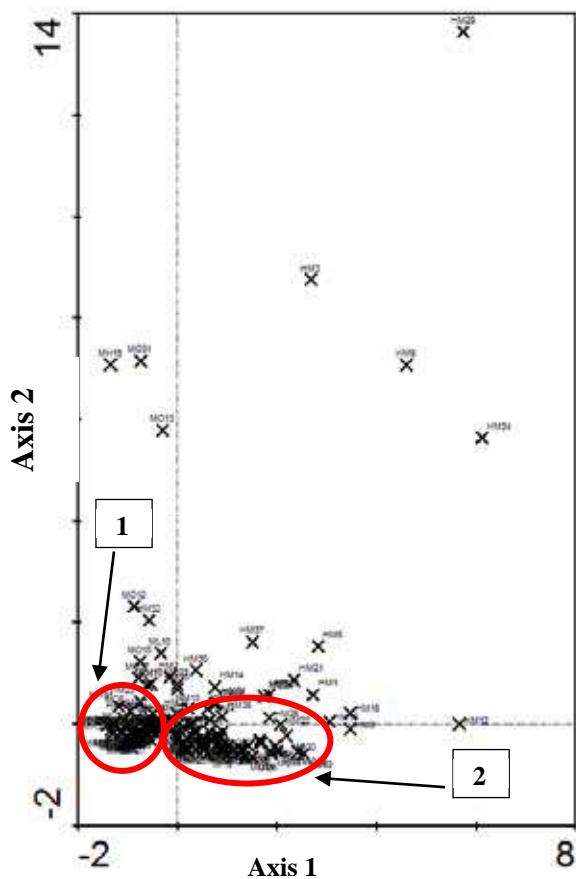


Figure 6 –Detrended correspondence analysis scatter plot for all suburbs

Sri Lanka with urbanization should think of relaxing its bank rules and policies on mortgage. Banks consider access road width as an important factor for loan approvals. As most suburbs are well connected by public transport. Also, on call taxi services are available and resident frequently use those, therefore, it is rather unnecessary to deprive loan facilities based on the access road width. This would decrease the land prices to a certain extent, as well as will help to optimize the use of available land.

5. Conclusion and Future Works

This research observed a suburb dependent land pricing as its main finding. In the larger picture Homagama showed a different land price signature to the other three suburbs. It is recommended to study the historical variation of land prices in these suburbs, and fine tune the results with the incorporation of more data and variables. This is particularly important

considering the relatively weak to moderate strength of correlations of some suburbs. This implies there are factors other than the factors that was considered, also impact the price. As an example real estate supply could be controlled by a group of companies/individuals result in a manipulated price.

Acknowledgement

Author wishes to acknowledge the two anonymous reviewers for their excellent review, and those who helped in data collection.

References

1. Ai, P., "Residential land value modelling," MSc Thesis, International institute for Geo-information Science and Earth Observation, Enschede, The Netherlands 2005.
2. Verheye, W. H., (Ed.). (2009). Land use, land cover and soil sciences. EOLSS Publ..
3. Guidry, K., Shilling, J. D., and Sirmans, C. F., "Land-Use Controls, Natural Restrictions , and Urban Residential Land Prices," vol. 29, no. 2, 1999.
4. Waddell, P., "Modeling urban deveopment for land use, transportation and environmental planning," *APA J.*, vol. 68, no. 3, pp. 297-314, 2002.
5. Ariyawansa, R. G., and Gunawardhana, T., "Guidelines for Real Estate Research and Case Study Analysis," *Department of Estate Management and Valuation, University of Sri Jayewardenepura*, 2016

Knowledge Management System for Mobile Telecommunication Sector in Sri Lanka

Jeewantha Nadeera, Shalanika Dayarathna and Eranda Ihalagedara

Abstract: Sri Lankan mobile telecommunication industry is a fiercely competitive market space where five key mobile service companies operate. Most operators provide their services island wide; therefore the coverage footprint is no longer a differentiating factor. On the other hand, knowledge is a tool, which companies can use to provide a better service quality, which is now in demand with customers.

In modern context with a dynamic environment, it is crucial to have a proper knowledge management system in the telecommunication field, because knowledge is the power for the success of many telecommunication area businesses. Mobile communication is so volatile, and a new technological revolution takes place in every five years and thus, all mobile telecommunication companies have to upgrade their networks frequently because of such technological advancement over the years. On other hand due to globalization and increasing opportunities for individuals, companies face a challenge to retain best employees within the organization. Now the focus has shifted to keep the knowledge within the organization even with the movement of skilled labour. When it comes to Sri Lankan context, Engineers who pass out from leading universities came up with excellent ideas to improve the performance of telecommunication services, optimize capital expenditure through creative solutions, and developed new business opportunities by combining unrelated technologies. However, they might change their job in telecommunication discipline, migrate to other countries, or upgrade into management field; this will diminish the transfer of tacit knowledge from generation to generation. It is vital to have a proper tacit knowledge management system to capture and conserve this valuable situational specific knowledge, and share such knowledge with future engineers. It will help to create new technical solutions, enhance robustness of the telecommunication network areas, and improve mobile customer experience.

The objective of this initiative was to study about knowledge management, select appropriate model, and develop most appropriate knowledge management system for mobile telecommunication sector in Sri Lanka.

Keywords: Knowledge, management, mobile, telecommunication, model

1. Introduction

This paper is intended to provide the detailed description of selecting an appropriate knowledge management model and how to develop and implement a knowledge management system for mobile telecommunication sector. In addition, suitability of knowledge management system for mobile telecommunication sector as well as barriers to implementing such system are discussed.

2. Suitability

Knowledge management systems are common throughout the world, however in Sri Lanka it is still a rising area. It is even rarer in mobile telecommunication sector.

Even though mobile telecommunication sector is a service oriented industry, people rarely have a platform to share their knowledge. Therefore, employees do not get the opportunity to share knowledge even if they wish to do so. Authors have identified one reason for this as the lack of focus in implementing knowledge sharing strategies by management, mainly because management focus is on competition with rival companies

Eng. Jeewantha Nadeera, B.Sc. Eng. Hons (University of Moratuwa), Manager-Radio Access Operations, Mobitel (Pvt) Ltd.

Eng. (Ms.) Shalanika Dayarathna, B.Sc. Eng. Hons (University of Moratuwa), CIMA Passed Finalist, Radio Access Operations Engineer, Mobitel (Pvt) Ltd.

Eng. Eranda Ihalagedara, B.Sc.Eng.Hons(University of Moratuwa), Radio Access Operations Engineer, Mobitel (Pvt) Ltd.



rather than preserving and sharing of the knowledge within. The diversity of employee age is another factor identified to demotivate new knowledge sharing strategies.

Mobile communication sector in Sri Lanka has begun around late 20th century. Thus, every mobile operator group consists of a wider employee base, which is likely to contain employees who are not familiar with computer technology and its advanced features. As knowledge management systems are more IT based, sometime it could be more complex for employees from older generations. Therefore, they rarely use complex knowledge management systems, even if they are willing to share their knowledge with younger generation. Even though, there are such concerns regarding knowledge management in mobile telecommunication sector, it can be considered as a highly effective and needed factor for this industry.

Service industry depends on the knowledge and experience of its people and loss of highly experience or highly intelligent employees could change the fate of a single company in this sector. Fate of mobile telecommunication sector is no different than that.

Currently, mobile telecommunication industry in Sri Lanka is in its saturated level. Therefore, in order to complete while retaining sufficient profits, companies need to move towards cost cutting strategies. Basic concepts in cost cutting strategy are to improve efficiency and effectiveness using same resources, in this case employees. Each operator has several highly efficient and experienced employees, who has less error rate and use shortcuts to complete more work in less time. That is where knowledge management system comes in handy. Imagine how much company would be able to save if every employee start to work like that.

Another restraining factor is time taken to find some useful information or old documents. Even after telecommunication sector moved towards more digital era, documents are rarely in a central location, thus making it harder and time consuming to find important documents. Knowledge management system runs in a single server and act as a central location to keep all knowledge related documents in one place. In addition, use of complex searching algorithms will make this task much easier and quicker.

Producing Technical experts of mobile telecommunication industry takes at least five to seven years with exposure to various areas of mobile telecommunication. If such an expert migrate to a different country for higher education, or for a new carrier, or even move to a different company within Sri Lanka, it would influence the existing organization because they have spent a significant amount to elevate such an expert to the current level by providing training and development opportunities. Hence, it is a duty and an obligation of the expert to share that knowledge with other employees. Also, if a technical expert move to a different job role, as an example a management role, there might be reduced opportunities to share such knowledge among the technical staff because he/she has to perform various tasks more related to management area. Thus, from the organization point of view, there is a strong requirement to share such a person's knowledge, experiences, and new ideas.

Situational knowledge will only be captured at the incident time. In most of the cases, this knowledge is limited to the people who have experienced the incident, even they might have forgotten about it after some time. In case a similar incident occurs with a different set of people, they will have to build up a solution from the scratch. Hence, it is needed to update such an incident-related knowledge immediately to knowledge forum, where it has happened. To achieve that objective, a proper knowledge management platform is required, as it gives opportunities to share the knowledge.

3. Implementation

Authors have successfully implemented a web based knowledge management system in one of the mobile operators in Sri Lanka. They have first performed a detailed analysis of available knowledge management techniques and their suitability to mobile telecommunication sector.

3.1 Preliminary Research

Initially, research has been conducted on different types of knowledge management and currently available knowledge management systems and their features. By understanding types of knowledge management systems, it was possible to identify the type that matches the requirement of the mobile telecommunication industry.

Even though there are several knowledge management systems such as,

- expert systems - perform problem diagnosis
- groupware - facilitate collaboration between workers
- document management system - share documents and enable search through documents more efficiently
- decision support system - present information to users in a manner they can make informed decisions easily
- database management system - store collection of data
- simulation systems - model and test real world scenarios

it has been identified that features of document management system, decision support system and database management system are required for the knowledge management systems in mobile telecommunication sector. Therefore, following key areas have been identified as essential implementation steps in knowledge management system by authors.

- Meta-search software - accepts a single query from users and return results from knowledge base.
- Knowledge mining software - allows query results to be sorted and clusters according to a set of predefined categories.
- Automated categorization tools - apply of both available data and incoming streams of knowledge.
- Knowledge warehouses - contain available data with substantially enhances functionality, security.
- Forms-base knowledge contribution schemes - end users can directly input their knowledge.
- Knowledge mapping software - pre-build knowledge maps designed for specific tasks.
- Knowledge directory software - automate the process of finding people with specific areas of expertise.

3.2 Basic Concepts of Knowledge

“Knowledge” has been defined in many ways by the philosophers since the ancient times. Basically every version of the definition can be simply put in to words as “knowledge is the understanding of something through experience or education”. Further, the knowledge can be classified based on different dimensions. However, the classification of

knowledge focused in this paper is tacit knowledge and explicit knowledge.

- Tacit Knowledge - the knowledge that is based on experience and pertaining to a specific context or incidents. This is difficult to be documented or transfer to another.
- Explicit Knowledge - the knowledge that can be easily put into verbal means or documented and hence easy to share.

3.3 Knowledge Management Model

This section explains the suggested knowledge management model for mobile telecommunication sector in Sri Lanka. Nonaka’s knowledge management framework [1] has been used as the basic model in order to develop a knowledge management model for Sri Lankan telecommunication sector. Leadership, knowledge sharing culture, socialization, externalization, combination, and internalization have been identified as the main areas in this knowledge management framework developed for Sri Lankan telecommunication sector [2].

They have introduced this “leadership” as one of the key concepts. It has been identified that the people are willing to support and contribute to knowledge management system if management (leader) introduces the knowledge management system. Thus, it is required the leadership to initiate, implement, and motivate people to share the knowledge through a knowledge management system. Therefore, following concepts were recommended by authors as required leadership practices in order to introduce a knowledge management system.

- Leaders shall create positive synergy among employees across the division
- Encourage employee participation in decision making
- It is required to absorb uncertainty currently encountered by employees in the organization

It is required to create a “knowledge sharing culture” in the organization to implement an effective and efficient knowledge management system. In order to form a knowledge sharing culture, management needs to encourage employees to work together more effectively by collaboration and sharing experiences. People are willing to share knowledge, however, they do not have a platform to share that knowledge. In the proposed knowledge



management framework, the second core layer would be the knowledge sharing culture. This is because, in Sri Lankan cultural dimension analysis, a high level of power distance is observed where people believe there is a significant power level difference. Therefore, the knowledge management framework in Sri Lankan context and knowledge share culture should be interconnected with leadership and rest of the knowledge management concepts as in Figure 1.



Figure 1 - Knowledge management Framework foundation

Therefore, authors recommend following knowledge sharing culture practices.

- Management encourages sharing quality information
- Managing excessive competition among the employees
- Allow constructive criticism to find optimal solutions

“Socialization” refers to how people in the organization interact with each other. When it comes to knowledge management, it is important to have a good relationship and a mutual understanding among organizational employees, as well as the interaction between subject experts with the rest of the employees in the organization. Therefore, there is a strong requirement to introducing socialization as a knowledge management platform for sharing knowledge among people, thus these socialization practices have been recommended.

- Providing a formal training program when employees are recruited to the organization
- Frequent engagement of newly recruited engineers and technical officers with technical experts
- Employees can easily reach a technical expert in the organization
- Frequent informal team gathering

During the “externalization” process, it is required to assess the method or process that supports converting tacit knowledge into explicit knowledge. This is a very important stage of the knowledge management process because it is the key factor that drive the knowledge management system in sustainable development in the long run. Hence, it is recommended to introduce the externalization concept with following practices in to knowledge management framework for mobile telecommunication sector in Sri Lanka.

- Convenient when accessing and updating information
- Frequent updating an internal forum to share new ideas, concepts, and trends
- Having brainstorming sessions when confronted with a new problem or when a critical decision has to be made
- Encourage to express their views, argue, and evaluate new ideas

According to Nonaka, the “combination” mode of knowledge conversion is ‘a process of assembling new and existing explicit knowledge held by individuals into a knowledge system’ [1]. It is also a process of exchanging, sorting, adding, disseminating, sharing, and therefore reconfiguring, different bodies of explicit knowledge among organizational members through documents, meetings, telephone conversations, and computerized communication methods. Nonaka terms the knowledge created through a combination process as systemic knowledge. It is required to combine various explicit knowledge with individual to single context. Hence, it is recommended to introduce the combination concept into knowledge management framework for mobile telecommunication sector in Sri Lanka with practises such as,

- Combining information such as network change history, network issue trouble shooting guides, and root cause analysis in the knowledge management system
- Combining different individual’s knowledge
- High level of contribution from technical experts

The “internalization” mode of knowledge conversion is ‘a process of embodying explicit knowledge into tacit knowledge’ [1]. It uses existing knowledge and creates new knowledge based on the existing knowledge. Generally

newly recruited engineers and technical officers access the internal knowledge management system to obtain knowledge. This might be the reason for the lack of an integrated knowledge management system. However, organization employees are willing to share knowledge, provided they have a system to share the knowledge. Therefore, a strong requirement exists from management to introduce such a system and provide leadership. As a recommendation based on this finding, an organization should introduce knowledge management system with following practices.

- Information quality rating mechanism
- Easy search mechanism and up to date information
- Structured way to retrieve information
- Encourage to build new knowledge based on existing available knowledge

Finally, considering all factors such as leadership, knowledge sharing culture, Socialization, externalization, combination, and internalization authors have come up with a suitable knowledge management framework for mobile telecommunication sector (Figure 2).



Figure 2 - Knowledge management Framework for mobile telecommunication industry in Sri Lanka

3.4 Methodology

Knowledge management system need to be implemented in a central location, thus most suitable method was to develop a web based system that runs in a single server. Therefore, knowledge management system was developed using basic web developing languages such as PHP, CSS, and JS as well as web developing tools such as XAMPP MySQL database. Some open source templates [2, 3] were also used to achieve an enriching appearance.

Knowledge management system was developed according to a pre-build knowledge map in order to ensure that the captured knowledge will be stored with categorization. This improves the searching ability by reducing

searching time and increasing the ability to cater to specific search requirements. This pre-build knowledge map is used to differentiate among divisions in the company as well as the knowledge categories.

Knowledge management system was developed in order to cater the different requirements in different levels of management. For example, uploading documents are done by lower management and below employees. Therefore, uploading option was given within each division. However, in addition to the search option within each division, another search option is given for senior management, which can capture the knowledge of every division as a whole. This was enabled to ensure that system support both senior and junior level employees requirements.

Having a knowledge management system is useless if the users can't rely on the system. In order for users to rely on the system, they need to have a trust towards the content of the documents in the systems. A rating system was introduced to ensure this as shown in Figure 3.



Figure 3 - Rating System implemented within Knowledge Management System.

In order to encourage people to use the system, extra steps were need to be taken to ensure handling feasibility and ability to force the system in to the mind of the entire employee base in the initial stage. Therefore, system should be able to operate easily. Authors have achieved this using several data capturing techniques including forms-base knowledge contribution schemes and automated data capturing schemes. They have used several automated data capturing mechanisms to capture performance and system oriented data while rely on user input for other sources of documents.

Another important factor is use of suitable data mining software. Final output need to be user friendly and provide effective and efficient searching for end users. Meta search software is used in combination with automated categorization tool to achieve this. Meta search specification used in the system is shown in Figure 6.





Figure 4 - Meta search specification used in the Knowledge Management System

Finally, important requirement of any system is feedback. Therefore, this knowledge management system has provide the opportunity for any user to provide their feedback anonymously.

4. Results

This section discuss the results of the implemented knowledge management system.

After conducting several training sessions, this system was initially introduced to one division within Mobitel, Sri Lanka. After several months, it was introduced to several other divisions as well as the next step. As authors continued to introduce new systems within the Engineering division, more and more people started to use and rely on the knowledge management system.

Currently, this system is being used in several sub divisions in Mobitel Engineering division as a platform to store and share knowledge among divisions as well as within each divisions.

5. Conclusions

It is expected that in the future, this system can be extended to entire engineering division. Thus, entire Mobitel team can benefit from sharing their knowledge while contributing to Mobitel as well. Hence, this would lead to a knowledge sharing culture within the organization.

References

1. Nonaka, I, "A Dynamic Theory of Organizational Knowledge Creation," Vols. Organization Science, Vol. 5, No. 1 (Feb., 1994), pp. 14-37, p. P207, 1994.
2. Nadeera, W. K. J. Knowledge Management Framework for mobile telecommunication sector in Sri Lanka, 2016.
3. <http://www.marcellop.com/bootmetro/>, Visited 14th July, 2016.

4. <https://themewagon.com/themes/free-bootstrap-3-admin-dashboard-template/> , Visited 5th December, 2016.

Effect of Technical & Non-Technical Competence on the Job Performance of Private Sector Engineers in Sri Lanka

With special reference to a group of large scale engineering companies

J.R. Ekanayake

Abstract: In any nation, engineers are expected to play a vital role in economic development while confronting the prevalent globalized rivalry and hence there is no exception for Sri Lankan engineers too. Majority of local engineers being employed by the private sector, their contribution for national economic progress is pivotal. However, it is commonly argued that whether the local engineers are competent enough to effectively contribute in aforesaid task and also it is observed that the relevant literature is scarce and hence the knowledge base as applicable to local context is not rich. The attempt of the paper is to enrich knowledge base of particular discipline in the local context, by exploring attributes and characteristics of competences and job performance sought in present-day engineers and also to investigate their inter-relationship.

This paper will present comprehensive details along with the findings of a methodically performed study based on a set of appropriate data (about competence & job performance) primarily collected by administering a suitably designed questionnaire. The study consisted of the detail facts and figures of both statistical and descriptive analysis. Ultimately, the paper presents the multiple dimensions of technical competence, non-technical competence and job performance as applicable to engineers. The findings of statistical analysis reveal that the average level of technical competence, non-technical competence and job performance are moderate. Further, this study statistically demonstrates, strong relationships in job performance vs technical competence, job performance vs non-technical competence and job performance vs overall competence.

Keywords: Engineers, Technical Competence, Non-technical Competence, Job Performance, Statistical Analysis

1 Introduction

It is obvious that, in any nation including Sri Lanka, engineers play a vital role in all nationally important sectors; it may be agriculture, industry or service. This significant nature of engineers' contribution for national economies makes it much important to explore and study about the attributes of competences sought in engineers and their effect on job performance.

With prevailing nature of rapidly advancing technical environment and speedy globalization, there exists a considerable consensus that the modern engineering profession requires not only technical excellence, but also some additional, non-technical competences. The problems faced by engineers today are increasingly complex and

require both strong technical knowledge and skills and an understanding of relevant environmental, social, economic and cultural contexts [5].

Above phenomenon is also applicable to local engineers who are predominantly employed by private sector organizations which operate in a globalized business environment. Hence it is obvious that contemporary Sri Lankan engineers requires not only technical excellence, but also some additional, non-technical competences. Irrespective of the nature of local establishment, as a result of the enduring phenomenon of globalization local companies also confront a severe rivalry in their business.

Eng. J. R. Ekanayake, B.Sc. Eng. (Hons), MBA, C. Eng., MIE(SL), MASME (USA), MIET (UK), Senior Lecturer in Mechanical Engineering, IESL College of Engineering.



The companies who try to achieve competitive advantage in an environment with continuing and enhancing competition, certainly demand their employees (engineers) to be competent in various facets in addition to essential technical competencies. But, it is argued that whether local engineers are competent enough to meet this demand of the industry.

As written by Wijesiri[11], the overwhelming consensus among employers is that, "too many graduates lack critical-thinking skills and the ability to communicate effectively, solve problems creatively, work collaboratively and adapt to changing priorities. In addition to these "soft skill" deficits, employers are also finding that young people lack the technical, or "hard", skills associated with specific jobs".

So, engineering graduates being a subset of graduates produced by the system of local universities, with equal standards and funding, governed by the same entity (i.e. by the University Grants Commission (UGC) under the Ministry of Higher Education and Highways), engineering graduates can't be expected to have an exception.

Based on author's 1st hand experience, it is understood that even at a highly technical working environment as in the case of his previous employment, also with sound technical competences, an engineer cannot become successful and climb up on the ladder in his career, unless he or she owns sufficient level of non-technical competences.

Further it is evident that, under prevailing economic situation and job market in Sri Lanka, the majority of graduates including engineering graduates are employed by the private sector [1]. So it is justified to do a research on this issue and it can be considered as a pertinent issue to the majority of private sector engineers graduated predominantly from local government universities.

As implied by the title itself, this study intends to identify the attributes of competence (i.e. the dimensions of technical and non-technical competence) and their influence on the job performance as applicable to Sri Lankan private sector engineers with special reference to a

group of large scale engineering companies and thereby to make recommendations to enhance the individuals' job performance and organizational performance.

2 Research Questions and Objectives

The research questions and objectives are as below.

1. What are the attributes and characteristics of the concept of competence and Job performance in relation to engineering profession?
2. How does competence influence job performance of engineers?
3. What are the recommendations to improve job performance of engineers?

Based on the above research questions, following research objectives are formulated.

1. To study and clarify the attributes and characteristics of the concept of competence and job performance in relation to engineering profession.
2. To analyse the relationship between competence and job performance
3. To make recommendations to improve job performance of engineers.

3 Methodology

This study adopts a commonly used scientific research method, where following hypotheses with relevant to the topic of interest are made based on the supporting evidences of available literature.

Hypothesis 1: High level of technical competence results in high job performance.

Hypothesis 2: High level of non-technical competence results in high job performance.

Hypothesis 3: High level of technical competence together with high level of non-technical competence will result in high job performance.

Subsequently those hypotheses are tested and proved by statistical analysis of gathered data relevant to the study.

The target population of this research study is the engineers of local private sector companies. A random sample consisting of fifty engineers employed in several private sector engineering companies (includes large scale manufacturing, design & engineering, construction, operations & maintenance and services sector companies) was selected from the entire population and the relevant data were collected through this sample by administering an appropriately designed questionnaire.

The questionnaire consisted of three main sections to gather data about demographic information, competence and job performance. Demographic data includes, age, sex, qualifications, designation, level of employment and experience. Competence data were gathered under the two categories of Technical and Non-Technical competence. Job Performance data were collected under the sub categories of Task Performance, Contextual Performance and Adaptive Performance. Except the demographic data, all others were collected through closed ended statements (representing measurable attributes) which were to be responded with a degree of agreement measured with 5-point Likert's scale of 1-5 from every employee's point of view

Finally, the analysis was carried out based on hypothesis deductive method using state of the art software "IBM SPSS Statistics Ver.24". For that purpose of analysis, the average level of competence and job performance of each respondent were calculated. Further, to find out the behaviour of dependent variable according to the movement of independent variables, two statistical methods namely the Correlation Analysis and Linear Regression Analysis were used.

4 Literature Review

There have been numerous researches done by scholars to identify and define the "competence" (or "competency"), "job performance" and to establish a relationship between them. In this study the literature review was narrowed down to the journals and publications which focus on competences and job performance dimensions particularly with a

special interest to engineers and engineering profession.

Based on the comprehensive literature survey it could be identified that engineering is no longer a matter of just engineering, as the profession of engineering and the roles of engineers have changed rapidly over the past few decades. The need to educate "holistic engineers" or "global engineers" is widely acknowledged. Previous studies suggest that present days' engineers need to be competent in both technical and non-technical competences in order to be successful in their job roles and to progress in career.

While taking various explanations and definitions about competence in to account, measurable dimensions of technical competences were derived from the studies of OECD [8] and Nguyen[7]. They are; Competence and updated knowledge in computer science and technology, Competence in mathematics skills and problem-solving skills, Competence in Engineering & Science fundamentals Competence in Engineering Practice, Competence in invention and development of new products/solutions.

Similarly, the measurable dimensions of non-technical competences were derived from the study of Heuristic Model of Engineering Nontechnical Competences [5] and those are; Professional ethics, Personal competences Interpersonal competences, Leadership, management, and administrative competences, Innovation and entrepreneurial competences and Law and legal system competences.

Measurable dimensions of Job Performance were identified from the study of Linda Koopmans [4]and Sabine Sonnentag J. V.[9]. These dimensions are categorized under three main dimensions and listed below namely; Task Performance, Contextual Performance and Adaptive Performance. Each of these dimensions are consist of multi-dimensions.

In various studies, around the world they highlight about the strong relationship between competences and job performance of engineers. With the speedy globalization and resultant



severe rivalry faced by contemporary organizations, there is a serious consensus that engineers need both technical and non-technical competences in almost equal proportions. Mare Teichmann states that “the “new century engineer” is expected to be technically competent, globally sophisticated, culturally aware, innovative and entrepreneurial, nimble, flexible and mobile” [5].

Accordingly, there exists considerable consensus that the modern engineering profession requires not only technical excellence, but also some additional, non-technical competences.

5 Analysis and Discussion

As the first step in the process of the analysis, the reliability analysis of the questionnaire was carried out by computing “Cronbach’s Alpha”. The Demographic Data, Competence Data and Job Performance Data which were collected by administering the questionnaire were subjected to a broad analysis which consist of both descriptive and statistical analysis. The details of the analysis are comprehensively presented in following paragraphs.

5.1 Reliability Analysis of Questionnaire

The reliability analysis of the questionnaire was done by computing the “Cronbach’s alpha”. The “Cronbach’s alpha” reveals the reliability, or internal consistency, of a set of questions designed to check any particular concept or principle [6]. Here, the reliability of any given measurement refers to the extent to which it is a consistent measure of a concept. Questionnaire used in this study consisted of main three sections to collect 1) Demographic information, 2) Data about competence and 3) Data about job performance. Among these three sections, section 2) and 3) were used to gather data about variables considered in this study and hence, the questions only in these sections are associated with answers on Likert scale.

Table 1 - Cronbach's Alpha - Questions to check Technical Competence

Reliability Statistics		
Cronbach's Alpha	Cronbach's Alpha Based on Standardized Items	N of Items
.650	.664	5

Table 2 - Cronbach's Alpha - Questions to check Non-Technical Competence

Reliability Statistics		
Cronbach's Alpha	Cronbach's Alpha Based on Standardized Items	N of Items
.704	.701	6

Table 3 - Cronbach's Alpha - Questions to check Technical and Non-Technical Competence together

Reliability Statistics		
Cronbach's Alpha	Cronbach's Alpha Based on Standardized Items	N of Items
.811	.813	11

Table 4 - Cronbach's Alpha - Questions to check Job Performance

Reliability Statistics		
Cronbach's Alpha	Cronbach's Alpha Based on Standardized Items	N of Items
.869	.865	17

As presented in above tables, for all sets of questions Cronbach’s Alpha was found to be between 0.65 and 0.90. Therefore, it was found that the entire questionnaire is reliable enough to serve the desired purpose of data gathering [2].

5.2 Descriptive Analysis

As per the findings of descriptive analysis, it can be resolved that the majority of private sector engineering jobs are occupied by middle aged engineers. Hence this study will contribute significantly to enhance the job performance of young & middle-aged engineers who are considered to be more productive in science and engineering tasks [3], and thereby to enhance the organizational performance and economic contribution.

Further the descriptive analysis suggests that the majority of engineers in targeted population are only BSc. Eng. qualified while a very less are qualified with post graduate and non-technical qualifications. Further it was revealed that the, engineers' turnover rate is less. This can be a result of good remuneration they are being offered by the present employer. When they are remunerated well by the present employer, they don't tend to look out for new jobs and therefore their interest on post graduate and non-technical qualifications could be very less. Ultimately all these matters get linked together and results in poor career progress.

5.3 Statistical Analysis

Univariate Analysis was carried out to find out the average levels of competence and job performance. Co-relation and regression analysis were carried out in order to formulate the relationship between variables and test the validity of collected data, investigate the significance and test the hypothesis.

5.3.1 Univariate Analysis

Univariate analysis, revealed that in average engineers' technical competence, non-technical competence and also the job performance are only at moderate level. This also can be a result of lack of post graduate and non-technical qualifications and finally this also will badly affect in long-term career progress while limiting engineers only to lower and middle management levels.

Table 5 - Descriptive Statistics of Technical Competence and Job Performance

Descriptive Statistics			
	Mean	Std. Deviation	N
Technical Competence	3.4520	.38926	50
Job Performance	3.3506	.37884	50

Table 6 - Descriptive Statistics of Non-Technical Competence and Job Performance

Descriptive Statistics			
	Mean	Std. Deviation	N
Non-technical Competence	3.1630	.42769	50
Job Performance	3.3506	.37884	50

As summarized in above both tables 5 and 6, it is evident that the Technical Competence, Non-Technical Competence and the Job Performance of the respondents are at Moderate Level (i.e. because $2.5 \leq \text{Mean} \leq 3.5$ and $\text{SD} < 0.43$)[10].

5.3.2 Correlation Analysis

Correlation analysis was carried out in order to determine what kind of relationship exists between variables. The results of correlation analysis of "Technical competence (TC)" vs "Job performance (JP)" and "Non-technical competence (NTC)" vs "Job performance (JP)" are as below.

Table 7 - Correlation of Technical Competence and Job Performance

Correlations			
		TC	JP
TC	Pearson Correlation	1	.769**
	Sig. (2-tailed)		.000
	N	50	50
JP	Pearson Correlation	.769**	1
	Sig. (2-tailed)	.000	
	N	50	50

** . Correlation is significant at the 0.01 level (2-tailed).



Table 8 - Correlation of Non-Technical Competence and Job Performance

Correlations			
		NTC	JP
NTC	Pearson Correlation	1	.756**
	Sig. (2-tailed)		.000
	N	50	50
JP	Pearson Correlation	.756**	1
	Sig. (2-tailed)	.000	
	N	50	50

** Correlation is significant at the 0.01 level (2-tailed).

According to above presented summarized results of correlation analysis, it is obvious that, a strong positive correlation exists between Technical Competence (TC) and Job Performance (JP) with $r = 0.769$, $p < 0.01$. Similarly, it is observed that, a strong positive correlation exists between Non-Technical Competence (NTC) and Job Performance (JP) with $r = 0.756$, $p < 0.01$ ($r = 0.5$ to 1.0 ; A Strong Positive Relationship as referred to V.J.Delima, [10]). Since both technical and non-technical competences are positively correlated with job performance and significant at 0.01 level (2-tailed), it can be resolved that, the linear relationship in the sample data is statistically significant and therefore the relationship between these variables can be fairly modelled by linear regression. These results conclude that, enhancement of either technical or non-technical competences will result in higher job performance of engineers. In comparison to the level of influence by non-technical competence on job performance, it can be identified that the technical competence influences slightly more on the job performance of engineers. This is because of the slightly high correlation coefficient between technical competence and job performance than the that of non-technical competence and job performance.

5.3.3 Regression Analysis

Research hypothesis was tested using the regression analysis and following three regression equations have been developed.

Case A: Technical Competence (TC) vs Job Performance (JP)

$$JP = a_0 + a_1 (TC) + error \quad \dots (1)$$

Case B: Non-Technical Competence (NTC) vs Job Performance (JP)

$$JP = \beta_0 + \beta_1 (NTC) + error \quad \dots (2)$$

Case C: Technical Competence (TC) together with Non-Technical Competence (NTC) vs Job Performance (JP)

$$JP = \gamma_0 + \gamma_1 (TC) + \gamma_2 (NTC) + error \quad \dots (3)$$

By ANOVA test for the linear regression it was found that, there is a relationship between the dependent variables and the independent variables in all above cases. Since the probability of the F statistic ($p < 0.000$) is less than to the level of significance (0.01), the research hypothesis that there is a relationship between the variables is supported and null hypothesis that coefficient of correlation is equal to 0 is rejected.

The coefficients; a_0 , a_1 , β_0 , β_1 , γ_0 , γ_1 and γ_2 of above equations were found using regression analysis.

Hence above equation (1) can be re-written as follows.

$$JP = 0.767 + 0.748 (TC) \quad \dots (4)$$

The coefficient for the independent variable "Technical Competence (TC)" found to be 0.748, indicating a positive relationship with the dependent variable "Job Performance (JP)". Thus, higher numeric values for the independent variable "Technical Competence (TC)" are associated also with higher numeric values for the dependent variable "Job Performance (JP)".

Therefore, the statement of hypothesis, high technical competence results in high job performance is proved.

Table 9 - Model Summary - Case A

Model Summary				
Model	R	R Square	Adjusted R Square	Std. Error of the Estimate
1	.769 ^a	.591	.583	.24470

a. Predictors: (Constant), Technical Competence

As per model summary above, the coefficient of determination (R^2) of 0.591 illustrates that; 59.1% of the total variation in "Job Performance" can be explained by the linear



relationship between “Technical Performance” and “Job Performance” (as described by the regression equation (4) stated above). The value of 0.591 obtained for coefficient of determination indicates that, the regression line represents the data reasonably well.

Similarly, above equation (2) can be re-written as follows.

$$JP = 1.234 + 0.669 (NTC) \quad \dots (5)$$

The coefficient for the independent variable “Non-technical Competence (NTC) ” found to be 0.669, indicating a positive relationship with the dependent variable “Job Performance (JP)”. Hence, higher numeric values for the independent variable “Non-technical Competence” are associated also with higher numeric values for the dependent variable “Job Performance”.

Therefore, the statement of hypothesis, high non-technical competence results in high job performance is proved.

Table 10 - Model Summary - Case B

Model Summary				
Model	R	R Square	Adjusted R Square	Std. Error of the Estimate
1	.756 ^a	.571	.562	.25071

a. Predictors: (Constant), Non-technical Competence

The coefficient of determination (R²) of 0.571 shows that; 57.1% of the total variation in “Job Performance” can be explained by the linear relationship between “Non-technical Performance” and “Job Performance” (as described by the regression equation (5) stated above). Further, the value of 0.571 obtained for coefficient of determination indicates that, the regression line represents the data reasonably well.

Finally, above equation (3) can be re-written as follows

$$JP = 0.562 + 0.460 (TC) + 0.380 (NTC) \quad \dots (6)$$

The coefficient for the independent variable “ Technical Competence (TC) ” found as 0.460,

and that for the other independent variable “Non-technical Competence (NTC)” found to be 0.380. This illustrates that there is a good positive relationship of both independent variables with the dependent variable “Job Performance”. This implies that, higher numeric values for both independent variables “Technical Competence” and “Non-technical Competence” or either of them will result in higher numeric values for the dependent variable “Job Performance”. Furthermore, the higher coefficient (0.460) associated with Technical Competence implies that the effect of Technical Competence on Job Performance is higher than the that of Non-Technical competence.

The coefficient of determination (R²) of **0.687** shows that; 68.7% of the total variation in “Job Performance” can be explained by the linear relationship as described by the regression equation (6) stated above. The value of 0.687 obtained for coefficient of determination indicates that, the regression line represents the data reasonably well.

Therefore, the statement of hypothesis, both higher technical and non-technical competence results in high job performance is proved.

6 Conclusions and Recommendations

The findings of the descriptive analysis suggest that, the majority of engineers are not qualified with the post graduate and non-technical qualifications and also they are not much attentive of the career prospectus with a new employer. In response to these findings it is recommended for engineers to take up relevant post graduate and non-technical studies on time and to look out for better job positions with new employers and thereby to maximize the opportunities of securing more senior management positions.

The results of statistical analysis (Univariate analysis) revealed that, the average level of technical competence (Mean = 3.45), non-technical competence (Mean = 3.16) and job performance (Mean = 3.35) of private sector engineers are moderate. Therefore, it is



required to further enhance both the technical and non-technical competences and also the job performance of private sector engineers.

As per the statistically significant findings of quantitative analysis (i.e. by Correlation and Regression Analysis), it is evident that high competence results in high job performance of engineers in local private sector. Further, the outcomes of comprehensive literature review clarified that, the competence as applicable to engineers consist of main two dimensions; technical competence and non-technical competence. The comprehensively performed quantitative analysis revealed that both types of competences are almost equally important to achieve high level of job performance, but with a slight higher importance of technical competence as applicable to engineering profession. In affirmative to these key findings of quantitative analysis, following recommendations are made to intensify the competences of local engineers. Hence those recommendations will pave the path towards enriched job performance of engineers and thereby to uplift the overall performance of private sector companies.

- It is recommended to review and upgrade the academic programmes of local engineering universities to broaden the non-technical content, while strengthening the technical core of course curriculum.
- It is suggested to introduce and conduct more and more education and training programmes by IESL at a subsidized price (or if possible free of charge for members) to enhance both technical and non-technical competence of local engineers. These programmes should be made attractive by making the content opportune, globally cognizant, industry oriented and interactive (or student-centred learning type).
- It is proposed for local private organizations to stress on appropriate competency management models and to concentrate on competency-based approaches to enhance job performance of their engineers (employees).
- It is recommended for individual engineers to make a self-assessment to check where I

am standing with respect to the level of technical competence and non-technical competence. Then having done the self-assessment with respect to competence, they shall concentrate on developing both technical and non-technical competences consistently and continuously.

Acknowledgement

Author wishes to thank Mr. Deepal BataduwaArachchi and Dr. Nalin Abeysekara for advising throughout the process of performing this study. Further the author conveys heart felt gratitude to Dr. K. E. D. Sumanasiri for providing very much needed encouragement and guidance during the process of preparing this paper.

References

1. Ariyawansa, R. G. (2008). Employability of Graduates of Sri Lankan Universities, Vol.2, No.1. *Sri Lankan Journal of Human Resource Management*.
2. Goforth, C. (2015, November). *Using and Interpreting Cronbach's Alpha*. Retrieved from University of Virginia Library, Research Data Services + Sciences: <http://data.library.virginia.edu/using-and-interpreting-cronbachs-alpha/>
3. Institute of Medicine (US) Committee on the Long-Run Macroeconomic Effects of the Aging U.S. Population. (2012, December). *Aging and the Macroeconomy: Long-Term Implications of an Older Population*. Retrieved from National Centre for Biotechnology Information, U. S. National Library of Medicine: <https://www.ncbi.nlm.nih.gov/books/NBK144283/>
4. Linda Koopmans, M. C. (2011, August). Conceptual Frameworks of Individual Work Performance; A Systematic Review. *Journal of Occupational and Environmental Medicine ; Vol:53*.
5. Mare Teichmann, V. P. (2013). *A Heuristic Model of Non-technical Competences for Engineers*.
6. Mohsen Tavakol, R. D. (2011). Making sense of Cronbach's alpha. *International Journal of Medical Education*.

7. Nguyen, D. Q. (1998). The Essential Skills and Attributes of an Engineer: A Comparative Study of Academics, Industry Personnel and Engineering Students. *Global J. of Engng. Educ., Vol. 2, No.1.*
8. OECD. (2009). *A Tuning-Ahelo Conceptual Framework Of Expected/Desired Learning Outcomes In Engineering.* Organisation for Economic Co-operation and Development.
9. Sabine Sonnentag, J. V. (2008). Job Performance. In J. Barling, *Micro Approaches - SAGE Handbook of Organizational Behaviour - Vol.1* (pp. 427-447). Los Angeles.
10. V.J.Delima. (2016). Influence of Employees' Functional Competencies on Employees' Job Performance: A Special Reference to Insurance Companies in Batticaloa District. *Journal for Studies in Management and Planning, e-ISSN: 2395-0463, Volume 02 Issue 6, 188-195.*
11. Wijesiri, L. (2016, March 5). Plugging Sri Lanka's skills gap. *Daily News.*



Artificial Bone Substitutes and Bone Tissue Engineering as Alternative Methods for Natural Bone Repair and Regeneration in Severe Traumas and Complex Clinical Conditions of Bones

B.R.M.G.W.U.B. Balagalla

Abstract: Human bone tissue has ability to develop and regenerate itself throughout the life. However, there is a need of alternative methods for natural bone repair and regeneration in severe traumas such as terrible bone fractures, infections, tumors and skeletal abnormalities. Additionally, the rate of bone disorders are increasing rapidly. Thus, it is necessity to conduct research on alternative cures for complex clinical conditions which compromises the natural repair process. One such method is bone grafting. However, there are some drawbacks which limit the grafting treatments. Researchers are working on improving more alternative methods such as artificial bone substitutes and bone tissue engineering. Biomedical engineering plays a major role in developing biocompatible, non-toxic biomaterials for artificial bone substitutes and testing their physical parameters to estimate the ability to mimic the natural bone. The latest trend of alternative methods for natural bone repair and regeneration is bone tissue engineering. Currently, bone tissue engineering is developing rapidly and in the near future it will become the major solution for severe traumas and complex clinical conditions. However, it is important to conduct more researches to find out the best scaffold materials, study them in micro and nano structural level, study the *in-vitro* cell developing and maintaining the physical parameters and growth factors in cell culture to obtain the bone tissue required. This review emphasizes the importance of artificial bone substitutes and bone tissue engineering, alternative methods for natural bone repair and regeneration in severe traumas and complex clinical conditions of bones, the current development and future directions.

Keywords: Biomedical Engineering, Artificial Bone Substitutes, Bone Tissue Engineering

1. Introduction

Bone tissue develops and remodels continuously itself throughout human life and it repairs and regenerates itself during bone fractures. It is a complex physiological process which can be seen during normal fracture healing. However, in severe traumas such as terrible bone fractures, infections, tumors and skeletal abnormalities and complex clinical conditions such as avascular necrosis, atrophic non-unions and osteoporosis. Moreover, in some cases such as avascular necrosis, atrophic non-unions and osteoporosis the regenerative process is compromised. To overcome these clinical problems of impaired and insufficient bone regeneration, bone grafting, bone tissue engineering and artificial bone substitutes are used[19].

2. Significance

The risk of bone fractures are increasing rapidly due to less exercises, lack of nutrition and accidents. It is estimated that 1.5 million individuals suffer bone fractures in each year. Risk of fractures is greater in elderly people and

women. United States estimated that 4 in 10 women after age of 50 experience hip, spine or wrist fracture. Furthermore, some fractures are life threatening or have some lifetime risks.

Additionally, genetic diseases caused by mutations such as deletion, insertion, RNA splicing, single base substitution cause some common ontogenesis diseases. One such significant problem is osteoporosis. It is estimated that around 10 million and 33.6 million individuals over age 50 suffer from hip osteoporosis and low bone mass/ osteopenia respectively in US. The risk of osteoporosis and osteopenia is increasing and by 2020 1 in 2 americans has the risk of having osteoporosis in any site of skeleton. Additionally, calculated percentage of osteoporosis risk for postmenopausal White women is 35 percent[4,5].

Eng. (Miss.) B.R.M.G.W.U.B. Balagalla, B.Sc. in Biomedical Engineering (General Sir John Kotelawala Defence University), Demonstrator, Department of Electrical and Electronics, Faculty of Engineering, University of Sri Jayewardenepura, Sri Lanka.



3. Bone Grafting Techniques

Bone tissue grafting is a commonly used surgical procedure which is used as a treatment for many bone defects. There are three types of grafting techniques, autograft, allograft and xenograft.

Autografting is re-implanting a tissue by another similar tissue taken from the same individual. Allografting is replacing a tissue by another similar tissue taken from a different individual in the same species. Xenografting is replacing a tissue by another similar tissue taken from a different individual in a different species.

Nevertheless, autografting and allografting is the commonly used techniques in bone grafting. Xenografting is not popular in bone grafting due to the biocompatibility, mechanical and chemical dissimilarities and immune rejections.

3.1 Autologous Bone Grafting

Autologous bone grafting is known as the gold standard method because of its advantages over other existing methods[6].

3.1.1 Advantages of Autologous Bone Grafting

Autologous bone grafts are biocompatible and non-immunogenic. They provide all the physical and chemical properties required as a bone graft material. In contrast, they are osteoinductive, osteogenic and osteoconductive. Moreover, it can be easily re-vascularized and it combines with the recipient site within less time period. Furthermore, possibility of pathogen transmission is rare in autologous bone grafting.

3.1.2 Disadvantages of Autologous Bone Grafting

Autologous bone graft is harvested from the same patient. Thus, it requires a second surgery in the donor site. It may result in significant morbidity or deformity in donor site. Possibility of excessive bleeding, inflammation and infection is high as there are two surgical sites in the same patient. If the defected site is larger than feasible or available donor sites, it is impossible to perform autologous bone grafting. Additionally, autologous bone grafts are comparatively expensive[7,8,12]

3.2 Allogenic Bone Grafting

Allogenic bone grafting is the most commonly used second bone grafting technique.

3.2.1 Advantages of Allogenic Bone Grafting

Allogenic bone grafts are histocompatible in most of the cases. Moreover, there are different forms of allogenic bone grafts are available according to the host-site requirements namely demineralized bone matrix, morcellised and cancellous chips, corticocancellous and cortical grafts, osteochondral and whole-bone segments.

3.2.2 Disadvantages of Allogenic Bone Grafting

Allogenic bone grafting is more susceptible to immune-rejections and pathogen transmission. Moreover, allografts show reduced osteoinductive properties because donor grafts are devitalized via irradiation or freeze-drying processing. Another problem associates with the allogenic bone grafting is unmet supply to the great demand. To be exact, there is a shortage in allograft bone grafts. Though the allogenic bone grafting costs less comparatively to the autologous bone grafting, it costs a significant amount[9,10].

4. Artificial Bone Substitutes

Artificial bone substitutes appeared in the clinical set-up as a solution for the disadvantages of gold standard method and allogenic bone grafting. There are continuous researches going on to find the ideal materials for bone replacement with adequate mechanical properties and biocompatibility which can be provided upto demand.

4.1 Different types of Bone Substitutes

4.1.1 Ceramics

Ceramics can be categorized as bioabsorbable ceramics, bioactive ceramics and bioinert ceramics based on the chemical reactivity and porosity. Mostly they are derived from coral which has a biological pore interconnectivity mesh network and hemihydrate of calcium sulphate known as Plaster of Paris which is prepared by heating gypsum.

Bioabsorbable ceramics is the first and most clinically used synthetic material in bone replacement. They bind to the host cells well and bioabsorption rate depends on the osteogenesis properties arises due to the chemical composition, crystal structure and surface area. For an example, tricalcium phosphate resorbed 10–20 times faster than hydroxyapatite. Tricalcium phosphate can be totally resorbed or converted into hydroxyapatite which may remain in the body significantly.

Porosity of the ceramics is important in grafting. The optimal osteoconductive pore sizes of ceramic bone grafts is 150 and 500 μm . Injured bone regenerates itself through pores during healing osteogenic process and the synthetic material is reabsorbed. However, the intrinsic strength of the callus site can be compromised due to weak synthetic ceramics and increased porosity can cause significant loss in compressive strength.

Hemihydrate of Calcium Sulphate which is generally known as Plaster of Paris is the first bone substitute used. It is reabsorbable ceramic with a high reabsorbable rates and indefinite shelf life. It does not compromise osteogenesis or increase the risk of infection when used in infected cavities. Additionally, it is easy to synthesize and sterilize. It allows drug administration and very inexpensive.

Nevertheless, Plaster of Paris does not provide internal strength or support. Accordingly, it can be used to fill small bone defects only.

Calcium phosphate is an osteoconductive bioabsorbable ceramic composed of hydroxyapatite, TCP or combination of the two. However, mixture of hydroxyapatite and TCP is used most of the time clinically. It is obtained by sintering calcium phosphate salts at high temperatures to evaporate water and high pressure compaction produces the powder which can be used to mold into pellet. Calcium Phosphate achieves higher percentage of its compressive strength within 24h after injected into bone cavity and more stable due to high density. Mechanical properties of porous calcium phosphate is similar to cancellous bone once they have been incorporated and remodeled. Possibility of early adverse effects namely inflammation and foreign-body responses to calcium phosphate are comparatively low. But the disadvantage is that it cannot be used where significant torsion bending or shear stress is required due to being a brittle material with insufficient tensile strength.

Calcium carbonate skeletal structure of sea coral is used to synthesize hydroxyapatite by a hydrothermal exchange method which replaces the original calcium carbonate with a calcium phosphate replicate. Structure of hydroxyapatite is more similar to human cancellous bone.

If porites are used as the synthesis material, microstructure structure becomes more similar to interstitial cortical bone. However, hydroxyapatite can be used only to fill the defects upto 7-8cm as it does not contain the intrinsic strength required. Additionally,

delayed degradation of coralline-derived hydroxyapatite is a most common problem occurs.

Bioglass contains SiO_2 less than 60%, high Na_2O and CaO . The ratio of $\text{CaO}/\text{P}_2\text{O}_5$ is almost similar to natural bone. The surface of the bioglass becomes highly reactive and forms hydroxyl carbonate apatite when it is exposed to an aqueous medium. Formation of hydroxyl rapidly is needed to make a good bond with host tissues as bioglasses are not reabsorbable. Bioglasses are used for the treatments of medium size bone defects due to the less mechanical strength.

Bioinert ceramics are biocompatible material with highest mechanical strength which do not react with the host tissue. Often, the composition of bioinert ceramics contain metal oxides such as zirconia, alumina or titanium. However, the applications of bioinert ceramics are limited due to less bonding capabilities with bone[1].

4.1.2 Polymers

Nonbiodegradable polymers such as polymethyl methacrylate have been used as osteoconductive artificial bone substitutes. Activity of PMMA is similar to bioinert ceramic and bioglasses. Though it does not bind to the new bone, it is adhesive to the bone surface without interrupting the regeneration. PMMA is selected as an artificial bone substitute over a decay due to its osteoinductive properties yet it is weak. However, polymers may even inhibit new bone growth and normal healing. Partially resorbable polymers such polyglycolide and poly-L-lactide are introduced to overcome the problems such as inhibition of new bone growth and healing process. Polymers have a great advantage over ceramics as they can be used in large bone fracture fixation and use as substances carriers[211,12]

4.1.3 Metals

A number of metals and their alloys, namely Fe, Cr, Co, Ni, Ti, Ta, Mo, and W have been used as an artificial bone substitutes for years. The first metallic implant developed known as Sherman Vanadium Steel is used as bone fracture plates and screws. Metals have good mechanical properties such as high durability and high strength. Moreover, they are readily available for the surgery and comparatively low cost. However, there is a great problem related with corrosion in metals which may weaken the



implant and cause toxic reactions. Additionally, metals are affected by electromagnetic environment. But Ti and its alloys are corrosion resistant and are not affected by the electromagnetic environment yet very expensive.

The common advantages of artificial bone substitutes are that they are readily available upto the demand, FDA approvals are provided and less ethical considerations has to be taken into account. Nevertheless, there are drawbacks such as low mechanical strengths, high foreign body immune reactions and toxicity[3].

5. Bone Tissue Engineering

Bone tissue engineering is the process of culturing osteogenic cells within three-dimensional scaffolds, under conditions supporting bone formation to obtain fully viable, biological bone grafts in vitro. Osteogenic cells, scaffolds, combinations of biochemical and biophysical signals can be given as the key components of bone tissue engineering[5,13,14].

5.1 Osteogenic Cells

There are different types of osteogenic cells used in bone tissue engineering namely, embryonic stem cells, bone marrow-derived mesenchymal stem cells, umbilical cord-derived mesenchymal stem cells and human amniotic fluid-derived stem cells.

Stem cells appear as the most valid and more promising solution in bone tissue engineering. Embryonic stem cells have nearly unlimited self-renewal capability and the capacity to differentiate via precursor cells. Disadvantage of embryonic cells is the tumorigenesis. Mesenchymal stem cells can be isolated from the intended recipient very easily. Therefore, there is a great advantage of minimized immune rejection. In addition, it has a high differentiation and proliferation capabilities. Mesenchymal stem cells have capability of self-renewal and multi-lineage differentiation. Human amniotic fluid-derived stem cells are isolated from amniotic fluid after routine amniocentesis. It expresses both embryonic and adult stem cell properties and is highly multipotent. Another advantage is that, it does not create tumorigenic reactions.

5.2 Scaffolds

In the bone tissue engineering, 3D scaffolds play an important role. There are many properties that should be fulfilled by a good scaffold for

proper functioning of cells and the new bone formation.

Scaffolds should be highly porous and highly interconnected to provide mass transport, cell to cell communication and vascularization. They should be hydrophilic to allow the cell attachment. Their anisotropic properties promote cell adhesion, proliferation and differentiation. Moreover, for an optimum performance, they should be available in a variety of shapes, sizes and structures according to the requirements. It is important to have the mechanical properties similar to those of the host and it should be structurally stable. Additionally, scaffold material should be a biodegradable, biocompatible and non-toxic.

There are different types of scaffold materials, namely bioactive ceramics, biological polymers, synthetic polymers and hybrid materials. Bioactive ceramics are used over many years. They can be divided into two as natural and synthetic based on the origin. Coralline hydroxyapatite is an example for natural origin and synthetic hydroxyapatite and β -tricalcium phosphate can be given as examples for synthetic origins. There are many advantages of bioactive ceramics namely, having high modulus non-toxicity, good osteo-integration, supporting osteoblast adhesion and proliferation. However, they are brittle and have a poor fatigue resistance. Additionally, if the Ca and P concentrations are increased, it may result in cellular death. Moreover, the degradation rate of bioactive ceramics is difficult to predict.

Biological polymers are extensively studied for bone tissue engineering as they have many advantages such as low immunologic response and have a good bioactive behavior. They interact with the host tissue properly. However, the degradation rate cannot be controlled and mechanical characteristics of biological polymers do not match those of the bone. Examples for biological polymers are collagen, chitosan and silk.

Synthetic polymers are biocompatible and have potential of delivering drugs and growth factors. The degradation rate of synthetic polymers can be controlled. Additionally, its mechanical properties can be tuned according to the requirement. Their capability of the cell attachment can be improved by negatively charged chemical groups. Moreover, they can be fabricated into complex shapes[15,16].

Composites consist of 2 phases, matrix phase and dispersed phase. These materials are mostly used to achieve additional good properties. For an example, polymer and ceramic composites

give the toughness of a polymer with the stiffness of a ceramic. Moreover, biocompatibility can be enhanced by using composites[17,18].

5.3 Biochemical and Biophysical Signals

Bioreactors and the growth factors are the most important signaling molecules in bone tissue engineering.

Bioreactors are the dynamic cell culture systems which allows more control to generate larger volumes of cells. They enhance the mass transfer of nutrients and gases and metabolites to regulate the size and structure of the tissue being generated.

Examples for the growth factors are recombinant human BMPs (rhBMPs), BMP-2, and BMP-7. They direct blend or coat on the scaffold or it adhere to the cell culture medium during the development of the cell/scaffold construction.

5.4 Advantages of Bone Tissue Engineering

In bone tissue engineering, the possibility of pathogen transmission is zero and the host has to undergo fewer surgeries. Possibility of immune rejections are rare. Moreover, it is advantageous as the host does not need to wait for a donor. It is a permanent solution and helpful in severe traumas. It avoids the permanent damages occurs to the donor site. There is a possibility of correcting incurable genetic defects with the aid of bone tissue engineering.

5.5 Disadvantages of Bone Tissue Engineering

The most prominent problem related to the bone tissue engineering is difficulty of constructing suitable scaffolds. Moreover, it is difficulty obtain the full functionality of the bone. It is comparatively high cost. Still there are fewer technologies are available.

5.6 Future Strategies of Bone Tissue Engineering

Biomedical engineer has a great role to play in bone tissue engineering developments. It is important to carry out research to figure out the new techniques and matrix materials will be developed to enhance the properties of needed bone tissue and scaffolds. In the future, there is a possibility in reprogramming of adult cells to form induced pluripotent stem cells. Moreover, it is important to look into cost-effective methods as bone tissue engineering has many advantages yet very expensive.

6. Conclusion

There is a great need of alternative methods for natural bone repair and regeneration due to the severe traumas and complex clinical conditions. There are many alternative methods are introduced. However, there are several drawbacks and limitations in each methods.

According to the review, researches should be done in every alternative methods for the further development. Tissue engineering will be the prominent solution for the need of alternative methods for natural bone repair and regeneration due to the severe traumas and complex clinical conditions in the near future.

References

1. Takao, Y. (1994) Bone bonding behavior and clinical use of A-W glass-ceramic, in *Bone Grafts, Derivatives and Substitutes* (Urist, M. R., O'Connor, B. T., and Burwell, R. G., eds.), Butterworth-Heinemann Ltd, pp. 245-259.
2. Hench, L. L. (1992) Bioactive bone substitutes, in *Bone Grafts and Bone Graft Substitutes* (Habal, M. B. and Reddi, A. H., eds.), Saunders, Philadelphia, pp. 263-275.
3. Park, J.B. and Lakes, R.S., 2007. Metallic implant materials. *Biomaterials*, pp.99-137.
4. Kuivaniemi, Helena, Gerard Tromp, and Darwin J. Prockop. "Mutations In Collagen Genes: Causes Of Rare And Some Common Diseases In Humans". *FASEB Journal* (1991).
5. Laurencin CT, Ambrosio AM, Borden MD, Cooper JA. Tissue engineering: orthopedic applications. *Annu Rev Biomed Eng.* 1999;1:19-46.
6. St John TA, Vaccaro AR, Sah AP, Schaefer M, Berta SC, Albert T, et al. Physical and monetary costs associated with autogenous bone graft harvesting. *Am J Orthop (Belle Mead NJ)* 2003;32(1):18-23.
7. Younger EM, Chapman MW. Morbidity at bone graft donor sites. *J Orthop Trauma.* 1989;3(3):192-195.
8. Banwart JC, Asher MA, Hassanein RS. Iliac crest bone graft harvest donor site morbidity. A statistical evaluation. *Spine (Phila Pa 1976)* 1995;20(9):1055-1060.
9. Delloye C, Cornu O, Druetz V, Barbier O. Bone allografts: What they can offer and what they cannot. *J Bone Joint Surg Br.* 2007;89(5):574-579.
10. Tomford WW, Starkweather RJ, Goldman MH. A study of the clinical incidence of infection in



the use of banked allograft bone. *J Bone Joint Surg Am.* 1981;63(2):244-248.

11. Glowacki, J., Jasty, M., and Goldring, S. (1986) Comparison of multinucleated cells elicited in rats by particulate bone, polyethylene, or polymethylmethacrylate. *J. Bone Miner. Res.* 1, 327.
12. Laurencin CT, Khan Y, El-Amin SF. Bone graft substitutes. *Expert Rev Med Devices.* 2006;3(1):49-57.
13. Cordonnier, T., Sohier, J., Rosset, P. and Layrolle, P. (2011). Biomimetic Materials for Bone Tissue Engineering - State of the Art and Future Trends. *Advanced Engineering Materials*, 13(5), pp.B135-B150.
14. Amini, A., Laurencin, C. and Nukavarapu, S. (2012). Bone Tissue Engineering: Recent Advances and Challenges. *Critical Reviews in Biomedical Engineering*, 40(5), pp.363-408.
15. Ulery BD, Nair LS, Laurencin CT. Biomedical applications of biodegradable polymers. *J Polym Sci B Polym Phys.* 2011;49(12):832-864.
16. Rossi, F., Santoro, M. and Perale, G. (2013). Polymeric scaffolds as stem cell carriers in bone repair. *Journal of Tissue Engineering and Regenerative Medicine*, 9(10), pp.1093-1119.
17. Karageorgiou V and Kaplan D. Porosity of 3D bio-material scaffolds and osteogenesis. *Biomaterials.*2005;26(27):5474-5491.
18. Stevens, B., Yang, Y., Mohandas, A., Stucker, B. and Nguyen, K. (2008). A review of materials, fabrication methods, and strategies used to enhance bone regeneration in engineered bone tissues. *Journal of Biomedical Materials Research Part B: Applied Biomaterials*, 85B(2), pp.573-582.
19. Dimitriou, R., Jones, E., McGonagle, D. and V Giannoudis, P. (2011). *Bone regeneration: current concepts and future directions.* [online] BioMed Central. Available at: <http://bmcmedicine.biomedcentral.com/articles/10.1186/1741-7015-9-66> [Accessed 27 Oct. 2016].

Condition Assessment of Power Transformers using Dissolved Gas Analysis

W.T.D. Samarasingha, J.R.S.S. Kumara and M.A.R.M. Fernando

Abstract: Power transformer is one of the key elements in an electrical power network. Therefore, in order to ensure reliable supply, proper condition assessment program of power transformers is an essential requirement. In the power transmission network of the Ceylon Electricity Board, there are over 160 numbers of power transformers (132/33 kV and 220/132/33 kV) in operation which are distributed in grid substations all over the country. They are from different manufacturers having different ratings and in the wide range of service life. This study has been carried out in order to seek the possibility of assessing the condition of power transformers based on the results obtained from Dissolve Gas Analysis. All the available Dissolve Gas Analysis data of the power transformers in grid substations were collected and analyzed in order to assess the condition of those power transformers. A health index (a numerical value which described the condition of the transformer) was calculated for each transformer based on Dissolve Gas Analysis test results. Several special cases were selected and further analyzed in order to investigate the potential of DGA for predicting of condition of power transformers. Other test results such as winding resistance and excitation current were also used in these case studies. Finally, it was identified that, Dissolve Gas Analysis can be effectively used in condition assessment of power transformer.

Keywords: Condition Assessment, Power Transformers, Dissolved Gas Analysis (DGA)

1. Introduction

Dissolved Gas Analysis (DGA) is a widely used tool in transformer condition monitoring which can be used to analyze the gas components dissolved in the insulating oil. Electrical disturbances and thermal decompositions can be identified as two common causes of gas formation in energized transformers.

Insulating mineral oil inside a transformer is a mixture of different hydrocarbons, and the decomposition processes for these hydrocarbons against a thermal or electrical fault are different to each other. Chemical reactions occurred at fault/stressed conditions are involving in breaking of carbon-hydrogen and carbon-carbon bonds [1]. During this process, active hydrogen atoms and hydrocarbon fragments are formed. Combination of few of these fragment may form hydrogen (H₂), methane (CH₄), ethylene (C₂H₄), ethane (C₂H₆) and acetylene (C₂H₂). In addition to that thermal decomposition of cellulose and electrical faults produce methane (CH₄), hydrogen (H₂), carbon monoxide (CO), and carbon dioxide (CO₂). In DGA, these gases are generally referred to as key gases and measured in Parts Per Million (PPM). Some of these gasses are considered as high risk indicators as they are generated only under

serious faults, while some of gasses are considered as not high risk indicators but should be at alarmed depend on their quantity has been formed [1].

The gases listed above are generally considered as combustible gases (except CO₂). Presence of these gas components can be due to thermal, electrical, or corona faults inside a transformer. The rate at which each of these key gases is produced basically depends on the fault temperature and volume of material. Because of the volume effect, amount of gases that a large volume of insulation at moderate temperature produced would be moreover equal to the amount of gases produced in a smaller volume at a higher temperature. Therefore, the concentrations of the individual gas component found in transformer insulating oil may be directly used and trended to evaluate the thermal history of the transformer in order to

Eng. W.T.D. Samarasingha, AMIE(SL), B.Sc. Eng. (Hons) (Peradeniya), Electrical Engineer, Ceylon Electricity Board.

Eng. (Dr) J.R.S.S. Kumara, AMIE(SL), SMIEEE, B.Sc. Eng.(Hons) & M.Phil (Peradeniya), Tech. Lic. & Ph.D. (Chalmers), Sweden, Senior Lecturer, Dept. of Electrical & Electronic Engineering, University of Peradeniya.

Eng. (Prof.) M.A.R.M. Fernando, C.Eng., FIE(SL), SMIEEE, B.Sc.Eng.(Hons) (Peradeniya), Tech Lic. (KTH), Sweden, Ph.D.(Chalmers), Sweden, Professor, Dept. of Electrical & Electronic Eng., University of Peradeniya.



evaluate any potential faults inside the transformer and hence assess condition of the transformer [2].

2. Literature Review

Among many diagnostic techniques developed for the interpretation of these gases below listed methods and techniques can be identified as the widely used once in transformer condition diagnostics [3].

1. Key Gas Method
2. Roger's Ratio Method
3. IEC Basic Ratio Method
4. Duval's Triangle Method
5. ANSI/IEEE C57.104

2.1 Key Gas Method

In this method, type of fault is identified based on the percentage amount of a specific gas. Table 1 summarizes the diagnostic criteria for key gas method. The percentage amount of gas is an approximated figure based on total dissolved combustible gases (TDCG) [3-5]. For example, large amount of H₂ with little amount of other hydrocarbons are produced by low intensity Partial Discharge (PD) or corona.

Further, relationship between fault temperature and gassing characteristics is described in the thermodynamic model proposed by Halstead [7]. This model assumes that all hydrocarbons in the oil are decomposed into same product and each of these products are in equilibrium with all the other products. According to the model, the generation rate of each gas can be calculated at any temperature.

Table 1 - Diagnostic criteria of the key gas method [3-5]

Fault	Key Gas	Criteria	Gas percentage
Arcing	C ₂ H ₂	High H ₂ and C ₂ H ₂ , low CH ₄ and C ₂ H ₄ , if cellulose involved CO, CO ₂	H ₂ : 60% C ₂ H ₂ : 30%
Corona (PD)	H ₂	High H ₂ , moderate CH ₄ , low C ₂ H ₆ , C ₂ H ₄ , if cellulose involved C O, CO ₂	H ₂ : 85% CH ₄ : 13%
Overheating of oil	C ₂ H ₄	High C ₂ H ₄ , low C ₂ H ₆ , moderate CH ₄ , H ₂ & CO	C ₂ H ₄ : 63% C ₂ H ₆ : 20%
Overheating of cellulose	CO	High CO & CO ₂ .	CO: 92%

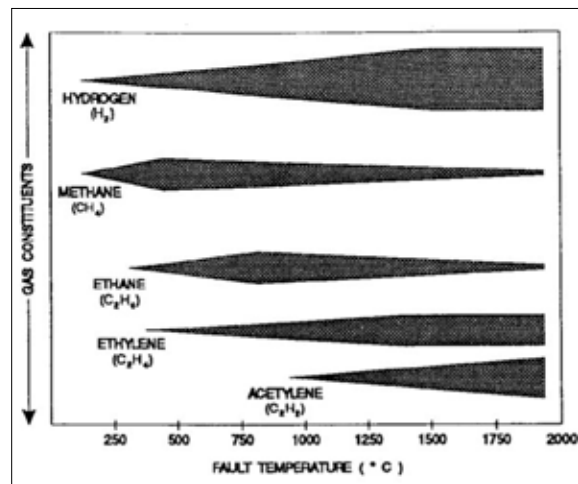


Figure 1 - Relationship between gas constituent vs. fault temperature [2,6]

Figure 1 shows the relationship between gas constituent vs. fault temperature. Study of these relationships reveals that gases are generated in following order with temperature increase H₂ → CH₄ → C₂H₆ → C₂H₄ → C₂H₂ [2], [6].

2.2 Roger's Ratio Method

Roger's ratio method can be identified as an extension of Doernenberg's ratio method. It described three ratios: R₁, R₂ & R₅ as defined below.

$$R_1 = \text{CH}_4/\text{H}_2 \quad \dots (1)$$

$$R_2 = \text{C}_2\text{H}_2/\text{C}_2\text{H}_4 \quad \dots (2)$$

$$R_5 = \text{C}_2\text{H}_4/\text{C}_2\text{H}_6 \quad \dots (3)$$

As shown in Table 2, there are 5 types of faults are described in Roger's ratio method.

Table 2 - Diagnostics Technique for Roger's Ratio Method [6]

Case	R ₂	R ₁	R ₅	Fault
0	< 0.1	0.1-1.0	<1.0	Normal
1	< 0.1	<0.1	<0.1	Low energy partial discharge
2	0.1-3.0	0.1-1.0	>3.0	Arcing
3	< 0.1	0.1-1.0	1.0-3.0	Low temperature thermal
4	< 0.1	>1.0	1.0-3.0	Thermal fault below 700°C
5	< 0.1	>1.0	>3.0	Thermal fault above 700°C

Table 3 - Diagnostics technique for IEC Basic Ratio Method [1,4,6]

Range of ratios	Code			
	C ₂ H ₂ /C ₂ H ₄	CH ₄ /H ₂	C ₂ H ₄ /C ₂ H ₆	
	R2	R1	R5	
<0.1	0	1	0	
0.1 to 1.0	1	0	0	
1.0 to 3.0	1	2	1	
>3.0	2	2	2	
Fault Types				Typical phenomena
Normal (No fault)	0	0	0	Normal aging
Partial discharge of low energy density	0 (but not significant)	1	0	Discharge in gas filled cavities resulting from incomplete impregnation or high humidity
Partial discharge of high energy density	1	1	0	Same as PD of low energy density but leading to tracking or perforation of cellulose
Discharge of low energy	1 to 2	0	1 to 2	Continuous sparking in oil or breakdown of oil between solid insulation
Discharge of high energy	1	0	2	Discharges with power follow-through. Arcing of oil between windings or coils or between coils and ground.
Thermal fault of low temperature < 150°C	0	0	1	General insulation conductor overheating
Thermal fault of low temperature range 150-300°C	0	2	0	Local overheating of the core, increasing hot spot temperatures, shorting links in the core, overheating of copper due to bad contacts/ joints, circulating currents.
Thermal fault of medium temperature range 300-700°C	0	2	1	
Thermal fault of high temperature >700°C	0	2	2	

Roger’s ratio method has not defined minimum gas level requirements regarding applicability of the method. However, it is suggested that the method be applied only when normal gas levels are exceeded [6].

2.3 IEC Basic Ratio Method

IEC Basic Ratio Method is further extension of the Roger’s Ratio method. IEC 60599: “Mineral oil-filled electrical equipment in service - Guidance on the interpretation of dissolved and free gases analysis” discusses a ratio method to analyze the concentrations of dissolved gases which can be interpreted to diagnose the condition of oil-filled electrical equipment in service. Diagnostics as per IEC 60599 is summarized under Table 3 [1], [4], [6].

2.4 Duval’s Triangle Method

A triangular graphical representation was used to analyze the gas concentration inside the transformer. As illustrated in Figure 2,7

zones are defined based on amount of CH₄,C₂H₂ and C₂H₄and each zone is corresponds to a particular fault.

The Triangle coordinates corresponding to DGA results in PPM are calculated as follows:

$$C_2H_2\% = 100 * x / (x + y + z) \quad \dots(4)$$

$$C_2H_4\% = 100 * y / (x + y + z) \quad \dots (5)$$

$$CH_4\% = 100 * z / (x + y + z) \quad \dots (6)$$

Where, x is C₂H₂ inppm, y is C₂H₄ in ppm andz is CH₄ in ppm. These coordinates are plotted in the Duval’s Triangle which is in Figure 2to evaluate the fault condition [5], [7].This method has proven to be accurate and dependable over many years and is now gaining in popularity.



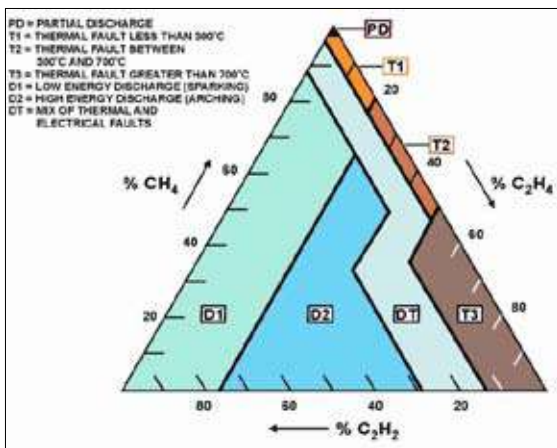


Figure 2 - Duval's Triangle [5,7]

2.5 ANSI/IEEE C57.104

Four condition levels have been introduced in order to assess the level of risks to transformers. Table 4 list the dissolved gas concentration levels allocated for each condition [2].

Condition 1: TDCG below 720 indicates the transformer is healthy. If any individual combustible gas exceeds specified levels, further investigations are recommended.

Condition 2: TDCG within 721-1920 indicates condition of the transformer is acceptable. Any individual combustible gas exceeding specified levels should prompt additional investigation. It is recommended to monitor the behavior of gas generation over the time.

Condition 3: TDCG within 1921-4630 indicates poor condition of the transformer. Immediate action should be taken to establish a trend over the time to monitor the behavior of gas generation. Faults are probably present.

Condition 4: TDCG exceeding 4630 indicates very poor condition and immediate attention is required to avoid possible failure of the transformer.

3. Tested Power Transformers

In this study, DGA tests were performed on 161 nos. of power transformers in Ceylon Electricity Board (CEB) which are spread all over the country. They are from different manufactures, with different characteristics and in the wide range of age groups (1 to 49 years range). Operating voltages of these

power transformers are 220kV, 132kV and 33kV. All these power transformers are ONAN/ONAF type with On Load Tap Changer (OLTC). Further, all these transformers are oil immersed type and suitable for outdoor operation.

MYRKOS portable dissolved gas analyzer manufactured by Morgan Schaffer was used to analyze the dissolved gas content in the transformer insulating oil. In this process, first, recommended amount of insulating oil quantity is sampled to a shake test syringe. Then, the oil sample is shaken as per the recommendation given by the instrument manufacturer in order to extract the dissolved gas components from liquid to air media.

Then the extracted gas amount is fed to the instrument as per the instruction given by the instrument manufacturer. The gases are evaluated using chromatography method in two columns inside the instrument and a test report is prepared for injected gas sample.

These test results were analyzed to evaluate the present health condition of the transformer. Some transformers were tested for several times to monitor the generation of a particular gas component(s).

4. Analysis of DGA Test Results

DGA test results are analyzed for transformer condition diagnostics. As per Duval's suggestions [8], 90% typical gas levels were calculated for each and every gas component. A comparison between calculated 90% gas levels for CEB network with threshold gas levels stated in ANSI/IEEE C57.104 and threshold gas levels stated in IEC 60599 are summarized in Table 5.

When considering gas levels in Table 5, 90% typical gas levels of H₂, CH₄, CO, C₂H₄ and C₂H₂ are substantially matched with IEEE or IEC standard. 90% typical values of CO₂ and C₂H₆ show a clear deviation from relevant values in IEEE or IEC standard.

Gas levels stated in ANSI/IEEE C57.104 and IEC 60599 are only recommended values which can be used to evaluate the health condition of a randomly selected power transformer. But, when it considers the

Table 4 - Dissolved gas concentration level allocated for each condition in ANSI/IEEE C57.104 [2]

Status	Dissolved key gas concentration limits [$\mu\text{L/L}$ (PPM)]							
	H ₂	CH ₄	C ₂ H ₂	C ₂ H ₄	C ₂ H ₆	CO	CO ₂	TDCG
Condition 1	100	120	1	50	65	350	2500	720
Condition 2	101-700	121-400	2-9	51-100	66-100	351-570	2501-4000	721-1920
Condition 3	701-1800	401-1000	10-35	101-200	101-150	571-1400	4001-10000	1921-4630
Condition 4	>1800	>1000	>35	>200	>150	>1400	>10000	>4630

Table 5 - Comparison of 90% gas levels for CEB network with threshold gas levels stated in ANSI/IEEE C57.104 and IEC 60599

Gas Component	Threshold gas levels stated in IEC 60599	Threshold gas levels stated in ANSI/IEEE C57.104	90% gas levels for CEB network
H ₂	60-150	100	68
CH ₄	40-110	120	112
CO	540-900	350	710
CO ₂	5100-13000	2500	4921
C ₂ H ₄	60-280	50	33
C ₂ H ₆	50-90	65	273
C ₂ H ₂	3-50	2	2

Table 6 - Threshold gas levels for power transformers in CEB network and Maximum detected gas levels in CEB network

Gas Component	H ₂	CH ₄	CO	CO ₂	C ₂ H ₄	C ₂ H ₆	C ₂ H ₂
Threshold level	70	110	710	5000	35	270	2
Maximum detected gas level	2737	7883	2282	11406	9956	3293	47

Table 7 - 11 nos. of cases that, all three diagnostics methods give same result for a given transformer and calculated health index for these transformers

Transformer	Duval's Triangle	Roger's Ratio	IEC Basic Ratio	HI
Kelanitissa TR02	Thermal fault (300°C - 700°C)	Thermal fault (below 700°C)	Thermal fault (300°C - 700°C)	1.2
Seethawaka TR02	Thermal fault (above 700°C)	Thermal fault (above 700°C)	Thermal fault (above 700°C)	1.2
Pannipitiya TR03	Low energy electrical discharges	Arcing	Low energy electrical discharges	1.6
Pannipitiya TR02	Thermal fault (above 700°C)	Arcing	High energy electrical discharges	1.8
Galle TR04	Thermal fault (above 700°C)	Thermal fault (above 700°C)	Thermal fault (above 700°C)	1.9
New Anuradhapura TR02-Y	High energy electrical discharges	Arcing	High energy electrical discharges	1.9
Veyangoda MT02	Thermal fault (300°C - 700°C)	Thermal fault (below 700°C)	Thermal fault (300°C - 700°C)	2.05
Galle TR01	High energy electrical discharges	Arcing	High energy electrical discharges	2.25
Kotugoda TR01-B	Thermal fault (300°C - 700°C)	Thermal fault (below 700°C)	Thermal fault (300°C - 700°C)	2.35
Veyangoda MT03	Thermal fault (above 700°C)	Thermal fault (above 700°C)	Thermal fault (above 700°C)	2.35
Biyagama TR01-B	Thermal fault (above 700°C)	Thermal fault (above 700°C)	Thermal fault (above 700°C)	2.9



batch, the level of dissolved gas components may differ from those recommended values due to difference in loading pattern, weather condition and fault levels. Therefore, threshold values defined in Table 6 were used for diagnostic of transformers in CEB network.

Transformers having at least one gas component higher than the threshold level were further diagnosed as per Duval's Triangle, Roger's Ratios and IEC Basic Ratios methods. In this analysis, there were 11 nos. of transformers that, all three diagnostics methods give same result as shown in Table 7. The output result "Arcing" which described in Roger's ratio method can be mapped with "high/ low energy electrical discharges" or "thermal faults with temperature above 700°C" in other two diagnostics methods.

Further, high concentration of CO₂ can be observed due to atmospheric air leakages through gaskets or breathers of the transformer. Therefore, concentration of CO₂ cannot be considered as a strong parameter in diagnostics of transformers.

5. Health Index based on DGA

A Health Index (HI) was defined for selected transformers. Equation 07 was used to calculate the health index [9-10].

$$HI = \frac{\sum_{i=1}^7 S_i * W_i}{\sum_{i=1}^7 W_i} \quad \dots(7)$$

Where, HI: Health Index, S_i: Score defined for each gas depends on concentration, W_i: Weighting factor allocated for each gas and i: Relevant gas component.

To define a score system for each gas component, the threshold gas levels for CEB network and maximum detected gas level for each gas component in CEB network (Table 6) and gas levels allocated for each condition (condition 01 to 04) in ANSI/IEEE C57.104 standards were taken into consideration. The score system is defined in Table 8.

Allocating of a weight factor for each gas component was basically depending on gas generating temperature described in Figure 1.

As per the score values assigned for each gas level, the maximum possible HI value that can obtained is 4.0 which indicates that the

particular transformer is in worst condition in the sense of DGA. The minimum possible HI value is 1.0 which indicates that the particular transformer is in satisfactorily normal condition in the sense of DGA. Health Index value was calculated for all the power transformers subjected to this study. Further, justification was carried out with calculated Health Index values with available diagnostic results of transformers.

Based on the variation of health index value, it is clear that the severity of fault condition becomes higher with increase of the health index value. Most of the transformers which have health index value less than 1.15, "normal" condition or "low temperature thermal faults" are dominated in other diagnostics techniques. For transformers which have health index value in between 1.15 and 1.8, thermal faults in mid temperature ranges, low density electrical discharges and partial discharges are dominated in other diagnostics techniques.

Table 8 - Score and weight defined for each gas component

Gas	Score				Weight
	1	2	3	4	
H ₂	< 70	71 to 700	701 to 1800	>1800	2
CH ₄	< 110	111 to 400	401 to 1000	>1001	2
CO	< 710	711 to 930	931 to 1750	>1751	2
CO ₂	< 5000	5001 to 8000	8001 to 10000	>10000	1
C ₂ H ₄	< 35	36 to 90	91 to 180	>181	4
C ₂ H ₆	< 270	271 to 400	401 to 800	>801	3
C ₂ H ₂	< 2	3 to 10	11 to 35	>35	6

For transformers which have a health index value greater than 1.8, high temperature thermal discharges and high density electrical discharges are dominated in other diagnostics techniques. Therefore, health index value can be further used to evaluate the fault conditions which are previously associated with transformer as previous fault conditions

directly related to the present condition of the transformer. Therefore, the conditions of the transformer gets deteriorate with the increase of the health index value.

Accordingly, 161 nos. of power transformers were tested for DGA and each power transformer were assigned with Health Index. Number of power transformers allocated for several ranges of Health Indexes is summarized in Table 9.

Table 9 - Number of power transformers vs. Health Index

Range of Health Index	No. of Power Transformers
1.0 - 1.5	146
1.5 - 2.0	09
2.0 - 2.5	05
2.5 - 3.0	01
3.0 - 3.5	00
3.5 - 4.0	00

In this sense, Biyagama TR01 - B, Veyangoda MT03, Kotugoda TR01 - B, Pannala TR01, Galle TR01, Veyangoda MT02, New Anuradhapura TR02 - Y, Galle TR04, Pannipitiya TR02, Mathugama TR01 can be identified as most critical 10 transformers (in condition based) in CEB transmission network.

6. Conclusion

This study has been carried out to seek the possibility of assessing the condition of power transformers based on a health index defined using results of Dissolve Gas Analysis.

All the power transformers in CEB transmission network were tested for DGA, and the test results were analyzed based on the guidelines given in international standards. Further, threshold limits for gas components were defined by taking not only the threshold limits given in international standards but also the distribution of each gas concentration in CEB network. Accordingly, a health index (a numerical figure varies from 1 to 4) was defined for each transformer. Based on the health index values, conditions of the transformers were evaluated and some transformers were found which are in high critical stage.

It is recommended to carryout DGA at least once a year for each power transformer. Further, it is required to carry out DGA test in

regular basis on power transformers which were identified as critical based on the health index. The duration of such two DGA tests shall be two weeks, one month or three months which depends on the criticality of the transformer.

It can be concluded that proposed health index based on DGA is an effective tool to evaluate the condition of a power transformer. Continuous monitoring of DGA will lead the development of a database of health condition of power transformers which is very helpful for a utility to manage and plan its future developments.

References

1. International Electro-technical Commission, "Mineral oil impregnated electrical equipment in service - Guide to the interpretation of dissolved and free gases analysis", IEC 60599, 1999.
2. Institute for Electrical and Electronics Engineers, "IEEE Guide for the Interpretation of Gases Generated in Oil-Immersed Transformers", IEEE Std C57.104-1998, 2009.
3. Jasim, S. Y. and Shrivastava, J. V., "Dissolved Gas Analysis of Power Transformers", International Journal of Electrical and Electronics Engineering Research (IJEEER), pp2., December 2013.
4. Borakhade, S. A., and Kunjal Jane, "Dissolved Gas Analysis in Transformer using Three Gas Ratio Method and Fuzzy Logic based on IEC Standard", SSRG International Journal of Electrical and Electronics Engineering (SSRG-IJEEE) - volume 2 Issue 4, pp 2, April 2015.
5. David Woodcock, William, H., Bartley, M. Duval, J. Dukarm, A. de Pablo and Lindgren, S. R., "Severon White Paper: DGA Diagnostic Methods", Severon Corporation, USA, pp 4, 2007.
6. Zhenyuan Wang, "Artificial Intelligence Applications in the Diagnosis of Power Transformer Incipient Faults", Faculty of the Virginia Polytechnic Institute and State University, Virginia, pp 9 - 11, August 2008.
7. M. Duval, "A Review of Faults Detectable by Gas-in-Oil Analysis in Transformers", IEEE Electrical Insulation Magazine, Vol. 18, No. 3, pp 8 - 17, 2002.
8. Duval, M., "Calculation of DGA Limit Values and Sampling Intervals in Transformers in Service", IEEE Electrical Insulation Magazine, Vol. 24, No. 5, pp 7 - 13, 2008.



9. Naderian, A., Piercy, R., Cress, S., Wang, F., Service, J., *"An Approach to Determine the Health Index of Power Transformers"*, 1988, Electrical Insulation, IEEE International Symposium, pp 2, July 2008, DOI: 10.1109/ELINSL.2008.4570308.
10. Jahromi, A. N., Piercy, R., Cress, S., Service, J. R. R., Fan, W., *"An Approach to Power Transformer Asset Management Using Health Index"*, IEEE Electrical Insulation Magazine, Vol. 25, No. 2, pp 2, 2009.

Battery - Supercapacitor Hybrid Energy Storage Control for Electric Vehicle

W.M.J. Madhusankha, G.A.T.P. Madhuranga, S.A.S. Indika,
B.G.L.T. Samaranayake, P.J. Binduhewa and J.B. Ekanayake

Abstract: The battery, the dc bus, the dc to ac inverter and the electrical machine are the main components of a conventional fully electric vehicle (EV) powertrain. However, it severely limits the absorption of regenerative electrical energy during the down-hill motion and braking due to the low power density of batteries. Therefore, researchers work on incorporating Supercapacitors, which has high power density even though energy density is lower than that of an EV battery, in harnessing the regenerative energy. The range of a light EVs, with limited battery capacity due to weight restrictions, can be significantly increased by harnessing the regenerative energy. In order to integrate the Supercapacitors and the battery, a three-port dc-dc converter is used which is realized by simple augmentation of two non-isolated dc-dc converters. The power flow of this converter is obviously bi-directional. The ports are connected to the battery, Supercapacitors and the dc bus respectively. In this paper, the average model of the non-isolated dc-dc converters were derived and thereby the small signal model of the three port bi-directional dc-dc converter was obtained. The system is presented in the linear state space format and classical control system design tools are used to derive the stability based minimum and maximum voltage and current limits of the converter. The controller of the non-isolated dc-dc converter between the Supercapacitors and the dc bus is used to control the dc link voltage while the controller of the other dc-dc converter between the battery and the dc bus is used to control the battery current. Both the controllers use simple Proportional Integral (PI) controllers. The powertrain is tested in simulation using standard drive cycles to show the effectiveness of adding the Supercapacitors.

Keywords: Battery, bi-directional dc-dc converter, electric vehicle, Supercapacitor.

1. Introduction

Energy storage system has a major role in electric vehicles. All the vehicles have a battery with the unique set of requirements to maintain, but the common disadvantage to all of them is the limited life time of the battery. The EV battery supplies the instantaneous power demand, which most of the time, gives rise to random sudden changes in the battery current. The high current derivatives lead to shorten the battery life time [1]. Coping up with this is a serious concern among the EV manufacturers [1]. Therefore, it is worthy to find a solution to extend the battery life time, while delivering the equivalent or better performance. In order to extend the battery life time by reducing the battery current derivatives, a hybrid energy storage system consisting of a battery and a supercapacitor with novel control strategy, has been proposed. In our study, we have used two bi-directional dc-dc converters coupled with the battery and the supercapacitor. This configuration is also aimed at decreasing the life cycle cost of the energy storage system of the EV.

In the past work, different control strategies have been adopted to control power sharing

between battery and supercapacitor (SC). These strategies include fuzzy logic, rule-based control, model predictive control, etc [1 - 7]. The basic idea of all these control strategies is that battery supports low frequency power component and SC supports high frequency power component momentarily. In this paper, a simple novel control strategy is proposed for battery and supercapacitor hybrid energy storage system (HESS). The proposed method is based on Kalman Filter [8]. Some parameters of the battery and supercapacitor have to be constrained within certain ranges to meet the objective of maintaining a long life.

The parameters are namely the State of Charge

Mr. W.M.J. Madhusankha, Mr. G.A.T.P. Madhuranga & Mr. S.A.S. Indika are undergraduates;

Eng. (Dr.) B. G. L. T. Samaranayake, AMIE(Sri Lanka), MIEEE(USA), B.Sc.Eng. (Hons) (Peradeniya), Tek. Lic., (KTH) Ph. D. (KTH), is a Senior Lecturer;

Eng. (Dr.) P. J. Binduhewa, AMIE(Sri Lanka), MIEEE(USA), B.Sc.Eng.(Hons) (Peradeniya), Ph.D. (Manchester), is a Senior Lecturer;

Eng. (Prof.) J. B. Ekanayake, C.Eng. (SL & UK), FIE(Sri Lanka), FIET(UK), SMIEEE (USA), B.Sc. Eng. (Hons) (Peradeniya), Ph.D.(UMIST), is a Chair Professor In the Department of Electrical and Electronic Engineering, Faculty of Engineering, University of Peradeniya.



(SOC) and State of Health (SOH). The SOC and the SOH can be defined [3] as follows:

$$\frac{d[SOH(t)]}{dt} = -\frac{|I_L(t)|}{2C_n N_{cyc}} \quad \dots(1)$$

$$\frac{d[SOC_{bat}(t)]}{dt} = \frac{I_L(t)}{C_n} \quad \dots(2)$$

$$\frac{d[SOC_{cap}(t)]}{dt} = \frac{I_c(t)}{C_{sc} V_{sc}} \quad \dots(3)$$

where,

- $I_L(t)$ = Current of the battery
- C_n = Capacity of the battery
- N_{cyc} = Life span of the battery
- $I_c(t)$ = Current of the capacitor
- V_{sc} = Voltage of the capacitor
- C_{sc} = Capacity of the supercapacitor.

These parameters are used in deriving the control decisions presented towards the later sections of the paper. This paper is organized as follows: in section 2, the theoretical models of the hybrid energy storage system is illustrated. Section 3 presents the proposed controller. In section 4, the simulation results are reported and the conclusions are presented in section 5.

2. General Information

The arrangement of Bi-directional dc-dc converter, battery, dc bus, supercapacitor and power demand is shown in Figure 1.

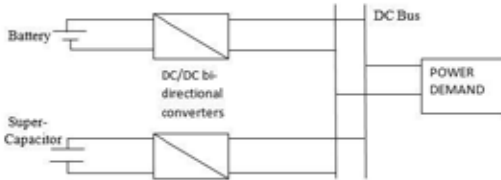


Figure 1 - Block diagram of the powertrain

2.1 Supercapacitor Model

Figure 2 shows the supercapacitor model used in this paper. In order to represent the capacitor internal resistance and leakage resistance of the SC respectively, series and parallel resistors are added to the ideal capacitor model.

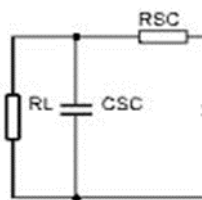


Figure 2 - Supercapacitor model

The variables used in bidirectional converter with Supercapacitor model are:

- \dot{I}_L = current of low voltage side of converter
- \dot{I}_{IND} = Inductor current of the converter
- \check{V}_L = voltage of low voltage side of converter
- \check{V}_H = voltage of high voltage side of converter
- V_H = voltage of the high voltage side at initial condition
- I_{IND} = inductor current at the initial condition
- \check{D}_{BUCK} = duty ratio of buck converter
- \check{D}_B = duty ratio of boost converter
- D_{BUCK} = initial duty ratio of the buck converter
- D_B = initial duty ratio of the boost converter
- R_L = leakage resistance of the supercapacitor
- R_{SC} = internal resistance of the supercapacitor
- R_p = resister in the converter
- C_{SC} = capacitance of the supercapacitor
- C_L = low voltage side capacitor
- C_H = high voltage side capacitor
- L = inductor in the converter

2.2 Supercapacitor with Buck Converter Model

The linearized governing equations averaged over one switching period of the bi-directional dc-dc converter, where the power flow takes place to the supercapacitor side from the dc bus side as shown in Figure 3 (converter operating in the Buck mode) can be derived as

$$\frac{d\check{I}_L}{dt} = -\left[\frac{1}{C_{SC}R_{SC}} + \frac{1}{C_{SC}R_L} + \frac{1}{C_L R_{SC}}\right]\check{I}_L + \frac{1}{C_L R_{SC}}\check{I}_{IND} + \frac{1}{C_{SC}R_{SC}R_L}\check{V}_L \quad \dots(4)$$

$$L\frac{d\check{I}_{IND}}{dt} = D_{BUCK}\check{V}_H + V_H\check{D}_{BUCK} - \check{V}_L - R_p\check{I}_{IND} \quad \dots(5)$$

$$C_H\frac{d\check{V}_H}{dt} = \check{I}_H - I_{IND}\check{D}_{BUCK} - D_{BUCK}\check{I}_{IND} \quad \dots(6)$$

$$C_L\frac{d\check{V}_L}{dt} = \check{I}_{IND} - \check{I}_L \quad \dots(7)$$

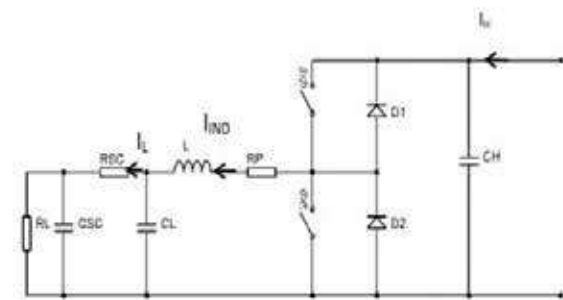


Figure 3 - Model Diagram of Buck Converter with Supercapacitor.

The above equations were presented in state space format with state vector being $[\check{I}_{IND} \check{V}_L \check{V}_H \check{I}_L]^T$ and the input vector being $[\check{D}_{BUCK} \check{I}_H]^T$ as:

$$\begin{bmatrix} \tilde{I}_{IND} \\ \tilde{V}_L \\ \tilde{V}_H \\ \tilde{I}_L \end{bmatrix} = \begin{bmatrix} -\frac{R_p}{L} & -\frac{1}{L} & \frac{D_{BUCK}}{L} & 0 \\ \frac{1}{C_L} & 0 & 0 & -\frac{1}{C_L} \\ -\frac{D_{BUCK}}{C_H} & 0 & 0 & 0 \\ \frac{1}{C_L R_{SC}} & \frac{1}{C_{SC} R_{SC} R_L} & 0 & -\left[\frac{1}{C_{SC} R_{SC}} + \frac{1}{C_{SC} R_L} + \frac{1}{C_L R_{SC}}\right] \end{bmatrix} \begin{bmatrix} \tilde{I}_{IND} \\ \tilde{V}_L \\ \tilde{V}_H \\ \tilde{I}_L \end{bmatrix} + \begin{bmatrix} \frac{V_H}{L} & 0 \\ 0 & 0 \\ \frac{1}{C_H} & \frac{1}{C_H} \\ 0 & 0 \end{bmatrix} \begin{bmatrix} \tilde{D}_{BUCK} \\ \tilde{I}_H \end{bmatrix}$$

and

$$Y = \begin{bmatrix} 0 & 0 & 1 & 0 \end{bmatrix} \begin{bmatrix} \tilde{I}_{IND} \\ \tilde{V}_L \\ \tilde{V}_H \\ \tilde{I}_L \end{bmatrix}$$

2.3 Supercapacitor with Boost Converter Model

The linearized averaged model equations of the same bi-directional dc-dc converter with the power flowing from the supercapacitor side to dc bus side as shown in Figure 4 were derived as

$$\frac{d\tilde{I}_L}{dt} = -\left[\frac{1}{C_{SC} R_{SC}} + \frac{1}{C_{SC} R_L} + \frac{1}{C_L R_{SC}}\right] \tilde{I}_L + \frac{1}{C_L R_{SC}} \tilde{I}_{IND} - \frac{1}{C_{SC} R_{SC} R_L} \tilde{V}_L \quad (8)$$

$$\tilde{V}_L = R_p \tilde{I}_{IND} + L \frac{d\tilde{I}_{IND}}{dt} + (1-D_B) \tilde{V}_H - V_H \tilde{D}_B \quad \dots(9)$$

$$C_H \frac{d\tilde{V}_H}{dt} = -\tilde{I}_H - I_{IND} \tilde{D}_B + (1-D_B) \tilde{I}_{IND} \quad \dots(10)$$

$$C_L \frac{d\tilde{V}_L}{dt} = \tilde{I}_L - \tilde{I}_{IND} \quad \dots(11)$$

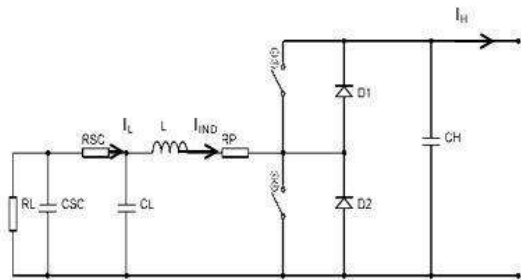


Figure 4 - Model Diagram of Boost Converter with Supercapacitor

The above equations were presented in state space format with state vector being $[\tilde{I}_{IND} \tilde{V}_L \tilde{V}_H \tilde{I}_L]^T$ and the input vector being $[\tilde{D}_B \tilde{I}_H]^T$ as:

$$\begin{bmatrix} \tilde{I}_{IND} \\ \tilde{V}_L \\ \tilde{V}_H \\ \tilde{I}_L \end{bmatrix} = \begin{bmatrix} -\frac{R_p}{L} & \frac{1}{L} & -\frac{(1-D_B)}{L} & 0 \\ -\frac{1}{C_L} & 0 & 0 & \frac{1}{C_L} \\ \frac{(1-D_B)}{C_H} & 0 & 0 & 0 \\ \frac{1}{C_L R_{SC}} & -\frac{1}{C_{SC} R_{SC} R_L} & 0 & -\left[\frac{1}{C_{SC} R_{SC}} + \frac{1}{C_{SC} R_L} + \frac{1}{C_L R_{SC}}\right] \end{bmatrix} \begin{bmatrix} \tilde{I}_{IND} \\ \tilde{V}_L \\ \tilde{V}_H \\ \tilde{I}_L \end{bmatrix} + \begin{bmatrix} \frac{V_H}{L} & 0 \\ 0 & 0 \\ \frac{1}{C_H} & \frac{1}{C_H} \\ -\frac{I_{IND}}{C_H} & -\frac{1}{C_H} \end{bmatrix} \begin{bmatrix} \tilde{D}_B \\ \tilde{I}_H \end{bmatrix}$$

2.4 Battery Model

Figure 5 shows the battery model used in this paper. It is the Thevenin equivalent model of a battery. This model reduces the complexities of modeling the HESS.

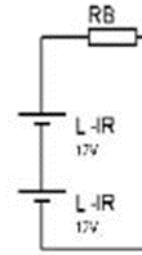


Figure 5 - Battery model

The variables used in bidirectional converter with battery model are:

- \tilde{I}_L = current of low voltage side of converter
- \tilde{I}_{IND} = Inductor current of the converter
- \tilde{V}_L = voltage of low voltage side of converter
- \tilde{V}_H = voltage of high voltage side of converter
- V_H = initial voltage at high side
- I_{IND} = inductor current at the initial condition
- \tilde{D}_{BUCK} = duty ratio of buck converter
- \tilde{D}_B = duty ratio of boost converter
- D_{BUCK} = initial duty ratio of the buck converter
- D_B = initial duty ratio of the boost converter
- R_B = internal resistance of the battery
- R_p = resistor in the converter
- C_L = low side capacitor
- C_H = high side capacitor
- L = inductor in the converter

2.5 Battery with Buck Converter Model

The linearized governing equations averaged over one switching period of the bi-directional dc-dc converter, where the power flow takes place to the battery side from the dc bus side as shown in Figure 6 (converter operating in the Buck mode) can be derived as



$$L \frac{d\tilde{I}_{IND}}{dt} = D_{BUCK} \tilde{V}_H + V_H \tilde{D}_{BUCK} - \tilde{V}_L - R_p \tilde{I}_{IND} \dots(12)$$

$$C_L \frac{d\tilde{V}_L}{dt} = -\tilde{I}_L + \tilde{I}_{IND} \dots(13)$$

$$C_H \frac{d\tilde{V}_H}{dt} = +\tilde{I}_H - I_{IND} \tilde{D}_{BUCK} - D_{BUCK} \tilde{I}_{IND} \dots(14)$$

$$\tilde{V}_L = R \tilde{I}_L \dots(15)$$

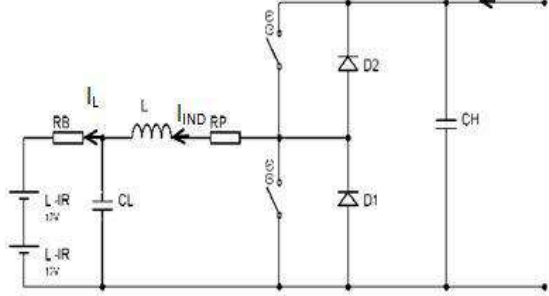


Figure 6 - Model Diagram of Buck Converter with Battery

The above equation set can be presented in state space format with state vector being $[\tilde{I}_{IND} \ \tilde{I}_L \ \tilde{V}_H]^T$ and the input vector being $[\tilde{D}_{BUCK} \ \tilde{I}_H]^T$.

$$\begin{bmatrix} \dot{\tilde{I}_{IND}} \\ \dot{\tilde{I}_L} \\ \dot{\tilde{V}_H} \end{bmatrix} = \begin{bmatrix} -\frac{R_p}{L} & -\frac{R_B}{L} & \frac{D_{BUCK}}{L} \\ 1 & -\frac{1}{C_L R_B} & 0 \\ -\frac{D_{BUCK}}{C_H} & 0 & 0 \end{bmatrix} \begin{bmatrix} \tilde{I}_{IND} \\ \tilde{I}_L \\ \tilde{V}_H \end{bmatrix}$$

$$+ \begin{bmatrix} \frac{V_H}{L} & 0 \\ 0 & 0 \\ -\frac{I_{IND}}{C_H} & \frac{1}{C_H} \end{bmatrix} \begin{bmatrix} \tilde{D}_{BUCK} \\ \tilde{I}_H \end{bmatrix}$$

$$Y = [0 \ 1 \ 0] \begin{bmatrix} \tilde{I}_{IND} \\ \tilde{I}_L \\ \tilde{V}_H \end{bmatrix}$$

2.6 Battery with Boost Converter Model

The linearized averaged model equations of the same bi-directional dc-dc converter with the power flowing from the battery side to dc bus side as shown in Figure 07 were derived as

$$\tilde{V}_L = R_p \tilde{I}_{IND} + L \frac{d\tilde{I}_{IND}}{dt} + (1-D_B) \tilde{V}_H - V_H \tilde{D}_B \dots(16)$$

$$C_H \frac{d\tilde{V}_H}{dt} = -\tilde{I}_H - I_{IND} \tilde{D}_B + (1-D_B) \tilde{I}_{IND} \dots(17)$$

$$C_L \frac{d\tilde{V}_L}{dt} = \tilde{I}_L - \tilde{I}_{IND} \dots(18)$$

$$\tilde{V}_L = -R \tilde{I}_L \dots(19)$$

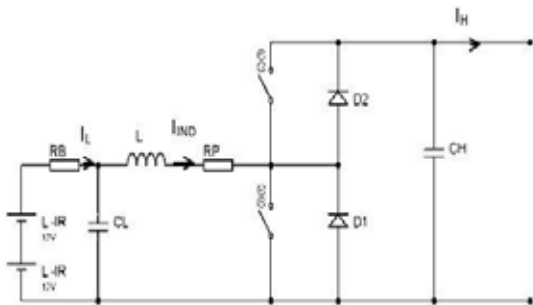


Figure 7 - Model Diagram of Boost Converter with Battery

The latter equations were presented in state space format with state vector being $[\tilde{I}_{IND} \ \tilde{I}_L \ \tilde{V}_H]^T$ and the input vector being $[\tilde{D}_{BOOST} \ \tilde{I}_H]^T$.

$$\begin{bmatrix} \dot{\tilde{I}_{IND}} \\ \dot{\tilde{I}_L} \\ \dot{\tilde{V}_H} \end{bmatrix} = \begin{bmatrix} -\frac{R_p}{L} & -\frac{R_B}{L} & -\frac{(1-D_B)}{L} \\ 1 & -\frac{1}{C_L R_B} & 0 \\ \frac{(1-D_B)}{C_H} & 0 & 0 \end{bmatrix} \begin{bmatrix} \tilde{I}_{IND} \\ \tilde{I}_L \\ \tilde{V}_H \end{bmatrix}$$

$$+ \begin{bmatrix} \frac{V_H}{L} & 0 \\ 0 & 0 \\ \frac{I_{IND}}{C_H} & \frac{1}{C_H} \end{bmatrix} \begin{bmatrix} \tilde{D}_B \\ \tilde{I}_H \end{bmatrix}$$

$$Y = [0 \ 1 \ 0] \begin{bmatrix} \tilde{I}_{IND} \\ \tilde{I}_L \\ \tilde{V}_H \end{bmatrix}$$

3. Control of Converters

3.1 Basic controllers for supercapacitor and battery

In order to implement the PI controller a linearized model was obtained by the actual system model as described Section 2. In this topology, the dc-dc converter connected to the Supercapacitor acts as a voltage regulator and the dc-dc converter connected to the battery acts as a current controller. To implement PI controllers for these two cases, it is necessary to have an idea about the poles of system. PI controllers were constructed using pole zero cancelation method while placing the poles as required. Time constant and damping ratios are the main parameters of the controllers.

In Figure 08, I_{demand} is the total demand current of the system. $I_{feedback}$ is the feedback from the power converter. The error is fed into the PI controller and the control signal (duty ratio) of converter were calculated. V_{ref} is equal to the bus voltage (48V). The PI controller of the converter with the Supercapacitor regulates the dc bus voltage. $V_{feedback}$ sense the bus voltage and error was fed into PI controller. Hence PI controller calculate the duty of the converter and fed it to the converter.

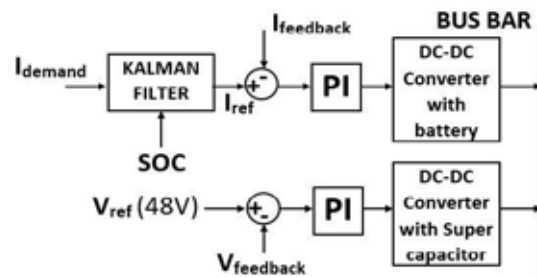


Figure 8 - Block Diagram of HESS Controller

I_{demand} is not the exact demand current. The demand current (I_{demand}) flows through the Kalman filter algorithm which has a variable gain according to the SOC of the Supercapacitor. However, dc bus voltage fluctuates due to the inequality of the demand current and the supply current. Supercapacitor acts as a voltage regulator and restores the bus voltage to the set point (48V), irrespective of whether it injects or draws current from the dc bus.

3.2 Power sharing between supercapacitor and battery

Currents components with high derivatives (high frequency components) of the demand current, cause rapid degradation of battery life. Simple one dimensional Kalman filter algorithm is utilized to share the power between supercapacitor and the battery. So that high frequency current is fed by supercapacitor and the low frequency components of current is fed by the battery. Following shows the simple Kalman filter algorithm used in this application.

$$I(k) = I(k-1) \quad \dots(20)$$

$$P(k) = P(k-1) + Q \quad \dots(21)$$

$$K(k) = P(k)(P(k) + R)^{-1} \quad \dots(22)$$

$$I(k) = I(k-1) + K(k) * (I_{demand}(k) - I(k)) \quad \dots(23)$$

$$P(k) = (1 - K(k)) * P(k) \quad \dots(24)$$

where,

$I(k-1)$	= Initial current value
$I(k)$	= Estimated current value
$I_{demand}(k)$	= Demand current
$P(k-1)$	= Initial error value
$P(k)$	= Initial estimated error value
$K(k)$	= Estimated Kaman gain
Q	= Process noise covariance
R	= Sensor noise covariance

4. Simulation Result & Discussion

In this section, we present the simulation results of the open loop models of the supercapacitor connected bi-directional dc-dc converter, battery connected bi-directional dc-dc converter, closed loop control of the same and the operation of the HESS.

4.1 Results of Supercapacitor connected bi-directional dc-dc converter

A step is applied with duty ratio 0.618 to achieve the 48V at the output side of the converter in the Buck mode. The converter is in

open loop control and the corresponding output is shown in Figure 9.

A step is applied with duty ratio 0.716 to achieve the 48V at the output side of the converter in the Boost mode. The converter is in open loop control and the corresponding output is shown in Figure 10.

Next a PI controller was introduced to the supercapacitor connected bi-directional dc-dc converter. A step of 48 V is applied as the reference input and the output of the Buck mode is shown in Figure 11. The same configuration in Boost mode is shown in Figure 12.

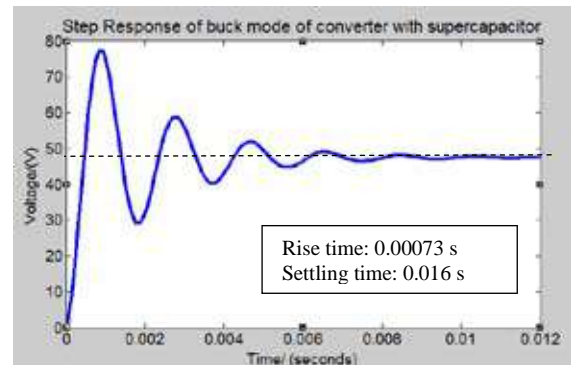


Figure 9 - Open loop step response of Supercapacitor connected bi-directional dc-dc converter in the Buck mode.

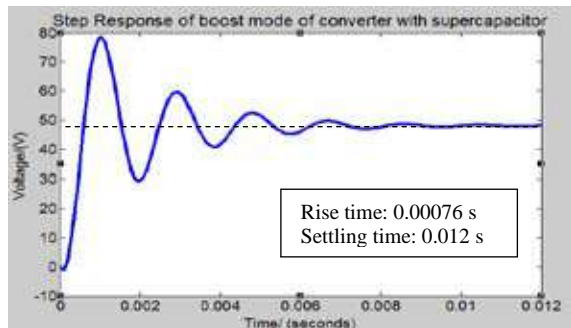


Figure 10 - Open loop step response of Supercapacitor connected bi-directional dc-dc converter in the Boost mode.

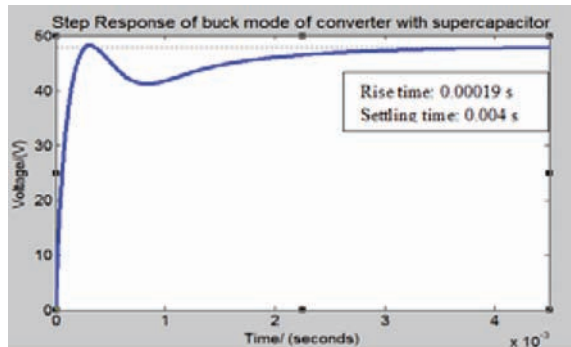


Figure 11 - Closed loop step response of the supercapacitor connected bi-directional dc-dc converter in Buck mode.



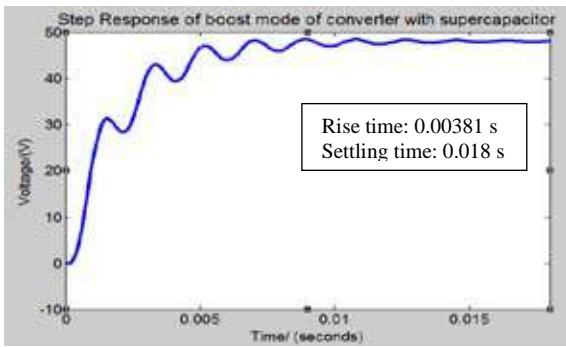


Figure 12 - Closed loop step response of the supercapacitor connected bi-directional dc-dc converter in Boost mode.

4.2 Results of Battery connected bi-directional dc-dc converter

The same procedure as in the previous section is followed for the battery connected bi-directional dc-dc converter.

A unit step was applied with unity duty ratio to achieve rated maximum current at the battery side of the converter. The converter is in Buck mode and open loop control and the corresponding response is shown in Figure 13.

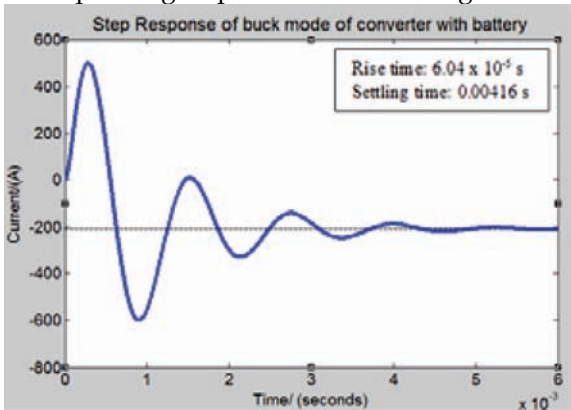


Figure 13 - Open loop Step response of the battery connected bi-directional dc-dc converter in the Buck mode.

The corresponding Boost mode operation is shown in Figure 14.

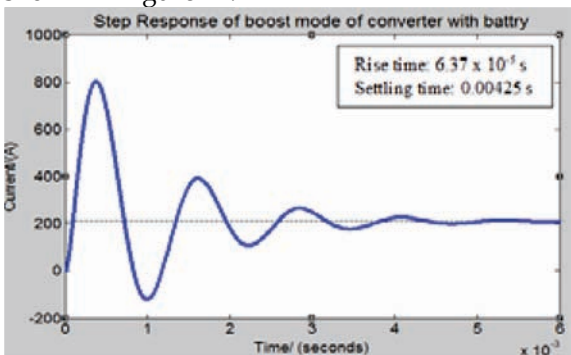


Figure 14 - Open loop Step response of the battery connected bi-directional dc-dc converter in the Boost mode.

Next a PI controller is added to the buck mode converter and the rated current step of -208.35 A was applied as the reference input. The corresponding output is shown in Figure 15.

Finally, the process is repeated in the Boost mode and the corresponding output is shown in Figure 16.

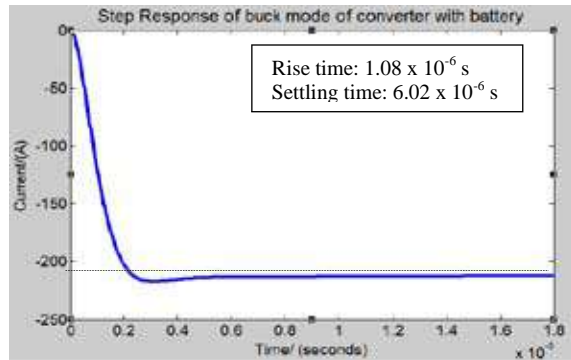


Figure 15 - Close loop step response of the battery connected bi-directional dc-dc converter in the buck mode.

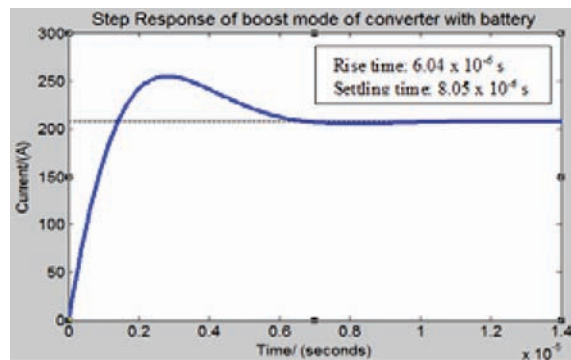


Figure 16 - Close loop step response of the battery connected bi-directional dc-dc converter in the buck mode.

4.3 Hybrid Controller Simulation Results

This result implies the hybrid current controller of the system works to its bi-directional maximum current demand. Step of -208.35 to 208.35 was applied to the hybrid current controller of the system as input and both buck and boost converters shares the current demand as shown in Figure 17.

Figure 18 shows the drive cycle simulation results for the first 70 s of the Cranfield drive cycle. Beyond 60 s, during de-acceleration, the Battery connected converter comes in to buck mode to store the energy in the battery.

Switching between buck and boost of the battery converter for the ARTEMIS drive cycle is shown in Figure 19.

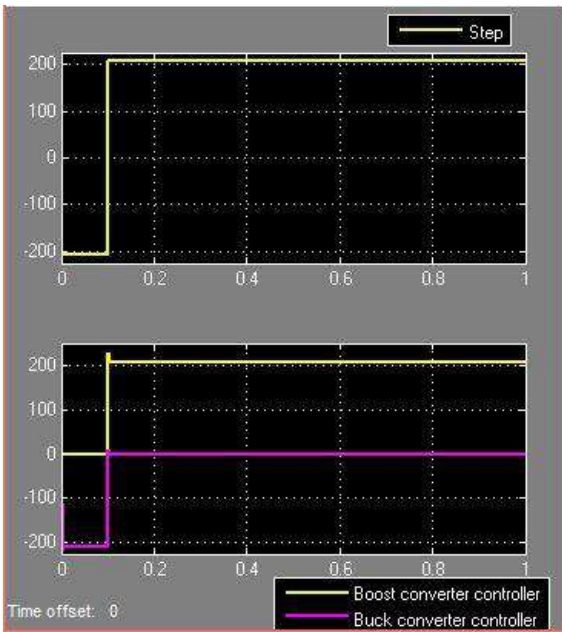


Figure 17 - Step Response of Battery Hybrid Controller

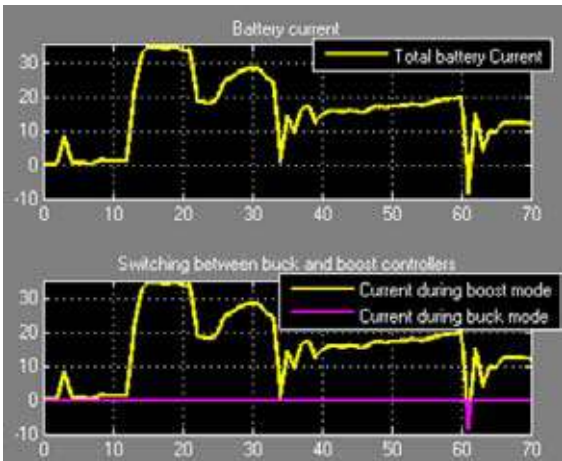


Figure 18 - Current Demand during the Cranfield drive cycle

4.4 Total system simulation results for ARTEMIS urban drive cycle

Figure 20 shows the total demand current, and its split between the battery and supercapacitor by using the Kalman filter proposed in this paper.

Figure 21 shows the improvement of Battery State of Health (SOH) in the Battery Supercapacitor Hybrid Energy Storage System as compared to the situation with Battery alone case without SC. The SOH reduction in the Battery is approximately 33% in the former case compared to the latter case for the 900 s drive cycle considered. Hence the HESS contributes to significantly lower the SOH reduction, which on the other hand means a significant improvement in the Battery useful life.

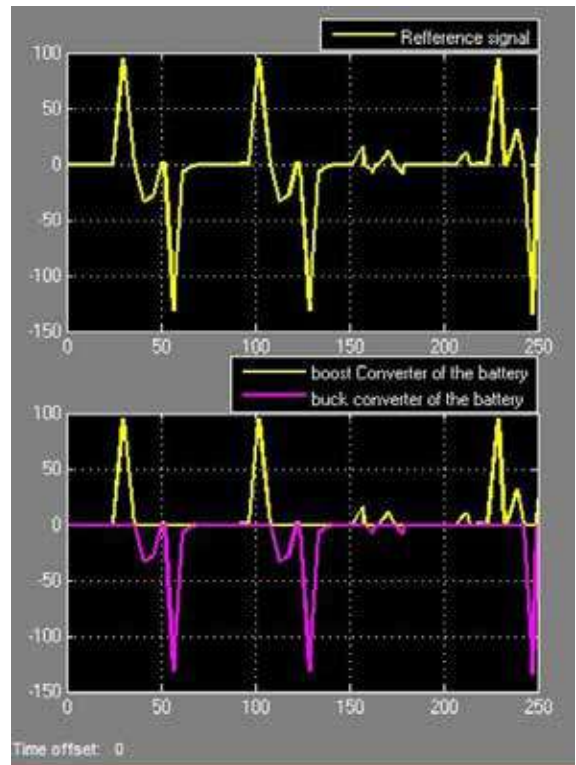


Figure 19 - Current demand being served by the battery connected dc-dc converter.

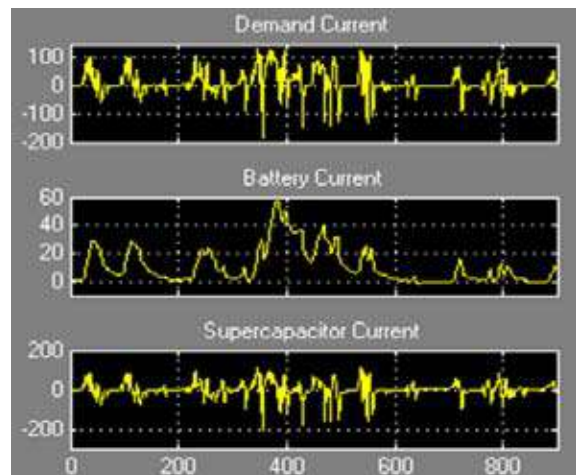


Figure 20 - Current sharing between battery and supercapacitor

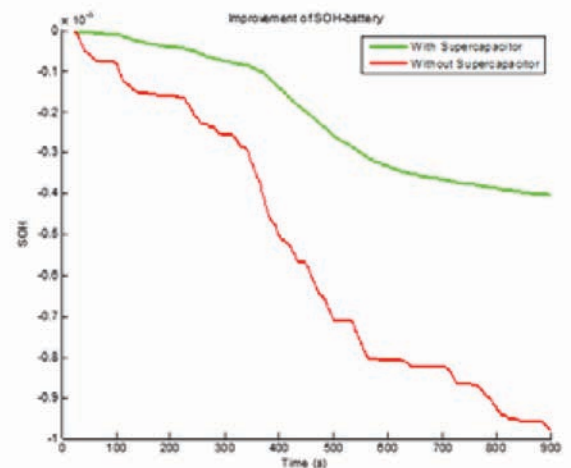


Figure 21 - Improvement of Battery SOH



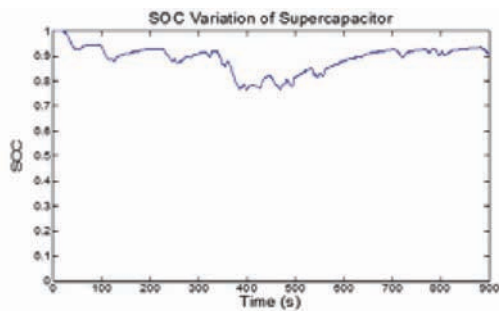


Figure 22 - Variation of SOC of the supercapacitor

5. Conclusions

Proposed control strategy is based on the linearized model of the HESS. The Kalman filter is used to filter out the rapid changes and obtain the reference for battery connected dc-dc converter. The remaining power is supplied by the Supercapacitor.

Based on the SOC of Supercapacitor, the optimum power sharing between Supercapacitor and Battery is assured. It will also ensure that high frequency current components will not flow through the battery so that the SOH reduction of battery is minimized. Voltage of the bus bar is in a fixed value since Supercapacitor ensure the voltage regulation of the bus bar so that the inverter input voltage is a constant.

Acknowledgement

Authors would like to acknowledge the University of Peradeniya Research Grant URG/2016/32/E for supporting this research.

References

1. Ziyou Song, Heath Hofmann, Jianqiu Li, Jun Hou, Xuebing Han, Minggao Ouyang, Energy management strategies comparison for electric vehicles with hybrid energy storage system, www.elsevier.com/locate/apenergy.
2. Jesús Armenta*, Ciro Núñez, Nancy Visairo, Isabel Lázaro, An advanced energy management system for controlling the ultracapacitor discharge and improving the electric vehicle range
3. Mid-Eum Choi, Seong-Woo Kim, and Seung-Woo Seo, Energy Management Optimization in a Battery/Supercapacitor Hybrid Energy Storage System, *IEEE Trans. On Smartgrid*, vol.3, no.1, pp 463 - 472, Mar. 2012

4. Omar Laldin, Mazhar Moshirvaziri, and Olivier Trescases, Predictive Algorithm for Optimizing Power Flow in Hybrid Ultracapacitor/Battery Storage Systems for Light Electric Vehicles, *IEEE Trans. On Power Electronics*, vol. 28, no. 8, pp 3882 - 3895, Aug. 2013
5. Sathish Kumar Kollimalla, Mahesh Kumar Mishra, and N. Lakshmi Narasamma, Design and Analysis of Novel Control Strategy for Battery and Supercapacitor Storage System, *IEEE Trans. On Sustainable Energy*, vol. 5, no. 4, pp 1137 - 1144, Oct. 2014
6. Branislav Hredzak, Vassilios G. Agelidis, and Minsoo Jang, A Model Predictive Control System for a Hybrid Battery-Ultracapacitor Power Source, *IEEE Trans. On Power Electronics*, vol. 29, no. 3, pp 1469 - 1479, Mar. 2014
7. Daniel J. Auger, Maxime F. Groff, Ganesh Mohan, Stefano Longo, Francis Assadian, Impact of battery ageing on an electric vehicle powertrain optimization, *Journal of sustainable development of energy, water and environment*, vol. 2, issue 4, pp 350-361, 2014
8. Ramsey Faragher, Understanding the Basis of the Kalman Filter Via a Simple and Intuitive Derivation, *IEEE Signal Processing Magazine*, pp 128 - 132, Sep. 2012

Pitch Control of a Twin Rotor System using Error Dynamics Based Nonlinear Controller

Yasitha Liyanage, Jagannath Wijekoon, Shirantha Welikala and
Lilantha Samaranayake

Abstract: In this paper we address the pitch axis control of the standard twin rotor multi-input-multi-output (MIMO) control system problem. Dynamic model of the pitch control system is derived using basic laws of physics, which results in a nonlinear plant model.

Some of the plant nonlinearities are able to linearize, while some, such as squared input, are not. In the conventional approach, this problem has been solved by linearizing the possible nonlinearities, while neglecting the others, at the cost of reduced performance. Most importantly, the latter partially linearized approach demands linearized plant model at every operating point, which makes the controller implementation complicated when considering a wide dynamic operating range.

In order to overcome limitations of the partially linearized approach, we derive a nonlinear controller. In that we use the tracking error dynamics to arrive at a compromise between the tracking performance of the pitch axis control and the smoothness of the actuator input.

The plant and the nonlinear controller have first been simulated in the MATLAB/Simulink™ environment and secondly, it has been implemented in hardware to control the pitch of an actual Twin Rotor MIMO system.

The performance is assessed using Integrated Absolute Error (IAE) and Accumulated Squared Input (ASI) representing the energy input. The performance of the controller is compared with a PID controller tuned to the partially linearized plant model and the results show approximately 50% improvement both in terms of IAE and ASI.

Keywords: Error dynamics, linearized plant model, nonlinear control, pitch control.

1. Introduction

Recent times the development of several approaches for controlling the flight of air vehicle such as helicopter and unmanned air vehicle (UAV) has been studied frequently. The modeling of the air vehicle dynamics is a highly challenging task due to the complicated nonlinear interactions among the various variables and also there are certain states which are not accessible for the measurement.

The twin rotor multi input multi output system (TRMS) is an experimental set-up that resembles with the helicopter model. The TRMS consist of two rotors at each ends of the horizontal beam known as main rotor and tail rotor which is driven by a DC motor and it is counter balanced by a pivoted beam. The TRMS can rotate in both horizontal and vertical direction. The main rotor generates a lift force due to this the TRMS moves in upward direction around the pitch axis. While, due to the tail rotor TRMS moves around the yaw axis. However TRMS resembles with the helicopter but there is some significant differences between helicopter and TRMS. In helicopter, by changing the angle of attack controlling has been done, while in TRMS it has been done by changing the speed of rotors.

Several models have been proposed for the twin rotor MIMO system. The conventional approach is to linearize the nonlinearities while neglecting some which in turn reduces the performance of the system. Furthermore, the plant model of the system has to be linearized at every operating point in the partially linearized model. Thus it complicates the implementation of the controller in a wide operating range.

This paper proposes a nonlinear controller to the pitch control based on state feedback linearization technique in order to overcome the limitation caused by partially linearized model.

Mr. Yasitha Liyanage, Student Member IEEE, Student Member of IESL, B.Sc.Eng. (Hons) Peradeniya, Temporary Instructor, Department of Electrical and Electronic Engineering, Faculty of Engineering, University of Peradeniya.

Eng. Jagannath Wijekoon, B.Sc.Eng.(Hons) Peradeniya, Temporary Instructor, Department of Electrical and Electronic Engineering, Faculty of Engineering, University of Peradeniya.

Eng. Shirantha Welikala, Student Member IEEE, AMIE (SL), B.Sc.Eng. (Hons) Peradeniya, Research Assistant, Department of Electrical and Electronic Engineering, Faculty of Engineering, University of Peradeniya.

Eng. (Dr.) B. G. L. T. Samaranayake, Senior Member IEEE, AMIE(SL), B.Sc.Eng.(Hons.) Peradeniya, Tech. Lic & Ph.D. KTH Sweden, Senior Lecturer, Department of Electrical and Electronic Engineering, Faculty of Engineering, University of Peradeniya.



The plant is first simulated in MATLAB/Simulink™ environment and secondly, it was implemented in hardware to control the actual system. The performance is assessed using Integrated Absolute Error (IAE) and Accumulated Squared Input (ASI) representing the energy input.

This paper is presented as follows. Methodology section describes the plant model, nonlinear control derivation, and performance evaluation scheme. It is followed by the implementation of the simulation model and experimental setup. The result and discussion section compare the results of simulation results and experimental results. Conclusions are presented in the final section.

2. Methodology

2.1 Plant Model

The Twin Rotor MIMO system has two degrees of freedom namely, the vertical axis and horizontal axis. The mechanical unit is presented in Figure 1.



Figure 1 - Twin Rotor MIMO System Model.

Using basis laws of physics, the model of the Twin Rotor MIMO system can be derived as follows. By applying the Newton's second law of motion to the vertical movement, it can be obtained that

$$I_1 \cdot \ddot{\Psi} = M_1 - M_{FG} - M_{B\Psi} - M_G \quad \dots(1)$$

Where, $\ddot{\Psi}$ is the angular acceleration in the vertical plane. M_1 is the nonlinearity caused by the rotor and it is estimated as a second order polynomial. A torque τ_1 is induced due to this.

$$M_1 = a_1 \cdot \tau_1^2 + b_1 \cdot \tau_1 \quad \dots(2)$$

The weight of the system produce a gravitational torque around the pivot point (M_{FG}) which is given by,

$$M_{FG} = M_g \cdot \sin \Psi \quad \dots(3)$$

Friction forces momentum ($M_{B\Psi}$) can be estimated using the following equation,

$$M_{B\Psi} = B_{1\Psi} \cdot \dot{\Psi} + B_{2\Psi} \cdot \text{sign}(\dot{\Psi}) \quad \dots(4)$$

The gyroscopic momentum (M_G) can be described by the following equation,

$$M_G = K_{gy} \cdot M_1 \cdot \dot{\phi} \cdot \cos \Psi \quad \dots(5)$$

The motor and the electrical control circuit is approximated by a first order transfer function thus in Laplace domain the motor momentum is described by,

$$\tau_1 = \frac{k_1}{T_{11}s + T_{10}} \cdot u_1 \quad \dots(6)$$

Where u_1 is the input signal.

Similar relationships can be derived to the horizontal plane motion. The net torque produced in horizontal plane motion is described by the following equation,

$$I_2 \cdot \ddot{\phi} = M_2 - M_{B\phi} - M_R \quad \dots(7)$$

Where, $\ddot{\phi}$ is the angular acceleration in the horizontal plane and M_R is the cross reaction momentum.

The nonlinear static characteristic of the main rotor (M_2) given by,

$$M_2 = a_2 \cdot \tau_2^2 + b_2 \cdot \tau_2 \quad \dots(8)$$

Frictional forces momentum is calculated as the same way as the main rotor

$$M_{B\phi} = B_{1\phi} \cdot \dot{\phi} + B_{2\phi} \cdot \text{sign}(\dot{\phi}) \quad \dots(9)$$

The cross reaction momentum M_R is described by,

$$M_R = \frac{k_c(T_0s + 1)}{(T_p s + 1)} \cdot \tau_1 \quad \dots(10)$$

The dc motor with the electrical circuit is given by,

$$\tau_2 = \frac{k_2}{T_{21}s + T_{20}} \cdot u_2 \quad \dots(11)$$

Table 1 - TRMS Model Parameters [6]

Parameter	Value
I_1 - moment of inertia of vertical rotor	$6.8 \times 10^{-2} \text{ kgm}^2$
I_2 - moment of inertia of horizontal rotor	$2 \times 10^{-2} \text{ kgm}^2$
a_1 - static characteristic parameter	0.00135
b_1 - static characteristic parameter	0.0924
a_2 - static characteristic	0.02

parameter	
b_2 - static characteristic parameter	0.09
M_g - gravity momentum	0.32 Nm
$B_{1\psi}$ - friction momentum function parameter	6×10^{-3} Nms/rad
$B_{2\psi}$ - friction momentum function parameter	1×10^{-3} Nms ² /rad
$B_{1\phi}$ - friction momentum function parameter	1×10^{-1} Nms/rad
$B_{2\phi}$ - friction momentum function parameter	1×10^{-2} Nms ² /rad
K_{gy} - gyroscopic momentum parameter	0.05 s/rad
k_1 - motor 1 gain	1.1
k_2 - motor 2 gain	0.8
T_{11} - motor 1 denominator parameter	1.1
T_{10} - motor 1 denominator parameter	1
T_{21} - motor 2 denominator parameter	1
T_{20} - motor 2 denominator parameter	1
T_p - cross reaction momentum parameter	2
T_0 - cross reaction momentum parameter	3.5
k_c - cross reaction momentum gain	-0.2

2.2 Nonlinear Controller Derivation

According to the plant model the horizontal plane motion is given in the equation 1 and the control input to the vertical plane motion is M_1 which is given in the equation 2.

Consider the error dynamics of the system where

$$e_1 = \Psi - \Psi_{ref} \quad \dots(12)$$

Here Ψ_{ref} is the desired yaw angle of the system.

$$e_2 = \dot{e}_1 \quad \dots(13)$$

Then,

$$\dot{e}_2 = \ddot{\Psi} - \ddot{\Psi}_{ref} \quad \dots(14)$$

The $\ddot{\phi}$ can be derived from equation 7. Hence \dot{e}_2 can be written as,

$$\dot{e}_2 = \frac{M_1 - M_{FG} - M_{B\psi} - M_G}{I_1 - \ddot{\Psi}_{ref}} \quad \dots(15)$$

Therefore the control law can be written as,

$$M_1 = \frac{M_{FG} + M_{B\psi} + I_1(\ddot{\Psi}_{ref} - c_1 \cdot e_1 - c_2 \cdot e_2)}{1 - K_{gy} \cdot \dot{\phi} \cdot \cos \Psi} \quad \dots(16)$$

Such that error dynamics become linear and in the form of controllable canonical form. Here c_1 and c_2 are constants which can be adjusted to have desired pole locations for second order linear error dynamics.

$$\dot{e}_1 = e_2 \quad \dots(17)$$

$$\dot{e}_2 = -c_1 \cdot e_1 - c_2 \cdot e_2 \quad \dots(18)$$

Error dynamics can be written as,

$$\begin{bmatrix} \dot{e}_1 \\ \dot{e}_2 \end{bmatrix} = \begin{bmatrix} 0 & 1 \\ -c_1 & -c_2 \end{bmatrix} \cdot \begin{bmatrix} e_1 \\ e_2 \end{bmatrix} \quad \dots(19)$$

The characteristic equation of error dynamics can be written as,

$$s^2 + c_1 \cdot s + c_2 = 0 \quad \dots(20)$$

By placing the poles on desired locations we can find out the values for c_1 and c_2 .

2.3 Performance Evaluation Scheme

Derived nonlinear controller is compared against conventional PID controller designed using classical techniques. In order to compare the performance of the nonlinear controller two methods are used. They are Integrated Absolute Error (IAE) as defined in equation 21 representing the tracking performance and Accumulated Squared Input (ASI) defined in equation 22 representing the energy input to the plant. The performance of both the partially linearized PID controller and the nonlinear controller are evaluated and compared using the latter indexes.

$$IAE = \int_0^t |\text{error}| dt \quad \dots(21)$$

$$ASI = \int_0^t |\text{controlled input}| dt \quad \dots(22)$$

3. Implementation

3.1 Software Model

Prior to implementing in hardware, the complete system consisting of the Twin Rotor MIMO system and the controller are implemented in MATLAB/Simulink™ environment. The performance of the new controller is tested for tracking and energy consumption. The simulation of the PID setup is presented in Figure 02 and the simulation setup of the nonlinear controller is presented in Figure 3.



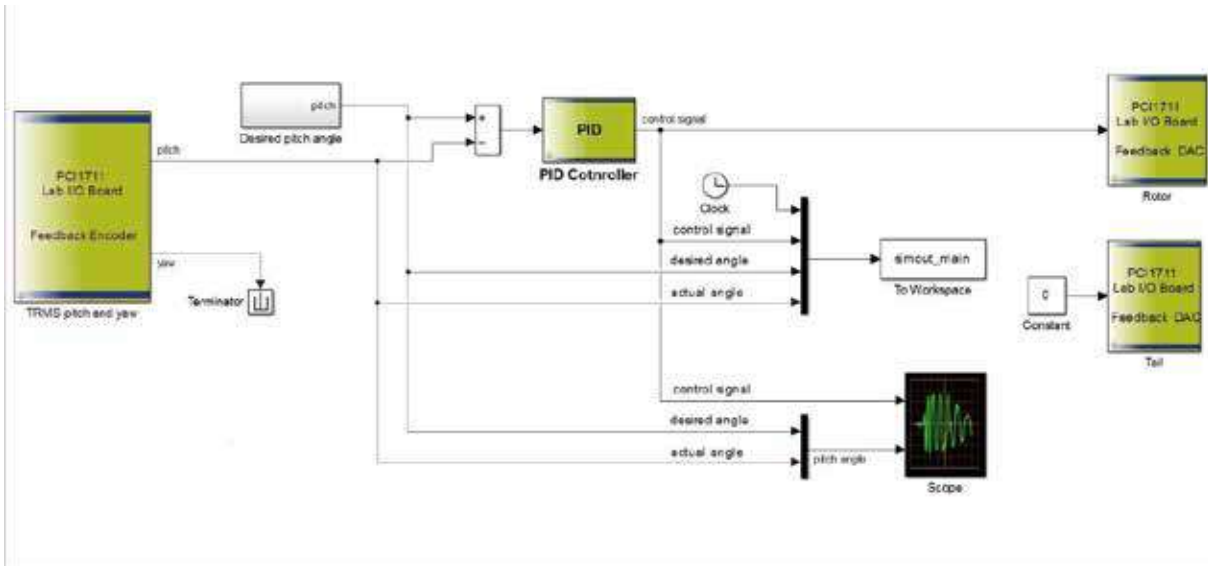


Figure 2 - Simulation Model of the PID Controller

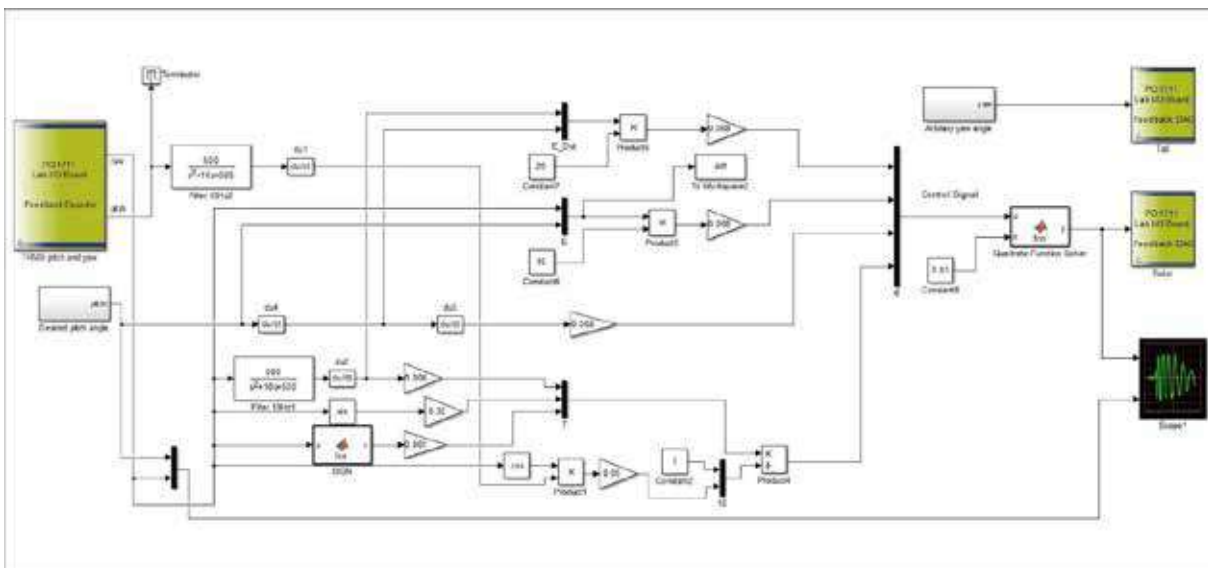


Figure 3 - Simulation Model of the Nonlinear Controller

3.2 Experimental Setup

Both the PID controller and the nonlinear controller ran on the experimental setup and the performance of the both systems were compared.

4. Results and Discussion

4.1 Simulation Results

Table 2 compares the simulation results of the PID controller and the nonlinear controller.

Table 2 - Comparison of the results of PID Controller and the Nonlinear Controller

Index	PID Controller	Nonlinear Controller
IAE	323.2708	46.0165
ASE	10507	3910.9

Figure 4 represents variation between actual pitch angle and the desired pitch angle with the PID controller. ($K_p=5$ $K_i=8$ $K_d=10$)

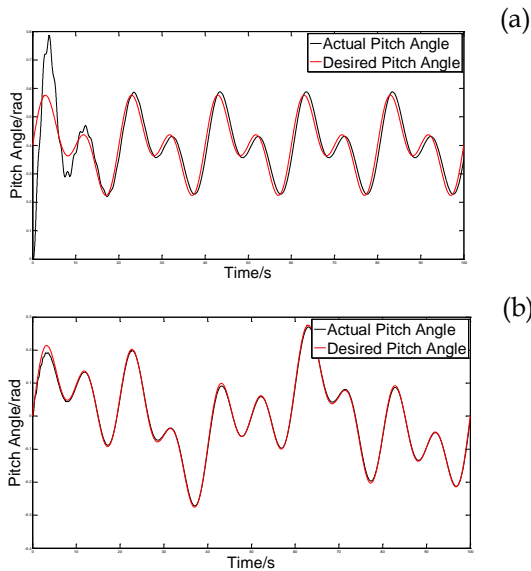


Figure 4 - Simulation Results of the PID Controller (a) and Simulation Results of the Nonlinear Controller (b)

4.2 Experimental Results

Table 3 compares the experimental results of the PID controller and the nonlinear controller. The experimental results of the PID controller is presented in Figure 5. ($K_p=5$ $K_i=8$ $K_d=10$)

Table 3 - Comparison of Experimental Results of PID Controller and Nonlinear Controller

Index	PID Controller	Nonlinear Controller
IAE	28.3148	21.2901
ASE	1300.8	1054.5

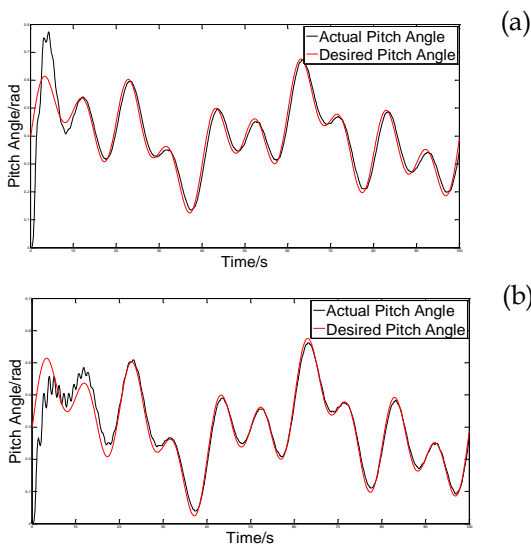


Figure 5 - Experimental Results of the PID Controller (a) and Experimental Results of the Nonlinear Controller (b)

5. Conclusions

The conventional PID controller is implemented on a linear system where the nonlinearities are neglected through assumptions. In the nonlinear controller design all the nonlinearities of the system were taken into consideration and they were cancelled off in controller design process. Therefore compared to the PID controller the system's performance was increased and the energy input of the system was reduced.

References

1. Pandey, S. K., and Laxmi, V., "Optimal Control of Twin Rotor MIMO System Using LQR Technique," in *Computational Intelligence in Data Mining - Volume 1*, vol. 31, L. C. Jain, H. S. Behera, J. K. Mandal, and D. P. Mohapatra, Eds. New Delhi: Springer India, 2015, pp. 11-21.
2. Pandey, S. K., and Laxmi, V., "Control of Twin Rotor MIMO System using PID Controller with Derivative Filter Coefficient," in *Electrical, Electronics and Computer Science (SCEECS), 2014 IEEE Students' Conference on*, 2014, pp. 1-6.
3. Prasad, G. D., Manoharan, P. S., and Ramalakshmi, A. P. S., "PID Control Scheme for Twin Rotor MIMO System using a Real Valued Genetic Algorithm with a Predetermined Search Range," in *Power, Energy and Control (ICPEC), 2013 International Conference on*, 2013, pp. 443-448.
4. Ramalakshmi, A. P. S., and P. S. Manoharan, "Non-Linear Modeling and PID Control of Twin Rotor MIMO System," in *Advanced Communication Control and Computing Technologies (ICACCCT), 2012 IEEE International Conference on*, 2012, pp. 366-369.
5. Wen, P. and Li, Y., "Twin Rotor System Modeling, De-Coupling and Optimal Control," in *Mechatronics and Automation (ICMA), 2011 International Conference on*, 2011, pp. 1839-1842.
6. "TRMS 33-949S User Manual." Feedback Instruments.



Museum Navigation System with Beacons

N.D.C.D. Kannangara and W.D.S.S. Bandara

Abstract: Bluetooth Low Energy (BLE) is a new specification of Bluetooth available for all new smart-devices. It is a new low power consumption technology aimed to transmit a small amount of data. In addition, to be able to transmit data, BLE can be used to locate objects. iBeacon® protocol, which uses BLEframe to navigate and find the artefacts. This is a new technology, and as yet it is unclear how it will be used. In conventional museums, information or explanation of the exhibited artefacts is presented by using panels or leaflets. Some museums are complicated places to navigate within. They may not have a clear path through the museum and may offer many alternatives. The problem is complicated even further given the fact that a visitor usually has limited time for a visit and may miss some important place. However, such paper maps are inconvenient and not easy to use, especially when a group of visitors is visiting the museum together. The objective of this project was to implement an Android app “Museum Navigation System” based on Bluetooth Low Energy beacons. Here an Android app illustrates approximate location and information on the smart device by using Received Signal Strength Indicator (RSSI) power and BLE frame (Universally Unique Identifier (UUID), major and minor). In the developed system three beacons were clustered to find the position. The system starts with a scan for beacons and then saving the RSSI power values in an array. Then sort the RSSI power in the descending order. RSSI-based triangulation method is used to find the position in the cluster. When the user moves to the next cluster region, it identifies route by the scanning. Then the user coordinates of the position and direction on the map are displayed by the Museum Navigation System app.

Keywords: Bluetooth Low Energy, BLE proximity location, Beacons, RSSI power, UUID, Triangulation.

1. Introduction

In conventional museums, information or explanation of exhibited materials is presented by using panels or leaflets. Some museums are complicated places to navigate within. They may not have a clear path through the museum and may offer many alternatives. The problem is complicated even further given the fact that a visitor usually has limited time for a visit and missed some important place. The classic navigation aid is the paper map of the museum, which is based on the museum floor plan and enables the visitor to orient themselves and find the way in the museum. However, such paper maps may be inconvenient and not easy to use, especially when a group of visitors is visiting the museum together. Current mobile technology opens new possibilities for supporting indoor navigation.

Beacons are small wireless sensors that communicate with Bluetooth-enabled smart devices such as smartphones or tabs by continuously advertising their location using a Bluetooth low energy radio transmitter. In turn, smart devices monitor the received signal strength indication (RSSI) and determine the device's proximity to the beacon.

This is a new technology, and as yet it is unclear how it will be used. Therefore the aim of the project is to develop a museum navigation system with beacon's delivering context-based information in museums.

2. Literature Review

Beacon is a small computer. Its 32-bit ARM® Cortex CPU is accompanied by the accelerometer, temperature sensor, and what is most important—2.4 GHz radio using Bluetooth 4.0 Smart, also known as BLE or Bluetooth low energy. Beacon other application is retail, stadium and airport navigation systems. But those applications are in trail condition.

Biggest Beacon manufacturers are BlueCats, BlueSenser, Estimote, Gelo, Kontakt and Sensorberg.

Eng. N.D.C.D. Kannangara, B.Tech.(Hons) in Eng. (OUSL), Dip in Software Eng.

Eng. W.D.S.S. Bandara, B.Sc.(Eng.) Hons.(Peradeniya), M.Eng (AIT) Lecturer, Department of Electrical & Computer Engineering, The Open University of Sri Lanka.



Beacons are low energy Bluetooth device. Therefore, it uses Bluetooth protocol stack to connect network and communicate like any network, Bluetooth has protocol layers that define the network and allow it to function.

2.1 Similar museum navigation systems

Augmented Reality Technologies introduced a system with a head-mounted display (HMD) which is introduced by Noboru Koshizuka. The issues and disadvantages of this system are high cost, difficult to use for everyone, limited no of HMD to use and need a person for an explanation.

PDMA(Personalized Digital Museum Assistant) is a tool and implementation of relatively high-speed wireless LANs which is introduced by Ken Sakamura. Issues and disadvantages are high cost and limited no of PDMA's.

3. Methodology

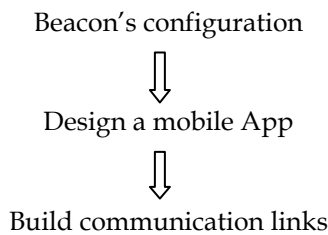


Figure 1 - Project steps

3.1 Beacon's configuration

The paired Bluetooth Beacons transmit with exact intervals (e.g. at about 100ms or 1 s). Beacons transmit their ID, which is contained in three parts, they are UUID (organization), Major (a specific group of items) and Minor (specific item). For example, whole museum area and location identify by UUID, a large group of items identify by major (King's jewellery), and the specific beacon identifies by a minor(crown).

3.2 Designing the Mobile Application

Bluetooth Low Energy technology is known as Bluetooth Smart technology. It support from Android 4.3 Jelly Bean version. Android smartphone requirements are greater than Android version 4.3 and Bluetooth Smart radio unit (v4.0)

3.3 Build communication links

Beacon frames are broadcasted by the Access Point. it is in Basic service set of infrastructures. The Android platform consists Bluetooth network stack, which allows a device to connect wirelessly and exchange. The Android Bluetooth APIs provided to access the application through Bluetooth. The beacon frame is one of the frames in IEEE 802.11.

4. Conceptual Design

Museum Navigation System is a novel system which gives the navigation information inside a museum to use with a smart device. Here the developed Android application illustrates navigation route and the artefact information on the smart device by using RSSI power, UUID, major and minor of the beacon frame.

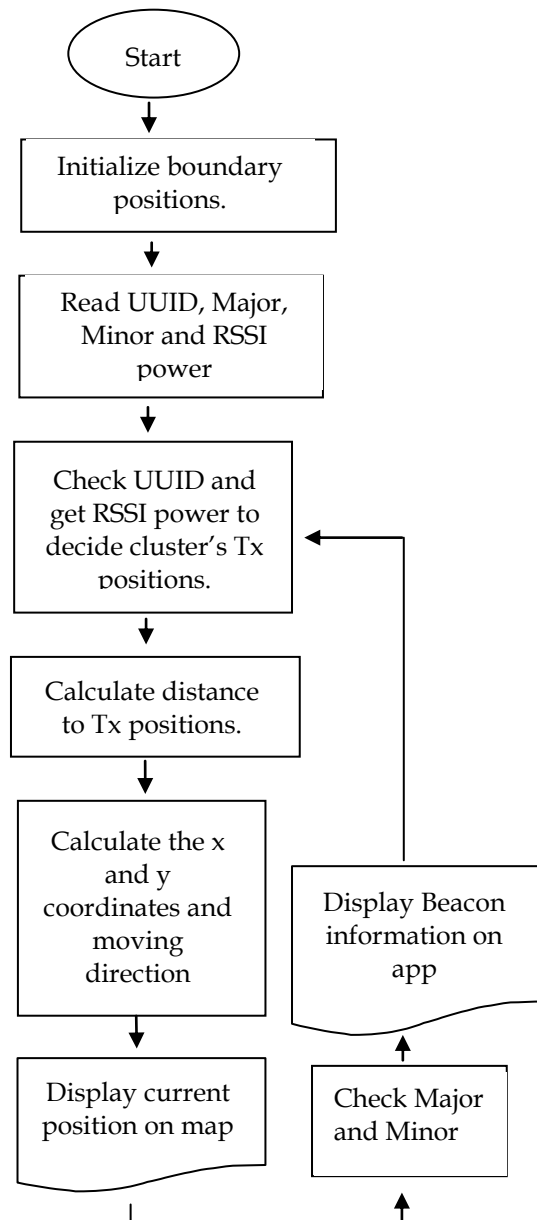


Figure 2 - Main flow chart of the app

The power of a Beacon's signal is captured by RSSI and Measured Power. Broadcasting Power is the power which it transmits its signal by beacon BLE module. Admin of the Beacon is able to change RSSI power. If the power is high, the range of the beacon is large, and it has a high ability of stable the signal, on the other hand, battery life is shorted.

Here three Beacons Cluster is used to find the position. The first scan for beacons and then RSSI power values are saved in an array. Then they are sorted ascending order of RSSI power. RSSI-based triangulation method is used to find the position in the cluster and when the user moves to next cluster region it identifies by scan route. Then it identified new beacon and previous beacon use to find anew position in the new region. Scan run within constant time and update beacons initial position with user position on the map.

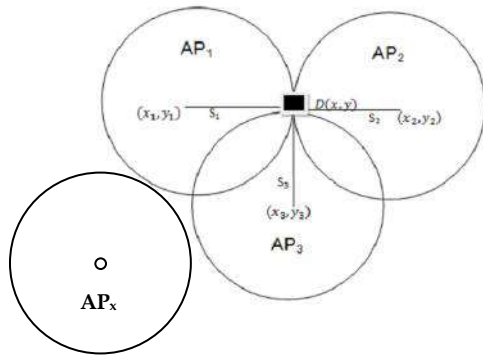


Figure 3 - Cluster plan

4.1 Bluetooth RSSI vs Distance

Anti et al. design and implementation of a Bluetooth Local Positioning Application in which the RSSI power level is converted to distance model as follows:

$$RSSI = P_{TX} + G_{TX} + G_{RX} + 20\log(4\pi cf) - 10n\log(d)$$

$$RSSI = P_{TX} + G - 40.2 - 10n\log(d)$$

Where P_{TX} is the transmit power; G_{TX} and G_{RX} are the antenna gains and G is the total antenna gain: $G = G_{TX} + G_{RX}$, c is light speed, f is the central frequency (2.44 GHz), n is the attenuation factor (2 in free space), and d is the distance between transmitter and receiver in meters. Then

$$d = 10[(P_{TX} - 40.2 - RSSI + G)/10n]$$

Due to multipath and noise, the relationship between RSSI and distance will differ from above. Further the, more environmental factors too effect for the RSSI power. In the case several

experiments were carried out to get the combination. However the, Bluetooth indicators fade with distance under these environmental influences. Let

$$A = P_{TX} + G - 40.2$$

Therefore:

$$RSSI = -10n\log(d) + A$$

where A is the received RSSI power at 1m.

4.2 Improved Algorithms for Beacon Navigation system

The algorithm is based on three Beacons which can communicate with the smart device and those Beacons measures the signal coming from the smart device.

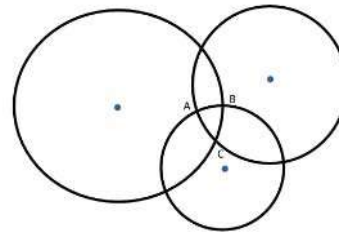


Figure 4 - Measuring the signal

Let beacons coordinates as $A(x_1, y_1)$, $B(x_2, y_2)$ and $C(x_3, y_3)$ and then

$$x^2 + y^2 - 2x_1x - 2y_1y + y_1^2 + x_1^2 = r_1^2 \dots (1)$$

$$x^2 + y^2 - 2x_2x - 2y_2y + y_2^2 + x_2^2 = r_2^2 \dots (2)$$

$$x^2 + y^2 - 2x_3x - 2y_3y + y_3^2 + x_3^2 = r_3^2 \dots (3)$$

Where r is represent as:

$$r = 10^{[A - RSSI] / 10n}$$

Solving (1) - (2) and (2) - (3), the above equations reduced to two equations as:

$$2(x_2 - x_1)x + 2(y_2 - y_1)y = r_1^2 - r_2^2 - x_1^2 + x_2^2 - y_1^2 + y_2^2 \dots (4)$$

$$2(x_3 - x_2)x + 2(y_3 - y_2)y = r_2^2 - r_3^2 - x_2^2 + x_3^2 - y_2^2 + y_3^2 \dots (5)$$

Let:

$$a = 2(x_2 - x_1), b = 2(y_2 - y_1), c = 2(x_3 - x_2), d = 2(y_3 - y_2),$$

$$e = r_1^2 - r_2^2 - x_1^2 + x_2^2 - y_1^2 + y_2^2 \& f = r_2^2 - r_3^2 - x_2^2 + x_3^2 - y_2^2 + y_3^2$$

So that;

$$ax + by = e \dots (6)$$

$$cx + dy = f \dots (7)$$

Finally, the coordinate of the device being tracked is:

$$x = \frac{de - bf}{ad - bc}, y = \frac{ce - af}{bc - ad} \dots (8) \& (9)$$

The actual motion is the very important things in order to improve model accuracy. In this case, higher order equation is used to



determine the distance that user moves in the time period. (Scan time duration is used).

$$S_x = U_x t + \frac{A_x}{2} t^2 + \frac{B_x}{6} t^3 + \frac{C_x}{24} t^4 + \dots \quad (10)$$

$$S_y = U_y t + \frac{A_y}{2} t^2 + \frac{B_y}{6} t^3 + \frac{C_y}{24} t^4 + \dots \quad (11)$$

Where,

S - distance, U - velocity, A - acceleration, B - variable acceleration and C - rate of variable acceleration. But in this application 3rd order equation is used to indicate motion. For the velocity

$$U_x = \frac{(x - x')}{t}, \quad U_y = \frac{(y - y')}{t} \dots (12) \& (13)$$

For the acceleration

$$A_x = \frac{(U_x - U'_x)}{t}, \quad A_y = \frac{(U_y - U'_y)}{t} \dots (14) \& (15)$$

For the variable acceleration

$$B_x = \frac{(A_x - A'_x)}{t}, \quad B_y = \frac{(A_y - A'_y)}{t} \dots (16) \& (17)$$

Assuming all beacons transmit the same signal power and therefore the average of velocity, acceleration and etc. can be obtained by substituting equation 8 and 9. Get the values of S which are related to x and y finally calculate position of x and y . Every dashed values are previous values and t scan time.

Error of the motion and distance $\sim Ct^4/24$

$$X_{final} = S_{previous} + S_x \quad \dots (18)$$

$$Y_{final} = S_{previous} + S_y \quad \dots (19)$$

The pointer rotates to indicate the user moving direction by using current and previous coordinates.

$$\theta = \tan^{-1} \left(\frac{y_{current} - y_{previous}}{x_{current} - x_{previous}} \right) \quad \dots (20)$$

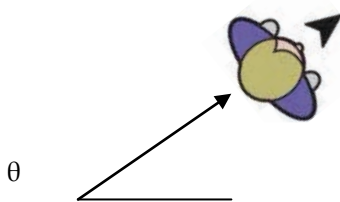


Figure 5 - Direction of pointer

4.3 Error calculation

It is used to find the error between actual point and calculated point. It is used a measure of the differences between values of predicted and actually observed. the standard deviation of the differences between predicted values and observed values represented by it.

Root Mean Square Error

$$= \frac{1}{N} \sum_{i=1}^N \sqrt{(x_{true} - x_{final,i})^2 + (y_{true} - y_{final,i})^2}$$

4.4 Android RSSI power test application

Android test application used to get *RSSI* power to find true values. Therefore considering three beacons and found true values to simulate and to get the results.

Block diagram for the RSSI testing app on Android device.

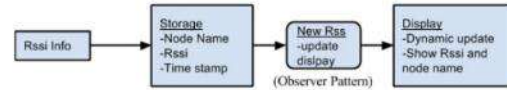


Figure 6 - RSSI test application block diagram

5. Implementation

The methodology used in this project, as well as the positioning algorithms, has been covered too. All these things are connected together and implemented into a navigation system which is consisting of a group of configured beacons and an Android application of the final product.

The system works like this: at first, few beacons are positioned as boundary and other used as artefact transmitters. The app scans beacons and received their RSSI readings. And calculate the distance between the user and each beacon. Then app calculated x and y coordinates to indicate direction of the user moving by substituting distance. After that beacons' and the user's position displayed by app, as well as the distance between them, are shown in the map.



Figure 7 - Screen prints of app

5.1 Testing environment

The app was tested inside a 30 m^2 part of department with the distance of three beacons, separated by approximately 5 m , were positioned. The map of the area as well as the position of the beacons is shown in figure.

The setting of the beacons and position environment is important to increase the testing value the accuracy of the system. Because of its capability to calculate the distance accuracy with low distance and high power transmit beacons. This situation will give an idea of how beacons should be configured regarding their output power. Which is affected the range of receive *RSSI* readings collected by the app. For example, if the area is less than 100 m^2 in this case no problem of using several beacons operating with 0 dBm transmit power with around 50 m range. This will only effect of the beacons battery life and affect the accuracy of the distance calculations as *RSSI* values will vary. It is able to increase update speed by reducing transition frame intervals.

5.2 The Android Application

At the start, the dialogue is displayed on the screen to get the permission from the user to turn on the Bluetooth adapter. On the other hand, the dialogue is professional and quickly starts the scan.

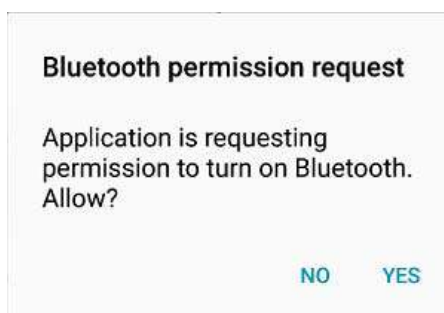


Figure 8 – Bluetooth permission request dialogue

5.3 Scanning

The app scans BLE devices and highest 3 *RSSI* power in every scan are passed through an algorithm of positioning. Then from that previous and current values calculate direction of moving and display on the map. And context base data display on the screen by using major and minor.

5.4 User's movement

Now the application estimates the distance of the user each of the beacon and indicates on the map by displaying a black arrow with a man, such as navigate pointer, user and user movement. Indicate the user navigation area.

According to the calculation, the user location, distance to the closest beacons and the round beacons how as accurately as possible on the map. However, the user position is located relative to the configured beacons is shown in figure 6.4

The thing is important to have in mind that the pointer is roughly showed the user position. The accuracy of the distance calculations differs from the pointer the actual position of the beacon. Because of multipath receive and noise level. On the other hand environment facts effect to the system. This inaccuracy may be tolerated due to the position. It is not too far from reality, and the user can get an idea of where he/she is.

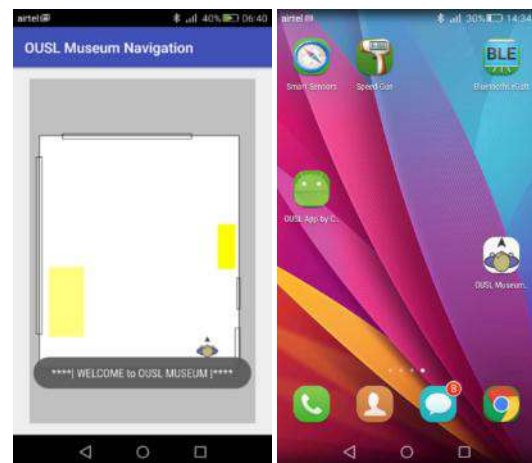


Figure 9 – Screen prints of navigation app

6. Simulation Results

Here used to get distance from measured *RSSI* power and accuracy of the improved algorithm of the Beacon navigation system for simulation purposes. To get the measured *RSSI* values a separate "OUSL App by Chanuka" Android app was used.

The *RSSI* power values were collected by changing Beacons and getting 20 values. Then decided the mean value for each considered distance.

AMATLAB Simulation was used to plot the data and to obtain the results.



Table 1 - Static result for data

Distance (m)	Coefficients (with 95% confidence bounds):		Goodness of fit:			
	P1	P2	SSE:	R-square:	Adjusted R-square:	RMSE:
0	-0.003 (-0.068, 0.06294)	-55.07 (-55.9, -54.23)	11.79	0.0005	-0.055	0.81
0.5	-0.0097 (-0.072, 0.0524)	-85.55 (-86.3, -84.8)	10.49	0.006	-0.049	0.763
1	-0.027 (-0.092, 0.037)	-90.62 (-91.4, -89.84)	11.31	0.04	-0.012	0.793
1.5	-0.015 (-0.075, 0.0436)	-95.08 (-95.1, -94.37)	9.584	0.017	-0.038	0.73
2	0.044 (-0.0114, 0.1002)	-97.22 (-97.8, -96.55)	8.441	0.13	0.086	0.685
3	0.0067 (-0.039, 0.0527)	-97.82 (-98.3, -97.27)	5.72	0.005	-0.049	0.564
4	0.012 (-0.045, 0.069)	-98.93 (-99.6, -98.23)	9.104	0.01	-0.04	0.711
5	0.01504 (-0.024, 0.05368)	-99.86 (-100, -99.39)	4.05	0.035	-0.018	0.474

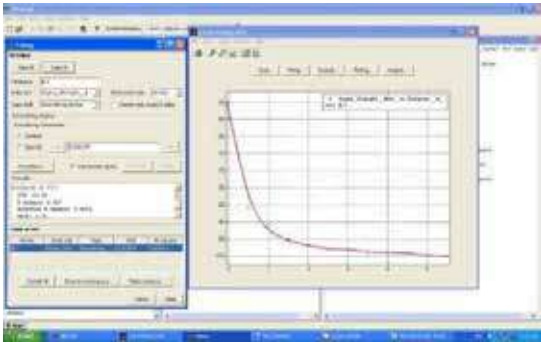


Figure 10 - Matlab simulation screenshot

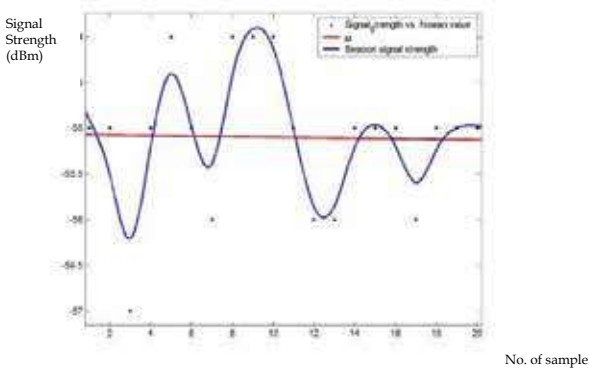


Figure 11 - RSSI power at 0 m

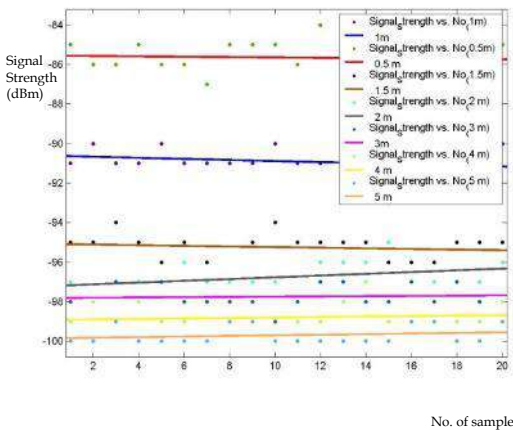


Figure 12 - RSSI power vs distance

Linear model Poly1: $F(x) = p_1x + p_2$

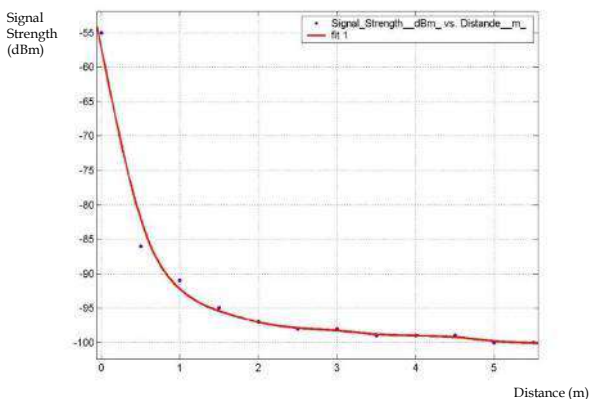


Figure 13 - Signal Strength vs Distance

6.1 Decision for getting value of RSSI power at 1m

It is very important to get "A" value for logarithm function.

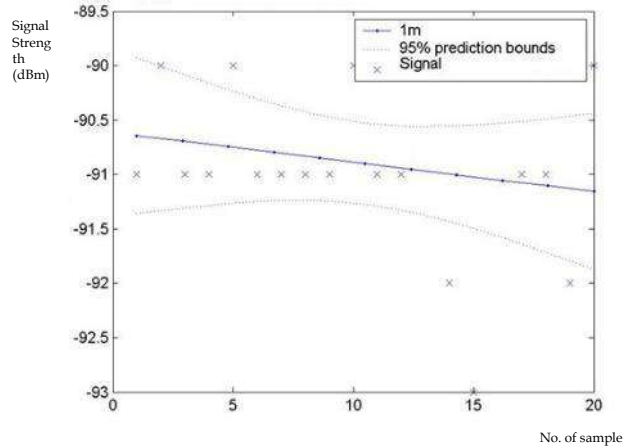


Figure 14 - Analysis of fit 1m for data set

Therefore,

$$RSSI = -10n \log(d) + A$$

$$RSSI = -10n \log(d) - 91$$

From the above data, $n = 1.5$; which is the attenuation constant and it is depend on the environment.

6.2 Simulation Results

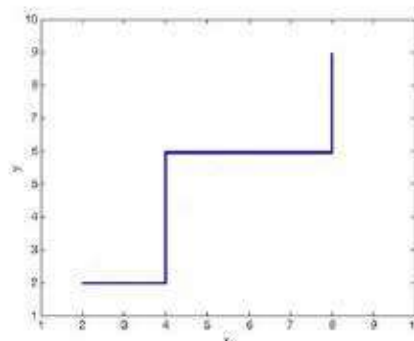


Figure 15 - Actual path of Smart device

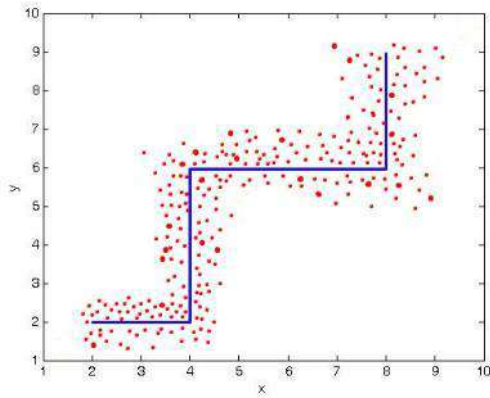


Figure 16 - Points measured by Smart device

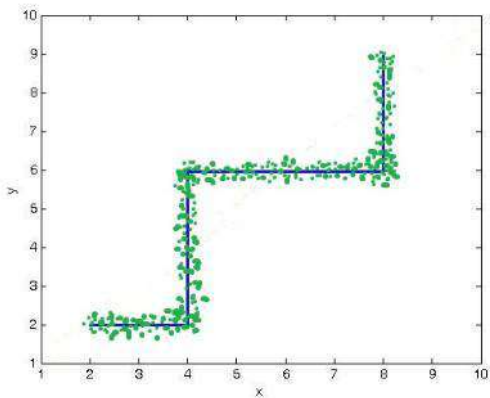


Figure 17 - Final points

6.3 Root Mean Square Errors

RMSE of reference = 12.1741

6.4 Product Test Result

The product was tested at Research Laboratory, Electrical and computer department.

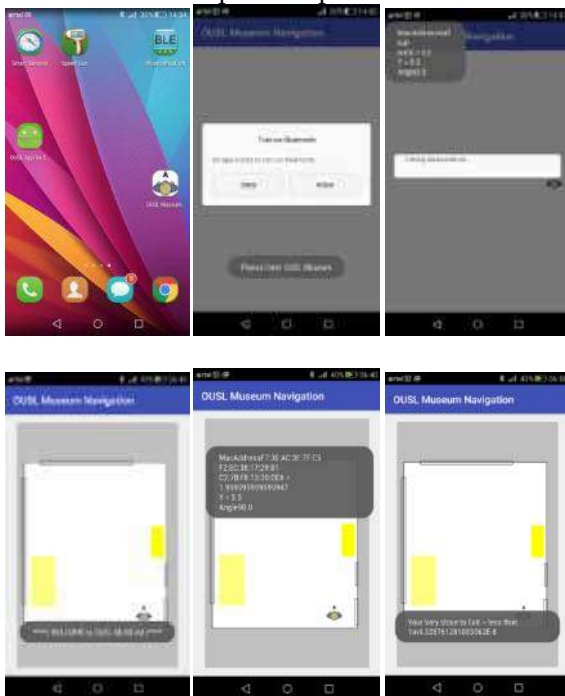


Figure 18 - Screen prints of product test

6.5 Future works

Furthermore, the developed app will improve and will eventually be published in the "playstore". Future work will focus on multipath receiving and improve the app functionality. Making the system stability for different environments will be a top priority to increase results of the distance calculations previously this system can only relate to a very specific testing environment.

7. Conclusions

iBeacon consist with apple simple ios and software protocols. In this case, BLE interface and linking problems were faced. No iBeacon support libraries were released for Android. But it was available for ios.

According to the well-established concept of outdoor navigation, indoor navigation must still face many challenges. For example is the limited technologies that can be used for it, as well as the accuracy. Furthermore, how to build indoor navigation systems available to the market is still the challenge.

The system will be more useful and will have access to these, and they will become part of the everyday life.

Acknowledgement

Authors wishes to pay their gratitude to the faculty of Engineering Technology, the Department of Electrical and Computer Engineering, the Department of Mathematics and Philosophy of Engineering, The Open University of Sri Lanka for the facilitate they received in carrying out this project work.

References

1. Heydon, Robin, 2013, Bluetooth Low Energy: The Developer's Handbook, New Jersey: Pearson.
2. Gupta, Naresh, 2013, Inside Bluetooth Low Energy, U.S.A: Artech House .
3. Townsend, K., Cufi, C., Akiba and Davidson, R., 2014, Getting Started with Bluetooth Low Energy, California: O'Reilly Media.
4. Bluetooth, 2016. Core specification v4.1. [online] Available at: <



<https://www.bluetooth.org/en-us/specification/adopted-specifications>>[Accessed 3 December 2013]. -

5. Bluetooth, 2016. Supplements to the Core Specification (CSS) v6. [online] Available at: <<https://www.bluetooth.org/en-us/specification/adopted-specifications>>[Accessed 14 July 2015]. -
6. Infoworld, 2014. What you need to know about using Bluetooth beacons. [online] Available at:<<http://www.infoworld.com/article/2608498/mobile-apps/what-you-need-to-know-about-using-bluetooth-beacons.html>>[Accessed 22 July 2014].
7. Umbel, 2016. 15 Companies From Airports to Retail Already Using Beacon Technology. [online] Available at:<<https://www.umbel.com/blog/mobile/15-companies-using-beacon-technology>>.
8. Bluetooth, 2016. Core System Architecture. [online] Available at:<<https://developer.bluetooth.org/TechnologyOverview/Pages/Core.aspx>>[Accessed 2016].

Adaptation of Scasa Technique for Surge Protective Devices for Equatorial Belt Countries

J.P.D.S. Athuraliya, N.L. Rathnayake, N.A.A.N. Dilrukshi, P. Mahadevan, R. Gihara, T.M.S. Dias, S.R.J.S. Bandara, H. Wijesooriya and Nihal Kularatna

Abstract: Modern electronic systems are very susceptible to failures due to high energy transients superimposed on the power input or the signal ports. In equatorial belt countries like Sri Lanka, lightning activity is high and it causes severe damage to equipment. To safe-guard electronics from such high energy transients, surge protection devices (SPD) rated to absorb repeated surges are required. Traditionally, SPDs use cascaded multiple non-linear devices (NLD) to clamp the transient overvoltage created by a transient. However, typical NLDs have energy absorption ratings based on short-term basis, and they have a limited life time.

Supercapacitor assisted surge absorber (SCASA) technique is a patented novel technique, where a very large capacitor's continuous energy absorption capability given by $\frac{1}{2} CV^2$ could be effectively coupled with NLDs and filters and a multi-winding magnetic component for a low component count based SPD where repeated transients can be absorbed.

In adopting this technique for absorbing severe transients with several orders of Joules dumped into a SPD, on a repeated basis, selection of the supercapacitor and the multi-winding magnetic core is a very critical design-task. Since the combination of the leakage and magnetizing inductances of the multi-winding magnetic core plays a dominant role, selection of the core is critical.

In absorbing repeated Class-B type surges, in equatorial belt locations like Sri Lanka, specific attention is required to come up with a reliable SPD design and this paper presents the design details and test results for an early-version of a prototype design of a differential-mode surge protector based on the SCASA technique. Experimental results generated using a lightning surge simulator with surge capability up to 6 kV/3 kA is used to validate the results. Performance of this technique with optimized magnetics is compared with some selected commercially available surge protectors sold in Sri Lanka. Test results clearly indicate, the developed device has a much higher energy absorption capability than tested commercial products and can be used in commercial surge protectors.

Keywords: Lightning Protection, Supercapacitors, Metal Oxide Varistors, Bidirectional Break-over Devices

1. Introduction

Lightning is a huge discharge originating in cumulonimbus clouds. As seen in figure 1, they can occur within a cloud, between clouds, down to earth or just expend their charge in air. Fortunately in the tropics, only about 10 % of the discharges terminate on the earth or earth bound objects. However, even this 10% can cause a disaster, and these disasters have occurred in a cyclical pattern in the world^[1].



Figure 1 - Propagation of lightning channel

Eng. J.P.D.S. Athuraliya, C.Eng., MIESL, MIET, MSc, BSc Eng (Hons), Director (Electronics Engineering), Electronic and Microelectronic Division, Arthur C Clarke Institute for Modern Technologies (ACCIMT), Katubedda, Sri Lanka

Eng. N.L. Rathnayake, BSc(Eng) in Electronic and Telecommunication, MEng, Senior Research Engineer, Electronic and Microelectronic Division, Arthur C Clarke Institute for Modern Technologies (ACCIMT), Katubedda, Sri Lanka

Eng. N.A.A.N. Dilrukshi, BSc(Eng) (Equivalent) Electronic Communication and Computer Eng, PG Dip (Industrial Automation), AMIESL, Research Engineer, Electronic and Microelectronic Division, Arthur C Clarke Institute for Modern Technologies (ACCIMT), Katubedda, Sri Lanka

Eng. P. Mahadevan, BSc(Eng) Electronic and Communication Eng (Hons), AMIESL, Research Engineer, Electronic and Microelectronic Division, Arthur C Clarke Institute for Modern Technologies (ACCIMT), Katubedda, Sri Lanka

Eng. R. Gihara, BSc. Electrical and electronics Eng. (Hons), AMIESL, Research Engineer, Electronic and Microelectronic Division, ACCIMT, Katubedda, Sri Lanka

Mr. T.M.S. Dias, NCT(Elect), Engineering Assistant, Electronic and Microelectronic Division, Arthur C Clarke Institute for Modern Technologies (ACCIMT), Katubedda, Sri Lanka

Mr. S.R.J.S. Bandara, IVQ Level 06, MIET, Engineering Assistant, Electronic and Microelectronic Division, Arthur C Clarke Institute for Modern Technologies (ACCIMT), Katubedda, Sri Lanka

Ms. H. Wijesooriya, BSc Physical Science, Engineering Assistant, Electronic and Microelectronic Division, Arthur C Clarke Institute for Modern Technologies (ACCIMT), Katubedda, Sri Lanka

Eng. (Prof.) N. Kularatna, BSc Eng (Hons), DSc, C.Eng, FIENZ, FIET, FIE, SMIEEE, Associate Professor in Electronic Engineering, The University of Waikato, New Zealand



Lightning causes damage to buildings, electronic and other equipment as well as causing injury and even death to people and livestock. This may be compared to typical temperate climates where the thunder days may be low, around 25 or 30 per year^[2]. Since the majority of high technology specialized military, communications, navigational and switching equipment is designed and generally manufactured in these temperate countries, scant regard is often paid to the need to protect this equipment from the devastating effects of lightning strikes whether they be direct or indirect. For this reason lightning protection against both direct and indirect lightning strikes at critical communications and navigational aid sites in tropical regions of the world should perhaps be mandatory^[2].

In most tropical countries, lightning and storm activity is high, compared to the more temperate regions of the world. For example in the equatorial belt, ten degrees north and south of the equator, thunder day statistics may vary from 150 to 200 days per year^[2].

In order to protect buildings against lightning, a structural protection system should be installed at the building^[3]. These do not protect domestic appliances which can usually be protected from lightning currents by unplugging them from service lines during thunderstorm periods. However, such an act is not realistic in most of the industrial and service sectors as even a short period of out-of-operation could cost the company a few million rupees. Therefore in such cases, lightning surges should be prevented from entering the building, or in particular sensitive equipment^[3].

This is done by installing surge protection devices (SPDs) to the power and communication lines^[3]. In the case of surge protection, both the quality of the product and the engineering of installation are equally important. It should be remembered that the provision of lightning protection both against direct strikes and indirect effects will only improve lightning immunity^[3].

It is unlikely that 100% protection can ever be achieved even by proper design at an early stage before equipment installation. It can both reduce later costs and substantially improve protection in the longer term. Most common surge protectors consist of non-linear devices in the market and they do not work well

during monsoon lightning times in equatorial belt countries like Sri Lanka and many other parts of the world due to their failure of components, such as capacitors. The use of high value capacitors (supercapacitors) could probably overcome some of these problems as they reduce the spikes.

A supercapacitor (SC) is a high-capacity electrochemical capacitor, with capacitance values much higher than other capacitors, but in lower voltage limits. It has the ability to absorb high-voltage (HV) transient surges with a short-duration occurrence^[4].

Early researchers^[5] have shown that a supercapacitor is not destroyed by the repeated application of HV transients and the gradual voltage rise across terminals after each hit is in the order of millivolt. This also indicates that the device still retains its capacitive behaviour and not adversely affected by the transient HV at the terminals. Therefore a supercapacitor can be used to absorb part of the surge energy in the SPD during a transient traveling through the incoming mains or the telecom/data circuits.

2. Methodology

2.1 Background

Researchers have shown^[5] that supercapacitors could have continuous energy storage capabilities in the range of energy carried in a transient surge into an electrical circuit. They are comparable with the transient energy absorption capabilities of non-linear devices used in typical surge protectors such as metal oxide Varistors (MOVs) and bidirectional break-over diodes (BBDs), coupled with LC-type filter stages.

However, at present commercially available supercapacitors have very low DC voltage ratings, such as less than 4 V for single-cell devices. (Ex: 2.5V 1 F, 2.7V 5F). This voltage is far below the instantaneous voltages occurring on the AC mains. Given this problem, a surge protector cannot just substitute a supercapacitor for a MOV or any other non-linear devices. Thus the necessity of testing is very important with the instantaneous voltage developed across the supercapacitor sub circuit for the entire design.

2.2 Design Approach

System design was done to achieve the expected results and there by selecting the suitable components after analyzing their characteristics.

Tests were carried out as per the IEC 61643-11^[6] with the 1.2/50 voltage - 8/20 current combination wave generator (EM TEST/UCS 500-M) which has a maximum transient voltage up to 6 kV and the maximum current up to 3 kA. Testing flow chart of the voltage protection level of the class III type SPDs is shown in figure 2.

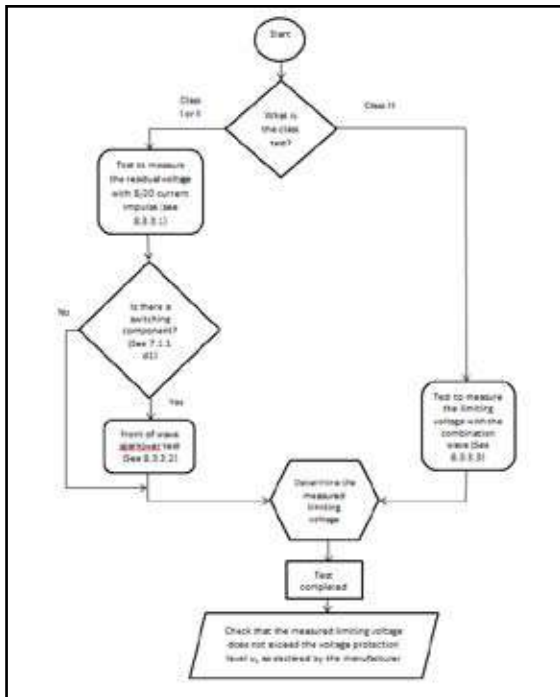


Figure 2 - Flow chart of testing the voltage protection level
Source : IEC 61643-11

2.3 Selection of components

2.3.1 MOVs

Two types of MOVs which have following characteristics were tested using the lightning surge simulator (UCS 500-M).

Table 1 - Characteristics of MOVs

Parameter	Type of MOV	
	Epcos - S20	B722 PANASONIC
Voltage Rating V AC	230 V	230 V
Voltage Rating V DC	300V	300V
Clamping Voltage Vc	595V	595V
Peak Surge Current @ 8/20µs	8kA	10kA
Operating Temperature Min	-40°C	-40°C
Operating Temperature Max	85°C	85°C
Peak Energy (10/1000uS)	130J	255J

2.3.1.1 Voltage buildup across MOVs

By applying 1 kV to 6 kV surges from the lightning surge simulator, different clamping output voltages could be observed.

Table 2 - Voltage build up across MOVs

Applied Surge Voltage (V)	Output Clamping Voltage (V) +/- 20%	
	Epcos - S20	B722 PANASONIC
1000	510	570
4000	630	710
6000	690	760

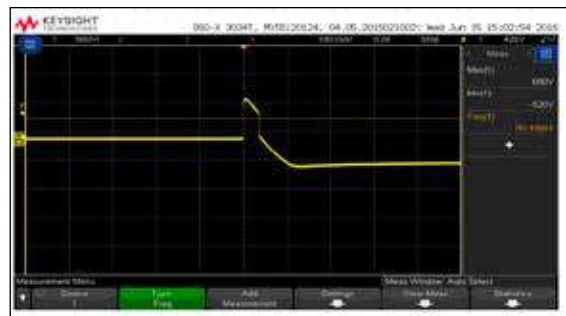


Figure 3 - Voltage build up across Epcos-S20

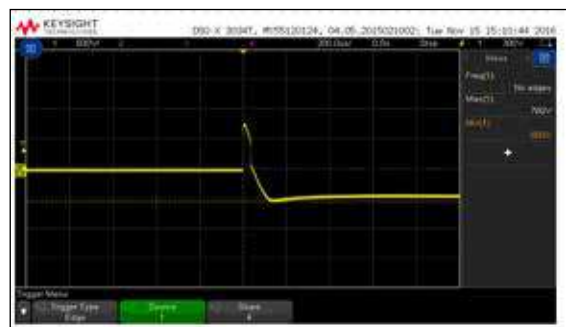


Figure 4 - Voltage build up across B722 Panasonic

Therefore, Epcos - S20 MOV which has the clamping voltage nearly 600 V, was selected for this design topology.

2.3.2 Supercapacitors

2.3.2.1 Voltage build up across super capacitors

Two types of supercapacitors were tested by applying different levels of transient voltages. Terminal voltage developed across supercapacitor after several strikes were measured using a multimeter. The test data set provides some valuable insight in estimating the capabilities of these new supercapacitors to withstand surges and transients, which in turn could lead to non-traditional applications^[5].

(a) 1F - 2.5V SC (B Series)- Initial voltage 0.20mV

Table 3 - Voltage build up across 1F-2.5 V SC

No. of strikes	mV (for 1.5 kV)	mV (for 4.5 kV)	mV (for 6.0 kV)
5	22.5	58.3	76.43
10	43.7	78.2	145.3
15	64.1	90.6	209.3
20	83.5	110.2	269.2

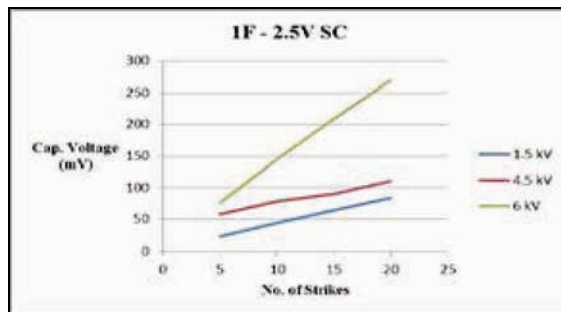


Figure 5 - Voltage build up across 1F-2.5 V SC

(b) 5F - 2.7V SC (Maxwell)- SC - Initial voltage 0.26 mV

Table 4 - Voltage build up across 5F-2.7 V SC

No. of strikes	mV (for 1.5 kV)	mV (for 4.5 kV)	mV (for 6.0 kV)
5	3.7	10	22.8
10	4.1	15	44.9
15	4.3	20	66
20	4.5	24	88

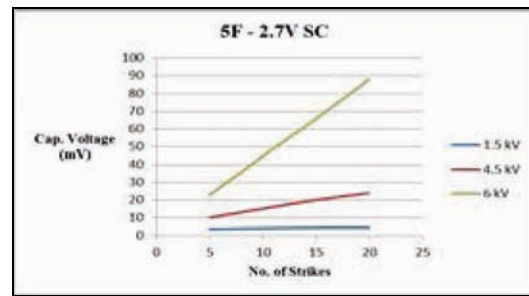


Figure 6 - Voltage build up across 5F-2.7 V SC

These results indicated that the supercapacitor is not destroyed by the repeated application of HV transients and the gradual voltage rise after each hit is in the order of millivolt. Also they still retain its capacitive behaviour and not adversely affected by the transient HV at the terminals^[5]. Therefore, 1F-2.5 V supercapacitor which has the highest voltage rise with 1 ohm resistor was selected as a supercapacitor sub circuit for this design.

2.3.3 Magnetic Core

2.3.3.1 Selection of magnetic core

In an inductor, the core provides the flux linkage path between the circuit winding and a non-magnetic gap, physically in series with the core. Virtually all of the energy is stored in the gap. These cores approach the ideal magnetic material characteristic - square loop with extremely high permeability (60,000), high saturation flux density (0.9 Tesla = 9000 Gauss) and insignificant energy storage. Unfortunately, resistivity of these metal alloys is quite low. To minimize losses due to induced eddy currents, these cores are built up with very thin tape wound laminations^[7].

Ferrites are ceramic materials made by sintering a mixture of iron oxide with oxides or carbonates of either manganese and zinc or nickel and zinc. MnZn ferrites are used in applications up to 1 or 2 MHz and include the power ferrite materials used in switching power supplies. The permeability of power ferrite materials is in the range of 1500 to 3000 (relative). As shown in the low frequency characteristic of Fig. 7, a ferrite core will store a small amount of energy, as shown by the areas between the hysteresis loop and the vertical axis. The permeability is high enough to keep the magnetizing current at a generally acceptable level in transformer applications^[7].

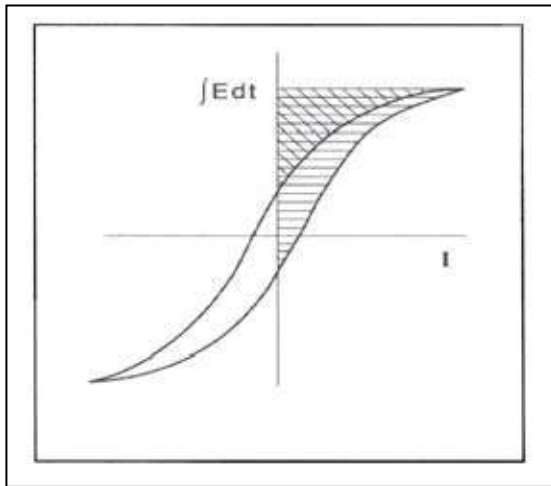


Figure 7 - Ferrite Core Characteristic

Composite powdered-metal cores, such as powdered iron, Kool M μ , and Permalloy powder cores do store considerable energy. However, energy is not stored in the very high permeability magnetic metal portions of the composite, but in the non-magnetic regions between the magnetic particles in the binder that holds the cores together^[7].

Essentially, these composite cores store their energy in a non-magnetic gap that is distributed throughout the entire core. These cores are manufactured and categorized by their effective permeability. Different effective permeability in the range of 15 to 200 (relative) are achieved by varying particle size and the amount of magnetically inert material in the composite mix. Their relatively low permeability results in high magnetizing current and energy storage undesired in a Transformer^[7].

Thus, Powdered core which has more energy storage capability and having relatively low permeability has been selected for this design.

3. System design

3.1 Design Overview

The implemented supercapacitor assisted surge absorber device was developed by using 2.5V/1F SC, 1 Ω resistor, transformer and a non-linear device(MOV). SC's continuous surge energy absorption capability given by $\frac{1}{2} CV^2$ could be effectively used with several other components such as MOVs, LC filters and a multi-winding magnetic components. This magnetic part works as a transformer when a surge travels through the power line and fires a nonlinear device such as a MOV or

a semiconductor device such as bidirectional break-over device^[8].

3.2 Main Configuration & Its Operation

Designed circuit of the surge protective device for the differential mode based on the supercapacitor concept is shown in Figure 8.

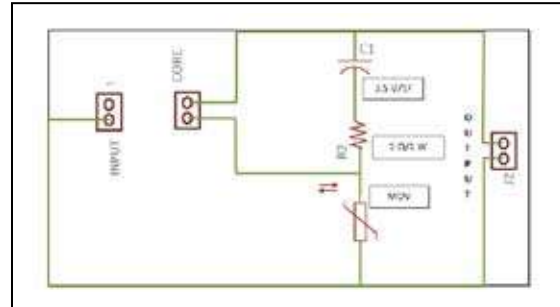


Figure 8 - Design Circuit Diagram

In this circuit, typical NLDs such as a MOV is combined with a magnetic component and an SC-based sub circuit. However, compared to a typical surge arrestor without supercapacitors, where NLDs are placed directly across the pairs of wires such as the neutral and the live (differential mode) or neutral or live and earth(common mode) as shown in figure 9.

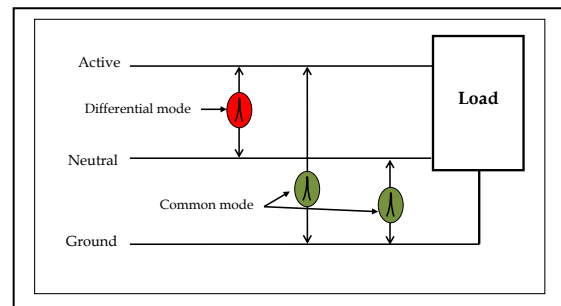


Figure 9 - Differential and common mode surges

As seen in figure 8, one end of the MOV is placed after the primary winding of the coil and the other end is connected to the return wire. A surge occurring at the mains input results in a voltage spike. At the instant the surge voltage increases above the MOVs firing voltage the high instantaneous current flows through the primary of the coil which results in an induced voltage in the secondary of the coil in the opposite direction. In order to achieve this, it is necessary for the primary and the secondary coils to be wound in the opposite direction. This drop in voltage across the coils will assist in reducing the voltage across the critical load that needs to be protected. The turns ratio can be adjusted to suit the voltage requirements of the supercapacitor based sub circuit^[8].



4. Results and analysis

In general practical circuit developments for low voltage surge protector for equipment are based on designing the protective circuit as an add-on block to the input wiring of the equipment. This block is used to attenuate the incoming transient using passive series impedances or bypassing the surge currents and absorbing the transient energy which is done using non-linear devices such as GDTs, MOVs, TVS, spark gaps, fuses, etc.

In the usual surge protector devices, the high transient energy can cause these non-linear devices to gradually deteriorate and eventually fail. If this energy can be taken out from the non-linear devices their life time will be greatly enhanced.

This paper presents the results of the use of supercapacitor based circuit together with non-linear devices to not only absorb the transient energy, but also to control the output clamping voltage to a lower value to give better protection for the equipment.

Since the protection circuit is for class III SPD, the equipment should be subjected to a 6 kV. Thus testing has been carried out at both 4 kV and 6 kV in the comparison.

4.1 Impact of The Supercapacitor Sub circuit and The Magnetic Component

As indicated in Figure 10, a supercapacitor-based subcircuit configuration could have few possible variations.

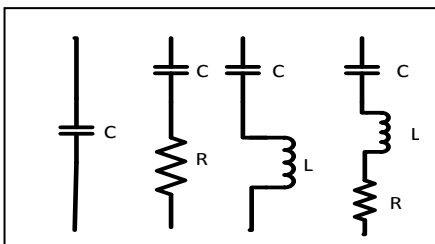


Figure 10 – Sub circuit combinations

SC-based sub circuit receives the voltage difference between primary and secondary coils. It creates a circulating current through the sub circuit and absorbing part of the surge energy into the supercapacitor. With this ability of supercapacitor, transient surge energy absorbed by the NLD is significantly reduced^[9]. The matlab simulation results for the sub circuit combinations is mentioned below.

4.1.1 Math lab simulation results for the sub circuit combinations

- Sub-circuit voltage variation for different capacitors

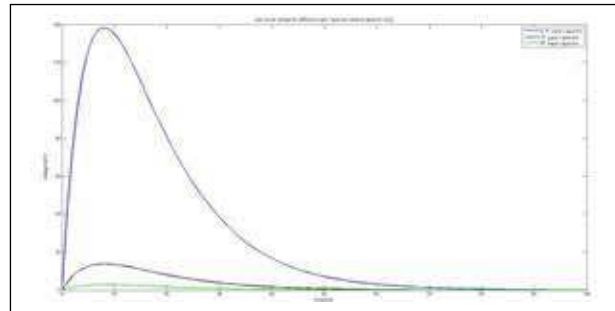


Figure 11 - Sub-circuit voltage variation for different capacitors

When capacitor value increased, voltage across sub circuit was decreased.

- Sub-circuit voltage variation for different resistors (R+1F sc)

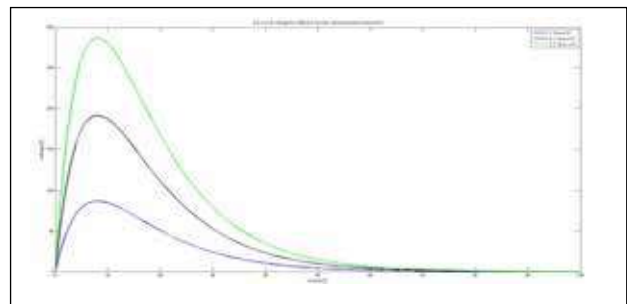


Figure 12 - Sub-circuit voltage variation for different resistors

When resistor value increased, voltage across sub circuit was increased.

- Sub-circuit voltage variation for different combinations (R+C, C+L, R+C+L)

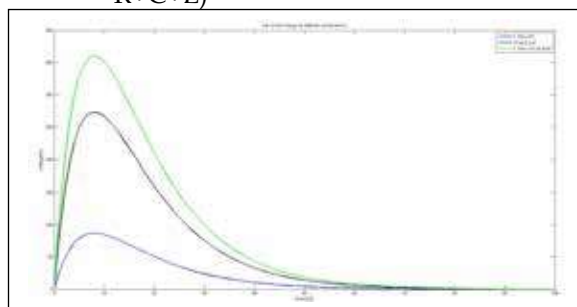


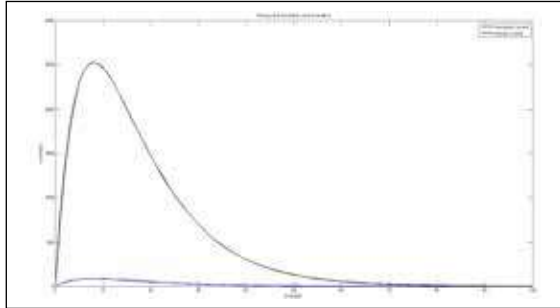
Figure 13 - Sub-circuit voltage variation for different combinations

$$V_{\text{sub}(R+C)} < V_{\text{sub}(C+L)} < V_{\text{sub}(R+C+L)}$$

Therefore, sub circuit with resistor, capacitor & inductor can have the ability of minimize the output voltage at the load end compared with other two combinations.

4.1.2 MATLAB simulation results for the complete circuit

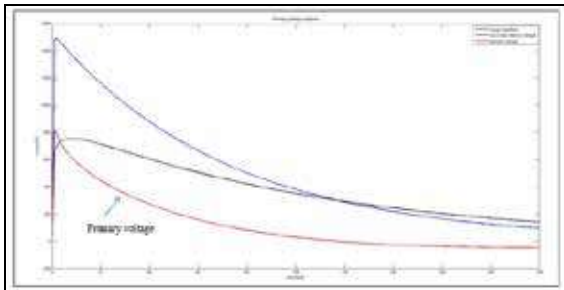
By applying surge input of 6 kV, the primary and secondary current variation of the magnetic core is shown as in figure 14.



$I_p(\max) = 2523 \text{ A}$ $I_s(\max) = 87 \text{ A}$

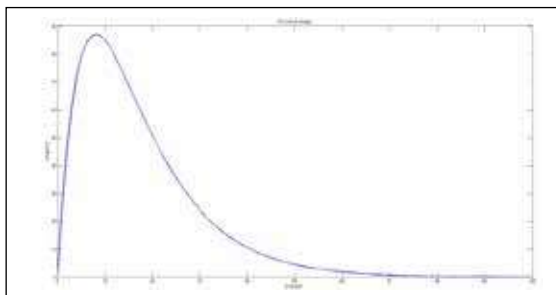
Figure 14 - Primary and secondary winding current variation

$$V_p = V_{\text{surge}} - V_{\text{NLD}}$$



$V_p(\max) = 794 \text{ V}$

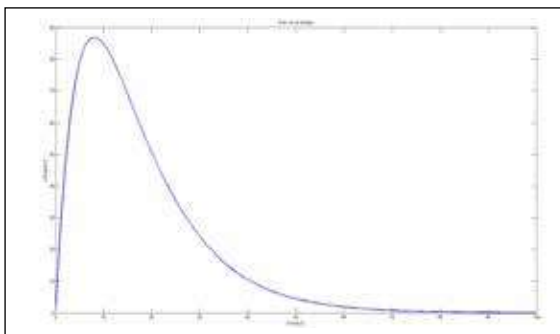
Figure 15 - Primary voltage variation



$V_{\text{sub}}(\max) = 87 \text{ V}$

Figure 16 - Sub-circuit voltage variation

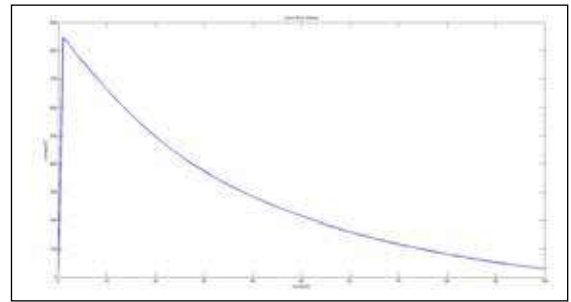
$$V_{\text{sub}} = I_{\text{sub}} * Z_{\text{sub}}$$



$V_{\text{sub}}(\max) = 87 \text{ V}$

Figure 17 - Sub-circuit voltage variation

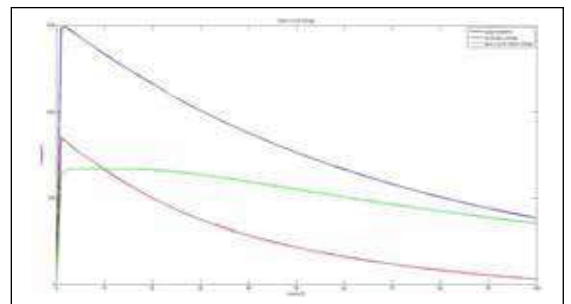
$$V_s = V_p + V_{\text{sub}}$$



$V_s(\max) = 821 \text{ V}$

Figure 18 - Secondary voltage variation

$$V_{\text{oc}} = V_{\text{surge}} - V_s$$



$V_{\text{oc}}(\max) = 667 \text{ V}$

Figure 19 - Open circuit voltage (No-load)

4.2 Energy Calculation

4.2.1 By using powdered core as a transformer

By applying 4 kV and 6 kV, total energy at the input and the energy absorbed by the MOV is calculated using the comma-separated values (CSV) from the oscilloscope trace.

4.2.1.1 For 4 kV Surge

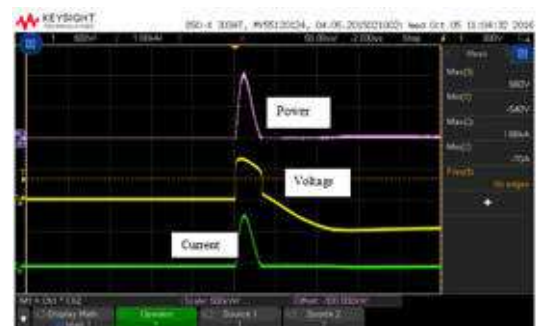


Figure 20 - Current, voltage & power waveforms across MOV



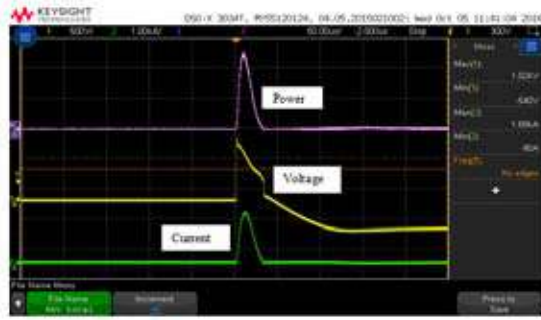


Figure 21 - Total current, voltage & power waveforms at the input

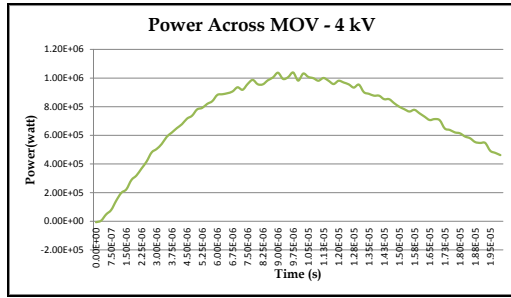


Figure 22 - Power across MOV



Figure 23 - Total power at the input

Output clamping voltage = 660 V

Total Energy = 17.2 J

Energy across MOV = 14.6 J

Energy absorbed by the supercapacitor subcircuit = (17.2-14.6) J
= 2.6 J

4.2.1.2 For 6 kV Surge

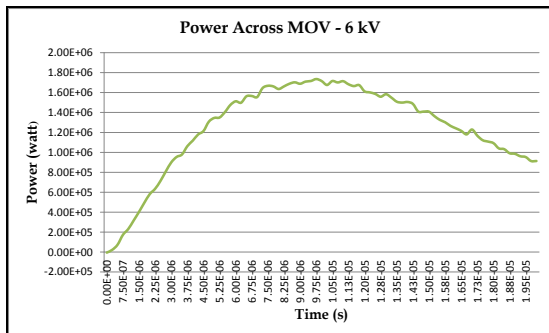


Figure 24 - Power across MOV



Figure 25 - Total power at the input

Total Energy = 30.8 J

Output clamping voltage = 720 V

Energy across MOV = 25.2 J

Energy absorbed by the supercapacitor subcircuit = (30.8-25.2) J
= 5.6 J

4.3 Energy Comparison of Powdered & Ferrite cores

Table 5 - Energy levels of powdered/ferrite cores

Surge Voltage (V)	Energy Absorbed by SC Sub-Circuit (J)	
	Powdered Core	Ferrite Core
4000	2.6	1.4
6000	5.6	5.1

Ferrite core stores less energy from the source which will be absorbed and dissipated by the SC sub-circuit. Hence, powdered core has more capability of absorbing surge energy than the ferrite cores.

5. Prototype implementation of the proposed system

5.1 Differential Mode

Final prototype implementation of the supercapacitor concept in a differential-mode protector circuit is shown in figure 26. The SC sub-circuit is formed by a 1 Ω resistor and a 1 F/2.5 V SC in series. The Epcos S-20 MOV with a maximum clamping voltage 595 V together with SC sub-circuit-created input/output voltages as shown in table 5.



Figure 26 - Proposed design of SPD (Differential Mode)

The output clamping voltage for the different voltages are tabulated as follows.

Table 6 - Output voltage at load end

Applied Surge Voltage (V)	Output Voltage At Load End L-N (V)
2000	600
4000	675
6000	690

6. Conclusions

The research study has been carried out to determine the best configuration of a supercapacitor (SC) to absorb excess energy during a transient. The study has shown that the large value supercapacitors are able to not only handle large amounts of energy but also their large time constants permit this stored energy to be released at a slow rate permitting a longer life to the surge protective device.

Compared to typical non-linear devices used in surge protective device (SPD) circuits, supercapacitors are capable of storing a large amount of energy despite their very low DC voltage rating. In the usual surge protector devices, the high transient energy can cause these non-linear devices to deteriorate and eventually fail. If this energy can be taken out from the non-linear devices their life time will be greatly enhanced.

The test results indicate that the supercapacitor is not destroyed by the repeated application of high voltage transients and the gradual voltage rise after each hit is in the order of millivolt. Also it still retain its capacitive behaviour and is not adversely affected by the transient high voltage at the terminals^[5]. Therefore, 1F-2.5 V supercapacitor which has the highest voltage rise with 1 ohm resistor was selected as a supercapacitor sub circuit for this design.

When applied input surge voltage of 6 kV, energy absorbed by the supercapacitor subcircuit with magnetic core is nearly 40% of total energy. Hence, supercapacitor subcircuit plays the role of absorbing part of the surge energy superimposed on the incoming pair of wires and increase the overall life time of the SPD device. Although the clamping voltage of SPD without supercapacitor is nearly 890 V, the supercapacitor assisted surge protective device has a 690 V at its output.

As the test results clearly indicate that the supercapacitor assisted surge protective device forms the basis of an entirely new on non-traditional applications that will yield not only longer life, but also a lower clamping voltage across a critical load to be protected. This proves that the new topology could be used as a base technique to develop full-scale common and differential mode surge capable, fully versatile, commercial surge protectors with better performance than traditional surge protectors with higher component counts. Overall performance of the supercapacitor technique with optimized magnetics is practically used to safeguard electronic systems against transient over-voltage related power quality issues. Further, this research can be developed to analyse the overall circuit, in order to predict its theoretical performance in detail^[11].

Acknowledgement

The authors would like to acknowledge the staff of the Electronic and Microelectronic division, ACCIMT for the great support given during the design and development of the device.

References

1. <https://www.britannica.com/science/lightning-meteorology>
2. Phillip R Tompson BE(Hons)FIE(Aust)CPEng MIEE, "PRINCIPLE OF LIGHTNING PROTECTION", 2008.
3. Chandima Gomes, "On the Selection and Installation of Surge Protection Devices in a TT Wiring System for Equipment and Human Safety", 4th February 2011, Elsevier Journal.
4. <https://en.wikipedia.org/wiki/Supercapacitor>



5. N. Kularatna, J. Fernando, S. James, A. Pandey, "Surge capability testing of supercapacitor families using a lightning surge simulator", *IEEE transactions on Industrial Electronics*, 2011, 58, 10 ,pp.. 4942 - 4949.
6. IEC61000-4-5 : Testing and measurement techniques - Surge immunity test, 2005-11
7. Texas Instrument, reference with "Magnetic Core Properties," originally titled "An Electrical Circuit Model for Magnetic Cores. " Unitrode Seminar Manual SEMIOOO, 1995.
8. Fernando, Jayathu, Nihal Kularatna, Howell Round, and Sadhana Talele. "Implementation of the supercapacitor-assisted surge absorber (SCASA) technique in a practical surge protector", *IECON 2014 - 40th Annual Conference of the IEEE Industrial Electronics Society*, 2014.
9. Jayathu Fernando, Nihal Kularatna "A supercapacitor based enhancement technique for stand-alone surge protection circuits" School of Engineering, The University of Waikato Hamilton, New Zealand.
10. Nihal Kularatna, "Energy Storage Devices For Electronic Systems-Rechargeable Batteries and, School of Engineering, The University of Waikato Hamilton, New Zealand, 8th September 2014.
11. Fernando, Jayathu, and Nihal Kularatna."Supercapacitor assisted surge absorber(SCASA) technique: Selection of supercapacitor and magnetic components",2014 *IEEE Energy Conversion Congress and Exposition (ECCE)*, 2014.
12. MdHisamHanapei and MohdRezadzudin Hassan, "Satellite Communication Equipments Reliability And Lightning Surge Measurement Results", *Lightning Protection And EMC Unit,CEEM'2006/Dalian 3A1-05*.
13. Kostas Samaras, Chet Sandberg, Chris J.Salmas and Andreas Koulaxouzidis, "Electrical Surge-Protection Devices for Industrial Facilities", *IEEE Transactions on Industrial Applications*, vol.43,No.1,January/February 2007.
14. <http://news.nationalgeographic.com/news/2013/11/131102-lightning-deaths-developing-countries-storms>, Visited, 15th January 2016.
15. http://batteryuniversity.com/learn/article/whats_the_role_of_the_supercapacitor, Visited, 5th March 2016.
16. <http://www.capacitorguide.com/supercapacitor>, Visited, 5th March 2016.
17. <https://www.maginc.com/Products/Powder-Cores/Learn-More-about-Powder-Cores.aspx>, Visited, 10th April 2016.

Detecting Key Actors in Multiple SIM Networks Via Centrality Measures and Mobile Service usage Behaviors

A.J.M. Korale and N.S. Weeraman

Abstract: The ubiquity of mobile service and the need for communication among small groups of individuals for personal and business use has prompted widespread registration of multiple Subscriber Identity Modules (SIM) under the ownership of a single individual. Operators desire to identify the key individuals in a multiple SIM network so that promotional messages and offers can be directed effectively and efficiently to the right customer where it will have the most impact and greatest chance of propagation through word of mouth.

In this paper we propose a novel algorithm that identifies key actors in a multi SIM network by way of their intra SIM call patterns, mobility information, demographic characteristics of the registered user and other information relating to the value added service (VAS) subscription portfolio. In this approach we associate a set of centrality related features with each SIM in the network based on the incoming and outgoing call patterns, their duration, the time of such calls, the location and mobility information of the SIM estimated at the time of the calls, the intra and inter operator traffic, average revenues and other ancillary information related to the age and gender of the registered user.

The algorithm provides a view of the hierarchical structure of the multiple SIM network and insights into the degree of importance of the individual SIMs and their relationships with each other. We also develop a set of criteria based on the features and detected leaders to help in the identification and validation of the key actors. These features and criteria also help to rank the SIMs in order of importance helping to prioritize an operator's approach to each individual SIM. They also help group multi SIM networks together according to a certain similarity criteria.

The detected key actors in the network are validated by matching their SIM with those SIMs registered for other services within the other operator's line of businesses such as contact numbers registered for customer services and other high value uses of the SIM such as roaming and international calls.

Keywords: Centrality, Social Network, Mobile Telecommunications, Eigen Vector Centrality, Multi-SIM Networks

1. Introduction

The ubiquitous availability of mobile services from a multitude of mobile service operators has resulted in the widespread registration of multiple mobile telecommunications service connections under the ownership of a single individual. It is usually the case that subscribers tend to register multiple service connections under a single network operator as the cost of calls to other networks is significantly higher than calls within a single network. Thus while these multiple Subscriber Identity Module (SIM) networks usually belong to a single network operator the identification of the key actor in the multi SIM network poses a significant challenge to the operator. The key actor in this respect refers to the leader of the

small multi SIM network. The attributes of what constitutes a leader may depend on such considerations as inter network call activity level, mobility, time and duration of calls in addition to what other products and services are used from the service portfolio of the mobile operator.

In the Sri Lankan mobile telecommunications market an individual is required to register the connection under ones National Identity Card (NIC) for security reasons.

Eng. (Dr.) A.J.M. Korale, C.Eng., MIE(SL), B.Sc. Eng. (Wisconsin), M.Sc. Eng. (Columbia), Ph.D. Eng. (Imperial College), MBA.(Sri Jayewardenepura), Senior Technology Consultant, Millennium Information Technology.

Mr. N.S. Weeraman, AMIE(SL), B.Sc. Eng. (Moratuwa), MBA. (Sri Jayewardenepura), Manager, Business Intelligence, Dialog Axiata PLC.



And mobile operators also place additional restrictions on the number of simultaneous or multiple connections an individual can register under a single NIC. In the case of the operator Dialog Axiata, an upper limit of five simultaneous connections per individual (NIC) is placed on the subscriber base.

These restrictions are to ensure that the mobile connections held are ones that serve a genuine purpose and are ones that will be in regular use. In these multiple SIM networks separate billing arrangements will be made for each connection under a particular NIC with detailed call analysis available for each connection but the ownership rests with a single individual and therefore so lies with the responsibility for making payments with respect to the multiple connections.

Business and other mercantile organizations have recourse to multiple connections through corporate accounts where many hundreds of connections can be obtained under the ownership of a corporate. In the case of such corporate multi-SIM networks it is clear where the ownership lies and any promotional messages or material on special offers can be delivered to the relevant representative of the corporate. Also the number of such corporate networks is relatively small in number so that an individual account manager from the mobile service operator can be assigned to handle all the affairs relating to that corporate multi SIM network.

Returning to the problem of the personal five connection multi-SIM networks under the ownership of a single owner, identification of the key actor in such networks poses a major problem for mobile operators. It may be that such multi SIM networks are used within a single family or in a small business or used both as a personal communication network between ones family members and with those employees of a small private enterprise. In such a scenario the operator cannot pay individual attention to the many thousands of such networks and requires an automated means of identifying the key individual at the centre of the multi-SIM network.

Operators therefor wish to have an efficient means of reaching the key actors in a network via an algorithm that can dispatch promotional materials and offers via electronic means such as SMS. SMS based advertising is now a key part of the digital advertising strategy of any

organization. Mobile operators leverage this opportunity by selling potential advertising “space” in the SMS domain to clients who wish to reach large groups of individuals in particular demographics.

2. Mobile operator specific criteria that help in detecting and validating key actors in multiple SIM networks

Certain mobile operators are in many lines of business and in the case of Dialog a quad play operator, has mobile telephone services, broadband internet, fixed line and television service in its service portfolio. This provides a unique opportunity for the operator to reach out to its customer base in one line of business to promote its other lines of business to subscribers who haven’t yet availed themselves the opportunity of trying out the other products on offer. When properly channelled, offers from one line of business can be promoted to consumers in its other lines of business presenting a unique cross sell opportunity.

This also provides the operator with a way of determining key actors in their subscriber base by identifying those mobile service contact numbers left by individual customers which are associated with different product lines of the company. For example an individual customer contact number associated with a Dialog Television service subscription may provide clues to the principal actor in a multi SIM network consisting of multiple mobile connections owned by an individual. If one of the multiple SIM numbers owned by a particular customer matches a customer contact number left with another Dialog product such as a TV, broadband or fixed line connection it may provide a means of identifying the main actor of that multi-SIM network.

While in this paper we do not rely exclusively on such heuristics to identify key actors in multi SIM network, we however do use them to validate the key actors found via our novel algorithm for detecting such key individuals.

Due to the particular nature of the mobile telecommunications service usage profile of individual customers we also may use other mobile service usage patterns, usage contexts and properties associated with mobile service assigned to a particular SIM in our quest to validate the key actors determined via the algorithm.

It is also very likely that the SIM that is used for high value services like International Direct Dialling (IDD) is in the hands of the key actor of the multi SIM network. Thus by monitoring the IDD service usage of each of the SIMs an idea to the key individual of the network may be arrived at. In this scheme it is the outgoing call pattern more than the incoming call pattern that will be most indicative. As it is the outgoing calls that are directly billed to a particular connection while incoming calls even from overseas are received without cost to the particular connection.

We may also use the overseas roaming profile of a subscriber (or SIM) to hazard a guess as to the importance placed on a SIM in a multiple SIM network. A customer that has activated roaming on a SIM or takes a particular SIM as his roaming connection when traveling overseas clearly places a priority on that SIM. In such a scenario we have grounds to believe that the key individual of the network is the one behind the use of that SIM.

Mobile service operators place internal rankings and priority handling tags on individual SIMs based on an internal assessment of the value of the customer to the network. In these schemes customers and SIMs associated with them are given high priority in customer care and are eligible for discounts and special offers on products and services on offer. This type of priority determination is made on the basis of the revenue contribution of each SIM (subscriber), the payment pattern which displays a history of prompt and on time settling of dues and subscription to numerous and high value products and services from across the quad play portfolio. In light of this a SIM ranked highly in the internal customer ranking is also bound to be a key actor in a potential multi SIM network.

All of these considerations can be used in the validation of potential key actors in the multi SIM networks determined through the proposed novel key actor detection algorithm.

3. Overview of the key actor detection algorithm

The key actor detection algorithm operates by processing the internetwork call pattern of a multi SIM network consisting of a maximum of five SIMs. In our quest to detect this key actor we employ the reasoning that the key individual in a network is the one who is most

“well connected”. In this respect we determine the SIM that has the most number of connections and connections of connections.

We believe a well-connected individual has many connections and also employ the thinking that the connections of the well-connected individual must themselves be well connected individuals. Using network theory and heuristics based on the incoming and outgoing call pattern of each of the members on the five member multi SIM network we are able to determine a set of properties or statistics for each node (or SIM) in the multi SIM network. These statistics then allow us to pick the node or SIM most “outstanding” in the network.

The outgoing and incoming calls between the nodes (actors) of the multi SIM network are used to populate two adjacency matrices. In one, the adjacency matrix is created using the number of calls between the actors of the network in a directed network configuration. In the other, the adjacency matrix is populated with the call durations between two actors in the network, in a directed network configuration.

3.1 Eigen vector centrality [1]

The magnitude of the elements of the principal Eigen vector of the adjacency matrix of the multi SIM network when sorted in descending order of magnitude indicates in that order the most well connectedness of actors in the network. Thus at the head of the sorted Eigen vector lies the most well-connected actor and our prime contender for the position of key actor of the multi SIM network.

The principal Eigen vector also accounts for the connections of connections of the actors in the network and so indicates the heuristic that the most well-connected actor is also the one who has the most well-connected friends (connections). Employing the idea that the importance of a connection is related to how many other important connections he has (employing the concept of having friends in high places)

In our framework we utilize both types of adjacency matrices discussed above and determine key actors based on their connections (the number of calls) and the strength of their connection (the duration of the calls).

It is quite frequently the case that some pre-filtering of calls is carried out prior to being



considered for inclusion in the adjacency matrix. This is to eliminate those calls that may not be the result of strong relationships between the calling and called party. In light of this we place a lower limit of 30 seconds call duration for a call to be considered valid and for inclusion in the adjacency matrix.

3.2 In-Degree

This measures the number of calls coming in to the node or calls received by the actor. In directed networks in-degree is considered more important than out-degree. The page rank algorithm also uses a similar heuristic which we too employ in our model [1].

We also consider the duration of incoming calls to a network node (actor). This is essentially to determine if there is a relationship between the number of calls received and the total duration of those calls. For it is likely that a key actor receives a large number of calls and also that those calls are of a relatively long duration when compared with the subordinate calls in the network.

3.3 Out-Degree

This measures the number of calls going out of the node or calls made by the actor.

We also consider the duration of total calls made by a network node (actor). For it is likely that a key actor in addition to receiving a large number of calls also makes a fairly large number of calls in return or in response to those calls. We may also surmise that those calls are of a relatively long duration when compared with the subordinate calls in the network.

3.4 Radius of Gyration

This is a measure of the degree of mobility of a SIM (actor). It is generally believed that a key actor may have a large radius of gyration. Meaning that in a day the calls taken and received by a key actor may happen in many more locations than that when compared to a subordinate SIM in the network.

We measure this mobility by determining the number of times the serving cell of the subscriber (SIM) changed during the day. We do this by noting the number of changes in the cell ID through which a call was made or received. As mobility level is an ancillary property of a node in the network and not directly related to the relationships between actors as evidenced by the calls between each of the SIMs, we do not place a limit on the

duration of a call for it to be considered valid for consideration in the radius of gyration measure.

3.5 Time stamp of incoming and outgoing calls to assess level of activity in making and receiving calls during the day

We also observe the number of calls coming in to and leaving a particular actor across the time of day by dividing the day in to periods 00:00-8:00, 8:00-16:00 and 16:00-00:00.

This measure is also an indicator which may tell us information relating to which calls may be related to official purposes and which calls may relate to more personal purposes as it is likely that calls received after business hours are generally due to personal reasons.

As activity level is also an ancillary property of a node in the network and not directly related to the relationships between actors we do not place a limit on the duration of a call for it to be considered valid for consideration in the activity during the day measure.

Clear outliers in this field also indicates a key actor in the network as the results will show.

4. Results and Validation

In the following figures and table we present some example results to demonstrate the working of the algorithm to detect the key actor(s) in a multi SIM network.

Table 1 - Multi SIM Call Node Properties.

Node No	In Degree	Out Degree	In MOU	Out MOU	Out Cell Change	In Cell Change	calls 0-8	calls 8-16	calls 16-24
1	51	0	4,025	-	24	21	9	63	29
2	101	139	3,731	11,954	40	38	10	149	117
3	9	17	671	748	7	5	1	12	15
4	65	93	5,440	3,441	29	16	3	82	73
5	42	19	2,884	608	6	6	5	52	16

In Table 1, we present the network statistics for each node in a multi SIM network to demonstrate how the properties of the internetwork call patterns can be used to detect the most well-connected (important) actors in the network. The 30 second call duration filter had been applied to the degree calculations but was not applied in determining the mobility level or time of day call activity levels.

With reference to Table 1, the first column gives the respective node number or identity of the actor, the second and third columns the number of incoming and outgoing calls to each node, the fourth and fifth columns present the total duration of calls (minutes of use) coming into and leaving a node. Columns 6 through 7 give the number of times the serving sell of the actor changed when receiving or making a call which is a measure of his mobility. Columns 8 through 10 give an indication of how busy the actor is in those hours giving an idea of the number of calls received or made that fall in to those time intervals.

From the table we can clearly conclude that actor 2 is the leader of the network or is the most well-connected as well as most active member of the network. Due to these reasons we consider node 2 to be the most important in the network and consider it the key actor of the five sim network.

The Figure 1 depicts the principal Eigen vector of the call based adjacency matrix. It too reinforces the finding that node 2 is the most central in the network. We also note that the Eigen vector centrality measure can also be used to rank the centrality of each of the nodes in the network. Thus it is a measure that can serve to prioritize the actors in the network in order of importance. Eigen vector centrality is the principal feature used to identify the central actor in the network while the radius of gyration and time of calls are of lesser importance. We give higher priority to the centralities obtained for the network based on the number of calls and then for the network based on call duration and consider radius of gyration and time of calls as the next most important criteria.

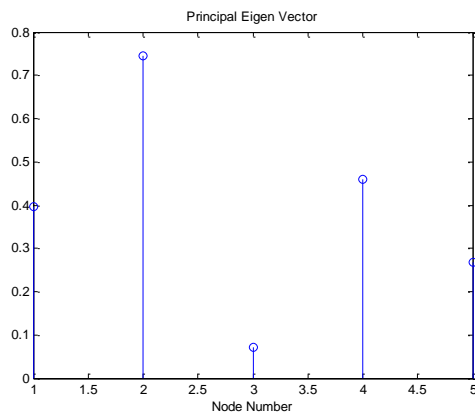


Figure 1 - Principal Eigen Vector of Call based Adjacency Matrix

The internetwork diagram of call patterns of Figure 2 and internetwork diagram of call

durations depicted in Figure 3 also confirm the earlier finding that node 2 is most central and that nodes 4 and 1 are perhaps next most important. This finding is also validated by the Eigen vector centrality measure and by the node level statistics found in Table 1.

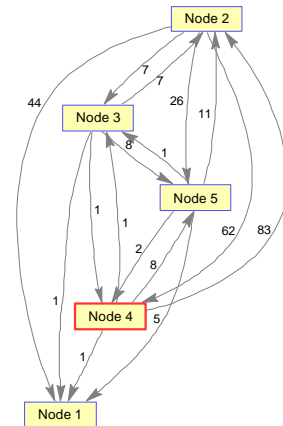


Figure 2 - Call based Multi SIM network

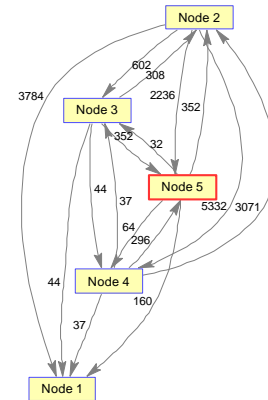


Figure 3 - Call duration (minutes of use - MOU) based Multi SIM network

5. Conclusions

Through this modelling we have shown that we are able to detect key actors in multi SIM networks. We are also able to rank the degree of well-connectedness or in this case a degree of importance by using the Eigen vector centrality measure as well as the tabulated properties of individual nodes that corresponds well with the Eigen vector centrality measure.

We were also able to independently verify that the key actors detected were in fact important actors in the network by using the criteria outlined in section 2 which acted as another level of validation for our findings.

References

1. Newman, MEJ, Networks, Oxford University Press, 2013, pp 109-149.



2. Smilkov et al, Identifying communities by influence dynamics in social networks
3. home.dei.polimi.it/matteucc/Clustering/tutorial_html/cmeans.html, extracted on 10 April 2017.

Intelligent Pest Repellent System for Sri Lankan Farming Industry

P.N. Karunanayake, W.H.H.N. de Soysa, J.A.C.L.C. Jayasundara,
Y.G. Wanniarachchi and A.P.I. Karunarathne

Abstract: Sri Lanka has a culture based on agriculture which has been descending from centuries. Currently in Sri Lanka cultivation activity from ploughing to harvesting and packing being carried out by machinery with less amount of labour. But even with such machines involved in the field, farmers find it very difficult to protect their crops from pests which cause maximal damages when strict supervision is absent. Though insects and rodents can be controlled by using pesticides, larger pests such as wild boars, warthogs, porcupines and birds cannot be controlled using such methods since it requires manpower to keep them away from the crops. The absence of advanced technology involved in this area has led the farmers to face many difficulties such as profit loss, the requirement of excess manpower to protect the crops from pests and usage of illegal and inhumane pest attack prevention mechanisms.

A novel approach is introduced as a solution for the mentioned difficulties. Wireless sensor network is used to detect pests in the field, and once a pest is detected, an appropriate repellent system which is harmless to animals and the environment is activated by the system. Emitting ultrasonic soundwaves and high-intensity flash lights are used as the repellent systems. Since there is a probability of sensor node failures, central node evaluates a pattern of the arrival of pests. When the central node detects a failure of one or more sensor nodes, it activates the repellent system automatically according to the evaluated arrival pattern of the pests and notifies about the node failure to the owner. Therefore this system is focused on the implementation of user-friendly, energy efficient, intelligent autonomous pest repellent system.

Keywords: Intelligent, Wireless Sensor Networks, Pest Repellent, Autonomous, Pattern Recognition

1. Introduction

Among the various agricultural sectors in Sri Lanka, the primary form of agriculture is rice production. Rice is the single most important crop occupying 708,000 hectares of land in Sri Lanka by 2016 [1].

In the past, the farmers used to the spent high amount of man power for cultivation, but nowadays with almost every cultivation activity from ploughing to harvesting and packing being carried out by machinery resulting minimization of labour requirement. The farmer is being transformed to a part time manager who coordinates various activities. But even with such machines involved in the field, Sri Lankan farmers find it very difficult to protect their crops from pests which cause maximal damages if strict supervision is absent. Though insects and rodents can be controlled using pesticides, larger pests such as wild boars, warthogs, porcupines and birds cannot be controlled using such methods since it requires manpower to keep them away from the crops.

As a result, pest controlling has become major problem leading to economic, social and ethical issues in the Sri Lankan society such as,

- Animal poacher.
- Animal attacks on humans.
- Usage of illegal pest control mechanisms.
- People being victims of their own traps (ex: Trap Guns)
- Crop Losses

The goal of this research project was to focus on an effective, user-friendly, humane, energy efficient and cost-efficient pest repellent system that can be used by Sri Lankan farmers. From all the pests that harm paddy fields in Sri Lanka, wild boar and sparrows are the pests which destroy the paddy mostly according to the farmers (apart from insect pests). Therefore this work only focused on repelling wild boars and sparrows.

Eng. P.N. Karunanayake, M.Eng.(SL), B.Sc. Eng. (Moratuwa), Department of Electrical, Electronic & Telecommunication Engineering, General Sir John Kotelawala Defence University, Sri Lanka.
Mr. W.H.H.N. de Soysa,
Mr. J.A.C.L.C. Jayasundara,
Mr. Y.G. Wanniarachchi
Mr. A.P.I. Karunarathne



The autonomous pest repellent system was designed by using wireless sensor networks (WSN) incorporating pattern recognition algorithm. Several techniques were used to increase the life time of the system since monitoring a paddy field should be done for few months in one cultivation season.

The remainder of this paper is organized as follows. Section 2 discusses on pest repellent systems, wireless sensor networks and its applicability for a pest repellent system. Also, it discusses on the behaviour of the targeted pests, wild boars and sparrows. Section 3 discusses the node construction which is used for the pest repellent system. Under section 4, the operation of the system is discussed. Section 5 discusses incorporated pattern recognition technique. The user interface and the SMS alert system is discussed in the section 6. Section 7 discusses the results obtained, and section 8 provides the conclusion. Future improvements are discussed under section 9.

2. Literature Review

2.1 Pest Repellent Systems

Conventional pest control mechanisms that are used in Sri Lankan farm fields can be named as, scarecrows, bells, electric fences, light bulbs, horns etc. These mechanisms are proven to be very inefficient and primitive. Among these, electric fences are used to repel considerably large animals but dangerous for both humans and animals. Even though electronic pest controlling mechanisms have a risk of danger, farmers tend to use them to save their crops or paddy.

Examples for electronically powered pest repellent are electronic pest chasers, electronic pest deterrent, electronic pesticides. These are generally known as electronic pest control devices. These repellent methods are more popular since their nature of environmental friendliness over the conventional pesticides. Two types of electronic pest control devices are available. The high-frequency devices and the electromagnetic are the two types of devices. They are popular for their reliable operation and availability. High-frequency devices operate by transmitting sound waves greater than 20,000 Hz. Although some animals such as dogs, bats, rodents, birds and wild boars can hear well in the high-frequency range, human ear lacks the capacity to hear such sound. Therefore high-frequency devices are designed and constructed to emit sound waves within

the range of frequencies that only targeted pests can hear. When the power of the sound wave is sufficiently large, the pests cannot withstand it. Thereby the sound wave repels them away from the area without affecting the environment and non-target organisms, including man. The second type of devices which are electromagnetic devices emit electromagnetic waves, inimical to pests. The advantages of these devices over other pest controlling devices are lower cost, environmental friendly and no known threat to the humans[2]. Therefore with the technological advancement, it can be seen that electronic pest repellent systems can be developed reducing the disadvantages and the risks of conventional pest repellent methods.

2.2 Wireless Sensor Networks (WSN)

Wireless sensor networks are applied in almost every application in nowadays to make life easier for the human. WSN systems have many advantages over wired networks such as easy deployment, and less amount of maintenance. But WSNs have many limitations such as limited amount of power, security, scalability, routing, node failures, data integrity, Localization, etc. According to the application, WSN should be designed considering all of its limitation to obtain its maximum output.

WSNs have been widely used for precision agriculture [3]. There are many goals for using precision agriculture as follows.

- To reduce Nitrogen, Methane and Carbon and other dangerous gases and liquid emission.
- To manage the available resources according to the requirements of the crops.
- To improve the output of the crops by monitoring their growth.

These goals can be accomplished by using WSNs. Although many research work has been done for precision agriculture and to control insect pests [4], [5], [6], research work for pests such as wild boars together with birds such as sparrows has not been done.

2.3 Behavioral Patterns of Wild Boars and Sparrows

Since this research project only focused on wild boars and sparrows, their behavioural information is important to design the repellent system.

Wild boars are highly capable of adapting to the environment and capable of learning from the environment. Usually, at night time they attack to paddy fields and destroy it for their food. The traditional method of repelling them is waving a flash light or a torch towards them. Within few seconds after a torch is flashed, wild boars leave the paddy. But if they understand flashing the torch is occurred only during a certain period of time, they change the time of their attack by learning the pattern. Therefore there are many disadvantages in this method.

1. The farmer needs to be awake and watchout throughout the night every day resulting in a requirement of man power in higher quantity.
2. If only flashing is done only for a certain period of time, wild boar realizes it with their capabilities and will visit the paddy at a different time.

Using this method is environmentally friendly. Therefore designing a system which identifies the wild boar and flashing a light towards them will provide an echo friendly system which saves a considerable amount of man power.

Sparrows damage the paddy fields at the day time. The traditional method of repelling them from harming the paddy is using a whistle which emits a sound wave higher than 20,000Hz.

This method is also environmental friendly. But it requires a higher amount of man power and time.

3. Device Construction

Two main units are being used in the system

1. Sink node
2. Sensor node

Each unit has distinctive characteristics which enable them to communicate with each other and execute operations as given by the sink node.

3.1 Sink Node

The Sink node consists of following main components:

- SIM800L GSM Module
- SD Card module
- FM Receiver
- LCD Panel
- Arduino Nano
- 12V Battery
- 8 Way Relay
- Solar Panel (10W)
- Real Time Clock
- PIR Sensors
- FM Receiver
- High-Frequency Speakers
- High intensity LED
- Solar charge controller and Frequency circuit

During the daytime, birds are the most likely to invade the crops. Therefore the high-frequency speaker unit will be activated throughout the day. Day and night are distinguished by using a real time clock attached to the sink node. At night the crops are prone to be attacked by larger animals such as wild boars and porcupines. Therefore both the speaker unit and the light unit will be in operation during the night till dawn. The light unit is switched off during the day time to save energy. Figure 1 illustrates the sink node. The solar panel was used to power up the sink node. During the night time, 12V battery was used to provide energy.



Figure 1 - Sink node

3.2 Sensor Node

Sensor node consists of following components.

- PIR sensors
- Pulse Generator circuit
- Battery level indicator LED Circuit
- 6V Battery
- FM Transmitter



Sensor nodes are simplified versions of the sink node. These nodes remain active all the time and are vigilant about the movements in the surrounding. Each node consists of 3 PIR sensors mounted on its head which cover a whole range of 360 degrees.



Figure 2 - Sensor node

4. Operation

Sensor nodes are placed to cover the area of the paddy field. For this research, nodes were placed within one hop distance from the sink node (Multi hop scenario is not considered). The nodes are placed in a known location. Each sensor node is given an individual address and ID. Node placement information is fed to the sink node to identify the direction of the arrival of the pest. Once a movement is detected by the sensor node, it sends a data packet to the sink node to indicate the presence of the pest. When a packet is received, the sink node activates either its flash light system or the speaker system which is directed towards the direction which the movement was detected. The high-frequency speaker System emits a range of frequencies ranging from 20 kHz above in order to repel any animal that is in its way. The flash light unit flashes the light during the night time to repel the wild boars.

If the sink node keeps on receiving signals from a certain stable target, it will automatically send an SMS to the user notifying about the presence of an unknown animal or pest which cannot be sent away from the system.

The sensor node sends a beacon periodically to the sink node to provide information about the presence of the sensor node. By using this beacon, the sink will be able to detect new nodes as well as the failure of the sensor nodes. If the sensor node ends its life time, it is identified by the sink node. When node failure is detected, an SMS is sent regarding the node failure with the node's ID to the assigned

phone number within a short period of time. The user can then inspect the sensor node and do the necessary actions.

Operation of the system is categorized as "Real mode" and "Demo mode". The purpose of these two modes is for real time deployment and for demonstration and testing purpose respectively. In "Real mode" the system functions considering night time as from 1800 hours to 0600 hours. The "Demo mode" is for testing and demonstration purpose. Hence night time is considered as 12 minutes.

5. Pattern Recognition

During a sensor node failure, until the node is replaced, any animal can disturb the paddy in the area which the failed sensor node provided coverage. Hence it will damage the paddy. To minimize the damage, sink node identifies a pattern of the arrival and the time of arrival of wild boars.

The Main purposes of Pattern Recognition are as follows,

- To Reduce excess energy consumption
- Function autonomously without any human interaction.
- Determine the times that the animals visit the field and repel them from entering the field.
- If a secondary node fails, the pattern recognition mechanism will still be in operation using the previously recorded data. The base station can, therefore, carry on normal functions in lieu of the failed secondary node. This enables the system to function smoothly and provides time for the user to look into the failed node and replace it.

Once packets are received informing the arrival of pests, the information such as the direction and the time of arrival is stored in the sink node. This information is collected for three consecutive days. Then sink node calculates a pattern of the arrival of pests with the direction and the time. This pattern is stored in the sink node and once a node failure is detected. The lighting system is activated according to the pattern, and the sound system is activated in a random manner for a period of the 40s. Since flash light requires more power, by using the pattern can reduce the time the flash light is activated. Hence can reduce the power consumption of the system.

For this pattern recognition mechanism, the arrival of wild boars was considered since the arrival of birds have a random pattern of arrival. When the sink node detects a node failure, it informs the user by sending an SMS and activates the flash light systems according to the recognized pattern. Therefore the time window that was identified as the most number

The interface which interacts with the sink node only is used to input the phone number which SMS alerts should be sent. Also mode selection between “Real Mode” and “Demo Mode” is selected using this interface.

The second interface is the graphical user interface (GUI). The GUI is used to analyze the collected data from the nodes. The GUI was

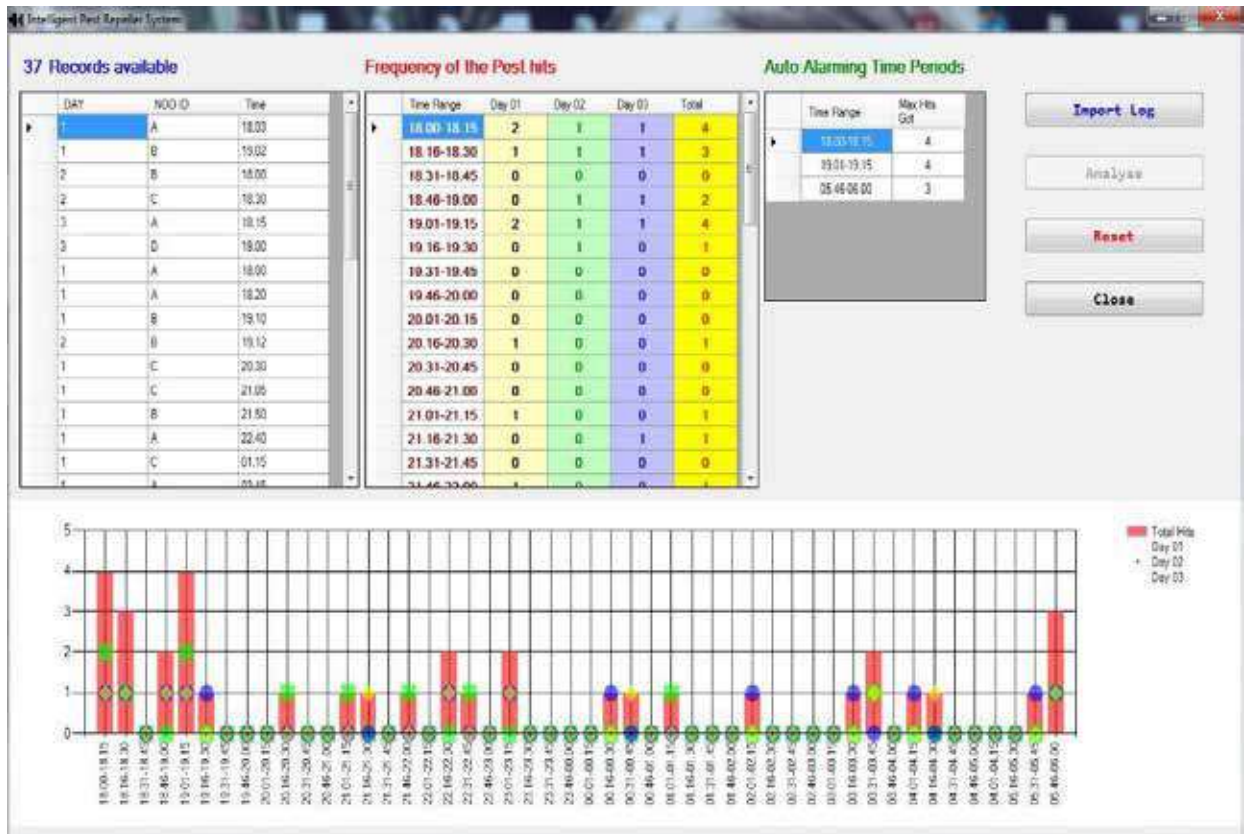


Figure 3 – Analysis of collected data

of the arrival of wild boars, the flash light system will be activated. The objective of this technique is to repel the wild boars even the sensor nodes are not activated for a period of time with lower power consumption.

The identified pattern is used for seven days. After seven days, anew pattern is identified. The pattern needs to be trained again since wild boars are able to identify patterns very easily. If the animals recognize that the flash light is activated only in a particular period of time, it will change the arrival of time. Therefore continues training of the pattern is important.

6. User Interface and SMS Alerts

The system has two main user interfaces. One interface interacts with the sink node only, and the other interface interacts with all the nodes.

created using Visual Basic.net. Figure 3 illustrates the analysis of collected data.

SMS messages are sent from the sink node to an assigned number alerting about the condition of the nodes and the detection.

Three types of messages are being programmed to be sent with three different alerts. They are,

1. Battery failure and Low battery levels of specific sensor nodes.
2. Malfunction of sink node.
3. Uncontrollable animal behaviour.

If the sensors keep on reporting detections for more than 5 minutes continuously, the base station will send a message to inform the presence of unwanted animal so that the user can inspect.



7. Results

Test results were analysed under two operating modes namely,

- Real Time Mode
 - From 0600 hours to 1800 hours
 - From 1800 hours to 0600 hours
- Demo Mode

The test environment was selected considering the habituation and the density of the birds.

Although lighting system was not able to test with real wild boars, motion detection, lighting system, user interfaces and the SMS alert mechanism were tested and provided more than 95% results.

8. Improvements

Since the prototype was not tested in a real paddy field for a longer period of time, it can be tested and identify the alteration which needed to be done.

The prototype used single hop WSN. Therefore coverage area by the sensor nodes is lower compared to actual paddy fields. Therefore by using multihop sensor networks, this system can be improved.

A cloud based data upload system can be implemented for the data to be stored and referred later. The user will be able to analyse and use the recorded data from anywhere, anytime via the internet.

A smart user interface can be implemented where the user can easily add / Remove nodes from the field and change the topological deployment of the nodes. This will enable anyone to be able to arrange and assign the desired number of nodes at desired locations.

A daily status report of the activities can be arranged as per the user's requirement.

9. Conclusion

This work is focused on autonomous, efficient and an intelligent system for pest repellent in various disciplines of agriculture but mainly focused on paddy fields. The system consists of integrated hardware components and an intelligent system which uses pattern recognition algorithms to operate. An initial survey was carried out to get an overall idea about the requirement of such a system to the Sri Lankan farming industry and to identify the key point which should be targeted in developing such a system.

A prototype design was made using WSN and tested thoroughly. The system can be visualized through a simple software which was built using Visual Basic.Net to analyse the collected data. A GUI enables the user to operate the system easily making it possible to let anyone operate the system.

SMS alerting system is activated with the sensor networks simultaneously. This service enables the user to remotely monitor the agricultural field and the equipment.

Therefore a system which is sustainable, autonomous and user-friendly was developed as a pest repellent system from this research project.

Acknowledgement

Authors wish to acknowledge the guidance provided by the Department members of Electrical, Electronic & Telecommunication Engineering - KDU.

References

1. <http://www.statistics.gov.lk/agriculture/Paddy%20Statistics/PaddyStats.htm>, Visited 14th May 2017.
2. O. O. D. et. al. Ibrahim A. G., "Electronic Pest Control Devices : A Review of their Necessity , Controversies and a submission of Design Considerations," *Int. J. Eng. Sci.*, pp. 26-30, 2013.
3. Azfar, S., Nadeem, A. and Basit, A. "Pest detection and control techniques using wireless sensor network: A review," *J. Entomol. Zool. Stud. JEZS*, vol. 3, no. 32, pp. 92-99, 2015.
4. C. Scientist, "Low Cost Sensor Based Embedded System for Plant Protection and Pest Control," pp. 179-184, 2015.
5. Aqeel-Ur-Rehman, Abbasi, A. Z., Islam, N. and Shaikh, Z. A. "A review of wireless sensors and networks' applications in agriculture," *Comput. Stand. Interfaces*, vol. 36, no. 2, pp. 263-270, 2014.
6. Akyildiz, Ian F., Weilian Su, Yogesh Sankarasubramaniam, and Erdal Cayirci. "Wireless sensor networks: a survey." *Computer networks* 38, no. 4 (2002): 393-422.
7. Schlageter, A. and Haag-Wackernagel, D. "A Gustatory Repellent for Protection of Agricultural Land from Wild Boar Damage: An Investigation on Effectiveness," *J. Agric. Sci.*, vol. 4, no. 5, pp. 60-68, 2012.

Land Cover Classification and Sub Component Analysis Using Hyperspectral Imagery

A. M. R. Abeysekara, T. S. J. Oorloff, S. S. P. Vithana, H. M. V. R. Herath,
G. M. R. I. Godaliyadda and M. P. B. Ekanayake

Abstract: This paper presents a classification of the land cover under soil, vegetation and water bodies in a strip along the north eastern region of Sri Lanka, using hyperspectral image data obtained by the Earth Observing (EO-1) satellite's Hyperion sensor. Using hyperspectral imagery in land-cover mapping is beneficial as it could capture the fine details of the region under consideration, which may not be achieved by other image processing techniques. In this paper, mathematical concepts and statistical tools such as Principal Component Analysis (PCA) and concepts of euclidean geometry have been used to develop an algorithm which classifies each pixel of the image under the above mentioned classes. In the process of classification, the pixels that are not classified with a clear cut boundary initially are identified as 'mixed' pixels, and are subjected to a separate algorithm in order to identify the percentages of fractional components of such pixels. Finally, the image is remapped according to the class that each pixel belongs to, and the mixed pixels are shown separately according the intensities of their fractional components.

Keywords: Hyperspectral Imagery, Hyperion, Principal Component Analysis, fractional components

1. Introduction

A collection of high resolution monochromatic pictures representing the reflectance values corresponding to a broad range of wavelengths is a hyperspectral image. Reflected radiation at a series of narrow and contiguous wavelength bands is measured in hyperspectral images. To identify the characteristic information of a given pixel, an appropriate frequency band can be used.

Land cover mapping using hyperspectral image data has both advantages and disadvantages. Since the finest details of the images are available, the accuracy of classification is high when the ideal spectral bands are chosen. The disadvantages of using Hyperspectral Imaging (HSI) data for land cover mapping are, redundancy of data, complexity in computations and excessive memory usage. [1]-[3].

The classification of the pixels under soil, water and foliage, HSI data which was obtained by the Hyperion Earth Observing - 1 (EO - 1) sensor [4] has been used. The sensor which was used in imaging is capable of resolving spectral bands from 0.4 to 2.5 μm with a 30 meter resolution and it has the ability of imaging a 7.5 km by 100 km land area per image, while providing detailed spectral mapping across all channels with high radiometric accuracy. The telescope provides for two separate grating image spectrometers to improve signal-to-noise ratio (SNR).

2. Area of Study and the Dataset

As shown in the Figure 1, the area of interest of our study comprises of a strip along the North Eastern region of Sri Lanka.

The Hyperion images of the aforementioned region seen in Figure 1 (a) and of geographical coordinates as in Table I, had been acquired on the 17th of September, 2005 starting at 04:40:57 and ending at 04:45:35 in local time (+5:30 GMT). Two cameras, VNIR (Visible and Near-Infrared) and SWIR (Short Wave Infrared) had been used to obtain the hyperspectral images of 242 bands spanning across a range of wavelengths, from 355.59nm to 2577.08nm [5]. However, 44 spectral bands have not been calibrated and cannot be used for data analysis.

Ms. A. M. R. Abeysekara, B.Sc. Eng. Undergraduate at the Department of Electrical and Electronic Engineering, University of Peradeniya.

Mr. T. S. J. Oorloff, B.Sc. Eng. Undergraduate at the Department of Electrical and Electronic Engineering, University of Peradeniya.

Ms. S. S. P. Vithana, B.Sc. Eng. Undergraduate at the Department of Electrical and Electronic Engineering, University of Peradeniya.

Eng. (Dr.) H. M. V. R. Herath, C. Eng., SMIEEE, MOSA, MIE(SL), B.Sc. Eng. (Hons) (Peradeniya), MS (Miami, US), Dr. - Ing. (Paderborn), Senior Lecturer at the Department of Electrical and Electronic Engineering, University of Peradeniya.

Eng. (Dr.) G. M. R. I. Godaliyadda, B.Sc. Eng. (Hons) (Peradeniya), Ph.D. (NUS, Sg), AMIE (Sri Lanka), Senior Lecturer at the Department of Electrical and Electronic Engineering, University of Peradeniya.

Eng. (Dr.) M. P. B. Ekanayake, B.Sc. Eng. (Hons) (Peradeniya), Ph.D. (Texas Tech, US), AMIE (Sri Lanka), Senior Lecturer at the Department of Electrical and Electronic Engineering, University of Peradeniya.



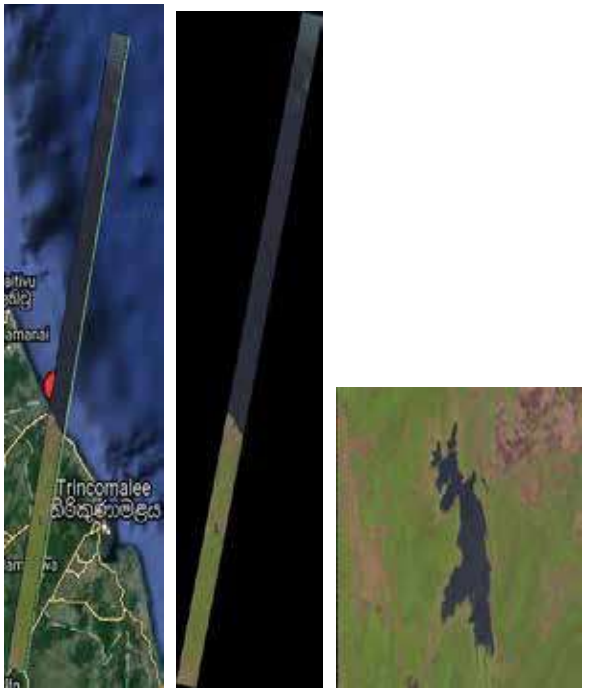


Figure 1 - (a) The geographical location of the study area (b) True color satellite image (c) The area chosen for classification.

Table 1 - Latitudes and Longitudes of the Chosen Region.

	Latitudes /°N	Longitudes /°E
Upper left corner	10.146810	81.251940
Upper right corner	10.133729	81.319533
Lower left corner	8.137243	80.818856
Lower right corner	8.124515	80.886088

Table 2 - The Structure of Data Files.

Col no.	Availability of Neighbouring pixel information								Spectral information			
	N	NE	E	SE	S	SW	W	NW	1	2	-	242
1 st index												
2 nd index												
3 rd index												
-												
262 nd index												

The Geo 'TIFF' images hence obtained was of resolution 7481 X 1851 pixels of which each pixel covers a geographical area of 30m X 30m. The data included in the images were radiance values of the respective wavelengths scaled by 40 for images obtained through the VNIR camera in the range of wavelengths from 400 nm to 1400 nm (bands 1 - 70) and by 80 for images obtained by the SWIR camera in the range of wavelengths from 900 nm to 1700 nm (bands 71 - 242) [6].

The true colour image, showed the region consists of foliage, water bodies and soil mainly.

3. Preprocessing

Preprocessing is deemed to be an important stage prior to any data analysis with the intention of providing qualitative and more productive data [7]. Preprocessing included extraction of data in a useful manner while removing the uncalibrated sets of data as indicated in [5] and conversion of the radiance values of the Geo 'TIFF' images to reflectance.

3.1 Extraction of Data

It is well evident that the useful information in the image is limited to a much less region compared to the total size of the image (approximately 14%) as seen in Figure 1 (b). Hence in order to improve efficiency and to the memory optimization, the important data were extracted in the following manner.

MATLAB® variable files (.mat) containing arrays of size 262 x 251 each, were created for each information containing row of the image in the structure shown in Table 2. Finally the uncalibrated data were removed creating a final matrix of size 262 X 207.

3.2 Conversion of Radiance to Reflectance

In Hyperspectral image analysis reflectance values of closely lying bands are used and hence the radiance values obtained from the raw data set had to be converted to reflectance values prior to any process of analyzing. The conversion process was done using [4],

$$\rho = (\pi \cdot L_{\lambda} \cdot d^2) / (ESUN_{\lambda} \cdot \cos \theta_s), \quad \dots (1)$$

where,

ρ = unitless planetary reflectance,
 L_{λ} = spectral radiance at the sensor's aperture,

d = Earth-Sun distance in astronomical units,
 $ESUN_{\lambda}$ = Mean solar exoatmospheric irradiances,

By substituting the spectral radiances obtained from the extracted data upon scaling with the scaling factors provided for the respective range of wavelengths, (1/40 for the first 70 spectral components and 1/80 for the rest) the earth-sun distance from, mean solar exoatmospheric irradiances and the Solar zenith angle based on the location, date and time of which the images were captured, obtained from [8], the respective reflectance values were obtained. Since the image spans across a small region and as the zenith angle doesn't vary considerably in the range of interest, the zenith angle was assumed to be constant throughout the region of interest.

4. Algorithm

Using the pre-processed Hyperspectral Image data obtained as mentioned in the above section, the land cover in a strip of the north eastern region of Sri Lanka was classified under 'soil', 'vegetation', 'water bodies' and 'mixed regions'. A total of 43975 pixels were individually classified with the aid of mathematical and statistical concepts and the tools available in MATLAB®. The pixels that did not have a prominent class were classified as 'mixed pixels' and the percentage of each end member (soil, vegetation and water) was calculated for such pixels.

The pre-processed Hyperspectral data contained reflectance values of 198 spectral bands for each pixel. These pixels were represented as points in a 198 dimensional space, in which the dimensions corresponded to the reflectance values of each spectral band. Since the algorithm requires normalized data for the classification to be completely based on the spectral characteristics of the image, the spectral signatures [9] of each of the pixels were shifted downwards, to have a mean of zero and were divided by the standard deviation of the reflectance values of each pixel.

As the large amount of data availability caused redundancy as well as complexity, along with the ability to detect fine features of the images, the 198 dimensional space was transformed into a 20 dimensional space which maximized the scatter of the pixels using principal component analysis (PCA) [3], [10], [11].

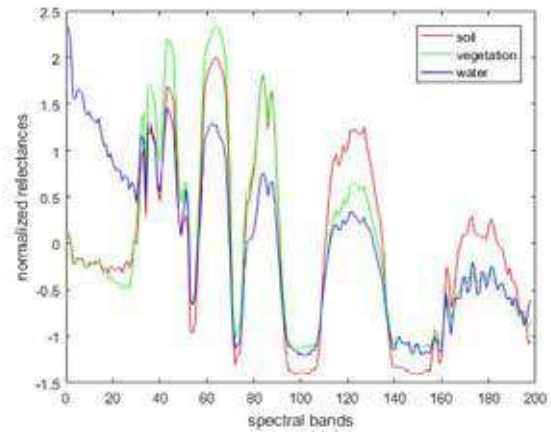


Figure 2 - Spectral signatures of the three classes soil, vegetation and water bodies, using the training sample data in the original space.

In order to find the transformation matrix for the dimensionality reduction, a training sample of 60 pixels were chosen, 20 from each class [12]. This selection was done with the aid of google maps and the image processing tools available in MATLAB®. The spectral signatures of the three classes based on the training sample data (considering the original spectral space) are shown in figure 1. The reduced space was obtained by using the PCA equations [3], [10], [11] given by,

$$C = E\{(X_n - \mu)(X_n - \mu)^T\} \quad \dots(2)$$

$$C = \frac{1}{N} \sum_{n=1}^N (X_n - \mu)(X_n - \mu)^T \quad \dots(3)$$

$$CV = \lambda V \quad \dots(4)$$

where,

C = covariance matrix, (198×198),

E = expected value operation,

X_n = vector representing the normalized 198 spectral band information (reflectance) of a pixel, (198×1),

μ = vector representing the mean spectral information (normalized reflectance) of all pixels, (198×1),

N = number of pixels in the training sample (60),

V = eigenvector of the covariance matrix, (198×1),

λ = eigenvalue of the covariance matrix.

The first 20 eigen vectors corresponding to the largest 20 eigen values were stacked as rows in the transformation matrix that transforms the original 198 dimensional space into the 20 dimensional space with maximum pixel scatter. The transformation matrix is given by,

$$TR = [V_1 \ V_2 \ V_3 \ \dots \ V_{20}]^T \quad \dots(5)$$

where,



TR - Transformation matrix,
 $V_1, V_2, V_3 \dots V_{20}$ - eigenvectors of the
covariance matrix.

All the pixels including the training sample, were transformed to the new reduced dimensional space using the transformation,

$$P1 = (TR) P \quad \dots (6)$$

where,

P = Matrix representing the pixels (in columns) in the original space (198x43925),
 $P1$ = Matrix representation of pixels (in columns) in the reduced space (20x43925).

The pixels are now represented as points (vectors directing to specific points) in a 20 dimensional space. The direction of each of these vectors characterizes the spectral behavior of the pixels compared to the magnitude of the vectors, as the magnitudes of the reflectance values could differ due to the effects of the environment, sensing equipment etc. Based on that conclusion, the direction of the vectors was selected as the basis of the classification algorithm. For this, the vectors representing all the pixels, including the training sample, were divided by its magnitude to convert them into unit vectors. Now all the pixels are represented as points (unit vectors directing to each of the points) on the surface of a sphere of unit radius, in a 20 dimensional space. The equation for obtaining the unit vectors is given by,

$$\omega = \frac{w}{|w|} \quad \dots (7)$$

where,

ω = Unit vector in the reduced space
 w = Original vector in the reduced space
 $|w|$ = Magnitude of the original vector in the reduced space

The reference spectral signatures (reference vectors) for the three classes were chosen to be the three mean unit vectors obtained by each of the 20 pixels in the training sample, from each class. The difference between each vector representing a pixel on the unit sphere and the three reference vectors were calculated to form a distance vector for each pixel, which is given by

$$\delta = (|\omega - \omega_s| \quad |\omega - \omega_v| \quad |\omega - \omega_w|)^T \quad \dots (8)$$

where,

δ = the distance vector
 ω = unit vector representing a given pixel
 ω_s = unit vector representing the reference spectral signature of soil

ω_v = unit vector representing the reference spectral signature of vegetation
 ω_w = unit vector representing the reference spectral signature of water

Since the requirement is to obtain a measure of affinity, the reciprocal of the distances was considered for the classification. The vector representing the percentage affinity of a given pixel, to the reference spectral characteristics of the three classes is given by,

$$\gamma = \begin{matrix} \frac{1}{|\omega - \omega_s|} \\ \frac{1}{|\omega - \omega_v|} \\ \frac{1}{|\omega - \omega_w|} \end{matrix} \quad \dots (9)$$

where,

γ = percentage affinity vector and the other terms are the same as before.

The unmixed pixels were selected using a threshold for the largest affinity percentage as follows.

$$\tau = \max(\gamma) \quad \dots (10)$$

Where γ is the maximum affinity percentage of the affinity vector .

If $\tau \geq 50\%$, the pixel under consideration was classified under the class which has the maximum affinity with it.

If $\tau \leq 50\%$, the pixel was labeled as 'mixed' and the percentage of each end member (soil, vegetation and water) was obtained by the percentage affinity vectory.

5. Results and Discussion

A portion comprising of 43925 pixels, of the image of a strip along the North Eastern region of Sri Lanka, taken by the Earth Observing - 1 satellite's Hyperion sensor was initially classified under soil, water and vegetation, based on the HSI data of the image. An algorithm based on classical feature reduction techniques, was used for the aforementioned classification. The results of the classification are tabulated in Table 3 and represented using a pie chart as in Figure 3 and the recreated image generated is shown in Figure 4 of which soil is represented in red, vegetation in green and water in blue which is comparable with the original true colour RGB image in Figure 1 (c).

Table 3 - Number of Pixels belonging to each Class

Substance	Soil	Vegetation	Water
Number of pixels	13236	27026	3663

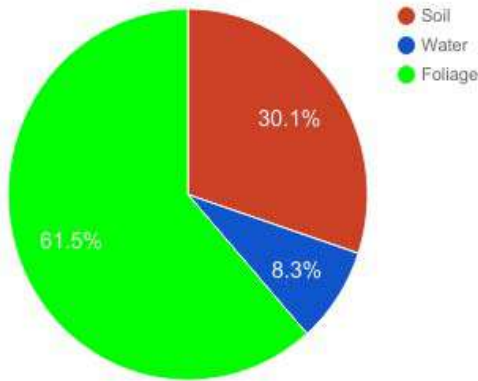


Figure 3 - Percentage of each substance in the chosen part of the image

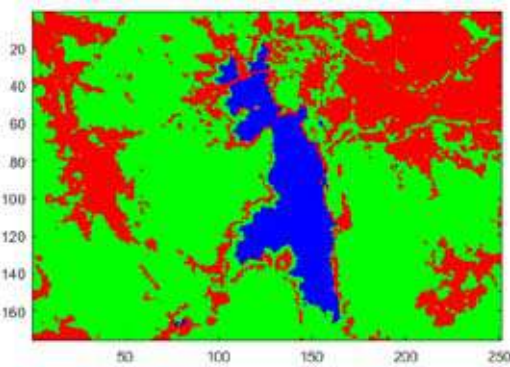


Figure 4 - Recreated image based on the results of Classification

However, it was evident that most of the pixels had more than one substance within the pixel. This is expected, as the size of a pixel correspond to an area of 30m x 30m. Even though the pixels have more than one substance, the substance that covers the majority of the area of the pixel was taken as the class of that specific pixel in this step. This practical interpretation corresponds to the shortest euclidean distance between the pixel and the three pure substances in the feature space.

Subsequently, the pixels which didn't have a majority percentage of affinity greater than 50%, was considered to be mixed, that contained substances belonging to more than one class. The mixed pixels hence identified, are shown in Figure 5 in yellow. The percentage of each end member; soil, vegetation and water are depicted through

Figure 6, 7 and 8 respectively.

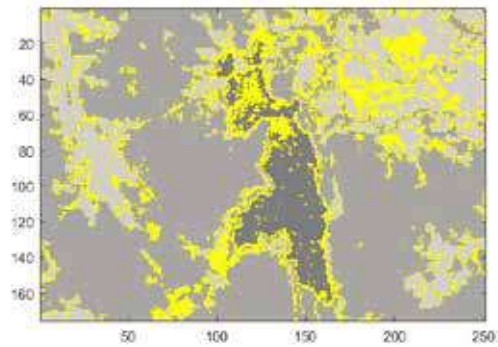


Figure 5 - Mixed pixels identified in the Recreated Image

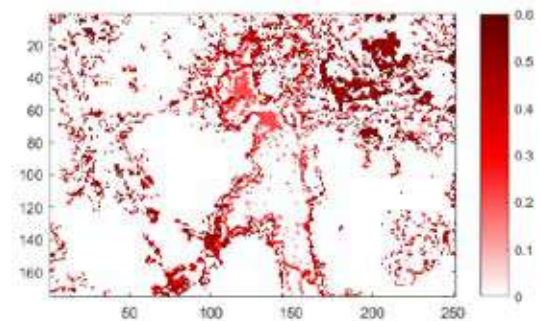


Figure 6 - Percentage of soil in each mixed pixel

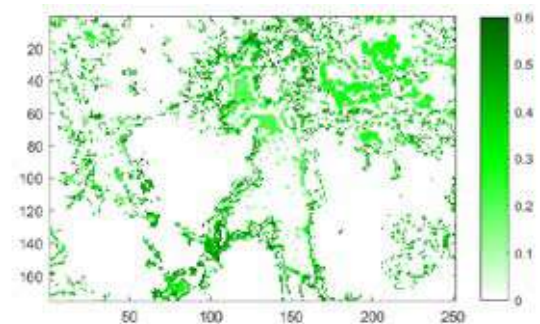


Figure 7 - Percentage of vegetation in each mixed pixel

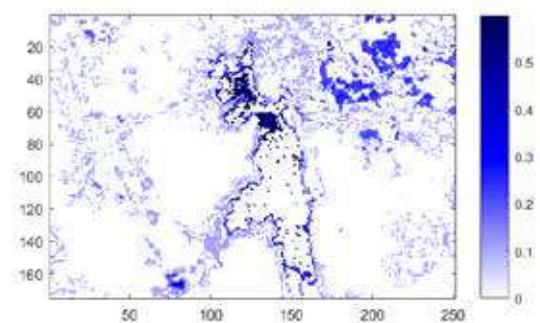


Figure 8 - Percentage of water in each mixed pixel



6. Conclusion

Since hyperspectral image data contains fine data which is indeed necessary for a fine classification, HSI image data analyzing approach results in better classification. The image considered in this paper consisted of 198 spectral bands which had calibrated data. Hence, it is possible to select the most useful spectral bands for better classification. However, excess information could also be challenging, especially in cases with computational limitations. In this paper, an algorithm which is based on the classical dimensionality reduction algorithm PCA and transformation of the spectral data of each pixel onto a unit sphere have been used in a logical manner as explained in the body of the paper. The classification algorithm in classifying the pixels was a combination of PCA and a comparison of mean spectral signatures of the training data set with unlabeled pixels based on euclidean geometry focusing on the directions of the vectors solely. The classification process resulted in an image similar to the true RGB image. It could further be concluded that, the part of the image of a strip in North Eastern Sri Lanka is mainly covered by soil, followed by foliage while water bodies are much less in the region of consideration. Considering the pixels that were classified as mixed, it could be concluded that the mixed pixels tend to appear mainly around borders of clustered pixels belonging to the same class.

Acknowledgement

We are immensely grateful to the United States Geological Survey (USGS) for making available the Hyperspectral images obtained by the EO - 1 satellite's Hyperion sensor and other related data which were used in applying the algorithm discussed in this paper.

References

1. Clark M. and Kilham, N. "Mapping of land cover in Northern California with simulated hyperspectral satellite imagery," *ISPRS J. Photogramm. Remote Sens.*, vol. 119, pp. 228-245, 2016.
2. Ntouros, K. D. Gitas, I. Z. and Silleos, G. N. "Mapping agricultural crops with EO-1 Hyperion data," presented at the Hyperspectral Image and Signal Processing: Evolution in Remote Sensing, 2009. WHISPERS '09. First Workshop on, Grenoble, France, 2009, pp. 1-4.
3. Zabaiza J. *et al.*, "Novel Folded-PCA for improved feature extraction and data reduction with HSI and SAR in remote sensing," *ISPRS J. Photogramm. Remote Sens.*, vol. 93, pp. 112-122, 2014.
4. "USGS EO-1." [Online]. Available: <https://eo1.usgs.gov/>. [Accessed: 11-Jan-2017].
5. Simon, K. "HYPERION LEVEL 1GST (L1GST) PRODUCT OUTPUT FILES DATA FORMAT CONTROL BOOK (DFCB) Earth Observing-1 (EO-1)." USGS Center for Earth Resource Observation and Science (EROS) Sioux Falls, South Dakota, Apr-2006.
6. Griffin, M. K. ., Hsu, S. M., Burke H., Orloff, K. S. M., Upham, C. A. and Misra, B. "Examples of EO-1 Hyperion Data Analysis," Lincoln Laboratory, MIT, Lexington, Massachusetts, HTAP-21, Jan. 2005.
7. Vaiphasa, C. "Consideration of smoothing techniques of hyperspectral remote sensing," *ISPRS J. Photogramm. Remote Sens.*, vol. 60, no. 2, pp. 91-99, 2006.
8. N. US Department of Commerce, "ESRL Global Monitoring Division - Global Radiation Group." [Online]. Available: <https://www.esrl.noaa.gov/gmd/grad/solcalc/>.
9. Filipczuk, P., Krawczyk, B. and Woźniak, "Classifier ensemble for an effective cytological image analysis," *Pattern Recognit. Lett.*, vol. 34, no. 14, pp. 1748-1757, Oct. 2013.
10. Tyo, J. S., Konsolakis, A., Diersen, D. I. and Olsen, R. C. "Principal-components-based display strategy for spectral imagery," *IEEE Trans. Geosci. Remote Sens.*, vol. 41, no. 3, pp. 708-718, Mar. 2003.
11. Raiko, T., Ilin, A. and Karhunen, J., "Principal component analysis for large scale problems with lots of missing values," presented at the 18th European Conference on Machine Learning (ECML 2007), Warsaw, Poland, 2007.
12. Tharshini, G., Dinesh, G., Godaliyadda, G. M. R. I. and Ekanayake, M. P. B. "A Robust Expression Negation Algorithm for Accurate Face Recognition for Limited Training Data," presented at the 10th IEEE International Conference on Industrial and Information Systems, ICIIS - 2015, Colombo, Sri Lanka, 2015.

Spatial Modulation for Indoor MIMO Visible Light Communication System

U.G.R.K.W.S. Palitharathna, A.G.D.U.K. Samarasinghe, Y.M.L.D. Wijayarathna,
S.A.H.A. Suraweera and G.M.R.I. Godaliyadda

Abstract: Power light emitting diodes (LED) are widely used in interior lighting systems due to the high energy efficiency and convenience of use. In addition, visible light communication (VLC) systems use light emitting diodes for communication purposes exploiting their high frequency capability. Though VLC systems are capable of achieving higher speeds, implementing multiple-input multiple-output (MIMO) systems is challenging due to co-channel interference. This paper presents the design and implementation of a VLC MIMO system using spatial modulation technique to suppress the co-channel effect of parallel VLC Links. Proposed controlling system can be used to obtain the optimum performance.

Keywords: Visible light communication, spatial modulation, multiple-input multiple-output system.

1. Introduction

The need for a new medium of wireless communication has emerged to satisfy the increasing demand of faster and more secure wireless communication, as the radio spectrum is already crowded [1]. In order to fulfil these requirements, visible light communication (VLC) technology is being developed to modulate and transfer data using visible light where light emitting diode (LED) is used as the transmitter, while photodiode is the receiver.

As a result of latest technology, power LEDs are widely used in interior lighting systems due to their high power handling capability, high energy efficiency, high reliability, and long lifetime than normal LEDs [2,3,6]. In addition, high frequency capability of LED enables the LED to be modulated with high rate digital data. Exploiting these inherent features, existing LED lighting systems like interior lighting systems, traffic lights [4], and LED display units can be adopted to use VLC.

VLC systems use visible light spectrum which is from 380nm to 780nm in the electromagnetic spectrum for data transmission. Since this range of frequencies doesn't interfere with radio frequency (RF) communications, VLC is a better solution for RF spectrum overcrowding. VLC is more secure since it is confined to the area where transmitted light signal reached. Visible light has smaller wavelength compared to RF which makes VLC systems to operate even at 1Gbps [5,6,7]. These advantages have made

VLC to be used in indoor wireless communication systems and for underwater communication [8].

Even though there are lot of advantages, VLC has several challenges too. Effect of ambient light and other light sources, enabling duplex communication, non-line of sight effect, and enabling multiple input multiple output (MIMO) communication are the major challenges to be addressed [9,10,11]. Using an adaptive algorithm to remove time varying DC offset voltage component at the receiver, ambient light effect can be removed. Various frequency selective filters are being used to remove flickering effect, fluorescent lamp effect etc. Among various methods that have been presented, most practical methods to enable duplex communication is using visible light as downlink while infrared is up link.

MIMO technique is used to have multiple VLC links in the same indoor environment to achieve a network of communication channels. Also MIMO can increase the performance of the system.

Mr. U.G.R.K.W.S. Palitharathna, B.Sc. Eng. (Peradeniya), Temporary Instructor, Dept. of Electrical & Electronic Engineering, University of Peradeniya.
Mr. A.G.D.U.K. Samarasinghe, B.Sc. Eng. (Peradeniya), Verification Engineer, Synopsis Lanka (Pvt) Ltd, Sri Lanka.
Mr. Y.M.L.D. Wijayarathna, B.Sc. Eng. (Peradeniya), Engineer, SysmexEngineering (Pvt) Ltd, Peradeniya.
Eng. (Dr.) S.A.H.A. Suraweera, B.Sc. Eng. (Peradeniya), Ph.D. (Monash), Senior Lecturer at Dept. of Electrical & Electronic Engineering, University of Peradeniya.
Eng. (Dr.) G.M.R.I. Godaliyadda, B.Sc. Eng. (Peradeniya), AMIESL(Sri Lanka), Ph.D.(NUS), Senior Lecturer at Dept. of Electrical and Electronic Engineering, University of Peradeniya.



Even though there are various techniques are being used to achieve MIMO, spatial modulation [12, 13, 14] that also use the position of the transmitter for the communication can be efficiently used for VLC. Even though spatial modulation is mainly used for RF, it is not commonly used with VLC.

In this paper, the design and implementation methodology of spatially modulated VLC MIMO system is described. A VLC MIMO system was implemented using eight power LEDs as transmitters and eight photodiodes as receivers. Furthermore, spatial modulation technique and special lens arrangement was introduced to mitigate co-channel interference and increase robustness of the system. Proposed controlling system of the lens adjustment was used to optimize the performance of the system for dynamic spatial coordinates of the transmitter and the receiver.

Following sections of this paper will describe the design and implementation of the system. Basics of implementing a single VLC link are presented under Section 2. Next, under Section 3, spatial modulation is introduced. Under Section 4, design and implementation of spatially modulated MIMO system are introduced. Finally, under Section 5, results for the experimental setup are introduced.

2. Basics of the VLC Link

Design and implementation aspects of a single directional VLC link are presented in this section. In spite of having a transmitter and a receiver as in every communication system, VLC uses a power LED as transmitter and a photodiode as the receiver. Light emitted from LED is modulated according to the data signal. The major sub modules of the VLC system are shown in the Figure 1.

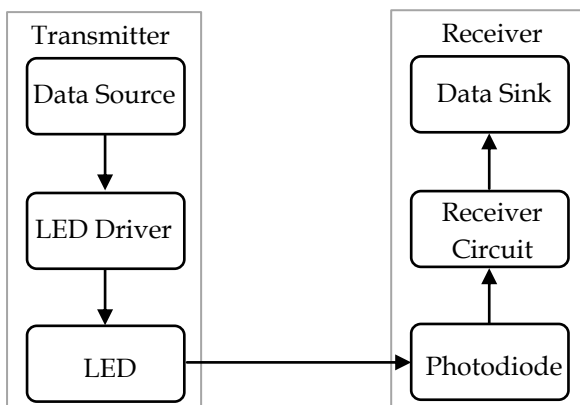


Figure 1 -Block diagram of the VLC link.

2.1. Theoretical Background

LED was assumed to be a Lambertian emitter where light intensity is constant along a circle and Lambertian emitter model was used to derive a mathematical equation for the power gain of the VLC channel for the geometric orientation shown in Figure 2 as follows [8]:

$$h = \frac{P_{TX}}{P_{RX}} = \frac{(m+1)A}{(2\pi d)^2} \cos^m(a) \cos(b) \quad \dots (1)$$

Where Lambertian order is given by,

$$m = -\frac{\ln(2)}{\ln(\cos(c))} \quad \dots (2)$$

Next, the maximum angle of the receiver with the vertical axis was derived to identify the geometrical limitations of the VLC link.

$$K = c - \tan^{-1}\left(\frac{x}{z}\right) \quad \dots (3)$$

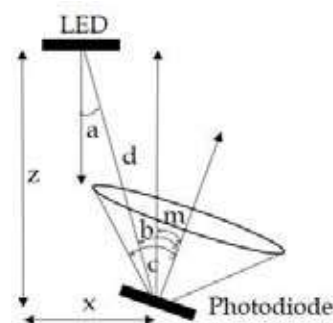


Figure 2 - Geometry of the VLC link.

Here, A is the detector physical area of the photodiode, d is the distance between the transmitter and the receiver, a is the angle of the line-of-sight (LOS) and the normal to the receiver, b is the angle between LOS and the vertical axis, c is the power angle at the receiver, K is the maximum tilting angle of the photodiode.

2.2. Transmitter

The main purpose of the VLC transmitter is to convert digital data signal into variation of light intensity. Modulated digital data stream to be transmitted is 0-5 V signal from the microcontroller. Since the power output from the microcontroller is not enough to drive a power LED, a LED driver circuit using 2N2222[15] power transistors is used to bridge the data source and the 1W power LED

transmitter due to high power handling and high frequency capabilities of transistors. On off keying (OOK) can be easily used for VLC systems. But due to variations of the data signal, the light intensity is changed with time making unnecessary fluctuations of light in indoor conditions. Pulse width modulation (PWM) is a good replacement for OOK. But since peak-to-average power ratio (PAPR) of PWM is 50%, pulse position modulation (PPM) which has a PAPR of 75% is used. In PPM, the light intensity is kept at a higher and constant value which is convenient for human eye. Four PPM patterns were selected to represent two bit data packet as shown in Figure 3.

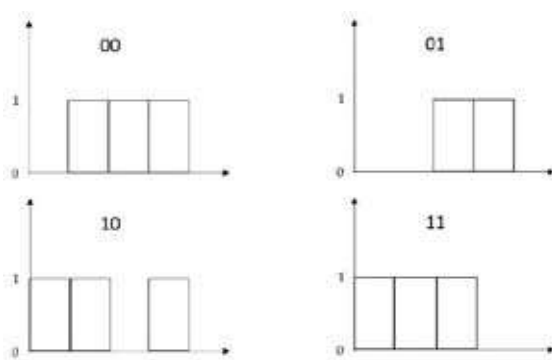


Figure 3 - PPM bit patterns.

2.3. Receiver

SFH 203P photodiode is used at the receiver as its spectral range of sensitivity is from 400nm to 1100nm which is in visible light range and it has high frequency capabilities [15]. Since the output of the photodiode is a current signal, it was converted to a voltage signal using a trans-impedance amplifier. The voltage output of the trans-impedance amplifier is fed into a microcontroller to extract transmitted data. Moreover, moving average and median filters are used at the microcontroller to remove noise components. DC voltage component due to the ambient light effect is removed by subtracting the minimum voltage from the received signal. Finally PPM signal was demodulated to get the original transmitted data signal.

2.4. Performance of the VLC link

Experiments were carried out to quantify the performance of the VLC link using bit error rate (BER) which is the most commonly used method in communication systems. BER was calculated taking the ratio between the numbers of bits received with an error and the total bits transmitted. Transmitter and receiver were placed in a vertical axis and BER was

measured for 200 kHz pulse stream by increasing the distance between transmitter and receiver in steps. Moreover, to observe the effect of BER having several LEDs at the transmitter, the number of LEDs at the transmitter were increased up to 3 by placing them in a circle with equal distances.

According to the results as shown in Figure 4, BER is higher for longer distances. With the increment of number of LEDs, BER can be reduced greatly. To achieve longer distance communication larger number of LEDs are needed.

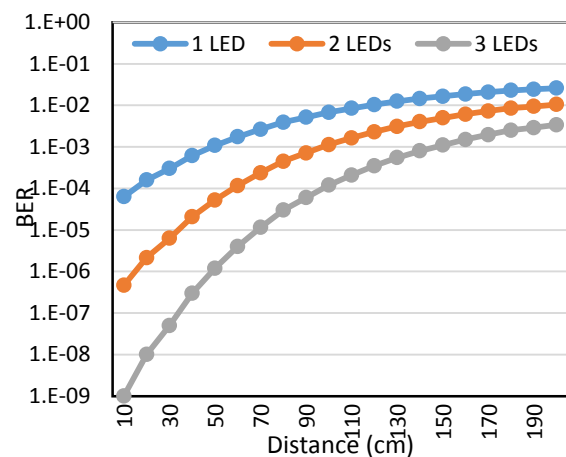


Figure 4 - BER vs. distance for VLC link.

3. Spatial Modulation

In MIMO VLC system multiple transmitters are transmitting and multiple receivers are used to receive signal on the same air channel [12, 13, 14]. Through this, parallel VLC links can be implemented to transmit different data streams. Even though phase shift keying (PSK), PPM can be used for multi-channel systems, they cause bandwidth to be reduced. To mitigate this effect spatial modulation technique can be used. Spatial modulation technique for four transmitters and four receivers are explained in Figure 5.



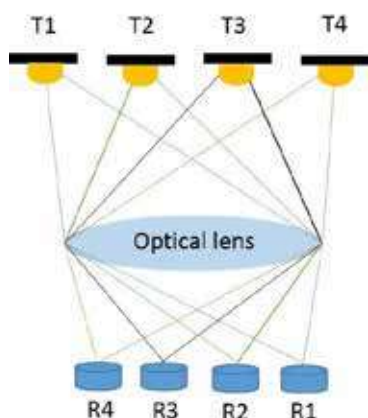


Figure 5 - Spatial modulation.

Four receivers R1, R2, R3, and R4 receive different data signals transmitted from T1, T2, T3, and T4 respectively. As an example optical lens focus light from T1 on R1 as shown in Figure 5. Due to the spatial distribution, R1 receives light signal only from T1. The interference from other transmitters are avoided using the optical lens arrangement. This method is used to differentiate distinct light signals from spatially distributed VLC transmitters in indoor environment.

4. Implementation of the Spatial Modulated MIMO system

Experiment setup for VLC MIMO link was designed and implemented to be able to handle eight different VLC channels. Block diagram of the MIMO system is shown in Figure 6.

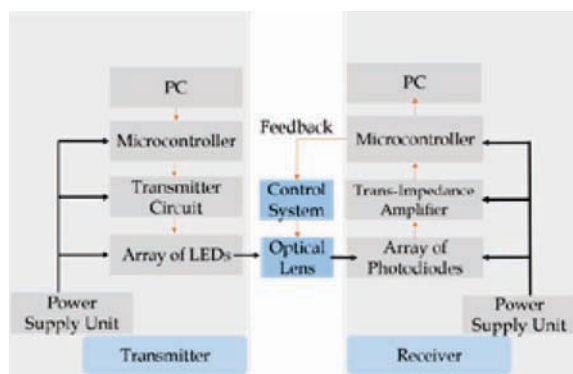


Figure 6 - Block diagram of experiment setup.

The transmitter consists of a power source, a microcontroller, LED driver circuit, and an array of eight LED transmitters each having three LEDs. The receiver consists of a power source, a microcontroller, trans-impedance amplifier, and eight photodiodes. In between the transmitter and the receiver an optical lens arrangement is used with the capability of moving along the vertical axis. Further, a

control system to control the position of the lens is implemented.

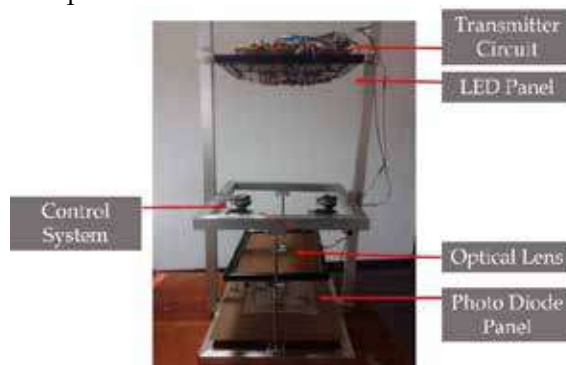
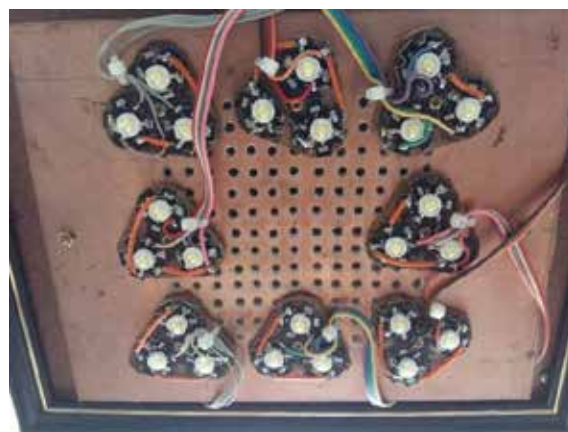


Figure 7 - Experiment setup.

4.1. Transmitter

Data that need to be transmitted are sent to the microcontroller using transmitting personal computer. In the microcontroller, data signals are separated into eight channels and modulated using PPM and are sent to the corresponding LED driver which is same as a single directional VLC link. Corresponding LED transmitters on the LED panel as shown in Figure 8 transmit the light signal. Each transmitter uses three power LEDs to have a higher light intensity at the receiver. The LED transmitter array was made in such a way that the x and y coordinates of a particular transmitter and the vertical distance of the transmitter from the receiver also can be



changed for experimental purpose.

Figure 8 - LED transmitter array.

4.2. Receiver

The receiver of the MIMO system has a photodiode bed which consists at least eight photo diodes to receiver transmitted signals as shown in Figure 9.

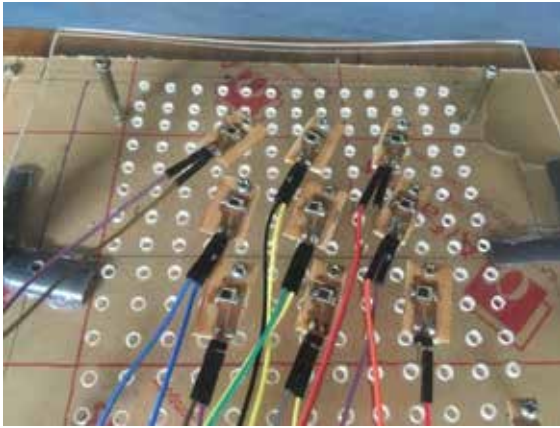


Figure 9 – Photodiode array.

Photodiode grid is made in such a way that the x and y coordinates of a photodiode can be changed. Those photodiodes are connected to a special receiver circuit with trans-impedance amplifiers for each photodiode separately. Outputs of the photodiodes are connected to an analog to digital converter. Digitized signals are fed into microcontroller to demodulate and separated data into each channel. After that those separate data signals are sent to data sinking personal computer using serial communication from microcontroller to the computer.

4.3. Optical lens

In spite of having eight transmitters and receivers, VLC needs modulation method to operate 8 channels at the same time since each channel make co channel interference from one to other. In spatial modulation double convex optical lens is used to reduce the co channel interference. In addition to the power level spatial modulation uses spatial distribution of transmitter and receiver. It can be easily derived using principles of optical lens. Focusing mechanism of double convex lens are shown in Figure 10.

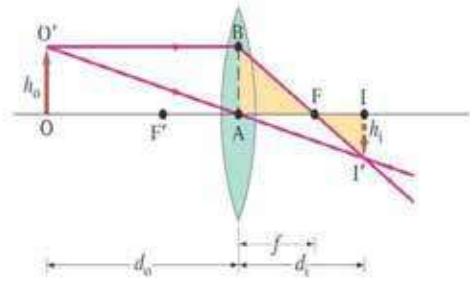


Figure 10 – Double convex lens arrangement.

Here O' is the position of the LED transmitter, I' is the position of the photodiode receiver, F is the focal point of the optical lens, d_o is the distance from LED panel to optical lens, d_i is the distance from photodiode panel to optical lens, f is the focal distance, h_o is the distance from axis of the optical lens to the LED, h_i is the distance from axis of the optical lens to the photodiode. Two equations can be derived using the principles of optical lens as follows.

$$\frac{1}{d_o} + \frac{1}{d_i} = \frac{1}{f} \quad \dots (5)$$

$$\frac{d_o}{h_o} = \frac{d_i}{h_i} \quad \dots(6)$$

Here f is known. For a particular spatial distribution of transmitter and receiver, since the angle between transmitter and receiver is known, h_o and h_i can be easily determined. Also $d_o + d_i$ is constant and can be determined. Using these two equations exact positions of the transmitting LED, receiving photodiode, and optical lens can be modelled. Position of the optical lens is fixed for optimum performance of the system.

4.4. Control system

Even though optimum lens position for static receiver can be calculated using above equations, when transmitter to receiver length changes optimum lens position changes. Special control system is designed that can be adopted to use with dynamic receivers to adjust the position of the lens before transmitting data. In this control system first transmitter transmit predefined bit sequence with ones and zeroes and optical lens moves using two servo motors from bottom to top while receiver calculates the output peak to peak voltage and stores in an array. Then maximum value among them is selected. Again lens moves from top to bottom. Once the maximum voltage with threshold value is reached it stops. Two limit switches are used to detect upper most and lower most



limits of the controller. Following algorithm is used on a separate microcontroller to detect the optimum position for the optical lens at a given instant.

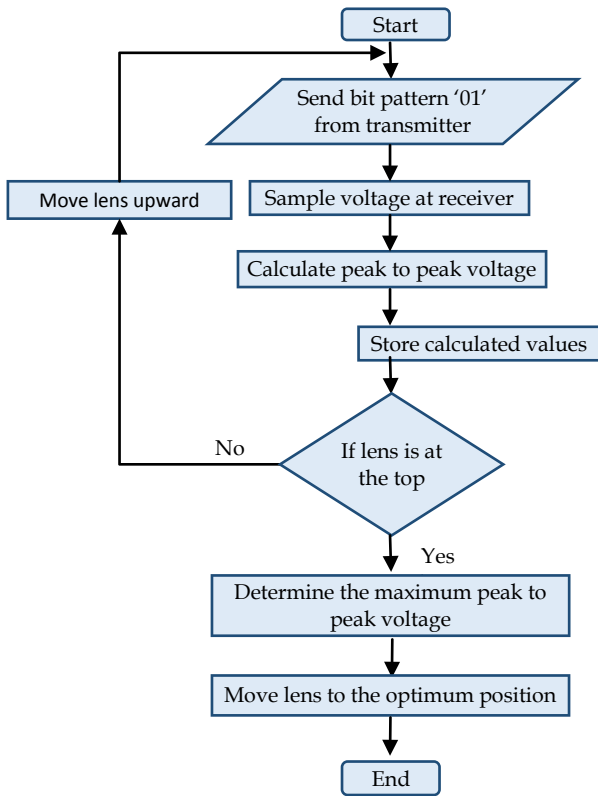


Figure 11 - Algorithm to detect the optimum lens position.

5. Experiment on performance

Even though spatial modulation method using optical lens enables multiple VLC links to be operated at same indoor environment without an interference, there are some disadvantages caused by this methodology. Specially, optical lens should be adjusted by the controlling system to get the light signal properly on to the effective area of the receiving photodiode. Otherwise there won't be any output at all. Also the distance between transmitter and the receiver, the distance among transmitters, and the distance among photodiodes are important factors to be considered. With proper performance analysis these effects can be identified.

To identify effect of different parameters on performance of the system set of experiments were done changing the parameters of the setup as shown in Figure 12.

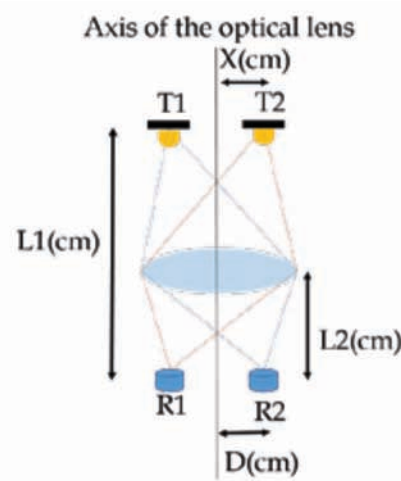


Figure 12 - Experiment setup.

Here X is the distance from axis of the optical lens to transmitting LED, $L1$ is the vertical distance between transmitter and receiver, $L2$ is the distance between receiver and optical lens. D is the distance between axis of the optical lens to receiving photodiode when peak voltage is detected.

Since at an indoor lighting systems transmitters are fixed, X was assumed to be fixed at 6cm. Also experiment was done for the static receiver assuming $L1$ to be 50cm. random data stream was sent from the transmitter at 200 kbps data rate.

The measured output peak to peak voltage at the output of the receiver $R2$ circuit with changing D for fixed $L2$ value at 10cm is as shown in Figure 13.

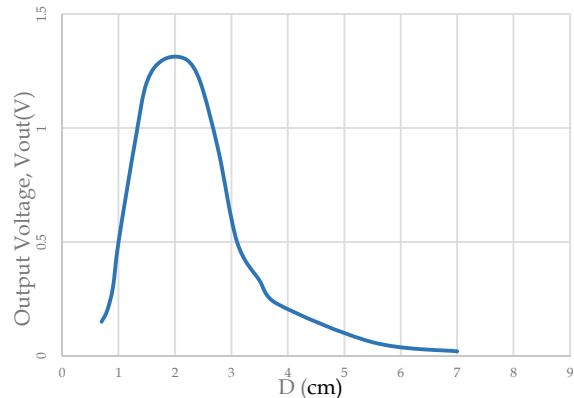


Figure 13 - Output peak to peak voltage (V) at $R2$ vs. D (cm).

According to the Figure 13, for a fixed position of the optical lens there is a peak value at the graph. It shows only at a particular D value it receives data. For $L2$ at 10cm this optimum value of D is 2cm. At that D value the performance of the system is very high. But with slightly changed D value output peak to peak voltage is low which results to have more errors at the receiving signal.

Next the D value was fixed at its optimum position which is 2cm for this setup and L2 was changed. The output peak to peak voltage was observed for different L2 values. Observed results are shown in Figure 14.

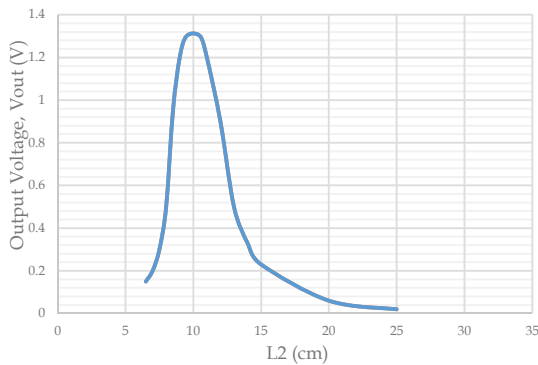


Figure 14 - Output peak to peak voltage (V) vs. L2 (cm).

According to the Figure 14 graph has a sharp peak at 10cm. Which means for fixed D value at 2cm, light signal focused on to the photodiode when L2 is 10cm. at slightly different L2 this system doesn't receive data well. This is a very important observation for this system. For a static receiver L1 is fixed. In practical situations D cannot be changed. Observing Figure 13 it was set to 2cm where L2 can be adjusted within the systems physical limits. Using this results for particular indoor environment D can be fixed considering Figure 13. For dynamic receivers, optical lens need to be adjusted to get the maximum output voltage at the receiver.

When designing a particular receiver for a spatially modulated VLC MIMO receiver, to limit its physical dimensions behaviour of L2 with D needs to be identified. For different L2 values D values at maximum output peak to peak voltage was observed by changing L2 values. Observed results are as in Figure 15.

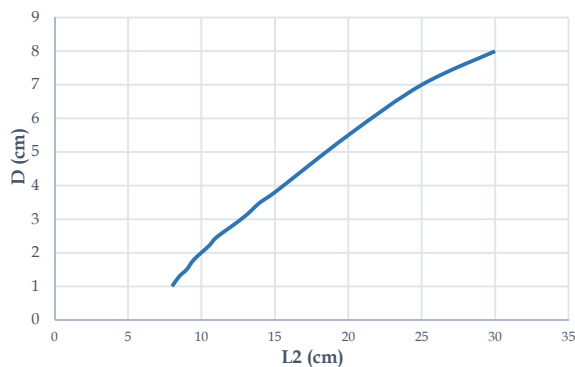


Figure 15 - D (cm) vs. L2 (cm).

Above results are important when designing a spatial modulated MIMO system. Designing parameters and dimensions of the system should be accordingly.

In this system BER is related to output peak to peak voltage. But for proper analysis BER value need to be observed. For the implemented system BER was measured at different L2 distances to ensure the performance of the system. Figure 16 shows the BER of the VLC MIMO system at different lens positions. Transmitter to receiver distance was set to 1m. X was set to 6cm and D was at 2 cm.

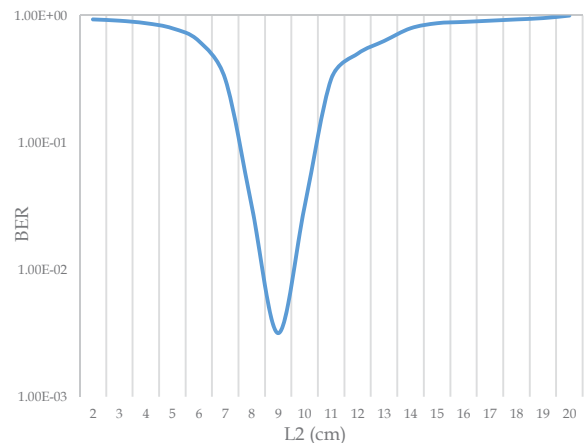


Figure 16 - Bit error rate vs. L2 (cm).

According to the Figure 16, optimum BER can be observed when light is focused on to the effective area of the photodiode.



(a) (b)
**Figure 17 - Light patterns at the receiver
(a) Focused, (b) Not focused.**

According to the Figure 17 when lights are focused on to the photodiodes sharp light pattern can be observed. It can be clearly seen that there is no interference when focused. When it is not properly focused light patterns interfere with each other resulting higher BER at each receivers.

6. Future work

For robust and continuous communication, adaptive algorithm for controlling system need to be implemented to optimize the spatially modulated MIMO system for continuously changing spatial coordinates of the receiver.



When extending this system for a mobile receiver closely placed photodiode array with more photodiodes need to be implemented to detect the small spatial variations of the receiver.

In this paper, the presented spatial modulation technique is applicable to downlink communication. However, in a complete communication system, both downlink and uplink needs to be operational. For the uplink infrared or RF can be used.

Moreover, the transmitters and receivers where designed as 2D arrays. However, there could be effects due to the 3D geometry of transmitters and receivers. To obtain the optimum performance of the system, geometric aspects of transmitters and receivers need to be further analysed.

In practical indoor environments, multipath, reflection, and refraction effect can occur due to shiny surfaces. To this end, suitable filtering methods are needed to remove the noise added due to the above effects.

7. Conclusion

In this paper, we presented a spatial modulation technique which can be used to implement parallel VLC channels in the same indoor environment without any interference from adjacent links. Although the implemented system works perfectly up to 200 kHz at a distance of 2m using general purpose electronics, using more sophisticated electronics, the system can be made to operate at a higher data rate.

The results of the paper demonstrate that co-channel interference can be mitigated using the developed spatial modulation technique. Also due to the use of optical lens arrangement to focus the light beam on each photodiode, effect from other light sources can be reduced.

This VLC MIMO technique can be used to implement an indoor wireless VLC MIMO system where several LED transmitters are mounted on the ceiling while receiving device is attached to the mobile device or personal computer on the use. Receiving device consists an optical lens and several photodiodes where light signals from different transmitters can be focused on to different photodiodes to reduce co-channel interference.

References

1. Karunatilaka, D, Zafar, F., Kalavally, V., and Parthiban, R., 'LED Based Indoor Visible Light Communications: State of the Art', *IEEE Communications Surveys & Tutorials*, vol. 17, pp. 1649 -1678, third quarter 2015.
2. Gancarz, J., Elgala, H., and Little, T.D.C., "Impact of Lighting Requirements on VLC Systems," *IEEE Communications Magazine*, vol. 51, no. 12, pp. 34-41, Dec. 2013.
3. Komine, T., and Nakagawa, M., 'Fundamental analysis for visible-light communication system using LED lights', *IEEE Transactions on Consumer Electronics*, vol. 50, no. 1, pp. 100-107, Feb. 2004.
4. Cailean, A., Cagneau, B., Chassagne, L., Topsu, S., Alayli, Y., and Blossville, J., 'Visible light communications: Application to cooperation between vehicles and road infrastructures', in *Proc. IEEE Intelligent Vehicles Symposium*, Alcalá de Henares, Spain, 2012, pp. 1055-1059.
5. Azhar, A., Tran, T., and O'Brien, D., "A Gigabit/s indoor wireless transmission using MIMO-OFDM visible-light communications," *IEEE Photon. Tech. Lett.*, vol. 25, no. 2, pp. 171-174, Jan. 2013.
6. O. Bouchet *et al.*, "Visible-light communication system enabling 73 Mb/s data streaming," in *Proc. IEEE Globecom2010 Workshops*, Miami, USA, Dec. 2010, pp. 1042-1046.
7. Grobe, L., Paraskevopoulos, A., Hilt, J., Schulz, D., Lassak, F., Hartlieb, F., Kottke, C., Jungnickel, V., and Langer, K., 'High-speed visible light communication systems', *IEEE Commun. Magazine*, vol. 51, no. 12, pp. 60-66, 2013.
8. Wang, C., Yu, H. Y., and Zhu, Y. J., "A Long Distance Underwater Visible Light Communication System With Single Photon Avalanche Diode," *IEEE Photonics Journal*, vol. 8, no. 5, pp. 1-11, Oct. 2016.
9. O'Brien, D. C., Zeng, L., Le-Minh, H., Faulkner, G., Walewski, J. W., and Randel, S., "Visible Light Communications: Challenges and Possibilities", in *Proc. IEEE PIMRC 2008*, Cannes, France, Sept. 2008, pp. 1.5.
10. Jovicic, A., Li, J., and Richardson, T., 'Visible Light Communication: Opportunities, Challenges and the Path to Market', *IEEE Commun. Magazine*, vol. 51, no. 12, pp. 26-32, 2013.
11. O'Brien, D., 'Visible Light Communications: Challenges and Potential', *IEEE Photonic Society 24th Annual Meeting*, Arlington, USA, 2011, pp. 365-366.

12. Di Renzo, M., Haas, H., Ghayeb, A., Sugiura, S., and Hanzo, L., "Spatial Modulation for Generalized MIMO: Challenges, Opportunities, and Implementation," *Proceedings of the IEEE*, vol. 102, no. 1, pp. 56-103, Jan. 2014.
13. Kumar, C. R., and Jeyachitra, R. K., "Power Efficient Generalized Spatial Modulation MIMO for Indoor Visible Light Communications," *IEEE Photonics Technology Letters*, vol. 29, no. 11, pp. 921-924, June 2017.
14. Alaka, S. P., Narasimhan, T. L., and Chockalingam, A., "Generalized Spatial Modulation in Indoor Wireless Visible Light Communication," in *Proc. IEEE Global Communications Conference (GLOBECOM)*, San Diego, USA, Dec. 2015, pp. 1-7.
15. Edirisinghe, E. S. S., Karunarathna, P. H. R. S. S., Dissanayake, D. M. T. B., and Godaliyadda, G. M. R. I. "Design and implementation of a bi-directional visible light communication system," in *Proc. IEEE 10th International Conference on Industrial and Information Systems (ICIIS)*, Peradeniya, Sri Lanka, Dec. 2015, pp. 519-524.



Energy Management System of a Solar Driven DC System

H.M.A.A.B. Herath, K.K.S.U. Kodithuwakku, D.R.D.S. Dasanayaka,
P.J. Binduhewa, J.B. Ekanayake and S.M.K.B. Samarakoon

Abstract: Today in the power sector the focus is shifting towards distributed power generation in the mode of renewable sources instead of fossil fuels. Solar photovoltaic is an attractive renewable energy source for Sri Lanka considering the location. Generation of solar power has some limitation with the time of the day as it only produces power in the day time. So, it is not going to be match with the load pattern of the consumer. There by this creates a need of a battery-storage for the non-power generation time. This sort of a system with a battery-storage creates a list of challenges which include intermittency of source, time of the day prices, sizing of solar panels and battery, limitations of charging and discharging rates of the battery. The task of the proposed system is to maximize the savings for the power consumer using some methodology. In order to do so, this paper introduces an algorithm for an energy management system of a Solar driven dc system. In fact this paper presents the decision making side of an Energy Management System which also includes a physical layer comprise of Power electronic converters. Outputs of the results of the system are fed into that controlling system's controllers as inputs. The charge controller of the battery uses this algorithm for making decision on charging or discharging of the battery or keeping it in the idle mode. Then the system commands when to use the grid and when to net meter the excess power. At the initial stage the algorithm is simulated in MATLAB with the use of realistic load and solar generation patterns. In the later stage a sensing circuit is developed to do a hardware simulation of the system. The proposed system with the algorithm helps in effectively deriving the potential benefits of a solar system with battery storage by providing an optimum usage routine.

Keywords: Algorithm, Solar, Battery, Load, Energy, Power, Management, MATLAB, Raspberry Pi

1. Introduction

Today all the Governments in the world are in search of ways to shift more of their power generating sources towards renewable energy sources. With the increased awareness of the depletion of traditional energy sources and environmental damage caused by increased carbon dioxide emissions from coal-fired power generation, the use of renewable energy has become the goal for energy development. Many countries have set a goal of increasing the usage of renewable energy above 20% of their total power consumption by the year 2020 [1]. Out of the renewable power sources solar energy is more straight forward, flexible and much easier to set up the power generation as well [2]. So, roof top solar turned out to a popular energy generation source. This also mainly due to the fact that roof top solar panels doesn't require a separate area and it can be easily installed on the roof of the power consumer's house or any sort of building. As the Solar power does not exist throughout the day there should be a proper management which utilize this renewable source generated power in the best possible manner. In order to do so battery storage need to be installed along with the solar

panels [3]. Today there are many solar power users use battery storages. Just having battery storage doesn't give the consumer all the available benefits of a solar power system. This is where an Energy Management System (EMS) is required to gain those available benefits.

The EMS should be with an effective algorithm which considers all the aspects related to gaining the benefits through the system. The base of the EMS should be cost as the amount of savings going to matter at the end of the day. So, initially the per unit power generation cost of each source was required to be calculated. Then the technical specifications of each power generating source need to be considered. Considering both of these aspects at a given time period Energy Management System should recommend the power sources usage to fulfil the load requirement.

Mr. H.M.A.A.B. Herath, B.Sc. Undergraduate at Dept. of E&E Engineering, Peradeniya.

Mr. K.K.S.U. Kodithuwakku, B.Sc. Undergraduate at Dept. of E&E Engineering, Peradeniya.

Eng. (Mrs.) D.R.D.S. Dasanayaka, B.Sc. Undergraduate at Dept. of E&E Engineering, Peradeniya.

Dr. P.J. Binduhewa, B.Sc. Eng. (Peradeniya), Senior Lecturer at Dept. of E&E Engineering, Peradeniya.

Eng. (Prof.) J.B. Ekanayake, B.Sc.Eng.(Peradeniya), Professor at Dept. of E&E Engineering, Peradeniya.

Eng. (Dr.) S.M.K.B. Samarakoon, B.Sc.Eng.(Peradeniya), Senior Lecturer at Dept. of Computer Engineering, Peradeniya.



This Paper presents an Energy Management System considering the above mentioned aspects. This study was done to implement the system on a Sri Lankan household consumer's power facility. As the electricity tariff household time based tariff was considered [4]. Initial implementation of the algorithm was done in MATLAB and the expected results were achieved. Then as the start of the hardware implementation the algorithm was implemented on a Raspberry Pi and the system gives a video output. This paper includes the work procedure up to that point. Here the raspberry pi model B was used. The MATLAB simulation results and hardware results are included in this paper.

2. Proposed distribution board and integrated Energy Management System

The Architecture of the power electronic interface is shown in Figure1. PV panel (Solar Panel), battery Storage and the utility supply are the power sources included in System and a household user's case is considered.

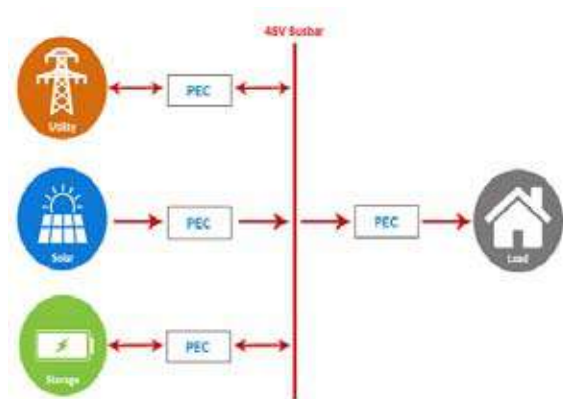


Figure 1 - Architecture of the System

The final output of our System is a set of decision to the Power Electronic Converters (PEC) which controls the power flow of the power sources whether to turn ON or OFF. At the start of the day a set of these decisions are given to the converters to follow throughout the day for an expected load and power generation pattern. Then the System monitors the decision set throughout the day and if a sudden change from the expected values is there, System is developed to react and change the set of decisions for the day from that point.

3. Development of load profile, PV profile and selecting Battery storage

3.1 Typical Load profile for a Domestic user

Power consumption of a medium type house in Sri Lanka is considered to develop the load profile in the proposed system. Table 1 shows the electrical loads in the house and their power ratings. For this analysis, it was assumed that dc-loads with power ratings given in Table 1 are used in the considered domestic house.

Table1 - Power Ratings of Electrical Loads

Appliance	Power Rating
Refrigerator	32W
Rice cooker	630W
Television	45W
Heater	1200W
Blender	110W
Laptop	40W
30W CFL (2 Nos)	60W
16W CFL (1 Nos)	16W
20W CFL (2 Nos)	40W
11W CFL (2 Nos)	22W

Following assumptions were made when developing the load profile. Even though the appliance like refrigerator, washing machine has varying power usage throughout the using time, an average on-off cycle for an appliance is considered [5]. A weekday load profile was considered. Further it was assumed that the people in the house start up their activities at 5 am and ends activities at 10.30 pm. Abnormal weather, national or international events were not considered in this study [6]. Figure 2 shows the load profile we have developed for a typical Sri Lankan household power consumer.

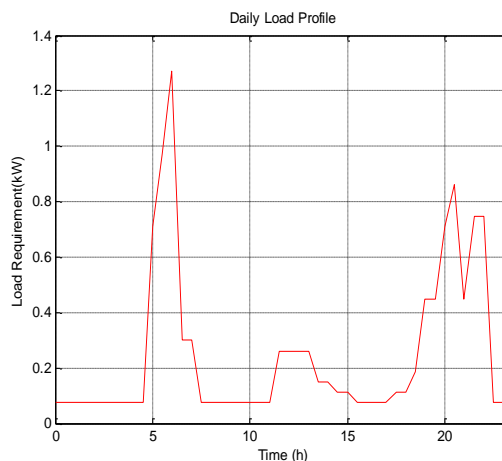


Figure 2 - Developed Load Profile

3.2 PV system power profile

Photovoltaic system is the local power generation source in the house. It was assumed that a rooftop 2 kW photovoltaic system is mounted. In this study, it was assumed that photovoltaic system consists of an inbuilt maximum power point tracker thus it always operates at its maximum power point [3]. So, any expected voltage or current variation in PV panel for the input power for our system is not considered. In order to generate the Power generation of the PV panel an irradiance level curve for a day is required. Irradiance is the solar power received by a surface for unit area. By considering Sri Lanka's earth positioning an irradiance curve for a day in Sri Lanka was obtained by applying Sri Lanka's latitude values to the Solar irradiance calculation equation set [7],[8]. The chosen day for the calculation was June 1st, the middle day of the year. As Sri Lanka is a country near to the equator, the day of the year doesn't matter much for the average irradiance curve for a day [7]. To account the effect of cloud cover for irradiance a sky clearness factor was used, which is the actual solar irradiation, divided by solar irradiation from a completely clear sky [9]. In our study, 3 cases considered as 100%, 60% and 40%. That means in our Energy Management System we are considering 3 types of days with 3 types of average cloud levels. This sky clearness factor causes to give wrong peak solar power generation values for a given time, but this gives an approximately correct PV energy value for the day. The MATLAB plots of these are shown in Figure 3.

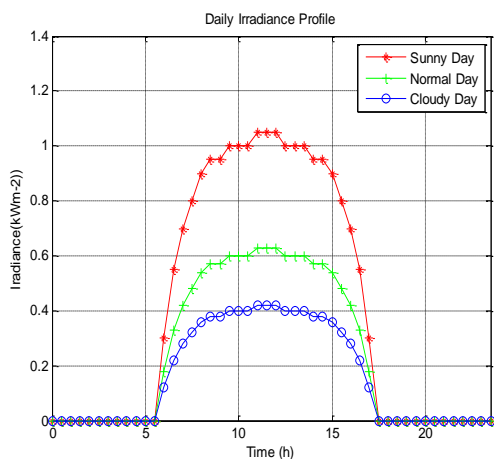


Figure 3- Daily Irradiance Profile of Sri Lanka

Using the Irradiance curve, the relevant power generation curve was obtained. For that temperature coefficient (TE) of the PV panel which is specified by the PV panel

manufacturer was used. Here, one average temperature value for the whole day is considered, deviations of temperature from that average value is not considered. The rated temperature of the PV panel is 25°C. The power generation of the PV panel is calculated through the following equations.

$$\text{For temperature, } T > 25 \quad \text{Power} = I \times 2 \times (1 - TE)^{(T-25)} \quad \dots(1)$$

$$\text{For temperature, } T = 25 \quad \text{Power} = I \times 2 \quad \dots (2)$$

$$\text{For temperature, } T < 25 \quad \text{Power} = I \times 2 \times (1 + TE)^{(25-T)} \quad \dots (3)$$

Figure 4 shows PV power generation profile for a cloudy day with 25°C average temperature.

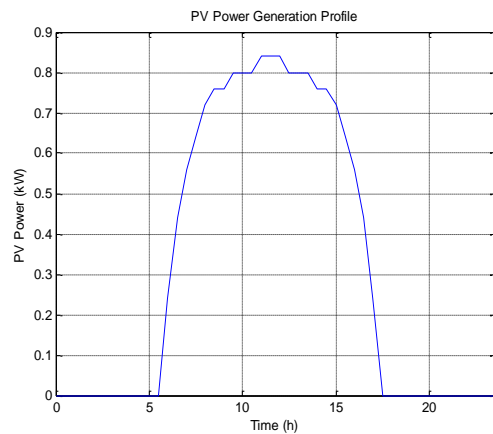


Figure 4 - PV Power Generation Profile

PV power generation cost is calculated by the following equation.

$$\text{Cost} = \frac{\text{Initial Installation Cost} + \text{Power Electronic Converters Cost}}{\text{Total Expected Power Units}} \quad \dots(4)$$

Selected PV panel generates 228kWh average per month and the guaranteed life time is 25 years, Installation and power electronic converters cost is LKR 650,000/= [10]. The calculation gave the answer as LKR 9.50/=.

3.3 Battery Storage

Most of the batteries used for PV systems are Lead acid batteries since they are cheap and they have a higher depth of discharge (DOD). Various types of Lead-acid batteries are available in the market and we have looked in to common electrical parameters of these batteries which include Battery Voltage, Charging and Discharging current, Number of cycles during the lifetime, Operating temperature, Capacity of the battery etc.



State of Charge (SOC) is an important factor required for the EMS as it decides whether to charge or discharge a battery. The SOC estimation methods available in the literature are open circuit voltage method, Specific gravity method, SOC estimation by battery impedance, Coulomb counting method [11]. In open circuit voltage method load needs to be disconnected before taking the measurement and it's not possible. Taking the specific gravity measurement of electrolyte is not practical at load conditions. To decide variation of battery impedance parameters with SOC needs lot of experiments. But coulomb counting method is much more practical to use in the proposed system since it determines the SOC by integrating the charging and discharging current over the time which is more simple and accurate.

$$\text{Unit Cost} = \frac{\text{Battery Price}}{\text{Energy per cycle} \times \text{No. of cycles}} \quad \dots(4)$$

By referring data sheets of industrial solar batteries, it was found that cycles of the battery are inversely proportional to the DOD. At higher DOD, total cycles of the battery are less and at lower DOD, total cycles of the battery are high [11]. According to the data obtained by the data sheet of DISCOVER 12VRE-300TF-L Battery, plot in Figure 5 was obtained in MATLAB simulations. In this study the effect of temperature is not considered.

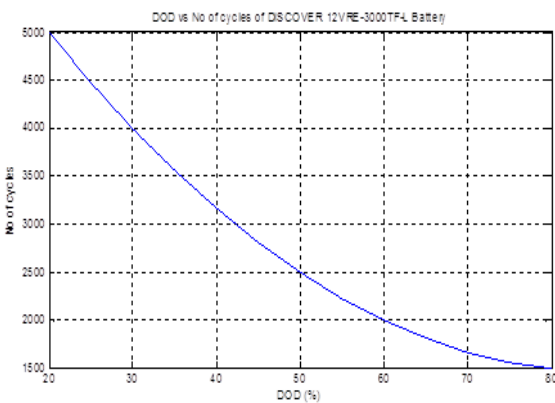


Figure 5- Battery cycles variation with DOD

By considering all of the above conditions, it was found that best DOD to operate the battery is 40% (60% of SOC). Figure 6 shows the plot obtained for the unit cost variation with DOD after a MATLAB simulation and it shows that cost is minimum at 40% DOD and the unit cost is LKR 16.50/= [12]. (200Ah Exide battery, LKR 31500/=, at 40% DOD)

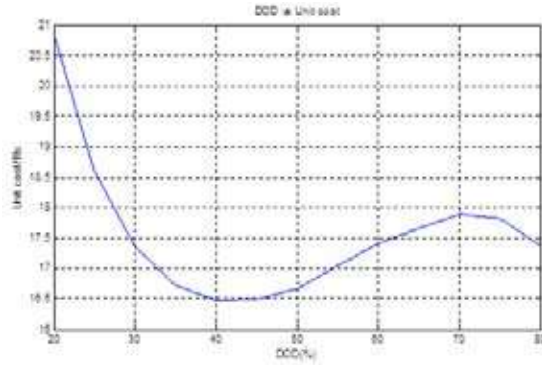


Figure 6 - Battery cost variation with DOD

4. Development of the Algorithm

This Proposed algorithm consists of cost and technical conditions. The main base is cost and main focus is cost reduction and increasing of savings. Initially we have defined the elements in our algorithm and those are of two kinds as fixed and variable. Fixed elements are initiated before the start of the algorithm and the variable elements either generated or changed with in the algorithm.

Fixed Elements:

Ebat,full	Battery Storage Capacity in kWh
Ebat,min	Minimum allowable battery storage level in kWh
Ichrg,rated	Battery charging current in A
Idchrg,rated	Maximum Battery discharging current in A
ChrgEff	Battery charging Efficiency
DChrgEff	Battery Discharging Efficiency
Cbat	1 kWh generation cost of Battery in LKR
Vbat	Battery Storage Voltage in V

Variable Elements:

t	time interval
Psolar,t	Generated Solar power at t in kW
PLoad,t	Load power requirement at t in kW
Ebat,t	Battery Storage level at t in kWh
Ichrg,t	Battery charging current at t in A
Idchrg,t	Battery discharging current at t in A
Cutility	1 kWh cost of the Utility Supply at t in LKR

Calculations:

$$I_{chrg,t} = \frac{(P_{solar,t} - P_{load,t}) \times ChrgEff}{V_{bat}} \quad \dots (5)$$

$$I_{dchrg,t} = \frac{(P_{load,t} - P_{solar,t}) \times DChrgEff}{V_{bat}} \quad \dots(6)$$

$$E_{bat,t+1} = E_{bat,t} + I_{chrg,t} \times V_{bat} \times \text{hours} \quad \dots (7)$$

$$E_{bat,t+1} = E_{bat,t} - I_{dchrg,t} \times V_{bat} \times \text{hours} \quad (8)$$

Load requirement and PV power generation for the considered time period and the current energy level of the battery storage are the inputs of the algorithm.

Figure 7 shows the algorithm we have developed for our Energy management System.

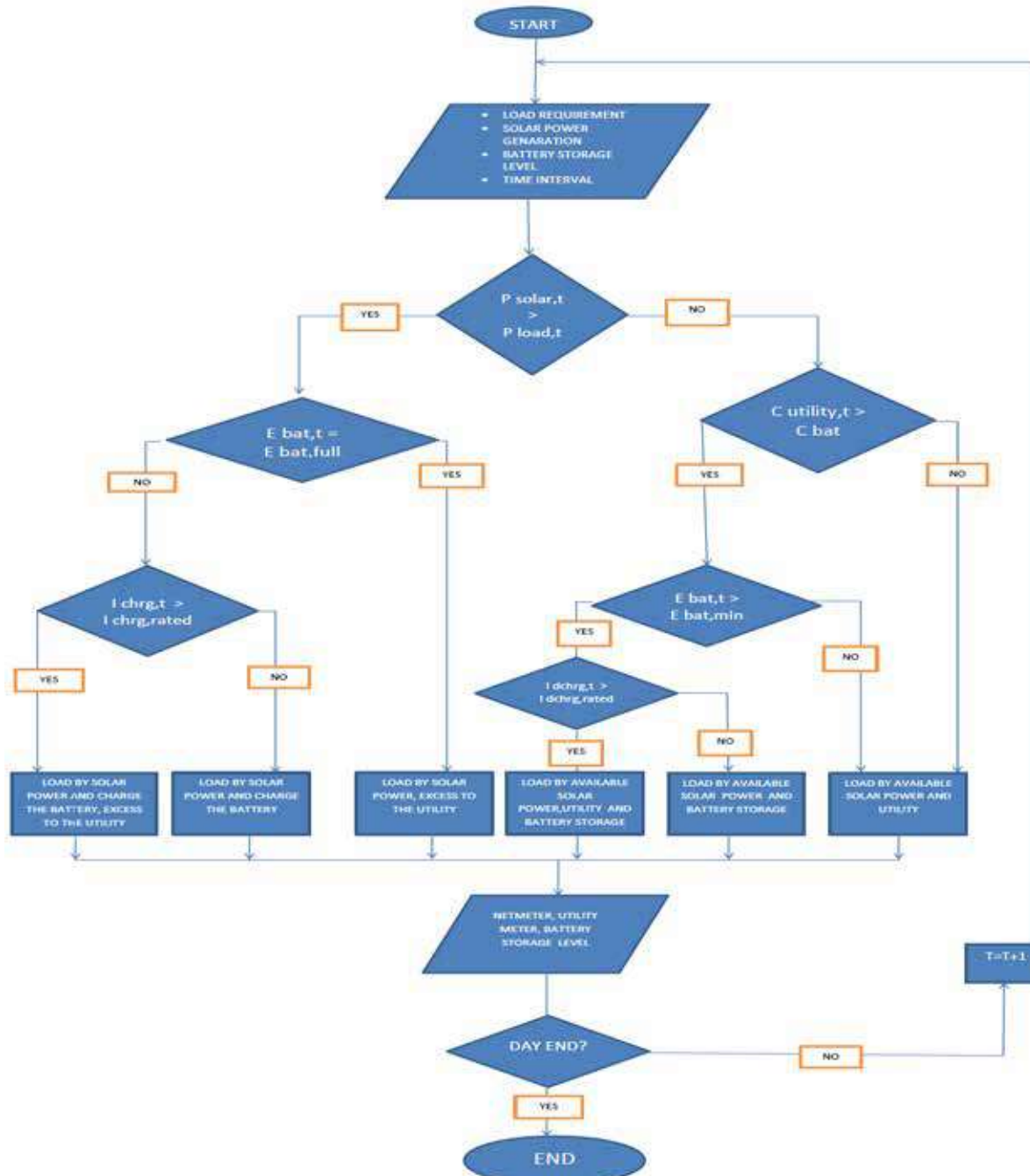


Figure 7 - Algorithm (1) For the Energy Management System

Out of the three available power sources it was evaluated that PV generation cost is the lowest. So, PV source stands above the rest two in any case. At the initial tier load and the PV power is compared and if PV power is greater total load of that interval is fulfilled by the PV power. In the next stage battery storage state is considered and if it is fully charged excess PV generated power is supplied to the utility. If

the battery is not fully charged excess PV power is used to charge the battery. If that charging current is higher than the rated battery charging current the remaining power is supplied to the utility. At the initial tier if the load is higher than the PV power there would be a PV power supply deficit. In order to cover that deficit next two options are considered. Per unit cost of both sources are compared and for



the whole day battery is a fixed value, but the utility cost changes with the time period [4]. That variation is shown in the Table 2.

Table 2 - Time of Day Tariff rates

Time Period/ hrs	Per kWh cost in LKR
2230-0530	13
0530-1830	25
1830-2230	54

If the utility is cheap the required power is fulfilled by the Utility. If the battery is cheap the battery storage status is checked and if it is

above the minimum allowable storage level battery is used to supply the power.

If the required current to the load is higher than the battery's rated discharging current utility supply is turned on and it is a situation where all the three supplies are with ON state decision. This algorithm runs for total number of time intervals for the day and Power source profiles of each source are generated. This happens at the start of the day and this sets the system a path to follow throughout the day.

If there is a sudden change in the value of the expected PV power value or Load value, EMS has an algorithm to react and to set up a new decision set. Figure 8 shows that algorithm.

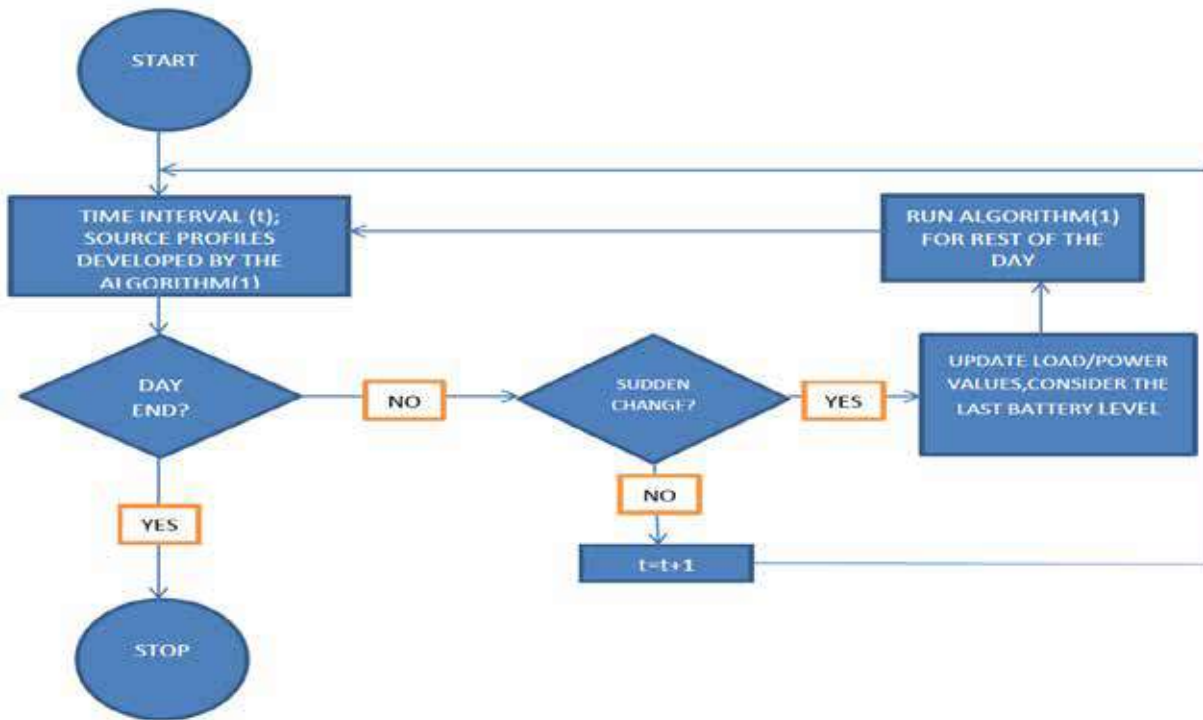


Figure 8- Algorithm (2) For the Energy Management System update for sudden Source changes

This algorithm was developed considering the fact that the only data affect to the next time cycle of the system is battery storage level. Both the load and the PV power values are independent of the future or past interval Values. So, what this algorithm does is update the change to the system, consider the battery storage level as the initial storage value and run the earlier algorithm for the rest of the day as the way did at the start of the day.

5. Results and Discussion

5.1 MATLAB Simulation

For the simulation of the algorithms, the time interval duration was considered as 5 minutes, which means 288 time intervals for a day. The two algorithms were simulated in MATLAB and the results are displayed in a plot. Figure 9 shows the implementation of the first algorithm which depicts the Power source and load profiles set by the Energy Management System at the start of the day for the Normal Day Case. 25°C was considered as the average temperature. Battery or Utility power is not required in the middle part of the day and they

are only ON in early morning and the later part of the day. Because of the utility cost variation with time of the day preference for battery and utility usage has varied and it is clearly shown in the plot.

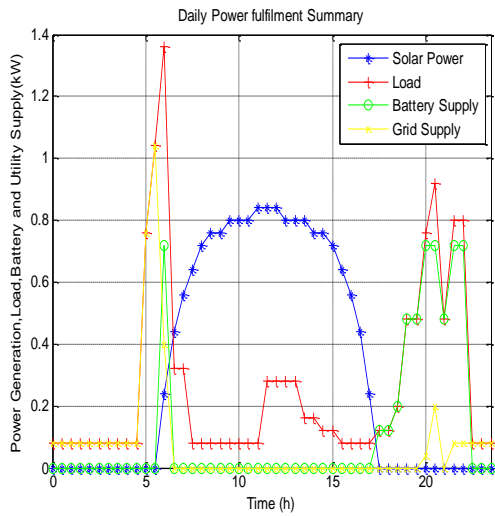


Figure 9- Algorithm (1) MATLAB Simulation

Figure 10 shows the implementation of the second algorithm in MATLAB. Here sudden changes to the solar power source and load were given (At 1300h PV power -400W, Load Requirement +400W/at 2100h Load Requirement -300W) and the plot for the day was obtained. These changes were given to the case we have considered in implementing the first algorithm. A comparison of the two plots figure 8 and figure 9 shows how our energy management system have reacted to a sudden changes in conditions. In the above expected profile battery is OFF at 1300h, Utility is ON at 2100h. In the new profile battery is ON at 1300h, Utility is OFF at 2100h.

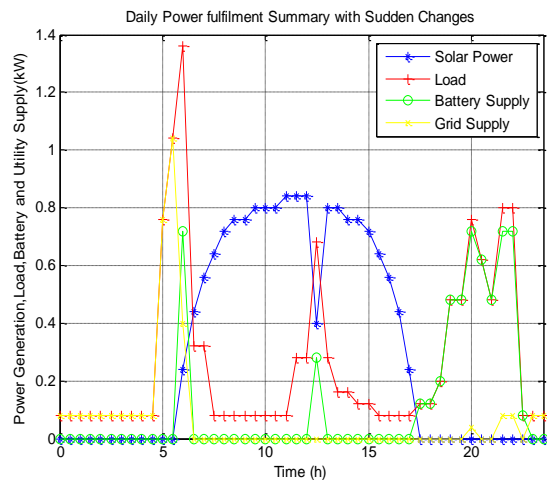


Figure 10 - Algorithm (2) MATLAB Simulation

5.2 Raspberry pi Implementation

The System Algorithm was also implemented on a Raspberry pi and Figure 11 shows a photo of the setup. Here raspberry pi is considered as our EMS and its output is displayed on the monitor. Figure 12 shows the Graphical interface developed to get a data entry from the user. If there is a considerable change from the Normal day routine for the next day the user can enter those specific cases to the system and he/she can build load pattern for the next day.



Figure 11 - EMS setup on Raspberry pi



Figure 12 - Load Profile User Interface

In this interface the major appliances of the user is given and the expected using time intervals can be selected. The interface also shows the load pattern as well as the expected power usage in values and the expected cost. So, the user can rethink on any of the plans on the power usage for the next day.

Implementation of the EMS algorithm on Raspberry pi was done and a screen shot of the video output obtained. It is shown in Figure 13. Here the raspberry pi gives a real time output of the System implementation the output is the four live plots of the power sources and the load.



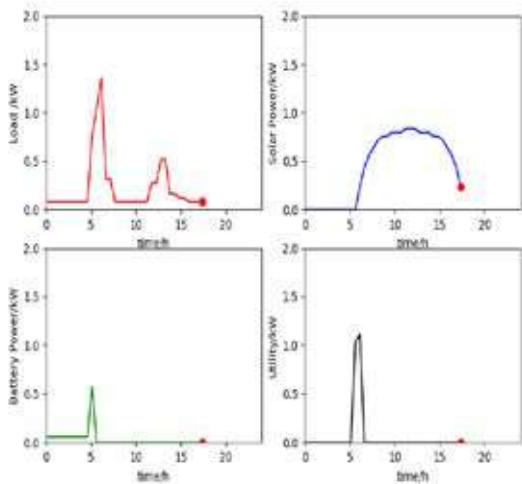


Figure 13- Real time Algorithm Implementation

These plots were plotted in real time and showed how the system shifts the sources within a day cycle. In the video output 24 hour day was scaled down to a 24 second time frame. Any time interval with the power value of any source is greater than 0 in these plots means that the system has considered ON decision for that source and if any power value is 0 means that either that power source is turned OFF by the system or it is not available.

5.3 Cost Comparison

A Cost comparison was done to show the potential benefits of our energy management System. For this comparison 4 cases were considered as for a normal utility user, normal solar power user, our EMS user with net metering connection and our EMS user with a net accounting connection. Equations for the cost calculations are as follows.

Normal Utility User

$$\text{Cost} = \text{Total Power Usage} \times \text{Time Based Utility Cost} \quad \dots(9)$$

Net Metering User

$$\text{Cost} = \text{PV generation} \times \text{PV unit Cost} + \text{Battery Usage} \times \text{Battery Unit Cost} \quad \dots(10)$$

Net Accounting User

$$\text{Cost} = \text{Utility Usage} \times \text{Time Based Utility Cost} + \text{PV generation} \times \text{PV unit Cost} + \text{Battery Usage} \times \text{Battery Unit Cost} - \text{Units to utility} \times \text{Net Accounting Rate} \quad \dots(11)$$

Solar and Utility User

$$\text{Cost} = \text{Utility Usage} \times \text{Time Based Utility Cost} + \text{PV generation} \times \text{PV unit- Units to utility} \times \text{Net Accounting Rate} \quad \dots(12)$$

In this comparison payment for a unit of a net accounting customer was taken as LKR 22/=, which is the rate which is only valid for the first 7 years of connection. Here, the cost for a month period was calculated and plotted. This comparison was done to a user with a load pattern which consumes 6 kWh per day, 180 kWh per month. Figure 14 shows the cost comparison and it clearly depicts that both types of EMS user have a considerable saving over the user who only uses the utility.

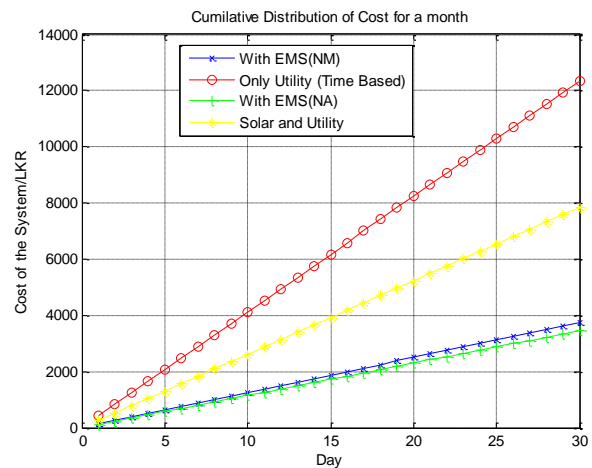


Figure 14- Monthly Cost Comparison

6. Conclusions and Future Work

In this study, an algorithm for an Energy management system was presented which controls the power system of a household with a utility connected solar power system and Battery storage. Software level implementation was completed and the hardware implementation would be developed around the Raspberry Pi with modelled PV panel and load modules. A Real system linked with the physical layer which sends decisions to the converters is to be developed. An algorithm which predicts the load pattern of the next day is to be added to the system. Adding the case of the power cut situation to the algorithm is under study and it would be added to the algorithm in the future. For further optimization of the system use of a FPGA instead of the Raspberry pi is to be considered.

References

1. Yu-Kai Chen, *Member, IEEE*, Yung-Chun Wu, Chau-Chung Song, and Yu-Syun Chen "Design and Implementation of Energy Management System With Fuzzy Control for DC Microgrid Systems" in *IEEE Transactions on Power Electronics*, VOL. 28, NO. 4, April 2013.
2. Sonal Gaurav, Chirag Birla, Aman Lamba, S. Umashankar, Swaminathan Ganesan, School of Electrical Engineering, VIT University, Vellore, 632014, India, Schneider Electric, Bangalore, 560072, India, "Energy Management of PV - Battery based Microgrid System", SMART GRID Technologies, August 6-8, 2015.
3. Nasim Jabalameh, Student Member, IEEE, Sara Deilami, Student Member, IEEE, Mohammad A.S. Masoum, Senior Member, IEEE, Farhad Shahnia, Member, IEEE "Rooftop PV with Battery Storage for Constant Output Power Production Considering Load Characteristics" in 2013 8th International Conference on Electrical and Electronics Engineering (ELECO).
4. <http://www.pucsl.gov.lk/english/news/press-release-3/>, Visited, 24th May 2017.
5. Manisa Pipattansomporn, Senior Member, IEEE, Murat Kuzlu, Member, IEEE, Safiur Rahman, fellow, IEEE, and Yonael Teklu, Member, IEEE "Load Profiles of major household appliances and their demand response opportunities".
6. Luo Chuan and Abishek Uku, Senior Member, IEEE "Modeling and Validation of Electrical Load Profile of Residential building in Singapore".
7. Anna Petrasova, Brendan Harmon, Vaclav Petras, Helena Mitsova of Center for Geospatial Analytics, North Carolina State University, Raleigh, NC, USA, "Tangible Modeling with Open Source GIS", Chapter 8 - "Solar Radiation Dynamics".
8. <http://www.pveducation.org/pvcdrom/calculation-of-solar-insolation>, Visited, 11th May 2017.
9. Exell, R.H.B., King Mongkut's University of Technology, Thonburi "The Intensity of Solar Radiation"-2000.
10. <http://www.jlankatech.com/net-metering-users/>, Visited, 24th May 2017.
11. Chang, W. Y., «The State of Charge Estimating Methods for Battery: A Review», *Int. Sch. Res. Not.*, vol. 2013, page953792, lug. 2013.
12. <https://www.quora.com/How-is-the-cost-for-batteries-per-kWh-calculated-Energy-storage-battery-companies-get-prices-of-800-per-kWh-for-their-cells-and-Tesla-says-their-Powerwall-costs-about-350-per-kWh-How-are-these-figures-calculated-with-grid-electricity-prices-around-0-12-per-kWh>, visited 27th May 2017.





Laser Ranging Based Intelligent System for Unknown Environment Mapping

T.H.M.N.C. Thelasingha, U.V.B.L. Udugama, E.M.S.P. Ekanayake,
G.M.R.I. Godaliyadda, M.P.B. Ekanayake, B.G.L.T. Samaranyake and
J.V. Wijayakulasooriya

Abstract: Autonomous systems are used in many applications like unknown terrain mapping, Reconnaissance, Explorations etc. in areas of impossible human access. They require an accurate and practically realizable Intelligent Navigation System(INS), which can handle the complexity in the environment and necessarily be ready for mobile platform implementation. Also, a method of error free localization is a major requirement for the practical realization of such a system. This work outlines implementation of a system, simple enough to be implemented on a mobile platform, focused on provision of a logical and computationally efficient algorithm which uses measurements from a Laser Range Finder (LRF) as input. Usage of LRFs for mapping is a trending research area in contrast to the usage of Ultrasonic Sensors with errors like cross talk and specular reflections or vision systems that are power hungry. As, the LRF readings too contain some noise due to reflectivity problems, methods were developed for pre-processing the measurements. INS analyses the data spectrum intelligently to determine the obstacle free path that should be traversed, which will in turn enable the mobile platform to canvas the whole environment and construct the map. Also, the localization methods have been implemented through usage of similarity transform and particle filter. The conceptual design was simulated in Python™ on Windows™ and was tested for robustness in artificially generated environments. Then the system was emulated in Python™ with real environment data fed from the LRF in real-time. Then it was implemented in the embedded system level in a Raspberry pi3™ on a 3WD Omni-directional mobile platform, and tested for real environments. Also, the separately running localization algorithm has been used to correct the generated map and the position of the platform. The system was able to generate a complete two-dimensional map of the locale accurately. A quantitative justification of the proposed methodology is presented in a comparative analysis of the execution time.

Keywords: Intelligent Navigation, LIDAR, Autonomous Mapping, Monte Carlo SLAM

1. Introduction

Environment mapping has been a key fact in endeavours like space explorations, excavations, disaster relief and reconnaissance applications. For that automation is highly essential when such tasks are carried out areas with restricted human access. Mapping an unknown environment autonomously has been an engineering problem that many researches have been focussed[1][2] on for years. For it to be successful, development has to be done in many fronts.

Initially a correct sensing method has to be implemented to sense the geometry of the environment. Many of the published work include the use of RADARs[3], SONARs[4], Vision systems and Laser Range Finders (LRFs)[5]. The use of methods like and SONARs are convenient for simple distance sensing but when considered for applications like mapping they contain much noise. Although vision sensors provide more accurate and vivid data spectrum of the environment,

the computational power required will make them less feasible for mobile platform implementation. In this work, a low cost LRF

Mr. T.H.M.N.C. Thelasingha, B.Sc. Eng. Undergraduate at Dept. of Electrical & Electronic Engineering, university of Peradeniya, Sri Lanka

Mr. U.V.B.L. Udugama, B.Sc. Eng. Undergraduate at Dept. of Electrical & Electronic Engineering, University of Peradeniya, Sri Lanka

Ms. E.M.S.P. Ekanayake, B.Sc. Eng. Undergraduate at Dept. of Electrical & Electronic Engineering, University of Peradeniya, Sri Lanka

Eng. (Dr.) M.P.B. Ekanayake, B.Sc. Eng. (Peradeniya), Ph.D. (Texas Tech, US), AMIE (Sri Lanka), Senior Lecturer at Dept. of Electrical & Electronic Engineering, University of Peradeniya, Sri Lanka

Eng. (Dr.) G.M.R.I. Godaliyadda, B.Sc. Eng. (Peradeniya), Ph.D. (NUS, Sg), AMIE (Sri Lanka), Senior Lecturer at Dept. of Electrical & Electronic Engineering, University of Peradeniya, Sri Lanka

Eng. (Dr.) B. G. L. T. Samaranyake, BSc Eng. Peradeniya, Tech. Lic & PhD KTH (Sweden), Senior Member IEEE, AMIE (SL), Senior Lecturer at Dept. of Electrical & Electronic Engineering, University of Peradeniya, Sri Lanka

Eng. (Dr.) J.V. Wijayakulasooriya, B.Sc. Eng. (Peradeniya), Ph.D. (Northumbria, UK), MIE (Sri Lanka), Senior Lecturer at Dept. of Electrical & Electronic Engineering, University of Peradeniya, Sri Lanka



[6]has been used as the distance sensor. A high-end sensor like Microsoft Kinect™ will render much accurate data but to keep the implementation realizable a simple sensor has been selected.

Another major problem is the method of traversing the unknown area. Various approaches like mobile robots and quadrotors[7] are possible solutions. But considering the accuracy and convenience in positioning and manoeuvrability an omni-directional 3WD mobile platform[8] has been used as the mapping agent in this work. It has been developed completely in house. And its size and the instant mobility in any direction due to omni directional nature has allowed it to traverse many complex environments effectively. A state feedback linearizing nonlinear controller has been implemented so that the platform can adjust itself to a given reference coordinate and orientation.

Additionally, a convenient sensor has been selected and a method of motion is developed. Most approaches lack a correct navigation system[1] where the agent can be guided through the obstacles in the environment so that it canvases the whole area. Obstacle detection[9]and traversable space identification methods[10] have already been developed. Also, algorithms for finding the minimum cost path has been developed for some time[11].



Figure 1 - The Practical Realization

But an approach to intelligently analyse the data from the distance measurements and decide the direction to be explored is a requirement. Hence a separate navigation algorithm has been developed which will analyse the information spectrum from the sensor and decides the path to be taken by the mobile platform to create a complete 2D overlay of the locale.

Here, to construct themap, the mobile platform traverses the area as guided by the navigation algorithm. And also the current position and

orientation of it will be computed and fed to the navigation system in order to find the direction it should travel in the next moment. But the errors in the measurements and actuation are always possible. Also, the encoder based position is prone to errors due to wheel slipping and data transmission errors. Hence, for correct localization and to provide a correction for the map data generated from the LRF, a separately running simultaneous localization and mapping (SLAM)[12] algorithm based on Monte Carlo approach has also been developed. It uses the LRF sweeps from short time frames when the agent traverses in its trajectory and correct the encoder based position estimate in real time.

The combined implementation of the above three aspects namely, the hardware setup (omni directional mobile platform and the LRF), the navigation and path planning algorithm and the SLAM algorithm has allowed to develop a successful attempt in generating a 2D overlay of an unknown obstacle filled environment. For the task of extension of the 2D map to a complete 3D map, incorporating a vision system would be an effective approach. Further research in this work would include such a combination.

2. The Hardware Implementation

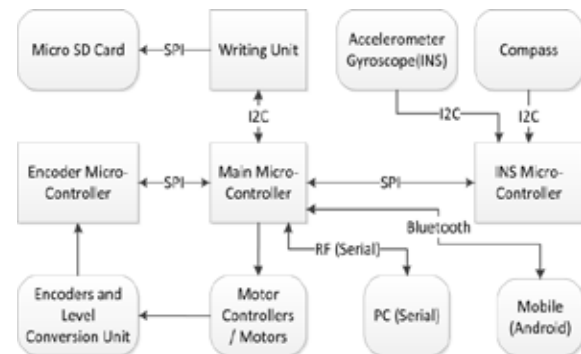


Figure 2 - The complete embedded system architecture

2.1 The Omni Directional Mobile Platform

The omni-directional mobile platform is the practical realization on which the proposed work has been implemented. It has been designed and constructed completely in house. A separate embedded system architecture has been developed, so that the control algorithms and also sensor fusion algorithms can be implemented on general purpose micro controllers. Also, the electronics of the system including the electronics of motor controlling

and other auxiliary systems has been implemented on a single board with sensor modules.

Here, it is to be noted that the usage of GPS is avoided as in the scenarios like explorations and excavations which the equipment is developed for, would not guarantee the availability of GPS everytime. An accurate estimation of the position and orientation of the mapping agent (pose or state) is obtained by fusing data from three different sensors that detect the orientation. The following sensors were used: a gyroscope (MPU6050), a compass (HMC5883L) and optical shaft encoders (OSE) (model - E50050030) attached to the wheels. To fuse the data from the above sensors, a centralized Kalman filter (CKF) was implemented in a general-purpose microcontroller. As odometrical measurement system is coupled with an inertial measurement unit and a compass the accuracy of the position estimate has been improved much, while the system moves in different motion conditions like slipping and jerky motion. As controller strategy, a nonlinear state linearization controller has been implemented on the main micro controller so that the ODR platform can be guided along any given trajectory while following a given orientation profile.

2.2 The Laser Range Finder (LRF) Data Processing

The LRF used, has a Neato laser sensor[6] driven by the Xv-11 LIDAR controller. The used LRF is a popular low-cost range finder compared to others in the market and has been used for many research and experimental applications. Although the accuracy is much

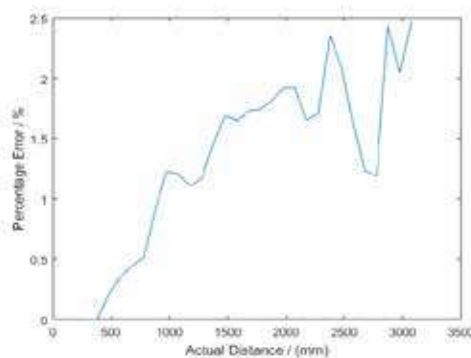


Figure 3 – The Error Characteristic of LRF

higher than SONAR, or simple vision systems, it also has some deviations in the measured distances. The error characteristics of the LRF is shown in the Fig. 3.

The laser sensor works by projecting a pulse stream of lasers around and measures the time it takes to reflect back. The distance to the reflection point can be accurately calculated (to 1mm) from the time of flight the sensor then encodes the distance data into a packet and forward it to the LIDAR controller. The data packets are then decoded in the controller and relayed through the serial port up to the host device which is the embedded system that the Intelligent Navigation System (INS) implemented on. As the percentage error is small, in distances less than 3m, the LRF measurement can be used as accurate estimation of distance. Separate method has been developed to mitigate the noise in the LRF measurements. Most of it was due to the reflectivity effects on the object surfaces and also the variation of the rotational speed of the LRF. To prevent overlapping of data points and incorrect angle measurements, A PID controller is implemented in the XV LIDAR controller to regulate the rotational speed of the sensor to the optimum speed of 200 rpm, where the device can send out a distance data point per a degree of rotation. Many of the reflectivity distortions could be rectified by sampling through multiple realizations. Here it was about five realizations, considering speed of operation and the power consumption.

A main capability that the system was intended to poses was its ability to be versatile and to be dynamically adaptive to any mobile platform. Hence, at the scanning step, the LRF is powered ON only at the scanning moment otherwise it is powered OFF, such that lesser power is consumed in the case of mobile implementation.

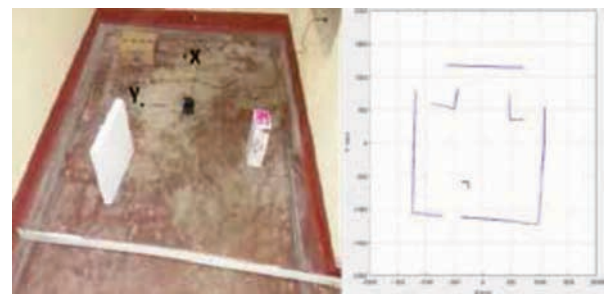


Figure 4 - A Polar LRF Sweep of 360°

3. The Intelligent Navigation System

The Intelligent Navigation System (INS) is the entity which analyses the data from the sensors and directs the mobile platform to the necessary place to explore [17]. The INS was run for the simulation environment in Fig. 5(a)



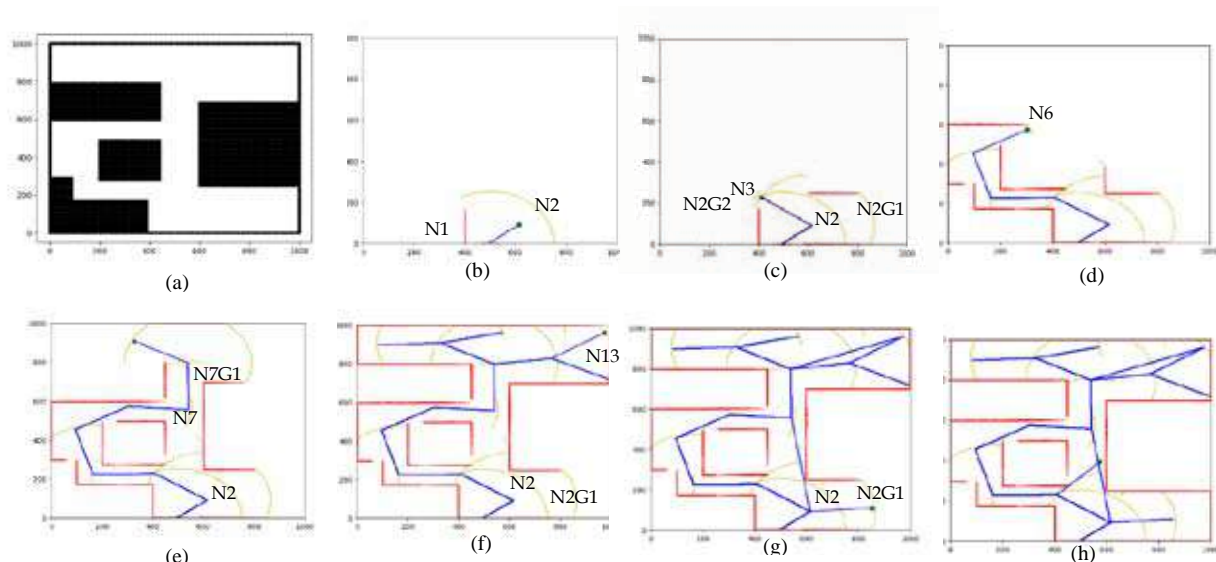


Figure 5 - Simulation of Navigation Algorithm

and the result was generated in the steps shown in the Fig. 5(b) to Fig. 5(h). It should be noted that the anchor points where the laser sweeps are done, are named as 'nodes' and respective nodes, which the agent can traverse to and from each other, are called as 'neighbours'. The procedure of the INS can be analysed through following explained steps,

1) Step 01: All the storage classes and data structures are initialized and current position and orientation is read. A node is created in the current position namely labelled as N1 in Fig.5(b). (if this is not the first node, new node is also added as a neighbour for the previous node and vice versa) scanning is done for 360° initially because agent has to localize and decide which direction to explore. The list of distance data per degree is obtained from the LRF.

2) Step 02: Next the gaps and the walls should be correctly identified. Gap points are selected as data points with a relative distance from the agent, which is longer than a given length. Because those places can be assumed as places where it can be expected to find new information about the environment. The distance data is analysed to classify them as walls or gaps. At the end of each classification, its properties (width and centroid) are calculated. Here in the example, a large gap is detected from the scan at N1 hence the agent is directed towards the centroid of it. Hence the scanning is done again at the node N2, where 2 gaps have been detected. Here in Fig.5(c), it can be seen that the agent has been directed towards the minimum width gap first which is N2G2. This approach is justified in the latter part of the document. Here it should be noted that the scanning is done forward biased after

the first scan. It is a 300° scan $\pm 150^\circ$ around the agents heading direction. In Fig. 5(d), it can be seen that the agent has now travelled up to the node N6 and further to node N7 in Fig. 5(e).

3) Step 03: It can be observed that direct travelling from N2 to N7 is possible. Hence, those two nodes should be neighbours. Also, it can be noticed that a scan down towards N2 from N7 is not necessary as the whole environment in between the nodes have been already mapped through the scans done at the respective nodes. Hence, to handle those kinds of situations a separate 'neighbour identification' is done as,

A.) If any two nodes are closer than twice the scan range, the whole area in between nodes can be assumed to be explored. Hence above situation occurs.

B.) Each gap of the corresponding two nodes are considered and checked if they intersect the line joining the two nodes. They are set as explored gaps as there is no new un-explored data in side those gaps, which are in between known nodes.

C.) Also if the widths of those gaps are larger than the size of the agent, they can be travelled through. Hence, the corresponding nodes are considered neighbours of each other (where node to node travelling is possible).

After the above analysis, the agent is now directed towards N7G1 because that is the information lacking area in the map. But INS has now learned that there is a path available to N2 from N7, without travelling or exploring any gap between them. This is kept track by constantly updating the travel cost map from each and every node to current node. The cost of travel (distance) is calculated to each node from the current node, through the

neighbouring nodes. The minimum cost, unexplored node is selected and it is analysed to find the minimum width unexplored gap in its corresponding gaps. But the gap should be wide enough so that it can be traversed through. The minimum cost unexplored node obviously is the node where the agent is currently positioned. But if it does not contain any unexplored gaps, means a dead end. Then the INS intelligently decides to travel to the minimum cost node instead of just backtracking to find an unexplored gap. (This minimum cost node is the first approach and the narrowest gap first approach is justified in next section)

4) Step 04: In the next step, Fig. 5(f) after agent has explored the upper part of the map, at node N13, it has decided through the above explained process in step 03, to go back to unexplored node N2 to the gap N2G1. As of now the INS knows the path from N7 to N2, hence it does not unnecessarily backtrack, but travels through middle part of the environment to node N2 as observable from Fig. 5(g). The minimum cost path is found to the selected node employing the Dijkstra's Shortest path algorithm[11]. The reference point to travel is generated for the agent to follow the path intended. After node N2, it explores another unexplored gap at N3 and finishes up mapping as in Fig. 5(h)

The algorithm has been implemented so that it uses minimum amount of external complex libraries. Also, program loops have been avoided as much as possible and functions have been implemented so that it will be faster in execution. Conditional switches have been used to handle errors caused by data dependencies. The lesser processing power needed and the usage of simple functions and libraries have made it much more feasible to implement the system on a mobile platform with limited resources.

4. Improvement of Mapping Efficacy

When the efficacy of mapping is considered, two key factors are the accuracy of the map and the time it takes to map the whole area. The accuracy of the map highly depends on the accuracy of the LRF measurements and also correct estimation of current position relative to the locale. The control strategy deployed in the agent will determine the accurate positioning of the platform to the coordinates directed by the INS. Hence to correctly localize the agent a special SLAM algorithm has been employed. It

uses the data from the LRF and compute necessary corrections needed for the position of the agent as well as the generated map.

Apart from the above approaches, the INS has been developed on several logics that improves the mapping time. one is the scanning method. Initially at the agents first scan of the environment, it is done for a full circle of 360°, so that the agent can localize itself and correctly decide that where should it explore first. But the scans followed after the initiation are done forward biased around $\pm 150^\circ$ around the heading direction. This approach limits the agent of collecting existing information again in the area it just explored and keep the information spectrum forward biased.

Another approach is the continuously updated cost of travel (distance) map of the nodes. If there are no gaps to explore in the current node the traditional approach is to backtrack and find the unexplored gaps in the past nodes according to the order of traversing. But in the proposed INS next node to explore is decided by analysing the cost of travel to the nodes and selecting the unexplored node with minimum cost of travel. This comes much effective in complex environments, when there exist two or more paths for node to node traversing, which are identified through the process of 'neighbour identification' explained in the above section. Hence, if the agent has found a lesser cost path to a past node, in its path planning, it will effectively utilize the found path instead of simple backtracking. It can be seen clearly in the example in Fig. 5, where a path has been found from N2 to N7 without an explicit scan.

Another approach towards improving mapping efficacy is selection of the minimum width gap to explore first. After selecting the respective node to travel as explained above, a gap need to be selected in the respective node.

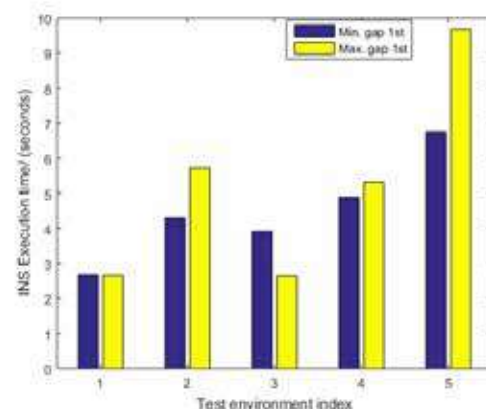


Figure 6 - INS execution time comparison

Here it's done under the general assumption that in the real world a smaller gap is much



probable to lead to a convergence and reach a dead-end, unlike a wider gap. Hence, the minimum width gap is selected to explore before heading out in to the wider area where the probability of convergence is much lower. As a quantitative analysis of the efficacy, figure 6 shows a comparison of the execution times of the INS in 'Min. gap vs. Max. gap first' approaches for five test environments. From the comparative analysis, it can be concluded that the min. gap first approach is an efficient method of exploration.

5. Localization - SLAM

The accurate localization or else knowing the exact position is critical in the mapping task. As the existing GPS systems provide accuracy of few meters and also fails in indoors, SLAM approach has been utilized as a localization method[16]. Although the usage of extended Kalman filter for SLAM is popular[13], due to its high computational complexity, solutions based on similarity transforms and particle filter (Monte Carlo Localization)[14][15] based methods have been used in this work.

In both methods, encoder readings are used to estimate the position, then the LRF data is used to correct the position estimate. Finding the relevant features/objects using LRF is done using differentiation.

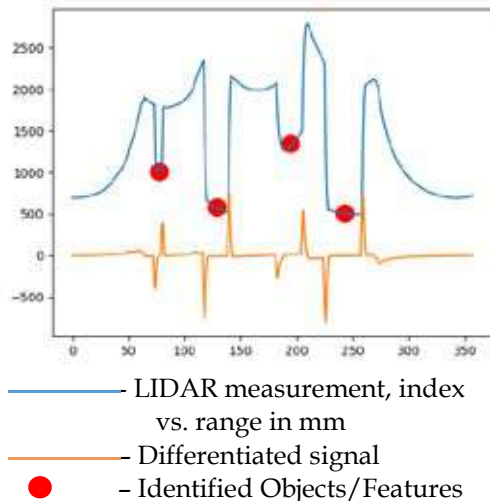


Figure 7 - Feature Identification

5.1 Similarity Transform

This method is based on finding an optimized parameter estimation for the transformation, to transform the agent back to its correct position. It has been assumed that the erroneous localization is occurred when it is

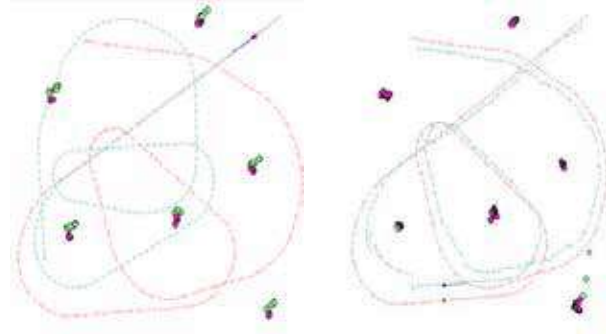
traveling on curved paths. The detected feature positions can be used for correction. Correspondences between erroneous object positions and previously determined positions of the same object are found through similarity transform and optimize the values of the transformation from using recursive method to minimise the error of the similarity transform. The transform can be found as;

$$\lambda Rl_i + t = r_i ;$$

$$R \text{ (rotation matrix)} = \begin{bmatrix} \cos\alpha & -\sin\alpha \\ \sin\alpha & \cos\alpha \end{bmatrix} \dots (1)$$

$$t \text{ (translation matrix)} = (t_x, t_y)$$

Equation (1) can be optimized by minimizing the sum of absolute error. The determined transform is then used to remap the objects and correct the position as shown in the Fig.7. (a) and (b) shows how the objects have been remapped and agent's path has been corrected.



- (a) Before (b) After
- - calculated Path
 - - Reference path
 - - observed features
 - - Reference objects

Figure 8 - Applying Similarity Transform

5.2 Particle Filter (Fast SLAM)

The major drawback of the similarity transform method is the difficulty to converge on an optimized parameter value set in real-time. Hence, another method based on Bayesian filtering called Particle filter has been used. Particle filter SLAM [15] is a better solution, as the convergence rate is very high and with the probabilistic inferences to the estimation, it will address the uncertainty in the LRF too. Initially, it is hypothetically assumed that the agent will be anywhere with any orientation. Then Position estimate is computed using the density of the particles, representing the position with orientation. This is a two-step process,

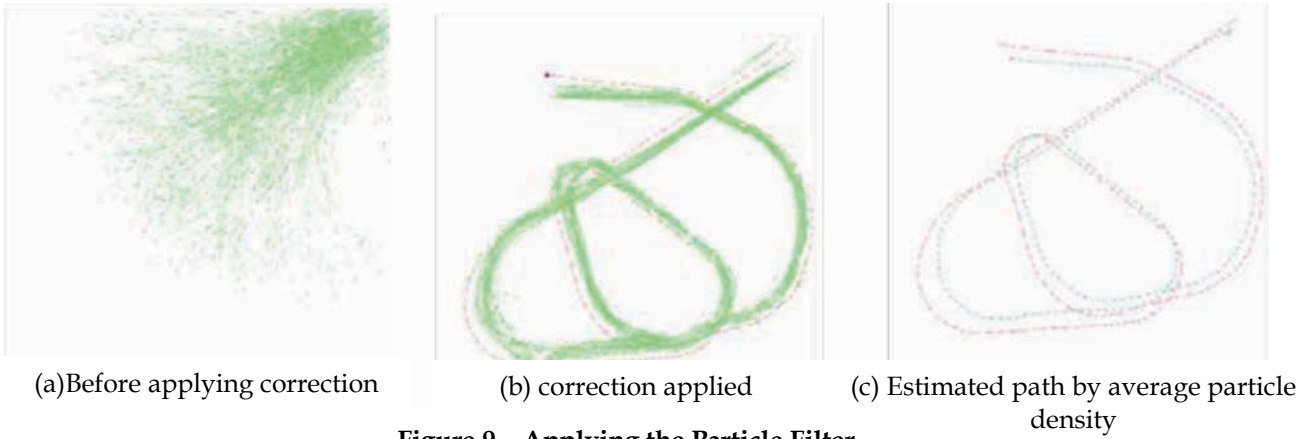


Figure 9 - Applying the Particle Filter

A). Prediction step- Particles are generated to represent the position, through iterative sampling of a normal distribution

$$\begin{aligned} & \text{for } i = 1 \text{ to } n; \\ & \text{sample } x^{(i)} \sim N(\mu, \sigma^2); \end{aligned} \quad \dots (2)$$

Then the particles are translated with the aid of the applied control signal and then resampled using resampling wheel technique.

It is a method that gives a higher chance to choose a particle from a position which has a higher weight (weighting is done in the correction step) rather than others.

$$\begin{aligned} & \text{for } i = 1 \text{ to } n; \\ & \text{sample } x^{(i)} \sim p(x_t | x_{t-1}^{[m]}, U_t); \end{aligned} \quad \dots (3)$$

B). Correction Step- This is done by weighting the particle by finding the match between obtained measurement and the position of the particle. This will reduce the outliers with the time and quickly converge to the actual path. Drawn samples with probability $\alpha w_t^{[i]}$

$$\begin{aligned} & \text{for } i = 1 \text{ to } n; \\ & w_t^{[m]} \sim p(z_t | \bar{x}_t^{[m]}, U_t); \text{ where } z \text{ is LRF measurement} \\ & p(z_t | \bar{x}_t^{[m]}) = \prod_i p(z_i | \bar{x}_t^{[m]}) \end{aligned} \quad \dots (4)$$

$$\begin{aligned} p(z_i | \bar{x}_t^{[m]}) &= p(d - \hat{d}) * p(\alpha - \hat{\alpha}) \\ &= N(d - \hat{d}, 0, \sigma_d^2) * N(\alpha - \hat{\alpha}, 0, \sigma_\alpha^2) \end{aligned}$$

$d - \hat{d}$ = error in the distance

$\alpha - \hat{\alpha}$ = error in orientation

After the calculations,

$$\text{position estimation} = 1/n * \sum_i x_i \quad \dots (5)$$

$$\text{orientation estimation} = \tan^{-1} \left\{ \frac{\sum_i \cos \theta_i}{\sum_i \sin \theta_i} \right\}$$

Through the above process, a particle filter SLAM can be implemented. A much accurate position estimation is rendered through that approach as seen from the Fig.8.

6. Conclusion

This work has been focussed on finding a simple and practically realizable solution to the engineering problem of constructing a map of an unknown environment. In the approach proposed, a low-cost laser range finder (LRF) has been selected as the sensor due to its high accuracy along with simplicity when compared with traditional ultra-sonic sensors and complex vision systems. Methods have been developed for correcting the distortions and acquiring the data from the LRF. But any convenient sensor capable of producing an accurate distance data spectrum can be easily used to replace the LRF.

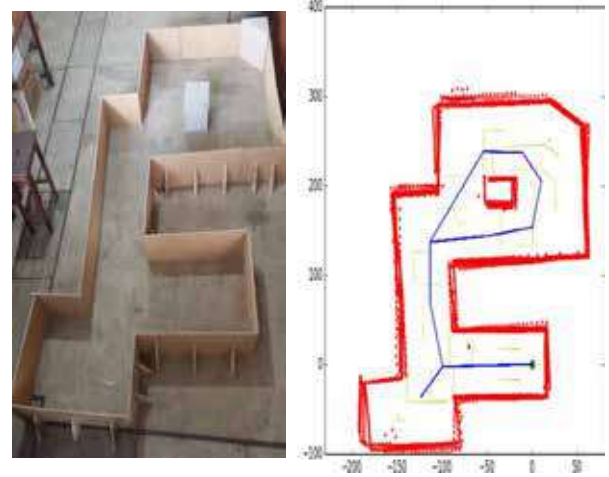


Figure 10 -The Test Environment and Generated 2D Map.

As the hardware platform, a 3WD Omni directional mobile platform has been chosen due to its convenient manoeuvrability into any direction intended. To guide it towards information gap in the data and to provide optimum path planning a separate navigation algorithm has been implemented. Key features like, 'Smallest gap first approach' and the 'Intelligent neighbour identification process'

has allowed the mapping efficacy to be at optimum.

Due to the errors in the encoder based position measurement of the system, a parallelly running simultaneous localization and mapping (SLAM) algorithm has been developed. Similarity transform based approach and Monte-Carlo method (Particle filter) has been experimented and the Particle filter based Fast SLAM has been implemented on the system.

Altogether taken the combined work on above approaches has enabled to create a simple and rapidly realizable solution to the problem of environment mapping. Although specific hardware set-up is considered in this work, the developed algorithms are quickly adaptable to any other hardware combination. Also, as further improvements if a suitable sensor like a vision system is available, it would be convenient to extend the 2D map, generated through the proposed approach to a complete 3D map of the locale.

Acknowledgement

This research work has been hosted and supported by the Department of Electrical and Electronic Engineering, Faculty of Engineering, University of Peradeniya, Sri Lanka.

References

- Hatao, N., Okada, K., and Inaba, M., "Autonomous Mapping and Navigation System in Rooms and Corridors for Indoor Support Robots," in *2008 IEEE International Conference on Mechatronics and Automation*, 2008, pp. 840-845.
- Ip, Y. L., Rad, A. B., and Wong, Y. K., "Autonomous Exploration and Mapping in An Unknown Environment," in *Proceedings of 2004 International Conference on Machine Learning and Cybernetics (IEEE Cat. No.04EX826)*, 2004, vol. 7, pp. 4194-4199 vol.7.
- Yuan, S., and Schumacher, H., "Vehicle microwave radar system for 2D and 3D environment mapping," in *2015 IEEE MTT-S International Conference on Microwaves for Intelligent Mobility (ICMIM)*, 2015, pp. 1-3.
- Dam, R. R., Biswas, H., Barman, S., and Ahmed, A. Q., "Determining 2D Shape of Object using Ultrasonic Sensor," in *2016 3rd International Conference on Electrical Engineering and Information Communication Technology (ICEEICT)*, 2016, pp. 1-5.
- Forouher, D., Besselmann, M. G., and Maehle, E., "Sensor Fusion of Depth Camera and Ultrasound Data for Obstacle Detection and Robot Navigation," in *2016 14th International Conference on Control, Automation, Robotics and Vision (ICARCV)*, 2016, pp. 1-6.
- Konolige, K., Augenbraun, J., Donaldson, N., Fiebig, C., and Shah, P., "A Low-Cost Laser Distance Sensor," in *2008 IEEE International Conference on Robotics and Automation*, 2008, pp. 3002-3008.
- Zhou, S., Kang, Y., and Shi, X., "Indoor Localization, Navigation and Mapping for Quad-Rotor," in *Proceedings of 2014 IEEE Chinese Guidance, Navigation and Control Conference*, 2014, pp. 2669-2674.
- Abeysekara, A. H. A. D., Liyanage, D. P., Welikala, W. R. C. B. S., Godaliyadda, G. M. R. I., Eakanayake, M. P. B., and Wijayakulasooriya, J. V., "Depth Map Generation for a Reconnaissance Robot via Sensor Fusion," in *2015 IEEE 10th International Conference on Industrial and Information Systems (ICIIS)*, 2015, pp. 320-325.
- Catapang, A. N., and Ramos, M., "Obstacle Detection using a 2D LIDAR System for An Autonomous Vehicle," in *2016 6th IEEE International Conference on Control System, Computing and Engineering (ICCSCE)*, 2016, pp. 441-445.
- Plonski, P. A., Hook, J. V., Peng, C., Noori, N., and Isler, V., "Navigation around an Unknown Obstacle for Autonomous Surface Vehicles using a Forward-Facing Sonar," in *2015 IEEE International Symposium on Safety, Security, and Rescue Robotics (SSRR)*, 2015, pp. 1-7.
- Dijkstra, E. W., "A Note on Two Problems in Connexion with Graphs.," *Numer. Math.*, vol. 1, pp. 269-271, 1959.
- M. T. Sqalli *et al.*, "Improvement of a Tele-Presence Robot Autonomous Navigation Using SLAM Algorithm," in *2016 International Symposium on Micro-NanoMechatronics and Human Science (MHS)*, 2016, pp. 1-7.
- Saman, A. B. S. H. M., and Lotfy, A. H., "An Implementation of SLAM with Extended Kalman Filter," in *2016 6th International Conference on Intelligent and Advanced Systems (ICIAS)*, 2016, pp. 1-4.
- Aini, F. R. Q., Jati, A. N., and Sunarya, U., "A Study of Monte Carlo localization on Robot Operating System," in *2016 International Conference on Information Technology Systems and Innovation (ICITSI)*, 2016, pp. 1-6.
- Zhao, L., Fan, Z., Li, W., Xie, H., and Xiao, Y., "3D Indoor Map Building with Monte Carlo Localization in 2D Map," in *2016 International Conference on Industrial Informatics - Computing Technology, Intelligent Technology, Industrial Information Integration (ICIICII)*, 2016, pp. 236-240.
- Galgamuwa, G.I.R.K., "A Novel Scan Matching Algorithm for Slam Problem," *M.Sc. Eng. thesis, Department of Electrical and Electronics Engineering, Faculty of Engineering, University of Peradeniya, Peradeniya, Sri Lanka, January 2017*
- Jayasuriya, D.M.N., Liyanage, W.L.Y.S., Herath, H.M.A.S., Godaliyadda, G.M.R.I., Ekanayake,

M.P.B., and Wijayakulasooriya, J.V.,
"Intelligent Navigation System for Mapping
Unknown Environments," in *2016 IEEE 8 th
International Conference on Information and
Automation for Sustainability (ICIAfS 2016), Galle,
Sri Lanka, December 2016.*



A Novel Handover Mechanism for Visible Light Communication Network

M.A.N. Perera, N.G.K.R. Wijewardhana, A.A.D.T Nissanka, S.A.H.A. Suraweera
and G.M.R.I. Godaliyadda

Abstract: Visible light communication (VLC) is an emerging technology and considered as an alternative to overcome some of the disadvantages of radio frequency communication technology in an indoor environment. However, the line of sight nature of the technology limits the user mobility and create new challenges to provides seamless network coverage under user mobility scenarios. In VLC multi access points and multi cell based network, co channel interference (CCI) between neighbor cells limits the overall performance. Therefore, by following the already existing VLC handover systems, this statistical parameter based novel handover method is designed. This paper proposes a handover mechanism for indoor VLC systems by introducing cell ID bits and statistical kurtosis values of the cell ID waveforms as metric for the handover initiation. As advantage of the method, effects from the CCI can be eliminate when measuring signal strengths in the signal overlapping cell boundary area. Also the handover criteria are adoptive to the different ambient lighting conditions compared to existing pre-configured light intensity threshold based handover systems. With the use of bit error rate (BER), the experiment results showed that Kurtosis value of the cell ID waveforms can be used as metric to initiate network handover in indoor VLC systems

Keywords: Visible light communication, handover, co channel interference, Indoor VLC

1. Introduction

Visible light Communication (VLC) has become a popular research area during recent years, due to the lack of bandwidth in the frequency spectrum for radio frequency (RF) communication [1,2]. The bandwidth frequency spectrum of visible light is larger than that of RF bandwidth. RF bandwidth ranges from 3 kHz to 300 GHz and VLC spectrum offers a bandwidth range from 400 THz to 800 THz. There are several other advantages in VLC compared to RF based mobile communication systems. Unlike RF mediums, visible light cannot penetrate walls in indoor environments. This characteristic provides an inherent network security for indoor environments. The use of visible light as a carrier of data reduces the VLC systems from electromagnetic interference and associated health concerns. Therefore, VLC systems can be implemented on places where RF communication systems have disadvantages. Such as hospitals, factories, under water, inside airplanes etc. Also VLC facilitates the reuse of existing light configuration for communication. [3] Since the characteristics of reusability and abundant spectrum compared to RF, VLC systems can be built with lesser efforts and at a lower cost.

In order to use VLC in mobile network systems, it is necessary that this system can provide uninterrupted high speed connectivity in presence of user mobility scenarios. To use VLC systems as an alternative for RF communication systems, it should be able to initiate handovers between access points to provide seamless connectivity for the mobile users [4]. Usually in RF communication systems handover is initiated on the basis of

Mr. M.A.N Perera, B.Sc.Eng.(undergraduate) Department of Electrical and Electronics Engineering, Faculty of Engineering, University of Peradeniya.

Mr. N.G.K.R. Wijewardhana, B.Sc.Eng.(undergraduate) Department of Electrical and Electronics Engineering, Faculty of Engineering, University of Peradeniya.

Ms. A.A.D.T Nissanka, B.Sc.Eng.(undergraduate) Department of Electrical and Electronics Engineering, Faculty of Engineering, University of Peradeniya.

Dr. S.A.H.A. Suraweera, B.Sc.Eng.(Peradeniya), Ph.D. (Monash University), Senior Lecturer, Department of Electrical and Electronics Engineering, Faculty of Engineering, University of Peradeniya.

Eng. (Dr.) G. M. R. I. Godaliyadda, B.Sc.Eng.(Peradeniya), Ph.D. (National university of Singapore), Senior Lecturer, Department of Electrical and Electronics Engineering, Faculty of Engineering, University of Peradeniya.



physical parameter measurements, such as received signal strength. To define optimal criteria for handover, there are several factors taken into consideration. such as energy consumption, positioning, end user quality of service etc.

This paper proposes a handover method for indoor multi cell based VLC networks. Cell ID bits and statistical parameters are introduced to eliminate the CCI. In indoor VLC systems, Intensity level can vary quickly due to reasons such as receiving height, receiving orientation, background light intensity etc. As an advantage of using statistical parameters, impact from above mentioned incidents can be minimized compared to other intensity threshold based handover methods. According to the purposed methodology, received visible light cell ID wave form is analyzed statistically. Handover initiation is decided when statistical parameters reached to their relative maximum value. Since there isn't any comparison between pre-configured constant threshold values, the system can be designed to adopt in different uniform lighting conditions.

The rest of the paper is organized as follows. Section 2 describes the existing methodologies for VLC networks and their drawbacks. The system model is explained in section 3. Section 4 gives the experiment details and observed results. Finally, conclusions are given in section 5.

2. Literature Review

Presently there are several technologies designed for achieving seamless connectivity for mobile users [5,6,7]. One of the most widely recognized standardized approaches to VLC is the exploitation of IEEE 802.15.7 standard for visible light data communication. IEEE 802.15.7 [8] supports high-data-rate visible light communication up to 96 Mb/s by fast modulation of optical light sources which may be dimmed during their operation. IEEE 802.15.7 provides dimming adaptable mechanisms for flicker-free high-data-rate visible light communication.

In [9] vertical handover initiating algorithm is proposed for VLC - LTE Hybrid communication system. since this method designed for hybrid communication system, it cannot apply on handovers in VLC only

systems. In [10] authors propose two handover mechanisms for overlapped uniform VLC cells and non - overlapped spotlight VLC cells. In overlapped uniform VLC cell, the user performs intensity test and detects the presence of overlapped area [11]. It initiates the handover when intensity reach the threshold level. In spotlight VLC cell method, there is buffer memory allocated to save data on mobile user to avoid connectivity interruptions in dead zones. In [12], there is an optical at to cell network proposed which can reduce the co channel interference by using joint transmission method from multiple access points. However, as the authors mentioned the downside of joint transmission systems is that they need extra signaling overhead. In a cell based network, using same frequency in adjacent cells causes co-channel interference [13]. This significantly reduce the network performance to a mobile user in overlap region. Therefore, interference coordination techniques are used to eliminate CCI. In [14] CCI is eliminated by splitting cells into clusters. Inside of a cluster, frequency resources are used in orthogonal manner.

3. System Model

The system model consists of multiple transmitters and multiple receivers. The block diagram of a single data link is shown in Fig. 1.

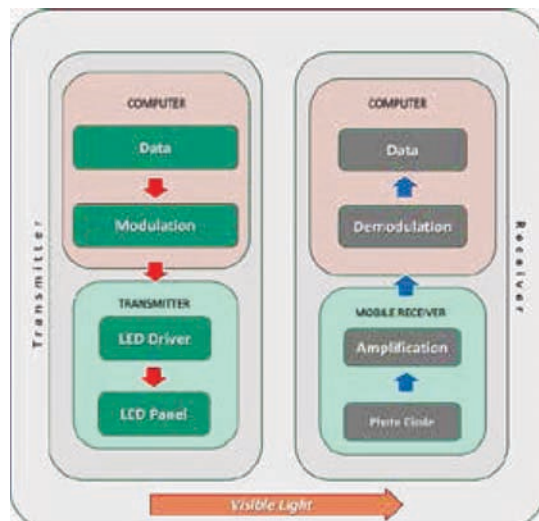


Figure 1 - Block diagram of system model.

3.1 Transmitter

The transmitters were designed to provide good indoor illumination in addition to data

transmission. Data communication by using higher illumination intensities can minimize the distortions to the transmitted data in the transmitting medium.

The Prototype transmitter unit consists of LED driver and power LED panel. Since power LEDs have the high speed switching capability and higher illumination intensity compared to the traditional LEDs, 5x 7w Chips on Board type (COB) cool white power LEDs were used in order to achieve large distance data transmission. COB power LED contain more light sources in the same area than standard LEDs could occupy. This will result a greatly increased illumination output per square meter.

In order to handle required current for the LED panel, TTL compatible metal-oxide-semiconductor field-effect transistors (MOSFET) were used. Transistor switching circuit was used for the LED driver. The MOSFETs were operated by switching signal from the Arduino output. The switching signal carries the data which was needed to be transmitted. The block diagram and the prototype transmitter are shown in Figure 2 & Figure 3.

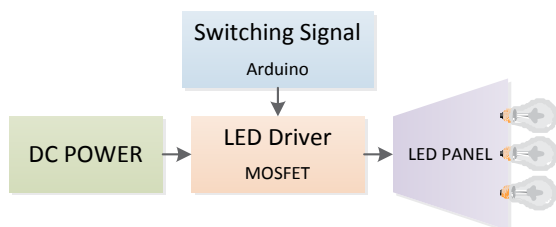


Figure 2 - Block diagram of prototype receiver.

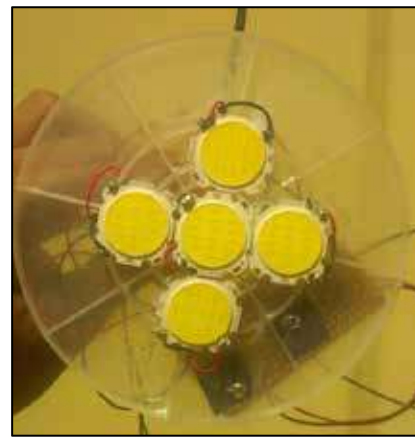


Figure 3 - Prototype transmitter with multiple power LEDs.

3.2 Receiver

Typically, in indoor environments, there is a highly possibility of distorting and interfering the incoming signal wave due to the DC components from ambient light and rectified sine wave emitted from filament, fluorescent lamps. [16] In order to minimize the impact from background disturbances, two photodiodes (PD) with noise cancellation method was used in the receiver unit. Two transimpedance amplifiers were used to convert PD's output current in to voltage signal. DC shift corresponding to ambient noise and light sources were reduced by using differential amplifier in the receiver. Also a reflector fixed on signal receiving PD to improve the signal receiving vertical distance. The reflector directs the signal receiving PD to transmitter direction. Therefore, it limits the signal receiving PD scope and minimize the exposure of the ambient noise. To further minimize the DC shifts of the incoming waveforms, a high pass filter was used in the receiver. The prototype receiver is shown in Figure 4.

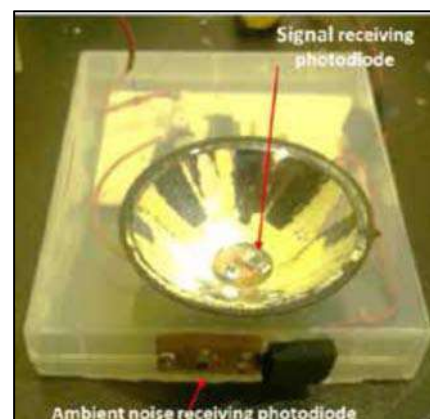


Figure 4 - Prototype receiver.



Then, received data is transmitted to receiver's ADC unit to sample the waveforms at higher sample rate. Block diagram of the prototype receiver is shown in Figure 5.

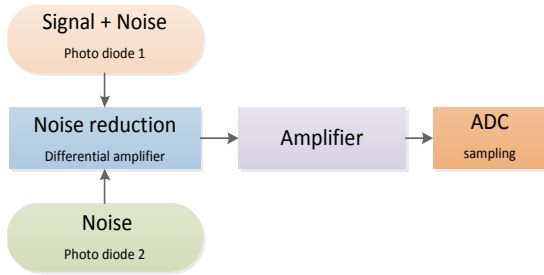


Figure 5 - Block diagram of prototype receiver.

Two ARDUINO UNO boards were used to the communicate with the prototype VLC system.

3.3 Handover Initiation

In VLC system model can be described as illustrated in Fig. 6. To initiate handover, system follow few steps.

- A data structure is defined to transmit data from transmitter to receiver. First two bit of the data structure is used for cell ID bit. each transmitter adds its cell id bits before data transmission [17]. The cell ID bits are transmitted by OOK (On Off Keying) modulation. Fig. 7 illustrates the received data frame structure.
- Then from the receiver, received wave form shape is analyzed. Mobile user separates the cell id segment and data segment of the data structure. Then it calculates the kurtosis value of the cell ID waveform to estimate position. As shown in figure, different shapes of cell id waveforms received for different user positions. Fig. 7 illustrates the received data frame structure.

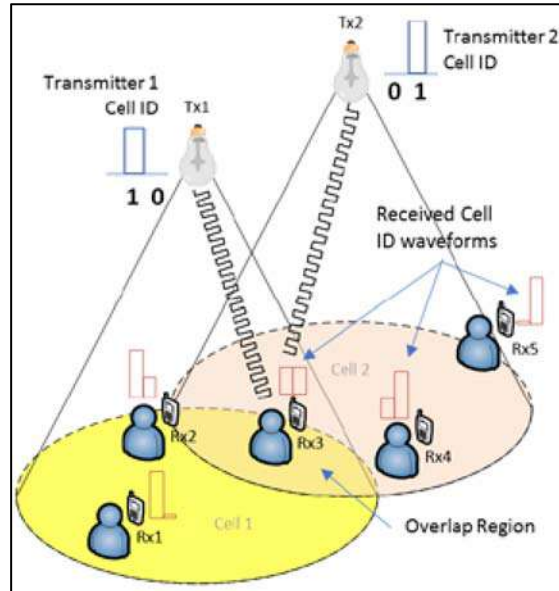


Figure 6 - VLC system with cell ID waveforms.

- Handover initiation decision is based on statistical characteristics of the ID wave form. According to the Fig. 6, Rx3 receives superimposed signals which have equal signal strengths on two cell bits while, Rx5 and Rx1 receive only one strong signal on cell bits. The waveform shape depends on the received signal strength of the transmitted cell ID. Received signal is shown in Figure 7.

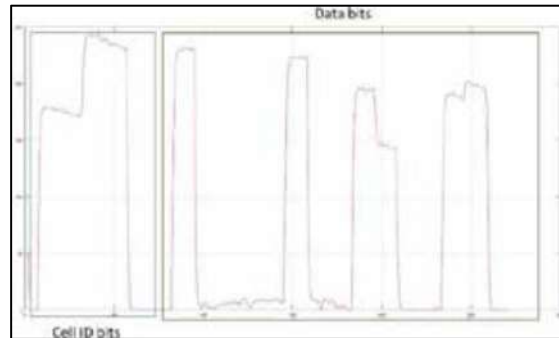


Figure 7 - Received data structure.

3.4 Mathematical Background

The shape of cell ID waveform varies with the received cell ID signal level strengths of adjacent transmitters. The variations of this type waveforms can be analyzed by calculating the kurtosis value of the waveform. User position for the handover initiation can be estimated based on the kurtosis values. For the calculation of the kurtosis, conditional probability density function (PDF) of the waveform was constructed using sampled

data of the received waveform. Mathematically, the sampled values constructed from the received waveform from the PD, $y(t)$ can be written as

$$y[n] = y(nT_s) \quad n = 1, 2, 3 \dots \quad \dots(1)$$

where T_s is the sampling time and $y[n]$ is the sampled value.

The sample values are mapped to a histogram to construct the PDF of distribution.

Kurtosis is a measure of whether the data are heavy-tailed or light-tailed with respect to a normal distribution. The kurtosis decreases as the tails become lighter and it increases as the tails become heavier. Kurtosis for a discrete set of data is

$$\text{Kurtosis} = \frac{\sum_{i=1}^N (Y_i - \bar{Y})^4 / N}{s^4} \quad \dots(2)$$

Where Y is sampled data point, \bar{Y} is mean of sampled data, S is standard deviation and N is the sample size.

If the kurtosis is close to 0, then a normal distribution is often assumed. These are called *mesokurtic* distributions. If the kurtosis is less than zero, then the distribution is light tails and is called a *platykurtic* distribution. If the kurtosis is greater than zero, then the distribution has heavier tails and is called a *leptokurtic* distribution [13].

Kurtosis is a component of both tailedness and peakedness of a distribution. It is basically because kurtosis represents a movement of mass that does not affect the variance. In the case of positive kurtosis, where heavier tails are accompanied, can be modeled to the waveform received for the cell identification on handover region. If the distribution is more concentrated towards the tails, then the variance will also be larger. To leave the effect of variance unchanged, standardized kurtosis is taken with respect to variance. Hence a high value for kurtosis is obtained at the handover position. It is also recognized that although tailedness and peakedness are often both components of kurtosis, kurtosis can also reflect the effect of primarily one of these components, such as light tails. Thus, for symmetric distributions, positive kurtosis indicates an excess in either the tails, or peakness which is used to identify the receiver location.

In this handover method, combination of kurtosis and bit error rate is used to initiate handover, hence a more reliable outcome is achieved. Bit error rate is calculated from the equation,

$$\text{BER} = \frac{\text{No. of bits in error}}{\text{No. of total bits transmitted}} \quad \dots(3)$$

4. Experiment & Results

4.1 System Setup

The experiment was carried out in an area of dimensions 1.6 m x 1.6 m. The experiment was carried for two transmitters and one mobile observer. Observed user moving path across boundary of the neighboring cells is shown in Fig. 8. Two transmitters are named as T1 and T2 in the figure. BER was calculated by using 8 x 8 grid with resolution of 0.2m x 0.2m placed over the area. Transmitters were fixed 2m above from receiver plane. Transmitters were the only light sources at the experiment premises.

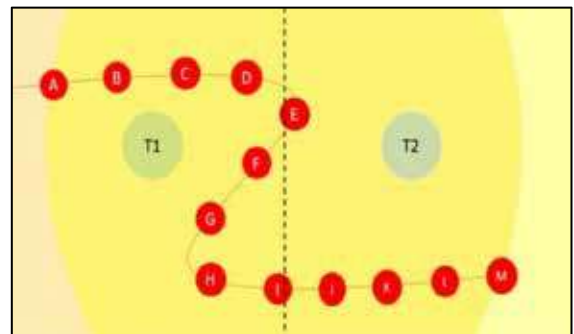


Figure 8 - Path of the mobile user

4.2 Results

To observe the receiving cell ID waveform patterns, 0 1 and 1 0 bit sequences transmitted as cell ID from T1 and T2 respectively. Fig. 9 shows the received Cell id waveforms when moving along A to M. Random walking pattern across the two transmitters was taken to consideration when creating the observing path. From position E to H user change the moving direction and from H onwards it continues to go across the two transmitters. Calculated kurtosis values variation for the received cell ID waveforms is given in Fig. 10. From the received waveforms shown in Fig. 9, it can be observed that waveforms corresponding to position (E) and (I) have the highest kurtosis values compared to other positions.



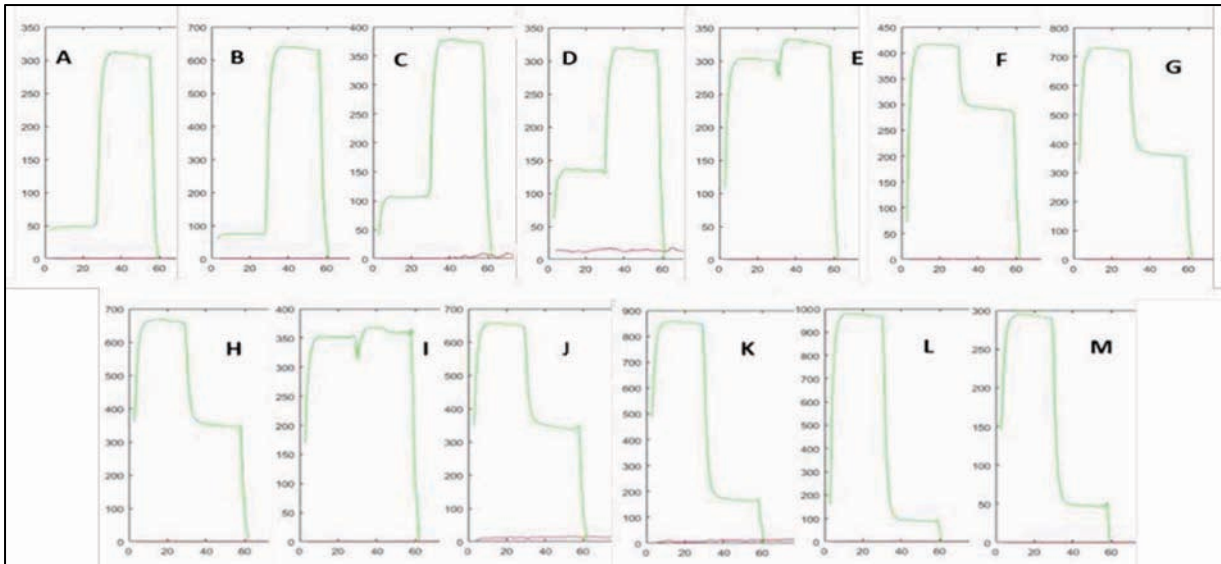


Figure 9 - Received cell ID wave form for different positions.

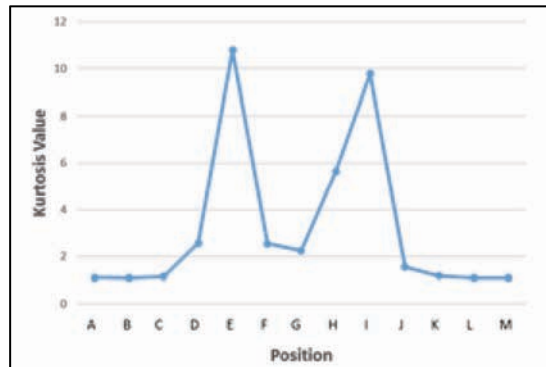


Figure 10 - Kurtosis values for different positions.

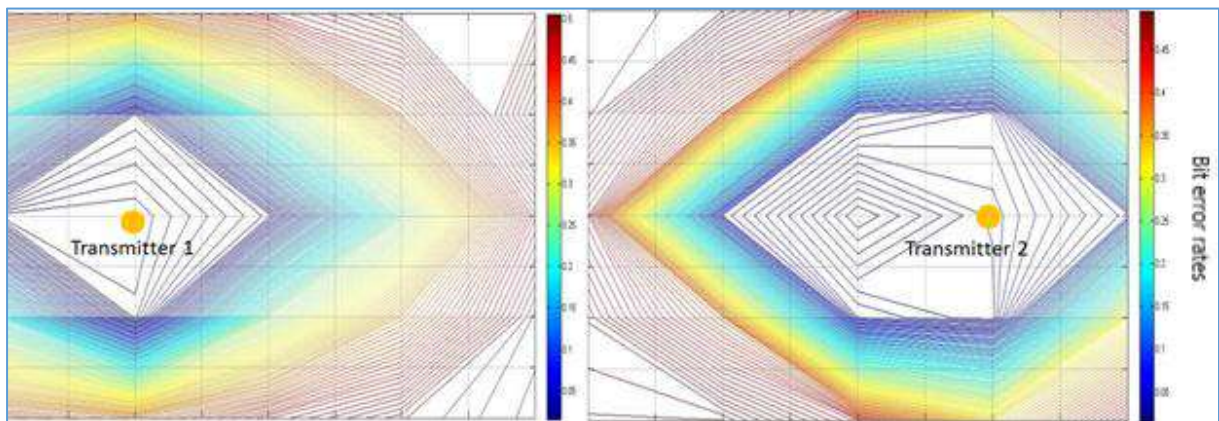


Figure 11 - BER for TX1 & TX2 in different positions of the grid.

Measured BER on different positions of the 8x8 grid is shown in Fig. 11. Each coloured contour lines represents a different BER value observed in the area.

4.3 Handover Based on Results

Fig.12 shows the BER variation with kurtosis along the A-M path. Position (E) and (I) have the minimum BER in both TR1 and TR2. Positions directly under the transmitters have low kurtosis values compared to the other positions. Such as position A, B, C, G, J, K, L, M. Therefore, it can be clearly observed that positions which have higher CCI results high Kurtosis values. According to the results position (I) and (E) which have equal signal strengths from the TR1 & TR2, can be used as a handover initiation positions. However, since user change its moving direction, handover initiation is not required in position E.

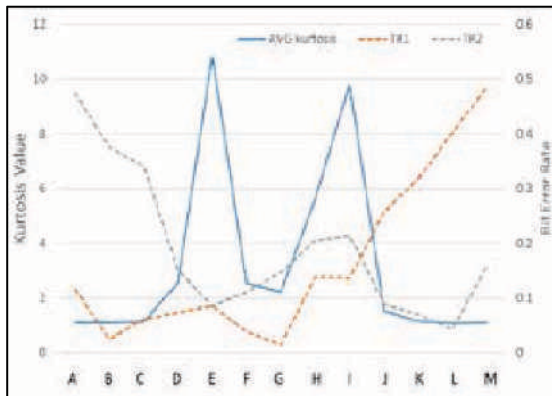


Figure 12 - Kurtosis values and BER variations for different positions

Therefore, experiment results shown in Fig. 12 concludes that higher kurtosis values of the cell ID bits directly related to the minimum BER positions of the multiple access points. Results of the prototype experiment demonstrate that kurtosis parameter can be used as metric for handover position together with minimum bit error rate.

5. Conclusions

This paper presents a novel handover mechanism for VLC network in order to mitigate CCI in neighbor cells and detect the accurate signal strengths of the neighbor transmitters in order to initiate handovers and achieve seamless coverage for the mobile users. To perform that, cell ID bits were

introduced and received waveforms were analyzed statistically. The kurtosis values and bit error rates from two transmitters were considered in the experiment and the results showed that the higher kurtosis values can be obtained when multiple transmitters have equal visible light signal intensity. Also low BERs were observed at the high kurtosis positions. Therefore, it can be showed that kurtosis values of the cell ID can be used as handover decision making metric for the indoor VLC networks. The system can be further improved in combination with other devices such as CCTV video cameras in order to track the walking patterns of the users and optimize the handover decision criteria.

References

1. H. Elgala, R. Mesleh, and H. Haas, "Indoor optical wireless communication: potential and state-of-the-art," *IEEE Communications Magazine*, vol. 49, Sept. 2011.
2. P. H. Pathak, X. Feng, P. Hu and P. Mohapatra, "Visible light communication, networking, and sensing: A survey, potential and challenges," *IEEE communications surveys & tutorials*, 17(4), pp. 2047-2077, 2015.
3. A. Jovicic, J. Li, and T. Richardson. "Visible light communication: opportunities, challenges and the path to market." *IEEE Communications Magazine* vol. 51, pp. 26-32. Dec. 2013.
4. Pollini, Gregory P. "Trends in handover design." *IEEE Communications magazine* 34.3 (1996): 82-90.
5. Dinc, E., Ergul, O., & Akan, O. B. (2015, September). Soft handover in OFDMA based visible light communication networks. In *Vehicular Technology Conference (VTC Fall), 2015 IEEE 82nd* (pp. 1-5). IEEE.
6. Xiong, J., Huang, Z., Zhuang, K., & Ji, Y. (2016). A cooperative positioning with Kalman filters and handover mechanism for indoor microcellular visible light communication network. *Optical Review*, 23(4), 683-688.
7. Hien, Dang Quang, and Myungsik Yoo. "Handover in outdoor Visible Light Communication system." *Information Networking (ICOIN), 2017 International Conference on*. IEEE, 2017.
8. Rajagopal, Sridhar, Richard D. Roberts, and Sang-Kyu Lim. "IEEE 802.15. 7 visible light



communication: modulation schemes and dimming support." *IEEE Communications Magazine* 50.3 (2012).

9. Liang, Shufei, et al. "A novel vertical handover algorithm in a hybrid visible light communication and LTE system." *Vehicular Technology Conference (VTC Fall), 2015 IEEE 82nd*. IEEE, 2015.
10. Vegni, Anna Maria, and Thomas DC Little. "Handover in VLC systems with cooperating mobile devices." *Computing, Networking and Communications (ICNC), 2012 International Conference on*. IEEE, 2012.
11. *Wu, Y., Yang, A., Feng, L., Zuo, L., & Sun, Y. N. (2012). Modulation based cells distribution for visible light communication. *Optics express*, 20(22), 24196-24208.
12. Chen, Cheng, Dobroslav Tsonev, and Harald Haas. "Joint transmission in indoor visible light communication downlink cellular networks." *Globecom Workshops (GC Wkshps), 2013 IEEE*. IEEE, 2013.
13. Cui, Kaiyun, Jinguo Quan, and Zhengyuan Xu. "Performance of indoor optical femtocell by visible light communication." *Optics Communications* 298 (2013): 59-66.
14. Marsh, Gene W., and Joseph M. Kahn. "Channel reuse strategies for indoor infrared wireless communications." *IEEE Transactions on Communications* 45.10 (1997): 1280-1290.
15. Bui, T. C., Kiravittaya, S., Nguyen, N. H., Nguyen, N. T., & Spirinmanwat, K. (2014, October). LEDs configuration method for supporting handover in visible light communication. In *TENCON 2014-2014 IEEE Region 10 Conference* (pp. 1-6). IEEE
16. Zhao, Yan, and Jayakorn Vongkulbhisal. "Design of visible light communication receiver for on-off keying modulation by adaptive minimum-voltage cancelation." *Engineering Journal* 17.4 (2013).
17. Bao, X., Zhu, X., Song, T., & Ou, Y. (2014). Protocol design and capacity analysis in hybrid network of visible light communication and OFDMA systems. *IEEE Transactions on Vehicular Technology*, 63(4), 1770-1778.
18. Mardia, Kanti V. "Measures of multivariate skewness and kurtosis with applications." *Biometrika* (1970): 519-530.

Technical, Economic, Operational and Dispatch Analysis of Optimum Integration of Renewable Energy in to the Sri Lankan Power system

Buddhika Samarasekara, Randika Wijekoon and Lathika Attanayake

Abstract: The application of more renewable energy based technologies is intensifying with the technological advances and global climatic concerns. Renewable energy sources have become increasingly important in the electricity sector and will continue to grow as a significant source of electricity generation in future. The Integration of renewable energy sources poses various technical and economic challenges depending on the characteristic of the resources and the system.

Sri Lanka, being a country with rich potentials of renewable energy sources, it is important to integrate optimum share of the indigenous renewable energy sources. At present nearly 45% of the country's electricity demand is met by renewable sources. This consists of 34% of major hydro and 11% of wind, solar, small hydro and biomass. In the future it is expected to increase the contribution from wind and solar. Increased penetration levels of variable renewable energy based generation sources pose various technical challenges for system planning and operation. Determining the optimum level of Renewable energy penetration requires the consideration of seasonality and intermittency of sources, daily electricity demand pattern, power system stability and system operational flexibility concerns are among the main system specific constraints for the country.

A detailed study was carried out to increase the renewable energy share from 11% in 2015 to an optimum share of more than 20% beyond 2020. The paper focuses on the analysis on the economic, operational and dispatch restriction aspects of the above renewable energy integration study. Detailed system studies that were carried out for the above work is not included in scope of this paper. Ultimately, it quantifies the results on generation of renewable energy sources and curtailments required under the given system's constraints. Further it highlights the key observation of the results and prospective mitigation measures to facilitate the integration of more renewable energy sources to the network.

The paper outlines the renewable energy resource estimation, optimized development plan, operational analysis and cost estimations to open a pathway to a paradigm shift in Sri Lankan electricity generation system in near future.

Keywords: Renewable Energy Integration, Intermittency, Operational Constraints, Curtailment

1. Introduction

1.1 Background

Sri Lanka being an island has an isolated power system and it was 100% renewable system until mid-nineties. With the growing demand, it has now evolved to a system with a mix of both renewable and thermal generation sources and the size of the existing generating system is nearly 4018 MW in 2016. This includes 1903MW (47%) of renewable energy sources and 2115MW (53%) of thermal energy sources.

Sri Lanka electricity requirement was growing at an average annual rate of around 6% during the past 20 years [1], and it is expected to continue in the foreseeable future with the

rising economic activities. An optimum strategy to meet the growing electricity demand of a developing island nation should mainly cover the aspects of supply reliability and security, economics of supply as well as environmental and social considerations. Total renewable and thermal installed capacity and the peak

Eng. Buddhika Samarasekara, B.Sc. Eng. (Hons), C.Eng. MIE(SL),MIET, PGDipBM (Col),Chief Engineer (Generation Planning)

Eng. Randika Wijekoon, B.Sc. Eng. (Hons), AMIE(SL), Electrical Engineer

Eng. Lathika Attanayake, B.Sc. Eng. (Hons), AMIE (SL),Electrical Engineer, Generation and Transmission Planning Branch, Ceylon Electricity Board



demand of the country over the last 30 years are shown in Figure 1 and the energy contribution of the renewable energy sources has been significant in past years.

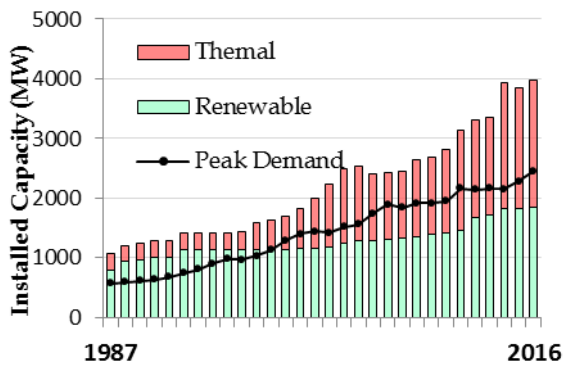


Figure 1 - Peak Demand and Installed Capacity of past 30 years

Sri Lanka, together with other countries, has expressed its national obligation towards mitigating the climate change impacts to United Nations Framework Convention on Climate Change (UNFCCC). Even though the greenhouse gas (GHG) emission of the country is as small as 0.05% of the global total[2], Sri Lanka has an ambitious program towards a reducing the overall GHG emissions. When considering the greenhouse gases, CO₂ is one of the primary gases which contribute towards warming of earths’ atmosphere. According to International Energy Agency [2], approximately 41% of CO₂ emission from the electricity sector while major contributor for CO₂ emission is the transport sector which account for 48% approximately. Indigenous renewable energy development is a key area for decarbonizing the electricity sector and that requires special analysis to explore the possibilities of renewable energy integration.

Technical and economic implications of renewable energy integration possibilities are different from system to system due to number of factors. System attributes such as size, plant composition, network features, stability levels, operational constraints, interconnectivity and demand characteristics as well as renewable energy resource characteristics such as seasonality, intermittency and geographical locations are important factors. Therefore, being the transmission system operator, Ceylon Electricity Board (CEB) conducts a comprehensive study, to determine the optimum extent of renewable energy integration covering its technical, economic, operational and environmental aspects prior to formulating the long term generation expansion plan. This paper presents the above

renewable energy integration study describing its methodology and results covering the renewable resource assessment; long term optimized planning, operational analysis and economic analysis. Detailed analysis conducted on the system stability as an integral part of the study carried out by transmission planning unit is not described in this paper. Renewable energy (RE) forms except major hydro are referred to as “Other renewable energy” (ORE) and intermittent renewable energy sources such as wind and solar are referred to as variable renewable energy (VRE) in this work.

2. Study Methodology

The main objective of the study is to determine the optimum extent of renewable energy integration subjected to the technical, operational and economic constraints. A new methodology was adopted considering the limitations in Sri Lankan Power System specifically to investigate the restrictions of integrating more ORE’s and that has an integrated approach of major steps of the system planning functions. A simplified approach of the overall study methodology is shown in the figure 2. The study process started with the assessment of the renewable energy potentials in the country followed by the preparation of the future RE deployment scenarios as necessary. Optimized plant sequences were then determined for each scenario which were then subjected to the transmission network study and the operational study. Additional scenarios were defined whenever necessary for the network and operational study to obtain practical results.

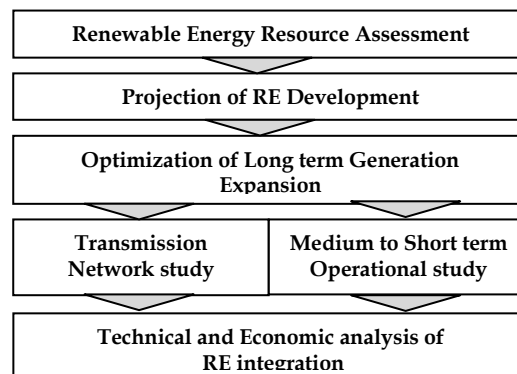


Figure 2 - Main Outline of the Methodology

Similar approaches have been adopted in other international studies such as Western wind solar integration [6], Hawaii solar integration [7] and have slight differences to suit the study objective and the system characteristics.

Figure 3 below illustrates the generation and transmission planning operation functions by timescale. The scope of this study covers most of the system constraints that are important from years to sub hourly time steps.

Years	Long-Term Planning
Weeks	Mid-Term Planning
Days	Unit Commitment
Hours	Economic Dispatch
Minutes	Generator Primary Control
Seconds	
Milliseconds	Protection

Figure 3 - System Planning functions by timescale

The methodology requires use of extensive amount of data and the use of number of modelling and simulation tools. Such details are presented in the relevant sections of this paper.

3. Renewable Energy Resource Assessment

Assessment of the performance of the each renewable energy sources is required for the detail modelling simulation and optimization work. Major Hydro, Wind, Solar, Mini Hydro and Biomass are separately modelled appropriately to assess capacity and energy contribution of while capturing all the necessary characteristics such as seasonality, intermittency and features of geographical dispersion. Effort is placed to best represent each resource while harnessing the maximum potential.

3.1 Assessment of Major Hydro Resources

Major hydro being the largest renewable energy contributor, accurate determination of its hydrological probabilities and total resource capability is important. However, this assessment is complex due to the cascade and multipurpose nature of reservoirs with numerous operational constraints. The software tool Stochastic Dual Dynamic Program (SDDP) which is a hydrothermal dispatch model that determines least-cost stochastic operating policy of a hydrothermal system for short, medium and long term operation studies was used for the purpose. The simulation tool uses the hydro inflow data on past 35 years to stochastically estimate the hydro potential for

multiple scenarios. Following Figure 4 illustrates the probabilistic variation of annual energy production of hydro system. It is important to note that the hydro energy can vary as much as 2250GWh depending on the hydrological condition which is a significant uncertainty. The average hydro condition yields 4155GWh of energy for power generation.

As illustrated in figure 5 the Even though the total capacity of the Major hydro is closely 1384 MW, the actual available capacity can vary from 85% to 45% seasonally depending on the month of the year and the hydrological condition.

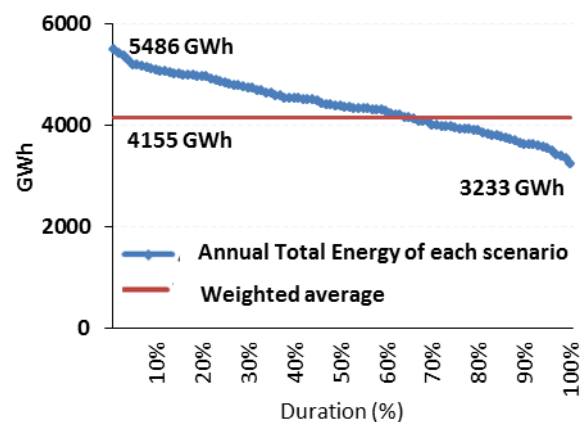


Figure 4 - Variation of Annual Energy

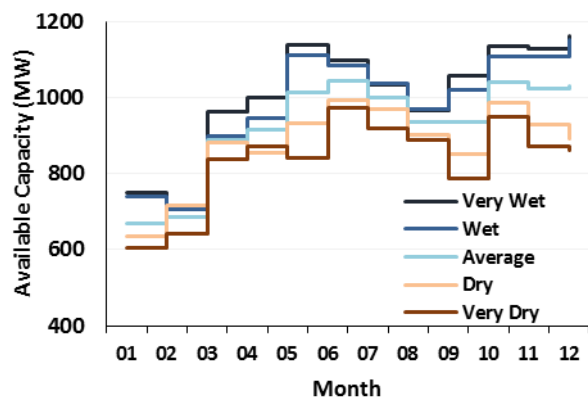


Figure 5 - Available monthly average capacity of the hydro for hydrological conditions

3.1 Assessment of Wind Resources

Assessing the performance of wind resources in the country is crucial as it is one of the best wind resource potential in the world. Therefore capacity and energy contribution, seasonality intermittency and geographical dispersion have been given importance in the modelling activity.

As the wind resources of different quality are spread across the country, this study considered five main wind regimes for the



modelling. 10 minute wind measurement data recorded by Sustainable Energy Authority (SEA) and the Ministry of Power and Renewable Energy (MOPRE) were used for the modelling purpose. Using the software tool System Advisor Model, wind plants were modelled for each wind regime and parameters of each wind plant are set considering multiple factors while ensuring maximum energy yield [3]. Table 1 provides the main wind plant parameters and results obtained for energy for each wind regime. The figure 6 shows the power production profiles obtained from simulation for the Mannar wind resource.

Table 1 - Characteristics of Wind plants modelled for each wind regime

Parameter	Turbine capacity (MW)	Block Capacity (MW)	Annual Energy (GWh)	Annual Plant Factor (%)	Wind Speed Data location
Mannar	2.5	25	80	36.7	Nadukuda 2015
Puttalam	2	20	55	31.4	Udappuwa 2009-2010
Hill Country	0.5	10.5	17	19.1	Seethaeliya 2012-2014
Northern	2	20	59.7	34.1	Pooneryn 2015
Eastern	2	20	47.9	37.3	Kokkilai 2015

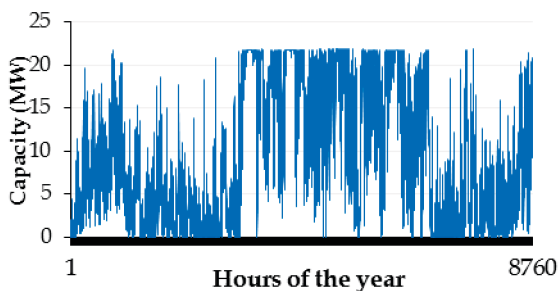


Figure 6- Power output variation of 25MW wind plant at Mannar

3.2 Assessment of Solar PV Resources

Performance of solar PV resources was assessed using the Sam Advisor Model through modelling and simulation. Solar irradiance measurements were obtained from the Sustainable Energy Authority (SEA) where the data were available for two locations in northern and southern areas of the country. Therefore two solar regimes were considered for this study. Global Horizontal Irradiance

(GHI) and Diffuse Horizontal Irradiance (DHI) measurements were available in ten minute time steps and the Direct Normal Irradiance (DNI) was estimated with the available GHI and DHI using solar zenith angle. Typical commercial PV modules and parameters were used modelling the solar PV plant. Figure below illustrates the estimated output of a 10MW Solar PV plant at Kilinochchi for consecutive five days.

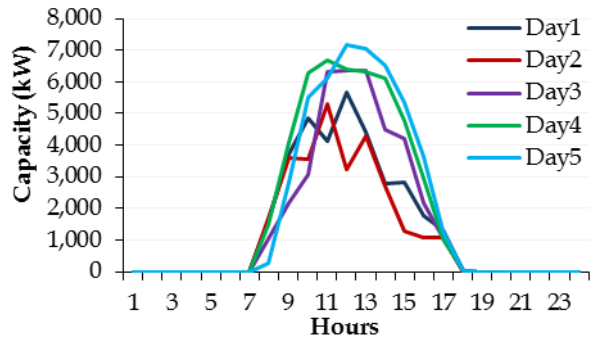


Figure 7 - Output of a simulated 10 MW solar PV plant at Kilinochchi area

3.3 Assessment of Mini Hydro Resources

The Model for Mini-hydro power plant was appropriately prepared based on 10 year historical data to reflect the seasonal energy and monthly average capacity variation and to obtain accurate results. The annual plant factor is estimated to be 37.4 % in the average hydro condition. Figure 8 below illustrate the average model used for the mini-hydro resources.

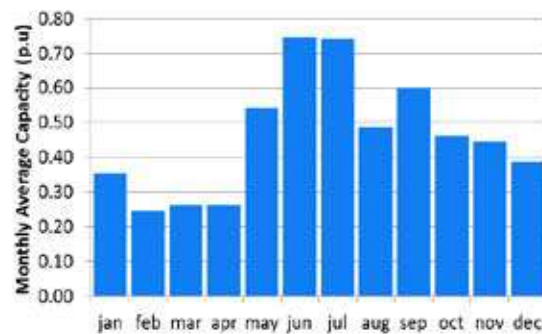


Figure 8 - Monthly average capacity Variation of the mini-hydro Plant in p.u

4. Optimized long term planning

Once the renewable energy resources are assessed, long term planning of the total system is then carried out. Development of renewable energy resources and other thermal generation sources is determined through the optimization process.

4.1 Renewable Energy Development Projection

Projection of the development of future renewable energy potentials is based on number of technical and other driving factors. Fundamentally, most attractive resources were given priority for the development.

Only few alternatives remain for the major hydro development as the county's potential is already harnessed to a greater extent. 241MW of Major hydro plants already planned [1] will be added during the period of this study. Capacity additions of other renewable energy sources have been projected for all five wind regimes, two solar regimes and for Mini-hydro and biomass resources. Quality of resource, availability and the development transmission infrastructure, maintaining optimum share of other renewable energy have been considered for future capacity additions. Factors such as past experience in renewable energy project development, reduction of global technology costs especially solar PV [4], availability of land and other infrastructure were given consideration when making the projection. It is was identified that increasing the total ORE share above 20-22% causes system to experience operational limitations where the VRE output have to be curtailed. Such knowledge has also been considered in making initial projections.

In this study considered two main ORE development cases that are defined optimum ORE share more than 20% by 2020. Basis for defining two cases considered mainly the curtailment levels due to system operational flexibilities with different future expansion scenarios of major power plants. Many other cases were defined on the basis of regulatory reserve availability under the transmission network study purpose and they were not covered under the scope of this paper. But the results of the system study have also been incorporated in preparing the projections. Projected ORE capacities for selected milestone years are given in the table 2 and the table 3 respectively.

Table 2 - ORE development case -1

Year	Mini Hydro (MW)	Wind (MW)	Biomass (MW)	Solar (MW)	Total Capacity
2018	344	144	39	210	737
2020	374	414	49	410	1246
2025	424	729	74	685	1912
2030	474	894	99	1009	2476
2035	524	1184	114	1283	3105

Table 3 - ORE development Case -2

Year	Mini Hydro (MW)	Wind (MW)	Biomass (MW)	Solar (MW)	Total Capacity
2018	344	144	39	210	737
2020	374	414	49	410	1246
2025	424	649	74	635	1782
2030	474	814	99	959	2346
2035	524	1104	114	1233	2975

4.2 Optimized development scenarios

Long term expansion planning was carried out using the WASP IV software tool to identify optimum plant development program. Several key long term development scenarios with various system flexibilities were analysed to evaluate impact of RE integration.

At this stage focusing on different RE integration method is important. Flexibility of power plants, storage technologies, demand side measures and grid support from renewables are among them [5], [9]. In this study, considering the Sri Lankan context, the grid support of pumped storage hydro power plant that has been planned mainly for the peak power requirement, was subjected to analysis.

Four main scenarios were defined and the technical, operational and economic impact of the introducing combined cycle units, coal fired units and the grid scale storage system such as pumped storage hydro power plant are key differences of these scenarios. Each scenario represents the least cost plant sequence for the corresponding renewable energy development Case (case1 or case 2). Additionally, a Reference scenario was created with no future ORE development for the comparison purpose. A summary and the capacity additions of the scenarios are given in the table 4 and table 5 below.



Table 4 –Optimized Long term planning scenarios

Scenario	Description
Reference scenario	Only the existing “other renewable energy” by 2016 is included and No future ORE development is assumed
Scenario 1	New Combined cycle power plants are restricted in western region. Coal and Pumped hydro plants included
Scenario 2	Development Coal units are limited with pumped hydro and more Combined cycle units are permitted in other locations
Scenario 3	Development coal units and pumped hydro units are restricted. All new additions are combined cycle units.
Scenario 4	All new additions are combined cycle power plants with pumped hydro development

Table 5 - New Major Capacity Additions in each scenario until 2036

Type of plant	Reference scenario	Scenario 1	Scenario 2	Scenario 3	Scenario 4
Major hydro	241	241	241	241	241
Gas Turbines	105	105	105	105	105
Combined Cycle	1500	1500	2700	4800	4200
Coal	3300	2400	1200	0	0
Pumped Hydro	600	600	600	0	600
ODE Dev. Case	Case 1	Case 1	Case 1	Case 2	Case 1

5. Operational analysis

In the power system operation process, maintaining supply and demand balance at all times is utmost important to ensure continuous and reliable supply of electricity. Intermittency of variable renewable energy sources such as wind and solar, specially introduce additional supply side fluctuation to the system. These fluctuations are compensated by the rest of the power plants in the system and their flexibility to that is often finite [8]. Therefore Sri Lankan power system, being a small isolated power system, its ability to integrate more variable renewable energy significantly depends on the operational flexibility of the system. The objective of the operational study is to examine in detail the operational flexibility and constraints of the system in integrating high levels of variable renewable energy sources.

Main operational constraints in VRE integration are limitation of operational flexibilities of different power plants [11]. Ramping rate of different plants that determines how quick the plant can respond to counter the changes in VRE output, Minimum stable loading level of the power plant which determines how much room and reserve can be allocated for the operation of VRE throughout the day. Additionally, plant start-up and shutdown constraints are also important to a certain extent. Observing these characteristics requires the operation to be simulation at least sub-hourly time step. In this study simulation were conducted in 30 minute time steps.

The software tool Stochastic Dual Dynamic Program (SDDP) was used for determining the medium term hydro-thermal operation policy and subsequently the software tool (NCP) was used for optimized short term dispatch simulation in 30 minute time steps. Both models requires extensive amount of input data and computation resources. The input data requirement ranges from 30 minute VRE output data, demand data, plant technical, operational parameters to system wide operational requirements such as reserves and largest single unit restrictions.

The key observation of the dispatch simulation results was the scale of over generation of VRE resource. In other words some parts of the VRE generation are seen as excessive due to the operational limitations of the system. In such instances VRE generation had to be curtailed. The requirement of such curtailment depends on many factors such as the VRE production level, intermittency, demand level and the type of power plants online at the time.

The study specially requires the dispatch information for entire year for multiple years and the short term model is capable of simulating limited number of days at a time. Therefore considering the scale of the study, a given year was divided into three periods as illustrated in Figure 9 and a weekday and a weekend day was simulated for each period that provide simulation of 6 days per each year to make a reasonable approximation,. This approximation is mainly to reasonably capture the seasonal variation of renewable energy production and the demand variations.

Dry Period	High Wind Period	Wet Period
Jan- April	May- Aug	Sep- Dec

Figure 9 - Approximation of a year

Considered plant operational constraints are crucial in determining the system's VRE absorption capability. Following key assumptions were used for this study.

- Future VRE Generation profiles are estimated based on measured data and past performance. No significant variation was assumed for future years.
- Maintenance plans of major power plants (Coal fired and Combined cycle Plants) were prepared as per the maintenance requirement and present practice.
- According to the past demand data, relatively low off-peak usually occur on Monday early mornings and relatively low Day time load is present in Sundays. To capture such bottlenecks a Sunday and a Monday is consecutively simulated in short term model.
- Wind, biomass, solar and mini hydro were considered as "Must run" power plants and curtailment of VRE is allowed subjected to operational constraints.

In terms of operation reserve, higher level of reserve is necessary with the increased penetration of VRE sources. For this study purpose 5% of reserve for load variability and 10% reserve from VRE share are included as regulation reserve requirements.

Simulations were conducted for four key years (2020, 2022, 2025 and 2028) covering 10 years period from 2018 for several scenarios. Sample of the results obtained for a day in high wind period weekend of 2025 is given in the figure 10 below.

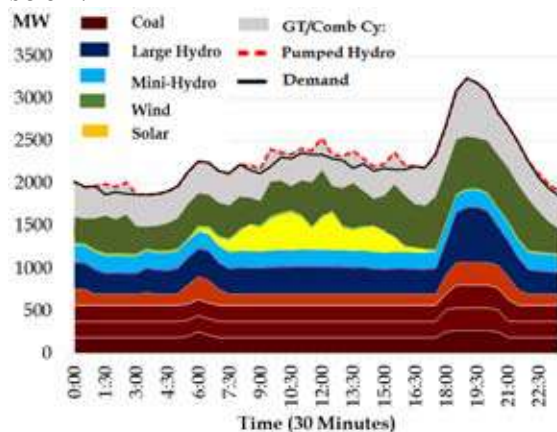


Figure 10 – 30 minute dispatch simulation of a 2025 weekend day in high wind season

The figure 11 illustrates the ORE production relative to the demand and the red coloured portion is the VRE over generation that need to be curtailed due to operational constraints.

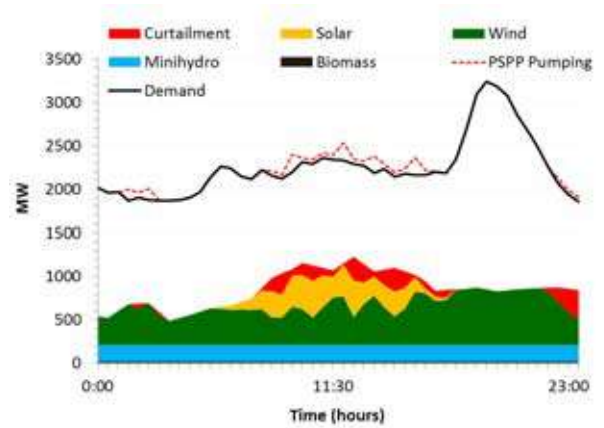


Figure 11 –curtailment Requirement of VRE 2025 weekend day in high wind season

6. Variable Renewable Energy Curtailment

Summary of the scale of curtailment observed through the operational study results are given in the table 6 below. No curtailment was observed in the year 2018 and Key observations of the operational analysis are as follows.

Table 6 – Observed Curtailment levels

Yr	High Wind Season (MW)				Wet Season (MW)			
	Weekday		Weekend		Weekday		Weekend	
	OP	DP	OP	DP	OP	DP	OP	DP
Scenario 1 (New Combined cycle power plants are restricted in western region. Coal and Pumped hydro plants included)								
2020	150	-	80	50	170	-	140	-
2022	220	-	140	100	-	-	-	-
2025	380	-	330	280	70	-	20	-
2028	70	-	60	185	-	-	-	-
Scenario 2 (Development Coal units are limited with pumped hydro and more Combined cycle units are permitted in other locations)								
2028	70	-	30	111	-	-	-	-
Scenario 3 (Development coal and pumped hydro units are restricted. All new additions are combined cycle units)								
2025	445	-	380	430	-	-	-	-
2028	80	-	200	276	-	-	-	-

*OP- Off peak, DP- Day peak

- No renewable energy curtailments were observed in dry periods, mainly due to the very low level of wind and mini-hydro production.
- Curtailments were observed on High wind period from 2020 onwards in all scenarios and gradually rising until 2015.
- Reduced curtailments can be observed in wet periods compared to high wind period.
- Weekend days required higher curtailment levels at day time than week days due to the relatively low demand levels.
- Off peak curtailments were significant in the lowest off-peak of the week.
- Both off-peak and daytime curtailments were observed in high wind periods.
- Introduction of pump storage units from 2025 to 2028 gradually decreases the curtailment requirement both in day time and off-peak time. Curtailment requirement increases when the pumped hydro development restricted. However, it slightly reduces when the combined cycle plants are operated with higher flexibility.

Approximated calculation yields that this level of curtailment can result 2-3% reduction in annual VRE (wind and solar PV) generation and such curtailment can negatively affect the economic viability of VRE projects.

7. Economic and Cost Analysis

Economic cost effectiveness of renewable energy technologies is also a crucial factor in determining the integration possibilities. There are number of cost components to be considered when evaluating the RE integration possibilities and the total Present Value (PV) cost for each scenario over the 25 year period (2017-2036) is considered in evaluating the cost effectiveness alternative scenarios. Addition to that the capacity, energy and emission benefits of RE can be assessed in comparison with the reference scenario.

The PV cost mainly includes the capital cost, operation costs, relevant infrastructure development cost and cost of additional system reserve for VRE integration. Capital costs data, plant factors and the levelized cost of electricity (LCOE) of ORE considered for the study is given in the table below. Most appropriate technology costs for the Sri Lankan context is considered and the falling capital cost of solar PV is incorporated to reflect the present trend. Table 8 below compares the total PV cost of each scenario against the reference scenario.

Table 7 - Levelized Cost of Other ORE technologies

Renewable Technology	Capital Cost	Plant Factor	LCOE (UScts/kWh)
Solar PV (2017-2020)	1412 USD/kW	17 %	11.80
Solar PV (2021-2025)	1100 USD/kW	17 %	9.34
Solar PV (2026 onwards)	900 USD/kW	17 %	7.76
Wind	7.26	35 %	8.19
Mini Hydro	6.22	37 %	7.80
Biomass	3.44	80 %	18.19

Table 8 - Levelized Cost of ORE technologies

Scenario	Total PV Cost up to 2036 (USD million)	Difference with Reference Scenario (USD million)
Reference	12382.0	-
Scenario 1	12872.0	490.0
Scenario 2	12979.3	597.3
Scenario 3	13653.3	1271.3
Scenario 4	13618.6	1236.6

It is observed that the cost of the reference scenario is the lower than other scenarios. The scenario 1 is the lowest among four scenarios. Therefore the most economically optimum strategy to increase system flexibility to integrate the level of renewable energy penetration envisage in this study, is to develop a combination of low cost base load power plants with pumped hydro power plant. When the system flexibility is increased by increasing the number of combined cycle units in the system, curtailments are reduced but the total cost increases is significantly.

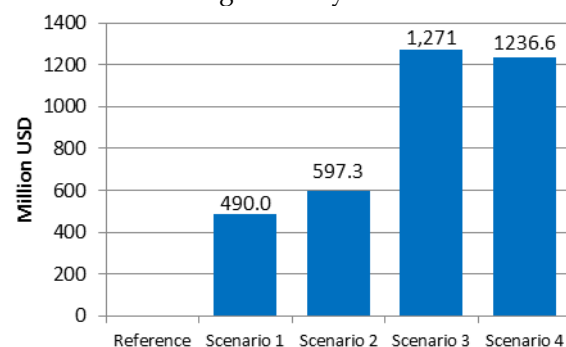


Figure 12 - Cost differences of Scenarios

8. CO₂ Emission Reduction

The renewable energy development significantly supports the country's obligation of reducing greenhouse gas emissions. The level of RE development projected in this study successfully contributes for the reduction of GHG emissions in-line with the nationally determined commitment (NDC) submitted to UNFCCC. Latest analysis of power sector emissions that incorporated the RE projection of this study, compares the CO₂ reduction potential in two scenarios with and without renewable energy development and it is illustrated in the figure 13 below.

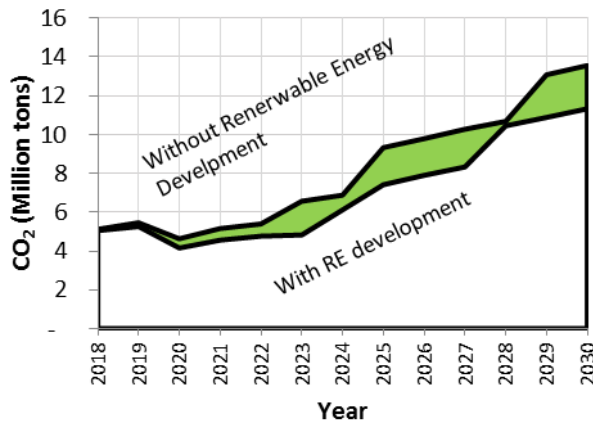


Figure 13 - CO₂ emission comparison of with and without renewable energy development

10. Conclusions

It is observed that the system flexibility is limited when increasing in variable energy share around 20% requires curtailment. According to the results, inclusion of hydro units with a combination of low cost base load plants and combined cycle units increases the system flexibility as well as the cost effectiveness for integrating RE share envisaged in this study.

Sri Lankan power system needs to adopt following measures for the effective integration of higher level of Renewable Energy sources in to the system.

- Establishing a day ahead, hourly basis wind and solar PV energy forecasting systems and a 24 hour (round the clock), Renewable Energy Desk for the national dispatch centre.
- Proving Variable Renewable Energy (VRE) curtailment rights to system operator and introducing a compensation mechanism has to be studied to future VRE plants.

- Designing the future base load power plants to be de-loaded with increased flexibility in order to minimize the VRE curtailment.
- Completing the planned network strengthening projects as scheduled.
- Prioritizing the development of ORE locations based on life cycle cost considering plant factors, availability and cost of transmission network.
- Incorporate the characteristics grid scale storage technologies to enhance the system flexibility.
- For small scale RE projects, competitive bidding process should be adopted to reflect the economic costs of development.
- If the proposed conventional plants are not commissioned as scheduled, the VRE addition in the plan has to be revised accordingly. Thus it is proposed to review this planning methodology once in two years.
- The LNG Power Plants may require minimum plant factors high as more than 70% in order for LNG contracts to be viable and competitive in the global market. This would lead to curtailment of more RE sources in order to dispatch the LNG operated power plants. Therefore, LNG procurements contracts should be negotiated to minimize the 'Take or Pay' risks.
- This study open a pathway for a paradigm shift to Sri Lankan Electricity Generation System in near future by enabling the integration of more renewable energy for future years as illustrated in the Figure 12.

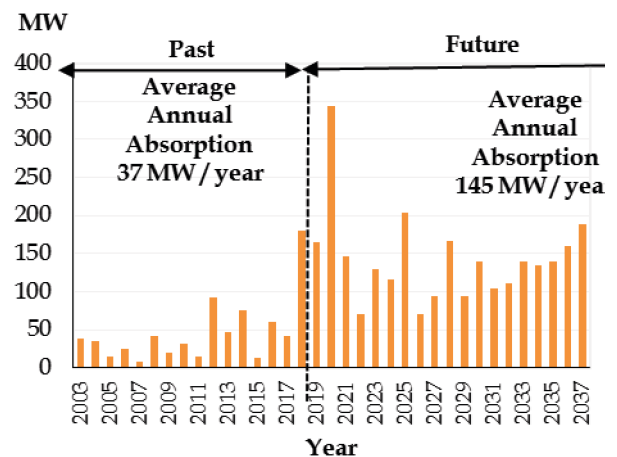


Figure 14 - Increased renewable energy integration



References

1. Long Term Generation Expansion Plan 2015-2034. Ceylon Electricity Board
2. CO₂ Emissions from Fuel Combustion, 2016 Edition, International Energy Agency
3. Wind resource assessment handbook, National Renewable Energy Laboratory (NREL), U.S. Department of Energy
4. World Energy Outlook 2016, International Energy Agency
5. Renewable Energy Road Map 2016 edition, International Renewable energy Agency
6. Western wind and solar integration study, National Renewable Energy Laboratory (NREL), U.S. Department of Energy
7. Hawaii solar integration study: National Renewable Energy Laboratory (NREL), U.S. Department of Energy
8. Emerging Issues and Challenges in Integrating High Levels of Solar into the Electrical Generation and Transmission System, National Renewable Energy Laboratory, U.S. Department of Energy
9. Grid Operations for Efficient Variable Renewable Integration, Dr. Michael Milligan, National Renewable Energy Laboratory, U.S. Department of Energy
10. The Evolution of Wind Power Integration Studies: Past, Present, and Future, Erik Ela, Michael Milligan, Brian Parsons, Debra Lew, David Corbus, 2009 IEEE
11. Integrating Variable Renewable Energy: Challenges and Solutions, L. Bird, M. Milligan, and D. Lew, National Renewable Energy Laboratory

Optimum Use of Solar Inverter by Feeding Reactive Power at the Night

K. Kanchanee Navoda and Asanka S. Rodrigo

Abstract: Due to the significant increase in the price of Grid Electricity, many countries are switching to Renewable sources. With the expanded Solar Net Metering system in Sri Lanka, domestic consumers and commercial consumers are benefited, after installing such a renewable energy system directly connected to the LV distribution system. However, LV distribution system in Sri Lanka has many issues related to the under voltages. The PV inverters are not utilized at the night peak. Therefore, it can be operated in feeding reactive power to eliminate the low voltage occurrence during the night peak. This paper describes the theoretical background of "How the solar PV inverters can be operated as a voltage controller in Sri Lankan Electricity Network by feeding reactive power". The study was conducted considering the existing PV inverters. An algorithm is developed to calculate operating power factors for existing PV inverters in the feeders, where the feeders are experiencing under voltage problems. The proposed algorithm was discussed with a case study, and the results are verified by modelling the same system in SynerGee. Based on the developed algorithm, a software tool with a user interface is developed to calculate the operating power factors. In order to promote this scheme, an economic evaluation was carried out by proposing an incentive scheme for customers. It is found that by implementing such system, the net benefit to the utility was positive. Furthermore, by utilizing distributed PV inverters at night peak by feeding reactive power, low voltage issues and line losses can be reduced.

Keywords: Power Factor, PV Inverter, Reactive Power

1. Introduction

Solar power is only available at the day time where the effectiveness of this solar installation is zero during the night time. However due to the rapid growth of solar PV installations, now the network is connected with many distributed generators [1-3]. It is shown that the solar PV installations with modern grid connected inverters can be used to ensure the voltage stability of the network by feeding reactive power [4-6].

Most of the utilities are experiencing system voltage unbalances at many feeders during the night time. This situation can be eliminated by using a net metering inverter as a VAR producer to the system. That can provide reactive power for maintaining the system voltage within its limits. The operating power factor of the inverter has to change for feed reactive power to the grid. The efficiency in the use of net metering installation is increased and helped to maintain the grid voltage stability by this concept. [7][9][12][13]

This method is not yet popular in Sri Lanka because the available tariff methodology does not address about a rate for reactive power. As this feed is important as an effective

improvement of the night grid performance, this can be promoted by proposing a new tariff for reactive power generation as well.

2. Literature Review

In the past, several research has been done on the methods for feed reactive power to distribution networks using different methods. One of those studies which are described in [10] by Huajun. Yu, Junmin. Pan, and An. Xiang. The theory behind the inverter use to produce VAR was described by these authors, and that was applying appropriate phase shift between reference current and grid.

The internal arrangement of the solar grid tie inverter use to as a VAR injector was described in the paper [12] by A. Ellis, B. Kirby, C. Barker, E. Seymour, E. Von Engeln, J. MacDowell, J. R. Williams, L. Casey, R. Nelson, R. Walling and W. Peter. Also, the same arrangement further

Eng (Ms.) K. Kanchanee Navoda, M.Sc.(Moratuwa), B.Sc.Eng.(Ruhuna), AMIE(SL), Electrical Engineer, Ceylon Electricity Board.

Eng. (Dr.) Asanka S. Rodrigo, Ph.D.(HKUST), M.Sc.(Moratuwa), B.Sc.Eng.(Moratuwa), AMIE(SL), Senior Lecturer, Department of Electrical Engineering, University of Moratuwa.



described with simulation results in the paper [11] by Maknouninejad, M. Godoy Simoes and M. Zolot. The simulation and practical results were obtained in the paper [8] by A.Cagnano and E.D. Tuglie with varying the parameters and tested with several scenarios.

According to the tariff system which was proposing in the reactive power feeding concept in Germany was described in the paper [1] by A. Kozinda, T. Beach and V. Rao, the concept was for the whole day. The cost comparison was made based on two factors in this paper; those were 'cost to the customer to produce reactive power' and 'cost to the utility to produce reactive power' with the absence of inverter feeding method. Under that 'cost to customer' was again considered with the cost if the customer downgrades power factor and cost if the customer over sizes the inverter. On the other hand, the cost to the utility of installing capacitor banks to compensate the reactive power requirement was instated feeding it by using an inverter.

Tariff method needs to be addressed a rewarding method to the customer who wishes to feed reactive power at the night peak. Before proposing such tariff, the tariff for reactive power consumption also needs to be introduced. The Maximum Demand Charge for Bulk Consumers which was the only consent on reactive consumption, introduced in Sri Lankan tariff system. The purpose of introducing Maximum Demand Charge was to encourage the customer for Demand Side Management and minimize the system voltage reduction and harmonics etc.

Considering the tariff systems in other countries, several methods were recommended to charging for reactive power. Per kVAr rates in three blocks for reactive power were introduced Singapore and Spain. From April 2010, a common charging method was forced across all UK Electricity Supply Companies. The way the reactive power charge was calculated; the customer was 'allowed' to use reactive power up to a third of the active power consumed for free, 'allowed' reactive power = 0.33 x total kWh. The charge was only applied by reducing the allowed reactive power from total consumed reactive power. In German distribution network operators were charged in averagely 1.1 c€/kVArh (0.0-2.7 c€/kVArh) for reactive power consumption only if the power factor was lower than 0.9 (in average). [5]

This research study was conducted using the existing PV inverters. Therefore, the capacities and the implemented locations were already set. All the research works carried out in the literature review was calculated the suitable capacities and the pre-defined locations (selected by another calculation) to minimize the low voltage issues in the feeder. The developed algorithm also specified to select operating power factors for each existing PV inverter only.

The economic evaluation mentioned in the paper was described the cost saving factors [1] according to the Sri Lankan tariff system, and the reactive tariff was proposed to reward such customers who were expected to feed reactive power to the network through their PV inverters. This total economic evaluation was newly discussed in the paper, and it was not previously mentioned in other research works mentioned in the literature review.

3. Mathematical Modelling

3.1 Technical Background

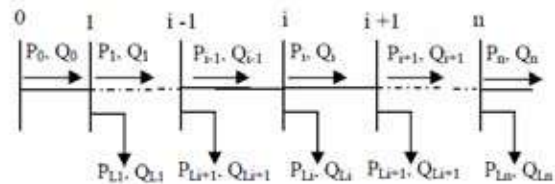


Figure 1- Line Diagram of Feeder Points

The active loads and reactive loads were obtained in each point, and power flow of throughout the line was represented according to the above line diagram. The i^{th} point active power load and reactive power load were represented as P_{Li} and Q_{Li} . The active and reactive power at point i was represented as P_i and Q_i (Figure 1).

Active Power at $i+1$ bus,

$$P_{i+1} = P_i - P_{Li+1} - R_{i,i+1} \cdot \frac{(P_i^2 + Q_i^2)}{|V_i|^2} \quad \dots (1)$$

Reactive Power at $i+1$ bus,

$$Q_{i+1} = Q_i - Q_{Li+1} - X_{i,i+1} \cdot \frac{(P_i^2 + Q_i^2)}{|V_i|^2} \quad \dots (2)$$

Line Loss between i^{th} and $i+1^{\text{th}}$ bus,

$$P_{\text{Loss}}(i, i+1) = R_{i,i+1} \cdot \frac{(P_i^2 + Q_i^2)}{|V_i|^2} \quad \dots (3)$$

Here the line resistance and line reactance between i^{th} and $i+1^{\text{th}}$ points were $R_{i,i+1}$ and $X_{i,i+1}$. S (kVA) was denoted the installed solar inverter capacity, the operating power factor of the solar inverter $\cos\alpha$ was needed to be fixed according to the requirement of the reactive power at the

particular location and the distribution line conditions (Minimum voltage, Power Loss, etc..).

Reduced distribution line loss between i^{th} and $i+1^{\text{th}}$ points was denoted as,

$$P_{\text{Loss new}}(i, i+1) = R_{i,i+1} \cdot \frac{P_i^2 + (Q_i - S_i \sin \alpha)^2}{|V_{i \text{ new}}|^2} \dots (4)$$

The current $I_{i,i+1}$ in figure 2 was represented as I_r and I_x where $I_r = I_{i,i+1} \cos \theta$, $I_x = I_{i,i+1} \sin \theta$ respectively ($\cos \theta$ is the power factor).

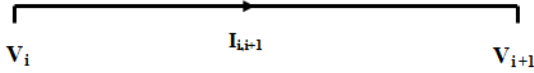


Figure 2 - Current between Two Points

$$V_i = V_{i+1} + I_{i,i+1} (R_{i,i+1} + jX_{i,i+1}) \dots (5)$$

$$V_i = V_{i+1} + (I_r - jI_x) (R_{i,i+1} + jX_{i,i+1})$$

$$V_i = V_{i+1} + I_r R_{i,i+1} + I_x X_{i,i+1} \dots (6)$$

$$V_i = V_{i+1} + I_{i,i+1} \cos \theta R_{i,i+1} + I_{i,i+1} \sin \theta X_{i,i+1} \dots (7)$$

Hence voltage drop between i^{th} and $i+1^{\text{th}}$ point,
 $V_i - V_{i+1} = I_{i,i+1} (R_{i,i+1} \cos \theta + X_{i,i+1} \sin \theta) \dots (8)$

Considering the scenario with feeding reactive power shown in figure 3,

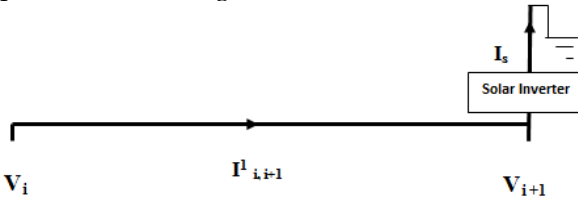


Figure 3 - Current between Two Points with PV Inverter

$$I_{i,i+1} = I_{i,i+1} + jI_s \dots (9)$$

Here I_s the current flow through the solar inverter,

$$I_{i,i+1} = I_r - jI_x + jI_s \dots (10)$$

Hence under above scenario voltage drop between i^{th} and $i+1^{\text{th}}$ point,

$$V_i - V_{i+1} = I_{i,i+1} (R_{i,i+1} + jX_{i,i+1})$$

$$V_i - V_{i+1} = I_r R_{i,i+1} + I_x X_{i,i+1} - I_s X_{i,i+1} \dots (11)$$

Before feeding of reactive power by solar inverter, the representing voltage at $i+1^{\text{th}}$ point was,

$$V_{i+1} = V_i - I_r R_{i,i+1} - I_x X_{i,i+1} \dots (12)$$

After feeding of reactive power by solar inverter, the representing voltage at $i+1^{\text{th}}$ point was,

$$V_{i+1} = V_i - I_r R_{i,i+1} - I_x X_{i,i+1} + I_s X_{i,i+1} \dots (13)$$

The voltage was improved, and this improved voltage was maintained between the accepted standard tolerances margin is $\pm 6\%$.

The current I_s was adjusted within the allowed voltage tolerance margin. I_s was denoted as,

$$Q = \frac{V \times I_s}{1000} \dots (14)$$

Here Q was in kVAR which is feeding by the solar inverter.

$$Q = S \sin \alpha \dots (15)$$

Here S was the apparent power of the solar inverter and the $\sin \alpha$ was the operating power factor ($\cos \alpha$) of the inverter which was set according to the requirement of voltage regulation.

3.2 Objective Function

The objective function was obtained as a sensitivity factor by considering the power loss function equation no (3) of a point. Line loss between i^{th} and $i+1^{\text{th}}$ sections,

$$P_{\text{Loss}}(i, i+1) = R_{i,i+1} \cdot \frac{(P_i^2 + Q_i^2)}{|V_i|^2}$$

Sensitivity factor was defined as,

$$\frac{\partial P_{\text{Loss}}}{\partial Q_i} = \frac{2Q_i R_{i,i+1}}{V_i^2} \dots (16)$$

The locations where the power losses are high were identified by the Sensitivity Factor. This was defined as a function of reactive power since the concept was to feed reactive power by a solar inverter and reduce line losses and maintain the system voltage within the margins.

3.3 General algorithm for VAR control with existing PV installations

The operational data of the selected existing system (LV feeder) with PV installations were considered as the inputs for the algorithm. The load data of each pole and the voltage profile on each pole were taken in to account for the model. Then by considering the data, the locations were identified where the low voltage profiles existed.

Existing installed solar inverter data such as the inverter capacity and the availability of the function of Q at night mode was collected.

The sensitivity factor was computed to each pole, and the locations were identified where the power losses are high considering as a factor of reactive power.

According to the information of installed solar inverters, the largest capacity of inverter was



selected which was the nearest location of the poles and which was having the highest loss. The operating power factor of the inverter was set where it feeds required reactive power, to eliminate low voltage issues and the voltage profiles of the poles were increased within the standards.

The voltage profiles were obtained again, and the low voltage affected areas were selected and if the issue was there then again the sensitivity factor for the selected feeder was computed with the modification, and the next highest loss locations were identified. The iterations were done by using Genetic Algorithm.

Next, the installed solar inverter was selected where having a high capacity to the nearest location among the poles which are having with highest losses and operation power factor was set as mention in above.

The function was repeated until eliminate or reduce the low voltage problems of the selected feeder with existing solar installations.

4. Case Study

A sample model was created for case study considering the features shown in Table 1. Parameters of the sample feeder were shown in Table 2.

The final operating power factors of each PV inverter installation which are to feed reactive power to minimize the low voltage problem were shown in the Table 3.

Table 1- System Features

Transformer Capacity (kVA)	100
Feeder Length (m)	1500
Average Pole Span (m)	40
Fly Conductor Resistance (Ohm/m)	0.000452
Fly Conductor Reactance (Ohm/m)	0.000321
Average Service Wire Length (m)	30
25mm ² ABC Service Wire Resistance (Ohm/m)	0.00149
25mm ² ABC Service Wire Reactance (Ohm/m)	0.0001
Total Customers per Feeder (1 Phase)	64

Table 2- Parameters of the Sample Feeder

Length of the Feeder (m)	No of service connections at the pole	Installed inverter Capacity (kVA)	Active Power Load (kW)	Reactive Power Load (kVAr)
0				
40	2	0.5	1.20	0.60
80	2		1.30	0.60
120	1		0.56	0.40
160	2	1	1.50	0.60
200	2		0.92	0.51
240	3		1.36	0.94
280	1	2	1.11	0.73
320	2		0.75	0.44
360	2		0.64	0.18
400	2		0.45	0.25
440	3	3	1.28	0.30
480	2		1.33	0.61
520	1		0.95	0.70
560	1	0.5	0.64	0.37
600	2		1.20	0.50
640	3	1.5	1.37	0.14
680	1		0.94	0.27
720	3	0.5	2.20	1.20
760	2		1.06	0.52
800	1	2	1.12	0.60
840	2	0.5	1.23	0.47
880	1		0.86	0.70
920	1		0.81	0.50
960	2	2	1.80	0.62
1000	3		2.21	0.72
1040	2		1.25	0.76
1080	1	0.5	0.94	0.45
1120	2		1.68	0.49
1160	1		0.85	0.73
1200	1	1	1.20	0.35
1240	1		0.76	0.27
1280	2	3.5	0.91	0.50
1320	1		0.80	0.20
1360	1	0.5	0.61	0.37
1400	1	1	0.68	0.34
1440	2		0.80	0.26
1480	1		1.50	0.31
1520	1		0.75	0.30

The results for voltage profiles were shown in Figure 4.

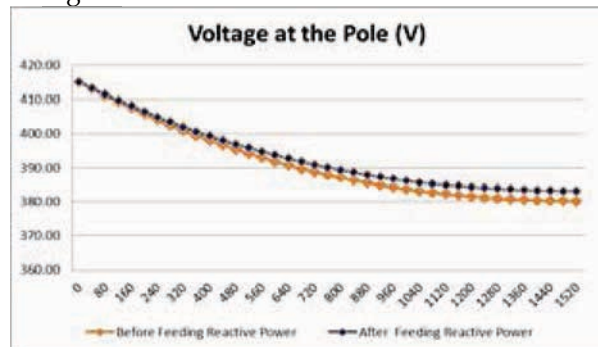


Figure 4 - Graph of Voltage Profiles

According to the resultant voltage profiles, it can be seen that when the absence of feeding reactive power, low voltage profile was obtained starting from 640m of feeder length and downwards. Once the reactive power feeding was enabled the low voltage profile was started from the 720 m length of the feeder. The point of 640 m and 680m feeder locations voltage were eliminated from low voltage issue. Considering all locations the voltage was increased slightly.

Table 3 - Computed Operating Power Factors

Length of the Feeder (m)	Installed inverter Capacity (kVA)	Final Operating Power Factor
40	0.5	0.00
160	1.0	0.80
280	2.0	0.93
440	3.0	0.99
560	0.5	0.67
640	1.5	0.99
720	0.5	0.00
800	2.0	0.95
840	0.5	0.28
960	2.0	0.95
1080	0.5	0.44
1200	1.0	0.94
1280	3.5	0.99
1360	0.5	0.67
1400	1.0	0.94

The obtained results for reactive power variation of the feeder were shown in Figure 5.

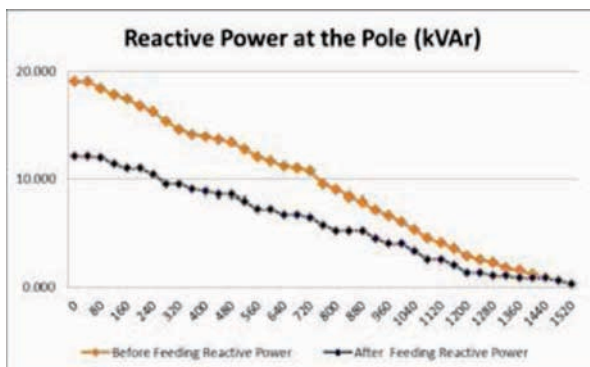


Figure 5 - Graph of Reactive Power Variation

According to the reactive power variation, it can be seen that the 19.045 kVAR of the reactive power feeding from transformer was

reduced and that balance was fed by the distributed solar PV inverters in the feeder. The obtained results for total current variation of the feeder were shown in Figure 6.

The obtained results for power loss variation of the feeder were shown in Figure 7.

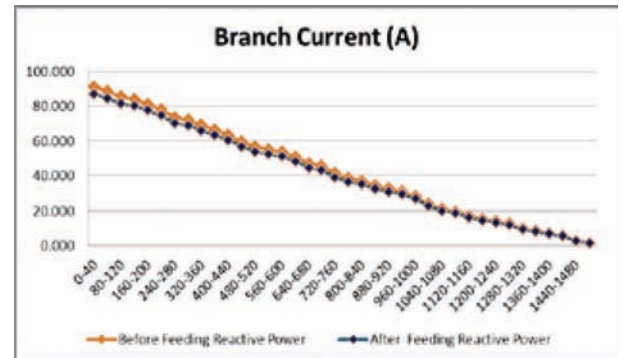


Figure 6 - Graph of Current Variation

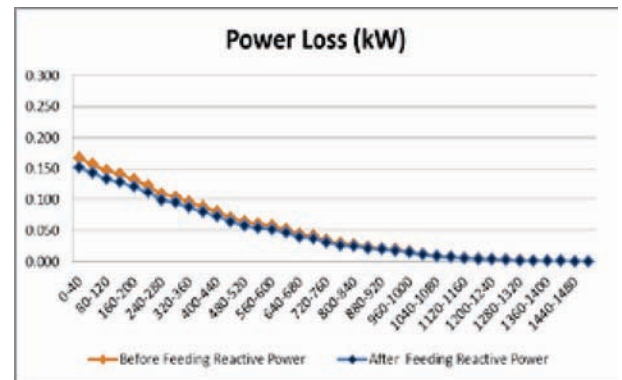


Figure 7- Graph of Power Loss Variation

According to the case study total power loss of all the branches before feeding reactive power was 1.95kW, and after feeding reactive power, the total power loss was 1.77kW. Total reduction of power loss was 9.26%.

5. Model Validation

The Case Study results obtained by the developed algorithm were compared with the results obtained by the SynerGee 3.5 software for the same Case Study.

The feeder loading at Table 2 have modelled in SynerGee was shown in Figure 8.

According to the parameter of the feeder and the connected loads, the low voltage scenario was shown after 640m of the feeder length.





Figure 8 - SynerGee Model of Case Study Feeder

The result obtained by the algorithm was used, and the inverters were placed in the feeder with the operating power factors according to the Table 3, and Figure 9 was shown the model that includes with PV inverter installations.



Figure 9- SynerGee Model of Case Study Feeder with PV Inverter Installations

After running the load flow analysis the low voltage issue was eliminated until 720m away the length of the feeder which was obtained as the same result by the implemented algorithm.

Compare to the results from the implemented algorithm and the SynerGee model the percentage of voltages with feeding reactive power obtained at the same nodes are almost same in both scenarios. Therefore the validity of proposed algorithm for reactive power feeding and its implemented software version was accepted.

6. Economic Evaluation

6.1 Energy Cost Saving due to Feeding Reactive Power

The economic evaluation was conducted considering the energy saving at selling end. The average cost per unit of selling end was taken at Rs 15.06 and the feeding time of reactive power was limited to peak hours. [2]

- Loss reduction due to reactive power feeding by solar inverter [4]

Reduced distribution line loss between i^{th} and $i+1^{\text{th}}$ points was denoted as,

$$P_{\text{Loss}}(i, i+1) = R_{i,i+1} I_{i,i+1}^2 \quad \dots (17)$$

The cost saving due to the reduction of loss was represented considering the distribution system loss.

$$\text{Saving of Cost (Per Year)} = \text{Saving of loss} \times \text{Average cost per unit} \times \text{Peak Hours} \times 365$$

Considering the Case Study the saving of cost due to the reduction of loss was Rs 3979.76.

- Increased line capacity due to reactive power feeding by solar inverter [4]

The line current without compensation was 91.365 A. The line current with compensation was 87.001 A.

Considering the Case Study the saving of cost due to the increased line capacity was Rs 45266.88.

- Increased Maximum Transfer Capability [4]

$$P_{\text{max}} = \frac{V^2 (-k + \sqrt{1+k^2})}{2X} \quad \text{Where } k = Q/P \quad \dots (18)$$

Considering the starting point of the feeder,

The maximum transfer capability without

$$\text{compensation} = \frac{V^2 \left(-\left(\frac{19.045}{48.07}\right) + \sqrt{1 + \left(\frac{19.045}{48.07}\right)^2} \right)}{2X}$$

The maximum transfer capability with

$$\text{compensation} = \frac{V^2 \left(-\left(\frac{12.078}{48.07}\right) + \sqrt{1 + \left(\frac{12.078}{48.07}\right)^2} \right)}{2X}$$

Considering the Case Study the saving of cost due to the increased line capacity was Rs 155593.07.

6.2 Proposal for Reactive Tariff in Sri Lanka

Proposing the reactive power tariff for Sri Lankan system was needed only to encourage the Demand Side Management. Therefore the rate was defined bit higher than the cost of the market price of per kVAR when installing the capacitor bank to improve the power factor. Then the customers were insisted to installed such system and improve the power quality

rather than paying a higher rate for each month.

Considering the Case Study results calculation was computed when a capacitor banks fixed at customer end. The assumptions were made in Table 4. [5]

Table 4 - Assumptions Made for Economic Analysis

Life time of the capacitor bank	5 years
Annual maintenance cost (% of capital cost)	2%
Cost of installing 1kVAr	Rs 3000
Rate of return on equity	20%

Considering the pole 40m away from the transformer required reactive power was 0.6 kVAr and assuming 1kVAr capacitor bank was installed operates at the peak time.

Total reactive energy required per year
= 876 kVArh

If the rate per kVArh was 'R' considering the annual cash flow,

$$R \times \sum_{x=1}^5 \frac{876}{(1+0.2)^x} = 3000 + \sum_{x=1}^5 \frac{60}{(1+0.2)^x} \dots (19)$$

$$R = \text{Rs } 1.830 \text{ per kVArh}$$

Levelized cost for "Reactive Energy" by each pole for Case Study was calculated, and the computed average cost per kVArh was Rs 1.809, when installing capacitor bank in customer end.

Therefore for encouraging customers to feed reactive power at the peak time by using installed solar PV inverters the reward was proposed by crediting Rs 2.00 per kVArh.

Cost benefit analysis was computed by using the case study results.

Total saving by reactive power feeding per year
= Rs 204839.71

Total rewards to the customers per year
= Rs 20032.66

Net saving to the utility per year
= Rs 184807.05

7. Conclusion

According to the case study when selecting the optimal operating power factor for the existing installed PV inverters, conclusions were finalized as follows;

- Even with the small capacities of distributed PV inverters can be used to eliminate the low voltage for some extent. According to the case study, it fixed the voltage around 80m length of the feeder.
- "Sensitivity Factor" was introduced to identify the critical locations where it is necessary to attend first, under the limitations of "over voltage".
- Since the concept was introduced for the night peak solar generation module is mostly utilized, and the efficiency of the installation increased.
- Due to the reduction of reactive power feeding from the transformer, it has reduced the total line current and caused to reduce the power loss of the total system. According to the case study, the reduction of power loss was 9.26%.
- Even after the rewarding back to the customers, the net saving to the utility was profit, and according to the case study, it was nearly 185000 LKR per year.

8. Recommendations

As per the research findings, when promoting feeding reactive power with existing installed PV inverters following recommendations were made;

- The behaviour of the feeder parameter values at the night peak needs to be analysed such as voltage, power loss along the feeder before computing the power factors. By analyzing the whole feeder under the limitations, the operating power factor for each inverter has to be decided by the utility and to be informed to the customer.
- Solar inverter manufacturers have to manufacture their products with the provision of changing the power factor set by the user and with the ability to program the setting on an hourly basis.
- General Public, including the customers who wish to connect solar power generation module, are need to be educated on the selection of proper PV inverters which are capable of operating in reactive mode as well.
- The rewarding method for reactive feeding by PV inverters needs to be introduced to customers in order to encourage them for maintaining the stability of the system voltage.



References

1. Kozinda, A., Beach, T., Rao, V., "Latent Opportunities for Localized Reactive Power Compensation," *Cal x Clean Coalition Energy C226*, 2013".
2. CEB Statistical Digest Report -2015.
3. Ceylon Electricity Board, "Manual for Interconnection of Micro Scale Renewable Energy Based Power Generating Facilities at Low Voltage Consumer Feeders of National Grid", August 2016.
4. Kutkut, N., "An AC PV Module with Reactive Power Capability: Need and Benefit," *Petra Solar, Inc.*, 2012".
5. Resource Management Associates (Pvt) Ltd "A Tariff for Reactive Power in Sri Lanka", *Final Report*, September 2011".
6. SMA Solar Technology, America "Q at Night," *Reactive power outside of feed-in operation with SUNNY CENTRAL 500CP XT / 630CP XT / 720CP XT /760CP XT / 800CP XT / 850CP XT / 900CP XT"*.
7. Ellis, A., Kirby, B., Barker, C., Seymour, E., Von Engeln, E., MacDowell, J., Williams, J. R., Casey, L., Nelson, R., Walling, R., Peter, W., "Reactive Power Interconnection Requirements for PV and Wind Plants - Recommendations to NERC" Sandia National Laboratories, USA, 2012.
8. Cagnano, A., Tuglie, E. D. "Online Optimal Reactive Power Control Strategy of PV Inverters" *Industrial Applications, IEEE Transactions on*, vol.58, no.10, pp.4549,4558, October 2011".
9. Rajesh, C. H., Reshma Kiran, S., "Harmonic and Reactive Power Compensation in a Grid Connected PV System with Source Side Control Technique." *The International Journal of Emerging Technology and Advanced Engineering*, vol. 3, pp.212-220, Sep 2013.
10. Huajun, Yu, Junmin, Pan, and An. Xiang, "A Multi-Function Grid Connected PV System with Reactive Power Compensation for the Grid" *Solar Energy*, vol. 79, no. 1, pp. 101-106, July. 2005.
11. Maknoungejad, M. Godoy Simoes, M. Zolot, "Single Phase and Three Phase P+Resonant Based Grid Connected Inverters with Reactive Power and Harmonic Compensation Capabilities" *IEEE Tr. IEMDC 09*, 3-6 May 2009, pp. 385-391.
12. A. Ellis, B. Kirby, C. Barker, E. Seymour, E. Von Engeln, J. MacDowell, J. R. Williams, L. Casey, R. Nelson, R. Walling, W. Peter." *Reactive Power Performance Requirements for Wind and Solar Plants" presented at the IEEE Power and Energy Society General Meeting, San Diego, CA, 2012.*
13. A. Maknoungejad, N. Kutkut, I. Batarseh, Z. Qu. "Analysis and Control of PV Inverters Operating in VAR Mode at Night" *presented at the IEEE PES Innovative Smart Grid Technologies (ISGT)*, Hilton Anaheim, CA, 2011.
14. Inverter Reactive Power Compensation (2014): <http://www.blueoakenergy.com/blog/inverter-reactive-power>, Visited, 24th November 2016.

Smart Electronic Analyzer for Determination of Chicken Meat Spoilage

M.P.U. Isuranga, H. Pasqual and N.S. Weerakkody

Abstract: People in the modern society pay more attention to food safety than the cost, since a lot of known diseases are transmitted through spoiled food. Freshness is the main factor considered by a customer when purchasing food items. Microbes can easily spoil perishable food. The traditional food spoilage detection methods are visual identification, physical detection, chemical detection, and microbial appraisal methods. However, these methods have many problems like long experiment cycle, high equipment cost, and necessity of relatively sophisticated laboratory environmental conditions. Thus, this study presents a spoilage status analyser which can detect evolving gas concentration of meat products. In this design, concentrations of gases are measured, which are emitted in the meat decaying process using gas sensors. The classifier operating on support vector machine based on many parameters gave a quality approach to obtain a final spoilage status of tested meat samples. The obtained results demonstrated good performance in discriminating meat samples in one of two quality classes, the accuracy of obtained data by the equipment was further confirmed by microbiological assay using total plate counts. The developed smart electronic analyser is a quick and low-cost detector with accuracy to detect freshness of meat.

Keywords: Electronic nose; Gas sensors; Meat spoilage; Support vector machines;

1. Introduction

Meat is easily being spoiled by microbes. As a product from animal sources, it can expose to bacteria that cause food spoilage during processing, transporting, and selling. Sri Lankan meat industry only large-scale entities have any state of the art facilities that can control the above processes following ISO 22000 [15] standard conditions. Presently, butchers openly slaughter the animals without considering the standard environmental conditions. Therefore, the chances of microbial contamination are significantly high.

The present society gives more attention to meat freshness because of food spoilage can cause many health problems. Therefore, meat products are regulated under the Laws which have specific guidelines to assess the quality of meat products. In Sri Lanka, meat products are regulated under the Food (Amendment) Act, No 20 of 1991. Food Act states that 10^6 CFU/g (colony-forming units per gram) is the limit that determines whether meat is spoiled or not (Microbial Population $\geq 10^6$ CFU/g - Spoiled, Microbial Population $\leq 10^6$ CFU/g - Fresh) [7,16].

Regular monitoring is required to determine whether butchers are selling fresh quality meat or not. Public health inspectors are the responsible officers to ensure the implementation of the Food Act. At present, public health inspectors collect samples from butcher shops and apply microbial appraisal

methods in the laboratories. After getting results from such samples, further investigations are carried out.

The early detection of microorganisms in meat is an essential part of any quality control or food safety plan. Conventional methods for identifying bacterial spoilage have involving basic steps like pre-enrichment, selective enrichment, selective plating, biochemical screening [11]. Commonly used methods like SPC (Standard Plate Count), DMC (Direct Microscopic Count) are inexpensive and can give both quantitative and qualitative information on the number and nature of bacteria. Moreover, preparation of the culture medium, inoculation of plates and colony counting make these conventional methods need expert personnel. Also, those methods require days to complete and to produce results.

Eng. M.P.U. Isuranga, B. Tech. Eng. (Hons) (OUSL), Student Member of IESL, Demonstrator, Department of Electrical & Computer Engineering, The Open University of Sri Lanka.

Ms. H. Pasqual, B.Sc. (Eng.) (Hons), MEng(Saitama), Senior Lecturer, Department of Electrical & Computer Engineering, The Open University of Sri Lanka.

Dr. N.S. Weerakkody, BSc Agri (Peradeniya), MSc (Peradeniya), Ph.D. (Australia), Senior Lecturer, Department of Agricultural and Plantation Engineering, The Open University of Sri Lanka.



The testing of microbial spoilage needs a method that can overcome problems from conventional methods. These methods are validated and evaluated using conventional culture methods as a reference. Most of these rapid detection devices are expensive. Because those devices use advanced technologies, which are very costly. For example, FT-IR (Fourier transform infrared) spectroscopy uses infrared rays for detection while mass spectrometer and gas chromatography use ionised detectors and external gases for measuring purposes[11]. Methods like PCR (Polymerase chain reaction) uses detecting DNA patterns which require expert labour intensive also. Rapid detection methods are needed to operate in a laboratory environment to get required conditions. An electronic nose introduced as rapid detection method which can detect and recognise certain item using their odour signature. These systems have sensors, pumps, valves, electronics, data extraction methods, data processing methods. However, most of the modern devices like Alabaster UV, FOX 2000, FOX 3000, and food sniffer provide excellent accuracy in their results, though they are very expensive. Several types of research done to design a low-cost, effective device [14].

Meat is made up of fibres which are held together by connective tissue. Most animal muscle is 75% water, 20% protein, and 5% fat, carbohydrates, and various proteins. The connective tissue is composed of proteins, collagen and elastin. The fat surrounds the fibres in small particles.

While the content of the fibres is called muscle juice. it is composed of water in which are proteins, salts and extractives. These extractives contain nitrogen which causes a flow of digestive juices in the stomach, which aids in the breakdown of food [4]. Meat decomposes like any other organic matter. Bacteria, Enzymes, fungi, Oxygen, and moisture all convert meat back to the core organic compounds. Protein will decompose into ammonia, the fat will become aldehydes and aldehyde acid, and the carbohydrate will decompose into alcohol, ketone and carboxylic acid [4]. Food would not decompose if not for bacteria, enzymes and fungi these microbes are primary decomposers of all food items. They decompose meat into volatile gases [8].

2. The Proposed System

Meat spoilage can be detected using, off-odours, off-flavours and discolouration. However, mainly this off-flavours, and discolouration are present when most of the

spoilage occurs. For early detection, odour/smell signatures are considered useful parametric resources for determining spoiled meat [1]. Apart from that temperature and humidity of environment make many variations to the spoiling process. [6,12] Proposed system can be used to sniff in the normal environment to identify spoiled items. The proposed system mainly consists two parts, identification and classification. Figure 1 shows the block diagram of the proposed model.

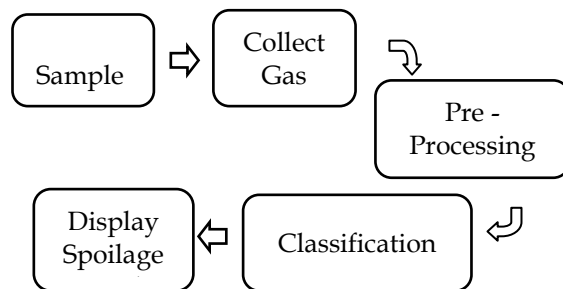


Figure 1 - Proposed Model

The developed system consists of five key components: sensor chamber, sampling unit, data acquisition system, Control unit, and Display Unit. Details of principal components explained in the following sections.

2.1 Sensor chamber

Sensor Chamber has a gas sensor array which has six different gas sensors. This measures concentrations of gases such as ammonia, carbon monoxide, natural gas, smoke, alcohol, and volatile organic compounds which associated with meat decaying process and microbial interactions. This sensor array fixed in the chamber that connects with the sample headspace collection chamber. Also, sensor chamber temperature and humidity are always monitored to avoid instability of stable conditions of sensors.



Figure 2 - Sensor Chamber

Perspex plastic container serves as a gas chamber. This chamber is airtight and non-

reactive to chemical or food odours. A tube connected to the sample section via a diaphragm-type air pump. This air pump is turned on for 20 seconds to drawing in the headspace gas from the meat sample via a tube. The odours directed by this pump directly access the sensors to get measurement according to the gas concentration.

There are no specific rules applied when selecting the type of sensors. A considered factor was the detection ability of the required gas. The type of sensors used and their sensitivity to a particular gas listed in Table 1.

Table 1 - Gas Model Sensitivity

Sensor Model	Sensitive Gases
MICS 5524	CO, C ₂ H ₅ OH, H ₂ , NH ₃ , CH ₄
MQ5	LPG, NPG, C ₄ H ₈ , C ₃ H ₈
MICS 5914	NH ₃ , C ₂ H ₅ OH, H ₂ , C ₃ H ₈ , C ₄ H ₁₀
MQ3	C ₂ H ₆ O, CO, LPG
MQ2	H ₂ , LPG, CH ₄ , CO, C ₂ H ₆ O
MICS 2714	NO ₂ , H ₂

MICS (Sensortech) gas sensors and MQ (Futurlec) gas sensors both operate with 5V supply for both heater section and sensing section. However, to maintain the required voltage level to get a proper heating temperature, a voltage divider circuits implement for each and every sensor according to datasheets.

When compared to the electrochemical gas sensors, MOS type gas sensors have several advantages. Some of them are simple operations, low manufacturing cost, significantly good sensing range, commercial availability and small size.

2.2 Sensor data acquisition

Voltage captured from the sensor connected to the LM358N operational amplifier. Op-Amp circuit with non-inverting configuration used as the amplifier model [13]. The gain of the operational amplifier was adjusted on a one to one basis, depending on the strength of each sensors' response. The amplified voltage signals of the six sensors connected to the ADC of the Arduino platform. Then this data was processed using the Analytical algorithm.

3. Calibration Method

Briefly, a small portion of the meat sample weighing approximately 10g was aseptically

removed and diluted into 1:10 ratio using 0.85% saline solution. The meat sample was homogenised in a stomacher (IUL masticator, torrent del'Estadella, Barcelona, Spain) for 2 minutes and serially diluted in 9 ml of diluent (0.85%, Saline) as necessary. Plate count obtained by plating out samples on the surface of nutrient agar with incubation of the plates at 37°C for 48 hours. Counts were achieved by enumerating typical colonies present and calculated as log₁₀CFU/g of the meat sample. From this calculation predetermination of meat samples quality was obtained before testing with the device.

4. Analytical Algorithm

Data measured with gas sensors react with one another quickly and may be distracted by the thermal noise. Moreover, before applying the classification, in this work we use the "moving average" technique as filtering method to reduce the noise factor from sensor signals. From getting moving averages, final sensor data can base on the all the sensory data gathered till sensors come to steady state. This process runs along the 20s to get decent data set from all six sensors.

The two most popular types of moving averages are Simple Moving Average (SMA) and the Exponential Moving Average (EMA). [5,9] From these two moving average algorithms, SMA formed by computing the average sensory data over a specific number of periods and old data dropped when the new data comes available. Therefore, it is necessary to determine an exact number of periods from which we want to get the average. In this work, twenty periods were used to get the average. In EMA algorithm, recent data get more weight than old data when getting the final average. However, in this situation, we want to get the average of sensory data when it is already in the steady state. So SMA is the most suitable algorithm for the system.

5. Classification algorithm

There are three popular algorithms which used in the several gas sensors based works considered when choosing the correct algorithm for the system. These three algorithms namely artificial neural networks (ANN), support vector machines (SVM), and K-nearest neighbour (KNN). Training and evaluation for classification of meat spoilage status use two classes, Spoiled and Fresh.

According to the researches done by several intuitions most accurate algorithm is KNN [10,12]. The most underperforming algorithm,



when used with gas sensors, is ANN algorithm. KNN and ANN both have a drawback that to get a considerably accurate result; these algorithms need a large amount of training data set. However, when using support vector machine, we can get acceptable accuracy with the much lower amount of training dataset [3,9]. So for this study, we use SVM as classification algorithm.

This algorithm is used to classify data based on features. SVMs hinge on two core mathematical operations: first, plotting the input data into high dimensional space using a kernel function and then splitting them into two different classes using hyperplane decision surface [5]. When training the SVM algorithm, SVM will identify the hyperplane that separates two classification class which leaves maximum margin from data of both classes as possible. The maximum margin hyperplane:

$$w^T x - b = 0 \quad \dots (1)$$

W and b are to be determined to maximise the separation between the two parallel hyperplanes as a state in figure 3 where “ m ” defines as the distance between two hyperplanes. Hence in the training process, can be definite that (x_i, y_i) is data points where “ x_i ” is the captured data while “ y_i ” is the class label [$y_i \in \{-1,1\}$] which each sample belongs.

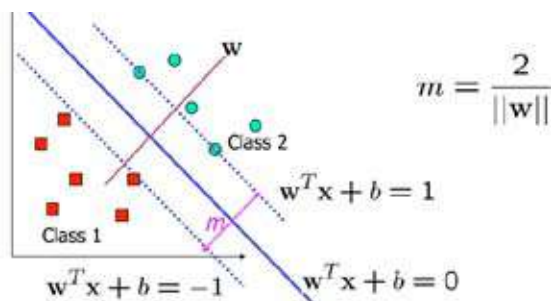


Figure 3- SVM determine the maximum margin for separation hyperplane

The decision boundary should classify all points correctly under the hyperplane which have a maximum distance to both classes. Then maximisation will reduce with the minimization of $||w||$ under the constraint $y_i (w^T x_i + b) \geq 1$ or $y_i (w^T x_i + b) \geq -1$.

6. Prototype implementation and testing

A prototype system was developed (figure 4) for obtaining concentration values and also training for classification algorithm which based on support vector machine. For this study, only one kind of meat samples (Chicken)

used. Meat decay rapidly compared to other items. If rotten meat exposed to the proposed system by placing it in the sampling chamber, identified the spoiled item using classification algorithm.



Figure 4 - Prototype implementation

The developed prototype system was capable of measuring gas concentration values which emit when the spoilage process happens. When training experiment conducting temperature inside the chamber kept almost constant (about 30°C) and the humidity value also kept 40-60% level in every experiment. The data measured after a regular interval of 15 minutes. The sampling and cleaning periods defined by obtaining sensor responses that have been tested by the system. For that allocation of the 20s were sufficient to clean and sample the headspace using a vacuum pump. Another 20s was given to get the moving average of sensors. Total time for the process is the 60s.

In this experiment, 60 randomly selected samples used from a local hospital, local butcher shops and supermarkets. The quality of the meat samples separately identifies with a microbiological assay using total plate counts. A support vector supervised training was carried for 50% of the samples, and decision boundary hyperplane parameters included in Atmel Mega 2560 microcontroller. Furthermore, other 50% of the samples used in testing the accuracy of the classifier.

Gas concentration of 30 Samples from the collected meat batch taken to train the support vector machine algorithm. The relevant parameter values received from the six sensors. However, these sensors did not provide exact gas concentration value of single gas. As an example, MICS5524 and MICS5914, both sensors detect Ammonia gas. So, sensor values are weighted according to the importance of parameter and obtained two different values for Sensortech (MICS) sensors and MQ sensors.

$$\text{MICS Value} = (\text{MICS5914} * 0.5) + (\text{MICS5524} * 0.3) + (\text{MICS2714} * 0.2) \quad \dots (2)$$

$$\text{MQ Value} = (\text{MQ3} \cdot 0.4) + (\text{MQ2} \cdot 0.3) + (\text{MQ1} \cdot 0.3) \dots (3)$$

7. Results & Discussion

The obtained “MICS value” and “MQ Value” 2D graph has been plotted in figure 5 to show freshness status distribution among training data set.

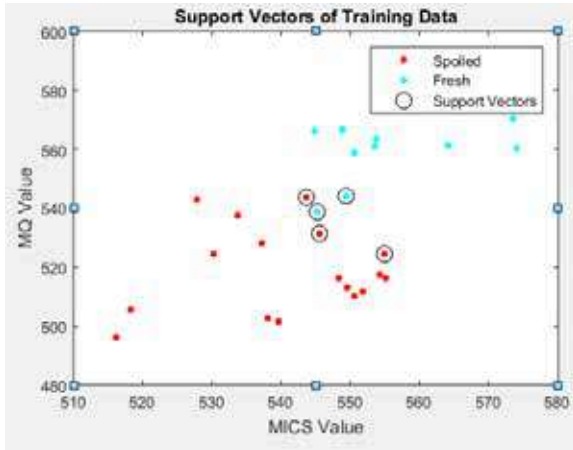


Figure 5- Support Vectors of Training Data

According to this graph, the fresh samples are in blue and the spoiled samples shown in red colours. When we examine Y, X axis, it clearly demonstrated that there is a separation between these two classes. With this data, the most suitable method for data classification can be found. The proper classification answers are given by the support vector machines. Below show the steps of hyperplane equation derivation of support vector machine.

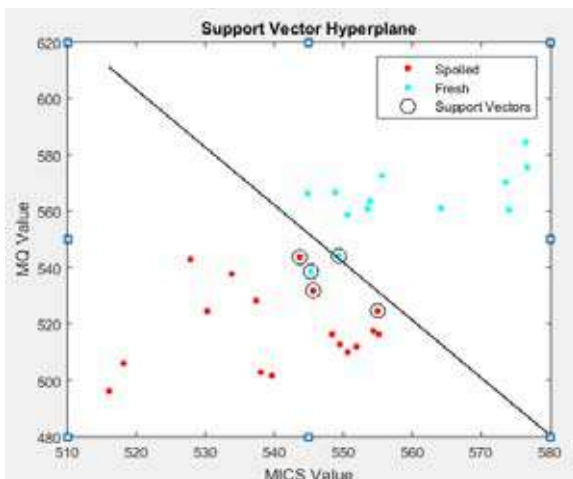


Figure 6 - Hyperplane support vectors

According to these data in feature space, there is a boundary that can separate these data into two classes as a good class and bad class. This boundary defined by the help of some data from both classes which is near to the border

and we get the support from these data as vector form to adjust the boundary well for classification process, and here we have five support vectors to define the optimum boundary (Figure 6). Below shows the used support vectors,

$$S_1' = \begin{pmatrix} 555 \\ 524.6 \\ 1 \end{pmatrix} \quad S_2' = \begin{pmatrix} 545.6 \\ 531.6 \\ 1 \end{pmatrix}$$

$$S_3' = \begin{pmatrix} 543.7 \\ 543.8 \\ 1 \end{pmatrix} \quad S_4' = \begin{pmatrix} 549.4 \\ 544 \\ 1 \end{pmatrix}$$

$$S_5' = \begin{pmatrix} 545.3 \\ 538.6 \\ 1 \end{pmatrix}$$

When we use the theory support vector, we need the bias input 1 to modify existing vectors into modified support vector form. Modified support vectors are S_1' , S_2' , S_3' , S_4' , and S_5' . Also, we need to find seven parameters α_1 , α_2 , α_3 , α_4 , and α_5 about the vectors by using seven equations.

$$\alpha_1 S_1^1 S_1^1 + \alpha_2 S_2^2 S_1^1 + \alpha_3 S_3^3 S_1^1 + \alpha_4 S_4^4 S_1^1 + \alpha_5 S_5^5 S_1^1 = -1 \text{ (-ve Class)} \dots (4)$$

$$\alpha_1 S_1^1 S_2^2 + \alpha_2 S_2^2 S_2^2 + \alpha_3 S_3^3 S_2^2 + \alpha_4 S_4^4 S_2^2 + \alpha_5 S_5^5 S_2^2 = -1 \text{ (-ve Class)} \dots (5)$$

$$\alpha_1 S_1^1 S_3^3 + \alpha_2 S_2^2 S_3^3 + \alpha_3 S_3^3 S_3^3 + \alpha_4 S_4^4 S_3^3 + \alpha_5 S_5^5 S_3^3 = -1 \text{ (-ve Class)} \dots (6)$$

$$\alpha_1 S_1^1 S_4^4 + \alpha_2 S_2^2 S_4^4 + \alpha_3 S_3^3 S_4^4 + \alpha_4 S_4^4 S_4^4 + \alpha_5 S_5^5 S_4^4 = +1 \text{ (+ve Class)} \dots (7)$$

$$\alpha_1 S_1^1 S_5^5 + \alpha_2 S_2^2 S_5^5 + \alpha_3 S_3^3 S_5^5 + \alpha_4 S_4^4 S_5^5 + \alpha_5 S_5^5 S_5^5 = +1 \text{ (+ve Class)} \dots (8)$$

Let substitute values for above equations S_1' , S_2' , S_3' , S_4' , and S_5' . From these seven equations, we obtain values for α_1 , α_2 , α_3 , α_4 , and α_5

$$\alpha_1 = 1.6745 \quad \alpha_2 = -2.4937 \quad \alpha_3 = 3.6123 \\ \alpha_4 = -2.3696 \quad \alpha_5 = -4.2355$$

Using previously obtained α values w' value obtained.

$$w' = \sum_i^n \alpha_i S_i' \dots (9)$$

w' value of the developed system can be obtained from above equation,

$$w' = \begin{pmatrix} 0.7720 \\ 0.3774 \\ -629.0450 \end{pmatrix} \dots (10)$$

Using above calculations, hyperplane equation is,



$$y = \left(\frac{0.7720}{0.3774}\right)x + c \quad \dots (11)$$

b (offset value) = -629.045

Gradient of a line = $\frac{0.7720}{0.3774}$; $\theta = 2.04$

From that, Hyperplane 30 samples were tested with spoilage early detection device to determine the accuracy. Figure 7 shows the test samples which categorised according to the above hyperplane.

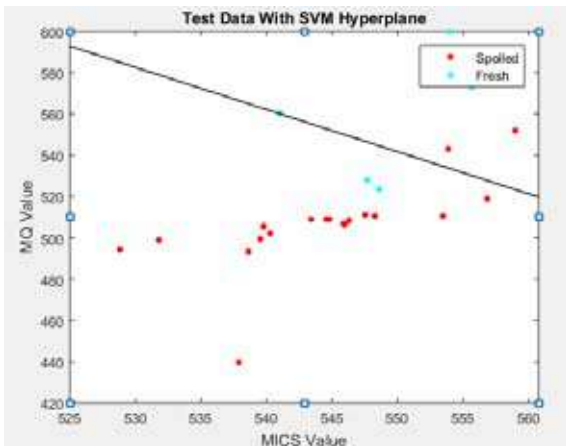


Figure 7- Test Data with SVM Hyperplane

the accuracy obtained according to test samples show below;

Accuracy of the selected algorithm

$$= \frac{\text{No. of Correct classification}}{\text{Total test data set size}}$$

$$= \frac{26}{30} * 100\%$$

$$= 86 \%$$

8. Conclusion and Future Work

Microbial spoilage of food caused major problems such as foodborne illnesses and significant food wastage. For controlling those diseases, early detection of foods is important. Existing methodologies for rapid detection like mass spectrometry, gas spectrometry, Fourier Transform Infrared Spectrometry, and electronic nose can identify the foodborne pathogens. Most of these methods operated under laboratory environment. Also, most of those devices are very complicated and very expensive. Due to these issues, regular food inspections occupied under traditional methods such as direct microscopic count and standard plate count which are time-consuming methods.

When Doing this study, problems like sample odours are not coming to sensor chamber were occurred. Therefore, two vacuum pumps introduced for cleaning and sample collection. Six gas sensors determined the gas concentration data from the sample headspace and displayed the status. The support vector machine; statistical data classification algorithm did the classification part of the device to get the outcome.

The smart electronic analyser is a kind of electronic nose. As far with all the electronic nose systems, it depends on gas sensor technology. The next step is integrated more advanced gas sensors with the device to make it universal food spoilage detection device which can detect freshness status of any food item. Also, can be developed a cloud database using device test data and rerun the classification algorithm in cloud platform to get more precise hyperplane boundary update will do in future improvements of the project.

References

1. Abdallah, S. A., Al-Shatti, L. A., Alhajraf, A. F., Al-Hammad, N. and Al-Awadi, B. (2013) 'The Detection of Foodborne Bacteria on Beef: The Application of the Electronic Nose', *SpringerPlus*, 2(1), p. 687. doi: 10.1186/2193-1801-2-687.
2. Anthony, C. R. M. and Balasuriya, D. N. (2016) 'Electronic Honey Quality Analyser', *Engineer: Journal of the Institution of Engineers, Sri Lanka*, 49(3), p. 41. doi: 10.4038/engineer.v49i3.7075.
3. Balasubramanian, S., Panigrahi, S., Logue, C. M., Gu, H. and Marchello, M. (2009) 'Neural Networks-Integrated Metal Oxide-Based Artificial Olfactory System for Meat Spoilage Identification', *Journal of Food Engineering*, 91(1), pp. 91-98. doi: 10.1016/j.jfoodeng.2008.08.008.
4. Eom, K.-H., Hyun, K.-H., Lin, S. and Kim, J.-W. (2014) 'The Meat Freshness Monitoring System using the Smart RFID tag', *International Journal of Distributed Sensor Networks*, 2014, pp. 1-9. doi: 10.1155/2014/591812.
5. Gutierrez-Osuna, R. (2002) 'Pattern Analysis for Machine Olfaction: A Review', *IEEE Sensors Journal*, 2(3), pp. 189-202. doi: 10.1109/jsen.2002.800688.
6. Hasan, N., Ejaz, N., Ejaz, W. and Kim, H. (2012) 'Meat and Fish Freshness Inspection System Based on Odor Sensing', *Sensors*, 12(12), pp. 15542-15557. doi: 10.3390/s121115542.

7. ICMSF - International Commission of Microbiological Specification (2011) *Microorganisms in foods*. (8 Vols). New York: Springer.
8. Kai Zhang, L. Z. (2014) 'Volatile Organic Compounds as Novel Markers for the Detection of Bacterial Infections', *Clinical Microbiology: Open Access*, 03(03). doi: 10.4172/2327-5073.1000151.
9. Kima, E., Lee, S., Lee, T., Shin, B.J., Lee, J., Byun, Y.T. and Kim, H.S. (2011) 'An Intelligent Real-Time odor Monitoring System using a Pattern Extraction Algorithm', *2011 IEEE Ninth International Conference on Dependable, Autonomic and Secure Computing*, doi: 10.1109/dasc.2011.92.
10. Mamat, M., Samad, S. A. and Hannan, M. (2011) 'An Electronic Nose for Reliable Measurement and Correct Classification of Beverages', *Sensors*, 11(12), pp. 6435–6453. doi: 10.3390/s110606435.
11. Mandal, P.K., Biswas, A.K., Choi, K. and Pal, U.K. (2011) 'Methods for Rapid Detection of Foodborne Pathogens: An Overview', *American Journal of Food Technology*, 6(2), pp. 87–102. doi: 10.3923/ajft.2011.87.102.
12. Panigrahi, S., Balasubramanian, S., Gu, H., Logue, C.M. and Marchello, M. (2006) 'Design and Development of a Metal Oxide Based Electronic Nose for Spoilage Classification of beef', *Sensors and Actuators B: Chemical*, 119(1), pp. 2–14. doi: 10.1016/j.snb.2005.03.120.
13. Pearce, T. C., Schiffman, S. S. and Nagle, H. T. (eds.) (2006) *Handbook of machine Olfaction: Electronic nose technology*. Germany: Wiley-VCH Verlag GmbH.
14. Schaller, E., Bosset, J. O. and Escher, F. (1998) "'Electronic Noses" and their Application to Food', *LWT - Food Science and Technology*, 31(4), pp. 305–316. doi: 10.1006/fstl.1998.0376.
15. Srilankabusiness.com. (2017). *Food & Beverage Product Standards in Sri Lanka | Food & Beverage Standards & Regulations*. [online] Available at: <http://www.srilankabusiness.com/exporters/standards/food-and-beverages-products-standards.html> [Accessed 12 Sep. 2017].
16. Health.gov.lk. (1980). *Regulations under the Food Act*. [online] Available at: <http://www.health.gov.lk/enWeb/FOODWEB/files/regulations.html> [Accessed 24 May 2017].



Power Electronic Interface of a Solar Driven DC System

W.W.M.D.B. Wijesinghe, H.M.K.C.B. Wijerathne, B.H.T.S. Gunaratne,
P.J. Binduhewa and J.B. Ekanayake

Abstract: The distributed grid connected PV systems are gradually increasing in Sri Lanka and around the globe, and will continue in the future. With the rapid development of energy storage techniques and dc loads, a domestic distribution should comprise of dc and ac multi-ports to integrate loads and sources in the forms of ac and dc. Such an interface would increase the efficiency by reducing the number of conversion stages. Further an Energy Management System would help to coordinate the resources effectively. This paper presents the design of a power electronic interface of a multi-port distribution board which enables to realize the above functionalities. This multiport power electronic interface combines the grid and a photovoltaic system along with an enhanced storage unit as power sources. The loads are connected to the dc and ac ports. The simulation results of the designed power electronic converters and their controllers will be presented in the full paper.

Keywords: boost converter, bidirectional converter, Grid connected voltage source inverter

1. Introduction

The modern day energy demand and rapid improvements of technology has created a question as to whether the power and energy is being well managed and optimized to match the economy as well. The usage of renewable energy sources to supply the demand, mainly in the means of solar power is becoming the future of power management. On the other hand, the traditional approach of grid supply has not disappointed the customers much, but the next step need to be improved. And uninterruptible power supply in domestic scale is the issue that needs to be addressed while the efficiency is maintained at a higher level.

The power electronic interface of solar driven dc system combines all the concerns that the modern world is seeking answers for. It enables the combination of a PV panel, the grid supply and a storage unit to the same bus bar of 48V, which is then expected to be used as the supply point for different kinds of ac and dc loads. The use of power electronic interface to perform energy management results in number of merits to the individual user as well as to the entire society in a whole. Since the usage of power is being optimized, the overall efficiency will increase while providing the user with multiple options in energy distribution. The majority of the utility

side will be handled by the PV panel and it can supply the other two units as well. The storage unit will ensure that an uninterruptible supply is maintained when it is required. Even though the initial cost will be on the high side, the maintenance and handling cost will not be considerable which supports the economy side as well.

2. Proposed System

The proposed multiport power electronic interface is shown in Figure 1. Power sources coupled to the system are utility supply, photovoltaic panels and a battery storage unit. The battery bank enables to store energy so that the stored energy can be utilized when the utility is not available or utility tariff is relatively high. The loads connected to the system can be either ac or dc.

All the sources and loads are connected to a dc-link through power electronic converters connected to each source and load. PV panels

Mr. W.W.M.D.B. Wijesinghe, B.Sc. Undergraduate, Faculty of Engineering, University of Peradeniya.
Ms. B.H.T.S. Gunaratne, B.Sc. Undergraduate, Faculty of Engineering, University of Peradeniya.
Mr. H.M.K.C.B. Wijerathne, B.Sc. Undergraduate, Faculty of Engineering, University of Peradeniya.
Dr. P.J. Binduhewa, B.Sc.(Peradeniya), Ph.D. (UK), Senior Lecturer at Dept. of Electrical and Electronic Engineering, UOP.
Eng.(Prof.) J.B. Ekanayake, B.Sc. Eng.(Peradeniya), Ph.D., FIEE, FIET, FIESL, CEng (SL & UK), Senior Lecturer at Dept. of Electrical and Electronic Engineering, University of Peradeniya.



are connected to the dc-link through a dc-dc converter. Utility is coupled using a Voltage Source Converter (VSC) which is capable of bi-directional power flow. A bi-directional dc-dc converter is used to integrate the battery bank to the dc-link. In order to facilitate the interconnection of ac loads, an inverter is used. A dc-dc converter can be used to match the dc-voltage of the load.

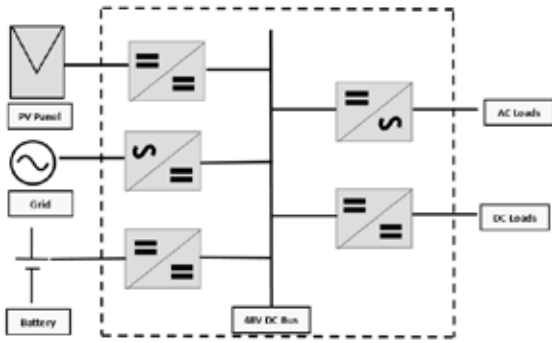


Figure 1 - System Diagram

This project aims to evaluate the controllers associated with the power electronic converters in the proposed system. Thus a scaled down grid supply is applied. The Grid supply is assumed to be 30 V and the DC bus bar is maintained as 48V.

3. Design of the Physical Interface

3.1 PV connected DC-DC converter

The photovoltaic panel produces a dc output thus a dc-dc converter is required to interface the PV panels to the dc-link of the proposed system. The output power of a PV panel varies with irradiance and temperature. Thus it is important to know the ranges of voltage and current. Equation (1) and (2) present the variation of short circuit current and open circuit voltage of the PV panel with irradiance and temperature. I_{sc} , G_a , T , V_{oc} , ΔI_{sc} , ΔV_{oc} and V_t are short circuit current, irradiance, temperature, open circuit voltage, temperature coefficient of I_{sc} , temperature coefficient of V_{oc} and thermal voltage. The 's' notation represents the parameter value at the standard conditions.

$$I_{sc} = \frac{G_a}{G_{as}} [I_{scs} + \Delta I_{sc}(T - T_s)] \quad .. (1)$$

$$V_{oc} = \Delta V_{oc}(T - T_s) + V_t \cdot \ln\left(\frac{I_{scs}}{I_{sc}}\right) \quad .. (2)$$

Thus a simple boost converter, which is shown in Figure 2, is used for this function.

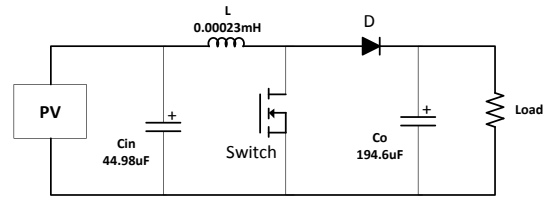


Figure 2 - Boost Converter

The component values and the necessary parameter values were calculated using the theoretical equations as given below [8].

$$D = 1 - \frac{V_{in}}{V_o} \quad \dots (3)$$

$$L = \frac{V_{in} D}{f_s \Delta i_L} \quad \dots (4)$$

$$C_{in} = \frac{\Delta i_L}{8 \cdot f_s \cdot V_{in} \cdot \left(\frac{\Delta V_{in}}{V_{in}}\right)} \quad \dots (5)$$

$$C_o = \frac{I_o \cdot D}{f_s \cdot V_o \cdot \left(\frac{\Delta V_o}{V_o}\right)} \quad \dots (6)$$

Function of the controller of the converter associated with PV panel is to ensure that the photovoltaic panel is operating at the maximum power point. The controller for the converter was designed to control the input voltage where the MPPT algorithm was used to maintain the PV output at the optimum level under varying conditions. Average equations of the converter operation were used to obtain the operating model and the equations obtained for the plant are given below [8], [11]. PI controller was established with suitable pole placements. The controller is shown in figure 3.

$$sL_p I_L(s) = V_{in}(s) - R_p I_L(s) - (1 - D_o)V_o(s) + V_{oo}D(s) \quad \dots (7)$$

$$sC_{po}V_o(s) = (1 - D_o)I_L(s) - I_{Lo}D(s) - I_o(s) \quad (8)$$

$$sC_{pin}V_{in}(s) = I_{in}(s) - I_L(s) \quad ..(9)$$

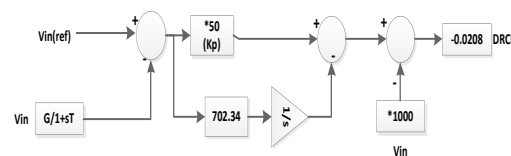


Figure 3 - Input Voltage Controller Block Diagram

3.2 Design of Bi-directional DC-DC Converter

A bi-directional dc-dc converter is being used in this system in order to connect the battery bank with dc bus bar. The main objectives of connecting a battery bank are to maintain the stability of the dc link according to the load requirement and a continuous power flow of the dc link.

Buck boost half bridge bi-directional converter topology as referred in figure 4 was selected to acquire this objective [10]. Switch Q1 operates for the buck mode power flow of the converter and the Q2 operates for the boost mode conduction. The switches are controlled by using a PWM signal. In the buck mode of the converter, power flow facilitates the battery bank charging and in the boost mode it converts to DC link power supply. For the boost mode operation, component value calculations were done by using equations 10-13 [8]. A similar set of equations can be obtained by considering the buck mode as well.

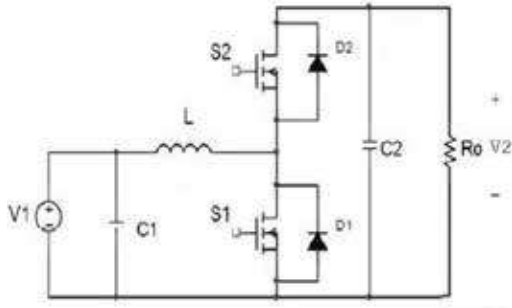


Figure 4 - Buck Boost Bi-directional Converter

$$D = 1 - \frac{V_{in}}{V_o} \quad \dots(10)$$

$$L = \frac{(V_{in}-V_o)D}{f_s \cdot \Delta i_L} \quad \dots(11)$$

$$C_{in} = \frac{\Delta i_L}{8 \cdot f_s \cdot V_{in} \cdot (\frac{\Delta V_{in}}{V_{in}})} \quad \dots(12)$$

$$C_o = \frac{I_o \cdot D}{f_s \cdot V_o \cdot (\frac{\Delta V_o}{V_o})} \quad \dots(13)$$

Voltage and current controlling of the converter has done in the both modes. In the buck mode, output voltage has been controlled to 24V or for an externally given desired value. Output current has been controlled for the constant current charging purposes.

The plant equations for buck mode, with the consideration of the operating point model, were obtained as follows [8]. In the boost

mode output voltage has been controlled to connect the dc bus bar, where the stored power is need to be used by loads. The plant equations for the boost mode were obtained as follows [8], [11].

$$sL_p I_L(s) = V_{in}(s) - R_p I_L(s) - (1 - D_o)V_o(s) + \frac{V_o D(s)}{D_o} \quad \dots(14)$$

$$sC_{po} V_o(s) = (1 - D_o)I_L(s) - I_{Lo}D(s) - I_o(s) \quad \dots(15)$$

$$sC_{pin} V_{in}(s) = I_{in}(s) - I_L(s) \quad \dots(16)$$

For the buck mode operation,

$$sL_p I_L(s) = D_o V_{in}(s) - R_p I_L(s) - V_o(s) + \frac{V_{ino} D(s)}{V_{ino}} \quad \dots(17)$$

$$sC_{po} V_o(s) = I_L(s) - I_{Lo}(s) \quad \dots(18)$$

$$sC_{pin} V_{in}(s) = I_{in}(s) - D_o I_L(s) - I_{Lo} D(s) \quad \dots(19)$$

The controller of this bi-directional converter is to control the charging and discharging current. A PI controller based controller was implemented for this purpose. The battery storage may need to regulate the dc-link voltage when the utility is not available. For such situations, an outer voltage control loop is required. Figure 5 and 6 presents the controller of the inner current controller and the output voltage controller loops.

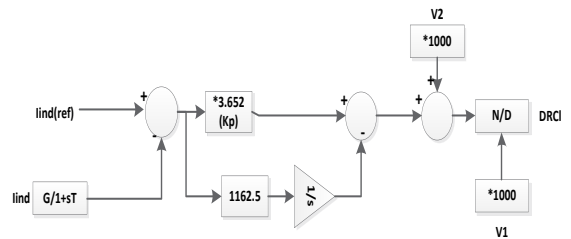


Figure 5 - Inner Current Loop of the Converter

PI controlling method was used by taking 25 kHz as the fundamental frequency level. Poles were selected accordingly making the outer voltage loop poles 10 times slower than the inner current loop poles. Necessary switching signals have provided to make changes within the control loops according to the mode being used in the converter.



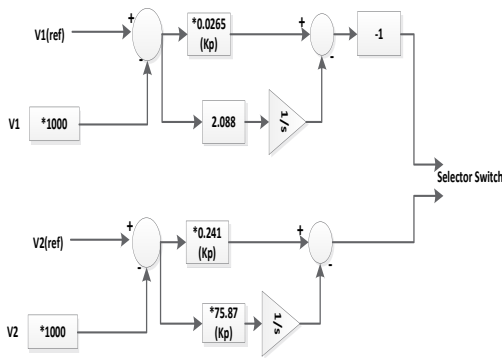


Figure 6 - Outer Voltage Loops of the Converter

3.3 Design of Grid Connected Voltage Source Converter

The voltage source inverter is the link between the utility and the dc-link. The converter is capable of bi-directional power flow. Power will be imported from the utility when the local generation is not enough and power will be exported when local generation is excessive than generation.

Even though there are several common topologies for a single phase inverter, full bridge inverter using sinusoidal PWM unipolar voltage switching was selected due to its low harmonic content compared with bipolar switching [8]. The schematic diagram of the full-bridge inverter is shown in Figure 7

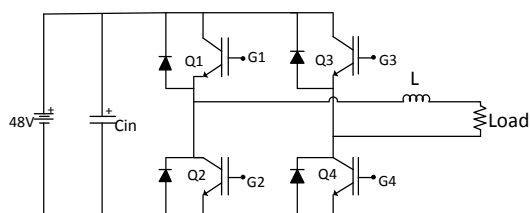


Figure 7 - Voltage Source Inverter

The switches are controlled using PWM signals. A sinusoidal signal (V_{ref}) is compared with a high frequency triangular waveform. The frequency of the sinusoidal signal is equal to the frequency of output voltage waveform. The operating pattern of switches are explained in Equation X. The output of the inverter is passed through an inductive filter (L) to filter out undesired harmonic content providing the desired sinusoidal waveform at 50Hz. The rectifier mode of operation can be

obtained by varying the magnitude and phase angle between the voltages at the ends of the inductor. A DC link capacitor (C_{in}) is used to reduce dc side voltage ripple [2], [7], [8].

$$\left. \begin{aligned} V_{ref} &\geq V_{tri} & Q_1 \text{ ON} \ \& \ Q_2 \text{ OFF} \\ V_{ref} &< V_{tri} & Q_1 \text{ OFF} \ \& \ Q_2 \text{ ON} \\ -V_{ref} &\geq V_{tri} & Q_3 \text{ ON} \ \& \ Q_4 \text{ OFF} \\ -V_{ref} &< V_{tri} & Q_3 \text{ OFF} \ \& \ Q_4 \text{ ON} \end{aligned} \right\} \dots (20)$$

The instantaneous inverter output voltage is given by [8],

$$E(t) = M_a V_{dc} \sin(2\pi ft) \quad \dots(21)$$

Where,

- E(t) - instantaneous output voltage of the inverter
- M_a - modulation index
- V_{dc} - DC bus voltage
- f - grid voltage frequency

Using the above equation M_a value was calculated and following theoretical equations were used to calculate the component values [2].

$$L = \frac{EV \sin(\delta)}{2\pi f P} \quad \dots(22)$$

$$C_{in} = \frac{V_{dc}}{32 L \Delta V f_s} \quad \dots(23)$$

- E -RMS value of inverter output voltage
- V - RMS value of grid voltage
- Δ - Phase angle difference between E

&

- P - Power rating of inverter
- ΔV - DC link voltage ripple
- f_s - Switching frequency

4. Implementation of the Physical Interface

4.1 PV Connected DC-DC Converter

For the development of the prototype, Mitsubishi PVUJ225GA6 panel was selected. The main specifications of the panel are given in Table 1.

Table 1- PV panel specifications

Parameter	Value
V_{mmp}	30V
I_{mpp}	7.50A
V_{oc}	36.4V
I_{sc}	8.30A
P_{mpp}	225W

Since the output of the PV panel was expected to vary under practical operation, the range of variation of the input voltage of the converter was calculated under limits of irradiance and temperature. The temperature range was taken as 10°C to 35°C and the irradiance level range was considered to vary from 600W/m² to 1400W/m². The effect of the conditions was calculated using the equations 1 and 2 [2]. With the system requirements the specifications of the converter are listed in the table below. The open circuit voltage values for extreme worst cases were found to be 33.07V and 41.19V. using the assumption of maximum power point voltage to be 80% of the open circuit voltage, the variation of PV panel output voltage range was calculated. Table 02 presents the specifications of the boost converter. Worst case condition analysis was performed considering both the limits of the input voltage value and the extreme worst case was found to 26.4V where the duty ratio was 0.313.

Table 2 - Design specifications of the converter

Parameter	Value
Power rating / (W)	250
Input voltage / (V)	26.4 – 32.9
Output Voltage / (V)	48
Switching frequency / (kHz)	25
Inductor current ripple	20% of average inductor current
Input voltage ripple	1% of rated input voltage
Output voltage ripple	1% of rated output voltage

The obtained parameter values considering the given equations under theory are listed in table 03.

The inductor current ripple was selected to be 20% since improving it further would cause the size of the inductor to be large and lowering the ripple would increase the size of capacitors.

Table 3 - Parameters of the converters

Parameter	Calculated Value
Inductance / (mH)	0.23
Input Capacitance / (uF)	44.98
Output Capacitance / (uF)	194.50

4.2 Bi-directional DC-DC Converter

It was decided to use two 12 V batteries connected in series as the storage method. The power rating of the bi-directional converter is made equal to the power rating of the solar converter when designing this prototype interface. Thus the total power generated from PV can be absorbed by the battery storage. The specifications of the bi-directional dc-dc converter is given in table 04.

Table 4 - Design specifications of the converter

Parameter	Value
Power rating / (W)	250
High side voltage / (V)	48
Low side voltage / (V)	24
Switching frequency / (kHz)	25
Inductor current ripple	20% of the inductor current
Input / output voltage ripple	1% voltage

According design specifications listed in table 04, the two instances of converter power flow, worst case conditions were reviewed through previous literature studies. By analyzing the battery charging and discharging characteristics of lead-acid batteries, two worst case scenarios were found as the battery bank voltage varies between 27.6V – 23V. Converter design was done according to the worst case conditions in order to withstand the variations and the parameter values are given in table 05.

Table 5 - Calculated parameters of the converter

	Buck mode operation	Boost mode operation	Selected value for the converter design
C1	226.12 μF	225.6 μF	226.12 μF
C2	54.17 μF	61.5 μF	61.5 μF
L	185.2 μH	184.39 μH	185.2 μH



4.3 Grid connected Voltage Source Inverter

Table 06 present the specifications of the voltage source converter to be implemented in the prototype interface.

Table 6 - Design specifications of the voltage source inverter

Parameter	Value
Power rating /(W)	250
AC side rms voltage /(V)	30
DC side voltage /(V)	48
Switching frequency /(kHz)	5
Grid voltage frequency /(Hz)	50
DC side voltage ripple	1% of the DC output

When calculating parameter values, the phase angle difference (δ) of the voltages at the ends of the inductor was set to be 10° and voltage drop across the inductor was assumed to be 10% of grid voltage.

Table 7- Calculated parameters of the voltage source inverter

Component	Calculated value	Selected value for the design
L	2.19 mH	-
C_{in}	57 μ H	67 μ H

5. Simulation Results of the proposed system

5.1. PV Connected DC-DC converter

The designed dc-dc converter was simulated in PSCAD. The open loop results of the converter are shown in Figure 8 and 9. For input of 30 V, the converter output voltage is 48 V. The current ripple of inductor current is around 2 A which corresponds to 20 % ripple. Thus the desired characteristics are shown by the converter.

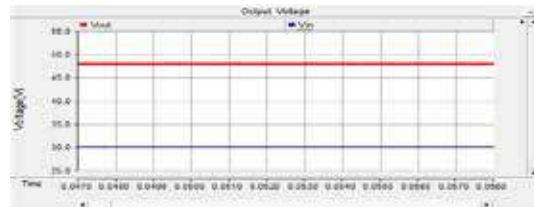


Figure 8 - Input Voltage and Output Voltage

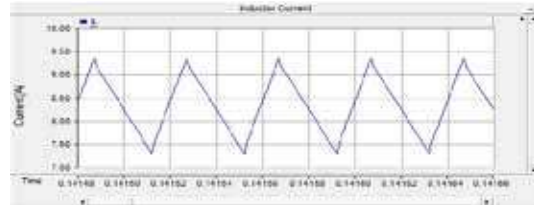


Figure 9 - Inductor Current at Open Loop Condition

Closed loop response of the converter is obtained by connecting the PV panel to the input of the converter. Step response of the controller is shown in Figure 10. It is clear that the controller follows the reference within 0.000s.

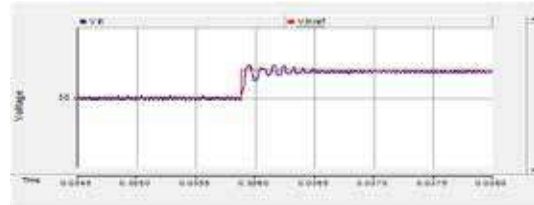


Figure 10 - Response of Input Voltage to a Step Variation in Reference

5.2 Bi-Directional DC-DC Converter

Open-loop operation of the bi-directional converter was first verified for the two operating modes. Figure 11 and 12 shows the results for the buck mode. A voltage source was connected to the low-voltage side and load to the high voltage side when testing the buck mode. For a low-voltage side 24 V is applied with 0.5 duty ratio. The corresponding output voltage is 48 V. The inductor current ripple corresponds to 20 %.

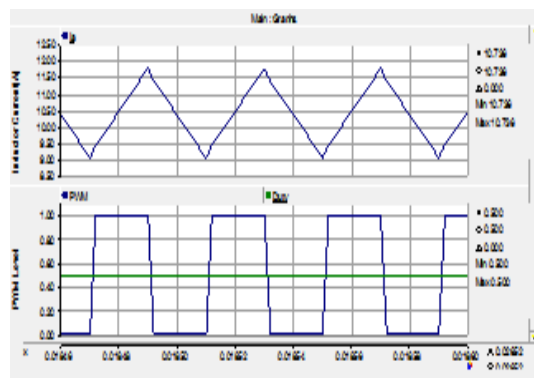


Figure 11- Inductor Current and PWM Signal

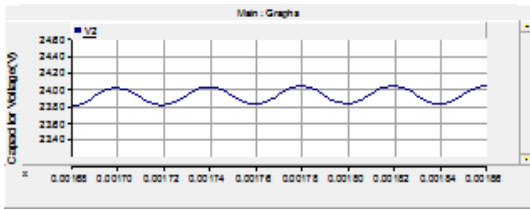


Figure 12 - Output Voltage

Boost mode results are shown in Figure 13 and 14. A voltage source of 48 V was connected to the high-voltage side of the converter while a load is connected to the low-voltage side. Duty ratio was set to 0.5. The corresponding low-voltage side voltage is 24 V and inductor current ripple is 20 %.

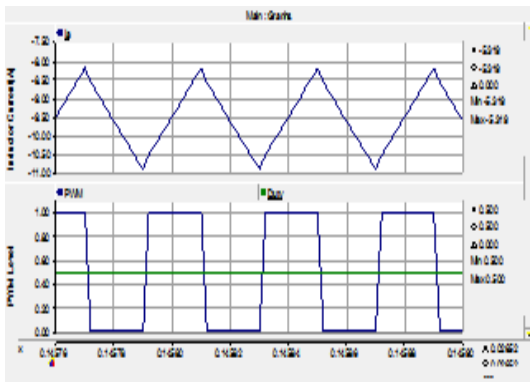


Figure 13 - Inductor Current Variation and PWM Signal

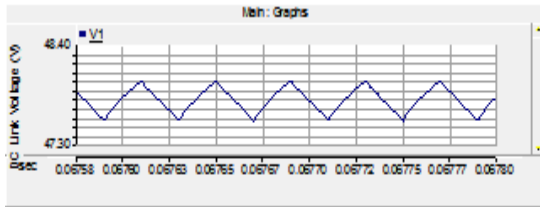


Figure 14 - Output Voltage

After the verification of open-loop operating, the closed loop controller was implemented for the bi-directional converter. First the current controller was implemented for the two operating modes. Figure 15 shows the step response during buck mode operation. Step response during the boost mode is shown in Figure 16. In both cases, the current response is tracked by the controller.

Then the outer voltage control loops were developed. Figure 17 shows the step response of the outer voltage loop for buck and boost modes. The controller is following the command. Further the results of the inner loop and outer loop has verified that the inner loop is faster than the outer loop in both operating modes.

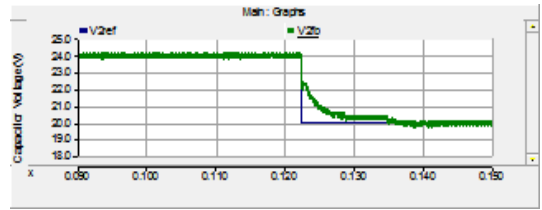


Figure 15 - Buck Mode Output Voltage Variation with Given Reference

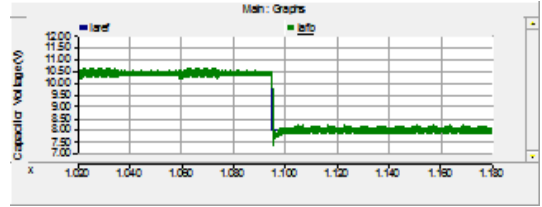


Figure 16 - Buck Mode Output Current Variation with Given Reference

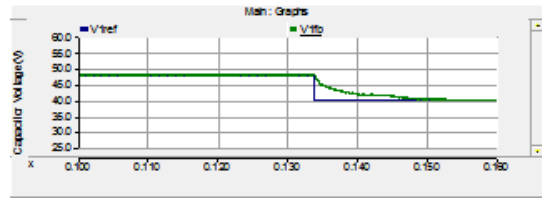


Figure 17 - Boost Mode Output Voltage Variation with Reference

5.3 Grid connected Voltage Source Inverter

First, the open loop operation of inverter mode was verified using PSCAD simulator for the calculated M_a value which is 0.97.

Figure 18 shows the inverter output voltage waveform which is a square wave with a varying duty ratio. Unipolar switching makes the output waveform pattern much similar to that of a sinusoidal waveform.

Figure 20 shows the sinusoidal waveform and its RMS value obtained after filtering via the inductive filter.

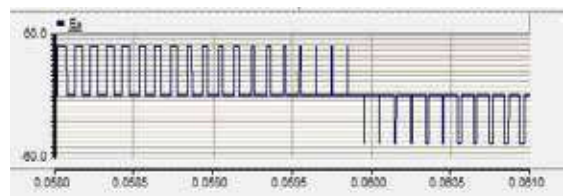


Figure 18- Inverter Output Voltage Waveform



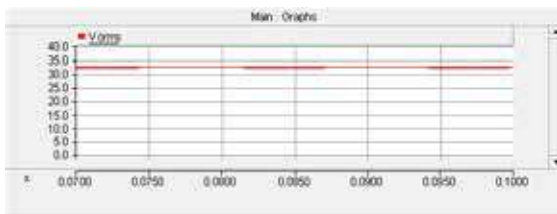
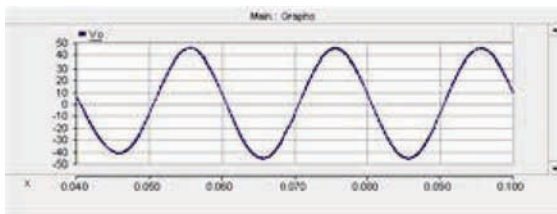


Figure 19 - Desired Output Voltage and its RMS Value Variation

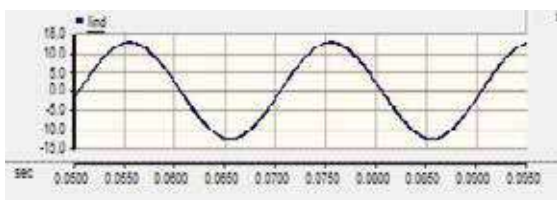


Figure 20 - Inductor Current Waveform

6. Conclusion

The proposed ac-dc multiport power electronic interface enables to integrate different energy sources and load operated by ac and dc.

This paper presented the design methodology of the converters and controlled related to this multiport power electronics interface. A prototype system was designed based on the theory. Then the system was simulated in EMTDC/PSCAD software. The simulation results verified the open-loop and closed-loop operating of the power electronic converters associated with the energy sources of the interface.

As future work, the power electronic converters related to the load side will be developed with controllers. Then the performance of the systems as a single unit will be evaluated.

References

1. Parhizi, S., Lotfi, H., Khodaei, A., and Bahramirad, S., "State of the Art in Research on Microgrids: A Review," *IEEE Access*, vol. 3, pp. 890-925, 2015.
2. Binduhewa, P. J., "Microsource Interface for a Microgrid," The University of Manchester, 2010.

3. Jasim farhood sultani "Modelling, Design and Implementation of d-q Control in Single-Phase Grid-Connected Inverters for Photovoltaic Systems Used in Domestic Dwellings" Faculty of technology, de montfort university, leicester, UK
4. Bhim Singh, Sagar Goel, Chinmay Jain and Umarshankar Subramaniam, " A Sustainable Solar Photovoltaic Energy System Interfaced with Grid-tied Voltage Source Converter for Power Quality Improvement", [Online], <http://www.researchgate.net/publication/311731886>.
5. Erickson, R. W., and Maksimović, D., *Fundamentals of power electronics*. Norwell, Mass.: Kluwer Academic, 2001.
6. Colonel W.M.T McLyman, " Transformer and Inductor Design Handbook" , Idyllwiled California USA , ch 8, pp 254
7. Mojgan Hojabri and Mehrdad Hojabri, "Design, Application and Comparison of Passive Filters for Three-Phase Grid-Connected Renewable Energy Systems"
8. NED Mohan, Tore M. Undeland & William P. Robbins, "Power Electronics, converters applications & design", second edition.
9. K.Suresh & Dr. R. Arulmozhiyal, "Design and Implementation of Bi-directional DC-DC Converter", [Online], <http://www.scirp.org/journal/cs> .
10. M Stadler, G.Cardoso, S.Mashayekh, T Forget, N.De.Forest, A.Agarwal, and A. Schobein, "Value Streams in Microgrids", 2015
11. Athimulam Kalirasu, Subharensu Sekar Dash, "Simulation of Closed Loop Controlled Boost Converter for Solar Installation", *Serbian Journal of Electrical Engineering*, vol. 7, No1, May 2010, 121-130
12. Nagisetty Sridhar and R. Kanagaraj "Modeling and Simulation of Controller for Single Phase and Three Phase PWM Rectifiers"

Indoor Navigation System with RFID Tags for Virtually Impaired Individuals

J.M.K.V. Jayalath, D.M.G.C. Jayathilake, M.A.C.I.U. Yapa
S.A.H.A. Suraweera and G.M.R.I. Godaliyadda

Abstract: This paper targets to deliver a comprehensive indoor navigation system especially for blind and elderly people for navigating safely and efficiently. In order to address the issue of navigating oneself in complex environments such as shopping complexes, hospitals, offices etc., we propose deploying RFID tags in a network connecting each and every strategic location in the area. The user is navigated through these RFID tags via the shortest and least obstructive path available. Fuzzy logic based deviation correction algorithm is developed to provide required voice commands to the user guiding him safely from the entrance to the destination. User specific step detection system, which is a major area in inter-waypoint navigation has been developed to track the user using his step count. Finally, a cloud system is proposed which can keep track of each and every user who is wearing the device in a particular environment.

Keywords: Indoor Navigation, RFID tags, step counting, fuzzy logic

1. Introduction

Navigating in an indoor environment has become a major issue for visually impaired individuals as the most popular navigation system, global positioning system (GPS) malfunctions inside buildings [1]. Generally, there might be several floors connecting several building sections where the user will not be localized by GPS. Furthermore, in most of massive structures, people experience less internet connectivity than outside due to attenuated signals.

On the other hand, people who have less eye sight or old enough to get lost inside buildings would still want to walk around and get their works done by themselves. For an example A visually impaired person would like to go to the eye clinic which is located at south wing ground floor which he cannot reach without getting help from someone around. In order to address this general problems, people have proposed various indoor navigating techniques such as Ultrasonic Beacons [2], Ultra-wideband, and indoor navigation with WIFI and Indoor localization [3] using KINECT sensors [4] etc. But all these methods use active equipment which may affect the effectiveness and the practicality of the navigation system when the power consumption factor is considered.

The discussed paper proposes RFID tags, a cheap passive element which can be deployed all over the building for a very low cost. These RFID tags form a local network in the building connecting almost all possible destinations that a single user is able to visit. A device which is capable of providing voice commands to the user and guide him to his desired destination and a white cane which can detect RFID tags will be the proposed user carrying equipment. A step recognition and counting system is proposed which can identify a stepping action of the user out of his other body movements. A deviation correction technique is proposed incorporating fuzzy logic to provide more linguistic and accurate results that will smoothly correct the user's deviation from the desired path without giving sharp turn commands time to time. Further, this device

*Eng. J.M.K.V. Jayalath, BSc.Eng(Peradeniya)
Automation Engineer, MAS Kreedaa.*

*Eng. D.M.G.C. Jayathilake,
BSc.Eng(Peradeniya).Engineer, IP Core Network
Operations, Dialog Axiata PLC.*

*Eng. M.A.C.I.U. Yapa, BSc.Eng(Peradeniya).Electrical
Engineer, ZPMC Lanka Company(PVT.) Limited.*

*Dr. S.A.H.A. Suraweera, BSc.Eng.(Peradeniya), Ph.D.
(Monash University), Senior Lecturer, Department of
Electrical and Electronics Engineering, Faculty of
Engineering, University of Peradeniya.*

*Eng. (Dr.) G.M.R.I. Godaliyadda
BSc.Eng.(Peradeniya), Ph.D. (National university of
Singapore), Senior Lecturer, Department of Electrical and
Electronics Engineering, Faculty of Engineering,*



connects to a common local network where someone can monitor the user throughout his/her journey.

2. Literature Review

Our proposed system is similar to the system proposed by [5] But the novel use of deviation correction method using Fuzzy logic and the step recognition technique developed using standard deviation of foot acceleration signals made the human navigation smoothly and accurately. The limitations of the existing system would be the lack of deviation correction which makes it necessary to use a large amount of RFID tags. But in the proposed system, the navigation primarily depends on deviation correction using fuzzy logic and distance estimation with the use of step recognition algorithm which drastically decreases the number of RFID tags required. Furthermore, in the existing system a network lag causes a difficulty in Navigation due to usage of GPRS signals, but in the proposed system, this issue is eliminated by Mainly relying on the deviation correction and distance estimation for navigation instead of relying on data obtained from the server

Most of the methods have been developed to identify steps using mobile phone's inbuilt gyro sensor and accelerometer [6] to use in health purposes such as identifying gait patterns etc. [7], [8] Since Mobile phones are normally carry in pockets, we could not get a better signal enough to count steps in a reasonable accuracy.

Some of those methods analyzed singles directly come from the foot by placing an accelerometer on the foot top [8]. Such methods can be categorized in to two as analytical methods and mathematical methods.

In mathematical prospective, researches were trying to model the foot dynamics in to a mathematical model. And trying to generate a foot stepping signal using the mathematical model and then match the template with the original signal [9]. Researches have also tried such as window overlapping method, Standard deviation based methods [6] Spectrogram analysis and template matching to count the steps accurately. Further, several experiments were made to optimize a filter to

design for this kind of movements of 3 axes [8],[10].

3. System Description

System initiates at the first point when a user step into the building from any given entrance. This happens when the cane detects a floor mounted RFID tag at the entrance. It is proposed to use few RFID tags placed in an array so that the user will not miss any waypoint. Passive RFID tags has a maximum detection range of around 10 mm.

Then the user receives a voice command through his earphone to select the destination he wants to go. After his selection using up down and enter buttons, the system calculates the best least distraction path to his destination.

There are two basic concepts we developed in this system, a technique which uses fuzzy logic to minimize the deviation of the user while walking on the desired path and a specific feature which is extracted from the limb acceleration signals. This feature helps to differentiate leg movements with step and random motion.

In the implementation, a centralized server which communicate with the wearable device via WIFI network in the building is proposed to accomplish the following criteria.

- Keep track on all users in the building.
- Perform the necessary communication with the user
- Running Dijkstra's algorithm.

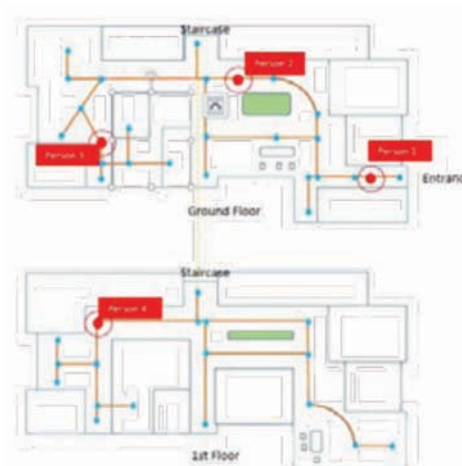


Figure 1 - RFID tag placement at every strategic location in each floor. Positions of all the users can also be demonstrated in the server room interface

4. Deviation Correction Technique Using Fuzzy Logic

Inter waypoint navigation system using direction and distance would not be robust enough to assist the user in navigating between waypoints due to environment complexities. Therefore, a new algorithm is proposed to guide the user in between waypoints using the perpendicular threshold method.

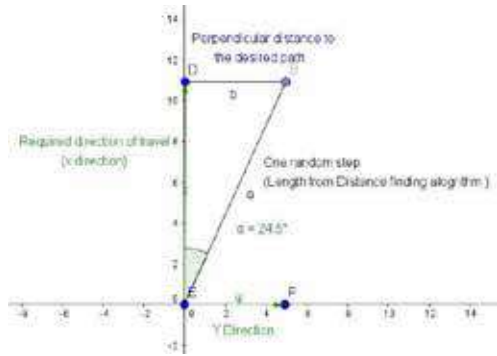


Figure 2 - The perpendicular threshold method with two parameters

After implementing the perpendicular threshold method, it was found that the accuracy of the system varies drastically with the walking pattern of the users. To remedy that issue and increase the adaptability of the guiding system, fuzzy logic is proposed to be incorporated to give more linguistic and probabilistic commands to user rather than straightforward turn commands.

For the Fuzzy control system, the two inputs; Distance travelled along the desired path and the distance travelled perpendicular path is obtained. Distance travelled along the desired path is obtained as a factor of the distance between two RFID waypoints which improves the system's adaptability to user's walking pattern.

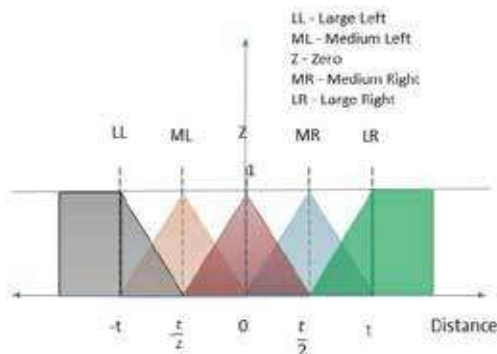


Figure 3 - Membership function for distance Moved perpendicular to desired path

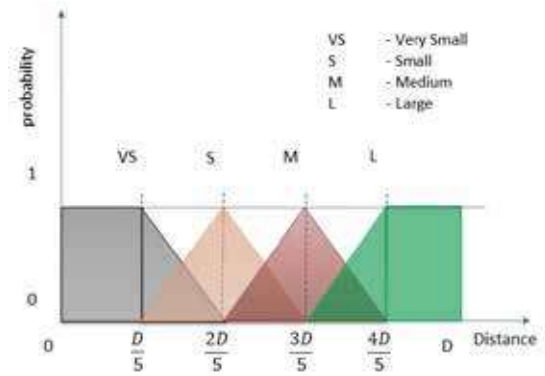


Figure 4 - Membership function for distance Moved along the desired path

during the implementation of the proposed method, turn commands such as turn left, Turn Right, turn left a lot etc. were issued not respective to some hard coded parameters but in a probabilistic way which improve the accuracy of the system. The commands such as proceed forward, turn right and turn left were issued all the time but commands such as turn right a lot and turn left a lot were issued very rarely proving the accuracy of the system.

Table 1 - Rule base for the fuzzy logic control

Rule Base					
	LL	ML	Z	MR	LR
VS	TRL	TR	-	TL	TLL
S	TR	-	-	-	TL
M	TR	-	-	-	-
L	TRL	TR	-	TL	TLL

TRL - Turn Right a lot TR - Turn Right

TLL - Turn Left a lot TL - Turn Left

5. Step Identification Using Moving standard deviation

In statistics, standard deviation is a measure that is used to quantify the amount of variation of a set of data from the mean. Low standard deviation indicates that the data points tend to be close to the mean while high standard deviation indicates that the data points are spread out over a wider range of values. This is a useful property to differentiate data from 'moving' segments to 'not moving' segments. Because when the leg moves, the data points vary in a high frequency. When the standard deviation is considered, getting a high value can be



predicted while low value is predicted for standard deviation when the user is not moving [6].

First, accelerometer data from low cost gyro sensor was collected and filtered against noise [11],[12]. Consider the standard deviation in a non-overlapping moving window, consider the size of the window 30. The whole data set is divided to non-overlapping windows of size 30 and e standard deviation in each window can be predicted as below.

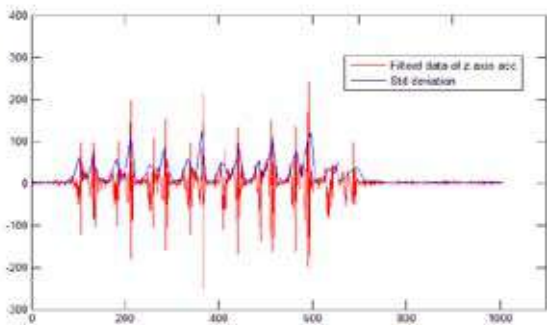


Figure 5 - Filtered foot acceleration data along z axis (top) and Plot of standard deviation on Acceleration data set along z axis (bottom)

As the graph depicts, the blue plot is clustered properly than the red one (filtered acceleration signal) proving the expected results. Through the experiment, the two mountain type segments gathered together can be identified as actual steps. In other words, 'moving' segments. There is a space between those two mountains which represents the interval between steps and is called 'not moving' segments.

Calculating moving standard deviation:

Standard deviation of the window I,

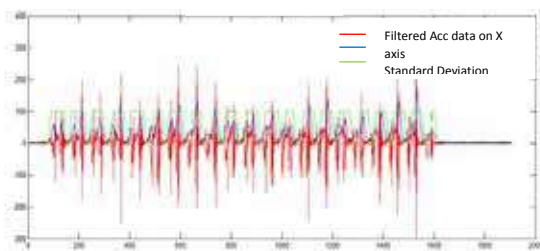


Figure 6 - Generation of candidate steps

$$S_x(i) = \sqrt{\sum_i \frac{\sum_j^{30} (x(j) - \mu)^2}{30}} \quad \dots (1)$$

5.1 Calibration stage

From the calibration it is expected to acquire few details which are unique from person to person. First the user is asked to walk up and down once, first a known number of steps and then a known distance. Then the program is executed and in the first turn, the standard deviation of the whole walking signal and the best value for a 'K' constant (which will be described later) is calculated. In the second turn the user is asked to walk down a known distance. It may be 10-15 meters. Program will calculate the average distance of a step and will use it to measure the distance.

5.2 Unique constant for each and every user

The K constant is a portion of standard deviation which will be used to compare with the real time moving standard deviation would be the unique constant for a particular person. As an example, if the user is a low weight, thin person, the stepping signal will contain much noisy data where the standard deviation is relatively high. Hence the K value will be larger. If the user is an obese person who has short steps, a less noisy stepping signal is expected which lead to a low K value.

5.3 Decision making criteria

In the proposed work the different standard deviation can be calculated as below using the data discussed above.

$$S_x(signal) = \sqrt{\frac{\sum_{n=1}^m (x(n) - \mu)^2}{m}} \quad \dots (2)$$

First the average standard deviation of 3 sets is obtained from set one to set 3.

If the average of standard deviation is greater than $K \cdot S_x(signal)$, it is considered to be a candidate step.

For $i=1$

$$S_{check} = \frac{S_x(i-1) + S_x(i) + S_x(i+1)}{3} \quad \dots (3)$$

Candidate step if;

$$S_{check} \geq K \cdot S_x(signal) \quad \dots (4)$$

And continue till $i = m$.

In the proposed work, if it is followed the same methodology with all the three axes, the parameters

$$K_z, K_x, K_y, S_x(\text{signal-z}), S_x(\text{signal-y}), S_x(\text{signal-x}),$$

can be obtained.

5.4 Voting

A voting method is proposed for the candidate plots generated earlier to get the final decision to the problem. As a first step AND rule as a voting strategy is considered. But it is proposed to use weighted average techniques to vote for a step.

P_x, P_y and P_z are the voting of axis x, y, z respectively

$$\text{Voting Marks} = \frac{W1 * P_x + W2 * P_y + W3 * P_z}{W1 + W2 + W3} \dots (5)$$

As an example, if we have given same weightage for each axis and the candidate plots vote for a step as, 2 axis vote for a step, one is not: $P_x = 1 P_y = 1 P_z = 0$

$$\text{voting marks} = \frac{1(1)+1(1)+1(0)}{3} = 0.67 \dots (6)$$

Decision- Step is not identified

Every axis vote for a step:

$$P_x = 1 P_y = 1 P_z = 1$$

$$\text{voting marks} = \frac{1(1)+1(1)+1(1)}{3} = 1 \dots (7)$$

Decision- Step has identified

6. Determining the weights of paths

According to the above explanation on Dijkstra's algorithm, weight should be determined between RFID tag points. Weights of the paths were determined considering several facts.

- Distance between two RFID tags:

This is the main factor to be considered to determine the weight. The blind person should have to be navigated through the shortest path as possible. Therefore, more weight is put on distance.

- Allowable and not allowable paths:

In an indoor environment some paths are not allowed to walk for blind

people. Some paths are too dangerous for blind people to walk. Sometimes, blind people walking through normal people disturb the community. So, weight between two RFID points is determined considering all those facts.

- Objects on paths should be avoided.

After determining weights with above mentioned facts, these weights are included to a matrix called "weighted matrix". Then weighted matrix is used in Dijkstra's algorithm with source as the input and destination as the output.

For the demonstration of applicability of Dijkstra's algorithm in RFID based navigation system, we have designed an interface. Source RFID point and the destination RFID point is given as the input and the most appropriate path is displayed on the map.

6.1 Experiment on Step counting and results

This method is tested using randomly selected 7 men and 2 women and they were asked to follow the procedure and collected the results. It was observed that the user walks fast the system found it difficult to recognize the steps differently because the variation curves segment together. Furthermore AND voting mechanism serves its best as three axis(x,y,z) are equally informative.

Table 2 - Experiment Results

Walking Pattern	Actual Steps	Counted Steps	Error
Normal Walking	10	10	0
	12	12	0
	14	14	0
	16	16	0
	18	18	0
	20	20	0
	22	22	0
	24	21	-3
	26	25	-1
	28	27	-1
Walking in a staircase	20	23	3
	15	18	3
Walking at human disturbance	20	22	2



7. Conclusion

The proposed work discusses the implementation of a RFID based navigation system which can be used by blind people. The system contains RFID tags placed in strategic locations. A shortest path calculating algorithm and inter waypoint navigation principle using step counting and deviation techniques. The key novelties of the work are the step counting algorithm and the deviation correction algorithm using fuzzy logic and the step distance estimation algorithm. The proposed step counting algorithm uses the acceleration data of the foot in all three perpendicular directions and provides a final result using a voting mechanism. The step distance measuring algorithm uses this output and the data obtained from user's walking pattern to estimate the distance travelled by the user. Once the distance is estimated, the user's location is obtained with the direction travelled and Turn commands are issued to correct the deviation of the user from the desired path. The deviation control is done through a fuzzy control system which adapts to the human nature of the user which improves the accuracy and overall reliability of the system. Using these three novel concepts, the accuracy of the system was improved immensely and after actual implementation of the system at the shopping mall, Kandy City Center. The system proved to be a complete indoor navigation system for visually impaired individuals.

Reference

1. Babu R and Wang J, "Real-time data analysis of ultra-tight GPS/INS integration", Springer-Verlag, 2008, doi:10.1007/s10291-008-0097-9
2. Rohan Kapoor et al., (2016 Oct 8), "A Novel 3D Multilateration Sensor Using Distributed Ultrasonic Beacons for Indoor Navigation"[Online], Available: www.mdpi.com/1424-8220/16/10/1637
3. Kai Dong et al., "Canoe: An Autonomous Infrastructure-Free Indoor Navigation System", MDPI AG, Basel, Switzerland, 2017, doi:10.3390/s17050996
4. Kourosh Khoshelham and Sander Oude Elberink, "Accuracy and Resolution of Kinect Depth Data for Indoor Mapping Applications", MDPI AG, Basel, Switzerland, 2012, doi:10.3390/s120201437
5. Sakmongkon Alessandro Chumkamon et al., "A Blind Navigation System Using RFID for Indoor Environments", in ECTI-CON 5th conference, 2008, DOI: 10.1109/ECTICON.2008.4600543
6. Aylar Seyrafi, "Real time Automatic Step Detection in the Three Dimensional Accelerometer Data", M.S. thesis, Appl. Signal Proc. Dept., Bleking Institute of technology, Karlskrona, SE, 2009
7. Joaquín Torres-Sospedra et al., "The Smartphone-Based Offline Indoor Location Competition at IPIN 2016: Analysis and Future Work", MDPI AG, Basel, Switzerland, 2017, doi:10.3390/s17030557
8. Akram Bayat et al., "A Study on Human Activity Recognition Using Accelerometer Data from Smartphone", International Conference on Mobile Systems and Pervasive Computing, Ontario, CA, 2014, pp 3-5.
9. Christopher M. Bishop, "Pattern Recognition and Machine Learning", New York, Springer Science+Business Media, 2006, ch. 7, sec. 1. pp.359-370
10. Xiaoping Yun, Eric R. Bachmann, "Self-contained Position Tracking of Human Movements Using Small Magnetic Sensor Modules", IEEE International conference on Robotics and Automation, Roma, Italy, 2007
11. Yongjian Zhang et al., (2017 April 28), "A Novel MEMS Gyro North Finder Design Based on the Rotation Modulation Technique"[Online], Available: <http://www.mdpi.com/1424-8220/17/5/973>
12. Ryo Takeda et al., (2014 Dec 5), "Drift Removal for Improving the Accuracy of Gait Parameters Using Wearable Sensor Systems"[Online], Available: <http://www.mdpi.com/1424-8220/14/12/23230/htm>

Energy Efficiency Benchmarking of Pumps in Water and Wastewater Industries in Sri Lanka

B.G.A. Dinesh

Abstract: Pumping of public portable water in Sri Lanka constitutes the largest power consumption in the country, 237 million kWh being utilized annually at present levels, but growing at a rapid rate. The overall efficiency of pumps bears a direct correlation to the efficient use of electric power. According to the energy audits carried out in the field, there is at least 20% economically redeemable energy wastage by conservative estimation, while actual loss percentage found was close to 30%.

To gauge the operating efficiency of pumps, there have to be benchmarks against which to compare actual efficiency and find out wastages of energy. Benchmarking of pumps poses a challenge due to the wide-ranging sizes, ranges of flow & head of pumps. Size of pumps ranges up to 850 kW, head up to 180 m flow rate up to 4,300 m³/h.

The achievable efficiency of pumps is directly related to the pump type, specific speed and similar parameters. There are widely published data on the empirical relationship among pump types, specific speed and related pump parameters.

Therefore, an empirical system of determination of efficiency benchmarking was developed and implemented which is undergoing field verification at the moment. The system is based on empirical correlation data published by reputed institutions supplemented by methodology devised by us.

Specific Energy Consumption (SEC) was calculated and used as a final extended parameter of comparison. Benchmark SEC was arrived at, using the empirical method of determination explained in this paper. From above SEC figures, it can be determined whether any pump is performing below acceptable benchmark levels.

This exercise needs the ongoing validation of the benchmarks against best efficiencies of pumps available on the market and results of the actual SEC figures found in the studies.

This paper summarizes the approach, formulation of methodology and findings in the field on the topic of this paper.

Keywords: Pump Efficiency, Motor Efficiency, Pump Specific Speed, Rotodynamic Pumps Characteristics, Specific Energy Consumption

1. Introduction

Conveyance of water and wastewater in the National Water Supply & Drainage Board (NWSDB), Sri Lanka is mainly carried out by pumping. Pumps used are of a rotodynamic type. NWSDB annually consumes 237 Million kWh of electricity for the pumping requirement of the water and wastewater systems. With the new mandatory regulations regarding energy efficiency coming into effect in Sri Lanka in the recent past, as well as the awareness created regarding the efficiency problems that might exist in the NWSDB pumping systems, NWSDB undertook a study programme. The programme mainly consisted of carrying out energy audits at the water supply systems in

the island, analyzing the study data and finding the causes of inefficiencies. Depending on the nature and the extent of the causes of inefficiencies, appropriate remedial actions were carried out.

The main cause of the energy wastage in pumping is the lower efficiencies at which the pumps are operated. This is found out in the energy audits carried out in the pumping stations.

Eng. B.G.A. Dinesh, AMIE(SL), M.Sc.(Sustainable Energy Engineering, KTH-Sweden), P.G. Dip. (Energy Technology-UOM), B.Sc.Eng.(Mechanical-UOM), Chief Engineer (M&E), RSC(S), NWSDB.



Pumps in the water and wastewater systems of the NWSDB, vary in size from 1.5 kW to 850 kW. Owing to the inherent characteristics of the pumps, their achievable highest efficiency depends on the size and several other factors.

There is no reliable way to gauge the acceptable efficiency of the pumps to determine whether pumps are wasting energy.

As a redress to this problem, NWSDB commenced establishing an effective benchmarking program. An empirical system was established based on data published by reputed bodies to determine the empirically possible highest efficiency for the pumps operating in the field.

A comparison was made between the above efficiency and the operating efficiency of the pumps in the field. This exercise facilitated in the determination of whether the pumps are working at the highest possible efficiency or wasting energy by working at sub-optimal efficiencies.

In case they are working at sub-optimal efficiencies, further investigations can be

carried out to find out the causes. Subsequently, the remedial solutions can be determined for implementation and saving energy.

2. Methodology

The efficiency of a pump is expressed in different forms such as Overall Pump Efficiency and Pump Hydraulic Efficiency. Motor efficiency also comes into the picture when determining these pump efficiencies. Any pump will have a single operating point where it exhibits the maximum efficiency of the particular pump, in its range of efficiencies (Figure 1). An operating point is any point on the Head vs Flow rate curve on which the pump operation range lies.

The maximum efficiency point is termed Guaranteed Duty Point in the industry. At operating points away from this point on either side will reduce the efficiency, thus increasing the wastage of energy.

Therefore in an effort to reduce energy wastage or to optimize the efficiency, we must make sure that the pumps are functioning at the guaranteed duty point or as close to it as possible.

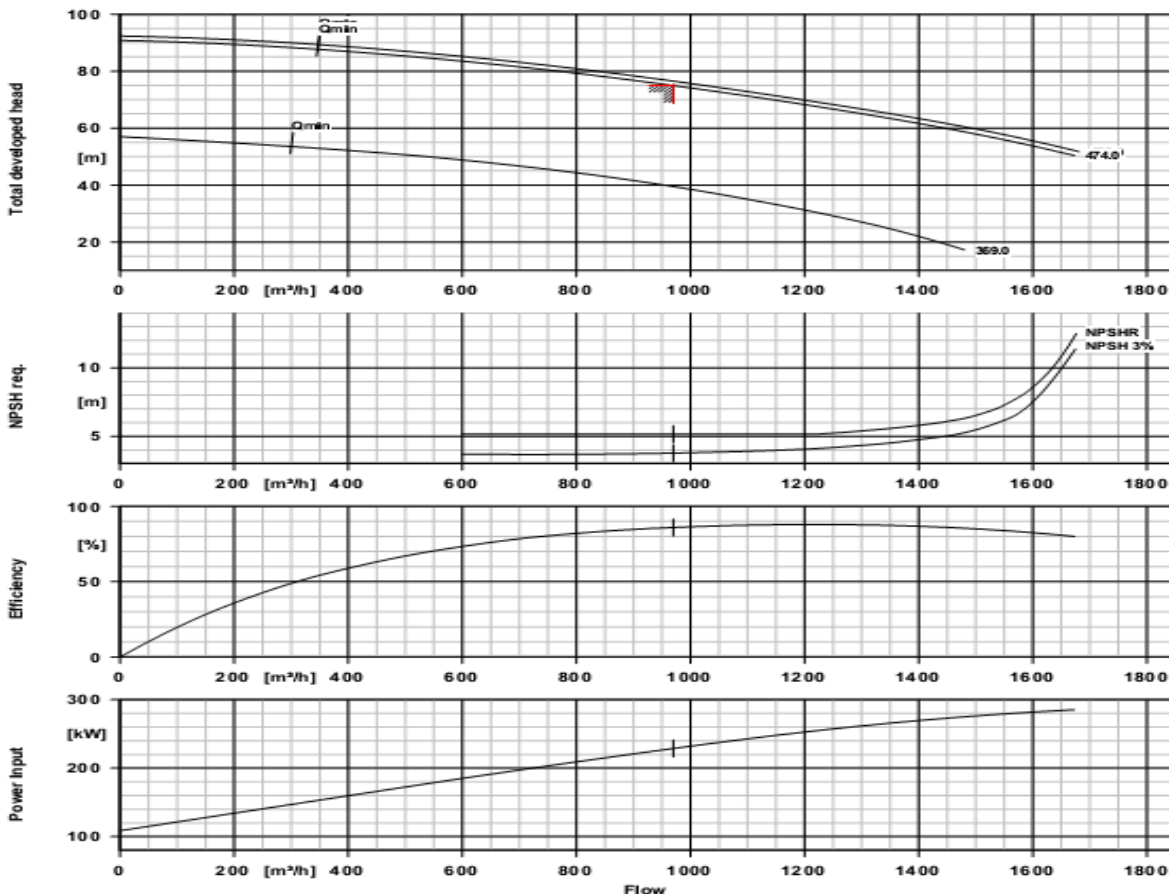


Figure 1 – Typical manufacturer published characteristics of a pump

Overall pump efficiency defines how efficiently the pump unit uses the electrical power drawn from the utility grid in the pumping operation which is given by,

$$\text{Overall Efficiency} = \frac{\text{Power Absorbed}}{\text{Power drawn from the Grid}} \quad \text{--- (1)}$$

$$\text{Power Absorbed} = \frac{q\rho gh}{(3.6 \times 10^6)}$$

q = flow capacity (m^3/hr)

ρ = density of fluid (kg/m^3)

g = gravity ($9.81 m/s^2$)

h = differential head (m)

$$\text{Pump hydraulic efficiency} = \frac{\text{Power absorbed by water}}{\text{Shaft power required to drive pump}}$$

Motor efficiency deterioration over time is rather slow compared to the deterioration of the pump efficiency due to the fact that wear and tear phenomena associated with pumps are relatively absent. Similarly, motors are built with narrow and accurate efficiency tolerances. However, in this benchmarking exercise, we also determined the actual operating efficiency of the motors. For this, we use typical motor characteristics published by IEC 60034-30 (2008) (Table 1).

Instantaneous pump efficiency is directly related to the instantaneous flow rate through it. This is evident from the manufacturer's characteristic curves issued for the performance of any particular pump (Figure 1).

At the same time, rotodynamic pump exhibits an inherent design characteristic termed Specific Speed which is directly related to the achievable efficiency as well as defining the configuration of the pump structure within the rotodynamic category.

When the specific speed of a particular pump is determined, it is possible to find out the maximum achievable efficiency for that pump by using the flow rate through the pump and empirical data published by a recognized body. In our study, we used the data published by the Hydraulic Institute (HI), USA, and McGraw

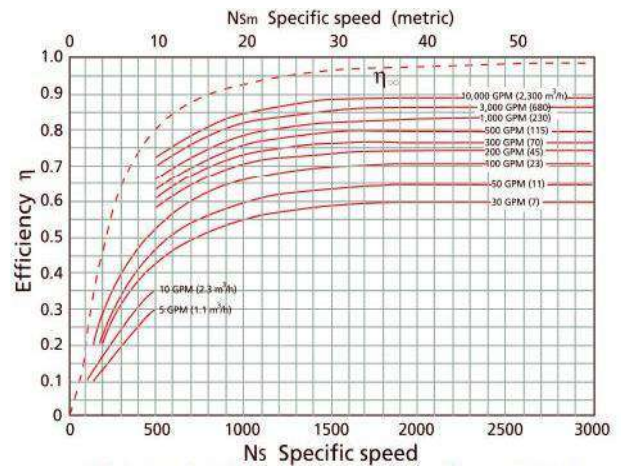


Figure 2 -Hydraulic efficiency vs Specific speed

Table 1 - Table with efficiency classes: IE 60034-30 (2008)

kW	HP	IE-1 - Standard efficiency						IE2 - High efficiency						IE3 - Premium efficiency					
		2 pole		4 pole		6 pole		2 pole		4 pole		6 pole		2 pole		4 pole		6 pole	
0.75	1	72.1	77.0	72.1	78.0	70.0	73.0	77.4	75.5	79.6	82.5	75.9	80.0	80.7	77.0	82.5	85.5	78.9	82.5
1.1	1.5	75.0	78.5	75.0	79.0	72.9	75.0	79.6	82.5	81.4	84.0	78.1	85.5	82.7	84.0	84.1	85.5	81.0	87.5
1.5	2	77.2	81.0	77.2	81.5	75.2	77.0	81.3	84.0	82.8	84.0	79.8	86.5	84.2	85.5	85.3	86.5	82.5	88.5
2.2	3	79.7	81.5	79.7	83.0	77.7	78.5	83.2	85.5	84.3	87.5	81.8	87.5	85.9	86.5	86.7	89.5	84.3	89.5
3	3	81.5	81.5	81.5	81.5	79.7	81.5	84.6	85.5	85.5	87.5	83.3	87.5	87.1	87.7	87.7	89.5	85.6	89.5
3.7	5	84.5	84.5	85.0	85.0	83.5	85.0	87.5	87.5	87.5	87.5	87.5	87.5	88.5	88.5	89.5	89.5	89.5	89.5
4	4	83.1	83.1	83.1	83.1	81.4	83.1	85.8	86.6	86.6	86.6	86.6	88.1	88.1	88.6	88.6	88.6	88.6	88.6
5.5	7.5	84.7	86.0	84.7	87.0	83.1	85.0	87.0	88.5	87.7	89.5	86.0	89.5	89.2	89.5	89.6	91.7	88.0	91.0
7.5	10	86.0	87.5	86.0	87.5	84.7	86.0	88.1	89.5	89.7	89.5	87.2	89.5	90.1	90.2	90.4	91.7	89.1	91.0
11	15	87.6	87.5	87.6	88.5	86.4	89.0	89.4	90.2	89.8	91.0	88.7	90.2	91.2	91.0	91.4	92.4	90.3	91.7
15	20	88.7	88.5	88.7	89.5	87.7	89.5	90.3	90.2	90.6	91.0	89.7	90.2	91.0	91.0	92.1	93.0	91.2	91.7
18.5	25	89.3	89.5	89.3	90.5	88.6	90.2	90.9	91.0	91.2	92.4	90.4	91.7	92.4	91.7	92.6	93.6	91.7	93.0
22	30	89.9	89.5	89.9	91.0	89.2	91.0	91.3	91.0	91.6	92.4	90.9	91.7	92.7	91.7	93.0	93.6	92.2	93.0
30	40	90.7	90.2	90.7	91.7	90.2	91.7	92.0	91.7	92.3	93.0	91.7	93.0	93.3	92.4	93.6	94.1	92.9	94.1
37	50	91.2	91.5	91.2	92.4	90.8	91.7	92.5	92.4	92.7	93.0	92.2	93.0	93.7	93.0	93.9	94.5	93.3	94.1
45	60	91.7	91.7	91.7	93.0	91.4	91.7	92.9	93.0	93.1	93.6	92.7	93.6	94.0	93.6	94.2	95.0	93.7	94.5
55	75	92.1	92.4	92.1	93.0	91.9	92.1	93.2	93.0	93.5	94.1	93.1	93.6	94.3	93.6	94.6	95.4	94.1	94.5
75	100	92.7	93.0	92.7	93.2	92.6	93.0	93.8	93.6	94.0	94.5	93.7	94.1	94.7	94.1	95.0	95.4	94.6	95.0
90	125	93.0	93.0	93.0	93.2	92.9	93.0	94.1	94.5	94.2	94.5	94.0	94.1	95.0	95.0	95.2	95.4	94.9	95.0
110	150	93.3	93.0	93.3	93.5	93.3	94.1	94.3	94.5	94.5	95.0	94.3	95.0	95.2	95.0	95.4	95.8	95.1	95.8
132	180	93.5	93.5	93.5	93.5	93.5	94.6	94.6	94.7	94.7	94.7	94.6	94.6	95.4	95.4	95.6	95.6	95.4	95.4
150	200	94.1	94.1	94.5	94.5	94.1	94.1	95.0	95.0	95.0	95.0	95.0	95.0	95.4	95.4	95.6	95.6	95.8	95.8
160	220	93.8	93.8	93.8	93.8	93.8	94.8	94.8	94.8	94.8	94.8	94.8	94.8	95.6	95.6	95.8	95.8	95.8	95.8
185	250	94.1	94.1	94.5	94.5	94.1	94.1	95.4	95.4	95.4	95.4	95.0	95.0	95.8	95.8	96.2	96.2	95.8	95.8
200	300	94.0	94.0	94.0	94.0	94.0	95.0	95.0	95.1	95.1	95.0	95.0	95.8	95.8	96.0	96.0	96.0	95.8	95.8
220	350	94.0	94.1	94.0	94.5	94.0	94.1	95.0	95.4	95.1	95.4	95.0	95.0	95.8	95.8	96.0	96.2	95.8	95.8
250	400	94.0	94.1	94.0	94.5	94.0	94.1	95.0	95.4	95.1	95.4	95.0	95.0	95.8	95.8	96.0	96.2	95.8	95.8
300	450	94.0	94.1	94.0	94.5	94.0	94.1	95.0	95.4	95.1	95.4	95.0	95.0	95.8	95.8	96.0	96.2	95.8	95.8
330	500	94.0	94.1	94.0	94.5	94.0	94.1	95.0	95.4	95.1	95.4	95.0	95.0	95.8	95.8	96.0	96.2	95.8	95.8
375	500	94.0	94.1	94.0	94.5	94.0	94.1	95.0	95.4	95.1	95.4	95.0	95.0	95.8	95.8	96.0	96.2	95.8	95.8



Hill (Figure 2).

Equation for the specific speed is,

$$N_s = N \cdot Q^{0.5} / H^{0.75} \quad \dots(2)$$

Where,

N_s = Specific speed

N = Rated rotational speed in revolutions per minute

Q = Rated flow rate in $\frac{m^3}{s}$ ($\frac{Q}{2}$ for double suction pumps)

H = Rated total dynamic head of the pump in m (per one stage for multi stage pumps)

Therefore, the achievable optimal efficiency of a pump under particular operating conditions is dependent on the actual flow rate through it and the specific speed of the particular pump.

In this programme, we also determined an extended parameter termed Specific Energy Consumption (SEC), which is the total amount of energy consumed per one cubic meter of water pumped. It is obvious that higher the efficiency figure for a pump, lower the SEC, which is the situation that we are striving for.

The objective of this study is to benchmark efficiency of the NWSDB pumps using the empirical method described and at the same time to find the actual operating efficiencies of the pumps. If the actual operating efficiency is lower than the benchmark, then it is subjected to further investigation action as well as remedial measures.

As the core of the methodology, the benchmark efficiency or the achievable optimal efficiencies were determined.

The first step of the process is to determine the Specific Speed of the pump. Design or rated values of the Q and H are used in the calculation. These Q and H values are the values corresponding to the guaranteed duty point.

Once the specific speed is calculated, the achievable optimal hydraulic efficiency of a particular pump is determined from the HI diagram (Figure 2).

Next, the actual power drawn by the pump is determined by the following formula,

$$\text{Shaft power} = \frac{\text{Hydraulic power}}{\text{Pump efficiency}} \quad \dots(3)$$

To make corrections for the actual operating efficiency of the motor due to the extent of instantaneous under loading, Load Factor (LF) of the motor has to be determined.

Equation for the Load Factor is,

$$LF = \frac{\text{Shaft power}}{\text{Motor rated power}} \quad \dots(4)$$

Where,

Motor rated power is the rating mentioned on the manufacturer's data plate on the motor.

Achievable optimal power consumption (OPC) of the motor was determined by the following formula.

$$OPC (kW) = \frac{\text{Shaft power}}{\text{Motor efficiency at LF}} \quad \dots(5)$$

Benchmark specific energy consumption (BSEC) is determined from the following equation,

$$BSEC = \frac{OPC (kW)}{\text{Flow rate (m}^3/\text{hr)}} = \text{kWh/m}^3 \quad \dots(6)$$

This is the maximum allowable energy consumption by a given pump to deliver 1 m³ of water under the operating conditions encountered during the study.

During the programme, NWSDB has benchmarked about 500 pumps and compared the actual operating efficiencies of about 200 pumps.

3. Results

From the results, it is evident that 127 nos. pumps show excessive SEC figures over the benchmark SEC's. These pumps are clearly using excessive power than necessary; are wasting energy.

The energy wasting pumps should be further investigated with guaranteed efficiencies of similar pumps in the market as an additional check on the achievable efficiency. Although this is an essential step of the analysis, it is yet to commence. After its commencement, changing or improving efficiency data will be

used to modify the HI diagram for achievable efficiencies. This will allow NWSDB to provide detailed analysis on this aspect as well.

4. Discussion and Constraints

Since this is mainly an empirical exercise, the results and deductions from the data must be compared with the achievable efficiency of similar pumps of the same specific speed range. This might reveal necessary adjustments to HI data used in this programme or elsewhere.

Pumps in the same specific speed range and operating in the same Head/Flow Rate ranges may show varying efficiencies because the detailed design of the pumps varies from manufacturer to manufacturer. Some manufacturers are able to achieve comparably higher efficiencies due to innovativeness and their R&D achievements. Therefore, the adjustment process must be a continuous process whenever necessary.

A considerable problem in the results is the inconsistent results are generated with respect to the SEC value. There are cases when SEC should show higher values theoretically, favourable results or lower SEC's result for example, when operating well away from the guaranteed optimal efficiency point, mostly on the higher flow rate side. This is due to the non-linear, different behaviour of the characteristics of the power, H - Q etc. of the pumps, which is again the result of marginal design improvements of similar pumps among different manufacturers. This peculiarity is interpreted case by case with the actual characteristics of the particular pumps.

5. Conclusions

The programme is greatly useful as an indicator to identify the possible energy wasting pumps. Thus this tool is very useful in screening problematic pumps. However, once identified, they must be subjected to further investigations, including an Investment Grade Energy Audit to find out the status of the performance of the pump. Depending on the results of such studies, remedial action could be taken, if necessary.

It must also ensure to compare the achievable efficiency level of compatible pumps from similar manufacturers in the market, in order to validate or calibrate the HI Efficiency diagram or other aspects of this tool to make it more

accurate. Also, the tool must be subjected to any necessary changes depending on the verification process. This must be an ongoing process to capture the technological and other changes in the market.

References

1. Ebara Pump system Engineering Handbook: *Ebara Corporation, 2001*
2. *Garr M. Jones , PE : Pumping Station Design - Third Edition , 2006*
3. Hydraulic Institute Standards for Centrifugal, rotary and reciprocating pumps: fourteenth edition -1983
4. *Igor J. Karassik , Joseph P. Messina , Paul Cooper , Charles C. Heald (2004) : Pump Hand Book - Fourth Edition , 2008*
5. *Pumping Station Engineering Handbook: Japan Association of Agricultural Engineering Enterprises - Tokyo , 1991*



Feasibility of Hybrid Reactors for Removal of Heavy Metals in Wastewater

G.S. Nallaperuma and W.M.K.R.T.W. Bandara

Abstract: The research carried out for the removal of heavy metals in wastewater is very much significant in the field of Environmental Engineering and Science. Although there are a number of chemical and physical treatment processes to remove heavy metals efficiently from wastewater, the drawbacks like high operational cost and excess sludge production limit the use of those methods. However, the biological treatment methods are still economical because the combination of anaerobic and aerobic treatment methods can be used more efficiently since they have a number of advantages like low operational cost, less sludge production and energy through gas production. Therefore, an Up-flow Anaerobic Sludge Blanket Reactor (UASB) and an activated sludge process were combined to form a hybrid reactor for the removal of heavy metals with less sludge. The hybrid system was operated with a flow rate of 20 ml/min and an HRT of 7hrs in the UASB reactor. The hybrid reactor was operated 12 times with the influent having 12 different characteristics as follows: each of four heavy metals, namely Pb, Cd, Zn and Cu contained wastewater in three different concentrations. The average COD removal efficiency was 84%. Heavy metal removal efficiencies achieved for Pb and Cu were above 80%, for Cd is above 75%, and Zn removal efficiency was above 90%. Through this study it was found that the hybrid reactor is feasible for the removal of heavy metals in wastewater and the heavy metal removal from the wastewater increases in the order of Cd<Cu<Pb<Zn. The initial heavy metal concentration is directly proportional to the removal efficiency. The same study can be carried out to investigate the technical feasibility of the hybrid reactor to treat the actual wastewater containing heavy metals.

Keywords: Hybrid reactor, UASB reactor, activated sludge process, HRT, COD removal, heavy metal removal, sludge volume

1. Introduction

It is known that the elements with an atomic weight between 63.5 and 200.6 and a specific weight of more than 5.0 are heavy metals [1]. It is well recognized that the industrialization has resulted in the collection and discharge of heavy metals into the environment. The common heavy metal pollutants in wastewater are Cadmium (Cd), Chromium (Cr), Copper (Cu), Iron (Fe), Lead (Pb), Nickel (Ni), Zinc (Zn), and Arsenic (As). Zn, Cu, and Ni have toxic effects in both very low and very high concentrations [2]. Heavy metals accumulate in living organisms since they are not biodegradable as organic compounds. Most of the heavy metals present in the environment are toxic or carcinogenic. As an example zinc cause severe health problems like stomach cramps, vomiting, skin irritations and anaemia [3]. Similarly, the U.S. Environmental Protection Agency says that the Cadmium is a probable human carcinogen.

Nowadays heavy metals are the most popular environmental pollutants and create most serious environmental and health [4]. Therefore, the removal of toxic heavy metals is significant in order to protect both the people and the environment. The methods available for the removal of heavy metals in wastewater can be categorized into three sections like biological, chemical and physical. Currently, the physical and/or chemical processes are the major processes of industrial wastewater treatment.

G. S. Nallaperuma, B.Sc.Eng.(Ruhuna), Civil Engineer, Sierra Construction Pvt Ltd, Colombo 6.

Dr. W. M. K. R. T. W. Bandara, Ph.D.(Hokkaido-Japan), M.Sc (Hokkaido-Japan), B.Sc.Eng. (Peradeniya, Senior Lecturer, Department of Civil and Environmental Engineering, Faculty of Engineering, University of Ruhuna.



Chemical precipitation, coagulation, solvent extraction comes under chemical treatment methods while ultra-filtration, electrolytic processes, and reverse osmosis, oxidation with ozone/hydrogen peroxide, membrane filtration, ion exchange, photocatalytic degradation, and adsorption comes under physical methods [5]. Many of these methods are not popular nowadays due to the high cost and disposal problems. Therefore, these methods for treating wastewater have not been widely applied at large scale. However, at present, there is no any single process capable of sufficient treatment due to complexity in the effluents. Therefore, a combination of different processes is often used to achieve the best water quality in the most economical way [5].

When compared with physical and chemical treatment processes, Biological treatment is the most economical processes. Biodegradation by microorganisms such as bacteria, yeasts, algae and fungi degrade various pollutants such as hydrocarbons, Pharmaceutical substances and metals [5]. Biological treatment mainly divides into two groups, aerobic and anaerobic treatment. The main units of most wastewater treatment plants are aerobic and anaerobic. Anaerobic processes produce biogas as a by-product which can be used to generate energy and produces less sludge other than in aerobic systems. However, aerobic processes have disadvantages like high energy requirement for the aeration to maintain the dissolved O₂ level which is necessary to maintain aerobic condition and at the same time produce excess sludge which requires handling, treatment and disposal [6].

In anaerobic treatment, the decomposition of organic and inorganic matter occurs in the absence of molecular oxygen [7]. They tend to produce sludge only 5-10% when compared with the aerobic process due to many reasons [8]. The main reason is the energy available for the microorganisms to create biomass is less due to the energy available in the wastewater is preserved in methane gas. This ultimately results in less sludge. This saves a significant amount of cost associated with the sludge disposal. Other than that CO₂ and CH₄ are produced as a result of the breakdown of organic molecules by microorganisms. Eighty percent (80%) of biogas which produced through anaerobic treatment is CH₄ and remainder is CO₂. The advantage is that CH₄ is a source of energy which is the primary biogas produced by anaerobic treatment [9]. There is a

greater demand for alternative energy sources as a result of increased demand for energy with the increasing of cost of available fuels. Due to the rapid industrialization, this resulted large quantity of wastewater with high organic content. Therefore, the primary biogas which is produced as a result of treating this waste water anaerobically will be one of solution for growing interest in alternative energy sources.

Anaerobic process does not require aeration. Thereby the cost associated with equipment, maintenance and energy consumption is low in anaerobic treatment when compare with aerobic treatment [8] due to above benefits, wastewater treatment process has forwarded towards the anaerobic treatment. However, anaerobic processes are not popular among treatment plants used for treatment of municipal wastewater. Reasons for the reluctance in the implementation of anaerobic processes are mainly the spreading of unpleasant odour, unstable behaviour of reactors and operation difficulties with the high load rate variations [6]. The effluent quality is also less in anaerobic treatment. As wastewater cannot be treated to low chemical oxygen demand level through anaerobic treatment, quality of the effluent is low. However aerobic treatment is capable of producing a good quality effluent without an unpleasant odour. Therefore, the combination of anaerobic and aerobic system was used in this research to limit the drawbacks in each process in a successful way.

2. Literature Review

In combined anaerobic-aerobic treatment, anaerobic digester is used to treat the influent of the aerobic treatment. It means that anaerobic digester acts as a pre-treatment for aerobic influent. Therefore, oxygen requirement in the aerobic system for degradation and nitrification of remaining organic matter from the anaerobic digester effluent is low due to the large fraction of organic matter is degraded earlier from the anaerobic digester. Also, this system can be used to prevent the separate sludge stabilization.

Less sludge production, low chemical consumption and operational simplicity with minimum equipment. However, anaerobic-aerobic systems have many limitations such as high HRT, difficulties in biogas collection and high space requirement.

Anaerobic-aerobic treatments have more attention than the other combinations throughout the research history since it has significant benefits like less energy requirement. These limitations can be successfully avoided by the use of developed high rate bioreactors which increase removal of organic compound at a shorter HRT and produce high methane yields for biogas production. In order to limit the problems arising with respect to space, odour and minimal sludge production, necessary steps have been implemented by combining the aerobic- anaerobic process in a single bioreactor. It is expected that these bioreactors will be able to treat a wide range of municipal and industrial wastewater which contains high organic strength with the advantages like simplicity, effective cost, production of renewable energy and high treatment efficiency. However, large scale implementation of the integrated bioreactors is need for the industry and operation and performance of these reactors should be investigating on a larger scale [10].

Use of high rate bioreactors in anaerobic-aerobic systems tends to achieve more than 70% of COD removal within a short HRT. Hence, the hybrid treatment can be used very effectively and efficiently to treat both industrial and municipal wastewater [10]. Treating high strength industrial wastewaters using anaerobic-aerobic processes couples the benefit of anaerobic digestion by producing biogas while removing COD and volatile suspended solid (VSS) through aerobic digestion. Therefore, the anaerobic-aerobic processes are operationally and economically advantageous in the treatment of industrial wastewaters. [11].

The reason for that is when using a single system some bio degradable organic matter can be remained. Due to the additional digestion, that residual part was degraded further. It caused to destruct VS additionally in hybrid system. Although, sludge reduction was achieved using hybrid system, the problem associated that was difficulty in maintenance and construction of the anaerobic reactor. Therefore, in this research, it is decided to use UASB reactor, as construction and maintenance of UASB is easy compared with other reactors. According to past researches, it is proved that a considerable amount of heavy metals can be removed by the aerobic treatment. As an example, in 1972 six number of municipal

sewage treatment plants were monitored for the heavy metal removal efficiency using activated sludge process. Under this study, the removal efficiencies of Cd, Cr, Cu, Zn, and Pb from each plant were monitored. According to the results a high removal efficiency of Cr, Cu, and Pb were identified in secondary treatment processes than in primary processes. Chromium was highly removed during aeration in the secondary process while copper was strongly adsorbed by the microbial floc, and lead was removed more efficiently because of increased settling time and larger particle size in secondary treatment. Zn removal efficiency was high and equal from all plant types. However, the removal of Cd could not be made during this study [12].

Similarly, Cheng carried out an investigation to check whether the sludge is capable of removing soluble metal species from wastewater and the attraction of the biological mass towards the selected heavy metals. There he found that, at lower metal concentrations, metal is taken up by the biofloc through the formation of metal organic complexes. At higher metal concentrations, metal ion precipitation from solution may occur in addition to sludge uptake.

The metal uptake by the biomass also depends on several factors, including pH and the concentration of organic matter and metals present in the system. Higher initial concentrations of metal ions or sludge increase the overall uptake. In general, the uptake capacity increases with increasing pH, up to a value at which metal hydroxide precipitation occurs. Among the metals studied, the preferred order of uptake by activated sludge was found to be in the sequence of $Pb > Cu > Cd > Ni$ [13].

Metal removal in the activated sludge process was observed by Stephenson and Lester. There, the least soluble metals in the influent such as Ag, Bi, Cd, Cr, Cu, Pb, and Zn showed removal efficiency greater than 67%. The most soluble metals in the influent such as Cobalt, Mn, Mo, Ni and Tl were poorly removed at approximately 40%. All the other metals except Mn were more soluble in effluent compared to influent. In order to remove insoluble metals, in total, the total was responsible for the total removal of metals for the metals to be removed [14].



In another study carried out by Chipasa, compared the heavy metal removal efficiency in wastewater using biological wastewater treatment system [15]. At the same time he compared the heavy metal contents in undigested and digested sludge as a further study. At the end, he concluded the study as follows, the heavy metal content of copper and zinc were highly varying in the influent wastewater than the cadmium and lead. The results of the wastewater treatment system investigated by Chipasa indicate that when the contents of cadmium and lead at 0.02 and 0.05 mg/l their removal efficiency is insignificant [15]. Therefore he concluded that the heavy metal removal from wastewater is influenced by the initial contents in the influent. Hence it is certain that the heavy metal removal is directly proportional to their influent concentrations. There, he found that the heavy metal removal increased in the order of $Cd < Pb < Cu < Zn$, with respect to their initial influent wastewater contents.

According to the varying heavy metal contents the digested and undigested sludge were characterized. Due to microbial decomposition of organic and inorganic compounds and anaerobic stabilization of sludge, the heavy metal content on dry weight basis was increased. However, the order of increase in heavy metal contents in digested sludge was opposite to that in the effluent. Therefore, the order of increase is as $Zn < Cu < Pb < Cd$ with the change in positions of copper and lead [15].

Hassani A.H in 2009 studied the performance of activated sludge system in treating wastewater containing chromium, lead and nickel [16]. A three section Plexiglas tank with a downward-flow aerated reactor, an upward-flow aerated reactor and a gravity sediment unit was fed with the synthetic wastewater. There the COD removal efficiency is about 96% and the acclimation time for microorganisms is short. In the above activated sludge system at 1 mg/l concentration the removal efficiency of chromium, lead and nickel was about 84%, 75% and 80% respectively. When the concentration of them is increased up to 5 mg/l, 10 mg/l and 50 mg/l the removal efficiency of chromium, lead and Nickel were increased. Finally by rising concentration of chromium, lead and nickel up to 100 mg/l the removal efficiency became 86%, 97.6% and 97% respectively. In every stage, with the increase of heavy metal concentration of chromium, lead and nickel, COD and MLSS removal efficiency was

decreased at the beginning of period but COD and MLSS removal efficiency re-increased due to micro-organisms adapted to changes. However the increase in the later part is less than the best previous stage condition of COD removal efficiency and it showed a downward trend. That concludes the heavy metal removal in the fixed activated sludge is not simply because of a biological process but also because of some part of these compounds is removed by adsorption on sludge. Although this part is negligible in comparison with biological removal of these compounds [16].

According to the past researches, it is found that the anaerobic treatment is not much popular in heavy metal removal from wastewater since heavy metals are toxic to micro-organisms in the anaerobic process. Fang & Hui in 1994 found that the order of heavy metal inhibition due to anaerobic starch-degradation in granules is $Zn > Ni > Cu > Cr > Cd$ [17]. Due to the layered structure of the sludge granules, it had higher toxicity-resistance than flocculent sludge. According to many researcher, the methanogenic bacteria are the most sensitive anaerobes to the toxic material in the waste [18]. However, another two researches show that, some of the acid-forming bacteria were more sensitive and highly affected due to the heavy metals than the methanogens [19] [20]. In an investigation carried out by Hickey *et al.* found that some anaerobic micro-organism groups might be severely inhibited with the addition of heavy metals than the methanogenic groups [20]. Also found that acidogens were severely affected with the addition of Cu and Zn than the methanogens.

Leighton and Forster investigated the effect of Lead and Nickel on biogas production and the VFA production [21]. However, Lead and Nickel was highly influenced on biogas production while they appeared to act quickly on acidogenesis than on the methanogenic bacteria. On the other hand, Lin and Chen investigated that biogranules have high sensitivity to metal toxicity in the methanogenesis process than in the acidogenesis process [18].

According to the above discussed past research facts, it is clear that the combination of anaerobic and aerobic process will be more effective when removing heavy metals from wastewater. Therefore, the objectives of this research are to study whether the hybrid

reactor is feasible in removing heavy metals from wastewater and the removal efficiencies.

3. Materials and Method

3.1 Experimental setup of the hybrid system

The experiment was conducted in the laboratory scale. The hybrid system was constructed by combining the aerobic treatment system with the UASB reactor. UASB reactor worked as a pre-treatment for aerobic system.

The UASB reactor has a working volume of 8.5L (height: 110 cm with 10 cm diameter). The reactor body was made using cylindrical Perspex pipes. The bottom of the reactor was filled up to 2 L level with anaerobic granular sludge obtained from a full-scale UASB reactor in Elephant house beverage and ice-cream company, Ranala, Sri Lanka. Anaerobic sludge granules had total and volatile solids concentrations of 26 g/L and 20 g/L respectively.

Aerobic system was constructed using an aeration tank (20L) and a sedimentation tank (13L). Aerobic treatment was initiated by introducing 100 ml of activated sludge into the aeration tank which was obtained from Hemas southern hospital wastewater plant, Galle, Sri Lanka.

A simplified flow sheet of lab scale model of hybrid system was shown in Figure 1.

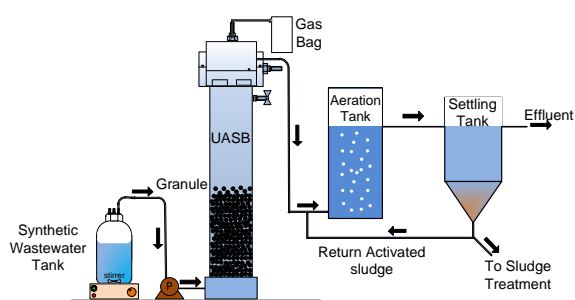


Figure 1 - Experimental set up of the hybrid system

3.2 Synthetic wastewater

Synthetic wastewater was prepared using milk powder as the main substrate. Table 1 shows the composition of synthetic wastewater.

Table 1 - Composition of synthetic wastewater

Chemical	Concentration (mg/L)
Milk powder	1000
Sucrose	300
Ammonium chloride (NH ₄ Cl)	30
Magnesium sulphate(MgSO ₄ .7H ₂ O)	150
Ferric chloride (FeCl ₃ .6H ₂ O)	1.5
Calcium chloride (CaCl ₂ .2H ₂ O)	25
Manganus sulphate (MnSO ₄)	0.1
Copper sulphate (CuSO ₄)	0.1
Sodium bicarbonate (NaHCO ₃)	200
KH ₂ PO ₄	5

3.3 System operation

Hybrid reactor was operated over 110 days. The methodology followed is in the flow chart shown in figure 2. Hybrid reactor was fed with synthetic wastewater and operated at 20 ml/min flow rate. Synthetic wastewater was introduced from the bottom valve of the UASB reactor using a peristaltic pump. To control the fluctuation of pH in the UASB reactor sodium bicarbonate was added to the wastewater. First, the reactor was operated without introducing any heavy metal.

According to the literature review it was found that the Cu, Cd, Zn and Pb are the most common heavy metals in municipal wastewater. Therefore by considering the maximum and minimum concentrations available on those wastewaters and the maximum tolerance limit that can be discharged in to the inland water surfaces, three concentrations were selected for each heavy metal as shown in table 2 and the treatment was started. Each heavy metal concentration was treated for a period of one week. After treating all the three concentrations of one heavy metal, the system was once again fed with synthetic wastewater without any heavy metal and operated for one week. This was done every time before adding a new heavy metal to the wastewater.



Table 2 - Heavy metal concentration used for synthetic wastewater

Heavy metal	Heavy metal concentration (mg/l)		
	Lead (Pb)	0.1	0.25
Zinc (Zn)	1	2	3
Cadmium (Cd)	0.1	0.25	0.5
Copper (Cu)	0.5	1	1.5

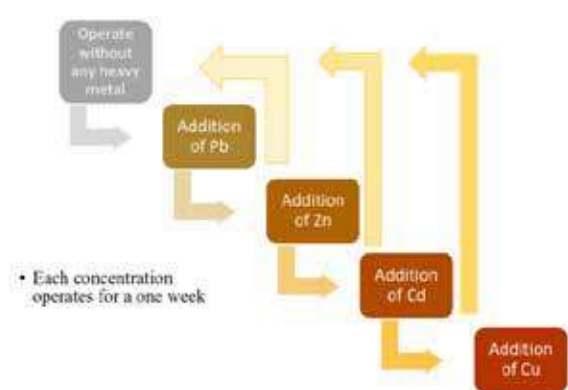


Figure 2 - Operational procedure of the system

3.4 Analysis

Table 3 and Table 4 shows the measured parameters and measurement methods, respectively.

Table 3 - Measured parameter

Parameter	Influent	Effluent	Reactor	Sludge
COD	√	√		
pH	√	√	√	
Temperature			√	
Heavy metal concentration	√	√		
Sludge Volume				√

Table 4 - Measurement methods

Parameter	Method/Apparatus
COD	Portable spectrophotometer
pH	pH meter
Temperature	Thermometer
Heavy metal concentration	Graphite furnace atomic absorption spectrometer
Sludge Volume	Settleable solid using imhoff cone

4. Results and Discussion

Hybrid system was operated over 110 days at 7 HRT and at ambient temperature. Reactor performance was observed by measuring COD, pH, temperature, heavy metal concentration and sludge volume to check whether the anaerobic-aerobic treatment was occurred within the hybrid reactor.

pH and temperature inside the UASB reactor during the operating period is shown in Figure 3. pH was maintaining within the range of 5.8 – 7. The temperature was above 30°C.

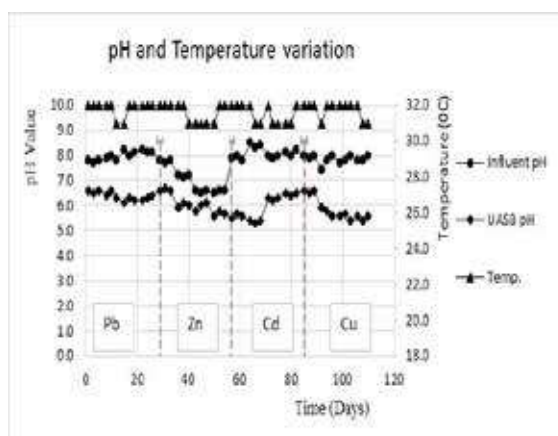


Figure 3 - pH value inside the UASB reactor

4.1 Reactor performance

The influent T-COD concentration and effluent T-COD concentration of hybrid system were measured. The average T-COD concentration of the influent was 1631 ± 92 mg-COD/L. The average COD removal efficiency and the sludge volume of the synthetic wastewater without adding any

heavy metal was around 94% and 38 ml respectively

4.1.1 Lead (Pb) removal

The COD removal efficiency of lead introduced wastewater was around 90% and sludge production also reduced with the increase of influent Pb concentration. However above 80% Pb removal efficiency was obtained from the hybrid reactor. Heavy metal removal efficiency has increased with the influent concentration.

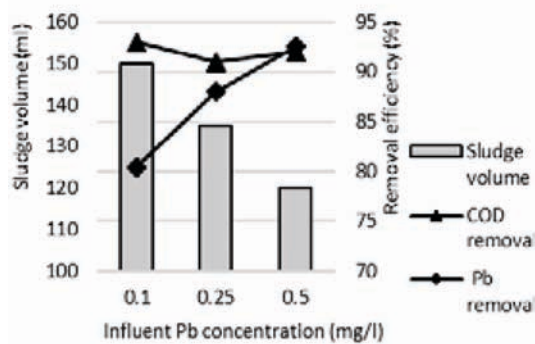


Figure 4 - COD removal efficiency, heavy metal removal efficiency and the sludge volume for the wastewater containing Pb

4.1.2 Zinc (Zn) removal

Around 90% COD removal efficiency was obtained for the Zinc introduced wastewater. However, the sludge volume has increased due to the reduction of treatment from UASB due to toxicity of Zinc for anaerobic sludge granules. Above 90% Zn removal efficiency was obtained from the hybrid reactor.

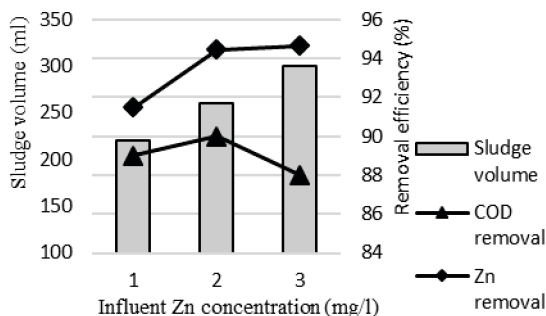


Figure 5 - COD removal efficiency, heavy metal removal efficiency and the sludge volume for the wastewater containing Zn

4.1.3 Cadmium (Cd) removal

Cadmium (Cd) was introduced to the wastewater in 0.1 mg/l, 0.25 mg/l, and 0.5 mg/l concentrations. The COD removal also

above 80% and sludge volume produced has also decreased with the increase of influent Cd concentration. The removal efficiency of Cd is less compared to other heavy metals because of its high solubility. However above 75% removal efficiency was obtained.

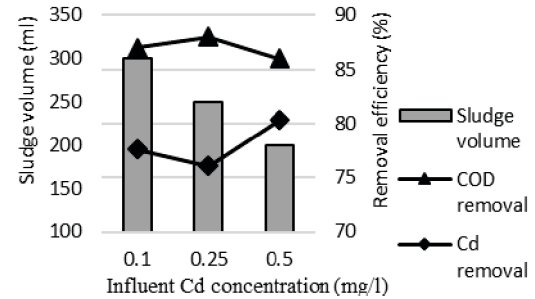


Figure 6- COD removal efficiency, heavy metal removal efficiency and the sludge volume for the wastewater containing Cd

4.1.4 Copper (Cu) removal

When Copper (Cu) was introduced to the wastewater in 0.5 mg/l, 1 mg/l, and 1.5 mg/l concentrations, the COD removal efficiency has been affected with the addition of Copper to the influent and the efficiency of removal has decreased. This is because of the reduction of treatment from UASB reactor. Therefore, the sludge volume is also high compared to other cases. However above 80% Cu removal efficiency was obtained from the hybrid reactor.

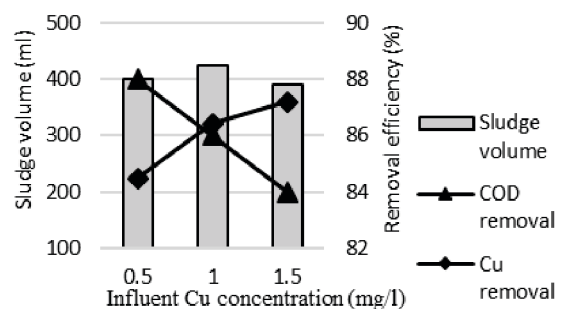


Figure 7- COD removal efficiency, heavy metal removal efficiency and the sludge volume for the wastewater containing Cu

Although there were no past researches have conducted on the heavy metal removal from UASB reactor, a comparison or a range for removal efficiencies cannot be shown. However the study carried out by Hawari & Mulligan in



2006 shows that the feasibility of anaerobic granules as a novel type of biosorbent, for lead, copper, cadmium, and nickel removal from aqueous solutions. Therefore, it can conclude that the anaerobic sludge granule used in the UASB reactor was able to remove heavy metals by the biosorption process. However more than 60% removal efficiency was obtained from the UASB reactor for all the heavy metals.

According to the literature review done on the removal efficiencies of Pb, Zn, Cd and Cu from activated sludge process it was found that the high heavy metal removal efficiency for Zinc was obtained due to the microbial floc produced in the activated sludge process efficiently adsorbed zinc in both the soluble form and in the finely-divided suspended particles. An experiment done by Brown *et al* in 1973 found that the removal efficiency of zinc when the influent concentration within 2.5 mg/l -20 mg/l is 95% - 74%. Stephenson & Lester in 1987 found that the removal efficiency of Zinc from activated sludge process is above 67%. According to Brown *et al* (1973), the overall lead removal efficiency varies within 33%-55%, Cadmium removal is around 25% and the Copper removal is round 63%. Copper is mainly adsorbed by the microbial floc, and lead is removed more efficiently because of increased settling time and larger particle size. These values are also tally with the research done by Chipasa in 2003, he found that the order of removal efficiency of Pb, Zn, Cd and Cu from wastewater is Cd<Pb<Cu<Zn. The removal efficiencies obtained from the ASP during this reasearch also tally with the above values.

Considering above facts the removal efficiencies of Pb, Zn, Cd and Cu obtained from the hybrid reactor can be acceptable.

5. Conclusions

The subject of this paper is the feasibility of hybrid reactor for removal of heavy metals from wastewater. Hybrid reactor is the combination of UASB reactor (Anaerobic) and the activated sludge process (Aerobic). The reactor was operated over 110 days by maintain a flow rate of 20 ml/min where HRT of UASB reactor is 7 hrs at ambient temperature of 32°C. Results showed that the T-COD removal is above 84% for all the heavy metals introduced wastewaters and more than 80% removal efficiency of Lead (Pb) and Copper (Cu). More than 75% removal efficiency of Cadmium (Cd) and more than 90% removal

efficiency of Zinc (Zn) from synthetic wastewater. From the above removal efficiencies, it can conclude that the reduction of heavy metal contents has increased in the order of Cd<Cu<Pb<Zn.

This study can be carried out further to investigate the technical feasibility of hybrid reactor for removal of heavy metals in actual wastewater because in the real case the heavy metals presence in the wastewater not limited to Pb, Zn, Cd and Cu. The heavy metal content in sludge is higher than that of the effluent. Although the sludge produced from the wastewater without heavy metals is much lower, with the heavy metal introduced wastewater the sludge volume has increased. Therefore a further investigation can be carried out to minimize the sludge production in the wastewater with heavy metals by changing reactor conditions, flow rate and the anaerobic sludge granule and activated sludge amount added to the UASB and ASP.

References

1. Srivastava, N. K. & Majumder, C. B., 2008. Novel biofiltration methods for the treatment of heavy metals. *Journal of Hazardous Materials*, Volume 151, pp. 1-8.
2. Dhokpande, S. R. & Kaware, J. P., 2013. Biological Methods for Heavy Metal Removal- A Review. *International Journal of Engineering Science and Innovative Technology (IJESIT)*, 2(5), pp. 304-309.
3. Oyaro, N., Juddy, O., Murago, E. M. & Gitonga, E., 2007. The contents of Pb, Cu, Zn and Cd in meat in Nairobi, Kenya. *Journal of Food, Agriculture & Environment*, 5(3,4), pp. 119-121.
4. Fu, F. & Wang, Q., 2011. Removal of heavy metal ions from wastewaters: A review. *Journal of Environmental Management*, Volume 92, pp. 407-418.
5. Ahmaruzzaman, M., 2011. Industrial wastes as low-cost potential adsorbents for the treatment of wastewater. *Advances in Colloid and Interface Science*, Volume 166, pp. 36-59.
6. Leitao, R. C., Haandel, A. V., Zeeman, G. & Lettinga, G., 2006. The effects of operational and environmental variations on anaerobic wastewater treatment systems: A review. *Bioresource Technology*, Volume 97, p. 1105-1118.

7. Metcalf & Eddy, 2003, wastewater engineering: Treatment and reuse. 4th ed., MacGraw hill companies, china.
8. Castillo, A., Cecchi, F. & Mata-alvarez, J., 1997. A combined anaerobic-aerobic system to treat domestic sewage in coastal areas. *water research*, 31(12), pp. 305-306.
9. Kassam, Z. A., Yerushalmi, L. & Guiot, S. R., 2003. A market study on the anaerobic wastewater treatment systems. *Water, Air, and Soil Pollution* 143, p. 179-192.
10. Chan, Y. J., Chong, M. F., Law, C. L. & Hassell, D. G., 2009. A review on anaerobic-aerobic treatment of industrial and municipal wastewater. *Chemical Engineering Journal*, Volume 155, pp. 1-18.
11. Ros, M. & Zupancic, G. D., 2004. Two-Stage Thermophilic Anaerobic-Aerobic Digestion of. *Environmental engineering science*, 21(5), pp. 617-626.
12. Brown, H. G., Hensley, C. P., McKinney, G. L. & Robinson, J. L., 1973. Efficiency of heavy metals removal in municipal sewage treatment plants. *Environmental letters*, 5(2), pp. 103-114.
13. Cheng, M. H., Patterson, J. W. & Minear, R. A., 1975. Heavy metals uptake by activated sludge. *Water Pollution Control Federation*, 47(2), pp. 362-376.
14. Stephenson, T. & Lester, J. N., 1987. Heavy metal behaviour during the activated sludge process- extent of soluble and insoluble metal removal. *The science of the total environment*, Volume 63, pp. 199-214.
15. Chipasa, K., 2003. Accumulation and fate of selected heavy metals in a biological. *Waste Management*, Volume 23, p. 135-143.
16. Hassani, A. H., Hossenzadeh, I. & Torabifar, B., 2010. Investigation of Using Fixed Activated Sludge System for Removing Heavy Metals (Cr, Ni and Pb) From Industrial Waste Water. *Journal of Environmental Studies*, 36(53), pp. 22-24.
17. Fang, H. P. & Hui, H. H., 1994. 'Effect of heavy metals on the methanogenic activity of starch-degrading granules', *Biotechnology letters*, 16(10), pp. 1091-1096.
18. Lin, C. Y. & Chen, C. C., 1999. Effect of heavy metals on the methanogenic UASB granule. *Wat. Res.*, 33(2), pp. 409-416.
19. Hickey, R. F., Vanderwielen, J. & Switzenbaum, M. S., 1989. The effect of heavy metals on methane production and hydrogen and carbon monoxide levels during batch anaerobic sludge digestion. *water research*, 23(2), pp. 207-218.
20. Lin, C. Y., 1993. Effect of heavy metals on acidogenesis in anaerobic digestion. *Water research*, 27(1), pp. 147-152.
21. Leighton, I. R. & Forster, C. F., 1998. The effect of heavy metals on a thermophilic methanogenic upflow sludge blanket reactor. *Bioresource Technology*, Volume 63, pp. 131-137.



Feasibility of UASB Reactor for Removal of Heavy Metal in Wastewater

U.L.N.C. Jayathileke and W.M.K.R.T.W. Bandara

Abstract: Even though there are many ways to remove heavy metals in wastewater, most of them are not cost effective and have many drawbacks. The feasibility of the Up-flow Anaerobic Sludge Blanket (UASB) reactor, for the removal of heavy metals, were studied through this research. A lab-scale reactor was operated for 110 days with synthetic wastewater influent and HRT of 7 hours. Pb, Zn, Cd and Cu were added to the influent to 4 different concentrations and one heavy metal at a time. The parameters analyzed in the treatment was COD, Biogas production rate, pH, temperature, heavy metal concentrations. The results show that Zn and Cd shows a toxic effect for the wastewater treatment, and Cu and Pb are not toxic. However heavy metal removal efficiency of more than 60% was achieved for each heavy metal. Therefore the UASB reactor is feasible for the removing of heavy metals from the UASB reactor.

Keywords: Biogas, COD removal, Heavy metal removal, HRT, Sludge granules, UASB reactor

1. Introduction

Environment contamination with toxic heavy metals has become one of the major concern for humankind in the current era of globalization and rapid industrialization. Discharge of heavy metal contaminated wastewater causes the accumulation of heavy metals to the water bodies, soil and crops. Heavy metals are naturally occurring substances that have a high atomic weight and a density at least 5 times greater than that of water [1].

Through the circulation of heavy metals from wastewater discharge to water bodies, soil and crops, finally, it can be consumed by the animals and humans. Through that, there are many toxic effects to the human and animal health through heavy metal consumption like Skin manifestations, visceral cancers, vascular disease Kidney damage, renal disorder etc. [2]. According to above description, heavy metal removal from wastewater has become a major concern in the present world. Therefore this study focuses on two objectives. The first objective is to identify whether the Up-flow Anaerobic Sludge Blanket (UASB) reactor is feasible for the removal of heavy metals and if feasible the removal efficiencies that can be obtained. The second objective is to identify the effect of heavy metals on UASB reactor treatment process.

2. Literature Review

In the present era, there are many methods used for heavy metal removal such as Ion exchange, Membrane filtration, Coagulation

and flocculation [3]. However, there are many drawbacks from these metals such as high capital cost, high maintenance cost, high operation cost, high usage of chemicals and high sludge production [4].

Therefore new methods with less cost and less sludge production are required. Such as anaerobic digestion. Anaerobic digesters are commonly used at municipal wastewater treatment plants to degrade sludge, which uses suspended bacterial growth. Most of the industrial wastewater treatment plants are using anaerobic digesters with the development of anaerobic digesters, having fixed-film bacterial growth. Anaerobic digesters use a method called catabolic (destructive) processes, which occur in the absence of free molecular oxygen (O_2). The process of anaerobic digestion involves biologically destroying a significant portion of the volatile solids in sludge, and to minimize the volume of sludge. The main products from anaerobic digesters are biogas and digested sludge. Biogas contains methane (CH_4) and carbon dioxide (CO_2) mostly. This involves four processes called Hydrolysis, Acidogenesis, Acetogenesis and Methanogenesis [5].

U.L.N.C. Jayathileke, B.Sc. Eng. (Ruhuna), Civil Engineer, Road Development Authority (RDA).

Dr. W.M.K.R.T.W. Bandara, Ph.D. (Hokkaido-Japan), M.Sc (Hokkaido-Japan), B.Sc. Eng. (Peradeniya, Senior Lecturer, Department of Civil and Environmental Engineering, Faculty of Engineering, University of Ruhuna..



UASB reactor is an attractive anaerobic treatment method because of its compactness, low operational cost, low sludge production, and production of biogas [6]. In the late 1970's the UASB reactor was developed by Dr. Gatzke Lettinga and his colleagues [7]. The UASB reactor has been used increasingly in recent years, to treat a variety of industrial wastes and municipal wastes. The treatment occurs with exposure to microorganisms in the granule to wastewater- substrates. All biological processes are taken place within the sludge bed, and the production of biogas occurs. The accumulation of incoming suspended solids and bacterial growth forms the sludge bed. Retention of active sludge within the UASB reactor facilitates good treatment performance at high organic loading rates [8].

Although most of the researchers have focused on the toxic effect of heavy metals on the anaerobic digestion [9] [10]. , there are some researchers who have focused on the removal of heavy metal using the anaerobic treatment methods .

Haytoglu studied the effectiveness of the anaerobic biomass in adsorbing heavy metals. This study focused on five heavy metals which are Pb, Cr, Cu, Ni and Zn [11]. The biomass used for the study were grown under the laboratory conditions using a synthetic wastewater composition. The adsorption capacity was measured for the anaerobic dead biomass. The maximum adsorptive capacity for the biomass for Pb, Zn, Cu, Ni and Cr were found as 1250, 625, 357, 227, and 384 mg/g dry biomass.

Packed Bed Biofilm Reactor (PBBR) is an anaerobic reactor used for wastewater treatment. Research carried out on this reactor was focused on the removal of Zn, Cd, Cu and Ni [12]. The heavy metals were injected to the influent, and then the removal efficiencies were checked. The higher removal efficiency was achieved when the influent heavy metal concentration was at 8 and 20 mg/l. The removal efficiency was higher than 71%. At the 28 and 40 mg/l, the removal efficiencies were reduced. The removal efficiencies were in the order of Cu>Zn>Ni>Cd. Also, a BOD removal of 90 % was achieved.

Removal of Cu, Cd, Pb and Zn were studied in an up-flow anaerobic packed bed reactor which was filled with porous volcanic rock to act as an

adsorbent. Two types of wastewater were used. One is high strength wastewater with 5mg/l of heavy metals from each and other is low strength wastewater with 10mg/l of heavy metals from each. For both, the cases good removal efficiencies of 86% were achieved. The order of heavy metal removal efficiencies was Cu>Pb>Cd>Zn [13]

However, the feasibility of the UASB reactor for the removal of heavy metals has not been taken into consideration. Therefore the objective of this study is to identify whether the UASB reactor is feasible for the removal of heavy metals and to identify the removal efficiencies. Also, the effect on wastewater treatment process by heavy metals are considered through this study.

3. Materials and Method

3.1 Setup of the UASB reactor

A lab-scale UASB reactor with a height 110 cm; diameter 10 cm; working volume 8.5 L was used for this study. Reactor body is made with cylindrical Perspex pipes. PVC conical shaped funnel with a valve is connected to the bottom of the reactor. The reason to use conical shape is to make the uniform flow throughout the reactor. The top part of the reactor is designed to collect gases that emit during anaerobic reactions and to collect treated wastewater.

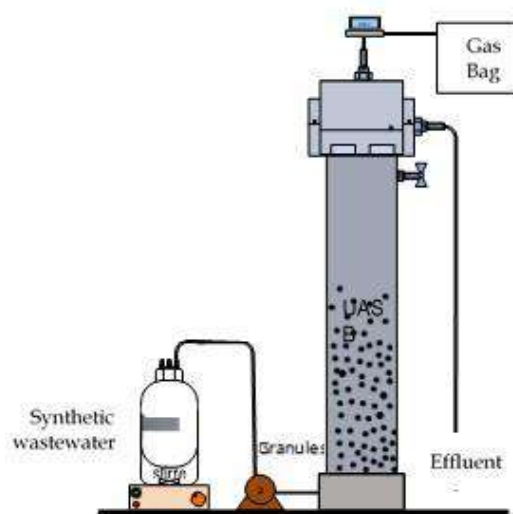


Figure 1 - Experimental setup of UASB reactor

Six valves were connected to the reactor at different places. Bottom valve is used to introduce wastewater into the reactor. Three valves were connected at the body of the reactor to collect a sample that is taken from inside the reactor. Top two valves are used to collect treated wastewater and headspace gases. The Synthetic wastewater is fed to the reactor using a mini pump from a PVC storage tank. A Cross-sectional view of lab scale UASB reactor is shown in Figure 1.

A synthetic wastewater composition was used as the influent to the reactor. First, a baseline was established for the performance of the reactor by running the reactor without adding any heavy metals. Then the four heavy metals Pb, Zn, Cd and Cu were added to the influent, as one heavy metal at a time in 3 different concentrations and the reactor was operated at 7 HRT. The influent and Effluent wastewater samples were collected to test the parameters mentioned in Table 2.

3.2 Synthetic wastewater

For the study, a milk powder based wastewater composition was prepared using the chemicals stated in table 1.

Table 1 - Composition of synthetic wastewater

Chemical	Concentration (mg/L)
Milk powder	1000
Sucrose	300
Ammonium chloride (NH ₄ Cl)	30
Magnesium sulphate (MgSO ₄ .7H ₂ O)	150
Ferric chloride (FeCl ₃ .6H ₂ O)	1.5
Calcium chloride (CaCl ₂ .2H ₂ O)	25
Mangenus sulphate (MnSO ₄)	0.1
Sodium bicarbonate (NaHCO ₃)	200
Monopotassium phosphate (KH ₂ PO ₄)	5

3.3 System operation

The reactor body was filled with 2l of granular sludge (which were taken from the

UASB reactor at Ranala Elephant house Ice-cream factory) blanket. After that system was commenced by introducing water for few days. Then synthetic wastewater was fed from the bottom of the UASB reactor. without heavy metals for a selected flow rate of 20ml/min, considering an HRT value of 7 hrs. As the wastewater flows upward through the granular sludge and with contact of sludge blanket the treatment occurred. Also, the gas produced from the treatment were collected from the top valve of the reactor. The heavy metals selected for testing of the feasibility of UASB reactor are as follows.

- I. Lead (Pb)
- II. Zinc (Pb)
- III. Cadmium (Cd)
- IV. Copper (Cu)

Then by introducing one heavy metal at a time, the system was run for treatment, and the required parameters were checked. For different concentrations of heavy metals using the HRT as 7hr, the removal of heavy metals and the effect of the reactions of the UASB were checked. The overall methodology is shown in Figure 2.

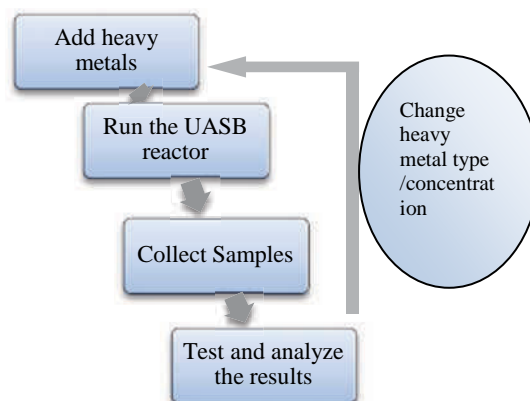


Figure 2 - Overall Methodology

3.4 Experiment

Table 2 and Table 3 shows the measured parameters and measurement methods, respectively.



Table 2 - Measured parameter

Parameter	Influent	Effluent	Reactor	Gas outlet
COD	√	√		
pH	√	√	√	
Temperature			√	
Headspace gas				√
Gas Composition				√
Heavy Metal Concentration	√	√		

Table 3 - Measurement methods

Parameter	Method/Apparatus
COD	Portable Spectrophotometer
pH	pH meter
Temperature	Thermometer
Headspace gas volume	Water replacement method
Gas Composition	Gas chromatograph
Heavy metal concentration	Atomic absorption spectrophotometer

4. Results and Discussion

4.1 pH and temperature

For the treatment in UASB reactor, three types of bacteria are involved, which were hydrolysis, acid-producing bacteria, and methane-producing bacteria. Therefore, due to acid-forming bacteria and the methane-producing bacteria the pH value should be in a range of 6 to 8. Otherwise, there can be less treatment from the bacteria performances. When considering the pH values inside the UASB within the operational period, it is at an acceptable level as per the figure 3. In general, the most of the anaerobic wastewater treatment processes are operated within the mesophilic temperature range which is 30°C - 40°C or in the thermophilic temperature range which is 45°C - 60°C. The temperature is within the mesophilic temperature range which is acceptable.

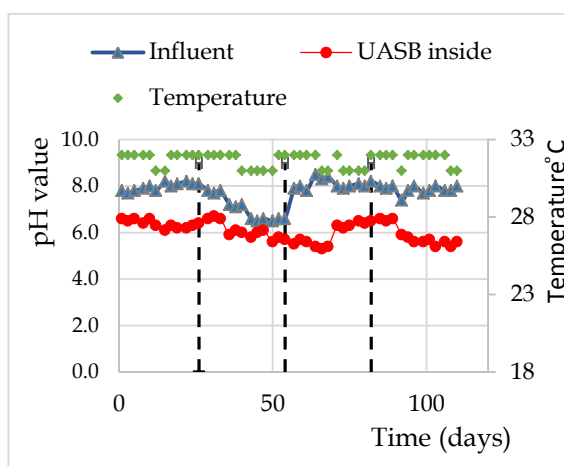


Figure 3 - pH and temperature variation

4.2 Pb removal

For the treatment of Pb introduced wastewater, Pb was added to wastewater in 3 concentrations which are 0.1 mg/l, 0.25 mg/l and 0.5 mg/l. These values were selected after considering the Pb concentration in domestic wastewater in Asia.

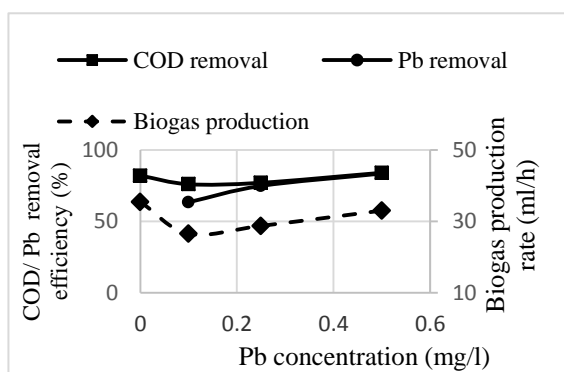


Figure 4 - Pb Introduced wastewater

As for the figure 4, the COD removal efficiencies and the biogas production have increased with the increase of Pb concentrations in the influent wastewater. Therefore, the adsorbent of the Pb into the granules has enhanced the performances of the granules. Also, the Pb removal is between 63% - 83%.

This matches with the fact that the presence of heavy metals enhances the biogas production in UASB, as studied by Nkemka & Murto [14]. Also, the enhanced performances have increased the adsorption capacity of the granules as the Pb removal efficiencies also have increased.

4.3 Zn removal

For the treatment of Zn introduced wastewater the Zn was added to wastewater in 3 concentrations which are 1 mg/l, 2 mg/l, and 3 mg/l (These values were selected after considering the Zn concentration in domestic wastewater in Asia). As for the Figure 5, Zn removal efficiency between 68% -74% were achieved (figure 5). With the increase in the Zn concentration, the COD removal efficiency and biogas production have reduced. One of the reasons for this might be because of the high concentrations of Zn than other heavy metals. Also, Atlas has found from his studies, that the methane production ability is reduced when the Zn is present [9]. Therefore, this is a reason for the reduction in biogas production and the COD removal. However anaerobic dead biomass has a high adsorption capacity of Zn after the Pb adsorption [11]. Therefore, it explains the increase in the Zn removal efficiencies although the COD removal decreased. So, the Zn is toxic for the reactions in the sludge granules.

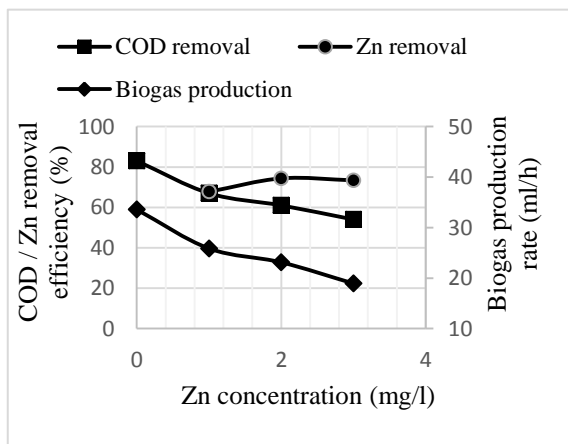


Figure 5 - Zn Introduced wastewater

4.4 Cd removal

For the treatment of Cd introduced wastewater the Cd was added to wastewater in 3 concentrations which are 0.1, 0.25 and 0.5mg/l (These values were selected after considering the Cd concentration in domestic wastewater in Asia). As for the Figure 6, COD removal efficiencies and the biogas production have increased and then decreased with Cd concentrations. A removal efficiency of 61-71% was achieved.

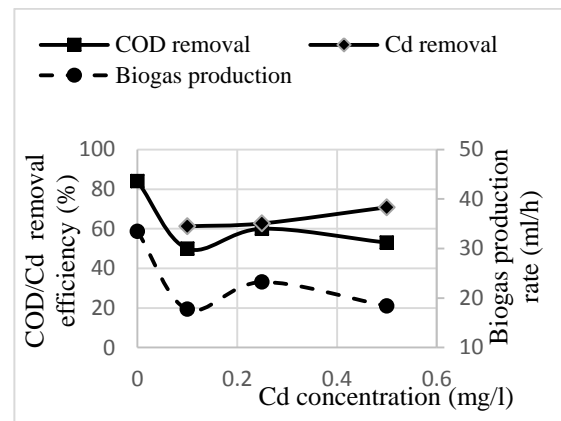


Figure 6 - Cd Introduced wastewater

The COD removal efficiencies and the biogas production have gained a peak value at 0.25mg/l concentration of Cd. Therefore, after that concentration the Cd it is toxic for the anaerobic digestion process. However, the Cd removal has increased further with the increase of Cd concentration. This may be due to the inorganic precipitation of Cd with increased Cd concentrations [15].

4.5 Cu removal

For the treatment of Cu introduced wastewater the Cu was added to wastewater in 3 concentrations which are 0.5 mg/l, 1 mg/l, and 1.5 mg/l (These values were selected after considering the Cu concentration in domestic wastewater in Asia). A Cu removal efficiency between 61% - 68% was achieved. For the COD removal (figure 7) and biogas production, there is no significant variation with an increase of Cu concentrations. Therefore, the increase in Cu concentrations has not affected the anaerobic digestion which indicates Cu is not toxic. Also for the Cu removal the efficiency there is no significant variations. Therefore' this Cu removal efficiency and COD removal efficiency can be enhanced with the change of the HRT. Also in the other anaerobic treatment methods, Cu has a high removal efficiency [11] [12]. However, when considering the observations done during the Cu treatment, the sludge granules started to float at the final concentration without settling at the bottom. As for Nnaji, large granules tend to possess a polymeric coat which traps evolved gases and thus make the granules fluffy [16]. The larger the granules, the more difficult it becomes for the substrate to diffuse into the core of the granule, hence reducing the rate of bioconversion. Therefore, this might be the reason for the no change is the COD removal and the Cu removal efficiencies.



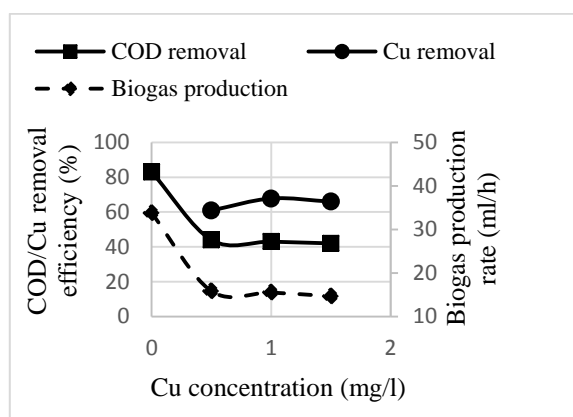


Figure 7 - Cu Introduced wastewater

5. Conclusions

With reference to the main objective of this study the UASB reactor is feasible for removing heavy metals. The removal efficiencies are different based on the heavy metal type and the concentrations. For Pb, the efficiencies were between 63% - 83%. For Zn, the removal efficiencies were between the 68% -74%. On the other hand, for Cd, the removal efficiencies were between 61-71% for the concentrations of 0.1, 0.25 and 0.5 mg/l. Finally, for Cu, the removal efficiencies were between 61% - 68%. The other objective of this research was to identify whether there is an effect on the wastewater treatment parameters from the heavy metals. Therefore, from the results, it can be concluded that the COD removal has enhanced by the increased Pb concentrations. However, there is a negative effect on the COD removal by the Cd and Zn. However, the effect is more significant when it comes to Cu. However, in each case at least 50% removal efficiencies can be achieved. This study can be developed considering the removal efficiencies of heavy metals when there is more than one heavy metal in influent wastewater and for different HRT values for better analysis.

References

1. Tchounwou, P. B., Yedjou, C. G., Patlolla, K. A. & Sutton, D. J., n.d., 'Heavy Metal Toxicity and the Environment', In: A. Luch (ed.), *Molecular, Clinical and Environmental Toxicology*, s.l.:Birkhäuser Basel, pp. 133-164.
2. Gunatilake, S., 2015, 'Methods of Removing Heavy Metals from Industrial Wastewater', *Journal of Multidisciplinary Engineering Science Studies (JMESS)*, 1, pp. 12-18.
3. Dhokpande, S. R. & Kaware, D. J. P., 2013, 'Biological Methods for Heavy Metal Removal', *International Journal of Engineering Science and Innovative Technology (IJESIT)*, 2(5), pp. 304-309.
4. Fu, F. & Wang, Q., 2011, 'Removal of Heavy Metal ions from Wastewaters: A Review', *Journal of Environmental Management*, 92, pp. 407-418.
5. Gerardi, M. H., 2003, *The Microbiology of Anaerobic Digesters*. s.l.: A John Wiley & Sons, Inc., Publication.
6. Mudhoo, A. & Kumar, S., 2013, 'Effects of Heavy Metals as Stress Factors on Anaerobic Digestion Processes and Biogas Production from Biomass', *Int. J. Environ. Sci. Technol.*, 10, pp. 1383-1398.
7. Bandara, W. M. K. R. T. W. et al., 2013. Introduction of a Degassing Membrane Technology into Anaerobic Wastewater Treatment. *Water Environment Research*, 85(5), pp.387-390.
8. Karthikeyan, K. & Kandasamy, J., 2009, 'Upflow Anaerobic Sludge Blanket (UASB) Reactor in Wastewater Treatment', *Water and wastewater treatment technologies*, 2, pp. 180-198.
9. Altas, L., 2008, 'Inhibitory Effect of Heavy Metals on Methane-Producing Anaerobic Granular Sludge', *Journal of Hazardous Materials*, pp. 1551-1556.
10. Azizi, S., Kamika, I. & Tekere, M., 2016, 'Evaluation of Heavy Metal Removal from Wastewater in a Modified Packed Bed Biofilm Reactor', *PLoS ONE*, 11(5).
11. Haytöglu, B., Demirer, G. & Yetis, U., 2001., 'Effectiveness of Anaerobic Biomass Adsorbing Heavy Metals', *Water Science and Technology*, 44(10), pp. 245-252.
12. Azizi, S., Kamika, I. & Tekere, M., 2016, 'Evaluation of Heavy Metal Removal from Wastewater in a Modified Packed Bed Biofilm Reactor', *PLoS ONE*, 11(5).
13. Sekomo, C., Kagisha, V., Rousseau, D. & Lens, P., 2012, 'Heavy Metal Removal by Combining Anaerobic upflow Packed Bed Reactors with Water Hyacinth Ponds', *Environmental Technology*, 33(12), pp. 1455-1464
14. Nkemka, V.N. & Murto, M., 2010, 'Evaluation of Biogas Production from Seaweed in Batch Tests and in UASB Reactors Combined with

the Removal of Heavy Metals', *Journal of Environmental Management*, 91, pp. 1573-1579.

15. Cheng, H., Patterson, J. & Minear, R., 1975, 'Heavy Metals Uptake by Activated Sludge', *Water Pollution Control Federation*, 47(2), pp. 362-376.
16. Nnaji, C. C., 2013, 'A Review of the upflow Anaerobic Sludge Blanket Reactor', *Desalination and Water Treatment*.



GIS-Based Site Suitability Analysis for Wastewater Treatment Plants

N.A. Nusky, S.I.S. Wijesingha, W.M.K.R.T.W. Bandara, B.M.L.A. Basanayake and Terrance M. Rengarasu

Abstract: Identifying a site for domestic wastewater treatment plant involves a comprehensive assessment to identify the best obtainable location(s) or site(s) that can simultaneously meet the requirements of minimise economic and regulations, health, environmental and social costs. While GIS has been a powerful tool to handle spatial data in site suitability analysis, application of this tool alone could not overcome the issue of unpredictability in expert opinion when trying to judge and assign relative importance to each of many criteria considered in a site suitability analysis. To overcome this issue, the Analytical Hierarchy Process method is used in combination with the GIS tools. This manuscript presents how the integrated tool has used effectively in the site suitability analysis for Unawatuna tourist area and Puttalam Municipal Council which considered simultaneously 8 different sub-criteria under 3 different main criteria such as soil texture, topography, surface water, groundwater, land use, residential area and roads.

Keywords: GIS, Treatment Plant, Site Suitability Analysis, Wastewater

1. Introduction

Wastewater has been defined as the water discharged from a community after it has been contaminated by various wastes. In the wastewater, 99% is water, and only 1% is solid waste. Wastewater is generated from domestic, industrial, agricultural sources and surface run-off due to rain. Eventually, it goes down to the drainage and ends up in wastewater treatment facility. Usually, surface water needs more filtration and treatment than the groundwater because rivers, streams and lakes contain more pollutants and sediments and are more vulnerable to be contaminated than groundwater. Some water supplies may also contain organic chemicals, disinfection by-products and inorganic chemicals.

Municipal domestic wastewater can be defined as wastewater from residential settlements and services which originates primarily from the domestic activities the human metabolism. It provides an essential community service that is vital for the protection of the environment and public health. The domestic wastewater treatment plant undergoes physical, chemical and biological processes for cleaning the wastewater and separate the solids. The treated wastewater can be used for irrigation of food crops. In addition, the nutrients in the wastewater can be recovered and provided to the water bodies. This gives benefits for

protecting public health from hotel wastewater and eliminates or reduces the migration of wastewater pollutants to the water bodies. Hence, it is necessary to take effective steps toward achievement of environmental goals of sustainability through developing treatment plants in suitable sites. But finding a suitable site for this purpose involves considering a wide range of criteria which makes decision-making complicated.

The principles of sustainable development of wastewater treatment make site suitability analysis more and more complex due to the concern of multiple criteria. It includes attention not only essential capacity of a land unit to support a particular land use for a long period of time without deterioration, but also environmental and the socio-economic feasibility.

N.A. Nusky, B.Sc. Eng. (Ruhuna), Planning Engineer, Sierra Construction Pvt Ltd, Colombo.

S.I.S. Wijesingha, B.Sc. Eng. (Ruhuna), Civil Engineer, Navaloka Construction Company Pvt Ltd.

Dr. W. M. K. R. T. W. Bandara, Senior Lecturer, Department of Civil and Environmental Engineering, Faculty of Engineering, University of Ruhuna.

B.M.L.A. Basanayake, Senior Lecturer, Department of Civil and Environmental Engineering, Faculty of Engineering, University of Ruhuna.

Dr. Terrance M. Rengarasu, Senior Lecturer, Department of Civil and Environmental Engineering, Faculty of Engineering, University of Ruhuna.



Therefore, when selecting appropriate site selection, the technical, social, environmental aspects need to be considered as main criteria during analysis. The criteria influencing the site selection were mainly determined by temperature, wind direction and speed, rainfall soil, topography, groundwater, surface waters, land use, residential area and roads [1].

The site selection studies usually utilize many parameters. Thus a systematic methodology is needed to combine the various information from a wide range of disciplines [2]. Multi-criteria decision analysis (MCDA) involves a set of processes that assign the alternatives values evaluating for a specific purpose. In spatial MCDA, geographical data are gathered, processed and transformed into a decision. For that, we have to implement a technique that allows an estimation of the weights. Analytic hierarchy process (AHP) is one such technique which was applied to assign weights for the selected influence criteria with a combination of GIS analysis tools to provide effective and efficient site identification promising results [3].

1.1 Role of GIS in Site Suitability Analysis

Recent technological advances made in the field of spatial technology created significant impact in planning activities. The purpose of using GIS is that maps provide an added dimension to data analysis which brings us one step closer to visualizing the complex patterns and relationships that characterize real-world planning and policy problems [4]. This field of planning is of prime importance for the countries which have various geographic patterns, cultural activities etc. It also offers an interpretation of physical (spatial) data with other socio-economic data, and thereby providing an important linkage in the total planning process and making it more effective and meaningful [5].

When we consider the site suitability analysis, every factor required for the suitability analysis can be represented in a digital layer which can be queried individually or overlaid with other layers. In contrast to manually querying and overlaying the different information sources, a GIS can prove to be very efficient, accurate and time-saving [6]. This is particularly true for large areas or for a great number of variables, as is the case for this research. Therefore, using a GIS allows a

relatively easy identification of those areas where all criteria are met. In addition to storing, retrieving, displaying spatial data, a GIS allows the user to create overlays, intersections, buffers, spatial joins, map algebra, proximity analysis, and other analytical processes. In the perspective of land or site suitability, GIS helps the user to determine what locations/sites are most/least suitable for development. In this means, the results of GIS analysis can offer support for decision-making.

Here the study was carried with the main objective to develop an approach of GIS suitability analysis to identify an optimal site for domestic wastewater treatment plant. The selected study areas are Unawatuna tourist area in the southern region and Puttalam Municipal Council of Sri Lanka which is the agriculture-based area. Here we are trying to find the feasibility of the application of this approach in various types of areas. That is the reason behind the selection two different types of the study area which is most common in Sri Lanka.

2. Materials and Method

2.1 Analytic Hierarchy Process (AHP)

AHP is a multi-criteria decision method that uses hierarchical structures to represent a problem and then develop priorities for alternatives based on the judgment of the user [7]. AHP shows that weighting activities in multi-criteria decision-making method can be effectively dealt with via hierarchical arranging and pair-wise contrasts. According to the statements, the AHP is based on three steps:

- Assemble the decision problem in a hierarchy
- Comparative judgment / Pair-wise Comparison of the elements
- Synthesis of the priorities

Advantages:

- The AHP method supports group decision-making through consensus by calculating the geometric mean of the individual pairwise comparisons [8].
- The advantages of AHP over other multi-criteria methods are its flexibility, intuitive appeal to the decision-makers and its ability to check inconsistencies [9].
- AHP is uniquely positioned to help model situations of uncertainty and risk since it is

capable of deriving scales where measures ordinarily do not exist [10].

- AHP method has the distinct advantage that it decomposes a decision problem into its constituent parts and builds hierarchies of criteria. Here, the importance of each criterion becomes clear [11].

2.2 Factors Influence on Site Selection

• Technical Aspects

Soil texture: Physical characteristics influence the permeability of the soil. The permeability must be within a range in which adequate residence time for renovation is given and prevent rapid downward movement of effluent. The bearing capacity of the soil also an important factor in site selection process for treatment. The allowable bearing capacity of the soils and the allowable differential settlement will control the need to support tanks and structures on piles. According to the permeability condition and bearing capacity of the soil, the red-yellow podzolic is preferable to the WWTP in the study area.

Slope (Topography): A low-lying site facilitates the wastewater flow from the network service area by a gravitational flow which minimizes the number of pumping stations in the collection system. If the slope is a too high surface runoff and soil erosion will be very high. And, such sites require flood protection. In addition, the steep slope will also affect cultivation. According to the wastewater treatment plant construction guideline, the appropriate slope is less than 35% which provides suitable irrigation of treated wastewater for agricultural purposes.

• Environmental Aspects

Surface Water: The wastewater will be discharged to the surface water bodies or sea directly or indirectly. It pollutes the inland and coastal surface water when the pollutant content increases. And also, the natural water bodies, wetlands, oceans quality can be deteriorated by wastewater nitrogen, phosphorus, chloride, faecal coliforms and salinity removals. The intentional and accidental discharges, leakages, seepage will cause this more. Therefore, an excluded area should be created between surface waters and WWTP site. According to the crown land ordinance (Chapter 454), there should be the

60m distance from any public stream or water body to the WWTP.

Ground Water: The groundwater protection responses are concerned with the site selection process for disposal effluent site and the associated design, operation and monitoring of disposal sites. Therefore, drinking water quality of groundwater should be protected from migrating pollutants and contaminants. The minimum distance to the groundwater table will be 1.5m [12]. Generally, greater depths are usually preferred.

• Social and Cultural Aspects

Land Use and Building Area: The sewage must be applied to land in a way that does not cause a nuisance and does not endanger health. Nuisance relates particularly to odour which is allocated with by buffer zones to be kept around building/residential areas. As our study area is a densely populated area, we cannot go for big buffer limit. Mainly to minimize odour, noise, aerosols and air particles, it is preferable to keep a 20m buffer. Regarding the land use, our study has a land-use type such as cultivation area, rock area, built-up area, sandy area, bare land, etc. Here we should avoid the area like built-up area, rock area, cultivation area and forest area. Bare lands are more suitable for the site.

Roads: Distance from the roads increases the cost of wastewater treatment plant construction and maintenance. However, the presence of the wastewater treatment plant close to the roads affects the landscape, climate, and the public health. According to the wastewater treatment plant construction guideline, it has to be a buffer zone of 500m from the highway and railways.

2.3 Methodology

All research procedures can be mainly categorized as defining site suitability criteria, AHP analysis and weighted overlay. Defining site suitability criteria was done by referring previous studies and laws on conservation. And relevant GIS maps were created using ArcGIS. For AHP analysis questionnaire survey was conducted among experts such as Galle irrigation chief engineer, engineers, doctors, undergraduates and the public in the study area. In the survey, the main and sub-criteria were compared pair-wise among them. The weights derived from the AHP analysis was used for weighted overlay



process using ArcGIS. The weighted overlay was done in two phases, with the sub-criteria and main criteria. Finally, field verification was carried out. The design flow chart is shown in Figure 1.

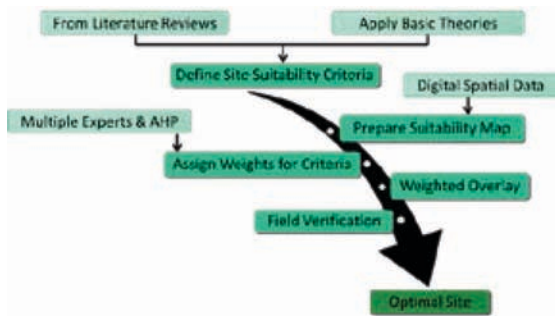


Figure 1 - Design Flow Chart

The digital layers used for spatial analysis were 1: 10000 map obtained from the department of surveying, Sri Lanka. The groundwater map was created by collecting the data around the study area using ArcGIS tools. Ultimately, based on the above procedures the final suitability map was created.

3. Results and Discussion

Criteria which have highest weights influence more in the output overlaid map. The weighting criteria for Unawatuna area is shown in table 1. Here, among main criteria social and cultural aspect influence around 61%.

Table 1 - Weightage of criteria for Unawatuna

Main criteria	Weight	Sub-criteria	Weight
Technical Aspects	0.090	Soil Texture	0.750
		Slope	0.250
Environmental Aspects	0.303	Ground Water	0.250
		Surface Waters	0.750
Social and Cultural Aspects	0.607	Land use	0.303
		Residential Area	0.607
		Roads	0.090

The criteria and the suitability classification with scores were developed which is a primary procedure to identify an optimal site for municipal WWTP for Unawatuna is shown in table 2.

Table 2 - Suitability Criteria for Unawatuna

Main Criteria	Sub Criteria	Class	Scores	
Technical Aspects	Soil	Soil Texture	Red-yellow Podzolic	3
		Regosol	2	
		Bog and half dog	1	
	Topography	Slope [%]	0 - 15	2
			15 - 30	3
			30 <	1
Environmental Aspects	Ground water	Depth [m]	0 - 1.5	1
		1.5 - 2.0	2	
		2.0 <	3	
	Surface Waters	Buffer [m]	0 - 60	1
			60 - 100	2
			100 <	3
Social and Cultural Aspects	Building/ Residential Areas	Buffer [m]	0 - 15	1
			15 - 30	2
			30 <	3
	Land Use	Type	Built-up area	1
			Boggy area	
			Forest area	
			Cloud area	
			Cultivation area	
			Rock area	
			Water area	
			Sand area	
	Bare area	3		
	Major Roads	Buffer [m]	0 - 400	1
			400 - 600	3
			600 <	2
Minor Roads	Buffer [m]	0 - 50	1	
		50 - 100	3	
		100 <	2	

3 - suitable 2 - Moderate 1 - Unsuitable

The criteria and the suitability classification with scores for Puttalam Municipal Council are shown in table 3.

Table 3 - Suitability Criteria for Puttalam Municipal Council

Main criteria	Sub criteria		Class	Scores
Social and cultural Aspects	Building/ Residential Areas	Buffer [m]	0 - 50	1
			50 - 100	2
			100 <	3
	Land Use	Type	Build up area	1
			Cultivation area	
			Water area	
			Rock area	
			Cloud area	2
			Sand	
			Forest	
			Boggy area	
	Barren land	3		
	Major Road	Buffer [m]	0 - 400	1
			400 - 600	3
			600 <	2
Minor Road	Buffer [m]	0 - 50	1	
		50 - 100	3	
		> 100	2	
Technical Aspect	Soil Texture	Type	Alluvial	3
			Red-Yellow Lotosois; gently undulating terrain	
			Reddish Brown Earths and Low Humic Gley Soils	
	Slope	Slope [%]	Regosols	2
			0 - 0.15	2
			0.15 - 0.3	3
Environmental Aspect	Ground Water	Depth [m]	0 - 1.5	1
			1.5 - 2	2
			2 <	3
	Surface Waters	Buffer [m]	0 - 60	1
			60 - 100	2
			100 <	3

3 - suitable 2 - Moderate 1 - Unsuitable

The weighting criteria for Unawatuna area is shown in table 4.

Table 5 - Weightage of criteria for Puttalam Municipal Council

Main criteria	Weight	Sub criteria	Weight
Technical Aspects	0.090	Soil Texture	0.750
		Slope	0.250
Environmental Aspects	0.303	Ground Water	0.250
		Surface Waters	0.750
Social and Cultural Aspects	0.607	Land use	0.303
		Residential Area	0.607
		Roads	0.090

The final suitability maps for Unawatuna and Puttalam area (see Figure 2 and Figure 3) were created from weighted overlaid maps and majority filtering processes. The particular sites were identified from field verification and land area requirement.

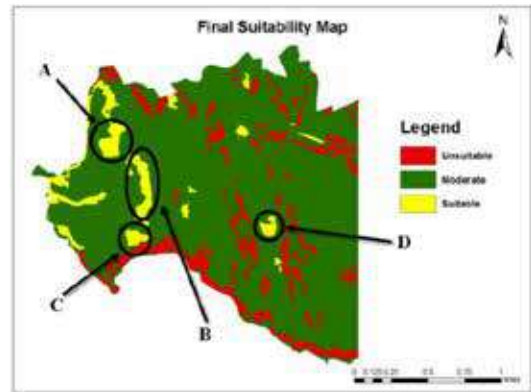


Figure 2- Final Suitability Map for Unawatuna

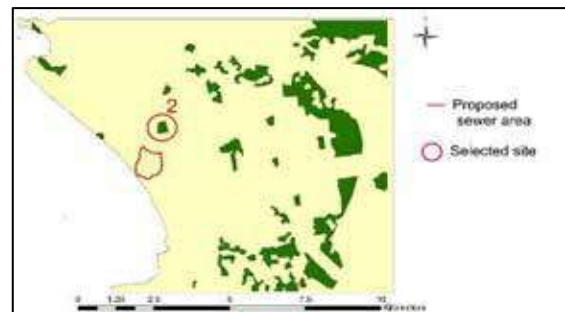


Figure 3 - Final Suitability Map for Puttalam Municipal Council

In the Puttalam Municipal Council, approximately 1200 hectare was identified as a suitable area. For Unawatuna final suitable areas A, B, C, D were identified according to



the land area requirement and field verification. The area requirement from the client (NWSDB Galle) was 16000m².

4. Conclusions

The defined criteria were more reliable for the selected study area. AHP method is superior for multi-criteria decision-making technique. GIS is greater flexibility and accurate tool for domestic wastewater site suitability analysis. Hence, Wastewater treatment plant site suitability has been very effective due to the application of spatial analysis tools and decision-making results in the GIS. Using AHP technique for multi-criteria weight assigning process is quantitatively and qualitatively reliable, and a priority order for each criterion selected in the study area had been easy to be obtained using this method. The integration of AHP technique and GIS analysis provided the efficient result of suitability analysis of wastewater treatment plant. Authorities can easily apply this new approach as it is fast and high accuracy. The approach applied in this thesis can be adopted in another part of Sri Lanka for sustainable future development.

References

- 1 Meinzinge, F., 2003, GIS Based Site Identification for the Land Application of Wastewater, Linclon University.
- 2 Siddiqui, M., Everett, J. & Vieux, B., 1996, 'Landfill Siting Using Geographic Information Systems: A Demonstration', *Journal of environmental engineering*, 122(6), pp.515-523.
- 3 Duc, T. T., 2006, 'Using GIS and AHP Technique for Land-Use Suitability Analysis', *International Symposium on Geoinformatics for Spatial Infrastructure Development in Earth and Allied Sciences*, pp.1-6.
- 4 Malczewski, J., 1996. 'A GIS-Based Approach to Multiplecriteria group Decision making. International', *Journal of Geographical Information Systems* 10(8), 955-971.
- 5 Verma, R., Kumari, K. & Tiwary, R., 2009, 'Application of Remote Sensing and GIS Technique for Efficient Urban Planning in India', *Geomatrix Conference Proceedings*, pp.1-23.
- 6 Fancek, M., Kloplic, J. & Kloplic, R., 1999, 'GIS Helps Return Sewage Sludge to Soils Where Nutrients Can Be Recycled', *GeoWorld*, Apr 1999, 12(4): 52-54.
- 7 Saaty, T.L., 1980, 'the Analytic Hierarchy Process', New York.
- 8 Zahir, S., 1999, 'Clusters in a Group: Decision Making in the Vector Space Formulation of the Analytic Hierarchy Process', *European Journal of Operational Research*, 112(3), pp.620-634.
- 9 Ramanathan, R., 2001. 'A Note on the Use of the Analytic Hierarchy Process for Environmental impact assessment', *Journal of Environmental Management*, 63, pp.27-35
- 10 Millet, I., Wedley, W.C., 2002. 'Modelling Risk and Uncertainty with the Analytic Hierarchy Process', *Journal of Multi-Criteria Decision Analysis*, 11: pp.97-107.
- 11 Macharis, C., Springael, J., De Brucker, K. and Verbeke, A., 2004, 'PROMETHEE and AHP: The Design of Operational Synergies in Multicriteria Analysis.: Strengthening PROMETHEE with ideas of AHP', *European Journal of Operational Research*, 153(2), pp.307-317.
- 12 USEPA (U.S. Environmental Protection Agency), 1988, 'Quality criteria for water. EPA 440/5-86-001. USEPA, Office of Water Regulations and Standards', U.S. Government Printing Office (PB81-226759), Washington, D.C., USA.

Air Pollution Monitoring Through Crowdsourcing

M.I.N.P. Munasinghe, G.I.U.S. Perera, J.K.W.D.B. Karunathilaka, B.C.S. Cooray
and K.G.D. Manupriyal

Abstract: Air pollution, a silent killer in the modern world, is responsible for 7 million deaths in 2012 according to WHO. Sri Lanka, as a developing country, does not possess a real-time air quality monitoring system but only has a mobile unit, which collects air quality data periodically according to the Central Environment Authority (CEA). The solution discussed in this paper addresses several critical aspects of the problem such as collecting, transmitting, storing, analyzing and finally giving active feedback to individual users as well as general public using a crowdsourcing solution. In our approach, we have developed a miniature micro-controller based handheld device, which collects hazardous gas levels (CO, SO₂, NO₂) using semiconductor sensors and sends data to an android device using a serial interface. An Android app provides real time warnings to users while it syncs data to a cloud based web application. This would provide analytical data from all devices using multiple visual dimensions giving air quality information to the general public through an Open API. The device, which we have developed is handheld, cheaper and is easily extensible to detect multiple gases compared to other devices currently in the market and provide rich information to the public regarding air quality in the country as well as anywhere in the world where the device is used.

Keywords: Air quality monitoring, Mobile data measurement, Air pollution, Crowdsourcing, Map Reduce

1. Introduction

Air pollution has become one of the most perilous problem in modern world, which causes harmful illnesses, dangerous smog and gravely affects to the people's everyday life. Unfortunately, despite the very real impacts air pollution cause on people's lives, it often goes unnoticed, unless the pollution is critically high, because of its invisible nature. That is to say, most developed countries have implemented effective processes to regulate air pollution. Nonetheless, air quality monitoring and relaying that information to public is at poor level because government maintained air quality monitoring networks are sparse and do not possess a proper method to deliver gathered information to public.

"Breathe Free" is a new generation of hand held device, paired with the android smart phone, which reveals various hazardous gas levels to users in real time. Moreover, air quality details are gathered through crowdsourcing and visualized in a web application. Aforementioned web application visualizes gas levels in a three-dimensional geographical map with time axis. This paper presents a detailed description regarding development of "Breath free" device and related applications.

2. Problem

Air pollution is a staggering worldwide problem. The impacts of air pollution rank it among the most serious and widespread human health hazards in the world. Air pollution occurs when any harmful gases, dust, smoke enters the atmosphere and makes it difficult for plants, animals and humans to survive as the air becomes dirty. Current atmosphere is quite different from the natural atmosphere that existed before the Industrial Revolution in terms of chemical composition [1].

Breathing polluted air causes chronic illnesses such as asthma and bronchitis and contributes to terminal illnesses such as cancer and heart disease. The World Health Organization (WHO) estimates that in 2012 around 7 million premature deaths resulted from air pollution, more than double the previous estimates [2].

In Sri Lanka, presently it is impossible to get real-time air quality details of any cities according to Central Environment Authority (CEA). CEA is the only institute, which

Eng. M.I.N.P. Munasinghe, Dept. of CSE, University of Moratuwa.

Eng. (Dr.) G.I.U.S. Perera, Dept. of CSE, University of Moratuwa.

Mr. J.K.W.D.B. Karunathilaka, Dept. of CSE, University of Moratuwa.

Mr. B.C.S. Cooray, Dept. of CSE, University of Moratuwa.

Eng. K. G. D. Manupriyal, Dept. of CSE, University of Moratuwa.



measures air quality in Sri Lanka and it follows a procedure to gather data in whole country. CEA possess a mobile unit which is taken to main town of every district and collects environmental data throughout a week by using instruments in this mobile unit. There is no real-time air quality monitoring and furthermore, general public cannot access to this collected data.

Similar products and their limitations

There are few devices that has been developed to monitor air pollution but clearly there are major limitations which have been addressed by proposed solution.

- **AirCasting**

This device aims to collect air pollution data using a device and android app. [3]However, its main limitations are the higher cost, being battery powered makes it bulky, and difficult to use since people have to charge it. Nowadays people even don't prefer to charge their mobile phone. Therefore, it would be highly unlikely they will be pleased to use a device, which require charging. Moreover, its data visualization is in very poor state since it uses 2D map with colored squares.

- **Mob Geo Sens**

This device use phones internal and other connected external sensors to collect data which use external power source [4]. Main limitation is it only works with old Nokia phones because it depends on Symbian operating system, which is obsolete now.

3. Solution

“Breathe Free” is a solution which is not only limited to monitoring real time air quality, but also a complete system to transmit, store, process and present data to public in simple easily understandable interface. It is composed with three major components. A hand-held device, android application and visualization platform.

In the problem mentioned above, one critical component is data collection method. At the moment, it was done by the CEA and it has some limitations as mentioned before. Therefore, in this new approach data collection is done via crowdsourcing.

3.1 Crowdsourcing

Crowdsourcing means act of a company or institution taking a function once performed by employees and outsourcing it to an undefined network of people in the form of an open call. This can take the form of peer-production, but is also often undertaken by sole individuals. The crucial prerequisite is the use of the open call format and the large network of potential laborers [4].When applying crowdsourcing to this application, function of collecting data is transferred from CEA to public. This is a strategic model to attract an interested, motivated crowd of individuals capable of providing solutions superior in quality and quantity to those that even traditional forms of methods can.

Furthermore, it would be better, if the people have the knowledge of what it might do to the crowd and how it may reinstitute long-standing mechanisms of oppression through new discourses. Following reasons are the key reasons to use crowdsourcing in this project.

- Low cost: Remunerations of Crowdsourcing can be relatively low cost [5].
- Higher accuracy: Large number of people contribute for same gas in particular area reduce the error percentage.
- Cover more area: Large number of people from diverse locations can contribute, system can cover more area than conventional systems.

Following components are the major components of the system.

3.2 Hand Held Device

This is an Arduino driven small device which consists of three main sense modules. Those are CO sensor module (MQ-7) [6], SO₂ sensor module (MQ-136) [7] and NO_x sensor module (MiCS-2714) [8]. This device is capable of collecting ambient gas level details and sending them using serial communication method to an Android smartphone. In order to connect the device and the phone, mini USB to micro USB cable is used and moreover this device is powered by the smartphone itself hence no need of external battery or Bluetooth/Wi-Fi transferring module for operating the device. Since this device is aimed to be a low-cost device, this method is more beneficial because battery cost and data transfer module costs are reduced from the manufacturing cost.

This device further has an ability to reduce the power consumption by sleeping the Arduino

module and other sense modules. "Sleep" is a special mode of the processor, which halts normal program execution and shuts down its internal components to reduce power consumption. Once a processor is asleep it can only be awakened by specific events such as an external interrupt from a button press, or a timer counting a period of time. Different sleep modes disable various internal clocks and components to reduce power consumption. In this product, to save the maximum amount of power, "SLEEP_MODE_PWR_DOWN" has been used. In this mode, all clocks and oscillators are turned off and this is the maximum power down mode that can be achieved in Arduino[9].

Detecting ranges of aforementioned gas modules are shown in the following table.

Table 1 - Sensor details

Sensor Module	Detection Gas	Detecting Range (ppm)
MQ-7	CO	20-2000
MQ-136	SO ₂	1-200
MiCS-2714	NO ₂	0.05-5

These sensors should be operated within their operational temperature levels in order to have good accuracy. Therefore, the circuit was designed to minimize heat exchange between sensors by keeping them apart while making the circuit footprint minimal in order to provide easy usage. The design of the circuit is shown in the figure below.



Figure 1 - Device Circuit

Final device with its housing is shown in the following figure.



Figure 2 - Device with housing

3.3 Android Application

An Android application is developed in order to provide an interface to handheld device by allowing user to control the device and providing readings from the device.

Functionalities of the Android application are,

1. Displaying current gas levels.
2. Warn user when gas levels are above a threshold value.
3. Send data to online server.
4. Change settings of the device.

Primary requirement of the Android application is to sync gathered data to online database which is also the crowdsourcing component. In order to achieve this, android application uses a NoSQL database called Couchbase as the medium to store data received by the device. Couchbase provides automatic syncing capability which satisfy the main requirement. Application syncs data to online server periodically when an internet connection is available. This sync is a one-way sync from the mobile phone to the online database server. Moreover, nature of the gathered data is not structured. Same app should be able to use with multiple type of devices since the device can be easily extensible by adding multiple sensors. Therefore, NoSQL type database is most suitable for requirement.

Measured gas level data are fed to the mobile phone via USB interface and Android application collects received data and saves to local Couchbase database. Real-time gas levels are displayed on the main screen of the application. User can easily view what are the pollution gas levels in the area the user is at.



Furthermore, application warns to the user of any increased reading of a pollution gas. The application produces an alert if it senses that a pollution gas level is above some threshold. These threshold values are determined according to standard maximum gas levels a human can withstand without a problem.

Another key feature in the application is it provides the user to control the device through few important settings. Application allows user to configure the time interval, which the device should collect data from the sensors. This is important since this interval becomes smaller, power consumption increases but provide more real-time data. Another configuration it provides is the device sleep settings which lets user to set a time which put device in to sleep mode in order to preserve battery power. Another setting is to select type of internet the connection which should be used to sync data like Wi-Fi or mobile data.

3.4 Visualization and Data Processing Platform

In this project this is the most important part that distinguishes this product from other similar products. Key thing to mention is that this visualization platform can be easily extended to add more maps to visualize data in rich formats.

Visualization platform consists of web server and Couchbase NoSQL database. Reason to use NoSQL database is that data which are gathered are schema less, as mentioned before. And the other advantage is that Couchbase server uses caching to optimize the data access. In the case of data growth Couchbase server can be easily extended by adding more nodes to the database.

3.4.1 Data Processing Using MapReduce

Major challenge in this solution is handling large amounts of data and process them in order to generate useful information to end user. To overcome this MapReduce has been used.

MapReduce is a programming model and an associated implementation for processing and generating large datasets that is amenable to a broad variety of real-world tasks. Users specify the computation in terms of a map and a reduce function, and the underlying runtime system automatically parallelizes the computation across large-scale clusters of machines, handles machine failures, and schedules inter-machine

communication to make efficient use of the network and disks [1]. MapReduce allows programmers with no experience with parallel and distributed systems to easily utilize the resources of a large distributed system. A typical MapReduce computation processes many terabytes of data on hundreds or thousands of machines [11].

In this application, large amount of data is gathered from large number of devices across various locations and data is distributed in multiple nodes. Because of this large volume and distributed manner, calculations include collected data is a challenging task. Therefore, MapReduce support in Couchbase DB is used do calculation which are required to produce maps. For example, in average map view it is required to calculate gas level averages in each city. In order to do that map function will emit key as city and gas values as value parameter. Corresponding reduce function will reduce that values and calculate average of each value and return a document with key as city and value as average values of each gas.

3.4.2 Outlier Detection and Removal

In this crowdsourcing approach, there is a higher probability of getting incorrect values to the online sever because of various reasons like malfunctioning sensors because of humidity and temperature differences and even intentional incorrect data inputs. Therefore, data cleaning or outlier removal is a very crucial aspect in order to filter accurate data set to visualize.

An outlier can be defined as an observation that lies an abnormal distance from other values in a random sample from a population. In a sense, this definition leaves it up to the analyst (or a consensus process) to decide what will be considered abnormal. Before abnormal observations can be singled out, it is necessary to characterize normal observations [12]. In [13] the authors define an outlying observation, or outlier, is one, that appears to deviate considerably from other members of the sample in which it occurs. Another definition as observed in [14] is, it is an observation that deviates so much from other observations so as to arouse suspicion that it was generated by a different mechanism.

One of the major tool in descriptive analysis is quartiles which divides the range of data in four parts each having 25% of the data. Q1 is the 25% point, Q2 which is also same as median, is the

50% point and Q3 is the 75% point [15]. In order to remove outliers in this application, data of each gas has been grouped by city and quantities are calculated for each city. Location data is gathered using mobile phone location information. Following method is used to identify lower and upper bound in each city.

1. Arrange data in order.
2. Calculate first quartile (Q1)
3. Calculate third quartile (Q3)
4. Calculate inter quartile range (IQR)=Q3-Q1
5. Calculate lower boundary= Q1-(1.5*IQR)
6. Calculate upper boundary= Q3+(1.5*IQR)
7. Anything outside the lower and upper boundary is an outlier [16].

Figure 3 shows the graphical representation of this calculation.

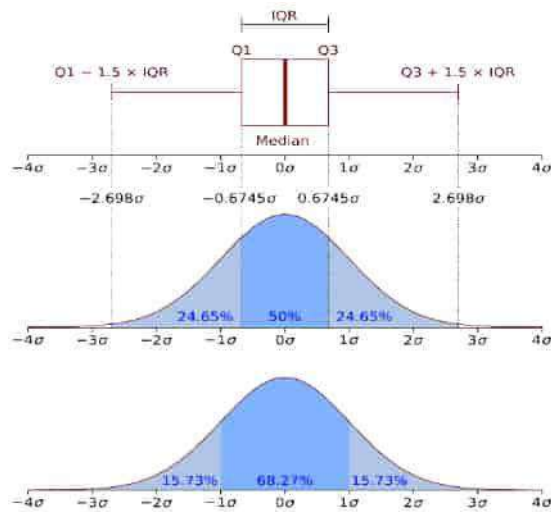


Figure 3 - Identifying outliers

3.4.3 Data Visualization

Visualization component of this project is intended to provide simple and informative representation of collected, cleaned and processed data to public. Following are the types of maps which are currently added in order to showcase the possible multiple modes of visualization and their related technologies.

Cesiumjs for 3D map visualization

With environmental pollution data, 3D visualization can provide users a better and more artistic picture. After considering multiple charting libraries, Cesiumjs [17] and Google Earth [18] were selected because they match with most of the requirements. Google earth provides better visualization options and proved to be better with a higher existing user base. Cesiumjs was the other library which comes after Google Earth in both feature wise and user base wise. Main issue with Google

Earth was its web plug-in was set to discontinue after December 2015 due to a security issue. With that problem, the only option was to use next best library. Cesiumjs has client side rendering of data which was much suitable for this use case since it leverages rendering the map to the client which reduce the load on server. Cesiumjs is also built on plugin free technology which gives assurance that there will not be problems like with Google Earth. For the past few years, progressively more users were moving to Cesiumjs from Google Earth. There were two main reasons for this migration [19]. The first reason is the lack of high resolution image content. Google lost its source of high quality imagery in few years back. Since then Google did not have a scalable high resolution image supply. The other reason was it is required to use a plugin to view Google Earth in web applications. This became a major issue when Google released a new 64-bit Chrome version which does not support Google Earth plug-in. On the other hand, Cesiumjs uses WebGL [21] to render 3D maps. Therefore, it does not have problems associated with Google Earth. As of now Cesiumjs does not have much high-quality imagery. But Cesiumjs is holding discussions with early imagery providers for Google Earth and future seems optimistic.

Google Maps for 2D visualization

In order to provide 2D visualization of city wise pollution data, several visualization libraries were considered as before. One of them was Google Maps [22] and other alternatives included Bing maps and open street maps. Google Maps has better and more features considering other visualization alternatives. Support for heatmaps is a one major concern and additionally Google maps consists with easy to use API (Application Programming Interface) and better documentation.

Following maps are the different visualization modes that has been implemented.

- **3D Map**

In this map, each bar represents a reading of a certain hazardous gas. Importance of this map compared to other maps is that it is more convenient to get an idea about gas level changes from the relative height of each bar. From other 2D maps that has been developed, it is difficult to get idea about relative levels from the just color and shown gas value. Moreover, the color of this map is related to the intensity



level of the gas. Higher intensity gives intense color.

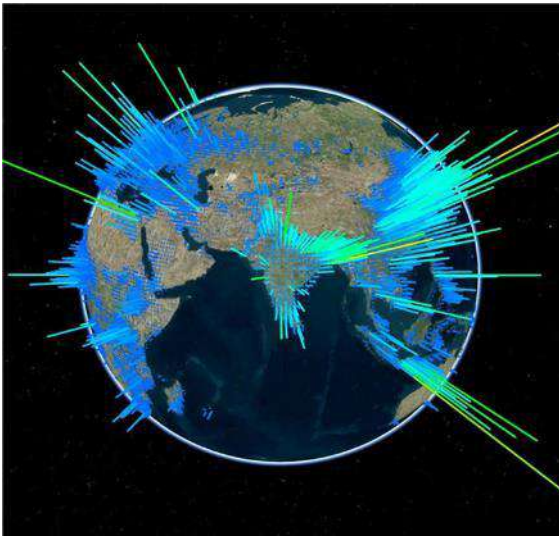


Figure 4-3D map

- **2D Dot Map**

Visualization of each data point as a dot with a color. Here each data point represents a single reading observed by a user. Advantage of this map it gives clear top down view of data and gives straight forward color representation of different gas levels rather than using intensity in 3D map. Which gives direct idea about gas level in particular location.



Figure 5- 2D dot map

- **Average Map**

Aim of this map is to visualize city wise data to provide overall notion. Here each cylinder represents a city. Height of the cylinder represents the average value of a certain pollution gas. Radius of the cylinder represents the radius covered by city. Importance of this map is it represents the average pollution of particular city. In order to calculate this

average, map reduce technique which was discussed before has been used.

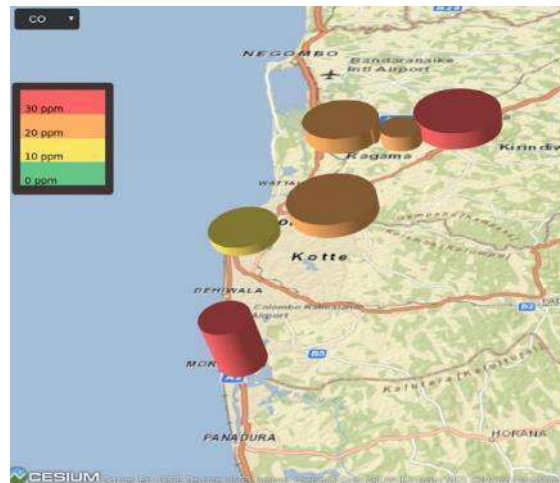


Figure 6 - Gas level average map

- **Heat Map**

This map represents the amount of data available for a given gas. If higher number of users are available, color becomes red. Importance of this map is, if there are large number of users in particular area, that means the accuracy of data in that area is high.

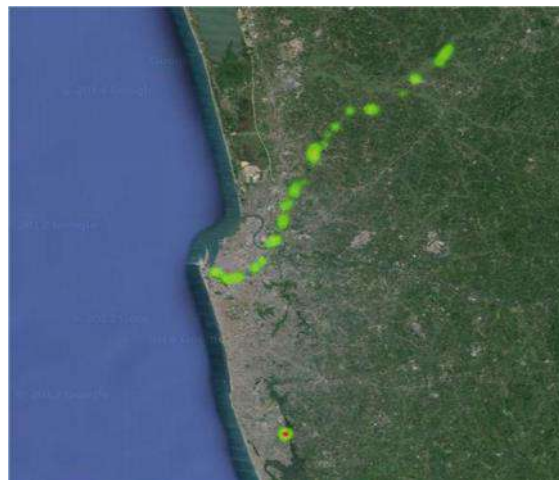


Figure 7 - Heat map

3.4.4 Public API (Application Programming Interface) to retrieve air pollution data

It was able to develop an API for public which can be used to retrieve air pollution data in particular area. By providing latitude and longitude to this API, it returns average pollution gas levels of that location. Development of this API is very useful because it facilitates large number of other types of applications in air quality monitoring domain which depends on data collected by this system. For an example, billboards in cities that shows real time air pollution data, desktop or mobile widgets that show air pollution like

weather apps which currently have or small devices which shows air pollution data can be developed.

4. Discussion

General use case of this device would be the ability to view air pollution details to the public using visualization platform, which is exposed via web application. In order to test that scenario, testing is carried out by using the device while traveling the train; Figure 5, Figure 6 and Figure 7 shows the actual data gathered from the device while traveling from Colombo Fort railway station to Gampaha railway station and near the University of Moratuwa premises. These are the maps which are generated by the visualization platform and exposed via web application. Test results shows bright red dot in heat map (Figure 7) indicating large number of data points near university area and this is due to higher amount of testing near the university premises. Moreover, average map (Figure 6) shows there are higher concentration of CO near university area and Gampaha area. But near Colombo Fort area, it is considerably low. This may be caused by the sea wind near Colombo area. Since only one device was used in small amount of time in one particular area, collected data is not sufficient to support these claims.

Major limitation of this project was lack of more devices and more data to support these claims with less error percentage. However, with the resources available to the project, only one device could be developed, and was used as a proof of concept.

5. Conclusion

It can be concluded that the authors were able to bring forward a vital solution to help support for improving human health, through real-time air pollution monitoring. The discussed work here presents a complete solution which is composed of parts for collecting, transmitting, processing, warning and providing information to public. The system fills the gap of awareness not only in Sri Lanka but also in any country in the world. Above all, data collected by the system will be crucial element for researches to study adverse effects and predict trends in air pollution. The device can be a cost-effective tool for research and field studies relevant to air-quality monitoring as well

Acknowledgement

Authors thanks to central environment authority for helping us by giving access to their laboratories to calibrate sensors and providing access to mobile air pollution monitoring vehicle to get more information regarding current air quality data gathering.

References

1. Daly, A., and Zannetti, P., *An Introduction to Air Pollution, California: The Arab School for Science and Technology*, 2007.
2. U. N. E. Programme, "Air Pollution: World's Worst Environmental," *UNEP Year Book 2014 emerging issues update*, December 2014, pp. 43-47.
3. <http://www.takingspace.org/airbeam-technical-specifications-operation-performance/>. Visited 9th Sept 2015.
4. Kanjo, E., Benford, S., Paxton, M., Chamberlain, A., Fraser, D. S., Woodgate, D., Crellin, D., and Woolard, A., "MobGeoSen: Facilitating Personal Geosensor Data Collection," *Pers Ubiquit Comput*, vol. 12, 2008, p. 599-607.
5. http://crowdsourcing.typepad.com/cs/2006/06/crowdsourcing_a.html, Visited August 2015.
6. Schenk, E., and Guittard, C., "Crowdsourcing: What can be Outsourced to the Crowd, and Why?", 2009.
7. <https://www.sparkfun.com/datasheets/Sensors/Biometric/MQ-7.pdf>, Visited 20th Jan 2016.
8. <http://www.china-total.com/Product/meter/gas-sensor/MQ136.pdf>, Visited 20th Jan 2016.
9. <http://sgx.cdistore.com/datasheets/e2v/1107-Datasheet-MiCS-2714.pdf>, 20th Jan 2016.
10. <http://playground.arduino.cc/Learning/ArduinoSleepCode>, 20th Jan 2017.
11. Jeffrey, D., and Sanjay, G., "MapReduce: simplified data processing on large clusters", *Communications of the ACM - 50th anniversary issue: 1958 - 2008*, vol. 51, no. 1, 2008, pp. 107-113.
12. Jeffrey, D., and Sanjay, G., "MapReduce: A Flexible Data Processing Tool," *Communications of the ACM - Amir Pnueli: Ahead of His Time*, vol. 53, no. 1, 2010, pp. 72-77.
13. <http://www.itl.nist.gov/div898/handbook/indx.htm>, Visited 23rd Jan 2016.



14. Mehmed Kantardzic, "Data Mining – Concepts, Models, Methods, and Algorithms " .
15. Hawkins D," Identification of Outliers", Chapman and Hall, 1980.
16. Goswami, S., and Chakrabarti, D. A., "Quartile Clustering: A quartile based," JOURNAL OF COMPUTING, vol. 4, no. 2, 2012.
17. D. M. D. J., E. R. L. Sunitha, "Automatic Outlier Identification in Data Mining," International Journal of Advanced Research in Computer and Communication Engineering, vol. 3, no. 6, 2014.
18. <https://cesiumjs.org/> , Visited 25th Jan 2016.
19. <https://www.google.com/earth/>, Visited 25thJan 2016.
20. <https://medium.com/@CyberCity3D/globetrotting-the-fall-of-google-earth-the-rise-of-cesium-and-what-it-all-means-for-the-virtual-1d261fdc25c9#.bg0olksk3>, Visited 25th Jan 2016.
21. <https://www.chromeexperiments.com/webgl> , Visited 25th Jan 2016.
22. <https://developers.google.com/maps/?hl=en>, Visited 25th Jan 2016.

A Conceptual Tool for Assessing Building Life Cycle Carbon Emissions in the Context of Sri Lanka

R.P. Kumanayake, H.B. Luo and R.M.P.S. Bandara

Abstract: At present, the world is facing an enormous challenge due to the adverse environmental impacts of various human activities including construction. Construction is one of the major industrial sectors of Sri Lanka, within which buildings sub-sector has the highest contribution to the value of work and raw material consumption. Consequently, buildings are responsible for a significant share of the total energy use and carbon emissions. Therefore, the development of suitable mechanisms for assessing building environmental performance with regard to energy use and carbon emissions is a timely requirement. Most of the existing systems are focused on the developed and temperate climate countries and these have a limited use in Sri Lanka, due to a range of climatic, geographical, technological, economic, social, political and cultural diversifications unique to the country. This paper presents the initial design for developing an automated tool for assessing life cycle carbon emissions of buildings in the specific context of Sri Lanka. Within the proposed tool, a building information database will be developed using MySQL database management system, by making use of existing databases such as Inventory of Carbon and Energy (ICE), relevant data from recent research literature and field data from building contractors, material manufacturers and equipment suppliers. The database is integrated with a computerized programme for estimating life cycle carbon emissions which is developed using Visual Studio C# Object Oriented Programming language in the .NET framework. Using the proposed tool, the life cycle carbon emission assessment of buildings from raw material extraction to the deconstruction can be estimated. The tool will facilitate the quantification of the impacts of life cycle carbon emissions of buildings and provide a much needed environmental decision making mechanism to the construction professionals, hence contributing to environmentally sustainable construction.

Keywords: Carbon emission, building life cycle, environmental assessment, sustainable construction

1. Introduction

Buildings have a significant environmental footprint which includes 40% of global energy consumption and one third of greenhouse gas (GHG) emissions worldwide [1]. On the other hand, it was found that the building sector has a considerable potential for energy efficient improvements and GHG reduction without significant increase in the investment cost [2].

The Kyoto protocol was targeted at reducing 5% of global GHG emissions within the time period of 2008–2012[3]. Carbon dioxide (CO₂) is considered as the predominant GHG and the CO₂ equivalent emission values of the other greenhouse gases are usually given in terms of global warming potential (GWP)[1]. Many studies related to the assessment of carbon emissions of buildings were initiated as a result of introducing the Kyoto Protocol. The energy consumption is identified as the main cause of carbon emissions in buildings. As buildings have long life spans, the decisions taken at present have the ability to affect the carbon

emissions over long term. For any improvements to take place, assessment of the current building performance is essential. Life cycle assessment (LCA), that assesses a range of environmental impacts throughout the lifetime of a product is considered to be the best technique to evaluate the full extent of the life cycle carbon emissions of a building [4].

Life cycle carbon emissions assessment is a specialized form of LCA, which evaluate the carbon emissions over the building life cycle, facilitating the selection of low-carbon emitting

*Eng. R.P. Kumanayake, B.Sc.Eng. (Hons.) (Moratuwa), M.B.A. (Colombo), AMIE(SL), Ph.D. Student, School of Civil Engineering and Mechanics, Huazhong University of Science and Technology, China.
Senior Lecturer, Department of Civil Engineering, General Sir John Kotelawala Defence University, Sri Lanka.*

Prof. H.B. Luo, B.A. (Civil Engineering), Ph.D., Deputy Dean, School of Civil Engineering and Mechanics, Huazhong University of Science and Technology, China.

Eng. R.M.P.S. Bandara, BSc.Eng. (Hons.) (Moratuwa), M.Eng. (Moratuwa), AMIE(SL), Senior Lecturer, Department of Mechanical Engineering, General Sir John Kotelawala Defence University.



materials, systems, and processes for buildings. In recent years, carbon emission assessment has gained attention worldwide due to its direct association with global warming. In conventional buildings, over 80% of carbon emissions take place in the operational phase due to energy used for heating, cooling, ventilation, lighting and appliance usage[5]-[7]. The other life cycle phases such as manufacturing of building materials, building construction, maintenance, renovation and demolition are responsible for the rest of the carbon emissions.

Although a variety of building environmental assessment systems are being used globally, most of these were established by the developed countries. Despite their effectiveness in assessing building environmental performance in their countries of origin, they are less successful in other regions of the world such as South Asia, due to a wide range of climatic, geographical, technological, economic, social, political and cultural diversifications unique to these regions[8]. In Sri Lanka, Construction is one of the major industrial sectors, within which the buildings sub-sector has the highest share of value of work and raw material usage[9]. Sri Lanka has already identified the importance of developing building environmental assessment systems, codes and standards which take the regional and national differences into account. The Energy Efficient Building Code developed by Sri Lanka Sustainable Energy Authority[10] and GREEN^{SL} Rating System developed by Sri Lanka Green Building Council [11] are two such initiatives. But the assessment tools necessary to monitor the compliance to the codes and to assist the green building certification are yet to be developed.

The objective of the present research is to develop the initial framework and the associated conceptual model for a computerized building life cycle carbon emission estimation tool, which is integrated with a carbon emission database. The insufficiency of the relevant regional and country specific data was found to be a huge challenge. Therefore, the data available in the recent literature and globally accepted databases such as Inventory of Carbon and Energy (ICE) [12] were referred and adjusted to match the specific context of Sri Lanka. The proposed program can be used as a decision making tool in low-carbon building design as

well as a carbon emission assessment tool for the green building certification in Sri Lanka.

2. Literature Review

Based on a detailed study of literature, it was found that the majority of the existing energy and carbon related research and databases focus on the developed and temperate climate countries. Only a few examples of developing, tropical countries exist[13]-[16]. Ruuska[17] investigated how the energy and carbon profiles of these two categories of countries differ. The specific areas which should be focused when applying the existing research findings to developing and tropical countries were identified as “ level of operational energy use, transition from traditional to modern building materials, role of insulation, role of advanced building systems, technology of material production, energy production methods and energy carriers”[17]. In their studies, Abeyundara et al. [13], Chau et al. [18] and Gonzalez and Navarro [19] made suitable adjustments to make the existing data compatible with the specific context of a particular country.

A significant lack of country specific research and related data on building energy and carbon emissions in Sri Lanka can be observed at present. Dias and Pooliyadda[20] developed a database management system to present and compute the embodied energy and carbon emission of a number of building materials commonly used in Sri Lanka. Although some Sri Lankan researchers have been using the existing building environmental assessment tools and life cycle inventory databases for their studies, these do not reflect the true conditions of the country as they were originally intended for a different country or region. Thus, the necessity of developing building environmental assessment programs to match the unique conditions of the country has emerged.

With the current level of integration of the construction industry with information technology, there are numerous software and other computerized tools developed globally for energy and carbon emission assessment of buildings. Most of these were developed by the researchers and organizations in developed countries with the use of databases and information readily available. These include SUSB-LCA (Korea), AIJ-LCA (Japan), GEM-21P (Japan), Carbon Navigator (Japan), BECOST (Finland), LISA (Australia), ENVEST2 (UK),

LCA-MCDM (U.S.) and Eco-Quantum (The Netherlands)[21].

Apart from the above, researchers from around the world have been developing frameworks, models and related computerized programs based on the existing green building certification systems, life cycle databases, standards and codes of the respective countries. BEGAS 2.0, a framework to support the Green Building Index (GBI) certification system of Korea was introduced by Roh et al.[22]. In order to assess life cycle carbon emissions and identify environmentally-friendly construction techniques for a specific CO₂ emission target, an optimum design program (SUSB-OPTIMUM) for apartment houses was developed[23]. A LCA model to estimate the energy use and carbon emission of buildings in Beijing, China was developed by Aden et al. [24]. A life cycle carbon emission program to be used in the schematic design stage was introduced by Baek et al. [25] which was based on the global environmental management system GEM-21P.

A simplified life cycle carbon emission assessment model and the associated tool (B-SCAT) was developed especially focusing on the early design stages, which is expected to support low carbon building design [26]. Fu et al. [27] developed a computer based carbon emissions calculation system for the construction phase of buildings. A computer-based model for assessing building life cycle carbon emission was developed by Kwok [28] and an assessment framework to evaluate the embodied carbon impacts of residential buildings in China was modelled by Li et al.[29]. In a subsequent research, an automated tool for estimating life cycle carbon emission of residential buildings in China, was developed[30]. Some researchers have integrated carbon emission estimation programs with Building Information Modelling to enhance the effectiveness of carbon emission estimation at early design stages [31], [32]. Moncaster and Symons [33] introduced "Embodied Carbon and Energy of Buildings (ECEB)" tool, designed as an approach for early design stage of UK buildings.

Reviewing of the processes, assumptions, specific features, highlights and limitations related to these existing frameworks and systems provide a good starting point for developing a similar system for Sri Lanka.

Kang et al.[34] suggested a systematic model for developing sustainable building assessment tools by establishing a logical performance assessment framework. It can also be used as a guideline in developing a building life cycle carbon emission assessment framework and the related model in the context of Sri Lanka.

For developing these systems, the existing carbon emission databases, standards and codes of the country concerned were used. In the existing literature a significant gap can be observed in relation to the availability of related research, data sources and carbon emission programs in the context of developing, tropical countries like Sri Lanka. The present study is expected to bridge this gap to some degree by establishing a framework and the associated conceptual model as an initial step in developing a life cycle carbon emission estimation program for buildings in the specific context of Sri Lanka.

3. Methodology

There are a number of LCA techniques available today. ISO 14040 standard series introduced by International Organization for Standardization (ISO) presents a general methodological framework, which make the comparisons of different LCAs easier. In recent years, it has emerged as a preferred framework and followed by many researchers [27], [35]–[37]. ISO 14040 Environmental Management - Life cycle assessment standard [38] identifies four interactive phases of a LCA: goal and scope definition, inventory analysis, impact assessment and interpretation. The framework for the proposed LCA tool which is illustrated in Figure 1 was developed according to it.

3.1 Goal and scope definition

The proposed tool is intended for assessing the life cycle carbon emissions of buildings in Sri Lanka. The system boundary includes both spatial boundary and life cycle process boundary for the calculation of carbon emissions. The spatial boundary is defined as the closed 3-dimensional space of the building. Life cycle process boundary includes all phases of cradle-to-grave life cycle process and 1m² of gross floor area of the building per year was considered as the functional unit of the study.



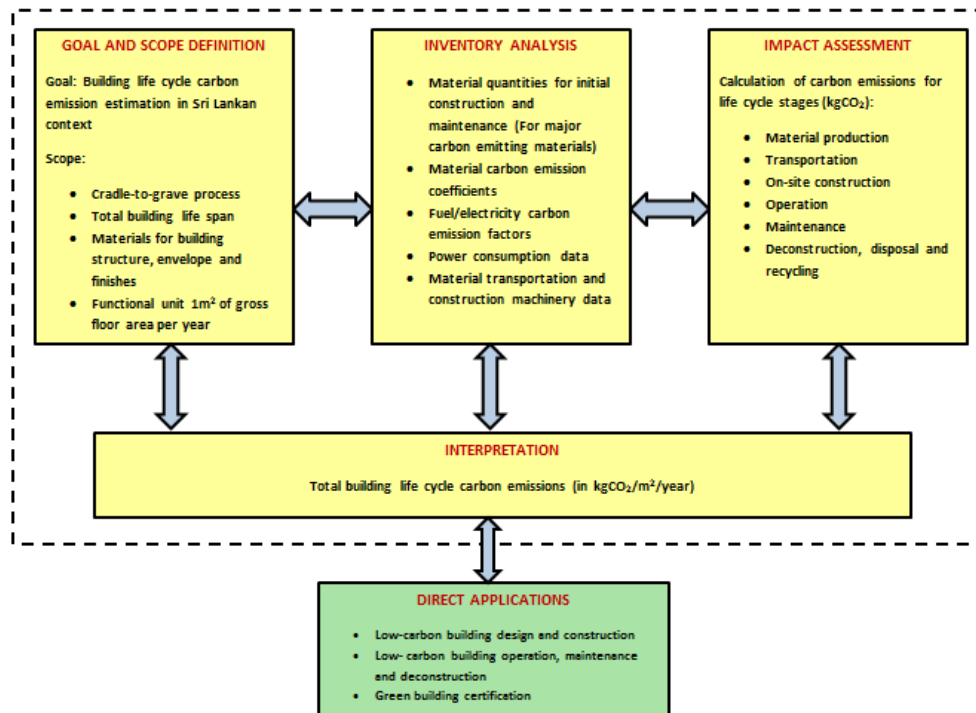


Figure 1- LCA framework for developing the building life cycle carbon emission estimation tool.

3.2 Inventory analysis

The life cycle inventory includes the inputs of the building life cycle process in the forms of energy and materials. By analysing a sample of buildings, the major construction materials that make up more than 80% of carbon emissions in typical Sri Lankan buildings were identified. A similar approach was followed in previous studies [21], [22], [29], [32], [39]. The material quantities and building information are obtained from design drawings, bill of quantities and technical specifications. The energy data are obtained from recent literature as well as local and international reports. Due to the lack of national databases in relation to construction machinery, transportation, demolition and waste disposal in Sri Lanka, suitable assumptions are made by consulting experienced construction professionals and referring to records of previous construction projects. Due to the common challenge of data unavailability in building life cycle studies, especially in developing countries, many researchers have followed a similar approach [14], [16], [40]. The computerized life cycle inventory is developed using MySQL database management system.

3.2.1 Impact assessment

The proposed tool is designed to compute the carbon emissions of each life cycle phase and

the life cycle carbon emission of the building will be produced as the final output. For this, the proposed carbon emission estimator program will be developed using Visual Studio C# programming language in .NET framework. Given the basic project information and material quantities, it will estimate the carbon emissions using the programmed formulae for each life cycle stage incorporating material and energy related data stored in the MySQL database. In order to make the LCA results more representative of Sri Lanka, the energy coefficient values obtained from the existing databases and research literature will be converted to carbon emission coefficients by considering the specific energy generation mix of the country at present.

3.2.2 Interpretation

The results will be interpreted to give the total life cycle carbon emissions of the building in kgCO₂/m²/year.

3.3 Estimation of carbon emissions

Based on the carbon emission coefficient method and the LCA approach, total life cycle carbon emissions of a building can be calculated as given in equation (1)[41].

$$C_{LC} = C_M + C_T + C_C + C_{O\&M} + C_D \quad \dots(1)$$

Where C_{LC} represents the total life cycle carbon emissions of a building (kgCO₂) and C_M , C_T , C_C , $C_{O\&M}$ and C_D represent the carbon emissions at material production, transportation, construction, operation and maintenance and deconstruction phases (kgCO₂) respectively. The carbon emissions at each life cycle stage are presented by equations (2)-(7).

3.3.1 Carbon emissions at material production

The carbon emissions at the material production stage C_M , which includes the raw material extraction and building material production can be calculated as in equation (2)[30]:

$$C_M = \sum_{i=1}^n (m_i \times f_{m,i}) \quad \dots(2)$$

Where n is the total number of material types, m_i and $f_{m,i}$ are the quantity (kg) and the carbon emission coefficient (kgCO₂/kg) of type i material respectively. The value of $f_{m,i}$ can be calculated using the equation (3)[41].

$$f_{m,i} = (e_i \times \beta_i) \quad \dots(3)$$

Where e_i and β_i are the embodied energy coefficient (MJ/kg) and the average carbon emission factor (kgCO₂/MJ) of the energy source used for manufacturing type i material respectively. As multiple sources are used for energy production, an average carbon emission factor (β_i) is generally used for a specific country. For example, the value of β_i for the power generation in Sri Lanka can be calculated by considering the primary energy mix of the country at present that comprises of biomass (38.8%), petroleum (38.9%), coal (9.9%) major hydro (9.5%) and new renewable energy (2.9%)[42]. In several previous studies, a similar process for computing an average carbon emission factor was carried out [19], [43].

3.3.2 Carbon emissions at material transportation

The equation (4) is used to calculate the carbon emitted during the delivery of materials to the construction site (C_T)[30].

$$C_T = \sum_{i=1}^n (m_i \times D_i \times f_{t,i}) \quad \dots(4)$$

Where D_i is the average transportation distance (km) of type i material and $f_{t,i}$ is the carbon emission coefficient for unit material transported over unit distance of type i material (kgCO₂/kg.km).

3.3.3 Carbon emissions of on-site construction

Carbon emission during on-site construction, C_c is due to the operation of construction machinery and equipment during various construction activities, which is given as:

$$C_c = \sum_{i=1}^j (Q_i \times R_i \times f_{c,i}) \quad \dots(5)$$

Where j is the total number of on-site construction activities, Q_i and R_i are the quantity (m³ or kg) and fuel/electricity use rate (l/m³, kwh/kg etc.) of the construction activity i respectively. $f_{c,i}$ (kgCO₂/l or kgCO₂/kwh) is the carbon emission coefficient of the type of energy used for the construction activity i .

3.3.4 Carbon emissions at building operation and maintenance

Carbon emission at the operation and maintenance stage, $C_{O\&M}$ is due to the fuel/electricity consumption of the building operation and the materials replaced in maintenance, which is estimated as[30]:

$$C_{E_{O\&M}} = (Q_e \times f_e \times Y) + (\sum_{i=1}^k r_i \times f_{m,i} \times \frac{Y}{R}) \dots(6)$$

Where Q_e is the average annual electricity consumption of the building (kWh/year), f_e the carbon emission coefficient of electricity (kgCO₂/kWh) and Y the assumed lifespan of the building (years). Electricity is considered as the energy source for building operation and it is calculated based on the monthly electricity bills. In the case of new buildings, the energy consumption can be computed based on the expected functions, power demands and working time of the building[44]. For the maintenance stage, k is the total number of material types required for repairs and replacement, r_i the amount of building material i that needed to be replaced or used for repairs (kg), $f_{m,i}$ is the carbon emission coefficient of type i material (kgCO₂/kg), Y is the assumed lifespan of the building (years) and R the renewal or repair interval (years) of material i . The value (Y/R) is the replacement factor of the material considered[18].

3.3.5 Carbon emissions at deconstruction

The carbon emissions at the deconstruction stage, C_D can be regarded as the summation of carbon emissions for demolition, transportation to landfill and recycling which is given as[30]:



$$C_D = \sum_{i=1}^m (Q_{d,i} \times f_{d,i}) + \sum_{i=1}^p (m_d \times D_d \times f_{t,i}) - \sum_{i=1}^r (m_r \times w_r \times f_{m,i}) \quad \dots (7)$$

The carbon emissions due to building demolition is given by the component $\sum_{i=1}^m (Q_{d,i} \times f_{d,i})$, where m is the total number of demolition activities, $Q_{d,i}$ and $f_{d,i}$ are the quantity and carbon emission coefficient of demolition activity respectively.

The carbon emissions due to the transportation of demolished material is given by the component $\sum_{i=1}^p (m_d \times D_d \times f_{t,i})$, where p is the total number of demolished materials, m_d the weight of demolished material to be transported for landfill or recycling (kg), D_d the distance from the demolition site to the landfill

site or recycling facility (km) and $f_{t,i}$ is the carbon emission coefficient for unit material transported over unit distance of type i material ($\text{kgCO}_2/\text{kg.km}$).

The carbon emissions due to recycling of materials is given by the component $\sum_{i=1}^r (m_r \times w_r \times f_{m,i})$, where r is the total number of recyclable material, m_r is the weight of recyclable material i (kg), w_r the proportion of recycling and $f_{m,i}$ the carbon emission coefficient of the type i recyclable material (kgCO_2/kg). The data related to building demolition, disposal and recycling are taken from the literature on similar studies and, whenever available, the existing practices in Sri Lanka are considered.

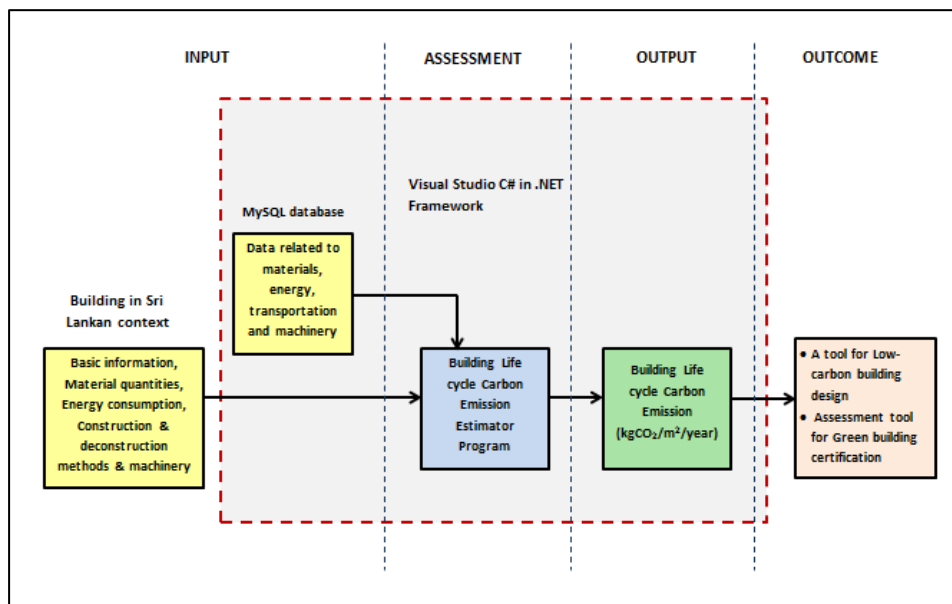


Figure 2 - The conceptual model for the building life cycle carbon emission estimation tool.

4. Development of the carbon emission estimator tool

The development of the building carbon emission estimation tool will be carried out in two stages; development of carbon emission database and development of the estimator program including the user interface.

4.1 Development of carbon emission database

The data needed for computing carbon emission of each life cycle phase according to equations (2) to (7) are of four types; energy, materials, transportation and construction activities. The lack of data availability for energy and carbon emission related studies has been a major challenge to the researchers of the developing countries. The carbon emission

coefficients for the relevant energy sources are referred from Sri Lankan and international data sources [1], [45], [46]. The embodied energy coefficients for building materials are taken from recent research literature and international databases [12], [47] and converted to the carbon emission coefficients by using the average carbon emission factor for Sri Lanka which is described in section 3.5.1. A similar approach in 'localization of data' has been followed in previous research [19], [43]. Transportation and machinery data are collected from research literature and by consulting construction professionals in Sri Lanka. In selecting most appropriate data, recent data from Sri Lanka and Asian countries with similar construction practices are given priority.

MySQL database management software is used to create the carbon emission database, which can be easily integrated with the estimator programme.

4.2 Development of carbon emission estimator program

The carbon emission estimator programme is developed using Visual Studio C# programming language in the .NET Framework. The model for developing the proposed tool is illustrated in Figure 2. The user interface of the program is developed using Visual Studio C# forms application. Upon entering the program, a user has to provide two types of input manually; (1) basic information of the project such as project name, location, type of building, type of structure, number of floors, gross floor area and building life span (2) building life cycle information such as major material quantities and annual energy consumption.

Using this data the building life cycle carbon emission estimator program calculates the carbon emissions of the each life cycle stage by using the programmed formula and the carbon emission database. As the output the total building life cycle carbon emission is given in kgCO₂/m²/year. The carbon emissions of different life cycle stages and material types can be viewed both in tabular and graphical forms, facilitating easy comparison of the results. The proposed tool can be used for multiple purposes. Low-carbon building design, evaluation of alternative project solutions and as an assessment tool in green building certification are a few among these.

5. Conclusion

This study aims at developing the initial framework and the conceptual model for a computerized building life cycle carbon emission estimation program in the context of Sri Lanka. The framework is based on a cradle-to-grave building life cycle assessment. The proposed tool integrates a computerized database and an automated estimator program with a user-friendly interface. The concept of the major building materials, which are responsible for 80% of carbon emission in a typical Sri Lankan building, is used for developing the tool. Due to the lack of country-specific energy and carbon emission data, the data taken from recent literature and international databases are adjusted to match

the unique conditions of the country. After the development of the proposed tool, it will be verified by using several case study buildings in Sri Lanka. The database will need periodical revision due to the changes in energy and carbon emission values in future. This tool can be used in different life cycle stages for multiple purposes including low-carbon building design and green building certification, hence promoting sustainable building practices in Sri Lanka.

References

1. United Nations Environment Programme, "Common Carbon Metric: Protocol for Measuring Energy Use and Reporting Greenhouse Gas Emissions from Building Operations", 2010.
2. Intergovernmental Panel on Climate Change, "Climate Change 2007: Synthesis Report", *Contribution of Working Groups I, II and III to the Fourth Assessment Report of the Intergovernmental Panel on Climate Change, Core Writing Team, Pachauri, R.K and Reisinger, A (eds.). IPCC, Geneva, Switzerland.* 2007.
3. Kim, S., Lee, S., Na, Y. J., Kim, J. T. "Conceptual Model for LCC-based LCCO2 Analysis of Apartment Buildings", *Energy Build.*, Vol. 64, 2013, pp. 285-291.
4. UNEP SBCI (Sustainable Buildings and Climate Initiative), Buildings and Climate Change. United Nations Environment Programme, 2009.
5. Junnila, S., "The Environmental Impact of an Office Building throughout its Life Cycle", *PhD Thesis -Helsinki University of Technology*, 2004.
6. Suzuki, M., Oka, T., "Estimation of Life Cycle Energy Consumption and CO₂ Emission of Office Buildings in Japan", *Energy Build.*, Vol. 28, No. 1, 1998, pp. 33-41.
7. Adalberth, K., Almgren, A., Petersen, E. H., "Life-Cycle Assessment of Four Multi-Family Buildings", *Int. J. Low Energy Sustain. Build.*, Vol. 2, 2001, pp. 1-21.
8. Ding, G. K. C., "Sustainable Construction-The Role of Environmental Assessment Tools", *J. Environ. Manage.*, Vol. 86, No. 3, 2008, pp. 451-464.
9. Survey of Construction Industries 2013, Department of Census and Statistics Sri Lanka, 2015.



10. "Innovative, Energy Efficient Building Concepts", [Online]. Available: <http://www.energy.gov.lk/your-business/building-energy/energy-efficient-building-design>, Accessed : May 7, 2017.
11. Green SI ® Rating System for Built Environment, Green Building Council of Sri Lanka, 2015.
12. "Inventory of Carbon and Energy (ICE) Version 2.0", University of Bath, UK, 2011.
13. Abeyundara, U. G. Y., Babel, S., Gheewala, S. H., "A Matrix in Life Cycle Perspective for Selecting Sustainable Materials for Buildings in Sri Lanka", *Build. Environ.*, Vol. 44, No. 5, 2009, pp. 997-1004.
14. Kofoworola, O. F., Gheewala, S. H., "Life Cycle Energy Assessment of a Typical Office Building in Thailand", *Energy Build.*, Vol. 41, No. 10, 2009, pp. 1076-1083.
15. Ramesh, T., Prakash, R., Shukla, K. K., "Life Cycle Energy Analysis of a Residential Building with different Envelopes and Climates in Indian Context", *Appl. Energy*, Vol. 89, No. 1, 2012, pp. 193-202.
16. Pinky Devi, L., Palaniappan, S., "A Case Study on Life Cycle Energy Use of Residential Building in Southern India", *Energy Build.*, Vol. 80, 2014, pp. 247-259.
17. Ruuska, A., "Role of Embodied Energy, Operational Energy and Related Greenhouse Gas Emission of Buildings in the Context of Developing Tropical Countries", in *SB13 Singapore-Realising Sustainability in Tropics*, 2013, pp. 205-211.
18. Chau, C. K., Yik, F. W. H., Hui, W. K., Liu, H. C., Yu, H. K., "Environmental Impacts of Building Materials and Building Services Components for Commercial Buildings in Hong Kong", *J. Clean. Prod.*, Vol. 15, No. 18, 2007, pp. 1840-1851.
19. González, M. J., García Navarro, J., "Assessment of the Decrease of CO2 Emissions in the Construction Field through the Selection of Materials: Practical Case Study of Three Houses of Low Environmental Impact", *Build. Environ.*, Vol. 41, No. 7, 2006, pp. 902-909.
20. Dias, W. P. S., Pooliyadda, S. P., "Quality Based Energy Contents and Carbon Coefficients for Building Materials: A Systems approach", *Energy*, Vol. 29, No. 4, 2004, pp. 561-580.
21. Tae, S., Shin, S., Woo, J., Roh, S., "The Development of Apartment House Life Cycle CO2 Simple Assessment System using Standard Apartment Houses of South Korea", *Renew. Sustain. Energy Rev.*, Vol. 15, No. 3, 2011, pp. 1454-1467.
22. Roh, S., Tae, S., Suk, S. J., Ford, G., Shin, S., "Development of a Building Life Cycle Carbon Emissions Assessment Program (BEGAS 2.0) for Korea's Green Building Index Certification System", *Renew. Sustain. Energy Rev.*, Vol. 53, 2016, pp. 954-965.
23. Roh, S., Tae, S., Shin, S., Woo, J., "Development of An Optimum Design Program (SUSB-OPTIMUM) for the Life Cycle CO2 Assessment of an Apartment House in Korea", *Build. Environ.*, Vol. 73, 2014, pp. 40-54.
24. Aden, N., Qin, Y., Fridley, D., "Lifecycle Assessment of Beijing- Area Building Energy Use and Emissions : Summary Findings and Policy Applications", China Energy Group, Energy Analysis Department, Environmental Energy Technologies Division, Lawrence Berkeley National Laboratory, September, 2010.
25. Baek, C., Park, S. H., Suzuki, M., Lee, S. H., "Life Cycle Carbon Dioxide Assessment Tool for Buildings in the Schematic Design Phase", *Energy Build.*, Vol. 61, 2013, pp. 275-287.
26. Roh, S., Tae, S., "Building Simplified Life Cycle CO2 Emissions Assessment Tool (B- SCAT) to Support Low- Carbon Building Design in South Korea", *Sustainability*, Vol. 8, No. 6, 2016.
27. Fu, F., Luo, H., Zhong, H., Hill, A., "Development of a Carbon Emission Calculations System for Optimizing Building Plan Based on the LCA Framework", *Math. Probl. Eng.*, 2014.
28. Kwok, K., "Assessment of Building Lifecycle Carbon Emissions", *PhD Thesis - Univ. Kansas*, 2013.
29. Li, X., Yang, F., Zhu, Y., Gao, Y., "An Assessment Framework for Analyzing the Embodied Carbon Impacts of Residential Buildings in China", *Energy Build.*, Vol. 85, 2014, pp. 400-409.
30. Li, D., Cui, P., Lu, Y., "Development of An Automated Estimator of Life-Cycle Carbon Emissions for Residential Buildings: A Case Study in Nanjing, China", *Habitat Int.*, Vol. 57, 2016, pp. 154-163.
31. Peng, C., "Calculation of a Building's life Cycle Carbon Emissions Based on Ecotect and Building Information Modeling", *J.*

- Clean. Prod.*, Vol. 112, 2014, pp. 453–465.
32. Knight, D., AddisB., “Embodied Carbon Dioxide as a Design Tool – A Case Study”, in *Proceedings of ICE - Civil Engineering*, Vol. 164, Nov. 2011.
 33. Moncaster, A. M., Symons, K. E., “A Method and Tool for ‘Cradle to Grave’ Embodied Carbon and Energy Impacts of UK buildings in Compliance with the New TC350 standards”, *Energy Build.*, Vol. 66, 2013, pp. 514–523.
 34. Kang, H. J., “Development of a Systematic Model for An Assessment Tool for Sustainable Buildings Based on a Structural Framework”, *Energy Build.*, Vol. 104, 2015, pp. 287–301.
 35. Scheuer, C., Keoleian, G. A., Reppe, P., “Life Cycle Energy and Environmental Performance of a New University Building: Modeling Challenges and Design Implications”, *Energy Build.*, Vol. 35, No. 10, 2003, pp. 1049–1064.
 36. Biswas, W. K., “Carbon Footprint and Embodied Energy Assessment of Building Construction Works in Western Australia”, *Int. J. Sustain. Built Environ.*, Vol. 3, 2014, pp. 179–186.
 37. Dong, Y. H., Jaillon, L., Chu, P., Poon, C. S., “Comparing Carbon Emissions of Precast and Cast-in-situ Construction Methods - A Case Study of High-Rise Private Building”, *Constr. Build. Mater.*, Vol. 99, 2015, pp. 39–53.
 38. “ISO 14040-Environmental Management - Life Cycle Assessment - Principles and Framework”, International Organization for Standardization, 1997.
 39. Roh, S., Tae, S., Shin, S., “Development of Building Materials Embodied Greenhouse Gases Assessment Criteria and System (BEGAS) in the Newly Revised Korea Green Building Certification System (G-SEED)”, *Renew. Sustain. Energy Rev.*, Vol. 35, 2014, pp. 410–421.
 40. Atmaca, A., Atmaca, N., “Life Cycle Energy (LCEA) and Carbon Dioxide Emissions (LCCO2A) Assessment of Two Residential Buildings in Gaziantep, Turkey”, *Energy Build.*, Vol. 102, 2015, pp. 417–431.
 41. Chau, C. K., Leung, T. M., Ng, W. Y., “A Review on Life Cycle Assessment, Life Cycle Energy Assessment and Life Cycle Carbon Emissions Assessment on Buildings”, *Appl. Energy*, Vol. 143, No. 1, 2015, pp. 395–413.
 42. “Sri Lanka Energy Balance 2015-- An Analysis of Energy Sector Performance”, Sri Lanka Sustainable Energy Authority, 2015.
 43. Aye, L., Ngo, T., Crawford, R. H., Gammampila, R., Mendis, P., “Life Cycle Greenhouse Gas Emissions and Energy Analysis of Prefabricated Reusable Building Modules”, *Energy Build.*, Vol. 47, 2012, pp. 159–168.
 44. Zhang, X., Wang, F., “Life-Cycle Assessment and Control Measures for Carbon Emissions of Typical Buildings in China”, *Build. Environ.*, Vol. 86, 2015, pp. 89–97.
 45. “IEA Statistics: CO2 Emissions from Fuel Combustion”, International Energy Agency, 2015.
 46. “Emission Factors for Greenhouse Gas Inventories”, US EPA Center for Corporate Climate Leadership, April, 2014.
 47. “Embodied Energy Coefficients”, Centre for Building Performance Research (CBPR), School of Architecture, Victoria University of Wellington, New Zealand. 2007.



Upgrading of the Existing Sedimentation Tank at Hemmathagama Water Supply Scheme

L. Wijesinghe and D.R.I.B. Werellagama

Abstract: Demand of a water supply scheme may exceed designed production capacity due to elapsing of design period, population growth, changing consumption patterns and water service extensions to adjoining areas. With increasing demand, existing water supply schemes need upgrading. Financial and time constraints should be resolved for best augmentation strategy. Efficiency of existing unit processes need increasing. With long settling times, large sedimentation tanks require large investment and longer construction period. This study researched capacity upgrading of plain sedimentation tank at Hemmathagama water supply scheme (HWSS) in 2005. Sediment removal efficiencies were compared for clarifier design discharge of 1000 m³/day and augmented discharge of 4000 m³/day. A conceptual design was proposed to improve the solid particles removal efficiency for increased flow rate in the same plain sedimentation tank by fixing plate settlers. Plate settler modules were designed and constructed. Removal efficiency was evaluated. Influent and effluent turbidity were measured weekly for six months; for three scenarios, namely plain sedimentation tank with 1000 & 4000 m³/day flow rates and same tank with plate settler for 4000 m³/day flow rate. Results showed that the plain sedimentation tank at HWSS could achieve 86% reduction of turbidity, when operated with the design flow rate of 1000 m³/day. Only 27% reduction of turbidity could be achieved when the design flow rate was increased by four times up to 4000 m³/day. When a properly designed plate settler module was fixed to the existing plain sedimentation tank, it achieved 82% reduction of turbidity with the increased flow rate of 4000 m³ /day. It was demonstrated that using a plate settler; the existing plain sedimentation tank at HWSS could be upgraded to cater for an increased flow rate, which is four times of its original design flow. Performance in 2017 (after 10 years in operation) is also reported.

Keywords: water treatment, high rate sedimentation, plate settlers

1. Introduction

The production capacity of a water supply scheme is decided considering the consumers within a defined service boundary and a specified design horizon [1]. The demand of the water supply scheme often exceeds the production capacity due to elapsing of design period, unpredicted population growth, changes in consumption pattern and requests for extensions to the adjoining areas. To cater for the increasing demand the existing water supply scheme can be augmented. When selecting the best augmentation strategy financial and time constraints must be resolved. Often there is no money available and the plant cannot be taken offline as it is already serving the consumers. Therefore, the engineer should plan to increase the efficiency of the existing unit processes as far as possible. This study showed the feasibility to carry out applied research on the full-scale model, under Sri Lankan (tropical) conditions, without disrupting the water supply.

Due to the long settling time needed, rectangular or circular sedimentation tanks are very large, thereby occupying large areas compared to the treatment plant area. Since the settling efficiency largely depends on the surface area of the sedimentation tank, further increasing settling area to upgrade the treatment plant capacity is a very difficult option due to financial and space constraints. Using tube or plate settlers, an internationally accepted option (relatively new to Sri Lanka in 2005) to increase the sedimentation efficiency was investigated in this study, to increase the settling efficiency in a working plant, within few weeks, with a limited budget.

Eng. (Dr.) D.R.I.B. Werellagama Int. PEng. (SL), C. Eng., MIE (SL), CMEngNZ, B.Sc. Eng. (Peradeniya), M.Eng. (AIT), Dr. Eng. (Nagoya), Principal Lecturer in Civil Engineering, School of Engineering, Wellington Institute of Technology, New Zealand.

Eng. Lalith Wijesinghe, C.Eng., MIE(SL), B.Sc. Eng. (Peradeniya), M.Sc.Eng. M.Eng. (AIT), MBA, District Manager (World Bank Funded Water Supply and Sanitation Improvement Project), National Water Supply and Drainage Board, Kegalle, Sri Lanka.



Plate settler technique has been successful in developed countries (with different feed waters and temperatures). As plate/tube settlers do not require any mechanical devices, except for a mechanical sludge scraper (required in any large clarifier), authors attempted a full-scale trial in 2005 as a cost effective option for water plant upgrading under local conditions. Presently (2017) Plate settlers are well accepted in Sri Lankan water treatment plants.

The objective of this 2005 study was studying possible capacity increase at Hemmathagama Water Supply Scheme (HWSS) after fixing plate settlers designed by authors, to the existing plain sedimentation tank. Quality parameter monitored was turbidity removal efficiency. Chemical coagulation and flocculation was not introduced to the HWSS, saving capital and maintenance costs.

The scope of this study was to:

- * Study the sediment removal efficiency of the existing plain sedimentation tank at HWSS for its design flow rate of 1000 m³/day and for an increased flow rate of 4000 m³/day.
- * If increased flow deteriorated water quality, then to propose a conceptual design to improve the solid particles removal efficiency in the same plain sedimentation tank, by fixing plate settlers (for the increased flow rate).
- * Carry out actual design, identify construction materials and locally construct an actual (Full) scale model.
- * Evaluate the removal efficiency for flow rate 4000m³/day after fixing the locally manufactured plate settlers in existing tanks.
- * Evaluate the turbidity removal efficiency for flow rate 4000m³/day in 2016 (after 10 years of fixing the plate settlers in existing tanks), to assess the reliability of introduced low-cost technology.
- * Evaluate the durability of the designed plate settlers after 10 years of operation.

2. Literature Survey

2.1. Sedimentation Theory

Sedimentation uses gravitational settling principle. Efficiency of sedimentation process relates to inlet water quality, particle/floc size and weight, tank geometry, etc. In a conventional sedimentation tank, the flow is usually horizontal. The main design criteria for a sedimentation tank with horizontal flow are the surface loading rate (discharge/surface area = Q/A), adequate depth and detention time for settling, suitable horizontal flow velocity and

weir loading rate to minimize turbulence to avoid re-suspension of settled particles [2]. Settling basins require large land areas. Plant upgrades increasing water demand are constrained by land availability. High-rate settler modules can be installed underwater in flow channels, increasing the tank loading rate without adding basin volume [3].

Shallow basins provide the same settling as deep basins. But horizontal shallow basins are subject to scouring action of the flow-through velocity and wind action, lowering removal efficiency. If horizontal shallow basins are stacked to reduce plant surface area, sludge removal becomes difficult. Therefore, plate settlers are designed to be vertically inclined. Settled solids can slide down inclined surfaces and drop into the basin below. Distance between plates is designed to provide an up-flow velocity lower than the setting velocity of the particles, allowing particles to settle on the inclined plate surfaces. The effective settling area is the horizontal projected area of the plate, calculated by multiplying the inclined area; by cosine of the angle of the plate to horizontal. Total settling area is the sum of the effective areas of each plate [4]. Depending on the type of plate setting modules, water enters either horizontally parallel to the plates or upward along the 60° tilted plates [5].

Main design criterion for plate settlers is the surface loading rate for each plate. Typical loading rates for plates range from 0.7 to 1.7 m/h, depending on the settling characteristics of the solids, water temperature, and desired effluent quality. These loading rates allow for overall basin loading from 5 to 15 m/h, which is a multiple of conventional basin loading rate [4]. Commercially available Plate settlers are typically manufactured in modules. Dimension of modules and plates vary by manufacturer and are proprietary (and therefore expensive). Basin dimensions are controlled by sludge removal method. In this 2005 research work, design was done in-house and plate modules were manufactured locally.

Materials selection for fabrication of settler modules is important. Plates can be made of plastic, wood, galvanized steel, and asbestos – cement. Each of them has its advantages and limitations. Asbestos – cement plates must be coated with plastic or a similar type of coating material to prevent corrosion from alum treated water. Galvanized steel needs anti-corrosive coatings. Wood needs preservatives and should

be cleaned often as sludge does not slide easily on wood [2]. Modules fabricated with paper-thin PVC plates were said to be deteriorate within 10 to 15 years due to weathering and wave actions in the basins. Settler modules made with thick plastic plates are more durable and may have a module height over 2m [5]. In this study 10 mm thick PVC sheets were selected, inclined by 60°.

3. Project Description

The Hemmathagama Water Supply Scheme (HWSS) is located 16km away from the Mawanella town, in Kegalle district. The existing water supply scheme constructed in year 2000 comprised an intake at Asupini Ella, a plain sedimentation tank without pre-treatment by coagulation/flocculation and a distribution network providing 1000 m³/day to Hemmathagama town and suburbs. By 2004 about 1000 service connections were provided by HWSS and the NWS&DB had to stop providing service connections as the production capacity was barely sufficient to supply the demand of existing customers. There were many requests for new service connections and pipe line extensions. A demand survey revealed that capacity of the HWSS needed to be increased to 4000 m³/day.

In 2005 funds were allocated to construct a new intake at a higher elevation at Asupini Ella and replace the existing 150 mm diameter GI raw water gravity main with 225 mm diameter uPVC pipes to increase inflow to the treatment plant. Sadly, no funds were allocated for capacity improvement of the treatment works.

Data collection for this study started from January 2005. Then discharge through the plant was 1000 m³/day (full design capacity). Samples were collected weekly for turbidity measurement, for six months. The WTP was performing well during this period (Table 1.1). In July 2005 construction of intake and new raw water main was completed. The discharge through the WTP increased to 4000 m³/day. From July 2005 NWS&DB started distributing the increased volume but without augmenting the treatment plant capacity. Samples collected weekly for turbidity measurement from July to December 2005 (Table 1.2) show water quality deteriorating with quadrupled discharge (existing plain sedimentation tank was overloaded). While augmenting the existing treatment plant was desirable, it was impossible to design and construct a plant with

full treatment within the limited budget allocation. Also, acquiring new lands to construct new civil structures within allocated time was impossible, and no usable land was available within the HWSS. Considering the inadequacy of funds to acquire lands & the limited time available to complete the augmentation, a plate settler module was considered for existing plain sedimentation tank to increase plant capacity to 4000 m³/day.

The plate settlers were designed by authors, fabricated and fixed within the month of January 2006 and samples were collected weekly for turbidity measurements from February 2006 to July 2006. As shown in table 1.3, it was observed that the performance of the sedimentation tank with plate settlers for a discharge of 4000m³/day met the required standard (of Turbidity less than 2 NTU).

4. Methodology

4.1 Sampling

Samples were collected from influent & effluent of the sedimentation tank at HWSS (without coagulation and flocculation) for three different scenarios and the turbidity was measured. Samples were collected in 250ml sterilized glass bottles. One sample each from influent and effluent of the plain sedimentation tank were collected (weekly) from first week of January 2005 to final week of June 2005 with volume flow rate at 1000m³/day. After discharge was increased up to 4000 m³/day, without modifying the plain sedimentation tank, one sample each from influent and effluent of the plain sedimentation tank were collected weekly from first week of July 2005 to final week of December 2005. Plate settlers were designed, assembled in to modules and fixed to the existing plain sedimentation tank in January 2006. One sample each from influent and effluent of the sedimentation tank were collected weekly from February 2006 to July 2006 with discharge at 4000 m³/day. Samples were transported to the district laboratory and the turbidity was measured. These (2005) results were used to assess the viability of installing plate settlers as plant capacity augmentation option.

To assess performance of plate settlers after 10 years, one sample each from influent and effluent of the sedimentation tank were collected monthly from January 2017 to June 2017 with discharge kept constant at 4000 m³/day (Table 1.4).



4.2 Turbidity measurement

The turbidity of the collected samples was measured using HACH Model 2100P turbidimeter. These results are tabulated in Tables 1.1, 1.2, 1.3 and 1.4. The HACH Model 2100P Portable Turbidimeter measures turbidity (in manual mode) in three ranges; 0.001 to 9.99, 10 to 99 and 100 to 1000 NTU [6].

4.3 Flow measurements

The flow rate to the sedimentation tank at HWSS was measured using the Arkon-iMag magnetic type flow meter fixed to the inlet line. The flowmeter shows Flow Rate (L/s or m³/hr) with Accuracy $\pm 0.5\%$ of reading [7].

4.4 Physical observations

Physical observations were made on PVC plates and fixing arrangement for durability.

Table 1 - Turbidity data for 3 Experimental Scenarios (2005-6) and 10 years later (2017)

Table 1.1 Turbidity in NTU in existing Plain Settling Tank for 1000m³/day design flow				Table 1.2 Turbidity in NTU in existing Plain Settling Tank for 4000m³/day augmented flow				Table 1.3 Turbidity in NTU with Settling tank improved with Plate Settlers for 4000m³/day increased design flow			
Date 2005	Inflow (NTU)	Outflow (NTU)	% Removal	Date 2005	Influent (NTU)	Effluent (NTU)	% Removal	Date 2006	Influent (NTU)	Effluent (NTU)	% Removal
05/1	25.0	1.9	92	05/7	6.0	4.0	27	03/2	6.5	1.3	80
13/1	30.0	2.0	93	12/7	8.0	6.0	25	12/2	7.3	1.9	74
18/1	15.5	1.8	88	17/7	7.8	5.8	26	24/2	6.4	1.2	81
25/1	17.0	1.9	89	24/7	4.8	2.5	48	07/3	8.0	1.6	80
09/2	0.7	0.6	14	04/8	7.6	5.6	26	15/3	8.8	1.8	80
18/2	6.5	1.5	77	12/8	8.0	5.7	29	27/3	6.0	1.1	82
25/2	5.5	1.3	76	17/8	8.3	6.3	24	02/4	8.0	1.7	79
13/3	8.8	2.0	77	27/8	2.8	2.0	29	10/4	6.1	1.0	84
19/3	8.0	1.9	76	06/9	6.2	4.5	27	18/4	4.0	1.0	75
27/3	8.5	1.9	78	13/9	7.4	5.9	20	29/4	7.5	1.2	84
05/4	8.0	1.9	76	21/9	4.2	2.1	50	05/5	3.8	0.9	76
10/4	6.1	1.3	79	26/9	7.5	6.0	20	10/5	8.3	1.9	77
19/4	6.1	1.0	84	06/10	8.1	5.0	28	17/5	6.0	1.0	83
25/4	8.8	2.0	77	14/10	7.6	5.7	25	26/5	7.6	1.3	83
04/5	3.5	1.0	71	19/10	5.3	3.1	42	06/6	25.0	4.0	84
09/5	8.2	1.5	82	25/10	9.7	5.9	39	11/6	20.0	3.1	84
19/5	8.1	1.2	85	05/11	5.4	3.1	43	18/6	13.5	2.0	85
25/5	8.0	1.8	77	18/11	8.0	5.0	38	26/6	12.0	1.9	84
07/6	16.3	1.6	90	17/11	17.0	12.0	26	07/7	15.8	2.3	85
13/6	25.0	1.9	92	26/11	20.0	15.4	23	09/7	20.0	3.2	84
16/6	7.8	1.4	82	07/12	9.3	4.8	48	15/7	6.0	1.0	83
27/6	7.4	1.0	86	15/12	8.5	6.4	25	25/7	7.8	1.3	83
				23/12	30.0	22.0	27				
				28/12	25.0	19.0	24				
All Effluent turbidity values satisfied SLS614(1983) Maximum desirable water quality value of 2 NTU				All Effluent turbidity values except on 27/8/2005 failed SLS614(1983) Maximum desirable water quality limit of 2 NTU				All Effluent turbidity values satisfied SLS614(1983) Maximum desirable water quality value of 2 NTU			

Table 1.4			
Turbidity in NTU after 10 years operation with Plate Settlers for 4000 m³/day flow			
<i>Date</i>	<i>Influent (NTU)</i>	<i>Effluent (NTU)</i>	<i>% Removal</i>
05/1	2.0	1.5	25
06/2	6.3	1.6	75
04/3	13.0	1.9	85
04/4	12.5	1.8	85
06/5	2.4	1.9	21
03/6	2.4	1.8	25
<i>All Effluent turbidity values satisfied SLS614 (1983) Maximum desirable water quality value of 2 NTU</i>			

5. Results and Discussion

The observations are shown in the Tables 1.1, 1.2, 1.3 & 1.4. The relevant data of final design are given (and compared with literature values) in Table 2. Table 1.1 gives effluent turbidity when discharge was 1000 m³/day. The percentage reduction of turbidity was more than 70% always (Figure 1) and the effluent turbidity was within the maximum desirable level of SLS 614 (1983).

When the discharge increased to 4000 m³/day (without modifying the existing sedimentation tank), the values of the major design parameters shifted out of the recommended ranges. The percentage reduction of turbidity (for this case) is tabulated in Table 1.2. Except one sample with the minimum raw water turbidity (2.8 NTU) all other samples failed to achieve the desirable treatment level. The effluent water quality deteriorated. The percentage reduction of turbidity ranged from 20% to 50% with varying raw water turbidities, the average percentage reduction being 27.3 % only.

The above findings showed that the turbidity of raw water can be reduced to maximum desirable level {SLS 614 (1983) standard} by sending the raw water at designed flow rate through a properly designed plain sedimentation tank. When discharge increased, shifting the surface loading beyond recommended range, the same plain

sedimentation tank could not reduce the turbidity to meet required standard (<2NTU).

As the remedial measure, Plate Settlers were designed and fixed to the existing plain sedimentation tank. The design was carried out following design recommendations by Vigneswaran & Viswanathan (1995) [2]; ASCE & AWWA (2005) [4], Kawamura (2000) [5] and NWS&DB Design Manual D3 (1989) [8]. Pre-treatment was not introduced.

- Surface loadings of the tank and plate settlers for 4000 m³/day flow rate were calculated and verified against above design recommendations. The design surface loading in the plate settler is 9.64 mm/min. It is less than 28 mm/min which is the recommended value by ASCE & AWWA [4].

- The upward velocity through the plates was calculated and checked against the design recommendations to verify it was less than the settling velocity.

- Material for the plates was selected considering the durability, non-corrosive nature & smooth texture of the surface, availability and economy.

- Angle of inclination of plates were selected as 60° satisfying the design standards.

- Detention time of plate settlers was calculated and checked against the design recommendations.

- The capacity of the existing inlet channel was checked to verify whether it could accommodate the increased flow rate. The existing inlet channel could accommodate a flow rate of 2.78 m³/s. However the design flow rate was 0.05 m³/s only.

- Inlet ports were designed to provide laminar flow in to the sedimentation basin. Recommended port velocity was 0.10 - 0.20 m/s [1]. Design flow velocity was 0.13 m/s.

- The clear height (of water) below plate settlers was provided as per the design recommendations to minimize turbulences due to localized velocity effects (Figure 4).

- The capacity of the existing outlet channel was checked to verify whether it could accommodate the increased flow rate.

- The scour chamber was checked against design recommendations.

After above calculations, Plate Settlers with following details were fixed (Figures 2, 3 and 4) to the existing plain sedimentation tank.



Design Capacity	4000 m ³ /day	Slope length of plates	1000 mm
Number of tanks	02 Nos.	Slope to horizontal plane	60°
Plate Thickness	10 mm	# Distance between plates	63 mm
Width of plates	2490 mm	# Length of the tank	9.50 m
Number of plates	101 per tank		

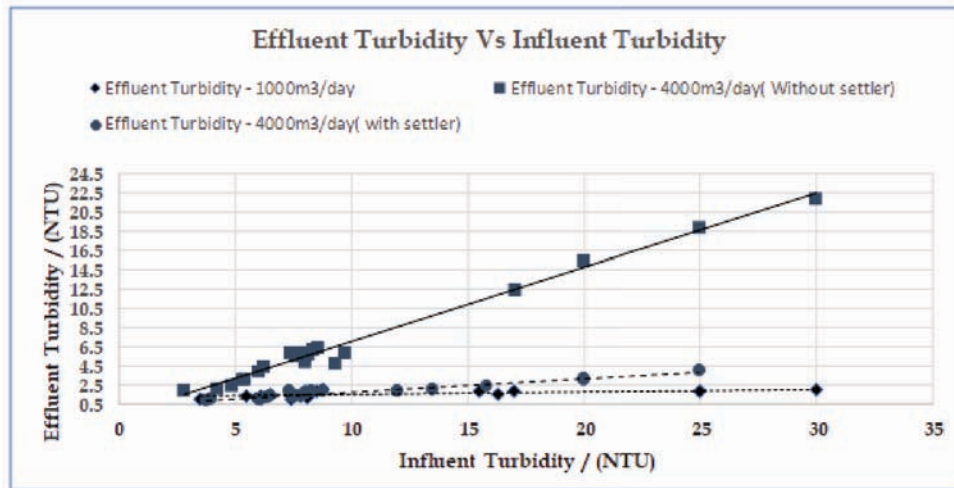


Figure 1 - Graph of Effluent Turbidity Vs Influent Turbidity for Three Different Scenarios

Table 2 - Comparison of selected values of design parameters with “recommended range for the plate settlers” for volume flow rate of 4000 m³/day

Design Criterion	Design Value (This study)	Recommended Range of Values		
		D3, NWS&DB, (1989) (with no pre-treatment)	Kawamura (2000)	ASCE & AWWA (2005)
Surface loading rate/(m/hr)	3.9	< 9.0	< 12.5	5.0 - 15.0
Surface loading in plate settler rate/(mm/min)	9.6	-	7.5 - 8.8	11.6 - 28.3
Tank depth / (m)	2.5	2.5 - 4.0	3.0 - 5.0	2.1 - 4.3
Length /width ratio	4:1	3:1 to 8: 1	4:1 to 5: 1	3:1 to 5: 1
Detention time/(min)	11	-	-	5 - 20
Weir overflow rate/ (m ³ /m.hr)	34	< 18	9.0 - 13.0	< 10
Sludge storage/ (m)	0.30	0.15 - 0.30	> 0.15	> 0.15
Upward velocity in basin / (m/s)	75.9	-	150 - 200	-
Velocity in inlet pipes/ (m/s)	0.13	< 0.2	< 0.01	< 0.3
Detention time / (min)	11	-	-	5 - 20



Figure 2 - Plate settler sedimentation tank after completion (2007)



Figure 3 - Fixing details of plate settlers

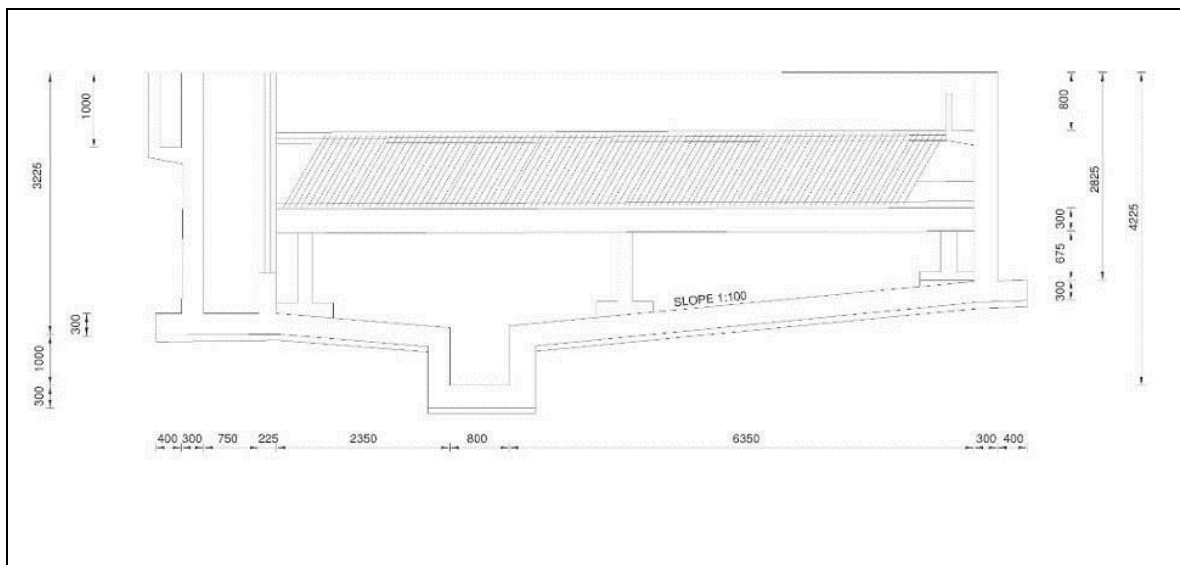


Figure 4 - Detail of Plate Settler (Section); (width is 5300mm with two channels)



Figure 5 - Plate settler sedimentation tank after 10 years



Figure 6 - Fixing details of plate settlers after 10 years



The performance of sedimentation tank with plate settler is tabulated in Table 1.3 and shown in Figure 1 too. The maximum influent raw water turbidity was 25 NTU and it was reduced up to 4 NTU, which is not within maximum desirable level but within the maximum permissible level (Turbidity reduction of 84%). The plate settlers could reduce the raw water turbidity up to the desirable level when the influent turbidity is ≤ 13.5 NTU. Turbidity reduction of more than 75% has been achieved for all the samples. Compared to the inferior performance of the plain sedimentation tank with increased flow rate (27% only), the turbidity removal significantly improved (to 82% removal) after fixing plate settlers. The whole augmentation process was achieved while the tanks were on-line too.

The performance status is further confirmed in Table 1.4 where the data of the % removal after 10 years is presented. These effluent turbidity data confirm that the plate settler continues to be a reliable technical option to remove high (and low) raw water turbidity inputs, even after a long service life.

The physical status of the plate settler (after 10 years of operation) is shown in Figures 5 and 6. The plates and the fixing arrangement are still intact except for minor discolouration of plates at few locations. This confirms that PVC plate settlers (with design values used) is a durable technical option in tropical conditions too.

6. Conclusions

The plain sedimentation tank at Hemmathagama WSS could reduce the turbidity up to the desirable level (2 NTU; SLS 614) for its design flow rate of 1000 m³/day, when the influent turbidity was less than 30 NTU, with average percentage reduction of turbidity of 86%. However, when the flow rate was increased by four times up to 4000 m³/day the quality deteriorated to 27% average percentage reduction of turbidity.

Therefore, plate settlers were designed, modules fabricated and fixed to the existing plain sedimentation tank. These plate settlers removed turbidity up to the desirable level of SLS 614 (1983) standard (for the augmented design flow 4000 m³/day), with average percentage turbidity reduction of 82%. The plate material selected was 10mm thick PVC, for availability, durability, smoothness, lightweight & low cost. Water quality testing

and physical observations made after 10 years showed that the installed plate settlers are still reliable and durable.

It was practically demonstrated (in a working full scale plant) that plate settlers can be used to upgrade the plain sedimentation tank within a short time frame without completely stopping the water supply. The upgrade produced 4 times more water in the same settling tank (with four times original design flow rate) with local design and fabrication (a limited capital input). Not having to introduce coagulation and flocculation to cater for an increased flow rate is an advantage both capital-cost wise and operations (O&M) cost wise.

Acknowledgement

Authors wish to acknowledge the assistance given by the National Water Supply & Drainage Board in preparation of this paper.

References

1. National Water Supply & Drainage Board (NWS&DB), (1989), "Design Manual D2 - Urban Water Supply & Sanitation", Sri Lanka Water Supply and Sanitation Sector project.
2. Vigneswaran, S. & Viswanathan C., (1995), "Water Treatment Processes - Simple Options", CRC press, Florida, USA.
3. MWH (Montgomery Watson Harza, Inc), (2005), "Water Treatment: Principles and Design"
4. ASCE (American Society of Civil Engineers) & AWWA (American Water Works Association), (2005), "Water Treatment Plant Design, 4th Ed.", McGraw Hill Publishing Company.
5. Kawamura S., (2000) "Integrated Design and Operation of Water Treatment Facilities", Wiley-Interscience Publishers.
6. HACH, (2005), "Model 2100P portable Turbidimeter. Instrument & Procedure Manual"
7. Arkon Flow Systems, (2005), "i-Mag Magnetic Flow Meter Manual"
8. National Water Supply & Drainage Board (NWS&DB), (1989), "Design Manual D3 - Water Quality and Treatment", Sri Lanka Water Supply and Sanitation Sector Project.
9. American Public Health Association, American Water Works Association & Water Pollution Contract Federation, (1995), "Standard Methods for the Examination of Water and Waste Water, 16th Ed."
10. Wijesinghe, L. (2007), Upgrading the existing sedimentation tank at Hemmathagama Water Supply Scheme, Unpublished Master of Engineering Thesis, Department of Civil Engineering, University of Peradeniya. (Research Supervisor Dr. D.R.I.B. Werellagama).

Risk Assessment of the Active Ingredient, Glyphosate of the Herbicide, *ROUNDUP*[®] Present in Water Sources of CKDu Prevalent Areas for Humans

S. Gunarathna, B. Gunawardana, M. Jayaweera and K. Zoysa

Abstract: Glyphosate, which is commercially available as *Roundup*[®], was the most widely used herbicide in Chronic Kidney Disease of unknown etiology (CKDu) prevalent areas in Sri Lanka until recently; hence, it has still been persistent in the soil and water environment. Ingestion of water contaminated with Glyphosate is believed to create adverse impacts on human health. Previous studies provide evidence of the presence of Glyphosate in trace levels in urine samples of CKDu subjects. Hence, Glyphosate is suspected to be a causal factor for CKDu. Therefore, this study focuses on (1) investigating the presence of Glyphosate in water sources of CKDu prevalent areas and, (2) risk assessment based on exposure levels of Glyphosate present in water for humans to determine whether daily consumption of water contaminated with Glyphosate would create any adverse health impacts. Water samples were collected from nine shallow wells and seven surface water sources in the CKDu prevalent areas, in Anuradhapura District. Glyphosate in water was quantified using LC/MS and GC/MS. Average daily dose and hazard quotient corresponding to Glyphosate was obtained according to USEPA guidelines on risk assessment. Glyphosate was detected both in well water and surface water samples tested. Concentrations of Glyphosate measured were in the range of 3-4 µg/l and 30-45 µg/l in well water and surface water samples respectively. Hazard quotient was calculated for Glyphosate concentrations measured in all water samples. With respect to well water, a maximum hazard quotient of 0.0001 was obtained for both male and female for body weight 71 kg and 59 kg, respectively. When considering surface water, maximum hazard quotients of 0.0010 and 0.0009 were obtained for male and female for the same group of body weight respectively. In conclusion, all hazard quotients determined in this study were profoundly less than 1 indicating no adverse health impacts from Glyphosate when present in the detected levels in the water sources tested. Nevertheless, it is advisable to conduct comprehensive studies on other possible pathways of human exposure to Glyphosate, such as direct ingestion of Glyphosate due to careless handling and consumption of food contaminated with Glyphosate and/or dermal exposure etc. before Glyphosate being ruled out as a triggering factor for CKDu.

Keywords: CKDu, Exposure assessment, Glyphosate, Hazard Quotient

1. Introduction

Consumption of water contaminated with agrochemicals is implicated to be one of the triggering causes of the Chronic Kidney Disease of unknown etiology (CKDu). Glyphosate, which is commercially available as *Roundup*[®], was the widely used herbicide in Sri Lanka until recently; hence, it is still persistent in the environment. Ingestion of water contaminated with Glyphosate is believed to create adverse impacts on human health[1]. Previous studies provide evidence of the presence of Glyphosate in trace levels in urine samples of CKDu subjects[2]. Hence, Glyphosate is suspected to be a triggering factor causing CKDu.

2. Literature Review

2.1. Chronic Kidney Disease of unknown etiology (CKDu)

CKDu is one of the critical health issues prevailing in Sri Lanka and found to be widely spreading in the North Central Province. To date, CKDu prevalent area is approximately

Eng. Ms. S. Gunarathna, AMIE(SL),
B.Sc.Eng.(Moratuwa), Research Assistant, Department of
Civil Engineering, University of Moratuwa.
Eng. (Dr) (Ms.) B. Gunawardana, AMIESL, B.Sc.Eng.
(Moratuwa), M.Sc. (Auckland), Ph.D.(Auckland), Senior
Lecturer, Department of Civil Engineering, University of
Moratuwa.
Eng. (Prof.) M. Jayaweera, C.Eng., FIE(SL), B.Sc.Eng.
(Moratuwa), Ph.D.(Saitama), Professor of Civil
Engineering, Department of Civil Engineering, University
of Moratuwa.
Mr. K. Zoysa, B.Sc. (Banglore), M.Sc. (Colombo),
Analytical Chemist, Department of Civil Engineering,
University of Moratuwa.



17,000 km²[3]with reported morbidities and mortalities over 400, 000 and approximately 20, 000respectively[1]. Majority of the reported CKDu victims is males above 40 years, whose occupation is farming [4].

The exact causal factors for the CKDu have not yet been determined. However, direct ingestion of toxins due to careless handling of agrochemicals, ingestion of toxins that are being absorbed/accumulated by various edible products and prolonged exposure to toxins through drinking water consumption is considered as potential pathways that are likely to cause CKDu[5]. Since the majority of the reported CKDu victims is from the farming communities and also above the age of 40 years, it is suspected that drinking water contamination due to agrochemicals (e.g. pesticides, herbicides) could be a leading cause of the disease[4].

2.2. Glyphosate

Glyphosate [N-(phosphonomethyl)glycine] is a broad-spectrum systemic herbicide and crop desiccant that has been widely used in the CKDu prevalent areas. Glyphosate is commercially available as the herbicide "Roundup®" which is a very powerful weed killer used worldwide for the past few decades due to its high effectiveness in weed killing [6].

Glyphosate is known to be strongly sorbed by soil minerals [7] showing a greater affinity to sorb onto variable-charge surfaces and not onto permanent-charge sites present on the soil surfaces [7].The sorption of Glyphosate depends on various factors such as soil organic matter, cation exchange capacity of the soil, minerals present in the soil matrix, soil type, pH and various cations that are present in the soil matrix[7].In addition, Glyphosate has shown a greater affinity to create bonds with trivalent cations such as Al³⁺ and Fe³⁺thus, the main sorption sites in the soil matrix for Glyphosate retention were reported as the surfaces of amorphous aluminium and iron oxides [7].

Glyphosate degradation occurs mainly due to the microbial activity of the soil microorganisms[8]. Microbial transformation of Glyphosate degrades the Glyphosate molecules to Aminomethylphosphonic acid (AMPA), which is the major derivative of Glyphosate due to direct cleavage of the C-N bond [8]. However, strong sorption characteristics of Glyphosate onto soil could have a negative

impact on the degradation of Glyphosate, where decreased levels of degradation of Glyphosate is expected when sorption affinity of Glyphosate onto soil matrix is strong [7].

Glyphosate can be mobilized into surface water sources as solutes or free compounds and as combined with the colloidal particles present in the top soil layers which get carried away with the surface runoff during the rainfall events[9]. However, due to the strong adsorption affinity of Glyphosate onto soil particles, percolation of Glyphosate into groundwater through the vertical soil profile is considered to be significantly low compared to the Glyphosate getting carried away with the surface runoff [7]. Hence, Glyphosate concentration in groundwater could be profoundly low compared to the detectable levels of Glyphosate in surface waters [9].

Glyphosate is recognized as a low acute toxic compound [10]. Nonetheless, due to the potential health risks that have been recognised with exposure to Glyphosate [10], the USEPA has imposed a maximum contamination level of 0.7 mg/L for Glyphosate when present in water [11]. In addition, the reference dose or the average daily dosage that will not create adverse effects throughout the life time is set as 2 mg/kg/day[10].

According to the WHO study conducted in the CKDu prevalent areas in Sri Lanka, the proportion of CKDu victims with a level above reference value for Glyphosate residue is 3.5%[2] Thus, Glyphosate seems to play an important role for CKDu. Furthermore, in animal studies, it was found that Glyphosate alone could cause adverse effects on Kidney function. Changes in proximal tubular cells in Kidney were observed in Nile Tilapia due to exposure to Glyphosate [12], and Ayoola et al. (2008) have noted changes in the proximal tubule, Bowman space and degenerated tubules in African catfish exposed to Glyphosate [13]. Furthermore, glutathioneperoxidase dependent reduction of cumenehydroperoxide in kidneys of rats exposed to Glyphosatehas also been observed [14]. Therefore, Glyphosate could be a triggering factor causing CKDu. However, there are no comprehensive studies reported in the literature to investigate the probable presence of Glyphosate in the water sources and the associated human health risk levels due to the consumption of waters contaminated with Glyphosate in the CKDu prevalent areas in Sri Lanka.

3. Objectives

This study focuses on (1) investigating the presence of Glyphosate in water sources of CKDu prevalent areas and, (2) risk assessment based on exposure levels of Glyphosate present in water for humans to determine whether daily consumption of water contaminated with Glyphosate would create any adverse health impacts.

4. Materials and Method

4.1 Selection of test sites and sample collection

Nine shallow wells and seven surface water sources were selected in the CKDu prevalent areas, in Anuradhapura District. All selected sites of water sources were located near the Chena cultivation sites, which have been subjected to intense application of *Roundup*[®] over long periods of time. Such sites have also been subjected to series of rainfall events, tilling, followed by cultivation of a variety of crops and application of fertilizers, especially Triple Super Phosphate. The locations of shallow wells were selected after identifying the greater possibility of seepage of percolated water from *Roundup*[®]-applied Chena cultivation sites, that would be occurring followed by the rainfall events, to the selected wells. Also, the surface water sources were selected on the basis where such surface water bodies are located in places exposed to the path of surface runoff occurring from *Roundup*[®]-applied Chena cultivation areas followed by rainfall events, and such runoff would eventually end up in the selected surface water bodies.

Water samples were collected from the selected wells and surface water sources. All water samples were properly sealed, carefully transported and stored below 4° C in the laboratory to ensure the preservation of chemical properties.

4.2 Glyphosate and AMPA analysis

Glyphosate and AMPA in water were quantified using Liquid Chromatography/Mass Spectrometer (LC/MS) Agilent 1200 Infinity series LC with G1600 series Mass Selective Detector coupled with Zorbax Eclipse XDB- C18 column was used for the quantification. Samples were derivatized using 9-fluorenylmethylchloroformate. Glyphosate

(PESTANAL[®], 98% purity) was used for the preparation of standards for the calibration and quantification.

4.3 Exposure Assessment

Exposure Assessment test was performed according to the USEPA guidelines on risk assessment [15]. Average daily dose (ADD) and hazard quotient (HQ) corresponding to Glyphosate levels detected were obtained according to equations (1) and (2) [15].

$$ADD = (C \times IR \times ED) / (BW \times AT) \quad \dots(1)$$

Where:

- ADD - Average Daily Dose
- C - Exposure Concentration (mg/L)
- IR - Ingestion Rate (L/hr)
- ED - Exposure Duration (hr)
- BW - Body Weight (kg)
- AT - Average Time period (day)

$$HQ = ADD / Rfd \quad \dots(2)$$

Where: Rfd- Reference dose (mg/kg/day)

Glyphosate concentrations measured in shallow wells and surface water sources were considered as the exposure concentration during calculations. Males and females in the age group of 20-50 were considered for the exposure assessment test due to high risk of exposure [4]. It was considered that daily consumption would be 13 and 9 cups of water by males and females, respectively, per cup volume to be 250 mL and water would be sustained in the human body for 2 hours. Average body weight for a male and female for the selected age group was considered as 71 kg and 59 kg, respectively [16]. These assumptions were used during determination of the ADD value for Glyphosate concentration present in wells and surface water sources.

5. Results and Discussion

Table 1 presents the detected levels of Glyphosate in surface water and well water samples. As shown in the results, Glyphosate was detected both in well water and surface water samples tested. Concentrations of Glyphosate measured were in the range of 3-4 µg/l and 30-45 µg/l in well water and surface water samples respectively (Table 1). Surface water sources near Chena cultivation sites 5 and 6 have been dried due to the absence of rain for long periods of time, and thus water



samples could not be collected from these two sites at the time of sampling.

Table 1 - Glyphosate concentration in wells and surface water sources

Chena Cultivation site	Glyphosate concentration in wells (µg/L)	Glyphosate concentration in surface water sources (µg/L)
1	3.94	36.00
2	ND*	38.00
3	2.80	33.00
4	ND*	45.00
5	3.90	-
6	ND*	-
7	3.60	28.00
8	ND*	34.00
9	3.70	43.00

*ND: Not detected

It is apparent that Glyphosate concentration present in well water is profoundly lower than Glyphosate concentrations detected in surface water sources (Table 1). Glyphosate is known to

Glyphosate can be mobilized into surface water sources along with the surface runoff followed by a rainfall and Glyphosate can be present as solutes and/or attached to colloidal particles [9]. Therefore, the probability of Glyphosate mobilization into surface water sources is greater compared to that of groundwater as was observed with the presence of higher concentration of Glyphosate in surface water sources compared to that in well waters.

ADD values for Glyphosate concentrations present in well water and surface water were calculated for both male and female groups. Based on the ADD values obtained, hazard quotient (HQ) was calculated for Glyphosate concentration measured in all water samples. ADD and HQ values obtained are presented in Table 2. HQ values of Glyphosate concentration present in well water were extremely lower than the HQ values for surface waters. Lower Glyphosate concentrations in well water have resulted in lower HQ values for well water. In

Table 2 - ADD and HQ values obtained for well water and surface water samples

Chena Cultivation site	Well water				Surface water			
	Male		Female		Male		Female	
	ADD (mg/kg/day)	HQ	ADD (mg/kg/day)	HQ	ADD (mg/kg/day)	HQ	ADD (mg/kg/day)	HQ
1	0.00018	0.00009	0.00015	0.00008	0.00165	0.00083	0.00137	0.00069
2	-	-	-	-	0.00174	0.00087	0.00145	0.00073
3	0.00013	0.00007	0.00011	0.00006	0.00151	0.00076	0.00126	0.00063
4	-	-	-	-	0.00206	0.00103	0.00171	0.00086
5	0.00018	0.00009	0.00015	0.00008	-	-	-	-
6	-	-	-	-	-	-	-	-
7	0.00016	0.00008	0.00014	0.00007	0.00128	0.00064	0.00107	0.00054
8	-	-	-	-	0.00156	0.00078	0.00130	0.00065
9	0.00017	0.00009	0.00014	0.00007	0.00212	0.00106	0.00164	0.00082

demonstrate a high affinity to adsorb onto soil particles [7]. Characterization of soil in the selected Chena cultivation sites showed the presence of amorphous Al and Fe oxides providing evidence of greater retention of Glyphosate onto these elements (data not shown). Thus, the strong adsorption behaviour of Glyphosate with soils in the selected sites would not permit Glyphosate to mobilize and percolate through the vertical profile of the soil to meet the groundwater sources.

summary, when considering both well water and surface water, all the HQ values obtained were profoundly less than 1 indicating no adverse health impacts from Glyphosate when present in the detected levels in the water sources tested. With respect to well water, maximum HQ of 0.0001 was obtained for both male and female groups respectively. When considering surface water, maximum HQs of 0.0010 and 0.0009 were obtained for male and female groups respectively (Table 2).

HQ values for the male population were slightly higher in surface water samples (Table 2), which could be attributed to the higher amounts of water consumptions by males compared to the females. Further, the majority of the people in the selected study areas were farmers. Hence there is a possibility that the actual amounts of water consumption would be greater than the values considered during the calculations. Therefore, HQ values for the male population could be higher than the average value considered.

6. Conclusions

In conclusion, all HQ values were profoundly lower than 1, which indicates no adverse health impact would be imposed from Glyphosate by consuming the water from the water sources tested. However, water consumption could be greater than the amounts taken during calculations due to the factors such as the prevailing dry climatic conditions and intense farming activities exposing to outdoor conditions. Hence, under such conditions, the HQ values could be greater than the obtained values in this study. Also, the reference value considered for Glyphosate is established for a healthy person, and the reference value for Glyphosate for a CKDu subject could be lower than that of the reference value. Hence, the HQ value for a CKDu subject could be greater than the values obtained. Furthermore, there are other pathways of human exposure to Glyphosate such as direct ingestion of Glyphosate due to careless handling and consumption of food contaminated with Glyphosate and/or dermal exposure etc. Therefore, it is advisable to conduct comprehensive studies on other possible pathways of human exposure to Glyphosate before Glyphosate being ruled out as a triggering factor for CKDu.

Acknowledgement

Authors wish to acknowledge the financial assistance given by the National Research Council, Sri Lanka and the Senate Research Committee Grant of the University of Moratuwa for providing funding for conducting the present study.

References

- Jayasumana, C., S. Gunatilake, and P. Senanayake, *Glyphosate, hard water and nephrotoxic metals: Are they the culprits behind the epidemic of chronic kidney disease of unknown etiology in Sri Lanka?* Int J Environ Res Public Health, 2014. **11**.
- WHO, *Investigation and evaluation of Chronic Kidney Disease of uncertain aetiology in Sri Lanka*, 2013, WHO.
- Noble, A., et al., *Review of literature on chronic kidney disease of unknown etiology (CKDu) in Sri Lanka*, 2014, Colombo, Sri Lanka: International Water Management Institute (IWMI). p. 41.
- Wanigasuriya, K., *Aetiological factors of Chronic Kidney Disease in the North Central Province of Sri Lanka: A review of evidence to-date*. Journal of the College of Community Physicians of Sri Lanka, 2012. **17**(1): p. 21-42.
- Dharma-wardana, M.W.C., et al., *Chronic kidney disease of unknown aetiology and ground-water ionicity: study based on Sri Lanka*. Environmental Geochemistry and Health, 2014. **37**(2): p. 221-231.
- Schuette, J., *Environmental fate of glyphosate., E.m.a.p. management., Editor 1998, Department of Pesticide Regulation: Sacramento, . p. 95824-5624*.
- Borggaard, O.K. and A.L. Gimsing, *Fate of glyphosate in soil and the possibility of leaching to ground and surface waters: a review*. Pest Management Science, 2008. **64**(4): p. 441-456.
- Sviridov, A.V., et al., *Microbial degradation of glyphosate herbicides (Review)*. Applied Biochemistry and Microbiology, 2015. **51**(2): p. 188-195.
- Vereecken, H., *Mobility and leaching of glyphosate: a review*. Pest Management Science, 2005. **61**(12): p. 1139-1151.
- EPA, U., *R.E.D. Glyphosate*, 1993, September.
- EPA, U., *National Primary Drinking Water Regulations, in Glyphosate*1995.
- Jiraungkoorskul, W., et al., *Biochemical and histopathological effects of glyphosate herbicide on Nile tilapia (Oreochromis niloticus)*. Environ. Toxicol, 2003. **18**: p. 260-267.
- Ayoola, S.O., *Histopathological effect of glyphosate on Juvenile African Catfish(Clarias gariepinus)*. Am. Eurasian J. Agric. Environ. Sci, 2008. **4**: p. 362-367.
- Larsen, K., et al., *Effects of sub-lethal exposure of rats to the herbicide glyphosate in drinking water: Glutathione transferase enzyme activities, levels of reduced glutathione and lipid peroxidation in liver*,



kidneys and small intestine. . Toxicol. Pharmacol.
, 2012. **34**: p. 811-818.

15. EPA, U., *Guidelines for Exposure Assessment*, 1992. p. 104.
16. WHO, *Measuring change in nutritional status; Guidelines for Assessing the Nutritional Impact of Supplementray Feeding programmes for Vulnerable Groups*, 1983.

Field-Scale Study on Treating Landfill Leachate Using Anaerobic Filters Packed with Low-Cost Filter Media

W.K.C.N. Dayanthi, B.S.R. Nanayakkara, K. Kawamoto, M.D.B.A. Premathilaka and O.V.N. Dulvin

Abstract: Though the anaerobic filters (AFs) are effective in treating landfill-leachate, it is an expensive treatment method mainly due to expensive filter materials. If low-cost materials can effectively be utilized as filter media, AFs can be made suitable for the day-to-day practice. This study included a treatment of leachate generated from a sanitary landfill model, using two types of AFs. One AF contained expensive plastic pall rings as filter media, while the other was filled with washed sea sand (WSS), dewatered alum sludge (DAS), saw dust (SD) and bio char (BC) in layers of equal thickness. The former acted as the control experiment while the latter was the experimental filter. BOD₅, COD, Nitrogenous compounds, pH, ORP, TSS, TDS, conductivity, turbidity, cations and heavy metals were analyzed for influent and effluent samples. Overall, the treatment efficiencies of TN, cations and heavy metals, especially Cu and Fe, of the experimental filter column were higher than those of the control column. Removal efficiencies of BOD and COD in the control and experimental filter columns were more or less similar. Therefore, it can be concluded that the identified low cost and locally available materials could potentially be used as efficient packing media in AFs to treat landfill-leachate.

Keywords: Field-scale experiments, Filter media, Heavy metals, Nitrogenous compounds, Organic matter

1. Introduction

Landfill-leachate is highly contaminated with carbonaceous materials, nitrogenous compounds, inorganic compounds, soluble and suspended particulate materials, heavy metals etc. It has a great potential to pollute the water bodies, streams and even ground water. Toxicity, turbidity, odor, bad taste and deposits are resulted due to the presence of heavy metals such as Zn, Pb, Ni, Cu, Cd and Fe. Therefore, treating landfill-leachate before releasing to the environment is a compulsory need.

As municipal solid waste is high in organic matters, biochemical treatments with attached growth anaerobic filters (AFs) are well suited for the leachate treatment. This process is widely used because it reduces volumes and masses of the input materials and generates useful byproducts as well.

However, the conventional packing media used in AFs are very expensive, therefore finding suitable low-cost and locally available efficient packing materials is a crucial and timely need. Dayanthi et al. [1] stated that the organic materials, namely coconut coir fiber (CCF), rice husk (RH) and rice straw (RS) and saw chips (SC) packed in separate up-flow and down-flow anaerobic filter columns were satisfactory

in treating landfill-leachate, with different media emerging as the best for different contaminants. Nanayakkara et al. [2] found that the same organic materials as layers in one media bed and inorganic waste materials, namely Dewatered Alum sludge (DAS), Sea Sand (SS), Fire wood Charcoal (FC) filled as single medium in separate experimental columns showed different efficiencies in removing different contaminants. Nanayakkara et al. [3] concluded that the filter media with a mixture of FC, SS and DAS showed high potential in removing Total-N and BOD, while it had a low potential in removing COD for both up and down flow loading conditions.

Eng.(Dr.) W.K.C.N. Dayanthi, Ph.D.(Kyoto), MEng(AIT), MEng-Moratuwa, B.Eng.(Peradeniya), C.Eng., Senior Lecturer, Department of Civil and Environmental Engineering, Faculty of Engineering, University of Ruhuna, Hapugala, Galle.

Eng. Mrs. B.S.R. Nanayakkara, BSc.Eng. (Moratuwa), C.Eng., Civil Engineer, Sri Lanka Ports Authority, MPhil Candidate, Department of Civil and Environmental Engineering, Faculty of Engineering, University of Ruhuna, Hapugala, Galle.

Prof. K. Kawamoto, Ph.D.(Tokyo), Professor, Graduate School of Science and Engineering, Saitama University, Saitama, Japan.

Eng. Mrs. M.D.B.A. Premathilaka and O.V.N. Dulvin, B.Sc. Eng.(Ruhuna), Civil Engineers, Maga Engineering Pvt. Ltd.



Therefore, this study focused on investigating the suitability of the materials, namely, washed sea sand (WSS), DAS, Bio Char (BC) and Saw Dust (SD) as filter media in field-scale anaerobic filters to treat the landfill-leachate.

2. Methodology

2.1 Experimental Set-Up and Experimental Run

Figure 1 and 2 show the isometric view and the image of the field-scale experimental set-up, respectively. The field-scale experimental set-up consisted of a lysimeter modelling a sanitary landfill; a receiving tank; two dilution tanks the inlet of each was connected to the receiving tank and the outlet of each was connected to an overhead tank; a control anaerobic filter column receiving influent from one overhead tank and an experimental anaerobic filter column receiving influent from the other overhead tank. The effluent of both the anaerobic filters flowed into a collection tank, water from which was recirculated back onto the lysimeter via a pump. The recirculated water together with rain water generated the leachate while passing through the municipal solid waste inside the lysimeter.

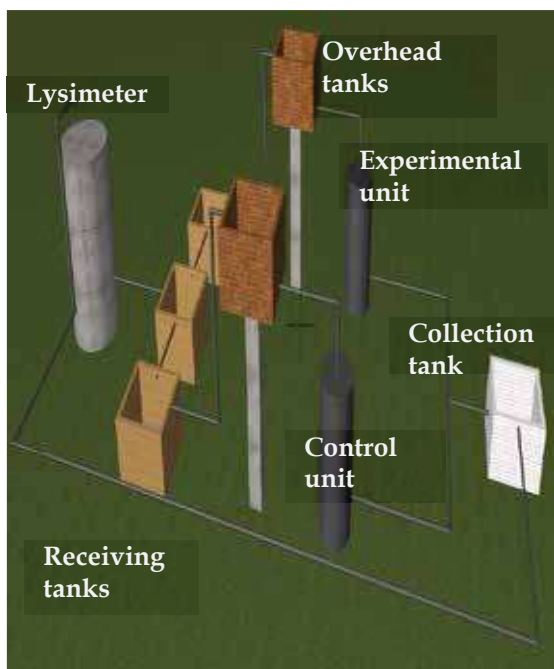


Figure 1 - Isometric View of the Field-Scale Experimental Set-Up

The control filter column was filled with 'plastic pall rings' (PPR), which is a conventional expensive filter media. BC, SD, DAS and washed sea sand (WSS) were filled in

layers of equal thickness in the experimental filter column (Figure 3). Influent was distributed in downward direction to the experimental and control filter columns under gravity. The approximate hydraulic retention time inside anaerobic filters were 2 days. The influent and effluent samples of both the filter columns were collected periodically, and they were analyzed in terms of several wastewater parameters as per the Standard Methods for the Examination of Water and Wastewater [4]

2.2 Characterization of the Filter Materials

Figure 4 shows the images of the selected filter materials. Material characterization was done mainly for the experimental low-cost materials. Physical properties such as specific gravity, porosity, surface area and packing density, and mechanical properties such as hydraulic conductivity, shear strength parameters such as friction angle and cohesion of the materials were measured using core samples extracted from the packed bed of the experimental column. Particle size distribution was obtained using the sieve analysis test. Table 1 to 4 and Figure 6 indicate the values of the above-mentioned properties of the selected filter materials



Figure 2 - Image of the Field-Scale Experimental Set-Up

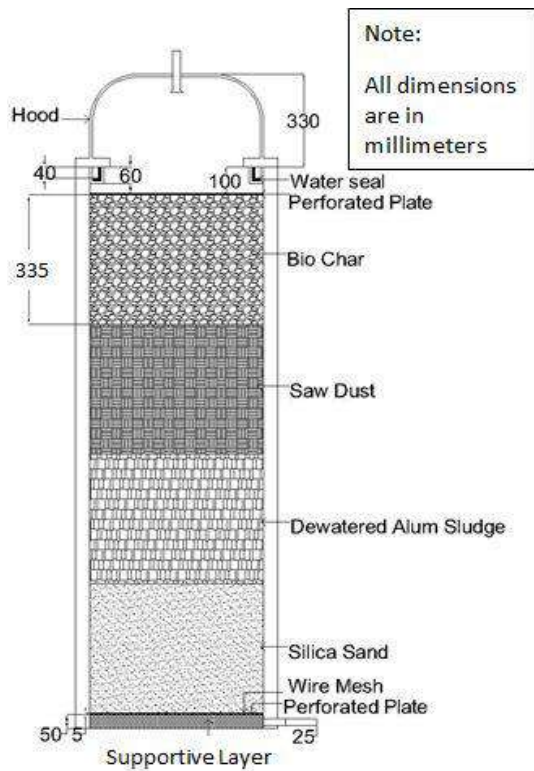


Figure 3 - Sectional View of the Experimental Filter Column

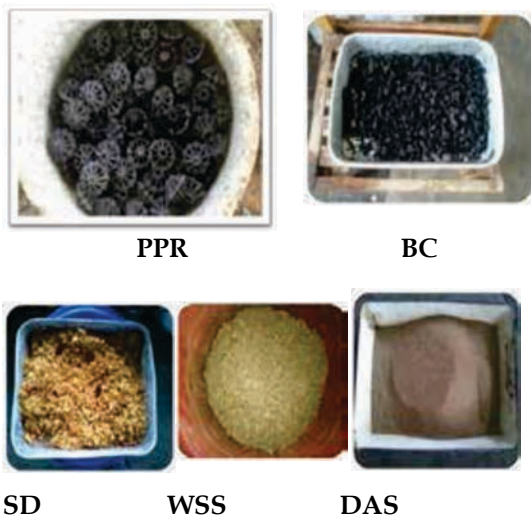


Figure 4 - Selected Filter Materials

Table 1- Specific Gravity and Porosity of the Filter Materials

Filter Materials	Specific Gravity	Porosity (n)
WSS	3.116	0.589
DAS	2.459	0.761
SD	0.790	0.801
BC	0.962	0.695

Table 2 - Packing Density, Surface Area and Particle Size Distribution of the Filter Materials

Filter Materials	Packing Density (kg/m ³)	Surface Area m ² /g	Particle Size (mm)
WSS	1279.1	1.0	0.3-5
DAS	670.5	32.9	1-20
SD	201.4	2.3	-
BC	386.9	281.6	4-20
PPR	105.7	-	-

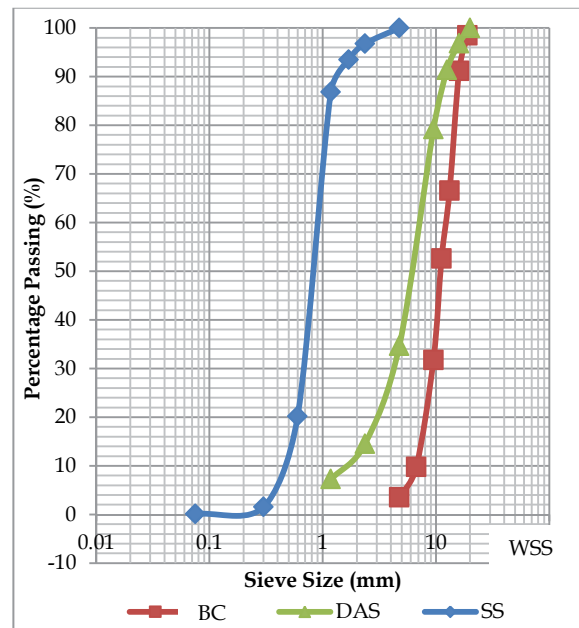


Figure 5 - Particle Size Distribution of the Filter Materials

Table 3 - Hydraulic Conductivity of Filter Materials

Filter Materials	Hydraulic Conductivity (cm/s)
WSS	0.01
DAS	0.01
SD	0.01
BC	0.01

Table 4 - Shear Strength Parameters of Filter Materials

Filter Material	Cohesion (kN/m ²)	Friction angle (Φ) ^o
WSS	1.1	0.09
DAS	2.9	0.09



3. Results & Discussion

Table 5 shows the mean values of the treatment efficiencies and their standard deviations. Figures 7 and 8 show the variation of removal efficiencies of BOD₅ and COD, respectively. Bodik et. al. [5] reported that the BOD removal is around 68% with the plastic tube media. However, in this study, PPR used as the filter material in the control unit gave a mean removal efficiency of 42.8%, which is slightly higher than the result of the experimental unit (40.3%). COD removal efficiencies of the experimental and control units were 40% and 44.4%, respectively. Attached growth processes in waste water treatment are very effective for BOD removal and denitrification. Young and McCarty [6] stated the potential of the anaerobic filter process for such treatments by treating a medium strength wastewater successfully.

The ORP (oxidation reduction potential) variation (Figure 9) indicates a reducing environment in both the filters.

Table 5- Mean and Standard Deviations of the Removal Efficiencies

Parameter	Control System		Experimental System	
	Mean (%)	Standard deviation	Mean (%)	Standard deviation
BOD ₅	42.9	9.0	40.3	7.3
COD	44.4	8.6	40.0	10.3
TSS	42.1	24.6	53.1	21.8
TDS	37.6	13.6	28.7	9.9
Turbidity	42.9	18.2	40.4	9.4
Cu ²⁺	60.7	25.6	69.5	19.8
Pb ²⁺	15.6	8.3	11.6	5.9
Fe ²⁺	22.5	10.2	59.5	30.8
TOC	25.0	14.5	5.4	2.4
TC	29.3	12.9	27.2	19.6
IC	31.2	17.5	36.0	30.8
TN	26.4	13.0	35.4	21.9
TP	16.0	5.2	11.3	1.4
PO ₄ ³⁻	10.1	5.4	6.4	6.1
Na ⁺	31.6	22.9	13.7	8.5
Ca ²⁺	16.7	15.3	31.9	18.8
K ⁺	30.8	30.2	10.3	11.0
Mg ²⁺	7.1	4.9	26.0	7.6

It could cause the removal of biodegradable organic matter and TN due to anaerobic decomposition and denitrification, respectively. The mean removal efficiency of TN (Figure 10)

in the experimental set-up was 35.3%, which is higher than PPR in the control column i.e. 26.4%. The removal efficiencies of cations such as Ca²⁺ and Mg²⁺ (Figure 11 and 12) and heavy metals such as Cu²⁺ and Fe²⁺ (Figure 13 and 14) in the experimental column were considerably greater than those of the control column. The mean removal efficiencies of Fe²⁺ and Mg²⁺ were 59.5, 26% respectively in the experimental column whereas those for PPR were 22.47, 7.1%, respectively. This could be due to the promotion of treatment mechanisms such as ion exchange, precipitation and adsorption in the experimental system owing to the different properties possessed by these materials.

Figure 15 shows the pH variation during the experimental run. The variation has an increase at the beginning and a decrease toward the end within a range of 6 to 10.

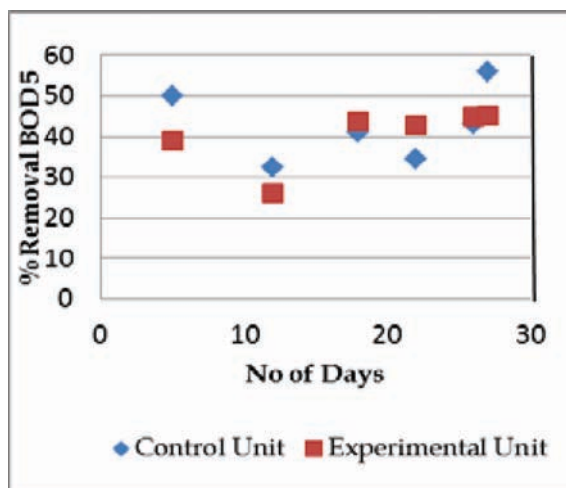


Figure 6 - Removal Efficiency of BOD₅

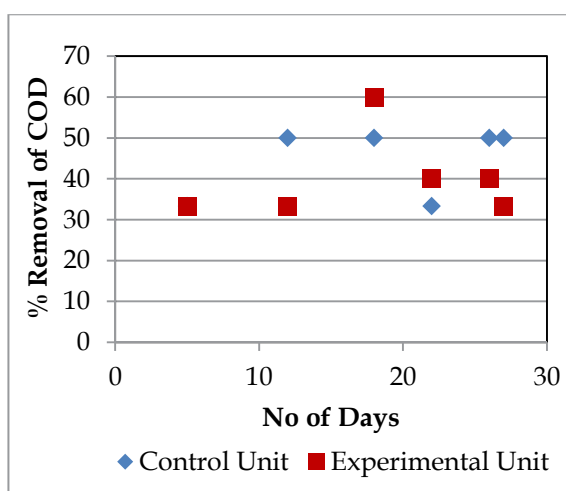


Figure 7 - Removal Efficiency of COD

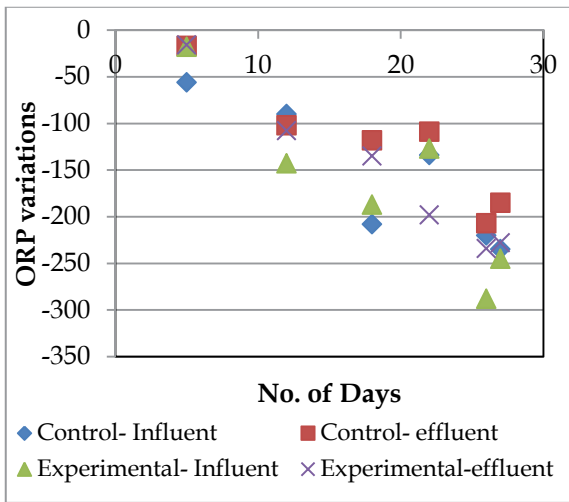


Figure 8 - Variation of ORP

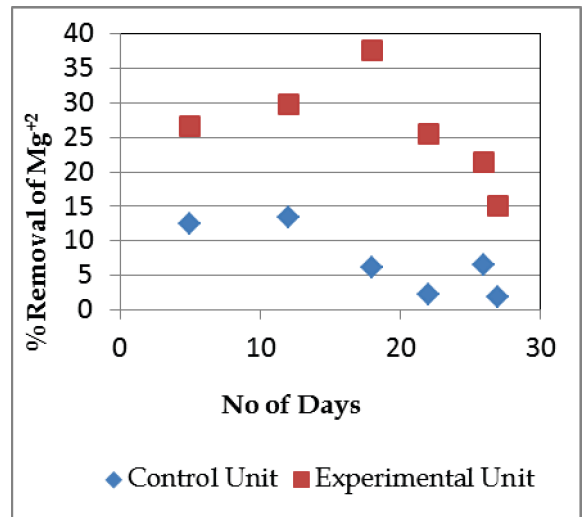


Figure 11 - Removal Efficiency of Mg²⁺

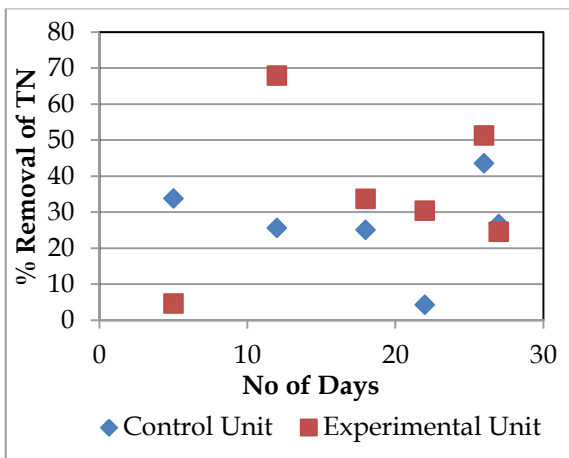


Figure 9 - Removal Efficiency of TN

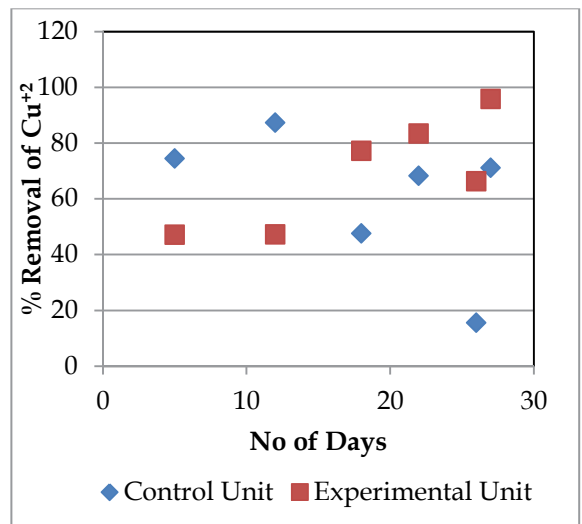


Figure 12 - Removal Efficiency of Cu²⁺

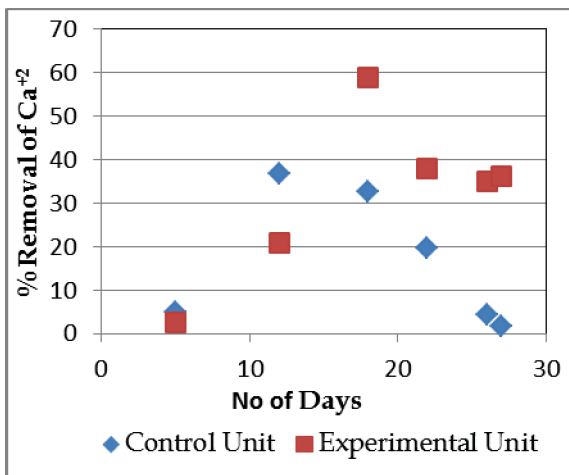


Figure 10 - Removal Efficiency of Ca²⁺

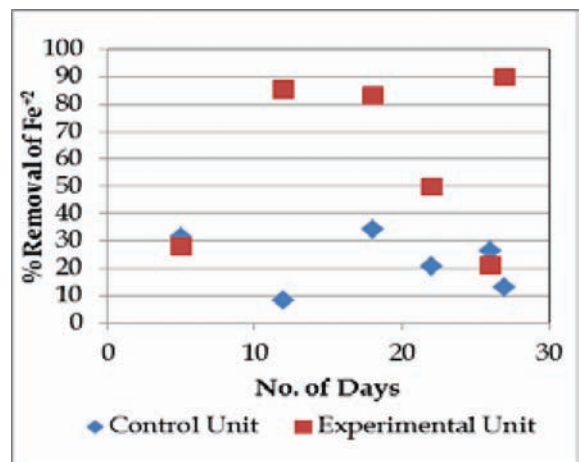


Figure 13 - Removal Efficiency of Fe²⁺



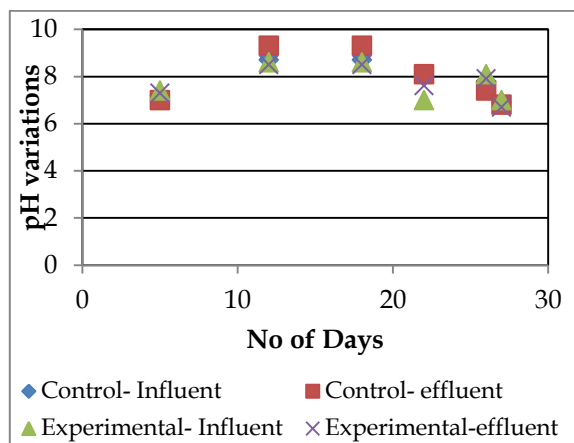


Figure 14 - Variation of pH value

4. Conclusions

The performances of the selected filter materials are on a par with conventional filter materials for organic compounds removal. The selected materials surpassed the conventional materials in treating several cations and heavy metals owing to the promotion of treatment mechanisms such as ion exchange, precipitation and adsorption due to different properties possessed by these materials. Therefore, these materials can effectively be applied to treat landfill leachate.

Acknowledgement

The authors would acknowledge the financial support given by the research grant from the JST/JICA Science and Technology Research Partnership for Sustainable Development (SATREPS). They would also like to offer their gratitude to Mr. Ganaila Paranawithana, a PhD student of the Saitama University for measuring surface areas of the packing media.

References

- Dayanthi, W.K.C.N., Ranga, U.K.S., Sanjeevani, H.K.M., "Applicability of Low-Cost Organic Materials as Packing Media in Anaerobic Filters to Treat Landfill Leachate" *Engineer Journal*, Annual transaction of IESL, pp. [72-79], 2013
- Nanayakkara, B.S.R., Dayanthi, W.K.C.N, Vidanapathirana, V.P.H.S, Siriwardana, M.P, "Up and Down- Flow Anaerobic Filters Using Firewood Charcoal, Dewatered Alum Sludge and Silica Sand for Landfill-Leachate Treatment" *Engineer Journal*, Annual transaction of IESL, 2014
- Nanayakkara, B.S.R, Dayanthi, W.K.C.N, "Landfill-Leachate Treatment in Up and Down Flow Anaerobic Filters with Combined Packing Media of Locally Available and Low-Cost Materials" 14th Academic Sessions, University of Ruhuna, 2017
- Standard Methods for the Examination of Water and Wastewater, American Public Health Association, 1015 Fifteenth Street, NW, Washington, DC, USA, pp.20005-2605, 1988.
- Bodik, I., Herdova, B., Krotovichil, K., "The Application of Anaerobic filter for Municipal Waste Water Treatment", 26th International Conference of the Slovak Society of Chemical Engineering, Jasná - Demänovská dolina, 24 – 28, May 1999.
- Young, J. C, McCarty P. L, 1968, "The Anaerobic Filter for Waste Treatment", Stanford University Technical Report No 87

Variations to Key Chemical Parameters during Dried Faecal Sludge and Municipal Solid Waste Co-Composting

H.M.N. Jayawardena, S.C. Fernando, S.H.P. Gunawardena and N. Jayathilake

Abstract: Co-composting of Municipal Solid Waste (MSW) together with one or more feedstock has been proven to be addressing typical drawbacks such as low nutrient density, nutrient imbalance, elemental deficiency, etc. when it is compared with compost that has been produced solely by MSW. Meantime the disposal of septage from onsite sanitation systems (such as pit latrines, septic tanks, etc.) has emerged as one of the major problems for local authorities because of rapid urbanization and land scarcity. This paper focuses on the co-composting of the dried faecal sludge (DFS) and organic fraction of MSW and its influence on pH, electrical conductivity, nutrient parameters, heavy metals and biological parameters.

Co-compost trials were conducted using turning windrow composting method consisting of 1000 kg of total mass; where one windrow was made solely with MSW as a control and other was made with 90% MSW and 10% DFS by mass. Each windrow was allowed to undergo a ten-week active composting period and a two-week curing period. Results show that addition of faecal sludge assist to improve pH of co-compost pile within the favourable range during the overall time span enhancing the microbial activity. Further, pile conditions were set up, so that Nitrogen loss could be expected to be at minimal level and hence higher Total Nitrogen (TN) content within the compost pile could be observed together with the high and favourable improvement of electrical conductivity. Improvement of Total Phosphorus availability and water-soluble Phosphorus availability could be observed. Heavy metal availability and pathogenic species availability were under allowable ranges under stipulated standards as well.

Keywords: Composting, Dried Faecal Sludge, Municipal Solid Waste.

1. Introduction

With the advanced technology development and the growth of urban population at an alarming rate change of consumption patterns of the modern world, which in turn has significantly increased the quantity of Municipal Solid Waste (MSW) generated. This MSW is not properly treated, disposed and managed in many parts of both developed and developing countries [1]. MSW contributes to the production of various types of gases such as methane, ammonia together with leachate, which could cause various problems ranging from simple odours to impacts on climate change. Environmental scientists adopt various solid waste management measures with appropriate modifications to match both quantity and characteristics of MSW [2]. Source reduction, recycling, composting, controlled burning where emissions are managed properly with well stipulated mitigation measures or landfilling are proven to be effective management measures [2]. However, the effectiveness of these conventional

techniques has to be revisited due to significant changes in characteristics and quantity of MSW that have taken place within last few years. Therefore, the interest for reusing and recycling of MSW based on novel technological aspects is developing currently in the world [3].

MSW consists of diverse types of raw materials, which can be classified into two main groups: agro-industrial and those derived from civil establishments [4]. These wastes can be further categorized into groups such as animal wastes, crop residuals, fruit and vegetable wastes, aquatic biomass and bio fertilizers, fish and marine wastes, industrial wastes and human habitation wastes [4]. The resource potential of mixed municipal solid waste deviates as it is

Eng. (Dr.) S.H.P. Gunawardena, B.Sc. Eng.(Moratuwa), Ph.D. (Birmingham), Senior Lecturer, Dept. of Chemical & Process Engineering, University of Moratuwa.

Eng. (Dr) S.C. Fernando, B.Sc. Eng.(Moratuwa), M.Sc. Eng. (Moratuwa), Ph.D.(Soton).

Eng. H.M.N. Jayawardena, B.Sc.Eng.(Moratuwa)

Eng. A.M. Jayathilake, M.Sc.Eng(Moratuwa), B.Sc.Eng. (Moratuwa).



dependent upon the waste consumption, which also differs considerably from country to country and in a particular country from a city to city due to income levels and consumer habits [5].

It was suggested that average MSW generation (mixed) between 0.4-0.6 kg per capita per day in low-income countries whereas 0.7-1.8 kg per capita per day in high-income countries. Typically, in low-income countries, the biodegradable fraction is significantly higher (40-85 %) than in high-income countries (20-50 %) [5].

Most commonly executed strategies such as recycling, reusing and resource recovery have proved to yield several considerable advantages; such as reducing the environmental impact, extending the existing landfill capacity and replenishing the soil humus layer. Reducing the organic fraction in the waste, allows reducing the collection, transportation and disposal costs as well as the health and environmental risks associated with appropriate waste handling and management [6]. Usage of organic fraction of MSW as a source of food for urban animal livestock, direct untreated application onto soils and production of fuel pellets as an energy source are other several novel applications, which are under discussion [7].

Controlled biological treatment of the organic fraction of MSW into compost for organic farming is getting wide attention these days due to its cost factor and health benefits in long term utilization. Composting is a process of controlled biological decomposition of raw organic material into stable humic substances with the presence of oxygen [8]. Once the compostable organic portion of solid waste streams is converted into compost, it can be used for landscaping, enhance crop growth, enrich topsoil etc. [2]. Apart from being a source of nitrogen, phosphorous, potassium and other plant nutrients, compost is also believed to suppress soil-derived diseases in plants [7]. Incomplete decomposition of complex constituents, the existence of pathogenic microorganisms, the existence of heavy metals in undesirable concentrations, and nutrient imbalance are on the top of discussions of MSW composting drawbacks [9]. The addition of several other bio-solids such as faecal sludge and inorganic salts to MSW is found to be addressing most of pre-mentioned

drawbacks associated with MSW composting and is known as Co-composting [10].

Several abundant and cheap organic materials can be utilized for co-composting such as animal manure, saw dust, wood chips, barks, slaughterhouse waste, sludge or solid residue from food and beverage industries. A considerable number of past studies that have been carried out related to MSW co-composting with animal manure, poultry manure [11] [12] and several other co-composting agents [13] [14] suggest that the finished co-compost has ensured higher stability than compost derived from MSW only. MSW co-composting with cow manure, poultry manure, and yard trimmings has found to maintain soil fertility while improving moisture holding capacity and acceptable release of plant nutrients [15].

The aim of this study was to evaluate the effectiveness of faecal sludge (FS) as low-cost nutrient enhancement agent while understanding the solubility of phosphorous containing constituents in the presence of organic acids that are likely to be formed during the process of decomposition.

2. Methodology

Compost piles with base dimensions of 1 m × 1 m were constructed. Each pile contained 1 tonne of total mass. The first pile was constructed solely with sorted market waste as the source of MSW in order to keep it as the control. The other pile was constructed with the addition of dried faecal sludge (DFS) as a fortifying agent.

Drying bed for FS was prepared by applying a single layer of medium size stone pellets together with three layers of gravel particle screened by 20 mm and 10 mm mesh. A metal net with appropriate mesh size was laid on top of all four layers in order to avoid mixing of gravel particles with faecal sludge. Black waters were fed onto the drying bed directly through gully trucks that are currently being utilized by the municipal council. DFS was obtained after 21 days of drying of black water in the drying bed.

100 kg of DFS was added to a pile in order to keep FS composition at 10% by mass so that initial C/N ratio is maintained around 30 [16] based on available values of carbon and nitrogen content of the market waste.

The addition of 100 kg of DFS with 900 kg of MSW was done by a series of constituent layering method. Where 90 kg of MSW was spread at the beginning to cover 1 m × 1 m base dimension. 10 kg of faecal sludge was then distributed on top of MSW layer and a hand rake was used to mix the content so that maximum possible homogeneousness can be expected. Once raked mixture was properly arranged on 1 m × 1 m base spread, another 90 kg of MSW and 10 kg of DFS were added and mixed with the rake. This process was followed until all the constituent quantities were introduced to the pile. DFS contains pathogen loads and should be handled with care. The co-compost can only be considered safe after the active composting period and appropriate personal protection equipment should be worn to avoid any possible health risks to the workers.

Each pile was first turned when the temperature exceeded 55°C of the windrow (usually 2 to 3 days after piling of windrow). Piles were turned weekly after the initial turning until 10 weeks were completed from the day of first turning. The moisture level of each pile was maintained in the range of 45 - 60% with the addition of water based on squeeze test [17] performed on site. The squeeze test is a simple field methodology where it is believed that water can be squeezed out if compost has moisture content above 60% and neither water is released nor remained when compacted.

Samples collected at each turning were subjected to testing in order to determine Electrical Conductivity (SLS 1219 / 1:6 V/V), pH Value (ISO - 10390:2005) and C/N Ratio (ISO - 11261/14235), which were pre-decided as characterization parameters.

Each pile was allowed to cure for two weeks after 10th turning. The organic municipal solid waste material used for this was market waste (vegetable and fruit waste). In general, the minimum curing time is considered 21 days but can be extended to many months. Bioassay can help to predict the success of the compost curing. By considering the input material, a reduced curing time was used. In this case the bioassay test was conducted successfully and confirmed the quality of the product. Any obstruction or water addition was not performed during this curing phase. Sample drawn after two weeks of curing (i.e. 12 weeks after first turning) were subjected to full-

parameter lab testing in order to determine Electrical Conductivity (SLS 1219 / 1:6 V/V), pH Value (ISO - 10390:2005) and C/N Ratio (ISO - 11261/14235), together with Total Nitrogen (as N) (ISO - 11261: 1995), Total Phosphorous (ISO 11263: 1994) and Water Soluble Phosphorous (SLS 645).

3. Results and Discussion

Co-composting of FS and MSW is expected to be beneficial since they complement with each other. Nitrogen and moisture content in human waste is relatively high whereas organic carbon content in MSW is relatively high. Meantime, high temperatures generated in composting may effectively inactivate pathogens present in both FS and MSW, eventually generate hygienically safe soil conditioner and a fertilizer.

Electrical Conductivity

Electrical conductivity is an indicator of soluble salts and ions prevailing in the compost. From the results presented in figure 01 it is clearly visible that the sample only with MSW has very low conductivity when compared with the MSW and DFS co-compost pile. This may be due to the fact that organic components are the prime element in MSW and it lacks inorganic ions and salts. Free ion availability will increase if more inorganic ions are added to the compost.

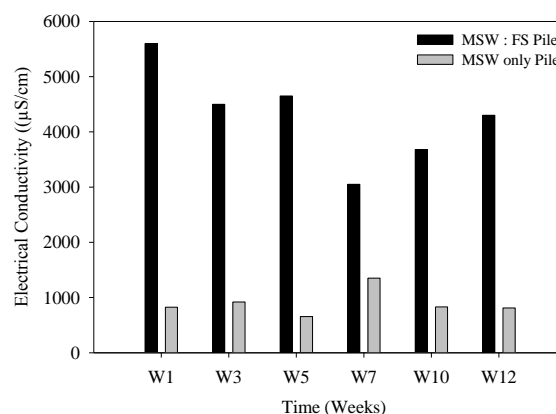


Figure 1- Electrical Conductivity Variation with composting time

Increased electrical conductivity in DFS added samples indicates the presence of inorganic matter in sludge. Salts and other water-soluble inorganic ions that have been consumed by



humans may have been transferred to the DFS. DFS added MSW pile shows gradual decrease in conductivity with time. This could be due to the irregularities in decomposing of constituent components available in the feedstock. It is reported that unnecessarily high conductivity is due to sodium chloride in soil and is not beneficial to plants. Further, soil salinity greater than 4000 $\mu\text{S}/\text{cm}$ could lead to inhibition of plant growth and germination [1]. The conductivity of final compost obtained in 12 weeks from this study has an acceptable conductivity value of 4300 $\mu\text{S}/\text{cm}$.

Throughout the time span of 12 weeks the electrical conductivity does not show a significant improvement in MSW only sample; it remained constant around 1000 $\mu\text{S}/\text{cm}$ throughout the monitoring period. According to reported work, less EC value tends to cause adverse effects compared to higher EC values in compost since composts are used as a soil conditioner in agriculture, which will be incorporated into the soil and thus diluted [18]. Therefore, an addition of DFS as a co-composting agent has positively affected the quality of compost.

pH

with reference to figure 02, it could be observed that the addition of faecal sludge, a significant increase in pH value of the contents in the pile can be seen from the week 1 onwards and remained around 8.0 (7.5 - 8.5). The pH increases from week 1 in DFS added pile should be due to the electron accepting ability of ions released with the process of decomposition as reflected in high electrical conductivity in figure 1.

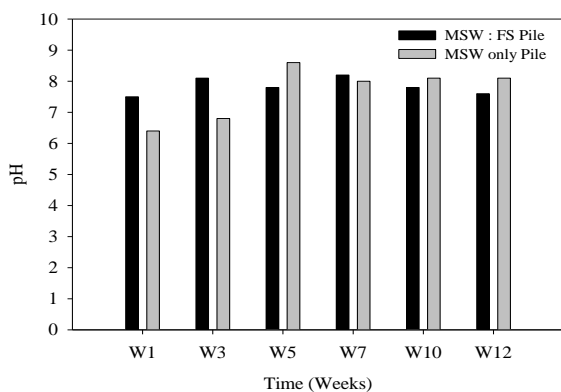


Figure 2 - pH Variation with Composting Time

At this pH, it could expect to enhance the kinetics of composting process due to prevalence of favourable condition for microbial existence as reported by (Chen, et al.) [19]. Further, this favourable pH environment will improve the nutrient value of co-compost by reducing nitrogen loss as ammonia which happens under alkaline pH conditions [9].

During the period from W7 to W12 a drop in pH could be observed in faecal sludge added pile when compared with the control, and this could be due to the neutralization of alkaline constituents by acidic waste generated during decomposition.

Carbon Nitrogen (C/N) Ratio

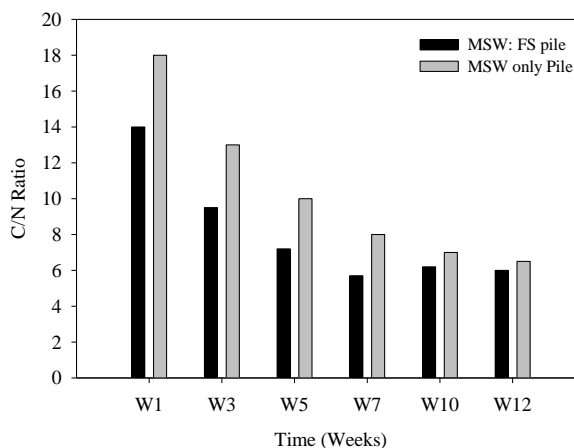


Figure 3 - C/N Ratio Variation with Composting Time

When analyzing results represented in figure 03, it can be clearly seen that addition of faecal sludge has decreased the C/N ratio initially. This is a clear indication of rich in Nitrogen components when compared with constituents of MSW. Higher water-soluble nitrate concentrations lead to faster discharging of nutrients enhancing the fertility value of compost since all nitrates are highly water-soluble. These results showcase the correlation of pH variation plot in figure 02, since significantly high pH conditions supposed to release Nitrogen in the form of ammonia and result in high C/N ratio. When it comes to end user, co-composting has added a considerable value in terms of Carbon to Nitrogen ratio. But it is better to have the proper C/N ratio so as it will maintain a favourable environment for microbes to proceed with degradation. It is accepted to have a C/N ratio in the

specifications of 20% to 30% for proper microbial action [20]. Results have shown acceptable C/N ratio below 20 at the maturity according to (Wong, et al.) [21] and even recommended level at maturation below 16 suggested by [22]. The rapid decrease in value of nitrogen for MSW: DFS with time may be due to the loss of ammonia with time.

Nutrient Content Parameters

Figure 4 shows the total Nitrogen (TN), total Phosphorus and water-soluble Phosphorus content in both compost samples after 12 weeks. According to figure 4, MSW based control pile has low TN content when compared with MSW: DFS co-compost pile. This is a reflection of figure 2 i.e. end of the line acidic condition is generated through an introduction of DFS has enhanced nitrogen availability in nitrite and nitrate forms by demoting nitrogen loss in the form of ammonia tendency in alkaline conditions.

The presence of acidic constituents that maintains pH within favourable range increases nitrogen availability in the forms of nitrites and nitrates where alkaline constituents decrease the nitrogen availability in the forms of nitrites and nitrates [23].

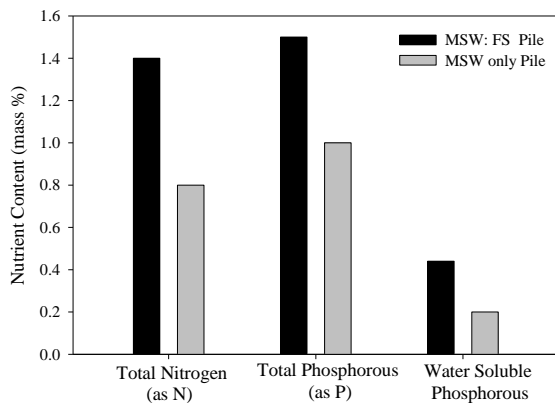


Figure 4 - Total Nitrogen, Total Phosphorous and Water Soluble Phosphorous content in finished compost

Variations observed in total phosphorous and water-soluble phosphorous content follow the characteristic low proportional relationship between total phosphorous and water-soluble phosphorous in both pile configurations. If the ratio between water-soluble phosphorous and

total phosphorous is taken as characterization parameter, it could be seen that MSW based control pile has got about 20% of its total phosphorous in water-soluble forms while the ratio is about 30% in MSW: DFS co-composting pile. This is due to low level of alkalinity maintained with the addition of faecal sludge as reflected in pH variation curve i.e. figure 2. According to (Kauwenbergh) [24] acidic nature of faecal sludge has assisted the task of the acidic constituent formation during decomposition process and hence has been promoted, phosphorous dissolution and ultimately shown the higher total and water-soluble phosphorous content. This would enhance further investigations for evaluating the effectiveness of the addition of faecal sludge as a phosphorous enhancement agent.

Heavy Metal Availability

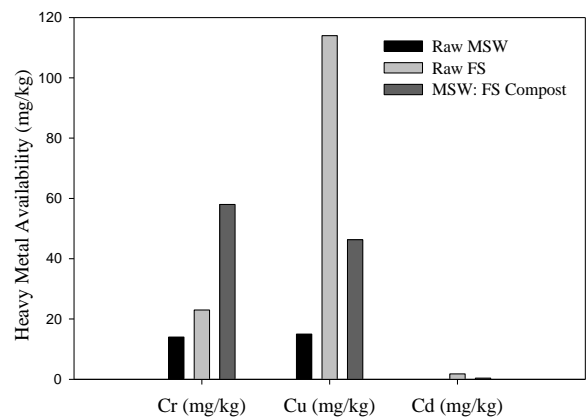


Figure 5 - Heavy Metal availability in raw materials and finished compost

Heavy metals availability in raw MSW, DFS and co-compost is shown in Figure 05. MSW and raw dried faecal sludge (DFS) contained a Cr concentration of 14 and 23 mg/kg on dry basis respectively while MSW: DFS co-compost sample contained 58 mg/kg Cr concentration at the maturity. This should be due to the mass loss occurred during the decomposition process [25]. However, Cr concentration is still satisfactory and has a value less than 60 mg/kg comply the strictest environmental regulation stipulated by European Compost Network (ECN) [26]. Cu availability and Cd availability also represent allowable values of 46.3 and 0.4 mg/kg, which are satisfactory when compared



with 70 mg/kg and 0.7 mg/kg guideline values [26].

Biological Parameters

Faecal coliform availability is believed to be one of the parameters of concern in evaluating FS application due to hygienic aspects and has been subjected to discussion in the recent times. It is reported that if faecal Coliforms below 1000 MPN/g then that particular DFS mixed compost is suitable for ground application [27].

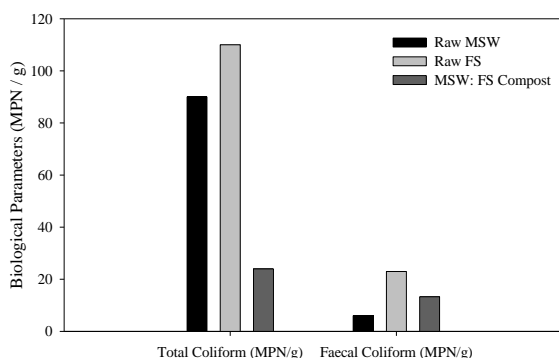


Figure 6 - Total and Faecal Coliform Availability in raw materials and Finished compost

According to figure 6, MSW: DFS co-compost produced in this study has a satisfactory level of biologically available pathogens with 13.3 MPN/g of faecal coliform. Therefore, the addition of 10% by weight DFS to MSW has not affected the hygienic parameters of the co-compost.

4. Conclusions

The following conclusions can be drawn from the study.

- The addition of DFS as the co-composting agent has improved Electrical Conductivity within the derived co-compost by increasing free ion availability and hence it favourably maintains soil characteristics.
- The addition of DFS leads to favourable pH maintenance within the derived co-compost compatible with the SLS standard.
- DFS acts as a compatible co-composting agent for Municipal Solid Waste and improves the

nutrient content especially Total Phosphorous (TP) and Water-Soluble Phosphorous (WSP) content availability within the derived co-compost, where Phosphorous is a non-renewable source

- The addition of 10% of the mass FS has not caused any serious safety consideration due to the availability of permissible concentrations of Heavy metals
- High temperatures were achieved during the co-composting process and has been confirmed biologically safe (sanitized final product).

Acknowledgement

Authors would like to acknowledge the support extended by CGIAR research program on water, land and eco systems in funding this study.

Authors would like to acknowledge the support extended by Municipal Council - Kurunegala, North Western Province in conducting this study

References

1. Cofie, O., Kone, D. & Rothenberger, S., 2009. Co-composting of Faecal Sludge and Organic Solid Waste for Agriculture: Process Dynamics. *Water research*, 43(1), pp. 4665-4675.
2. Sherman, R., 1999. *Large scale organic materials composting*, Carolina: NC State university.
3. Mollazadeh, N., 2014. Composting: A New Method for Reduction of Solid Waste and Waste Water. *International Research Journal of Applied and Basic Sciences*, 8(3), pp. 311-317.
4. Sharma, V. K., Canditelli, M., Fortuna, F. & Cornacchia, G., 1997. Processing of Urban and Agro-Industrial Residues by Aerobic Composting: Review. *Energy conservation and management*, 38(05), pp. 453-478.
5. Strauss, M., Drescher, S., Zurbrugg, C. & Montangero, A., 2003. *Co-composting of Faecal Sludge and Organic Municipal Solid Waste*, Ghana: International Water Management Institute.
6. Tweib, S. A., Rahman, R. A. & Kalil, M. S., 2011. *A literature review on the Composting*. Singapore, International Conference on Environmental and Industrial Innovation.

7. Hirrel, S. s. & Riley, T., 2005. *Understanding the Composting process*, Fayetteville: University of Arkansas.
8. Kathryn, P., 2003. *Chemistry and Compost*, Washington: American Chemical Society.
9. Kokhila, M. S., 2015. *Composting: Advantages and Disadvantages*. Tbilisi-Georgia, Ilia state university.
10. Dinis, M., 2009. *Co-composting: A Brief Review*, Porto-Portugal: University Fernando Pessoa-Porto-Portugal.
11. Varma, S. V. & Kalamdhad, A. S., 2013. Composting of Municipal Solid Waste (MSW) mixed with cattle manure. *International Journal of Environmental Sciences*, 6(3).
12. Ferreira, N. L. & Oliveira, R., 2013. *Co-composting cow manure with food waste: The influence of lipids content*. dubai, World Academy of Science, Engineering and Technology, pp. 986-991.
13. Hasanimehr, M., Rad, H. A., Babae, V. & baei, M. S., 2011. Use of Municipal Solid Waste Compost and Waste Water Biosolids with Co-Composting Process. *World Applied Sciences Journal*, 11(Special Issue of Food and Environment), pp. 60-66.
14. Ogunwande, G. A., Osunade, J. A. & Ogunjimi, L. A. O., 2008. Effects of Carbon to Nitrogen Ratio and Turning Frequency on Composting of Chicken Litter in Turned-Windrow Piles. *Agricultural Engineering International: the CIGR Ejournal*, x(07).
15. Davidson, G., 2011. *Waste management practices*, Halifax, Norva Scotia: Dalhousie university.
16. Cooperband, L., 2002. *The Art and Science of Composting*. [Online]
Available at: <https://www.cias.wisc.edu/wp-content/uploads/2008/07/artofcompost.pdf> [Accessed 14 November 2016].
17. David, A. & Gamble, S., 2013. *Municipal Solid waste Organics Processing*. s.l.:ISBN: 978-1-100-21707-9.
18. Dimambro, M., Lillywhite, R. & Rahn, C., 2006. *Biodegradable municipal waste composts: analysis and application to agriculture*, United Kingdom: the university of Warwick.
19. Chen, L., Morti, M. d. H., Moore, A. & Falen, 2011. *The Composting Process*. [Online]
Available at: <http://www.extension.uidaho.edu/nutrient/wastemanagement/PDF/dairycomposting.pdf> [Accessed 17 January 2017].
20. Kutzner, H. J., 2008. Microbiology of Composting. In: H. Rehm & G. Reed, eds. *Biotechnology set*. Ober-Ramstadt: Wiley library, pp. 34-47.
21. Wong, J. et al., 2001. Co-composting of Soybean Residues and Leaves in Hong Kong. *Bioresource Technological Journal*, 76(02), pp. 99-106.
22. Bernal, M., Navarro, A., Roig, A. & Cegarra, J., 1996. Carbon and Nitrogen Transformation during Composting of Sweet Sourghm Bagasse.
23. Ameen, A. & Ahmad, J., 2016. Effect of pH and Moisture Content on Composting of. *International Journal of Scientific and Research Publications*, Volume 6(Issue 5), pp. 35-37.
24. Kauwenbergh, V. S., 2010. *World Phosphate rock reserves and resources*, Alabama-USA: IFDC
25. Brinton, F. W., 2000. *Compost Quality Standards and Guidelines*, New York: New York State Association of Recyclers.
26. Cofie, O. et al., 2016. *Co-composting of Solid Waste and Faecal Sludge for Nutrient and Organic matter recovery*. 3rd ed. Germany: CGIAR Research Program on Water, Land and Ecosystems (WLE).
27. Miller, C. M., 2015. *Microbiological Safety of Organic Fertilizers Used to Produce Production*. Carolina: Clemson University.



Life Cycle Assessment Based Tool to Visualize Environmental Impact of Construction Materials & Products

H.M.M.M. Jayawickrama, K.G.N.H. Weerasinghe, R.L. Peiris and A.K. Kulatunga

Abstract: The construction industry has boomed significantly in Sri Lanka after the 30 years of war. This has created unprecedented demand for some construction materials, and some of them are extracted or mined from virgin sources. Even several building materials such as cement, roofing sheets, etc. need to manufacture before they are being used which contribute substantially to the environment during the manufacturing phase. Conversely, due to the growing interest towards sustainable built environment or greener buildings has made curiosity within the construction industry to move towards sourcing of greener materials or to secure greener supply chains for the construction industry. However, it is difficult to identify the environmental impacts of construction material and specially to assess or compare in a quantifiable manner. Therefore, this research focuses on developing a tool to indicate environmental impacts taken into account the phases of the supply chain which are rarely come to the surface. This tool has been developed based on life cycle assessment concept. Life Cycle Assessment is a well-recognized methodology used for quantifying the magnitude of the potential environmental impact of a particular system during a selected period of its lifetime. Commercial software's have been developed to conduct these studies, but they are dependent on the primary databases which have been prepared considering regional geographical representations. Therefore, it is difficult to use these software due to non-availability of country and region-specific data/information in the commonly used databases. However, this research overcomes this barrier with some alternative means to develop the final tool. Based on the developed tool, it is easier to compare environmental hotspots for the selected impact categories specifically highlighting the particular phase which has a significant impact in the way of different colour coding system which can be easily compared by the construction industry professionals without deep knowledge in Sustainability or Greenness of the supply chains.

Keywords: Life Cycle Assessment, Environmental performance, Construction Material

1. Introduction

Construction industry has evolved enormously during the last two centuries all over the world while consuming gigantic amount of resources and covering free lands available [1]. Since it directly links with the economic development of a country [2], all over the world this industry continued to be developed rapidly in developing countries and operate at stable state in developed countries alike. Due to the rapid development of the technologies and population increase, size of buildings also keeps on increasing continuously in to larger scale and the impact of buildings and this industry on environment also increasing in parallel. This has created severe damage to many eco systems as most of the materials use for constructions or to manufacture construction materials are virgin and extracted from earth. (Ex: Sand, Clay and Lime). Due to stringent regulations available in developed countries material extraction process happening in controlled manner with minimal effect to the

eco systems. Conversely, developing countries have been unable to control illegal material extraction processes [3, 4]. Sri Lanka also as a developing country, has been contributing to this damage for a while [5]. After the 30 year of civil war, the development of construction industry is rapidly increasing (Figure. 1). This has increased the construction material consumption. For instance, LKR 38 billion used for construction raw materials during 2010 [6] and it has been increased up to LKR 221 billion for 2015 [7].

Mr. H.M.M.M. Jayawickrama, B.Sc. Eng. Hons (Peradeniya), MPhil Candidate, Department of Manufacturing and Industrial Engineering, University of Peradeniya

Mrs. K.G.N.H. Weerasinghe, B.Sc. in Export Agriculture (Uva Wellassa University, MSc.in Environmental Science, University of Peradeniya

Eng. R.L. Peiris, BSc. Eng. Hons (Ruhuna), MPhil Candidate, Department of Manufacturing and Industrial Engineering, University of Peradeniya

Eng. (Dr.) A.K. Kulatunga, BSc.Eng. Hons (Peradeniya), Ph.D. (Australia), Senior Lecturer, Department of Manufacturing and Industrial Engineering, University of Peradeniya.



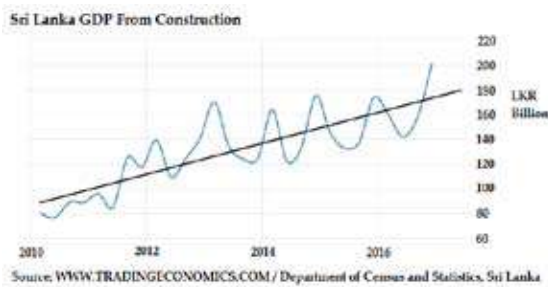


Figure 1 - Sri Lanka GDP - construction [8]

When considering above statistics it is a fact that the construction material consumption is escalating at an alarming rate resulting a great loss of the ecosystem and associated bio diversity. The availability of low quality materials at low cost, and availability of materials without having safe end use mechanisms are the facts identified for the above issue [5]. Consequently, the necessity of consideration of all four phases of the life cycle that are Pre Manufacturing, Manufacturing, Use and Post -Use when selecting of environmental friendly construction materials has been raised by recent studies [9, 10, 11] as well.

Meantime the attention of local industrialists has gone towards environmental friendly buildings or green buildings with global trend towards sustainable Built environment. Some of the land mark buildings such as Kandalama Hotel, MAS Thuruliya apparel plant etc. has gone into LEED [12] certification and many other buildings have been accredited by the GREEN^{SL}® [13] of Green Building Council of Sri Lanka (GBCSL). In both LEED and GREEN^{SL}® accreditation schemes, considerable percentage has been given to construction material and in GREEN^{SL}® to disposal. Though selection of construction materials is a paramount factor for environmental friendly buildings, available tools and methods are not sufficient in visualizing the environmental impact in all four life cycle phases. Mainly the lack of awareness of the decision makers in environmental impact calculation methods has to be addressed via such a methodology. Therefore, it is better to develop a country specified tool to visualize the environmental impacts of construction materials and products considering whole life cycle.

International Organization for Standardization (ISO) has introduced ISO14020 series of standards for environmental labelling [14] with three types of environmental labels such as Type I, Type II and Type III which are

voluntary in nature. Type I is done by stakeholders and advisory committees which considers product life as a whole. Type II is a self-declaration claim without pre-clearance in criteria development and it leads less consumer trust. Type III is a LCA approached criterion which the setting and verification is done by a third-party. Though the standards discussed above have addressed the total product life cycle, the detailed quantification of environmental impacts generated by each life cycle phase targeting the eye open on responsible party is not addressed [15, 16, 17, 18, 19]. However, regional divergences can be identified in such methods as LCA base line data are not applicable to the geographical representation of developing countries and therefore, wide range of assumptions are used in analysis which cause to reduce the credibility of LCA results. The limitation of a baseline/ benchmark to compare is the main weakness identified. Providing a roadmap to above issue, a decision making methodology by evaluating environmental performance of products against a pre-defined benchmark specifically calculated to each country /region is suggested by Finkbeiner in his research [19].

When look at in to locally developed environmental performance monitoring tools or methodologies developed aiming construction materials, Green Label Scheme introduced by GBCSL [20] focus on issuing a Green Label to construction material manufactures. This methodology specified for providing a green label through evaluating greenness of manufacturing phase of the construction materials by observing the company's adherence to the country regulations where the final rating is based on the evaluators without having an overall representation of the environmental impacts. Moreover, the major gap of this methodology is lack of influence in Pre-manufacturing, Manufacturing, Use and Post-use phases for the evaluation process. Therefore, the final green label does not visualize the overall impact of the labeled material. Other than GBCSL Green Label there are no any Eco-Labeling systems which are focus on Sri Lankan requirement. However, there are tools [21, 22, 23] developed based on LCA which focused on sustainable construction material selection. Though these can be used as decision making tools in sustainable material selection it is unable to visualize the environment performance in different life cycle phases. When consider the local requirement, still there is no any tool or method which is able

to visualize the environmental performance of the different phases of a product life cycle. Since there is a big requirement for such a system specially for construction industry, the proposed study focuses on develop a tool to evaluate the environmental performance of construction materials throughout the life cycle and visualize them via Eco-Labeling system. This tool will be elaborated in research methodology and then results interpretation and decision making strategies will be described through a case study, discussion and conclusion.

2. Methodology

The methodology of the study mainly consists of six phases and the structural overview of the methodology is given in Figure 2. Phases of methodology are, Goal and scope definition of the study, Identification of assessment indicators, Inventory preparation for data collection, Development of analytical framework, Introduction of a technique for results interpretation and validating the proposed methodology through a case study.

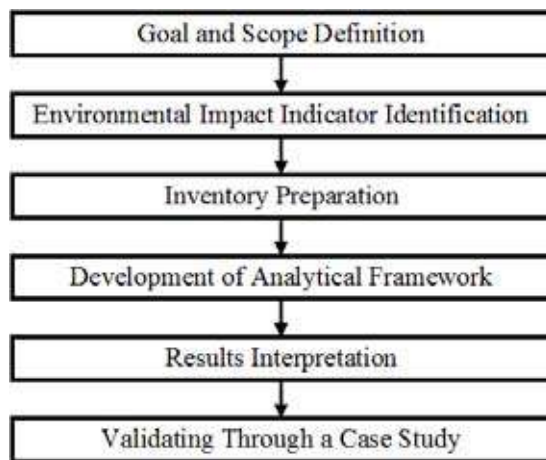


Figure 2 - Methodology

2.1 Goal and Scope definition

The goal of the study is to develop a tool to compare environmental impact of construction materials throughout the life cycle phases under selected environmental impact categories specifically highlighting the particular phases which has a significant impact which can be easily compared by the construction industry professionals without deep knowledge in Sustainability or Greenness of the supply chains. The life cycle phases considered here are Pre-manufacturing, Manufacturing, Use and Post-use. Activities such as material

extraction, pre-processing and transportation to the manufacturing plant are considered under pre-manufacturing phase. Gate to gate processing inside the manufacturing facility is considered under manufacturing phase. Distribution of finished products and impact generating during consumption of the product are considered at use phase. Finally reuse, recycle, recover or disposal of the product after its use is considered at post-use phase. This has been elaborated in Figure 3. It is expected to develop a data collection format to collect environmental impact related data of construction materials use in Sri Lanka and to develop a methodology to issue a graphically represented Eco- Label for construction materials.

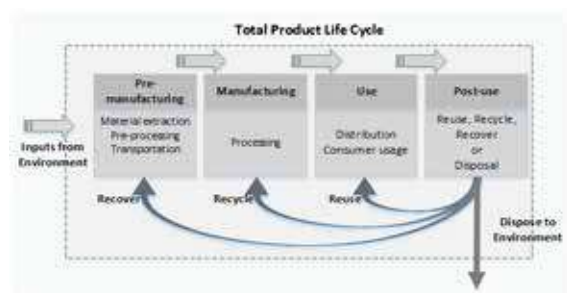


Figure 3 - Total Life Cycle representation of a product

2.2 Impact indicator identification

There are 14 impact categories defined for LCA. However, to calculate the impact under each category will require software assistant and database support. Commercially available software such as SimaPro, Gabi and Athena or freely available Open LCA can be used with the support of a database such as Eco-invent. Apparently the available data sets in currently available databases does not represent Sri Lankan data. Other than that conducting a LCA for total life cycle is time taken effort which requires expertise knowledge. Therefore, for a convenient and user-friendly tool, number of impact indicators were limited to four. Otherwise decision makers will face complications. Following impact categories for each phase of the product life cycle are selected for the proposed tool. Selection of impact categories was subjected to the data availability and calculation simplicity for the better understanding of consumers and users.

1. GHG emission = I_{GHG}
2. Material Consumption = $I_{Material}$
3. Energy Consumption = I_{Energy}
4. Solid Waste = I_{Waste}



GHG emission and Energy consumption directly considered in each phase. Solid waste amount considered under two categories such as hazardous waste and non-hazardous wastes. Since the material consumption occurs in different ways along life cycle phases, virgin raw material percentage in pre-manufacturing, packing and indirect material in manufacturing, supportive materials consumption in use and total of the ratio of reusability and recyclability under post use are considered.

2.3 Inventory Preparation

Considering above indicators, a data collection sheet was prepared by covering all four life cycle phases. It is expected to collect data for all the construction materials manufacturing in Sri Lanka. And also, the data from published research papers and recommended web sites also need to be collected for the imported construction materials. The sample inventory table which was completed for the case study is given in Table 1.

2.4 Development of Analytical Framework

Analytical frame work developed in an Excel work book which calculates the resulted values for above four measuring indicators in each life cycle stage for defined functional unit. Calculation process consists three steps such as: calculation of performance scores, calculation of weighted impact under each phase for indicators, calculation of overall impact. The calculation methodology has been presented bellow for the GHG emission indicator by deriving equations for each step. The same methodology can be applied for other three indicators. Within this analytical frame work the problem oriented approach (mid-point) was used for the simplification and final results also presented directly for impact categories.

Calculation of performance scores

Performance score is the 0-1 scaled value for each indicator. Scaling has done by considering minimum and maximum values identified for Sri Lankan construction materials under each phase. However, still in Sri Lanka there is no such database available. In this proposed tool, it is assumed that these data are available for the decision making and all calculation steps of analytical framework was developed based on that. Let,

- Absolute value of GHG emission in manufacturing phase = $I_{mfg.,GHG}$
- Maximum value of the GHG emission in manufacturing phase among all construction materials = $Max I_{mfg.,GHG}$
- Minimum value of the GHG emission in manufacturing phase among all construction materials = $Min I_{mfg.,GHG}$
- Indicator score of GHG emission in manufacturing phase = $S_{mfg.,GHG}$

Then,

$$\{S_{mfg.,GHG} = \frac{Max I_{mfg.,GHG} - I_{mfg.,GHG}}{Max I_{mfg.,GHG} - Min I_{mfg.,GHG}} \dots (1)\}$$

Calculation of weighted impact under each phase of GHG emission

After calculating the performance scores they were normalized along the phases by considering the weighted average of maximum indicator value under each phase.

Let,

- Maximum values of GHG emissions at four phases for all construction materials are; $Max I_{pre,GHG}$, $Max I_{mfg,GHG}$, $Max I_{use,GHG}$ and $Max I_{post,GHG}$
- Weight assign for GHG emission in manufacturing phase = $W_{mfg.,GHG}$
- Weighted impact of GHG emissions at manufacturing phase = $WI_{mfg,GHG}$ (X_{12} in Table 2)

Then,

$$\{W_{mfg.,GHG} = \frac{Max I_{mfg.,GHG}}{Max I_{pre,GHG} + Max I_{mfg.,GHG} + Max I_{use,GHG} + Max I_{post,GHG}} \dots (2)\}$$

$$\{WI_{mfg,GHG} = S_{mfg,GHG} \cdot W_{mfg,GHG} \dots (3)\}$$

Calculation of overall impact

After calculating the weighted impact for all indicator values in each phase, weighted impact matrix (Table 2) can be developed. Total life cycle impact of each indicator can be calculated by taking the summation of values in each phase. In this study it has considered that all four indicators are equally important for a simplified calculation methodology. However, if it is not applicable the Analytical Hierarchical Process is recommended to calculate weights for each indicator. Overall impact can be obtained by taking the average of total life cycle impact values which is a value between 0 - 1.

Table 1 - Completed Inventory for S1 clay roof tile

Parameter	Unit	Pre-mfg	Mfg	Use	Post-use
Virgin Raw Material	kg per Product	4.52			
Recycled Raw material	kg per Product	0.502	2.62		
Packing material	kg per Product		14.59		
Other material required for use	kg per Product	0.015	2.33	0.72	
Water	l per Product		4.2		
Electricity (National grid)	kWh per product	0.28	0.79		
Electricity (Generator)	kWh per product		0.24		
Process fuel oil consumption	kg per Product	0.9	38.5		
Process Gas consumption	kg per Product		0.44		
Process wood consumption	Kg per Product				
Transport distance (air)	tkm per product	0.049			
Transport distance (land)	tkm per product	0.291	0.010	0.003	0.16
Transport distance (water)	tkm per product	0.140			
Solid waste amount (Hazardous)	g per product				
Solid waste amount (Non-hazardous)	kg per product		0.021		
Recycle Amount	% from product				20
Landfilling Amount	g per product				336
Reuse Amount	% from product				65

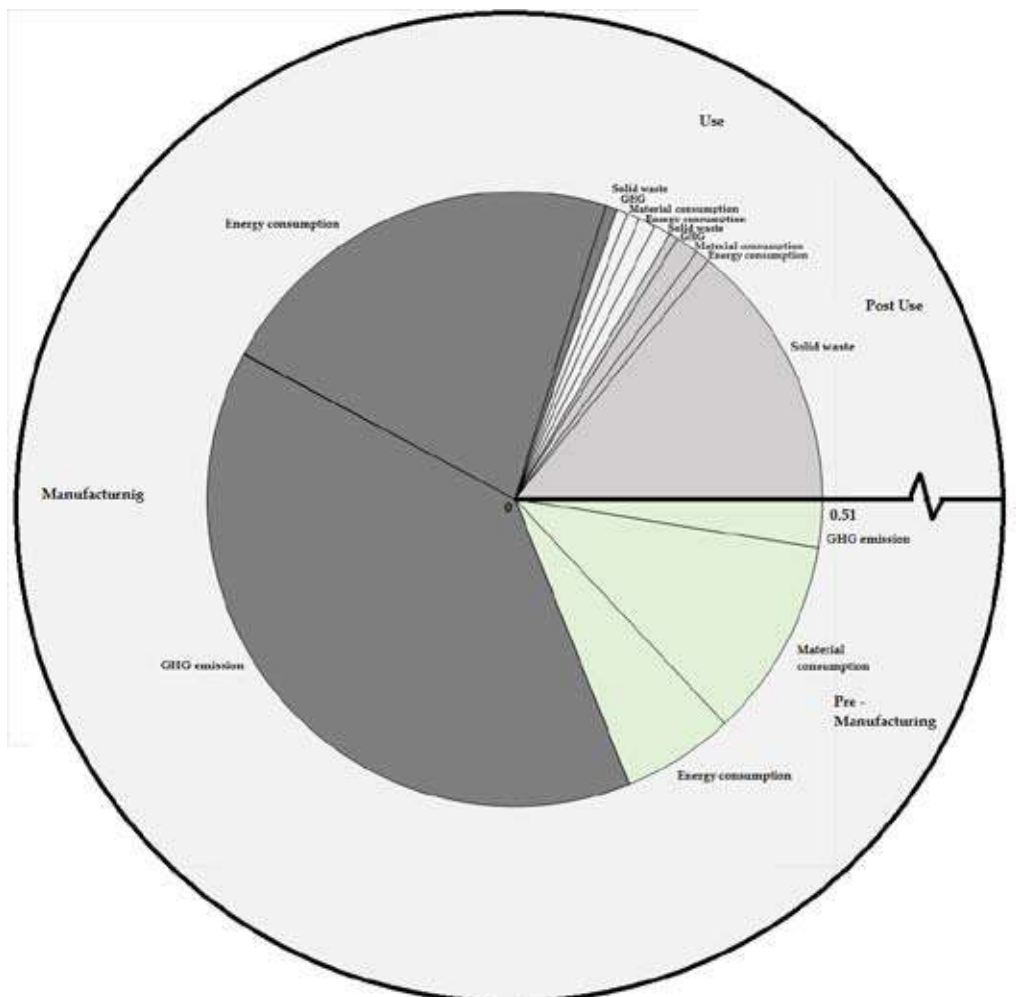


Figure 4 - Graphical representation of environmental impact



Table 2 – Weighted impact matrix

Indicator	Pre mfg	Mfg	Use	Post use	Total life cycle
GHG emission	X ₁₁	X ₁₂	X ₁₃	X ₁₄	$\sum X_1$
Material consumption	X ₂₁	X ₂₂	X ₂₃	X ₂₄	$\sum X_2$
Energy consumption	X ₃₁	X ₃₂	X ₃₃	X ₃₄	$\sum X_3$
Solid waste	X ₄₁	X ₄₂	X ₄₃	X ₄₄	$\sum X_4$
Overall impact	-	-	-	-	$\sum X/4$

2.5 Results Interpretation

The results obtained through the weighted impact matrix are to be represented graphically using a pre-defined criterion (Figure 4). The radius of the outer most circle represent the value range from 0 to 1. And the radius of the inner circle represents the total impact of the particular product which is to be considered in the environmental labelling.

The four phases of production that are, pre-manufacturing, manufacturing, use and post use phases were named separately in the diagram against the area govern by each phase. Then each phase was sub divided in to four areas that represent the relative proportions of impact categories naming, GHG emission, Material Consumption, Energy Consumption and Solid Waste generation. There are occasions, where you can find the manufacturing phases only with three sub divisions where the value related to the category is zero. To find the area to be covered by each indicator under each phase can be found by normalizing the values of weighted impact matrix.

Since such a graphical representation interprets the environmental impact through entire life cycle of a particular product, this can be recommended as an environmental label which will be a solution to the identified research gap.

2.6 Validating through a case study

The case study was conducted for validating the developed tool. The study was done for S1 clay roof tiles manufactures in Anuradhapura, Sri Lanka. Further data available [24, 25] for Asbestos roofing sheets and Calicut roof tile were referred for selecting minimum and maximum values for each indicator. The functional unit selected was the amount of each roofing options required to cover one square metre (1 m²) area of the roof. The results

obtained through the case study were given in the next chapter.

3. Case Study

Selected manufacturing industry process more than 2000MT of clay per month and produces over 300,000 clay tiles per month. Cradle to Gate data were collected through monitoring their available data and taking measurement during the process. Data for use phase and post use phase were collected from expertise and through calculations. Calculated results for each indicator are presented herewith Table 2.

Table 3 – Calculated results of each indicator for S1 clay roof tile

Indicator	Unit	Pre mfg	Mfg	Use	Post use
GHG emission	kg CO ₂ Eq	185.4	2848.5	42	34.5
Material consumption	kg	75.6	0.27	10.8	-
Energy consumption	MJ	22.05	79.2	4.95	3.3
Solid waste	kg	0	0.315	0.45	7.2

Material consumption under post use phase has measured as the total of reusability and recyclability ratios. That value has been estimated 0.85. The results above founded were scaled to the performance score and converted to the weighted impact values following the equations 1,2,3. Calculated weighted impact values are given in Table 4. Further the total impact for the entire life cycle of S1 clay roof tile according to the proposed tool was calculated as 0.51. The resulted Eco-Label representation is illustrated at Figure 4.

Table 4 – Weighted impact of each indicator for S1 clay roof tile

Indicator	Pre mfg	Mfg	Use	Post use	Total life cycle
GHG emission	0.056	0.863	0.013	0.010	0.942
Material consumption	0.214	0.001	0.013	0.025	0.253
Energy consumption	0.090	0.345	0.014	0.012	0.461
Solid waste	0	0.008	0.011	0.38	0.399
Overall impact	-	-	-	-	0.514

4. Discussion

According to the results, the overall environmental impact of S1 clay roof tile is 0.514 out of 1. Since it is at the middle of the impact scale, it can be recommended as an environmental friendly product comparatively.

However, in order to have a fair result it is required to expand the data set so that benchmark values cover a large distribution. In this case study, it has only considered the data for 3 products which cause to deliver a more relative outcome.

As shown in Figure 4, the highest impact occurs at manufacturing phase and next at pre-manufacturing. Most critical indicator for S1 tile is GHG emission and it contributes more at manufacturing phase. Material consumption at pre-manufacturing, and energy consumption at both manufacturing and pre-manufacturing are the other significant indicators. By reducing these high impacts, the radius of the impact circle can be got closer to the centre and it will be a more environmental friendly material.

5. Conclusions

The tool developed as the result of this research can be recommended as an initial approach of achieving the product environmental impact representation for Sri Lanka. The unique features which can be highlighted in this tool out of the other tools developed are;

- Simple representation of the environmental impacts using a graphical representation which can be understand by any person without deeper knowledge on manufacturing, LCA, Environmental impacts etc.
- Representation of the four phases of product the life cycle in one pictorial diagram
- The easiness of comparing two or more products together as a better decision making support system

However, the developed tool is to be validated by applying it to different construction materials available in Sri Lanka to overcome the pros and cons before introducing it to the interested parties including manufactures, consumers, contractors, certification bodies, and other third party.

The main disadvantage of this proposed tool is that it only developed based on the environmental perspective of a product. Since the economic and social aspects also important in making purchasing decisions the representation of other two aspects is important and that makes the entire overview of a product. The developed tool is consisting with a graphical representation that elaborates the magnitude of each impact as per each phase. And also, this tool development is not based on

a strong analytical method and it represents a deterministic approach.

References

1. Krausmann, F., Gingrich, S., Eisenmenger, N., Erb, K. H., Haberl, H. and Fischer-Kowalski, M., 2009. Growth in Global Materials Use, GDP and population during the 20th century. *Ecological Economics*, 68(10), pp.2696-2705.
2. Crosthwaite, D., 2000. The Global Construction Market: A Cross-Sectional Analysis. *Construction Management & Economics*, 18(5), pp.619-627.
3. Ofori, G., 2000, November. Challenges of Construction Industries in Developing Countries: Lessons from Various Countries. In *2nd International Conference on Construction in Developing Countries: Challenges Facing the Construction Industry in Developing Countries*, Gaborone (pp. 15-17).
4. Othman, E. and Ahmed, A., 2013. Challenges of Mega Construction Projects in Developing Countries. *Organization, Technology & Management in Construction: An International Journal*, 5(1), pp.730-746.
5. Pereira, K. and Ratnayake, R., 2013. Water Integrity in Action: Curbing.
6. <http://www.tradingeconomics.com/sri-lanka/gdp-from-construction>, Visited, 19th May 2017.
7. http://www.statistics.gov.lk/industry/SCI_Final_Report_2010.pdf, Visited, 19th May 2017.
8. http://www.statistics.gov.lk/industry/SCI_Final_Report_2015.pdf, Visited, 19th May 2017.
9. Reiter, S., July, 2010. Life Cycle Assessment of Buildings-A review. In *Proceedings of the Sustainability Workshop and Third Plenary Meeting*, Brussels, Belgium (pp. 1-19).
10. Borg, M., Paulsen, J., and Trinius, W, 2001, Proposal of a Method for Allocation in Building-Related Environmental LCA Based on Economic Parameters, *International journal of Life Cycle Assessment*, pp. 219 – 230.
11. Frischknecht, R., Wyss, F., Knöpfel, S.B. and Stolz, P., 2015. Life Cycle Assessment in the Building Sector: Analytical Tools, Environmental Information and Labels. The



- International Journal of Life Cycle Assessment, pp.421-425.
12. U.S. Green Building Council (USGBC). LEED® for New Construction & Major Renovations (LEED-NC), 2005, Version 2.2”.
 13. Green Building Council Sri Lanka. GREEN^{SL}® Rating System for Built Environment. Version 1.
 14. ISO 14020, Environmental labels and declarations – General principles.
 15. Mungkung, R., De Haes, H.U. and Clift, R., 2006. Potentials and limitations of Life Cycle Assessment in Setting Ecolabelling Criteria: A Case Study of Thai Shrimp Aquaculture Product (5 pp). The International Journal of Life Cycle Assessment, 11(1), pp.55-59.
 16. Fet, A. M. and Skaar, C., 2006. Eco-labeling, Product Category Rules and Certification Procedures Based on ISO 14025 Requirements (6 pp). The International Journal of Life Cycle Assessment, 11(1), pp.49-54.
 17. Thrane, M., Ziegler, F. and Sonesson, U., 2009. Eco-labelling of Wild-Caught Seafood Products. Journal of Cleaner Production, 17(3), pp.416-423.
 18. Canals, L. M., Domènèch, X., Rieradevall, J., Puig, R. and Fullana, P., 2002. Use of Life Cycle Assessment in the Procedure for the Establishment of Environmental Criteria in the Catalan eco-label of leather. The International Journal of Life Cycle Assessment, 7(1), p.39. G. L. Baldo, S. Rollino, G. Stimmeder and M. Fiesch, The Use of LCA to Develop Eco-Label Criteria for Hard Floor Coverings on Behalf of the European Flower, International Journal of LCA (2002) 269-275.
 19. Finkbeiner, M. and Hoffmann, R., 2006. Application of Life Cycle Assessment for the Environmental Certificate of the Mercedes-Benz S-Class (7 pp). The International Journal of Life Cycle Assessment, 11(4), pp.240-246. GBCSL labelling scheme.
 20. Green Building Council Sri Lanka. GREEN Labeling System for Construction Materials. Version 1.
 21. Abeyundara, U. Y., Babel, S., Gheewala, S. and Sharp, A., 2007. Environmental, Economic and Social Analysis of Materials for Doors and Windows in Sri Lanka. Building and Environment, 42(5), pp.2141-2149.
 22. Abeyundara, U. Y., Babel, S. and Gheewala, S., 2007. A Decision Making Matrix with Life Cycle Perspective of Materials for Roofs in Sri Lanka. Materials & design, 28(9), pp.2478-2487.
 23. Abeyundara, U.Y., Babel, S. and Gheewala, S., 2009. A Matrix in Life Cycle Perspective for Selecting Sustainable Materials for Buildings in Sri Lanka. Building and Environment, 44(5), pp.997-1004.
 24. Kurupparachchi, K. A. B. N., Life Cycle Assessment of Two Different Clay Roofing Tiles KABN Kurupparachchi, RK Ihalawatta, AK Kulatunga Department of Production Engineering, Faculty of Engineering, University of Peradeniya, Sri Lanka.
 25. Charles, C. V., Jeyamathan, S. J. and Rameezdeen, R., 2008. Sustainability Index for Roof Covering Materials. Building Resilience, p.140.

Safety Analysis of Anaerobic Digestion Plant Operation

Deshai Botheju and P. G. Rathnasiri

Abstract: Biogas generation by anaerobic digestion is rapidly gaining ground as a popular option for sustainable energy generation in Sri Lanka (SL). More importantly, it also contributes to formulating a successful waste management strategy SL is desperately in need for. However, despite the great attention put on research and development related to efficiency enhancement, process control, degradation of resilient organic matter, and gas utilisation techniques, only a marginal focus is so far being made on the essential safety technologies that must be incorporated into industrial and pilot scale biogas plants. This technical paper aims to provide a general overview of various safety dimensions related to biogas plants and offer guidance to plant designers and operators to incorporate essential technical, procedural, and organizational barriers with respect to process safety, occupational safety, and environmental care. A case study is also presented where it relates to the context of the paper.

Keywords: Anaerobic digestion, Biogas, Environment, Explosion, Process Safety.

1. Introduction

The anaerobic digestion (AD) is accepted as a sustainable process in the context of waste management and carbon-neutral energy generation in the form of biogas. Mostly free from the issues that infested old generation AD reactors like unstable operation, poor methane yield, and low reliability, the new era of biogas energy is promising and is rapidly becoming adopted in Sri Lanka as a workable technology for organic waste treatment and energy generation. The Sri Lankan experience at this point has shown that, with proper use of process technologies, biogas generated from organic waste streams, such as the organic fraction of MSW, can effectively be utilized in multiple platforms such as electricity generation, transport fuel for vehicles, or as a heating/cooking fuel. However, only a peripheral attention has so far been made on the important process safety and HSE considerations of AD plant operation and biogas handling.

We emphasize here that process safety aspects are critically important as biogas contains highly flammable methane that poses a significant safety risk when mixed with air within its flammability range (≈ 5 -15 vol % for methane in air). AD reactors can also lead to significant HSE risks such as exposure to the toxic H_2S byproduct gas, asphyxiation danger, and biological hazards associated with wastes feeds and reactor sludge. Accelerated corrosion resulting from H_2S is another risk factor.

1.1 Biogas safety - current perspective

In the early days of biogas generation, the processes were rudimentary, the generated volumes were quite small, and the large scale plants were rare, thereby safety was not perceived as a challenge. However, during last two decades, biogas generation has been steadily rising throughout the globe, as a result of the focus on climate neutral energy generation. Many governments supported this trend by heftily subsidising the biofuel and renewable energy industry. The increased number of biogas plants, as well as the significant increase in the size (scale) of biogas installations during recent times, demand high attention on associated safety risks. In addition, dramatic shifts in the social acceptability and perception of industrial risks [1] have led to the adoption of stricter safety standards and regulatory controls all over the globe.

1.2 Scope

Eng. (Dr.) Deshai Botheju, Ph.D.(NTNU), M.Sc.Tech (Norway), M.Sc. & B.Sc.Eng. (Moratuwa), AIChE, AMIE(SL). Currently working for Norwegian Petroleum industry, as an expert consultant in Safety Engineering and HSE Management.

Eng. (Dr.) P. G. Rathnasiri, Ph.D.(NTNU, Norway), M.Sc. (UK), B.Sc.Eng (Moratuwa), AMIE(SL). Senior Lecturer & the former Head of the Dept. of Chemical and Process Engineering, University of Moratuwa.



This technical paper presents a comprehensive safety analysis covering AD plant operation. The work is founded on long term experience of the authors related to the fields of Anaerobic Digestion and Safety Engineering. Further, a case study is presented based on the pilot AD plant treating canteen food wastes at the University of Moratuwa

In this paper, we intend to analyse related safety considerations under three (3) main categories. They are: (i) Process safety, (ii) Occupational health and working environment, and (iii) Environmental care. Note that, "safety" can be briefly defined as "freedom from unacceptable risk" [2]. Accordingly, the concept of industrial safety encompasses many discretely recognized disciplines such as Process Safety and Loss Prevention, Occupational Health & Safety, Environmental Management, etc.

It is emphasized that only through a systematic and holistic approach to process safety and HSE can avert catastrophic plant accidents like explosions and process fires, tragic incidents of personal injuries, as well as unwarranted damages to plant equipment and client utilities.

2. Process safety considerations

The loosely defined feed and gas compositions, and varying production rates are among the key challenges related to biogas safety. Biogas is generated as a result of a multitude of biochemical reactions; thereby the product composition and the volumetric gas generation rate depend on a number of less-controllable parameters such as feed material composition, ambient temperature, the presence of inhibitory agents, etc. In many cases, the digester feed is a mixture of organic waste material (such as municipal solid waste, waste water sludge, agricultural residue, food wastes, etc.) of which the composition and mixing proportions can vary throughout the year. Therefore, the gas composition and the volumetric generation rates to be used at the plant design stage are often the best possible estimates available at that time. All process safety measures and other safety procedures must, therefore, be determined after careful consideration of the foreseeable worst-case scenarios.

Table 1 illustrates some of the key physicochemical parameters, important for safety considerations, applicable for a "typical"

biogas stream. In most cases, it is sufficient to consider biogas primarily as a mixture of methane (CH₄) and carbon dioxide (CO₂) with some minor amounts of Hydrogen sulphide (H₂S), ammonia (NH₃), and water vapour. Nevertheless, biogas generated (naturally) from highly complex sources such as landfills might contain a large number of other trace compounds[3].

The composition of the main flammable agent of biogas, i.e. methane, may also widely vary (from about 10 % to 80 % vol.) depending on the biochemical state of the process. Methane and carbon dioxide compositions close to 50 - 60 % and 38 - 34 %, respectively, are quite common for the digestion of municipal organic wastes[20].

Table 1 - Typical composition and flammable properties of biogas constituents [4, 5, 3, 22].

Components	Typical composition	LEL (% in air at STP)	UEL (% in air at STP)
CH ₄	50 - 70 %	5	15
CO ₂	30 - 50 %	Non-flammable	
H ₂ S	1 - 2 %	4.3	46
NH ₃	< 1 %	15	28
H ₂	< 1 %	4	75
VOC	< 1 %	vary	vary
H ₂ O vapour	< 1 %	Non-flammable	
Biogas	As a mixture (of 60 % CH ₄)	10	30

2.1 Flammability / Explosivity

Methane, the main energy generating component of biogas, with 36 MJ/m³ of gross calorific value [6], creates explosive mixtures with atmospheric air within the concentration range of $\approx 5 - 15$ % [4]; i.e. the limits of explosion (Lower explosion limit -LEL, and Upper explosion limit - UEL). Therefore, it is critically important to avoid biogas being allowed to mix with air either within the digester or inside any gas storage vessel. Biogas must only be allowed to mix with combustion air within a suitable burner device at a final energy releasing step (e.g. gas burners, internal combustion engines, orgasflares). Table 1 further shows the flammable and explosive properties of the other constituents of biogas. H₂S, NH₃, and H₂ can, in standalone mode, also act as flammable agents, although their typical concentrations in biogas mixtures are so low that they do not normally pose a significant explosion hazard.

2.2 Hazardous zone classification

Hazardous zone classification (HZC) is a safety engineering technique used in process plants handling potentially flammable and /or explosive substances (i.e. flammable liquids, gases, and combustible dust particulates). The intention of this technique is to tag the areas surrounding hazardous installations (e.g. reactor vessels, process areas, storage areas, engine and boiler rooms, etc.) based on the likelihood of presence (or release) of flammable materials. Table 2 indicates a generally accepted criterion for the four (4) different types of zones often defined for process plants.

Table 2 - Hazardous zone classification*(abstract definitions are based on IEC 60079 Part 10-1 standard; [7])*

Zone classification	Abstract definition	Example
Zone 0	Explosive gas atmosphere is present continuously	Inside the digester
Zone 1	Explosive gas atmosphere is likely to occur periodically during normal operation	The adjacent area near pressure relief valve.
Zone 2	Explosive gas atmosphere might be present for short durations occasionally	Process area /process buildings near the digester.
Non-hazardous zone	Explosive gas is not perceived as a danger in this area.	Office buildings of the plant.

2.3 Ignition source control

If a flammable gas cloud (e.g. methane from biogas mixed in air) is formed within the plant (e.g. due to a gas leak or failure of process containment), the last barrier preventing a catastrophic fire or an explosion is to keep ignition sources (such as electrical sparks or hot surfaces) from igniting the flammable gas cloud. Therefore it is important to use explosion proof (EX rated) equipment, tools, and electric & electronic equipment within areas where flammable gases are likely to be present. Accordingly, proper hazardous zone classification (HZC) is the first step towards a sound ignition source control (ISC) philosophy.

All electrical and electronic devices (e.g. pumps, motors, light fixtures, control circuits, instrumentation and sensors, fire and gas detectors, etc.) that are to be used within a Zone 1 or Zone 2 environment must be EX certified

(explosion protected) for the respective zone. Zone 0 environments must usually be devoid of any potential ignition sources (e.g. inside of the digester), as only a handful of devices exists if at all, that can be used within a zone 0 environment. Explosion protected electric equipment utilise different techniques to avoid or minimise the likelihood of spark generation (such as low energy non-sparking equipment, encapsulated equipment, oil submerged equipment, etc.).

2.4 Gas detection

The only reliable way to identify gas hazards during the early phase of a leakage is to use gas sensors which could warn the impending danger by audio-visual alarms (i.e. sounds and light flashes). For biogas plants, two types of gas detectors, i.e. flammable gas detectors, and toxic gas detectors, are relevant.

2.4.1 Flammable gas detection

Fixed gas detection devices that can identify flammable methane at about 20 – 40 % of the LEL must be installed at strategic locations where a flammable biogas cloud is likely to be present during a gas leak event (e.g. near digester top, gas storage tanks, near gas utilization devices such as electric generators or boilers, etc.).

2.4.2 Toxic gas detection

Continuous detection of H₂S is recommended near medium to large scale biogas plants. Being a highly toxic gas, it is necessary to identify the presence of H₂S even at low concentrations (See Table 3). If a permanently mounted H₂S detector is not available, it is vital to use a handheld H₂S detector when working near active digesters with low ventilation conditions (e.g. a digester located inside a plant house).

In addition, carbon monoxide (CO) detectors must be installed at enclosed machine rooms containing power generators and fired boilers where combustion might generate deadly CO gas.

2.4.3 Portable gas detectors

Portable gas detectors are often used as a part of occupational safety procedures whenever operational or maintenance tasks are to be conducted near or within digester tanks and pits. These are handheld devices that can indicate both the presence and concentration of dangerous gases (flammable and toxic). They are also useful for recognizing



potentially asphyxiating environments if they could indicate the available oxygen level in the environment. There are many handheld gas detectors which could simultaneously detect multiple gases and indicate their concentrations, and also emit alarm sounds if dangerous levels are detected. It is, however, important to keep such devices properly calibrated all time.

2.5 Fire detection and fire fighting

The biogas plants must be protected with fire detection devices (e.g. infrared flame detectors, smoke detectors, etc.) and firefighting means such as deluge nozzles, sprinklers, fire hoses, portable fire extinguishers etc.

2.5.1 Fire and gas detector actions

Medium to large scale biogas plants need automatic safety actions based on input from gas detectors and fire detectors. Confirmed detection of gas (based on multiple detectors) must preferably deactivate /shutdown potential ignition sources such as electrical equipment, electronic circuitry, hot surfaces (e.g. electric heaters), flames (e.g. gas burners, boilers), and internal combustion engines (biogas powered electricity generators). Fire or gas detection must preferably shut the main gate valve of the gas supply connected to the digester or the gas storage vessel. In addition, various other safety actions such as activation of deluge or sprinkler systems, change of ventilation conditions, etc. may be required according to the plant design and the Fire & Gas control logic defined based on actual risk levels.

2.6 Corrosivity

Anaerobic digesters and the surrounding plant equipment can be subjected to highly corrosive conditions due to the presence of corrosive digester liquors and the gaseous components such as H₂S, CO₂ (through carbonic acid formation), and also H₂. Therefore, the plant design must incorporate such considerations and the material selection must be done with due care. High corrosion, if not properly taken care of, is a safety threat to the plant's functional integrity as well as to the structural strength. Corrosion could lead to dangerous gas leaks also. Various process equipment such as pipes, valves, vessels must have inbuilt resilience against the highly corrosive environment.

2.7 Ventilation

Plant buildings near digesters must have suitable ventilation arrangements, in order to avoid accidental accumulation of flammable and toxic gases. A ventilation air change rate of 5 air exchanges per hour [4] is recommended. If natural ventilation is the only available ventilation mean, then large openings must be used with ample air circulation access to ensure adequate ventilation could be realized even under unfavourable stagnant atmospheric conditions.

For mechanical (forced draft) ventilation systems, it is recommended to install at least 2 gas detectors (one for flammable methane and the other one for toxic H₂S) at the ventilation air inlet. Upon detection of gases at this location, the mechanical ventilation system must automatically stop.

Special ventilation conditions required for maintenance and repair activities within digesters is briefly described in section 3.3.2.

2.8 Pressure safety

An anaerobic digester is a biochemical reactor which gradually builds up pressure due to the gas generation. If gas is not removed from the system, the pressure will continue to build up until it leads to a material failure (e.g. pipe rupture, or vessel blow up). Therefore, medium to large scale biogas plants, require dedicated pressure safety designs to avoid such dangerous failures which could then lead to process fires and explosions. If normal process control system fails to maintain the operating pressure conditions (e.g. by controlling digester feeding rate and controlling gas removal flow rate), an emergency safety system must kick in to bring the digester into a "safe status". The intended safe status, in this case, can be achieved by depressurizing the digester (i.e. lowering the energy content of the system). This could be achieved by using emergency pressure safety devices such as the opening of a pressure safety valve (PSV) and venting or allowing to burst a rupture disk. In more advanced designs, various instrumented safety functions shall be used to bring the entire plant to a safe shutdown (together with ignition source control and depressurization) when detecting such dangerous developments.

Continuous monitoring of digester pressure using process instrumentation is a sound safety strategy for any biogas plant irrespective of the

scale. For larger plants, it is advisable to incorporate two independent pressure safety barriers (e.g. a PSV and a rupture disk; or a PSV and an instrumented pressure safety function).

2.8.1 Negative pressure development

An anaerobic digester must always run with a positive pressure inside. In case, a negative pressure development is allowed, then air could draw into the digester and mixed with biogas to create an explosive methane-air mixture. A negative pressure development could occur if a gas treatment and utilization systems such as a gas blower or a compressor draw more biogas from the digester than the system is capable of producing. This situation must be avoided by incorporating necessary process control strategies (such as gas flow control), and also by designing emergency safety barriers such as instrumented safety functions to shut down gas blowers or pumps upon the detection of low digester pressure.

2.9 Flame arresters

Installation of flame arresters on biogas supply lines is recommended in order to avoid a flame travelling back through a gas pipe and igniting the gas vessel (i.e. digester or a gas storage vessel). A flame arrester is simply a short pipe segment filled with a mesh of fine metal wires (see Figure 1). The wire mesh must be corrosion resistant against H₂S (e.g. copper is a suitable material). The metal wire mesh absorbs heat from a propagating flame and quenches it within the flame arrester.

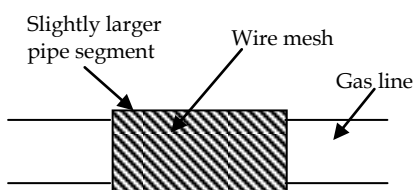


Figure 1 - A simple flame arrester

A flame arrester must be located upstream the gas burner (or a flare). In addition, it is recommended to include a flame arrester downstream the main gas valve of a digester or gas storage vessel.

2.10 Lightning protection.

Taller digesters and the digesters in open landscapes must be lightning protected. If lightning strikes a digester and damages its

vessel containment or gas piping, it can quickly develop into a fire and explosion scenario. Various lightning protection means,[8] such as air termination & down conductor systems, may be utilized for this purpose.

Plant electric supply and the electronic control systems (e.g. process control and emergency control systems) must also have suitable surge protection devices installed so that critical instrumented safety functions remain operational even if the plant is struck with a lightning induced surge current.

2.11 HAZID, HAZOP, and Risk Assessments

Hazard identification (HAZID), hazards and operability studies (HAZOP), and various risk assessment techniques must diligently be used based on the plant capacity and other relevant risk factors affecting the particular plant. For small to medium scale plants, a HAZOP study (based on plant P&IDs) and a qualitative risk assessment study must suffice. Large scale plants and the plants with significant risks to surrounding third parties must be based on more rigorous risk assessment and safety techniques such as quantitative risk assessments, gas dispersion studies, working environment and health risk studies, etc.

2.12 Dispersion analysis

For large biogas plants, it is advisable to conduct a numerical simulation of gas dispersion together with actual plant geometry and surroundings. This will be used to generate a realistic picture of a gas leak scenario and to acquire more accurate details on potential impacts. Hazardous zone classification and locating of gas detectors must then be based on this information. Often, such numerical studies are a part of a wider quantitative risk assessment.

3. Occupational safety, health, and working environment considerations

Apart from critical process safety concerns and safety barriers introduced at the design stage, day-to-day operation of biogas plants requires attention to various occupational hazards, health impacts, and working environment considerations.



3.1 Asphyxiation

Asphyxiation is the greatest working environment hazard for those who perform work near digesters, especially the inside of anaerobic digesters, during occasional maintenance works or breakdowns. Asphyxiation happens when rapidly generating biogas pushed out air from a confined space, or when biogas is accumulated within an enclosed area such as a pit or a digester vessel. When the oxygen level in the air is diluted below 10 % [9], a person may quickly succumb. However, already at 19 - 16 % oxygen levels, a person would be subjected to impaired judgement [5, 9]. Therefore it is not generally recommended to enter any area with less than 19 % oxygen unless a self-contained breathing device is worn.

Wet waste storage pits or a manure tanks can inadvertently act as anaerobic digesters, depending on the environmental conditions (temperature, humidity, etc.). A worker used to enter such area without harm in previous occasions may suddenly succumb to asphyxiation if the waste material is now undergoing digestion process generating biogas. Also, even an open top pit (or a tank) that could look like safe enough due to its open nature might be a hazardous location to enter as the rate of gas generation may be so high to drive out oxygen (air) from the tank /pit interior.

3.1.1 Gas layering

Layering refers to the stratification of various biogas components based on the relative density of various gases. Methane has a lower density than air; therefore it floats upwards and usually accumulates at higher levels of a pit or a tank. If biogas ingress happens into a closed building (e.g. plant house), the methane will be accumulating close to the ceiling level. On the other hand, CO₂ has a higher density than air; therefore it accumulates close to the bottom of a tank or a pit (or a closed building). Considering the minor components; H₂S is heavier than air and accumulates at bottom layers, and NH₃ is lighter than air and rises to upper layers.

3.2 Toxicity

Even though it is a minor component in biogas, H₂S could pose a formidable threat to personnel as it is a highly toxic gas. The possibility of varying biogas composition (as explained before) makes judging the H₂S level more

challenging at the design stage of a biogas plant. Therefore, it is always advisable to use H₂S detectors near digesters.

Table 3 illustrates toxicity information on various biogas components.

Table 3 - Toxicity and Health hazards of gases found in biogas plants [10, 11, 12, 21].

Gas	Toxicity limit (ppm)	Olfactory sense	Impact
CH ₄	Non toxic	Odourless	Asphyxiating
CO ₂	1000	Odourless	Drowsiness and headache, Asphyxiating
H ₂ S	20	Rotten egg smell at low concentrations	Highly Toxic
NH ₃	50	"ammonia" smell	Eye, throat, and lung irritation. Fatal
CO	50	Odourless	Highly Toxic

CO₂, though not considered as a toxic gas, can have negative health impacts at elevated concentrations. If breathing CO₂ concentration increases beyond 1000 ppm level [12], impaired thinking and difficulty of concentration may occur. At further increasing concentrations, symptoms like dizziness increases respiration rate, and heart rate will occur. Eventually passing out would occur as CO₂ displaces oxygen supply in the blood stream. OSHA recommends 5000 ppm [11] as the permissible limit of CO₂ in the air for an 8 hour work day and a 40 hour work week for a lifetime of exposure.

NH₃ also acts similar to CO₂ in displacing blood oxygen levels [13].

Carbon monoxide (CO), even though not a component of biogas itself, can be a safety hazard when internal combustion engines (such as electric power generators running on biogas), are operated within enclosed buildings. Exhaust gas from internal combustion engines contains CO in deadly amounts. In addition, some burners (e.g. biogas operated boilers) can generate CO if complete combustion does not occur. Use of CO detectors at such locations is recommended.

3.3 Confined area entry

Entering a confined area (like a manure pit or an anaerobic digester) must only be carried out

if it is really needed, and with a range of safety precautions.

3.3.1 Eliminate entry requirements

The “safety in design” concept must always be adopted. Digesters must be designed with minimum need of entry for maintenance; like installing mechanical devices such as mixers that can be replaced or repair from outside.

3.3.2 Ventilation

Whenever possible, excessive forced ventilation must be used before and during any confined area entry. Either dedicated ventilation air blowers may be installed as a part of the design, or else, if such arrangements are not available, external temporary fans or blowers must be used to expel gases from the confined area before and during the entry. Oxygen level measurements and readings for toxic gases (H₂S) must be taken using portable gas detectors before entry.

3.3.3 Rescue

If a person is found unconscious within an enclosed environment, one should never attempt a rescue by directly entering, without safety precautions. It is all more common that multiple victims succumb to asphyxiation (or to toxic gases) by trying to rescue previous victims[5]. Such chain casualties can be avoided by only letting professional or trained rescuers attempt rescuing victims. An enclosed area with suspected asphyxiation or toxic gas presence must only be entered by wearing a self-contained breathing apparatus. Further, the enterer must have a rescue rope attached to his body and a second person must be present with full attention on the enterer. The second person must have some sort of pulling arrangement (like a pulley) to withdraw the enterer by pulling on the rescue rope while standing outside the danger zone (e.g. out of the pit or tank). The use of the self-contained breathing apparatus requires special training, and often such use is restricted to fire fighters and professional rescuers. Therefore, whenever, an enclosed area entry with suspected gas presence is attempted during normal maintenance or repair work in a biogas plant, the other aforementioned safety precautions must be followed (i.e. rope attachment, a second person outside the area, and pulling arrangement).

3.4 Biological hazards

Biogas is generated in a digester due to the activity of a variety of microorganisms acting on, often, waste materials such as manure, sewage, wastewater sludge, organic fraction of municipal solid wastes, food wastes, etc. Such feed materials can also easily carry various pathogenic microorganism and parasites (e.g. worms). Workers looking after digester operations usually exposed to these biohazards. Therefore it is critical to use proper safety procedures and use good housekeeping practice within the plant facility. Digester residence time and the operating temperature play a key role in determining the sanitary condition of the digested sludge which must be handled after exiting the reactor. For example; in one study related to a plug flow digester feeding dairy manure and operating under mesophilic temperature conditions (i.e. $\approx 37\text{ }^{\circ}\text{C}$), with a retention time of about 36 days, a Fecal coliform destruction of 99.9 % was achieved [14]. This is considered to be a safe level of pathogen destruction. However certain parasitic worms such as roundworms can survive at a much greater percentage. Therefore digester sludge, especially the sludge resulting from digesting human and animal excretes, must be handled with care, and must be considered as a biohazardous material for plant workers.

3.4.1 Vaccination

Exposed personnel such as plant workers, researchers, and research students, must get appropriate vaccination shots at regular intervals as recommended by immunologists.

3.4.2 Personnel protective equipment

Proper use of personal protective equipment is essential. Gloves, overalls, safety goggles, masks, and boots are required for the personnel who are exposed to hazardous materials.

3.4.3 Plant house keeping

Standard cleaning and sorting procedures must be followed throughout the plant facility. The use of 5S concept [15] is a proper approach to this. Workers must also pay attention to proper personal hygiene practice.

3.5 Safety signs

Safety signs are vital for delivering critical safety related information to the plant workers as well as to any occasional / first-time visitors to the plant, in a simple and effective way.



Prohibition of open flames, attention on alarms and light signals, escape directions, assembly stations, the location of first-aid and firefighting equipment etc. are among many things that must be indicated by proper signage. A mix of illustrations and wording should be used in such a way that the maximum comprehension is possible within the shortest possible time.

3.6 Heat radiation

Potential heat radiation impact from biogas flaring should be evaluated. Intense heat radiation can be hazardous for plant workers. Expected heat radiation levels at exposed plant locations must be estimated /calculated. For a person without special protection suits (but with ordinary clothing), maximum bearable heat radiation exposure is given as 6.31 kW/m² for 30 seconds period[16]. This factor should especially be evaluated for very large scale biogas plants. The height of the flare stack must be designed to minimize this heat radiation impact on the plant, and also to properly disperse air pollutant emissions (section 4.1).

Further, installation of a knock out drum before the biogas flare is recommended in order to avoid any liquids (such as reactor liquor or any condensate from the gas stream) entering the gas burner /flare stack. Liquids could not only increase the level of air emissions (section 4.1) but also, at worst cases, could result in a dangerous "burning rain" type scenario where fiery liquid droplets / mists raining down from the flare stack.

3.7 Noise

Exposure to high noise levels near machinery like electric power generators, gas compressors, biogas flares can be an occupational safety concern in biogas plants. Procedural controls must be in place to avoid workers being exposed to high noise levels for extended period of times. Maximum allowable work duration shall be determined based on the expected noise levels. For short exposure intervals, ear protection devices such as ear plugs and earmuffs must be used.

4. Environmental considerations

As described elsewhere [17] various environmental care perspectives are also a part of the concept of "safety". Therefore any environmental impacts related to the building and operation of a biogas plant must be

investigated, and necessary mitigation measures must be taken.

4.1 Emissions

Emissions can primarily occur when the generated biogas is combusted to utilise its useful energy (e.g. burning to generate heat or combustion within an internal combustion engine to produce electricity, or to achieve vehicle mobility). Also, emissions occur when unused or extra biogas is burned in a gas flare (e.g. in a flare stack, or in an open flare burner). Even though the emission of air pollutants and climate gases such as CO₂, SO_x, NO_x, unburnt and molecularly rearranged hydrocarbon components, and particulates are not expected to be a serious problem in relation to biogas (unlike liquid and solid fuels), particular attention must still be paid to the air emission standards within the relevant regulative regime. The content of CO and unburnt hydrocarbons can most often be avoided by realizing > 850 °C flame temperatures and > 0.3 sec. residence times [6]. At higher flame temperatures (>1200 °C) increasing amounts of atmospheric N₂ oxidizes to form thermal NO_x; often explained by a mechanism called extended Zeldovich mechanism that comprised of a set of highly temperature dependent chemical reactions [23]. The cleanliness of the generated biogas is an important factor here. If there is a gas cleaning stage within the process, then the level of CO₂, H₂S, NH₃, and various other trace components (such as various volatile organic components) will be significantly low, thereby leading to a cleaner combustion flue gas stream.

4.2 Odour

Due to the handling of various types of organic waste material, the odour might become a problem if not properly managed. Odours often spread well beyond plant perimeters and may impact neighbourhood areas.

Following key steps must be considered in order to minimize odour issues:

- Waste transportation, unloading, and feeding the plant must be done with minimum exposure to open air.
- Digester residence time must be long enough for the waste to undergo complete degradation. Only partially digested waste would emit significant odours.
- Reactor sludge stabilization and suitable disposal means must be adopted.

4.3 Contaminated sludge

The sludge resulting from biogas reactor operation has to be disposed of using sustainable means. It usually needs further stabilization or treatment before release to the environment. Use of anaerobically digested sludge as a soil conditioner or fertilizer is quite common. However, attention must be paid to the fact that such sludge quite often contains high concentrations of heavy metals [18]. Therefore, it is perceived as unsafe to use them on food crops without careful analysis of the content of heavy metals. Metals like Pb, Ni, Cd, etc. can gradually accumulate in living organisms and could lead to chronic health problems [19].

5. Case study

A pilot scale demonstrative anaerobic digester (high rate reactor) was constructed on the premises of University of Moratuwa (UoM) with the objective of utilizing food wastes generated in university canteens as the feed material and then using the generated biogas as a transport fuel (for three wheel vehicles) after upgrading. The project was aimed at technology demonstration related to waste management, process, biochemical, reactor, and safety technologies. Figure 2 illustrates the schematic arrangement of this pilot facility.

The digester was designed to operate on 20 days retention time and at a maximum pressure of 1.5 bar. The bulk liquid capacity was 4.9 m³ and the total reactor volume including head space was 5.2 m³. This designed gas production rate is 11.4 m³/d with an average CH₄ composition of 55 %.

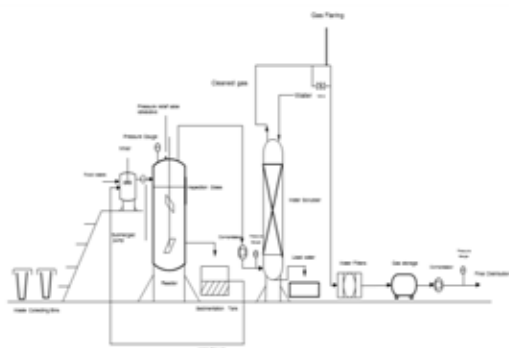


Figure 2 - Pilot scale anaerobic digester at UoM aimed at technology demonstration.

The following is a brief description of the key safety considerations evaluated during the

design and operation phases of this pilot facility.

Pilot plant building

By taking into account, safety aspects and proper natural ventilation, the plant building was located in a remote part of the university land, well away from the building clusters with student lecture rooms and laboratories. All sides of the building were kept half way open enabling proper natural ventilation and dispersion of any potential gas leakage.

Feed preparation system

A crusher was installed to reduce the particle size of the feed stock (food waste). A mesh guard was installed around the crusher by taking into account of the working environment considerations related to the personal safety of the operator.

Feed transfer system

A submersible sewage pump was installed to pump the food waste slurry into the anaerobic reactor. A submersible pump does not act as an ignition source even if a flammable gas cloud is present.

Material selection

Based on the project budget, the selected construction material was mild steel. However, with proper attention to the corrosive atmosphere, inside of the reactor vessel was surfaced coated with high-grade marine paints and the outside with anti-corrosive paints.

Pressure safety instrumentation

A pressure gauge and safety valve were fixed on the top of the vessel so that a continuous pressure reading can be obtained by the operators.

Gas cleaning and pressure safety

A water scrubber was designed and fabricated to remove CO₂ and H₂S from the biogas mixture. This should greatly reduce the corrosive nature of the product biogas stream. The raw gas enters the scrubber at 10 bar pressure from the bottom and water is sprayed from top of the column. Operating pressure is also 10 bars inside the vessel. Safety valve for 10 bars has been fixed on the top of the scrubber which is fabricated from stainless steel.

Intermediate gas storage and compression

Biogas is required to storage at two stages. i.e. between the reactor and scrubber and before pumping to the vehicle. The compressor used was a scuba type compressor which is operated



by gasoline and has a maximum capacity of 250 bars. Upgraded biogas was stored in high-pressure cylinders at 20 bar pressure. The cylinders were of proper safety design and approved for the application and the pressure condition.

Inspection for gas leaks

Before starting up of the pilot plant, the piping and anaerobic reactor were tested for possible gas leaks. To conduct this test, the system was over pressurized and then kept one hour at test pressure condition.

Waste handling and sludge disposal

Canteen food waste is transported into the pilot plant using closed containers in order to avoid odour and contamination due to spilling. Sludge generated from the digester is transferred to a nearby isolation pit and then subsequently utilized as a fertilizer for gardening (non-food crops).

6. Conclusions

This technical paper presents a detailed outlook on various safety dimensions that have to be properly assessed in the design phase as well as in the operation phase of anaerobic digestion processes. The presented process safety, occupational safety & working environment, and environmental care considerations are critical to the sustainable and safe operation of biogas plants. It is emphasized that safety and sustainability are the most vital aspects that could determine the social acceptance and the economic viability of any industrial technology.

A case study is presented where a pilot scale anaerobic digester was designed, constructed and operated as a technology demonstration project. A wide attention is given to the relevant safety considerations during all life cycle phases of this pilot scale digester.

References

1. Botheju, D., and Abeysinghe, K. 2014. Public risk perception towards chemical process industry: Comprehension and response planning. *Safety & Reliability: Methodology and Applications*, Nowakowski et al. (Eds.) (Book), pp. 453-60, Taylor & Francis Group, London, ISBN 978-1-138-02681-0. (Also presented at European Safety & Reliability Conference, ESREL 2014, Wroclaw, Poland. Organized by European Safety & Reliability Association (ESRA).
2. International Electrotechnical Commission (IEC). 2004. Functional safety and IEC 61508; A basic guide. Available online: http://www.ida.liu.se/~simna73/teaching/SCRTS/IEC61508_Guide.pdf
3. Walsh, J. L., Ross, C. C., Smith, M. S., Harper, S. R., Wilkins, W. A. 1988. Handbook on biogas utilization. Published by U. S. Department of Energy.
4. CH4Biogas. 2017. Hazardous zones in CH4 biogas systems. Technical article. Available online: http://www.chfourbiogas.com/uploads/1/4/1/9/14199462/hazardous_zones_in_our_biogas_systems.pdf
5. NIOSH (The national institute for occupational safety and health). 1990. Preventing deaths of farm workers in manure pits. NIOSH publication number 90-103. Available online: <https://www.cdc.gov/niosh/docs/90-103/>
6. International Energy Agency (IEA). 2000. Biogas flares: State of the art and market review. Topic report of the IEA Bioenergy Agreement Task 24 – Biological conversion of municipal solid waste.
7. International Electrotechnical Commission (IEC). 2015. Explosive atmospheres – Part 10-1: Classification of areas – Explosive gas atmospheres. International Standard IEC 60079-10-1. Edition 2.
8. DEHN International. 2015. Lightning and surge protection of biogas plants. White paper. Article online: <https://www.dehn-international.com/sites/default/files/uploads/dehn/pdf/white-papers/ab-juli15/wp003-e-biogas.pdf>
9. Air Products and Chemicals. 2014. Dangers of oxygen-deficient atmospheres. Safetygram 17. Article available online: <http://www.airproducts.com/~media/files/pdf/company/safetygram-17.pdf>
10. Heezen, P. A. M., Gunnarsdottir, S., Gooijer, L., Mahesh, S. 2013. Hazardous classification of biogas and risks of large scale biogas production. *Chemical Engineering Transactions*, Vol. 31.
11. Aldrich, B. S., Brown, N. J., Hallman, E. M. 2005. Innovations in manure management: Manure gas can be deadly. Cornell Manure Management Program. Article online: <http://extension.psu.edu/natural-resources/energy/waste-to-energy/resources/biogas/links/biogas-and-anaerobic-digestion-safety/manure-gas-can-be-deadly.pdf>
12. Renewable Fuels Association (RFA). 2015. Carbon dioxide safety program. Report; Available online: http://ethanolrfa.3cdn.net/2d1bea9178e0e876bd_idm6i8enq.pdf

13. Aria, A. 2006. Ammonia emissions and safety. Agri-Facts, June 2006. Available online: [http://www1.agric.gov.ab.ca/\\$department/deptdocs.nsf/all/agdex8271/\\$file/086-6.pdf?OpenElement](http://www1.agric.gov.ab.ca/$department/deptdocs.nsf/all/agdex8271/$file/086-6.pdf?OpenElement)
14. P. E. Wright, P. E., Inglis, S. F., Stehman, S. M., Bonhotal, J. 2003. Reduction of selected pathogens in anerobic digestion. In Proceedings of the 9th international symposium of ani mal, agricultural and food processing wastes. Article available online: http://www.manuremanagement.cornell.edu/Pages/General_Docs/Papers/Reduction_Selected_Pathogens_A D.pdf
15. Michalska, J. and Szewieczek, D. 2007. The 5S methodology as a tool for improving the organization. J. of Achievements in Materials and Manufacturing Engineering. Vol. 24, No. 2., pp. 211- 214. Available online: http://www.academia.edu/10065153/5S_methodology_as_a_tool_for_improving_the_organization
16. American Petroleum Institute (API). 2014. Pressure relieving and depressurizing systems. API standard 521. Ed. 6, pp. 106.
17. Botheju, D., Abeysingha, K. and Rathnasiri, P. G. 2014. Safety and emergency preparedness in oil and gas industry: Experience based on North Sea offshore platforms. Annual proceedings of the Institution of Engineers of Sri Lanka (IESL) 2014, pp. 163-170.
18. Botheju, D., Svalheim, Ø., Rydtun, B., Johansen, J., Haraldsen T. K. and Bake R. 2007. Fertilizer production by digestate nitrification. In proceedings of the 12th European Biosolids and Organic Resources Conference, Manchester, UK, November 2007.
19. Stasinou, S., Nasppoulou, C., Tsikrika, C., Zabetakis, I. 2014. The bioaccumulation and physiological effects of heavy metals in carrots, onions, and Potatoes and dietary implications for Cr and Ni: A review.
20. Biogas Renewable Energy. 2009. Biogas composition. Information page available online. http://www.biogas-renewable-energy.info/biogas_composition.html
21. NIOSH (The national institute for occupational safety and health). 1994. Table of IDLH values – Carbon monoxide. Available online. <https://www.cdc.gov/niosh/idlh/630080.html>
22. Coward, H. F., Jones, G. W. 1952. Limits of flammability of gases and vapors. Bulletin 503, US Bureau of Mines.
23. Niska, J., Kaufmann, B., Mortberg, M., Almeida, S. M., Zanusso, E., M., Gitzinger, H-P., Fernandez, J. M., Mori, M. F. C. 2007. Minimizing NOx emissions from reheating furnaces. Final Report – Research Programme of the Research Fund for Coal and Steel. Tecnico Lisboa. Available online: <http://projects.ctn.tecnico.ulisboa.pt/Dioxinas/18.pdf>



Simulating the Effect of Modifying Reversed A2O Process on Combined Removal of Nitrogen, Phosphorous and Organic Matter in Municipal Wastewater

W.B. Roshen P.S. Fernando and P.G. Rathnasiri

Abstract: In evolution of biological wastewater treatment processes, extended aeration, A2O (combination of anaerobic, anoxic and oxic (aerobic) processes) and Reversed-A2O (RA2O) (combination of anoxic, anaerobic and oxic processes) processes are significant milestones. While other methods (than RA2O) have been subject for improvements, improvements for RA2O process have been minimal. Thus, the effect of modifying Reversed-A2O (RA2O) process via mixed liquor recirculation, activated sludge recycling and optimizing the percentage recycled on efficiency of combined removal of nitrogen, phosphorous and organic matter in municipal wastewater has been studied via mathematical modelling and simulation. The results suggest that mixed liquor recirculation from aerobic to anoxic reactor reduces nutrient removal efficiency and that RA2O process can be improved to achieve significant nutrient and organic matter removal efficiencies by recycling activated sludge only to anaerobic reactor without recycling activated sludge to anoxic reactor.

Keywords: Reversed-A2O process, Nutrient and organic matter removal, Municipal wastewater, Activated Sludge Modelling

1. Introduction

When wastewater treatment practices improved its focus on nutrient removal, biological nutrient removal (BNR) methods were more attractive compared to chemical nutrient removal methods due to savings in investment in machinery, less energy requirement (Lettinga, 1996 [1]) and lower environmental impacts (Arbuckle and Griggs, 1982 [2]). Following the various BNR models, such as University of Cape Town model, Anaerobic/Anoxic/Aerobic (A2O) model (Spector, 1993 [3]), in 1997, Zhang and Gao [4] proposed the ability to further improve A2O process, by changing the sequence of anaerobic and anoxic reactors, and this process was named Reversed-A2O (RA2O).

The main arguments supporting this improvement were the preference given to denitrification by the carbon source, from influent and returned activated sludge, and the greater biochemical efficiency in aerobic reactor, due to deeper anaerobic conditions in the anaerobic reactor with the exhaustion of nitrates in the anoxic reactor. This innovation was supported to be higher in efficiency with respect to nutrient removal by Xuejun and Bo in 2006 [5] and Bi et al. in 2009 [6]. Furthermore,

Kang et al. in 2011 [7], proved that the RA2O process was also more economically competitive with respect to installation, construction and operation than the A2O process.

However, Zhang and Gao (2000) [8] did not observe significant improvements in removal of organic matter in the RA2O process compared to the A2O process. Furthermore, in 2014, Xu et al. [9] argued that the RA2O process to be significant only in phosphorous removal, in a comparative study among the two processes, under same operating conditions, including mixed liquor recirculation from aerobic zone to anoxic zone. This had also been supported by Zhou et al. in 2011 [10] via a simulation study. Nevertheless, via the projection pursuit method, Fang et al. in 2016 [11], showed that still the A2O process to be predominant, compared to the RA2O process, in both organic matter and nutrient removal.

Eng. W. B. Roshen P. S. Fernando, B.Sc. Eng. (Hons) (Moratuwa).

Eng. (Dr.) P. G. Rathnasiri, B.Sc.Eng.(Hons) (Moratuwa), M.Sc. (UMIST-UK), PhD (NTNU-Norway), Senior Lecturer, Department of Chemical and Process Engineering, University of Moratuwa.



Accordingly, it is observed that there exists, still, wide spread opinions on the efficiency and effectiveness of the RA2O process, even though it is currently, widely applied all over the world. Moreover, application of mathematical modelling for the RA2O is at a fairly young stage. Thus, it was decided to investigate the possibility to improve the RA2O process with respect to combined removal of nutrients and organic matter by changing intermediate recycling streams and percentage quantities recycled, and thereby, suggest modifications to the RA2O process, via a modelling approach.

2. Materials and Methods

With the intention of extending the findings from the study to real world practices, a municipal wastewater treatment plant, already employing RA2O, was selected for the study. It was one of the two RA2O municipal wastewater treatment plants operated by National Water Supply & Drainage Board (NWSDB) at Ratmalana, handling a daily flow of 17,009 m³, on average. Even though, the plant currently meets the discharge standards, stipulated by Central Environment Authority, Sri Lanka, in order to identify further room for improvement, the performance of the plant for a period of 18 months, from January, 2015 to June, 2016 was analyzed.

Thereafter, in order to build the simulation platform for modelling, using Aquasim 2.1 (Reichert, 1998), the guidelines given in Activated Sludge Modelling (ASM) 2d framework (Henze et al., 2000), were followed. Nine soluble components and ten particulate components, given in ASM 2d, were developed as Dynamic Volume Variables, and their initial values were given as Formula Variables. The empirical constants, given in ASM 2d, as they

were within the operational parameters of the actual plant, too were input as Formula Variables, and four more Formula Variables were defined for COD (Chemical Oxygen Demand), TN (Total Nitrogen), TP (Total Phosphorous) and TSS (Total Suspended Solids) removal efficiencies from effluent. The twenty-one processes, specified in ASM 2d, were developed as Dynamic Processes, and their rate equations and stoichiometric coefficients were, thereafter, fed to the software. Four mixed reactor compartments were developed for the anaerobic, anoxic and aerobic reactors and secondary clarifier, using the actual volumes of the reactors and average inflow and outflow rates. After that, three links among the four compartments and three bifurcations from the clarifier for effluent, waste activated sludge and recycled activated sludge were developed.

After that, two samples taken from the inflow to the actual plant were characterized for the nineteen model components, according to the experimental procedures stated in Standard Methods for Water and Wastewater Characterization by APHA. The obtained values were, then, input to the model as the initial values of the model components.

Following that, the links among the compartments were modified to reflect the standard RA2O process (Fig. 1) and three modified configurations of the RA2O process (Fig. 2-4). Then, the results from simulation for them, for four Formula Variables, removal efficiencies of COD, TN, TP and TSS from the effluent were evaluated. After identifying the optimum placement of recycling streams from the simulation, the recycling percentages were changed, and the resulting removal efficiencies for the same four Formula Variables were evaluated.

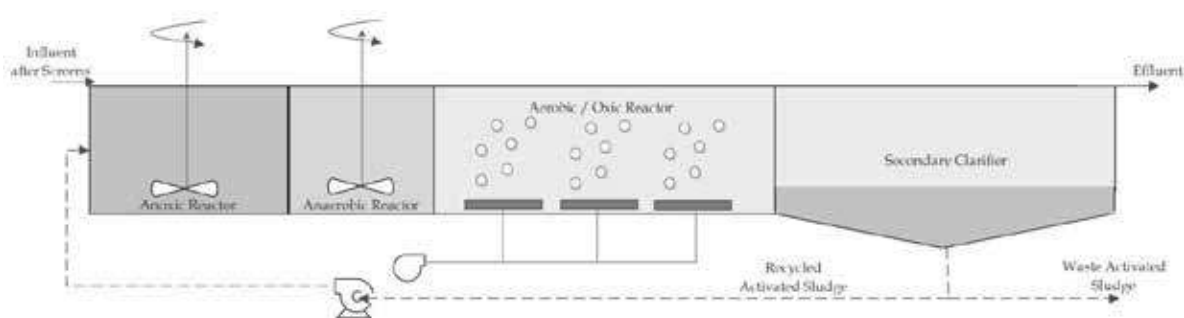


Figure 1 - Reversed A2O Process

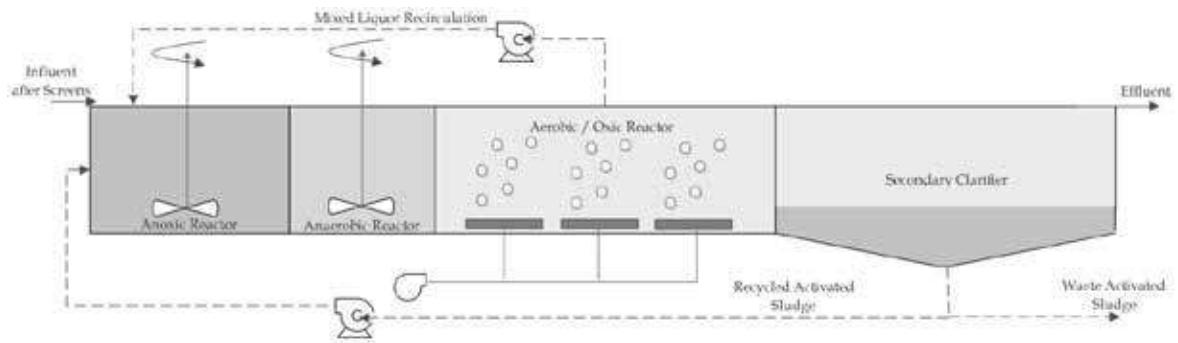


Figure 2 - Modified RA2O Configuration 01

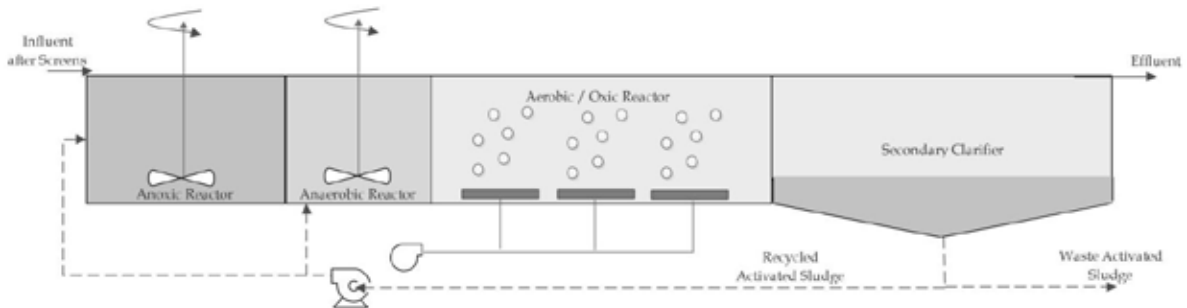


Figure 3 - Modified RA2O Configuration 02

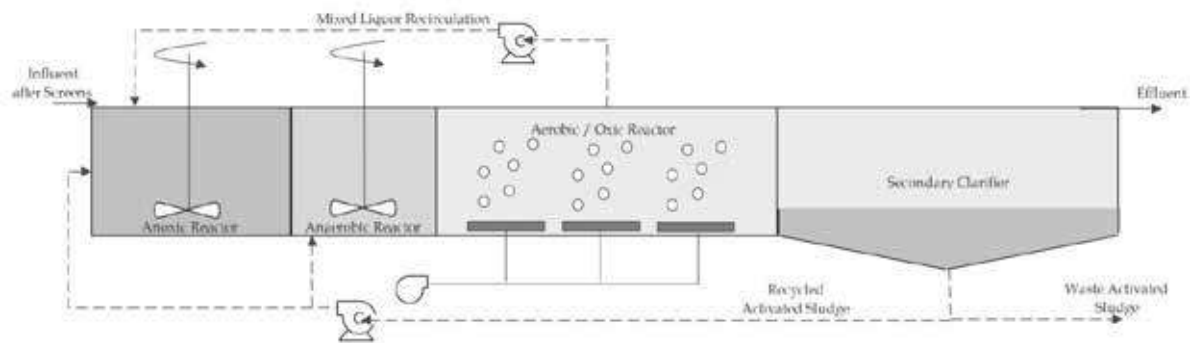


Figure 4 - Modified RA2O Configuration 03

3. Results

3.1 Influent Characterization

Table 1 - Results from Influent Characterization

Component	Characterizati on I (mg/l)	Characterizati on II (mg/l)	Component	Characterizati on I (mg/l)	Characterizati on II (mg/l)
S _{O2}	0.86	0.11	X _I	157.036	102
S _F	105.636	195.84	X _S	166.67	173.8293
S _A	95.87	122.4	X _H	0.65	0.01
S _{NH4}	60	65.88	X _{PAO}	0.03	0.01
S _{NO3}	1.95	2.95	X _{PP}	0.01	2.626
S _{PO4}	1.975	6.69	X _{PHA}	0.02	27.2451
S _I	40.914	307.2629	X _{AUT}	0.32	97.68
S _{ALK}	5	5	X _{TSS}	425	342
S _{N2}	0.1	0.01	X _{MeOH}	89.12	13.865
			X _{MeP}	92.7642	10.504



3.2 Removal Efficiencies

Table 2 - Results for the Removal Efficiencies

Configuration	COD	TN	TP	TSS
Standard RA2O Process	29.47%	39.76%	36.55%	8.16%
Modified RA2O Process 01	29.34%	39.59%	36.38%	8.13%
Modified RA2O Process 02	29.50%	39.80%	36.60%	8.22%
Modified RA2O Process 03	29.36%	39.62%	36.44%	8.16%

As per Table 2, it is observed that the highest removal efficiencies for all the parameters considered have been obtained in Modified RA2O Process 02. As this involved recycling of activated sludge both to anoxic and anaerobic reactors, thereafter, the percentage recycled to each reactor from the total recycled flow was optimized. There, the percentage recycled from the total recycled flow, from the secondary clarifier, to anaerobic reactor was changed from 0% to 100%, and the variations in removal efficiencies were observed (Fig. 5-8).

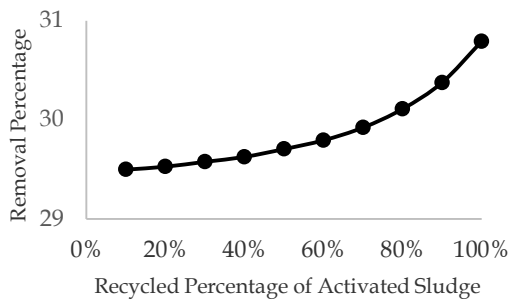


Figure 5 - COD Removal Efficiency

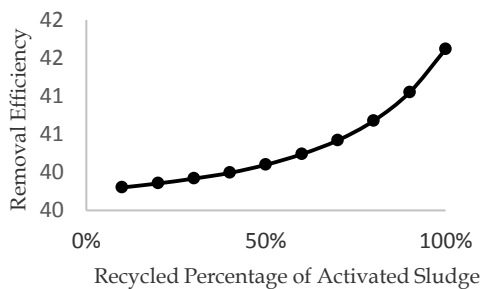


Figure 6 - TN Removal Efficiency

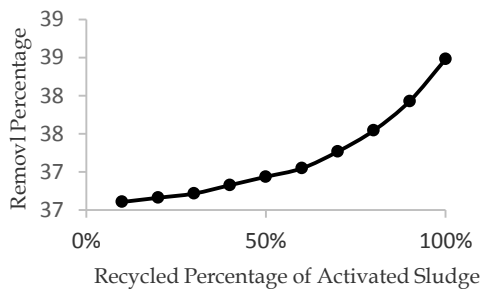


Figure 7 - TP Removal Efficiency

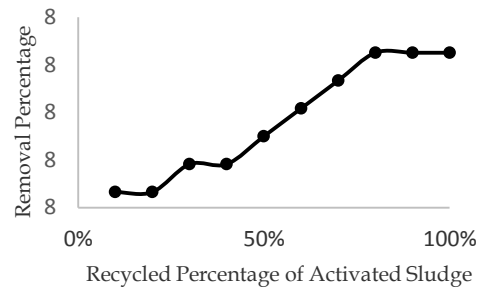


Figure 8 - TSS Removal Efficiency

Thus, it was observed that the removal efficiencies of all the parameters improved, with the highest improvement being in phosphorous removal, when the activated sludge was completely recycled to the anaerobic reactor, without recycling anything to the anoxic reactor.

4. Discussion

The main reason for changing the sequence of anaerobic and anoxic reactors in the previously used A2O process was to give preferential treatment to denitrification by the carbon source for nitrogen removal, thereby, improve achievement of deeper anaerobic conditions, in the anaerobic reactor, due to exhaust of nitrates (Zhang and Gao, 1997 [4]) and to enhance the efficiency of nitrification in the aerobic zone, due to higher non-aerobic retention time and greater energy generation for PAOs in the previous reactors (Bi et al., 2009 [6]).

One of the major modifications introduced in previous studies to improve the RA2O process has been in recirculation of mixed liquor from aerobic zone to anoxic zone. However, the results, via modified configuration 01, portray that recirculation of mixed liquor from aeration reactor decreases both the organic matter and nutrient removal efficiencies, compared to the standard RA2O process. This reduction is observed in modified configuration 03, compared to modified configuration 02 as well, where the difference among the two

configurations are in recirculation of mixed liquor. Thus, the results are in disagreement with the findings of Zhou et al. (2011) [10] and Xu et al. (2014) [9], who had observed increased efficiency in TP removal, at an expense of TN removal, with mixed liquor recirculation. This deviation from previous findings is possibly due to the higher concentration of dissolved oxygen in the recirculation stream from aerobic reactor, which prevents achieving anoxic conditions in the anoxic reactor, which is in line with the findings of Fang et al. (2016) [11].

Furthermore, although previous researchers (Zhang and Gao, 2000 [8] and Bi et al., 2009 [6]) have claimed that recycling activated sludge to the anoxic zone from the secondary clarifier to improve the nutrient removal efficiency, due to remaining generated nitrates from aerobic zone to be exhausted in the anoxic zone prior to transfer to the anaerobic zone, the results, from modified configuration 02 and optimization of recycling percentages, suggest that organic matter and nutrient removal efficiencies to be greatest when activated sludge is solely recycled to the anaerobic reactor. This is partly due to the increased sludge concentration in the anaerobic reactor, which helps it achieving deeper anaerobic conditions faster. Moreover, the sludge is expected to be richer in oxygen compared to nitrate, due to a highly efficient aeration process. As PAOs can generate energy at a higher efficiency using oxygen as electron acceptors compared to nitrate, this would lead to a higher biochemical efficiency in the phosphorous uptake in aeration process. Thus, although remaining nitrates in activated sludge would slightly inhibit the anaerobic conditions (Bi et al., 2009 [6]), due to the higher aggregate favourable impact, the overall efficiency of the anaerobic reactor would improve. Consequently, this would result in increased phosphorous removal.

Furthermore, prevention of contamination of anoxic reactor with oxygen in the activated sludge has improved nitrogen removal, via denitrification, as well. However, still, the highest improvement in nutrient removal is observed in phosphorous removal, indicating the higher potential for RA2O to improve phosphorous removal efficiency.

Moreover, although attempts to improve RA2O process largely were focused in spheres of nutrient removal, it is observed that organic matter removal too could be improved. Due to improved activity of autotrophs and

heterotrophs, resulting from optimized favourable conditions, the organic matter removal efficiency too has got improved in modified configuration 02, compared to the standard RA2O process.

Thus, it can be claimed that in order to further improve the RA2O process, from its standard, there should be no recirculation of mixed liquor from aerobic reactor to anoxic reactor and activated sludge from secondary clarifier should only be recycled to the anaerobic reactor.

5. Conclusions

RA2O process could achieve a higher efficiency in removal of organic matter and nutrients, highest being in phosphorous removal, from municipal wastewater, when activated sludge is recycled only to the anaerobic reactor.

Recirculation of mixed liquor from aerobic reactor to anoxic reactor inhibits achievement of anoxic conditions in the anoxic reactor, and hence, deteriorates the efficiency of RA2O process.

Acknowledgement

The support received in this study from Eng. (Mr.) Dhanesh Gunatillake, Eng. (Mr.) Lasantha Rupasinghe, Eng. (Mr.) A. Ranatunge, Chemist (Ms.) Lakmini Dhanawardhane, staff at the wastewater treatment plant of NWSDB at Ratmalana and Eng. (Dr.) Sanjeewa Wickramaratne from Lanka Hydraulics Institute is much appreciated.

References

1. Lettinga, G., "Sustainable Integrated Biological Wastewater Treatment", *Water Science and Technology*, 1996, Vol. 33, No. 3, pp. 85-98.
2. Arbuckle, W. B. & Griggs, A. A., "Determination of Biomass MLVSS in PACT Sludges", *Journal of Water Pollution Control Federation*, 1982, pp. 1553-1557.
3. Spector, M., "Biological Process for Enhanced removal of Ammonia, Nitrite, Nitrate, and Phosphate from Wastewater", US5182021A, 1993.
4. Zhang, B. & Gao, T., "Enhancement of Nitrogen and Phosphorus Removal by Reversal of Anaerobic and Anoxic Zones Sequence", *China Water & Wastewater*, Vol. 13, No. 3, 1997, pp. 7-9.



5. Xuejun, B. & Bo, Z., "The Principle and Full-Scale Application of Reversed A2O Process for Removing Nitrogen and Phosphorous", *Environmental Engineering*, Vol. 3, 2006, pp. 008.
6. Bi, X., Liu, C.Q., Cheng, L., Zhang, F. & Zhang, B., "The Principal and Full-Scale Application of Reversed A²/O Process for Removing Nitrogen and Phosphorus from Municipal Wastewater", *3rd International Conference on Bioinformatics and Biomedical Engineering*, June, 2009, pp. 1-4.
7. Kang, X. S., Liu, C. Q., Zhang, B., Bi, X. J., Zhang, F. & Cheng, L. H., "Application of Reversed A2/O Process on Removing Nitrogen and Phosphorus from Municipal Wastewater in China", *Water Science and Technology*, 2011, Vol. 63, No. 10, pp. 2138-2142.
8. Zhang, B. & Gao, T., "An anoxic/anaerobic/aerobic Process for the Removal of Nitrogen and Phosphorus from Wastewater", *Journal of Environmental Science & Health Part A*, 2000, Vol. 35, No. 10, pp. 1797-1801.
9. Xu, S., Bernards, M. and Hu, Z., "Evaluation of Anaerobic/anoxic/oxic (A2/O) and Reverse A2/O Processes in Biological Nutrient Removal", *Water Environment Research*, 2014, Vol. 86, No. 11, pp. 2186-2193.
10. Zhou, Z., Wu, Z., Wang, Z., Tang, S., Gu, G., Wang, L., Wang, Y. & Xin, Z., "Simulation and Performance Evaluation of the anoxic/anaerobic/aerobic Process for Biological Nutrient Removal", *Korean Journal of Chemical Engineering*, 2011, Vol. 28, No. 5, pp. 1233-1240.
11. Fang, F., Qiao, L. L., Cao, J. S., Li, Y., Xie, W. M., Sheng, G. P. & Yu, H. Q., "Quantitative Evaluation of A²O and reversed A²O Processes for Biological Municipal Wastewater Treatment using a Projection Pursuit Method", *Separation and Purification Technology*, 2016, Vol. 166, pp.164-170.
12. Reichert P., *AQUASIM 2.0 - User Manual Computer Program for the Identification and Simulation of Aquatic Systems*, Switzerland, 1998.
13. Henze M., Gujer W., Mino T., Matsuo T., Wentzel M. C., Marais G. v. R., Van Loosdrecht M.C.M., *Activated Sludge Model No. 2d*, The Netherlands, 2000.

Extraction of Cellulose from Sri Lankan Agricultural Waste for Engineering Applications

M.P.A. Nanayakkara, W.G.A. Pabasara, A.M.P.B. Samarasekara,
D.A.S. Amarasinghe and L. Karunanayake

Abstract: Polymers play a critical role in engineering applications today. Cellulose is the most abundant renewable natural biopolymer on earth. It is present in a wide variety of living species including plants and some marine animals. Rice is the main food of the inhabitants of Sri Lanka. The total land devoted for paddy is estimated to be about 708,000 Hectares at present in Sri Lanka. Rice straw is a rice by-product produced after harvesting paddy. Rice straw is a major agricultural waste product in Sri Lanka. Farmers are not economically using rice straw today. It is noted that rice straw contains a considerable amount of cellulose with hemicelluloses and lignin. This research is based on investigating the possibility of extraction of cellulose from most frequently used traditional rice varieties (Suwandel and Raththal) and technically modified rice varieties (BG300 and BG352) in Sri Lanka. The dried and cleaned rice straw was milled using a grinder to produce a fine powder of rice straw. Sieve analysis method was used to analyze the rice straw powder, and equal or less than 150 μm particle size was selected for the cellulose extraction. Pure cellulose was extracted from BG 352 rice straw variety after following de-waxing, delignification, hemicellulose and silica removal processes. The Same extraction procedure was followed for BG 300, Suwandel and Raththal rice varieties. The complete removal of non-cellulosic materials from rice straw was confirmed by FTIR spectroscopy after each chemical purification step. According to the experimental results, highest cellulose yield was obtained from rice straw of Suwandel (35.2%). Other types of rice varieties showed cellulose yield of BG300 (27.8%), BG352 (29.3%) and Raththal (26.8%). This research finding proves that this developed environmental friendly chemical purification process can be successfully utilized to isolate pure cellulose from rice straws. This extracted cellulose material can be used for different engineering applications.

Keywords: Agro waste, Cellulose, Rice straw

1. Introduction

Paddy is the leading cereal crop grown in Sri Lanka. The total land devoted for paddy is estimated to be about 708,000 Hectares [1]. But regrettably, it has resulted in a large amount of agro waste. Among them, the highest percentage is occupied by rice straw. Each 1 kg of milled rice produced results in roughly 0.7–1.4 kg of rice straw depending on varieties, cutting-height of the stubbles, and moisture content during harvest [2]. It is estimated that 800 GT of rice straw is produced in Sri Lanka per year [3]. Generally, this rice straw produced is surplus and is either left in the field as uncollected or to a large extent open-field burnt which is neither an environmental friendly nor a productive method. Several researchers have studied the adverse effects of rice straw burning on the environment and reported that toxic emissions from rice straw result in air pollution, water pollution, soil degradation and overheating which ultimately generate risk factor towards human health [4]. Therefore, it is

necessary to explore the capabilities and options regarding maximization of value generation in rice straw.

Rice straw, being a lignocellulosic biomass, consists of cell wall polymers: lignin, hemicellulose and cellulose [5]. Among them, cellulose is known as the most abundant natural biopolymer on earth which satisfies the criteria for being an excellent engineering material including as reinforcing fibres in bio composites [6].

Ms. M.P. A. Nanayakkara, B.Sc. Eng. (Moratuwa), Dept. of Materials Science & Engineering, University of Moratuwa.

Ms. W.G.A Pabasara, B.Sc. Eng. (Moratuwa), Dept. of Materials Science & Engineering, University of Moratuwa.

Eng. A.M.P.B. Samarasekara, B.Sc. Eng. (Moratuwa), M.Phil. (Moratuwa), AMIE(Sri Lanka), Senior Lecturer, Dept. of Materials Science & Engineering, University of Moratuwa.

Dr. D.A.S. Amarasinghe, BSc. (Kelaniya), MSc. (Moratuwa), M.Phil. (CUNY, USA), Ph.D. (CUNY, USA), Senior Lecturer, Dept. of Materials Science & Engineering, University of Moratuwa.

Prof. L. Karunanayake, B.Sc. (USJP), Ph.D. (North London), Professor, Department of Chemistry University of



Rice straw can be considered as the most abundant source of cellulose from all agricultural residues with 32 - 47% cellulose [7]. By considering above facts, developing an environmentally friendly method to isolate cellulose from Sri Lankan rice straws would be most effective way of value addition to rice straw. Since, there have been hardly any researches on evaluating and analyzing the yield of cellulose from rice straws of various rice varieties, this research is significant not only because as this focuses on a unique area of research but also the rice straws were used in this research consist of both frequently used traditional and technically improved rice varieties in Sri Lanka.

Under the most abundant traditional rice varieties, Suwandel and Raththal were chosen and under the most abundant technically modified varieties BG300 and BG352 were chosen. These technically modified rice varieties are created by a process known as hybridization. They have been modified to acquire some characteristics that the traditional rice varieties lack such as increased yield potential, increased resistant to pest and disease etc. The traditional rice varieties are cultivated by using completely traditional methods while the technically modified rice varieties are cultivated using conventional methods [8]. Hence, these rice varieties are cultivated in completely different agronomic, soil and climatic conditions besides their genetic variations.

The main objectives of this research are to establish an environmental friendly method to isolate cellulose from rice straws of frequently used traditional (Suwandel, Raththal) and technically modified (BG300, BG352) rice varieties and analyzing the cellulose yield from above varieties in order to identify the most suitable rice straw variety for commercial cellulose production. Up to date, high-quality cellulose was separately isolated from above rice straws varieties by streamlining and optimizing extraction and dissolution conditions to remove wax, lignin, hemicellulose and silica in a step-wise manner.

2. Experimental

2.1 Material

Rice straws of BG300, BG352 were collected at maturity after harvesting in 2016 Yala season from Rice Research Center, Batalegoda, Kurunegala, Sri Lanka. Rice straws of Raththal were collected at maturity after harvesting in 2016 Yala season from Hela Suwaya paddy

cultivation area, Padaviya, Anuradhapura, Sri Lanka. Rice straws of Suwandel were collected at maturity after harvesting in 2016 Yala season from a traditional paddy cultivation area, Kurunegala, Sri Lanka. Toluene ($C_6H_5CH_3$, $\geq 99.7\%$, ACS, Sigma-Aldrich), ethanol (H_3CCH_2OH , Min. 99.85 %, ACS, VWR Chemicals), acetic acid (CH_3COOH , $\geq 99.8\%$, ACS, Sigma-Aldrich), hydrogen peroxide (H_2O_2 , 50% (w/v), AR, Glorchem), sulfuric acid (H_2SO_4 , 95.0 - 97.0%, ACS, Sigma-Aldrich), potassium hydroxide (KOH, ≥ 85.0 %, GR, MERCK Chemicals) were used for separation of cellulose from rice straw. Hydrochloric acid (HCl, $\geq 37.0\%$, ACS, Sigma-Aldrich) was used for determination of silica content and used as received without further purification. All water used was purified by Barnstead™ Smart2Pure™ Water Purification System (Thermo Fisher Scientific, Waltham, MA).

2.2 Determination of Inorganic and Silica Content in Rice Straw Varieties

1 g of rice straw powder sample of each rice variety was transferred to a crucible and carbonized gently in a chamber furnace (Nabertherm, Germany) at 550°C for 6 h. The weight of the ash obtained was measured. The ash was treated with concentrated HCl. The acid-insoluble residue was filtered, washed with hot water until no chlorides were detectable, ignited, and finally weighed as silicon dioxide. All the tests were carried out in triplicate.

2.3 Isolation of Cellulose from Rice Straw Varieties

Pure cellulose was isolated from rice straw by step wise removal of non-cellulosic materials. The quantity utilized was 200g for each variety. Initially, foreign material such as dried grass, rice husk and other plant residues were removed from rice straw. Then rice straw was thoroughly washed with warm water followed by washing with normal tap water twice to remove dirt and aqueous soluble substances. Then cleaned rice straw was subjected to air drying at room temperature for 48 h followed by oven drying (Memmert GmbH, Germany) at 60 °C for 5h. The dried and cleaned rice straw was milled using SINGER Easy Blend grinder (Model No - KAEASYBLEN, SINGER, Sri Lanka). Sieve analysis of rice straw powder was done with the use of 250 μ m, 150 μ m, 106 μ m, 75 μ m and, 53 μ m aperture sized screens. Then the rice straw powder retained in each screen (except for 250 μ m screen), and the pan was mixed together in order to obtain a

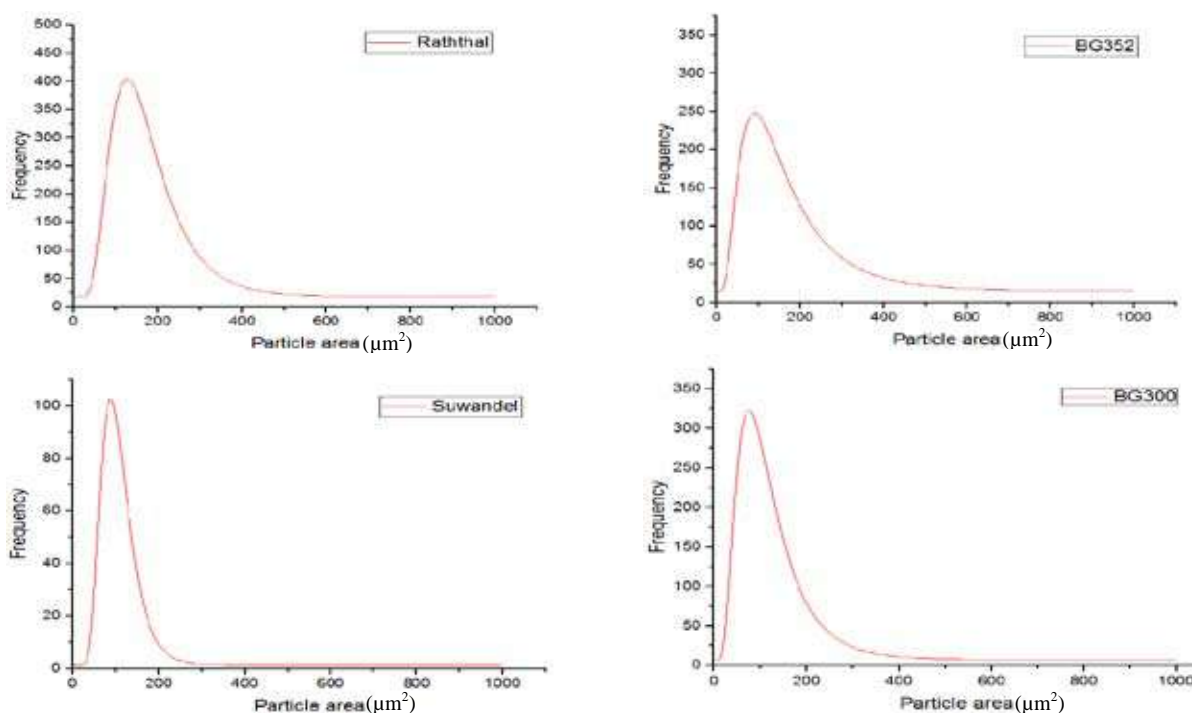


Figure 1 - Log Normal Particle Area Distributions of Rice Straw Varieties

homogeneous mixture. Rice straw powder (10 g) was first extracted in Soxhlet apparatus with 2:1, v/v toluene/ethanol (450 mL) mixture at 400°C for 15 h to remove wax, pigments and oils, followed by oven-drying at 55°C for 24 h. Then the dry weight of the dewaxed rice straw was measured. The dewaxed powder was then immersed in 3:10, v/v H₂O₂/CH₃COOH solution with solid: liquid ratio 1: 60, w/v at 70°C for 3h to dissolve lignin. H₂SO₄ was used as a catalyst. Extraction mixture was constantly stirred at 125 rpm. The insulated flask containing extraction mixture was heated with water from the thermostatically-controlled water bath. Extraction was conducted in a flask with volumes two to three times those of extraction mixtures to prevent oxygen evolution and substantial frothing during initial stages. The insoluble residue was collected by vacuum filtration (Whatman 1, Maidstone, Kent, England), washed with deionized water until the pH of the filtrate was neutral, and then dried at 60°C. Then the dry weight of the delignified rice straw was measured. Hemicellulose and silica in the delignified rice straw were leached with 110 mL 5% KOH at room temperature for 24 h and then at 90°C for 2 h. The insoluble residue was collected by vacuum filtration (Whatman 42, Maidstone, Kent, England), washed with deionized water until the pH of the filtrate was neutral, and then oven dried to remove water. Then the dry weight of the cellulose was measured. All the

tests were carried out in triplicate separately for four rice straw varieties.

2.4 Characterization

2.4.1 Optical Microscopy

Unbiasedly spread distributions of rice straw powder of above four rice varieties were imaged under an optical microscope (MT, Meiji Techno Co. Ltd, Japan) at 50 magnification. The area distributions of rice straw powder from above four varieties were analysed using ImageJ software (ImageJ 1.46, National Institute of Health (NIH), USA) by analysis of micrographs. The statistical analysis was performed using Origin Pro 2016 software.

2.4.2 Fourier Transform InfraRed (FTIR) Spectroscopy

FTIR Spectra were obtained using a Bruker ALPHA spectrometer (Bruker Corporation, Billerica, MA) at ambient conditions. Samples were prepared by grinding with KBr (1:100, w/w) and pressing into transparent pellets. The spectra were obtained in the transmittance mode from an accumulation of 128 scans at a 4 cm⁻¹ resolution over 4000–600 cm⁻¹ range.

2.4.3 Scanning Electron Microscopy (SEM)

The microstructures and surface morphologies of cellulose from above four rice straw varieties were examined by a scanning electron microscope (EVO 18, Carl Zeiss AG, Germany). The samples were mounted on aluminum stubs



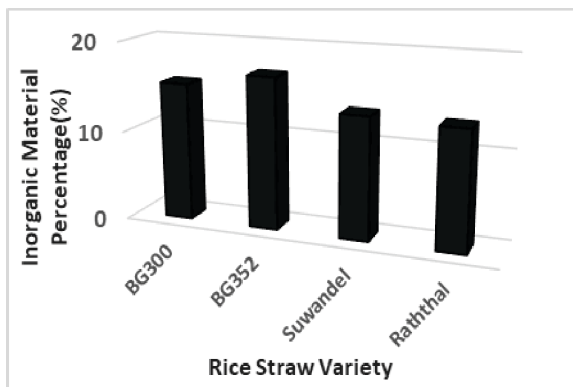


Figure 2 - Inorganic Material Percentage of Rice Straw Varieties

with conductive carbon tape and sputtered with gold under vacuum at 10 mA for 90 secs (Sc7620 sputter coating system). The samples were observed and imaged at 14.5 mm working distance and 20 kV accelerating voltage.

3. Results and Discussion

3.1 Particle Size Distribution of Rice Straw Varieties

Prior to cellulose isolation process, particle size distributions of rice straw powder of above-mentioned rice varieties were studied using microscopy analysis. This method involved spreading rice straw powder on a glass slide unbiasedly to obtain a very thin layer of rice straw powder followed by microscopy imaging. These microscopy images were analysed using ImageJ software to obtain particle area distributions of each rice straw varieties assuming that particle size is proportional to the particle area. Particle area distributions were fitted to a log normal curve using Origin Pro 2016 software. The observations showed that most particles of these varieties have particle area between 100-200 μm^2 range (Figure 1).

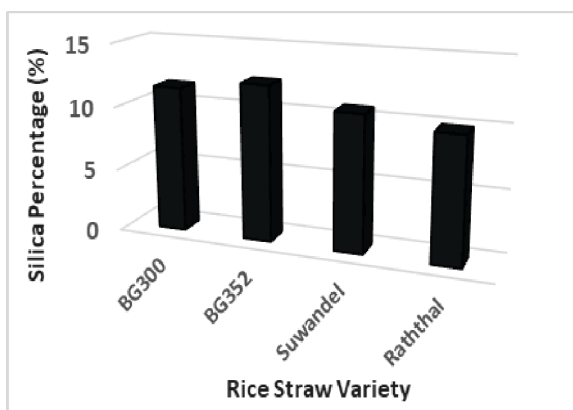


Figure 3 - Silica Percentage of Rice Straw Varieties

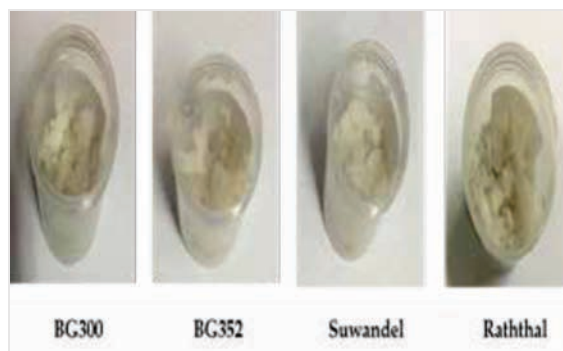


Figure 4 - Cellulose Extracted from Rice Straw Varieties

3.2 Determination of Inorganic and Silica Percentage of Rice Straw Varieties

Inorganic (Ash) content of rice straws of BG300 (15.4%) and BG352 (16.8%) was higher than that of rice straws of Suwandel (13.5%), Raththal (13.1%) (Figure2). These values were similar to the inorganic content reported for Asian and Californian rice straw varieties [9]. Since around 75% of the inorganic material present in rice straw is silica [10], variation in inorganic content of rice straws should be directly influenced by the variation in the silica content. Rice straw is unique compared to other cereal straws due to its high silica content. It is absorbed as monosilicic acid from soil and deposited as amorphous silica in the plant. Silica content is affected by its concentration in soil and on the uptake capacity of the plants [11]. Highest Silica content was showed by rice straws of BG300 (11.5%), BG352 (12.3%) while lowest was showed by rice straws of Suwandel (10.8%), Raththal (9.9%) (Figure 3). Hence, this variation in silica content may be due to the genetic variation in rice varieties as well as variation in monosilicic acid concentration in the soil in straw retrieved locations.

3.3 Isolation of Cellulose from Rice Straw Varieties

Cellulose was successfully isolated from cleaned and dried rice straw powder of above mentioned four rice varieties through three-step de-waxing, delignification and hemicellulose (and silica) removal process. The faded light brown colour of rice straw reduced with each step of delignification and hemicellulose (and silica) removal to become pure white (Figure4).

The surface of the rice straw is covered with a protective epicuticular wax layer which is a complex mixture of different hydrocarbons [12]. Hence its presence prevents the permeation of water and organic solvents into rice straw, preventing it from further treatment

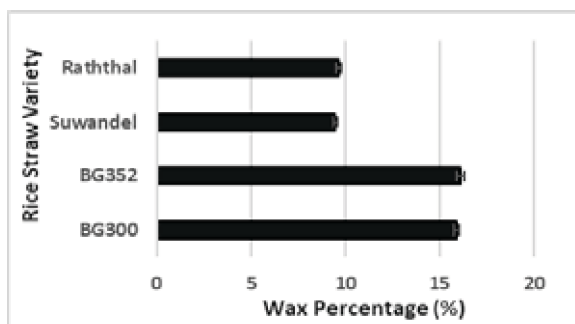


Figure 5 - Wax Percentage of Rice Straw Varieties

to isolate cellulose. Hence, removal of wax was achieved using conventional Soxhlet extraction method. It was observed that rice straws of BG300 (15.9%), BG352 (16.8%) varieties had more wax content than rice straws of Suwandel (9.5%), Raththal (9.6%) (Figure5).

Removal of lignin from dewaxed rice straw was essential to proceed forward with the research. Acidified NaClO_2 treatment was the most conventional de-lignification method found in the literature [13]. However, the use of chlorinated compounds has been restricted due to its adverse impact on the environment. Therefore, this research focuses on using an environmental friendly de-lignification method which satisfies Totally Chlorine Free (TCF) conditions. Therefore, next option was to proceed de-lignification with the hydrogen peroxide treatment in an alkaline medium [14]. Even so, there were two constraints associated with this method. First one was that this treatment does not provide sufficient level of de-lignification and bleaching and the second one was the unavailability of the jacketed reaction vessel which was required to host the reaction of this method. Due to these short comings, it was decided that a new method was required to get the expected level of results in this research. Therefore, peracetic acid treatment was chosen which possess high bleaching and de-lignifying action with higher selectivity compared to other TCF oxidizing agents [15].

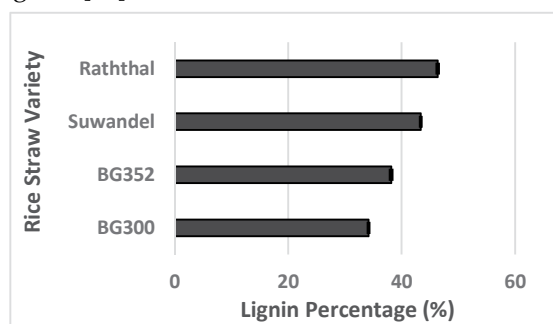


Figure 6 - Lignin Percentage of Rice Straw Varieties

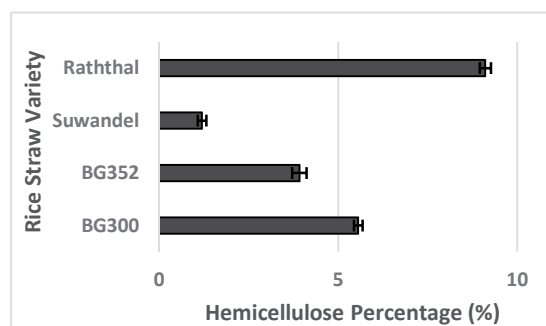


Figure 7 - Hemicellulose Percentage of Rice Straw Varieties

Peracetic acid treatment was generally used for wood de-lignification and also it was a time-consuming treatment since it was done under static conditions. Regardless of the above difficulties, when adopted this treatment to the research, it did not return the expected bleaching level. Due to that reason, it was necessary to modify the conditions in the peracetic acid treatment to get the expected results.

In order to do so, concentrations of acetic acid and H_2O_2 and liquid: solid ratio used were modified. Also, time, temperature and agitation conditions were modified accordingly. In order to accommodate these changes to the original method, insulated reaction vessel (by concerning the jacketed reaction vessel design) was created. Due to these process optimizations complete de-lignification and bleaching with minimum deterioration of the cellulose structure was achieved.

Highest lignin content was observed from rice straws of Suwandel (43.4%), Raththal (46.4%) while rice straws of BG300 (39.2%), BG352 (38.2%) showed the lowest (Figure6). These observations were significantly higher compared the lignin contents (<7%) reported for the international rice straw varieties [16]. Nevertheless, these observations suggest that besides genetic variations, environmental conditions may also greatly influence the lignin content.

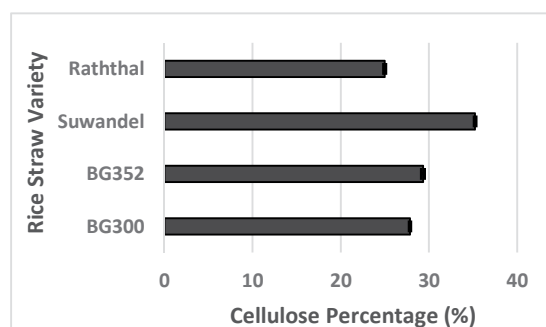


Figure 8 - Cellulose Yield from Rice Straw Varieties



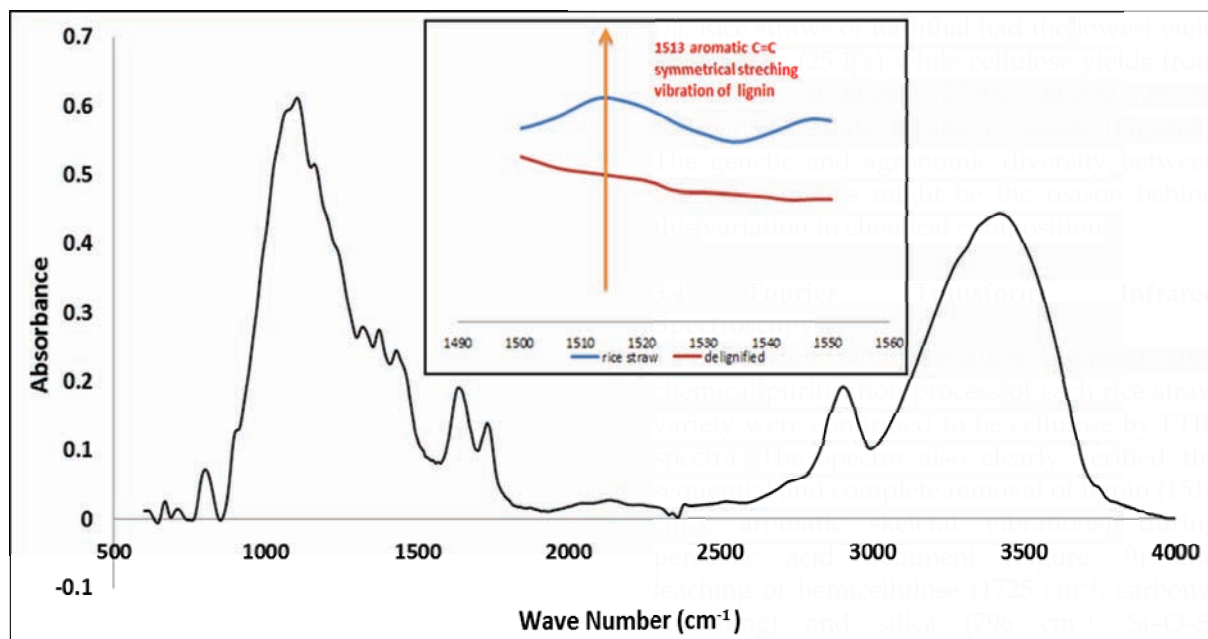


Figure 9 - FTIR Spectrum of Delignified Rice Straw - Suwandel

Removal of hemicellulose and silica was achieved with the conventional alkaline treatments mentioned in the literature. Rice straws of Raththal (9.1%) showed highest hemicellulose content while rice straws of Suwandel (1.2%) showed the lowest (Figure 7). However, hemicellulose percentages (19.8%-31.6%) observed for international rice straw varieties [17] were considerably lower than these results.

The highest yield of cellulose was observed from rice straws of Suwandel variety (35.3%). Cellulose yields reported for international rice straw varieties were similar to this observation

stretching) during the alkaline treatment (Figure. 10).

3.4 Morphological Analysis of Cellulose Extracted from Rice Straw Varieties

SEM micrographs (Figure 11) showed that cellulose isolated from rice straw was mostly in the form of fibres with diameters ranging from 2-8 μm . Moreover, large aggregates of cellulose consisted of bundles of cellulose fibres with clear boundaries, which indicated the potential to break down these bundles to individual fibers further. occurred during the oven drying step.

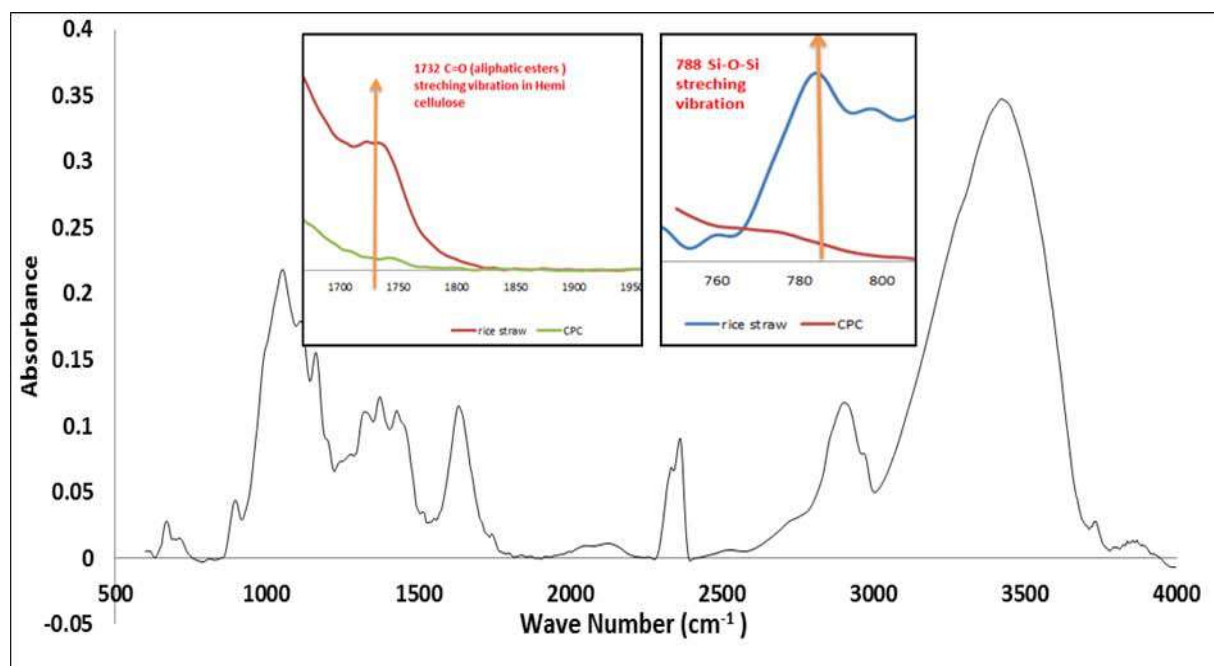


Figure 10 - FTIR Spectrum of Chemically Purified Cellulose - Suwandel

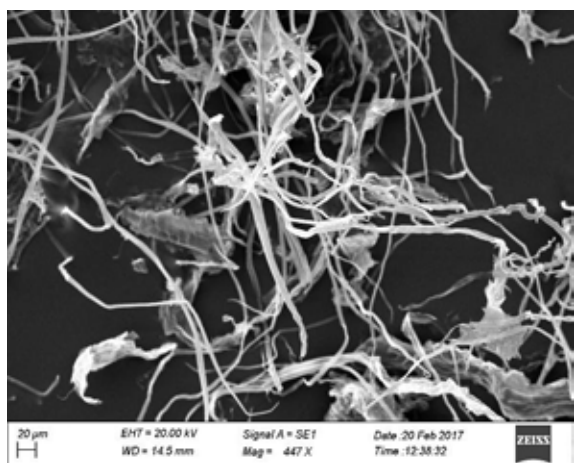


Figure 11 - SEM Micrograph of Cellulose from BG300 Rice Straw Variety

4. Conclusions

The established environmental friendly chemical purification process can be successfully utilized to isolate pure cellulose from rice straws of frequently used traditional (Suwandel, Raththal) and technically modified (BG300, BG352) rice varieties. This process consisted of three steps: dewaxing, de-lignification, and removal of hemicellulose and silica treatments. Highest cellulose yield was observed from rice straws of Suwandel variety (35.2%). Modified peracetic acid treatment can be used successfully for de-lignification of rice straw as it was able to provide the required level of bleaching and de-lignification with less time consumption. This study shows that promisingly effective results for extraction of cellulose from rice straw can be given by this chemical purification method.

References

1. http://www.cbsl.gov.lk/pics_n_docs/10_pub/_docs/statistics/other/econ_&_ss_2011.pdf, Visited 26th August 2016.
2. <http://irri.org/networks/rice-straw-project>, Visited 25th October 2016.
3. http://nerdc.lk/en/sub_pgs/1_dept_6_renew.html, Visited 20th November 2016.
4. Romasanta, R. R., Sander, B. O., Gaihre, Y. K., Alberto, M. C., Gummert, M., Quilty, J., Castalone, A. G., Balingbing, C., Sandro, J., Correa, T. and Wassmann, R., "How does Burning of Rice Straw Affect CH₄ and N₂O Emissions? A Comparative Experiment of different on-Field Straw Management Practices". *Agriculture, Ecosystems & Environment*, 239, 2017, pp.143-153.
5. Kadam, K. L., Forrest, L. H. and Jacobson, W.A., "Rice Straw as a Lignocellulosic Resource: Collection, Processing, Transportation, and Environmental Aspects". *Biomass and Bioenergy*, vol. 18(5), 2000, pp.369-389.
6. Bledzki, A. K. and Gassan, J., "Composites Reinforced with Cellulose Based Fibres", *Progress in polymer science*, vol. 24(2), 1999, pp.221-274.
7. Sarkar, N., Ghosh, S.K., Bannerjee, S. and Aikat, K., "Bioethanol Production from Agricultural Wastes: An Overview", *Renewable Energy*, 2012, vol. 37(1), pp.19-27.
8. <http://dh-web.org/botany/Paddycultivation.pdf>, Visited 10th August 2016.
9. Balasta, M. L. F., Perez, C. M., Juliano, B. O., Villareal, C. P., Lott, J. N. and Roxas, D. B., "Effects of Silica Level on Some Properties of Oryza Sativa Straw and Hull", *Canadian Journal of Botany*, vol. 67(8), 1989, pp.2356-2363, Guzmán, A., Delvasto, A. and Sánchez, V., "Valorization of Rice Straw Waste: An Alternative Ceramic Raw Material", *Cerâmica*, vol. 61(357), pp.126-136, 2015.
10. Guzmán, A., Delvasto, A. and Sánchez, V., Valorization of Rice Straw Waste: An Alternative Ceramic Raw Material. *Cerâmica*, 61(357), Guzmán, A., Delvasto, A. and Sánchez, V., 2015. Valorization of Rice Straw Waste: An Alternative Ceramic Raw Material. *Cerâmica*, vol. 61(357), 2015, pp.126-136.
11. Raven, J. A., "The Transport and Function of Silicon in Plants", *Biological Reviews*, vol.58 (2), 1983. pp. 179-207.
12. Buschhaus, C. and Jetter, R., "Composition differences between Epicuticular and Intracuticular Wax Substructures: How do Plants Seal their Epidermal Surfaces?", *Journal of experimental botany*, vol. vol.62(3),2011, pp.841-853.
13. Lu, P. and Hsieh, Y.L., "Preparation and Characterization of Eellulose Nanocrystals from Rice Straw", *Carbohydrate Polymers*, vol. 87(1), 2012, pp.564-573.
14. Lewis, S. M., Holzgraefe, D. P., Berger, L. L., Fahey, G. C., Gould, J.M. and Fanta, G.F., "Alkaline Hydrogen Peroxide Treatments of Crop Residues to Increase Ruminant Dry Matter Disappearance in Sacco", *Animal Feed Science and Technology*, vol.17 (3), 1987, pp.179-199.
15. Jääskeläinen, A. S., Poppius-Levlin, K. and Sundquist, J., Kraft Pulp Delignification with



peroxy Compounds. *Paperi ja puu*, 82(4), 2000, pp.257-263.

16. Abou-El-Enin, O. H., Fadel, J. G. and Mackill, D. J., "Differences in Chemical Composition and Fibre Digestion of Rice Straw with, and without, Anhydrous Ammonia from 53 Rice Varieties", *Animal feed science and technology*, vol.79(1), 1999, pp.129-136.
17. Jin, S. and Chen, H., "Near-Infrared Analysis of the Chemical Composition of Rice Straw", *Industrial Crops and Products*, vol.26 (2), 2007, pp.207-211.

Environmental Impacts of Organic Fertilizer Produced from Industrial Zone Central Effluent Treatment Plant Sludge using Delta-D Technology

M.F.H.M. Aadhil and S.A.S. Perera

Abstract: Conversion of Central Effluent Treatment Plant Sludge (CETPS) from industrial zones, consisting textile and garment processing plants, into a nutrient rich organic fertiliser (OF) using Delta-D Technology has been explored by Perera et al. CETP primary and tertiary sludge is not acceptable to be sent to landfills. As a result, CETPS is transported and incinerated in the rotary kiln of a cement plant at high temperatures. This solution is expensive and non-sustainable as it has many negative environmental impacts. A comparative study reveals that the high cost and the negative environmental impacts of incineration can be greatly reduced by converting CETPS to produce OF. An acute toxicology test on aquatic life revealed that this fertilizer is non-threatening to marine and aquatic life.

A deeper analysis of the compounds in the OF by conducting FTIR and GC-MS tests have been carried out and discussed in detail in the paper affirming scientifically that the production of OF is ecofriendly and is a sustainable solution to CETPS.

Keywords: Solid Waste Disposal, Waste Management, Delta-D Technology, Rapid Digestion, Organic Fertiliser Production, CETP Sludge Sludge

1. Introduction

Delta-D Technology (DDTech) is a patented technology (Sri Lanka Patent No: 12544 and Patent No: 12947) developed by a Professor in the Department of Chemical and Process Engineering of the University of Moratuwa [7,8,9,10,11]. In DDTech, a digestive fluid called Delta-D rapidly digests organic waste (OW), by a combination of enzymetic and acidic action and finally converts OW into a nutrient rich organic fertiliser (OF). DDTech removes bad odour and destroys pathogenic microorganisms as well [7,8,9,10,11].

A leading apparel manufacturer in Sri Lanka approached the research team to develop a low cost solution to dispose 800 tons/year of sludge generated at the Central Effluent Treatment Plant (CETPS) of a major industrial park. CETPS had around 70% moisture and emanated a bad smell. The disposal method practiced was to transport CETPS to Puttalam and hand over to incinerate in the rotary kiln of a cement manufacturing plant. The annual cost of CETPS disposal was around Rs. 24 million.

The team selected DDTech to rapidly digest CETP Sludge and to convert it into organic fertilizer with the addition of saw dust, Eppawela Rock Phosphate (ERP) and Dolomite. The main objective was to produce a nutrient rich organic fertilizer (OF) which

could be sold and the cost recovered. Moreover it was found that the objectionable smell emanating from the CETP Sludge was completely removed resulting in an odorless environment in the vicinity. At the experimental stage the manufacturing cost of OF produced was approximately Rs. 18.75 per kg. [1] However, in depth analysis revealed that the OF manufactured on a commercial scale, DDTech based OF manufacture and sale could result in a lower cost of production and an income of over Rs. 40 million per annum. This solution was found to have major economic benefits, as well as, improved environmental conditions due to removal of bad odour of CETPS [12,13,14,15].

The environmental sustainability of the proposed solution was analyzed and is presented in this paper. The composition of CETPS and OF produced were analysed and impacts of components at the given concentrations were studied. Further an acute toxicology test was carried out at high concentration level to study the toxicity to marine life due leachate produced by application of OF on agricultural land.

Eng. (Prof.) S.A.S. Perera, DSc, B.A.Sc.(ChEng&FSc), CEng, PE(SL), IntPE(SL), FIE(SL), MAChE (USA), Professor,, Department of Chemical and Process Engineering, University of Moratuwa.

Eng. M.F.H.M. Aadhil, B.Sc. Engineering (UoM), Post Graduate Research Student, Department of Chemical and Process Engineering, University of Moratuwa.



2. Literature Review

Sanitary land filling, composting, bio gas production incineration, artificial drying and combustion to recover thermal energy, disposal of combustion ash by mixing with cement mortar and concrete are some of the methods of CETPS disposal in the world. Some of the problems associated with the above techniques are; landfilling and composting–slow OW digestion rate, foul smell, high land consumption and leachate production with pathogens that could contaminate soil and ground water table.; incineration and combustions – air pollution, volatile organic compounds, chlorinated organic compounds and ash containing heavy metals. A recently developed method issu per critical water oxidation based sludge processing[17]. All these methods are expensive in terms of capital cost and operational cost. In literature, there is no rapid digestion process to produce OF, to recover the cost and to earn an income. References pertaining to this section are [17,18,19,20,21,22,23].

3. Objectives

The main objectives were to provide a low cost, environment friendly, economically viable, sustainable disposal method by using DDTech to produce a nutrient rich organic fertilizer (OF) which could be sold and the cost recovered and to remove the objectionable foul smell emanating from the CETPS. The objectives of testing the OF produced from CETPS using DDTech, by, Chemical Composition, GC-MS, FTIR and acute toxicology tests, were to determine the elements present, main chemicals and their structures and the toxicity plant and marine life.

4. Experimental material and methods

The CETPS sample received was well mixed and a representative sample was used for laboratory analysis. The stepwise experimental procedure, as recommended by the inventor of DDTech is given below.

(a) A quantity of 15.059 kg of de-watered ETPS with 20% moisture content was well mixed with 2L of Delta-D solution in a 50L plastic barrel. After a few hours the thick CETPS became a uniform slurry. 1 day was allowed for further digestion.

(b) After 1 day, 10 kg of sawdust and 5L of water were added and to the digested CETPS slurry and well mixed.

(c) Two days later, 5kg's of ERP was added and well mixed.

(d) Two days later 10 kg of Dolomite was added and the mixture was left closed for 5 days to obtain the final nutrient rich organic fertilizer (OF), of which the total weight was approximately 44.35 kg.

(e) A well-mixed sample of OF was taken and was sent to Bureau Veritas for GC-MS, FTIR, Microbial Testing.

(f) A representative sample of OF was applied to plants and the plant growth was compared with several other types of fertilizers available in the market.

The applicability of any fertilizer into soil directly depends on the constituents of the fertilizer and the form each constituent is present in. It also helps to understand the complementary behavior certain chemical compounds display in the presence of other chemical compounds. However though the above is necessary it may not be sufficient to prove the harmfulness or otherwise of a fertilizer. While the above may result in predictions being drawn the reality check of how the environment will respond to fertilizers of unknown composition is revealed only by studying the changes it exerts on the environment in the short term and the long term.

Therefore the paramount test to establish that a fertilizer is safe for application in the short term is to study the soil fertility and carryout acute toxicology tests for aquatic and marine life due to the potential leachate the fertilizer will produce when applied on land. To establish the long term suitability chronic diseases have to be evaluated. However it requires long term studies of the fertilizer. As in the case of any fertilizer many of the chronic conditions can be prevented by strictly adhering to the fertilizer guideline especially in managing the heavy metal content in fertilizer.

4.1 Acute toxicology test on marine and aquatic life

Aquatic toxicology is the study of the effects of manufactured chemicals and other anthropogenic and natural materials and

activities on aquatic organisms at various levels of organization, from subcellular through individual organisms to communities and ecosystems.

There are different types of toxicity tests that can be performed on various test species. Different species differ in their susceptibility to chemicals, most likely due to differences in accessibility, metabolic rate, excretion rate, genetic factors, dietary factors, age, sex, health and stress level of the organism. Common standard test species are the fathead minnow (*Pimephalespromelas*), daphnids (*Daphnia magna*, *D. pulex*, *D. pulicaria*, *Ceriodaphniadubia*), midge (*Chironomustentans*, *C. riparius*), rainbow trout (*Oncorhynchus mykiss*), sheepshead minnow (*Cyprinodonvariegatu*), rosy barbs (*Pethiaconchonus*), scud (*Hyalalla Azteca*), grass shrimp (*Palaemonetespugio*), goldfish (*Carassiusauratus*). As defined by ASTM, these species are routinely selected on the basis of availability, commercial, recreational, and ecological importance, past successful use, and regulatory use. [3]

A static non-renewal test is appropriate to test the acute toxicology of the sludge by dissolving known weights of the sludge sample in incremental dosage (10g per day) to the same static water tank with *Carassiusauratus* (gold fish (GF)) and *Pethiaconchonus* (rosy barbs (RB)) to ensure the validation is done precisely. The test samples should be monitored for a minimum of 1 week prior to renewal of water and change of dosing rate if required. However sample there is a higher possibility of dissolved oxygen (DO) depletion from high chemical oxygen demand (COD) and/or biological oxygen demand (BOD), and ill effects from metabolic wastes from organisms in the test solutions. Therefore it is important to provide nutrients and oxygen to the test and control sample to ensure these shortcomings are eliminated. It is important to select a fish food that does not contain toxic organics and metals or whenever difficulty is encountered in meeting minimum test acceptability criteria for control survival and reproduction or growth. If the concentration of total organochlorine pesticides exceeds 0.15 µg/g wet weight, or the concentration of the total organochlorine pesticides plus Polychlorinated biphenyl's (PCBs) exceeds 0.30 µg/g wet weight, or toxic metals (Al, As, Cr, Co, Cu, Pb, Ni, Zn, expressed as total metal) exceed 20 µg/g wet weight, the food should not be used

(for analytical methods see AOAC, 1990 and USDA, 1989).

For the test results to be acceptable, control survival must equal or exceed 90%. Therefore if 10 fishes are used in the control sample and one die due to the conditions in the control sample the experiment is terminated and the number of living species are counted. Further the accuracy of the test can be improved by using a facility that is well ventilated and free of toxic fumes. Sample preparation, culturing, and toxicity testing areas should be separated to avoid cross contamination of cultures or toxicity test solutions with toxic fumes. Laboratory ventilation systems should be checked to ensure that return air from chemistry laboratories and/or sample handling areas is not circulated to test organism culture rooms or toxicity test rooms, or that air from toxicity test rooms does not contaminate culture areas. When the toxicity test is concluded, all test organisms (including controls) should be humanely destroyed and disposed of in an appropriate manner. [3]

For the purpose of the acute toxicology test 10 fish each was used in the fish tank used as the control set up and the fish tank which was supplied with the fertilizer. The ten fish selected included 8 *Pethiaconchonus* (rosy barbs) and 2 *Carassiusauratus* (gold fish) for each tank. All the fish were from the same aquarium and were of same age. The tanks were suitable to accommodate 8L of water each and was supplied oxygen at a constant rate. Nontoxic readymade fish food was supplied as per daily recommendations sufficient for the fish in the tanks. One of the tanks were supplied with the fertilizer 10g every day up to 7 days. The daily fish count was obtained in both the tanks.

4.2 Determining the composition of the produced fertiliser

It is tedious to find the exact composition of a fertilizer derived from various waste raw materials of relatively unknown composition. As often is the case most of the types of compost fertilizers do not measure an exact composition. However it is important to minimize the environmental and human health risk by identifying the nature of the fertilizer. The following parameters were analysed using Inductive coupled plasma - Optical Emission

Spectroscopy (ICP-OES) according to standard Environmental Protection Agency (EPA) 3051



A. Total Potassium (K), Sodium (Na), Magnesium(Mg), Lead (Pb), Nickel (Ni), Copper (Cu), Iron (Fe), Chromium (Cr), Zinc (Zn), Mercury (Hg) Cadmium (Cd) and Arsenic (As). Nitrogen (N) was determined using standar SLS 645: Part 1: Section C: 2009, and Phosphorous (P) was determined using SLS 645: Part 5:1985. Organic Carbon (C) was determined using SLS 1246: Appendix D: 2003.

A separate Gas chromatography and Mas spectroscopy (GC-MS) test was carried out to determine organic compounds present in the fertilizer sample. Further a Fourier Transform - Infrared Spectroscopy (FT-IR) was carried out to identify organic classes such as O-H groups, C=O groups, C=N groups, C≡N groups and C-N groups. Through carryout various tests the composition of the fertilizer has become relatively clear and the harmfulness can be predicted thereby.

4.3 Determining the composition of the produced fertiliser

The total coliform of the produced fertilizer was analyzed as the raw material sludge was detected with coliform. Further fecal coliforms, *Escherichia coli* and *Salmonellaspp* was analyzed. The following standards were used for each of the parameters.

Table 1 - Mixed mass ratios of sawdust and rice husk

Parameter	Test Method
Total Coliform	ISO 4831: 2006 / SLS 516 Part 3 Section 1 :2013
Fecal coliforms	ISO 7251: 2005 / SLS 516 Part 12 Section 1 :2013
<i>Escherichia coli</i>	ISO 7251: 2005/ SLS 516 Part 12 Section 1 :2013
<i>Salmonellaspp</i>	ISO 6579: 2002 / Amd 1:2007 SLS 516 Part 5:2013

5. Results and Discussion

5.1 Results of the acute toxicology test

7 samples of approximately 10g each of fertilizer was mixed in one of the tanks over 7 days gradually increasing the dissolved fertilizer in water assimilating the runoff into streams. The solubility of over 60 g in 4 litres

of water was validated prior to the toxicology experiment to ensure the components dissolved or remain as a suspension in the fish tank.

The number of remaining fish species was recorded up to 7 days on a daily basis in both the tanks. The results proved to be positive in the environmental toxicology test after 70 g of fertilizer was added 10g a day and the living number of fish were counted. All fish species survived during the 7 day period indicating no acute toxicology risk. The results are presented in Table 2 below.

However it has to be noted that there are several vulnerabilities of this examination as some times fish may harm each other and some fish may die due to these kind of behavioral aspects. This factor is uncontrollable. Therefore the test data would be more accurate if both the control and test samples contained a large amounts of fish. However this may lead to inaccurate counting as it has to be done manually.

Table 2 acute toxicology test results

Sample	Fish type	Day						
		1	2	3	4	5	6	7
Control	RB	8	8	8	8	8	8	8
	GF	2	2	2	2	2	2	2
Fertilizer	RB	8	8	8	8	8	8	8
	GF	2	2	2	2	2	2	2

The survival rate expected is 90% whereas the resulting survival rate was 100%. This implies that the fertilizer will not be of toxic nature in the short term for aquatic or marine life even if they are very sensitive to toxics.



Analysis of the composition of the fertiliser

Figure 1 - Acute toxicology test set up

5.2 Effects of Heavy metals

Heavy metals present in compost fertilizers cause pollution in the soil. Uptake of these metals by the plants from the soil leads to reduction in crop productivity by inhibiting physiological metabolism. Metals such as As, Cd, Hg, Pb or Se are not essential for plant growth since they do not perform any physiological function on the growth of the plants. Others, Co, Cu, Fe, Mn, Mo, Ni and Zn are required for the metabolism and normal growth of plants. However, these metals may cause poisoning if the available amounts are higher than their optimal values.

Heavy metal poisoning by compost is a matter of concern if applied to food crops since they can easily get transferred to humans and animals via edible parts.

Absorption and accumulation of heavy metals in plant tissues depends on many factors including temperature, moisture, organic matter, pH and nutrient availability. Accumulation of heavy metals in plants depends on the species. Elevated Pb in soils causes decrease in soil productivity, and a very low Pb concentration may inhibit some vital plant processes, such as photosynthesis, mitosis and water absorption with toxic symptoms of dark green leaves, wilting of older leaves, stunted foliage and brown short roots. [2]

Heavy metals are phytotoxic to plants and causes chlorosis which decolorizes plant leaves. Furthermore, they have negative effects such as yield depression, reduced nutrient uptake, disorders in plant metabolism and reduced ability to fixate molecular nitrogen in leguminous plants. [2]. The maximum allowable limits of the heavy metals in any commercial fertiliser and the concentration of heavy metals present in the produced fertiliser is given in table 3 below.

Table 3 - heavy metal composition

Heavy Metal	Max allowable	Amount present
Lead (Pb)	30	ND
Chromium(C)	50	11
Cadmium	3	ND
Arsenic (As)	50	ND
Mercury (Hg)	1	ND

ND : Not detected
 LOQ : Limit of
 Quantification = 0.04 mg/kg

5.3 Organic matter from GC-MS

The components present in the fertilizer can be interpreted in many ways as many studies can be carried out how each chemical behaves in different environments and how the behavior of a chemical is altered in the presence of other chemicals.

The GC-MS test identified over 16 organic compounds present in the fertilizer which may have given rise due to the sludge or other additives. The results are presented in figure 2 below. The components detected and toxicity and toxic concentration is given in Table 4 below. [4][5]

Table 4 - organic compounds detected and toxicity

No	Detected Compound	Acute Toxicity	Ground water contaminat
1	Cyclohexasiloxane		
2	2H-Naphthol[1,2-b]pyrane-3-carbonitrile		
3	Silane		
4	Carbazole		
5	Hexadecanoic acid		
6	3,6-Dioxa-2,4,5,7-tetrasilaoctane		
7	Hexasiloxane		
8	Octadecanoic acid		
9	Mercaptoacetic acid		
10	Heptasiloxane		
11	1H-Indole-2-carboxylic acid		
12	N-Benzhydrylidene-1-(2,4,6-trimethylphenyl)ethylamine N-oxide		
13	Piperdine		
14	Tetrasiloxane		
15	2,4,6-Cycloheptatrien-1-one		
16	4-Methyl-2-trimethylsilyloxy-acetophenone		

No detected toxicity in past research
 Toxicity detected

Most of the chemicals used do not display an acute toxicity even when administered orally. However the lethal dosage varies in each component. Considering Silane and Piperdine, though the lethal dosage is relatively low the acute toxicology test proved to be positive indicating the concentrations were below the lethal dosage for marine and aquatic life. Further ground water contamination is not present in any of the substances.



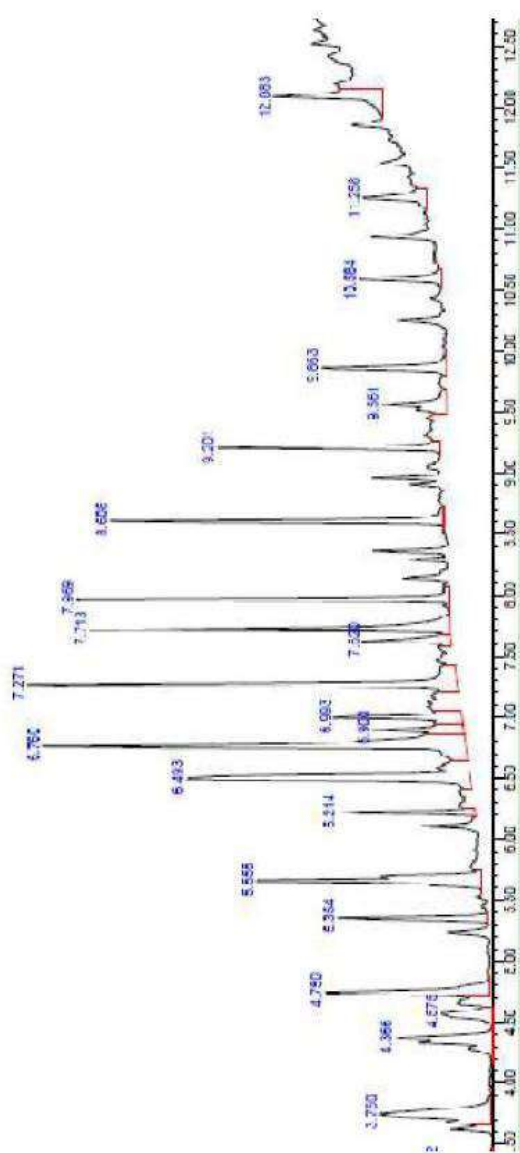


Figure 2 GC-MS results

5.4 Pathogenic nature of produced OF

The pathogenic nature of the feed sludge and the produced fertilizer were compared by carrying out microbial tests on the feed sludge and the produced fertilizer according to the standards mentioned in the methodology. The comparison revealed that although the feedstock contained high microbial counts the final product was free from any form of microbes. Table 5 contains the results.

Table 5 - Microbial Test Results

Parameter	Result of sludge	Result of Fertilize	Unit
Total Coliform	N/A	ND	MPN/
Fecal Coliforms	460	ND	MPN/
Escherichia coli	N/A	ND	MPN/
Salmonella spp	Absent	Absent	In 25g

Total coliform and Escherichia coli was not tested in the sludge. Only the critical parameter of fecal coliforms and Salmonella spp were tested. However all four parameters were tested in the fertilizer that was produced. The Delta-D process inhibits all pathogenic microbes and results in the fertilizer being pathogen free.

When the fertilizer is applied to the earth, microbial digestion takes place from microorganisms in the earth further digesting any large molecules present in the fertilizer and break it down to smaller fractions to be able to be absorbed into the plants.

5.6 Results of the FT-IR test:

The FT-IR test was carried out to identify functional groups in the produced fertilizer. The Table 6 contains the results of the FT-IR test. Figure 3 is the graph obtained from the test.

Table 6 - FT-IR Test Results

Type of bond	Wavenumber (cm ⁻¹)	Intensity
O-H	3650-3200	Strong,
C=O	1750-1650	Strong
C=N	1650-1550	Medium
C≡N	2260-2100	Medium
C-N	1230-1020	Medium

6. Conclusions

The study revealed that the fertilizer produced using the CETPS through DDtech conversion process was far superior to other fertilizers, available in the local market, that were used in the experiment.

Chemical composition, GC-MS, FTIR and microbial test results (carried out by Bureau Veritas Laboratory, Katubedde, Sri Lanka) indicate that there are no toxic chemicals or pathogenic microorganisms in the OF produced.

Acute toxicology test on marine and aquatic life carried out at the University of Moratuwa, clearly indicate that the OF produced can be applied to agricultural fields, without causing any harm to marine organism living in waterbodies in the vicinity.

Acknowledgement

The research group is thankful to the great support and corporation rendered by Mr. Harsha Deraniyagala, The General Manager of MAS Fabric Park at Thulhiriya in making the research a success.

References

1. Perera, S.A.S. Aadhil, M.F.H.M. Gunarathne, K.K.D.I.K. Dananjina, A.M.U. "Conversion of textile industry effluent treatment plant sludge into a valuable organic fertilizer using Delta-D technology," Moratuwa, 2017.
2. Singh, J. and Kalamdhad, A. S. "Effects of Heavy Metals on Soil, Plants, Human Health and Aquatic Life," *International Journal of Research in Chemistry and Environment*, vol. I, no. 2, pp. 15-21, 2011.
3. US-EPA, "acute-freshwater-and-marine-wet-manual_2002.pdf," October 2002. [Online]. Available: https://www.epa.gov/sites/production/files/2015-08/documents/acute-freshwater-and-marine-wet-manual_2002.pdf. [Accessed 26 December 2016].
4. PAN Pesticide Database, "pesticideinfo," PAN Pesticide Database, 2006. [Online]. Available: <http://www.pesticideinfo.org>. [Accessed 25 5 2017].
5. OSHA, "www.osha.gov," [Online]. Available: https://www.osha.gov/dts/chemicalsampling/data/CH_231525.html. [Accessed 31 05 2017].
6. Perera, S.A.S. *Influence of Organic Fertiliser Fortified with Eppawela Rock Phosphate on the Cultivation of Spinach and Curry Chillies*. Proceedings of The International Seminar on "The Engineer in Sustainable, Social and Economic Development - Regional Contribution Towards Agenda 21, organised by The Institution of Engineers Sri Lanka (IESL), World federation of Engineering Organisations (WFEO) and the Federation of Engineering Institutions of South and Central Asia (FEISCA), 20 Oct. 2002, pp. 62-74, © The Institution of Engineers, Sri Lanka
7. Perera, S.A.S. Patented Process for Rapid Digestion of All Types of Biomass into Organic Fertiliser, a Solution to the Urban Solid Waste (USW) and to the Fertiliser Problem in Sri Lanka, The Proceedings of the 22nd International Conference on Solid Waste Technology and Management March 2007, pp. 1312-1319, ISSN 1091-8043 © 2007 JSWTM, Widener University, Philadelphia, USA.
8. Perera, S.A.S. Manufacture of Organic Fertiliser from Vegetable Market Garbage (VMG) Using Eppawela Rock Phosphate and Its' Effects on Rice Cultivation, The Proceedings of the 22nd International Conference on Solid Waste Technology and Management March 2007, pp. 1301-1311, ISSN 1091-8043 © 2007 JSWTM, Widener University, Philadelphia, USA.
9. S.A.S. Perera, P. Ratnaweera, J.N. Meegoda,, Sustainable Agricultural Practices for Developing Countries, The Proceedings of The First International Conference on Soil and Rock Engineering August 2007, Colombo, Sri Lanka , pp. 1-7 © The Geotechnical Society of Sri Lanka.
10. Perera, S.A.S. **Delta-D Technology, a Technically, Economically and Environmentally Feasible Solution to the Urban Solid Waste (USW) Problem and the Fertiliser Problem in Sri Lanka** Annual Transactions of IESL-2007, pp.129-39, © The Institution of Engineers, Sri Lanka.
11. Perera, S.A.S. Delta-D Initiated Microorganic Digestion of Saw Dust into Organic Fertiliser - A Technically, Economically and Environmentally Feasible Solution to the Saw Dust Problem in Sri Lanka Engineer (Journal of The Institution of Engineers, Sri Lanka), Vol XXXX1, No: 04, October 2008, ISSN-1800-1122, pp.50-65, 2007, © The Institution of Engineers, Sri Lanka.
12. Perera, S.A.S. Conversion of Coconut Water Waste Produced in Desiccated Coconut Mills into Liquid Organic Fertiliser Using Delta-D Technology by S.A.S. Perera, The Proceedings of the 24th International Conference on Solid Waste Technology and Management March 15-18, 2009, pp. 1601-1612, ISSN 1091-8043 © 2009 JSWTM, Widener University, Philadelphia, USA.
13. Perera, S.A.S. Sustainable Agriculture Through Delta-D Technology, a Solution to Urban Solid Waste and Global Warming The Proceedings of the 24th International Conference on Solid Waste Technology and Management March 15-18, 2009, pp. 1601-



1612, ISSN 1091-8043 © 2009 JSWTM, Widener University, Philadelphia, USA.

14. Perera, S.A.S. Delta-D Technology - A Patented Technology That Could Be Used To Prevent Emission Of Green House Gases From Urban Solid Waste, Agricultural Waste and Farm Waste International Conference on Climate Change, Biodiversity and Food Security in the South Asian Region, Organised by Punjab State Council for Science and Technology of Govt. of Punjab and UNESCO - New Delhi, pp. 87-89, ISBN No: 978-81-88362-24-0, © Punjab State Council for Science and Technology.

**Published in Abstract Form / Single Author
Marks Claimed = 1.5**

15. Perera, S.A.S. Manufacture of Organic Fertiliser from Poultry Slaughterhouse Waste Rendering Plant Sludge Using Delta-D Technology

The Proceedings of the 24th International Conference on Solid Waste Technology and Management March 15-18, 2009, pp. 1601-1612, ISSN 1091-8043 © 2009 JSWTM, Widener University, Philadelphia, USA.

**Published in Abstract Form / Single Author
Marks Claimed = 1.5**

16. Robinson, T. McMullan, G. Marchant, R. P Nigam, Remediation of dyes in textile effluent: a critical review on current treatment technologies with a proposed alternative, Bioresource technology, 2001 - Elsevier

17. Griffith, J.W., Raymond, D.H. The first commercial supercritical water oxidation sludge processing plant
- Waste Management, 2002 - Elsevier

18. Suh, Y.J. Rousseaux, P. An LCA of alternative wastewater sludge treatment scenarios,
- Resources, Conservation and Recycling, 2002 - Elsevier

19. KD North, Tracking polybrominated diphenyl ether releases in a wastewater treatment plant effluent, Palo Alto, California - Environmental Science & Technology, 2004 - ACS Publications

20. Fytili, D., Zabaniotou, A. Utilization of sewage sludge in EU application of old and new methods—a review
- Renewable and Sustainable Energy Reviews, 2008 - Elsevier

21. Rulkens, W., Sewage sludge as a biomass resource for the production of energy: overview and assessment of the various options- Energy & Fuels, 2007 - ACS Publications

22. I.S. Turovskiy, P.K Mathai, Wastewater sludge processing, .google.com

23. Fullana, A., Conesa, J.A., Font, R. Formation and destruction of chlorinated pollutants during sewage sludge incineration- Environmental science & ..., 2004 - ACS Publications

24. Dai, J., Xu, M., Chen, J., Yang, X., Z KePCDD/F, PAH and heavy metals in the sewage sludge from six wastewater treatment plants in Beijing, China
- Chemosphere, 2007 - Elsevier

Field Experiments on Low-Cost Combined-Media an Anaerobic Filter System for the Treatment of Landfill-Leachate

D.M.T.P. Fernando, W.K.C.N. Dayanthi, K.G.D. Chamenuka,
B.S.R. Nanayakkara and K. Kawamoto

Abstract: Anaerobic filter (AF) is commonly applied in the treatment of landfill-leachate, and one major drawback is the use of expensive packing media. Hence, investigations on the applicability of low-cost materials as efficient packing materials in anaerobic filters are timely and crucial. Thus, the present study was focused on assessing the applicability of low-cost materials as packing media in an anaerobic filter treatment system at field conditions, in which two AFs (AF1 and AF2) were connected in series. The treatment was processed through the anaerobic filter 1 filled with dewatered alum sludge (DAS) and washed sea sand (WSS) and then through the anaerobic filter 2 filled with sawdust (SD) and biochar (BC). Removal efficiencies of organic compounds, nutrients and heavy metals found in land fill-leachate; and the variation of physical and mechanical properties of the packing media subjected to the interactions between the packing media and the landfill-leachate were obtained throughout the experimental period of 133 days. Average overall removal efficiencies of BOD₅ and COD were 43.6 ± 17.7 % and 54.6 ± 17.0 %, respectively. Average removal efficiencies of TN and TP were 61.5 ± 15 % and 68.9 ± 16 %, respectively. The mean values of the overall removal efficiencies of the AF system for Cu, Fe, Mn, Pb and Cd were 85%, 79%, 74%, 72% and 67 %, respectively. The physical and mechanical properties of the packing materials did not undergo a significant variation as a result of the interaction with the landfill-leachate.

Keywords: Anaerobic filters, Contaminants, Field conditions, Low-cost media, Landfill-leachate

1. Introduction

Industrialization, population growth and urbanization have caused a rapid generation of solid waste. Solid waste can be classified into three main types depending on different sources: municipal waste, industrial waste and biomedical waste [1]. One of the major pollution problems caused by the municipal solid waste (MSW) landfill is the leachate, which is generated as a result of mixing water from precipitation and surface run-off with the MSW.

Generally, landfill-leachate may contain a large amount of organic matter, which are biodegradable, materials refractory to biodegradation, as well as ammonia -nitrogen, heavy metals (e.g. copper, iron, zinc, lead, manganese etc.), chlorinated organic and inorganic salts (e.g. Chloride, sulphate, sodium etc.) All these contaminants are a great threat to the surrounding soil, groundwater and even surface water [2], [3].

Therefore, proper treatment of the landfill-leachate is essential in landfill handling in order to mitigate environmental risks and to protect the surface and groundwater. The landfill-

leachate treatment processes can be categorized into physical, chemical and biochemical. Due to the reliability, simplicity and high cost-effectiveness, biochemical treatment is commonly used for the removal of the bulk of leachate containing high biochemical oxygen demand (BOD). When treating biodegradable leachate, biochemical techniques can yield a reasonable treatment performed with respect to the chemical oxygen demand (COD) and NH₃-N [4].

*Eng. (Ms.) D.M.T.P Fernando, Student member of IESL, B.Sc.(Eng. Ruhuna), Civil Engineer, Nawaloka Piling Pot(Ltd)
Email: thanujafernando26@gmail.com*

*Eng. (Dr) W.K.C.N Dayanthi, MIE(SL), B.Sc.(Eng. Peradeniya), M.Eng.(Moratuwa), M.Eng.(AIT), Dr.Eng. (Kyoto), Senior Lecturer, Department of Civil and Environmental Engineering, Faculty of Engineering, University of Ruhuna.
Email: neeth02@gmail.com*

Eng. (Ms.) K.G.D Chamenuka, Student member of IESL, B.Sc. (Eng. Ruhuna), Civil Engineer, Sanken Construction Pot(Ltd)

Eng. (Mrs.) B.S.R. Nanayakkara, C.Eng., B.Sc.Eng.(Moratuwa), MIE(SL), M.Phil. Student (Ruhuna), Civil Engineer. Ports Authority, Colombo.

Prof. K. Kawamoto, Graduate School of Science and Engineering, Saitama University, Saitama, Japan.



Landfill-leachate treatment mechanisms can be divided into two categories, namely, pump-and - treat methods and in-situ methods. Among the advantages of pump - and- treat method over in-situ method is the less adverse impacts on the ecological conditions, groundwater issues, and the less requirement of the long-term monitoring activities [5].

Anaerobic filter (AF) is a notable 'pump-and-treat' method because it is a kind of anaerobic digester containing a packing medium that anaerobic bacteria can grow in as well as remove contaminants while the leachate flows through the media. One merit of using an anaerobic filter for treating the landfill-leachate is the absence of the secondary clarifiers and reduction of all the associated cost and operational problems [5]. Anaerobic filters have emerged as a promising technology to treat the landfill-leachate.

However, its application has been limited due to the requirement of expensive packing media. Plastic pall rings, tubes and flakes are conventional packing materials, which have to be manufactured in a factory, thus causing these materials to be quite expensive. If low-cost materials can effectively be utilized as packing media in anaerobic filters, it will enhance the applicability of the AF as a treatment technique for landfill-leachate in a developing country.

Thus, it is a timely need to perform experiments on low-cost packing media and their appropriate quantities and placement techniques in AFs to treat the landfill-leachate. According to a previous research conducted at field conditions, by the authors of this paper, materials, namely washed sea sand (WSS), dewatered alum sludge (DAS), sawdust (SD) and biochar (BC) are efficient as packing materials in anaerobic filters to treat organic compounds, nutrients and heavy metals [6]. In the above research, the performances of the selected packing materials for the removal of organic compounds were on a par with plastic pall rings, which is a conventional packing material. Further, the selected materials surpassed the performances of plastic pall rings in treating the cations, Ca^{2+} and Mg^{2+} and heavy metals, Cu and Fe, owing to the promotion of treatment mechanisms such as ion exchange, precipitation and adsorption due to different properties possessed by these materials. The experimental set-up of the above research consisted of two AFs, each of which

had been filled with WSS, DAS, SD and BC in layers of equal thickness; and plastic pall rings, respectively. The AF filled with plastic pall rings was the control experiment.

The aim of the present study was to assess the landfill-leachate treatment potential of a system of two anaerobic filters connected in series, filled with low-cost, locally and readily available materials. The first objective of the study was to find out the removal efficiencies of the organic compounds, nutrients and heavy metals. Removal efficiencies of organic compounds were obtained in terms of BOD_5 and COD and nutrients in terms of ammonia nitrogen ($\text{NH}_3\text{-N}$), total nitrogen (TN), total phosphorus (TP) and orthophosphate phosphorus ($\text{PO}_4^{3-}\text{-P}$). Similarly, the removal efficiencies of heavy metals were measured in terms of Cu, Fe, Mn, Pb and Cd. The removal efficiency of total dissolved solids (TDS) was also measured. The second objective was to find out the changes in the physical and mechanical properties of the packing media due to them being interacted with the landfill-leachate.

As the selected packing materials are low- cost and readily available, the present study is significant in the context of developing countries. The study will also find a solution for the disposal issue of DAS, which is regarded as a waste material.

2. Methodology

2.1 Experimental Set-Up

The experimental set-up (Figure 1) includes a sequence of components connected to each other in the following order: a lysimeter (1.5 m diameter and 5 m height), a receiving tank, an overhead storage tank, an anaerobic filter filled with packing materials of high particle densities (DAS and WSS), a storage tank, an overhead storage tank, an anaerobic filter filled with packing materials of low particle densities (SD and BC) and a storage tank. The lysimeter consisted of five layers of expansive soil, metals, sand, MSW and in-situ soil. The sectional view of the lysimeter is shown in Figure 2. This lysimeter acted as a model landfill, of which the leachate was used as the influent of the AF system.

The experimental set-up was located in Hambantota. Hence, the rainfall received by the lysimeter was relatively less, and tap water was applied onto the lysimeter to increase the

leachate production rate. The leachate generated in the lysimeter was applied on AFs in the down-flow direction. The layer thickness of each layer packing material was 67 cm. The leachate generated in the lysimeter was stored in the storage tank 1, and using a pump it was flown to the overhead tank 1. By gravity, the flow was passed through AF 1. The effluent of AF 1 was collected in the receiving tank 1 and then pumped to the overhead tank 2. The effluent in the overhead tank 2 was drained onto AF 2 under gravity. The effluent of AF 2 was collected temporarily in a storage tank before being recirculated onto the lysimeter.

2.2 Packing Configuration of the Media and the Experimental Run.

Figure 3 depicts the packing configurations of the media beds of AF1 and AF2. The height and the diameter of the cylindrical AF columns were 2 m and 600 mm, respectively. AF 1 and AF 2 consisted of a bed of coarse aggregates (200 mm layer thickness) at the bottom in order to collect the drained effluent through the media bed, and direct toward the effluent port. The packing media of the AF columns were arranged considering the particle densities of the packing materials. In AF 1, packing materials with relatively higher particle densities, DAS and WSS, were filled with layers. In AF 2, packing materials with relatively lower particle densities, BC and SD, were filled in layers. The layer height of each packing material was 670 mm. After compacting the packing materials, two AF units were connected in series.

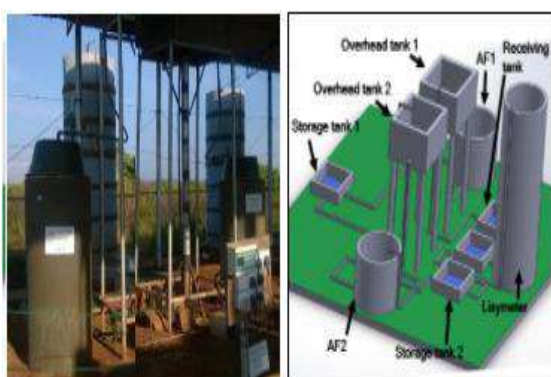


Figure 1 - Image and the Isometric View of the Experimental Set-Up.

After loading the AF system, the influent was applied, and its flow rate was adjusted to give a pore volume retention time approximately equal to 2 d in each AF. Table 1 indicates the flow rates and the hydraulic loading rates of the AF units. The flow rate was manually measured several times during one loading

cycle of leachate onto the respective overhead tank of AF1 and AF2. The loading cycle was approximately 2 weeks. Then, the surface loading rates were obtained by multiplying the flow rate with the value of each parameter and then dividing by the surface area of the respective reactor.

Wastewater samples were collected from the influent of the AF1 and the effluent lines of both AF1 and AF2, once in the two-week period. Influent characteristics and the surface loading rates of the selected wastewater parameters are mentioned in Table 2 and 3, respectively. pH of AF1 influent varied between 6.5 and 9.5. The target wastewater parameters were organic compounds (BOD₅ and COD), nitrogenous compounds {Total Nitrogen, Ammonia Nitrogen} and phosphorous compounds {Total Phosphorus and Ortho Phosphates Phosphorus}. In addition, heavy metals namely Cu, Fe, Mn, Pb and Cd, and TDS were also analysed. In the partial run of the experiment (after 98 days), the influent was added with heavy metals artificially to obtain heavy metal characteristics typical for the landfill-leachate. This was done to find the capability of the treatment system to bear high heavy metal loading rates. Table 4 indicates the heavy metal loading rates before and after addition of heavy metals artificially in the influent.

Core samples of the packing media bed were collected before applying the influent and at the end of the experimental run in order to find out the variation of the physical and mechanical properties of the packing media with the progression of the treatment.

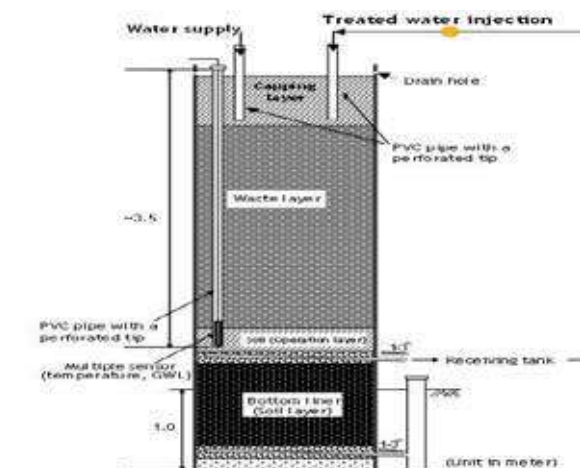


Figure 2 - Sectional View of the Lysimeter.

2.3 Analysis of the Physical and Mechanical Properties of the Packing Media.

For the analysis of physical and mechanical properties of the packing media, specific gravity test and hydraulic conductivity tests were conducted. These test results demonstrate the influence of the treatment mechanisms inside the packing media on their physical and mechanical properties.

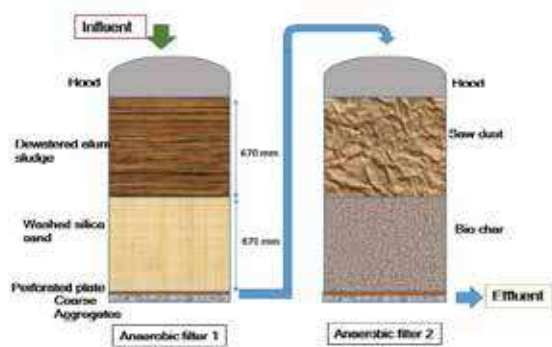


Figure 3- Packing Configuration.

Table 1 - Flow Rates and the Hydraulic Loading Rates of the AF Units.

AF unit	Packing material	Flow Rate of individual material (m ³ /d)	Average flow rate (m ³ /d)	Hydraulic loading rate (m ³ /d/m ²)
AF 1	DAS	0.07	0.06	0.23
	WSS	0.06		
AF 2	BC	0.06	0.07	0.25
	SD	0.08		

Table 2 - Influent Characteristics.

Parameter	AF 1	AF 2
	Average influent concentration (mg/L)	Average influent concentration (mg/L)
BOD ₅	219.50	137.00
COD	882.36	493.48
TN	74.10	58.29
TP	0.79	0.31

Table 3 - Surface Loading Rates on the AF System.

Parameter	AF 1	AF 2
	Surface loading rate (g/m ² . d)	Surface loading rate (g/m ² . d)
BOD ₅	49.7	34.3
COD	199.7	123.6
TN	16.8	14.6
TP	0.18	0.08

Table 4 - Heavy Metal Loading Rates Before and After the Addition of Heavy Metals Artificially.

Parameter	Surface loading rate (mg/m ² . d)	
	Before adding heavy metals artificially	After adding heavy metals artificially
Cu	4.7	35.9
Pb	11.0	2.5
Cd	0.1	3.1
Mn	0.8	9.3
Fe	0.3	27.7
TDS	169.0	266.4

3. Results and Discussion

3.1 Removal of Organic Matters

Removal efficiencies of organic matters with time were obtained in terms of BOD₅ and COD during the experimental period. Figure 4 indicates the removal efficiencies of BOD₅ with respect to the time. According to the graph, removal efficiency of AF 1 was in the range of 20% -30% in the first half of the experimental run. However, a continuous increment of the removal efficiency was obtained in the second half of the experimental run. The overall removal efficiency of BOD₅ in the treatment system was 43.6 ± 17.7 %.

As stated by McCarty (1982) [7], in anaerobic conditions, three physiological groups of bacteria are involved in the anaerobic conversion of organic materials to methane. In wastewater treatment applications, biomass is produced continuously as the substrate in the wastewater is consumed, and thereby biodegrade [8]. Therefore, the rate of biodegradation may increase with time. The low treatment efficiencies of BOD₅ at the initial stage could be caused by the less microbial

population in the filtration media. In line with the above phenomenon, the treatment efficiency of BOD₅ in the present study increased with time.

COD is another important parameter, which measures the organic matter content. COD removal efficiencies of the AF units are illustrated in Figure 5. According to the graph, COD removal efficiency was significantly higher in AF 1, and fluctuations of the removal efficiencies could also be seen. In the mid experimental run, the removal efficiencies were lesser compared to the initial and later stages. The overall COD removal efficiency of the treatment system was $54.6 \pm 17.0\%$.

Sorption refers to the exchange of molecules and ions between the solid phase and the liquid phase [9]. Adsorption is a very important method for removing contaminants, particularly dissolved organic contaminants from wastewater streams [8]. Hence, adsorption can be considered a potential removal mechanism of organic materials in AF1 and AF2. With time, adsorption capacity decreases, and hence another mechanism should govern the treatment process to keep the consistency in treatment. The explanation of Coony (1999) [9] on biodegradation process, can be used to explain the COD removal in the latter part of the experimental run. As the rate of biodegradation may increase with time, the biodegradation could be the possible dominant treatment mechanism in both AFs to obtain removal of COD at the latter stage.

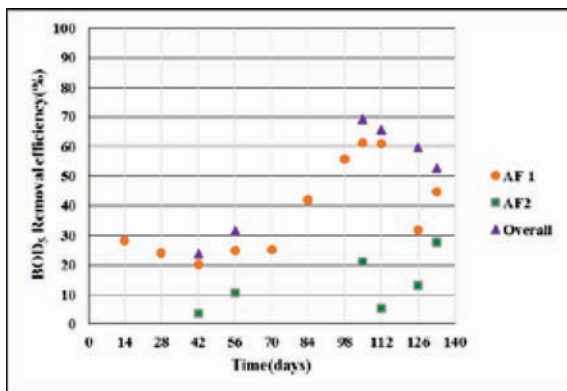


Figure 4 - BOD₅ Removal Efficiency with Time.

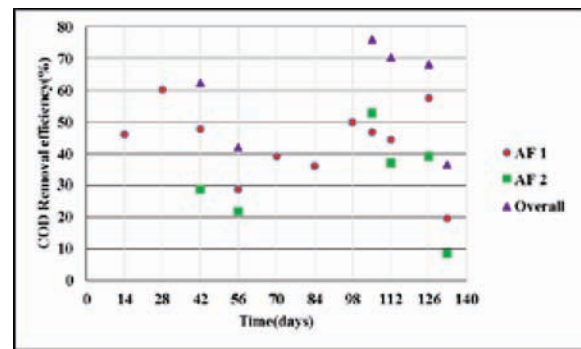


Figure 5 - COD Removal Efficiency with Time.

3.2 Removal of Nitrogenous Compounds

In this analysis of nitrogen compounds, mainly NH₃-N and TN were considered. Figure 6 indicates the removal efficiencies of NH₃-N with time. The mean efficiencies of NH₃-N removal by AF 1 and AF 2 were $77.9 \pm 17.94\%$ and $55.1 \pm 28.5\%$, respectively. Nitrification and the adsorption of ammonium could be the possible mechanisms, which can eliminate NH₃-N [10]. At the initial stage, NH₃-N adsorption could be the process, which contributed to the removal of most of the NH₃-N. Here, adsorbent could most probably be the packing materials. Large surface areas provide high adsorption capacities, and small particles have relatively large surface areas. At the initial stage of the experimental run, the dominant mechanism for NH₃-N treatment could be adsorption. The adsorption capacity of the packing materials decreases with the gradual occupation of the vacant sites with time.

Average removal efficiencies of TN were $25.63 \pm 15.30\%$ and $54.33 \pm 11.37\%$ for AF 1 and 2, respectively as shown in Figure 7. Mainly the biochemical nitrogen removal is accomplished by anoxic denitrification process. When compared to AF 1, AF 2 gained higher removal efficiency in the latter part of the experimental run.

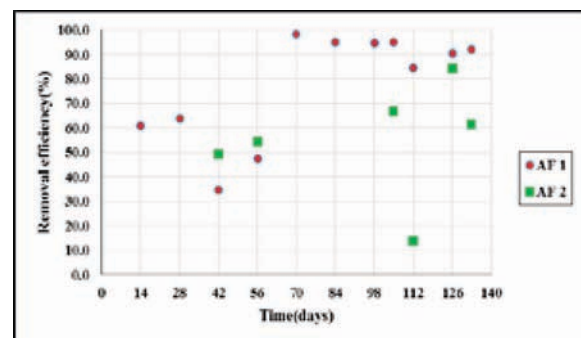


Figure 6 - NH₃-N Removal Efficiency with Time.

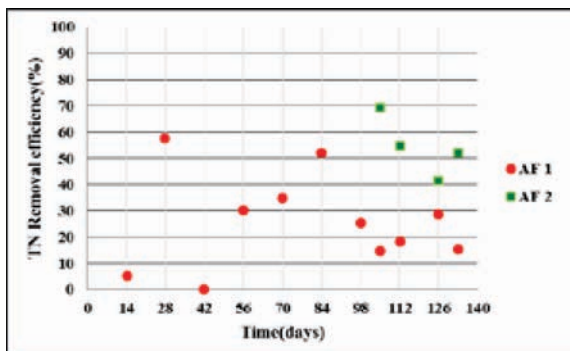


Figure 7 - TN Removal Efficiency with Time.

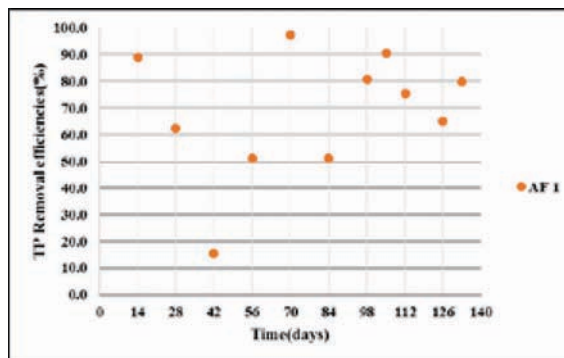


Figure 9 - TP Removal Efficiency with Time.

3.3 Removal of Phosphorus Compounds

Phosphorus compounds in terms of TP and PO_4^{3-} -P were considered in the analysis. A considerable treatment occurred in the AF 1 unit. According to Figure 8 and 9, it is obvious that AF 1 unit directly contributed to the PO_4^{3-} -P removal. The average overall removal efficiency was $75.4 \pm 14.53\%$. According to Razali et al. [11], DAS is an effective absorbent for phosphorus compounds. Because there are some polymeric forms of aluminium that are not completely neutralized, the alum sludge may carry a small net positive charge. As phosphorus is normally present in the form of negatively charged anions, it is readily adsorbed by the positively charged aluminium hydroxide. It is the principal mechanism for removal of phosphorus from the wastewater in sewage treatment plants [12]. Hence these results verify that DAS is a suitable packing material to treat phosphorus compounds in the landfill-leachate.

3.4 Removal of TDS and Heavy Metals with Time

The mean values of the overall removal efficiencies of the AF system for Cu, Fe, Mn, Pb, Cd and TDS were 85%, 79%, 74%, 72%, 67%, and 47%, respectively. Figure 10, 11, 12, 13 and 14 depict the variation of the removal efficiencies of TDS, Cu, Fe, Pb and Mn, respectively with the progression of the experiment.

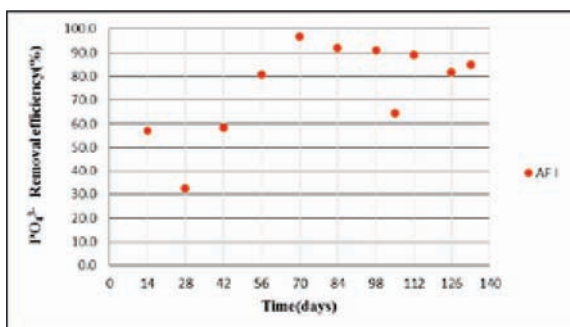


Figure 8 - PO_4^{3-} -P Removal Efficiency with Time.

According to Bagchi [9], the surfaces of organic matter provide some adsorption sites, and the adsorption process has demonstrated to be widely effective for removing dissolved organic substances from the wastewater. Therefore, adsorption could also contribute to the removal of inorganic dissolved solids in AFs.

Presence of coagulants such as alum, iron salts, and organic polymers in DAS can cause the removal of heavy metals as a hydroxide precipitate. As microorganisms consume substrates and carry out oxidation/reduction reactions, metal ions can be oxidized/reduced. In addition, the sulphides available in the packing media can react with heavy metal ions and form insoluble precipitates. The precipitates such formed can be separated from the influent by sedimentation or filtration as it flows through WSS. The removal of heavy metals could occur due to the packing media favouring adsorption such as DAS, SD and BC [14]. Biosorption activities also may remove heavy metals due to the availability of the microbial biomass in packing materials [15]. Further BC and SD contain various organic compounds (lignin, cellulose and hemicellulose) with polyphenolic groups that could bind heavy metal ions through different mechanisms. Ion-exchange reactions could also cause the heavy metal removal. Zeolites and silicate minerals contained in WSS could be able to exchange its cations with the heavy metal ions.

3.5 Variation of Physical and Mechanical Properties

Table 5 shows the physical and mechanical properties of the packing materials before and after loading the influent onto the system. The physical properties of the packing media did not undergo much change during the 4-month long experimental run. The slight changes of these properties could be attributed to the occurrences of treatment mechanisms such as

coagulation, flocculation, sedimentation, filtration, adsorption and ion exchange. In addition, a slight wearing off of the materials could contribute to these variations.

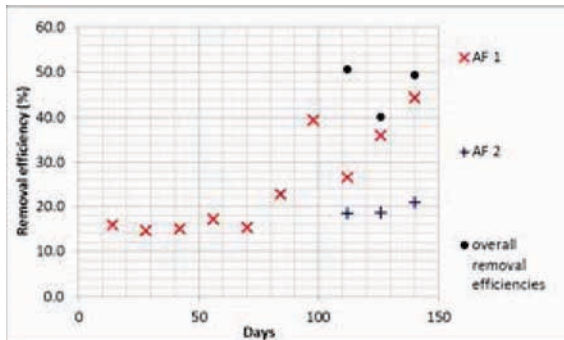


Figure 10 - TDS Removal Efficiency with Time.

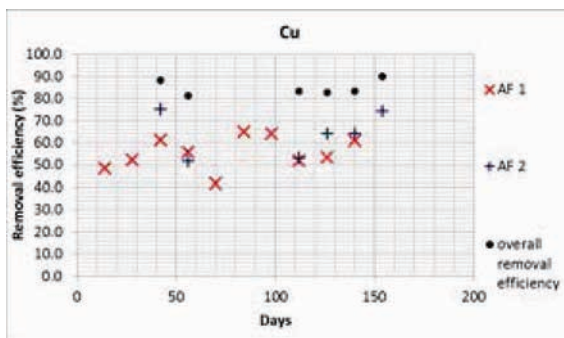


Figure 11 - Cu Removal Efficiency with Time.

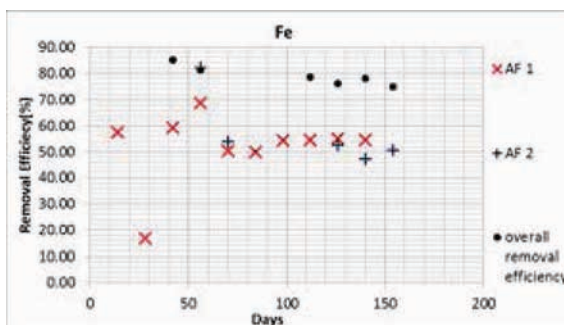


Figure 12 - Fe Removal Efficiency with Time.

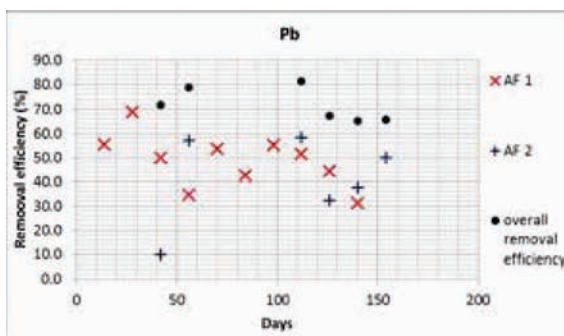


Figure 13 - Pb Removal Efficiency with Time.

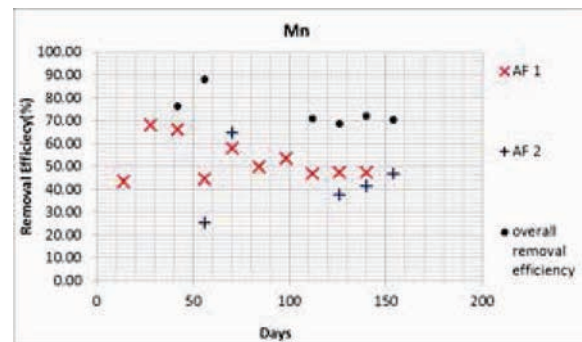


Figure 14 - Mn Removal Efficiency with Time.

Table 5 - Physical and Mechanical Properties of Packing Materials.

Filter media	Porosity		Hydraulic conductivity(cm/s) ($\times 10^{-3}$)	
	Initial	Final	Initial	Final
DAS	0.663	0.697	3.8	3.6
WSS	0.401	0.392	6.9	6.5
SD	0.756	0.807	3.8	3.2
BC	0.541	0.446	4.1	3.6

4. Conclusions

The anaerobic filter treatment system described in this study had the potential to treat the organic and nutrient compounds as well as heavy metals in the landfill-leachate with significant efficiencies. There was no significant variation of the physical and mechanical properties of the packing media due to the interactions between packing materials and leachate. The AF treatment system could withstand high heavy metal loading rates. It was also proved to some extent that these low-cost, locally and readily available filter materials can effectively be applied in anaerobic filters to treat landfill-leachate partially, without rapid deterioration of the physical and mechanical properties of the reactive media.

The key feature of this study was the use of low-cost, locally and readily available materials instead of the expensive packing media in a system of anaerobic filters connected in series. The selected packing media were expected to provide effective treatment for the organic compounds and nutrients due to the diverse properties possessed by these materials.

The study showed that all four materials were satisfactory in treating landfill-leachate in terms of organic compounds and nutrients. As the anaerobic filter 1 was packed with dewatered alum sludge and washed sea sand, a significant removal of phosphorus was obtained. That was a key finding of this study, which verifies that the DAS is a suitable adsorbent to treat



phosphorus compounds (Total-P and orthophosphate phosphorus) in the leachate at the field conditions prevailing in the dry zone of Sri Lanka.

As the future improvements of this research study, better and alternative arrangements of low-cost and readily available materials in the AFs and alteration of the hydraulic retention time can be highlighted in order to enhance the removal efficiencies. Further experiments with increased packing densities and hydraulic retention times will give better results. Chemically modified packing materials will also provide higher efficiencies. The effect of the long-run operation of the system on the variation of the physical and mechanical properties of the packing materials should be investigated.

Acknowledgement

This work was supported by the research grant from the JST/JICA Science and Technology Research Partnership for Sustainable Development (SATREPS). Authors would like to acknowledge Ms D.A.M. Nimal Shanthi for her assistance in laboratory analyses.

References

1. Liu, S., *Landfill leachate treatment methods and evaluation of Hedeskoga and Måsalöcke landfills*, Water and Environmental Engineering, Department of Chemical Engineering, Lund University, Sweden, 2013.
2. Renou, S., Givaudan, J. G., Poulain, S., Dirassouyan, F. & Moulin, P., "Landfill Leachate Treatment: Review and Opportunity", *Journal of Hazardous Materials*, vol. 150, 2008, pp. 468-493.
3. Robinson A. H., *Landfill leachate treatment membrane technology*, June 6-12, 2005.
4. Kurniawan, T. A., Lo, W. H. & Chan, G. Y., "Physico-Chemical Treatment for Removal of Recalcitrant Contain from Landfill Leachate", *Journal of Hazardous materials*, 129(1), 2006, pp.80-100.
5. Madu, J. I., *Water and Environmental Engineering*, Department of Chemical Engineering, Lund University, Sweden, Master Thesis number: 2008-02
6. Dayanthi, W. K. C. N, Nanayakkara B. S. R., Kawamoto K., Premathilaka M.D.B.A. & Dulvin O.V.N., "Field-Scale Study on Treating Landfill Leachate Using Anaerobic Filters Packed with Low-Cost Filter Media", *IESL Annual Transaction 2017* (In review)
7. McCarty, P. L. In: (D.E. Hughes, D. A. Stafford, B. F. Weatley, W. Beader, G. Lettinga, E. J. Nuns, W. Verstraete and R. L. Wentworth, eds.) *Anaerobic Digestion*. Elsevier Biomedical, Amsterdam, pp. 3-22. McCoy, J.H. (1962) *J. Appl. Bact.* 25:213-224. cited by the Director, Publications Division, Food and Agriculture Organization of the United Nations, Viale delle Terme di Caracalla, 00100 Rome, Italy, 1982.
8. Coony, D. O., *Adsorption Design for Wastewater Treatment*, Lewis Publishers, 1999.
9. Bagchi, A., *Design of Landfills and Integrated Solid Waste Management*, John Wiley & Sons, Inc., 2004.
10. Metcalf & Eddy, "Wastewater Engineering Treatment and Reuse", 4th edition, McGraw-Hill, Inc., New York, chapter 9, pp. 888-889.
11. Manoj, V. R. & Vasudevan, N., "Removal of Nutrients in Denitrification System using Coconut Coir Fibre for the Biological Treatment of Aquaculture Wastewater", *J. Environ. Biol.*, Vol.33, pp.271-276, 2012.
12. Razali, M., Zhao, Y.Q., & Bruen, M., "Effectiveness of a Drinking-Water Treatment Sludge in Removing Different Phosphorus Species from Aqueous Solution", *Separation and purification technology*, Vol. 55, No. 03, July, 2007, pp.300-306.
13. Norvell, W. A., 1982," Feasibility of Inactivating Phosphorus with Aluminium Salts in Ball Pond. CT. Conn. Agr. Exp. Sta. Bull.806.10p.
14. Wan, N. W. S & Hanafiah, M. A. K. M., "Removal of Heavy Metal ions from Wastewater by Chemically Modified Plant Wastes as Adsorbents: A Review", *Bioresource Technology*, Volume 99, Issue 10, July 2008, pp. 3935-3948.
15. Friis, N. & Myers-Keith, P., "Biosorption of Uranium and Lead by *Streptomyces longwoodensis*", *Biotechnol. Bioeng.* 28., 1986, pp 21-28.

Low-Cost drinking Water Filter

U.A.C. Perera and S.C.S. Karunaratne

Abstract: Sri Lanka could be identified as more fortuitous land owning about 85 % of its drinking water in the safe zone. But still, in most parts of the country, people are battled against water borne diseases since they don't have access to safe drinking water. Hence need of the society is to have a drinking water filter with the ability to outflow clean potable water at domestic level. Reviews on existing filter systems in Sri Lanka and contamination levels different physicochemical and bacteriological parameters were identified in ground water sources. The filter was designed to fabricate with filter materials such as clay, activated carbon and two different types of ion exchange resins to remove contaminants, treat total hardness and improve physical parameters. The effectiveness of the filter was analysed for reducing and treating various contaminants and physical parameters in raw water under provided Sri Lankan Standards. Results showed that designed filter is capable of treating hardness, removal of Nitrogen based contaminants and improving physical parameters. But it was found that used filter materials were not capable of treating total alkalinity and removing bacteria such as Coliform and E-coli. Through the cost analysis, it was rated that fabricated filter could be manufactured at a unit price of LKR 6030.00 whereas most of the existing filters in Sri Lanka cost more than LKR 10,000.00 per unit with some having a very high maintenance cost.

Keywords: Low cost, drinking water, filtration

1 Introduction

In the present people are being faced the issue of not having safe drinking water with adequate quality for the consumption. In certain situations, people have to pay for their water, and it too has limitations. Reasons for unavailability of water have been identified as the presence of contaminants such as nitrates, nitrites, chlorides, fluorides, hardness due to calcium and magnesium, heavy metals and bacterial contaminants such as coliform and E-coli [1]. Presence of this kind of contaminants affects human body cells if they are consumed in bulk. Furthermore, it has been identified that unavailability of safe drinking water is a reason for diseases like Chronic kidney diseases, tooth decay due to fluorides and chlorides, diarrhoea and Cholera [2],[3]. Although currently available filters are capable of treating and removing these contaminants to some extent, they are priced high and poor people face problems in acquiring one of them. Therefore, the objective of the research was to design a Filter at a reasonable cost to remove contaminants such as nitrates, nitrites, ammonia and treat hardness and capable of treating parameters such as turbidity and colour. During this research scope of the study was based on qualities of ground water in the western province.

2 Methodology.

2.1 Approach

The research was approached in a way that filter was fabricated and tested with collected and prepared water samples for identifying

the capabilities of the filter. For that, both artificial and natural materials were used in filter and tested for their abilities in treating parameters aforementioned. While ground water samples were collected from different areas in the western province and they were tested before and after filtration through the designed filter for selected parameters such as pH, conductivity, level of several contaminants and hardness etc. Detailed information in each step is given below. Also, two commercially available filters were used to compare results with designed filter

2.2 Filter Fabrication

2.2.1 Clay core fabrication.

For the fabrication of clay cores, normal brick clay was collected from Kaduwela, Ranala and Atigala area. Rice husk was collected from a rice mill in Athurugiriya. They were thoroughly washed and dried under sunlight prior to fabrication. Initially, clay cores were planned to fabricate using clay and rice husk. Sample cores were prepared with following clay to rice husk proportions given in Table 1.

Mr. U.A.C. Perera, B.Sc.Eng. Hons. (SLIIT), Temporary Assistant Lecturer, Department of Civil Engineering, Faculty of Engineering, Sri Lanka Institute of Information Technology.

Eng. (Dr.) (Ms.) S.C.S. Karunaratne, B.Sc.Eng. Hons. (Moratuwa), M.Eng. (Saitama), Ph.D. (Saitama), C.Eng., MIE(SL), MIEP(SL), Senior Lecturer, Department of Civil Engineering, Faculty of Engineering, Sri Lanka Institute of Information Technology.



Clay cores were fabricated with dimensions of 150mm x 50mm x 50mm yielding surface area of 325 cm² per each core, and four cores were used instead of one to increase the surface area for filtration and avoid issues due to clogging during operation. These cores were burnt in a muffle furnace at 200 °C for 2 hours, then at 400 °C for 2 hours and another 4 hours at 900 °C and these increments were followed to avoid cracking of cores.

Table 1 - Mix proportions used for clay cores

Sample	Core 1	Core 2	Core 3	Core 4	Core 5
Clay %	100%	95%	90%	85%	80%
Rice husk %	0	5%	10%	15%	20%
Flow rate (L/h)	19.5	19.2	20.6	20.0	19.8

2.2.2 Selection of materials for filter fabrication

Drinking water parameters which are intended to improve during the filtration process of water through expected design are as follows.

- Turbidity.
- Colour.
- Chemical contaminants.
 - Nitrates and nitrites
 - Phosphates
- Hardness.
- Electrical conductivity

For the removal of these unpleasant characteristics and contaminated chemical compounds following mechanisms and filtering, materials were used for the filter. At the first stage, cuboidal shaped clay cores were used. Considering the disadvantages of filters mentioned above, Intention was to fabricate the filter for the research project using a combination of activated carbon, SCR-B ion exchange resin and Nitrate selective ion exchange resin. These were finalized based on their performance in filtration. Normal clay was used to cast the clay core used in the initial stage of filtration. The basis for the selection of materials has been discussed below.

2.2.2.1 Filter materials

Activated carbon - Based on the capability of activated carbon to remove and treat contaminants and physical properties in water it was decided to use Granular Activated Carbon of size 12 x 30 in the cuboidal cage as the third level of filtration. 775 cm³ of activated carbon was used in 30mm depth chamber with

a surface area of 225 cm² based on specifications in the mineral pot filter.

SCR-B cation exchange resin - Trilite is a gel type strongly acidic cation exchange resin which is capable of deionization of water, separation and recovery of metals, refining of chemicals, desiccation of organic solvents and catalysts. The resin was backwashed prior to use in order to remove any resin fines and small particles. Grade used for the research was SCR- B and data sheet for the resin is provided in Table 2. This resin was used at the second level of filtration chamber with same quantity as activated carbon [4].

Table 2 - Data sheet for Trilite SCR-B

Type	Gel type
Grade	Trilite SCR-B
Matrix	Polystyrene + DVB
Functional group	SO ₃ ⁻
Ionic form	Na
Specific gravity	1.29
Shipping weight (g/l)	830
Moisture retention	43 - 50
Total capacity (eq/l)	2.0
Effective size (mm)	0.40
Uniformity coefficient	Max. 1.6
Particle size (mm)	0.3 - 1.2
Operating temperature (Celsius)	Max 120
Operating pH range	0 - 14

Nitrogen selective ion exchange resin - INDION NSSR is a microporous strongly basic anion resin which is a ready-made resin used to remove nitrate ions from water. Its proper mix of physicochemical properties gives ideal exchange kinetics of nitrate making this suitable for removing nitrate ions in the presence of chloride ions. This resin was used as the first filter material in the filtration chamber in same quantity as other two filter materials. Data sheet for the resin is given in Table 3. sequence of filter material usage in the filtration chamber is shown in Figure 1 [5].

Table 3 - Data sheet for INDION NSSR

Type	Gel type
Appearance	Opaque off white to brown beads
Matrix	Styrene DBC
Functional group	Quaternary ammonium
Ionic form	Chloride

Shipping weight kg/m ³	670
Moisture holding capacity	45 - 55 %
Total capacity (meq/ml)	Min 0.9
Effective size (mm)	0.40
Uniformity coefficient	Max. 1.7
Particle size (mm)	0.4 - 0.5
Operating temperature (Celsius)	Max 100 in Cl form
Operating pH range	0 - 14

INDION NSSR Anion resin	For Nitrates, Nitrites and Free Ammonia
SCR - B Cation resin	For Total hardness
Activated carbon	For Chlorides, Bacteria and Viruses

Figure 1 - Arrangement of filter materials in filter chamber

2.2.2.2 - Casing and adhesive.

Casing material - Case was fabricated using clear acrylic sheets with 3mm thickness and laser trimming technology was used cut the sheets and shapes in the design.

Adhesive material - Cyanoacrylate (Commonly termed as Super glue) was used as the adhesive to glue acrylic sheets. Cyanoacrylate is known as a non-toxic adhesive in solid form although it shows toxic properties in its aqueous form [6].

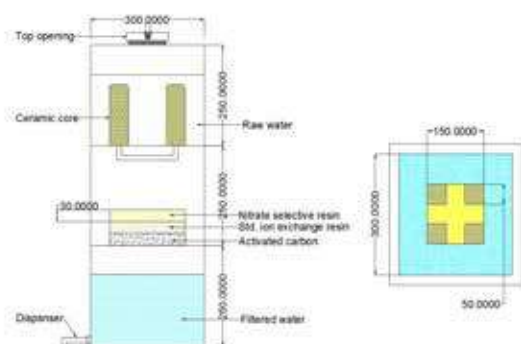


Figure 2 - Side elevation and plan view of the designed filter

2.2.3 Fabrication method

The filter was designed and planned to fabricate with three main chambers to store raw water, store filter materials and store filtered water. For each chamber, dimensions were selected to make the capacity of cuboid as 20 litres approximately, and dimensions are shown in Figure 2

Three of these chambers were planned to rest on top of each other, and top most chamber would be composed of four clay cores. Middle chamber would compose of filter materials, and the bottom chamber has been designed to use for storage of filtered water. During filtration process water would be seeped through clay cores at a rate of 19.5 litres per hour and at the second step water would be collected at cuboidal shaped storage compartment. Then Water would be seeped to filter materials evenly, and filtered water will be collected in the bottom chamber with a volume of 20 litres at a rate of 18 litres per hour.

2.2.4 Cost analysis

One of the prominent factor considered during the design of this filter was the cost of production of the filter. Hence detailed Cost breakdown of the filter has been calculated tabulated in Table 4. Based on above calculation it can be finalized that filter could be fabricated at a rate of LKR 6030.00 per unit.

Table 4 - Cost analysis chart

Material	Quantity	Unit cost	Total cost
Acrylic board for chamber	1.36 m ²	3,000.00	4,080.00
Activated carbon	0.50 kg	340.00	170.00
SCR-B cation exchange resin	0.50 litre	700.00	350.00
Nitrate selective IER	0.5 litre	220.00	110.00
Clay	2.4 kg	50.00	120.00
Adhesive	10 No	20.00	200.00
Water dispenser	1	150.00	150.00
PVC tubes	1	250.00	250.00
Plastic Sieving nets	4	25.00	100.00
Indirect cost and overheads	-	-	500.00
Total cost			<u>LKR</u> <u>6030.00</u>

2.3 Sample collection and locations

Samples were collected from different areas in the Western province according to the standards given in ISO 566-11 :2009 - Part II to

test for different parameters and the responsiveness of filter for those parameters. Locations are given in Table 5 [7].

Table 5 - Sample locations in Western Province

No	Location	Latitude (°N)	Longitude (°E)
01	Godagama	6.8630639	80.031118
02	Maharagama	6.849661	79.923288
03	Athurugiriya	6.891224	80.006153
04	Malabe	6.906096	79.956835
05	Pokunuwita	6.708166	80.042156
06	Kaduwela I	6.926053	80.001271
07	Rajagiriya	6.920425	79.903393
08	Kadawatha	6.994726	79.646420
09	Kaduwela II	6.924859	79.999439
10	Horana	6.724919	80.093851

2.4 Test methods

Collected samples were tested for following parameters based on standard methods given in American Public Health Association (APHA, 2005). These test methods are given in Table 6. [8].

Table 6 - Test methods used

Parameter	Test method used
Electrical Conductivity (S/cm)	APHA, 2510 B
Colour (Hazen units)	APHA, 2120 C
Turbidity (NTU)	APHA, 2130 B
Nitrate (NO ₃ ⁻) (mg/l)	APHA, 4500 NO ₃ . E
Nitrite (NO ₂ ⁻) (mg/l)	EPA 35.1
pH	APHA, 4500 HB
Free Ammonia (NH ₃) (mg/l)	APHA 4500 NH ₃ - C
Total Hardness (as CaCO ₃) (mg/l)	APHA, 2340 B
Phosphates (PO ₄ ³⁻) (mg/l)	APHA 4500 PE:2012

2.5 Ground water quality standards.

Sri Lankan Standards for potable water is given in SLS 614: 2013 (SLS-Sri Lanka Standards). Based on the cap values given in for drinking water filter was tested whether it could filter raw water to be within given limits. Highest Desirable level (HDL) and Maximum Permissible Level (MPL) for selected parameters are shown in Table 7 [9].

Table 7 - SLS for drinking water

Parameter	HDL	MPL
Electrical Conductivity (S/cm)	0.75	3.5

Colour (Hazen units)	5	30
Turbidity (NTU)	2	8
Nitrate (NO ₃ ⁻) (mg/l)	10	45
Nitrite (NO ₂ ⁻) (mg/l)	-	0.01
pH	7.0 - 8.5	6.5 - 9.0
Free Ammonia (NH ₃) (mg/l)	-	0.06
Total Hardness (as CaCO ₃) (mg/l)	250	600
Phosphates (PO ₄ ³⁻) (mg/l)	-	2.0

3 Results and Discussion

3.1 Selection of clay core

Rice husk percentages of 5 - 20 % were selected for finally produced clay cores due to failures in fabrication for higher percentages of rice husk. Cores were tested for treating turbidity and colour. Also, Flowrates were tested for each core and had been tabulated in Table 1. Based on the test results for flow rate in Figure 3 and Figure 4, no major variation was identified between different proportions used in cores for treating turbidity and colour. Therefore, clay cores were fabricated using clay as the only material.

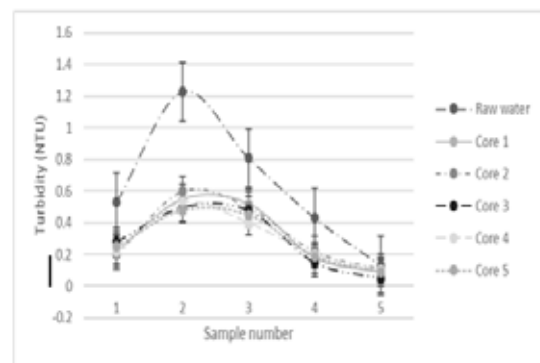


Figure 3 - Variation of turbidity of water for clay cores

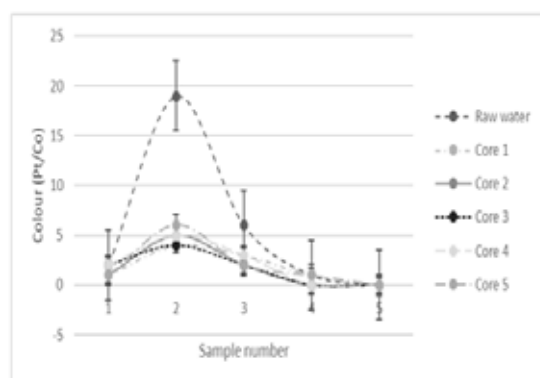


Figure 4 - Variation of colour of water for clay cores

3.2 Comparison of results for prepared solutions.

3.2.1 Nitrate variation

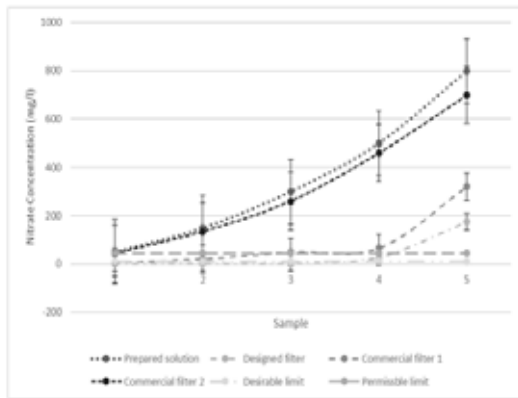


Figure 5 - Variation of nitrate concentration of prepared solution

Based on the results shown in Figure 5 for the prepared nitrate solutions using NaNO_3 with different concentrations given in the graph, identification can be made that designed filter has optimum ability to remove nitrate contaminants in raw water where filter has shown capabilities to treat nitrate concentrations up to 500mg/l which is normally not found in drinking water sources. While Commercial filter 1 has shown a closer trend but not as effective as the designed filter. Commercial filter 2 has not shown the ability to treat higher level of nitrates which are greater than the permissible limit. Removal effectiveness is shown in

Table 8. Hence, the judgement could be made such that designed filter is highly effective against Nitrates.

3.2.2 Nitrite variation

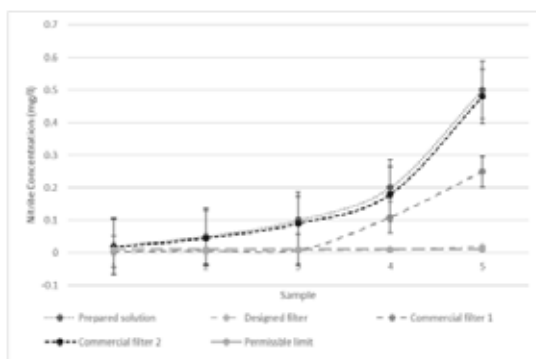


Figure 6 - Variation of nitrite concentration in prepared samples

According to Figure 6, similar pattern can be identified as in nitrates where designed filter

has shown capabilities of removing nitrites with concentrations up to 0.3 mg/while Commercial filter 1 has shown its maximum treatable concentration as 0.1 m/l. But Commercial filter 2 has not shown any ability in treating nitrates to permissible limit of 0.01 mg/l. Considering average nitrite removal percentages given in

Table 8, it can be judged that Designed filter is highly effective in treating Nitrite contaminants in water.

3.2.3 Turbidity variation.

Considering the results given in Figure 7, it can be seen that all the filters are capable of treating turbidity of water to permissible limit of 8 NTU. That is all the filters are capable of treating water with turbidity varying from 0 – 150 NTU to the allowable limit. But it can be seen that Commercial filter 1 and Commercial filter 2 has shown slightly better results and reason for this can be identified as fabrication errors in clay cores produced in designed filter. Percentages of treating turbidity are given in Table 8.

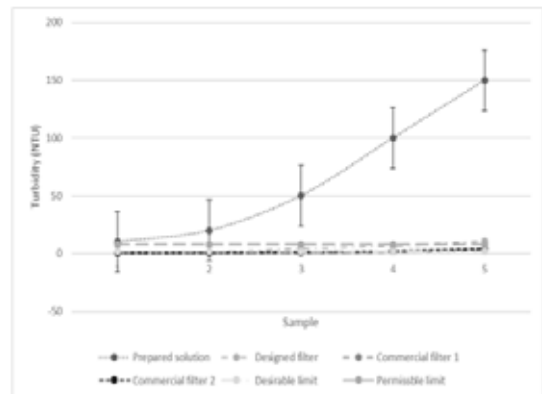


Figure 7 - Variation of Turbidity of prepared solution

3.2.4 Colour variation.

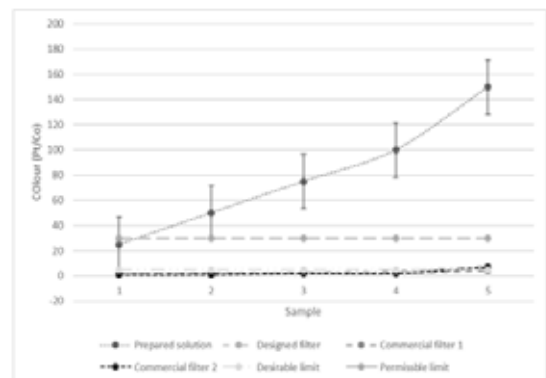


Figure 8 - Variation of colour for prepared solution



As per Figure 8, a similar pattern can be identified for treatment of colour and as in turbidity removal Commercial filter 1 and Commercial filter 2 have shown better effectiveness. It could be identified that similar reason as in turbidity has affected that. From Figure 8, it can be seen that all three filters tested are capable treating colour with 150 Pt/Co to permissible limit of 30 Pt/Co and in most cases below the desirable limit of 5 Pt/Co. Average treatment percentages are shown in Table 8.

But during the experiments, only these tests were performed for prepared solutions due to constraints in time and resources. Also, these results for Commercial filter 1 and Commercial filter 2 might have slight variations since old and modelled filters of them were used for tests.

Average capabilities of designed filter and selected two commercial filters to remove/treat parameters nitrates, nitrites, turbidity and colour for prepared solutions are given in Table 8.

Table 8 - Percentages of average capabilities to remove/ treatment for prepared solution

Filter	Designe d filter	Comm ercial filter 1	Commerci al filter 2
Nitrate	93.14 %	80.58 %	11.84 %
Nitrite	94.54 %	70.00 %	2.00 %
Turbidity	92.41 %	96.80 %	95.5 %
Colour	94.93 %	96.93 %	96.92 %

3.3 Comparison of test results for raw water and filtered water.

3.3.1 pH value variation

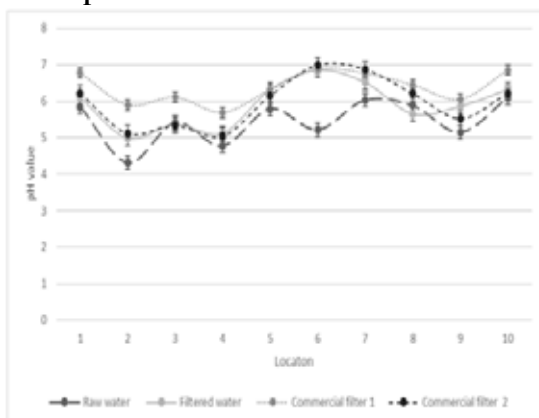


Figure 9 - Variation of pH value

Based on the test results shown in Figure 9 it can be identified that pH value of the water samples has approached the provided limits for suitable drinking water. A possible cause

for this increment can be identified as impact due to the increment of Total alkalinity after filtration. Cause for total alkalinity increment could be the use of ion exchange resins and impact due to the exchange of ions to remove nitrates and nitrites. From these results, it is clear that designed filter and Commercial filter 1 is almost similarly capable of adjusting the pH value of water. That is maximum and minimum adjustment identified through this filter was an increment of pH value from 5.22 to 5.86 and 5.85 to 6.11.

3.3.2 Turbidity variation.

From Figure 10, the ability of each filter to treat turbidity in raw water has been shown. It is clear that considerable percentage of turbidity has been treated with each type of filter. Highest removal percentage was identified in Commercial filter 1 and Commercial filter 2. The maximum level of treatment can be identified for the sample 9, where turbidity level has reduced to 1.65 NTU from an initial value of 4.37 NTU. It could be finalized that designed filter has adequate capacity to treat turbidity. Also, it is understandable that for all samples repetitive pattern has been shown.

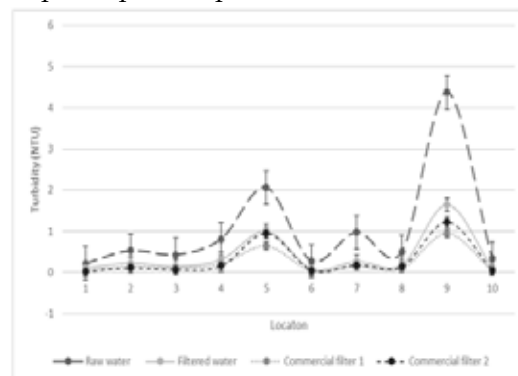


Figure 10 - Variation of turbidity

3.3.3 Electrical conductivity variation

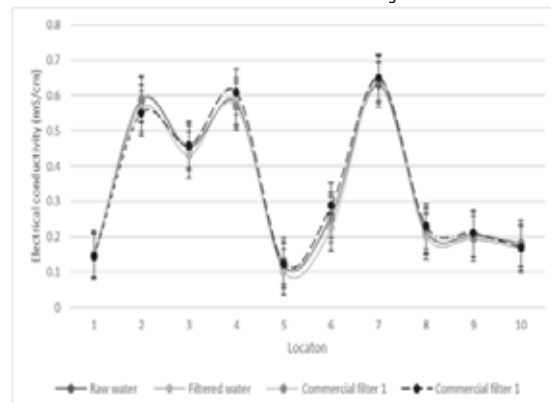


Figure 11 - Variation of Electrical conductivity

According to Figure 11, it is clear that for all the filter types tested for filtration of raw water samples, a considerable change has not been identified for the electrical conductivity measurement. Where a maximum change of electrical conductance identified was positive 0.035 for sample location 6 where conductance has increased from 0.226 ms/cm to 0.261 ms/cm. Therefore, a conclusion could be made that designed filter has a very minimal impact on the change in conductance of raw water when filtered.

3.3.4 Colour variation

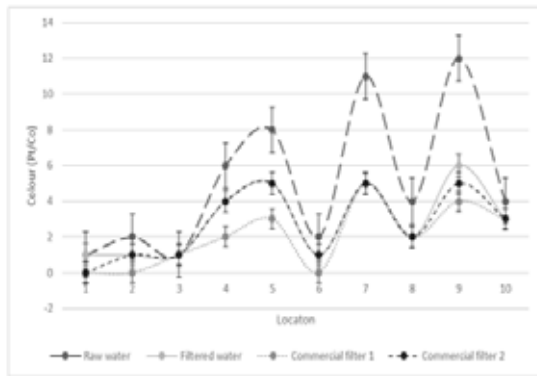


Figure 12 - Variation of colour intensity

From Figure 12, decision could be made such that intensity of colour measured in Pt/Co has been reduced when filtered through designed filter and possible reason for this reduction can be identified as use of clay core in the initial step of filtration and the use of activated carbon as a filter material in the final step of filtration. From this figure, it can be understood that filtration ability of designed filter is almost similar to other filters used in the comparison. Maximum colour adjustment identified was 8 Pt/Co units. This reduction of colour intensity from 12 Pt/Co to average of about 4 Pt/Co was identified for sample location 9.

3.3.5 Nitrate variation

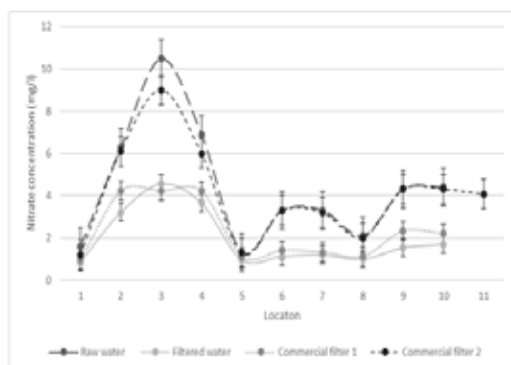


Figure 13 - Variation of nitrate contamination

As per Figure 13, the decision could be made that fabricated filter can remove nitrates in the raw water. Possible reason in the filter for this outcome can be identified as use of nitrogen selective resin in the filtration process. Also, one of the main objectives of the filter design was to reduce nitrate contaminants in water. Compared to other filters contrast can be seen in the ability of nitrate removal from the designed filter. In numerical terms for the designed filter, nitrate concentration has been diminished to 4.22 mg/l from its initial value of 10.5 mg/l for sample 3. While minimum removal was identified for sample 5 where concentration has been reduced to 0.96 mg/l from the initial value of 1.3 mg/l.

3.3.6 Nitrite variation

Based on Figure 14, it can be understood that nitrite presence has been reduced when water is filtered through a designed filter and Commercial filter 1. But no considerable reduction has been detected in nitrite contaminants when water is filtered through Commercial filter 2. That is a maximum reduction of nitrite concentration was 0.007 mg/l for sample location 2 and reduction were observed from 0.015 mg/l to 0.008 mg/l for the designed filter. But more precision was observed for Commercial filter 1 where concentration has been reduced to 0.006 mg/l. The main cause for reduction of nitrite when filtered through the designed filter can be again identified as the presence of nitrogen selective resin as a filter material.

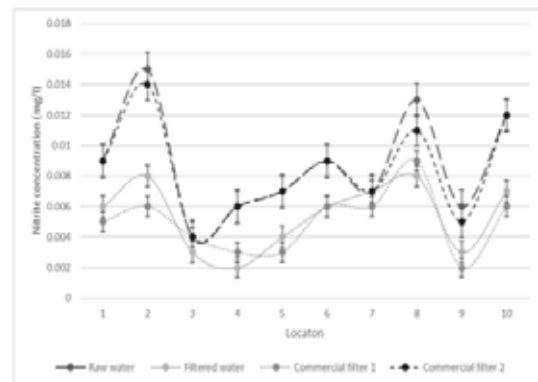


Figure 14 - Variation of nitrite contamination



3.3.7 Phosphates variation

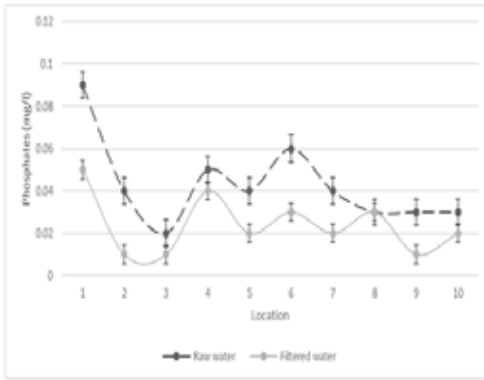


Figure 15 - Variation of phosphates

According to Figure 15, a reduction in phosphate concentration can be seen when raw water is filtered through the designed filter. But the conclusive decision could not be made on which material caused this reduction. Maximum concentration reduction from 0.09 mg/l to 0.05 mg/l was observed for the sample collected from location 1 and minimum concentration reduction observed for sample 8 where no reduction was identified. The average percentage of reduction of phosphates is shown below. Based on samples 1,6 and 2 it can be said that reduction capacity of filter for phosphates is considerably adequate although the same pattern has not been noticed for other sample locations.

3.3.8 Total hardness variation

From the chart given in Figure 16 decision could be made such that total hardness in raw water has been treated through the filtration process and possible cause for this reduction could be marked as the ability of SCR-B cation exchange resin to soften water. Numerically observation is that maximum reduction in hardness was from 85 mg/l to 12mg/l for sample location 7 while the minimum reduction was observed for sample 5 while increment was detected for sample location 1 where hardness has been increased to 18mg/l from 12mg/l. Hence it can be decided that one of the primary objective of the design to treat Hardness has been achieved during the process.

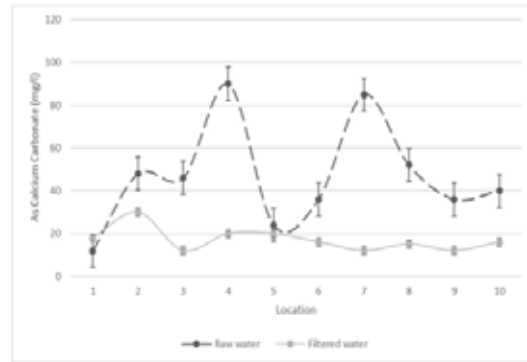


Figure 16 - Variation of total hardness

3.3.9 Free ammonia variation

Based on Figure 17, it can be seen that free ammonia content of the filtered water has been reduced in some samples and some samples have not undergone considerable reduction. But maximum reduction was identified for sample 7, and it was 1.6 mg/l to 0.17 mg/l while a minimum of zero reduction was read for sample location 3. While maximum increment in concentration was observed for sample 5 and it was 0.01 mg/l to 0.27 mg/l. A potential cause of the reduction could be identified as use of nitrogen selective ion exchange resin in the filter. But totally clear judgement could not be made on the ability of the designed filter to remove free ammonia from raw water due to scenarios discussed above. But derivation could be made that filter can remove them.

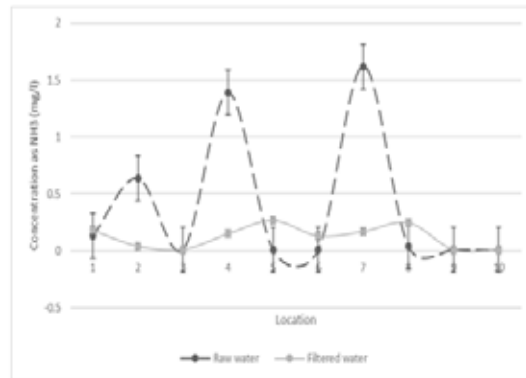


Figure 17 - Variation of free ammonia concentration

4. Conclusions

Based on the Results obtained for the test procedures carried out conclusion could be made in a way that designed and fabricated filter can remove nitrates, nitrites and free ammonia and treat total hardness, colour and turbidity prominently based on test results for prepared solutions with above contaminants and physical parameters. Summary of effectiveness of the designed filter in treating these are shown in Table 9.

Table 9 - Contaminant removal effectiveness of designed filter

Parameter	Nitrates	Nitrites	Turbidity	Colour
Removal effectiveness (%)	93.14	94.54	92.41	94.93

while filter has shown capabilities in removing certain other parameters such as phosphates to a certain extent. But it can be concluded that filter is not capable of treating total alkalinity, and the filter has not shown ability in removing chlorides contaminated in water. Based on the results obtained conclusion can be made that bacteriological parameters such as Coliform bacteria and E-Coli would not be treated at a considerable level although reduction has been notified for several samples. Considering the results, Conclusion can be made on removal percentage of contaminants present in raw water. contaminants reduction percentages are shown in Table 10.

Table 10 - Summary of treatment level

	Contaminant	Percentage (%)
01	Nitrates	55.09
02	Nitrites	38.63
03	Total Hardness	63.54
04	pH adjustment	8.44
05	Colour correction	43.14
06	Phosphates	44.19
07	Turbidity removal	60.67

Considering the cost of the existing filters, commercial filter 1 analysed earlier for its performance is priced at about LKR 10,000 to 12,000 in the market. Therefore, it is considered as expensive filter although its performance is high in treating water. Commercial filter 2 is priced at LKR 4,000 – 6,000 in the market and it was found that for most parameters it is not good as a designed filter in filtration. Also, most of the filters

which use Reverse Osmosis as its principle for filtration are priced around LKR 20,000 to 30,000 in the market. Therefore, considering both variables cost and performance of the designed filter which is about LKR 6,000 in price could be nominated as a low cost and good in performance filter to be used in the domestic level.

Acknowledgement

We would like to acknowledge the financial support given by Sri Lanka Institute of Information Technology (SLIIT) to carry out this study successfully.

References

1. Dissanayake, C. and Weerasooriya, S. *The Hydrogeochemical atlas of Sri Lanka*. Peradeniya: Natural Resources Energy and Science Authority of Sri Lanka, 1985.
2. Dissanayake, C. B. "The fluoride problem in the ground water of Sri Lanka – environmental management and health," *Int. J. Environ. Stud.*, vol. 38, no. 2-3, pp. 137-155, Sep. 1991.
3. Dissanayake, C. B. "Water quality and dental health in the Dry Zone of Sri Lanka," *Geol. Soc. London, Spec. Publ.*, vol. 113, no. 1, pp. 131-140, 1996.
4. Iontec, "Trilite SCR-B," 2006. [Online]. Available: http://www.iontec.co.kr/pds_files/130701.pdf. [Accessed: 30-Nov-2016].
5. Ion resins, "Ion resins." [Online]. Available: <http://www.ionresins.com/pds/NSSR Brochure.pdf>. [Accessed: 01-Dec-2016].
6. Soehendra, N. Grimm, H. Nam, V. C. and Berger, B. "N-Butyl-2-Cyanoacrylate: A Supplement to Endoscopic Sclerotherapy," *Endoscopy*, vol. 19, no. 6, pp. 221-224, Nov. 1987.
7. Google, "Google maps," 2016. [Online]. Available: <https://www.google.lk/maps>. [Accessed: 30-Nov-2016].
8. Greenberg, A. E. and A. D. (eds) Eaton, "Standard Methods for the Examination of Water and Wastewater," 1999.
9. SLS, "Drinking water standards - First Revision (Sri Lanka Standards for potable water - SLS 614: 2013)," 2013.





Monitoring Carbon Monoxide (CO) Levels at Five Major Schools in Kandy City using Real Time Air Quality Monitoring Sensor Network

R.G.R.N.K. Ariyaratne, D.G.G.P. Karunaratne, M.A. Elangasinghe, A. Manipura, S.P. Kodithuwakku, A.D. Siribaddana and K.H.N. Abayalath

Abstract: Ambient air quality in Sri Lanka is rapidly deteriorating due to an addition of a large number of motor vehicles, traffic congestions, combustion of fossil fuel and poor quality of fossil fuels. Previous researchers have found that Kandy city has a higher degree of ambient air pollution owing to its geographical location and heavy traffic congestions. However, lack of continuous monitoring has hindered assessing the impact of air quality on human health in Sri Lanka. In recent years, low-cost yet reliable air quality monitoring solutions have been developed using open-source hardware systems. A variety of such electrochemical gas sensors is available for monitoring pollutants such as NO_x, CO, CO₂, O₃, SO₂ and H₂S at parts per billion levels (ppb). Six air quality monitoring units using such electrochemical gas sensors measuring CO, NO, NO₂, SO₂, O₃, temperature and humidity were developed and setup in Kandy city at selected locations. Emission data from these stations are being acquired on real time basis using the web based data acquisition system. In this paper we present the data of CO levels obtained for the months of March and April, 2017 at five different schools in Kandy city. CO sensors were calibrated to identify the effects of temperature and their linearity. They have shown 5-7% increase of sensor response with temperature and they were highly linearly correlated ($R^2 > 0.9816$) between 0-10 ppm CO concentrations. When comparing the average CO levels at different schools Mahamaya College has shown the highest 24 hour average of 2.05 ppm and Girls High School has shown the least value of 0.165 ppm in the above months.

1. Introduction

Not like many other environmental problems, air pollution is directly related to human health even at low doses, and it is the single largest environmental risk to health globally [1]. According to the World health organization (WHO), more than 6 million premature deaths were caused due to air pollution exposure in 2012 [2]. Health impacts of air pollution result in significant financial and economic consequences, not only in terms of societal costs of mortality and morbidity but also in terms of hospital and public budgets [3]. So, maintaining healthy ambient air quality levels is essential for the well-being of the general community. However, the increasing urbanization, industrialization and rapid growth of vehicle usage have deteriorated the urban ambient air quality all over the world.

Ambient air quality in Sri Lanka is rapidly deteriorating due to the addition of large number

of motor vehicles, traffic congestion, combustion of fossil fuel in thermal power

plants, and the poor quality of fossil fuels [4]. It is observed that Kandy city has a higher degree of ambient

Eng. R.G.R.N.K Ariyaratne, B.Sc. Eng. (Peradeniya), AMIESL, Research Assistant, Department of Chemical and Process Engineering, University of Peradeniya.

Eng. (Dr.) D.G.G.P Karunaratne, B.Sc. Eng. (Peradeniya), P.hD. (Nova), Senior Lecturer, Department of Chemical and Process Engineering, University of Peradeniya.

Eng. (Dr.) M.A. Elangasinghe, B.Sc. Eng. (Peradeniya), M.Phil (Peradeniya), P.hD. (Auckland), Senior Lecturer, Department of Chemical and Process Engineering, University of Peradeniya.

Eng. (Dr.) A. Manipura, B.Sc. Eng. (Peradeniya), M.Eng. (Moratuwa), P.hD. (Rhodes), Senior Lecturer, Department of Chemical and Process Engineering, University of Peradeniya.

Dr. S.P. Kodithuwakku, B.Sc. Agri. (Peradeniya), P.hD. (Hong Kong), Senior Lecturer, Department of Animal Science, University of Peradeniya.

Dr. A.D. Siribaddana, MBBS (Peradeniya), Consultant Respiratory Physician, Teaching Hospital, Kandy

Mr. K.H.N. Abayalath, Research Assistant, Department of Animal Science, University of Peradeniya.



air pollution owing to its geographic location and heavy traffic congestions [4]. Moreover, in Kandy, almost all schools, hospitals, and other public working places are situated nearby the main roads increasing the public exposure to air pollution for longer time periods. So, taking immediate actions to reduce air pollution and setting up an air quality management plan for Kandy is a timely necessity.

Monitoring air quality and the establishment of air quality inventory database for the Kandy city is the first step of implementing an air quality management plan. Due to the complexities of the behaviour of air pollutants, emission sources, topographical and meteorological conditions, an air quality monitoring system should have the ability to monitor pollutants with broad spatial and temporal variability with having high accuracy of monitored data (at parts per billion (ppb) levels), low-cost of operation, low power consumption, capability for mobility and selectivity for multiple gases [5]. But, when compared to traditional air quality instruments they do not meet the above requirements except the higher accuracy.

Nowadays throughout the world, research studies are being done to introduce low-cost, yet reliable real time air quality monitoring systems. Use of electrochemical gas sensors is found to be a more reliable solution for high-cost air quality monitoring with having the ability to monitor pollutants at ppb levels [6]. In this research study, we have developed such electrochemical air quality monitoring sensor network for Kandy city. Initially, data are being collected on real time basis at six different locations in Kandy city. This paper presents preliminary results of this study with the measures to be taken to improve the accuracy and reliability of data for future long-term monitoring.

2. Literature review

2.1 Air pollution and its impacts

Ambient air pollution occurs due to a wide variety of sources, which are broadly classified as

stationary (point), mobile (line) and area sources. In urban environments, air quality is mainly deteriorated due to the traffic related air pollution. In Colombo, about 60% of the total emissions are due to vehicular emissions [7]. Since there are no large industries that release gaseous or particulate matter (PM) in Kandy city, it can be assumed that vehicular emissions are the primary cause of air pollution in Kandy too.

Air pollutants can be primary or secondary. Primary pollutants are released into the atmosphere from ground sources and secondary pollutants are formed within the atmosphere due to the reactions of primary pollutants with natural components of atmosphere. Though there are many such air pollutants, the most significant pollutants are particle pollution (often referred to as particulate matter (PM)), ground-level ozone (O_3), carbon monoxide (CO), Sulphur oxides (SO_x), nitrogen oxides (NO_x), Hydrogen Sulphide (H_2S), heavy metals (e.g., lead (Pb)), volatile organic compounds (VOCs) and polycyclic aromatic hydrocarbons (PAHs) which are found in the ambient air [7].

NO_2 is identified as a pollutant which can affect the mortality rates. Both NO_2 and CO have the capability to act as respiratory sensitizers. Long term exposure to NO_2 can lead to having adverse effects on lung function. CO can reduce the body's capacity to transport oxygen to cells [6]. O_3 is formed during the periods of sunny weather conditions by the reaction of pollutants such as NO_x and VOCs with the sunlight. Ground level O_3 can cause breathing problems, lung function reduction, and lung diseases. SO_2 can also affect the respiratory system and function of the lungs and causes the irritation of the eyes. Exposure to PM increases the risk of respiratory infections, cardiovascular diseases and lung cancers [1]. In most of the developing countries, PM concentrations are higher at both indoors and outdoors [8].

Deterioration of the ambient air quality in Sri Lanka has made significant health impacts to the people of the country. Respiratory related diseases are the most significant issue of the air pollution. In Sri Lanka since 1995, respiratory

system related diseases have ranked as the second

highest cause of hospitalization, and it is among the first five leading causes of death in most of the

age groups in Sri Lanka [9]. And also asthma has become a major respiratory disease in Sri Lanka according to the statistical data of hospitalization and hospital deaths [10]. Cancer has also become one of the main health issues in Sri Lanka, especially in Kandy [11]. Polycyclic aromatic hydrocarbons (PAHs), which can be found at very high concentrations in Kandy is one of the major organic pollutants in the atmosphere. This can be the prime etiological cause for lung cancers too [11].

The economic costs related to these adverse health effects are very high. The potential financial loss due to outdoor air pollution in Colombo owing to PM_{2.5} has been estimated to be about Rs. 886 million, and due to PM₁₀, it was

overcome above serious health and economic consequences.

2.2 Traditional air quality monitoring methods

Air quality monitoring allows us to establish the status of air quality in a particular area, which is the preliminary step in setting up air quality management plans. At present air quality data are being collected by environmental or government authorities using fixed or mobile air quality monitoring stations. These monitoring stations use analytical instruments such as optical and chemical analysers, gas chromatographs and mass spectrometers [5]. Traditional monitoring methods are expensive to operate and maintain. They are complex in nature in terms design, operation and maintenance, mostly stationary and consume more power and resources [13]. In the UK, setting up of these fixed air quality monitoring stations could cost between £ 5000 to

Table 1 - Comparison of the characteristics of different low-cost sensor technologies available

Analyzer	Sensor technology	Range	Precision	Response time (s)	Price (USD)
CO					
Alphasense B4	Electrochemical	0-1000 ppm	0.004 ppm	<25	100
TECO model 48c	IR absorption	0.3-3000 ppm	0.1 ppm	60	12K
Aeroqual Series 500	Metal oxide semiconductor	2-100 ppm	0.1 ppm	<150	1.5K
Membrapor CF-200	Electrochemical	0-200 ppm	0.1 ppm	<40	280
CiTicel 7E/F	Electrochemical	0-1000 ppm	0.5 ppm	<30	140
NO₂					
Alphasense B4	Electrochemical	0-50 ppm	0.015 ppm	<60	100
API model 200EM	chemiluminescence	0.05 -1 ppm	0.05 ppm	20	8-14K
Aeroqual Series500	Metal oxide semiconductor	0.01-200 ppm	0.001 ppm	<180	2K
Membrapor C-1	Electrochemical	0-1 ppm	0.05 ppm	<60	320
CiTicel 7NDH	Electrochemical	0-20 ppm	0.1 ppm	<40	225
NO					
Alphasense B4	Electrochemical	0-50 ppm	0.015 ppm	<45	100
Membrapor CF-100	Electrochemical	0-100 ppm	0.5 ppm	<25	340
Citichel 7NT	Electrochemical	0-100 ppm	0.5 ppm	<15	200
	Unloaded WO ₃	2-300 ppm	2 ppm	<160	N/A
O₃					
Alphasense B4	Electrochemical	0-50 ppm	0.015 ppm	<45	100
API Model 400	UV absorption	0.6-200 ppb	0.001 ppm	<20	8-14K
2B technologies, 202	UV absorption	1.5 -200 ppb	0.0001 ppm	10	5K
Aeroqual Series500	Metal oxide semiconductor	8-50 ppm	0.001 ppm	<60	2K
OMC - 1108	Electrochemical	0.01-100 ppm	0.01 ppm	<70	1.2K
SO₂					
Alphasense B4	Electrochemical	0-200 ppm	0.005 ppm	<30	100
Membrapor CF-20	Electrochemical	0-20 ppm	0.2 ppm	<20	340
Envirocel A3Oz	Electrochemical	0-10 ppm	0.02 ppm	<40	500
	Unloaded SnO ₂	5-100 ppm	5 ppm	<35	N/A

about Rs. 30 billion per annum in 2003 [12]. Thus, air pollution mitigation plans are required to

£ 60000 (Reference). Though these have proven higher accuracy and precision of the measurements, above drawbacks associated with



these, have hindered the capability to use them in networks with higher densities [6]. Currently, in Sri Lanka only one such air quality monitoring station is located in Colombo Fort [7]. So, with the traditional air quality monitoring methods it is difficult to understand the behaviour of air pollutants in the atmosphere. Therefore, there is an urgent need to introduce air quality monitoring methods with flexible and affordable techniques having the capability to use them for both scientific and legislative purposes with the aim to improve the understanding of health impacts of air pollution.

2.3 Low-cost air quality monitoring networks

Due to the different types of emission sources and atmospheric flow conditions, air quality varies over a relatively small-scale environment and with temporal scale resulting the high level of unpredictability. To predict the behaviour of air flow masses sophisticated air quality modelling tools and real time high-resolution air pollution concentration maps are required for covering a whole urban area [5]. Hence, to fulfil the above requirements, low-cost air quality monitoring methods with remote data acquisition capabilities are being developed around the world nowadays [5]. Gas sensor devices tied with the advances in computing and communication have provided the ability to monitor air pollutants with high spatial and temporal resolutions having relatively very low costs. Most widely used sensor types are based on two major principles: (1) those depend on interactions with sensing material and detecting gas (e.g.,- metal oxide semiconducting sensors, electrochemical sensors) and (2) those that measure the absorption of light (e.g.,- non-dispersive infrared sensors, chemiluminescence) [13]. Comparison of these different low-cost air quality monitoring methods is given in Table 02.

2.4 Electrochemical sensors

Use of electrochemical sensors in ambient air quality monitoring is widely used around the world due to its low cost and capability to measure various air pollutants at parts per billion (ppb) levels with the use of low noise circuitry [5]. An electrochemical sensor consists of

four electrodes namely a working electrode (WE), a reference electrode, a counter electrode and an auxiliary electrode (AE). These electrodes are separated by hydrophilic wetting filters, which allow the electrolyte to transport via capillary action and keep the ionic contact in between electrodes [6].

Measuring gas that comes in to contact with the sensor diffuses through a gas permeable membrane to reach the WE surface. The WE either oxidizes or reduces generating an electronic charge which is balanced by the reaction at the counter electrode, forming a redox pair of reactions. These reactions are catalysed by the electrode materials specifically developed for the gas of interest. Current output by the sensor is directly proportional to the concentration of the measuring gas. During the operation, the WE is kept at a fixed potential while the counter electrode potential is allowed to change. Working electrode potential is kept at a defined value during the operation using the third reference electrode. Three-electrode sensor design means that the sensor sensitivity is stable and operates linearly within the range of use. To measure the effect of temperature and background current arising from solid electrode processes or from electrochemistry involving the electrolyte other than the gas of interest the AE is used. This AE current could then be subtracted from the WE total current to give a corrected WE current corresponding solely to the electrochemical reaction of the sampled gas. However, the sensing electrode potential does not remain constant due to the continuous electrochemical reaction taking place on the surface of the electrode causing a deterioration of the performance of the sensor over an extended period of time [6]. With the use of correction algorithms, these errors can be minimized. Sensors for this research were purchased from Alphasense (Pvt) Ltd. of United Kingdom, which is the largest manufacturer of electrochemical air quality monitoring sensors.

3. Methods

3.1 Sensor unit design and data acquisition method

Six sensor units were made with each including CO, NO₂, NO, SO₂ and O₃ pollutant sensors and DHT 11 temperature and humidity sensors. Sensor unit enclosure was designed to operate at extreme weather conditions, and they were placed about 1.75m above the ground. Power supply for the sensor units was obtained using AC power supply from nearby.



Figure 1 - Sensor unit placed at Faculty of Engineering, University of Peradeniya

Data acquisition was made using an open source hardware unit called Arduino Mega 2560. The acquired data were then sent to the web based server created using MySQL and PHP (kandyair.eu5.org) via a GPRS module. Until the sensor characteristics were clearly identified data were downloaded, and further processing was done manually to obtain the concentration values.

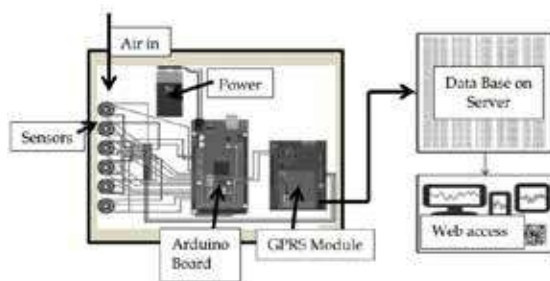


Figure 2- Schematic of the sensor unit and data acquisition method

3.2 Calibration of sensors

Issues concerned with the application of electrochemical sensors include: calibration of the sensor sensitivity to the target gas, the drift of the sensor sensitivity, cross sensitivities within complex gas mixtures, the effect of temperature, and humidity on sensor response and competition between the various gases at the active site of the detector which reduces the sensitivity [14]. These factors need to be evaluated in detail for accurate detection of gas concentrations and to characterize the emissions.

All the sensors purchased were calibrated initially by the sensor manufacturer. For each sensor, they have given their calibration data done at 23 °C. But the percentage change of sensor sensitivities with the temperature was given as a typical value for all sensors. And the effect of humidity on the sensors was not given. To identify two parameters our in-house developed calibration procedure was conducted. Those calibration parameters were 1). Effect of temperature on the sensor sensitivity and 2). Linearity of the sensor responses within the range.

Sensors were tested using different gas concentrations inside a gas tight chamber. Standard calibration gases used were obtained from GASCO, LTD, USA. The gas tight chamber was fabricated using rubber enclosure with the ability to change the volume and to create vacuum condition. Six gas sensors and DHT 11 sensors were inserted into the chamber using a wooden frame. Initially, the chamber was vacuumed using a pump and filled with zero grade air. Then different pollutant gas volumes were injected using syringes to the chamber filled with zero air to create step increases in the gas concentrations, and the respective sensor responses were obtained subsequently. Temperature effects were also tested changing the temperature of the chamber filled with zero grade air. And humidity effects were tested using a dehumidifier by changing the humidity of the exposing environment.

Since the CO levels at the ambient conditions vary between 0.2-50 ppm and CO sensor cross



interferences are less compared to the other sensors CO concentration values were finalised using the calibration data and data given by the sensor manufacturer. According to the manufacturer data sheets, CO sensors are affected by having cross sensitivity percentages of < 1 to NO₂, <0.1 to SO₂ and < -3 to NO. Since the NO, NO₂, O₃, and SO₂ concentrations are at ppb levels (<100 ppb) their cross sensitivities are significant. Thus, those data are yet to be finalised comparing with the high accurate air quality monitoring station. The results present here are of those CO sensors only.

3.3 Monitoring locations and their characteristics

Kandy town is about 465 m above the sea level and has an area of about 26 km². The city area is surrounded mainly by Hanthana, Bahirawa, Kurusa, and Dharmaraja mountain ranges and its condition is like a bottom of a basin. The residential population of the city area is about 120,000 and about 100,000 people arrive the city for daily activities. Daily vehicle arrivals are about 100,000 approximately causing heavy traffic congestions, which eventually leads to heavy air pollution in the city area [15].

To identify the importance of different places in Kandy city for monitoring air quality city area is gridded according to figure 3 and index was created by considering the emission sources that are the road network and traffic conditions, receptors that are the locations where people are mostly engaged in their work and the age limits

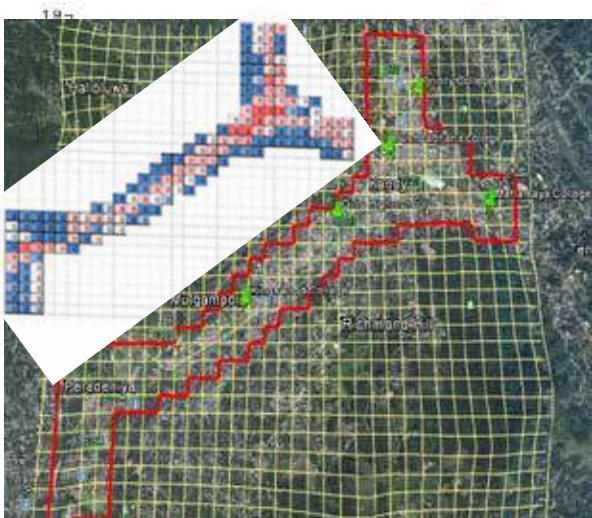


Figure 3- Gridded map of the Kandy city along with the developed guide map to select optimal monitoring locations on the left side. Five of the initial monitoring sites are shown.

of the people.

36 monitoring locations were identified to obtain a good spatial distribution of monitoring locations. However, to cover all these locations using only six sensor units monitoring will be taken for about two months at each location up to a period of one year. As our initial monitoring locations, we have selected five schools and Faculty of Engineering. These initial locations were selected considering the index values and safety, power supply and accessibility for the sensor units.

4. Results and discussion

4.1 Calibration results of CO sensors

- **Linearity of the sensors responses**

According to the Figure 4, all the six sensors were highly correlated linearly ($R^2 > 0.9816$) with gas concentrations varying from 0-10 ppm. Data were obtained at 27C⁰ and 60-65% humidity range. Therefore, the linear relationship between sensor response and gas concentrations was verified, and the manufacturer's data and linear equations were used to convert sensor responses into corresponding concentration values.

Figure 4 - Linear correlation plots of CO sensor responses with calibration gas mixing ratios

- **Effect of temperature**

It can clearly be seen (Figure 5) that sensitivities of the sensors have shown a linear ($R^2 > 0.953$) increment with the temperature. Sensitivity varied between 5 - 7% with the temperature.

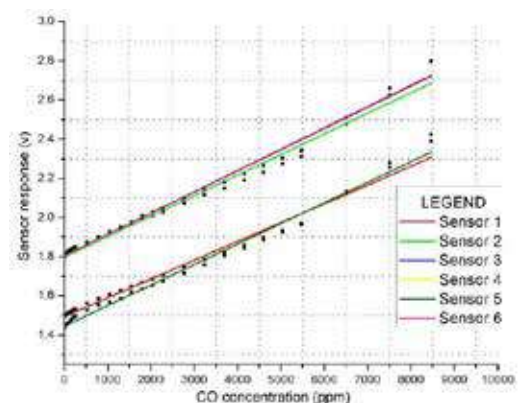


Figure 5- Variation of CO sensor responses with temperature

According to the manufacturer's data sheets, the average change of sensitivity for a CO sensor is 6% with the temperature. The results obtained from the calibration has shown similar values.

Further significant changes of sensor responses due to humidity changes could not be identified.

4.2 Variation of CO concentrations at different locations

Following equation was used to convert the sensor responses into concentration values.

$$C = [(WE_u - WE_0) - n(AE_u - AE_0)]/S \quad \dots(1)$$

Of the equation 1, C is the concentration (ppb), WE_u is the uncorrected WE output voltage (mV) which is the measured value, WE_0 is the WE output voltage (mV) in zero air. n is a factor calculated for temperature corrections using temperature values and manufacturer's data, AE_u and AE_0 are respective AE output voltages (mV), and S is the sensitivity (mV/ppb). n is a function of temperature and calculated using the temperature measurements. S values were corrected with the calibrated data and temperature measurements.

According to Sri Lanka national air quality standards 1 hour, 8 hour and anytime values are 26 ppm, 9 ppm, and 50 ppm respectively. Sensor units were programmed to obtain data at every 3 minutes intervals so that high temporal variation of the data could be obtained.

Figure 6 shows sample data obtained at 3 minutes intervals during a week at Kingswood College, Kandy. Location of the sensor unit was about 15m away and about 8m above from the main road. There were no obstacles between the sensor unit and road. So vehicle density at the road directly affected the pollutant levels near the sensor unit. Especially due to the variations of the wind fields around the sensor units significant variations of air quality data could be observed. So when averaging the air quality data, having data with high temporal resolution is essential.

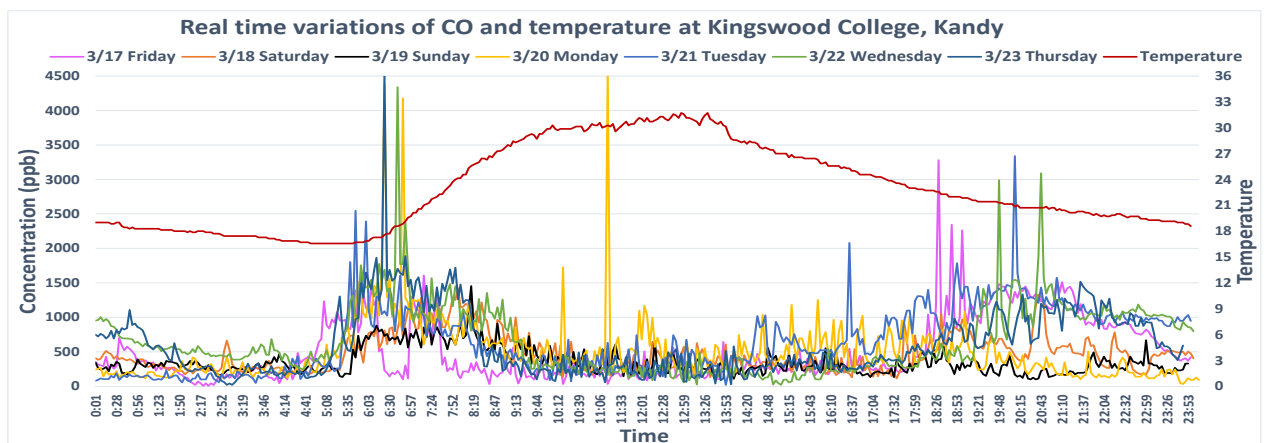


Figure 6 - Sample real time data of CO and temperature values at Kingswood College, Kandy obtained for a week period



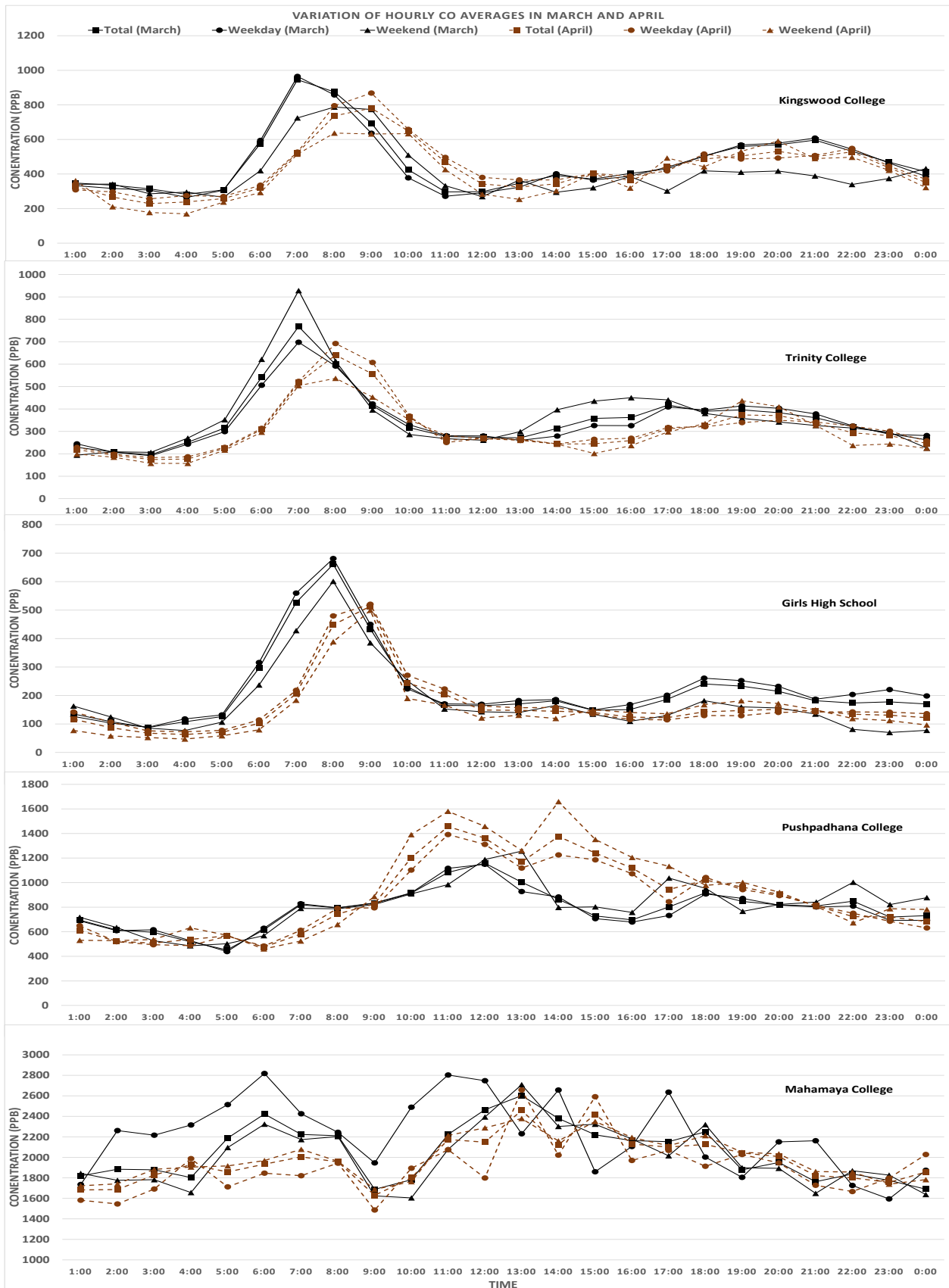


Figure 7 - Hourly averages of CO levels in the months of March and April, 2017 at five different schools in Kandy city

Table 2 - Sensor locations, their characteristics and averages of CO levels in March and April, 2017

Location	Surrounding of the sensor unit	Traffic condition	Distance, Elevation to road (m)	CO levels (ppb)	
				March (ppb) 24 hour average Day time average Peak value (time)	April (ppb) 24 hour average Day time average Peak value (time)
Kingswood College (KC)	Nearby main road, outside city area, no disturbing trees or buildings, bus stop	Average traffic and vehicle speed	16, 8	470 460 945 (6-7)	430 450 780 (8-9)
Girls High School (GHS)	Nearby main road, bus stop, near city area have disturbing trees and buildings	Heavy traffic, Very slow vehicle speed	40, 5	220 250 660 (7-8)	165 200 515 (8-9)
Pushpadhana College (PC)	Nearby main road, road junction, inside city area, have disturbing buildings, no trees	Heavy traffic, Very slow vehicle speed	40, 20	790 820 1160 (11-12)	880 1000 1460 (10-11)
Trinity College (TC)	Nearby main road, inside city area, road crossing, have disturbing trees, no buildings	Heavy traffic, slow vehicle speed	10, 6	355 370 770 (6-7)	310 330 640 (7-8)
Mahamaya College (MC)	Nearby main road, bus stop, no disturbing trees or buildings, outside city area	Heavy traffic, slow vehicle speed	5, 8	2050 2030 2600 (12-13)	1970 1930 2460 (12-13)

In figure 6 it could be clearly observed that in the morning and late evening significant increases in the CO levels, mainly due to the high traffic congestions on the road. Further the diurnal variation of pollutants can be clearly seen. During the morning due to the low temperature in the environment, the mixing height of the atmosphere is low, so that with the influx of vehicles the pollutant levels increase quickly. When the environment temperature increases, the mixing height increases and air pollutants disperse over a large volume of atmosphere decreasing the ground level pollution levels. During the evening again the pollutant levels increase due to the influx of vehicles. But due to the decreasing temperature, CO levels increase slowly and pollutants tends to be more stable in the air than the morning due to the decreasing atmospheric mixing height.

Figure 7 shows the variation of hourly averaged CO levels at five different schools in March and April, 2017. The data were obtained at every 3 minutes intervals daily and hourly averages were calculated for the whole month. Table 2 shows the location characteristics and summary of the average CO levels in different locations. Morning

peaks, evening peaks and diurnal variation of the CO levels could be clearly visible at KC, GHS and TC. Further peak and average CO levels have decreased in April compared to March. And the peak hours has also moved towards day time during the month of April. This is clearly due to the school vacation period in April. At KC in both March and April during the weekend CO levels have decreased and in March the peak values have moved towards day time clearly indicating the effect of school time heavy traffic conditions. Since TC is in the middle of the city weekend CO levels have increased in the month of March compared with the weekday values. One other reason can be the private tuition classes at weekend in nearby. CO levels in GHS during weekends have decreased compared with weekday values.

Sensor unit of the PC was situated about 20m height and about 40m distance from the road. Further there were disturbing buildings in front of the sensor unit. So due to above reasons pollutants take time to travel and peak CO levels were obtained during mid-day period. Further when comparing the CO level in weekdays and weekends, during the morning time CO levels



have decreased in weekends and during mid-day period CO levels have increased clearly indicating the effect of traffic conditions. Since the location is at a junction entering to the city relatively heavy traffic could be observed.

Near the MC highest CO levels could be observed. Since the surrounding is covered with trees and buildings wind variation is less around the sensor unit. So throughout the whole day high levels of CO could be observed. In March morning peak CO levels could be observed during 6.00 am and 8.00 am. Then the CO levels have reduced significantly between 8.00 am and 10.00 am. After CO levels have again increased during the mid-day period. During weekends in the month of March there is a significant reduction of CO levels due to lack of school and office vehicles. In April CO levels have compared with CO levels in March.

When comparing the overall data, national air quality standards have not been violated any location. Mahamaya College had the highest levels of CO levels among all the locations. Variation pattern of the CO levels clearly indicate the traffic conditions of the road. Atmospheric mixing height and wind velocities directly affects the spread of air pollutants in the environment.

5. Conclusions and future work

The results presented here are the preliminary results of our study. We have developed sensor units to monitor pollutants CO, NO, NO₂, SO₂ and O₃. Accuracy of the sensor data is highly important in these kind of studies. Compared to CO other four pollutants present in the environment at very low concentrations (below 100ppb), so that those sensors need to be accurately calibrated comparing with high precision air quality monitoring instrument. Currently we are in the process of verifying the sensor data. Since CO concentrations are at higher levels and their cross interferences are negligible the results present here are accurate. Further to increase the data accuracy interchanging of monitoring instruments and using multiple monitoring instruments at one location could be done.

Ambient air in urban environments has complex mixtures of gases where the gas abundances can fluctuate rapidly due to the inhomogeneous dilution by the variations in the wind field or by turbulent eddies and due to the changes in traffic flows. Considering the overall data, this could be clearly observed that the surrounding of the sensor units and distance from the road significantly affect the CO levels monitored. So, by changing the monitoring locations continuously can generate high-resolution air pollution maps according to macro environmental conditions.

Further, the sensor responses drift over the time due to the decaying of the electrolyte. To understand the issue of this long term data need to be obtained (>6 months) and an algorithm will be developed to correct the sensor responses comparing data with high precision instrument.

Since this is the first time we have used such sensor network to monitor air quality in Sri Lanka, there are a lot of improvements need to be done before enabling such systems in the country. Development of standard calibration method for these sensor units is the major future work that we plan to do with long term data. These real time air quality monitoring systems are a promising solution for the higher costs associated with air quality monitoring. And also they provide real time data which is highly useful when understanding the behaviour of pollutants.

As our future work we are working on developing a comprehensive air quality model for the Kandy city. For that we aim to monitor weather and traffic data simultaneously with air quality data to identify the effects of them on air pollution in Kandy city. Weather instruments are being setup now. But monitoring real time traffic data is difficult since there are no established traffic monitoring systems in Sri Lanka.

As our observations clearly indicate that the traffic congestions in the Kandy city area is the main source of air pollution, implementing methods to reduce the number of incoming vehicles to the city can be the best possible solution. Having good public transportation systems can reduce the number of incoming

vehicles significantly and also public community can be motivated for using public transportation at least once a week. Further better maintenance of vehicles, specially the old busses to reduce air pollution. By assessing and comparing the impacts of public, private and electric transportation methods or air pollution levels in the Kandy can clearly aware the public about this issue.

Acknowledgement

Authors would like to acknowledge kindly the funding provided for the project by Vehicle Emissions Testing Trust Fund, Department of Motor Traffic, Central Province Education Department and all the schools involved for their cooperation for this project.

References

1. WHO, WHO Expert Consultation : Available evidence for the future update of the WHO Global Air Quality Guidelines (AQGs), (2015).
2. Evolution of WHO air quality guidelines: past, present and future. Copenhagen: WHO Regional Office for Europe; 2017.
3. World Health Organisation, Economic cost of the health impact of air pollution in Europe, 2015.
4. O.A. Ileperuma, V.D.K. Abeyratne, MONITORING AIR POLLUTION LEVELS IN KANDY USING PASSIVE AND ACTIVE GAS SAMPLING TECHNIQUES, Ceylon J. Sci. Phys. Sci. 9 (2002) 54–61.
5. P. Kumar, L. Morawska, C. Martani, G. Biskos, M. Neophytou, S. Di, M. Bell, L. Norford, R. Britter, The rise of low-cost sensing for managing air pollution in cities, Environ. Int. 75 (2015) 199–205. doi:10.1016/j.envint.2014.11.019.
6. M.I. Mead, O. a. M. Popoola, G.B. Stewart, P. Landshoff, M. Calleja, M. Hayes, J.J. Baldovi, M.W. McLeod, T.F. Hodgson, J. Dicks, a. Lewis, J. Cohen, R. Baron, J.R. Saffell, R.L. Jones, The use of electrochemical sensors for monitoring urban air quality in low-cost, high-density networks, Atmos. Environ. 70 (2013) 186–203. doi:10.1016/j.atmosenv.2012.11.060.
7. Y.L.S. Nandasena, A.R. Wickremasinghe, N. Sathiakumar, Air pollution and health in Sri Lanka: a review of epidemiologic studies., BMC Public Health. 10 (2010) 300. doi:10.1186/1471-2458-10-300.
8. M.A. Elangasinghe, R. Shanthini, Determination of atmospheric PM concentration in Kandy in relation to traffic intensity, 36 (2008) 245–249.
9. S. Nandasena, A.R. Wickremasinghe, N. Sathiakumar, Air pollution and public health in developing countries : Is Sri Lanka different?, J. Coll. COMMUNITY PHYSICIANS SRI LANKA.17(2012)21–42.
10. M.J. Bunch, V.M. Suresh, T.V. Kumaran, C.S. Hons, P. Merit, AN OVERVIEW OF AIR POLLUTION AND RESPIRATORY ILLNESSES IN SRI LANKA, in: Proc. Third Int. Conf. Environ. Heal. Chennai, India, 2003: pp. 489–501.
11. A.P. Wickramasinghe, D.G.G.P. Karunaratne, R. Sivakanesan, PM(10)-bound polycyclic aromatic hydrocarbons: biological indicators, lung cancer risk of realistic receptors and “source-exposure-effect relationship” under different source scenarios., Chemosphere. 87 (2012) 1381–7. doi:10.1016/j.chemosphere.2012.02.044.
12. S. Yalgama, G. Bathan, Clean Air in Sri Lanka: Summary of progress on improving air quality, Country Network Sri Lanka, Clean Air Sri Lanka: (2008) 7.
13. E.G. Snyder, T.H. Watkins, P. a Solomon, E.D. Thoma, R.W. Williams, G.S.W. Hagler, D. Shelow, D. a Hindin, V.J. Kilaru, P.W. Preuss, The changing paradigm of air pollution monitoring., Environ. Sci. Technol. 47 (2013) 11369–77. doi:10.1021/es4022602.
14. T.J. Roberts, J.R. Saffell, C. Oppenheimer, T. Lurton, Electrochemical sensors applied to pollution monitoring : Measurement error and gas ratio bias – A volcano plume case study, J. Volcanol. Geotherm. Res. 281 (2014) 85–96. doi:10.1016/j.jvolgeores.2014.02.023.
15. H.D.S. Premasiri, I.H.K. Samarasinghe, K.M.N. Lakmali, Population exposure risk assessment to air pollution in Kandy city area, Environmental Division, National Building Research Organisation (2010).



Dense Graded Asphalt for Sri Lanka: Considerations related to Climate and Different Traffic Conditions

W.W. Bandara and R.P.M.M. Premathilaka

Abstract: High standard crushed rock aggregates, and 60/70 penetration grade bitumen which have a high stiffness at 25°C (testing temperature) are used to produce dense graded asphalts (DGAs) in Sri Lanka. Hence it is considered in pavement structure design that asphalts have a high stiffness (Modulus) approximately 2500MPa. Pavement temperature is measured in terms of weighted mean annual pavement temperature (WMAPT). WMAPTs of different geographic locations in Sri Lanka are calculated to be between 35°C and 41°C. It is revealed that 60/70 bitumen has a low stiffness and DGAs made with 60/70 bitumen also have a low stiffness (Modulus) at WMAPTs of Sri Lanka and low heavy vehicle speed. Further, this is verified by in-situ asphalt moduli which are back-calculated from surface deflection measurements. Nevertheless, 60/70 bitumen can be used up to heavy traffic load which is 20 Million Equivalent Standard Axles (ESAs). Then modulus of DGAs can be taken from 1000MPa to 2200MPa for WMAPTs of Sri Lanka and 30km/h to 70km/h heavy vehicle speed. Moreover, an equivalent viscosity grade bitumen class shall be used to mitigate reduction of modulus due to the poor coating of bitumen with aggregate, compaction and consistency in the mix.

Keywords: Asphalt Pavement, Bitumen Grade, Stiffness, Modulus, Defects, Sri Lanka Climate, Traffic Conditions

1. Introduction

In basic terms, asphalt is a mixture of coarse and fine aggregates, filler and bitumen. Dense graded asphalts (DGAs) are widely used in the construction of new road pavements and strengthening of existing road pavements in Sri Lanka. DGAs are manufactured from 60/70 penetration grade bitumens and 20mm nominal size aggregates [4]. DGA is placed on the aggregate base course or an existing bituminous pavement as a wearing course in conjunction with or without an asphalt binder course.

Alligator (or map) cracking and formation of waves and corrugation (caused by stop-and-go vehicles) are observed on asphalt surface of moderate-to-heavily trafficked road pavements. This kind of defects occurs on loaded areas even after several years from construction. The defects occur due to insufficient resistance to fatigue and permanent deformation effected by the asphalt modulus. Modulus of DGAs made with selected nominal size aggregate depends on the stiffness of bitumen at pavement temperature and heavy vehicle speed, a coating of bitumen with aggregate, compaction and consistency in the mix. Hence the study is conducted to review a selection of the bitumen class for Sri Lankan climate and different traffic conditions, and mixing and compaction temperatures of DGAs. "Austroads Guide to

Pavement Technology" (Austroads) has been principally used for the study.

2. Methodology

Asphalt stiffness modulus values along a good condition road section for known asphalt thickness are estimated from in-situ surface deflections measured by a falling weight deflectometer (FWD). Here rutting roughness data are used to evaluate the condition of the pavement and coring results in the road pavement are used to determine asphalt thickness.

A viscosity grade classification has been adopted by countries like Australia, South America and India [1]. For Sri Lanka climate and different traffic conditions, a viscosity grade bitumen class is selected from Austroads [3]. Selected bitumen class is compared with 60/70 bitumen class use in Sri Lanka. Here stiffness and operating temperature limits of both bitumen are estimated from their basic properties given in specifications [3] and [4]. It is documented the significance of the use of a viscosity grade bitumen class for road pavements in Sri Lanka.

Eng. W.W. Bandara, M.Eng. (Moratuwa), B.Sc.Eng. (Peradeniya), Director, Engineering Design and Project Management Consultants (Pvt) Ltd.

Eng. R.P.M.M. Premathilaka, B.Sc. Eng. Hons. (Peradeniya), Engineer, Engineering Design and Project Management Consultants (Pvt) Ltd.



Finally, design modulus of DGAs is estimated for pavement structure designs.

3. Literature Review

The performance of asphalts, in both the short and long term, is influenced by the bitumen properties, aggregate and grading characteristic, and the composition. Here the bitumen play a critical role [1]. In Sri Lanka, DGAs are manufactured from 20mm nominal maximum size aggregates of high standard crushed rocks and 60/70 penetration grade bitumen. Properties of 60/70 bitumen are given in Table 1. The bitumen and aggregate are mixed at temperatures within absolute limits of 145 °C and 170 °C. The final rolling are completed before the temperature of mix falls below 90°C. Air void in compacted aggregate are from 3% to 7%. However, it is generally less than 5% in the mix design. [4]

Table 1 - Properties of 60/70 Grade Bitumen

Penetration at 25°C 100g, 5s	60/70
Softening point (°C)	48/56
Loss on heating for 5 hrs. at 163°C (1) Loss in weight percent (2) Loss in penetration, (% of original value)	1.0 max 75 min
Solubility in trichloroethylene (%)	99 min
Flash point (°C)	232 min

In Australia, bitumen is classified by its consistency expressed as viscosity at 60°C and comprise three major grades: Class 170, Class 320 and Class 600. Class 170 bitumen is the softest grade and provides the greatest flexibility and durability for use in asphalt in cool climates, and for light traffic. Class 320 is a slightly harder grade of bitumen that is the most versatile and commonly used binder for hot mix asphalt in a wide range of applications. Compared to Class 170 bitumen, it provides greater resistance to rutting and deformation at high service temperatures or heavy traffic. Class 600 is a harder grade of bitumen than Class 320. The use of Class 600 is generally confined to heavy-duty asphalt base layers where greater asphalt mix stiffness is required. Class 600 is not generally recommended for use as a wearing course layer as increased stiffness can result in reduced resistance to cracking and fatigue in thin layers. Where greater stiffness for rutting resistance is required in wearing course layers, it is generally more effective to use polymer modified bitumen (PMBs). [3]

The selection of binder for hot mix asphalt applications is generally based on traffic levels and expected maximum temperatures. A summary of binder type for common dense graded asphalt wearing course and base course (binder course) applications is provided in Table 2 and Table 3 respectively for the categories of traffic in equivalent standard Axles (ESAs) and maximum pavement temperature [3]. Mampearachchi in 2012 revealed that 7-day average maximum pavement temperature in different geographical areas of Sri Lanka is between 52°C and 58°C [5].

Table 2 - Australian Binder Types for Dense Graded Asphalt Wearing Course [3]

Traffic Category	Maximum Pavement Temperature (°C)		
	>58	52-58	< 52
Light (<0.5x10 ⁶ ESAs)	C320	C170 C320	C170 C320
Medium (0.5x10 ⁶ -5x10 ⁶ ESAs)	C320	C320	C170 C320
Heavy (5x10 ⁶ -20x10 ⁶ ESAs)	C320 PMB	C320 PMB	C320
Very Heavy (>20x10 ⁶ ESAs)	PMB	PMB	PMB

Table 3 - Australian Binder Types for Dense Graded Asphalt Base Course [3]

Traffic Category	Maximum Pavement Temperature (°C)		
	>58	52-58	< 52
Light (<0.5x10 ⁶ ESAs)	C320	C170 C320	C170 C320
Medium (0.5x10 ⁶ -5x10 ⁶ ESAs)	C320	C320	C320
Heavy (5x10 ⁶ -20x10 ⁶ ESAs)	C320 C600 PMB	C320 C600 PMB	C320
Very Heavy (>20x10 ⁶ ESAs)	C320 C600 PMB	C320 C600 PMB	C320 C600 PMB

The bitumen test data chart developed (BTDC) by Heukelom in 1969, can be used for comparing the temperature, penetration and viscosity characteristics of different type of bitumen. The chart consists of one horizontal scale for the temperature and two vertical scales for the penetration and viscosity. The temperature scale is linear, the penetration scale is logarithmic, and viscosity scale has been devised so that penetration grade bitumen with penetration indices give straight line relationship. Then the test data for a large

group of bitumen can be represented by a straight line on BTDC. [1]

The monograph is used to estimate the stiffness modulus of a bitumen from the time of loading (heavy vehicle speed), the pavement temperature, the temperature (°C) at which the penetration of the bitumen is 800 (0.1mm) (T_{800Pen}) and temperature susceptibility measured in terms of the penetration index (PI). [1]

$$PI = \frac{20 - 500A}{1 + 50A} \quad \dots (1)$$

where A is the change in log (penetration) per °C change in temperature.

Thus, A and T_{800Pen} for conventional bitumen can be figured out from the BTDC. Also, the BTDC is a useful tool for ensuring that the correct operating temperatures are selected to achieve the appropriate viscosity of any grade of bitumen. When the aggregate and the bitumen are mixed together, the viscosity should be approximately 0.2Pa.s for satisfactory coating and not be below 0.5Pa.s. Also, it is widely recognised that the optimum bitumen viscosity for compaction is between 2Pa.s and 20Pa.s. [1]

Pavement temperature is measured in terms of weighted mean annual pavement temperature (WMAPT). The monograph is used to estimate the stiffness modulus of bitumen at the WMAPT and the rate of loading. Heavy vehicle traffic speed (V) is used to calculate the rate of loading (1/V). The WMAPT is estimated from the monthly average air temperatures by averaging the maximum and minimum air temperatures (T_{air}) in an area. Firstly, temperature weighting factor (WF) is calculated for each month by substituting T_{air} in Equation 2, and secondly, the weighted mean annual air temperature (WMAAT) are estimated by substituting WFs in Equation 3 and averaging. Finally, the WMAPT is estimated by substituting the WMAAT in Equation 4. [2]

$$WF = 10^{(-1.224 + 0.06508T_{air} - 0.000145T_{air}^2)} \quad \dots (2)$$

$$WMAAT = 19.66 + 16.91 \log WF + 0.3117 (\log WF)^2 \quad \dots (3)$$

$$WMAPT = -12.4 + \frac{6.32(WMAAT)}{\ln(WMAAT)} \quad \dots (4)$$

Modulus of DGAs made with known bitumen, and nominal size of aggregate can be calculated from the percentage of air void, temperature and heavy vehicle traffic speed (V). Modulus of Australian DGAs, made with 20mm nominal maximum size aggregate, determined on laboratory manufactured samples using the indirect tensile test procedure and standard test conditions and 5% air voids (AV_{Test}) are shown in Table 04. Standard test conditions are 40ms rise time and 25 °C test temperature. This modulus is corrected for the in-service air voids ($AV_{Service}$), temperature (WMAPT) and loading rate by Equation 5, Equation 6 and Equation 7 respectively. [2]

$$\frac{\text{Modulus at } AV_{Service}}{\text{Modulus at } AV_{Test}} = \frac{21 - AV_{Service}}{21 - AV_{Test}} \quad \dots (5)$$

$$\frac{\text{Modulus at WMAPT}}{\text{Modulus at test temperature (T)}} = \exp(-0.08[WMAPT - T]) \quad \dots (6)$$

$$\frac{\text{Modulus at speed V}}{\text{Modulus at test loading rate}} = 0.19V^{0.365} \quad \dots (7)$$

Table 4 - Laboratory Moduli of Australia DGAs

Bitumen	Modulus, MPa	
	Range	Typical
Class 170	2000-4500	4000
Class 320	3000-7500	5500
Class 600	4000-9500	7000

Roughness (longitudinal unevenness) describes the surface condition of a road. Roughness can be measured in terms of International Roughness Index (IRI). The IRI is a property of the true profile of the pavement. An overall description of the pavement condition is measured in terms of present Serviceability Index (PSI). Serviceability of pavement is its ability to serve traffic in its present condition. According to AASHTO Guide for Design of Pavement Structures (AASHTO Guide), when PSI reduces to 2.0, the road pavement shall be an overlay. Also, PSI equal to 4.2 is considered as initial serviceability index of newly constructed pavement [6]. Since the PSI is mostly affected by roughness, measured IRI values can be converted to PSI by Equation 8 developed by Paterson, 1986. Rutting (Transverse Unevenness) is load associated deflection will appear as longitudinal depressions in wheel paths. Permissible rut depth for asphalt pavement surface is 10mm [8].



$$PSI = 5e^{(-0.18 \times IRI)} \quad \dots (8)$$

The Falling Weight Deflectometer (FWD) is an excellent device for evaluating moduli of pavement layers and subgrade. BAKFAA program hosted by Federal Aviation Administration (FAA) are used to calculate moduli of pavement layers from FWD data [9].

4. Analysis

The section from 58+000 to 62+400 (Variyapola to Padeniya) of Katugastota - Kurunegala - Puttalam (A10) road is selected to calculate in-situ asphalt stiffness moduli as road pavement is visually in good condition and insignificant cracks are observed on the road surface. FWD data at 50m intervals and roughness and rutting data at 100m intervals are obtained from RDA. 10th percentile values of the PSI calculated from IRI values are 3.13 and 3.18 for LHS and RHS respectively, and 90th percentile value of rut depth is 5.07mm. Then calculated IRI and rutting values are well matched to a good condition road (i.e. 4.0 IRI and 10mm maximum rutting for a newly constructed road). Hence, it is confirmed that the road pavement is in good condition. According to asphalt coring result that is carried out at 250mm, thicknesses of asphalt at coring location are more than 200mm. Then modulus values of upper 200mm asphalt layer at test locations are back calculated by BAKFAA program using FWD data. 10th percentile value of Modulus is 880MPa. Modulus values of upper 200mm asphalt layer along the selected section of A10 road are presented in Figure 1. Measured temperatures of the pavement surface along this road section are varied from 31°C and 37°C.

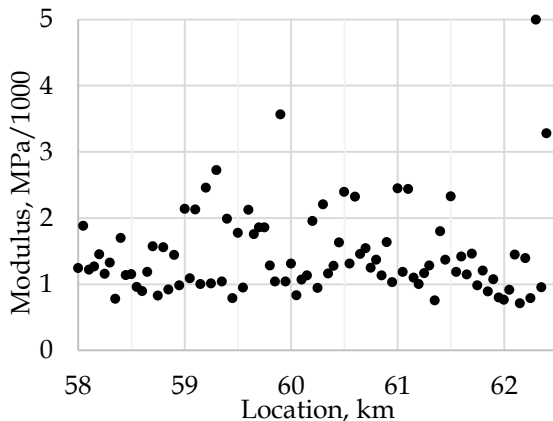


Figure 1 - Modulus values of Upper 200mm of asphalt in selected locations of A10 Road

Historical average monthly temperature data of all districts in Sri Lanka is obtained from the URL <https://www.msn.com/en-gb/weather/today/> [5]. Validation is done for the figures obtained from the given URL against the actual data obtained from Metrological Department of Sri Lanka.

Furthermore the WMAPT values calculated from the URL is compared with the actual figures given for Melbourne City. In both the cases results closer to the actual figures are given by the data obtained from the URL. WMAPTs of all districts are calculated and presented in Table 5. WMAPTs in Sri Lanka is between 35°C, and 41°C. WMAPT of several areas is 40°C. Since WMAPTs in Sri Lanka are in a narrow region, single bitumen class is sufficient for Sri Lanka. Also, there are many practical difficulties to use two grade of bitumens in deferent layers of pavement or different regions in Sri Lanka. Since maximum pavement temperature is between 52°C and 58°C, according to Austroads refer Table 2 and Table 3, a suitable viscosity grade bitumen class for Sri Lanka climate and traffic up to 20 million ESAs (heavy traffic) is C320. Its properties are shown in Table 6.

Table 5 - Weighted Mean Annual Pavement Temperatures (WMAPTs) of Sri Lanka

Group	WMAPT	District
1	35°C	Nuwara Eliya, Badulla, Rathnapura
2	36°C	Kandy, Matale, Monaragala
3	39°C	Kegalle, Kurunegala, Anuradhapura, Polonnaruwa, Trincomalee, Vavuniya
4	40°C	Colombo, Gampaha, Kalutara, Galle, Matara, Hambantota, Jaffna, Kilinochchi, Mullaittivu, Mannar
5	41°C	Puttalama, Ampara, Batticaloa

Table 6 - Properties of C320 Grade Bitumen [3]

Viscosity at 60°C (Pa.s)	260-380
Penetration at 25°C 100g, 5s	40 min
Viscosity at 135°C	0.40-0.65
Viscosity at 60°C after Rolling Thin Film Oven Test (% of original)	300 max
Matter insoluble in toluene (%)	1.0 max
Flashpoint (°C)	250 min
Loss on heating (%)	0.5 max

In order to compare C320 bitumen class with 60/70 bitumen class, four bitumen from each class are selected considering their boundary limits. (Bitumen A, B, C and D for Bitumen Class C320 and Bitumen E, F, G and H for Bitumen Class 60/70 respectively) Boundary limits of C320 bitumen class are taken as upper and lower limit of viscosity at 60°C (Vis@60) and 135°C(Vis@135). As well as Boundary limits of 60/70 bitumen class are taken as upper and lower limit of penetration at 25°C (Pen@25)and softening point (T_{800Pen}). The bitumen stiffness at 40°C is estimated from Monograph given in Austroads, and upper and lower limits of mixing temperature compaction temperature are estimated from BTDC. To estimate bitumen stiffness, viscosity at mixing and compaction limits are taken as 0.2Pa.s to 0.5Pa.s and 2Pa.s and 20Pa.s respectively, and heavy vehicle traffic speed is assumed practically as 30kmph. All specified and estimated properties are shown in Table 7 and Table 8.

Table 7 - Properties of Selected C320 Bitumen

Bitumen	A	B	C	D
Vis@60,Pa.s	260	380	260	380
Vis@135,Pa.s	0.40	0.65	0.65	0.4
A/1000	44	41	39	46
PI	-0.7	-0.2	0.1	-0.9
T800Pen,°C	49	51	48	52
T800pen-40°C	9	11	8	12
Stiffness@40, MPa	0.4	0.5	0.3	0.7
Upper Mixing Limit,°C	148	159	160	148
Lower Mixing Limit,°C	131	140	140	131
Upper Compaction Limit, °C	109	116	116	110
Lower Compaction Limit, °C	82	93	85	90

Table 8 - Properties of Selected 60/70 Bitumen

Bitumen	E	F	G	H
Pen@25,dmm	60	70	60	70
Softening Pt.,°C	48	56	56	48
A/1000	49	34	36	46
PI	-1.3	1.1	0.7	-0.9
T800pen-40°C	8	16	16	8
Stiffness@40,MPa	0.5	0.6	0.7	0.4
Upper Mixing Limit,°C	138	185	178	144

Lower Mixing Limit,°C	122	163	156	127
Upper Compaction Limit,°C	103	135	130	106
Lower Compaction Limit,°C	78	99	96	80

A stiffness range of both class of bitumen at 40°C is almost equal. Hence it can be concluded that modulus of asphalt made with both classes of bitumen is equal. Then modulus of Sri Lankan DGA, made with 60/70 bitumens and 20mm nominal maximum size aggregates, are considered as the modulus of DGA given for C320 bitumen in Table 4. However given modulus DGA should be corrected for the in-service air voids, WMAPT and heavy vehicle traffic speed by Equation 5, Equation 6 and Equation 7. Modulus of DGAs in different WMAPTs in Sri Lanka and different heavy vehicle traffic speed are calculated and presented in Figure 2. Also, modulus of Sri Lankan DGAs in different zones shown in Table 5 and different heavy vehicle traffic speeds are presented in Table 9 for the purpose of pavement structure designs.

There are no large variations in upper and lower temperatures of mixing and compaction of DGA made with C320 viscosity grade bitumen. Hence temperature limits can be specified for C320 bitumen. However variations of mixing and compaction of DGAs made with 60/70 penetration grade bitumen are huge, and some limits are out of specification limits (Specified mixing limits are 145°C and 170°C, and specified lower compaction limit is 90°C). Then there is a risk to produce poor DGA mixes due to the poor coating of bitumen with aggregates, compaction and consistency in the mix and it leads the insufficient resistance to fatigue and permanent deformation affected by the modulus of DGAs. Defining new specified limits are not possible because of huge variations. In order to mitigate the mixing and compaction issues, viscosity grade bitumen class similar to 60/70 bitumen class should be used in Sri Lanka for quality service of road pavements.



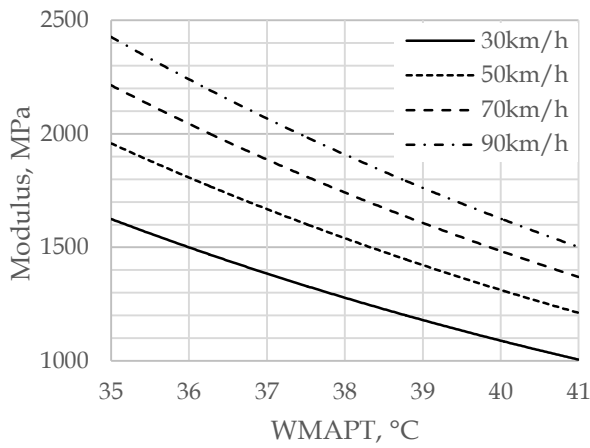


Figure 2 - Modulus of Sri Lankan Dense Graded Asphalt

Table 9 - Modulus of Dense Graded Asphalt of Deferent Zones in Sri Lanka

WMAPT Group	Heavy Vehicle Traffic Speed, km/h			
	30	50	70	90
1	1600	2000	2200	2400
2	1500	1800	2000	2200
3	1200	1400	1600	1800
4	1100	1300	1500	1600
5	1000	1200	1400	1500

5. Conclusions

The thickness of the asphalt for decided ESAs depends on the modulus of the asphalt. Since Sri Lankan DGAs varies from 1000MPa to 2400MPa and precise modulus shall be selected according to pavement temperature (WMAPT) and heavy vehicle traffic speed from Table 9. Then only road pavements in Sri Lanka provide their service without a premature failure. Further laboratory and field studies are required to improve modulus of Sri Lankan DGAs given in Table 9.

Although 60/70 bitumen can be used to produce GDAs up to 20 million ESA traffic loads, excessive asphalt thickness has to be used for high traffic loads with low heavy vehicle speed or high WMAPT. High-grade bitumen cannot be recommended for use as a wearing course layer as increased stiffness can result in reduced resistance to cracking and fatigue in thin layers. Then a polymer modified bitumens or composite pavement structure can be used to reduce asphalt thickness. For this reason, typical pavement structures used in Sri Lanka for high traffic have to be reviewed.

Low asphalt modulus at low heavy vehicle speed and high pavement temperature in Sri

Lanka together with a poor coating of bitumen, compaction and consistency in the mix, causes insufficient resistance to fatigue and permanent deformation in trafficked road pavements and leads to alligator cracking and formation of waves and corrugation caused by stop-and-go vehicles. In this condition, defects can occur on loaded areas even after a few years from construction. Hence, it is very essential to control viscosities of bitumen at mixing and compaction temperatures. Since viscosity grade, bitumen calcification controls viscosities at 60°C, and 135°C near mixing, viscosity grade bitumen calcification shall be introduced to Sri Lanka for the performance of roads.

Acknowledgement

The Authors wish to acknowledge Prof W.K. Mampearachchi and other engineers for sharing knowledge. The Authors express their gratitude to Asian Development Bank (ADB) Division of Road Development Authority (RDA) and Engineering Design and Project Management Consultants (Pvt) Ltd for providing relevant data for the study.

References

1. Robert N. Hunter, Andy Self, & John Read, *The Shell Bitumen Handbook*, 6th ed., ICE Publishing, One Great George Street, Westminster, London, 2015, pp.87-145, 503-542, 750-752.
2. Austroads, *Guide to Pavement Technology Part 2: Pavement Structural Design*, Sydney, 2012, pp.64-83.
3. Austroads, *Guide to Pavement Technology Part 4F: Bituminous Binders*, Sydney, 2008, pp.10, 23-25.
4. ICTAD, *Standard Specification for Construction and Maintenance of Road and Bridges*, 2th ed., Colombo, 2009, pp.143-151, 459-463.
5. Mampearachchi, W. K., "Review of asphalt binder grading systems for hot mix asphalt pavements in Sri Lanka", *Journal of the National Science Foundation of Sri Lanka* 40 (4), 2012, pp. 311-320.
6. <https://www.msn.com/en-gb/weather/today/>, Visited, January 2017.
7. AASHTO, *Pavement Guide for Design of Pavement Structure*, Washington, 1993, ii-10 p.
8. Transport & Road Research Laboratory, *Overseas Road Note 18: A guide to the pavement evaluation and maintenance of bitumen-surfaced roads in tropical and sub-tropical countries*, Berkshire, 1999, 34 p.
9. <http://www.airporttech.tc.faa.gov/Download/Airport-Pavement-Papers-Publications-Detail/dt/Detail/ItemID/34/BAKFAA-version-20-update-04012013>, Visited, February 2017.

Suitability Recycled Pet Fiber and Carbonized Wood Ash in Hot Mix Asphalt Concrete

N. Jegatheesan, T.M. Rengarasu and W.M.K.R.T. Wasala Bandara

Abstract: This study was aimed at investigating the suitability of Polyethylene Terephthalate (PET) fibres having a diameter of 0.5 mm and a length of 4 to 6 mm and Carbonized Wood Dust (CWD) having a nominal size of 1.18 mm, as alternative materials of Hot Mix Asphalt (HMA) by following the Marshall Method. Accordingly, conventional materials of HMA which are binder and aggregates were partially substituted with PET and CWD in three different ways. First, PET was added as a binder additive in a wet process. Next, stone dust (Filler) was replaced by CWD. Finally combined modification was done using PET and CWD which were added as binder additive and filler respectively in same HMA mix. Due to the less specific gravity of CWD, bulk density and void of Modified HMA (MHMA) with CWD were reduced. However, the Marshall properties of MHMA with CWD were impaired, due to the lack of bond between aggregates and CWD. Maximum 2.73% of CWD can be added to satisfy the minimum stability requirement given in CIDA specification. Modification with PET increased the Marshall Strength, bulk properties and bonding ability as well. Therefore, to improve the Marshall Stability of MHMA with 2.73% of CWD, PET was added as an additive that resulted in 30% - 103% increment in Marshall Stability compared to MHMA with CWD only. However, a reduction in stability was observed in comparing with the control mix. Furthermore, the bulk density of combined MHMA was reduced with the addition PET modification. The absorption rate of combined MHMA was increased at 5% to 10% addition of PET. Beyond 10% addition of the PET, the absorption rate was considerably reduced. Eventually, it was discovered that minimum 5% PET and maximum 2.73% of CWD can be added in the combined MHMA to satisfy the medium and the low traffic limitation of CIDA specification.

Keywords: PET fibre, Carbonized wood dust, Modified Hot Mix Asphalt, Wet process

1. Introduction

The rapid development of the country amplifies the number of expressway, highway and road construction to enhance the connectivity between lagging and developed area. Around 80% of the roads are paved with Hot Mix Asphalt Concrete (HMA) by using more than 90% of aggregates by the total weight of the mix [6, 7, 12, 29]. However, materials used in HMA can be able to withstand the traffic load that is usually spread out through the structural layer of the pavement [14] in such a way that the stress at the sub-grade soil is low enough not to cause major damage to the pavements [1, 7, 8].

The surface wearing course makes direct contact with the traffic load in the flexible pavement [6, 8]. Therefore, it should consist of proper materials to withstand traffic load without undergoing to any failure during their design life [6, 15, 20]. Because of the high cost of aggregates, conventional method with usual materials is not an economical way to follow in the case of medium and the low traffic class pavement. Therefore, Engineers are paying

attention on using alternative materials like waste or recycled materials to reduce the usage of convention aggregate and the overall cost of HMA.

2. Literature review

In developing countries like Sri Lanka, more efforts have to be taken to tackle the waste disposal problem, due to lack of space. About 85% of collecting waste in Sri Lanka is subjected to open or ocean dumping [11, 18, 30]. At present, nearly 4000 saw mills including pit-sawing units and excluding 680 mills owned by

Eng. N.Jegatheesan, B.Sc.Eng.(Hons) (Ruhuna), Postgraduate Student (MPhil), Department of Civil Engineering, Faculty of Engineering, University of Ruhuna.

Eng. (Dr.) Terrance M. Rengarasu, Ph.D.(Hokkaido), M.Eng. (Hokkaido), B.Sc.Eng.(Hons) (Peradeniya), AMIE(SL) Senior Lecturer, Department of Civil and Environmental Engineering, University of Ruhuna.

Eng. (Dr.) W.M.K.R.T. Wasala Bandara, Ph.D.(Hokkaido), M.Eng. (Hokkaido), B.Sc.Eng.(Hons) (Peradeniya), AMIE(SL), AMSSE(SL), MBEA(SL), Senior Lecturer, Department of Civil and Environmental Engineering, University of Ruhuna.



furniture manufacturers, are running in Sri Lanka. Annually, around 112,000 MT sawdust is produced from the saw mills [26]. In general, 12% of the input wood is wasted as sawdust during milling operations [23, 31]. Only a considerable amount of sawdust is used as fuel, ultimately remaining part is dumped or burned in the direct surroundings of the mills [26]. In Sri Lanka, it was estimated that, around 10.5% of total waste are non-biodegradable plastic and polythene in 2015 [11]. Approximately 4.8 to 12.7 million MT plastic waste is floating in the world's oceans which causes negative impacts on the environment [13].

As an environmentally friendly construction method, a considerable number of researches have been conducted on HMA with different kind of waste materials such as waste glass, rubber, steel slag, marble and ceramic dust, cement dust, rice husk ash, sawdust, sawdust ash, recycled concrete aggregates, tyres, demolished building waste, plastic, polythene etc [2, 3, 5, 12, 25]. Wood dust ash having 5–30% of carbon, can be used as filler or modifier, because it can be ground finer and become more activated due to the metastable state of surface structure [21, 27]. Wood dust ash as asphalt binder modifier, improves the rutting resistant, viscosity and complex modulus. Further, sawdust as filler produces light weight concrete; however, stability was reduced by lack of bonding ability and high absorption of the binder [17, 22].

Polyethylene Terephthalate (PET) recycled material form plastic also can be used as aggregate and binder modifier [2, 9, 20]. PET replaced with aggregate, improves performance of pavement in rutting and fatigue cracking compared to conventional one by the reduction of permanent strain [16, 20]. The viscosity of modified binders was simultaneously increased with both mixing time and adding PET percentages [4, 9]. PET coated aggregate MHMA resulted in higher Marshall Stability (MS) and less penetration [16, 28]. The 20% (weight of coarse aggregate) of PET as aggregate reduce the bulk density. However, result obtained from Marshall Test was almost same for control and modified mixture. The flow value of the modified mixture was somewhat lower than conventional one [2, 10]. PET as fine aggregate also reduced the permanent deformation of HMA mixture [19, 24]. This study aimed at investigating the properties of single modified HMA with CWD

using as filler and PET using as binder additive separately and combine modification.

3. Materials

3.1 Conventional materials

In this study, crushed rocks were taken at the required nominal size (Coarse – 20 mm, Fine – 14 mm and Filler – Quarry dust). The materials were tested based on American Standards. Based on particle size distribution of aggregate, the mix proportion of three types of aggregates (20%: 20%: 60% of coarse, fine and filler respectively) and binder percentage were selected. According to the CIDA specification mix design was categorized as Type 3 wearing course. The 80/100 penetration grade binder with a melting point at 43°C was used in this study.

3.2 Waste materials

Wood dust which was belonged to one type, *Albesia (Albizia Julibrissin)*, was burned in a sealed oxygen-less incinerator (Figure 1). Carbonized Wood Dust (CWD) having a nominal size of 1.18 mm was used as filler in the order of 1.77%, 2.73% and 3.75% of total weight of aggregate (respectively 1133.1g, 1099.7g and 1066.2g). Because of less specific gravity (0.61) of the CWD, the filler replacement was done at volume basis to keep the standard sample size.



Figure 1 - Carbanized wood dust (1.18 mm)



Figure 2 - Polyethylene Terephthalate (PET) of 0.5 mm, specific gravity 1.2 and melting

point - 252°C) was collected from PET manufacturing company (Figure 2). It was mixed with bitumen as an additive at 5%, 10% and 15% of total binder weight.

4. Methodology

In this study, Marshall Mix design was followed to investigate the bulk and Marshall properties of modified HMA (MHMA) with PET and CWD. The major scope of this mix design is to find out the optimum requirement of materials. Figure 3 shows the summary of the experimental study. According to the CIDA specification, binder content was selected as 4 to 6% at 0.5% interval with respect to the aggregate gradation (from Sieve analysis test).

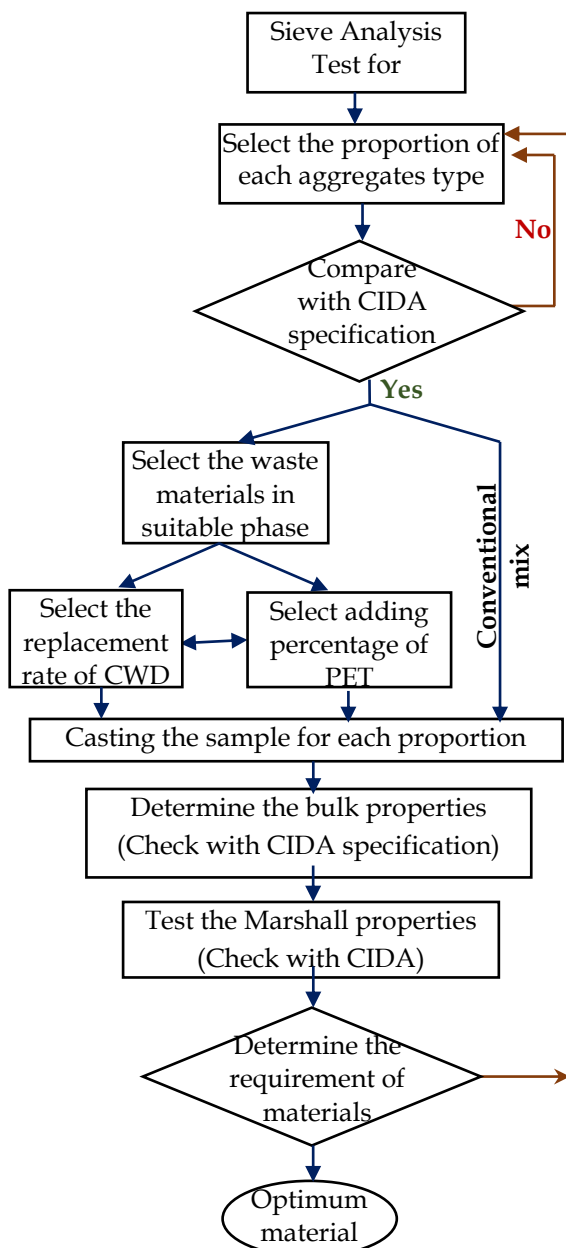


Figure 3 - Methodology flowchat

Control mix was prepared to compare the result of MHMA. As a first modification, PET was properly mixed with bitumen at high temperature (200 °C to 250 °C) to make the homogeneous modified binder. After that, PET modified binder was commingled with convention aggregate mix. In the second modification, pure bitumen was mixed with aggregate partially replaced with CWD. Finally, modification was done with PET modified bitumen and CWD replaced aggregate.

50 blows (For medium traffic load) per side were applied at 145°C to compact a sample. Bulk properties (Specific gravity, Void in Mix (VIM), Voids in Mineral Aggregate (VMA) and Void filling Bitumen (VFM)) was determined before test the stability of the sample. Marshall Properties (MP) which are Marshall Stability (MS) and Marshall Flow (MF) value, of the preheated specimens at 60°C for 30 minutes, were determined by using the Marshall Test apparatus. Finally, optimum requirement of materials were determined by analysing the obtained result. Absorption of wood dust is higher than the aggregate. Therefore, absorption test was conducted to determine the absorption rate of MHMA.

5. Result and discussion

5.1 HMA with PET as binder additive

The properties of the binder and the overall performance of MHMA were improved with addition of PET. When the PET content was increased, the specific gravity of MHMA was gradually reduced. However, compared to the control sample, the specific gravity was less. Variation of the specific gravity of control mix and the modified HMA with binder content are shown in Figure 4. There was no considerably different was observed, because of the specific gravity of the PET (1.2) which was nearly equal to the bitumen (0.94). In the case of air void percentage, the PET modified HMA resulted in greater value compared to control sample. Even though the air void percentage was greater, the value of air void at optimum bitumen content, was between the allowable ranges (3 < VIM < 5, CIDA specification). The air void of the modified HMA concrete was decreased with the addition of PET (Figure 5). The proper variation was observed on voids in mineral aggregate of PET fibre MHMA with respect to the addition of PET. However, modified HMA with PET resulted in greater percentage which was within allowable range, compared to the



control sample. Void filling ability also somewhat less compared to the control sample.

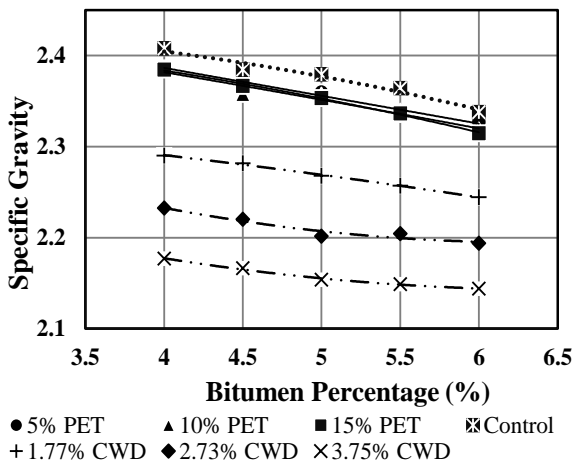


Figure 4 - Specific gravity of single MHMA

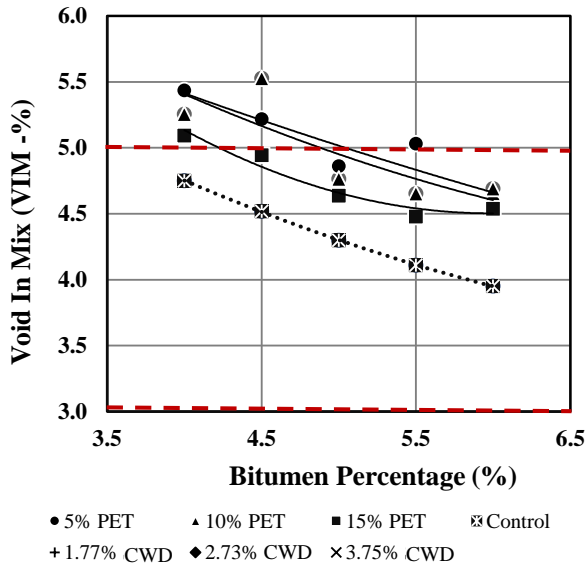


Figure 5 -Void of single MHMA

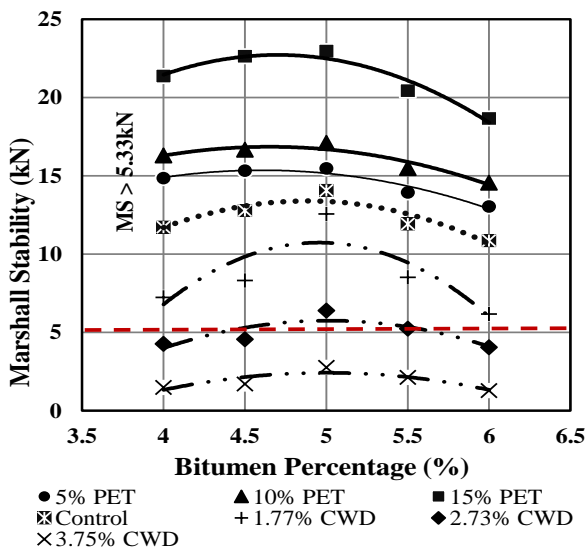


Figure 6 - MS of single MHMA

Marshall Stability of the PET modified HMA was increased with the addition of the PET. Even though, optimum bitumen percentage of the modified binder was less compared to control; it was increased with the addition of PET. PET improved the stiffness and the bonding strength of the binder which improves the load bearing ability of the pavement (Figure 6). At 5% of PET modification, the stability was increased by maximum 14%. Likewise, 10% of PET addition showed 25% increment in stability at 4.65% of modified binder content.

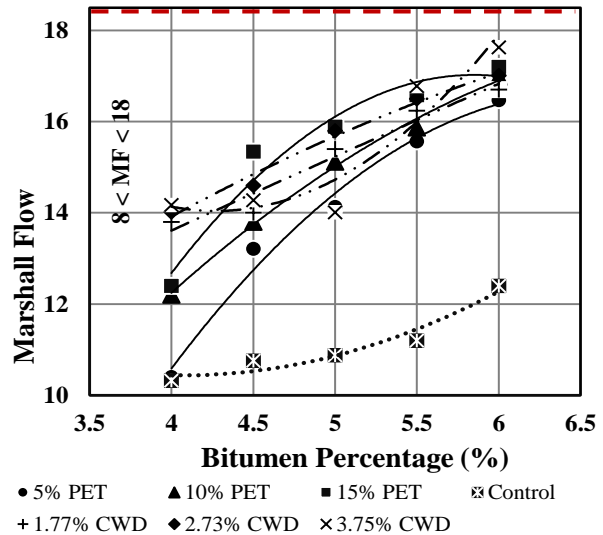


Figure 7 - MF of single MHMA

At 4.7% of modified bitumen, the 15% of PET modified sample resulted in 67% improvement in stability compared to HMA. Similarly, Marshall Flow (deflection) was increased due to the increment of air void. However, the occurred deflection was within the accepted range ($8 < \text{Marshall Flow} < 18$, CIDA specification) (Figure 7). Flow value was increased with binder content like control sample. However, the increasing percentage was decreased with percentage of modified bitumen. According to Sengoz & Topal [25] research, that variation also was acceptable. Up to 15% of PET modification, MHMA showed better performance compared to conventional HMA.

5.2 HMA with CWD as a filler - replacement

The replacement of CWD as filler produced the light weight concrete due to the low bulk density of CWD (Figure 4). When the amount of CWD was increased in the sample, they became as low-quality mix due to lack of binding ability of the binder. Therefore, with the increment of binder content, the samples displayed more consistency in the visual inspection due to the increased requirement of

binder to bind up the aggregates together. However, the CWD particles were affixed to the aggregate surface during the mixing and casting stages of the samples. Therefore, a better surface finish was achieved. Due to the low bulk density (0.61) of CWD, it was replaced in volume basis (Weight of CWD having volume equal to volume of filler aggregate) to keep the standard sample size. The addition of 1g CWD replaced the 4.3g of conventional filler (Stone dust). Maximum 24% of the weight of filler was substituted with 40g CWD. Due to the absorptive nature of CWD, the bitumen added to the mix was partially absorbed by the CWD particles. After being saturated, the rest of the bitumen added, was acted as the binder to tie up the aggregate skeleton.

Addition of CWD reduced the specific gravity by 5-10% at 1.77% to 3.75% of CWD replacement. Due to the fineness of the particles, void in the modified HMA was reduced (Figure 5). Moreover, the tiny particles of CWD filled the small cracks of aggregates. Compared to the control mix, the VIM also was less. However, it was within the allowable range. VMA of the modified HMA was less compared to the control mix and that satisfied the specification (VMA > 13).

The stability of MHMA with CWD was reduced by the addition of the CWD. The replacement of 1.77% (20g) showed better result compared to the other replacement. Even though, 2.73% of CWD replacement had less stability which satisfied the minimum requirement ($MS_{min} = 5.33kN$, CIDA specification) at 4.8 to 5.2% of binder content. MHMA at 3.75% of CWD replacement was completely failed under the loading (Figure 6). Flow value was also higher due to the softness of the CWD particles (Figure 7). Except for 3.75% of replacement, other flow values was within the allowable range. The flow value was increased by the increment of replacement rate of CWD. As the result of this modification, optimum replacement rate of CWD should be 2.73% (around 30g).

5.3 HMA with CWD as filler and PET as binder additive

In the previous case, due to the lack of bonding ability, CWD particles were removed from the sample during the casting process. In the combined modification, due to the modified binder with PET, bonding ability was improved well. In the low binder percentage also, the samples showed better finishing surface

compared to the modification with CWD only. Due to the addition of CWD and the PET, combine MHMA showed less bulk density compared to all other modification. Maximum 15% of bulk density was reduced compared to the control mix at 15% addition of PET. The variation of bulk density of combined MHMA was considerably small at 5% to 15% of PET (Figure 8). When the bitumen percentage was increased the air void of the modified sample, was decreased like control. Air void was also reduced with the addition of PET. At the low binder content, the air void was a little high compared to the control sample. Beyond 4.5% of modified binder percentage, the air void was less (Figure 9). VMA was within the allowable range of specification (VMA > 13); however, compared to the control that was significantly less.

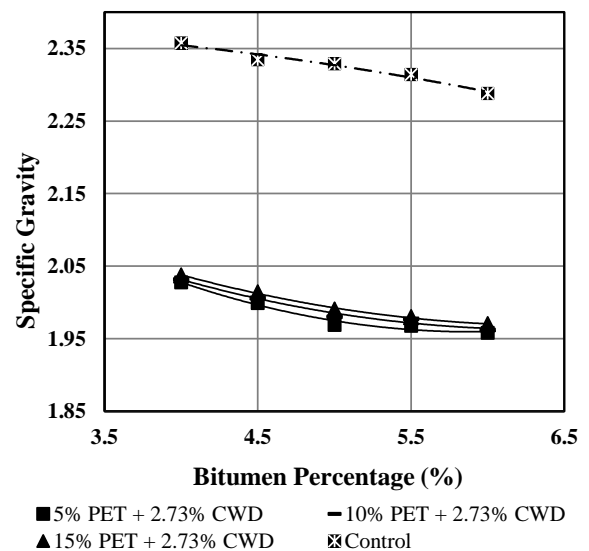


Figure 8 - Specific gravity of combine MHMA

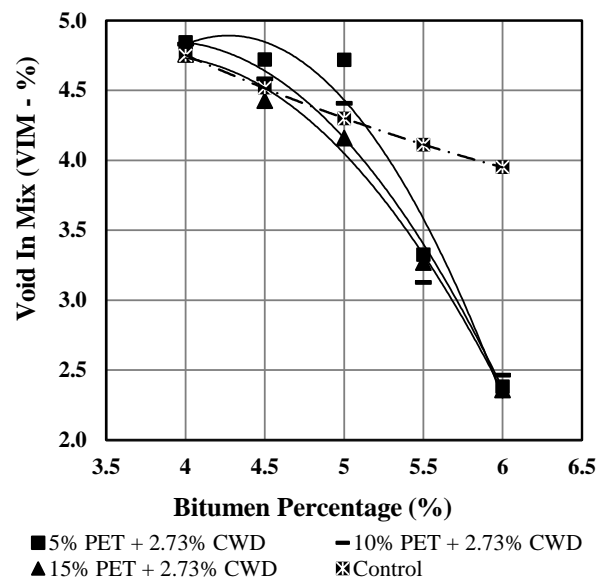


Figure 9 - VIM of combine MHMA



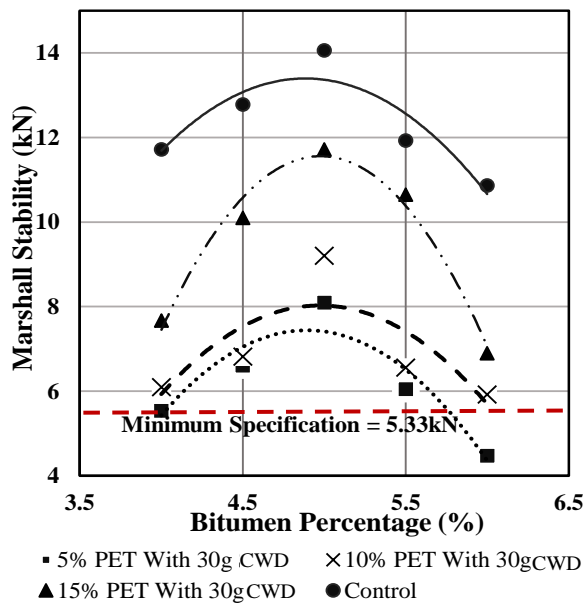


Figure 10 - MS of combine MHMA

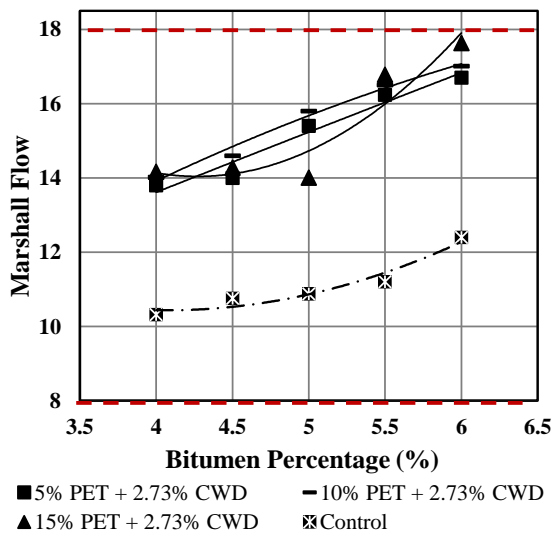


Figure 11 - MF of combine MHMA

The addition of the modified binder with PET improved the Marshall properties of the modified HMA with CWD and PET. Even though the stability was lesser than the control, while adding the PET with CWD, stability was increased compared to the single MHMA concrete with CWD as a filler (Figure 10). Even though the 2.73% of CWD modified sample partially satisfied the stability requirement by single modification, the 5% of PET modified binder improved the stability by 30%. The addition of 15% of PET modified binder improved the stability of the modified mix with CWD by 103%. However, compared to HMA stability was reduced by 13.3%. In the 5% of PET MHMA with CWD, sample was not satisfied the CIDA specification for the medium

traffic load condition at 5.65 to 6 % of modified bitumen. The flow value of the modified HMA with PET and CWD was higher than the control sample (Figure 11). However, the flow value was within the allowable range. Compared to modified sample with CWD only, deflection was less due to the addition of PET. Because of PET modification, the stiffness of the combined modified mix was improved. It was found that to improve the properties of the 2.73% of CWD MHMA, minimum 5% of PET is required.

5.4 Absorption

The absorption of the single modification of HMA with CWD was increased with the CWD content. With time, the absorption of the modified sample was increased until reach to the saturation point. The period for the saturation (15days) did not vary with the CWD content. At the saturation stage, the absorption of MHMA having 2.73% of CWD was increased by 26.7% compared to the MHMA with 1.77% of CWD. When the PET and CWD added in the same mix, the absorption was increased with the addition of the 5% to 10% of PET.

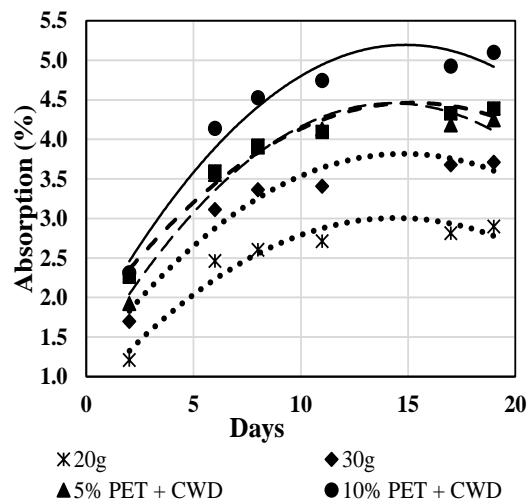


Figure 12 - Absorption rate

The 5% of PET modification resulted in 50% increment in the absorption, compared to the 1.77% of CWD modified HMA mix. The addition of PET increased the percentage of the void, because the molecular size of the binder particles may become as bigger after the addition of the PET. During the mixing process, bitumen was absorbed by the CWD. However, CWD absorbed more conventional bitumen than modified bitumen with PET. Up to 10% of the PET addition, the absorption was increased. Then beyond the 10% of PET, the absorption of the combine modified HMA was decreased. Maximum 73% of increment was resulted at the 10% of PET modification. At 15% of PET

modification, absorption rate was reduced by 18.2% compared to 10% of PET modified HMA mix. When the PET content increased, the CWD particles were covered with impermeable modified binder film. Due to this process, the absorption of the combined modified HMA was reduced. Therefore, the absorption can be controllable with the addition of the PET in the combined MHMA with CWD and PET.

6. Conclusions

The PET modified HMA showed better performance against Marshall and bulk properties. PET as an additive, improved the bonding ability. The 15% of PET modification resulted in maximum 67.4% increment in stability. Marshall Flow was increased with PET. However it was satisfied the specification.

In the CWD modified HMA, even though the bulk density was improved by 10%, Marshall Stability was reduced by 60% at 2.73% of CWD when compared to control. However, stability requirement was satisfied. Maximum 2.77% of CWD can be replaced with conventional filler. The deflection of MHMA with CWD was increased with the addition of CWD.

The modification with both PET and CWD in the same mix, improved the Marshall Stability of the sample, compared to MHMA with CWD only. When Marshall Stability was compared with 2.73% of CWD only, stability was increased by 30% to 103% due to the addition of 5 to 15% of PET respectively. However, stability of combined MHMA was reduced by 13.3% at 15% PET content compared to control. The bulk properties also showed better improvement because of the CWD having tiny particles. Light weight MHMA was produced with maximum 15% of weight reduction.

Further, the absorption of combined MHMA was controlled by the addition of PET modified binder. Beyond 10% of PET modification, the absorption reduced well compared to single MHMA with CWD.

7. Future direction

In this study maximum 5 to 10% of PET was good enough to modify the MHMA with CWD to the medium traffic load. However, Up to 15% the stability increased with the addition of the PET. Therefore, the optimum PET content should be greater than 15%.

The CWD can undergo to the carbon caption which may reduce the amount of the CWD with the time. Therefore, the design life of this modified sample should be investigated to fulfil the design requirements.

Acknowledgement

Special gratitude of the Authors goes to the Province Road Development Department (Southern Province) who provided various in kind support to conduct this study.

References

1. Mallick, R. B. and El-Korchi, T., 2013. *Pavement engineering: principles and practice*. CRC Press.
2. Ahmadinia, E., Zargar, M., Karim, M.R., Abdelaziz, M. and Shafigh, P., 2011. Using waste plastic bottles as additive for stone mastic asphalt. *Materials & Design*, 32(10), pp.4844-4849.
3. Akbulut, H. and Güreer, C., 2007. Use of aggregates produced from marble quarry waste in asphalt pavements. *Building and environment*, 42(5), pp.1921-1930
4. Al-Hadidy, A. I. and Yi-qiu, T., 2009. Effect of polyethylene on life of flexible pavements. *Construction and Building Materials*, 23(3), pp.1456-1464.
5. Arabani, M., Tahami, S. A. and Taghipoor, M., 2017. Laboratory investigation of hot mix asphalt containing waste materials. *Road Materials and Pavement Design*, 18(3), pp.713-729.
6. Arasan, S., Yenera, E., Hattatoglu, F., Hinislioglu, S. and Akbuluta, S., 2011. Correlation between shape of aggregate and mechanical properties of asphalt concrete: Digital image processing approach. *Road Materials and Pavement Design*, 12(2), pp.239-262.
7. Chen, J. S., Shiah, M. S. and Chen, H. J., 2001. Quantification of coarse aggregate shape and its effect on engineering properties of hot-mix asphalt mixtures. *Journal of testing and evaluation*, 29(6), pp.513-519.
8. Chen, J.S. and Liao, M.C., 2002. Evaluation of internal resistance in hot-mix asphalt (HMA) concrete. *Construction and Building Materials*, 16(6), pp.313-319.
9. Earnest, M.D., 2015. Performance Characteristics of Polyethylene Terephthalate (PET) Modified Asphalt.
10. Hassani, A., Ganjidoust, H. and Maghanaki, A.A., 2005. Use of plastic waste (poly-ethylene terephthalate) in asphalt concrete mixture as



aggregate replacement. *Waste Management & Research*, 23(4), pp.322-327.

11. Hikkaduwa, H. N., Gunawardana, K. W., Halwatura, R. U. and Youn, H. H., 2015. Sustainable Approaches to the Municipal Solid Waste Management in Sri Lanka. *6th International Conference on Structural Engineering and Construction Management 2015, Kandy, Sri Lanka*, 11th - 13th on. December
12. Huang, Y., Bird, R. N. and Heidrich, O., 2007. A review of the use of recycled solid waste materials in asphalt pavements. *Resources, Conservation and Recycling*, 52(1), pp.58-73.
13. Jambeck, J. R., Geyer, R., Wilcox, C., Siegler, T. R., Perryman, M., Andrady, A., Narayan, R. and Law, K. L., 2015. *Plastic waste inputs from land into the ocean*. *Science*, 347(6223), pp.768-771.
14. Kandhal, P., Lynn, C. and Parker, F., 1998. Characterization tests for mineral fillers related to performance of asphalt paving mixtures. *Transportation Research Record: Journal of the Transportation Research Board*, (1638), pp.101-110.
15. Kandhal, P. S. and Parker, F., 1998. *Aggregate tests related to asphalt concrete performance in pavements* (No. 405). Transportation Research Board.
16. Liang, Z. Z., Woodhams, R. T., Wang, Z. N. and Harbinson, B. F., 1993. Utilization of recycled polyethylene in the preparation of stabilized, high performance modified asphalt binders. In *Use of Waste Materials in Hot-Mix Asphalt*. ASTM International.
17. Marteano, D., 2002. *The performance evaluation of hot rolled asphalt mixed with sawdust ash as a filler*, Ph. D. Doctoral dissertation, Magister Teknik Sipil.
18. Menikpura, S.N.M., Gheewala, S.H. and Bonnet, S., 2012. Sustainability assessment of municipal solid waste management in Sri Lanka: problems and prospects. *Journal of Material Cycles and Waste Management*, 14(3), pp.181-192.
19. Modarres, A. and Hamed, H., 2014. Effect of waste plastic bottles on the stiffness and fatigue properties of modified asphalt mixes. *Materials & Design*, 61, pp.8-15.
20. Moghaddam, T. B., Soltani, M. and Karim, M. R., 2014. Experimental characterization of rutting performance of polyethylene terephthalate modified asphalt mixtures under static and dynamic loads. *Construction and Building Materials*, 65, pp.487-494.
21. Nair, D. G., Fraaij, A., Klaassen, A. A. and Kentgens, A.P., 2008. A structural investigation relating to the pozzolanic activity of rice husk ashes. *Cement and Concrete Research*, 38(6), pp.861-869.
22. Osinubi, K., Edeh, J. and Onoja, W., 2012. Sawdust ash stabilization of reclaimed asphalt pavement. In *Testing and Specification of Recycled Materials for Sustainable Geotechnical Construction*. ASTM International.
23. Perera, K. K. C. K., Rathnasiri, P. G., Senarath, S. A. S., Sugathapala, A. G. T., Bhattacharya, S. C. and Salam, P. A., 2005. Assessment of sustainable energy potential of non-plantation biomass resources in Sri Lanka. *Biomass and Bioenergy*, 29(3), pp.199-213
24. Rahman, W. M. N. W. A. and Wahab, A. F. A., 2013. Green pavement using recycled polyethylene terephthalate (PET) as partial fine aggregate replacement in modified asphalt. *Procedia Engineering*, 53, pp.124-128.
25. Sengoz, B. and Topal, A., 2005. Use of asphalt roofing shingle waste in HMA. *Construction and Building Materials*, 19(5), pp.337-346.
26. Shyamalee, D., Amarasinghe, A. D. U. S. and Senanayaka, N. S., 2015. Evaluation of different binding materials in forming biomass briquettes with saw dust. *International Journal of Scientific and Research Publications*, 5(3), pp.2250-3153.
27. Sinsiri, T., Kroehong, W., Jaturapitakkul, C. and Chindaprasirt, P., 2012. Assessing the effect of biomass ashes with different finenesses on the compressive strength of blended cement paste. *Materials & Design*, 42, pp.424-433.
28. Sojobi, A. O., Nwobodo, S. E. and Aladegboye, O.J., 2016. Recycling of polyethylene terephthalate (PET) plastic bottle wastes in bituminous asphaltic concrete. *Cogent engineering*, 3(1), p.1133480.
29. Tillson, G. W., 1900. *Street Pavements and Paving Materials: A Manual of City Pavements: the Methods and Materials of Their Construction*.
30. Viswanathan, C., 2006. Domestic solid waste management in South Asia. *Environmental Engineering and Management Program Asian Institute of Technology Thailand*. http://www.iges.or.jp/en/ltip/pdf/activity08/07_viswanathan.pdf.
31. Introduction to Uva Province (2009), Waste Quantification and Characterization – Sri Lanka, visited 10th May 2016 http://www.unep.or.jp/ietc/spc/activities/GP_WM/data/T1/AB_3_WasteQC_SriLanka.pdf

Evaluating Road user Cost for Highway Work Zones - Case Study for Urban Upgrading Projects in Sri Lanka

M.H.M. Hamsath and H.R. Pasindu

Abstract: A work zone is defined as a segment of highway in which maintenance and construction operations affect the number of lanes available for traffic or affect the operational characteristics of traffic flowing through the segment. Work Zone Road User Cost (WZRUC) is the additional cost borne by the road users as a result of the work zone activities. It is a combination of Value of Time Cost (VoTC), Vehicle Operating Cost (VOC), and Vehicle Emission Cost (VEC), Accident Cost (AC) and some non-monetary values such as noise and impact on social inconvenience. This paper is to identify the impact of Work Zone Road User Cost from upgradation projects in Sri Lanka compared with the real economic costs.

This study evaluated the five road upgrading projects in Colombo district and based on the study finding the economic cost during the construction in upgradation. WZRUC is in the range of 13-45 % of the total project cost. The major cost component of which is delay cost which is in the range of 8-27% of the total project cost. By evaluating the WZRUC, the real economic cost of upgradation projects can be assessed. This can be used in evaluating its economic impact of the project, in assessing work zone management strategies that may reduce the additional economic cost during construction stage. Thereby, the contractors can be given more specific guidelines to implement a proper work zone management plan.

Keywords: Road user cost, Value of time cost, Vehicle operating cost, Emission cost

1. Introduction

There has been a rapid increase in trip generation in urban areas in Sri Lanka and urban upgradation projects are very common in urban areas. As a result of increased upgradation projects in urban area, the traffic congestion has been increased and this has caused severe concern regarding the liveability in urban areas especially in Colombo area and its suburbs. As a result of increased road works in urban areas, these activities cause traffic disruptions, safety aspects to road users and construction workers and negative impact on local business and community.

The impact of the WZRUC are neglected in Sri Lankan practice, in the estimation of benefits from an upgradation project. As it is neglected in the benefit cost analysis, the contractors do not consider the impacts at the construction stage. Since they do not consider about the impacts, the work zone management is very poor in Sri Lankan urban upgradation projects. But in developed countries, the WZRUC is estimated through various tools and it is used to estimate the incentives to the contractors to decrease the project duration, early completion

of the projects and disincentives to the contractors for the delay in projects as well[1].

Delay in completions is one of the major problem in highway construction projects in Sri Lanka and all around the world as well[2]. As a result of delay in completion a huge amount is wasted by the government (by additional traffic control measures & maintenance) and road users (Road User Cost - RUC). Also Work zones formed by construction works lead to delay in travelling to road users. Main inconvenience causes by the work zones to the road users in urban area is the delay in travelling. Proper management of available lanes to road users is a major role of the contractors and they fail to maintain it properly in Sri Lankan practice because the contractors do not consider the inconvenience to the public and additional cost borne by the road users. This study will estimate the additional cost borne by the road users as a result of high way work zones in urban upgrading projects in Sri Lanka.

M.H.M. Hamsath B.Sc. Eng. Hons (Moratuwa)

Eng. (Dr.) H.R. Pasindu, B.sc. Eng. Hons (Moratuwa), Ph.D. (NUS)

Senior lecturer, Department of Civil Engineering, University of Moratuwa.



2. Objectives

Since there are no prior studies available on the estimation of WZRUC in Sri Lanka, the objective of this research is to estimate the WZRUC as a percentage of total construction cost of the project in urban upgradation projects in Sri Lanka. A case study is done in 05 selected urban upgrading roads with work zone and the WZRUC is estimated as a percentage of total construction cost of the project.

3. Literature Review

WZRUC is a combination of Travel delay cost, Vehicle operating cost, emission test and Accident cost as described in previous literatures.[2]&[3]

3.1 Estimation of WZRUC

There are no specific studies available on the evaluation of WZRUC in Sri Lankan practice. This research produces a method to evaluate the WZRUC for Sri Lankan urban upgrading projects. When a road is upgrading, at the economic analysis of benefit cost analysis the major benefits are considered as Travel time reduction, reduction in Vehicle operating cost, reduction in Vehicular emission and reduction in accident costs. For the evaluation of WZRUC this approach is used to estimate the additional cost borne by the road user as a result of work zones.

The benefits are estimated according to the report of Assessing Public Investments in the Transport Sector [2] the estimations are available in Rupees value in 2000. Estimation of Travel time saving - It is estimated by the potential time saving after the project implementation, Estimation of Value of time - The report described the value of time for passenger vehicles and freight consignee differently. Vehicle operating cost was estimated by HDM -III model for passenger car. The following inputs were added as cost of inputs - Fuel cost, Lubricant cost, Tires, Maintenance labor, Maintenance parts and crew costs. Relationship between speed, roughness and costs has not been developed for Sri Lanka. The most detailed work done to date

was by the road user charges studies, which calculated roughness - cost relationships for eight representative vehicle type using HDM-III models. Emission cost was estimated according to the fuel consumption rate (from HDM-III model) and the amount of pollutants per liter of fuel consumed.[4] The cost of pollutants was estimated for four pollutants (CO, NO_x, SO_x& PM) - emitted by thermal power generating projects. Current exchange rate was used to convert the value for Sri Lankan values[5]. Accident cost was also estimated according to the damage type from the accident. Since there are no studies available on estimating accidents in work zones, this cost is neglected in this research.

3.2 Application of WZRUC

Feasibility studies -At the feasibility analysis WZRUC analysis should be considered whether the project is going to be a real benefit to the society. Likewise, at the Benefit cost analysis WZRUC should be included to estimate the real benefits from the upgradation.

Selecting the contract type - Delay in completion has been a major issue in the delivery of highway construction projects in Sri Lanka. Delay in highway projects do not only result in cost over turn but also cause adverse economic impacts and disruptions on public travelling. The Highway agency in United States provides measure to shortening project delivery to manage the overall impacts of construction delays and associated road user costs by evaluating WZRUC and shorten the construction time by selecting various contract types.

- Incentives/Disincentives for early/late completion -

In this approach, the Contractor is required to complete the project by the Engineer's estimation of the contract time specified in the bid document. Upon completion the contractor is rewarded with bonus payments for early completion and penalized with disincentives for late completions. The incentive payments should be higher than the additional costs incurred by the contractor for accelerating the work.

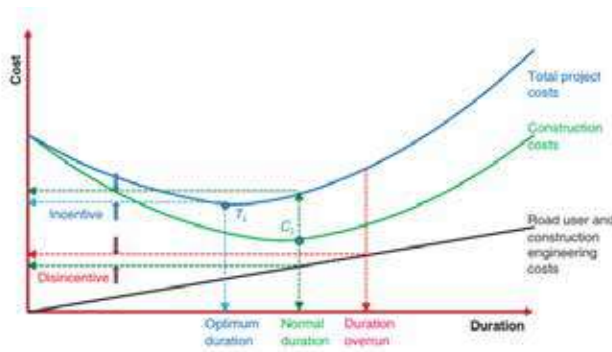


Figure 1- Relationship between project cost and duration

- Lane rental – The contractor pays a rental fee for the time period for a lane when it is closed for traffic as a result of work zones. This is intended to minimize the disruption of the work zone traffic and to motivate minimum use of lanes for construction activities. The owner agency determines the numbers and the duration of the lane closures. The lane rental fee is estimated using the WZRUC of the closure period. Therefore, contractors are motivated to close the lane in off peak hours because of low WZRUC in off peak hours. In some cases, the contractor may be allowed to propose the required amount of closure time and number of closures in their bid submissions. Generally, lane rental is suitable when detours are long, unavailable, impractical, or when peak hour traffic is impacted adversely. It is well suited for multiple lane roads with high traffic volumes where there is flexibility for intermittent or temporary lane closures to keep at least one lane open to traffic through the work zone. Typical projects include mill and overlay, temporary widening, patching, diamond grinding, dowel retrofitting, reclamation and recycling, guardrails, striping, signing, bridge painting, crack sealing, signal systems, and traffic management projects. Lane rental is not appropriate for the projects where long-term permanent lane closures are required, such as bridge re-deck or concrete rehabilitation projects.
- A+B Bidding – Allow the agency to request bids for the cost of work items and the time to complete the work and procedure them in

a single contract. This method involves two components –

Cost (A) – The dollar amount of contract items (Equipment, material & Man power) for all works to be conducted under traditional low – Bid contract.

Time (B) – The dollar for the component of a contract, estimated by multiplying the number of calendar days to complete the work by the daily road user cost.

Bid Value = (A) + (B * Daily road user cost)

The contract is then awarded to the lowest bid value for contract award. This formula is not used in determining the payment to the contractor. The contractor receives incentives for early completion and is required to pay disincentives (and liquidated damages) for delaying beyond the completion date agreed in the contract. Generally, A+B bidding is suitable for time-critical projects such as high-traffic volume roadways, business, tourist, and environmentally sensitive areas. Typical projects include new/reconstruction, rehabilitation projects, simple bridge replacement projects, detour projects, intersection upgrades, and bridge rehabilitation projects.

4. Methodology

4.1 Scope

- 05 numbers of urban upgrading roads were selected for the case study
 - B295 – (2+620 km – 5+120 km)
 - B389– (5+700 km – 7+840 km)
 - B267– (0+000 km – 6+150 km)
 - AB10 – (8+650 km – 9+100 km)
 - Old Kottawa road– (0+000 km – 1+900 km)
- 02 Segments were identified along each road – Normal segment (Before upgradation), Work zone.
- All other relevant details of the project were collected (Type of upgradation, duration, project cost & length of the road to be upgraded)

- Speed survey was done by video matching method in each road, each segment in a peak and off peak hours.
- From the speed survey - Vehicle count, Average Speeds of different vehicles, and reduction in speeds from a normal segment to work zone was calculated in peak and off peak hours.
- Road user cost values are updated to 2016 values by the guideline to estimate the road user costs from the Department of National Planning (DNP).
- WZRUC cost was evaluated and compared with the total project cost.

4.2 Data collection

Table 1 - Result of speed survey in B295 road in peak hour

Peak hour 5.00 pm - 6.00 pm				
Vehicle	Nos	Percent age	Average Speed (kmph)	
			Normal	Work zone
Car	416	29%	25	10
3 Wheel	373	26%	30	13
Mo. Bike	458	32%	40	25
Bus	57	4%	22	8
Truck	43	3%	22	7
MGV	85	6%	25	10

Table 2 - Result of speed survey in B295 road in off peak hour

Off Peak hour 10.00 am - 11.00 am				
Vehicle	Nos	Percentage	Average Speed (kmph)	
			Normal	Work zone
Car	180	20%	40	15
3 Wheel	283	31%	35	20
Mo. Bike	326	36%	50	30

Bus	32	4%	37	12
Truck	17	2%	35	10
MGV	65	7%	40	15

From the speed survey - Speeds were close to the speeds in the B295 road in other roads as well.

4.3 Estimation of RUC in 2016 values

4.3.1 Travel Delay cost

Travel delay cost is calculated by multiplying the additional delay to passenger vehicle and freight consignees caused by the work zone (hr) by the value of time (Rs / hr).

4.3.2 Delay time calculation

Delay time = Time taken to travel in effective work zone - Time taken to travel in normal road

Some assumptions were made to calculate the delay time cost in this research case study. They are,

- Effective work zone length = (150 + 100 + 150) = 400 m (Average queue length observed in peak time was 150 m & length of work zone is 100 m)
- Queue were formed in peak hours only & no queue in off peak times
- Peak day time (07.00 -10.00), off peak day time (05.00 - 07.00 & 10.00 - 16.00), Peak evening time (16.00 - 19.00) & off peak evening time (19.00 - 23.00)
- Evening 23.00 pm - morning 5.00 am no value was assumed
- Its assumed that Saturdays = 75% of week day value and Sunday = 25% of week day value (6 week days per week)
- Only one work zone exist along the road at a day and construction works equally interrupt the users along the entire construction period.

4.3.3 Monetary Value of time

The monetary value of travel time is defined in Federal Highway Administration [1] as it is based on the concept that time spent traveling otherwise would have been spent productively, whether for remunerative work or recreation.

Saving in travel time is major concern in upgrading a road. The system used in Sri Lanka to estimate the saving in travel time while upgrading a road is based on a survey/estimation done in 2000 by the DNP[2]. This research updates the monetary values according to the DNP guideline to 2016 values. The monetary value of time is calculated in two categories, Passenger Vehicle and Freight consignees.

4.3.3.1 Passenger Vehicles

Travel time saving for the passengers is the most important aspect when considering the benefits from the urban upgrading road projects. When we consider the work zone stage of an upgrading work, the additional travel time spend in the road is more significantly affects the road users than the other factors. From the analysis done by the DNP of the Ministry of finance and planning, the value of travel time depends on the passenger income and the purpose of the trip. The value of time of the same person undertaking trips for different purposes can vary accordingly. VoTC is calculated on the basis of

- Hourly income rate of the passengers
- Trip purpose of the passengers
- Quantum of travel time saved

▪ Hourly Income Rate(HIR) of the passengers

Hourly income rate is determined by obtaining the average annual income for the user and dividing by the number of working hours per year.

$$\text{HIR} = \frac{\text{Monthly income (Rs/month)} \times 12 \text{ (months in a year)}}{2000 \text{ (hrs/year)}}$$

Table 3 - Monthly income rate comparison

User group	Assumed Income Group		Mean monthly Income (Rs)		HIR Rs/hr
	1999	2015	1999	2015	2015
Car	10 th Decile	8 th - 10 th Decile	21,465	685	411
Motor bike	7 th &9 th Decile	4 th - 7 th Decile	4770	316	190
Three wheel	NA	5 th - 8 th Decile	NA	385	231
Bus	1 st to 8 th Decile	1 st - 7 th Decile	3387	243	146

*NA - Not Available

- Weighted Hourly Income (WHI) - HIR depends on the average income of the respective group. However, mobility indices for travel time in Sri Lanka, which means higher income earners within a particular user group make relatively more trips than lower income earners in the group. Therefore, Hourly income rate is multiplied by 1.5 to adjust for mobility

$$\text{WHI} = \text{Mean monthly Income of user group (Rs/Month)} \times 1.5 \times 12 \text{ (Months/year)} / 2000 \text{ (hrs/year)}$$

▪ Trip purpose

As the literature reveals trips undertaken in working time and hence referred to as work time trips, should be valued at the hourly income rate plus an allowance for employer's overhead.

$$\text{Work time VoTC} = \text{Hourly income rate} \times 1.2$$

$$\text{Non Work time VoTC} = \text{Hourly income rate} \times 0.2$$

Table 4 - Assumption of work time trips percentage

User group	In 1999	In 2016			
		Mor. Peak	Day Off peak	Eve. peak	Night time
Car/Je	15 %	85 %	40 %	75 %	5 - 10 %



ep					
Mo. Bike	10 %	80 %	55%	70 %	5 - 10 %
3 wheel	NA	80 %	45 %	65%	5 - 10 %
Bus	4 %	60 %	15%	55%	5 - 10 %

Value of User group = WHI of user group x (1.2 x Percent of Work Trips + 0.2 x Non - Percent of Work Trips)/100

▪ Quantum of travel time saved

In some circumstances even a smaller value of travel time can have very high value (E.g.: - Salary reduction for late arrivals) this reflect value of reliability rather than value of time per second. But in this study it is not considered and assumed that the value of time is randomly distributed.

Table 5 - Monetary value of time in 2016

User group	WHI	Value of time (Rs/hr) - 2016			
		Morning Peak	Day Off peak	Eve ning peak	Nig ht time
Car	617	687	392	621	180
Motor Bike	285	302	227	272	83
Three wheel	356	377	245	321	104
Bus	219	186	81	174	64

4.3.3.2 Freight Consignees

Table 6 - Capacity of freight vehicles & Value of freight

Type of vehicle		Percentage	Capacity (tons)	Cost/ ton/hr
Medium Good Vehicle (MGV)	Delivery Vans	35 %	0.5	Rs 1200
	Small truck	65 %	1-2	Rs 1000
Large Good Vehicle (LGV)	Medium Truck	75 %	5-15	Rs335
	Large Truck	25 %	15-40	Rs215

Travel time is an important function in the movement of freights as well. Increased travel time induces higher transport cost.

▪ Value of time (VoT) = Number of trucks x (Corresponding) Percentage x (Corresponding) Capacity x (Corresponding) Cost per ton per hour.

▪ VoT for Perishable Commodities

Perishable commodities can have an additional VoT arising from the prevention of deterioration in quality of the product being transported. From the user estimates the following values assumed.

Table 7 - Cost of refrigeration

Size of truck	Cost of Refrigeration (RS per hr)
Small (0.5 -2 ton)	150
Medium (2- 10)	250

It is assumed that 50 % of Delivery vans and 25 % of Small trucks are transporting Perishable commodities.

- Average VoT of a freight vehicle (MGV) = (0.35 x 0.5 x 1200 + 150) + (0.65 x 1.5 x 1000 + 250) = **1640 Rs/hr**
- Average VoT of a freight vehicle (LGV) = (0.75x10x335) + (0.25 x 25 x 215) = **3850 Rs/hr**

4.3.4 Vehicle Operating Cost

Vehicle operating costs are fuel cost, lubricants cost, tire depreciation, labour and parts for repair and maintenance, operator (crew) labour if applicable, depreciation and interests and overheads such as insurance and license fees and administration. From a HDM - 4 model developed in 2016, it is concluded that, VOC in 2016 is 3.165 times greater than VOC value in 2000[6].

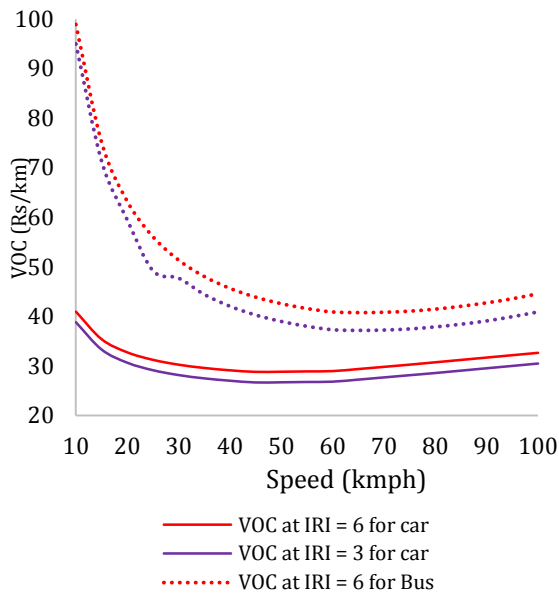


Figure 2 - VOC comparison of Passenger cars and Bus

4.3.5 Vehicular Emission Cost

Transport activities lead to air pollution directly from emission and indirectly from refining petrol and diesel. The following components are from vehicle emission to the air - Ozone, Carbon Monoxide (CO), Particulate Matter (PM), Lead, Carbon Dioxide, Methane, Hydrocarbons and Sulphur oxides.

From a research of Vehicle Emission Inventory for Sri Lanka[7] conducted by Liyange, the following graph was drawn for the Carbon Monoxide (CO) emission from passenger car at different speeds. Other emission gases also follow very similar pattern. Since there are no researches available on vehicle emission studies, this study assumed that the emission ratio at speed 10-15 kmph is 3 times greater than speed 40 kmph. For the estimation of Emission cost, it is assumed that vehicles are moving at 40 kmph speed in normal road segment and 10-15 kmph speed in Work zone.

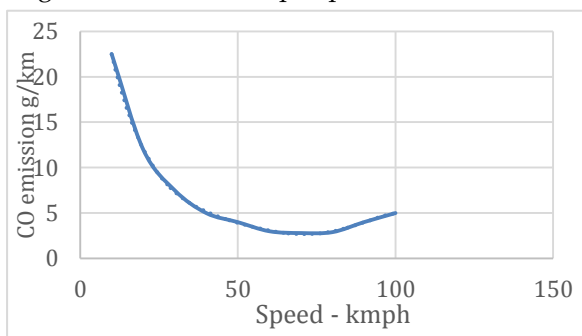


Figure 3 - CO Emission rate with speed for passenger car

- Estimation of emissions per liter of fuel consumed

The estimation of emissions per liter of fuel consumed is based on DNP guideline and the monetary value of emissions were estimated from the Caltrans report of California Department of transportation.[8].The monetary value of emissions is defined as “Emission costs are social costs that are borne directly by the road users, but are estimated based on the impact borne by the society in general”. There is no consensus on how to assign a dollar value to quantify the impact of each pollutant type. Unit cost of emissions typically used in practice is derived based on the economic analysis of health impacts caused by air pollutants and greenhouse gases.

- Estimation of cost of emission per liter of fuel consumed was calculated by multiplying grams of emission per pollutant, by respective costs of damage.
- Estimation of cost of Emission per kilometer by vehicle type at 40 kmph were calculated by dividing the cost of emission per liter fuel (Rs/l) by fuel consumption rate (km/l) [(Rs/l) / (km/l) = (Rs/km)]. Fuel consumption rate was calculated from the HDM - 4 model

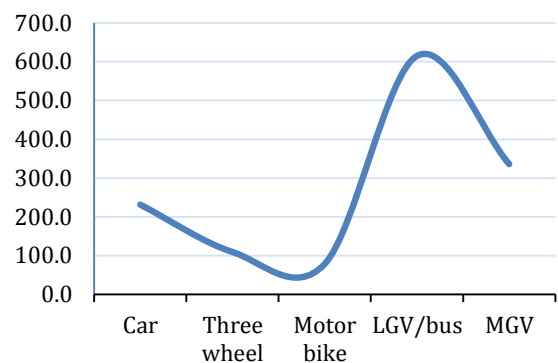


Figure 4 - Emission cost at kmph speed (Rs/1000km/veh)

5. Results

- Speed survey & Speed reduction percentage

From the speed survey - Speed reduction from normal segment to work zone was analyzed and there was a significant reduction in speeds in work zones were identified.



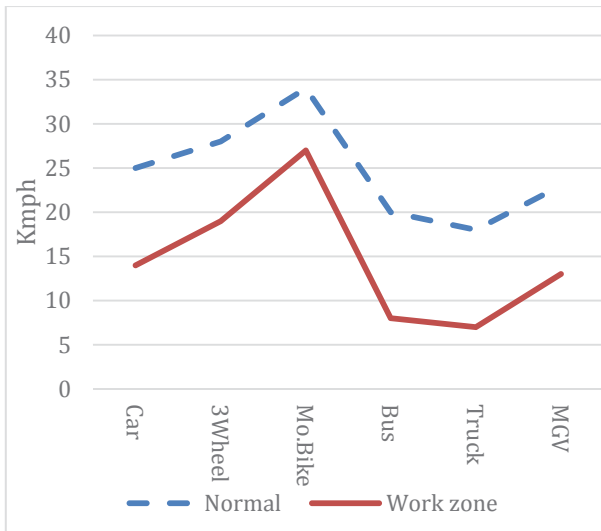


Figure 5 - Speeds in Normal road and work zone in B295 road

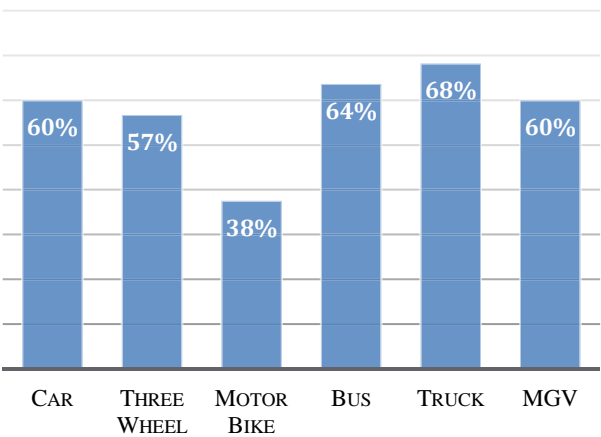


Figure 6 - Speed reduction from normal road to work zone in peak hour in B295

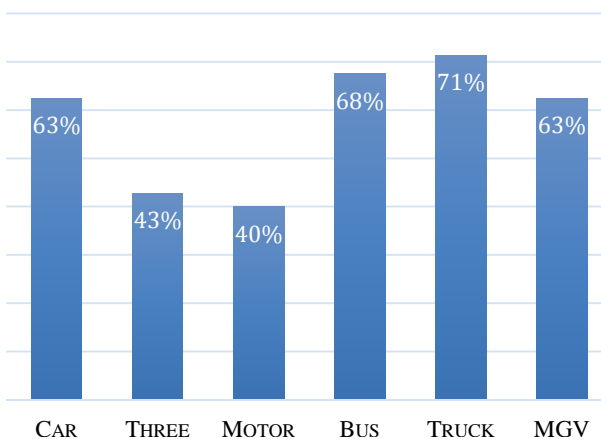


Figure 7- Speed reduction from normal road to work zone in off peak hour in B295

- Estimation of work zone travel delay cost - The speeds in work zone and normal road segment are calculated from the speed survey and the work zone travel delays for different vehicle are estimated. The travel delay cost is calculated by multiplying the delays by monetary value of time for different vehicle types.

Table 8 - Estimation of work zone travel delay cost

Road	Travel delay Cost
B295	Rs. 58,159,960.00
B389	Rs. 53,389,771.00
B267	Rs. 25,877,947.00
Old Kottawa road	Rs. 20,158,396.00
AB 10	Rs. 41,933,546.00

- Estimation of additional VOC - The speeds in work zone and normal road segment are calculated from the speed survey and the road roughness (IRI measurement) is measured by Roadroid Android application and it is concluded that, the road roughness in work zones are IRI = 6 and road roughness in normal segment IRI = 3. The vehicle operating cost for different speed and different vehicles are adjusted to 2016 monetary values.

Table 9 - Estimation of additional VOC

Road	VOC
B295	Rs. 18,967,084.00
B389	Rs. 21,463,383.00
B267	Rs. 14,971,848.00
Old Kottawa road	Rs. 7,667,771.00
AB 10	Rs. 12,277,143.00

- Estimation of additional vehicular emission cost - The speeds in work zone and normal road segment are calculated from the speed survey and additional emission cost is calculated as described above in methodology.

Table 10 - Estimation of additional vehicular emission cost

Road	Emission Cost
B295	Rs. 13,391,817.00
B389	Rs. 17,520,958.00
B267	Rs. 9,858,991.00
Old Kottawa road	Rs. 8,709,446.00
AB 10	Rs. 14,690,224.00

- Estimation of WZRUC - Is the addition of Travel delay cost, Vehicle operating cost & Emission cost caused by the work zones. Following table elaborates the summary of Work zone Road user cost in different work zones.

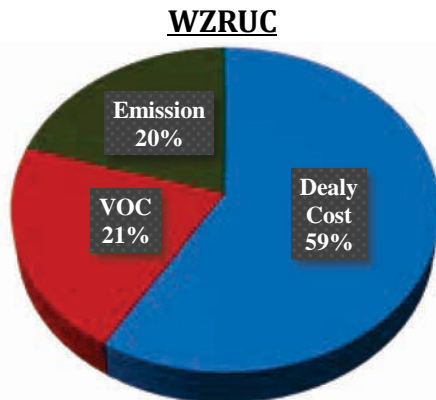


Figure 8 - Estimation of WZRUC

- Comparison of WZRUC with Total Construction cost is the major indication of the impacts of the WZRUC Evaluation and the scope of this research as well. When comparing the real economic benefits from an upgradation project, this kind of negative impacts should be included to the benefit cost analysis of upgradation projects and with the identification of the impacts by the work zones, the work zones can be managed efficiently. Following table shows the comparison of WZRUC with construction costs in prices for different work zones.

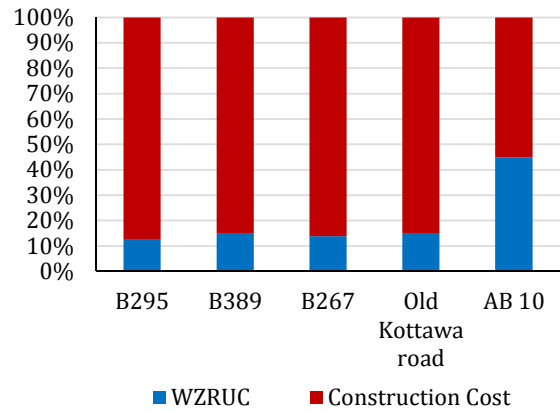


Figure 9 - Comparison of WZRUC with construction cost

6. Conclusion

The WZRUC is varies from 13 – 45 % compared to the total project cost and the major component of the cost is travel delay cost which is around 60% of the WZRUC and 08- 27 % of the project cost. The WZRUC is affected by the traffic volume of the road, Vehicle composition, Project duration and Type of upgrading works. When we consider the first four roads (B295, B389, and B267 & Old Kottawa road) the percentage of WZRUC compared to total project cost is almost same and which is in the range of 12.7 – 15.1 % of the total project cost. It is huge amount borne by the road users as a result of the work zone activities in urban upgradation projects. Since these roads are rehabilitating roads (road widening) it can be concluded that the WZRUC is within the range of 12.7 – 15.1 % of the project cost. Since the total project cost is comparably low for pipe laying projects (Water and waste water management) the WZRUC is very highin percentage of the total project cost. It is recommended to develop a proper work zone management plan for all the upgradation projects in urban areas in Sri Lanka. When considering two, similar traffic volumes with different upgradation works performing roads, WZRUC for a unit duration is same but when comparing with the project cost, the percentage of WZRUC is getting higher for low project cost works. The condition of temporary lanes allowed for traffic movement is maintained at very poor level and traffic management schemes are not implemented often.



7. Recommendation

- Improving monitoring mechanism to ensure work zone management practices are implemented.

Since The Road Development Authority is the client for all the road projects, they have to implement a proper monitoring mechanism to confirm the work zones are properly managed in a way to reduce the WZRUC by increasing the mobility in work zones. The mobility cannot be increased at all the times but it should be maximized.

- Providing incentives to contractors to work during off peak hours and expediting project completion.

Motivating the contractors to complete the project with optimum duration by providing incentives if they complete the project early and deduction of disincentives for the delays.

- Selecting a proper contract method when requesting for bids. The impact of WZRUC is included in some contract types described in Application of WZRUC. With the identification of the impacts of the WZRUC, contractors will be encouraged to reduce the WZRUC as much as possible.
- Reviewing and updating the existing guidelines on work zone management.

5. Munasinghe and Meier, "Incorporation Environmental Concerns into Power sector Decision Making - A case study of Sri Lanka," Environmental Policy and Research Division, 1992.
6. Ranawaka, D. "Estimating the Vehicle Operating Cost used for Economic Feasibility Analysis of Highway Construction Projects," in *Moratuwa Engineering Research Conference 2017*, Moratuwa, 2017.
7. Preethika, L. U. "Vehicle Emission Inventory for Sri Lanka," 2005.
8. Department of Transportation -California,, "Caltrans estimates," Californiya, 2011.
9. Highway capacity Manual, Washington DC, 2000.
10. Mallela J, and S. Sadasivam, "Work zone road user cost Concept and Application," US Department of Transport, 2011.
11. D. o. N. Planning, "Assesing Public Investment in the Transport sector," 2000.

Acknowledgement

Authors would like to express their gratitude to all the individuals and organizations, which help to accomplish this research.

References

1. FHA, F. H. A. "Work Zone Moblity and Safety program - Work Zone Road User Cost," U.S. Department of Transportation, Washington, 2012.
2. Department of National Planning, "Assesing Public Investent in the Transport Sector," Ministry of Finanace and Planning, 2000.
3. Federal Highway Administration, "Work Zone Moblity and Safety program - Work Zone Road User Cost," U.S. Department of Transportation, Washington, 2012.
4. NBRO - Environmental Division, "Air pollution from motor vehicles," 1998.

Development of a Methodology for Road Maintenance Planning of Low Volume Roads Based on Roughness Data

M.A.D. De Silva and H.R. Pasindu

Abstract: Sri Lanka has one of the highest road densities in the region, with most regions in the country having connectivity to a road network. Successive governments have invested billions of rupees to upgrade or expand the national road network, especially at provincial or local government level to improve the accessibility in rural areas. However, there is no systemic process in place to maintain these roads. Often maintenance is done on ad-hoc basis and there is high political influence and other societal pressure. The main reason is the lack of a maintenance management system, budgetary constraints and lack of resources to evaluate the condition of the road and make objective decisions with regard to implementing maintenance work. The study proposes a new methodology to assist local authorities make decisions on maintenance works considering the existing condition and cost of repair works. The existing condition is measured via smartphone based pavement roughness measurement method. These roughness values are correlated to representative cost values using HSR based on distress and roughness data. This can be used to select roads for maintenance works based on the current road condition as well considering the budgetary constraints. Using a prioritizing criteria and optimization methods such as integer programming, proposed in the study, candidate roads for maintenance can be selected. The methodology will provide an objective process to make maintenance decision making which allow the authorities to optimize their budget utilization and improve the network road condition.

Keywords: Low volume roads, pavement roughness, pavement maintenance, decision support system, maintenance budget

1. Introduction

Low volume roads (LVR) provide the primary links to the national highway network. They provide connectivity from homes and farms to markets, and they provide public access to essential health, education, civic facilities etc. These are critical to economies locally and nationally in all countries of the world. Low volume roads are defined as roads having an average daily traffic (ADT) less than 400 vehicles per day but typically roads with ADT up to 2000 is considered in this category [4]. Many low volume roads consist of single lane with gravel or even more native surfacing. In Sri Lanka there are about 70% of low volume rural roads among all the roads while 30% is the other highways. Very few data concerning LVR performance, use, cost and so forth is available within road agencies [7]. Fewer the road users, lesser the funding for LVR maintenance, restoration. Insufficient funding and inconsistent fund allocation is the most relevant issue associated with LVRs. Another major issue with financing and planning LVRs is the shortage of sufficient data. With incomplete data, investment strategies and funding justifications are fairly weak, and

agencies are unable to define priorities, quantify disinvestment, or support maintenance needs [4].

There is no adequate maintenance planning for low volume roads in Sri Lanka. Most of the time maintenance is carried out often on ad-hoc basis, due to external influence, lack of proper plans, and irregularity of funds. One reason for this is the lack of consistent objective method to evaluate the pavement condition and a simple tool/guideline to help local agencies to make decisions with regard to maintenance work.

In consideration of the above, road roughness, can be considered as a good indicator of pavement condition, provided that roughness measurements can be gathered at a low expense and with lesser manpower. Using the roughness data, road agencies are able to decide on the required maintenance operation for the road and thus, prepare a preliminary budget for the maintenance work with

Mr. M.A.D. De Silva, Undergraduate, Department of Civil Engineering, University of Moratuwa.

Eng. (Dr) H.R. Pasindu, Senior Lecturer, Transportation Engineering Division, Department of Civil Engineering, University of Moratuwa, pasindu@uom.lk



prioritizing of the road considering its condition.

2. Literature Review

2.1 Pavement Roughness

Pavement roughness is generally defined as an expression of irregularities in the pavement surface such as potholes, depressions, cracking, rutting, ravelling etc. Pavement roughness affects in many ways such as ride quality, vehicle delay cost, safety, asset management, fuel consumption and maintenance cost etc. Globally accepted indicator to measure pavement roughness is International Roughness Index (IRI). It is also possible that future pavement conditions might be more accurately predicted from the components of the index [3].

International Roughness Index was developed by World Bank in 1982. The IRI was first recommended as a standard for roughness measurements at the International Road Roughness Experiment conducted in 1982 [12]. International Roughness Index (IRI) is a scale for roughness based on the simulated response of a generic motor vehicle to the roughness in a single wheel path of the road surface. Its true value is determined by obtaining a suitably accurate measurement of the profile of the road, processing it through an algorithm that simulates the way a reference vehicle would respond to the roughness inputs, and accumulating the suspension travel.

Roughness can be measured in several ways depending on the accuracy of the measurement. Profilometers, Response type road roughness meters (RTRRMs) are examples that require high capital cost and high maintenance cost, but these methods produce very accurate measures. Profiling devices are used to provide accurate, scaled, and complete reproductions of the pavement profile within a certain range. They are available in several forms, and can be used for calibration of RTRRMs [8]. But these methods have few limitations when implementing to low volume roads. These devices are mounted on to a standard vehicle and the vehicle has to travel in the respective road to obtain the measures. Most of the time, it is not practical to travel in such vehicles in low volume roads as they do not provide sufficient space for the vehicle to travel. For low volume roads in Sri Lanka, a cost effective, more

accessible and simple method is applicable for measurements.

As a solution to this, there are new methods developed in order to obtain road roughness data. One such popular example is using smartphones for road roughness estimation [5]. Using smartphones to collect data is a promising alternative because of its low cost and ease of use. Moreover, smartphones are very popular devices all over the country, thus the technology easily accessible to any road agency. Furthermore, a non-technical employee of an organization can operate a simple mobile application and collect the required roughness data, thus reducing the burden on the technical staff which is often in shortage in the provincial level road agencies.

2.2 Low volume road maintenance management

There are many issues when authorities try to implement these maintenance works. Some of the issues would be [2],

- Insufficient road maintenance funding
- Limited construction material
- Limited capacity and number of qualified staff
- Inadequate maintenance
- Lack of decision supporting system.

Typical types of distresses that were observed on the sample of roads selected for the study are fatigue cracking, block cracking, edge cracking, longitudinal and transverse cracks, potholes, rutting, ravelling etc. The evaluation of current condition of the pavement and selection of the correct maintenance type is vital to ensure the functionality of the roads. By introducing a proper pavement management system, better decisions can be made in order to optimize the pavement condition with maintenance work.

Pavement management system performs an analysis of the collected rating data and reports on the current and projected condition of the road system in order to evaluate the effectiveness of the planning and funding priority and provide guidance in decision making process [9].

Using a pavement management system, there will be effective and efficient directing of the various activities involved in providing and sustaining pavements in a condition acceptable to the traveling public at the least life cycle cost.

[1] According to research, it has shown that it is far less expensive to keep a road in good condition than it is to repair it once it has deteriorated. Pavement management system performs the tasks of inventorying pavement conditions, identifying good, fair and poor pavements, assigning importance ratings for road segments, based on traffic volumes, road functional class, and community demand, scheduling maintenance of good roads to keep them in good condition and scheduling repairs of poor and fair pavements as remaining available funding allows.

There are key measures used to define the condition of a pavement [13].

- Roughness
- Surface Distress
- Structural Capacity
- Surface Friction

Roughness is directly related to both user satisfaction and user cost. It is an integral component of the pavement quality assessment in a PMS. In addition, as discussed earlier with the smart phone base application, roughness measurements can be gathered within a budget constraint and less manpower in data collection.

3. Evaluation of roughness of low volume roads and assessing road condition

Roughness and distress data collection of low volume roads were carried out covering few districts in Sri Lanka such as Kandy, Galle, Matara, Kurunegala, Kaluthara. Roads for data collection were selected to include, low volume roads with varying lengths, pavement conditions and pavement types. 20 number of roads were selected for the purpose of the study.

For the data collection the study follows the method proposed by Gamage et.al., 2016 [6]. The android mobile application, "Roadroid Classic" is used in getting roughness measurements. Smartphone equipped with this app is fixed on the windshield of the vehicle keeping in a steady position. Thus, we assume that the acceleration coordinates of the vehicle and smartphone are the same. A Toyota Hilux 4WD cab is used in data collection as most of the road agencies in Sri Lanka use such vehicles in their field work.



Figure 2 - Capturing the road condition using video

Figure 1 - Roughness Measuring from "Roadroid Classic"



Time	Latitude	Longitude	Altitude(m)	Speed(km/h)	IRI(m/km)	Grade (%)	IRI	IRI	RoadId
11/20/2018 9:42	7.28012323	80.8903888	260	20.85	484.77	-2.37	0.12	0.20	sdmatalana rd
11/20/2018 9:42	7.27948184	80.8904712	285	20.85	484.77	0	0.12	4.55	sdmatalana rd
11/20/2018 9:42	7.27912467	80.8904712	200	20.85	484.77	0	0.12	4.55	sdmatalana rd
11/20/2018 9:42	7.28077987	80.8905218	240	20.86	484.9	0	0.79	1.95	sdmatalana rd
11/20/2018 9:42	7.27948184	80.8904712	268	21.52	484.77	0.12	4.61	1.88	sdmatalana rd
11/20/2018 9:42	7.27948184	80.8904712	232	23.35	487.2	2.17	4.91	1.89	sdmatalana rd
11/20/2018 9:42	7.27847114	80.8903884	340	23.51	484.8	-0.5	1.01	1.58	sdmatalana rd

Figure 3 - Accelerometer data transferred to spread sheet

While traveling, the road surface is captured by a video camera for cross checking a validation. Roadroid Classic application is available in Google Play Store for free. This app registers the vibrations from the road and correlates to the International Roughness Index. It displays eIRI, cIRI and location data (speed of the vehicle, longitude, latitude and Altitude). The Application calculates eIRI for every 20-meter road section. Roadroid application can only calculate eIRI when driving speed of experiment vehicle is 20 kmph or faster. After calibrating the smartphone, accelerometer data from the app is obtained and transferred to spread sheet. Then those spreadsheets are thoroughly checked and IRI values are matched to the location of the road for the respective IRI using the images from the video camera. This is done for assessing of the current condition of the road. Table 1 shows how sample roads are evaluated using Roadroid Classic app, which shows that it gives satisfactory roughness values.



Table 1 - Sample of estimated IRI from mobile application and condition of the Kuliypatiya - Bowatta road

Road section	IRI from mobile application	Road Condition
	1.5	Excellent
	13.0	Very Poor

4. Determination of typical maintenance cost for low volume roads

Along with the roughness of the road, the distresses that are present in the road section are recorded as well. Based on the existing distresses, the corrective maintenance treatment required can be decided by the maintenance engineer or decision criteria as given in the Road Development Authority National Road Master Plan [10].

The representative cost of the identified maintenance treatment for each road section is estimated using the HSR (Highway Schedule of Rates) [11]. Sample rates in HSR are as follows.

Table 2 - Sample rates in HSR

Proposed maintenance operation	HSR-2016 Item No	Cost (Rs.)
Pothole patching	MS1-002	209 per sq.m
	MS1-007	949 per sq.m
	MS1-008	905 per sq.m
Patching ruts	MS1-011	1202 per sq.m
	MS1-010 +MS1-010A	1,433 + 24 =1457per sq.m
Sand Sealing	S1-036	135 per sq.m
Edge Repair	MS1-015	1485 per sq.m

This will give representative corrective maintenance cost for each road section evaluated, along with its roughness value. Furthermore, sections are categorized into IRI ranges such as IRI <2, 2-5, 5-7, 7-10, 10+ to indicate the condition of the roads that are selected such as very good condition, satisfactory, poor condition, very poor condition respectively.

From the data available, the average maintenance cost variation with IRI is plotted in Figure 4. The analysis also be extended to estimate average cost for each IRI range (representing different road condition categories), which is given in Table 3.

The information can be used to make preliminary estimates on the maintenance budget requirement for each road section, based on its roughness value.

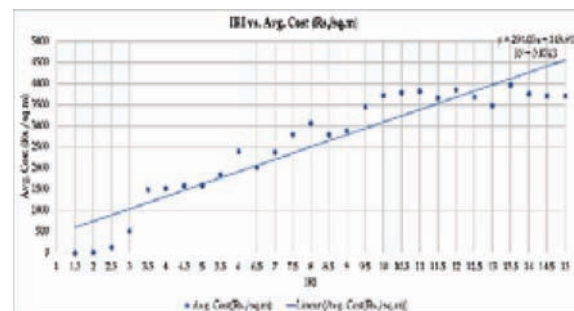


Figure 4 - IRI vs. Maintenance Cost (Rs./sq.m) Plot

Table 3 - Cost per sq.m in Rs. for IRI ranges

IRI Range	Avg. Cost
<2	6.43
2 to 5	1,158.41
5 to 7	2,172.57
7 to 10	3,097.85
>10	3,766.13

5. Selection of roads for maintenance based on roughness data

5.1. Prioritizing roads based on pavement condition

In order to select the priority of a road to be selected for maintenance work, there should be a proper prioritization criteria. Roughness, safety, importance of road and traffic etc. can be the criteria which are considered in

prioritization. Among them roughness data can be used in the preliminary stage as data collection and analysis is rather easy and cost effective. This is especially relevant for local authorities who have resource limitations to implement large scale pavement evaluation schemes.

Considering the IRI values of the road sections, they are ranked from worst roads to best roads. The roads can be selected based on the three ranks until the budget is utilized.

Table 4 - Maintenance Priority

IRI Range	Condition	Priority Rank
>10	Very Poor	1
7-10	Poor	2
5-7	Fair	3
2-5	Good	4
<2	Excellent	5

However, simple ranking of road sections based on road condition alone does not accurately represent the overall network condition, the minimum standards that should be maintained etc. Furthermore, this method may not be able to account for other parameters that should be incorporated in prioritizing roads.

5.2. Selection of candidate roads using optimization methods

Optimization based approach alleviates some of the problems identified in earlier section. For example, the proposed Integer Programming model can be used to select candidate roads for maintenance. Lingo software was used as the Integer Programming tool in this research. It is a comprehensive tool designed to make building and solving Linear, Nonlinear, Quadratic etc and Integer optimizations models [14].

Objective function of the model is to minimize the network roughness value, i.e. improve the network road condition.

$$\text{Objective function: } \min \sum_{i=1}^n \text{IRI}(2) * X(i) * L(i)$$

where i is the road section no, n is number of all road sections in the network, IRI(2) is IRI after maintenance (to be defined at the time of selecting the maintenance treatment for road i), L(i) is the length of road section i and X(i) is 1 if the road is selected for repair and 0 if the road is not selected for repair.

Other aspects such as safety, road hierarchy (roads used to access civic centres) can be incorporated into the objective function with priority factors.

Constraints can be included to represent the other requirements the authority seeks to implement. For the model proposed in this section the following constraints are given.

$$\begin{aligned} \text{IRI}(1) * X_i &\geq 4 \\ \sum_{i=1}^n X_i * C_i &\leq B \end{aligned}$$

where IRI(1) is IRI before maintenance, C_i is the cost of maintenance of road section i based on the maintenance treatment selected and B total budget.

6. Illustrative Example

To illustrate the proposed methodology the following case study is presented using the roads included in the study. There are 20 roads selected for the sample, and they have varying pavement conditions.

Total cost of maintenance for each road is determined using the regression model developed earlier. IRI after maintenance is formulated by considering types of operations, and the input of experienced highway engineers.

Table 4, shows the Worst first ranking of the road network is formulated considering the current average IRI of the road sections. The selection of the roads for maintenance depends on the budget available. For example, selecting all roads for maintenance would require approximately Rs. 950 mn. For the given budget of Rs. 500 mn road sections 6, 19, 16, 4, 2 and 3 is selected. Alternatively, the engineer could propose alternative maintenance treatments (which would change the cost) and change the number of roads selected considering the budgetary constraints



Table 5 - Worst first ranking of road sections for a budget of Rs. 500 Mn.

Road ID	Length [m]	Average IRI	IRI [after maintenance]	Total Cost [Rs.]	Cumulative Total Cost [Rs.]
6	5100	8	2	68,066,583	68,066,583
19	3120	8	2	40,017,734	108,084,298
16	13460	7	5	178,402,686	286,486,983
4	5140	7	5	39,933,846	326,420,829
2	380	7	2	4,221,378	330,642,207
3	9000	6	5	96,140,455	426,782,662
18	8980	6	6	115,171,954	
15	13300	6	5	160,325,688	
17	13080	6	2	130,383,620	
13	1020	6	2	12,786,877	
8	80	5	4	18,000	
11	160	5	4	1,796,000	
14	320	5	2	3,147,600	
10	460	5	2	3,972,675	
12	660	5	4	6,084,788	
9	300	4	3	2,006,700	
5	440	3	2	705,467	
7	540	3	2	4,307,040	
1	3340	2	1	19,901,181	
20	5960	2	1	31,309,370	

The proposed optimization model is then applied to select the roads. The selected and not selected roads from the Integer Programming model are given below.

Table 6 - Selected and not selected roads from Integer Programming

Selected Roads	Not Selected Roads
3*,4*,5,7,8,9,11,12,15,16*	1,2,6,10,13,14,17,18,19

*- roads selected under both methods

The results show that the both methods produce different results and second method includes a higher number of roads in the selected category.

The proposed methodology can also be adopted to estimate the required budget to,
 a) maintain all roads above a min IRI value – using the first approach, i.e prioritizing based on road condition;
 b) considering the network road condition (using a parameter such as network IRI)

As illustrated in Figure 6, as the budget allocation is increased the network IRI value can be reduced, thus indicating an overall improvement to the road condition in the network.

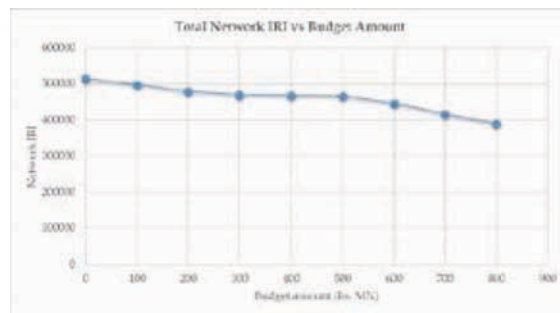


Figure 6 - Network IRI for various budget

7. Conclusion

The study has proposed a novel methodology to prioritize roads for maintenance planning for a low volume/provincial road network. Pavement condition evaluation is based on road roughness data that can be obtained easily using mobile application. Estimating budget requirement is based on the roughness value of the roads. A simplified prioritization method is given to select roads for maintenance planning considering both the condition and the budget availability. This can also be used to determine budget requirement and other factors can be incorporated to the optimization model to represent variables such as importance of the road, safety considerations etc.

This proposed approach provides a logical and objective methodology which can be implemented easily to select roads sections for maintenance planning. This study presents a decision support system for a maintenance engineer or decision makers to implement maintenance work in a local/ provincial road network without any external influence but with proper planning.

Acknowledgement

Assistance received from Mr. Lalith Sumanasiri (Road Development Authority) and Mr. Ajith Panagoda (Sabaragamuwa Provincial Road Development Authority) is acknowledged.

References

1. AASHTO. (1985). *Guidelines on Pavement Management*. American Association of State Highway and Transportation Officials, Washington D.C.
2. ADB. (2013). *2013 Annual Evaluation Review*. Asian Development Bank.
3. Camahan, J. V., ASCE, M., Davis, W. J., Shahin, M. Y., Keane, P. L., & Wu, M. I. (n.d.).

4. Coghlan, G. T. (2000). *Opportunities for Low-Volume Roads*. U.S. Department of Agriculture Forest Service. Transportation Research Board.
5. Douangphachanh, V., & Oneyama, H. (2013). A Study on the Use of Smartphones for Road Roughness Condition Estimation. *Proceedings of the Eastern Asia Society for Transportation Studies*, 9.
6. Gamage, D., Pasindu, H., & Bandara, S. (2016). Pavement Roughness Evaluation Method for Low Volume Roads. *Proc. of the Eighth Intl. Conf. on Maintenance and Rehabilitation of Pavements*. Research Publishing, Singapore.
7. Kinigama, G. (2010). Development of methodology to estimate esal values for low volume roads in provincial sector.
8. Pavia Systems, Inc. (n.d.). *Roughness*. Retrieved from Pavement Interactive: <http://www.pavementinteractive.org/roughness/>
9. Public Works Maintenance, Eugene. (2015). *Pavement Management Report*. Public Works Maintenance, Eugene.
10. Road Development Authority. (2007). *National Road Master Plan 2007-2017*.
11. Road Development Authority. (2015). Road Development Authority - HSR Analysis (Metric).
12. Sayers, M. W., Gillespie, T. D., & Queiroz, C. A. (1986). The International Road Roughness Experiment. *Establishing Correlation and a Calibration Standard for Measurements*.
13. US Department of Transportation Federal Highway Administration. (2002). *Use of PMS Data For Performance Monitoring*. US Department of Transportation Federal Highway Administration.
14. Lindo Systems. (2017). <http://www.lindo.com/index.php/products/lingo-and-optimization-modeling> , (Accessed 1.4.2017)



Travel Time Estimation Based on Dynamic Traffic Data and Machine Learning Principles

Sakitha P. Kumarage, V.M. Jayawardana, Dimantha De Silva and J.M.S.J. Bandara

Abstract: Travel time estimation is an important function in Transport Planning Activities. Applications such as Advanced Transport Information Systems (ATIS), Dynamic Route Guidance (DRG) and Network Performance Monitoring require travel time data. These applications, when deployed for an urban area, require models that estimate travel times on urban arterial corridors with temporal and spatial variations. Most of the travel time estimation models in the literature are inductive in nature, which require vehicle travel time observations for calibration. Obtaining vehicle travel time data is both a time consuming and costly process for a single link and it is impractical to collect this information for all the links across the road network. Hence, there is a need for travel time estimation models that do not require reference vehicle travel time data for calibration.

This paper presents a model for addressing the commodity of effective travel time estimation based on dynamic traffic data on top of data mining and machine learning foundations. Rather based on aforementioned reference vehicle travel time data, the proposed model incorporates dynamic and concurrent traffic data collection on multiple links based on google maps distance matrix application programming interface. Streaming data being fed into machine learning model, a rigorous estimation of travel time and formation of bottlenecks is calculated. The proposed solution performed well within an experimental workbench and the model is constantly learning with experience leading to better calculations with time.

Keywords: *Advanced transport information systems, Data mining, Urban traffic networks, Machine learning*

1 Introduction

Urban traffic congestion is one of the most severe problems of everyday life in Metropolitan areas. In an effort to deal with this problem, intelligent transportation systems (ITS) technologies have concentrated in recent years on dealing with urban congestion [1]. One of the most critical aspects of ITS success is the provision of accurate real-time information and short-term predictions of traffic parameters such as traffic volumes, travel speeds and occupancies [1].

Predicting car travel times along road segments is an increasingly important component of today's car navigation systems [2]. Johns et.al explored the problem of predicting travel times from floating car data (FCD) using geospatial inference method [2]. Floating car data are traces of GPS positions from actual cars driving on a road network. It provides speed or travel time estimates across the entire road network this is an advantageous feature in geospatial inference method when compared to stationary sensors, which typically only provide speed or flow estimates on highways or major roads [2]. A major disadvantage of floating car data is that, unlike data from stationary sensors, the

floating car data occur at irregular intervals and are typically much less frequent for any particular road segment [2]. Hence integrated stochastic estimation methods based on machine learning principles are proposed to adopt in estimation of travel time.

Most of the travel time estimation models in the literature are inductive in nature, which require vehicle travel time observations for calibration[3]. Obtaining vehicle travel time data is both a time consuming and costly process for a single link and it is impractical to collect this information for all the links across the road network[3]. Hence, there is a need for travel time estimation models that do not require reference vehicle travel time data for calibration.

Mr. Sakitha P. Kumarage, B.Sc.Eng(Hons)(Moratuwa), B.Sc(Hons)London, Research Assistant, University of Moratuwa .

Mr. V.M. Jayawardana, Undergraduate, Faculty of Engineering, University of Moratuwa.

Dr. Dimantha De Silva, B.Sc.Eng.(Hons) (Moratuwa), M.Sc (Moratuwa), Ph.D. (Calgary), P. Eng.(Alberta), Senior Lecturer, Department of Civil Engineering, University of Moratuwa.

Eng. (Prof.) J.M.S.J. Bandara, BSc. Eng (Moratuwa), Ph.D. (Calgary), FCILT, Professor, Department of Civil Engineering, University of Moratuwa.



The main objective of the paper is to identify the use of google travel time data in planning and management of traffic in urban road networks. On this regard the possibility of using Google travel time data in identifying bottlenecks on an urban road network. Data mining for travel time data and weather data was supported by the Google distance matrix API and Dark-Sky weather API which analyzed using Support Vector Machine for prediction of bottlenecks on an urban road network.

Use of travel time data to analyze the efficiency of utilizing traffic management plans was discussed with reference to the pilot project on implementing bus priority lanes for public buses of Colombo metropolitan area.

2 Literature Review

2.1 Data Mining

On the aspects of collecting data related to traffic models the literature provides many solutions. Such solutions are elaborated here. Real travel time data is typically measured and recorded in one of two ways: using stationary observers or moving observers[2]. Stationary observers include loop detectors and video surveillance. Moving observers, involving floating cars or probe cars, are becoming popular travel time collection methods since they can cover almost any road segment as needed[2].

The information on transport networks has improved with the emergence of crowd sourced data generated by social media, smartphones, Satellite navigation and other technologies[4]. According to Geurs et al websites like Here, Bing Maps, Google Maps, Google Transit, Open-Street-Map and the public availability of Transit Feed Specification (GTFS) data from transit authorities, enables vast area of research on evaluating accessibility and travel time. [5]

Georgios et al shows that use of crowd sourced data is an efficient way of data mining with the wide spread availability of smart mobile phones and the multi sensing features such as geolocation light, movement, audio and visual sensors[6].

Data gathered from crowd sourced applications could be used in identifying mobility patterns or popularity of a given trajectory. Such a

contribution can be utilized in large-scale urban and transit planning[6].

Venessa and Enrique identified that individuals generate vast amounts of geo-located content through the use of mobile social media applications[7]. The results have shown that geolocated tweets can constitute a good complement for urban planners to model and understand traditional land uses) in an affordable and near real-time manner[7]. Another informative way of data mining is by using Foursquare place data[8]. Spyrtos et al suggest Foursquare place data for estimating nonresidential building blocks and land use mapping purposes[8].

On the aspects of travel time estimation using crowd sourced data Dewulf et al. (2015) took Floating Car Data (FCD) from the Be-Mobile system to calculate car travel times[9]. In which the research estimated travel time by using geolocated positions of 400,000 vehicles equipped with track and trace devices. The obtained results were further aggregated to produce a generic travel time for peak and off-peak periods[9].

Further on this regards Araghi et al discusses the Accuracy of Travel Time Estimation using Bluetooth Technology in which results show that Bluetooth Technology can be used as a relatively new cost-effective source of travel time estimation[10].

As stated by Jones et al, one of the disadvantages in use of crowd sourced data is frequent unavailability of data[2]. When compared with travel time estimation, frequent floating car data is not available both on the link being predicted and succeeding links[2]. Thus a geospatial inference method to deal with such scenarios, which utilizes the data from geographically nearby links to predict the travel time of the designated link need to be incorporated[2]. On this regards, Giannotti et al presents the theory of trajectories which elaborates on a sequence of geo-referenced objects S of size ' m ' and a list of Temporal Annotations A of size $(m - 1)$, whose values represent the temporal distance between two consecutive geo-referenced objects belonging to S . Developing on this principle[11] Masiero et al propose a mechanism based on machine learning principles for estimating the travel time between any two points that: pre-processes raw trajectory data to create aggregated data; and learns the behavior of the vehicles using this aggregated data[12].

2.2 Data analysis and inferences

It was identified that there are many sources in which data could be mined and stored for analysing purposes. The basic theory was presented by Cho et al. To predict the travel time he identifies a function which relates the predicted travel time for an interval on a link to the available parameters such as speed, flow data[13]. The optimisation criteria would be to reduce the percentage error of predicted travel time with the observed [13].

In prediction of the travel time data many approaches could be observed in such Zhang and Jones propose to use historical means of the training data set at time t as the predictor for travel time[14]. Cho et al propose the current time predictor method in which the travel predictor is obtained by assuming the speeds of all segments at time t remain the same as the speeds at $t - \Delta$ throughout the entire travel[13]. Further Cho et al suggest time varying linear regression method in which they identify the travel time predictor as a linear combination of a time dependant constant and the the current travel time predictor of the previous segment[13]. Improving the time varying regression methods Kwon and Varaiya suggests time varying linear regression per segment by considering the current time predictor of the entire route as the key feature[15].

Deriving from these basic concepts Idé et al. proposed the probabilistic prediction of the travel time along an unknown path such that the similarity between paths is defined as a kernel function[16]. In this method authors emphasised on application of the Gaussian process regression for predicting the travel time[16].

Incorporating machine learning principles Wu et al suggest to use support vector regression (SVR) for travel-time prediction[17]. Since support vector machines have greater generalization ability and guarantee global minima for given training data, it is believed that SVR will perform well for time series analysis[17]. According to authors comparative to other baseline predictors which were mentioned above, their results show that the SVR predictor can significantly reduce both relative mean errors and root-mean-squared errors of predicted travel times[17]. Moreover authors emphasis that SVR had better results

than Artificial Neural Networks because SVR is more amenable to generalization than Artificial Neural Networks[17].

3 Methodology

3.1 Data gathering

From the previous literature, it was identified that travel time given by crowd sourced data could be utilized in estimating the travel time between origin and destination points with a significant accuracy and reliability.

In obtaining data for travel time variation between two points google ETA given by Google Maps could be incorporated into the data mining procedure[13]. Travel time estimations given by this method is quite reliable and highly efficient source of data collection for developing countries such as Sri Lanka which face a broader gap in funding for dedicated traffic sensors which can cover the whole urban arterial network[14].

Although google does not reveal the exact algorithm which they use for travel time prediction, the basis on which the travel time is calculated is crowd sourced data[15]. When a user enables Google services on a smart phone it sends anonymous bits of data back to Google describing how fast the user is moving[15]. The travel time prediction algorithms on google servers combine users speed with the speed of other phones on the road, across thousands of phones moving around a city at any given time in which a significantly reliable estimate on traffic conditions could be gained[15]. This process is continuously carried out to make predictions accurate based on machine learning principles[15].

According to ex-googler Richard Russel, to come up with the best prediction for travel times the google consider data available in a particular area[16]. The data range from official speed limits and recommended speeds, likely speeds derived from road types, historical average speed data over certain time periods (sometimes just averages, sometimes at particular times of day), actual travel times from previous users, and real-time traffic information[16]. Hence the gained travel times are scientifically justifiable to be accurate and reliable [16].

In this paper, data was gathered from Google Distance Matrix API where, it is possible to



collect travel time and distance values of a given route between start and end points. The collected data over a period of 3 months were analyzed.

The main objective of the paper is to identify the usability of google travel time data in planning and management of traffic in urban road networks. On this regard the possibility of using Google travel time data in identifying bottlenecks on an urban road network and using data to analyze the efficiency of utilizing traffic management plans are discussed.

3.2 Identification of bottlenecks

A bottleneck on a road is a point space that has a reduction in capacity as compared to the upstream and downstream capacity. Usually these are at facilities such as a bridge or an intersection at a given point along the road considered. When the road segments on each side of the bottleneck have sufficient capacity then no congestion occurs on them. The bottleneck, whose capacity is finite, is subject to congestion. Queuing will develop when the arrival rate of flow at the bottleneck exceeds its capacity [17]. The travel time along such a segment will increase when the bottle neck reaches its capacity[17]. Therefore, observing the increase in travel time along road segments will indicate the existence of any bottlenecks[17]. The study focuses on identifying the formation of bottlenecks along road segments subjected to the spatial and temporal variations. On that regard the such identification will enable efficient traffic management plans considering the spatial and temporal variations suitably.

According to Chien et al travel time in an urban traffic environment is highly stochastic and time dependent due to random fluctuations in travel demands, interruptions caused by traffic control devices, incidents, and weather conditions[18]. As discussed by Leong et al weather conditions tend to have a significant impact on the driving conditions, temperature precipitation and visibility tends to increase the road traffic and reduce roadway capacity[18]. Therefore, when formation of bottlenecks, these interruptions will have a significant influence. Hence its is required to consider weather conditions on propagation of bottlenecks[18].

Thus, travel time variation data was analyzed by taking following parameters into consideration; Day of the week, time, rainfall,

temperature, average speed of the road. It is possible to extend the model into parameters such as road pavement conditions, vehicle distribution, road geometry, accessibility of the road etc. Such extension could be included in the future work with the availability of data.

Based on past research it is suggested to identify of bottlenecks is by training a support vector machine which runs a machine learning algorithm in identifying extreme outliers of travel time data along a road segment varying with space and time. In inducing the SVM algorithm the factors which can cause bottlenecks were considered. Support Vector Machines (SVM) is a supervised learning tool well known for its discriminative power. SVM starts separating the data with a hyperplane and then extends this procedure to non-linear decision boundaries.

3.3 Effectiveness of traffic management plans

It was identified with the literature review; travel time data can be used to evaluate the traffic management of a particular link or a network[2]. As an application of the concept the travel time variation of Rajagiriya area with the implementation of a Bus Priority Lane (BPL) was studied to test the variations traffic speeds/times that can be found with the method which could be used to evaluate the effectiveness of the implemented plan.

BPL was suggested in the CoMTrans Master plan [14] and the Megapolis Transport Master Plan[19]. Hence BPL was implemented as a pilot project at Parliament Road from 12th to 23rd March 2017 by the Ministry of Megapolis and Western Development with the assistance of Korean International Cooperation Agency[20]. At the pilot project a single lane of the study area was separated for public buses[20]. The effect on overall traffic movement was analyzed from the collected data by Google Distance Matrix API. A situation analysis on variation of travel times before and after the implementation of BPL was studied.

4 Data Verification

The data collected from Google Map APIs was validated using Floating Car data collection method. Floating car data collection is a commonly used traveltime collection method. The test is conducted by dispatching a vehicle

to travel with the traffic stream and collect the travel time in-between specified locations[21]. The speed of the floating car was controlled to follow the usual traffic to set the driving guidelines of an average moving vehicle [21].

Data collected from the manual method was compared with the API travel times obtained parallel to floating car data collation. The results observed showed a minor variation from the traveltime collected from floating car data and Google Distance Matrix API. The correlation in between the FCD and API travel time was observed very high with a R^2 value of 0.9802, which indicates that the traveltime estimates given by Google Distance Matrix API do not indicate a significant difference from the observed floating car data. (see Figure 1)

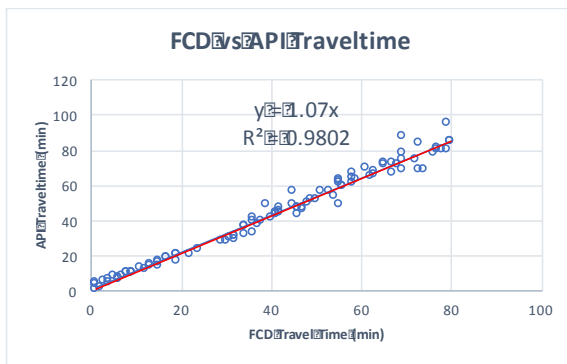


Figure 1 - FCD vs API Traveltime

5 Data Collection

Data collection for bottleneck identification and evaluation of traffic management plans was conducted using a data set collected on travel time and weather at Rajagiriya Junction.

Travel time data was collected using Google Distance Matrix API. Data was collected in 15 minute intervals from 0530h to 2359h. A PHP script was run on a server which collected data for the scheduled time. At every data collection interval travel time data between two links were recoded for 3 pre-identified road segments. Figure 2 shows the segments used for the analysis. Weather data which included precipitation, max. temperature and min. temperature of the Rajagiriya area was collected from Dark Sky API which was recorded in hourly intervals for the observed duration. Road profile data was not included in the estimation model as it is a generic parameter of the considered road segment in which the predictions were made. As the objective was to estimate traveltime of a particular link, road profile parameters will be kept a constant value for short term estimates.

Collected data was structured on a data set with following attributes: Road-segement, date, time, distance, travel-time, avg-speed, precipitation, tempMax, tempMin. The data set was prepared to identify patterns of variations in traveltime based on machine learning principles.



Figure 2 - Map of segments Used

6 Analysis

6.1 Identification of bottlenecks

SVM is used in the process of identifying the formation of traffic bottlenecks. Collected data set was fed into the SVM algorithm to predict the formation of bottlenecks. The algorithm was based on attributed identified earlier.

The basic algorithm was fine tuned to the situation in which it enables to train separate model for each road segment in the urban road network considered. Based on the trained models, it was checked the severity of traffic condition using the test data.(see Figure 3)

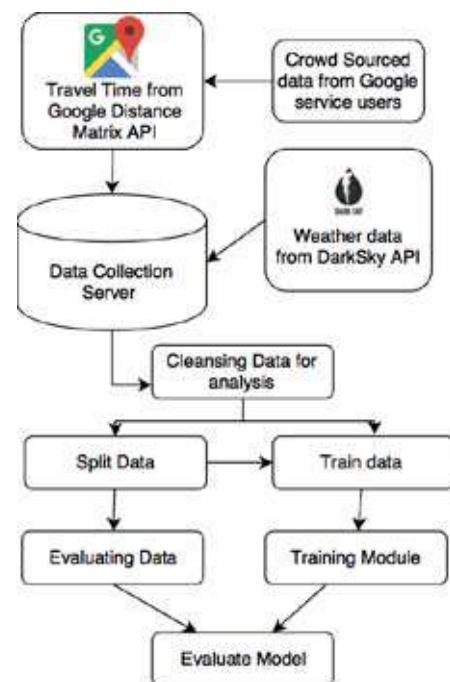


Figure 3 - Flow diagram of analysis



The prediction gave following results which are quite satisfactory.

Table 1 – Summary of estimation results

Segment	Precision	Recall	F1
M1-S1	91.84%	100 %	95.75
S1 -S2	98.90%	99.45%	99.17
S2 - S3	94.88%	100 %	97.37

precision also called positive predictive value is the fraction of relevant instances among the retrieved instances, while recall also known as sensitivity is the fraction of relevant instances that have been retrieved over the total number of relevant instances. F1 is a measure calculated by using both precision and recall. Thus, the estimates have given highly accurate results in all three instances.

Identification of bottlenecks along the three road segments were carried out using the SVM algorithm and spatial and temporal variation bottleneck formation was identified.



Figure 4 – Bottlenecks along road segments

In Figure 4 the spatio-temporal variation of speeds(km/h) is illustrated for the considered segments. According to the Figure 4 it could be identified that the segment S1-S2 (kotte road to HSBC junction) forms a bottleneck in the road segment considered where the segment speed is considerably less than the upstream and downstream segments, The speeds have localised minimum between at 0715h and 0830 most likely to the movement of school traffic along the segment. The segment M1-S1 speed reduction from 0800h to 0815h shows that the capacity of the road is been reached during the said time period. The results show that in the morning peak hours, M1-S1 segment and S1-S2 segment should be given high priority in traffic management to improve the traffic flow in the segment considered.

6.2 Effectiveness of traffic management plans

The variation of travel time along the M1-M6 road segment from Polduwa bridge to Senanayake Junction (see Figure 5) was recorded from the data collection method described above.

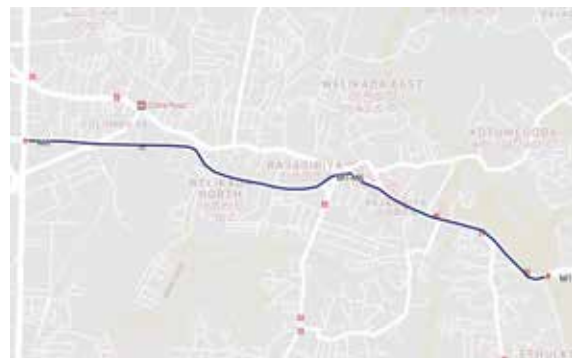


Figure 5 – Map of road segment M1-M6

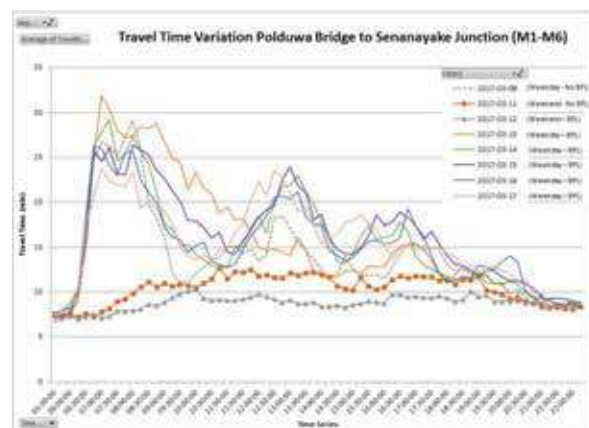


Figure 6 – Variation of traveltime along M1-M6

Figure 6 above shows an illustration on the variation of travel time along time for several days with and without BPL. A BPL was implemented for a 1km distance between Rajagiriya Junction and Ayurvedha Junction from 12th March (Sunday) to 17th March (Friday) for the whole day. The analysis shows that there is a significant difference in travel time with the weekday and weekend travel patterns where the weekends are represented by the 11th March and 12th March data

The data shows that there has been daily variation in travel times with the BPL implementation and could be compared with the 9th March data as base data for weekday and 11th March as base data for weekend where the BPL was not operational.

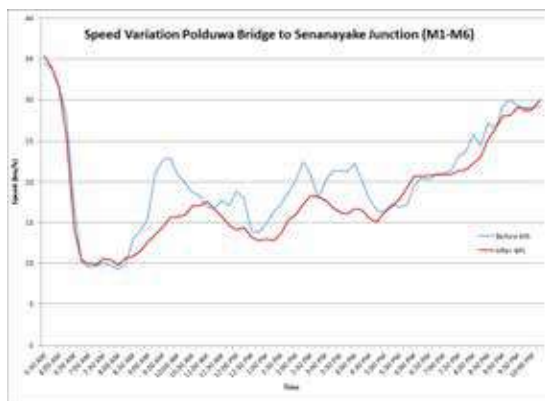


Figure 7 - Average Speed variation before and after implementation of BPL

Figure 6 and Figure 7 illustrate the variation in travel time and average moving speed of the passengers before and after the implementation of BPL. The illustration shows that there is a marginal decrease in average travel time, thus a marginal increase in speed during 6:30 am to 8:30am with the implementation of the Bus Priority Lane (BPL), but a considerable increase in average travel time, thus a considerable decrease in speed during other times of the day with BPL implementation. Therefore, it could be noted that when the existing speeds is already low the BPL has performed marginally positively during the peak time period.

However, it should be noted caution should be made when making judgement based on just a 1km of section of BPL since the impact to the overall network will only be evident with sufficient length of such implementation.

7 Discussion

The use of crowdsourced data in estimation of travel time was emphasized on the paper and the applications of travel time estimation by crowd sourced data were evaluated. From the literature review it could be identified that information required for transport analysis could be obtained from data sources such as APIs provided by Google, Twitter and other social media. Data mining based on these platforms will enable to identify mobility patterns of vehicles and people, travel time and accessibility. Although the data provided by mobile phone companies for research work is a primary source of data reliability and consistency of such data is questionable. Hence use of public data APIs provided by Goggle and other social media platforms will enable consistent collection of data. One of the main advantage of using travel time data provided by Google APIs, that it is cost effective and available consistently. Further availability of travel time data on any given time for a very large network of urban road networks will enable further advancement of travel pattern analysis. Incorporation of machine learning algorithms could be identified as a constructive approach. It is confirmed by the past research that use of machine learning is the novel approach as it will reduce the errors more than that of probabilistic models when the analysis spreads to a large urban network.

Based on the data mining principals of frequent collection of current traffic conditions and travel time data for a longer period of time has enabled to identify the traffic patterns of a given network which is dependent on spatial and temporal parameters. Data collected on the Rajagiriya junction has showed how the bottlenecks are formed on selected road segments with time. The use of support vector machine (SVM) has enabled to extend the analysis to a larger urban network in which cluster data of each road segment with a hyperplane and then extends this procedure to non-linear decision boundaries and predict the formation of bottleneck on a road segment for given conditions. As suggested in the methodology the algorithm could be extended to incorporate other parameters which can cause bottlenecks but in our analysis, we have limited only to parameters such as day, time, distance, travel-time, average-speed, precipitation, maximum-temperature, minimum temperature. Incorporation of these attributes have shown overall improvement in



identification and prediction of bottle necks. But the influence of maximum and minimum temperature has shown less significance as they are parameters which have lesser variation. In future work, it is expected to incorporate parameters such as road pavement and geometry, vehicle distribution, road accessibility etc

Regarding the study on travel time variation with the implementation of bus priority lane, the analyzed data reveals the pilot project has reduced the overall link speeds in the considered link after implementation. Therefore, it is questionable whether bus priority lane is a suitable solution for the considered route. Hence, it cannot be justified the opinion that there will be a considerable saving of time or money by implementing the bus priority lane.

As the limitations of the study it is identified that the study area used for data collection was not a large urban network. Further the collected data set cannot portray the variations which are dependent on months as the data was collected only for a one month duration. The experiment was carried out in the dry season therefore influence of high rainfalls and changing weather was not possible to identify. The extension of the methodology to rural areas has limitations as the data was collected using Google distance matrix API which collect data of moving smart phones. Hence availability of many people in a road network is a significant factor which can cause reliability issues.

8 Conclusion

In this paper, we reveal the use of google travel time data for effective estimation of travel time and identify bottlenecks based on data mining and machine learning foundations.

Use of google Distance Matrix API can surpass the cumbersome work of developing models to estimate travel time data. Further improving the prediction based on these estimates can be a constructive approach in prediction of bottlenecks of an Urban network.

It could be concluded that the main objective of the paper is reached as it was able to identify the usability of google travel time data in planning and management of traffic in urban road networks. The approach was confirmed by successful use of data in identifying bottlenecks

on an urban road network subjected to spatial and temporal variations.

The use of data to analyze the impact of utilizing traffic management plans was discussed by evaluating the pilot project on bus priority lane.

References

1. Stathopoulos, A., and Karlaftis, M. G., "A Multivariate State Space Approach for Urban Traffic Flow Modeling and Prediction," *Transp. Res. Part C Emerg. Technol.*, vol. 11, no. 2, pp. 121-135, 2003.
2. Jones, M. Geng, Y. Nikovski, D., and Hirata, T. "Predicting Link Travel Times from Floating Car Data," *IEEE Conf. Intell. Transp. Syst. Proceedings, ITSC*, no. Itsc, pp. 1756-1763, 2013.
3. Herring, R. J. "Real-Time Traffic Modeling and Estimation with Streaming Probe Data using Machine Learning," *Vasa*, 2010.
4. van Wee, B., "Accessible Accessibility Research Challenges," *J. Transp. Geogr.*, vol. 51, pp. 9-16, 2016.
5. Geurs, K. T. L. La Paix, and Van Weperen, S., "A Multi-Modal Network Approach to Model Public Transport Accessibility Impacts of Bicycle-Train Integration Policies," *Eur. Transp. Res. Rev.*, vol. 8, no. 4, pp. 1-15, 2016.
6. Chatzimilioudis, G., Konstantinidis, A., Laoudias, C., and Zeinalipour-yazti, D., "Crowdsourcing with Smartphones," pp. 1-7.
7. Frias-Martinez, V., and Frias-Martinez, E., "Spectral Clustering for Sensing Urban Land Use using Twitter Activity," *Eng. Appl. Artif. Intell.*, vol. 35, pp. 237-245, 2014.
8. Spyrtos, S., Stathakis, D., Lutz, M., and Tsinaraki, C., "Using Foursquare Place Data for Estimating Building Block Use," *Environ. Plan. B Plan. Des.*, 2016.
9. B. Dewulf *et al.*, "Examining Commuting Patterns using Floating Car Data and Circular Statistics: Exploring the Use of New Methods and Visualizations to Study Travel Times," *J. Transp. Geogr.*, vol. 48, no. August, pp. 41-51, 2015.
10. Araghi Namaki, B., Pedersen Skoven, K., Christensen Torholm, L., Krishnan, R., and Lahrman, H., "Accuracy of Travel Time Estimation Using Bluetooth Technology: Case Study Limfjord Tunnel Aalborg," pp.

- 166-191, 2012.
11. F. Giannotti *et al.*, "Unveiling the Complexity of Human Mobility by Querying and Mining Massive Trajectory Data," *VLDB J.*, vol. 20, no. 5, pp. 695-719, 2011.
 12. Masiero, L. P., Casanova, M. A., and de Carvalho, M. T. M., "Travel Time Prediction using Machine Learning," *Proc. 4th ACM SIGSPATIAL Int. Work. Comput. Transp. Sci. - CTS '11*, no. November, pp. 34-38, 2011.
 13. Massimino, B., "Accessing Online Data: Web-Crawling and Information-Scraping Techniques to Automate the Assembly of Research Data," *J. Bus. Logist.*, vol. 37, no. 1, pp. 34-42, 2016.
 14. Japan International Coporation Agency; Oriental Consultants Co LTD, "Ubnan Transport System Development Project For Colombo Metropolitan Region."
 15. Google, "The Bright Side of Sitting in Traffic: Crowdsourcing Road Congestion Data," *Googleblog*, 2009.
 16. E.-G. (2006-2012) Richard Russell, "How Does Google Maps Calculate Your ETA," *FORBES*, 2013. [Online]. Available: <https://www.forbes.com/sites/quora/2013/07/31/how-does-google-maps-calculate-your-eta/#241f6c01466e>.
 17. Yang, H., and Hai-Jun, H., "Analysis of the Time-Varying Pricing of a Bottleneck with Elastic Demand using Optimal Control Theory," *Transp. Res. Part B Methodol.*, vol. 31, no. 6, pp. 425-440, 1997.
 18. L. W. Leong *et al.*, "Improving Traffic Prediction by Including Rainfall Data," no. January 2016, 2014.
 19. Ministry of Megapolis and Western Development, "Western Region Megapolis Transport Master Plan," 2016.
 20. Department of Government Information Sri Lanka, "DECISIONS TAKEN BY THE CABINET OF MINISTERS AT ITS MEETING HELD ON 25-04-," *State Print. Coporation*, 2017.
 21. Turner, S. M., Eisele, W. L., Benz, R. J., and Douglas, J., *Travel time data collection handbook*, vol. 3, no. 5. 1998.



Infrastructure Feasibility Analysis of Inland Water Transportation from Peliyagoda to Hanwella along Kelani River

K.P.H.S. Kalaha and R.M.N.T. Sirisoma

Abstract: In the ancient times, people used to settle near waterways for their agricultural activities as well as to fulfil their mobility requirements. With the urbanization and development of technology, people began to shift to land transportation neglecting the waterways. When the land transportation system prevailing in the country is declining gradually, and it arises a need for a transport mode which does not use the existing road network. Therefore, transport planners have again eyed to identify the potential of inland waterways to cater transportation needs and recreational purposes. Inland water transport is a preferred mode throughout the world because it is a low cost, fuel efficient, environment-friendly, less capital needed, safe and a pleasant transportation mode. This paper focuses on the infrastructure feasibility of the proposed Mattakkuliya- Hanwella Inland waterway line. Through a detailed literature review, specifications of the vessel that should be operated, environmental impacts and safety measures related to water transportation and facilities at the stations were identified. A site survey was carried out to find the minimum horizontal and vertical clearance at the overhead structures along the river. Using the bathymetry data gathered for the Kelani River, navigable path and areas to be dredged were recognized. Water Intake and salinity barrier at Ambatale are major concerns in this waterway line and therefore, solutions have been identified to overcome these impacts. Data regarding on bathymetry of the river, has found that the entire water stream is navigable. Optimizing the number of boat stations with respect to the access, demand and the availability of transfer modes it was identified that 13 boat stations are required. Demand for the system was identified using a Logit Model. Highest and lowest demands per stations are at Malwana with 9700 passengers per day at Embulgama with 2000 passengers per day respectively. The new system will help to minimize the traffic congestion on the High-Level Road (A4) providing passengers with a safer journey.

Keywords: Navigable Path, Least Available Depth, Inland water transport

1. Introduction

Sri Lanka owns a rich history in inland water transportation where inland waterways such as rivers, canals and lakes were recognized as vital arteries for transportation. During ancient times in Sri Lanka, inland waters were used for international trade. There have been ports situated at estuaries of rivers such as Salwathura at Deduru Oya, Wattala at the Kelani Ganga, Kalathilaka at the Kalu Ganga, Nilwalatittha at the Nilwala Ganga and Kirinda at Kirindi Oya. [4]. But with globalization, traditional transport using inland waterways were substituted by road, rail, air and marine systems.

Waterborne transport is one of the oldest modes of transport compared to other modes of transportation prevailing in the world. Inland water transport can be divided into three sectors like public transport, freight transport and recreational. And it comprises

transportation through rivers, canals and lakes. This paper focuses on, public transportation and recreational aspects of inland waterways.

For a transport mode to be usable, the factors such as time, cost and intermodality are critical. Inland water transportation can serve as a convenient mode of transport in congested cities. Inland water transport has many inborn direct and indirect advantages. As for the direct advantages, its cost is low, capacity is high, safe, energy efficient, the capital need is less and pollution is limited. The indirect advantages are it attracts new industries, creates new business opportunities, boosts the economy in the area and generates tourism and recreation activities [1].

*Eng. (Dr.) R.M.N.T. Sirisoma, Ph.D., B.Sc. Eng (Hons),
C.Eng, CMILT(UK), MITE(US), MIE(SL)
Senior Lecturer, Department of Management and Finance,
General Sir John Kotelawala Defence University.*

*Mr. K.P.H.S Kalaha, undergraduate, Department of Civil
Engineering, General Sir John Kotelawala Defence
University.*



Because of these reasons, inland water transport is being used all around the world, especially in the countries such as Bangladesh, Germany, USA, UK, Russia, China, Thailand etc. In the Western Province of Sri Lanka, water ways are exploited in small scale for transporting commodities like bricks, tiles, sand and timber in the construction industry [11].

The Kelani is the second longest river in Sri Lanka. The Kelani River and its tributaries provide the portable and industrial water requirements for the people in Greater Colombo area. Starting from the Sri Pada mountain range in the Central hill country, it flows mainly in the western direction and falls into the sea at Modara, Colombo. The river section passing via Western Province has the most potential to use in public transport mode due to the land use pattern in the area. The study area consists of fifty-six Grama Niladhari Divisions, and the main cities are Peliyagoda, Kaduwela, Kelaniya, Malwana and Hanwella. Along the study area the river runs for a total distance of 31 km, and on the bank, on either side of the river, there are a number of important economic, religious and recreational places such as Kelani Maha Vihara, Water World Lanka and Water Board Pump Division, Ambatale.

2. Need for an Inland Waterway Line

Colombo, being the capital of Sri Lanka, has an average annual growth ratio of 8%, the number of vehicles in the Western Province has increased by a factor of 2.5 in 12 years and average speed of vehicles in major transport corridors during the peak time have fallen below 10 km/h. Colombo attracts more than one million daily commuters by 160,000 vehicles from the suburbs of Colombo [9]. The following table shows the average daily passenger flows along the corridor.

Table 1 - Average Daily Traffic: Mattakkuliya-Hanwella Line [8]

Corridor Name	Average Daily Traffic-2013(Passengers/day)
Negombo Road	20,455
Negombo- Colombo Main Road	92,662
New Kelani Bridge	119,903
Biyagama Road	25,945
New Kandy Road	55,344

Malwana Road	47,718
Awissawella Road	25,518
Colombo-Hanwella Low-Level Road	15,742
Hanwella- Urapola Road	16,476

(Source - Western Region Megapolis Transport Master Plan)

Due to reasons, such as traffic congestion in the area, shortage of parking spaces and pedestrian walkways, high rate of road traffic accidents and lack of comfort, safety and efficiency in public transport service the prevailing transport system has failed to cater to the mobility requirements of the people. Therefore, wastage of valuable man hours, wastage of fuel and other resources and environmental pollution is unbearable.

For declining of the level of service of commuters, constructing new roads is not a solution. Construction of new road networks, railway networks is always costly. The investment needed for inland waterways is 5%-10% of the investment for an equivalent road or rail line. Its maintenance cost is 20% of road maintenance cost [1]. Therefore, Colombo Metropolitan Region needs a transport mode which does not depend on the present road structure. Hence developing inland water transportation as a transit mode is a better solution to reduce the traffic congestion and to provide a pleasant, time-saving, economical and safer journey for the commuter.

Therefore, with the aim of reducing the heavy traffic burdens on the main road corridors and to capitalize the existing water bodies as a minor public transport medium Western Region Megapolis Transport Masterplan has identified 3 potential inland waterway lines. And the inland waterway line from Mattakkuliya to Hanwella is one of them [8].

3. Literature Review

3.1 Station Facilities

To attract passengers to the new system, station facilities are important. Jugović, Mezak and Lončar(2007) state that terminal capacities should be sized and profiled for quick flow of passengers. To provide passenger comfort, factors such as service and maintenance shops, sanitary facilities, parking lots, refreshment and

service areas, level of service of employees at the station and offer in the station is vital. [6].

During the daytime, the system can be used for public transportation minimizing the traffic congestion in the road network. During the off-peak time where the demand is low, they can be used to promote recreational activities. A study done by Transportation Engineering Division of the University of Moratuwa in 2003 has suggested that with the gradual development of the system, restaurants, children parks, leisure activities will develop around the river bank. This will boost the economy of the people living nearby. Hence a station has the ability to promote local and regional development. Local employment opportunities are vast when a wide range of value-added services are provided. Furthermore, Information Technology related infrastructure, aggressive marketing, public/private cooperation are some important assets for the success of a station/jetty. [2]

3.2 Safety and Environmental Pollution

In inland water transportation, the probability of accidents is less, and the costs of the accidents are low in economic and human terms. Awal (2015) states that accidents cannot be caused by a single factor, it is a result of various complex interactions. They may be mechanical failures, human errors and natural cases. According to most of the studies that have been carried out, especially in Bangladesh, the main factors related to accidents are human factors, operating environment factors, enforcement and educational factors and vessel design factors. Some of the causes related to human factors are overloading and overcrowding, stability problems due to the rush of passengers and collision due to handling errors. By making overloading passengers unlawful, instructing service providers about the safety of the passengers, establishing vessel traffic monitoring systems and enhancing manpower and infrastructural facilities needed for the system, the number of accidents can be minimized. [7]

Water is a scarce resource in the country. Use of water for transport is sometimes difficult to justify. Kalyani, Vidyasagar and Srinivas (2015) express that Inland water transport is a more environment-friendly mode of transport compared to other modes of transport. But depending on the individual characteristics of the river, its physical and ecological state it has

some negative impacts. Pollution is the major negative impact, and some of the others are bank erosion, loss of habitat, barriers to migration and species dispersal. Further, the pollution can be due to 6 major sources, and they are operational oil pollution, solid waste disposal, accidental spills, air pollution and construction and maintenance of stations and the waterway channel. Dredging poses a direct threat to the areas where it is carried out as it introduces sediment into the adjacent water column where sediment is redeposited at the bottom. This has short-term effects on pelagic fish and the benthic community. Dredging also increases turbidity because of the suspended sediments. It decreases light penetration and photosynthetic activity [5].

4. Horizontal and Vertical Clearance

Navigational channel with desired width, depth and clearance height is one of the basic Inland water transport related infrastructure for the development of waterways. In the study area, the Kelani River passes through 6 highway bridges, a footbridge and a railway bridge. These bridges were identified using the "Google Earth Pro" software, and a site survey was carried out to measure the clearance levels. The results showed that the river has sufficient horizontal and vertical clearance for navigation. This survey was done during the low tide, and the results are as follows.

Table 2 - Minimum horizontal and vertical clearance

Bridge	Min: Vertical Clearance(m)	Horizontal Clearance(m)
New Kelani Bridge	4.90	25.84
Railway bridge-Peliyagoda	5.85	18.74
Kelansiri Bridge at Kelanimulla	6.5	35.58
Footbridge at Mabima West	>5m	30
Bridge at Outer Circular Highway	8.4	33.5
Kaduwela bridge	8.6	20.5



Nawagamuwa bridge at Nawagamuwa - Mapitigama Road	9.45	11.1
Hanwella bridge at Hanwella-Urapola Road	13.14	10.2

5. Determining the Navigable Channel

The least available depth (LAD) is a critical parameter for navigability of a waterway. From the literature studied, it was found that for transportation, the least available depth must be 1.5 m. To decide the navigable path, the bathymetry data is important. In order to obtain accurate information, these data were collected from two institutes namely, Survey Unit of Sri Lanka Navy and Irrigation department of Sri Lanka.

From Sri Lanka Navy, centreline river depth variation values (Figure 1), river cross section at different locations and depth values at different locations in the river of the entire study area were collected. 1:10,000 digital data in the study area were obtained from the Survey Department of Sri Lanka. Using the software "ArcGIS 10.3.1," the bathymetry data obtained from Sri Lanka Navy were merged with the 1:10,000 digital data obtained from the Survey Department. Using the river depth details, the contours were obtained differentiating the bed levels of the river into 4 depth ranges. These depth ranges are depths above 4 m, depths from 4-3 m, depths in the range 3-2 m and river depths below 2 m.

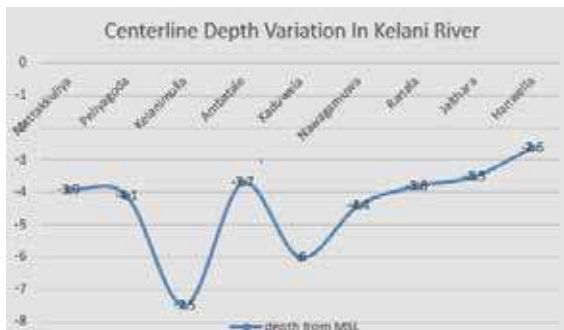


Figure 1 - Centreline Depth variation in Kelani River

The navigable line was then drawn connecting points with high bed levels, and it was discontinued at several locations as given in Figure 2, where least available depth for

navigation was not found. The navigable line was then buffered for 2 paths of 10 m and 20 m in size, where 10 m path is the safest path for navigation.

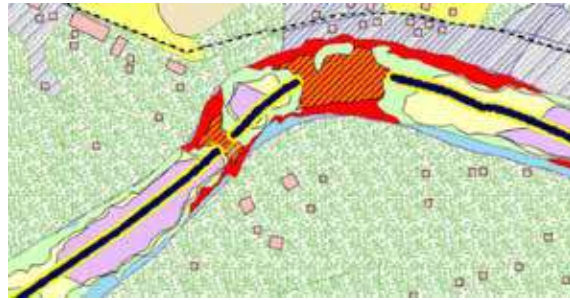


Figure 2 - Section of the navigational path

From the river depth analysis, it was found that areas such as downstream to salinity barrier at Ambatale, below the Outer Circular Highway bridge, near to Nawagamuwa Bridge and some areas in Hanwella have to be dredged for safe navigation especially during low flow periods.

6. Salinity Barrier at Water Intake Ambatale

Impact of the salinity barrier and the two water intakes namely, Water intake Ambatale and Kelani Right Bank (KRB) Intake are critical for the navigability of this inland water line. That is because on average 540,000 m³ of water is abstracted at the Ambatale Intake and another 180,000 m³ of water is abstracted at Kelani Right Bank intake per day accounting for more than 70% of the drinking water supply in the Colombo Metropolitan Region. [3]

The water level of the Kelani River is below 0 MSL up to about Hanwella during the dry season. When there is high tide, salt water of the sea propagates along the river and reach Ambatale water intake inducing a limitation in the treated water production experienced almost every year. After examining several solutions to overcome this problem, authorities have decided to erect a salinity barrier across the Kelani River in the vicinity of Ambatale Water Intake. At present, a sandbag barrier is used to control the salinity intrusion and control the water flow. But this has not been effective as maintenance is difficult and also as salinity intrusion cannot be stopped completely. Thus, they have decided to construct a permanent barrier across the river with the main objectives of ensuring the quality of water by preventing salinity intrusion during low flow periods, maintaining minimum flow requirement during low flow situations and

ensuring a more flexible operation and maintenance of the barrier where maintenance of a sandbag barrier is extremely difficult.

The barrier is situated 20 m to 30 m downstream of the Water Intake, Ambatale and its construction have been proposed to be executed in 2 phases, and the phase I, which is the construction of the foundation has already been implemented. The foundation has been constructed by filling boulders and sand in between 2 sheet piles. The top of the foundation is at -0.5 m from MSL level. At one corner of the barrier, a raft passage has been designed for the movement of vessels. It is a trapezoidal passage, and the top of its base is at -2 m from MSL level. The dimensions and the location of the barrier are as follows as given in Figure 3.

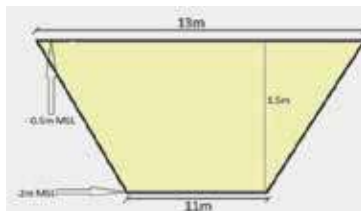


Figure 3 - Section of the raft passage

Phase II of the project is the installation of an inflatable rubber balloon across the river. It is going to be installed in 2 sections; a larger balloon across the raft passage and a smaller balloon across the rest of the structure. The inflatable balloon will only be inflated during the dry season up to +1 m MSL level usually from January to March, and it will be deflated during normal conditions.

Hence during normal conditions movement of vessels through the salinity barrier is possible, but movement during the dry season is completely restricted. In this time of the year, the river will be navigable only from Peliyagoda to Gonawala West and from Hanwella to Mabima West. Therefore, the only possible solution that can be implemented is having a shuttle bus service connecting 2 stations on either side of the barrier along the Biyagama Road and Sedawatta- Ambatale Road via Avissawella Road. Although dredging a new channel is an option it is too costly, and it can increase the salinity intrusion in fresh water in the upstream intakes. Furthermore, another objective of having a barrier is to store water and to control the flow. If another channel is dredged, controlling of water flow will not be possible.

7. Locations of the Stations/Jetties

Inland water stations are always and should be inter-modal. People travelling by water must arrive and depart by another transportation mode. Typically, roads and rail services which provide access to the inland stations/jetties can be called intermodal connectors to inland water stations. Improvements to the access of the ports can increase the efficiency of the ports, benefit trade and contribute to employment growth and regional productivity.

To attract more passengers to the system, the location of jetties and the distances between them are vital. When deciding the locations and distances of the stations, the demand generated in the area, land use details, access to the identified stations/jetties, connectivity with other transport modes, availability of main transport corridors and amount of dredging which need to be done at the proposed location were considered. In the analysis, the top priority was given to the demand generated in the area. These demand data were obtained from the demand estimation model use by Megapolis Transport Planning team. The demand data were forecasted for 2035 with the assumption that other modes such as rapid transit systems, electrified railways etc. will come up simultaneously.

When locating the jetties, the area around the river was analysed using the 1: 10,000 digital data from the software "ArcGIS 10.3". Then the possible locations of the stations were marked considering the demand in the area and the land use. The land use information was obtained from the Survey Department of Sri Lanka, and they were classified to identify the suitable lands for the stations/jetties. In order to minimize land acquisition costs, an attempt was made to use bare lands at each possible location. Further to reduce the construction costs, dredging need to be done was also considered at this stage.

To identify the connectivity with other public transportation modes, information regarding bus routes in and crossing the study area were collected from Road Passenger Transport Authority, and their routes were drawn on the map using "Google Earth Pro" software. The main bus routes in the area are Kaduwela-Biyagama (237), Bambalapitiya- Wattala (104), Kohuwela- Kelaniya (135), Fort-Kadawatha(138/1), Kiribathgoda- Angulana (154), Dekatana- Pettah (226), Kaduwela-



Gampaha(228), Colpity- Kohilawatta (175), townhall- Salmal Uyana (164) and Pettah-Kaduwela (143). The marked locations in the "Arcgis" document, were imported to the "Google Earth Pro" software in order to recheck the suitability of the locations marked. As given in figure 4, marked locations were adjusted considering the connectivity to other transport modes, access facilities available at each marked location and availability of main transport corridors.

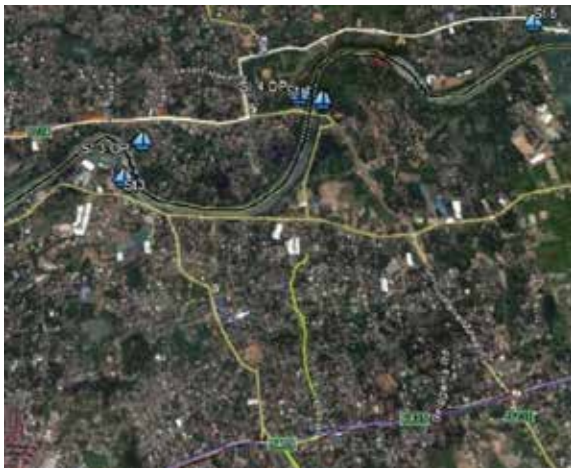


Figure 4 - Access to the proposed stations/jetties

After the analysis, the locations of the proposed stations and corresponding expected daily bi-directional demand obtained from Megapolis Transport Planning Team are as follows in Table 3.

available, the solutions are the construction of a bridge connecting river banks or construction of a station while developing access facilities to it. Out of these solutions, the most economical solution must be taken considering the characteristics at the location. In the station 12, land use is very high on only one side of the river, which is Embulgama area and in the other side land use and the population density is very low. Thus having 2 stations on either bank is an additional cost.

After locating the stations, it was seen that the station to station distance between first 11 stations ranges from 1.5 km to 2 km and in the last few stations, the distance between station to station is more than 3 km. That is because population density and demand around last 2-3 stations are very low compared to other stations. Therefore, having stations in between them will not be effective in the present conditions.

Table 3- Locations of stations/jetties

Station	Location	Expected Daily Bi-directional Demand
1	Next to New Kelani Bridge	4,133
2	Pethiyagoda	4,160
3	Kelaniya	4,465
4	Kelanimulla	6,552
5	Gonawala	3,560
6	Mabima West	2,547
7	Next to OCH Bridge	4,340
8	Next to Kaduwela Bridge	5,985
9	Yabaraluwa	1,850
10	Near to Malwana Town	9,701
11	Navagamuwa	4,477
12	Embulgama	1,999
13	Hanwella Bridge	565

In the stations 1,3,4,6,7,8,9,10,11 and 13, two jetties/stations were marked on either bank in order to provide the facility for people on both sides of the river. At stations 2 and 5, for one side of the bank, access facilities are unavailable. Therefore, to supply the demand on the side where access facilities are not

8. Features of the Boat/Vessel

The type of vessel that can be used for waterways depend on the water body, passenger capacity requirements, length of trip, depth and width of the waterway and docking requirements. There are different kinds of vessels operating in the inland waterways throughout the world. Some of them are passenger trawlers, passenger steamers, hydrofoil boats, electric boats where it can be solar powered, battery powered or hybrid, passenger launches, hovercraft and ferries.

Considering the features of the vessel to be used in the Kelani River, the most important aspect to consider will be the pollution the vessel creates. Since two major water intakes namely Ambatale water intake and Kelani Right Bank intake which supplies 70% of the total amount of water supply in the area are located in the study area, special attention must be given to minimizing the adverse effects on them. Since fuel powered boats emit various types of chemicals to the water body, a solar

powered or battery powered boat will be feasible to the Kelani River as they do not emit any harmful substances to the water body. Since the depth variation in the Kelani River is significant, a low draught boat like a hydrofoil will be more suitable. The demand for Mattakkuliya-Hanwella line is not high when compared to other 2 inland waterway lines. And another significant feature of this line is the distance between 2 stations. Compared to other waterway lines station to station distance is greater in Mattakkuliya-Hanwella line. Therefore, a boat with a capacity around 30-40 passengers and speed up to 30 km/h will be ideal for this line. And also, the boats should be of good quality, unsinkable and air-conditioned.

9. Conclusion & Recommendations

Although the potential of water bodies was neglected in the recent past, traffic planners have realized its potential as it is a good solution for the existing traffic in the road structure and also as it is a cost-effective, environment-friendly, flexible transportation mode.

In this paper, the infrastructural aspects of the inland transportation line from Peliyagoda to Hanwella along Kelani River was focused. Bathymetric data, land use data, data regarding other transportation modes were collected from various institutes and using "ArcGIS" and "Google Earth Pro" software's, navigational path was drawn. A site survey was carried out to examine the horizontal and vertical clearance of the channel. Impact of salinity barrier at Ambatale was studied, and it was found that the navigational path would be blocked during the dry season. Therefore, a shuttle bus service was proposed to mitigate that issue.

It can be concluded that Kelani River is a navigable river although there are some areas to be dredged. After developing the system, traffic congestion in the road network will be minimized, passengers will be able to have an efficient, safe and a pleasant journey, air and sound pollution will be minimized, and the area will be economically upgraded.

Further studies must be done to reduce the siltation and bank erosion which makes the navigable sections shallow and hinder the movement of the boats. A detailed environmental impact assessment must be carried out. IT related applications must be introduced to improve the quality of the

facility. And also, a detailed survey of the river must be carried out to find locations of the rock outcrops that can hinder the movement of boats.

References

1. De Silva, G. L. D. I., 2003. The Study of the Feasibility of Water Transportation in Colombo Metropolitan Region, Colombo: University of Moratuwa.
2. Bandara, J. M. S. J., Sirisoma, R. M. N. T., Pushpakumara, T. D. C., Jayarathne, P., and Cooray, L. H. C. (2004). Canal Commuter Transit Study. Colombo: Transportation Engineering Division, Department of Civil Engineering, University of Moratuwa.
3. Abeykoon, A. M. H. K. and Nawarathna, N. M. A. L. B., 2011. Enhancing Water Quality by Salinity Barriers and its Impact on Environment. XIVth IWRA World Water Congress, p. 9
4. Jayawardane, C., 2009. Ancient Modes of Inland Water Transportation in Sri Lanka; Stability Analysis of Craft Excavated from Attanugala Oya. The Institution of Engineers, Sri Lanka, 43(3), pp. 14-21.
5. Kalyani, T., Vidyasagar, D. and Srinivas, V., 2015. Accident analysis of river boats capsized in Indian Inland Waters and safety aspects related to passenger transportation. International journal of innovative research and development, 4(7).
6. Jugović, A., Mezak, V. and Lončar, S., 2007. Organization of Maritime Passenger Ports, s.l.: PREGLEDNI RAD.
7. Awal, Z., Islam, M. & Hoque, M., 2015. *Analysis of Passenger Vessel Accidents in the Inland Waterways of Bangladesh*. s.l.:ResearchGate.
8. Western Region Megapolis Planning Project Transport Master Plan, Ministry of Megapolis and Western Development, <https://www.megapolis.gov.lk/>, Visited, 20th September 2016.
9. Perera, D., 2014. Colombo Metropolitan Transport Master Plan \$ Areas for International Cooperation. Colombo: Ministry of Transport.
10. <http://www.google.com/earth/download/ge/>, Visited, 10th September 2016.
11. Senanayake, I., Pushpakumara, T. and Puswewala, U., 2013. A GIS Based Analysis on Use of Inland Waterways for Public Transportation in the Western Province of Sri Lanka. The Institution of Engineers Sri Lanka, 46(2), pp. 1-11.



Hydroplaning Risk Evaluation in High Speed Low Traffic Volume Highways

M.D.M. Sheranie and S. Senevirathne

Abstract: During high-intensity rainfall events, a significantly thick water film builds up on the surface of a highway. Hydroplaning occurs when water pressure builds up in front of a moving tire resulting in an uplift force sufficient to separate the tire from the pavement. The loss of steering and drag force produced during hydroplaning. During the rain, due to the decreased visibility, the traveling speed usually exceeds 80 kmph can drop by ten percent (10%) of its initial value. According to the current studies, the effect of hydroplaning can be significant even at a speed less than 70 kmph. Since the travel speed is well above this value in Sri Lankan expressways there is a higher probability of occurrence of hydroplaning hazard in expressways in Sri Lanka. A preliminary evaluation was performed to compare and test the wet weather crash frequencies and rates across different pavement materials. In this study, Florida crash database used for the analysis to identify the critical crash locations in Sri Lanka. The effects of the generated water film are considered as primary sources of investigation in crown and transition sections. It is found that the conditions are quite different for superelevation transition sections compared to normal crown sections. The combined effect of lateral and longitudinal slopes in superelevation transition sections causes a significant increment in Water Film Thickness (WFT) and the magnitude of the maximum Water Film Thickness (WFT) increases at superelevation transitions compared to normal crown conditions. Finally, the current study evaluates the hydroplaning effect by each factor and identified the safe speed limit for high crash locations in expressway network of Sri Lanka based on a case study of Southern Expressway. Criterion for pavement surface design must include a hydroplaning risk evaluation in the design stage of expressways and posted speed limits can be redefined for already constructed expressways.

Keywords: Heavy rain, water film thickness, travel speed, crown and transition sections, safe speed limit

1. Introduction

Driving risk under inclement weather conditions has long been considering higher than under normal weather conditions. Among several variables pertaining to weather conditions, rainfall is recognized as a critical factor that affects traffic crash occurrences [1]. Heavy rainfall often results in reduced visibility, increased stopping distance and hydroplaning.

During highly intense rainfall events, a significantly thick water film builds upon highway surfaces. When a vehicle is hydroplaning, the driver will lose control of the vehicle. Hydroplaning is caused when water on a roadway is deep enough to lose contact between tires of the vehicle and the road. Many people assume that water has to be deep enough to cause hydroplaning, but even a thin film of water can cause problems, especially if someone is driving at a higher speed. It is obvious that the risk of hydroplaning is higher on high-speed roadway facilities.

Expressway network in Sri Lanka (Figure 1) was designed to have a high speed. Even though there are some expressway projects are taking place, Southern expressway and Katunayake expressway are the operational and implemented expressways out of the entire expressway network in Sri Lanka.

When the travel speed exceeds 80 kmph, the speed can be dropped by ten percent (10%) during the rain due to the decreased visibility [2]. According to the studies in developed countries, the effect of hydroplaning can be significant even at speed less than 70 kmph [3].

Eng. (Ms.) M.D. M. Sheranie, BEng (Hons, UK), AMIE(SL), ICIOB(UK), AMCPM(SL).

Eng. (Mrs.) S. Seneviratne, C. Eng., MIE(SL), B.Sc. Eng. (Moratuwa).



Since the travel speed on Southern Expressway is well above this value (i.e. minimum travel speed is 80 kmph), it is very important to evaluate risk factors that contribute to hydroplaning. Even though there are several kinds of situations which produce the hydroplaning effect in expressway, mostly where water is assembling as a pond such as the bottom of sag vertical curves, horizontal transition curve sections, and pavements with wheel tracks or ruts are the most common situations [4].

The water film conditions are different in superelevation transition section compared to normal crown sections. The magnitude of the maximum Water Film Thickness (WFT) increases at superelevation transition section when compared with normal crown sections. Therefore, the hydroplaning can present a server safety issue at transition sections than at normal crown sections in highways.

But unfortunately, this has not been considered in most highway geometric design guidelines (ie: - AASTO, TRL Road note and Australian guideline). As mentioned by Torbic [5], even though the design speed has been estimated based on the mechanistic properties of the vehicle at curved segments, there is a high probability for accidents to be occurred in curved sections due to high speed.

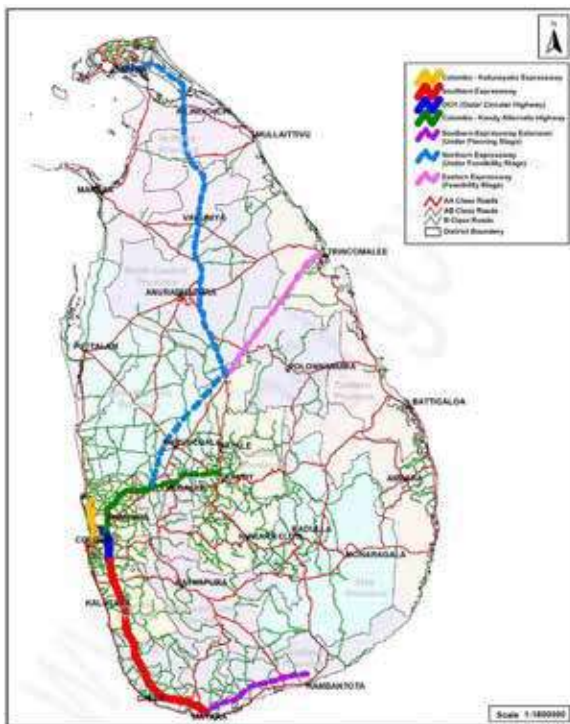


Figure 1 - Expressway Network in Sri Lanka (RDA)

There were a number of accidents occurred in the expressway during the rainy time including

hydroplaning accidents. Since the Southern Expressway is the first expressway in Sri Lanka, people have less awareness of the effect of hydroplaning.

An accident occurred in Southern Expressway at the 8th-mile post in Kahatuduwa on the very first day after the expressway was declared open. This was the first accident occurred in Expressway and it was a viscous hydroplaning crash [6].

Practical methods have to be followed in experimentation and analysis of the effect of hydroplaning in wet weather condition in expressway network of Sri Lanka since Sri Lankan expressway network has been designed using ASSHTO and TRL Road Design.

The objective of this research is to identify the potentially high crash locations in a road section and propose a safe speed to minimize the consequences of hydroplaning.

2. Literature Review

2.1 Impact of Weather and Climate

Fwa and Ong [7] have stated that “impact of the weather and climate is a major part of the hydroplaning accident”.

The wet climate of a major part of Sri Lanka is strongly governed by the monsoon seasons, the associated air masses and planetary wind regimes over South Asia. Due to alternating monsoon circulation systems through the year, two principal monsoon rainfall seasons and two transitional periods, called Inter-monsoon seasons can be identified in Sri Lanka.

Rainfall intensity at any time scale is one important aspect of monsoon climatology. Mean statistics reveal comparably high rainfall intensity with a maximum of 25 mm in the interior part of the south-western region, where the mean number of rainy days is higher than 100 [8].

2.2 Water Film Thickness with Rainfall Intensity

The thickness of the water film that contributes to hydroplaning is the Mean Texture Depth (MTD) plus the water film above the tops of the surface asperities. The flow path (L) for a particle of water falling on a pavement surface is simply defined as the line determined by the slope (S) of the pavement surface. Thus, the maximum flow path for a pavement section is the longest flow path for the section. The maximum distance that a rain droplet can flow

between the point of contact with the water film and its point of exit from the pavement. For a given quantity of rainfall, with known pavement parameters, the following relation can utilize to evaluate water film thickness t , from PAVDRN program [2].

$$t = \left[\frac{nLI}{36.1S^{0.5}} \right]^{0.6} - MTD \quad \dots(1)$$

Where,

- I = Rainfall intensity
- n = Manning coefficient

2.3 Effect of Cross Slope on Water Film Thickness

Typically, the cross slopes on either side are symmetric about the centre line and they are denoted as normal crown. But at a curve (super-elevation) the cross slopes about the centre line changes as shown in Figures 2 and 3. The cross slopes of the lanes between the centre line and inside edge remains constant and is equal to the normal crown. However, the cross slopes between the centre line of the road and the outside edge change and its' magnitude becomes equal but higher that the cross slope on the other side in super-elevation sections.

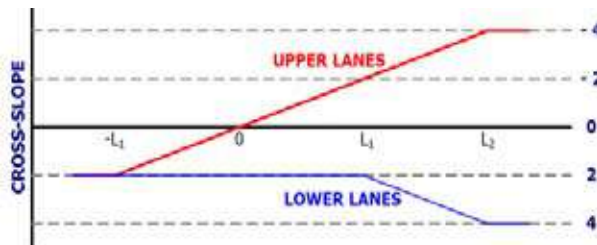


Figure 2 - Lateral alignment of super-elevation transition with cross slope = 4% [9]

Figure 2 shows that the slope of the normal crown is 2% and the slope of the full super-elevation is 4%. In this, fully super-elevated section can be seen at a distance of L_2 and cross-sectional details can be seen as Figure 3.

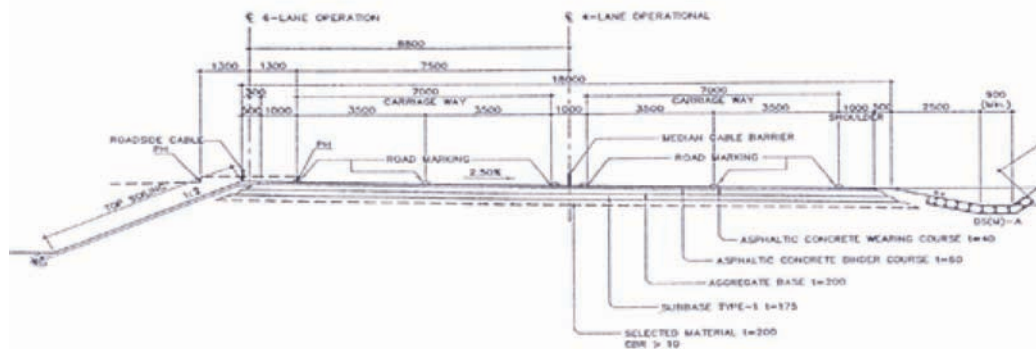


Figure 3 - Typical Cross Section of Southern Expressway

In this transition sections, cross slope reaches to zero value. With a longitudinal slope, the flow path of water can be extended and it leads to higher water film thickness near to transition sections.

2.4 Water Film Thickness in Transitions Sections

When pavement rotates with a super-elevation section, the flow path of water get extended and as a result of that, it can lead to higher water film thickness.

Maximum runoff depth (Water Film Thickness, WFT) was estimated using numerical simulation modelling for different roadway configurations [10]. Figure four shows the results for a roadway with 4 travel lanes for an Asphalt roadway surface with a Manning (n) = 0.015 and rainfall intensity of 100 mm/hr. The roadway alignment is based on a design speed of 96.6 kmph, which corresponds to a maximum relative gradient of 0.45 %. The 'zero' distance corresponds to the Zero Cross Slope (ZCS) station.

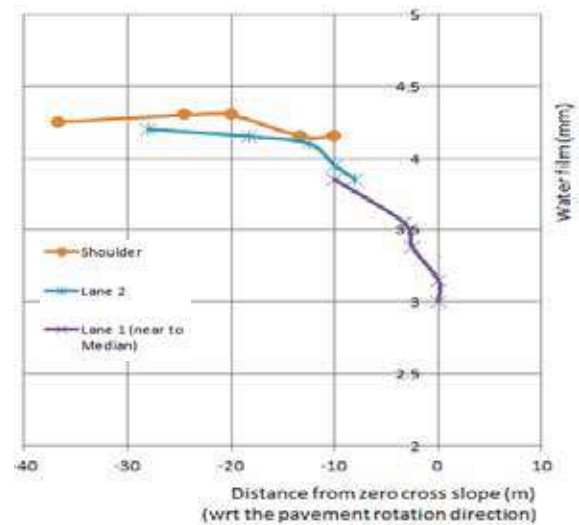


Figure 4 - Variation of the WFT with distance from ZCS (100 mm/h rainfall, longitudinal slope varies from 0.5% to 6% [10])



It can be seen that the water film near to ZCS can be increased up to 4.3 mm at outer lanes. Further, it can be seen that when longitudinal slope varies from 0.5% to 6% effect of that does not contribute to much change of maximum water film.

With regard to vehicle safety at superelevation transitions, it is not clear whether the magnitude of WFT or the changes in WFT in the longitudinal and lateral directions are the most critical variables. According to Figure 4, it is clear that maximum water film that can be generated by the super elevated transition section is always less than 5 mm due to a rainfall intensity of 100 mm/h.

2.5 Friction Number Vs Water Film Thickness

With a known water film thickness, the effect of dynamic friction has been evaluated as shown in Figure 5 [10]. The dynamic friction lowered by 35% once the pavement surface gets wet. Further, it can be seen that the dynamic friction coefficient can be further lowered up to 0.15 with the increment of water film thickness.

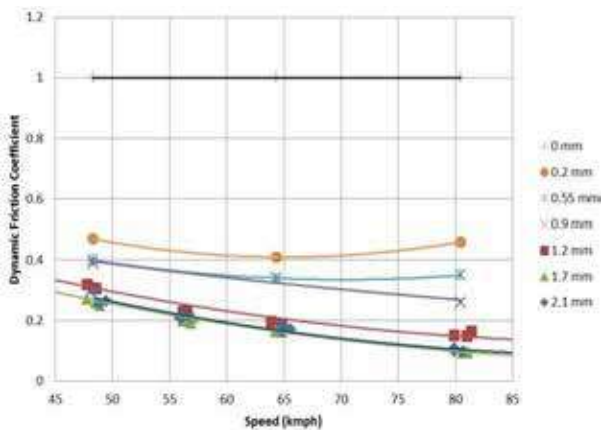


Figure 5 - Variation of Friction Coefficient with Speed and Water Film Thickness [10]

2.6 Hydroplaning Speed Vs Water Film Thickness

As stated by Glennon [4], the vehicle speed at incipient hydroplaning depends on the storm water runoff depth, tire pressure, tire tread depth, average pavement texture depth and other factors. From above-mentioned factors, storm water runoff depth (water film depth) is the primary variable.

Following equations are used in PAVDRN [2];

- Water film thickness less than 2.4 mm,

$$HPS = 26.04 WFT^{-0.259} \quad \dots(2)$$

Where,

HPS = Hydroplaning speed (mi/h)

WFT = Water film thickness (in)

- Water film thickness greater than or equal to 2.4 mm,

$$HPS = 3.09 A \quad \dots(3)$$

Where,

A is the greatest of the values calculated using equations (4) and (5);

$$\left[\frac{28.952}{WFT^{0.06}} - 7.817 \right] MTD^{0.14} \quad \dots(4)$$

$$\left[\frac{10.409}{WFT^{0.06}} + 3.507 \right] \quad \dots(5)$$

Where,

MTD - Mean Texture Depth (in)

3. Methodology

As described in the section 1, Sri Lankan expressway network has been designed using the road manuals in the USA and the UK. In this research, significant efforts have been devoted to data acquisition, processing, and compilation. A preliminary evaluation was performed to compare and test the wet weather crash frequencies and rates across different pavement materials to compare the pavement parameters with Sri Lankan expressways.

Project Methodology flowchart shown in Figure 6 has been used for the current study to evaluate the hydroplaning effect by each factor and also to identify the safe speed limit for high crash locations in expressway network of Sri Lanka based on a case study of Southern Expressway.

Florida crash database used for the analysis of crash locations in Sri Lanka since it is difficult to find a highway crash database in Sri Lanka. Florida is a tropical state as Sri Lanka, but few assumptions have been made such as both Southern expressway and Florida state road segment have similar driver behavior, demographic, environmental and vehicle factors.

In this analysis, data for four years (2007 to 2010) obtained from Florida Department of Transportation (FDOT) was considered. Two

major data source used in this evaluation as follows;

- Crash Analysis Reporting System (CARS) database of Florida
- Pavement Condition Survey (PCS) database

Data compilation process used to identify wet weather crashes and rainfall intensity at the crash location. Filtering criteria has been used to identify the wet weather crashes from the crash analysis reports.

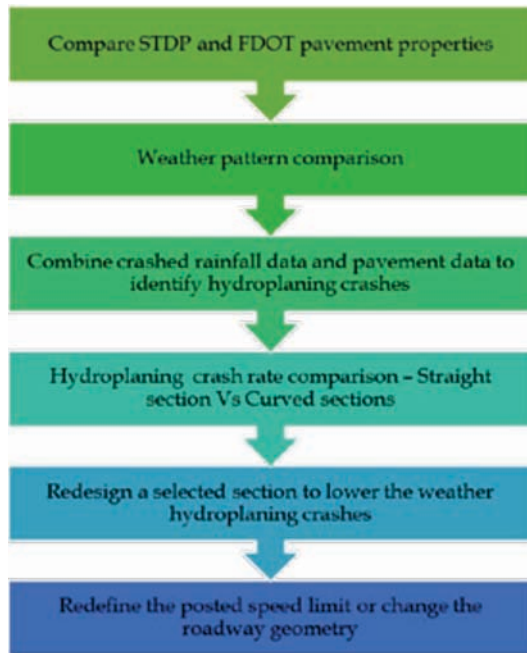


Figure 6 - Methodology Flow Chart

4. Weather Data Collection

4.1 Florida State

All the identified crashes have been assigned with geological locations. According to that, all the crashes were located in high-speed pavement facilities like interstate roadway network.

deliver the most reliable and real-time weather data for Florida State. Considering crash distribution in the study area and weather station proximity to each crash location, 72 airport weather stations were selected to obtain microscopic weather data measured on hourly based intervals in this study from year 2007 to 2010. For each crash observation, three weather stations out of the 72 weather stations were used by their proximity to the crash location to estimate the hourly weather data.

However, when it was difficult to find out three weather stations nearby for these one-dimensional points must be applied to two-dimensional areas. This was accomplished by creating Thiessen Polygons around the weather station location points [11].

4.2 Southern Expressway

As described in section 2.1, since the Southern Expressway is located in South-western region rainfall is an utmost important factor to consider. Rainfall intensities are calibrated on the basis of accumulated storm water during 15 min, 30 min or during 1-hour rainfall. Irregular variation can be observed many times as shown in Figure 8.

According to the Figure 8, it can be seen that rainfall intensity can be such different during that considered time period. So it is important to consider the immediate rainfall effect with respect to total rainfall. The effect of generating water film thickness can be varied on the pavement geometry and the pavement materials.

5. Results & Analysis

5.1 Pavement Properties Comparison

Sample data set used to compare the pavement



Figure 7 - Fluctuation in Rainfall Intensity (mm/h) Vs Time at Interstate Highway (I-275) Segment

National Climatic Data Centre (NCDC) in the USA affiliated 'Weather Source' was found to

properties of Southern Expressway (SE) and Florida Department of Transportation (FDOT) highways (Table 1).



A statistical analysis was done for both data sets to find the mean and standard deviation. The results are shown in Table 2.

Table 1 - Extracts of the SE and FDOT comparing data set

Section	EX_005	EX_005	EX_005	EX_010	EX_010	EX_015
IRI (m/km)	1.99	1.00	1.43	1.21	0.85	0.94

SE roadway sections

Roadway ID	1010000	1040000	1050000	1050000	1075000	1075000
IRI (m/km)	1.572	1.366	1.143	1.397	0.905	0.826

FDOT roadway sections

Table 2 - One Sample Statistics

	N	Mean	Std. Deviation	Std. Error Mean
FDOT	2124	1.258946	.4051048	.0087900
SE	293	1.250171	.4882191	.0285221

A sample t - Testing to compare pavement parameters of SE and FDOT highways. The result is shown in Table 3.

Table 3 - One Sample t - Test

	Test Value = 0					
	t	df	Sig. (2-tailed)	Mean Difference	95% Confidence Interval of the Difference	
					Lower	Upper
FDOT	143.22	2123	.000	1.2589	1.2418	1.2762
SE	43.832	292	.000	1.2502	1.1941	1.3064

From Table 3, it is seen that variance of lower and upper values of FDOT data set is in between 95% confidence interval of SE data set. Therefore, from above t-testing that pavement parameters of FDOT are similar to the SE pavement properties.

5.2 Critical Section Identification

Hypothesis testing to compare wet-weather crashes Vs crashes during dry condition on

curves. In this analysis, two crash rates have been considered,

1. Straight sections and
2. Curved section.

Formulation of the null hypothesis and alternative hypothesis are shown in below;

$$H_0: \mu_1 = \mu_0$$

- During wet weather conditions, the nature of hydroplaning related crashes that have occurred on straight roadway segments is the same as that in curved segments.

$$H_1: \mu_1 \neq \mu_0$$

- A significant difference in hydroplaning related crashes on curved sections with corresponding to the straight roadway segments.

Reject the null hypothesis if there is no difference between means at designated significance levels. The four-year crash data from 2007 to 2010 were considered. Then the data set was screened to identify the hydroplaning related accidents as shown in Table 4.

Table 4 - Hydroplaning Related Crash Screening and Analysis

Year	Straight Sections			Curved Sections		
	Total Crashes on Straight Sections	Hydroplaning related crashes on Straight Sections	Crash rate on Straight Sections	Total Crashes on Curved Sections	Hydroplaning related crashes on curved sections	Crash rate on Curved Sections
2007	301818	5257	1.74%	25603	1720	6.72%
2008	290101	5087	1.75%	23156	1648	7.12%
2009	285683	5604	1.96%	22675	1717	7.57%
2010	293053	6823	2.33%	23385	1617	6.91%

Since the variances and means of the two populations are known, hypothesis testing has been considered to avoid any Type I error, i.e. considering the very low significant level of 0.1%. It was assumed that data populations are normally distributed.

From Table 5 it is seen that there is a significant hydroplaning risk in curved sections compared to straight portions. It could be concluded from the above hypothesis testing that the hydroplaning risk at curvature segment is three times higher than on normal crown straight roadway segments.

It should be noted that hypothesis tests performed in this preliminary evaluation considered pavement width as the sole factor to explain the difference in wet weather crash frequencies and rates. It can be viewed as a qualitative analysis. More sophisticated multivariate analyses, such as Poisson and Negative Binominal regression, will be employed to evaluate and quantify the potential risk of hydroplaning and the effects of other contributing factors, such as pavement condition, speed, visibility, curvature, etc.

Table 5 - Hypothesis Test Verification of Hydroplaning Related Crashes

	Crashes on Straight Sections	Crashes on Curved Sections
Mean	1.95%	7.08%
Standard Deviation	0.24%	0.32%
Calculated Z	25.93	
Critical Value $Z_{0.001}$	3.29	

5.3 Case Study Based on Southern Expressway

In this analysis, I-275 roadway segment of the Southern expressway had been considered at a chainage of 0+700 distance, which highway behaves with a 0.1% cross slope and 0.667% longitudinal slope. Based on the probable rainfall pattern occurring on the southwestern part of Sri Lanka, water film thicknesses have been predicted as shown in Figure 9.

The PAVDRN equation (1) stated in section 2.2 has been used to predict the water film thickness for given parameters. Typical roughness parameters for different pavements used in PAVDRN are shown in Table 6.

It is obvious that dynamic friction reduces with the increment of water film thickness. With that, the safer vehicle speed calculated using equations (2), (3), (4) and (5) stated in section 2.6. It can be seen that, when rainfall intensity increases more than 20 mm/h, the safer speed reduces than the design speed. Based on the lane geometry and pavement parameters it can be further reduced i.e. 74 kmph. Likewise following Figure 10 was developed to identify the safer speed limit at a specific transition location (chainage 0+700 of I-275 roadway segment) of the Southern expressway.

Table 6 - Typical Roughness Parameters Used in PAVDRN [2]

Pavement type	MTD (mm)	Manning's n
PCC	0.91	0.031
DGAC	0.91	0.0327
OGAC	1.5	0.0355

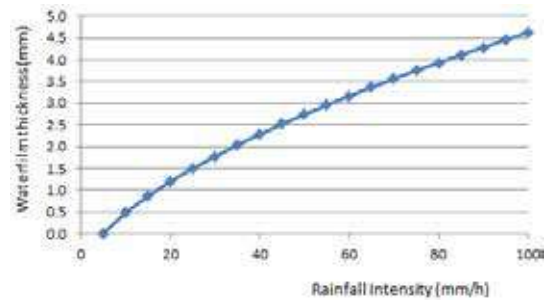


Figure 9 - Probable Water-film Thickness Vs Rainfall Intensity Based on Southern Expressway Pavement Characteristics

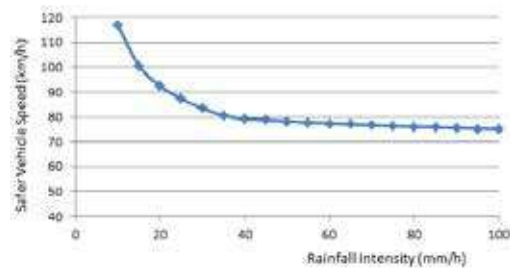


Figure 10 - Safe Vehicle Speed Limit for Southern Expressway Road Segment

6. Conclusions

Hydroplaning occurs when water pressure builds up in front of a moving tire resulting in an uplift force sufficient to separate the tire from the pavement. During rain, due to the decreased visibility, the traveling speed which usually exceeds 80 kmph can drop by ten percent (10%) of its initial value. But according to the current study, the effects of hydroplaning can be significant even at speeds around 70 kmph. This is applicable for Southern Expressway since the design speed is well above 70 kmph.

The effects of the generated water film thickness on superelevation sections are quite different with compared to normal crown sections. When compared regard to vehicle safety at superelevation transitions, it is not clear whether the reduction of friction across the pavement or changes in WFT in the longitudinal and lateral directions are the most critical variables.



It is realized that hydroplaning can present a severe safety issue at transition sections than the normal crown sections. Due to the numbers of different causative factors are involved in hydroplaning and their relative contributions, there is a great deal of uncertainty in the initiation of hydroplaning.

The safe speed limit for the critical sections such as curve sections and super elevated transition sections has been identified using factors. Redefine the posted speed limit can be done for already constructed expressways.

To increase the safety level of the expressways, it is an advantage to identify critical locations in the expressway network by analysing many sections. Based on the analysis, high priority must be given for drainage design at horizontal curve sections with superelevation in order to minimize the water level builds on the surface. It is always better to do the skid test for identified critical locations and skid proof if necessary and also pavement grooving will help to reduce the thick water film builds up on the surface of a highway [12].

Consideration of the effect of hydroplaning when designing the highway geometry and pavements will lead to a safe drive during the wet weather.

References

1. Gallaway, B. M., et al., "Tentative Pavement and Geometric Design Criteria for Minimizing Hydroplaning", No. FHWA-RD-75-11 Final Report, 1975.
2. Anderson, D. A., et al., "Improved Surface Drainage of Pavements", *The Pennsylvania Transportation Institute, The Pennsylvania State University*, No. Project 1-29 Final Rpt., 1998.
3. Cheng, G., et al., "Speed Analysis of the Radial Tire on Hydroplaning Pavement", *3rd International Conference in Material, Mechanical and Manufacturing Engineering, IC3ME*, 2015, pp. 1485-1489.
4. Glennon, J. C., *Roadway hydroplaning - A framework to determine critical wheel rut depths*, 2015.
5. Torbic, D. J., et al., "A Guide for Reducing Collisions on Horizontal Curves." *NCHRP, Report 500*, Vol. 7, 2004.
6. <http://www.dailymirror.lk/article/accident-on-southern-expressway-15065.html>. Visited 21st September 2017.
7. Fwa, T. F., & Ghim P. O., "Wet-Pavement Hydroplaning Risk and Skid Resistance: Analysis." *Journal of Transportation Engineering, ASCE*, Volume134, No. 05, 2008, pp. 182-190.
8. Ranatunge, E., et al., "Changes in the Southwest Monsoon Mean Daily Rainfall Intensity in Sri Lanka: Relationship to the El Niño-Southern Oscillation." *Palaeogeography, Palaeoclimatology, Palaeoecology*, Volume 197, No. 01, 2003, pp. 1-14.
9. http://onlinemanuals.txdot.gov/txdotmanuals/hyd/pavement_drainage.htm, Visited, 25th August 2016.
10. Charbeneau, R. J., Jaehak J., & Michael E. B., "Highway Drainage at Superelevation Transitions", *Centre for Transportation Report, The University of Texas at Austin*, Report No. FHWA/TX-08/0-4875-1, 2008.
11. Kyte, M., et al., "Effect of Weather on Free-Flow Speed." *Transportation research record: Journal of the transportation research board*, Report 1776, 2001, pp. 60-68.
12. Enustun, N. "Study to Identify Hydroplaning Crashes" TSD 330-77. Final Report submitted to Michigan Department of State Highways and Transportation, 1976.